

I. DEVELOPMENT OF NICKEL- AND PALLADIUM-CATALYZED
ASYMMETRIC ALLYLIC ALKYLATION REACTIONS
II. ENANTIOSELECTIVE SYNTHESSES OF TETRAHYDROISOQUINOLINE–
BASED NATURAL PRODUCTS AND UNNATURAL ANALOGS

Thesis by
Aurapat (Fa) Ngamnithiporn

In Partial Fulfillment of the Requirements
for the Degree of
Doctor of Philosophy

CALIFORNIA INSTITUTE OF TECHNOLOGY

Pasadena, California

2021

(Defended March 4, 2021)

© 2021

Aurapat Ngamnithiporn

ORCID: 0000-0002-5389-8171

All Rights Reserved

*To my family,
for their unconditional love and support*

ACKNOWLEDGEMENTS

My graduate studies and the research described in this thesis would not have been possible without the support of many people. First and foremost, I would like to express my deepest gratitude to my advisor, Professor Brian Stoltz. Brian has been the most supportive, encouraging, and understanding graduate advisor a student could ask for. His mentorship style, which provides freedom to explore chemistry of our own interest, has greatly benefited me to become an independent chemist. I am indebted to him for all his guidance and his unwavering support during the past five years, and I am honored to be part of the Stoltz Team.

I would also like to extend my appreciation to the chair of my committee, Professor Robert Grubbs, and the rest of my committee members, Professors Harry Gray and Gregory Fu for their valuable feedback and insightful comments. Thank you for creating such a welcoming environment while providing constructive criticism during all those meetings and examinations. Furthermore, I also wish to thank Professor Sarah Reisman for her expertise and advice during the joint Stoltz-Reisman group meetings. I have learned a lot from her during these past years, especially from her classes during the first year of my graduate studies.

I would not be where I am today without previous trainings from my undergraduate education. For that, I need to acknowledge my undergraduate research advisors, Professors David Alberg and Gretchen Hofmeister. I am sincerely thankful for the opportunity to work in their labs, as well as the trainings they provided during my years at Carleton College.

At Caltech, we are fortunate to have excellent facility staffs. I would like to especially express my gratitude to Dr. Scott Virgil for his relentless support in keeping the catalysis center running smoothly, particularly during these difficult pandemic times. Scott has also been a phenomenal source of advice for any problems I encountered in the lab, and his expertise in spectroscopy and product purification is greatly appreciated. I also need to thank another spectroscopic expert, Dr. David VanderVelde. I am thankful for his willingness to answer any of my questions in addition to his tireless support in maintaining the NMR facility in such an amazing condition. Dr. Mike Takase and Larry Henling are thanked for their assistance obtaining X-ray crystallography data and refining them into publishable structures. I also thank Dr. Mona Shahgholi and Naseem Torian for helping with mass-spectrometry data acquisition. Finally, I would like to thank Joe Drew, Alison Ross, and the rest of the graduate support staff for keeping everything running so well in the CCE department.

One of the most enjoyable aspects of my graduate school journey was being surrounded by amazing people and working with incredibly talented scientists. I am sincerely thankful to my first mentor, Dr. Shoshana Bachman, for teaching me necessary lab skills and techniques to work on a method project. We have become friends during the whole process, and I have truly enjoyed the time we spent outside of lab getting lunches and coffee. Dr. Carina Jette and Dr. Toshihiko Iwayama are acknowledged for their assistance with the allylation projects. I am also grateful to have been part of the THIQ team at the same time as Dr. Eric Welin and Dr. Gerit Pototschnig. Eric is an amazing chemist, a fantastic teacher, and a great friend. His vast knowledge of chemistry has made him become an invaluable source of ideas not just for me, but for many Stoltz

group members. Dr. Gerit Pototschnig, who is also my baymate, is a remarkable experimentalist. We both enjoyed working early mornings, so I need to thank her for the companionship during those times. Additionally, her many photos and videos of adorable Pablo, her golden retriever, have brightened my days recently.

The highly collaborative nature of the Stoltz group also landed me the opportunity to work with Dr. Michael Yamano and Professor Neil Garg from UCLA. This experience has broadened my perspective in chemistry, so I am thankful for that. Furthermore, I also need to thank Alexia Kim for being an amazing project partner. Alexia is a dedicated chemist, and it has been a productive two years working with her. Apart from chemistry, she is also a great musician, singer, hip-hop dancer, and a very skilled video game player. I admire her work-life balance, and I appreciate the memorable times we spent on Animal Crossing, Overcooked, as well as those random conversations we have had over the last two years.

Throughout my studies, I have overlapped with many more brilliant chemists. I would like to recognize the Stoltz's alums: Drs. Seo-jung Han, Kelly Kim, Nick O'Connor, Beau Pritchett, Sam Shockley, David Schuman, Steven Loskot, Elizabeth Goldstein, and Austin Wright for their friendship and intellectual discussions during my first few years at Caltech. I am also thankful for getting to know Dr. Jaika Doerfler, who is so lively and always the life of the party. I need to thank Tyler Fulton and Nick Hafeman for being amazing friends and labmates. I have enjoyed the time we spent during ping-pong sessions, as well as those entertaining conversations we have had over coffee breaks. Nick Hafeman is also especially thanked for his proofreading services on this thesis. And lastly, the younger students in the Stoltz group: Zach Sercel, Alex

Cusumano, Tyler Cassleman, Joel Monroy, and Melinda Chan, I appreciate the excitement and enthusiasm you all have brought to the team.

To my cohort on the 3rd floor of Schlinger, which includes Carina Jette, Eric Alexy, Chris Reimann Sean Feng, and Zainab Al Saihati, thank you for making my PhD journey unforgettable. I need to especially thank Carina, my hoodmate, as she has been with me since the very first day in lab. I truly admire her tenacity and determination in working on any project, and I am thankful for her friendship during these past years. Eric Alexy, who is my neighbor in the large office, has been a fun person to talk to. He is not only good at chemistry, but also surprisingly good at sports, as evident from the times we played tennis, ping pong, football, and volleyball. For Chris Reiman, who is the most sociable person within the Stoltz cohort, I really respect his passion for total synthesis. He, in my opinion, is the best party planner the Stoltz group has had because he always planned the party with extra packs of White Claw.

Outside of lab, I am grateful to be part of the Thai students community at Caltech. Thank you for the weekend dinners, karaoke nights, and many uplifting conversations we have had over the years. In addition, I need to especially thank Earth Jaika and Tee Warakkagun for everything we have gone through together. Ten years ago, we made the decisions to come to the US, and now we are so close to the finish line. I am so proud that we have made it this far!

Finally, I would like to acknowledge my family who made my graduate studies possible. My mom and dad have been there for me whenever I need them, and I am thankful for all their unconditional love and support. To my twin sister, Fern, thank you for being the best friend I could have, and I am looking forward to spending more time

with you very soon. Lastly, I am incredibly fortunate to have my husband, Dr. Nat Pombubpa, by my side through highs and lows. Thank you for celebrating both small and big successes with me these past five years, and I cannot wait to celebrate many more with you in the next chapter of our lives back in Thailand.

The work presented in this thesis would not have been possible without the continued support of all these people and many others not specifically mentioned by name. I am deeply grateful to each of them.

ABSTRACT

Described in this thesis are four projects related to the development of synthetic methodologies for the preparation of enantioenriched building blocks, and the total syntheses of complex tetrahydroisoquinoline natural products. In Chapter 1, the development of nickel-catalyzed asymmetric allylic alkylation of lactones and lactams with allylic alcohols is presented. In Chapter 2, the development of palladium-catalyzed enantioselective decarboxylative allylic alkylation of silicon-containing heterocycles is detailed. In these chapters, the utilization of prochiral enolates as nucleophiles has enabled access to enantioenriched all-carbon quaternary stereocenters.

Chapter 3 describes the total syntheses of bis-tetrahydroisoquinoline alkaloids, (–)-jorumycin and (–)-jorunnamycin A. A general synthetic strategy, which exploits the tandem cross-coupling/hydrogenation approach, represents the first non-biomimetic synthetic route and allows for an efficient construction of the pentacyclic core in a highly modular fashion. Additional bis-tetrahydroisoquinoline analogs were prepared, and preliminary studies to probe their cytotoxicity against cancer cell lines were conducted. Finally, an extension of the enantioselective and diastereoselective hydrogenation technology to include simple 1,3-disubstituted isoquinolines is described in Chapter 4.

PUBLISHED CONTENT AND CONTRIBUTIONS

1. Ngamnithiporn, A.; Jette, C. I.; Bachman, S.; Virgil, S. C.; Stoltz, B. M. “Nickel-Catalyzed Enantioselective Allylic Alkylation of Lactones and Lactams with Unactivated Allylic Alcohols.” *Chem. Sci.* **2018**, 9, 2547–2551. (Highlighted in *Synfacts* **2018**, 14, 0491). DOI: 10.1039/c7sc05216b.

A.N. participated in reaction design, reaction optimization, experimental work, data analysis, and manuscript preparation.

2. Welin, E. R.; Ngamnithiporn, A.; Klatte, M.; Lapointe, G.; Pototschnig, G. M.; McDermott, M. S. J.; Conklin, D.; Gilmore, C. D.; Tadross, P. M.; Haley, C. K.; Negoro, K.; Glibstrup, E.; Grünanger, C. U.; Allan, K. M.; Virgil, S. C.; Slamon, D. J.; Stoltz, B. M. “Concise Total Syntheses of (–)-Jorunnamycin A and (–)-Jorumycin Enabled by Asymmetric Catalysis.” *Science* **2019**, 363, 270–275. DOI: 10.1126/science.aav3421.

A.N. participated in reaction optimization, experimental work, data acquisition and analysis, and manuscript preparation.

3. Yamano, M. M.; Knapp, R. R.; Ngamnithiporn, A.; Ramirez, M.; Houk, K. N.; Stoltz, B. M.; Garg, N. K. “Cycloadditions of Oxacyclic Allenes and a Catalytic Asymmetric Entryway to Enantioenriched Cyclic Allenes.” *Angew. Chem. Int. Ed.* **2019**, 58, 5653–5657. DOI: 10.1002/anie.201900503.

A.N. participated in reaction optimization, experimental work, data analysis, and manuscript preparation.

4. Kim, A. N.;[‡] Ngamnithiporn, A.;[‡] Welin, E. R.; Daiger, M. T., Grünanger, C. U.; Bartberger, M. D.; Virgil, S. C.; Stoltz, B. M. “Iridium-Catalyzed Enantioselective and Diastereoselective Hydrogenation of 1,3-Disubstituted Isoquinolines.” *ACS Catal.* **2020**, *10*, 3241–3248. DOI: 10.1021/acscatal.0c00211.

A.N. participated in reaction optimization, experimental work, data analysis, and manuscript preparation.

5. Ngamnithiporn, A.;[‡] Iwayama, T.;[‡] Bartberger, M. D.; Virgil, S. C.; Stoltz, B. M. “Enantioselective Synthesis of Highly Oxygenated Acyclic Quaternary Center-Containing Building Blocks via Palladium-Catalyzed Decarboxylative Allylic Alkylation.” *Chem. Sci.* **2020**, *11*, 11068–11071. DOI: 10.1039/d0sc04383d.

A.N. participated in reaction optimization, experimental work, data analysis, and manuscript preparation.

TABLE OF CONTENTS

Dedication	iii
Acknowledgements	iv
Abstract	ix
Published Content and Contributions	x
Table of Contents	xii
List of Figures	xviii
List of Schemes	xxxix
List of Tables	xlii
List of Abbreviations	xlvi

CHAPTER 1

1

Nickel-Catalyzed Enantioselective Allylic Alkylation of Lactones and Lactams with Unactivated Allylic Alcohols

1.1	Introduction	1
1.2	Reaction Optimization	3
1.3	Substrate Scope Exploration	5
1.4	Preliminary Mechanistic Insights	8
1.5	Product Transformations	9
1.6	Conclusions	10
1.7	Experimental Section	11
1.7.1	Materials and Methods	11
1.7.2	Experimental Procedures and Spectroscopic Data	13
1.7.2.1	Synthesis of Nucleophiles	13
1.7.2.2	General Procedure for the Nickel-Catalyzed Allylic Alkylation	18
1.7.2.3	Additional Optimization Results	20
1.7.2.4	Spectroscopic Data for the Alkylation Products	24
1.7.2.5	Experimental Procedures and Spectroscopic Data for the Product Transformations	39
1.7.3	Determination of Enantiomeric Excess	45
1.8	References and Notes	49

APPENDIX 1 **54**
Spectra Relevant to Chapter 1

APPENDIX 2 **117**
X-Ray Crystallography Reports Relevant to Chapter 1

A2.1	General Experimental	118
A2.2	X-Ray Crystal Structure Analysis of Allylic Alkylation Product 3af	118

CHAPTER 2 **128**
Palladium-Catalyzed Enantioselective Decarboxylative Allylic Alkylation of Cyclic Siloxyketones

2.1	Introduction	128
2.2	Substrate Synthesis.....	130
2.3	Reaction Optimization.....	131
2.4	Substrate Scope Exploration	132
2.5	Product Transformations	134
2.6	Conclusions	136
2.7	Experimental Section	137
2.7.1	Materials and Methods.....	137
2.7.2	Experimental Procedures and Spectroscopic Data	138
2.7.2.1	Synthesis of Allyl β -Ketoester Starting Materials.....	138
2.7.2.2	General Procedure for the Palladium-Catalyzed Allylic Alkylation	149
2.7.2.3	Spectroscopic Data for the Alkylation Products	150
2.7.2.4	Experimental Procedures and Characterization Data for Product Transformations	157
2.7.3	Determination of Enantiomeric Excess	162
2.7.4	Determination of Absolute Configuration	164
2.7.4.1	Determination of Absolute Configuration of 17g via VCD and OR.....	164
2.7.4.2	Determination of Absolute Configuration of 17a via VCD and OR.....	167
2.6	References and Notes	170

APPENDIX 3 **174**
Spectra Relevant to Chapter 2

APPENDIX 4 **229**
Cycloadditions of Oxacyclic Allenes and a Catalytic Asymmetric Entryway to Enantioenriched Cyclic Allenes

A4.1	Introduction	229
A4.2	Computational Analysis of Oxacyclic Allene 31	232
A4.3	Substrate Synthesis.....	233
A4.4	Cycloadditions of Oxacyclic Allene	234
A4.5	Catalytic Asymmetric Approach to Oxacyclic Allenes and Evaluation of Enantiospecificity	238
A4.6	Conclusions	241
A4.7	Experimental Section	242
A4.7.1	Additional Optimization Results for Asymmetric Allylic Alkylation	242
A4.8	References and Notes	244

CHAPTER 3 **249**
Concise Total Syntheses of (–)-Jorunnamycin A and (–)-Jorumycin Enabled by Asymmetric Catalysis

3.1	Introduction	249
3.2	General Synthetic Strategy	252
3.3	Total Synthesis of Jorumycin	253
3.4	Biological Evaluation of Bis-THIQ Analogs	261
3.5	Conclusions	263
3.6	Experimental Section	264
3.6.1	Materials and Methods.....	264
3.6.2	Experimental Procedures and Spectroscopic Data.....	264
3.6.2.1	Synthesis of Isoquinoline N-Oxide	266
3.6.2.2	Synthesis of Isoquinoline Triflate	270
3.6.2.3	Fagnou Cross-Coupling Reaction	278
3.6.2.4	First-Generation Synthesis of Bis-Isoquinoline 83	280
3.6.2.5	Second-Generation Synthesis of Bis-Isoquinoline 83	286
3.6.2.6	Asymmetric Hydrogenation of Bis-Isoquinoline 83	290
3.6.2.7	Endgame Synthesis of Jorumycin	294
3.6.2.8	Synthesis of Derivatives 102–105	304
3.6.2.9	Preparation of 98 for Crystal Structure Analysis.....	304
3.6.3	Comparison of NMR Data to Known Samples.....	315

3.6.4	Optimization of the Enantioselective Hydrogenation	317
3.6.5	Explanation of Selectivity Differences	319
3.6.6	Biological Evaluation of Non-Natural Analogs	320
3.6.6.1	Cell Culture and Proliferation Assays.....	320
3.6.6.2	Biological Activity of Non-Natural Analogs.....	321
3.7	References and Notes	323

APPENDIX 5 **327**

Synthetic Summary of Chapter 3

APPENDIX 6 **330**

Spectra Relevant to Chapter 3

APPENDIX 7 **397**

X-Ray Crystallography Reports Relevant to Chapter 3

A7.1	General Experimental	398
A7.2	X-Ray Crystal Structure Analysis of sulfonamide 98	398

APPENDIX 8 **425**

Progress Toward the Syntheses of Bis-Tetrahydroisoquinoline Analogs

A8.1	Introduction	425
A8.2	Approach	426
A8.2.1	Synthesis of Difluorinated Isoquinolines 132 and 133	428
A8.2.2	Fagnou Coupling	429
A8.2.3	Preparation of the Hydrogenation Precursors	430
A8.2.4	Ir-Catalyzed Enantioselective Hydrogenation	434
A8.2.5	End-Route Toward Bis-THIQ Analogs 126–128	435
A8.3	Conclusions and Future Directions	437
A8.4	Experimental Section	439
A8.4.1	Materials and Methods.....	439
A8.4.2	Experimental Procedures and Spectroscopic Data	440
A8.4.2.1	Synthesis of Difluorinated Isoquinoline N-Oxide 132	440
A8.4.2.2	Synthesis of Difluorinated Isoquinoline Triflate 133	443
A8.4.2.3	Fagnou Cross-Coupling Reaction	444

A8.4.2.4	Syntheses of Hydrogenation Precursors 144 , 151 , and 155	448
A8.4.2.5	Ir-Catalyzed Enantioselective Hydrogenation	459
A8.4.2.6	Completion of Bis-THIQ Analogs	463
A8.4.2.7	Preparation of PMB-Protected Bis-Isoquinoline	470
A8.5	References and Notes	476

APPENDIX 9 **480**

Synthetic Summary of Appendix 8

APPENDIX 10 **485**

Spectra Relevant to Appendix 8

CHAPTER 4 **547**

Iridium-Catalyzed Enantioselective and Diastereoselective Hydrogenation of 1,3-Disubstituted Isoquinolines

4.1	Introduction	547
4.2	Substrate Synthesis	551
4.3	Reaction Optimization	552
4.4	Substrate Scope	554
4.5	Synthetic Utility	560
4.6	Conclusions	563
4.7	Experimental Section	563
4.7.1	Materials and Methods.....	563
4.7.2	Experimental Procedures and Spectroscopic Data.....	565
4.7.2.1	Syntheses of Hydroxymethyl 1,3-Disubstituted Isoquinolines.....	565
4.7.2.2	Syntheses of Isoquinolines with Different Directing Groups	603
4.7.2.3	Procedure for Hydrogenation Reactions and Spectroscopic Data for the Hydrogenated Products.....	607
4.7.2.4	Product Transformations	632
4.7.3	Additional Optimization Results	637
4.7.4	Determination of Enantiomeric Excess	638
4.7.5	Determination of Relative and Absolute Configuration via VCD and OR.....	643
4.8	References and Notes	648

APPENDIX 11 **653**
Spectra Relevant to Chapter 4

APPENDIX 12 **867**
X-Ray Crystallography Reports Relevant to Chapter 4

A12.1	General Experimental	868
A12.2	X-Ray Crystal Structure Analysis of THIQ 183p	868

APPENDIX 13 **879**
Notebook Cross-Reference for New Compounds

Comprehensive Bibliography.....	911
Index	927
About the Author.....	930

LIST OF FIGURES

CHAPTER 1*Nickel-Catalyzed Enantioselective Allylic Alkylation of Lactones and Lactams with Unactivated Allylic Alcohols*

Figure 1.1	Additional ligands examined.....	20
-------------------	----------------------------------	----

APPENDIX 1*Spectra Relevant to Chapter 1*

Figure A1.1	¹ H NMR (500 MHz, CDCl ₃) of compound 4a	55
Figure A1.2	Infrared spectrum (Thin Film, NaCl) of compound 4a	56
Figure A1.3	¹³ C NMR (125 MHz, CDCl ₃) of compound 4a	56
Figure A1.4	¹ H NMR (400 MHz, CDCl ₃) of compound 4b	57
Figure A1.5	Infrared spectrum (Thin Film, NaCl) of compound 4b	58
Figure A1.6	¹³ C NMR (100 MHz, CDCl ₃) of compound 4b	58
Figure A1.7	¹ H NMR (400 MHz, CDCl ₃) of Boc-protected lactam	59
Figure A1.8	Infrared spectrum (Thin Film, NaCl) of Boc-protected lactam	60
Figure A1.9	¹³ C NMR (100 MHz, CDCl ₃) of Boc-protected lactam	60
Figure A1.10	¹ H NMR (400 MHz, CDCl ₃) of Ts-protected lactam.....	61
Figure A1.11	Infrared spectrum (Thin Film, NaCl) of Ts-protected lactam.....	62
Figure A1.12	¹³ C NMR (100 MHz, CDCl ₃) of Ts-protected lactam	62
Figure A1.13	¹ H NMR (400 MHz, CDCl ₃) of Ph-protected lactam	63
Figure A1.14	Infrared spectrum (Thin Film, NaCl) of Ph-protected lactam	64
Figure A1.15	¹³ C NMR (100 MHz, CDCl ₃) of Ph-protected lactam	64
Figure A1.16	¹ H NMR (400 MHz, CDCl ₃) of compound 3aa	65
Figure A1.17	Infrared spectrum (Thin Film, NaCl) of compound 3aa	66
Figure A1.18	¹³ C NMR (100 MHz, CDCl ₃) of compound 3aa	66
Figure A1.19	¹ H NMR (400 MHz, CDCl ₃) of compound 3ba	67
Figure A1.20	Infrared spectrum (Thin Film, NaCl) of compound 3ba	68
Figure A1.21	¹³ C NMR (100 MHz, CDCl ₃) of compound 3ba	68
Figure A1.22	¹ H NMR (400 MHz, CDCl ₃) of compound 3ca	69
Figure A1.23	Infrared spectrum (Thin Film, NaCl) of compound 3ca	70
Figure A1.24	¹³ C NMR (100 MHz, CDCl ₃) of compound 3ca	70
Figure A1.25	¹ H NMR (400 MHz, CDCl ₃) of compound 3ab	71
Figure A1.26	Infrared spectrum (Thin Film, NaCl) of compound 3ab	72

Figure A1.27	^{13}C NMR (100 MHz, CDCl_3) of compound 3ab	72
Figure A1.28	^1H NMR (400 MHz, CDCl_3) of compound 3ac	73
Figure A1.29	Infrared spectrum (Thin Film, NaCl) of compound 3ac	74
Figure A1.30	^{13}C NMR (100 MHz, CDCl_3) of compound 3ac	74
Figure A1.31	^1H NMR (400 MHz, CDCl_3) of compound 3ad	75
Figure A1.32	Infrared spectrum (Thin Film, NaCl) of compound 3ad	76
Figure A1.33	^{13}C NMR (100 MHz, CDCl_3) of compound 3ad	76
Figure A1.34	^1H NMR (400 MHz, CDCl_3) of compound 3ae	77
Figure A1.35	Infrared spectrum (Thin Film, NaCl) of compound 3ae	78
Figure A1.36	^{13}C NMR (100 MHz, CDCl_3) of compound 3ae	78
Figure A1.37	^{19}F NMR (282 MHz, CDCl_3) of compound 3ae	79
Figure A1.38	^1H NMR (400 MHz, CDCl_3) of compound 3af	80
Figure A1.39	Infrared spectrum (Thin Film, NaCl) of compound 3af	81
Figure A1.40	^{13}C NMR (100 MHz, CDCl_3) of compound 3af	81
Figure A1.41	^1H NMR (400 MHz, CDCl_3) of compound 3ag	82
Figure A1.42	Infrared spectrum (Thin Film, NaCl) of compound 3ag	83
Figure A1.43	^{13}C NMR (100 MHz, CDCl_3) of compound 3ag	83
Figure A1.44	^{19}F NMR (282 MHz, CDCl_3) of compound 3ag	84
Figure A1.45	^1H NMR (400 MHz, CDCl_3) of compound 3ah	85
Figure A1.46	Infrared spectrum (Thin Film, NaCl) of compound 3ah	86
Figure A1.47	^{13}C NMR (100 MHz, CDCl_3) of compound 3ah	86
Figure A1.48	^1H NMR (400 MHz, CDCl_3) of compound 3ai	87
Figure A1.49	Infrared spectrum (Thin Film, NaCl) of compound 3ai	88
Figure A1.50	^{13}C NMR (100 MHz, CDCl_3) of compound 3ai	88
Figure A1.51	^1H NMR (400 MHz, CDCl_3) of compound 3aj	89
Figure A1.52	Infrared spectrum (Thin Film, NaCl) of compound 3aj	90
Figure A1.53	^{13}C NMR (100 MHz, CDCl_3) of compound 3aj	90
Figure A1.54	^1H NMR (400 MHz, CDCl_3) of compound 3ak	91
Figure A1.55	Infrared spectrum (Thin Film, NaCl) of compound 3ak	92
Figure A1.56	^{13}C NMR (100 MHz, CDCl_3) of compound 3ak	92
Figure A1.57	^1H NMR (400 MHz, CDCl_3) of compound 3al	93
Figure A1.58	Infrared spectrum (Thin Film, NaCl) of compound 3al	94
Figure A1.59	^{13}C NMR (100 MHz, CDCl_3) of compound 3al	94
Figure A1.60	^1H NMR (400 MHz, CDCl_3) of compound 3am	95
Figure A1.61	Infrared spectrum (Thin Film, NaCl) of compound 3am	96

Figure A1.62	^{13}C NMR (100 MHz, CDCl_3) of compound 3am	96
Figure A1.63	^1H NMR (400 MHz, CDCl_3) of compound 3an	97
Figure A1.64	Infrared spectrum (Thin Film, NaCl) of compound 3an	98
Figure A1.65	^{13}C NMR (100 MHz, CDCl_3) of compound 3an	98
Figure A1.66	^1H NMR (400 MHz, CDCl_3) of compound 5aa	99
Figure A1.67	Infrared spectrum (Thin Film, NaCl) of compound 5aa	100
Figure A1.68	^{13}C NMR (100 MHz, CDCl_3) of compound 5a	100
Figure A1.69	^1H NMR (400 MHz, CDCl_3) of compound 5ba	101
Figure A1.70	Infrared spectrum (Thin Film, NaCl) of compound 5ba	102
Figure A1.71	^{13}C NMR (100 MHz, CDCl_3) of compound 5ba	102
Figure A1.72	^1H NMR (400 MHz, CDCl_3) of compound 5ab	103
Figure A1.73	Infrared spectrum (Thin Film, NaCl) of compound 5ab	104
Figure A1.74	^{13}C NMR (100 MHz, CDCl_3) of compound 5ab	104
Figure A1.75	^1H NMR (400 MHz, CDCl_3) of compound 6	105
Figure A1.76	Infrared spectrum (Thin Film, NaCl) of compound 6	106
Figure A1.77	^{13}C NMR (100 MHz, CDCl_3) of compound 6	106
Figure A1.78	^1H NMR (400 MHz, CDCl_3) of compound 7	107
Figure A1.79	Infrared spectrum (Thin Film, NaCl) of compound 7	108
Figure A1.80	^{13}C NMR (100 MHz, CDCl_3) of compound 7	108
Figure A1.81	^1H NMR (400 MHz, CDCl_3) of compound 8	109
Figure A1.82	Infrared spectrum (Thin Film, NaCl) of compound 8	110
Figure A1.83	^{13}C NMR (100 MHz, CDCl_3) of compound 8	110
Figure A1.84	^1H NMR (400 MHz, CDCl_3) of compound 9	111
Figure A1.85	Infrared spectrum (Thin Film, NaCl) of compound 9	112
Figure A1.86	^{13}C NMR (100 MHz, CDCl_3) of compound 9	112
Figure A1.87	^1H NMR (400 MHz, CDCl_3) of compound 10	113
Figure A1.88	Infrared spectrum (Thin Film, NaCl) of compound 10	114
Figure A1.89	^{13}C NMR (100 MHz, CDCl_3) of compound 10	114
Figure A1.90	^1H NMR (400 MHz, CDCl_3) of compound 11	115
Figure A1.91	Infrared spectrum (Thin Film, NaCl) of compound 11	116
Figure A1.92	^{13}C NMR (100 MHz, CDCl_3) of compound 11	116

APPENDIX 2

X-Ray Crystallography Reports Relevant to Chapter 1

Figure A2.1	X-ray crystal structure of allylic alkylation product 3af	118
--------------------	--	-----

CHAPTER 2

Palladium-Catalyzed Enantioselective Decarboxylative Allylic Alkylation of Cyclic Siloxyketones

Figure 2.1	Experimental and computed IR and VCD spectra for 17g	166
Figure 2.2	Experimental and computed IR and VCD spectra for 17a	169

APPENDIX 3

Spectra Relevant to Chapter 2

Figure A3.1	¹ H NMR (500 MHz, CDCl ₃) of compound 14	175
Figure A3.2	Infrared spectrum (Thin Film, NaCl) of compound 14	176
Figure A3.3	¹³ C NMR (125 MHz, CDCl ₃) of compound 14	176
Figure A3.4	¹ H NMR (400 MHz, CDCl ₃) of compound 23	177
Figure A3.5	Infrared spectrum (Thin Film, NaCl) of compound 23	178
Figure A3.6	¹³ C NMR (100 MHz, CDCl ₃) of compound 23	178
Figure A3.7	¹ H NMR (400 MHz, CDCl ₃) of compound 15	179
Figure A3.8	Infrared spectrum (Thin Film, NaCl) of compound 15	180
Figure A3.9	¹³ C NMR (100 MHz, CDCl ₃) of compound 15	180
Figure A3.10	¹ H NMR (400 MHz, CDCl ₃) of compound 16a	181
Figure A3.11	Infrared spectrum (Thin Film, NaCl) of compound 16a	182
Figure A3.12	¹³ C NMR (100 MHz, CDCl ₃) of compound 16a	182
Figure A3.10	¹ H NMR (400 MHz, CDCl ₃) of compound 16a	181
Figure A3.11	Infrared spectrum (Thin Film, NaCl) of compound 16a	182
Figure A3.12	¹³ C NMR (100 MHz, CDCl ₃) of compound 16a	182
Figure A3.13	¹ H NMR (400 MHz, CDCl ₃) of compound 16b	183
Figure A3.14	Infrared spectrum (Thin Film, NaCl) of compound 16b	184
Figure A3.15	¹³ C NMR (100 MHz, CDCl ₃) of compound 16b	184
Figure A3.16	¹ H NMR (400 MHz, CDCl ₃) of compound 16c	185
Figure A3.17	Infrared spectrum (Thin Film, NaCl) of compound 16c	186
Figure A3.18	¹³ C NMR (100 MHz, CDCl ₃) of compound 16c	186
Figure A3.19	¹⁹ F NMR (282 MHz, CDCl ₃) of compound 16c	187
Figure A3.20	¹ H NMR (400 MHz, CDCl ₃) of compound 16d	188
Figure A3.21	Infrared spectrum (Thin Film, NaCl) of compound 16d	189
Figure A3.22	¹³ C NMR (100 MHz, CDCl ₃) of compound 16d	189
Figure A3.23	¹ H NMR (400 MHz, CDCl ₃) of compound 16e	190
Figure A3.24	Infrared spectrum (Thin Film, NaCl) of compound 16e	191

Figure A3.25	^{13}C NMR (100 MHz, CDCl_3) of compound 16e	191
Figure A3.26	^1H NMR (400 MHz, CDCl_3) of compound 16f	192
Figure A3.27	Infrared spectrum (Thin Film, NaCl) of compound 16f	193
Figure A3.28	^{13}C NMR (100 MHz, CDCl_3) of compound 16f	193
Figure A3.29	^1H NMR (400 MHz, CDCl_3) of compound 16g	194
Figure A3.30	Infrared spectrum (Thin Film, NaCl) of compound 16g	195
Figure A3.31	^{13}C NMR (100 MHz, CDCl_3) of compound 16g	195
Figure A3.32	^1H NMR (400 MHz, CDCl_3) of compound 16h	196
Figure A3.33	Infrared spectrum (Thin Film, NaCl) of compound 16h	197
Figure A3.34	^{13}C NMR (100 MHz, CDCl_3) of compound 16h	197
Figure A3.35	^1H NMR (400 MHz, CDCl_3) of compound 16i	198
Figure A3.36	Infrared spectrum (Thin Film, NaCl) of compound 16i	199
Figure A3.37	^{13}C NMR (100 MHz, CDCl_3) of compound 16i	199
Figure A3.38	^1H NMR (400 MHz, CDCl_3) of compound 17a	200
Figure A3.39	Infrared spectrum (Thin Film, NaCl) of compound 17a	201
Figure A3.40	^{13}C NMR (100 MHz, CDCl_3) of compound 17a	201
Figure A3.41	^1H NMR (400 MHz, CDCl_3) of compound 17b	202
Figure A3.42	Infrared spectrum (Thin Film, NaCl) of compound 17b	203
Figure A3.43	^{13}C NMR (100 MHz, CDCl_3) of compound 17b	203
Figure A3.44	^1H NMR (400 MHz, CDCl_3) of compound 17c	204
Figure A3.45	Infrared spectrum (Thin Film, NaCl) of compound 17c	205
Figure A3.46	^{13}C NMR (100 MHz, CDCl_3) of compound 17c	205
Figure A3.47	^{19}F NMR (282 MHz, CDCl_3) of compound 17c	206
Figure A3.48	^1H NMR (400 MHz, CDCl_3) of compound 17d	207
Figure A3.49	Infrared spectrum (Thin Film, NaCl) of compound 17d	208
Figure A3.50	^{13}C NMR (100 MHz, CDCl_3) of compound 17d	208
Figure A3.51	^1H NMR (400 MHz, CDCl_3) of compound 17e	209
Figure A3.52	Infrared spectrum (Thin Film, NaCl) of compound 17e	210
Figure A3.53	^{13}C NMR (100 MHz, CDCl_3) of compound 17e	210
Figure A3.54	^1H NMR (400 MHz, CDCl_3) of compound 17f	211
Figure A3.55	Infrared spectrum (Thin Film, NaCl) of compound 17f	212
Figure A3.56	^{13}C NMR (100 MHz, CDCl_3) of compound 17f	212
Figure A3.57	^1H NMR (400 MHz, CDCl_3) of compound 17g	213
Figure A3.58	Infrared spectrum (Thin Film, NaCl) of compound 17g	214
Figure A3.59	^{13}C NMR (100 MHz, CDCl_3) of compound 17g	214

Figure A3.60	^1H NMR (400 MHz, CDCl_3) of compound 17h	215
Figure A3.61	Infrared spectrum (Thin Film, NaCl) of compound 17h	216
Figure A3.62	^{13}C NMR (100 MHz, CDCl_3) of compound 17h	216
Figure A3.63	^1H NMR (400 MHz, CDCl_3) of compound 17i	217
Figure A3.64	Infrared spectrum (Thin Film, NaCl) of compound 17i	218
Figure A3.65	^{13}C NMR (100 MHz, CDCl_3) of compound 17i	218
Figure A3.66	^1H NMR (400 MHz, CDCl_3) of compound 18	219
Figure A3.67	Infrared spectrum (Thin Film, NaCl) of compound 18	220
Figure A3.68	^{13}C NMR (100 MHz, CDCl_3) of compound 18	220
Figure A3.69	^1H NMR (400 MHz, CD_3OD) of compound 19	221
Figure A3.70	Infrared spectrum (Thin Film, NaCl) of compound 19	222
Figure A3.71	^{13}C NMR (100 MHz, CD_3OD) of compound 19	222
Figure A3.72	^1H NMR (400 MHz, CD_3OD) of compound 20	223
Figure A3.73	Infrared spectrum (Thin Film, NaCl) of compound 20	224
Figure A3.74	^{13}C NMR (100 MHz, CD_3OD) of compound 20	224
Figure A3.75	^1H NMR (400 MHz, CDCl_3) of compound 21	225
Figure A3.76	Infrared spectrum (Thin Film, NaCl) of compound 21	226
Figure A3.77	^{13}C NMR (100 MHz, CDCl_3) of compound 21	226
Figure A3.78	^1H NMR (400 MHz, CDCl_3) of compound 22	227
Figure A3.79	Infrared spectrum (Thin Film, NaCl) of compound 22	228
Figure A3.80	^{13}C NMR (100 MHz, CDCl_3) of compound 22	228

APPENDIX 4

Cycloadditions of Oxacyclic Allenes and a Catalytic Asymmetric Entryway to Enantioenriched Cyclic Allenes

Figure A4.1	Highlights of benzyne and cyclic allene chemistry and cycloadditions of oxacyclic allenes described in this study.....	231
Figure A4.2	Ground State Structure of Oxacyclic Allene 31	233
Figure A4.3	(3+2) cycloadditions with nitrones	236

CHAPTER 3

Concise Total Syntheses of (–)-Jorunnamycin A and (–)-Jorumycin Enabled by Asymmetric Catalysis

Figure 3.1	Bis-tetrahydroisoquinoline natural products	252
Figure 3.2	Biological evaluation of non-natural analogs	263

APPENDIX 6*Spectra Relevant to Chapter 3*

Figure A6.1	^1H NMR (400 MHz, CDCl_3) of compound 107	331
Figure A6.2	^1H NMR (400 MHz, CDCl_3) of compound 86	332
Figure A6.3	^1H NMR (400 MHz, CDCl_3) of compound 88	333
Figure A6.4	Infrared spectrum (Thin Film, NaCl) of compound 88	334
Figure A6.5	^{13}C NMR (100 MHz, CDCl_3) of compound 88	334
Figure A6.6	^1H NMR (400 MHz, CDCl_3) of compound 84	335
Figure A6.7	Infrared spectrum (Thin Film, NaCl) of compound 84	336
Figure A6.8	^{13}C NMR (100 MHz, CDCl_3) of compound 84	336
Figure A6.9	^1H NMR (400 MHz, CDCl_3) of compound 109	337
Figure A6.10	^1H NMR (400 MHz, CDCl_3) of compound 110	338
Figure A6.11	^1H NMR (400 MHz, CDCl_3) of compound 89	339
Figure A6.12	^1H NMR (400 MHz, CDCl_3) of compound 91	340
Figure A6.13	Infrared spectrum (Thin Film, NaCl) of compound 91	341
Figure A6.14	^{13}C NMR (100 MHz, CDCl_3) of compound 91	341
Figure A6.15	^1H NMR (400 MHz, CDCl_3) of compound 111	342
Figure A6.16	^1H NMR (400 MHz, CDCl_3) of compound 85	343
Figure A6.17	Infrared spectrum (Thin Film, NaCl) of compound 85	344
Figure A6.18	^{13}C NMR (100 MHz, CDCl_3) of compound 85	344
Figure A6.19	^{19}F NMR (282 MHz, CDCl_3) of compound 85	345
Figure A6.20	^1H NMR (400 MHz, CDCl_3) of compound 93	346
Figure A6.21	Infrared spectrum (Thin Film, NaCl) of compound 93	347
Figure A6.22	^{13}C NMR (100 MHz, CDCl_3) of compound 93	347
Figure A6.23	^1H NMR (400 MHz, CDCl_3) of compound 114	348
Figure A6.24	^{13}C NMR (100 MHz, CDCl_3) of compound 114	349
Figure A6.25	^1H NMR (400 MHz, CDCl_3) of compound 112	350
Figure A6.26	Infrared spectrum (Thin Film, NaCl) of compound 112	351
Figure A6.27	^{13}C NMR (100 MHz, CDCl_3) of compound 112	351
Figure A6.28	^1H NMR (400 MHz, CDCl_3) of compound 113	352
Figure A6.29	Infrared spectrum (Thin Film, NaCl) of compound 113	353
Figure A6.30	^{13}C NMR (100 MHz, CDCl_3) of compound 113	353
Figure A6.31	^1H NMR (400 MHz, CDCl_3) of compounds 115 and 116	354
Figure A6.32	Infrared spectrum (Thin Film, NaCl) of compounds 115 and 116	355
Figure A6.33	^{13}C NMR (100 MHz, CDCl_3) of compounds 115 and 116	355

Figure A6.34	^1H NMR (400 MHz, CDCl_3) of compound 83•DCM	356
Figure A6.35	Infrared spectrum (Thin Film, NaCl) of compound 83•DCM	357
Figure A6.36	^{13}C NMR (100 MHz, CDCl_3) of compound 83•DCM	357
Figure A6.37	^1H NMR (400 MHz, CDCl_3) of compound 95	358
Figure A6.38	Infrared spectrum (Thin Film, NaCl) of compound 95	359
Figure A6.39	^{13}C NMR (100 MHz, CDCl_3) of compound 95	359
Figure A6.40	^1H NMR (400 MHz, CDCl_3) of compound 96	360
Figure A6.41	Infrared spectrum (Thin Film, NaCl) of compound 96	361
Figure A6.42	^{13}C NMR (100 MHz, CDCl_3) of compound 96	361
Figure A6.43	^1H NMR (400 MHz, CDCl_3) of compound 81	362
Figure A6.44	Infrared spectrum (Thin Film, NaCl) of compound 81	363
Figure A6.45	^{13}C NMR (100 MHz, CDCl_3) of compound 81	363
Figure A6.46	^1H NMR (500 MHz, CDCl_3) of compound 117	364
Figure A6.47	Infrared spectrum (Thin Film, NaCl) of compound 117	365
Figure A6.48	^{13}C NMR (125 MHz, CDCl_3) of compound 117	365
Figure A6.49	^1H NMR (500 MHz, CDCl_3) of compound 99	366
Figure A6.50	Infrared spectrum (Thin Film, NaCl) of compound 99	367
Figure A6.51	^{13}C NMR (125 MHz, CDCl_3) of compound 99	367
Figure A6.52	^1H NMR (500 MHz, CDCl_3) of compound 100	368
Figure A6.53	Infrared spectrum (Thin Film, NaCl) of compound 100	369
Figure A6.54	^{13}C NMR (125 MHz, CDCl_3) of compound 100	369
Figure A6.55	^1H NMR (400 MHz, CDCl_3) of compound 105	370
Figure A6.56	Infrared spectrum (Thin Film, NaCl) of compound 105	371
Figure A6.57	^{13}C NMR (100 MHz, CDCl_3) of compound 105	371
Figure A6.58	^1H NMR (500 MHz, CDCl_3) of compound 79	372
Figure A6.59	Infrared spectrum (Thin Film, NaCl) of compound 79	373
Figure A6.60	^{13}C NMR (125 MHz, CDCl_3) of compound 79	373
Figure A6.61	^1H NMR (400 MHz, CDCl_3) of compound 101	374
Figure A6.62	Infrared spectrum (Thin Film, NaCl) of compound 101	375
Figure A6.63	^{13}C NMR (100 MHz, CDCl_3) of compound 101	375
Figure A6.64	^1H NMR (400 MHz, CDCl_3) of compound 77	376
Figure A6.65	Infrared spectrum (Thin Film, NaCl) of compound 77	377
Figure A6.66	^{13}C NMR (100 MHz, CDCl_3) of compound 77	377
Figure A6.67	^1H NMR (400 MHz, CDCl_3) of compound 102	378
Figure A6.68	Infrared spectrum (Thin Film, NaCl) of compound 102	379

Figure A6.69	^{13}C NMR (100 MHz, CDCl_3) of compound 102	379
Figure A6.70	^1H NMR (400 MHz, CDCl_3) of compound 118	380
Figure A6.71	Infrared spectrum (Thin Film, NaCl) of compound 118	381
Figure A6.72	^{13}C NMR (100 MHz, CDCl_3) of compound 118	381
Figure A6.73	2D NOESY NMR of compound 118	382
Figure A6.74	^1H NMR (400 MHz, CDCl_3) of compound 118	383
Figure A6.75	Infrared spectrum (Thin Film, NaCl) of compound 118	384
Figure A6.76	^{13}C NMR (100 MHz, CDCl_3) of compound 118	384
Figure A6.77	2D NOESY NMR of compound 118	385
Figure A6.78	^1H NMR (500 MHz, CDCl_3) of compound 120	386
Figure A6.79	Infrared spectrum (Thin Film, NaCl) of compound 120	386
Figure A6.80	^{13}C NMR (100 MHz, CDCl_3) of compound 120	387
Figure A6.81	^1H NMR (600 MHz, CDCl_3) of compound 103	388
Figure A6.82	Infrared spectrum (Thin Film, NaCl) of compound 103	389
Figure A6.83	^{13}C NMR (100 MHz, CDCl_3) of compound 103	389
Figure A6.84	^1H NMR (400 MHz, CDCl_3) of compound 121	390
Figure A6.85	Infrared spectrum (Thin Film, NaCl) of compound 121	391
Figure A6.86	^{13}C NMR (100 MHz, CDCl_3) of compound 121	391
Figure A6.87	^1H NMR (400 MHz, CDCl_3) of compound 122	392
Figure A6.88	Infrared spectrum (Thin Film, NaCl) of compound 122	393
Figure A6.89	^{13}C NMR (100 MHz, CDCl_3) of compound 122	393
Figure A6.90	^1H NMR (400 MHz, CDCl_3) of compound 104	394
Figure A6.91	Infrared spectrum (Thin Film, NaCl) of compound 104	395
Figure A6.92	^{13}C NMR (100 MHz, CDCl_3) of compound 104	395
Figure A6.93	^1H NMR (400 MHz, CDCl_3) of compound 98	396

APPENDIX 7

X-Ray Crystallography Reports Relevant to Chapter 3

Figure A7.1	X-ray crystal structure of sulfonamide 98	399
--------------------	--	-----

APPENDIX 8

Progress Toward the Syntheses of Bis-tetrahydroisoquinoline Analogs

Figure A8.1	Non-natural bis-THIQ analogs with their corresponding in vivo half-lives.....	426
--------------------	---	-----

APPENDIX 10*Spectra Relevant to Appendix 8*

Figure A10.1	^1H NMR (500 MHz, CDCl_3) of compound 171	486
Figure A10.2	^{13}C NMR (100 MHz, CDCl_3) of compound 171	487
Figure A10.3	^1H NMR (300 MHz, CDCl_3) of compound 135	488
Figure A10.4	^1H NMR (300 MHz, CDCl_3) of compound 132	489
Figure A10.5	^{13}C NMR (100 MHz, CDCl_3) of compound 132	490
Figure A10.6	^{19}F NMR (282 MHz, CDCl_3) of compound 132	490
Figure A10.7	^1H NMR (500 MHz, CDCl_3) of compound 133	491
Figure A10.8	^1H NMR (400 MHz, CDCl_3) of compound 138	492
Figure A10.9	^{13}C NMR (100 MHz, CDCl_3) of compound 138	493
Figure A10.10	^{19}F NMR (282 MHz, CDCl_3) of compound 138	493
Figure A10.11	^1H NMR (400 MHz, CDCl_3) of compound 139	494
Figure A10.12	Infrared spectrum (Thin Film, NaCl) of compound 139	495
Figure A10.13	^{13}C NMR (100 MHz, CDCl_3) of compound 139	495
Figure A10.14	^{19}F NMR (282 MHz, CDCl_3) of compound 139	496
Figure A10.15	^1H NMR (300 MHz, CDCl_3) of compound 140	497
Figure A10.16	^{19}F NMR (282 MHz, CDCl_3) of compound 140	498
Figure A10.17	^1H NMR (400 MHz, CDCl_3) of compound 141	499
Figure A10.18	Infrared spectrum (Thin Film, NaCl) of compound 141	500
Figure A10.19	^{13}C NMR (100 MHz, CDCl_3) of compound 141	500
Figure A10.20	^{19}F NMR (282 MHz, CDCl_3) of compound 141	501
Figure A10.21	^1H NMR (300 MHz, CDCl_3) of compound 142	502
Figure A10.22	^1H NMR (300 MHz, CDCl_3) of compound 144	503
Figure A10.23	^1H NMR (400 MHz, CDCl_3) of compound 146	504
Figure A10.24	Infrared spectrum (Thin Film, NaCl) of compound 146	505
Figure A10.25	^{19}F NMR (282 MHz, CDCl_3) of compound 146	505
Figure A10.26	^1H NMR (400 MHz, CDCl_3) of compound 149	506
Figure A10.27	Infrared spectrum (Thin Film, NaCl) of compound 149	507
Figure A10.28	^{13}C NMR (100 MHz, CDCl_3) of compound 149	507
Figure A10.29	^{19}F NMR (282 MHz, CDCl_3) of compound 149	508
Figure A10.30	^1H NMR (400 MHz, CDCl_3) of compound 151	509
Figure A10.31	^{13}C NMR (100 MHz, CDCl_3) of compound 151	510
Figure A10.32	^{19}F NMR (282 MHz, CDCl_3) of compound 151	510
Figure A10.33	^1H NMR (400 MHz, CDCl_3) of compound 152	511

Figure A10.34	^{13}C NMR (100 MHz, CDCl_3) of compound 152	512
Figure A10.35	^1H NMR (400 MHz, CDCl_3) of compound 153	513
Figure A10.36	^{13}C NMR (100 MHz, CDCl_3) of compound 153	514
Figure A10.37	^{19}F NMR (282 MHz, CDCl_3) of compound 153	514
Figure A10.38	^1H NMR (400 MHz, CDCl_3) of compound 155	515
Figure A10.39	^{13}C NMR (100 MHz, CDCl_3) of compound 155	516
Figure A10.40	^{19}F NMR (282 MHz, CDCl_3) of compound 155	516
Figure A10.41	^1H NMR (400 MHz, CDCl_3) of compound 129	517
Figure A10.42	Infrared spectrum (Thin Film, NaCl) of compound 129	518
Figure A10.43	^{13}C NMR (100 MHz, CDCl_3) of compound 129	518
Figure A10.44	^{19}F NMR (282 MHz, CDCl_3) of compound 129	519
Figure A10.45	^1H NMR (400 MHz, CDCl_3) of compound 130	520
Figure A10.46	Infrared spectrum (Thin Film, NaCl) of compound 130	521
Figure A10.47	^{13}C NMR (100 MHz, CDCl_3) of compound 130	521
Figure A10.48	^{19}F NMR (282 MHz, CDCl_3) of compound 130	522
Figure A10.49	^1H NMR (400 MHz, CDCl_3) of compound 131	523
Figure A10.50	^{13}C NMR (100 MHz, CDCl_3) of compound 131	524
Figure A10.51	^1H NMR (400 MHz, CDCl_3) of compound 156	525
Figure A10.52	Infrared spectrum (Thin Film, NaCl) of compound 156	526
Figure A10.53	^{13}C NMR (100 MHz, CDCl_3) of compound 156	526
Figure A10.54	^{19}F NMR (282 MHz, CDCl_3) of compound 156	527
Figure A10.55	^1H NMR (400 MHz, CDCl_3) of compound 126	528
Figure A10.56	Infrared spectrum (Thin Film, NaCl) of compound 126	529
Figure A10.57	^{13}C NMR (100 MHz, CDCl_3) of compound 126	529
Figure A10.58	^{19}F NMR (282 MHz, CDCl_3) of compound 126	530
Figure A10.59	^1H NMR (400 MHz, CDCl_3) of compound 157	531
Figure A10.60	^{13}C NMR (100 MHz, CDCl_3) of compound 157	532
Figure A10.61	^{19}F NMR (282 MHz, CDCl_3) of compound 157	532
Figure A10.62	^1H NMR (400 MHz, CDCl_3) of compound 158	533
Figure A10.63	^{13}C NMR (100 MHz, CDCl_3) of compound 158	534
Figure A10.64	^{19}F NMR (282 MHz, CDCl_3) of compound 158	534
Figure A10.65	^1H NMR (400 MHz, CDCl_3) of compound 159	535
Figure A10.66	^{19}F NMR (282 MHz, CDCl_3) of compound 159	536
Figure A10.67	^1H NMR (500 MHz, CDCl_3) of compound 160	537
Figure A10.68	^1H NMR (400 MHz, CDCl_3) of compound 173	538

Figure A10.69	^1H NMR (400 MHz, CDCl_3) of compound 174	539
Figure A10.70	^1H NMR (300 MHz, CDCl_3) of compound 175	540
Figure A10.71	^1H NMR (300 MHz, CDCl_3) of compound 164	541
Figure A10.72	^1H NMR (400 MHz, CDCl_3) of compound 165	542
Figure A10.73	^1H NMR (500 MHz, CDCl_3) of compound 176	543
Figure A10.74	^1H NMR (500 MHz, CDCl_3) of compound 177	544
Figure A10.75	^1H NMR (500 MHz, CDCl_3) of compound 166	545
Figure A10.76	^1H NMR (500 MHz, CDCl_3) of compound 167	546

CHAPTER 4

Iridium-Catalyzed Enantioselective and Diastereoselective Hydrogenation of 1,3-Disubstituted Isoquinolines

Figure 4.1	Limitations in enantioselective hydrogenation of N-heterocycles and previous examples of iridium-catalyzed enantioselective hydrogenation of mono- and di-substituted isoquinolines	549
Figure 4.2	Our research on iridium-catalyzed enantioselective and diastereoselective hydrogenation of 1,3-disubstituted isoquinolines	550
Figure 4.3	Experimental and computed IR and VCD spectra for cis-187e	645
Figure 4.4	Experimental and computed IR and VCD spectra for trans-187e	646

APPENDIX 11

Spectra Relevant to Chapter 4

Figure A11.1	^1H NMR (400 MHz, CDCl_3) of compound 179a	654
Figure A11.2	Infrared spectrum (Thin Film, NaCl) of compound 179a	655
Figure A11.3	^{13}C NMR (100MHz, CDCl_3) of compound 179a	655
Figure A11.4	^1H NMR (400 MHz, CDCl_3) of compound 179b	656
Figure A11.5	Infrared spectrum (Thin Film, NaCl) of compound 179b	657
Figure A11.6	^{13}C NMR (100 MHz, CDCl_3) of compound 179b	657
Figure A11.7	^{19}F NMR (282 MHz, CDCl_3) of compound 179b	658
Figure A11.8	^1H NMR (400 MHz, CDCl_3) of compound 179c	659
Figure A11.9	Infrared spectrum (Thin Film, NaCl) of compound 179c	660
Figure A11.10	^{13}C NMR (100MHz, CDCl_3) of compound 179c	660
Figure A11.11	^1H NMR (400 MHz, CDCl_3) of compound 179d	661
Figure A11.12	Infrared spectrum (Thin Film, NaCl) of compound 179d	662
Figure A11.13	^{13}C NMR (100MHz, CDCl_3) of compound 179d	662

Figure A11.14	^1H NMR (400 MHz, CDCl_3) of compound 180a	663
Figure A11.15	Infrared spectrum (Thin Film, NaCl) of compound 180a	664
Figure A11.16	^{13}C NMR (100 MHz, CDCl_3) of compound 180a	664
Figure A11.17	^{19}F NMR (282 MHz, CDCl_3) of compound 180a	665
Figure A11.18	^1H NMR (400 MHz, CDCl_3) of compound 180b	666
Figure A11.19	Infrared spectrum (Thin Film, NaCl) of compound 180b	667
Figure A11.20	^{13}C NMR (100 MHz, CDCl_3) of compound 180b	667
Figure A11.21	^{19}F NMR (282 MHz, CDCl_3) of compound 180b	668
Figure A11.22	^1H NMR (400 MHz, CDCl_3) of compound 180c	669
Figure A11.23	Infrared spectrum (Thin Film, NaCl) of compound 180c	670
Figure A11.24	^{13}C NMR (100 MHz, CDCl_3) of compound 180c	670
Figure A11.25	^{19}F NMR (282 MHz, CDCl_3) of compound 180c	671
Figure A11.26	^1H NMR (400 MHz, CDCl_3) of compound 180d	672
Figure A11.27	Infrared spectrum (Thin Film, NaCl) of compound 180d	673
Figure A11.28	^{13}C NMR (100 MHz, CDCl_3) of compound 180d	673
Figure A11.29	^{19}F NMR (282 MHz, CDCl_3) of compound 180d	674
Figure A11.30	^1H NMR (400 MHz, CDCl_3) of compound 181a	676
Figure A11.31	Infrared spectrum (Thin Film, NaCl) of compound 181a	676
Figure A11.32	^{13}C NMR (100 MHz, CDCl_3) of compound 181a	676
Figure A11.33	^1H NMR (400 MHz, CDCl_3) of compound 181b	677
Figure A11.34	Infrared spectrum (Thin Film, NaCl) of compound 181b	678
Figure A11.35	^{13}C NMR (100 MHz, CDCl_3) of compound 181b	678
Figure A11.36	^1H NMR (400 MHz, CDCl_3) of compound 181c	679
Figure A11.37	Infrared spectrum (Thin Film, NaCl) of compound 181c	680
Figure A11.38	^{13}C NMR (100 MHz, CDCl_3) of compound 181c	680
Figure A11.39	^1H NMR (400 MHz, CDCl_3) of compound 181d	681
Figure A11.40	Infrared spectrum (Thin Film, NaCl) of compound 181d	682
Figure A11.41	^{13}C NMR (100 MHz, CDCl_3) of compound 181d	682
Figure A11.42	^1H NMR (400 MHz, CDCl_3) of compound 181e	683
Figure A11.43	Infrared spectrum (Thin Film, NaCl) of compound 181e	684
Figure A11.44	^{13}C NMR (100 MHz, CDCl_3) of compound 181e	684
Figure A11.45	^{19}F NMR (282 MHz, CDCl_3) of compound 181e	685
Figure A11.46	^1H NMR (400 MHz, CDCl_3) of compound 181f	686
Figure A11.47	Infrared spectrum (Thin Film, NaCl) of compound 181f	687
Figure A11.48	^{13}C NMR (100 MHz, CDCl_3) of compound 181f	687

Figure A11.49	^{19}F NMR (282 MHz, CDCl_3) of compound 181f	688
Figure A11.50	^1H NMR (400 MHz, CDCl_3) of compound 181g	689
Figure A11.51	Infrared spectrum (Thin Film, NaCl) of compound 181g	690
Figure A11.52	^{13}C NMR (100 MHz, CDCl_3) of compound 181g	690
Figure A11.53	^1H NMR (400 MHz, CDCl_3) of compound 181h	691
Figure A11.54	Infrared spectrum (Thin Film, NaCl) of compound 181h	692
Figure A11.55	^{13}C NMR (100 MHz, CDCl_3) of compound 181h	692
Figure A11.56	^1H NMR (400 MHz, CDCl_3) of compound 181i	693
Figure A11.57	Infrared spectrum (Thin Film, NaCl) of compound 181i	694
Figure A11.58	^{13}C NMR (100 MHz, CDCl_3) of compound 181i	694
Figure A11.59	^{19}F NMR (282 MHz, CDCl_3) of compound 181i	695
Figure A11.60	^1H NMR (400 MHz, CDCl_3) of compound 181j	696
Figure A11.61	Infrared spectrum (Thin Film, NaCl) of compound 181j	697
Figure A11.62	^{13}C NMR (100 MHz, CDCl_3) of compound 181j	697
Figure A11.63	^1H NMR (400 MHz, CDCl_3) of compound 181k	698
Figure A11.64	Infrared spectrum (Thin Film, NaCl) of compound 181k	699
Figure A11.65	^{13}C NMR (100 MHz, CDCl_3) of compound 181k	699
Figure A11.66	^1H NMR (400 MHz, CDCl_3) of compound 181l	700
Figure A11.67	Infrared spectrum (Thin Film, NaCl) of compound 181l	701
Figure A11.68	^{13}C NMR (100 MHz, CDCl_3) of compound 181l	701
Figure A11.69	^1H NMR (400 MHz, CDCl_3) of compound 181m	702
Figure A11.70	Infrared spectrum (Thin Film, NaCl) of compound 181m	703
Figure A11.71	^{13}C NMR (100 MHz, CDCl_3) of compound 181m	703
Figure A11.72	^1H NMR (400 MHz, CDCl_3) of compound 181n	704
Figure A11.73	Infrared spectrum (Thin Film, NaCl) of compound 181n	705
Figure A11.74	^{13}C NMR (100 MHz, CDCl_3) of compound 181n	705
Figure A11.75	^1H NMR (400 MHz, CDCl_3) of compound 181o	706
Figure A11.76	Infrared spectrum (Thin Film, NaCl) of compound 181o	707
Figure A11.77	^{13}C NMR (100 MHz, CDCl_3) of compound 181o	707
Figure A11.78	^1H NMR (400 MHz, CDCl_3) of compound 181p	708
Figure A11.79	Infrared spectrum (Thin Film, NaCl) of compound 181p	709
Figure A11.80	^{13}C NMR (100 MHz, CDCl_3) of compound 181p	709
Figure A11.81	^1H NMR (400 MHz, CDCl_3) of compound 181q	710
Figure A11.82	Infrared spectrum (Thin Film, NaCl) of compound 181q	711
Figure A11.83	^{13}C NMR (100 MHz, CDCl_3) of compound 181q	711

Figure A11.84	^1H NMR (400 MHz, CDCl_3) of compound 181r	712
Figure A11.85	Infrared spectrum (Thin Film, NaCl) of compound 181r	713
Figure A11.86	^{13}C NMR (100 MHz, CDCl_3) of compound 181r	713
Figure A11.87	^1H NMR (400 MHz, CDCl_3) of compound 192a	714
Figure A11.88	Infrared spectrum (Thin Film, NaCl) of compound 192a	715
Figure A11.89	^{13}C NMR (100 MHz, CDCl_3) of compound 192a	715
Figure A11.90	^{19}F NMR (282 MHz, CDCl_3) of compound 192a	716
Figure A11.91	^1H NMR (400 MHz, CDCl_3) of compound 192b	717
Figure A11.92	Infrared spectrum (Thin Film, NaCl) of compound 192b	718
Figure A11.93	^{13}C NMR (100 MHz, CDCl_3) of compound 192b	718
Figure A11.94	^{19}F NMR (282 MHz, CDCl_3) of compound 192b	719
Figure A11.95	^1H NMR (400 MHz, CDCl_3) of compound 192c	720
Figure A11.96	Infrared spectrum (Thin Film, NaCl) of compound 192c	721
Figure A11.97	^{13}C NMR (100 MHz, CDCl_3) of compound 192c	721
Figure A11.98	^{19}F NMR (282 MHz, CDCl_3) of compound 192c	722
Figure A11.99	^1H NMR (400 MHz, CDCl_3) of compound 192d	723
Figure A11.100	Infrared spectrum (Thin Film, NaCl) of compound 192d	724
Figure A11.101	^{13}C NMR (100 MHz, CDCl_3) of compound 192d	724
Figure A11.102	^1H NMR (400 MHz, CDCl_3) of compound 192e	725
Figure A11.103	Infrared spectrum (Thin Film, NaCl) of compound 192e	726
Figure A11.104	^{13}C NMR (100 MHz, CDCl_3) of compound 192e	726
Figure A11.105	^1H NMR (400 MHz, CDCl_3) of compound 192f	727
Figure A11.106	Infrared spectrum (Thin Film, NaCl) of compound 192f	728
Figure A11.107	^{13}C NMR (100 MHz, CDCl_3) of compound 192f	728
Figure A11.108	^1H NMR (400 MHz, CDCl_3) of compound 182a	729
Figure A11.109	Infrared spectrum (Thin Film, NaCl) of compound 182a	730
Figure A11.110	^{13}C NMR (100 MHz, CDCl_3) of compound 182a	730
Figure A11.111	^1H NMR (400 MHz, CDCl_3) of compound 182b	731
Figure A11.112	Infrared spectrum (Thin Film, NaCl) of compound 182b	732
Figure A11.113	^{13}C NMR (100 MHz, CDCl_3) of compound 182b	732
Figure A11.114	^1H NMR (400 MHz, CDCl_3) of compound 182c	733
Figure A11.115	Infrared spectrum (Thin Film, NaCl) of compound 182c	734
Figure A11.116	^{13}C NMR (100 MHz, CDCl_3) of compound 182c	734
Figure A11.117	^1H NMR (400 MHz, CDCl_3) of compound 182d	735
Figure A11.118	Infrared spectrum (Thin Film, NaCl) of compound 182d	736

Figure A11.119	^{13}C NMR (100 MHz, CDCl_3) of compound 182d	736
Figure A11.120	^1H NMR (400 MHz, CDCl_3) of compound 182e	737
Figure A11.121	Infrared spectrum (Thin Film, NaCl) of compound 182e	738
Figure A11.122	^{13}C NMR (100 MHz, CDCl_3) of compound 182e	738
Figure A11.123	^{19}F NMR (282 MHz, CDCl_3) of compound 182e	739
Figure A11.124	^1H NMR (400 MHz, CDCl_3) of compound 182f	740
Figure A11.125	Infrared spectrum (Thin Film, NaCl) of compound 182f	741
Figure A11.126	^{13}C NMR (100 MHz, CDCl_3) of compound 182f	741
Figure A11.127	^{19}F NMR (282 MHz, CDCl_3) of compound 182f	742
Figure A11.128	^1H NMR (400 MHz, CDCl_3) of compound 182g	743
Figure A11.129	Infrared spectrum (Thin Film, NaCl) of compound 182g	744
Figure A11.130	^{13}C NMR (100 MHz, CDCl_3) of compound 182g	744
Figure A11.131	^1H NMR (400 MHz, CDCl_3) of compound 182h	745
Figure A11.132	Infrared spectrum (Thin Film, NaCl) of compound 182h	746
Figure A11.133	^{13}C NMR (100 MHz, CDCl_3) of compound 182h	746
Figure A11.134	^1H NMR (400 MHz, CDCl_3) of compound 182i	747
Figure A11.135	Infrared spectrum (Thin Film, NaCl) of compound 182i	748
Figure A11.136	^{13}C NMR (100 MHz, CDCl_3) of compound 182i	748
Figure A11.137	^{19}F NMR (282 MHz, CDCl_3) of compound 182i	749
Figure A11.138	^1H NMR (400 MHz, CDCl_3) of compound 182j	750
Figure A11.139	Infrared spectrum (Thin Film, NaCl) of compound 182j	751
Figure A11.140	^{13}C NMR (100 MHz, CDCl_3) of compound 182j	751
Figure A11.141	^1H NMR (400 MHz, CDCl_3) of compound 182k	752
Figure A11.142	Infrared spectrum (Thin Film, NaCl) of compound 182k	753
Figure A11.143	^{13}C NMR (100 MHz, CDCl_3) of compound 182k	753
Figure A11.144	^1H NMR (400 MHz, CDCl_3) of compound 182l	754
Figure A11.145	Infrared spectrum (Thin Film, NaCl) of compound 182l	755
Figure A11.146	^{13}C NMR (100 MHz, CDCl_3) of compound 182l	755
Figure A11.147	^1H NMR (400 MHz, CDCl_3) of compound 182m	756
Figure A11.148	Infrared spectrum (Thin Film, NaCl) of compound 182m	757
Figure A11.149	^{13}C NMR (100 MHz, CDCl_3) of compound 182m	757
Figure A11.150	^1H NMR (400 MHz, CDCl_3) of compound 182n	758
Figure A11.151	Infrared spectrum (Thin Film, NaCl) of compound 182n	759
Figure A11.152	^{13}C NMR (100 MHz, CDCl_3) of compound 182n	759
Figure A11.153	^1H NMR (400 MHz, CDCl_3) of compound 182o	760

Figure A11.154	Infrared spectrum (Thin Film, NaCl) of compound 182o	761
Figure A11.155	^{13}C NMR (100 MHz, CDCl_3) of compound 182o	761
Figure A11.156	^1H NMR (400 MHz, CDCl_3) of compound 182p	762
Figure A11.157	Infrared spectrum (Thin Film, NaCl) of compound 182p	763
Figure A11.158	^{13}C NMR (100 MHz, CDCl_3) of compound 182p	763
Figure A11.159	^1H NMR (400 MHz, CDCl_3) of compound 182q	764
Figure A11.160	Infrared spectrum (Thin Film, NaCl) of compound 182q	765
Figure A11.161	^{13}C NMR (100 MHz, CDCl_3) of compound 182q	765
Figure A11.162	^1H NMR (400 MHz, CDCl_3) of compound 182r	766
Figure A11.163	Infrared spectrum (Thin Film, NaCl) of compound 182r	767
Figure A11.164	^{13}C NMR (100 MHz, CDCl_3) of compound 182r	767
Figure A11.165	^1H NMR (400 MHz, CDCl_3) of compound 184a	768
Figure A11.166	Infrared spectrum (Thin Film, NaCl) of compound 184a	769
Figure A11.167	^{13}C NMR (100 MHz, CDCl_3) of compound 184a	769
Figure A11.168	^{19}F NMR (282 MHz, CDCl_3) of compound 184a	770
Figure A11.169	^1H NMR (400 MHz, CDCl_3) of compound 184b	771
Figure A11.170	Infrared spectrum (Thin Film, NaCl) of compound 184b	772
Figure A11.171	^{13}C NMR (100 MHz, CDCl_3) of compound 184b	772
Figure A11.172	^{19}F NMR (282 MHz, CDCl_3) of compound 184b	773
Figure A11.173	^1H NMR (400 MHz, CDCl_3) of compound 184c	774
Figure A11.174	Infrared spectrum (Thin Film, NaCl) of compound 184c	775
Figure A11.175	^{13}C NMR (100 MHz, CDCl_3) of compound 184c	775
Figure A11.176	^{19}F NMR (282 MHz, CDCl_3) of compound 184c	776
Figure A11.177	^1H NMR (400 MHz, CDCl_3) of compound 184d	777
Figure A11.178	Infrared spectrum (Thin Film, NaCl) of compound 184d	778
Figure A11.179	^{13}C NMR (100 MHz, CDCl_3) of compound 184d	778
Figure A11.180	^1H NMR (400 MHz, CDCl_3) of compound 184e	779
Figure A11.181	Infrared spectrum (Thin Film, NaCl) of compound 184e	780
Figure A11.182	^{13}C NMR (100 MHz, CDCl_3) of compound 184e	780
Figure A11.183	^1H NMR (400 MHz, CDCl_3) of compound 184f	781
Figure A11.184	Infrared spectrum (Thin Film, NaCl) of compound 184f	782
Figure A11.185	^{13}C NMR (100 MHz, CDCl_3) of compound 184f	782
Figure A11.186	^1H NMR (400 MHz, CDCl_3) of compound 186a	783
Figure A11.187	Infrared spectrum (Thin Film, NaCl) of compound 186a	784
Figure A11.188	^{13}C NMR (100 MHz, CDCl_3) of compound 186a	784

Figure A11.189	^1H NMR (400 MHz, CDCl_3) of compound 186b	785
Figure A11.190	Infrared spectrum (Thin Film, NaCl) of compound 186b	786
Figure A11.191	^{13}C NMR (100 MHz, CDCl_3) of compound 186b	786
Figure A11.192	^1H NMR (400 MHz, CDCl_3) of compound 186c	787
Figure A11.193	Infrared spectrum (Thin Film, NaCl) of compound 186c	788
Figure A11.194	^{13}C NMR (100 MHz, CDCl_3) of compound 186c	788
Figure A11.195	^1H NMR (400 MHz, CDCl_3) of compound 186d	789
Figure A11.196	Infrared spectrum (Thin Film, NaCl) of compound 186d	790
Figure A11.197	^{13}C NMR (100 MHz, CDCl_3) of compound 186d	790
Figure A11.198	^1H NMR (400 MHz, CDCl_3) of compound 186f	791
Figure A11.199	Infrared spectrum (Thin Film, NaCl) of compound 186f	792
Figure A11.200	^{13}C NMR (100 MHz, CDCl_3) of compound 186f	792
Figure A11.201	^1H NMR (400 MHz, CDCl_3) of compound cis-183a	793
Figure A11.202	Infrared spectrum (Thin Film, NaCl) of compound cis-183a	794
Figure A11.203	^{13}C NMR (100 MHz, CDCl_3) of compound cis-183a	794
Figure A11.204	^1H NMR (400 MHz, CDCl_3) of compound trans-183a	795
Figure A11.205	Infrared spectrum (Thin Film, NaCl) of compound trans-183a	796
Figure A11.206	^1H NMR (400 MHz, CDCl_3) of compound 183b	797
Figure A11.207	Infrared spectrum (Thin Film, NaCl) of compound 183b	798
Figure A11.208	^{13}C NMR (100 MHz, CDCl_3) of compound 183b	798
Figure A11.209	^1H NMR (400 MHz, CDCl_3) of compound 183c	799
Figure A11.210	Infrared spectrum (Thin Film, NaCl) of compound 183c	800
Figure A11.211	^{13}C NMR (100 MHz, CDCl_3) of compound 183c	800
Figure A11.212	^1H NMR (400 MHz, CDCl_3) of compound 183d	801
Figure A11.213	Infrared spectrum (Thin Film, NaCl) of compound 183d	802
Figure A11.214	^{13}C NMR (100 MHz, CDCl_3) of compound 183d	802
Figure A11.215	^1H NMR (400 MHz, CDCl_3) of compound 183e	803
Figure A11.216	Infrared spectrum (Thin Film, NaCl) of compound 183e	804
Figure A11.217	^{13}C NMR (100 MHz, CDCl_3) of compound 183e	804
Figure A11.218	^{19}F NMR (282 MHz, CDCl_3) of compound 183e	805
Figure A11.219	^1H NMR (400 MHz, CDCl_3) of compound 183f	806
Figure A11.220	Infrared spectrum (Thin Film, NaCl) of compound 183f	807
Figure A11.221	^{13}C NMR (100 MHz, CDCl_3) of compound 183f	807
Figure A11.222	^{19}F NMR (282 MHz, CDCl_3) of compound 183f	808
Figure A11.223	^1H NMR (400 MHz, CDCl_3) of compound 183g	809

Figure A11.224	Infrared spectrum (Thin Film, NaCl) of compound 183g	810
Figure A11.225	^{13}C NMR (100 MHz, CDCl_3) of compound 183g	810
Figure A11.226	^1H NMR (400 MHz, CDCl_3) of compound 183h	811
Figure A11.227	Infrared spectrum (Thin Film, NaCl) of compound 183h	812
Figure A11.228	^{13}C NMR (100 MHz, CDCl_3) of compound 183h	812
Figure A11.229	^1H NMR (400 MHz, CDCl_3) of compound 183i	813
Figure A11.230	Infrared spectrum (Thin Film, NaCl) of compound 183i	814
Figure A11.231	^{13}C NMR (100 MHz, CDCl_3) of compound 183i	814
Figure A11.232	^{19}F NMR (282 MHz, CDCl_3) of compound 183i	815
Figure A11.233	^1H NMR (400 MHz, CDCl_3) of compound 183j	816
Figure A11.234	Infrared spectrum (Thin Film, NaCl) of compound 183j	817
Figure A11.235	^{13}C NMR (100 MHz, CDCl_3) of compound 183j	817
Figure A11.236	^1H NMR (400 MHz, CDCl_3) of compound 183k	818
Figure A11.237	Infrared spectrum (Thin Film, NaCl) of compound 183k	819
Figure A11.238	^{13}C NMR (100 MHz, CDCl_3) of compound 183k	819
Figure A11.239	^1H NMR (400 MHz, CDCl_3) of compound 183l	820
Figure A11.240	Infrared spectrum (Thin Film, NaCl) of compound 183l	821
Figure A11.241	^{13}C NMR (100 MHz, CDCl_3) of compound 183l	821
Figure A11.242	^1H NMR (400 MHz, CDCl_3) of compound 183m	822
Figure A11.243	Infrared spectrum (Thin Film, NaCl) of compound 183m	823
Figure A11.244	^{13}C NMR (100 MHz, CDCl_3) of compound 183m	823
Figure A11.245	^1H NMR (400 MHz, CDCl_3) of compound 183n	824
Figure A11.246	Infrared spectrum (Thin Film, NaCl) of compound 183n	825
Figure A11.247	^{13}C NMR (100 MHz, CDCl_3) of compound 183n	825
Figure A11.248	^1H NMR (400 MHz, CDCl_3) of compound 183o	826
Figure A11.249	Infrared spectrum (Thin Film, NaCl) of compound 183o	827
Figure A11.250	^{13}C NMR (100 MHz, CDCl_3) of compound 183o	827
Figure A11.251	^1H NMR (400 MHz, CDCl_3) of compound 183p	828
Figure A11.252	Infrared spectrum (Thin Film, NaCl) of compound 183p	829
Figure A11.253	^{13}C NMR (100 MHz, CDCl_3) of compound 183p	829
Figure A11.254	^1H NMR (400 MHz, CDCl_3) of compound 183q	830
Figure A11.255	Infrared spectrum (Thin Film, NaCl) of compound 183q	831
Figure A11.256	^{13}C NMR (100 MHz, CDCl_3) of compound 183q	831
Figure A11.257	^1H NMR (400 MHz, CDCl_3) of compound 183r	832
Figure A11.258	Infrared spectrum (Thin Film, NaCl) of compound 183r	833

Figure A11.259	^{13}C NMR (100 MHz, CDCl_3) of compound 183r	833
Figure A11.260	^1H NMR (400 MHz, CDCl_3) of compound 185a	834
Figure A11.261	Infrared spectrum (Thin Film, NaCl) of compound 185a	835
Figure A11.262	^{13}C NMR (100 MHz, CDCl_3) of compound 185a	835
Figure A11.263	^{19}F NMR (282 MHz, CDCl_3) of compound 185a	836
Figure A11.264	^1H NMR (400 MHz, CDCl_3) of compound 185b	837
Figure A11.265	Infrared spectrum (Thin Film, NaCl) of compound 185b	838
Figure A11.266	^{13}C NMR (100 MHz, CDCl_3) of compound 185b	838
Figure A11.267	^{19}F NMR (282 MHz, CDCl_3) of compound 185b	839
Figure A11.268	^1H NMR (400 MHz, CDCl_3) of compound 185c	840
Figure A11.269	Infrared spectrum (Thin Film, NaCl) of compound 185c	841
Figure A11.270	^{13}C NMR (100 MHz, CDCl_3) of compound 185c	841
Figure A11.271	^{19}F NMR (282 MHz, CDCl_3) of compound 185c	842
Figure A11.272	^1H NMR (400 MHz, CDCl_3) of compound 185d	843
Figure A11.273	Infrared spectrum (Thin Film, NaCl) of compound 185d	844
Figure A11.274	^{13}C NMR (100 MHz, CDCl_3) of compound 185d	844
Figure A11.275	^1H NMR (400 MHz, CDCl_3) of compound 185e	845
Figure A11.276	Infrared spectrum (Thin Film, NaCl) of compound 185e	846
Figure A11.277	^{13}C NMR (100 MHz, CDCl_3) of compound 185e	846
Figure A11.278	^1H NMR (400 MHz, CDCl_3) of compound 185f	847
Figure A11.279	Infrared spectrum (Thin Film, NaCl) of compound 185f	848
Figure A11.280	^{13}C NMR (100 MHz, CDCl_3) of compound 185f	848
Figure A11.281	^1H NMR (400 MHz, CDCl_3) of compound 187a	849
Figure A11.282	Infrared spectrum (Thin Film, NaCl) of compound 187a	850
Figure A11.283	^{13}C NMR (100 MHz, CDCl_3) of compound 187a	850
Figure A11.284	^1H NMR (400 MHz, CDCl_3) of compound 187b	851
Figure A11.285	Infrared spectrum (Thin Film, NaCl) of compound 187b	852
Figure A11.286	^{13}C NMR (100 MHz, CDCl_3) of compound 187b	852
Figure A11.287	^1H NMR (400 MHz, CDCl_3) of compound 187c	853
Figure A11.288	Infrared spectrum (Thin Film, NaCl) of compound 187c	854
Figure A11.289	^{13}C NMR (100 MHz, CDCl_3) of compound 187c	854
Figure A11.290	^1H NMR (400 MHz, CDCl_3) of compound 187d	855
Figure A11.291	Infrared spectrum (Thin Film, NaCl) of compound 187d	856
Figure A11.292	^{13}C NMR (100 MHz, CDCl_3) of compound 187d	857
Figure A11.293	^1H NMR (400 MHz, CDCl_3) of compound 187e	857

Figure A11.294	Infrared spectrum (Thin Film, NaCl) of compound 187e	858
Figure A11.295	^{13}C NMR (100 MHz, CDCl_3) of compound 187e	858
Figure A11.296	^1H NMR (400 MHz, CDCl_3) of compound 188	859
Figure A11.297	Infrared spectrum (Thin Film, NaCl) of compound 188	860
Figure A11.298	^{13}C NMR (100 MHz, CDCl_3) of compound 188	860
Figure A11.299	^1H NMR (400 MHz, CDCl_3) of compound 189	861
Figure A11.300	Infrared spectrum (Thin Film, NaCl) of compound 189	862
Figure A11.301	^{13}C NMR (100 MHz, CDCl_3) of compound 189	862
Figure A11.302	^1H NMR (400 MHz, CDCl_3) of compound 190	863
Figure A11.303	Infrared spectrum (Thin Film, NaCl) of compound 190	864
Figure A11.304	^{13}C NMR (100 MHz, CDCl_3) of compound 190	864
Figure A11.305	^1H NMR (400 MHz, CDCl_3) of compound 191	865
Figure A11.306	Infrared spectrum (Thin Film, NaCl) of compound 191	866
Figure A11.307	^{13}C NMR (100 MHz, CDCl_3) of compound 191	866

APPENDIX 12

X-Ray Crystallography Reports Relevant to Chapter 4

Figure A12.1	X-ray crystal structure of THIQ 183p	869
---------------------	---	-----

LIST OF SCHEMES

CHAPTER 1

Nickel-Catalyzed Enantioselective Allylic Alkylation of Lactones and Lactams with Unactivated Allylic Alcohols

Scheme 1.1	Metal-catalyzed enantioselective allylic alkylation of α -acyl lactone and lactam prochiral nucleophiles	3
Scheme 1.2	Product transformation of allylic alkylation product 3aa	9
Scheme 1.3	Product transformation of allylic alkylation product 5aa	10

CHAPTER 2

Palladium-Catalyzed Enantioselective Decarboxylative Allylic Alkylation of Cyclic Siloxyketones

Scheme 2.1	Enantioselective synthesis of cyclic siloxanes	130
Scheme 2.2	Siloxy- β -ketoester substrate synthesis	131
Scheme 2.3	Synthesis of highly oxygenated, chiral, acyclic quaternary stereocenters	135
Scheme 2.4	Synthesis of lactone bearing vicinal quaternary-trisubstituted stereocenters	136

APPENDIX 4

Cycloadditions of Oxacyclic Allenes and a Catalytic Asymmetric Entryway to Enantioenriched Cyclic Allenes

Scheme A4.1	Synthesis of silyl triflate	234
Scheme A4.2	Catalytic asymmetric approach and cycloaddition results	240

CHAPTER 3

Concise Total Syntheses of (–)-Jorunnamycin A and (–)-Jorumycin Enabled by Asymmetric Catalysis

Scheme 3.1	Retrosynthesis of (–)-jorumycin	253
Scheme 3.2	Synthesis of isoquinoline monomers 84 and 85 and Fagnou coupling	254
Scheme 3.3	Synthesis of hydrogenation precursor 83	256
Scheme 3.4	Stereochemical rationale for the hydrogenation of bis-isoquinoline 83	257
Scheme 3.5	Completion of jorunnamycin A and jorumycin	260
Scheme 3.6	Observed discrepancy in enantioenrichment of products 97 and 81	319
Scheme 3.7	Possible reaction pathways to generate pentacycle 81	320

APPENDIX 5*Synthetic Summary of Chapter 3*

Scheme A5.1	Synthesis of isoquinoline <i>N</i> -oxide 84	328
Scheme A5.2	Synthesis of isoquinoline triflate 85	328
Scheme A5.3	Total Syntheses of jorunnamycin A and jorumycin.....	329

APPENDIX 8*Progress Toward the Syntheses of Bis-tetrahydroisoquinoline Analogs*

Scheme A8.1	Targeted polyfluorinated bis-THIQ analogs 126–128	427
Scheme A8.2	Syntheses of isoquinoline <i>N</i> -oxide 132 and isoquinoline triflate 133	428
Scheme A8.3	Syntheses of bis-isoquinolines 138–140	429
Scheme A8.4	Attempt to prepare bis-IQ methyl ester 142	430
Scheme A8.5	Synthetic route to access tetrafluorinated hydrogenation precursor 144	431
Scheme A8.6	Synthetic route to access difluorinated hydrogenation precursor 151	433
Scheme A8.7	Synthetic route to access difluorinated hydrogenation precursor 155	433
Scheme A8.8	Ir-catalyzed diastereo- and enantioselective hydrogenation.....	434
Scheme A8.9	Syntheses of tetrafluorinated bis-THIQ analog 126 and its derivatives	435
Scheme A8.10	End-route toward difluorinated bis-THIQ analog 127	436
Scheme A8.11	Alternative strategy to access difluorinated bis-THIQ analog 127	438
Scheme A8.12	End-route toward difluorinated bis-THIQ analog 128	439

APPENDIX 9*Synthetic Summary of Appendix 8*

Scheme A9.1	Syntheses of isoquinoline <i>N</i> -oxide 132 and isoquinoline triflate 133	481
Scheme A9.2	Construction of tetrafluorinated bis-THIQ core 129	481
Scheme A9.3	Syntheses of tetrafluorinated analog 126 and its derivatives 157–158	482
Scheme A9.4	Construction of difluorinated bis-THIQ core 130	482
Scheme A9.5	Synthetic route toward analog 127	483
Scheme A9.6	Alternative Strategy to access difluorinated bis-THIQ analog 127	483
Scheme A9.7	Construction of difluorinated bis-THIQ core 131	484
Scheme A9.8	Proposed endgame toward difluorinated analog 128	484

CHAPTER 4*Iridium-Catalyzed Enantioselective and Diastereoselective Hydrogenation of 1,3-Disubstituted Isoquinolines*

Scheme 4.1	Syntheses of 1-(hydroxymethyl)-3-aryl isoquinoline substrates	552
Scheme 4.2	Substrate scope of different aryl substituents	556
Scheme 4.3	Substrate scope of heteroaryl substituents	557
Scheme 4.4	Substrate scope of IQ backbone substituents.....	559
Scheme 4.5	Substrate scope of different directing groups	560
Scheme 4.6	Derivatization of a hydrogenated product	561

LIST OF TABLES

CHAPTER 1

Nickel-Catalyzed Enantioselective Allylic Alkylation of Lactones and Lactams with Unactivated Allylic Alcohols

Table 1.1	Optimization of reaction parameters	4
Table 1.2	Nucleophile and electrophile scope.....	6
Table 1.3	α -acyl lactam prochiral nucleophiles	7
Table 1.4	Linear vs. branched cinnamyl alcohol.....	8
Table 1.5	Results from additional ligands	20
Table 1.6	Solvent effects in nickel-catalyzed asymmetric allylic alkylation of 1a	22
Table 1.7	Optimization of reaction parameters for lactam 4a	23
Table 1.8	Determination of enantiomeric excess	45

APPENDIX 2

X-Ray Crystallography Reports Relevant to Chapter 1

Table A2.1	Crystal data and structure refinement for allylic alkylation product 3af	119
Table A2.2	Atomic coordinates ($\times 10^4$) and equivalent isotropic displacement parameters ($\text{\AA}^2 \times 10^3$) for 3af	120
Table A2.3	Bond lengths [\AA] and angles [$^\circ$] for 3af	121
Table A2.4	Anisotropic displacement parameters ($\text{\AA}^2 \times 10^3$) for 3af	124
Table A2.5	Hydrogen coordinates ($\times 10^4$) and isotropic displacement parameters ($\text{\AA}^2 \times 10^3$) for 3af	125
Table A2.6	Torsion angles [$^\circ$] for 3af	126

CHAPTER 2

Palladium-Catalyzed Enantioselective Decarboxylative Allylic Alkylation of Cyclic Siloxyketones

Table 2.1	Optimization of reaction parameters	132
Table 2.2	Substrate scope	134
Table 2.3	Determination of enantiomeric excess	162

APPENDIX 4*Cycloadditions of Oxacyclic Allenes and a Catalytic Asymmetric Entryway to Enantioenriched Cyclic Allenes*

Table A4.1	Mild generation of oxacyclic allene 31 and its trapping in Diels-Alder cycloadditions	235
Table A4.2	Additional (3+2) and (2+2) cycloadditions	237
Table A4.3	Effects of ligands, solvents, and temperatures	242
Table A4.4	Substrate, temperature, and concentration optimization experiments	243

CHAPTER 3*Concise Total Syntheses of (–)-Jorunnamycin A and (–)-Jorumycin Enabled by Asymmetric Catalysis*

Table 3.1	Optimization of the hydrogenation reaction.....	259
Table 3.2	Tabulated NMR data for (–)-jorunnamycin A (79).....	315
Table 3.3	Tabulated NMR data for (–)-jorumycin (77).....	316
Table 3.4	Additional ligands investigated in the optimization of the enantioselective hydrogenation.....	317
Table 3.5	Geometric mean of IC ₅₀ values and their statistics.....	321
Table 3.6	IC ₅₀ 's (nM) of compounds 101–105	322

APPENDIX 7*X-Ray Crystallography Reports Relevant to Chapter 3*

Table A7.1	Crystal data and structure refinement for product 98	399
Table A7.2	Atomic coordinates ($\times 10^4$) and equivalent isotropic displacement parameters ($\text{\AA}^2 \times 10^3$) for 98	400
Table A7.3	Bond lengths [\AA] and angles [$^\circ$] for 98	402
Table A7.4	Anisotropic displacement parameters ($\text{\AA}^2 \times 10^3$) for 98	414
Table A7.5	Hydrogen coordinates ($\times 10^4$) and isotropic displacement parameters ($\text{\AA}^2 \times 10^3$) for 98	417
Table A7.6	Torsion angles [$^\circ$] for 98	419
Table A7.7	Hydrogen bonds for 98 [\AA and $^\circ$]	423

APPENDIX 8*Progress Toward the Syntheses of Bis-tetrahydroisoquinoline Analogs*

Table A8.1	Optimization of the alcohol oxidation to access bis-IQ 149	432
-------------------	---	-----

CHAPTER 4*Iridium-Catalyzed Enantioselective and Diastereoselective Hydrogenation of 1,3-Disubstituted Isoquinolines*

Table 4.1	Optimization of the enantioselective hydrogenation of isoquinolines.....	553
Table 4.2	Additional ligand screen	637
Table 4.3	Additive effects in Ir-catalyzed hydrogenation.....	638
Table 4.4	Determination of enantiomeric excess	638

APPENDIX 12*X-Ray Crystallography Reports Relevant to Chapter 4*

Table A12.1	Crystal data and structure refinement for product 183p	869
Table A12.2	Atomic coordinates ($\times 10^4$) and equivalent isotropic displacement parameters ($\text{\AA}^2 \times 10^3$) for 183p	870
Table A12.3	Bond lengths [\AA] and angles [$^\circ$] for 183p	871
Table A12.4	Anisotropic displacement parameters ($\text{\AA}^2 \times 10^3$) for 183p	875
Table A12.5	Hydrogen coordinates ($\times 10^4$) and isotropic displacement parameters ($\text{\AA}^2 \times 10^3$) for 183p	875
Table A12.6	Torsion angles [$^\circ$] for 183p	876
Table A12.7	Hydrogen bonds for 183p [\AA and $^\circ$]	878

APPENDIX 13*Notebook Cross-Reference for New Compounds*

Table A13.1	Notebook cross-reference for compounds in Chapter 1	880
Table A13.2	Notebook cross-reference for compounds in Chapter 2	884
Table A13.3	Notebook cross-reference for compounds in Chapter 3	887
Table A13.4	Notebook cross-reference for compounds in Appendix 7.....	892
Table A13.5	Notebook cross-reference for compounds in Chapter 4	898

LIST OF ABBREVIATIONS

$[\alpha]_D$	specific rotation at wavelength of sodium D line
$^{\circ}\text{C}$	degrees Celsius
Å	Ångstrom
Ac	acetyl
AcOH	acetic acid
APCI	atmospheric pressure chemical ionization
app	apparent
aq	aqueous
Ar	aryl
atm	atmosphere
Bn	benzyl
Boc	<i>tert</i> -butoxycarbonyl
bp	boiling point
br	broad
Bu	butyl
Bz	benzoyl
c	concentration for specific rotation measurements (g/100 mL)
ca.	about (Latin circa)
calc'd	calculated
cat	catalytic
CDI	1,1'-carbonyldiimidazole
cm^{-1}	wavenumber(s)
cod	1,5-cyclooctadiene
CPME	cyclopentyl methyl ether

Cy	cyclohexyl
d	doublet
D	deuterium
DABCO	1,4-diazabicyclo[2.2.2]octane
dba	dibenzylideneacetone
DBU	1,8-diazabicyclo[5.4.0]undec-7-ene
DCE	1,2-dichloroethane
DDQ	2,3-dichloro-5,6-dicyano- <i>p</i> -benzoquinone
DIAD	diisopropyl azodicarboxylate
DIBAL	diisobutylaluminum hydride
DIPEA	<i>N,N</i> -diisopropylethylamine
DMA	<i>N,N</i> -dimethylacetamide
DMAP	4-dimethylaminopyridine
dmdba	bis(3,5-dimethoxybenzylidene)acetone
DME	1,2-dimethoxyethane
DMF	<i>N,N</i> -dimethylformamide
DMP	Dess–Martin periodinane
DMS	dimethyl sulfide
DMSO	dimethyl sulfoxide
dr	diastereomeric ratio
e.g.	for example (Latin <i>exempli gratia</i>)
<i>ee</i>	enantiomeric excess
EI+	electron impact
equiv	equivalent(s)
ESI	electrospray ionization
Et	ethyl
EtOAc	ethyl acetate

EWG	electron withdrawing group
FAB	fast atom bombardment
g	gram(s)
GC	gas chromatography
gCOSY	gradient-selected correlation spectroscopy
h	hour(s)
HG-II	Hoveyda-Grubbs catalyst 2 nd generation
HFIP	hexafluoroisopropanol
HMBC	heteronuclear multiple bond correlation
HMDS	1,1,1,3,3,3-hexamethyldisilazane
HPLC	high-performance liquid chromatography
HRMS	high-resolution mass spectroscopy
HSQC	heteronuclear single quantum correlation
Hz	hertz
$h\nu$	light
<i>i</i> -Pr	isopropyl
i.e.	that is (Latin id est)
IPA	isopropanol, 2-propanol
IQ	isoquinoline
IR	infrared (spectroscopy)
<i>J</i>	coupling constant
K	Kelvin(s) (absolute temperature)
kcal	kilocalorie
KHMDS	potassium hexamethyldisilazide
L	liter; ligand
LAH	Lithium aluminium hydride
L*	chiral ligand

LDA	lithium diisopropylamide
LG	leaving group
lit.	literature value
m	multiplet; milli
<i>m</i>	meta
M	metal; molar; molecular ion
<i>m</i> -CPBA	<i>meta</i> -chloroperoxybenzoic acid
<i>m/z</i>	mass to charge ratio
Me	methyl
mg	milligram(s)
MHz	megahertz
min	minute(s)
MM	mixed method
mol	mole(s)
mp	melting point
MS	molecular sieves
n	nano
N	normal
<i>n</i> -Bu	butyl
NBS	<i>N</i> -bromosuccinimide
NHSI	<i>N</i> -hydroxysuccinimide
NMR	nuclear magnetic resonance
Nu	nucleophile
<i>o</i>	ortho
<i>p</i>	para
Pd/C	palladium on carbon
Ph	phenyl

pH	hydrogen ion concentration in aqueous solution
Phth	phthalimide
PHOX	phosphinooxazoline ligand
PIDA	Phenyliodine(III) diacetate
Pin	2,3-dimethylbutane-2,3-diol (pinacol)
Piv	trimethylacetyl, pivaloyl
pK_a	pK for association of an acid
pMBz	4-methoxy-benzoyl
pmdba	bis(4-methoxybenzylidene)acetone
ppm	parts per million
Pr	propyl
Py	pyridine
q	quartet
R	generic for any atom or functional group
RCM	ring-closing metathesis
Ref.	reference
R_f	retention factor
s	singlet or strong or selectivity factor
sat.	saturated
SFC	supercritical fluid chromatography
STAB	Sodium triacetoxyborohydride
t	triplet
<i>t</i> -Bu	<i>tert</i> -butyl
TBABr	tetrabutylammonium bromide
TBAF	tetrabutylammonium fluoride
TBAI	tetrabutylammonium iodide
TBME/MTBE	<i>tert</i> -butyl methyl ether

TBS	<i>tert</i> -butyldimethylsilyl
TES	triethylsilyl
Tf	trifluoromethanesulfonyl (triflyl)
TFA	trifluoroacetic acid
TFAA	trifluoroacetic anhydride
TFE	2,2,2-trifluoroethanol
THF	tetrahydrofuran
THIQ	tetrahydroisoquinoline
TIPS	triisopropylsilyl
TLC	thin-layer chromatography
TMEDA	<i>N,N,N',N'</i> -tetramethylethylenediamine
TMS	trimethylsilyl
TOF	time-of-flight
Tol	tolyl
t_R	retention time
Ts	<i>p</i> -toluenesulfonyl (tosyl)
UV	ultraviolet
v/v	volume to volume
w	weak
w/v	weight to volume
X	anionic ligand or halide
λ	wavelength
μ	micro

CHAPTER 1

Nickel-Catalyzed Enantioselective Allylic Alkylation of Lactones and Lactams with Unactivated Allylic Alcohols[†]

1.1 INTRODUCTION

Since the seminal report in 1965 by Tsuji,¹ transition metal-catalyzed allylic alkylation has emerged as one of the most powerful methods for the construction of stereocenters.² In particular, with the use of prochiral nucleophiles that proceed through tetrasubstituted enolates, the transition metal-catalyzed enantioselective allylic alkylation has proven to be a formidable strategy for accessing chiral quaternary stereocenters in catalytic enantioselective fashion.³ Although this transformation has been studied for more than 50 years,⁴ the use of α -substituted

[†] This research was performed in collaboration with Carina I. Jette, Dr. Shoshana Bachman, and Dr. Scott Virgil. Portions of this chapter have been reproduced with permission from Ngamnithiporn, A.; Jette, C. I.; Bachman, S.; Virgil, S. C.; Stoltz, B. M. *Chemical Science*. **2018**, 9, 2547–2551. © 2018 Royal Society of Chemistry.

lactones or lactams as prochiral nucleophiles remains significantly underdeveloped.^{5,6}

As part of our ongoing research program directed at the development of new strategies for constructing quaternary stereocenters,⁷ we were drawn to the α -acyl lactones and lactams, as we envisioned that the α -acyl substituent would provide an additional functional handle for further synthetic manipulations. In addition, lactone products could also provide access to acyclic quaternary stereocenters via ring-opening reactions⁸ and reduction of the lactam products would enable direct access to functionalized piperidine rings, the most prevalent nitrogenous heterocycle in drug molecules.⁹ However, to the best of our knowledge, there has been only one report of a transition metal-catalyzed enantioselective allylic alkylation of monocyclic α -acyl lactone or lactam prochiral nucleophiles to furnish products bearing a quaternary stereocenter.^{5d}

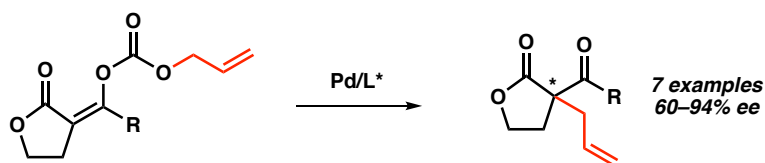
Recently, Cossy disclosed a palladium-catalyzed decarboxylative enantioselective allylic alkylation of enol carbonates derived from γ -butyrolactones (Scheme 1.1a). Various enol carbonates can be used to obtain diverse α -acyl quaternary butyrolactones in moderate to high levels of enantioselectivity. Nonetheless, the limited electrophile scope and challenging nucleophile synthesis limits the practicality of this transformation.

To address this limitation, we chose to investigate the enantioselective allylic alkylation of α -acyl lactones and lactams by using an inexpensive transition metal catalyst and easily accessible prochiral nucleophiles. Mashima's recent report on nickel-catalyzed enantioselective allylic alkylation of β -keto esters with allyl alcohol prompted us to probe nickel in our system.^{10,11} Furthermore, we

anticipated that an intermolecular allylic alkylation would simplify the substrate synthesis and provide a more convergent approach to these α -quaternary products.¹² Herein, we report the first example of nickel-catalyzed intermolecular enantioselective allylic alkylation using easily accessible α -acyl lactones and lactams as prochiral nucleophiles in conjunction with allylic alcohols as electrophilic coupling partners (Scheme 1.1b).

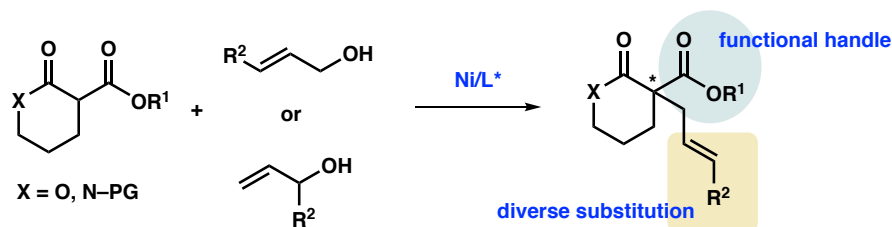
Scheme 1.1 Metal-Catalyzed Enantioselective Allylic Alkylation (AA) of α -Acyl Lactone and Lactam Prochiral Nucleophiles.

a) Previous Work (1 report):



- Limited to γ -butyrolactone substrates and an allyl group
- Substrates require low yielding, multistep synthesis

b) This Research:



- Inexpensive catalyst and commercially available ligand
- Easily accessible substrates

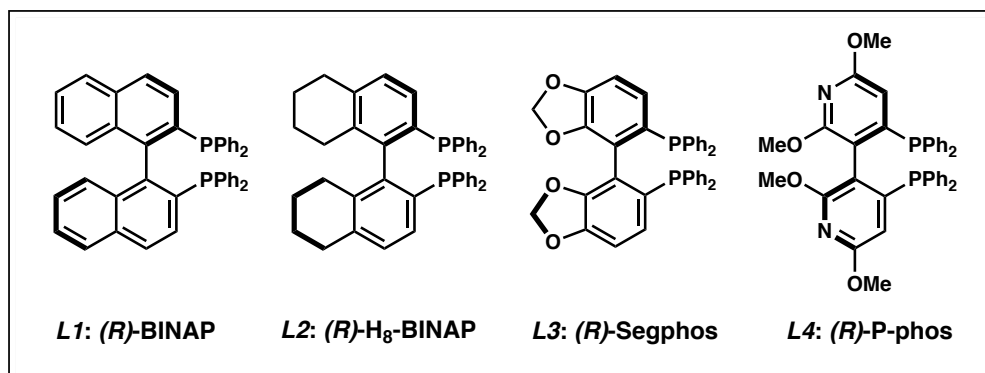
1.2 REACTION OPTIMIZATION

Our studies commenced with an investigation of the enantioselective allylic alkylation between α -ethoxycarbonyl lactone **1a** and allyl alcohol (**2a**) using Ni(COD)₂ and (*R*)-BINAP (**L1**) in diethyl ether at 0 °C. Although the α -quaternary lactone product **3aa** was obtained in good yield, only moderate enantioselectivity was achieved (Table 1.1, entry 1).¹³

Table 1.1 Optimization of reaction parameters.^a

$\text{1a} + \text{2a} \xrightarrow[\text{Et}_2\text{O (0.1 M), Temp, 19 h}]{\text{Ni(COD)}_2 \text{ (10 mol \%), Ligand (12 mol \%)}} \text{3aa}$

entry	ligand	temp (°C)	% yield ^b	% ee ^c
1	L1	0	53	75
2	L2	0	76	78
3	L3	0	93	79
4	L4	0	82	82
5 ^d	L4	0	62	81
6	L4	23	86	74
7	L4	−10	69	84
8 ^e	L4	−10	80	85
9	–	0	0	–



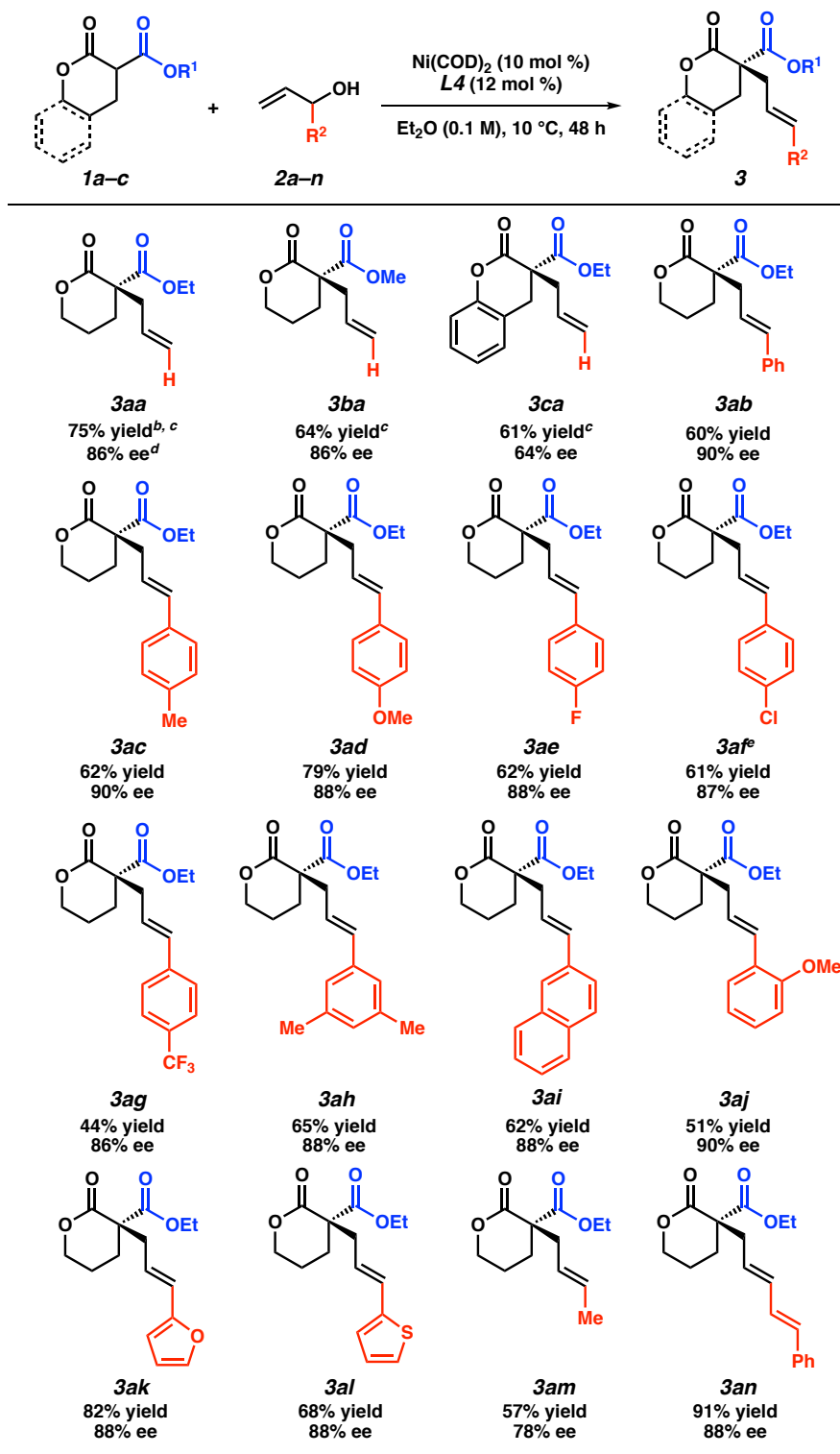
[a] Conditions: **1a** (0.1 mmol), **2a** (0.1 mmol), Ni(COD)₂ (10 mol %), ligand (12 mol %) in Et₂O (1.0 mL). [b] Yields determined by ¹H NMR of crude reaction mixture using 1,3,5-trimethoxybenzene as a standard. [c] Determined by chiral SFC analysis of the isolated product. [d] Ni(COD)₂ (5 mol %) and **L4** (6 mol %) were used. [e] Reaction time = 48 h.

Seeking to improve the enantioselectivity, we elected to survey a wide variety of commercially available ligand scaffolds. Chiral bisphosphine ligands were discovered to exhibit superior enantioselectivity to other classes of ligands, including those commonly used in asymmetric allylic alkylations such as phosphinooxazolines (PHOX) or C2-asymmetric ligands pioneered by the Trost group.¹⁴ In the presence of Ni(COD)₂ (10 mol %) and chiral bisphosphine ligands **L1–L4** (12 mol %) in Et₂O, the reaction proceeds with moderate levels of

enantioselectivity (Table 1.1, entries 1–4). Using toluene or other ethereal solvents results in lower ee.¹⁵ The highest enantiomeric excess (ee) was achieved with (*R*)-P-phos (**L4**), which delivers α -quaternary lactone **3aa** in 82% yield and 82% ee (entry 4). Decreasing the catalyst loading to 5 mol % requires exceedingly long reaction time (entry 5). An examination of different temperatures revealed that decreasing the temperature improves ee (entries 6–7), albeit with slightly diminished yields. Prolonged reaction time (48 h) at –10 °C affords product **3aa** in 80% yield and 85% ee (entry 8). Importantly, a control experiment performed in the absence of the chiral ligand shows no background reaction (entry 9).

1.3 SUBSTRATE SCOPE EXPLORATION

With the optimized reaction conditions in hand, we examined the scope of this asymmetric transformation (Table 1.2). The reaction of α -methoxycarbonyl lactone **1b**, possessing a smaller alkyl group at the ester fragment, with allyl alcohol (**2a**) provides α -quaternary lactone **3ba** in comparable yield and ee to the allylated product **3aa**. Bicyclic lactone **1c** could also be used to furnish product **3ca** in slightly diminished yield and enantioselectivity. With respect to the electrophile scope, reactions between lactone **1a** with various substituted allyl alcohols proceed with good ee (78–90% ee) at increased temperature (10 °C). Although a trend in enantioselectivity was not observed, we found that the electronic nature of the aryl substituent does affect the reactivity. Electrophiles containing electron rich aryl substituents provide the corresponding products in greater yields than their electron-deficient counterparts (**3ac–3ag**).

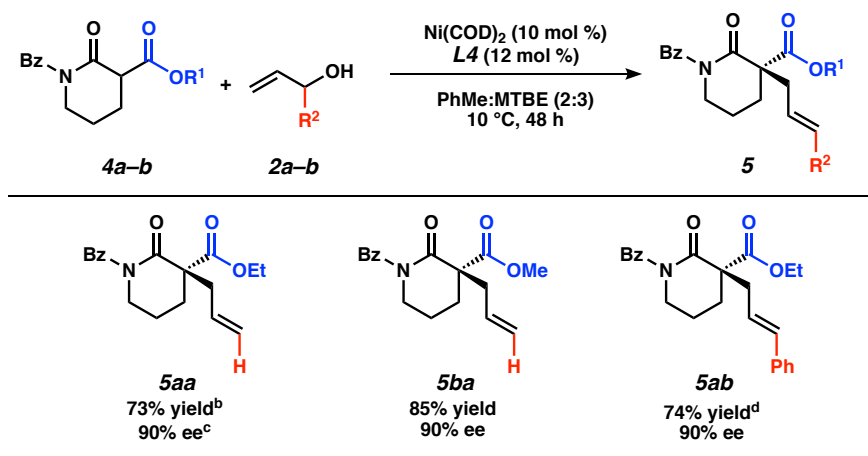
Table 1.2 Nucleophile and electrophile scope.^a

[a] Reactions performed on 0.2 mmol. [b] Yield of isolated product. [c] Reaction performed at -10 °C. [d] Determined by chiral SFC analysis. [e] Absolute configuration determined via single crystal x-ray analysis.

Furthermore, we found that *para*- and *meta*-substituted aryl rings exhibit higher reactivity as compared to the *ortho*-substituted aryl ring (**3ac**, **3ah–ai** vs. **3aj**). Apart from the aryl-substituted electrophiles, we were pleased to find that heteroaryl substitution is also well-tolerated (**3ak–3al**). The reaction with an aliphatic electrophile affords product **3am** in slightly diminished yield and ee. In addition, an alkenyl-substituted electrophile fares well under our reaction conditions, delivering product **3an** in an excellent 91% yield and 88% ee.

At this stage, we questioned whether we could leverage this transformation to include nitrogen-containing lactam nucleophiles. To our delight, under slightly modified reaction conditions using the same chiral bisphosphine ligand **L4**,¹⁶ α -ester lactams **4a–4b** furnish products **5aa–5ba** in good yields and with even higher enantioselectivity as compared to their lactone counterparts (Table 3). Examination of different protecting groups revealed that the benzoyl-protecting group is optimal.¹⁷ Reaction of α -ethoxycarbonyl benzoyl-protected lactam **4a** with branched cinnamyl alcohol affords linear product **5ab** in 74% yield and 90% ee.

Table 1.3 α -acyl lactam prochiral nucleophiles.^a

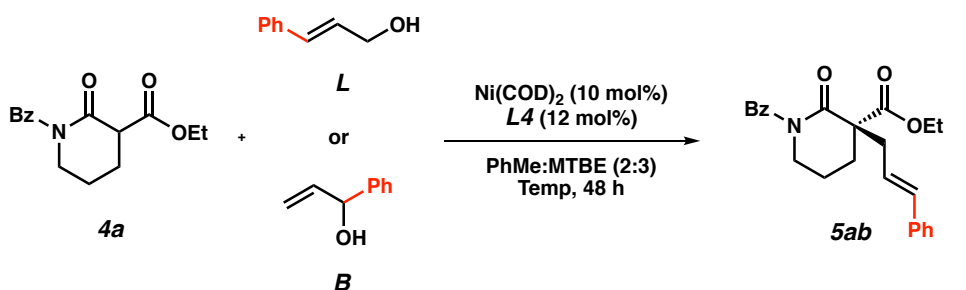


[a] Reactions performed on 0.2 mmol. [b] Yield of isolated product. [c] Determined by chiral SFC analysis. [d] Reaction performed at 30 °C.

1.4 PRELIMINARY MECHANISTIC INSIGHTS

In order to gain mechanistic insights into this transformation, we compared the results from reactions using linear and branched cinnamyl alcohols (Table 1.4). Only the linear product was detected, indicating that a nickel π -allyl is likely an intermediate in the catalytic cycle.¹⁸ While additional studies are needed to establish the full reaction mechanism and stereocontrolling factors in the process, the ability of this catalyst combination to access a single product from two electrophilic coupling partners highlights its flexibility in potential synthetic applications.

Table 1.4 Linear vs. branched cinnamyl alcohol.^a



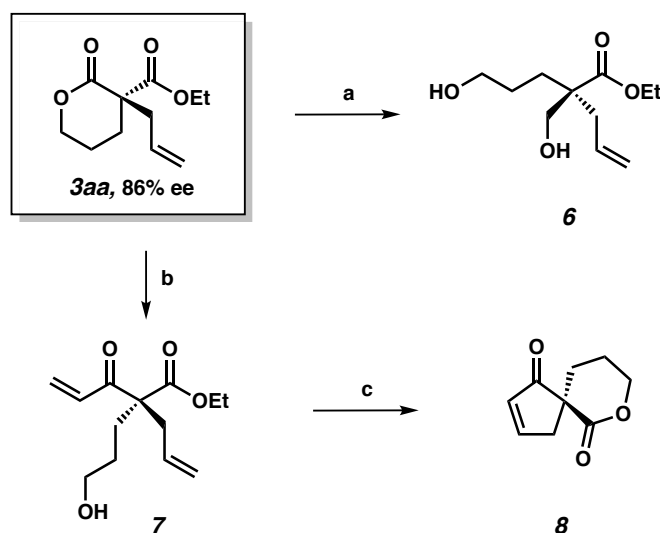
entry	elec	temp (°C)	% conversion ^b	% yield ^b	% ee ^c
1	L	10	60	59	92
2	B	10	58	55	92
3	L	30	>95	86	91
4	B	30	90	83	91

[a] Reactions performed on 0.1 mmol scale. [b] Yields determined by ¹H NMR of crude reaction mixture using benzyl ether as a standard. [c] Determined by chiral SFC analysis of the isolated product.

1.5 PRODUCT TRANSFORMATIONS

To demonstrate the synthetic utility of the α -quaternary products, we performed a number of product transformations on both α -quaternary lactone **3aa** (Scheme 1.2) and lactam **5aa** (Scheme 1.3). Selective reduction of the lactone functionality in **3aa** provides diol **6** in 88% yield. Additionally, vinyl Grignard addition into lactone **3aa** affords enone **7** in 67% yield with no erosion of enantioselectivity. These enantioenriched acyclic products **6** and **7** bearing a quaternary stereocenter are envisioned to be useful chiral building blocks as they contain multiple functional handles for further manipulations. For example, enantioenriched spirocycle **8** can be accessed via ring-closing metathesis followed by lactonization of enone **7**.

Scheme 1.2 Product transformations of allylic alkylation product **3aa**.

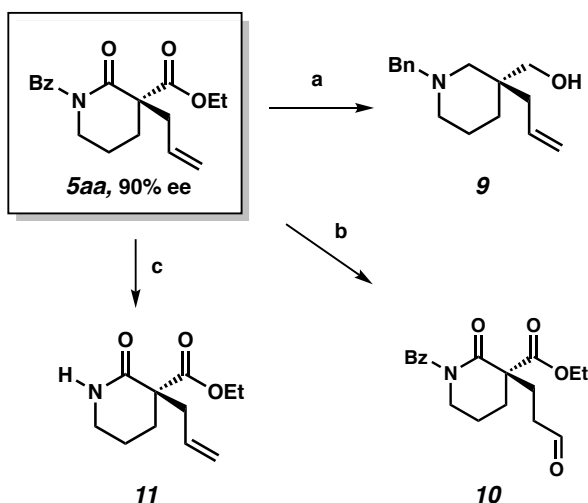


[a] NaBH_4 , $\text{CeCl}_3 \cdot 7\text{H}_2\text{O}$, THF/MeOH, 0°C , 88% yield; [b] Vinyl–magnesium bromide, THF, -78°C , 67% yield, 86% ee; [c] Grubbs' II (5 mol %), Toluene, 40°C ; DBU, MeCN, 23°C , 53% yield.

We also performed experiments to probe the reactivity of our α -quaternary lactam products. Reduction of lactam **5aa** with lithium aluminium hydride delivers chiral piperidine derivative **9**, which is of potential value to medicinal chemists.⁹ Use of the

aldehyde selective Wacker procedure¹⁹ affords aldehyde **10** in 75% yield. Lastly, cleavage of the benzoyl protecting group under basic conditions provides unprotected lactam **11** in 84% yield.

Scheme 1.3 Product transformations of allylic alkylation product **5aa**.



[a] LAH, Ether, 65°C, 80% yield; [b] CuCl·H₂O (12 mol %), PdCl₂(PhCN)₂ (12 mol %), AgNO₂ (6 mol %), t-BuOH, Nitromethane under O₂, 75% yield; [c] NaOEt, EtOH, 23 °C, 84% yield.

1.6 CONCLUSIONS

In summary, we have developed the first nickel-catalyzed enantioselective allylic alkylation of α -substituted lactones and lactams with free allylic alcohols. Utilizing a commercially available chiral bisphosphine ligand, α -quaternary lactones and lactams can be constructed in good yield (up to 91% yield) and with high enantiomeric excess (up to 90% ee). A broad range of functional groups are compatible with the reaction conditions. A number of product derivatizations showed the synthetic utility of this methodology for constructing small chiral building blocks with multiple functional handles. Future work to further elucidate the mechanism of this transformation is underway and will be reported in due course.

1.7 EXPERIMENTAL SECTION

1.7.1 MATERIALS AND METHODS

Unless otherwise stated, reactions were performed in flame-dried glassware under an argon or nitrogen atmosphere using dry, deoxygenated solvents. Solvents were dried by passage through an activated alumina column under argon. Reaction progress was monitored by thin-layer chromatography (TLC) or Agilent 1290 UHPLC-MS. TLC was performed using E. Merck silica gel 60 F254 precoated glass plates (0.25 mm) and visualized by UV fluorescence quenching, *p*-anisaldehyde, or KMnO₄ staining. Silicycle SiliaFlash® P60 Academic Silica gel (particle size 40–63 μm) was used for flash chromatography. ¹H NMR spectra were recorded on Varian Inova 500 MHz, Bruker 400 MHz, or Varian Mercury 300 MHz spectrometers and are reported relative to residual CHCl₃ (δ 7.26 ppm). ¹³C NMR spectra were recorded on Varian Inova 500 MHz spectrometer (125 MHz) and Bruker 400 MHz spectrometer (100 MHz) and are reported relative to CHCl₃ (δ 77.16 ppm). ¹⁹F NMR spectra were recorded on Varian Mercury 300 MHz spectrometer (282 MHz). Data for ¹H NMR are reported as follows: chemical shift (δ ppm) (multiplicity, coupling constant (Hz), integration). Multiplicities are reported as follows: s = singlet, d = doublet, t = triplet, q = quartet, p = pentet, sept = septuplet, m = multiplet, br s = broad singlet, br d = broad doublet, app = apparent. Data for ¹³C NMR are reported in terms of chemical shifts (δ ppm). IR spectra were obtained using Perkin Elmer Spectrum BXII spectrometer or Nicolet 6700 FTIR spectrometer using thin films deposited on NaCl plates and reported in frequency of absorption (cm⁻¹). Optical rotations were measured with a Jasco P-2000 polarimeter operating on the sodium D-line (589 nm), using a 100 mm path-length cell and are reported as: [α]_D^T (concentration in 10

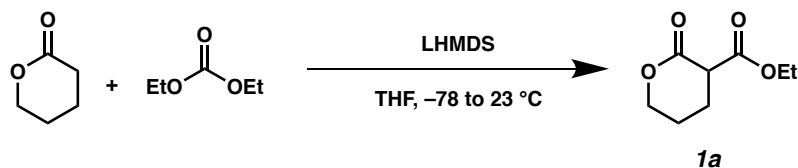
mg/1 mL, solvent) . Analytical SFC was performed with a Mettler SFC supercritical CO₂ analytical chromatography system utilizing Chiralpak (AD-H, AS-H or IC) or Chiralcel (OD-H, OJ-H, or OB-H) columns (4.6 mm x 25 cm) obtained from Daicel Chemical Industries, Ltd. High resolution mass spectra (HRMS) were obtained from Agilent 6200 Series TOF with an Agilent G1978A Multimode source in electrospray ionization (ESI+), atmospheric pressure chemical ionization (APCI+), or mixed ionization mode (MM: ESI-APCI+), or obtained from Caltech mass spectrometry laboratory. Low-temperature diffraction data (ϕ - and ω -scans) were collected on a Bruker AXS D8 VENTURE KAPPA diffractometer coupled to a PHOTON 100 CMOS detector with Cu K_{α} radiation ($\lambda = 1.54178$ Å) from an I μ S micro-source for the structure of compound P17471. The structure was solved by direct methods using SHELXS²⁰ and refined against F^2 on all data by full-matrix least squares with SHELXL-2016²¹ using established refinement techniques.²² All non-hydrogen atoms were refined anisotropically. All hydrogen atoms were included into the model at geometrically calculated positions and refined using a riding model. The isotropic displacement parameters of all hydrogen atoms were fixed to 1.2 times the U value of the atoms they are linked to (1.5 times for methyl groups).

Reagents were purchased from Sigma-Aldrich, Acros Organics, Strem, or Alfa Aesar, and used as received unless otherwise stated.

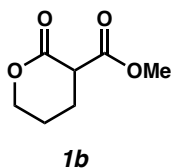
1.7.2 EXPERIMENTAL PROCEDURES AND SPECTROSCOPIC DATA

1.7.2.1 Synthesis of Nucleophiles

General procedure 1: α -acylation of lactones

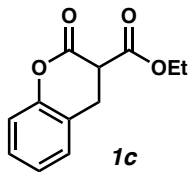


Ethyl 2-oxotetrahydro-2H-pyran-3-carboxylate (1a):²³ To a solution of LHMDS (3.43 g, 20.5 mmol, 2.05 equiv) in THF (20 mL) was added a mixture of delta-valerolactone (1.00 g, 10.0 mmol, 1.00 equiv) and diethyl carbonate (1.3 mL, 11.0 mmol, 1.10 equiv) at -78 °C. After stirring at room temperature for 6 hours, the reaction was quenched with glacial acetic acid (5 mL), diluted with Et₂O (20 mL), and stirred for 5 minutes. The insoluble white solid was filtered off and rinsed with more Et₂O. The filtrate was concentrated and purified by column chromatography (50% to 65% Et₂O in PET) to afford **1a** as a colorless oil (1.20 g, 70% yield); ¹H NMR (300 MHz, CDCl₃) δ 4.46–4.31 (m, 2H), 4.25 (qd, J = 7.1, 1.7 Hz, 2H), 3.56 (dd, J = 8.3, 7.5 Hz, 1H), 2.38–2.08 (m, 2H), 2.08–1.80 (m, 2H), 1.30 (t, J = 7.1 Hz, 3H). All characterization data match those reported.²⁴



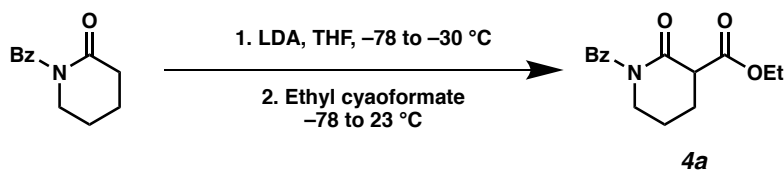
Methyl 2-oxotetrahydro-2H-pyran-3-carboxylate (1b): Compound **1b** was prepared from dimethyl carbonate using general procedure 1 (1.38 g, 87% yield); ¹H NMR (300

MHz, CDCl₃) δ 4.46–4.32 (m, 2H), 3.80 (s, 3H), 3.58 (dd, J = 8.4, 7.5 Hz, 1H), 2.38–2.06 (m, 2H), 2.02–1.81 (m, 2H). All characterization data match those reported.²³



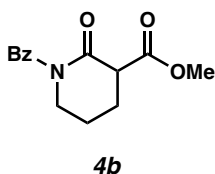
Ethyl 2-oxochromane-3-carboxylate (1c): Compound **1c** was prepared from dihydrocoumarin and diethyl carbonate using general procedure 1 (0.28 g, 25% yield); ¹H NMR (300 MHz, CDCl₃) δ 7.33–7.18 (m, 2H), 7.17–6.99 (m, 2H), 4.34–4.08 (m, 2H), 3.76 (dd, J = 8.5, 6.1 Hz, 1H), 3.42 (dd, J = 16.0, 8.5 Hz, 1H), 3.18 (dd, J = 16.0, 6.0 Hz, 1H), 1.21 (t, J = 7.1 Hz, 3H). All characterization data match those reported.²⁵

General procedure 2: α -acylation of lactams



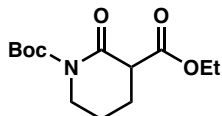
Ethyl 1-benzyl-2-oxopiperidine-3-carboxylate (4a):²⁶ To a solution of diisopropylamine (1.7 mL, 12 mmol, 1.2 equiv) in THF (65 mL) at 0 °C, *n*-BuLi (4.6 mL, 11 mmol, 2.4 M in hexanes, 1.1 equiv) was added dropwise over 10 minutes. After stirring for 30 min at 0 °C, the solution was cooled to –78 °C and a solution of benzoyl-protected lactam²⁷ (2.0 g, 12 mmol, 1.2 equiv) in THF (17 mL) was then added over 5 minutes. The reaction mixture was stirred at –78 °C for 2 hours and warmed to –30 °C for 1 hour. Ethyl cyanoformate (1.1 mL, 11 mmol, 1.1 equiv) was then added at –78 °C. The reaction was allowed to slowly warm to room temperature overnight. Upon complete consumption of the starting material by TLC, the reaction was quenched with saturated

NH₄Cl. The aqueous layer was extracted with EtOAc (50 mL × 4). The combined organic phases were washed with brine (50 mL), dried over Na₂SO₄, filtered, and concentrated under vacuum. The crude residue was purified by column chromatography (30% EtOAc in hexanes) to provide product **4a** as a white amorphous solid (1.47 g, 53% yield); ¹H NMR (500 MHz, CDCl₃) δ 7.73–7.66 (m, 2H), 7.52–7.44 (m, 1H), 7.43–7.34 (m, 2H), 4.25 (q, *J* = 7.1 Hz, 2H), 3.89–3.75 (m, 2H), 3.58–3.50 (m, 1H), 2.40–2.27 (m, 1H), 2.22–2.00 (m, 2H), 2.00–1.89 (m, 1H), 1.32 (t, *J* = 7.1 Hz, 3H); ¹³C NMR (125 MHz, CDCl₃) δ 174.7, 170.0, 169.6, 135.6, 132.0, 128.3, 128.2, 62.0, 51.2, 46.4, 25.6, 20.7, 14.2; IR (Neat Film, NaCl) 3062, 2980, 1734, 1701, 1683, 1476, 1449, 1392, 1285, 1258, 1185, 1152, 1113, 1026, 999, 730, 670, 638 cm⁻¹; HRMS (MM) *m/z* calc'd for C₁₅H₁₈NO₄ [M+H]⁺: 276.1230, found 276.1237.

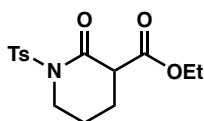


Methyl 1-benzoyl-2-oxopiperidine-3-carboxylate (4b): Compound **4b** was prepared from Bz-protected lactam and methyl cyanoformate using general procedure 2 and purified by column chromatography (40% EtOAc in hexanes) to provide a colorless amorphous solid (0.33 g, 51% yield); ¹H NMR (400 MHz, CDCl₃) δ 7.73–7.65 (m, 2H), 7.48 (m, 1H), 7.43–7.36 (m, 2H), 3.86–3.80 (m, 2H), 3.79 (s, 3H), 3.59 (t, *J* = 6.4 Hz, 1H), 2.39–2.27 (m, 1H), 2.23–2.03 (m, 2H), 2.02–1.89 (m, 1H); ¹³C NMR (100 MHz, CDCl₃) δ 174.7, 170.5, 169.6, 135.6, 132.0, 128.3, 128.3, 52.9, 51.1, 46.4, 25.6, 20.9; IR (Neat Film, NaCl) 2953, 1738, 1681, 1600, 1449, 1392, 1284, 1258, 1200, 1151, 1115,

1065, 973, 954, 857, 796, 731, 701, 639; HRMS (MM) m/z calc'd for $C_{14}H_{16}NO_4$ $[M+H]^+$: 262.1074, found 262.1066.

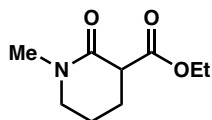


1-(*tert*-butyl) 3-ethyl 2-oxopiperidine-1,3-dicarboxylate: This compound was prepared from Boc-protected lactam²⁸ using general procedure 2 and purified by column chromatography (20% EtOAc in hexanes) to provide a colorless oil (0.47 g, 70% yield); 1H NMR (400 MHz, $CDCl_3$) δ 4.30 – 4.13 (m, 2H), 3.75 – 3.62 (m, 2H), 3.49 (dd, J = 8.7, 6.8 Hz, 1H), 2.24 – 2.02 (m, 2H), 1.96 (dt, J = 14.1, 6.6, 5.2 Hz, 1H), 1.81 (dddt, J = 14.1, 8.8, 7.5, 5.3 Hz, 1H), 1.52 (s, 9H), 1.29 (t, J = 7.1 Hz, 3H); ^{13}C NMR (100 MHz, $CDCl_3$) δ 170.05, 167.60, 152.75, 83.51, 61.72, 51.61, 45.93, 28.13, 24.35, 21.16, 14.23; IR (Neat Film, NaCl) 2980, 2939, 1772, 1717, 1478, 1458, 1393, 1369, 1297, 1252, 1146, 1115, 1096, 1056, 1029, 937, 852, 778, 748, 642; HRMS (MM) m/z calc'd for $C_{13}H_{21}NO_5Na$ $[M+Na]^+$: 294.1312, found 294.1315.

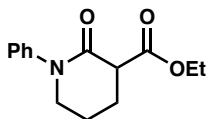


Ethyl 2-oxo-1-tosylpiperidine-3-carboxylate: This compound was prepared from tosyl-protected lactam²⁹ using general procedure 1 and purified by column chromatography (35% to 40% EtOAc in hexanes) to provide a colorless oil (0.32 g, 41% yield); 1H NMR (400 MHz, $CDCl_3$) δ 7.90 (d, J = 8.4 Hz, 2H), 7.31 (d, J = 7.9, 2H), 4.12 (qd, J = 7.1, 1.2 Hz, 2H), 4.03–3.84 (m, 2H), 3.41 (dd, J = 7.5, 6.3 Hz, 1H), 2.43 (s, 3H), 2.19–1.97 (m, 3H), 1.96–1.82 (m, 1H), 1.18 (t, J = 7.1 Hz, 3H); ^{13}C NMR (100 MHz, $CDCl_3$) δ 169.3,

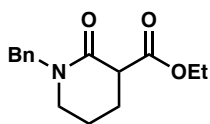
166.6, 145.06, 135.7, 129.5, 128.9, 61.9, 50.9, 46.6, 24.3, 21.8, 21.5, 14.1; IR (Neat Film, NaCl) 2980, 1737, 1694, 1456, 1353, 1289, 1169, 1089, 1036, 1008, 827, 815, 706, 670, 653; HRMS (MM) m/z calc'd for $C_{15}H_{20}NO_5S$ $[M+H]^+$: 326.1057, found 326.1066.



Ethyl 1-methyl-2-oxopiperidine-3-carboxylate: This compound was prepared from methyl-protected lactam using previously reported procedure;³⁰ 1H NMR (300 MHz, $CDCl_3$) δ 4.31–4.08 (m, 2H), 3.44–3.20 (m, 3H), 2.96 (s, 3H), 2.24–1.89 (m, 3H), 1.89–1.69 (m, 1H), 1.28 (t, $J = 7.1$ Hz, 3H). All characterization data match those reported.³¹



Ethyl 2-oxo-1-phenylpiperidine-3-carboxylate: This compound was prepared from phenyl-protected lactam³² using general procedure 2 and purified by column chromatography (40% EtOAc in hexanes) to provide a pale yellow solid (0.53 g, 42% yield); 1H NMR (400 MHz, $CDCl_3$) δ 7.42–7.35 (m, 2H), 7.29–7.22 (m, 3H), 4.31–4.15 (m, 2H), 3.76–3.61 (m, 2H), 3.57 (dd, $J = 7.8, 6.4$ Hz, 1H), 2.35–2.04 (m, 3H), 2.00–1.88 (m, 1H), 1.30 (t, $J = 7.1$ Hz, 3H); ^{13}C NMR (100 MHz, $CDCl_3$) δ 171.1, 166.2, 142.9, 129.3, 127.0, 126.1, 61.5, 51.4, 49.7, 25.3, 21.5, 14.3; IR (Neat Film, NaCl) 2943, 1734, 1654, 1595, 1494, 1462, 1427, 1371, 1353, 1308, 1259, 1197, 1171, 1036, 763, 697, 659; HRMS (MM) m/z calc'd for $C_{14}H_{18}NO_3$ $[M+H]^+$: 248.1281, found 248.1278.

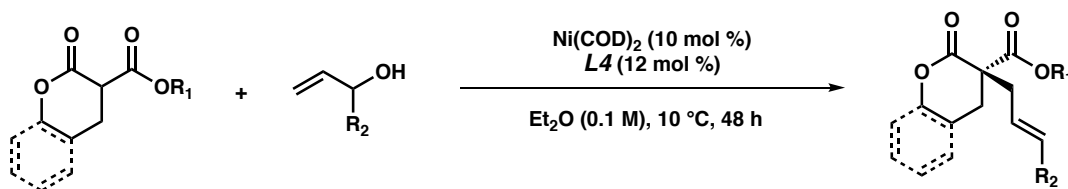


Ethyl 1-benzyl-2-oxopiperidine-3-carboxylate: This compound was prepared from benzyl-protected lactam³³ using general procedure 2 (0.32 g, 56% yield); ¹H NMR (300 MHz, CDCl₃) δ 7.37–7.23 (m, 5H), 4.73 (d, *J* = 14.7 Hz, 1H), 4.51 (d, *J* = 14.7 Hz, 1H), 4.24 (qd, *J* = 7.1, 4.0 Hz, 2H), 3.59–3.43 (m, 1H), 3.36–3.12 (m, 2H), 2.29–1.97 (m, 2H), 1.97–1.83 (m, 1H), 1.82–1.64 (m, 1H), 1.31 (t, *J* = 7.2 Hz, 3H). All characterization data match those reported.³⁴

1.7.2.2 General Procedure for the Nickel-Catalyzed Allylic Alkylation

Please note that the absolute configuration was determined only for compound **3af** via x-ray crystallographic analysis. The absolute configuration for all other products has been inferred by analogy. For respective HPLC and SFC conditions, please refer to Table S3.

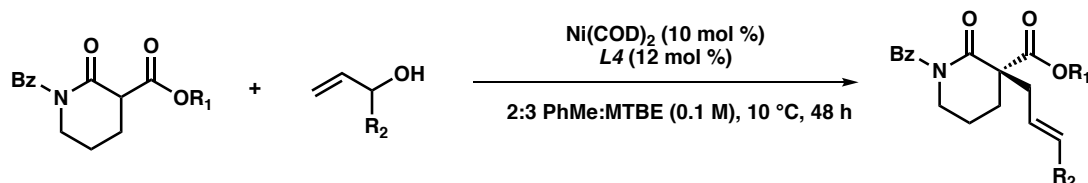
General procedure 3: Ni-catalyzed asymmetric AA of lactones



In a nitrogen-filled glovebox, to an oven-dried 4-mL vial equipped with a stir bar was added (*R*)-P-Phos ligand **L4** (15.5 mg, 0.024 mmol, 12 mol%) and Ni(COD)₂ (5.5 mg, 0.02 mmol, 10 mol%) in Et₂O (1.2 mL). The vial was then capped with a PTFE-lined septum cap and stirred at room temperature. After 30 minutes, the catalyst mixture was cooled to 10 °C. Precooled nucleophile (0.2 mmol, 1 equiv) in Et₂O (0.4 mL) and electrophile (0.2 mmol, 1 equiv) in Et₂O (0.4 mL) at 10 °C were prepared and then added

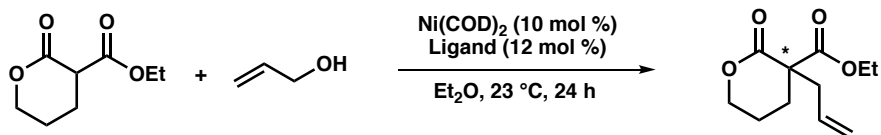
to the catalyst mixture at 10 °C. The vial was sealed with a PTFE-lined septum cap and stirred at 10 °C. After 48 h, the vial was removed from the glovebox. The crude reaction mixture was filtered through a silica plug with Et₂O, concentrated under vacuum, and purified by silica gel flash chromatography to furnish the product.

General procedure 4: Ni-catalyzed asymmetric AA of lactams



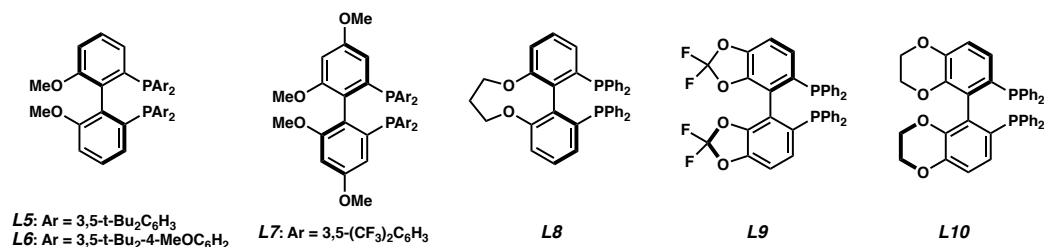
In a nitrogen-filled glovebox, to an oven-dried 4-mL vial equipped with a stir bar was added (*R*)-P-Phos ligand **L4** (15.5 mg, 0.024 mmol, 12 mol%) and Ni(COD)₂ (5.5 mg, 0.02 mmol, 10 mol %) in MTBE (1.2 mL). The vial was then capped with a PTFE-lined septum cap and stirred at room temperature. After 30 minutes, the catalyst mixture was cooled to 10 °C. Precooled nucleophile (0.2 mmol, 1 equiv) in toluene (0.4 mL) and electrophile (0.2 mmol, 1 equiv) in toluene (0.4 mL) at 10 °C were prepared and then added to the catalyst mixture at 10 °C. The vial was sealed with a PTFE-lined septum cap and stirred at 10 °C. After 48 h, the vial was removed from the glovebox. The crude reaction mixture was filtered through a silica plug with Et₂O, concentrated under vacuum, and purified by silica gel flash chromatography to furnish the product.

1.7.2.3 Additional Optimization Results

Table 1.5 Results from additional ligands ^a

Entry	Ligand	ee (%) ^b	Entry	Ligand	ee (%) ^b
1	<i>L5</i>	14	19	<i>L23</i>	0
2	<i>L6</i>	20	20	<i>L24</i>	−34
3	<i>L7</i>	–	21	<i>L25</i>	–
4	<i>L8</i>	−60	22	<i>L26</i>	−6
5	<i>L9</i>	57	23	<i>L27</i>	3
6	<i>L10</i>	67	24	<i>L28</i>	–
7	<i>L11</i>	−63	25	<i>L29</i>	31
8	<i>L12</i>	–	26	<i>L30</i>	9
9	<i>L13</i>	8	27	<i>L31</i>	−15
10	<i>L14</i>	19	28	<i>L32</i>	−22
11	<i>L15</i>	–	29	<i>L33</i>	–
12	<i>L16</i>	11	30	<i>L34</i>	−73
13	<i>L17</i>	24	31	<i>L35</i>	–
14	<i>L18</i>	–	32	<i>L36</i>	–
15	<i>L19</i>	12	33	<i>L37</i>	–
16	<i>L20</i>	–	34	<i>L38</i>	–
17	<i>L21</i>	–	35	<i>L39</i>	–
18	<i>L22</i>	17	36	<i>L40</i>	−44

[a] Reactions performed on 0.02 mmol scale using 3CS high-throughput setup. [b] Determined by chiral SFC analysis.

Figure 1.1 Additional ligands examined.

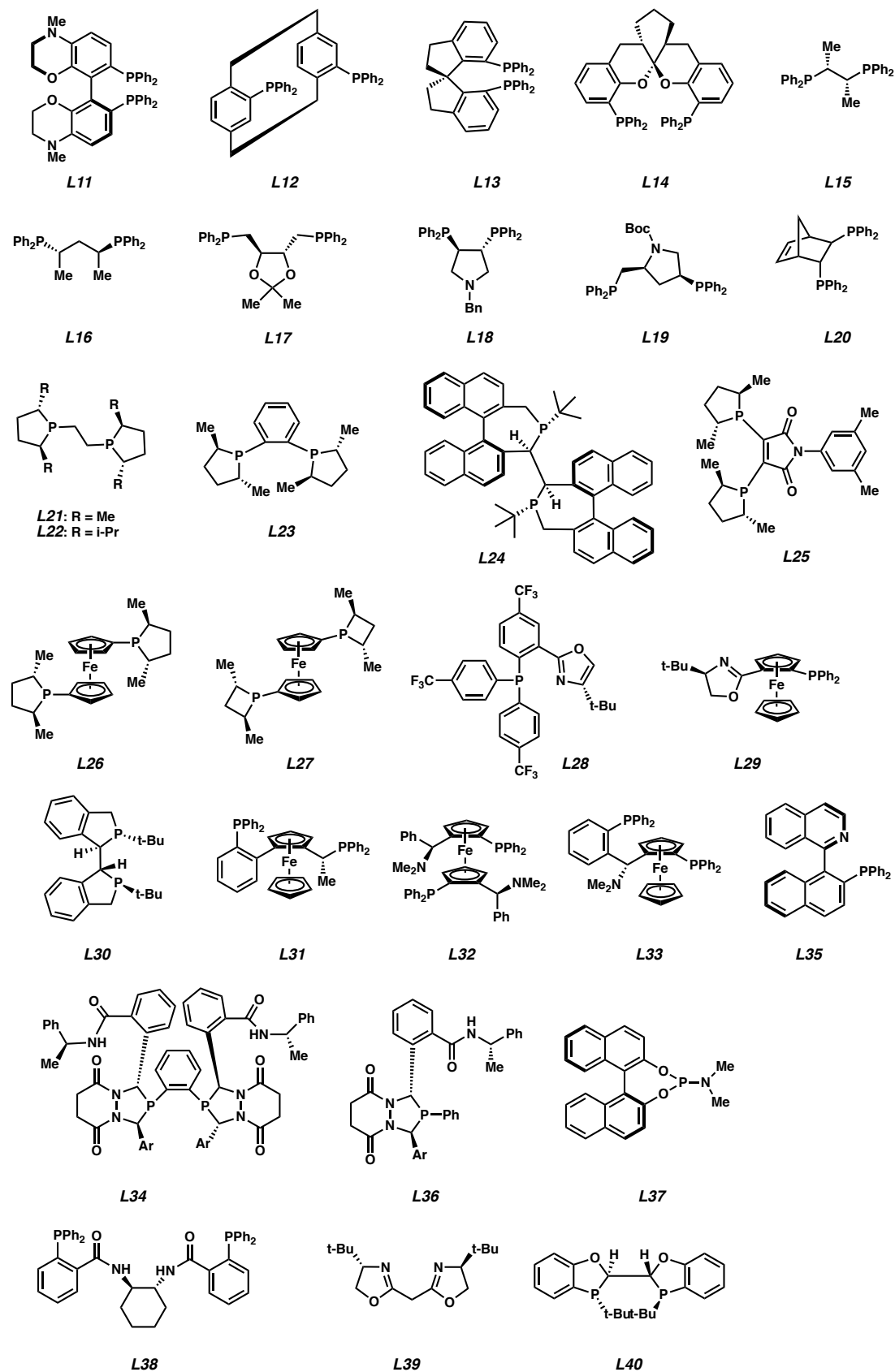


Table 1.6 Solvent effects in nickel-catalyzed AA of **1a**^a

<p style="text-align: center;"> 1a 2a $\xrightarrow[\text{Solvent (0.1 M), 23 }^{\circ}\text{C, 19 h}]{\text{Ni(COD)}_2 \text{ (10 mol \%)} \atop \text{Ligand (12 mol \%)}} \text{3aa}$ </p>					
Ligand	Solvent (% ee) ^[b]				
	Et ₂ O	MTBE	THF	Dioxane	Toluene
L1: (R)-BINAP	62% ee	65% ee	41% ee	18% ee	45% ee
L2: (R)-H₈-BINAP	74% ee	72% ee	60% ee	22% ee	46% ee
L3: (R)-Segphos	72% ee	70% ee	45% ee	28% ee	46% ee
L4: (R)-P-phos	74% ee	67% ee	52% ee	25% ee	51% ee

[a] Reactions performed on 0.05 mmol scale. [b] Determined by chiral SFC analysis of the isolated product.

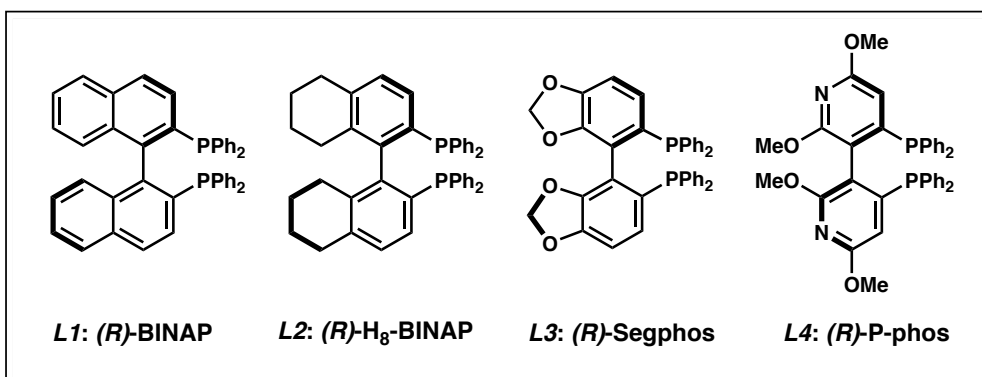
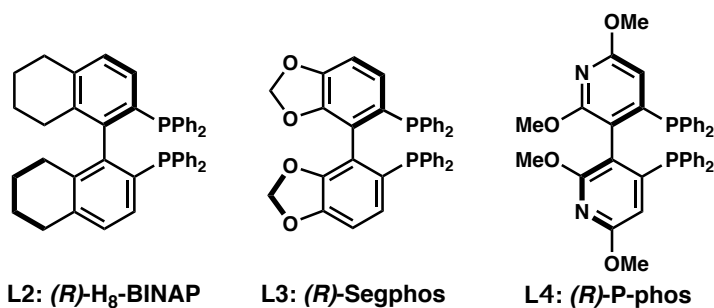


Table 1.7 Optimization of reaction parameters for lactam **4a**^a

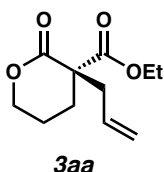
$\text{PG-N} \begin{array}{c} \text{O} \\ \parallel \\ \text{C} \end{array} \text{C} \begin{array}{c} \text{O} \\ \parallel \\ \text{C} \end{array} \text{OEt} + \text{CH}_2=\text{CHCH}_2\text{OH} \xrightarrow[\text{solvent (0.1 M), 10 }^\circ\text{C, 48 h}]{\text{Ni(COD)}_2 \text{ (10 mol \%), ligand (12 mol \%)}} \text{PG-N} \begin{array}{c} \text{O} \\ \parallel \\ \text{C} \end{array} \text{C} \begin{array}{c} \text{O} \\ \parallel \\ \text{C} \end{array} \text{OEt} \text{CH}_2=\text{CHCH}_2$

entry	PG	ligand	solvent	yield [%] ^[b]	ee [%] ^[c]
1	Bz	L2	PhMe:MTBE (2:3)	95	77
2	Bz	L3	PhMe:MTBE (2:3)	>95	88
3	Bz	L4	PhMe:MTBE (2:3)	79	90
4 ^[d]	Bz	L4	PhMe:MTBE (2:3)	28	88
5	Bz	L4	PhMe:Et ₂ O (2:3)	70	88
6	Bz	L4	Toluene	51	88
7	Bz	L4	THF	15	76
8 ^[e]	Bz	L4	PhMe:MTBE (2:3)	>95	88
9	Boc	L4	PhMe:MTBE (2:3)	38	52
10	Ts	L4	PhMe:MTBE (2:3)	0	–
11	Me	L4	PhMe:MTBE (2:3)	ND ^[f]	31
12	Ph	L4	PhMe:MTBE (2:3)	21	53
13	Bn	L4	PhMe:MTBE (2:3)	ND ^[f]	58

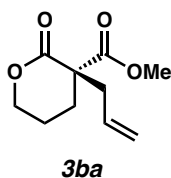
[a] Reactions performed on 0.1 mmol scale. [b] Yields determined by ¹H NMR of crude reaction mixture using 1,3,5-trimethoxybenzene as a standard. [c] Determined by chiral SFC analysis of the isolated product.



1.7.2.4 Spectroscopic Data for the Alkylation Products

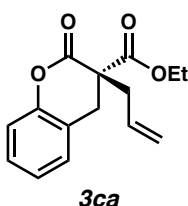


Ethyl (*R*)-3-allyl-2-oxotetrahydro-2*H*-pyran-3-carboxylate (3aa): Product **3aa** was prepared using general procedure 3 at $-10\text{ }^{\circ}\text{C}$ and purified by column chromatography (15% EtOAc in hexanes) to provide a colorless oil (31.8 mg, 75% yield); 86% ee, $[\alpha]_{\text{D}}^{25} +3.84$ (c 0.99, CHCl_3); ^1H NMR (400 MHz, CDCl_3) δ 5.84–5.69 (m, 1H), 5.19–5.08 (m, 2H), 4.34–4.23 (m, 2H), 4.21 (q, $J = 7.1$ Hz, 2H), 2.73 (ddt, $J = 13.8, 6.8, 1.2$ Hz, 1H), 2.59 (ddt, $J = 13.9, 7.9, 1.0$ Hz, 1H), 2.38–2.25 (m, 1H), 2.05–1.88 (m, 1H), 1.92–1.79 (m, 2H), 1.27 (t, $J = 7.1$ Hz, 3H); ^{13}C NMR (100 MHz, CDCl_3) δ 171.2, 170.0, 132.6, 119.9, 69.0, 62.2, 54.0, 40.8, 28.0, 20.6, 14.2; IR (Neat Film, NaCl) 2981, 1732, 1457, 1399, 1367, 1348, 1244, 1200, 1162, 1108, 1026, 974, 925, 857, 640 cm^{-1} ; HRMS (MM) m/z calc'd for $\text{C}_{11}\text{H}_{17}\text{O}_4$ $[\text{M}+\text{H}]^+$: 213.1121, found 213.1120; SFC Conditions: 25% IPA, 2.5 mL/min, Chiralpak IC column, $\lambda = 210$ nm, t_{R} (min): major = 2.77, minor = 3.39.

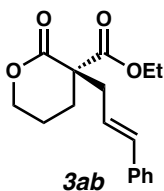


Methyl (*R*)-3-allyl-2-oxotetrahydro-2*H*-pyran-3-carboxylate (3ba): Product **3ba** was prepared using general procedure 3 at $-10\text{ }^{\circ}\text{C}$ and purified by column chromatography (30% EtOAc in hexanes) to provide a colorless oil (25.5 mg, 64% yield); 86% ee, $[\alpha]_{\text{D}}^{25} + 5.071$ (c 0.896, CHCl_3); ^1H NMR (400 MHz, CDCl_3) δ 5.85–5.66 (m, 1H), 5.20–5.10 (m, 2H), 4.33–4.26 (m, 2H), 3.76 (s, 3H), 2.75 (ddt, $J = 13.8, 6.8, 1.3$ Hz, 1H), 2.61 (ddt,

$J = 13.8, 7.8, 1.0$ Hz, 1H), 2.39–2.26 (m, 1H), 2.03–1.77 (m, 3H); ^{13}C NMR (100 MHz, CDCl_3) δ 171.8, 169.9, 132.5, 120.1, 69.2, 54.1, 53.2, 40.9, 28.1, 20.6; IR (Neat Film, NaCl) 3079, 2955, 2920, 1733, 1640, 1480, 1436, 1401, 1349, 1321, 1277, 1247, 1204, 1164, 1122, 1108, 1076, 1000, 978, 126, 844, 716, 659, 640; HRMS (MM) m/z calc'd for $\text{C}_{10}\text{H}_{15}\text{O}_4$ $[\text{M}+\text{H}]^+$: 199.0965, found 199.0970; SFC Conditions 20% IPA, 2.5 mL/min, Chiralpak IC column $\lambda = 210$ nm, t_R (min): major = 3.35, minor = 3.99.

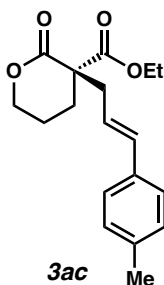


Ethyl (*S*)-3-allyl-2-oxochromane-3-carboxylate (3ca): Product **3ca** was prepared using general procedure 3 at -10 °C and purified by column chromatography (5% EtOAc in hexanes) to provide a colorless oil (31.9 mg, 61% yield); 64% ee, $[\alpha]_{\text{D}}^{25} -30.75$ (c 0.92, CHCl_3); ^1H NMR (400 MHz, CDCl_3) δ 7.33–7.13 (m, 2H), 7.13–7.00 (m, 2H), 5.91 (ddt, $J = 16.6, 10.6, 7.3$ Hz, 1H), 5.23–5.12 (m, 2H), 4.05 (qq, $J = 10.8, 7.1$ Hz, 2H), 3.26 (d, 15.9 Hz, 1 H), 3.04 (d, $J = 15.9$ Hz, 1H), 2.84–2.67 (m, 2H), 1.02 (t, $J = 7.1$ Hz, 3H); ^{13}C NMR (100 MHz, CDCl_3) δ 169.5, 167.2, 151.2, 132.1, 128.7, 128.5, 124.8, 121.4, 120.4, 116.5, 62.2, 53.3, 38.6, 32.5, 14.0; IR (Neat Film, NaCl) 3079, 2982, 2936, 1774, 1738, 1653, 1640, 1590, 1541, 1490, 1460, 1344, 1232, 1190, 1145, 1096, 1020, 921, 858, 759, 658; HRMS (MM) m/z calc'd for $\text{C}_{15}\text{H}_{17}\text{O}_4$ $[\text{M}+\text{H}]^+$: 261.1121, found 261.1123; SFC Conditions: 15% IPA, 2.5 mL/min, Chiralcel OB-H column, $\lambda = 210$ nm, t_R (min): minor = 2.23, major = 2.64.



Ethyl (*R*)-3-cinnamyl-2-oxotetrahydro-2*H*-pyran-3-carboxylate (3ab): Product **3ab**

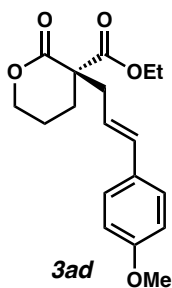
was prepared using general procedure 3 and purified by column chromatography (15% EtOAc in hexanes) to provide a colorless oil (34.4 mg, 60% yield); 90% ee, $[\alpha]_D^{25} -12.15$ (*c* 0.64, CHCl₃); ¹H NMR (400 MHz, CDCl₃) δ 7.38–7.25 (m, 4H), 7.27–7.17 (m, 1H), 6.47 (dt, *J* = 16.0, 1.4 Hz, 1H), 6.19 (ddd, *J* = 15.8, 8.0, 7.0 Hz, 1H), 4.35–4.17 (m, 4H), 2.91 (ddd, *J* = 13.8, 7.0, 1.4 Hz, 1H), 2.74 (ddd, *J* = 13.8, 8.0, 1.2 Hz, 1H), 2.45–2.31 (m, 1H), 2.11–1.77 (m, 3H), 1.27 (t, *J* = 7.1 Hz, 3H); ¹³C NMR (100 MHz, CDCl₃) δ 171.2, 170.1, 136.9, 134.8, 128.7, 127.7, 126.4, 124.1, 69.1, 62.3, 54.4, 40.1, 28.1, 20.6, 14.2; IR (Neat Film, NaCl) 2980, 2342, 1955, 1733, 1577, 1449, 1399, 1367, 1243, 1198, 1164, 1026, 971, 910, 858, 746, 695, 642, cm⁻¹; HRMS (MM) *m/z* calc'd for C₁₇H₂₁O₄ [M+H]⁺: 289.1430, found 289.1434; SFC Conditions: 10% IPA, 2.5 mL/min, Chiralpak AD-H column, λ = 254 nm, *t*_R (min): major = 5.43, minor = 6.24.



Ethyl (*R,E*)-2-oxo-3-(3-(*p*-tolyl)allyl)tetrahydro-2*H*-pyran-3-carboxylate (3ac):

Product **3ac** was prepared using general procedure 3 and purified by column chromatography (15% EtOAc in hexanes) to provide a white amorphous solid (37.5 mg,

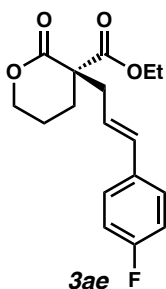
62% yield); 90% ee, $[\alpha]_{\text{D}}^{25} -14.42$ (c 0.95, CHCl_3); ^1H NMR (400 MHz, CDCl_3) δ 7.24 (d, J = 8.1 Hz, 2H), 7.15–6.98 (m, 2H), 6.51–6.33 (m, 1H), 6.13 (ddd, J = 15.8, 8.1, 7.0 Hz, 1H), 4.31–4.26 (m, 2H), 4.23 (q, J = 7.1 Hz, 2H), 2.90 (ddd, J = 13.8, 7.0, 1.4 Hz, 1H), 2.72 (ddd, J = 13.8, 8.1, 1.2 Hz, 1H), 2.41–2.25 (m, 4H), 2.02–1.78 (m, 3H), 1.27 (t, J = 7.1 Hz, 3H); ^{13}C NMR (100 MHz, CDCl_3) δ 171.3, 170.1, 137.5, 134.7, 134.2, 129.3, 126.3, 123.0, 69.1, 62.3, 54.4, 40.2, 28.1, 21.3, 20.6, 14.2; IR (Neat Film, NaCl) 2978, 1731, 1513, 1456, 1399, 1367, 1269, 1242, 1197, 1163, 1096, 1025, 972, 859, 803, 642 cm^{-1} ; HRMS (MM) m/z calc'd for $\text{C}_{18}\text{H}_{23}\text{O}_4$ $[\text{M}+\text{H}]^+$: 303.1591, found 303.1591; SFC Conditions: 10% IPA, 2.5 mL/min, Chiralpak AD-H column, λ = 254 nm, t_{R} (min): major 6.47, minor = 7.71.



Ethyl (R,E)-3-(3-(4-methoxyphenyl)allyl)-2-oxotetrahydro-2H-pyran-3-carboxylate

(3ad): Product **3ad** was prepared using general procedure 3 and purified by column chromatography (15% EtOAc in hexanes) to provide a colorless oil (50.5 mg, 79% yield); 88% ee, $[\alpha]_{\text{D}}^{25} -15.9$ (c 0.95, CHCl_3); ^1H NMR (400 MHz, CDCl_3) δ 7.32–7.24 (m, 2H), 6.89–6.79 (m, 2H), 6.41 (d, 15.8 Hz, 1H), 6.03 (ddd, J = 15.7, 8.0, 7.0 Hz, 1H), 4.29 (t, J = 5.9 Hz, 2H), 4.22 (q, J = 7.2 Hz, 2H), 3.79 (s, 3H), 2.89 (ddd, J = 13.8, 7.0, 1.4 Hz, 1H), 2.71 (ddd, J = 13.7, 8.1, 1.2 Hz, 1H), 2.43–2.29 (m, 1H), 2.05–1.87 (m, 2H), 1.92–1.79 (m, 1H), 1.27 (t, J = 7.1 Hz, 3H); ^{13}C NMR (100 MHz, CDCl_3) δ 171.3, 170.2,

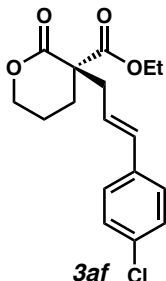
159.2, 134.2, 129.8, 127.5, 121.7, 114.0, 69.1, 62.2, 55.4, 54.5, 40.1, 28.1, 20.6, 14.2; IR (Neat Film, NaCl) 2978, 2837, 1732, 1608, 1577, 1512, 1457, 1400, 1349, 1367, 1249, 1198, 1108, 1032, 972, 840, 757, 667, 640 HRMS (MM) m/z calc'd for $C_{18}H_{25}O_6$ $[M+H_3O]^+$: 319.1840, found 319.1525; SFC Conditions: 15% IPA, 2.5 mL/min, Chiralpak AD-H column, λ = 254 nm, t_R (min): major = 5.37, minor = 6.37.



Ethyl (R,E)-3-(3-(4-fluorophenyl)allyl)-2-oxotetrahydro-2H-pyran-3-carboxylate

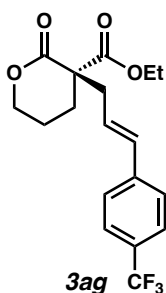
(3ae): Product **3ae** was prepared using general procedure 3 and purified by column chromatography (15% EtOAc in hexanes) to provide a colorless oil (38.2 mg, 62% yield); 88% ee, $[\alpha]_D^{25}$ -10.19 (c 0.86, $CHCl_3$); 1H NMR (400 MHz, $CDCl_3$) δ 7.34 – 7.27 (m, 2H), 7.05 – 6.90 (m, 2H), 6.53–6.34 (m, 1H), 6.20–6.02 (m, 1H), 4.29 (t, J = 5.6 Hz, 2H), 4.22 (q, J = 7.1 Hz, 2H), 2.87 (ddd, J = 13.9, 7.1, 1.4 Hz, 1H), 2.72 (ddd, J = 13.8, 7.9, 1.2 Hz, 1H), 2.47–2.31 (m, 1H), 2.07 – 1.78 (m, 3H), 1.26 (t, J = 7.1 Hz, 3H); ^{13}C NMR (100 MHz, $CDCl_3$) δ 171.2, 170.1, 162.4 (d, J = 246.8 Hz), 133.5, 133.1 (d, J = 3.3 Hz), 127.9 (d, J = 8.0 Hz), 123.9 (d, J = 2.2 Hz), 115.5 (d, J = 21.7 Hz), 69.0, 62.3, 54.4, 40.1, 28.2, 20.6, 14.2; ^{19}F NMR (282 MHz, $CDCl_3$) δ -114.56 (tt, J = 8.6, 5.3 Hz); IR (Neat Film, NaCl) 2981, 2342, 1733, 1602, 1508, 1456, 1400, 1368, 1349, 1298, 1269, 1226, 1198, 1160, 1095, 1025, 972, 847, 767, 711, 668, 639 cm^{-1} ; HRMS (MM) m/z

calc'd for $C_{17}H_{20}FO_4$ $[M+H]^+$: 307.1340 found 307.1343; SFC Conditions: 10% IPA, 2.5 mL/min, Chiralpak AD-H column, $\lambda = 254$ nm, t_R (min): major = 5.12, minor = 5.95.

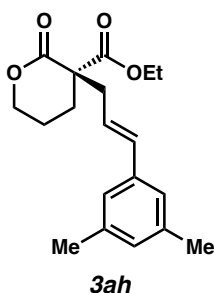


Ethyl (R,E)-3-(3-(4-chlorophenyl)allyl)-2-oxotetrahydro-2H-pyran-3-carboxylate

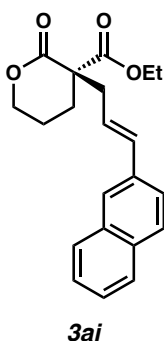
(3af): Product **3af** was prepared using general procedure 3 and purified by column chromatography (15% EtOAc in hexanes) to provide a colorless oil (39.5 mg, 61% yield); 87% ee, $[\alpha]_D^{25} -10.81$ (c 0.83, $CHCl_3$); 1H NMR (400 MHz, $CDCl_3$) δ 7.26 (s, 4H), 6.42 (dt, $J = 15.7, 1.3$ Hz, 1H), 6.18 (ddd, $J = 15.9, 7.9, 7.1$ Hz, 1H), 4.29 (t, $J = 5.7$ Hz, 2H), 4.22 (q, $J = 7.1$ Hz, 2H), 2.87 (ddd, $J = 13.9, 7.1, 1.4$ Hz, 1H), 2.74 (ddd, $J = 13.8, 7.9, 1.2$ Hz, 1H), 2.46–2.32 (m, 1H), 2.15–1.80 (m, 3H), 1.26 (t, $J = 7.1$ Hz, 3H); ^{13}C NMR (100 MHz, $CDCl_3$) δ 171.1, 170.1, 135.4, 133.5, 133.2, 128.8, 127.6, 124.9, 69.0, 62.3, 54.4, 40.1, 28.2, 20.6, 14.2; IR (Neat Film, NaCl) 2979, 2358, 1729, 1490, 1455, 1404, 1243, 1197, 1164, 1092, 971, 820, 760, 679 cm^{-1} ; HRMS (MM) m/z calc'd for $C_{17}H_{20}ClO_4$ $[(M+H)^+]$: 323.1045, found 323.1041; SFC Conditions: 30% IPA, 2.5 mL/min, Chiralpak AD-H column, $\lambda = 254$ nm, t_R (min): major = 2.29, minor = 2.57.



Ethyl (R,E)-2-oxo-3-(3-(4-(trifluoromethyl)phenyl)allyl)tetrahydro-2H-pyran-3-carboxylate (3ag): Product **3ag** was prepared using general procedure 3 and purified by column chromatography (15% EtOAc in hexanes) to provide a colorless oil (31.2 mg, 44% yield); 86% ee, $[\alpha]_D^{25} -6.52$ (*c* 0.98, CHCl₃); ¹H NMR (400 MHz, CDCl₃) δ 7.60–7.47 (m, 2H), 7.47–7.38 (m, 2H), 6.50 (d, *J* = 15.8 Hz, 1H), 6.32 (dt, *J* = 15.8, 7.5 Hz, 1H), 4.30 (dd, *J* = 6.3, 5.2 Hz, 2H), 4.23 (q, *J* = 7.1 Hz, 2H), 2.90 (ddd, *J* = 13.8, 7.1, 1.3 Hz, 1H), 2.77 (ddd, *J* = 13.8, 7.7, 1.2 Hz, 1H), 2.47–2.34 (m, 1H), 2.05–1.81 (m, 3H), 1.26 (t, *J* = 7.1 Hz, 3H); ¹³C NMR (100 MHz, CDCl₃) δ 171.1, 170.0, 140.4 (d, *J* = 1.6 Hz), 133.4, 129.4 (q, *J* = 32.4 Hz), 127.2, 126.5, 125.6 (q, *J* = 3.7 Hz), 122.9, 69.0, 62.4, 54.4, 40.1, 28.3, 20.6, 14.2; ¹⁹F NMR (282 MHz, CDCl₃) δ –62.52 (s); IR (Neat Film, NaCl) 2982, 1733, 1684, 1616, 1540, 1414, 1326, 1244, 1198, 1163, 1120, 1068, 1016, 972, 862, 833, 652; HRMS (MM) *m/z* calc'd for C₁₈H₂₀F₃O₄ [M+H]⁺: 357.1308, found 357.1307; SFC Conditions: 10% IPA, 2.5 mL/min, Chiralpak AD-H column, λ = 254 nm, *t*_R (min): major = 4.02, minor = 4.72.

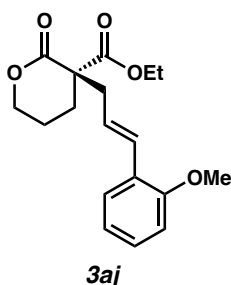


Ethyl (R,E)-3-(3-(3,5-dimethylphenyl)allyl)-2-oxotetrahydro-2H-pyran-3-carboxylate (3ah): Product **3ah** was prepared using general procedure 3 and purified by column chromatography (15% EtOAc in hexanes) to provide a colorless oil (41.0 mg, 65% yield); 88% ee, $[\alpha]_D^{25} -13.58$ (c 0.84, CHCl_3); ^1H NMR (400 MHz, CDCl_3) δ 7.00–6.94 (m, 2H), 6.87 (dt, $J = 1.9, 1.0$ Hz, 1H), 6.46–6.36 (m, 1H), 6.15 (ddd, $J = 15.7, 8.2, 6.8$ Hz, 1H), 4.32–4.27 (m, 2H), 4.27–4.20 (m, 2H), 2.91 (ddd, $J = 13.8, 6.8, 1.4$ Hz, 1H), 2.71 (ddd, $J = 13.7, 8.2, 1.2$ Hz, 1H), 2.43–2.26 (m, 7H), 2.04–1.87 (m, 2H), 1.92–1.79 (m, 1H), 1.28 (t, $J = 7.1$ Hz, 3H); ^{13}C NMR (100 MHz, CDCl_3) δ 171.3, 170.2, 138.1, 136.8, 135.0, 129.4, 124.3, 123.6, 69.1, 62.3, 54.4, 40.2, 28.1, 21.3, 20.6, 14.2; IR (Neat Film, NaCl) 2978, 2917, 1731, 1602, 1456, 1398, 1367, 1350, 1242, 1198, 1163, 1096, 1026, 972, 853, 759, 693, 638 cm^{-1} ; HRMS (MM) m/z calc'd for $\text{C}_{19}\text{H}_{25}\text{O}_4$ $[\text{M}+\text{H}]^+$: 317.1747, found 317.1749; SFC Conditions: 5% IPA, 2.5 mL/min, Chiralpak AD-H column, $\lambda = 254$ nm, t_R (min): minor = 9.68, major = 11.56.



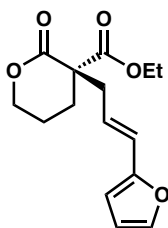
Ethyl (R,E)-3-(3-(naphthalen-2-yl)allyl)-2-oxotetrahydro-2H-pyran-3-carboxylate

(3ai): Product **3ai** was prepared using general procedure 3 and purified by column chromatography (15% EtOAc in hexanes) to provide a colorless oil (42.1 mg, 62% yield); 88% ee, $[\alpha]_{\text{D}}^{25} +27.34$ (*c* 0.82, CHCl_3); ^1H NMR (400 MHz, CDCl_3) δ 7.84–7.73 (m, 3H), 7.72–7.67 (m, 1H), 7.57 (dd, *J* = 8.5, 1.8 Hz, 1H), 7.52–7.38 (m, 2H), 6.68–6.59 (m, 1H), 6.34 (ddd, *J* = 15.8, 8.0, 7.0 Hz, 1H), 4.30 (t, *J* = 5.8 Hz, 2H), 4.24 (q, *J* = 7.1 Hz, 2H), 2.96 (ddd, *J* = 13.7, 7.0, 1.4 Hz, 1H), 2.81 (ddd, *J* = 13.7, 8.0, 1.2 Hz, 1H), 2.48–2.34 (m, 1H), 2.03–1.81 (m, 3H), 1.28 (t, *J* = 7.1 Hz, 3H); ^{13}C NMR (100 MHz, CDCl_3) δ 171.2, 170.1, 134.8, 134.3, 133.6, 133.0, 128.2, 128.0, 127.7, 126.3, 126.1, 125.9, 124.5, 123.6, 69.0, 62.3, 54.4, 40.2, 28.1, 20.6, 14.13; IR (Neat Film, NaCl) 2980, 1732, 1597, 1507, 1456, 1399, 1367, 1243, 1198, 1097, 1023, 971, 896, 861, 815, 751, 667, 639, 624; HRMS (MM) *m/z* calc'd for $\text{C}_{21}\text{H}_{23}\text{O}_4$ $[\text{M}+\text{H}]^+$: 339.1591, found 339.1595; SFC Conditions 30% IPA, 2.5 mL/min, Chiralpak AD-H column λ = 254 nm, t_{R} (min): major = 3.36, minor = 4.24.



Ethyl (R,E)-3-(3-(2-methoxyphenyl)allyl)-2-oxotetrahydro-2H-pyran-3-carboxylate

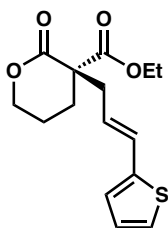
(3aj): Product **3aj** was prepared using general procedure 3 and purified by column chromatography (15% EtOAc in hexanes) to provide a colorless oil (32.4 mg, 51% yield); 90% ee, $[\alpha]_D^{25} -11.96$ (*c* 0.87, CHCl₃); ¹H NMR (400 MHz, CDCl₃) δ 7.40 (dd, *J* = 7.7, 1.7 Hz, 1H), 7.21 (ddd, *J* = 8.2, 7.4, 1.7 Hz, 1H), 6.90 (td, *J* = 7.6, 1.1 Hz, 1H), 6.88–6.75 (m, 2H), 6.16 (ddd, *J* = 15.9, 8.2, 6.9 Hz, 1H), 4.29 (dd, *J* = 6.2, 5.5 Hz, 2H), 4.23 (q, *J* = 7.1 Hz, 2H), 3.83 (s, 3H), 2.92 (ddd, *J* = 13.8, 6.8, 1.5 Hz, 1H), 2.77 (ddd, *J* = 13.7, 8.2, 1.2 Hz, 1H), 2.44–2.29 (m, 1H), 2.03–1.81 (m, 3H), 1.28 (t, *J* = 7.1 Hz, 3H); ¹³C NMR (100 MHz, CDCl₃) δ 171.3, 170.2, 156.5, 129.5, 128.7, 126.8, 126.0, 124.5, 120.7, 110.9, 69.2, 62.2, 55.5, 54.4, 40.6, 28.1, 20.7, 14.2; IR (Neat Film, NaCl) 2978, 2838, 1732, 1598, 1489, 1464, 1399, 1244, 1198, 1163, 1104, 1051, 1027, 976, 858, 755, 641; HRMS (MM) *m/z* calc'd for C₁₈H₂₃O₅ [M+H]⁺: 319.1540, found 319.1542; SFC Conditions 10% IPA, 2.5 mL/min, Chiralcel OD-H column λ = 254 nm, *t_R* (min): major = 9.05, minor = 9.85.



3ak

Ethyl (*R,E*)-3-(3-(furan-2-yl)allyl)-2-oxotetrahydro-2*H*-pyran-3-carboxylate (3ak):

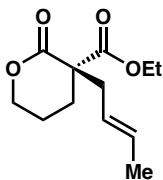
Product **3ak** was prepared using general procedure 3 and purified by column chromatography (15% EtOAc in hexanes) to provide a colorless oil (45.5 mg, 82% yield); 88% ee, $[\alpha]_D^{25} -11.85$ (*c* 0.99, CHCl₃); ¹H NMR (400 MHz, CDCl₃) δ 7.32–7.27 (m, 1H), 6.37–6.23 (m, 2H), 6.17 (d, *J* = 3.2 Hz, 1H), 6.14–6.01 (m, 1H), 4.29 (dd, *J* = 6.3, 5.5 Hz, 2H), 4.22 (q, *J* = 7.1 Hz, 2H), 2.86 (ddd, *J* = 13.9, 7.2, 1.3 Hz, 1H), 2.70 (ddd, *J* = 13.9, 8.0, 1.2 Hz, 1H), 2.40–2.29 (m, 1H), 2.05–1.91 (m, 1H), 1.96–1.78 (m, 2H), 1.26 (t, *J* = 7.1 Hz, 3H); ¹³C NMR (100 MHz, CDCl₃) δ 171.2, 170.0, 152.4, 141.9, 123.2, 122.7, 111.3, 107.6, 69.1, 62.3, 54.4, 39.8, 28.1, 20.6, 14.1; IR (Neat Film, NaCl) 2980, 1732, 1456, 1399, 1244, 1200, 1166, 1097, 1017, 969, 926, 858, 749, 640 ; HRMS (MM) *m/z* calc'd for C₁₅H₁₉O₅ [M+H]⁺: 343.1329, found 343.1327; SFC Conditions 10% IPA, 2.5 mL/min, Chiralpak AD-H column λ = 254 nm, t_R (min): major = 3.97, minor = 4.62.



3al

Ethyl (R,E)-2-oxo-3-(3-(thiophen-2-yl)allyl)tetrahydro-2H-pyran-3-carboxylate

(3al): Product **3al** was prepared using general procedure 3 and purified by column chromatography (15% EtOAc in hexanes) to provide a colorless oil (39.9 mg, 68% yield); 88% ee, $[\alpha]_D^{25} -15.7$ (c 0.98, CHCl_3); ^1H NMR (400 MHz, CDCl_3) δ 7.12 (dt, J = 4.9, 1.0 Hz, 1H), 6.97–6.87 (m, 2H), 6.59 (dtt, J = 15.7, 1.4, 0.6 Hz, 1H), 6.00 (ddd, J = 15.4, 8.0, 7.2 Hz, 1H), 4.29 (t, J = 5.9 Hz, 2H), 4.22 (q, J = 7.1 Hz, 2H), 2.86 (ddd, J = 13.9, 7.2, 1.4 Hz, 1H), 2.70 (ddd, J = 13.8, 8.0, 1.2 Hz, 1H), 2.42–2.29 (m, 1H), 2.06–1.80 (m, 3H), 1.27 (t, J = 7.1 Hz, 3H); ^{13}C NMR (100 MHz, CDCl_3) δ 171.2, 170.0, 142.0, 127.9, 127.4, 125.5, 124.2, 123.7, 69.1, 62.3, 54.4, 40.0, 28.2, 20.6, 14.2; IR (Neat Film, NaCl) 3107, 2980, 1731, 1446, 1367, 1348, 1244, 1199, 1165, 1096, 1024, 965, 855, 750, 704, 643; HRMS (MM) m/z calc'd for $\text{C}_{15}\text{H}_{19}\text{O}_4\text{S}$ $[\text{M}+\text{H}]^+$: 295.0999, found 295.0994; SFC Conditions 10% IPA, 2.5 mL/min, Chiralpak AD-H column λ = 254 nm, t_R (min): major = 9.05, minor = 9.85.

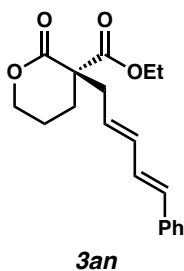


3am

Ethyl (R,E)-3-(but-2-en-1-yl)-2-oxotetrahydro-2H-pyran-3-carboxylate (3am):

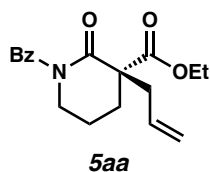
Product **3am** was prepared using general procedure 3 and purified by column

chromatography (15% EtOAc in hexanes) to provide a colorless oil (25.6 mg, 57% yield); 78% ee, $[\alpha]_D^{25} -0.22$ (c 1.13, CHCl_3); ^1H NMR (400 MHz, CDCl_3) δ 5.55 (dqt, J = 15.0, 6.2, 1.1 Hz, 1H), 5.47–5.30 (m, 1H), 4.27 (t, J = 5.7 Hz, 2H), 4.20 (q, J = 7.1 Hz, 2H), 2.72–2.61 (m, 1H), 2.51 (ddt, J = 13.8, 7.7, 1.1 Hz, 1H), 2.35–2.26 (m, 1H), 2.02–1.90 (m, 1H), 1.90–1.78 (m, 2H), 1.65 (dq, J = 6.5, 1.2 Hz, 3H), 1.26 (t, J = 7.1 Hz, 3H); ^{13}C NMR (100 MHz, CDCl_3) δ 171.4, 170.2, 130.7, 124.9, 69.0, 62.1, 54.3, 39.7, 27.9, 20.6, 18.1, 14.2; IR (Neat Film, NaCl) 2965, 2938, 1730, 1447, 1400, 1272, 1223, 1198, 1163, 1107, 1077, 973, 856; HRMS (MM) m/z calc'd for $\text{C}_{12}\text{H}_{19}\text{O}_4$ $[\text{M}+\text{H}]^+$: 227.1278, found 227.1275; SFC Conditions 25% IPA, 2.5 mL/min, Chiralpak IC column λ = 210 nm, t_R (min): major = 2.87, minor = 3.69.

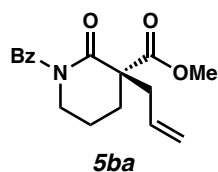


Ethyl (R)-2-oxo-3-((2E,4E)-5-phenylpenta-2,4-dien-1-yl)tetrahydro-2H-pyran-3-carboxylate (3an): Product **3an** was prepared using general procedure 3 and purified by column chromatography (15% EtOAc in hexanes) to provide a colorless oil (57.3 mg, 91% yield); 88% ee, $[\alpha]_D^{25} -22.45$ (c 0.96, CHCl_3); ^1H NMR (400 MHz, CDCl_3) δ 7.39–7.35 (m, 2H), 7.30 (ddd, J = 7.7, 6.8, 1.2 Hz, 2H), 7.24–7.17 (m, 1H), 6.74 (ddd, J = 15.7, 10.4, 0.8 Hz, 1H), 6.49 (d, J = 15.7 Hz, 1H), 6.28 (ddq, J = 15.4, 10.5, 1.1 Hz, 1H), 5.83–5.69 (m, 1H), 4.29 (t, J = 5.8 Hz, 2H), 4.23 (q, J = 7.1 Hz, 2H), 2.84 (ddd, J = 13.9, 7.2, 1.3 Hz, 1H), 2.68 (ddd, J = 13.8, 8.1, 1.1 Hz, 1H), 2.41–2.26 (m, 1H), 2.03–1.80 (m, 3H), 1.28 (t, J = 7.1 Hz, 3H); ^{13}C NMR (100 MHz, CDCl_3) δ 171.2, 170.0, 137.2, 135.3,

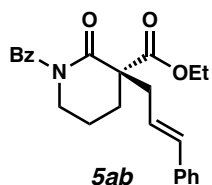
132.1, 128.7, 128.5, 128.3, 127.6, 126.4, 69.0, 62.3, 54.4, 39.9, 28.1, 20.6, 14.2; IR (Neat Film, NaCl) 3058, 3024, 2980, 1732, 1490, 1478, 1448, 1400, 1367, 1347, 1241, 1198, 1097, 1025, 994, 910, 857, 750, 694, 667, 640; HRMS (MM) m/z calc'd for $C_{19}H_{23}O_4$ $[M+H]^+$: 315.1585, found 315.1585; SFC Conditions 15% IPA, 2.5 mL/min, Chiralpak AD-H column λ = 254 nm, t_R (min): major = 5.30, minor = 6.23.



Ethyl (S)-3-allyl-1-benzoyl-2-oxopiperidine-3-carboxylate (5aa): Product **5aa** was prepared using general procedure 4 and purified by column chromatography (15% EtOAc in hexanes) to provide a colorless oil (45.9 mg, 73% yield); 90% ee, $[\alpha]_D^{25} +42.42$ (c 0.968, $CHCl_3$); 1H NMR (400 MHz, $CDCl_3$) δ 7.84–7.70 (m, 2H), 7.54–7.44 (m, 1H), 7.44–7.34 (m, 2H), 5.80–5.62 (m, 1H), 5.17–5.03 (m, 2H), 4.30 (q, J = 7.2 Hz, 2H), 3.84–3.71 (m, 2H), 2.72 (ddt, J = 13.8, 6.8, 1.2 Hz, 1H), 2.56 (ddt, J = 13.8, 7.9, 1.0 Hz, 1H), 2.43–2.25 (m, 1H), 2.04–1.83 (m, 3H), 1.36 (t, J = 7.1 Hz, 3H); ^{13}C NMR (100 MHz, $CDCl_3$) δ 175.1, 171.9, 171.8, 135.9, 133.0, 131.8, 128.2, 128.1, 119.7, 62.1, 56.4, 46.6, 40.0, 30.3, 20.3, 14.3; IR (Neat Film, NaCl) 3074, 2936, 2341, 1734, 1700, 1684, 1450, 1388, 1278, 1147, 1177, 1050, 1027, 919, 824, 726, 694, 668 cm^{-1} ; HRMS (MM) m/z calc'd for $C_{18}H_{22}NO_4$ $[M+H]^+$: 316.1543, found 316.1543; SFC Conditions: 20% IPA, 2.5 mL/min, Chiralpak IC column, λ = 254 nm, t_R (min): minor = 3.77, major = 4.39.



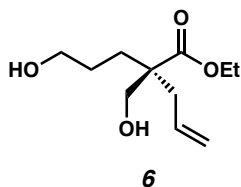
Methyl (*S*)-3-allyl-1-benzoyl-2-oxopiperidine-3-carboxylate (5ba): Product **5ba** was prepared using general procedure 4 and purified by column chromatography (20% EtOAc in hexanes) to provide a colorless oil (51.0 mg, 85% yield); 90% ee, $[\alpha]_{\text{D}}^{25} +48.58$ (*c* 0.890, CHCl₃); ¹H NMR (400 MHz, CDCl₃) δ 7.77–7.59 (m, 2H), 7.55–7.44 (m, 1H), 7.40 (ddt, *J* = 8.3, 6.6, 1.2 Hz, 2H), 5.84–5.63 (m, 1H), 5.20–5.02 (m, 2H), 3.83 (s, 3H), 3.77 (dd, *J* = 6.7, 5.4 Hz, 2H), 2.73 (ddt, *J* = 13.7, 6.8, 1.2 Hz, 1H), 2.57 (ddt, *J* = 13.7, 7.7, 1.1 Hz, 1H), 2.41–2.29 (m, 1H), 2.07–1.85 (m, 3H); ¹³C NMR (100 MHz, CDCl₃) δ 175.1, 172.4, 171.8, 135.9, 133.0, 131.8, 128.2, 128.1, 119.8, 56.5, 52.9, 46.6, 39.9, 30.3, 20.2; IR (Neat Film, NaCl) 3075, 2953, 1738, 1702, 1683, 1640, 1583, 1478, 1449, 1436, 1349, 1277, 1252, 1177, 1147, 1078, 1052, 1027, 1001, 844, 819, 796, 726, 695, 651; HRMS (MM) *m/z* calc'd for C₁₇H₂₀NO₄ [M+H]⁺: 302.1387, found 302.1377; SFC Conditions 10% IPA, 2.5 mL/min, Chiralpak AD-H column λ = 254 nm, *t_R* (min): minor = 4.00, major = 4.57.



Ethyl (*S*)-1-benzoyl-3-cinnamyl-2-oxopiperidine-3-carboxylate (5ab): Product **5ab** was prepared using general procedure 4 at 30 °C and purified by column chromatography (20% to 40% Et₂O in hexanes) to provide a colorless oil (59.0 mg, 75% yield); 91% ee, $[\alpha]_{\text{D}}^{25} +71.0$ (*c* 0.88, CHCl₃); ¹H NMR (400 MHz, CDCl₃) δ 7.81–7.73 (m, 2H), 7.55–

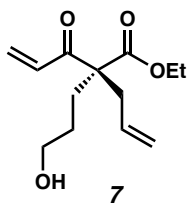
7.45 (m, 1H), 7.45–7.18 (m, 7H), 6.46 (dt, $J = 15.7, 1.3$ Hz, 1H), 6.14 (ddd, $J = 15.8, 8.0, 6.9$ Hz, 1H), 4.32 (q, $J = 7.1$ Hz, 2H), 3.86–3.73 (m, 2H), 2.91 (ddd, $J = 13.8, 7.0, 1.4$ Hz, 1H), 2.72 (ddd, $J = 13.8, 8.0, 1.2$ Hz, 1H), 2.49–2.35 (m, 1H), 2.10–1.98 (m, 1H), 2.03–1.91 (m, 2H), 1.37 (t, $J = 7.1$ Hz, 3H); ^{13}C NMR (100 MHz, CDCl_3) δ 175.0, 172.0, 171.9, 137.0, 135.9, 134.6, 131.9, 128.6, 128.2, 128.2, 127.6, 126.4, 124.5, 62.2, 56.9, 46.6, 39.3, 30.5, 20.3, 14.3; IR (Neat Film, NaCl) 2979, 1728, 1684, 1600, 1578, 1449, 1390, 1277, 1194, 1172, 1150, 1026, 970, 923, 934, 857, 822, 795, 745, 725, 694, 661 cm^{-1} ; HRMS (MM) m/z calc'd for $\text{C}_{24}\text{H}_{26}\text{NO}_4$ $[\text{M}+\text{H}]^+$: 392.1856, found 392.1849; SFC Conditions: 30% IPA, 2.5 mL/min, Chiralpak AD-H column, $\lambda = 254$ nm, t_{R} (min): minor = 2.56, major = 2.94.

1.7.2.5 Experimental Procedures and Characterization Data for Product Transformations



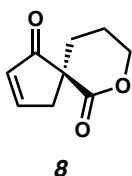
Ethyl (S)-2-(hydroxymethyl)-2-(3-hydroxypropyl)pent-4-enoate (6): To a solution of allylated product **3aa** (42.5 mg, 0.2 mmol, 1 equiv) in 4:1 methanol:THF (1.4 mL), $\text{CeCl}_3 \cdot 7\text{H}_2\text{O}$ was added (149.0 mg, 0.4 mmol, 2 equiv). After cooling the reaction mixture at 0°C for 10 minutes, NaBH_4 (37.5 mg, 1.0 mmol, 5 equiv) was added in three portions over the course of 20 minutes. Additional methanol (1.5 mL) was added to rinse the side of the flask and the reaction mixture was stirred for another 10 minutes. The reaction was quenched with glacial acetic acid. The crude mixture was then concentrated under reduced pressure. The resultant residue was extracted with EtOAc, washed with

NaHCO₃ and brine, dried over anhydrous MgSO₄, filtered, and purified by column chromatography (70% EtOAc/hexanes) to afford diol **6** as a colorless oil (54.1 mg, 88% yield). [α]_D²⁵ +1.2 (*c* 0.92, CHCl₃); ¹H NMR (400 MHz, CDCl₃) δ 5.71 (ddt, *J* = 17.4, 10.1, 7.4 Hz, 1H), 5.14–4.99 (m, 2H), 4.15 (q, *J* = 7.1 Hz, 2H), 3.72–3.62 (m, 2H), 3.59 (td, *J* = 6.2, 1.6 Hz, 2H), 2.65 (br s, 2H), 2.38 (ddt, *J* = 14.0, 7.3, 1.2 Hz, 1H), 2.30 (ddt, *J* = 13.9, 7.5, 1.1 Hz, 1H), 1.75–1.58 (m, 2H), 1.58–1.42 (m, 2H), 1.25 (t, *J* = 7.1 Hz, 3H); ¹³C NMR (100 MHz, CDCl₃) δ 176.0, 133.4, 118.6, 64.5, 62.9, 60.8, 50.8, 38.0, 29.3, 27.1, 14.4; IR (Neat Film, NaCl) 2281, 3078, 2940, 1725, 1641, 1465, 1447, 1372, 1329, 1300, 1219, 1191, 1138, 1112, 1053, 920, 862, 824, 782, 748, 679, 634; HRMS (MM) *m/z* calc'd for C₁₁H₂₁O₄ [M+H]⁺: 217.1434, found 217.1427.



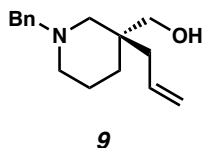
Ethyl (S)-2-allyl-2-(3-hydroxypropyl)-3-oxopent-4-enoate (7): A 0.5 M solution of vinylmagnesium bromide in THF (0.3 mmol, 1.5 equiv) was added dropwise to a solution of allylated product **3aa** (42.5 mg, 0.2 mmol, 1 equiv) in THF (0.7 mL) at –78 °C over 15 minutes. After 9 hours at –78 °C, the reaction was quenched with NH₄Cl. The mixture was diluted with EtOAc, washed with brine, and dried over anhydrous Na₂SO₄. Flash column chromatography (50% EtOAc in hexanes) of the crude residue afforded compound **7** as a colorless oil (80.0 mg, 67% yield); 86% ee, [α]_D²⁵ –9.9 (*c* 0.798, CHCl₃); ¹H NMR (400 MHz, CDCl₃) δ 6.53 (dd, *J* = 16.9, 10.2 Hz, 1H), 6.39 (dd, *J* = 17.0, 1.8 Hz, 1H), 5.70 (dd, *J* = 10.1, 1.8 Hz, 1H), 5.57 (ddt, *J* = 16.8, 10.1, 7.4 Hz, 1H),

5.16–5.04 (m, 2H), 4.19 (qd, $J = 7.1, 0.7$ Hz, 2H), 3.62 (td, $J = 6.4, 1.1$ Hz, 2H), 2.79–2.55 (m, 2H), 2.04–1.82 (m, 2H), 1.51–1.30 (m, 3H), 1.23 (t, $J = 7.1$ Hz, 3H); ^{13}C NMR (100 MHz, CDCl_3) δ 195.5, 172.1, 132.2, 131.8, 129.5, 119.3, 62.9, 61.7, 61.6, 35.9, 27.5, 27.0, 14.2; IR (Neat Film, NaCl) 340, 3079, 2924, 1732, 1698, 1642, 1612, 1447, 1402, 1368, 1299, 1262, 1200, 1137, 1096, 1057, 1029, 983, 923, 856, 808, 739, 670, 686, 654; HRMS (MM) m/z calc'd for $\text{C}_{13}\text{H}_{21}\text{O}_4$ $[\text{M}+\text{H}]^+$: 241.1440, found 241.1443.



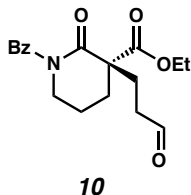
(S)-7-oxaspiro[4.5]dec-2-ene-1,6-dione (8): Compound **7** (68.9 mg, 0.29 mmol, 1 equiv) in degassed toluene (3.0 mL) was added to a stirred solution of Grubbs' II catalyst (12.2 mg, 5 mol%) in toluene (15 mL) at 23 °C. After stirring at 40 °C for 4 hours under argon atmosphere, the dark brown solution was filtered through silica plug, flushed with acetone, and concentrated under vacuum. The crude residue was then redissolved in acetonitrile, 1,8-Diazabicyclo[5.4.0]undec-7-ene (DBU) was added (52 μL , 0.35 mmol, 1.2 equiv), and the reaction mixture was stirred at room temperature. Upon complete consumption of the starting material by TLC, the reaction was quenched with NH_4Cl , extracted with EtOAc, washed with brine, dried over Na_2SO_4 , filtered, and concentrated under vacuum. The crude residue was purified by column chromatography (30% acetone in hexanes) to provide spirocycle **8** as a colorless oil (25.6 mg, 53% yield). $[\alpha]_{\text{D}}^{25} -62.2$ (c 0.75, CHCl_3); ^1H NMR (400 MHz, CDCl_3) δ 7.77 (dt, $J = 5.6, 2.7$ Hz, 1H), 6.14 (dt, $J = 5.7, 2.2$ Hz, 1H), 4.66–4.50 (m, 1H), 4.47–4.40 (m, 1H), 3.39 (dt, $J = 18.9, 2.5$ Hz, 1H), 2.58 (dt, $J = 18.9, 2.4$ Hz, 1H), 2.41–2.25 (m, 1H), 2.25–2.13 (m, 1H), 1.92–1.75 (m,

2H); ^{13}C NMR (100 MHz, CDCl_3) δ 206.2, 170.1, 163.8, 131.2, 71.0, 53.9, 44.5, 30.7, 20.4; IR (Neat Film, NaCl) 3082, 2932, 2871, 1728, 1699, 1592, 1422, 1403, 1343, 1272, 1217, 1160, 1108, 1080, 963, 816, 763; HRMS (MM) m/z calc'd for $\text{C}_9\text{H}_{11}\text{O}_3$ $[\text{M}+\text{H}]^+$: 167.0703, found 167.0696.



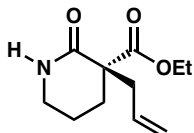
(S)-(3-allyl-1-benzylpiperidin-3-yl)methanol (9): To a flame-dried microwave vial under argon was added lactam **5aa** (63 mg, 0.2 mmol) and dry diethyl ether (2.0 mL). Lithium aluminum hydride (91 mg, 2.4 mmol) was added slowly. The reaction was allowed to stir at room temperature for 10 minutes, after which it was sealed and heated to 65°C for 36 h. The reaction was quenched with water and 15% sodium hydroxide solution, and extracted with ethyl acetate (5 mL \times 4). The combined extracts were dried with Na_2SO_4 , filtered, and concentrated under vacuum. The crude residue was purified by column chromatography (50% EtOAc in hexanes) to afford alcohol **9** as a colorless oil (39.3 mg, 80% yield). $[\alpha]_{\text{D}}^{25} +29.4$ (c 0.965, CHCl_3); ^1H NMR (400 MHz, CDCl_3) δ 7.36–7.22 (m, 5H), 5.74 (ddt, J = 16.7, 10.4, 7.6 Hz, 1H), 5.06–4.95 (m, 2H), 3.63 (qd, J = 10.6, 1.6 Hz, 2H), 3.52–3.39 (m, 2H), 2.78–2.66 (m, 2H), 2.10–2.00 (m, 3H), 1.91 (d, J = 7.5 Hz, 2H), 1.69–1.54 (m, 2H), 1.36–1.19 (m, 2H); ^{13}C NMR (100 MHz, CDCl_3) δ 138.0, 133.9, 129.1, 128.5, 127.3, 117.8, 72.4, 63.5, 62.8, 54.0, 37.2, 33.2, 29.8, 23.0; IR (Neat Film, NaCl) 3392, 3065, 3028, 3003, 2932, 2858, 2797, 2759, 1949, 1822, 1730, 1638, 1586, 1603, 1586, 1553, 1494, 1466, 1453, 1415, 1392, 1370, 1352, 1311, 1300, 1259, 1248, 1208, 1180, 1162, 1127, 1116, 1072, 1045, 1028, 1045, 1001, 913, 875, 834,

810, 739, 699, 635, 619; HRMS (MM) m/z calc'd for $C_{16}H_{24}NO$ $[M+H]^+$: 246.1852, found 246.1847.



Ethyl (S)-1-benzoyl-2-oxo-3-(3-oxopropyl)piperidine-3-carboxylate (10): To a flame dried vial was added $CuCl_2 \cdot H_2O$ (4.1 mg, 0.024 mmol), $PdCl_2(PhCN)_2$ (9.2 mg, 0.024 mmol), $AgNO_2$ (1.9 mg, 0.012 mmol), *t*-BuOH (3.75 mL), and nitromethane (0.25 mL). The solution was sparged with O_2 for 15 minutes, and then neat lactam **5aa** (63.1 mg, 0.2 mmol) was added. The solution was then sparged for another 3 minutes and allowed to stir for 14 hours under an oxygen atmosphere. Upon reaction completion by TLC, water (4 mL) was added and the aqueous layer was extracted with DCM (4 mL \times 3). The combined organic layers were dried with Na_2SO_4 , filtered, and concentrated under reduced pressure. The product was purified by column chromatography (50% EtOAc in hexanes) to yield 75% of product **5aa**. $[\alpha]_D^{25} +3.2$ (c 0.685, $CHCl_3$); 1H NMR (400 MHz, $CDCl_3$) δ 9.69 (t, J = 1.1 Hz, 1H), 7.78–7.69 (m, 2H), 7.52–7.44 (m, 1H), 7.44–7.35 (m, 2H), 4.38–4.24 (m, 2H), 3.89–3.70 (m, 2H), 2.73–2.59 (m, 1H), 2.55–2.38 (m, 2H), 2.23–2.13 (m, 2H), 2.06–1.91 (m, 2H), 1.82 (ddd, J = 13.6, 9.9, 5.4 Hz, 1H), 1.37 (t, J = 7.1 Hz, 3H); ^{13}C NMR (100 MHz, $CDCl_3$) δ 200.9, 175.0, 172.1, 171.9, 135.8, 132.0, 128.2, 128.2, 62.4, 55.8, 46.6, 39.9, 31.5, 27.8, 20.2, 14.3; IR (Neat Film, NaCl) 2924, 2853, 2727, 1723, 1704, 1681, 1601, 1449, 1391, 1348, 1275, 1195, 1174, 1150, 1062, 1023,

959, 916, 856, 824, 796, 726, 695, 659; HRMS (MM) m/z calc'd for $C_{18}H_{22}NO_5$ $[M+H]^+$: 332.1492, found 332.1483.



11

Ethyl (*S*)-3-allyl-2-oxopiperidine-3-carboxylate (11)³⁵: To a flame dried vial under argon was added NaOEt (17.4 mg, 0.26 mmol) and EtOH (1.3 mL). Lactam **5aa** (63.1 mg, 0.20 mmol) was added and the resulting mixture was stirred for 48 h at 65 °C. The reaction was quenched with citric acid (154 mg, 0.80 mmol) and the EtOH was removed in vacuo. The resulting oil was then diluted with water (2 mL) and extracted with chloroform. The combined organic layers were dried with sodium sulfate and the solvent was removed in vacuo. The product was purified by column chromatography (80% EtOAc in hexanes) to afford amide **8** as a colorless oil (35.6 mg, 84% yield). $[\alpha]_D^{25} +36.2$ (c 0.89, $CHCl_3$); 1H NMR (400 MHz, $CDCl_3$) δ 6.40 (s, 1H), 5.76 (dddd, J = 16.8, 10.2, 8.1, 6.5 Hz, 1H), 5.20–5.05 (m, 2H), 4.29–4.10 (m, 2H), 3.40–3.18 (m, 2H), 2.78 (ddt, J = 13.8, 6.5, 1.3 Hz, 1H), 2.66–2.50 (m, 1H), 2.14–2.04 (m, 1H), 1.93–1.68 (m, 3H), 1.26 (t, J = 7.1 Hz, 3H); ^{13}C NMR (100 MHz, $CDCl_3$) δ 172.7, 170.8, 133.7, 119.2, 61.6, 53.5, 42.5, 40.0, 29.4, 19.6, 14.3; IR (Neat Film, NaCl) 3213, 3077, 2978, 2941, 2873, 1732, 1668, 1490, 1469, 1417, 1392, 1356, 1326, 1314, 1297, 1282, 1241, 1193, 1153, 1116, 1094, 1026, 1005, 921, 856, 812, 763, 719, 663; HRMS (MM) m/z calc'd for $C_{11}H_{18}NO_3$ $[M+H]^+$: 212.1281, found 212.1280.

1.7.3 DETERMINATION OF ENANTIOMERIC EXCESS

Table 1.8 Determination of enantiomeric excess

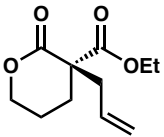
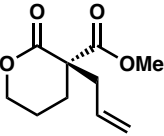
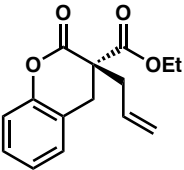
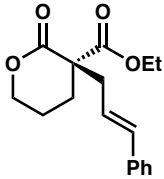
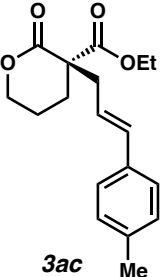
entry	compound	SFC analytic conditions	ee (%)
1	 <p>3aa</p>	Chiralpak IC, $\lambda = 210$ nm 25% IPA/CO ₂ , 2.5 mL/min t_R (min) major 2.77, minor 3.39	86
2	 <p>3ba</p>	Chiralpak IC, $\lambda = 210$ nm 20% IPA/CO ₂ , 2.5 mL/min t_R (min) major 3.35, minor 3.99	86
3	 <p>3ca</p>	Chiracel OB-H, $\lambda = 210$ nm 5% IPA/CO ₂ , 2.5 mL/min t_R (min) minor 2.23, major 2.64	64
4	 <p>3ab</p>	Chiralpak AD-H, $\lambda = 254$ nm 10% IPA/CO ₂ , 2.5 mL/min t_R (min) major 5.43, minor 6.24	90
5	 <p>3ac</p>	Chiralpak AD-H, $\lambda = 254$ nm 10% IPA/CO ₂ , 2.5 mL/min t_R (min) major 6.47, minor 7.71	90

Table 1.8 Determination of enantiomeric excess

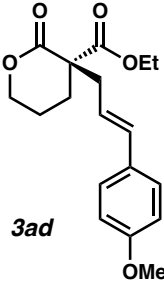
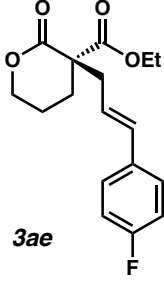
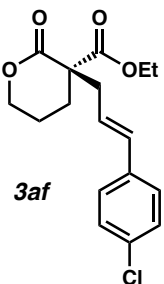
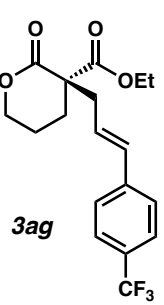
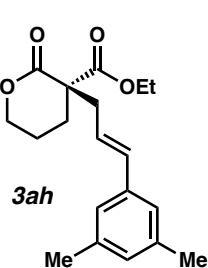
entry	compound	SFC analytic conditions	ee (%)
6	 <p>3ad</p>	Chiralpak AD-H, λ = 254 nm 15% IPA/CO ₂ , 2.5 mL/min tr (min) major 5.37, minor 6.37	88
7	 <p>3ae</p>	Chiralpak AD-H, λ = 254 nm 10% IPA/CO ₂ , 2.5 mL/min tr (min) major 5.12, minor 5.95	88
8	 <p>3af</p>	Chiralpak AD-H, λ = 254 nm 30% IPA/CO ₂ , 2.5 mL/min tr (min) major 2.29, minor 2.57	86
9	 <p>3ag</p>	Chiralpak AD-H, λ = 254 nm 10% IPA/CO ₂ , 2.5 mL/min tr (min) major 4.02, minor 4.72	86
10	 <p>3ah</p>	Chiralpak AD-H, λ = 254 nm 5% IPA/CO ₂ , 3 mL/min tr (min) major 9.68, minor 11.56	88

Table 1.8 Determination of enantiomeric excess

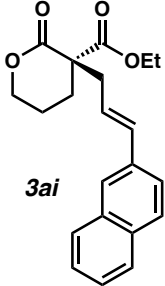
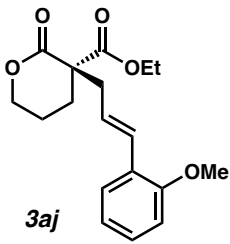
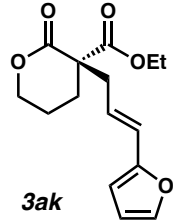
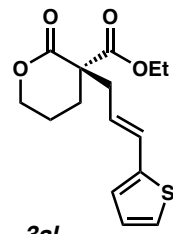
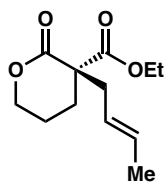
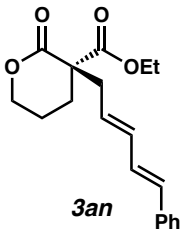
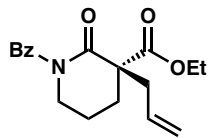
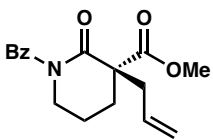
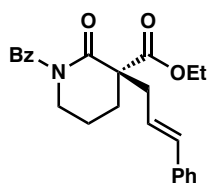
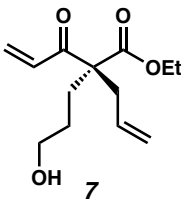
entry	compound	SFC analytic conditions	ee (%)
11	 <p>3ai</p>	Chiralpak AD-H, $\lambda = 254$ nm 30% IPA/CO ₂ , 2.5 mL/min tr (min) major 3.36, minor 4.24	88
12	 <p>3aj</p>	Chiralcel OD-H, $\lambda = 254$ nm 10% IPA/CO ₂ , 2.5 mL/min tr (min) minor 9.05, major 9.85	90
13	 <p>3ak</p>	Chiralpak AD-H, $\lambda = 254$ nm 10% IPA/CO ₂ , 2.5 mL/min tr (min) major 3.97, minor 4.62	88
14	 <p>3al</p>	Chiralpak AD-H, $\lambda = 254$ nm 10% IPA/CO ₂ , 2.5 mL/min tr (min) major 6.33, minor 7.51	88
15	 <p>3am</p>	Chiralpak IC, $\lambda = 210$ nm 25% IPA/CO ₂ , 2.5 mL/min tr (min) major 2.87, minor 3.69	78

Table 1.8 Determination of enantiomeric excess

entry	compound	SFC analytic conditions	ee (%)
16	 <p>3an</p>	Chiralpak AD-H, $\lambda = 254$ nm 15% IPA/CO ₂ , 2.5 mL/min t_R (min) major 5.30, minor 6.23	88
17	 <p>5aa</p>	Chiralpak IC, $\lambda = 254$ nm 20% IPA/CO ₂ , 2.5 mL/min t_R (min) major 3.77, minor 4.39	90
18	 <p>5ba</p>	Chiralpak AD-H, $\lambda = 254$ nm 10% IPA/CO ₂ , 2.5 mL/min t_R (min) minor 4.00 major 4.57	90
19	 <p>5ab</p>	Chiralpak AD-H, $\lambda = 254$ nm 30% IPA/CO ₂ , 2.5 mL/min t_R (min) minor 2.56, major 2.94	90
20	 <p>7</p>	Chiralpak IC, $\lambda = 210$ nm 10% IPA/CO ₂ , 2.5 mL/min t_R (min) major 7.01, minor 7.54	86

1.8 REFERENCES AND NOTES

- (1) Tsuji, J.; Takahashi, H.; Morikawa, M. *Tetrahedron Lett.* **1965**, 6, 4387–4388.
- (2) a) Trost, B. M.; Van Vranken, D. L., *Chem. Rev.* **1996**, 96, 395–422; b) Trost, B. M.; Crawley, M. L. *Chem. Rev.* **2003**, 103, 2921–2943; c) Trost, B. M. *J. Org. Chem.* **2004**, 69, 5813–5837.
- (3) a) Liu, Y.; Han, S.-J.; Liu, W.-B.; Stoltz, B. M. *Acc. Chem. Res.* **2015**, 48, 740–751; b) Bhat, V.; Welin, E. R.; Guo, X.; Stoltz, B. M. *Chem. Rev.* **2017**, 117, 4528–4561; c) Hethcox, J. C.; Shockley, S. E.; Stoltz, B. M. *ACS Catal.* **2016**, 6, 6207–6213.
- (4) For reviews, see a) Mohr, J. T.; Stoltz, B. M. *Chem. Asian. J.* **2007**, 2, 1476–1491; b) Oliver, S.; Evans, P. A. *Synthesis*. **2013**, 45, 3179–3198.
- (5) For α -quaternary lactones, see; a) Li, X.-H.; Wan, S.-L.; Chen, D.; Liu, Q.; Ding, C.-H.; Fang, P.; Hou, X.-L. *Synthesis*, **2016**, 48, 1568–1572; b) Akula, R.; Guiry, P. J. *Org. Lett.* **2016**, 18, 5472–5475; c) James, J.; Guiry, P. J. *ACS Catal.* **2017**, 1397–1402; d) Oliveira, M. N.; Fournier, J.; Arseniyadis, S.; Cossy, J. *Org. Lett.* **2017**, 19, 14–17.
- (6) For α -quaternary lactams, see a) Behenna, D. C.; Liu, Y.; Yurino, T.; Kim, J.; White, D. E.; Virgil, S. C.; Stoltz, B. M. *Nature Chem.* **2012**, 4, 130–133; b) Trost, B. M.; Frederiksen, M. U. *Angew. Chem. Int. Ed.* **2005**, 44, 308–310; *Angew. Chem.* **2005**, 117, 312–314.
- (7) For selected examples, see a) Alexy, E. J.; Virgil, S. C.; Bartberger, M. D.; Stoltz, B. M. *Org. Lett.* **2017**, 19, 5007–5009; b) Shockley, S. E.; Hethcox,

- J. C.; Stoltz, B. M. *Angew. Chem. Int. Ed.* **2017**, *56*, 11545–11548; *Angew. Chem.* **2017**, *129*, 11703–11706; c) Starkov, P.; Moore, J. T.; Duquette, D. C.; Stoltz, B. M.; Marek, I. *J. Am. Chem. Soc.* **2017**, *139*, 9615–9620; d) Hethcox, J. C.; Shockley, S. E.; Stoltz, B. M. *Angew. Chem. Int. Ed.* **2016**, *55*, 16092–16095; *Angew. Chem.* **2016**, *128*, 16326–16329; e) Hayashi, M.; Bachman, S.; Hashimoto, S.; Eichman, C. C.; Stoltz, B. M. *J. Am. Chem. Soc.* **2016**, *138*, 8997–9000; f) Behenna, D. C.; Mohr, J. T.; Sherden, N. H.; Marinescu, S. C.; Harned, A. M.; Tani, K.; Seto, M.; Ma, S.; Novák, Z.; Krout, M. R.; McFadden, R. M.; Roizen, J. L.; Enquist, J. A.; White, D. E.; Levine, S. R.; Petrova, K. V.; Iwashita, A.; Virgil, S. C.; Stoltz, B. M. *Chem. Eur. J.* **2011**, *17*, 14199–14223.
- (8) a) Liu, W.; Xu, D. D.; Repič, O.; Blacklock, T. J. *Tetrahedron Lett.* **2001**, 2439–2441; b) Delhayé, L.; Merschaert, A.; Diker, K.; Houpiš, I. N. *Synthesis*, **2006**, *9*, 1437–1442.
- (9) Vitaku, E.; Smith, D. T.; Njardarson, J. T. *J. Med. Chem.* **2014**, *57*, 10257–10274.
- (10) Kita, Y.; Kavthé, R. D.; Oda, H.; Mashima, K. *Angew. Chem. Int. Ed.* **2016**, *55*, 1098–1101; *Angew. Chem.* **2016**, *128*, 1110–1113.
- (11) For recent success in Ni-catalyzed allylic alkylations from the past 15 years, see a) Bernhard, Y.; Thomson, B.; Ferey, V.; Sauthier, M. *Angew. Chem. Int. Ed.* **2017**, *56*, 7460–7464; *Angew. Chem.* **2017**, *129*, 7568–7572; b) Sha, S. C.; Mao, J.; Bellomo, A.; Jeong, S. A.; Walsh, P. J. *Angew. Chem. Int. Ed.* **2016**, *55*, 1070–1074; *Angew. Chem.* **2017**, *128*, 1082–1086; c)

Wang, J.; Wang, P.; Wang, L.; Li, D.; Wang, K.; Wang, Y.; Zhu, H.; Yang, D.; Wang, R. *Org. Lett.* **2017**, *19*, 4826–4829; d) Son, S.; Fu, G. C. *J. Am. Chem. Soc.* **2008**, *130*, 2756–2757; e) Shields, J. D.; Ahneman, D. T.; Graham, T. J. A.; Doyle, A. G. *Org. Lett.* **2014**, *16*, 142–145; f) Srinivas, H. D.; Zhou, Q.; Watson, M. P. *Org. Lett.* **2014**, *16*, 3596–3599.

- (12) These α -quaternary products could alternatively be accessed via phase-transfer catalysis, see a) Ha, M. W.; Lee, H.; Yi, H. Y.; Park, Y.; Kim, S.; Hong, S.; Lee, M.; Kim, M.-h.; Kim, T.-s.; Park, H.-g. *Adv. Synth. Catal.* **2013**, *355*, 637–642; b) Park, Y.; Lee, Y. J.; Hong, S.; Kim, M.-h.; Lee, M.; Kim, T.-s.; Lee, J. K.; Jew, S.-s.; Park, H.-g. *Adv. Synth. Catal.* **2011**, *353*, 3313–3318.
- (13) The quaternary lactone product **3aa** was isolated in 86% yield and with 65% ee under Mashima's optimized conditions.
- (14) Additional 36 ligands were examined, see Experimental Section (Table 1.5) for details.
- (15) See Experimental Section, Table 1.6 for the investigation of different solvents.
- (16) Additional optimization of reaction parameters for lactam nucleophile is required due to the insolubility of substrate in Et₂O. See Experimental Section for results from the optimization.
- (17) Results from other protected-acyl lactams are included in the Experimental Section (Table 1.7).

- (18) Previous reports also proposed a nickel π -allyl intermediate in the catalytic cycle, see ref 10, 11a–b.
- (19) Kim, K. E.; Li, J.; Grubbs, R. H.; Stoltz, B. M. *J. Am. Chem. Soc.* **2016**, *138*, 13179–13182.
- (20) Sheldrick, G. M. *Acta Cryst.* **1990**, *A46*, 467–473.
- (21) Sheldrick, G. M. *Acta Cryst.* **2015**, *C71*, 3–8.
- (22) Müller, P. *Crystallography Reviews* **2009**, *15*, 57.
- (23) Procedure adapted from: Jakubec, P.; Farley, A. J. M.; Dixon, D. J. *Beilstein J. Org. Chem.* **2016**, *12*, 1096–1100.
- (24) (a) Szosak, M.; Spain, M.; Choquette, K. A.; Flowers II, R. A.; Procter, D. J. *J. Am. Chem. Soc.* **2013**, *135*, 15702–15705; (b) Parmar, D.; Duffy, L. A.; Sadasivam, D. V.; Matsubara, H.; Bradley, P. A.; Flowers II, R. A.; Procter, D. J. *J. Am. Chem. Soc.* **2009**, *131*, 15467–15473.
- (25) Suljić, S.; Pietruszka, J. *Adv. Synth. Catal.* **2014**, *356*, 1007–1020.
- (26) Adapted from synthesis of a similar compound, see ref 6a.
- (27) (a) Filippis, A.; Pardo, D. G.; Cossy, J. *Synthesis*. **2004**, *17*, 2930–2933; (b) Foti, C. J.; Comins, D. L., *J. Org. Chem.* **1995**, *60*, 2656–2657.
- (28) Garnier, E. C.; Liebeskind, L.S. *J. Am. Chem. Soc.* **2008**, *130*, 7449–7458.
- (29) Deng, J. Z.; Paone, D. V.; Ginnetti, A. T.; Kurihara, H.; Dreher, S. D.; Weissman, S. A.; Stauffer, S. R. *Org. Lett.* **2009**, *11*, 345–347.
- (30) Sauerberg, P.; Kindtler, J. W.; Nielsen, L.; Sheardown, M. J.; Honoré, T. *J. Med. Chem.* **1991**, *34*, 687–697.

- (31) Loreto, A.; Migliorini, A.; Tardella, P. A.; Gambacorta, A. *Eur. J. Org. Chem.* **2007**, 14, 2365–2371.
- (32) Hosseinzadeh, R.; Tajbakhsh, M.; Mohadjerani, M.; Mehdinejad, H. *Synlett.* **2004**, 9, 1517–1520.
- (33) Cossy, J.; de Filippis, A.; Pardo, D. G. *Org. Lett.* **2003**, 5, 3037–3039.
- (34) Hoshiya, N.; Takenaka, K.; Shuto, S.; Uenishi, J. *Org. Lett.* **2016**, 18, 48–51.
- (35) Adapted from: Davies, S. G.; Haggitt, J. R.; Ichihara, O.; Kelly, R. J.; Leech, M. A.; Mortimer, A. J. P.; Roberts, P. M.; Smith, A. D. *Org. Biomol. Chem.* **2004**, 2, 2630–2649.

APPENDIX 1

Spectra Relevant to Chapter 1:

*Nickel-Catalyzed Enantioselective Allylic Alkylation of Lactones and
Lactams with Unactivated Allylic Alcohols*

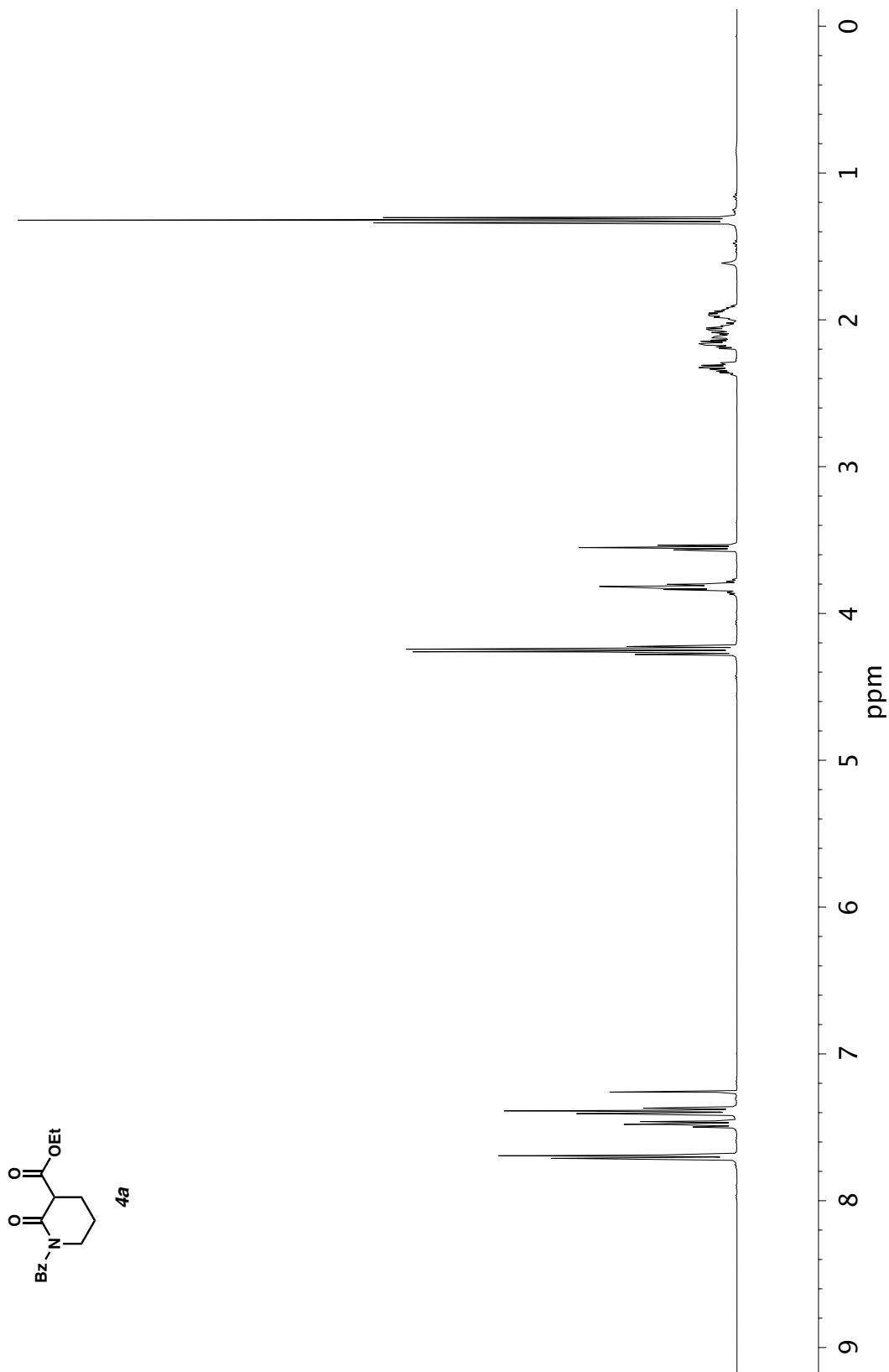


Figure A1.1 ^1H NMR (500 MHz, CDCl_3) of compound **4a**.

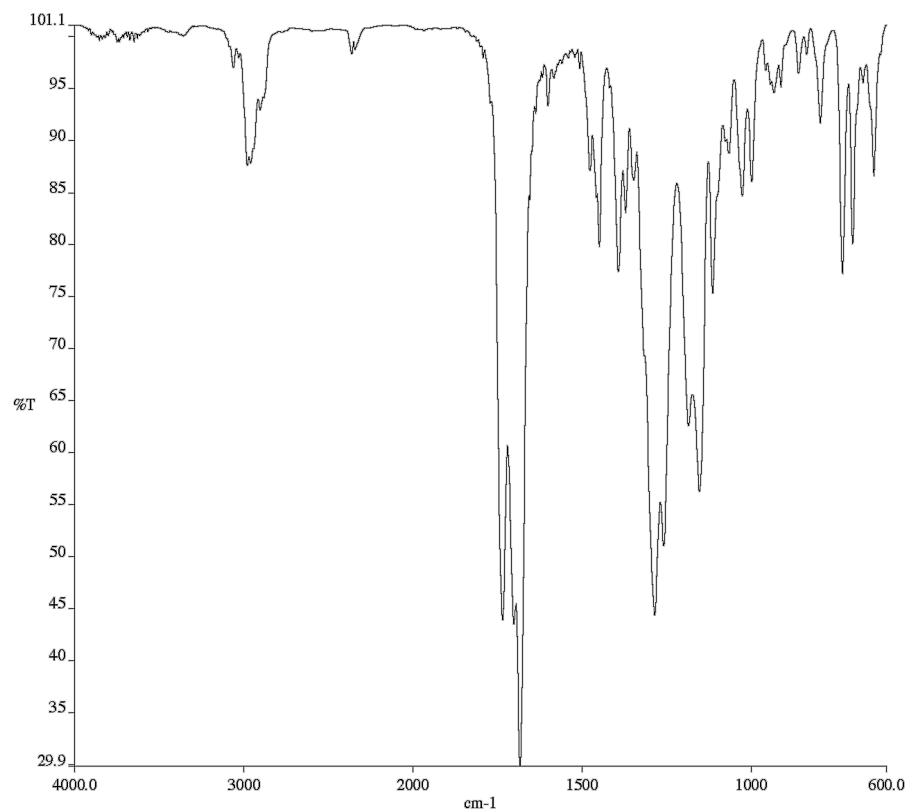


Figure A1.2 Infrared spectrum (Thin Film, NaCl) of compound **4a**.

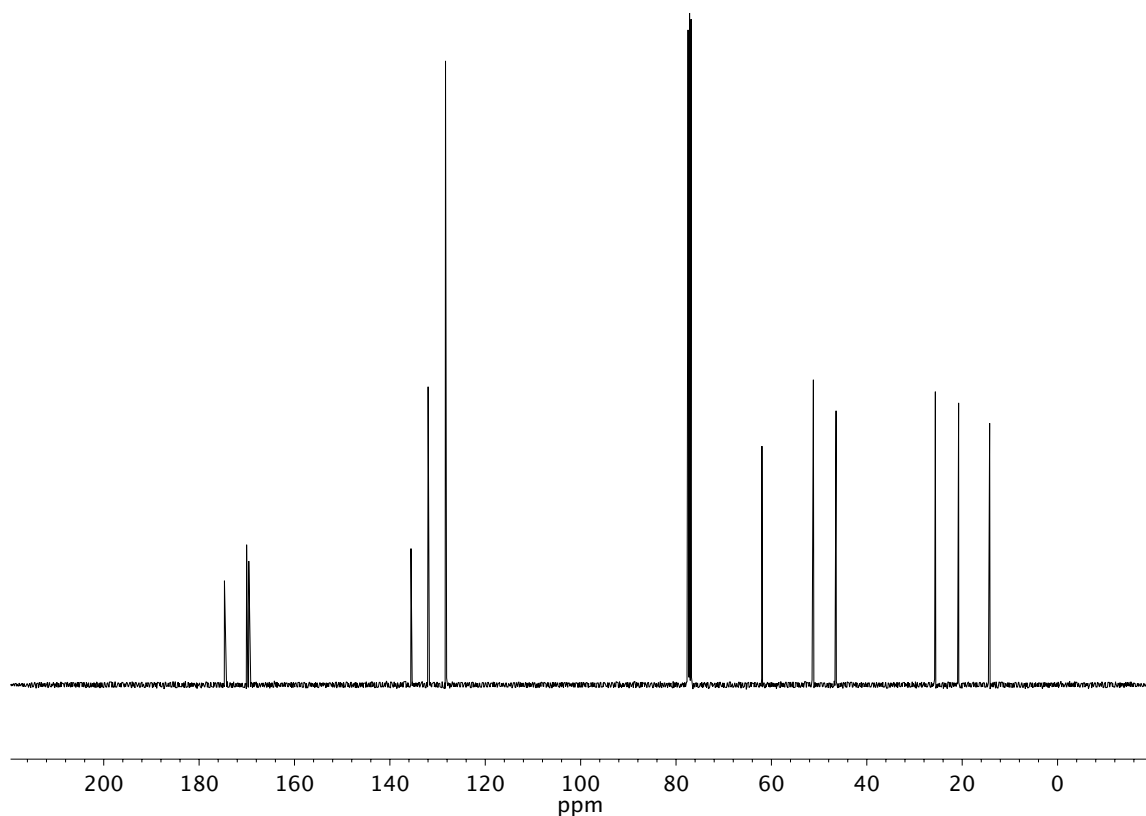


Figure A1.3 ¹³C NMR (125 MHz, CDCl₃) of compound **4a**.

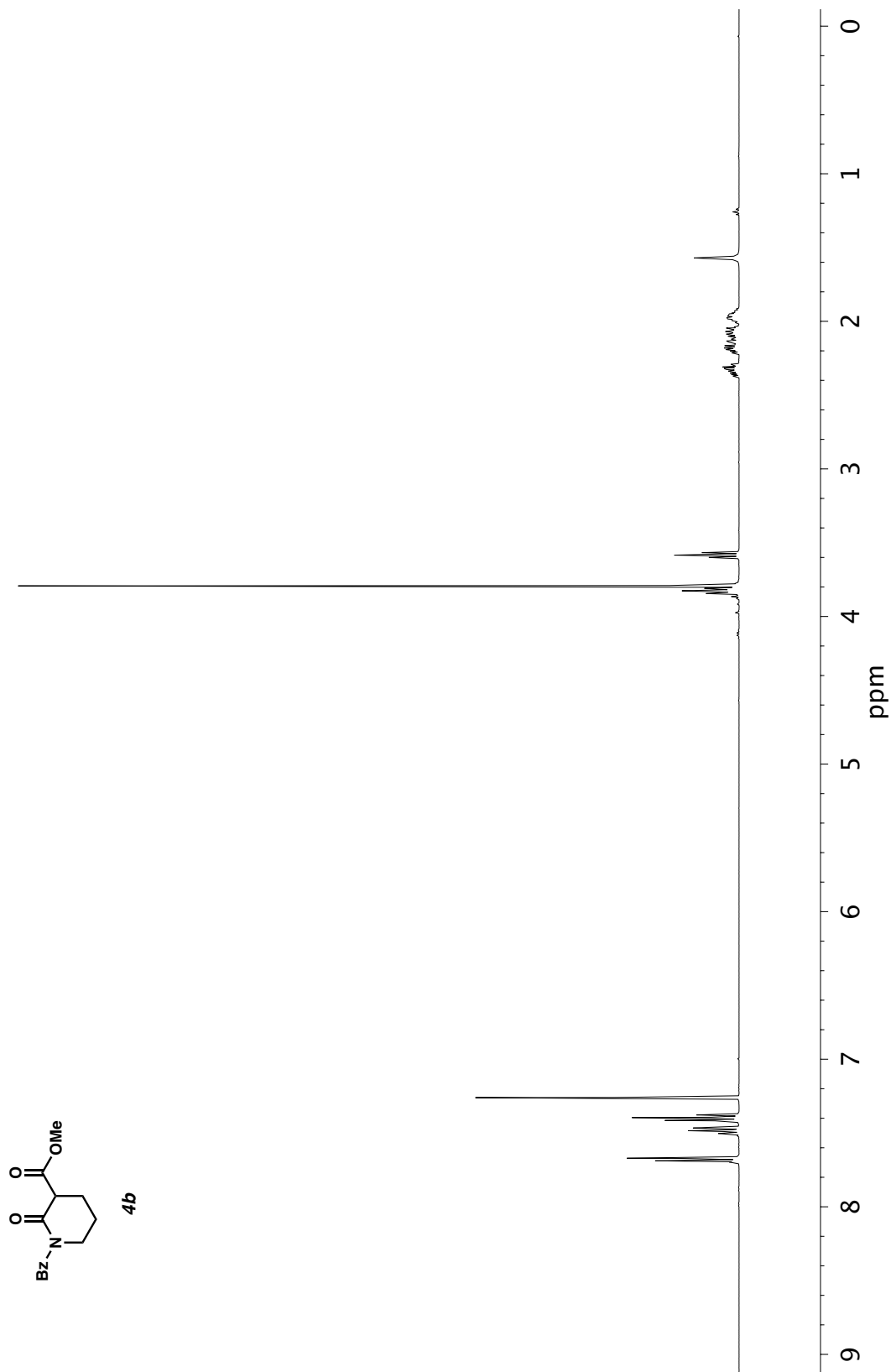


Figure A1.4 ^1H NMR (400 MHz, CDCl_3) of compound **4b**.

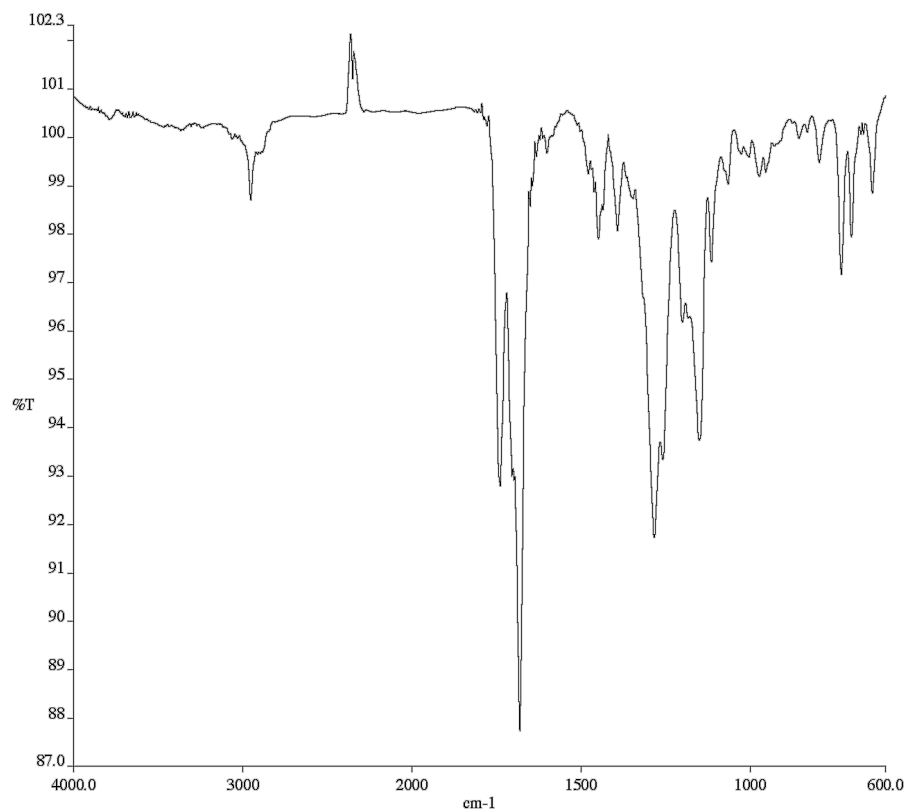


Figure A1.5 Infrared spectrum (Thin Film, NaCl) of compound **4b**.

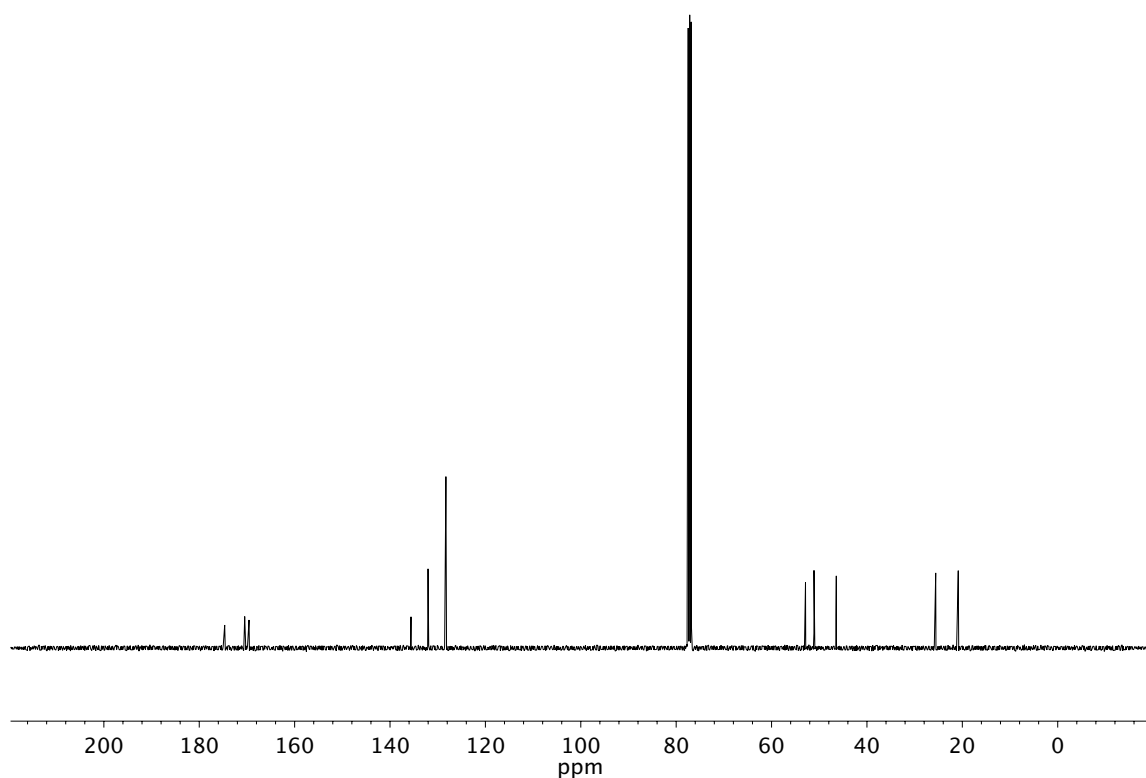


Figure A1.6 ^{13}C NMR (100 MHz, CDCl_3) of compound **4b**.

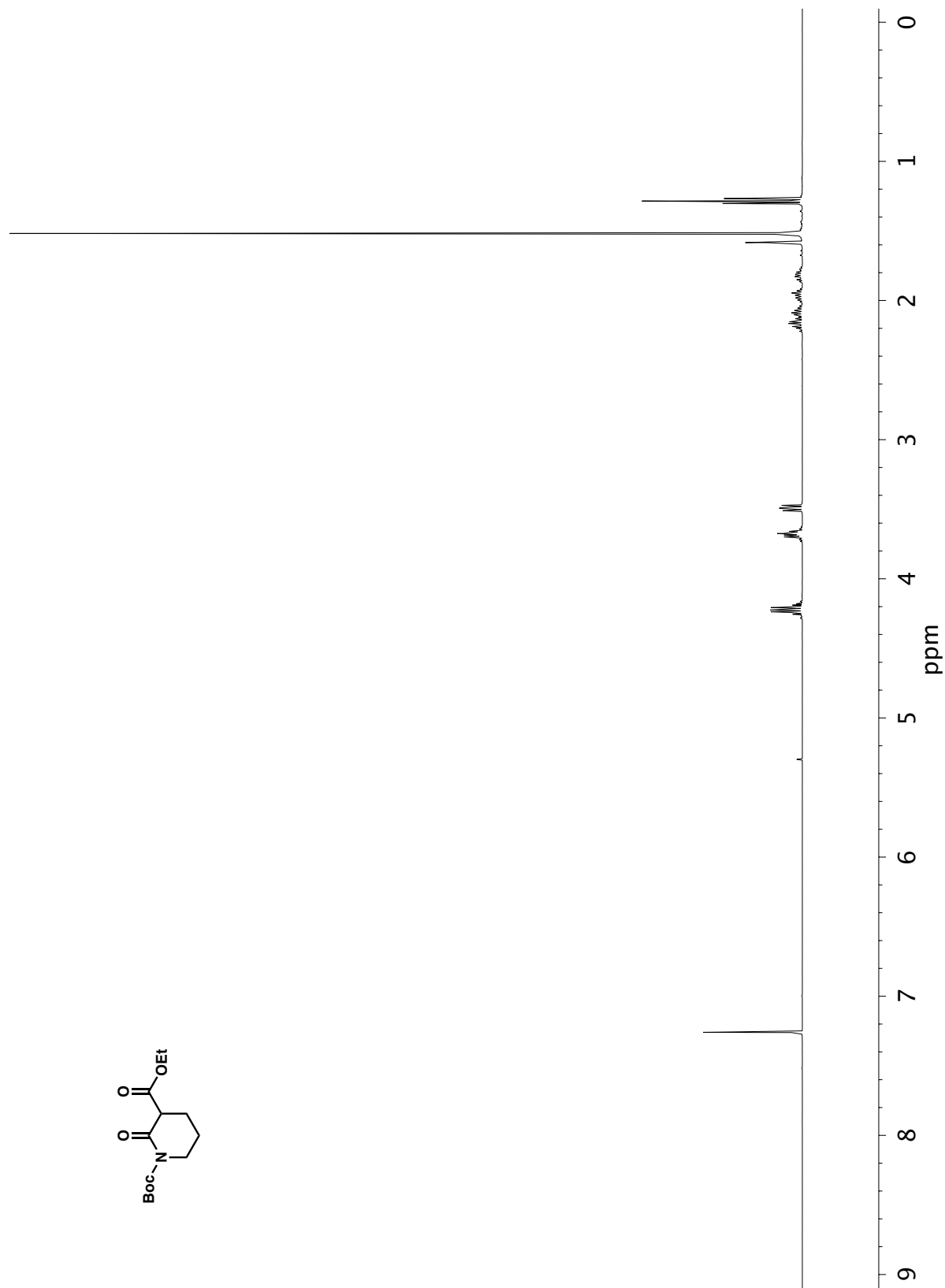


Figure A1.7 ¹H NMR (400 MHz, CDCl₃) of Boc-protected lactam.

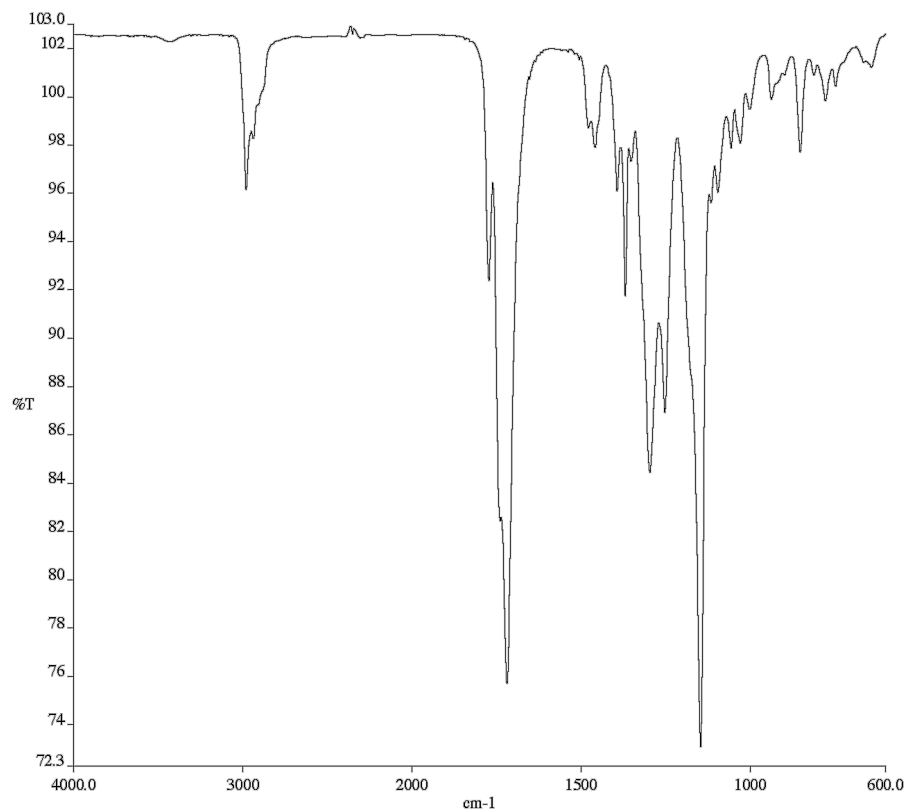


Figure A1.8 Infrared spectrum (Thin Film, NaCl) of Boc-protected lactam.

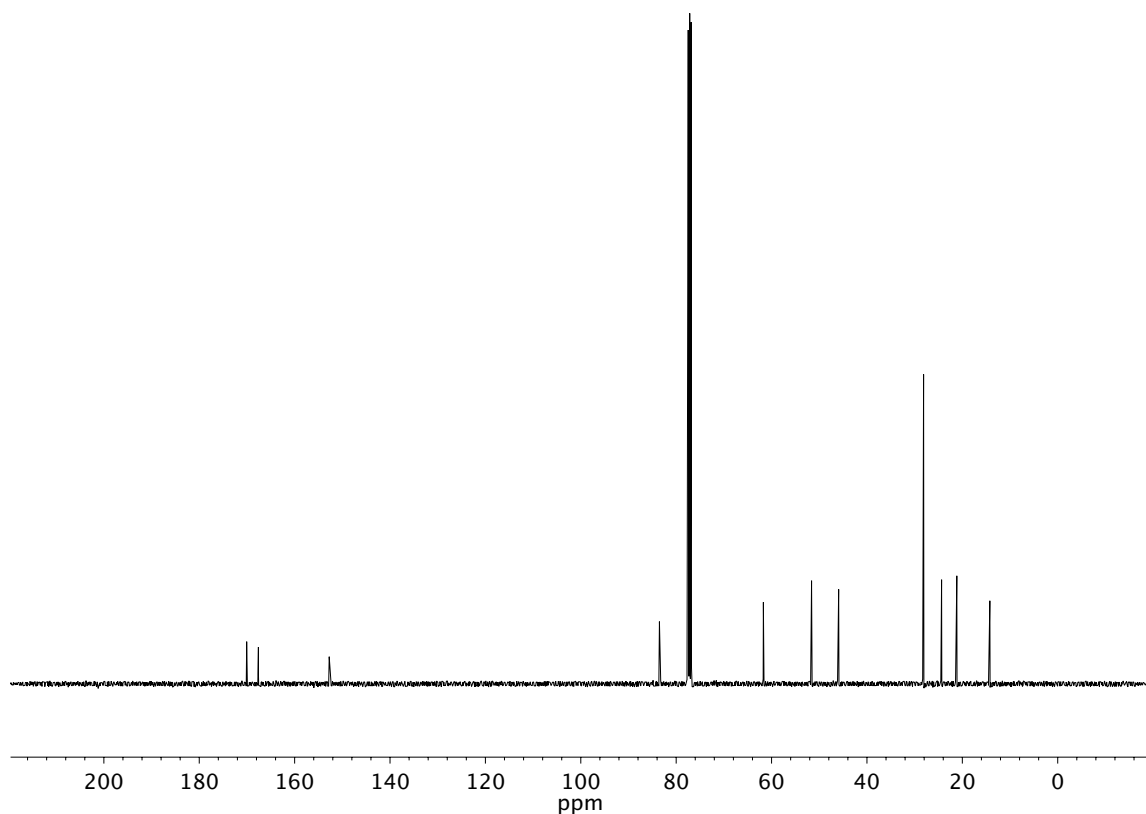


Figure A1.9 ¹³C NMR (100 MHz, CDCl₃) of Boc-protected lactam.

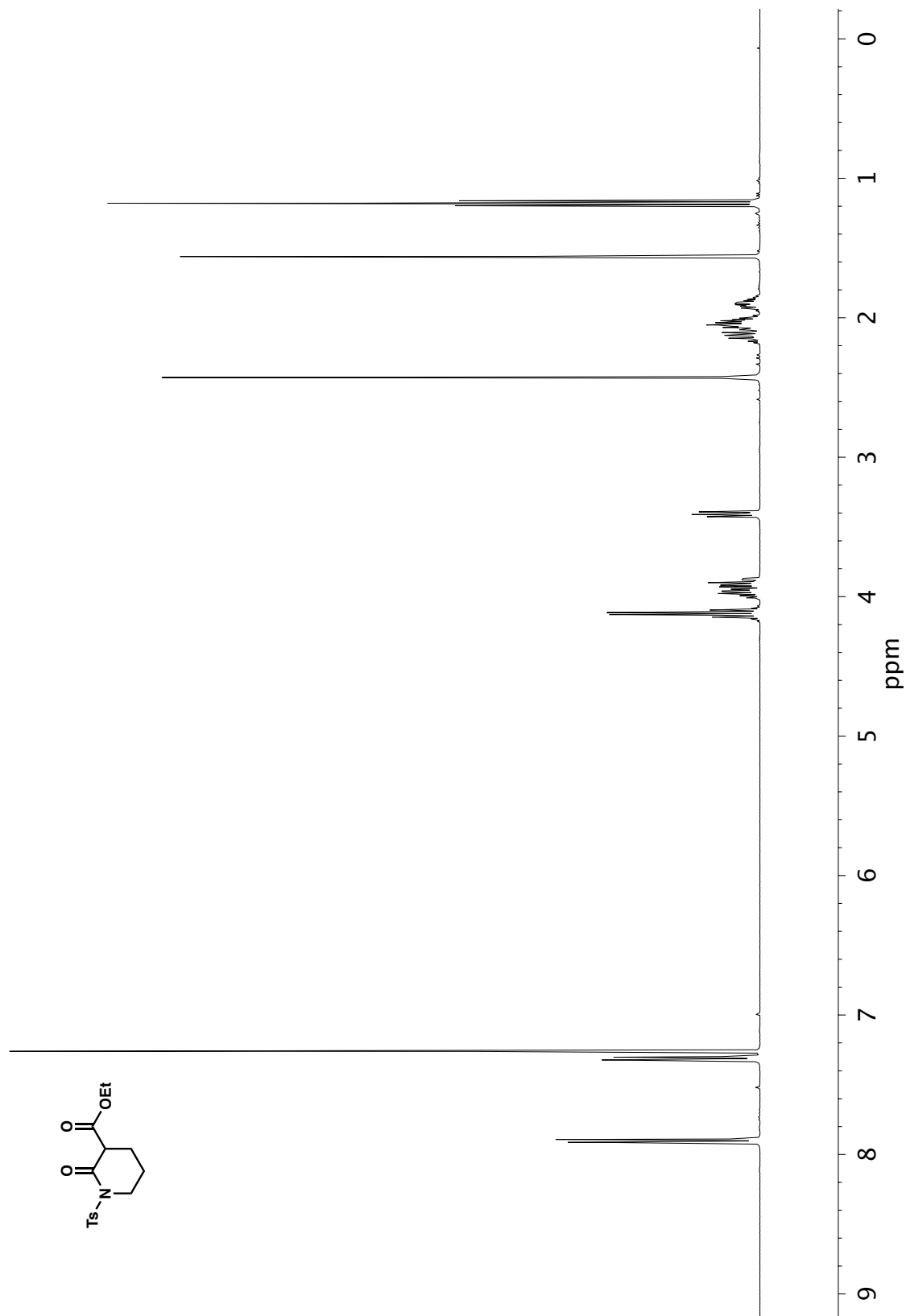


Figure A1.10 ^1H NMR (400 MHz, CDCl_3) of Ts-protected lactam.

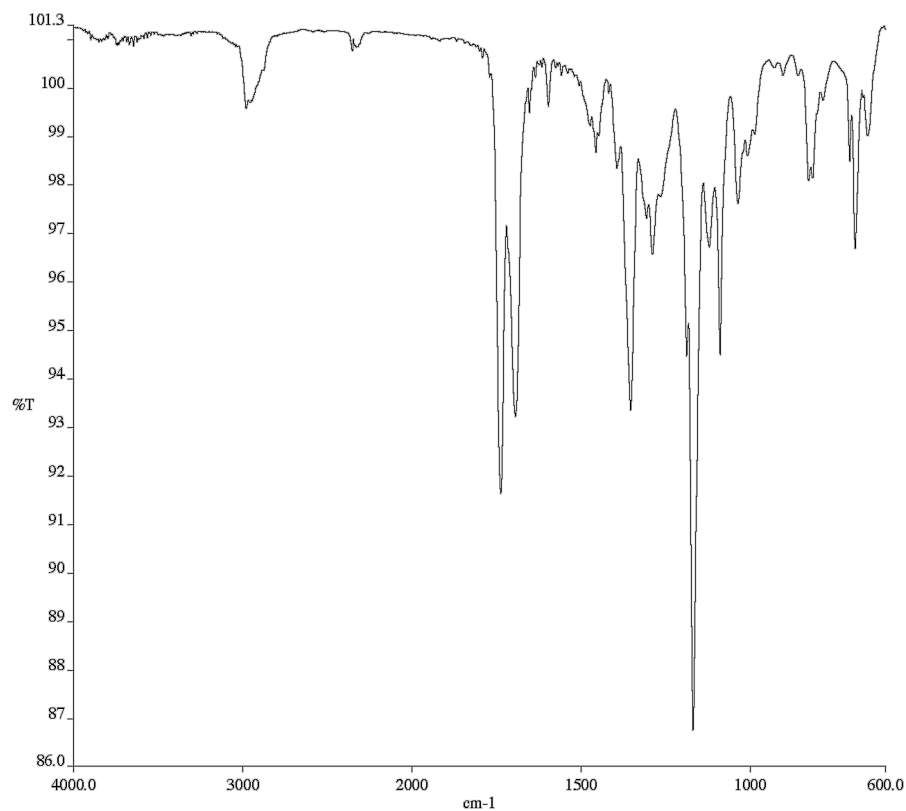


Figure A1.11 Infrared spectrum (Thin Film, NaCl) of Ts-protected lactam.

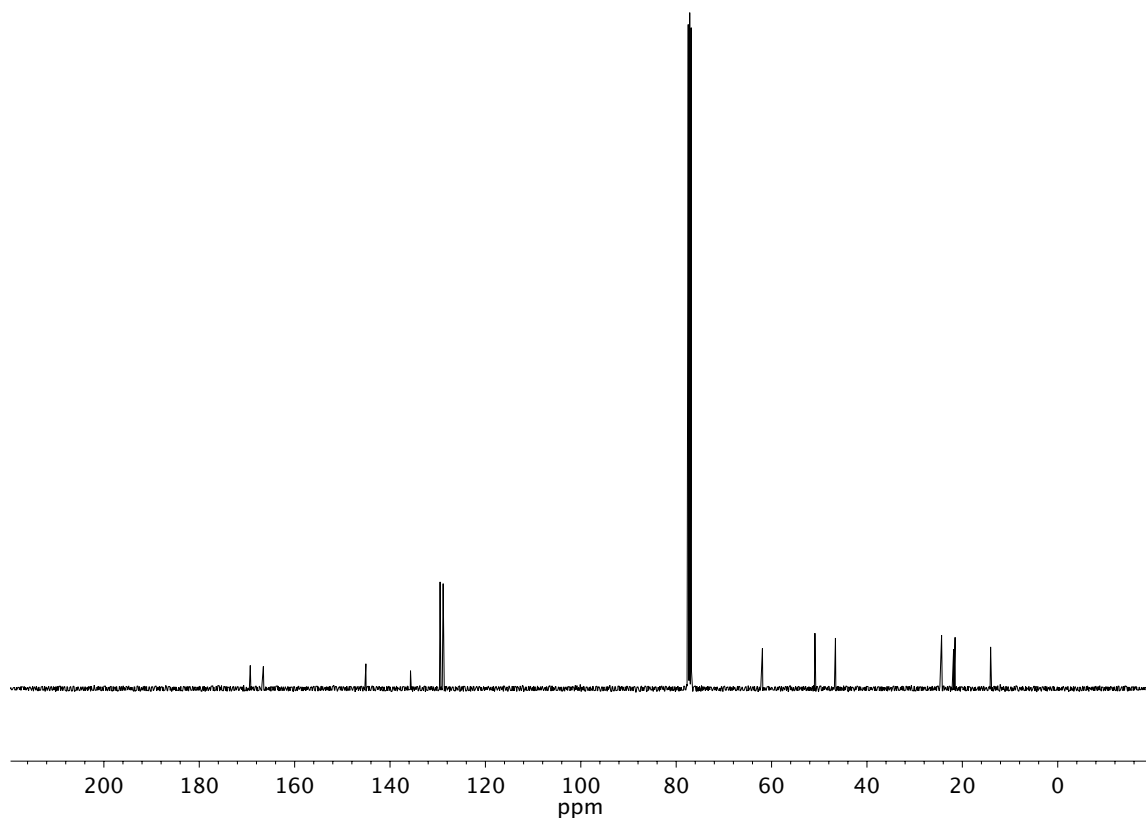


Figure A1.12 ¹³C NMR (100 MHz, CDCl₃) of Ts-protected lactam.

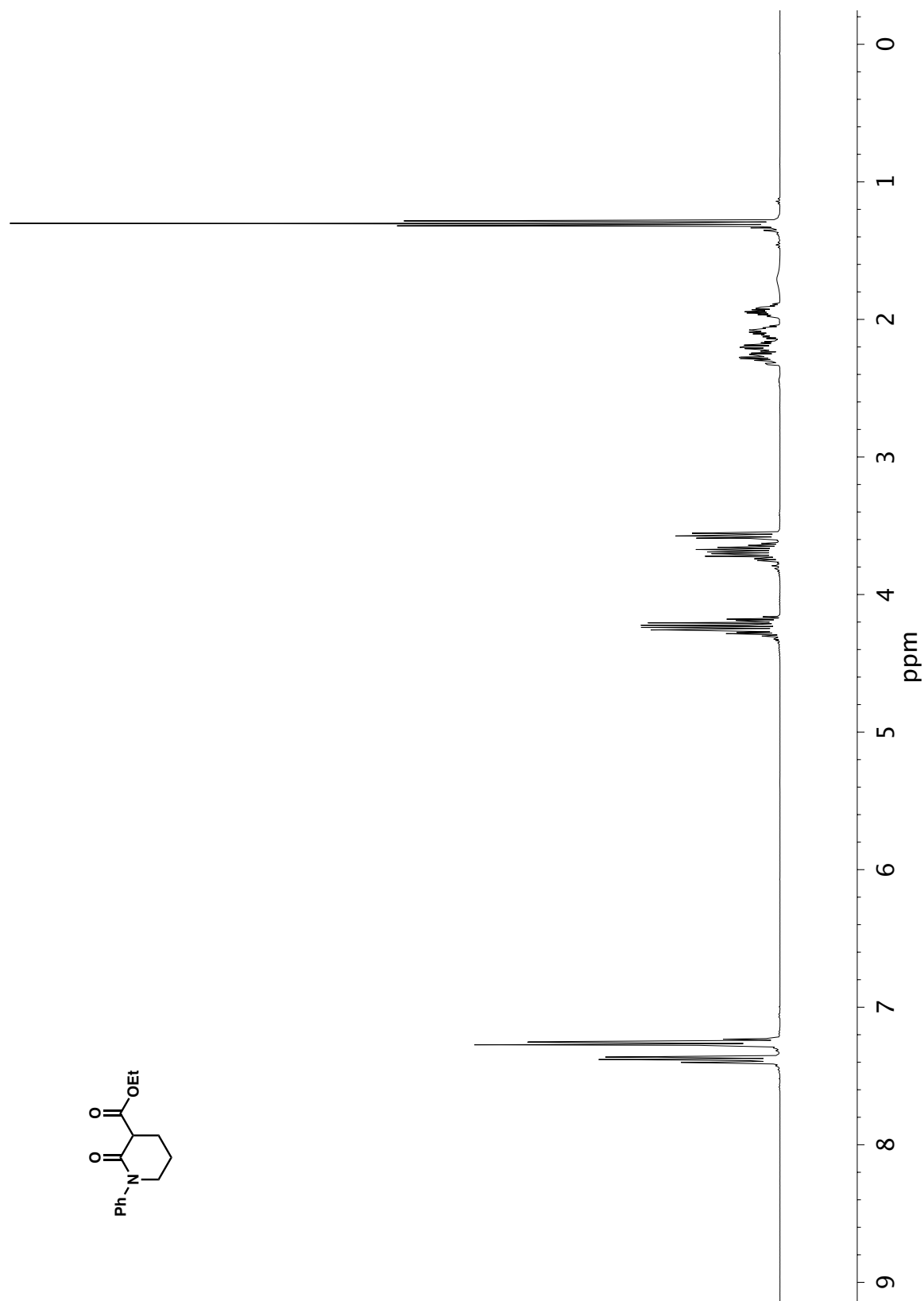


Figure A1.13 ^1H NMR (400 MHz, CDCl_3) of Ph-protected lactam.

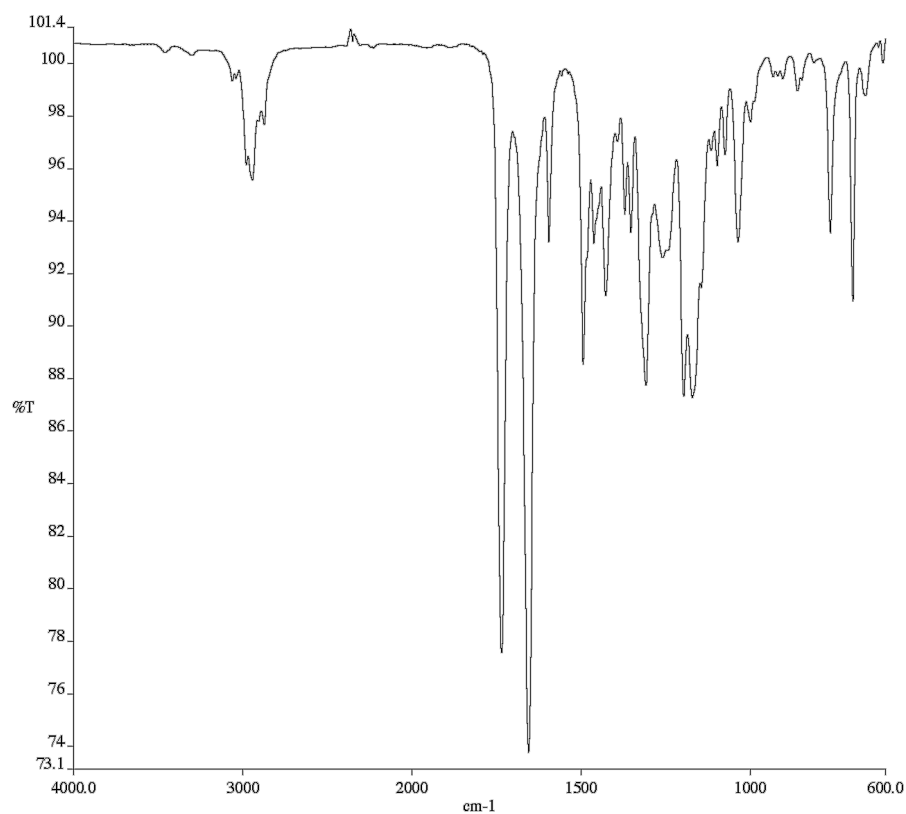


Figure A1.14 Infrared spectrum (Thin Film, NaCl) of Ph-protected lactam.

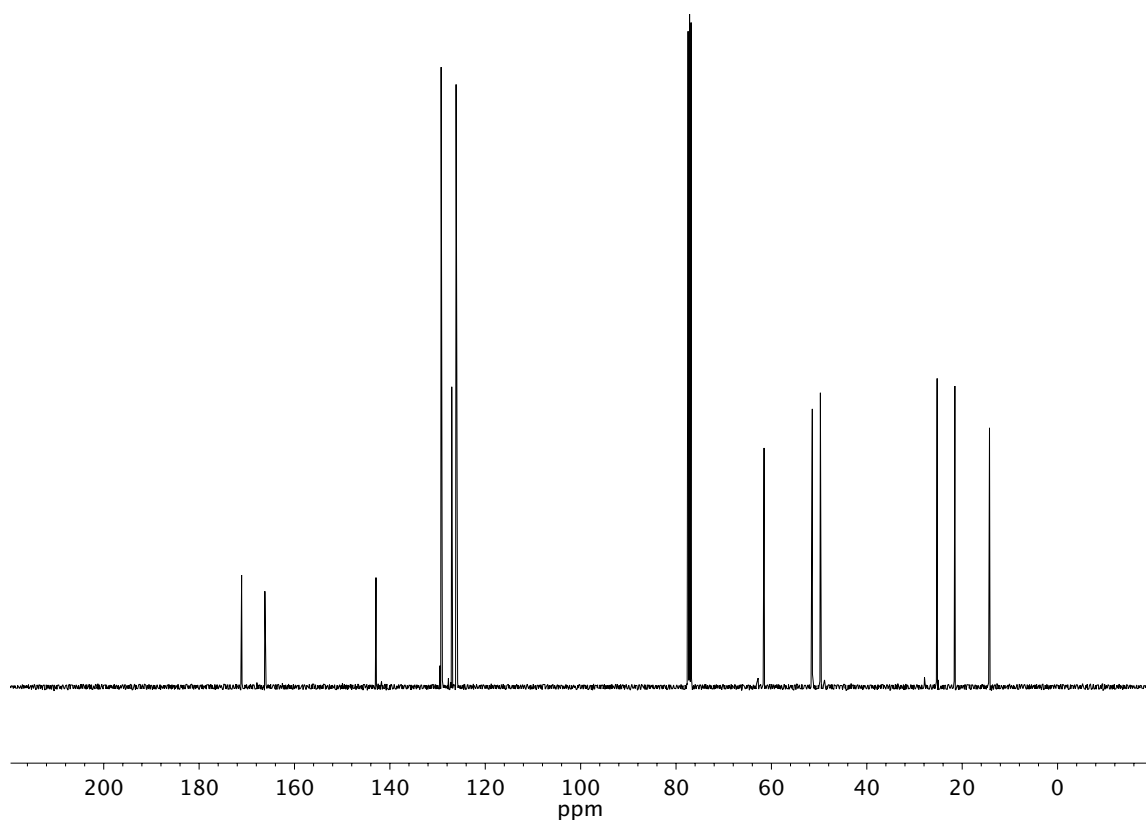


Figure A1.15 ¹³C NMR (100 MHz, CDCl₃) of Ph-protected lactam.

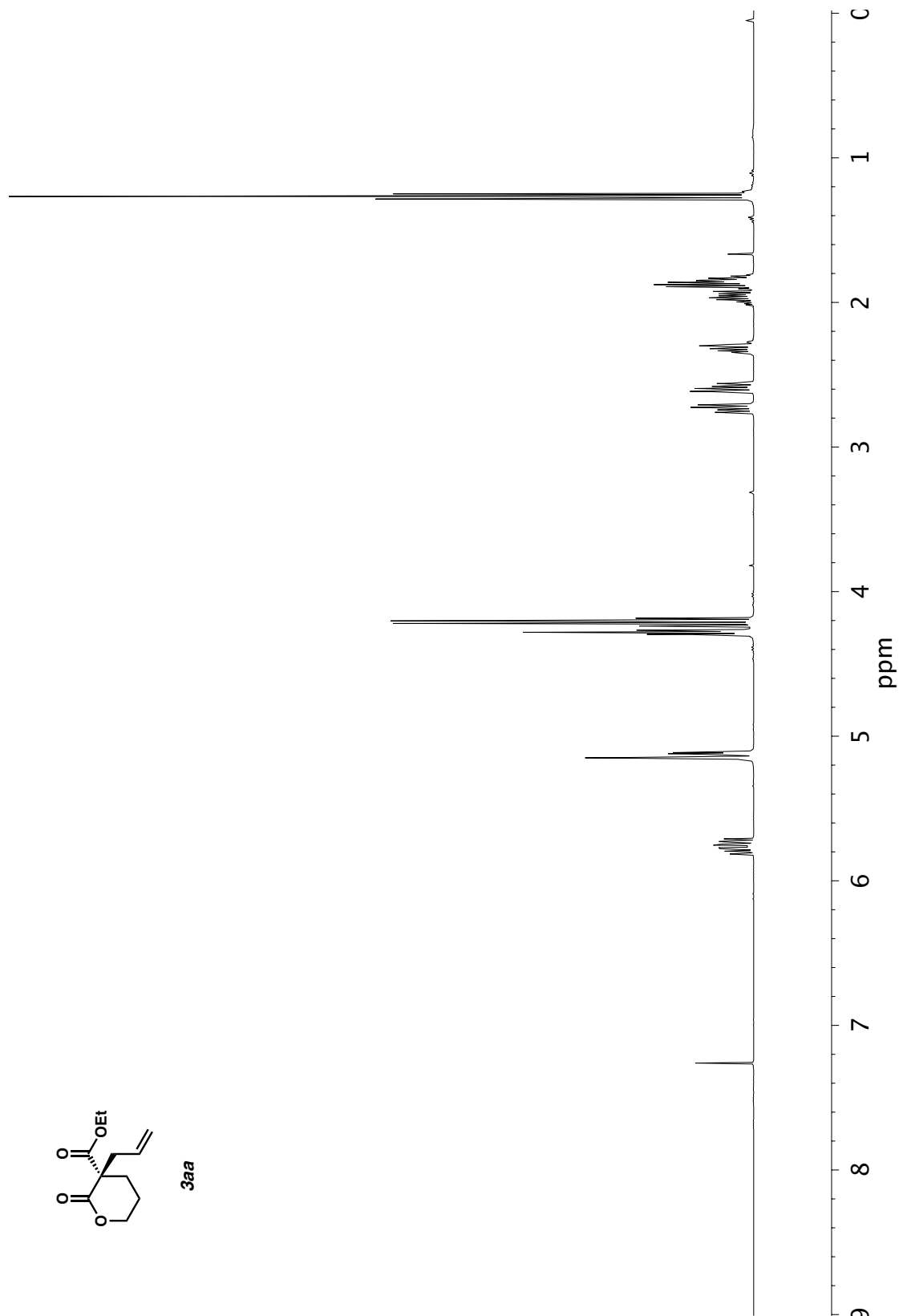


Figure A1.16 ¹H NMR (400 MHz, CDCl₃) of compound **3aa**.

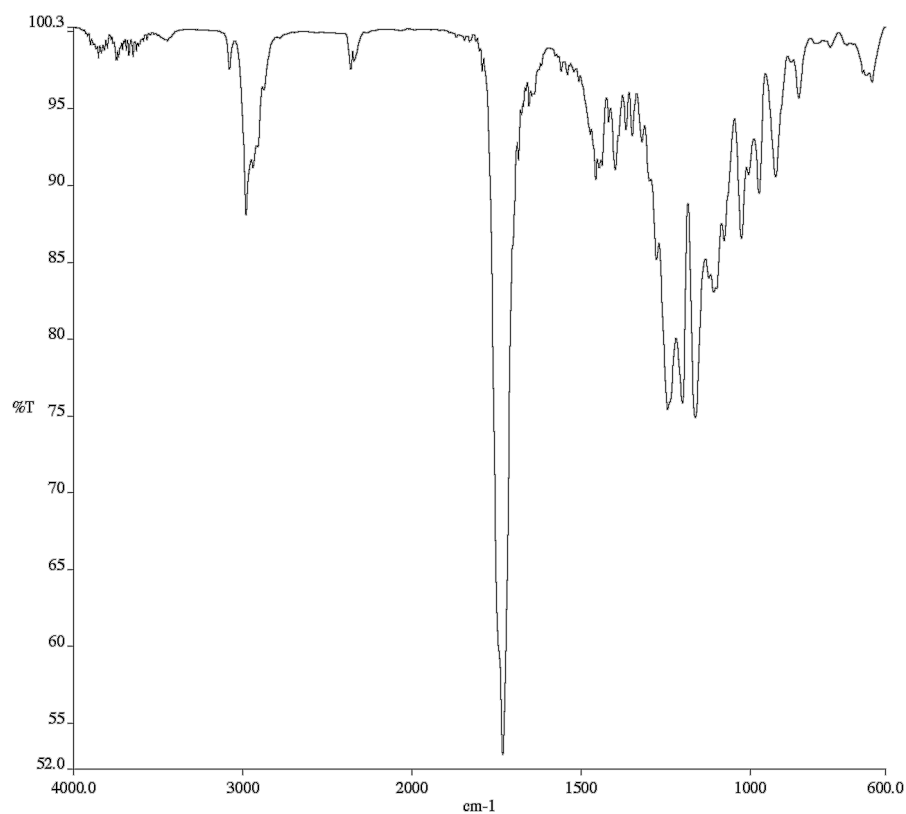


Figure A1.17 Infrared spectrum (Thin Film, NaCl) of compound **3aa**.

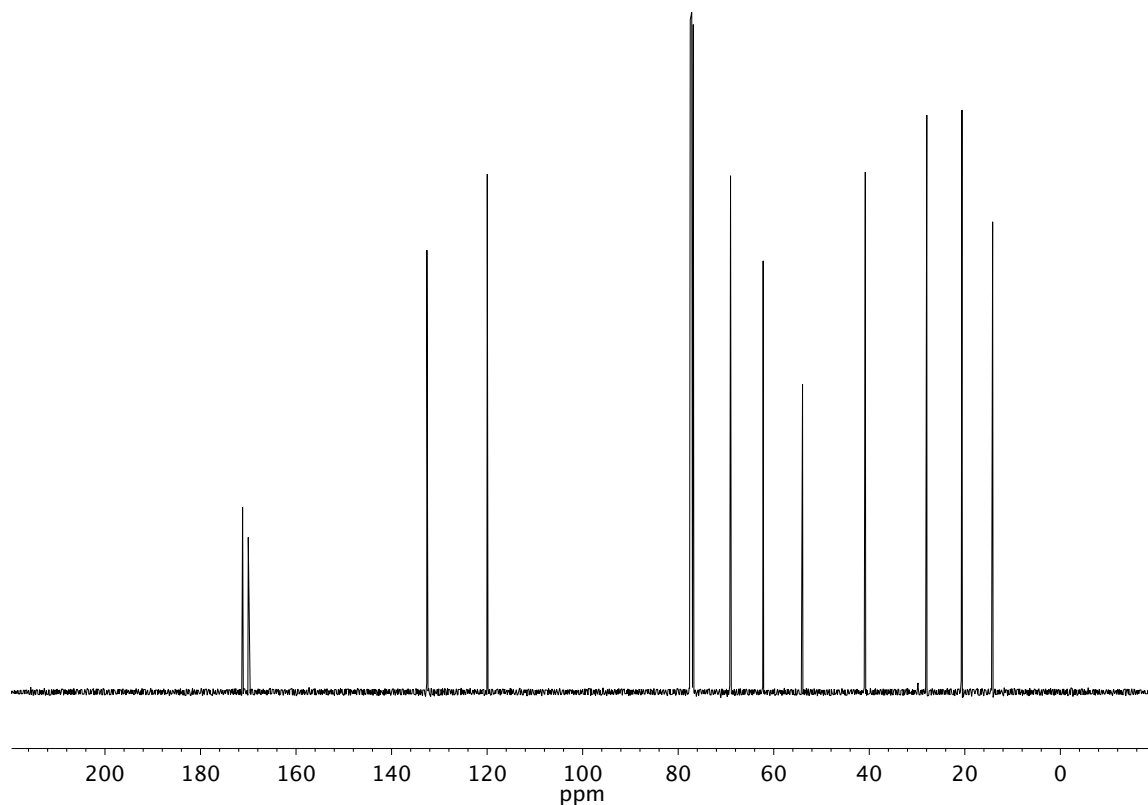


Figure A1.18 ¹³C NMR (100 MHz, CDCl₃) of compound **3aa**.

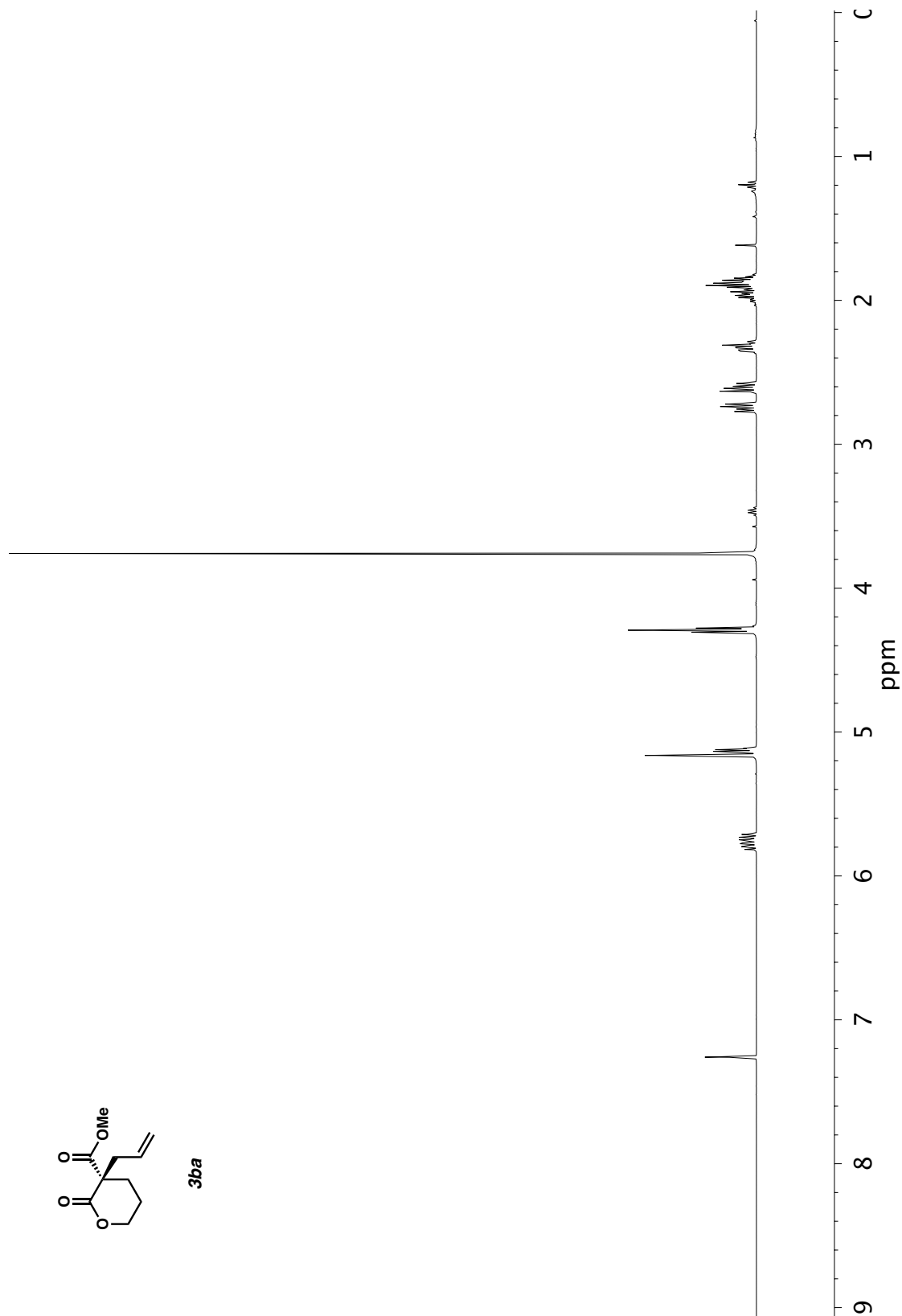


Figure A1.19 ¹H NMR (400 MHz, CDCl₃) of compound **3ba**.

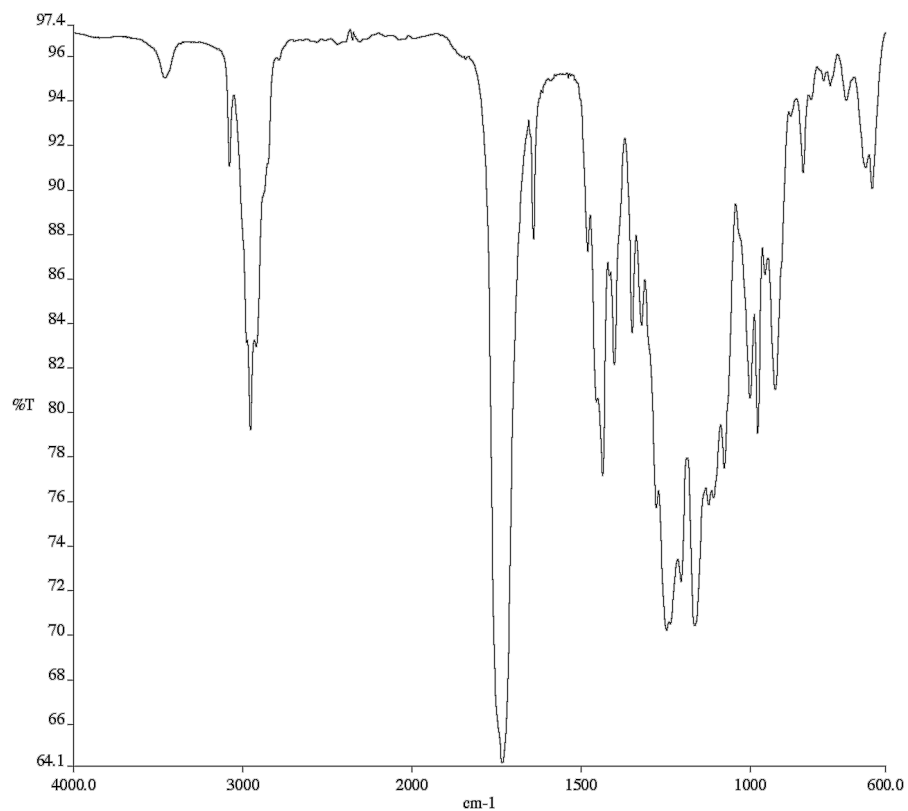


Figure A1.20 Infrared spectrum (Thin Film, NaCl) of compound **3ba**.

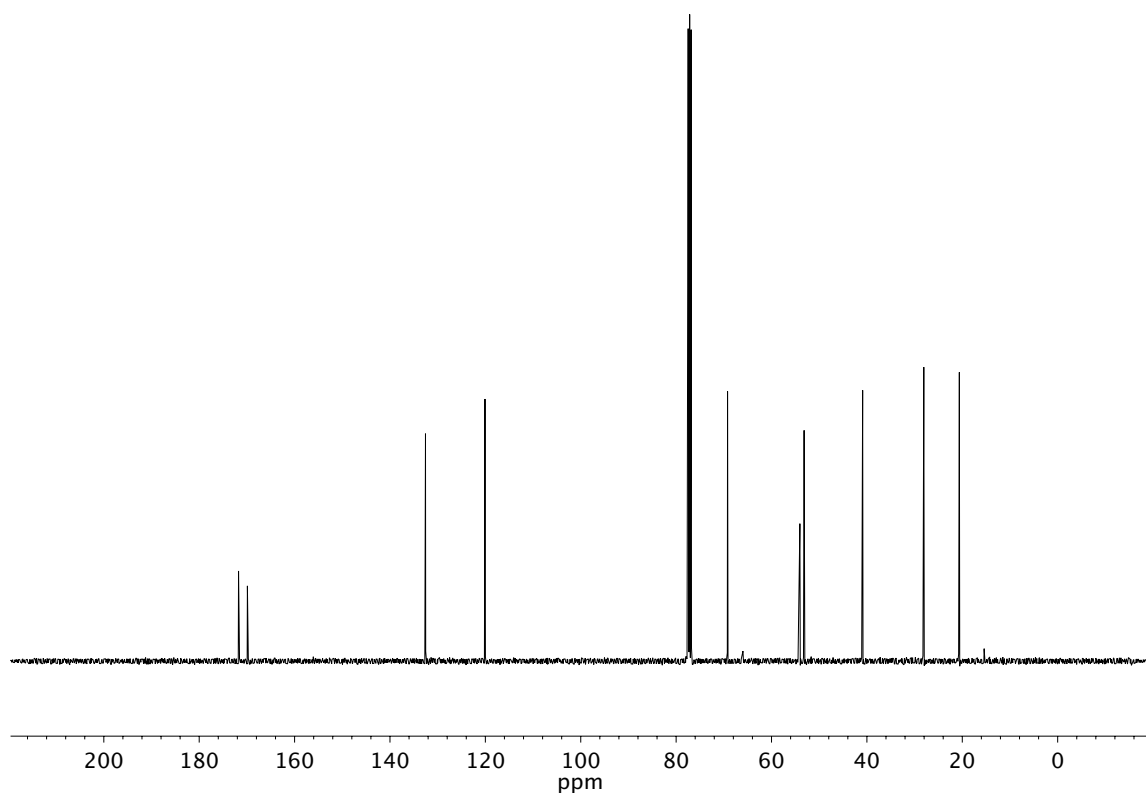


Figure A1.21 ¹³C NMR (100 MHz, CDCl₃) of compound **3ba**.

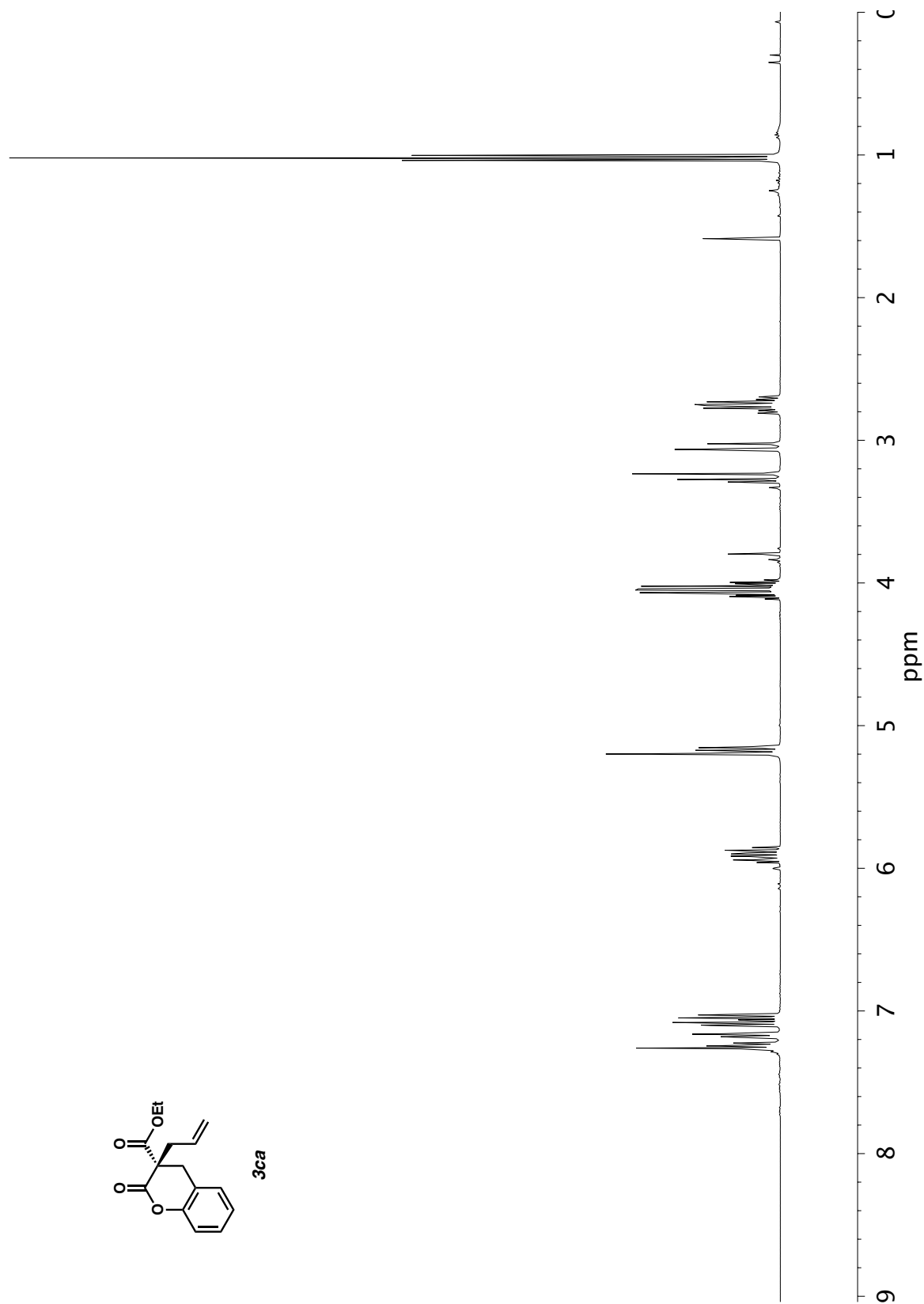


Figure A1.22 ^1H NMR (400 MHz, CDCl_3) of compound **3ca**.

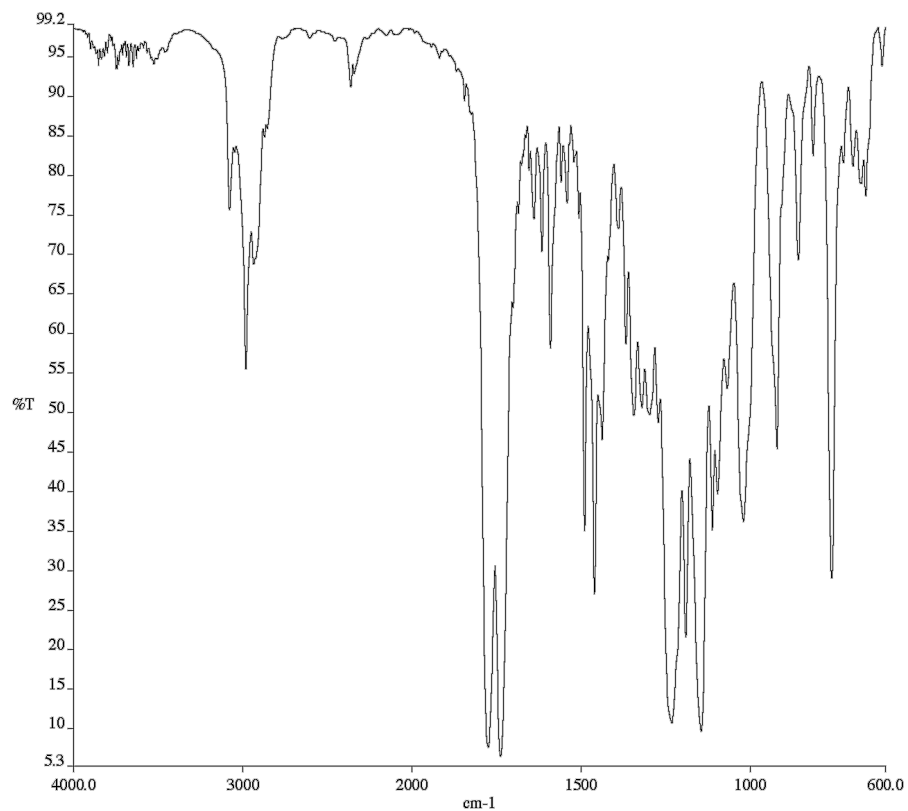


Figure A1.23 Infrared spectrum (Thin Film, NaCl) of compound **3ca**.

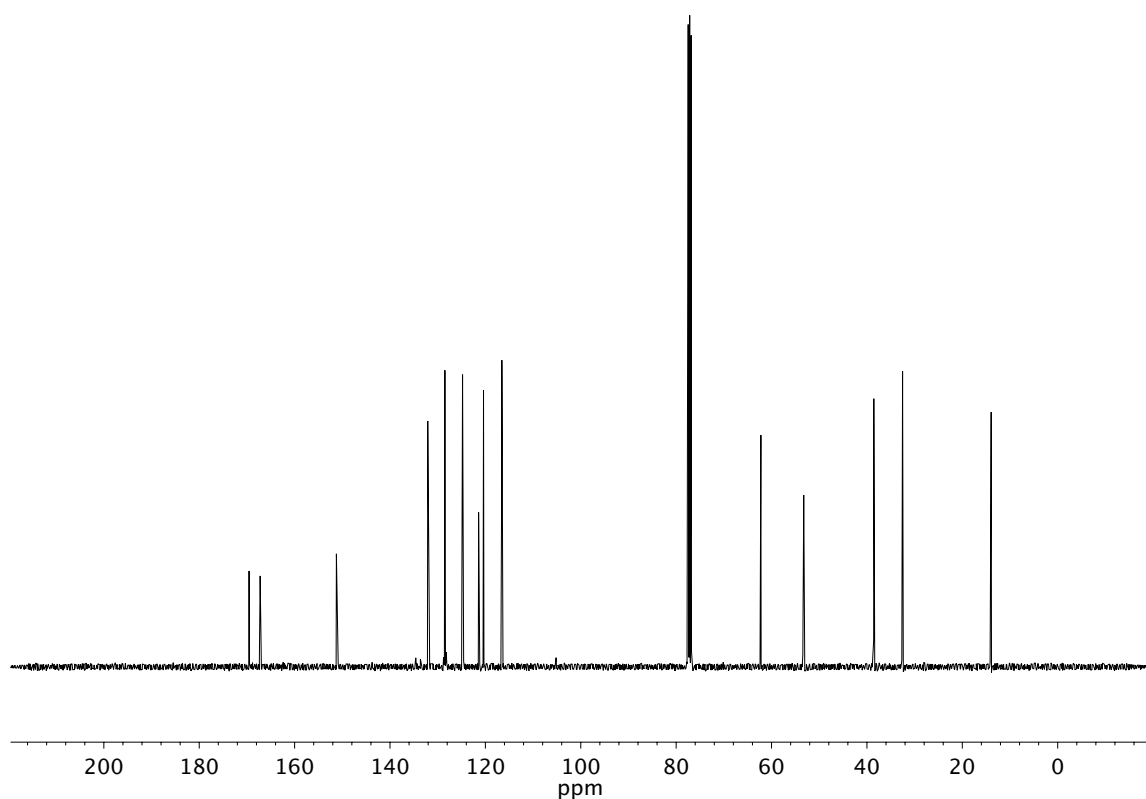


Figure A1.24 ¹³C NMR (100 MHz, CDCl₃) of compound **3ca**.

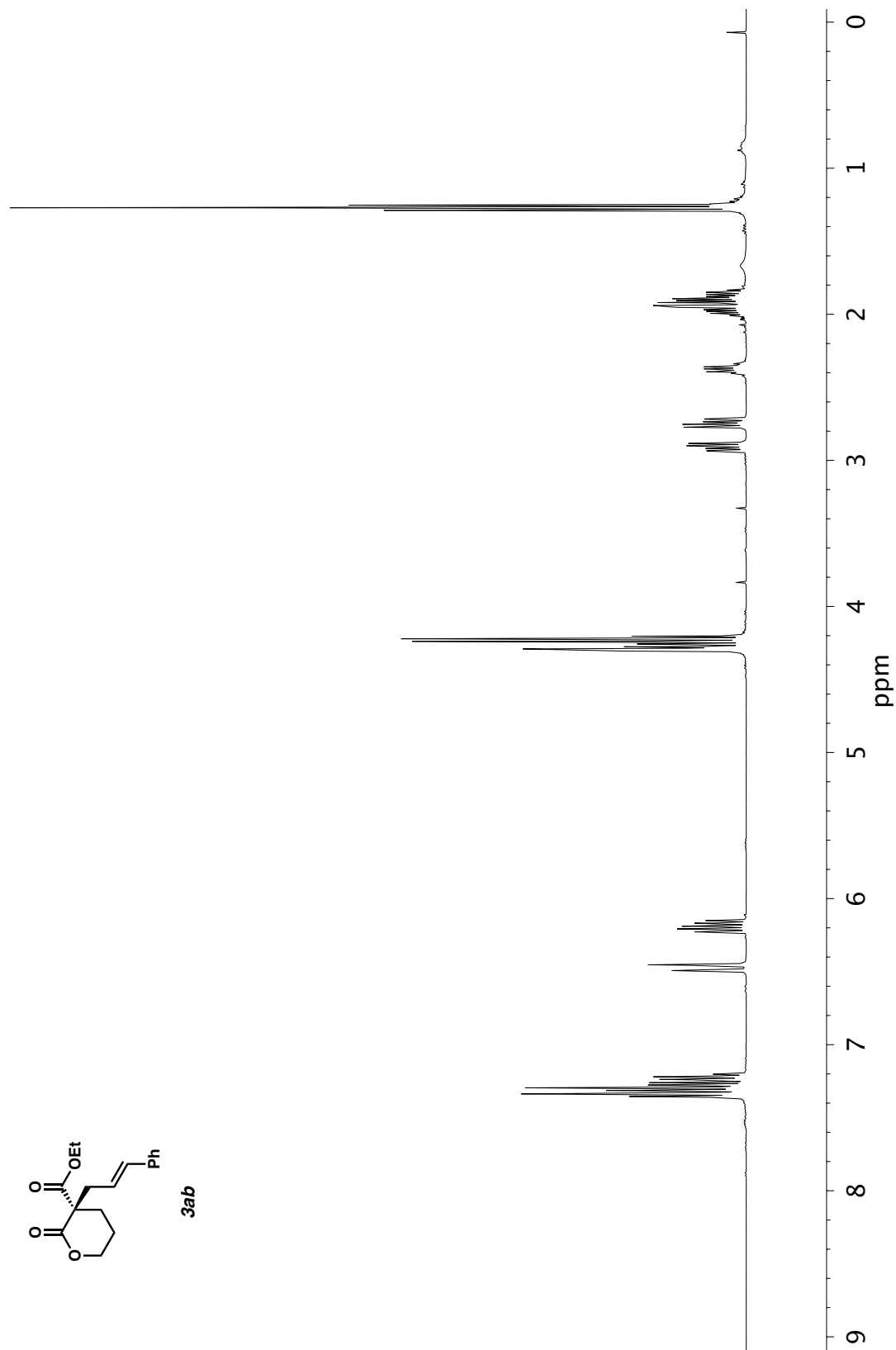


Figure A1.25 ^1H NMR (400 MHz, CDCl_3) of compound **3ab**.

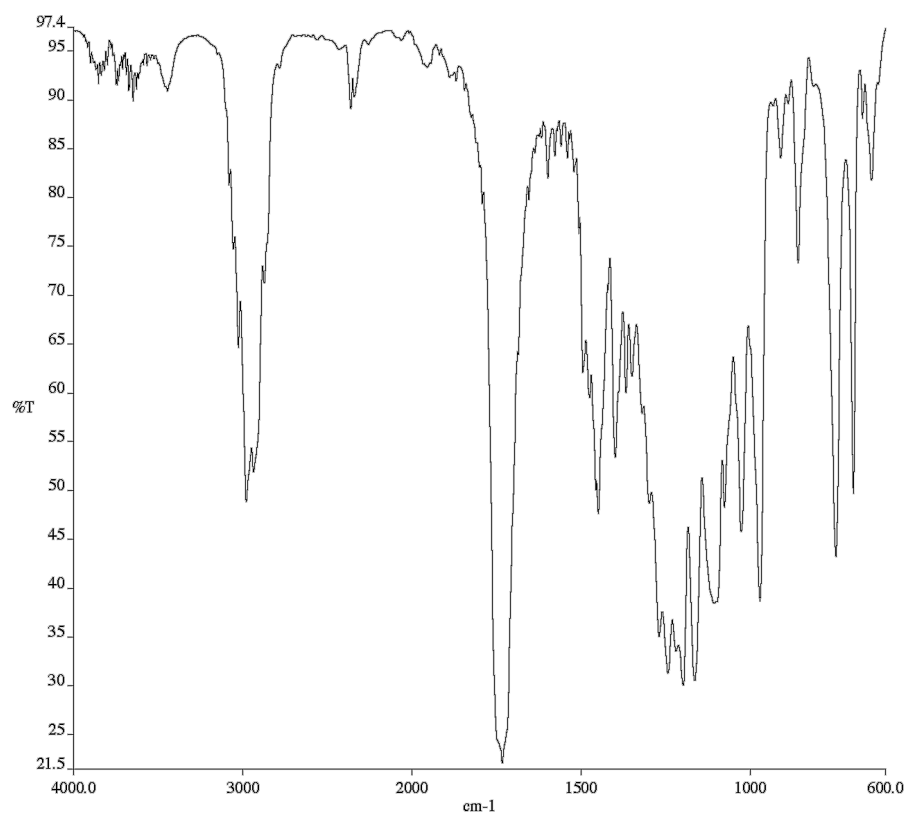


Figure A1.26 Infrared spectrum (Thin Film, NaCl) of compound **3ab**.

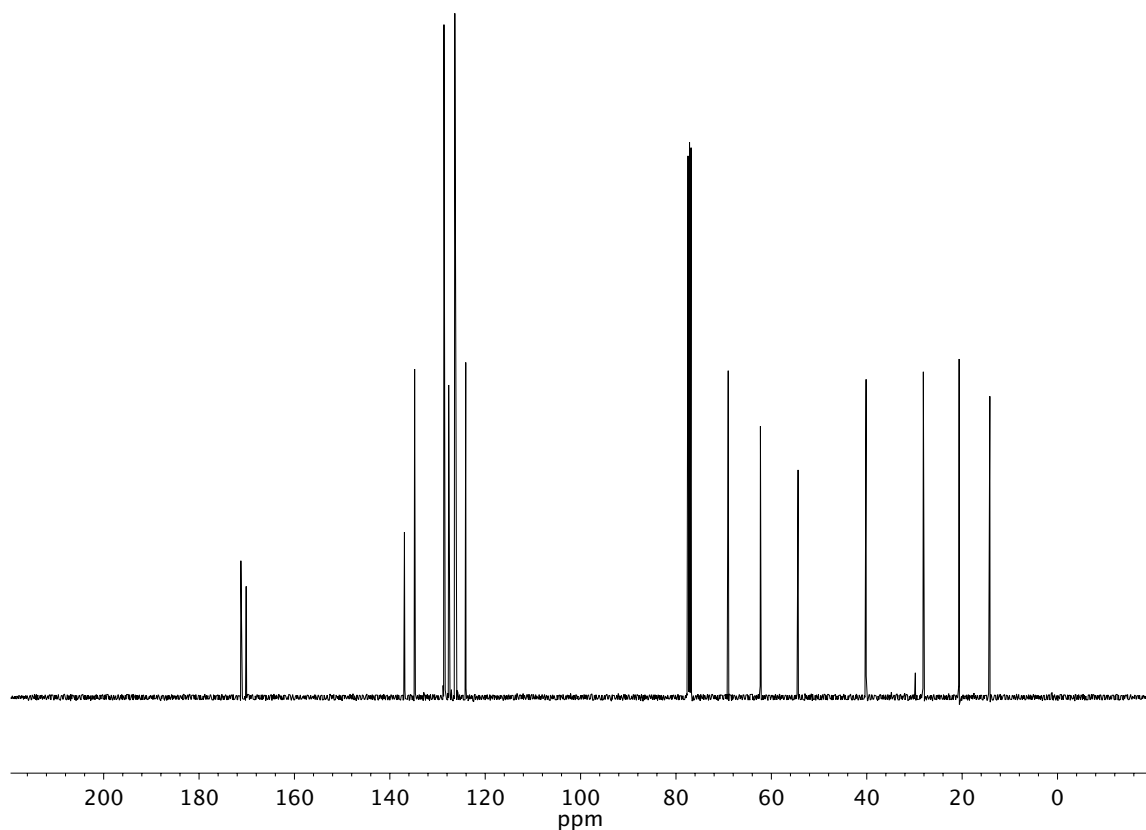


Figure A1.27 ¹³C NMR (100 MHz, CDCl₃) of compound **3ab**.

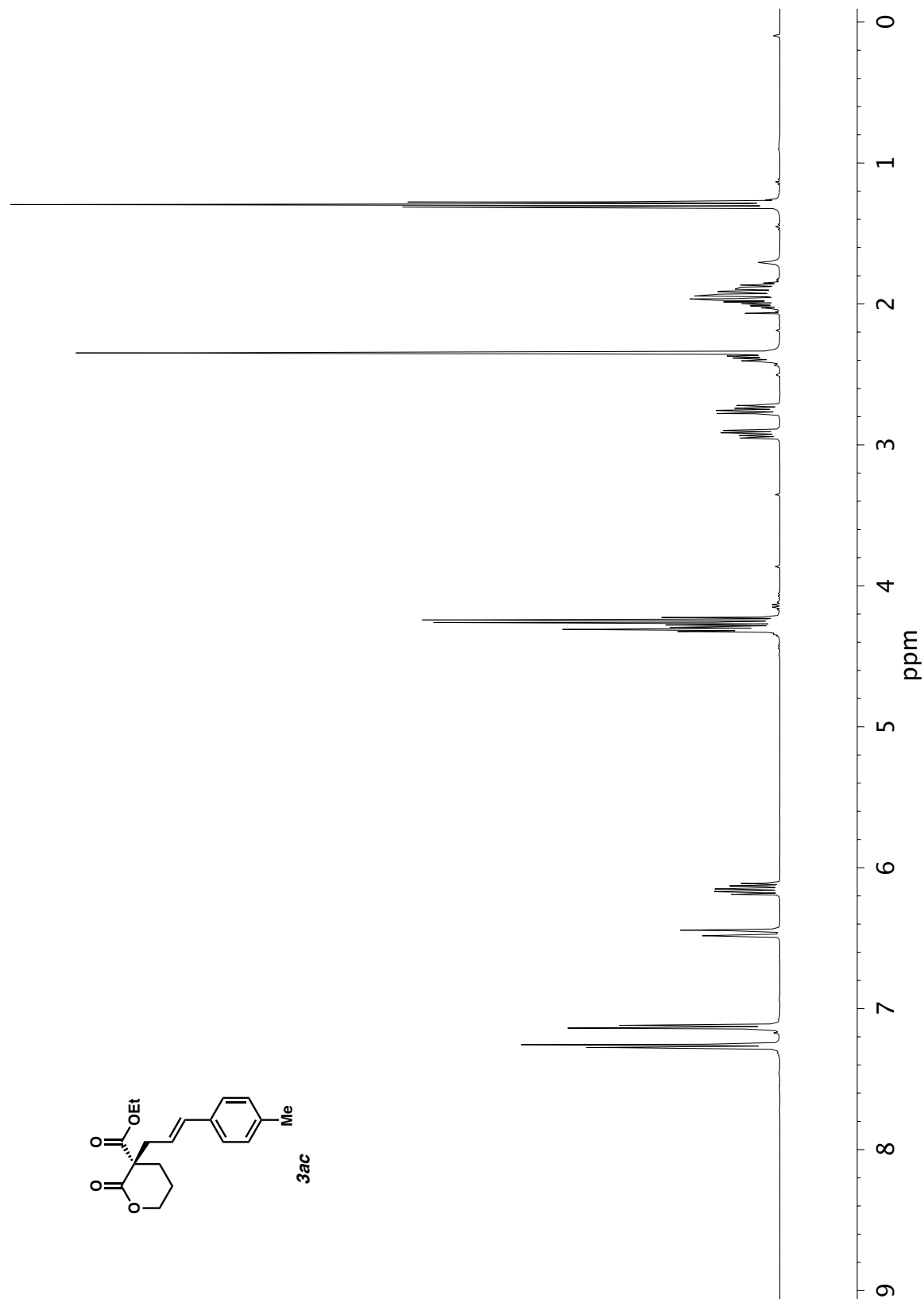


Figure A1.28 ¹H NMR (400 MHz, CDCl₃) of compound **3ac**.

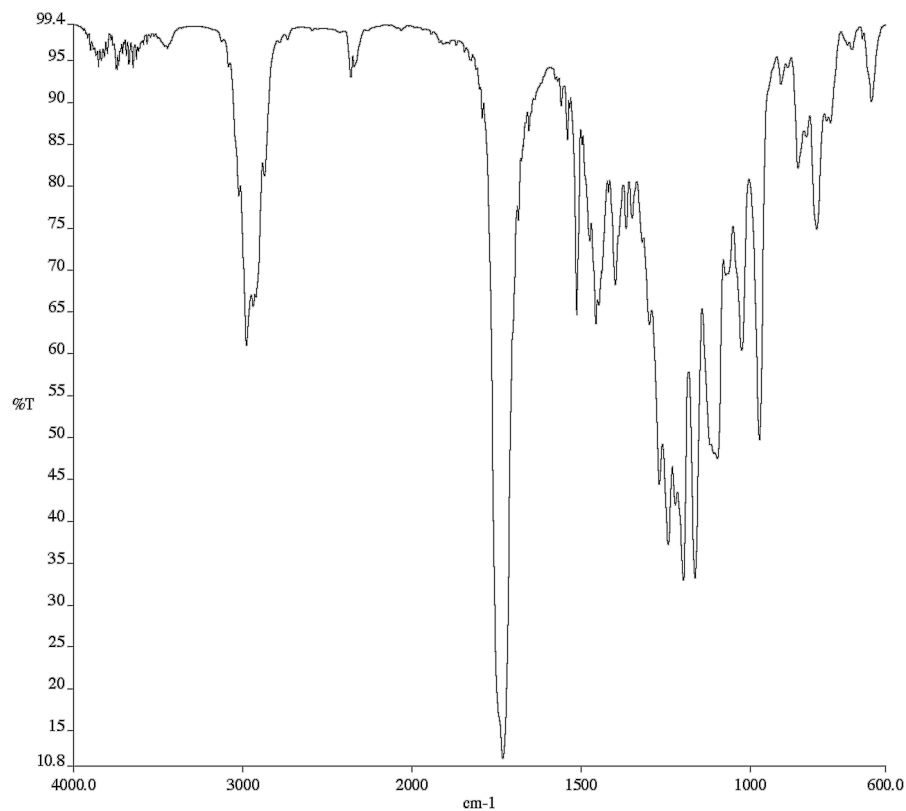


Figure A1.29 Infrared spectrum (Thin Film, NaCl) of compound **3ac**.

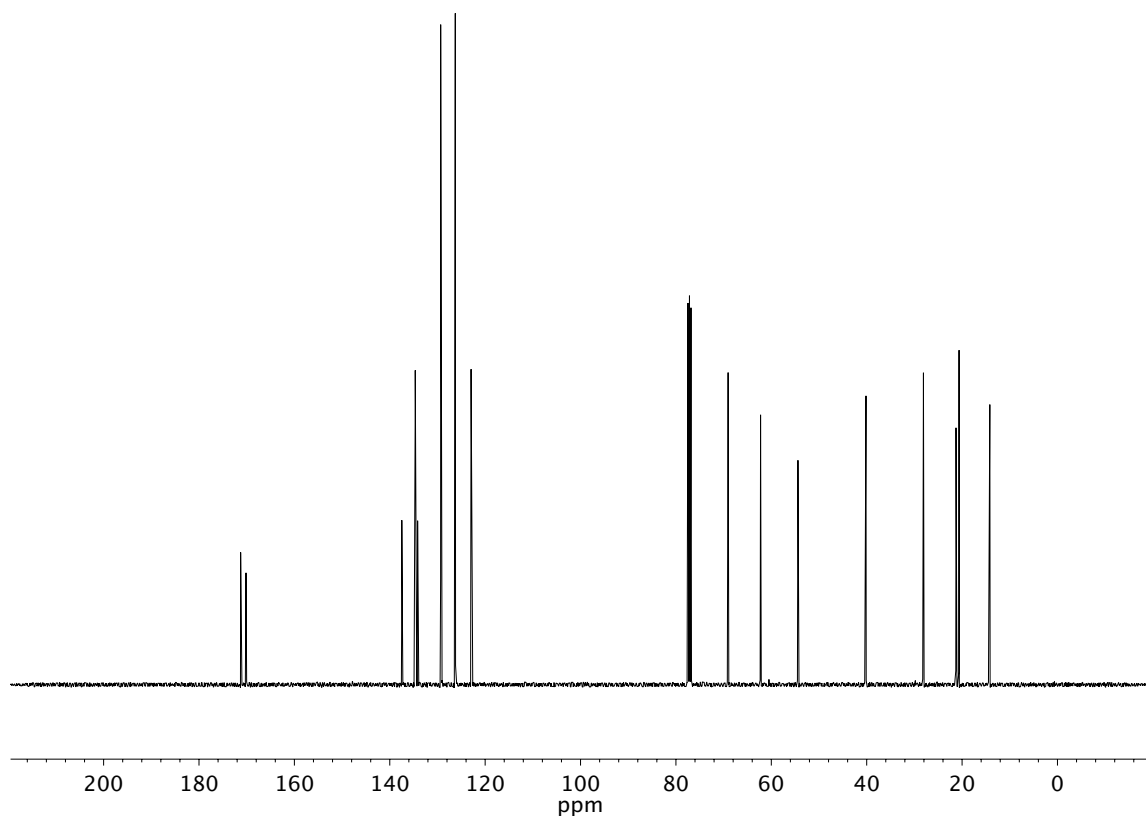


Figure A1.30 ¹³C NMR (100 MHz, CDCl₃) of compound **3ac**.

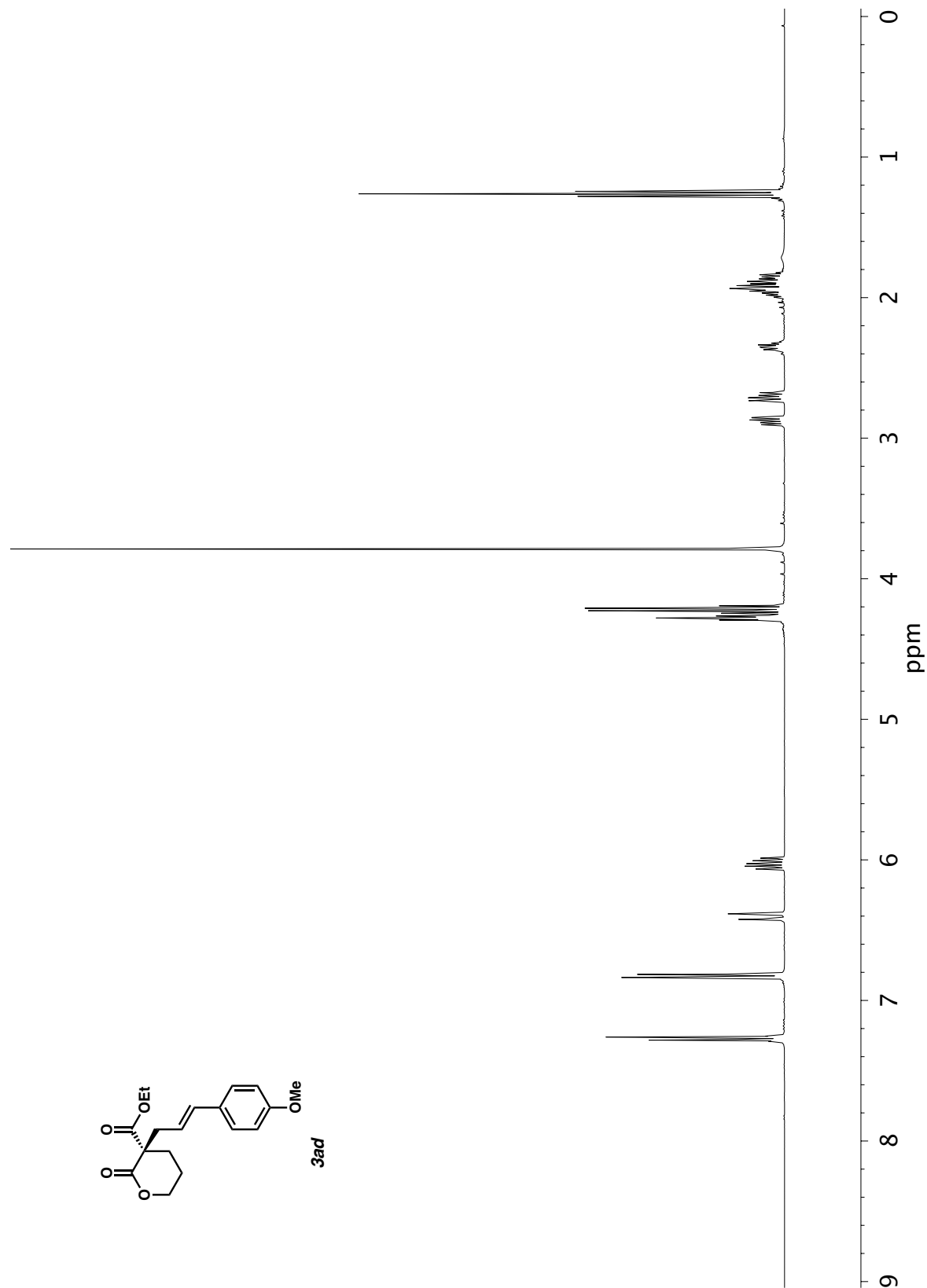


Figure A1.31 ^1H NMR (400 MHz, CDCl_3) of compound **3ad**.

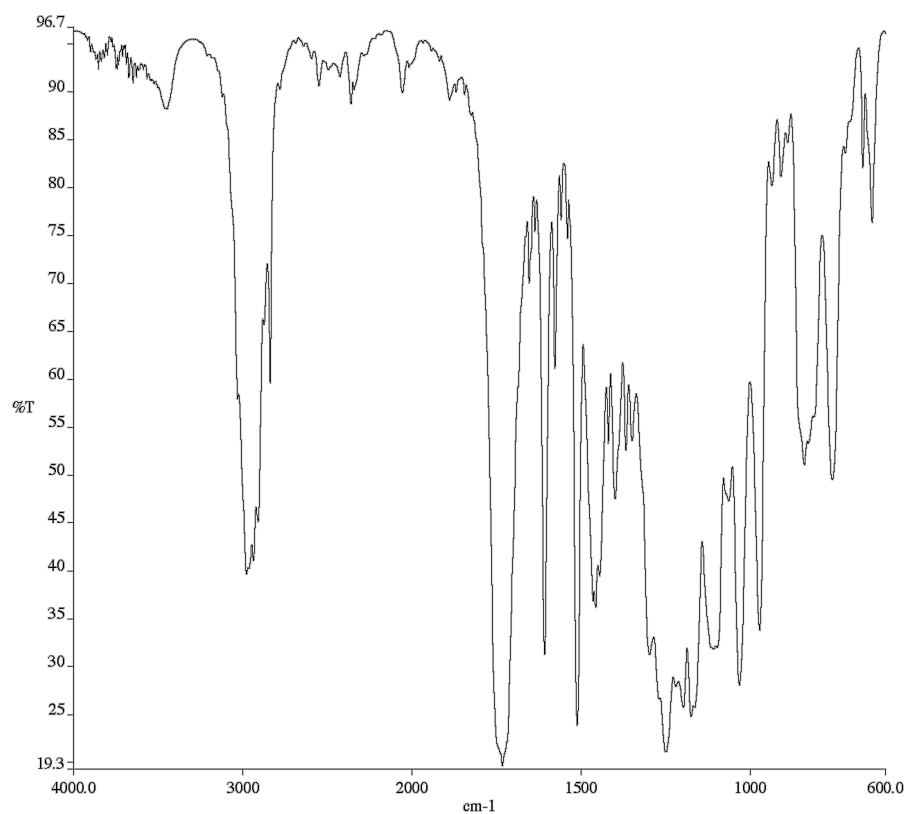


Figure A1.32 Infrared spectrum (Thin Film, NaCl) of compound **3ad**.

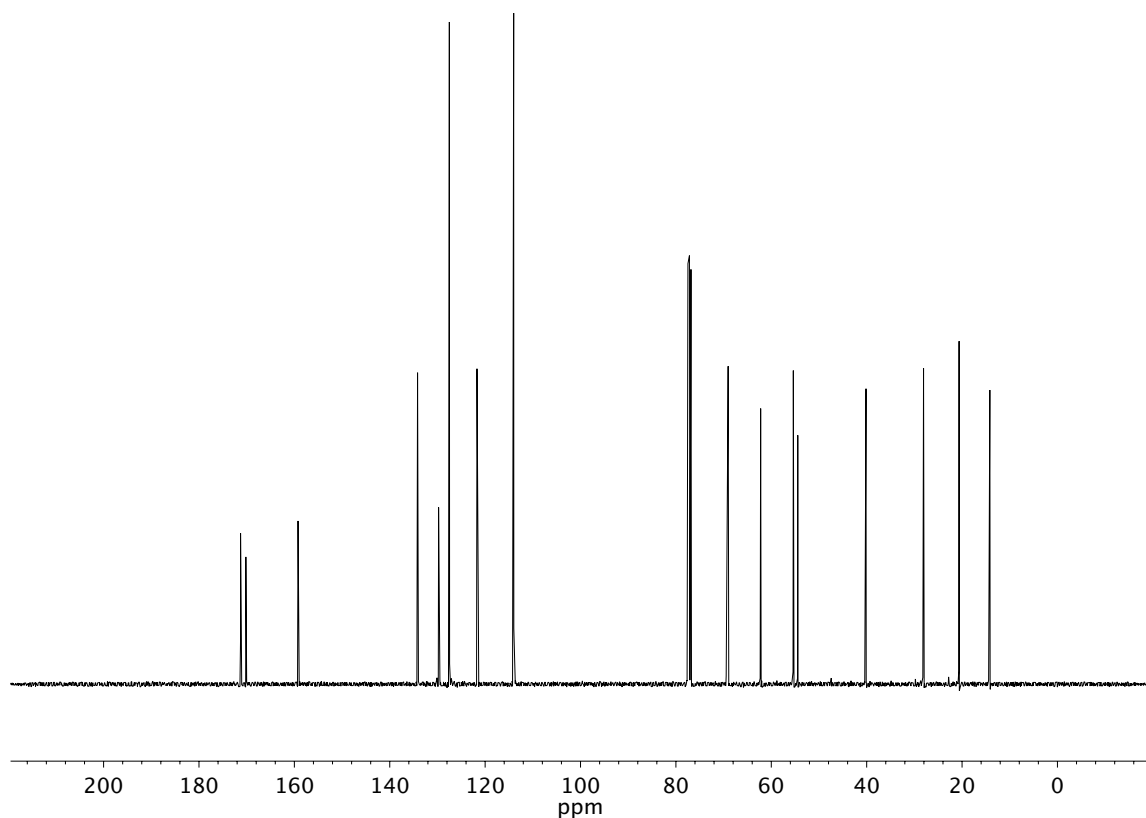


Figure A1.33 ¹³C NMR (100 MHz, CDCl₃) of compound **3ad**.

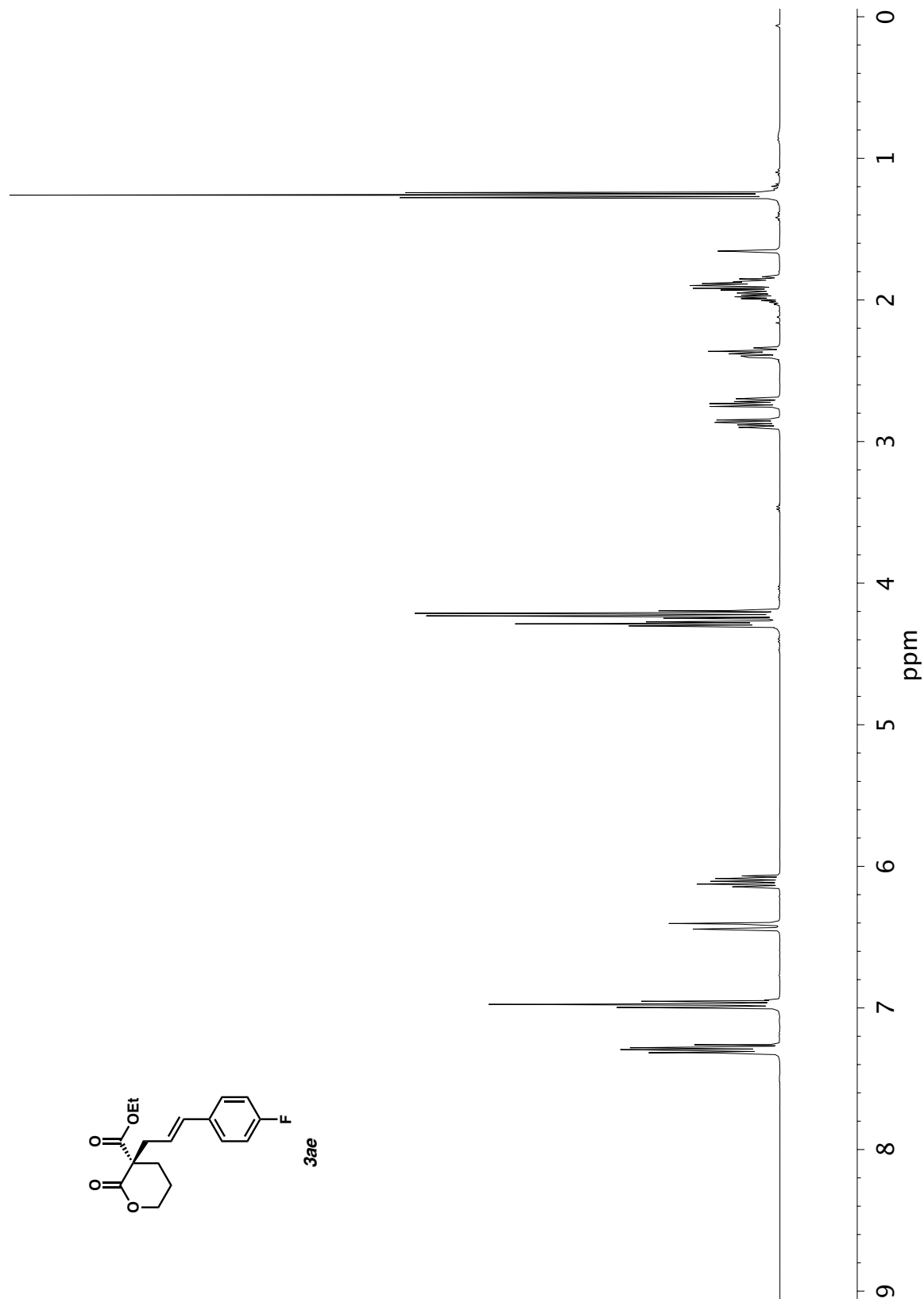


Figure A1.34 ^1H NMR (400 MHz, CDCl_3) of compound **3ae**.

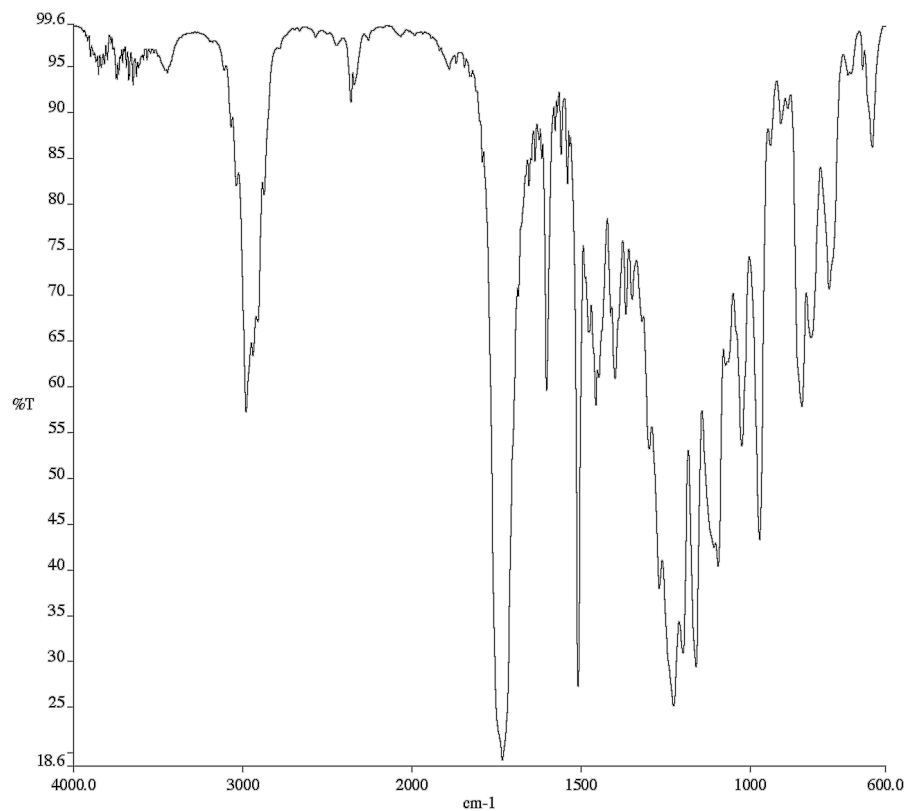


Figure A1.35 Infrared spectrum (Thin Film, NaCl) of compound **3ae**.

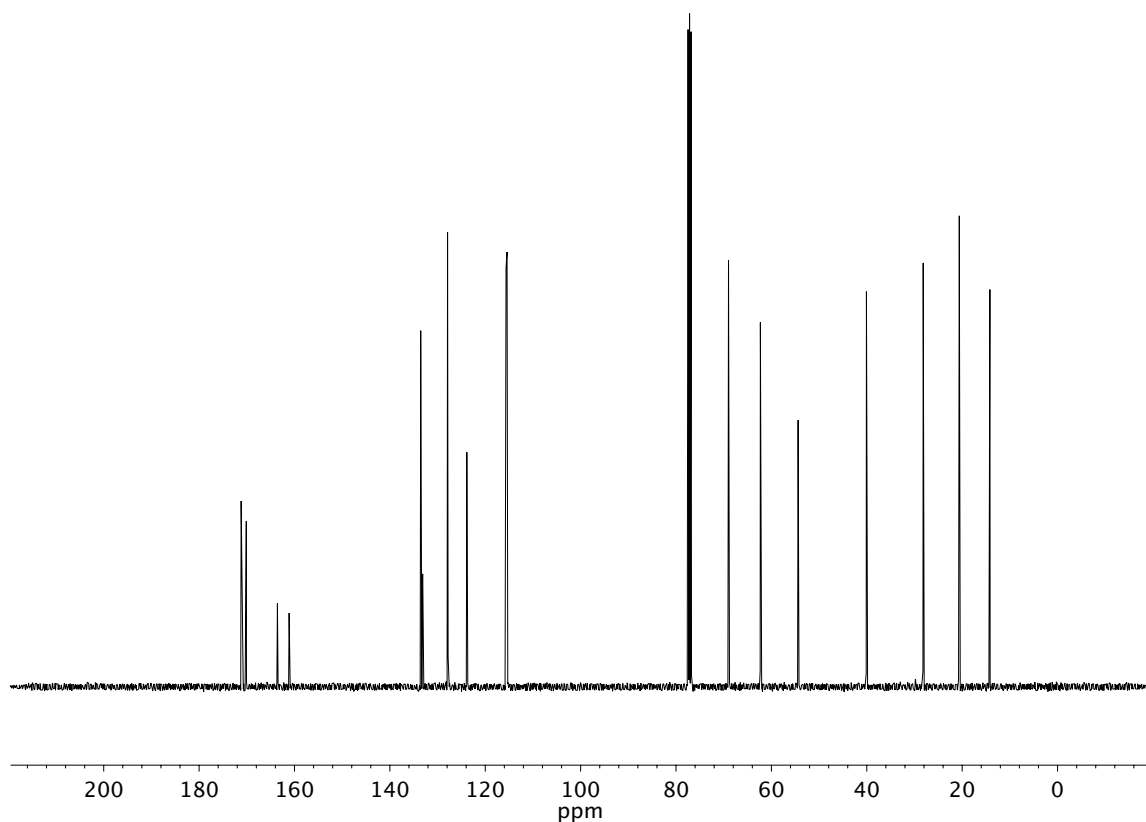


Figure A1.36 ¹³C NMR (100 MHz, CDCl₃) of compound **3ae**.

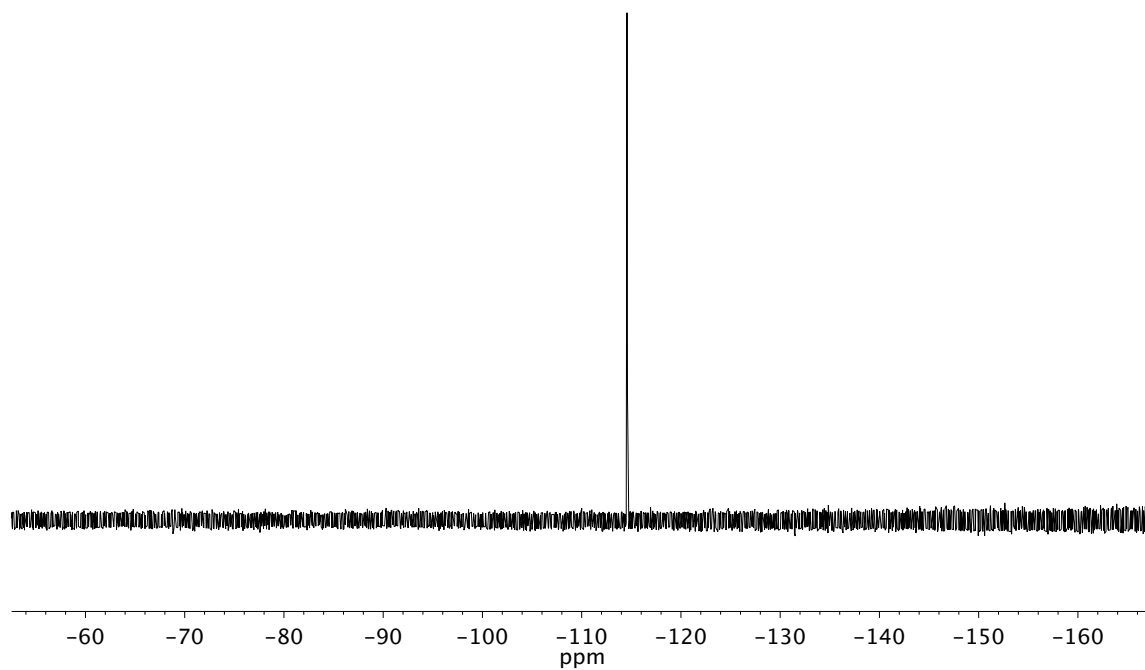


Figure A1.37 ^{19}F NMR (282 MHz, CDCl_3) of compound **3ae**

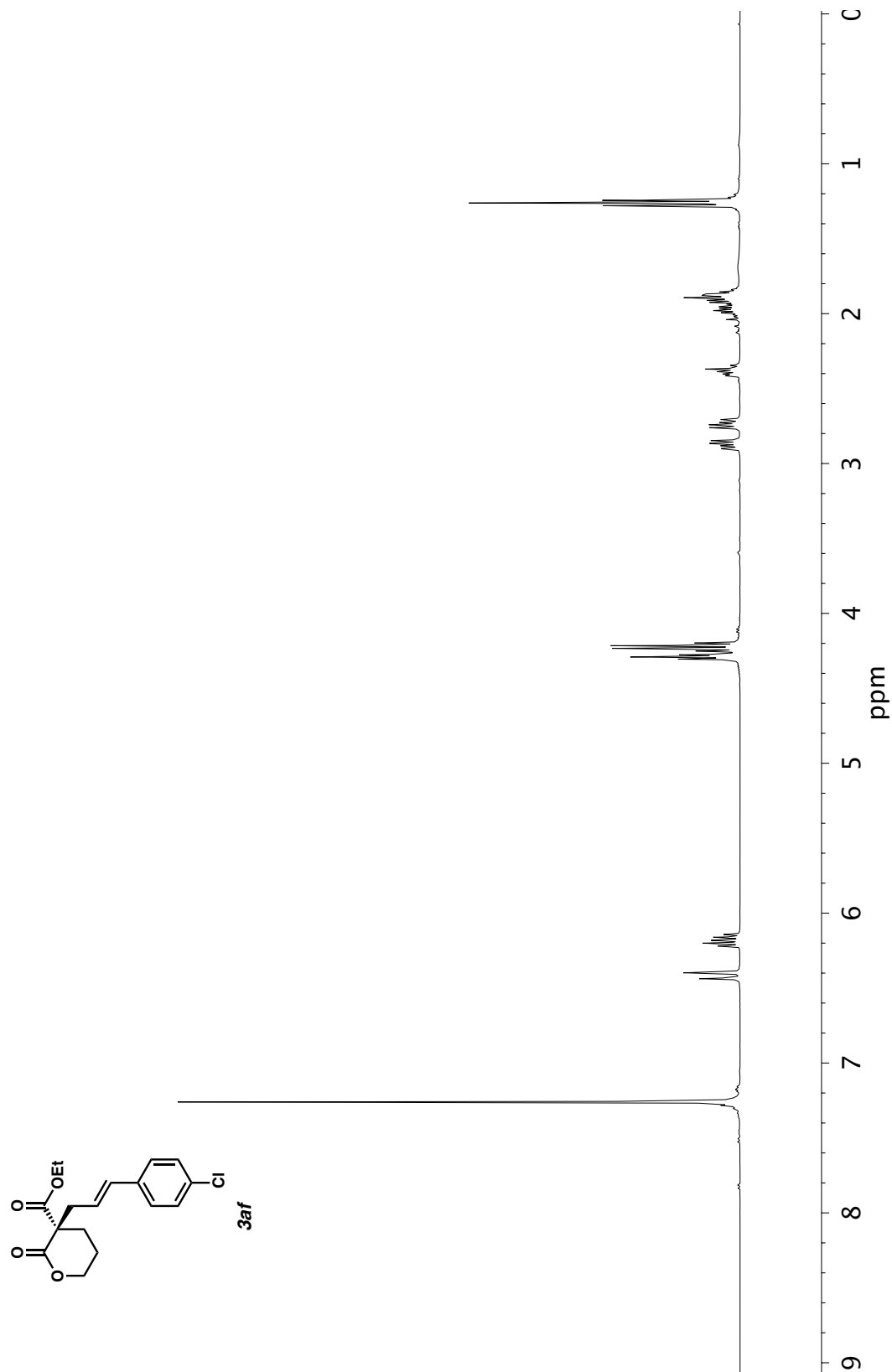


Figure A1.38 ^1H NMR (400 MHz, CDCl_3) of compound **3af**.

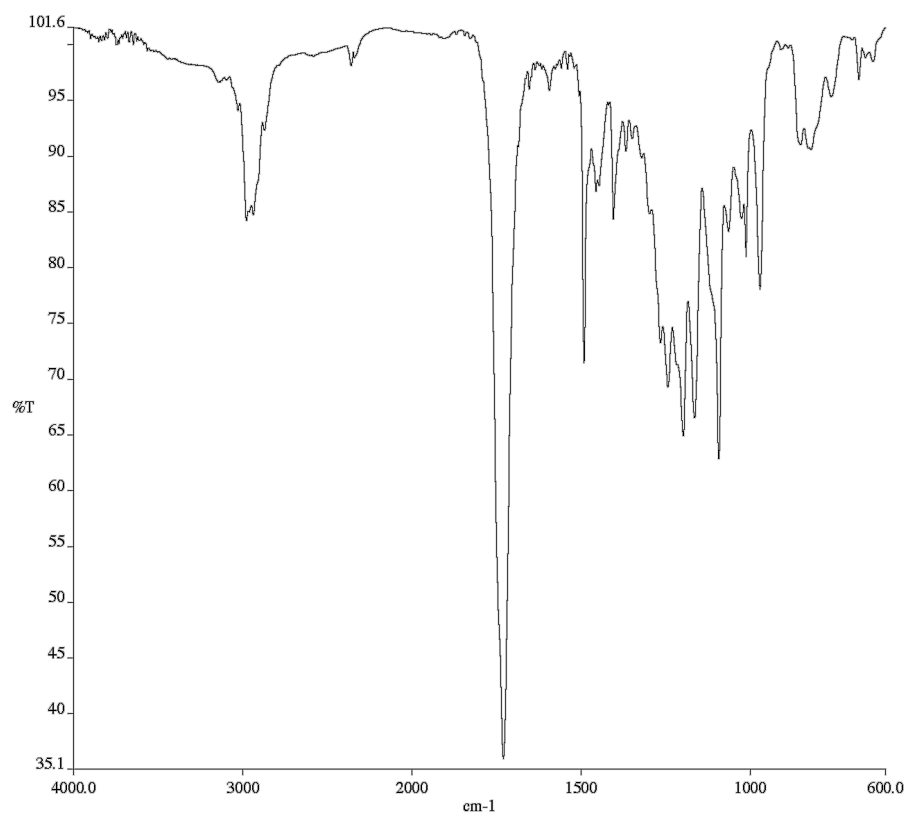


Figure A1.39 Infrared spectrum (Thin Film, NaCl) of compound **3af**.

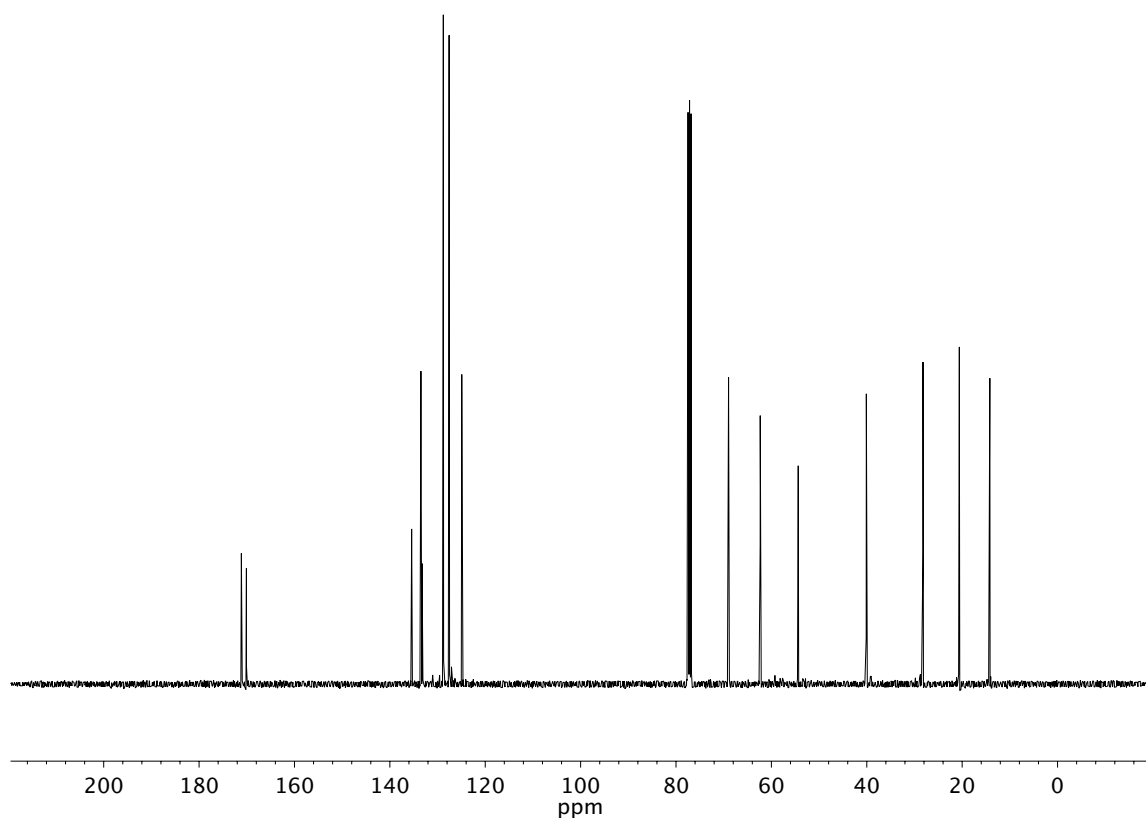


Figure A1.40 ¹³C NMR (100 MHz, CDCl₃) of compound **3af**.

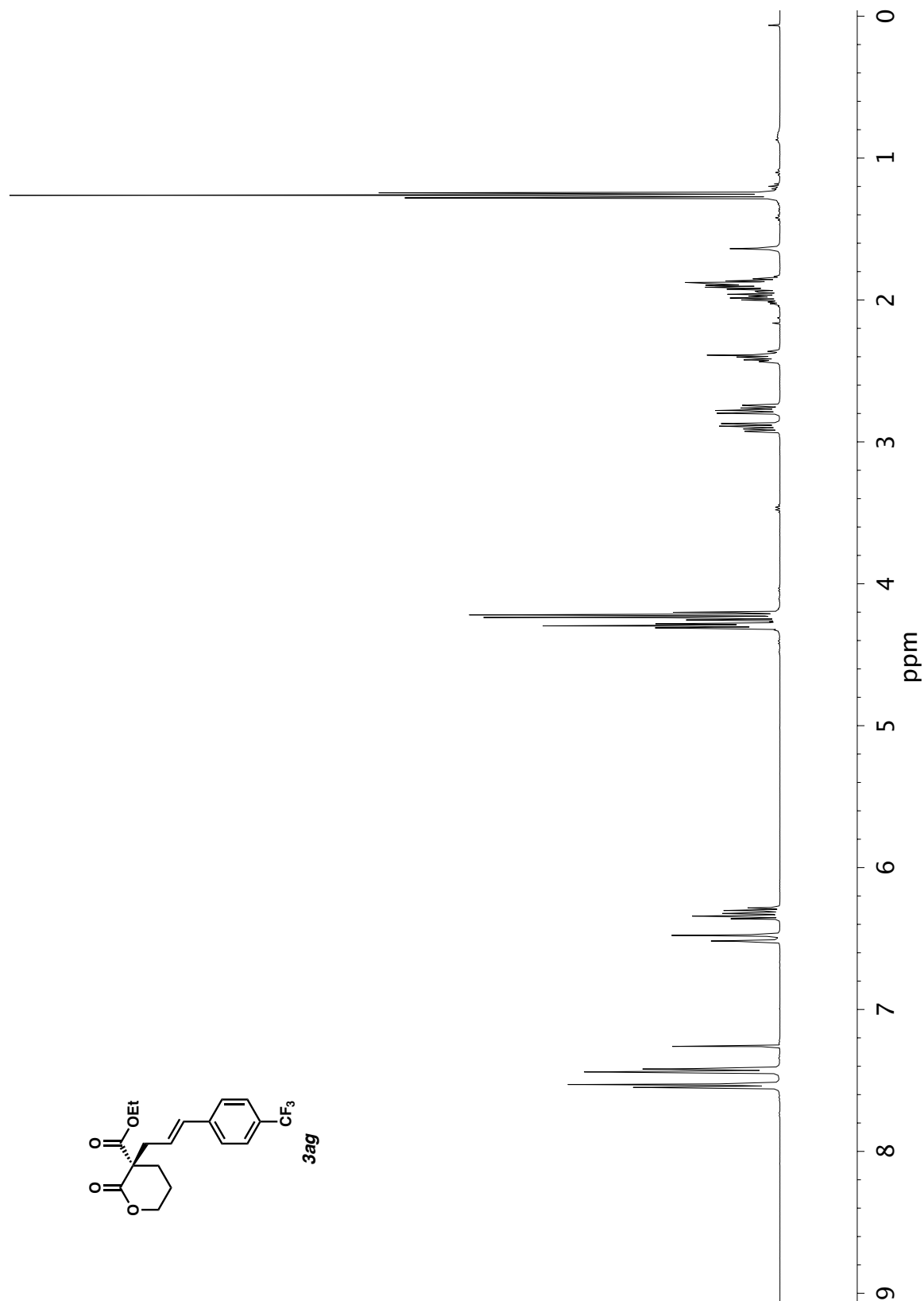


Figure A1.41 ^1H NMR (400 MHz, CDCl_3) of compound **3ag**.

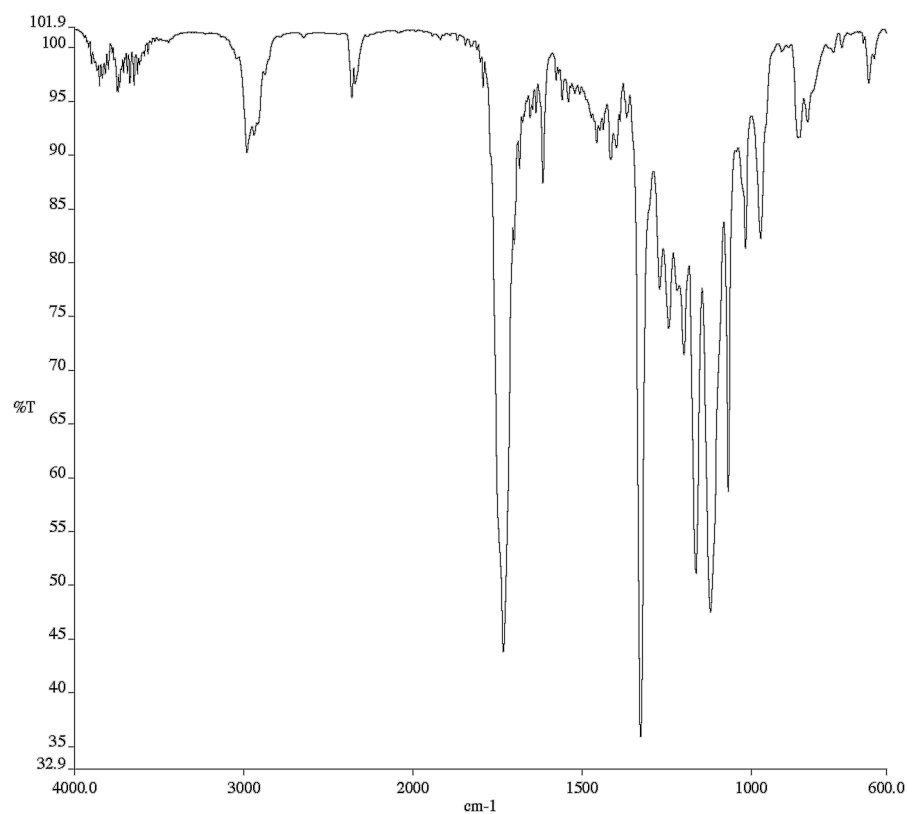


Figure A1.42 Infrared spectrum (Thin Film, NaCl) of compound **3ag**.

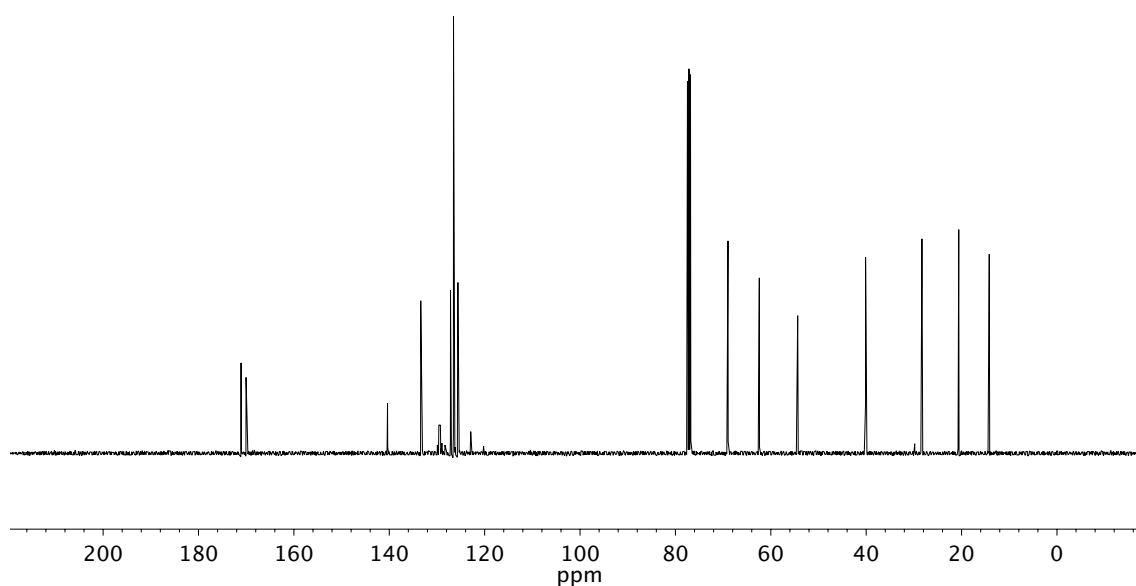


Figure A1.43 ¹³C NMR (100 MHz, CDCl₃) of compound **3ag**.

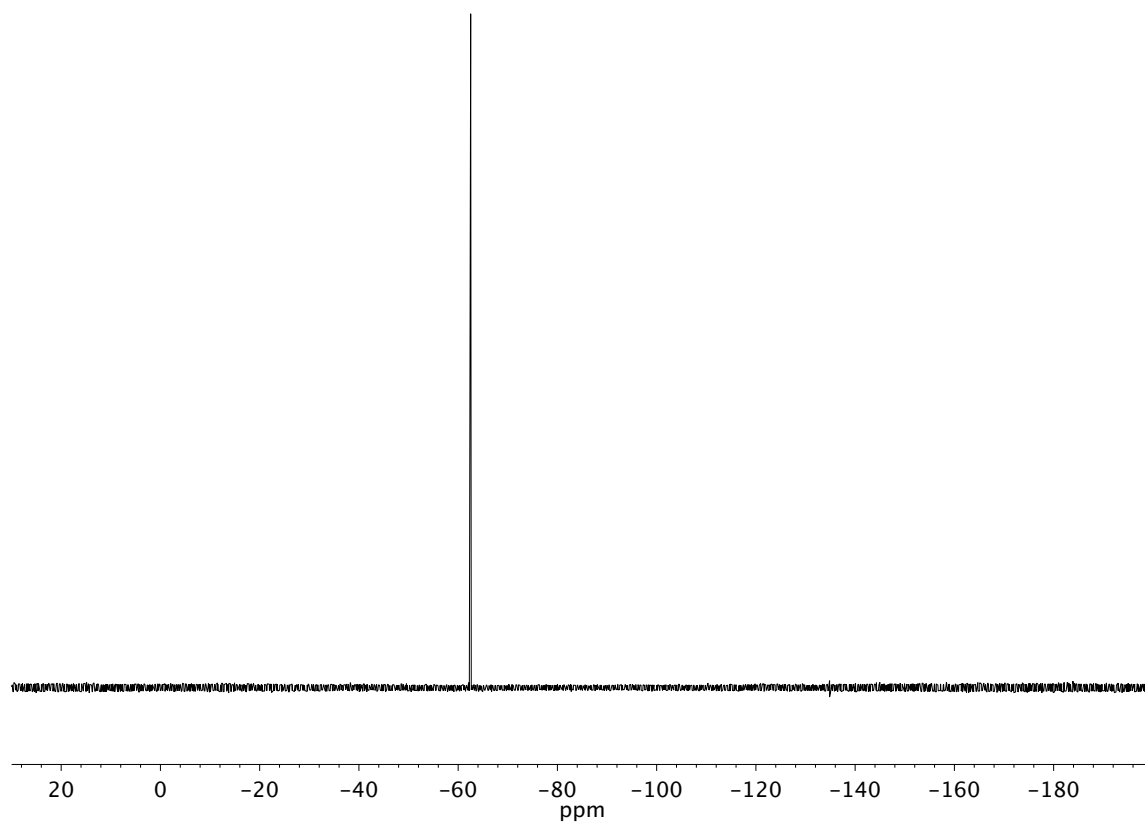


Figure A1.44 ^{19}F NMR (282 MHz, CDCl_3) of compound **3ag**.

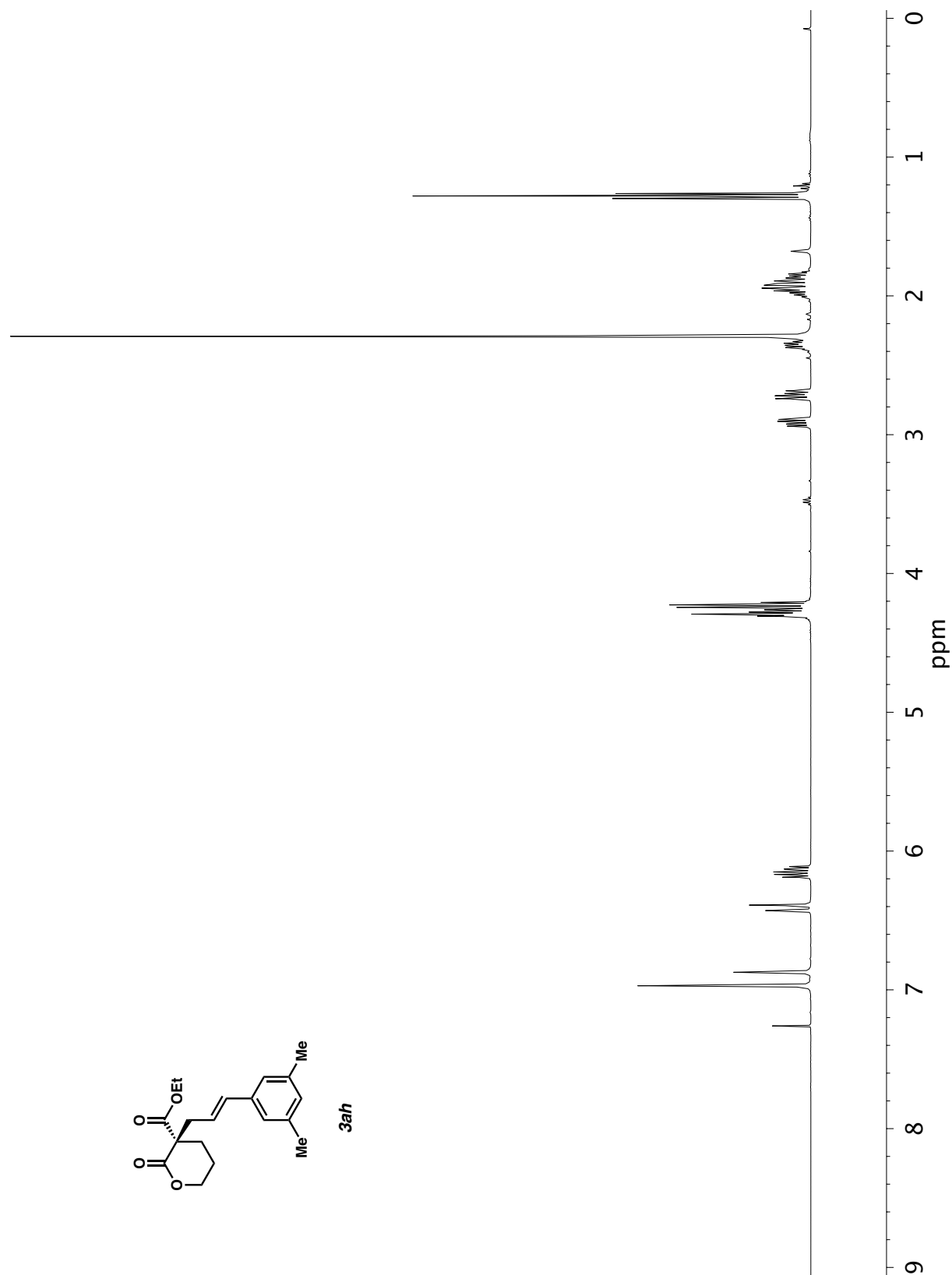


Figure A1.45 ^1H NMR (400 MHz, CDCl_3) of compound **3ah**.

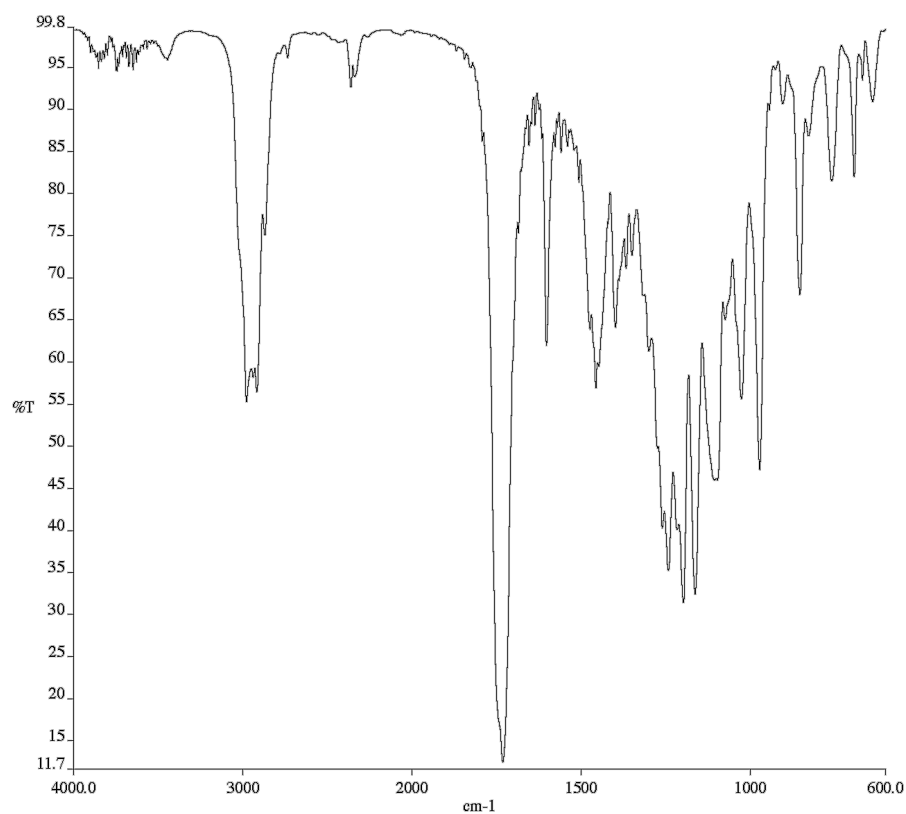


Figure A1.46 Infrared spectrum (Thin Film, NaCl) of compound **3ah**.

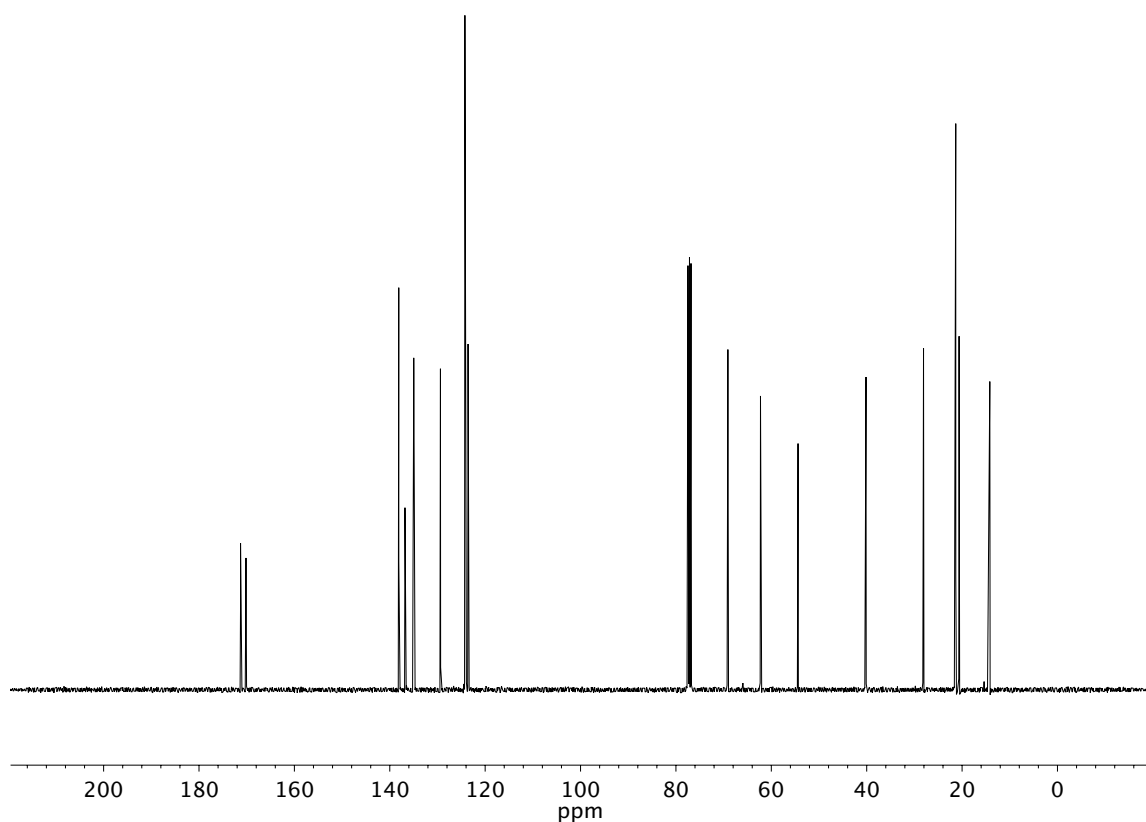


Figure A1.47 ¹³C NMR (100 MHz, CDCl₃) of compound **3ah**.

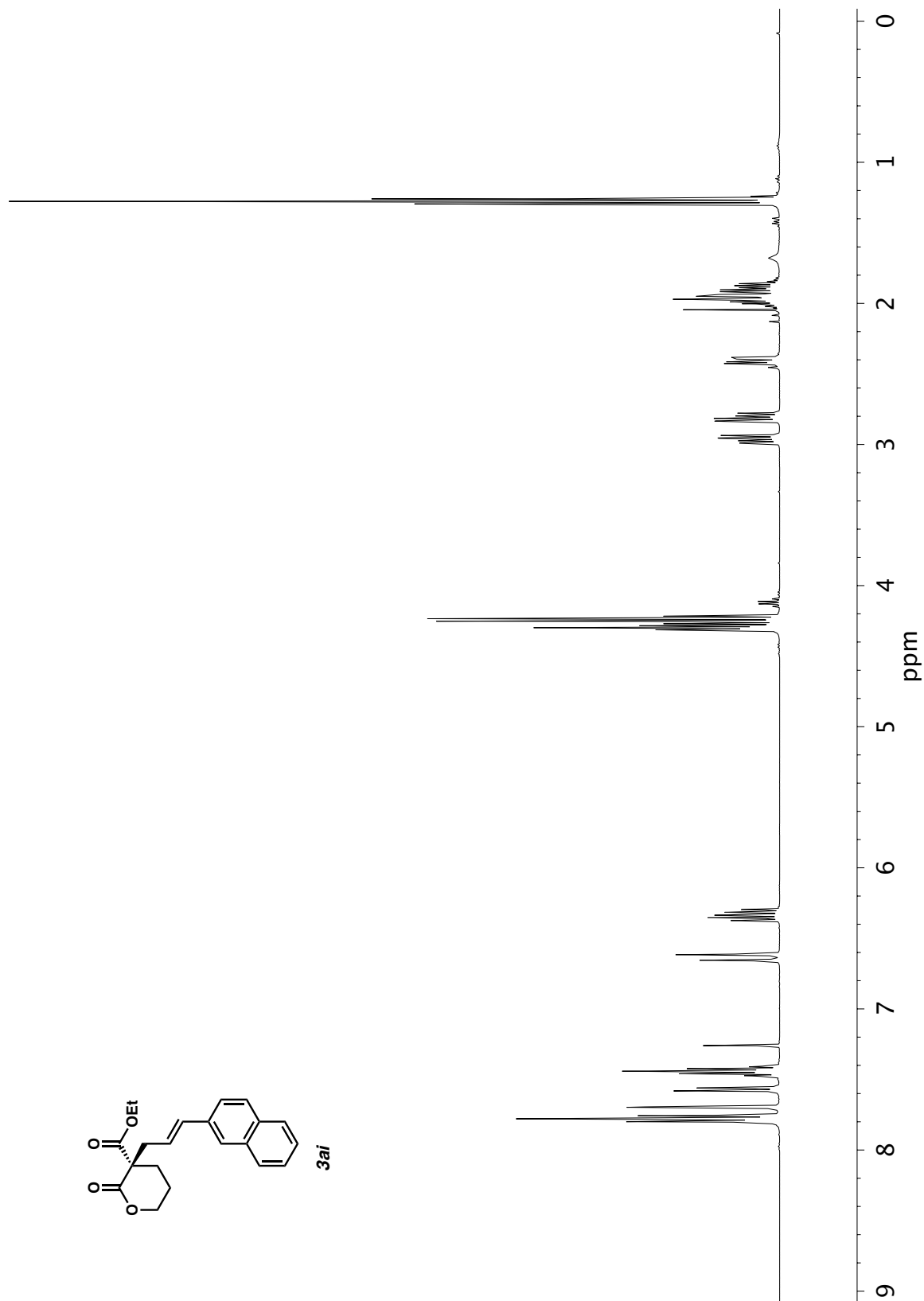


Figure A1.48 ^1H NMR (400 MHz, CDCl_3) of compound **3ai**.

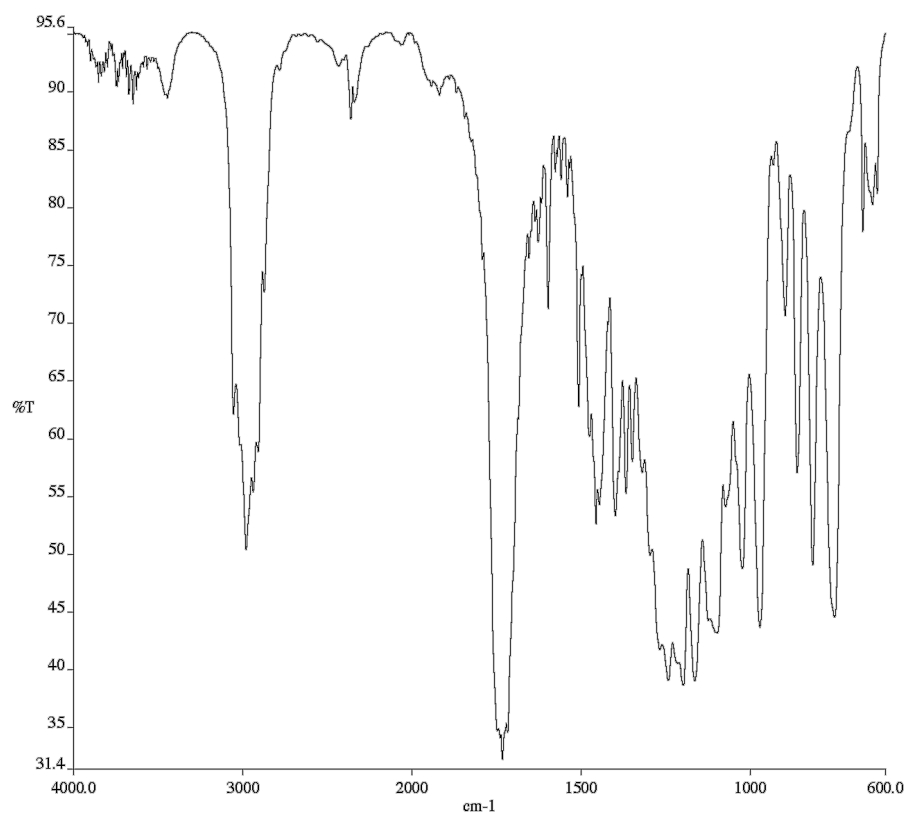


Figure A1.49 Infrared spectrum (Thin Film, NaCl) of compound **3ai**.

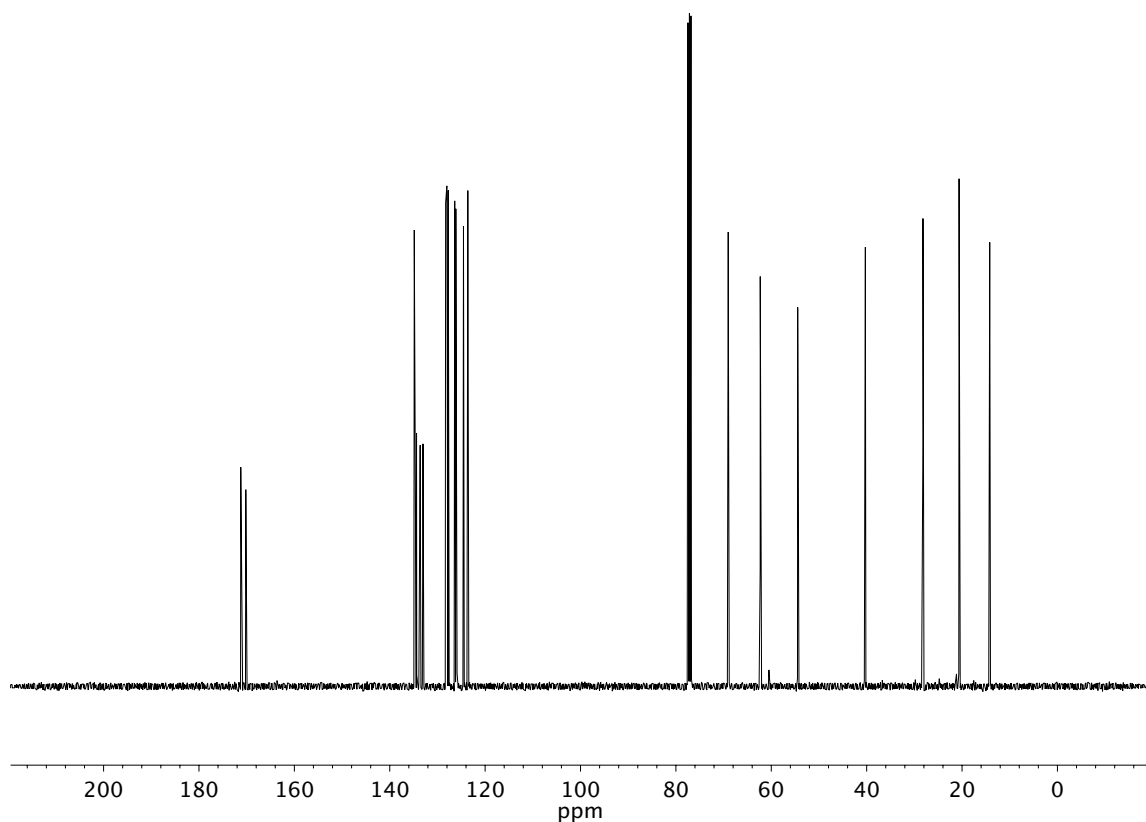


Figure A1.50 ¹³C NMR (100 MHz, CDCl₃) of compound **3ai**.

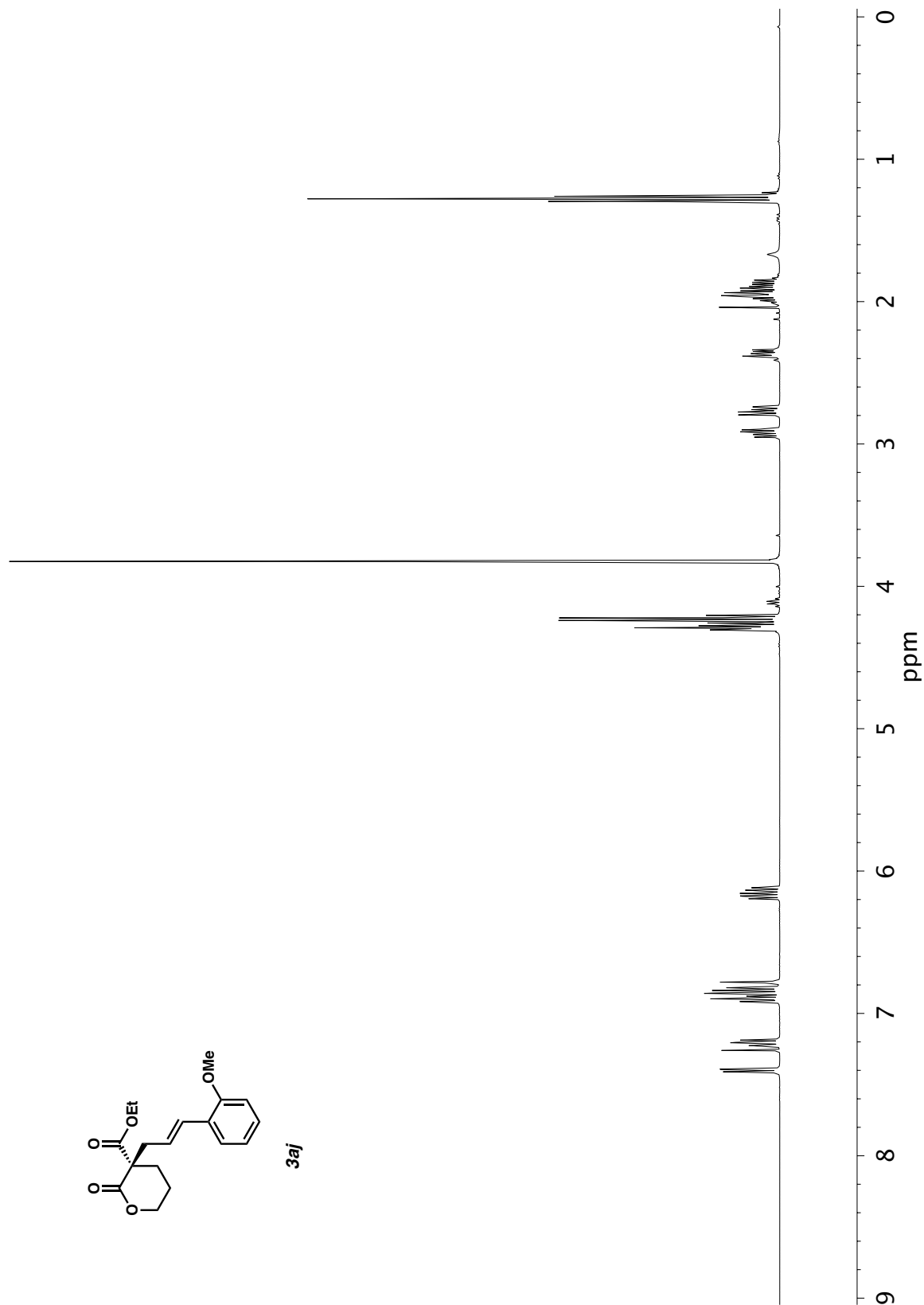


Figure A1.51 ^1H NMR (400 MHz, CDCl_3) of compound **3aj**.

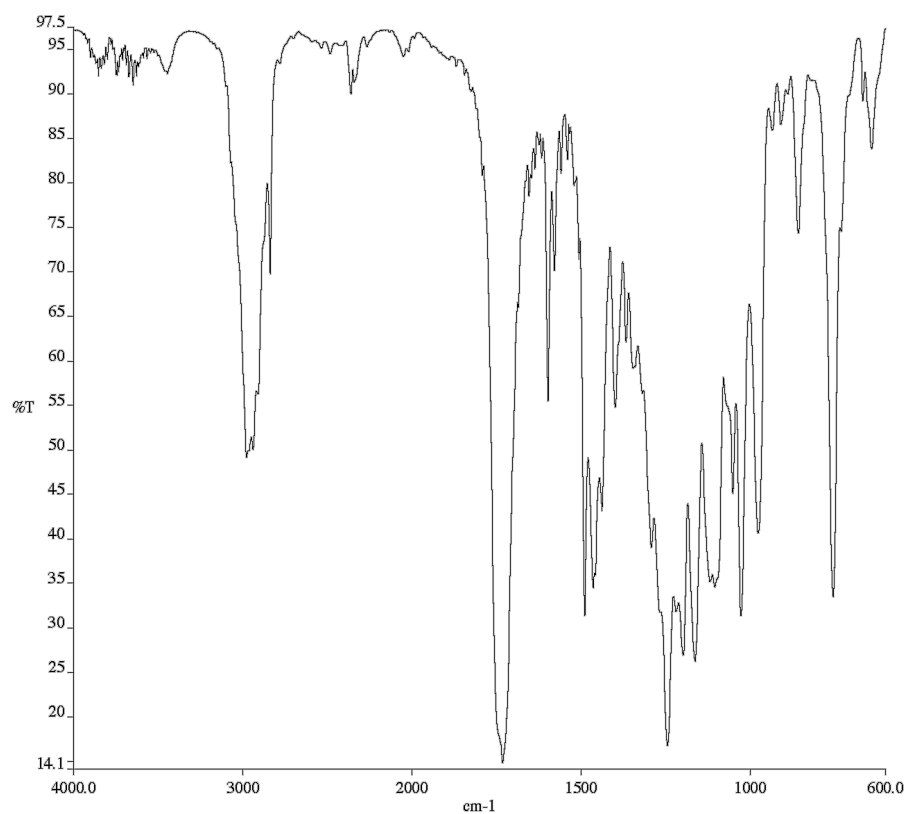


Figure A1.52 Infrared spectrum (Thin Film, NaCl) of compound **3aj**.

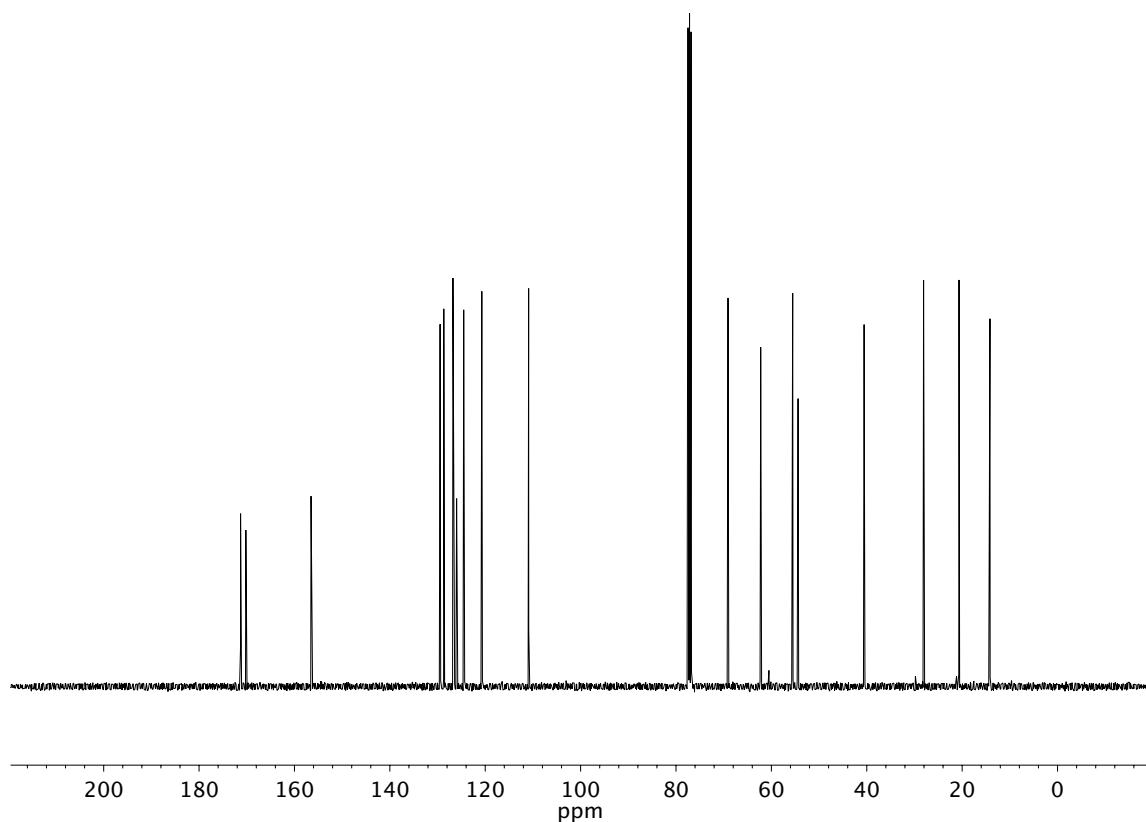


Figure A1.53 ¹³C NMR (100 MHz, CDCl₃) of compound **3aj**.

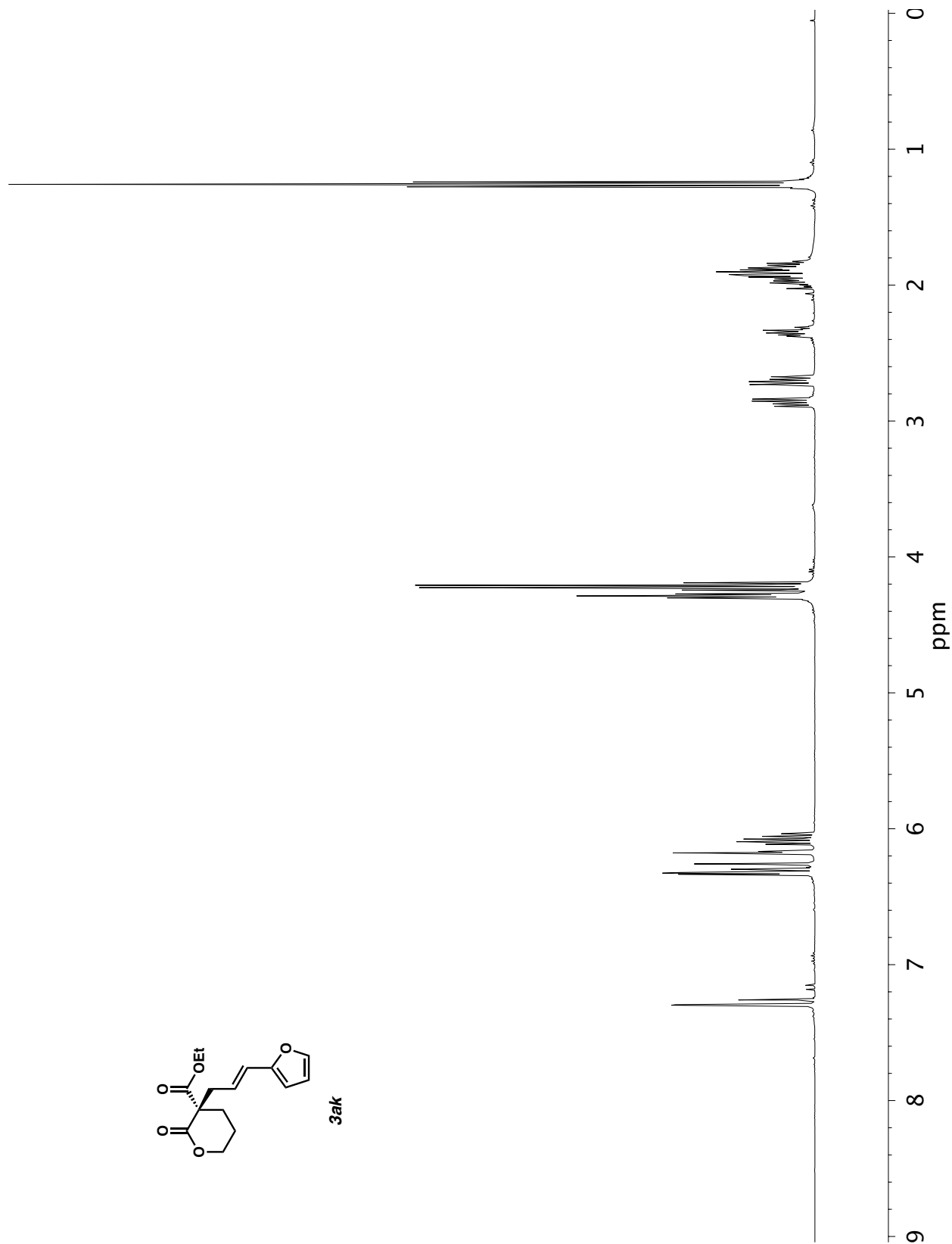


Figure A1.54 ^1H NMR (400 MHz, CDCl_3) of compound **3ak**.

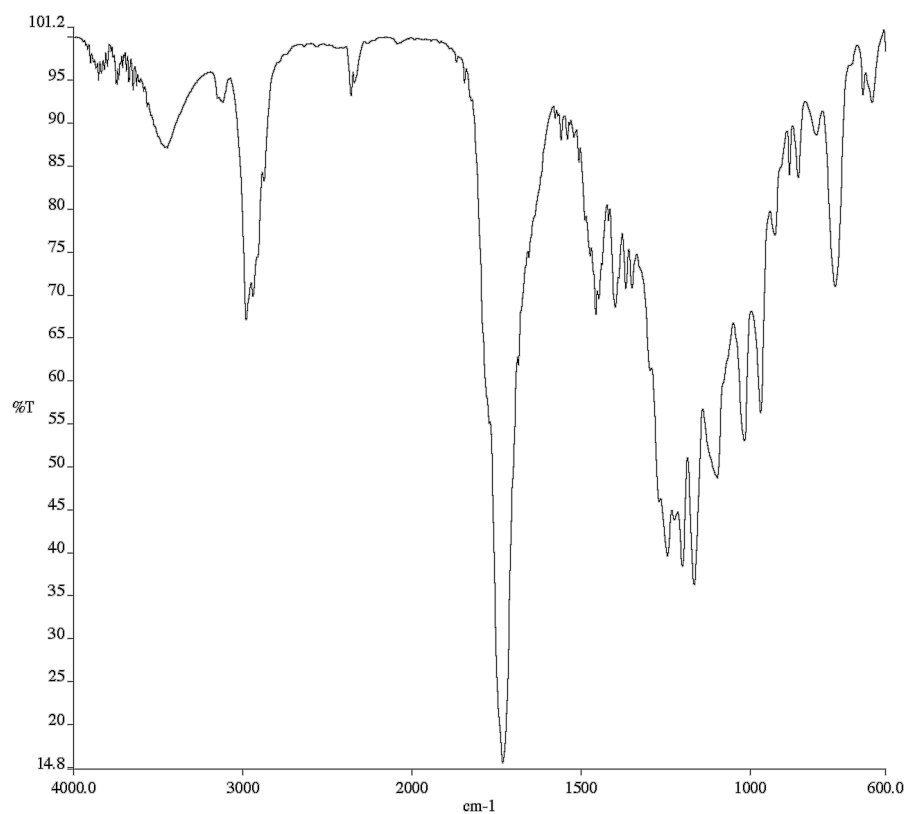


Figure A1.55 Infrared spectrum (Thin Film, NaCl) of compound **3ak**.

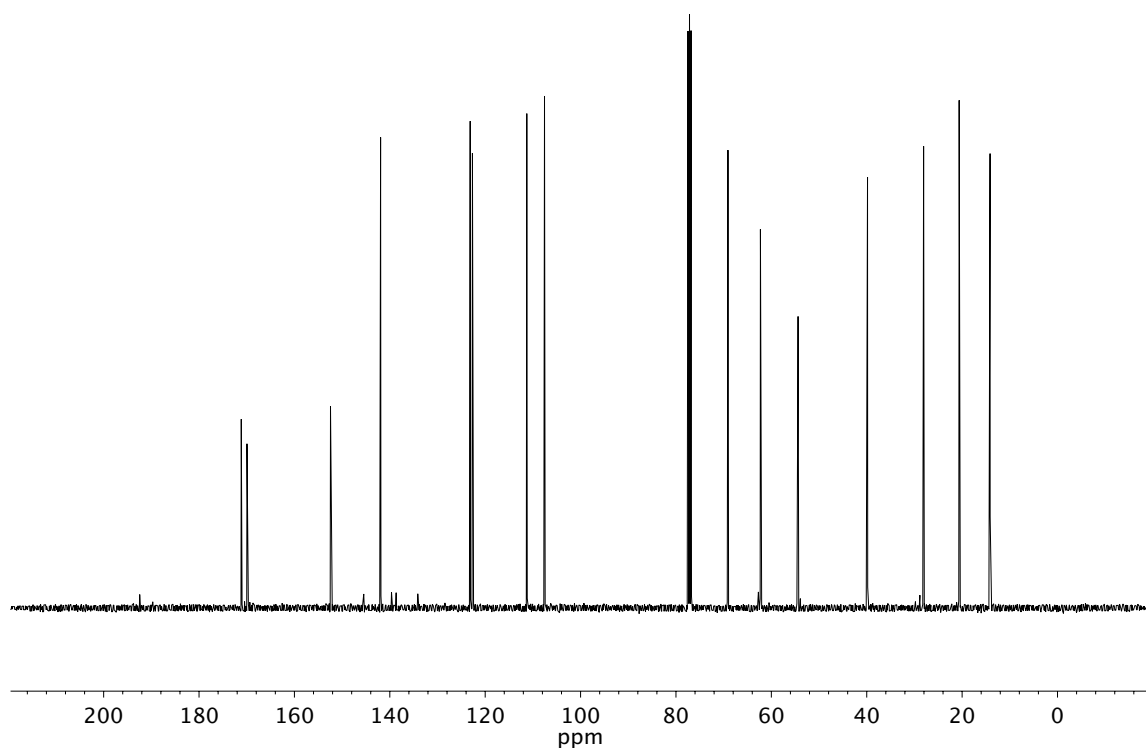


Figure A1.56 ¹³C NMR (100 MHz, CDCl₃) of compound **3ak**.

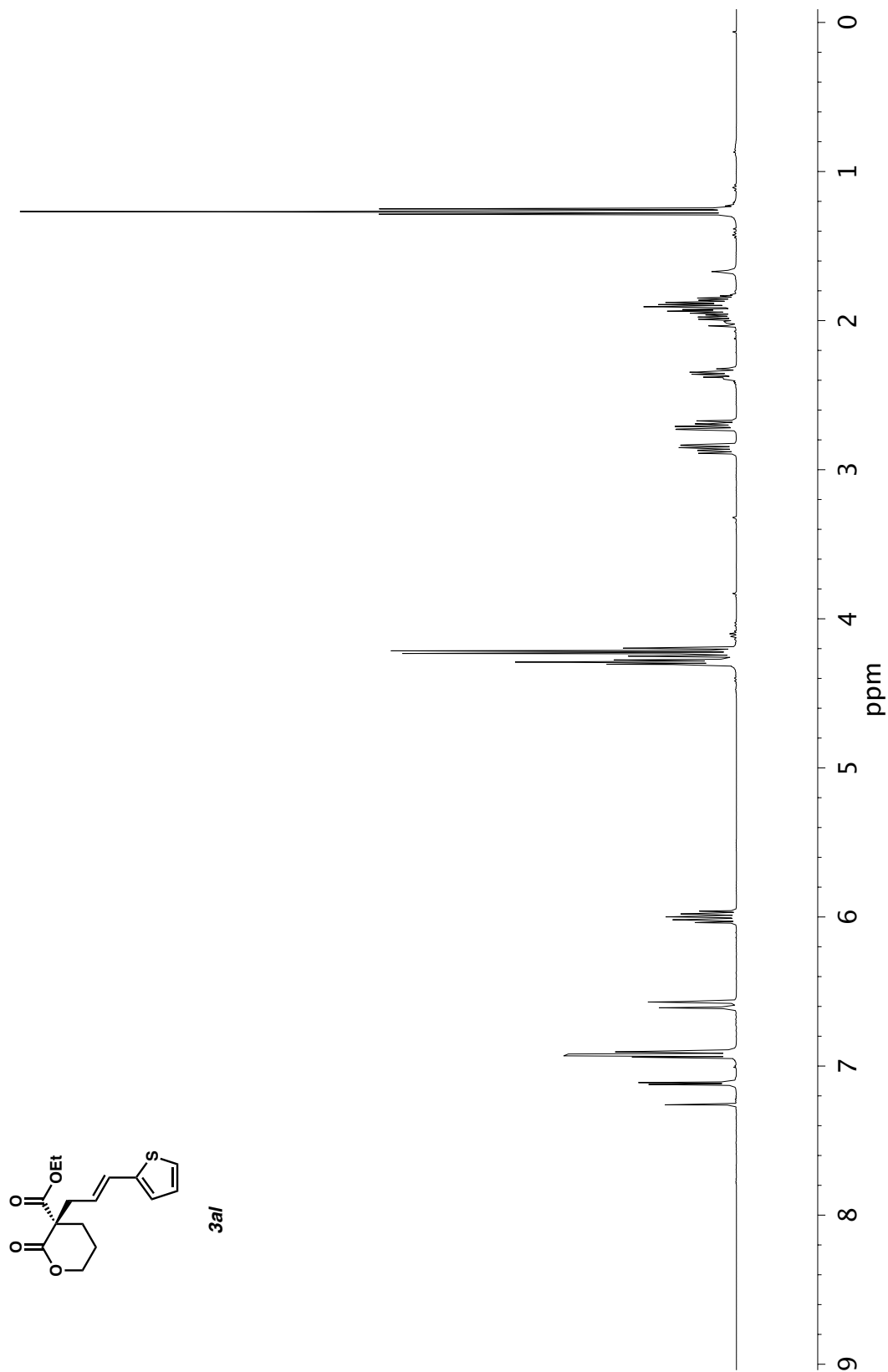


Figure A1.57 ¹H NMR (400 MHz, CDCl₃) of compound **3al**.

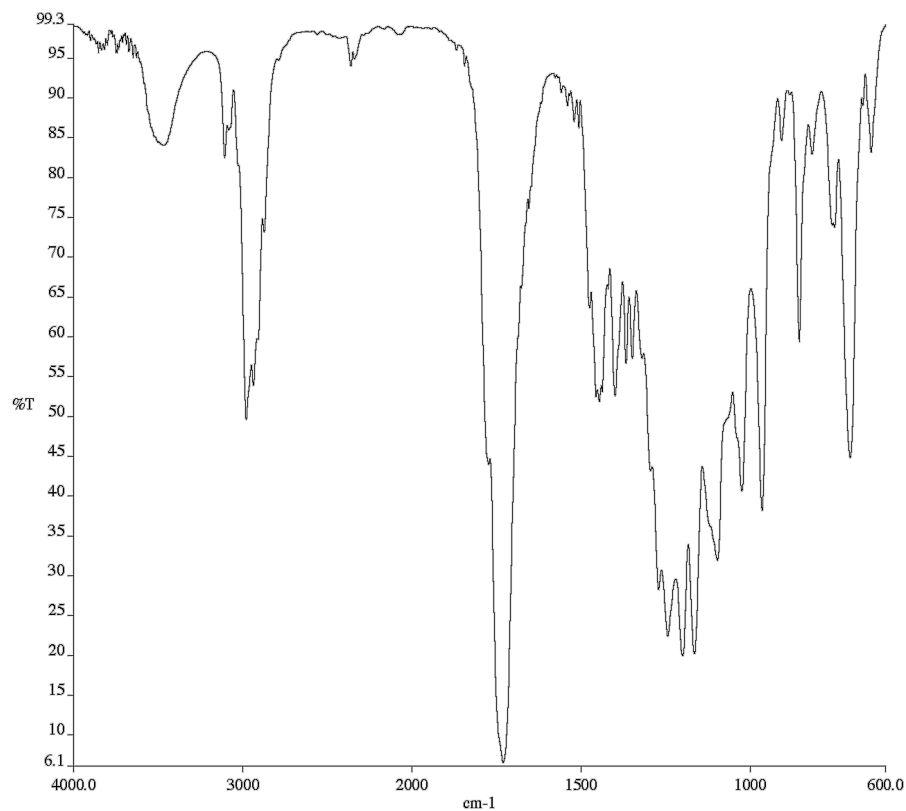


Figure A1.58 Infrared spectrum (Thin Film, NaCl) of compound **3al**.

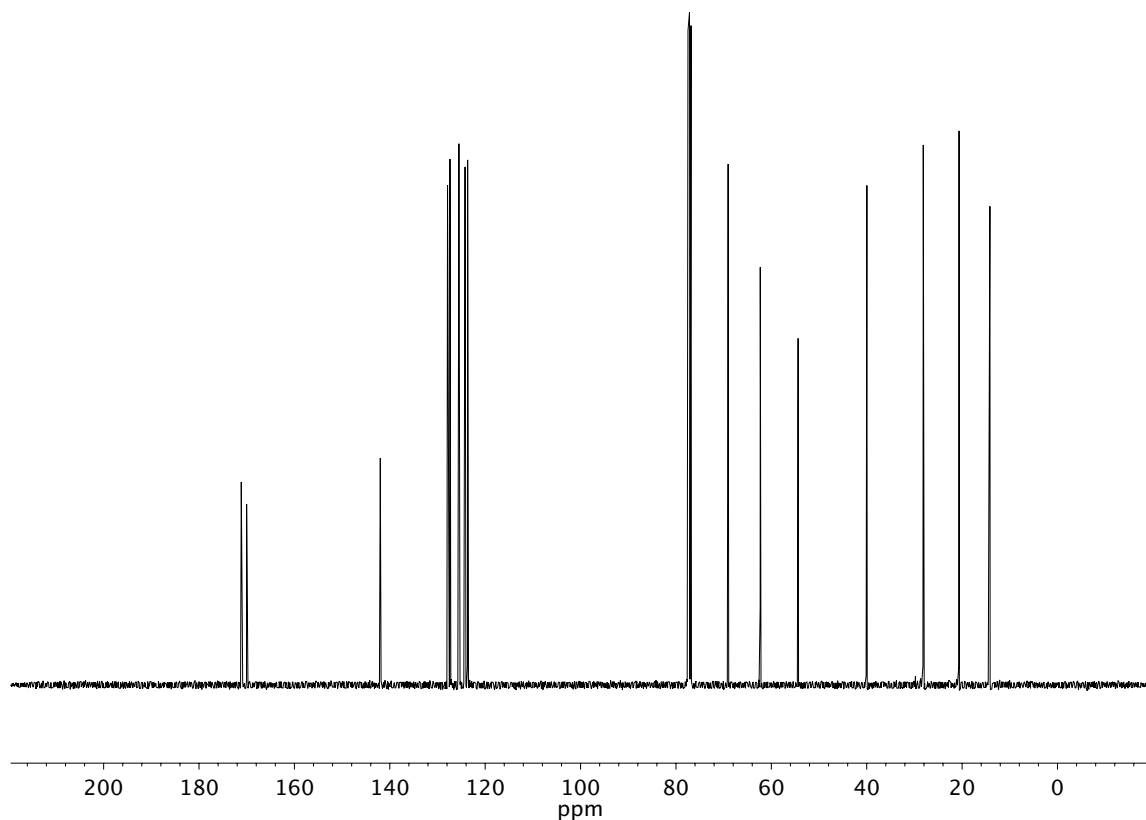


Figure A1.59 ¹³C NMR (100 MHz, CDCl₃) of compound **3al**.

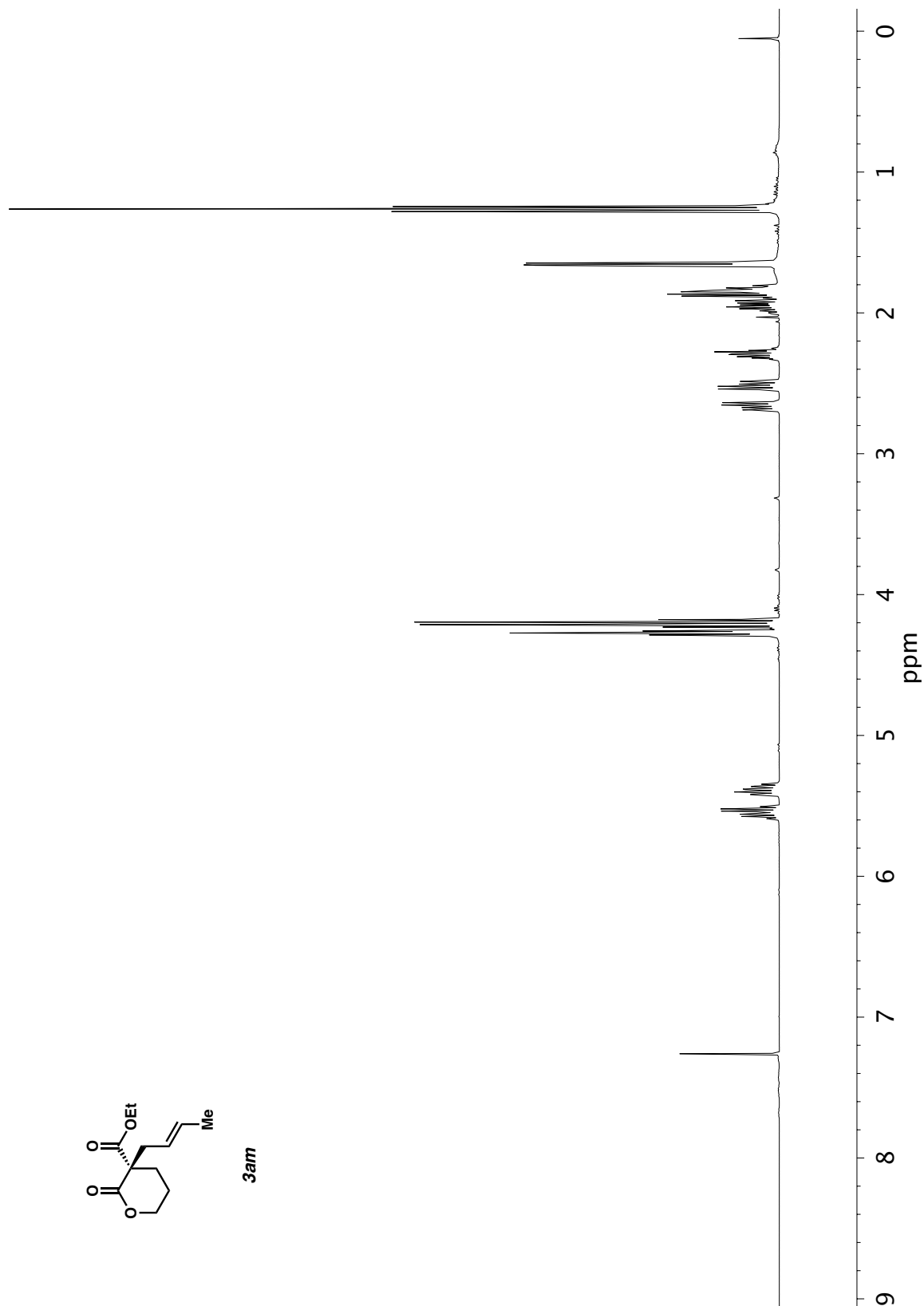


Figure A1.60 ¹H NMR (400 MHz, CDCl₃) of compound **3am**.

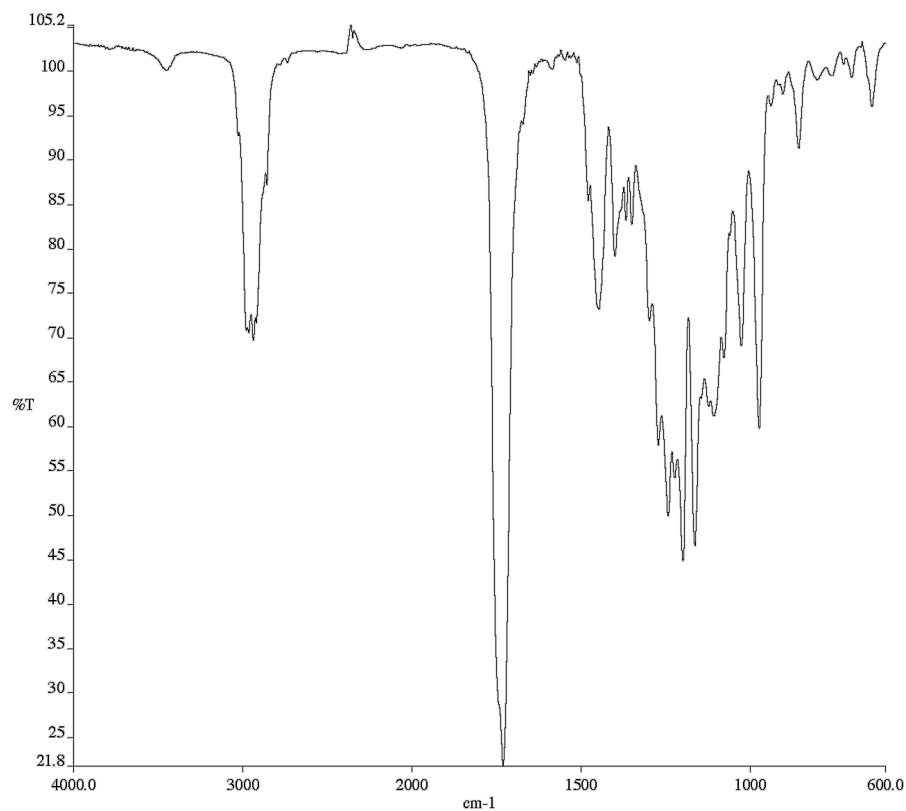


Figure A1.61 Infrared spectrum (Thin Film, NaCl) of compound **3am**.

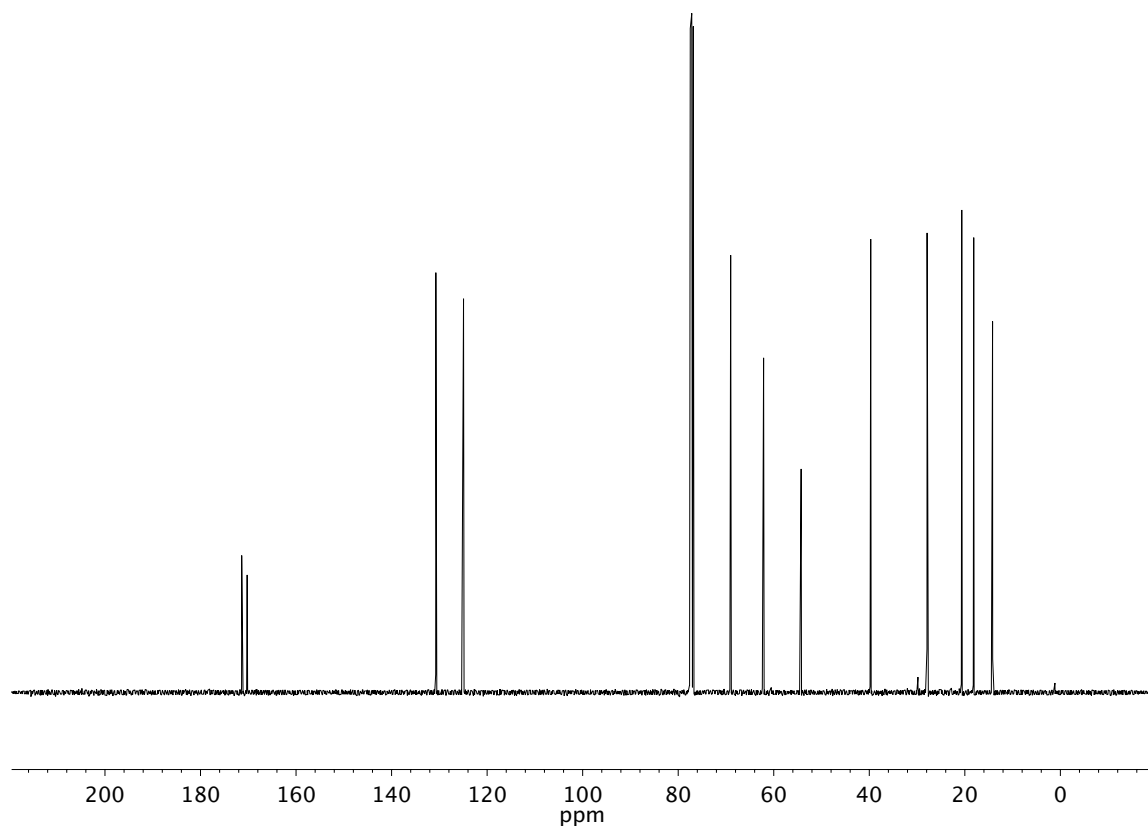


Figure A1.62 ¹³C NMR (100 MHz, CDCl₃) of compound **3am**.

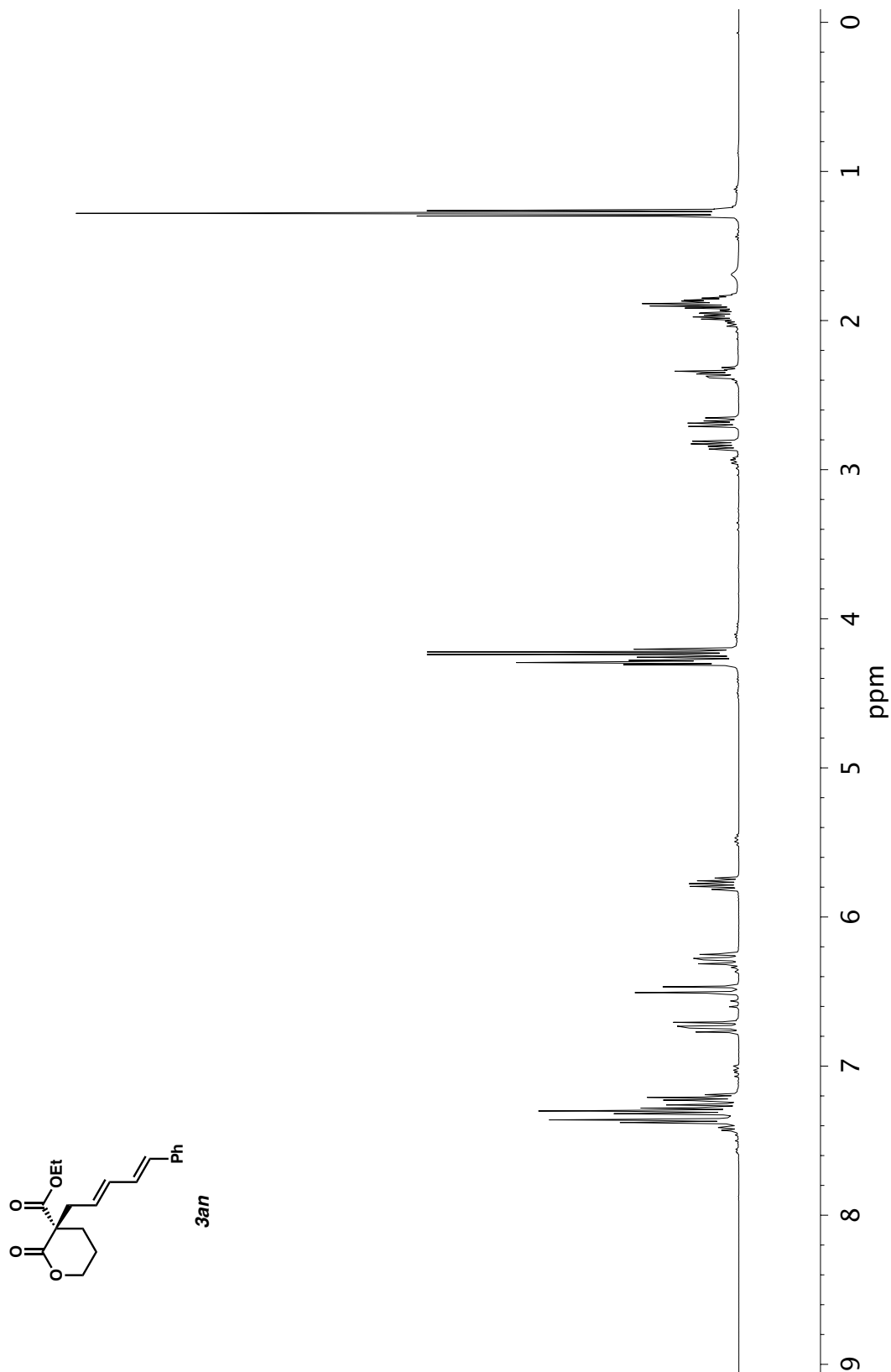


Figure A1.63 ¹H NMR (400 MHz, CDCl₃) of compound **3an**.

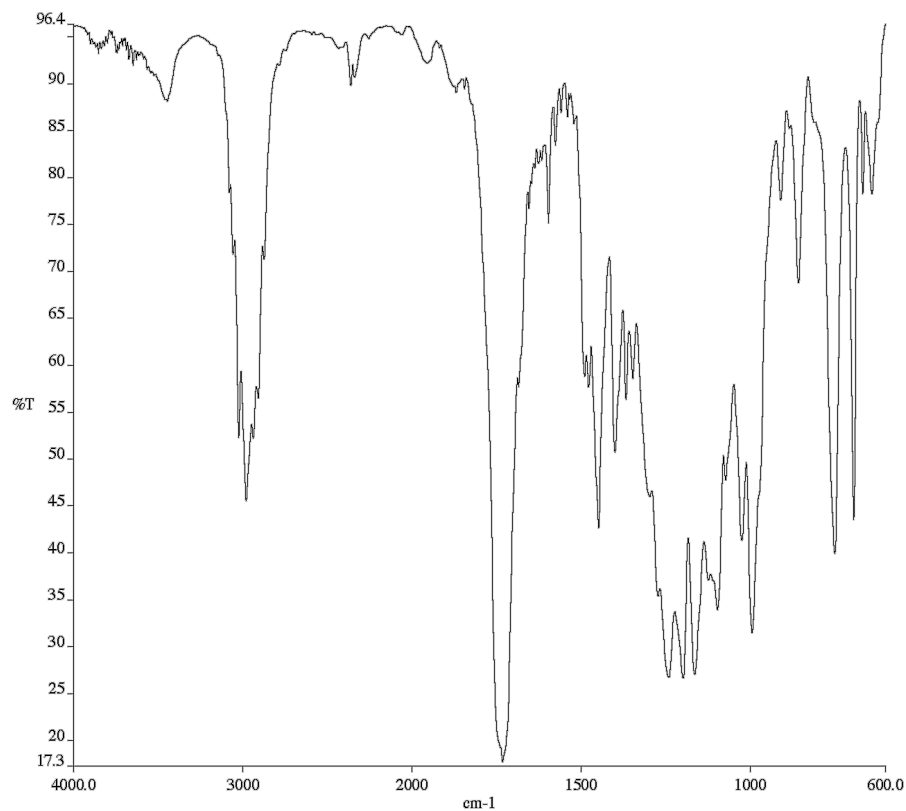


Figure A1.64 Infrared spectrum (Thin Film, NaCl) of compound **3an**.

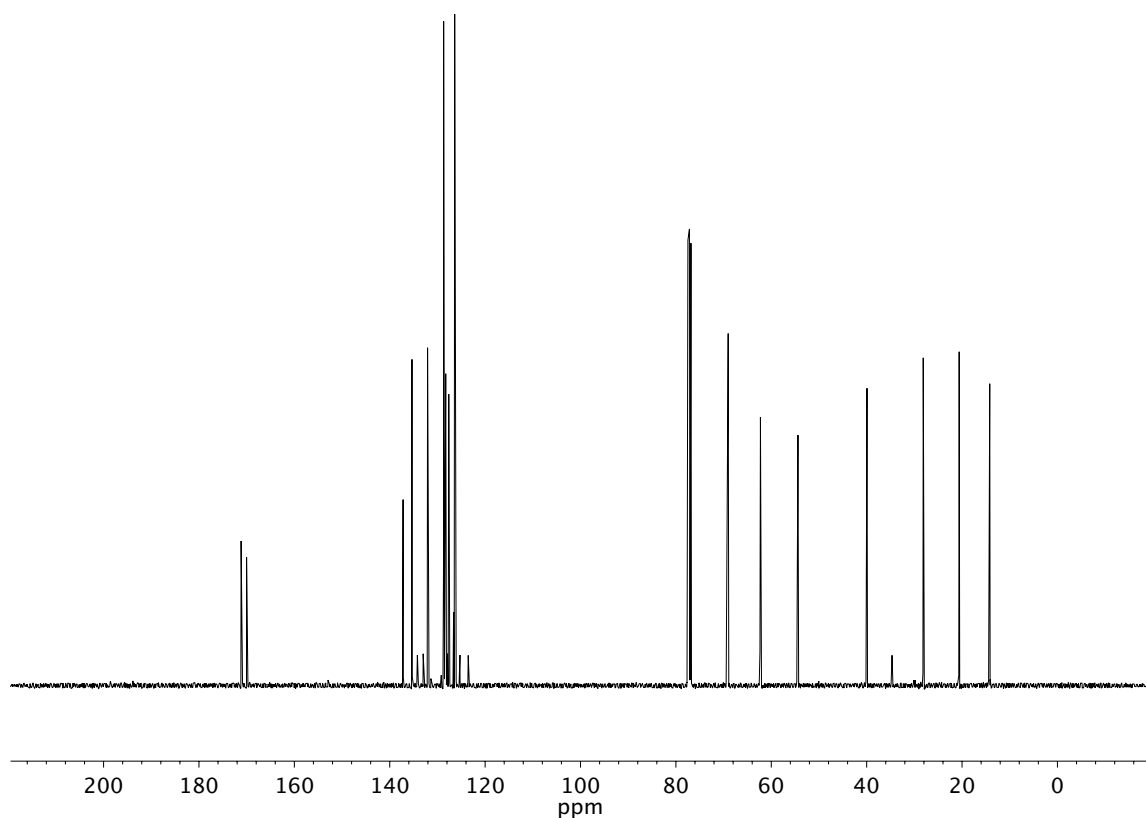


Figure A1.65 ¹³C NMR (100 MHz, CDCl₃) of compound **3an**.

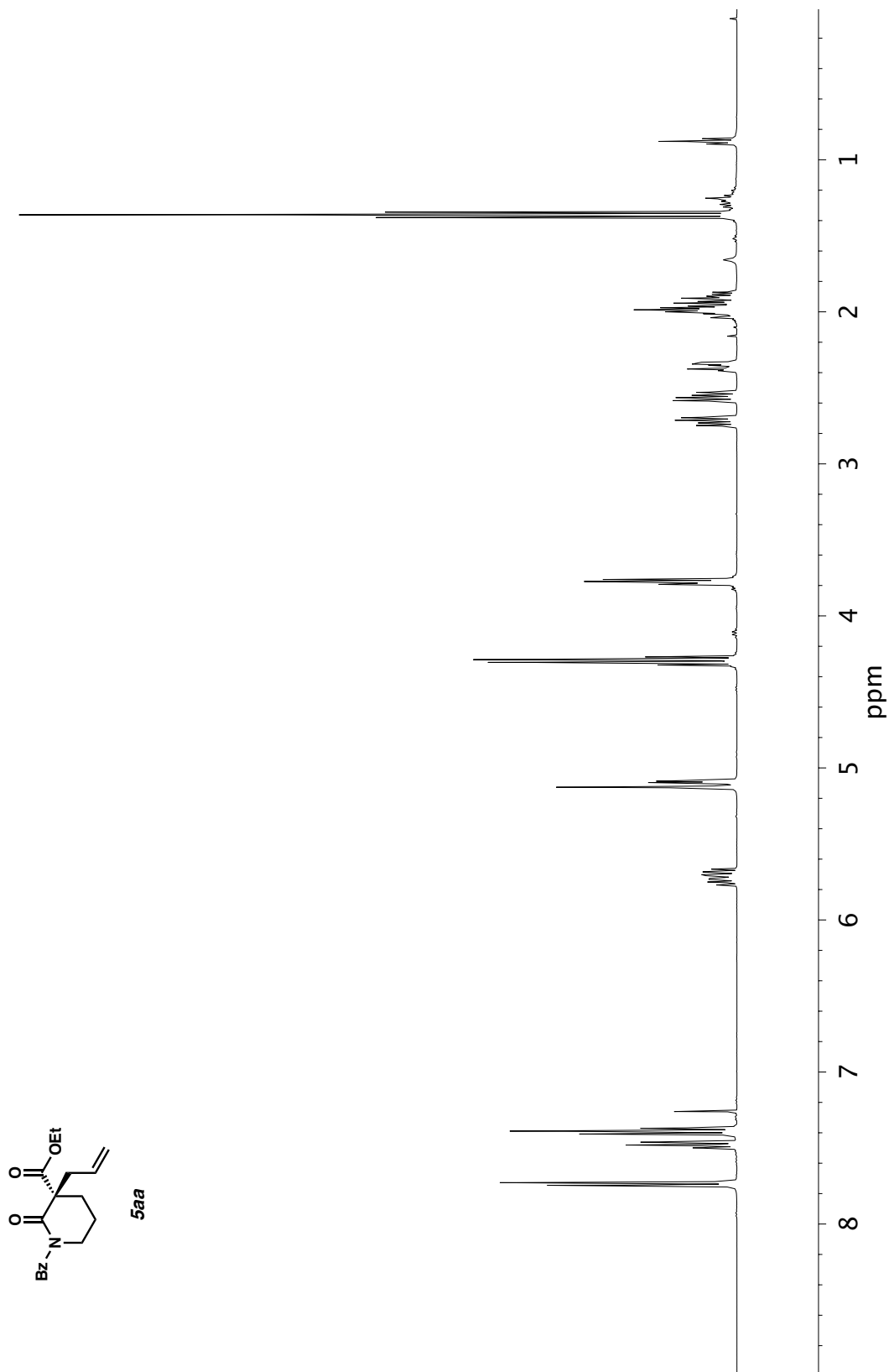


Figure A1.66 ¹H NMR (400 MHz, CDCl₃) of compound **5aa**.

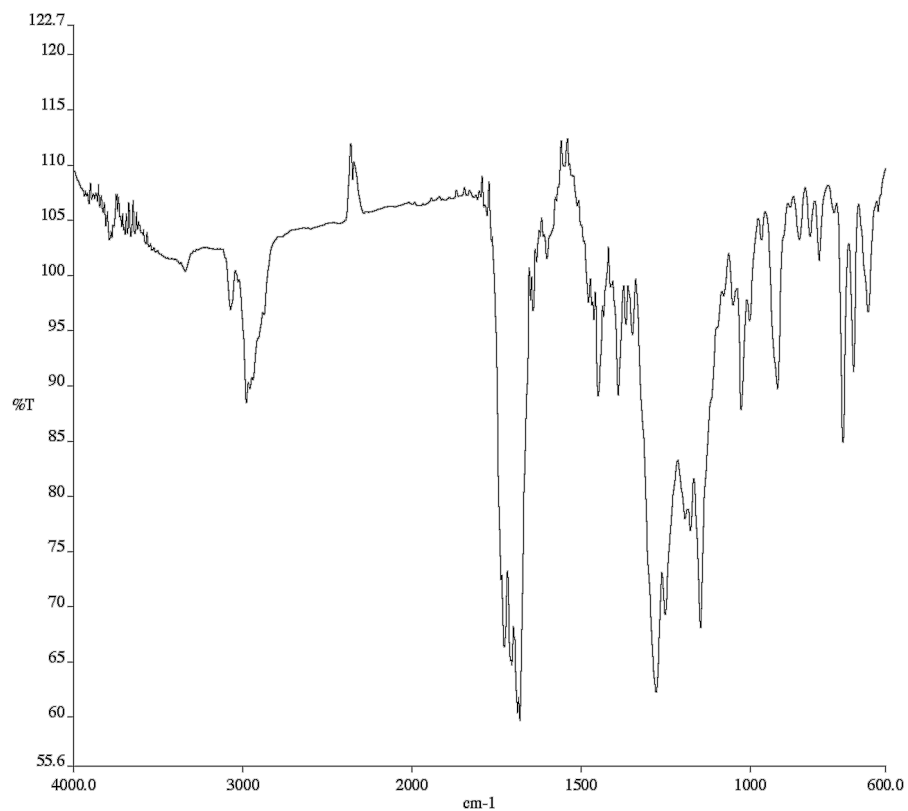


Figure A1.67 Infrared spectrum (Thin Film, NaCl) of compound **5aa**.

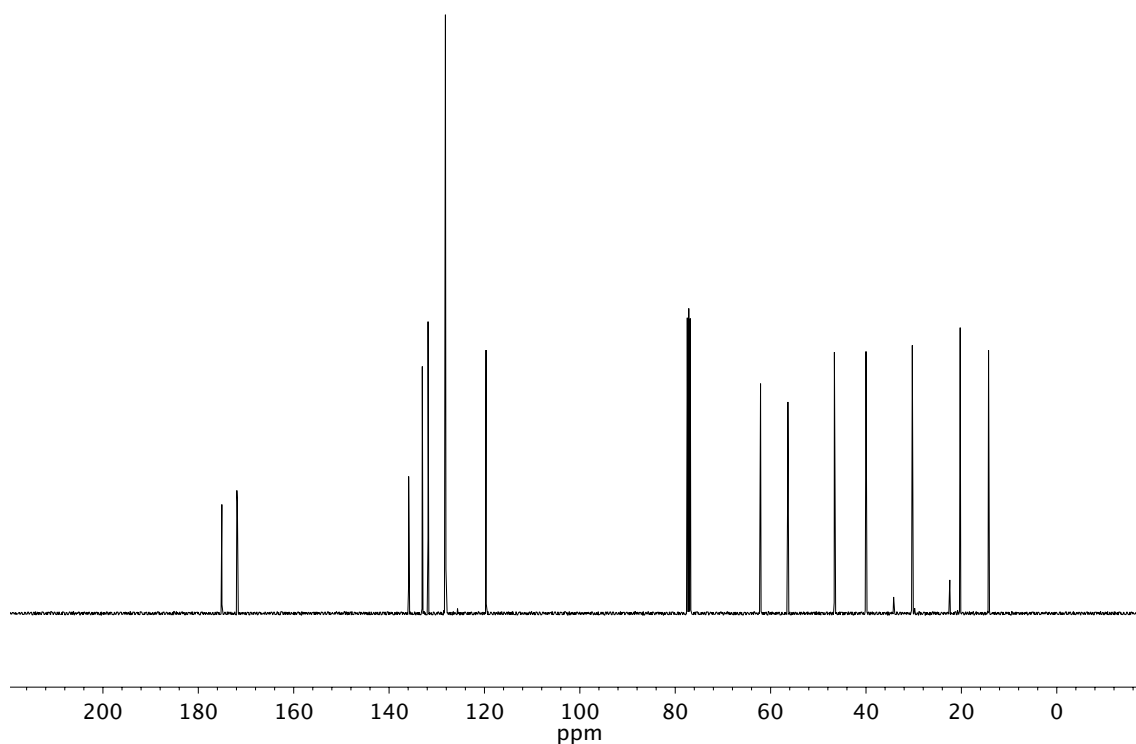


Figure A1.68 ¹³C NMR (100 MHz, CDCl₃) of compound **5aa**.

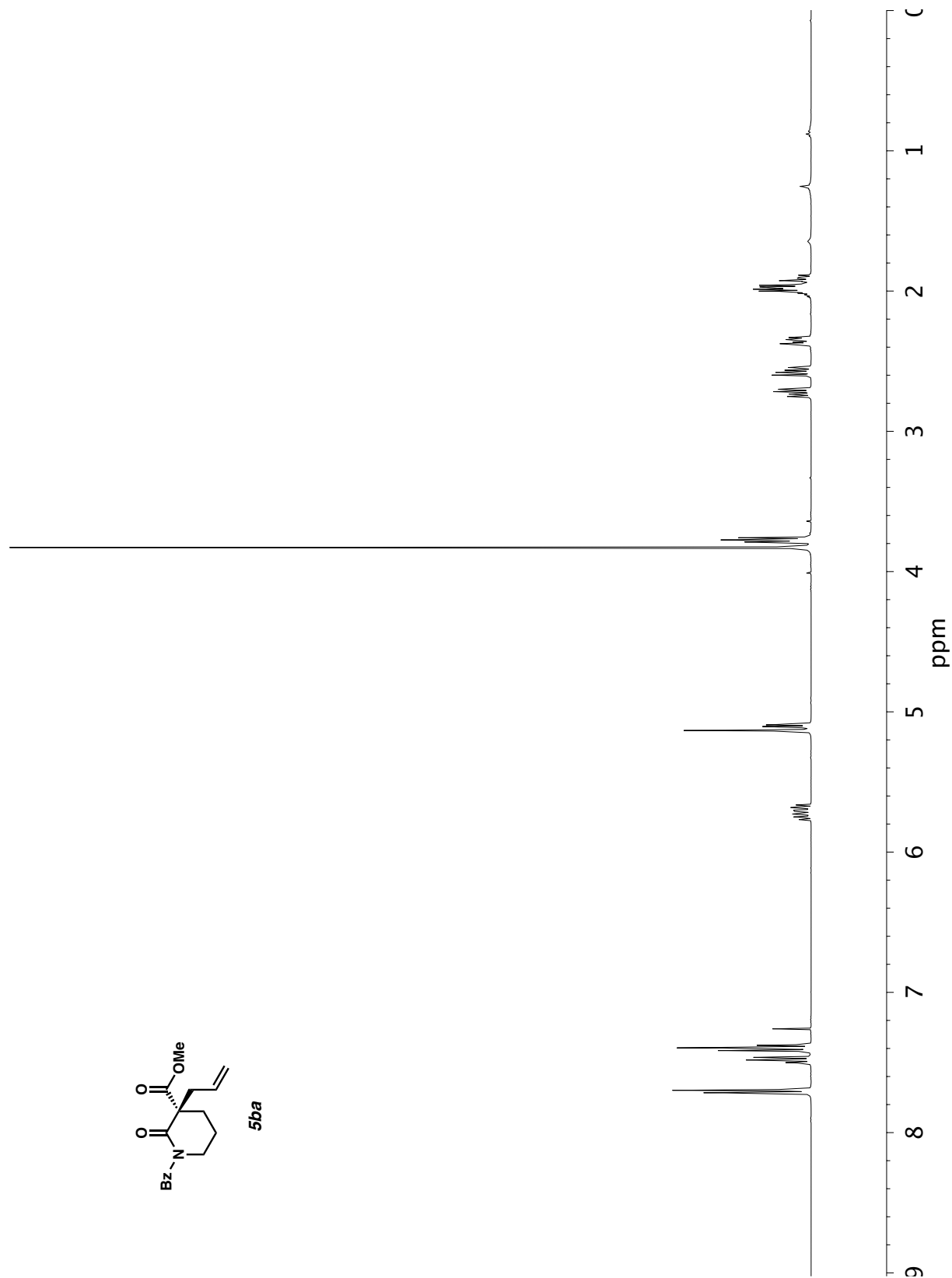


Figure A1.69 ^1H NMR (400 MHz, CDCl_3) of compound **5ba**.

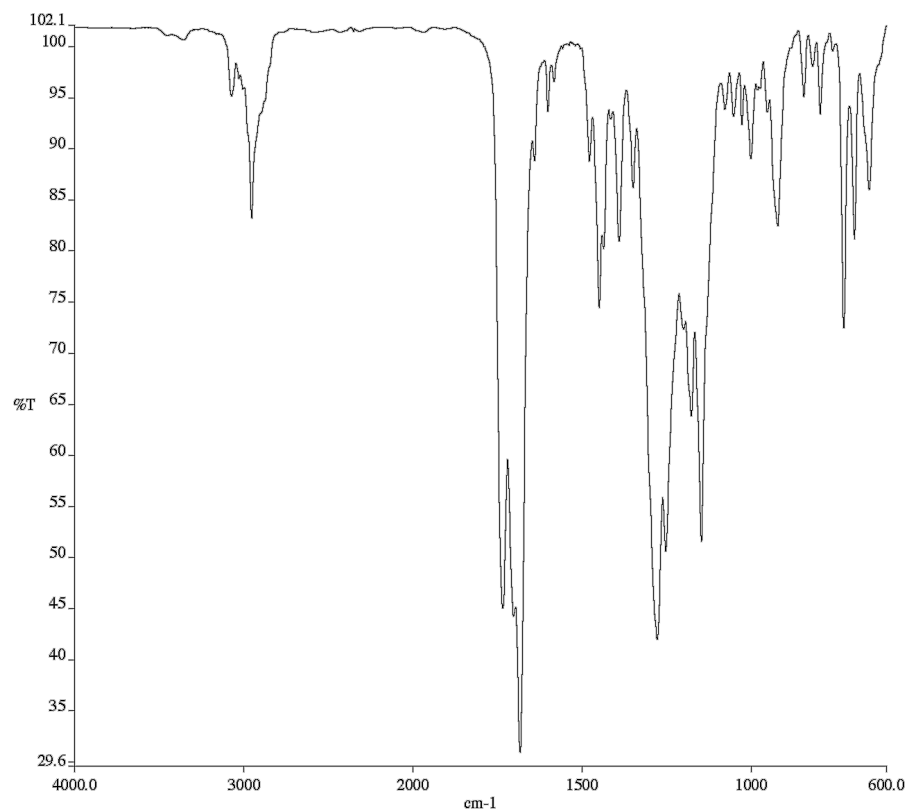


Figure A1.70 Infrared spectrum (Thin Film, NaCl) of compound **5ba**.

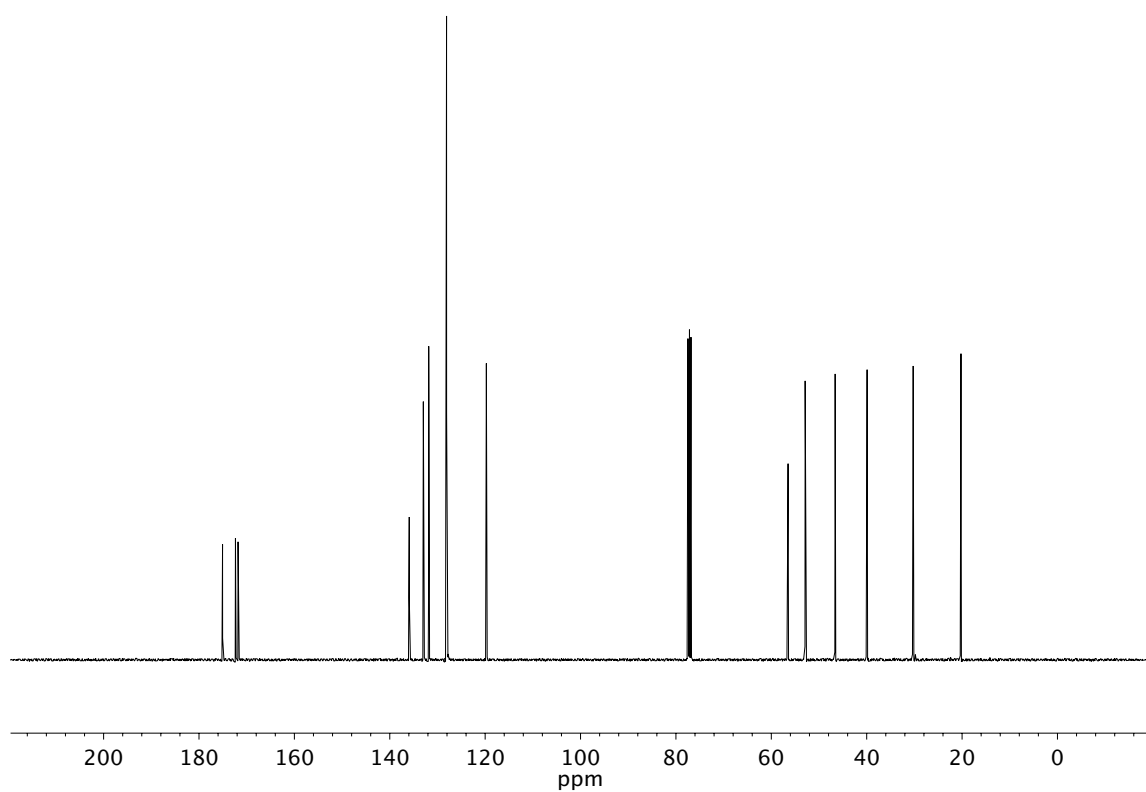


Figure A1.71 ¹³C NMR (100 MHz, CDCl₃) of compound **5ba**.

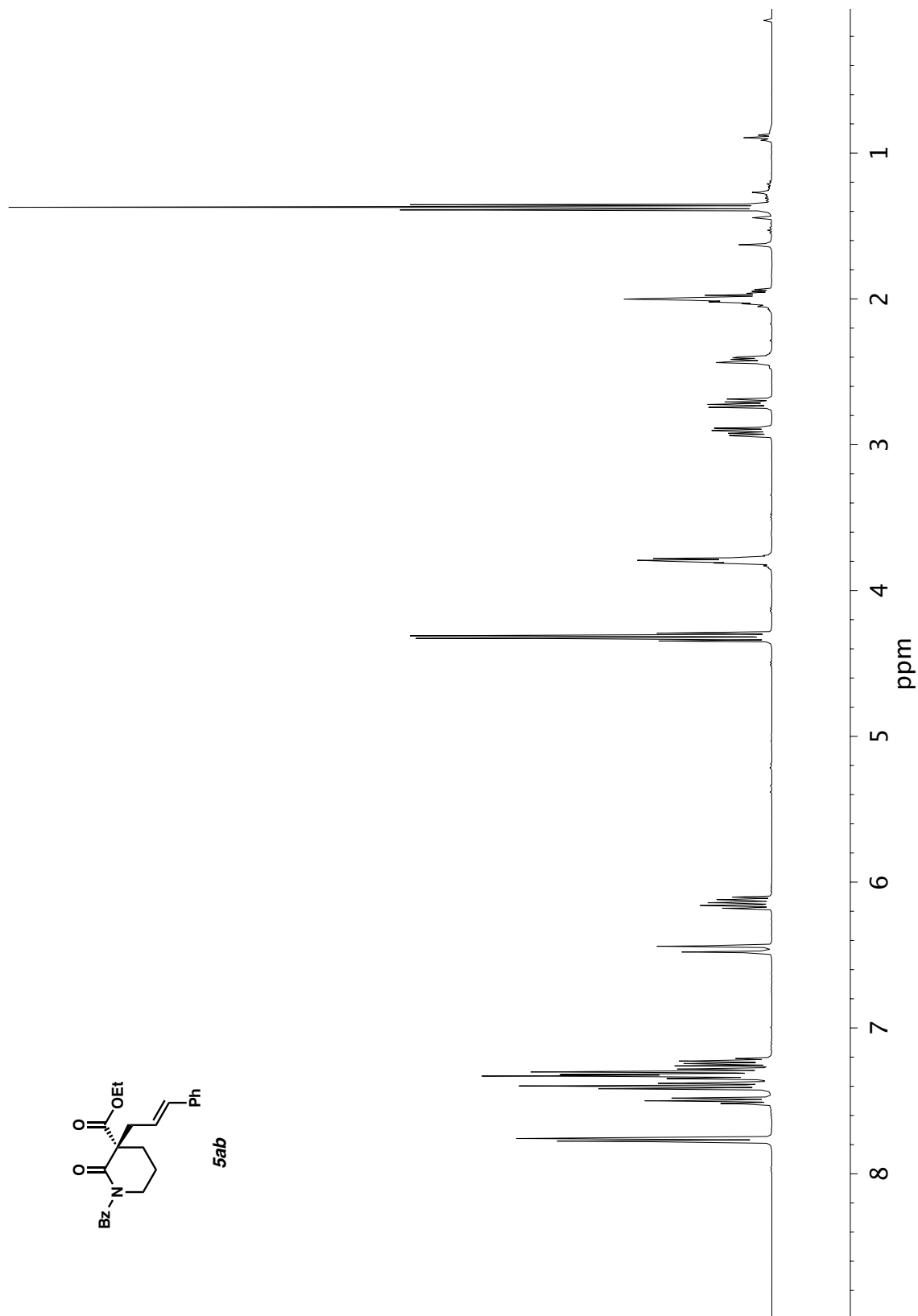


Figure A1.72 ^1H NMR (400 MHz, CDCl_3) of compound **5ab**.

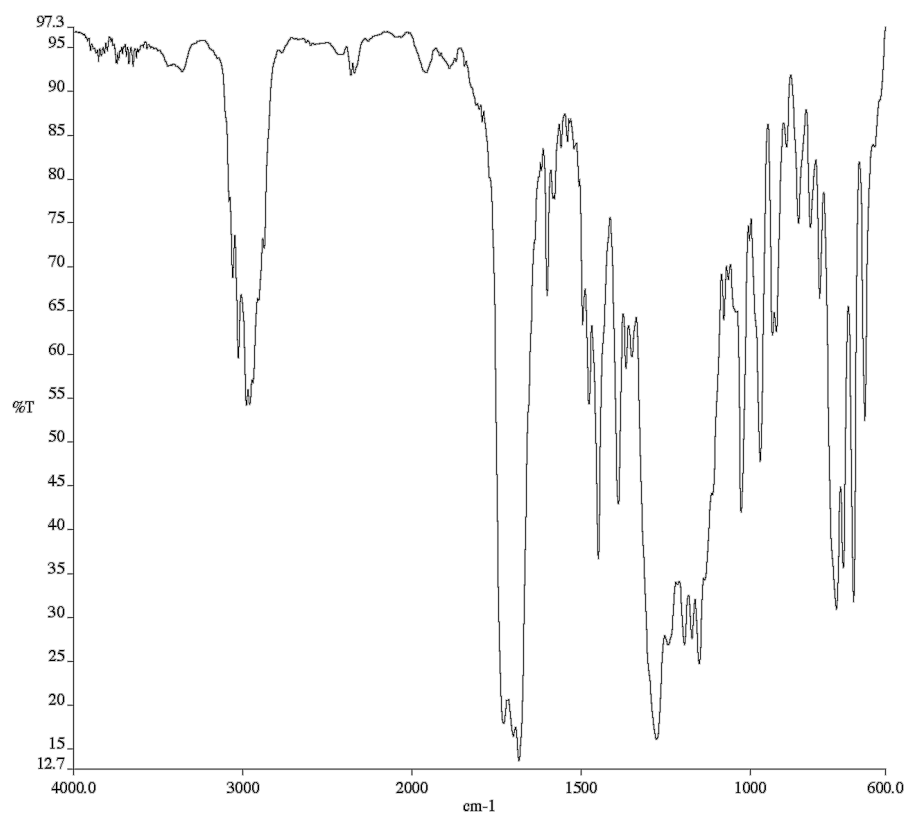


Figure A1.73 Infrared spectrum (Thin Film, NaCl) of compound **5ab**.

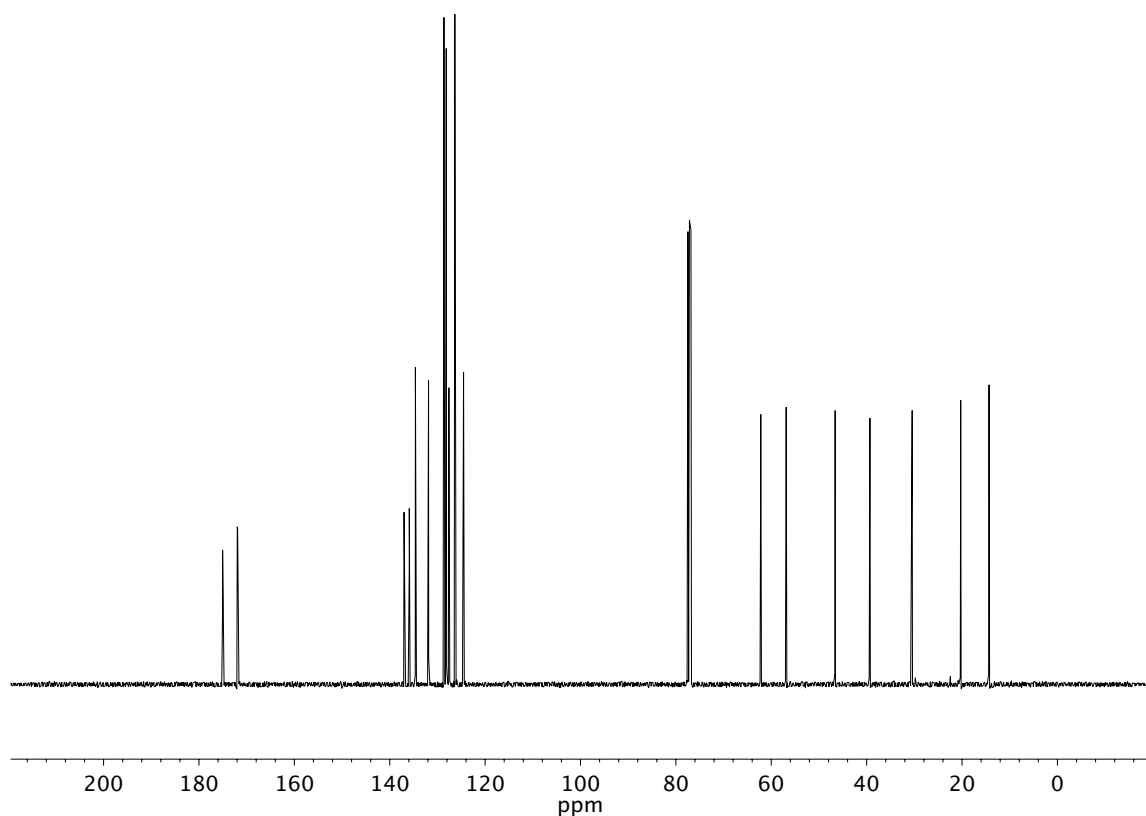


Figure A1.74 ¹³C NMR (100 MHz, CDCl₃) of compound **5ab**.

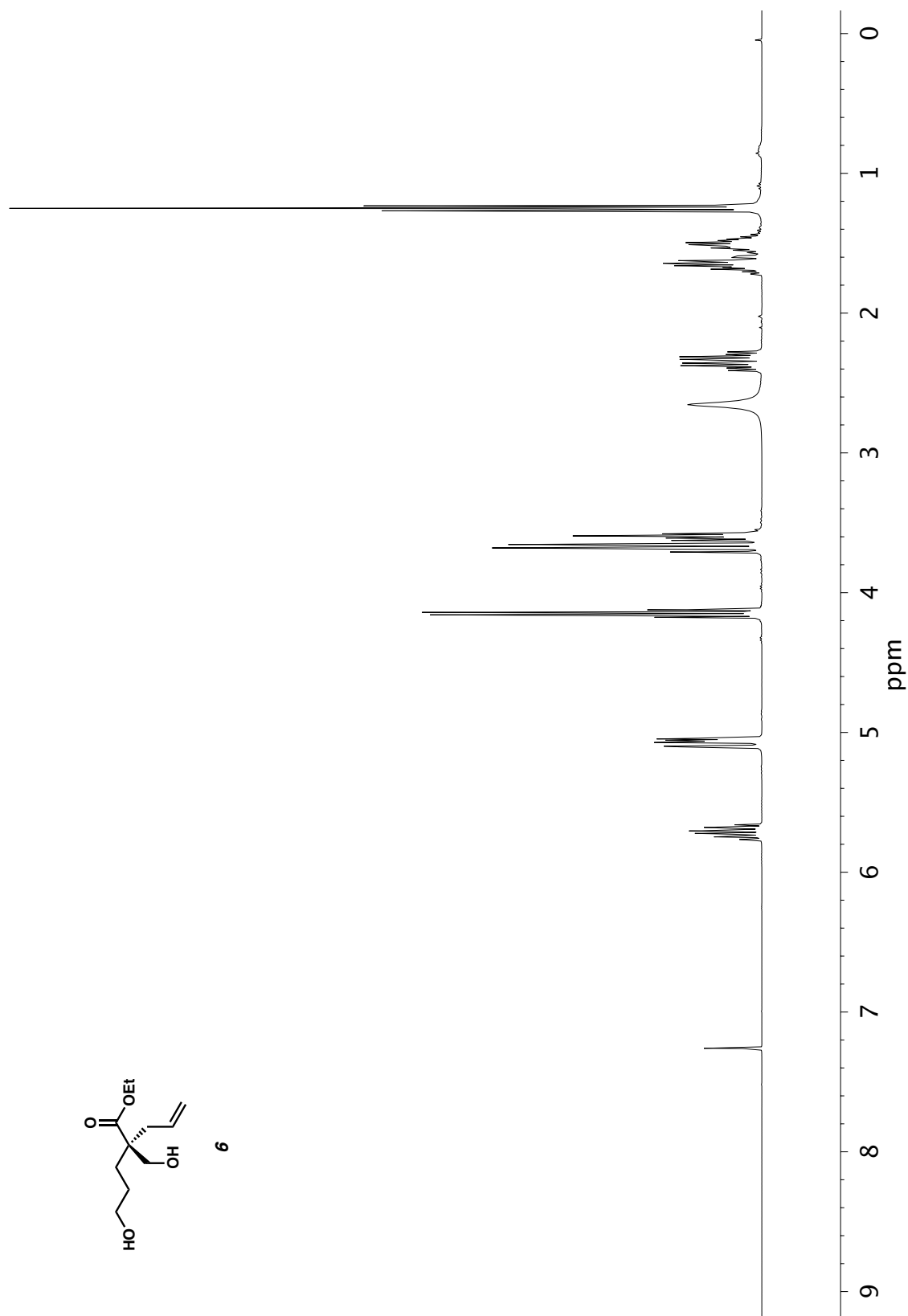


Figure A1.75 ^1H NMR (400 MHz, CDCl_3) of compound **6**.

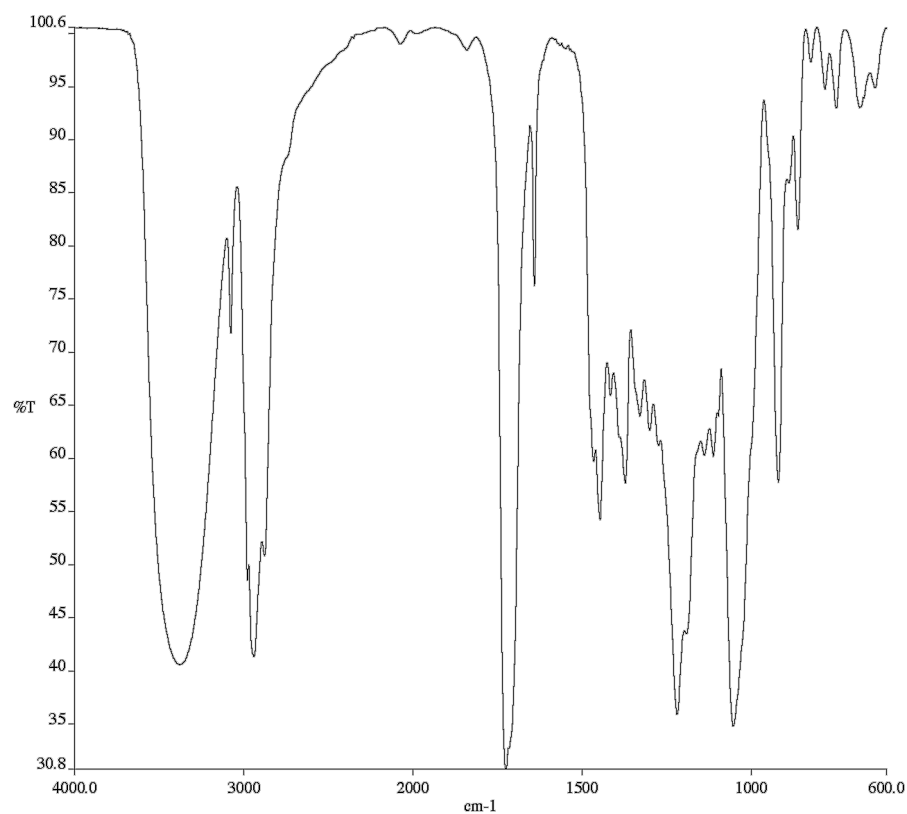


Figure A1.76 Infrared spectrum (Thin Film, NaCl) of compound **6**.

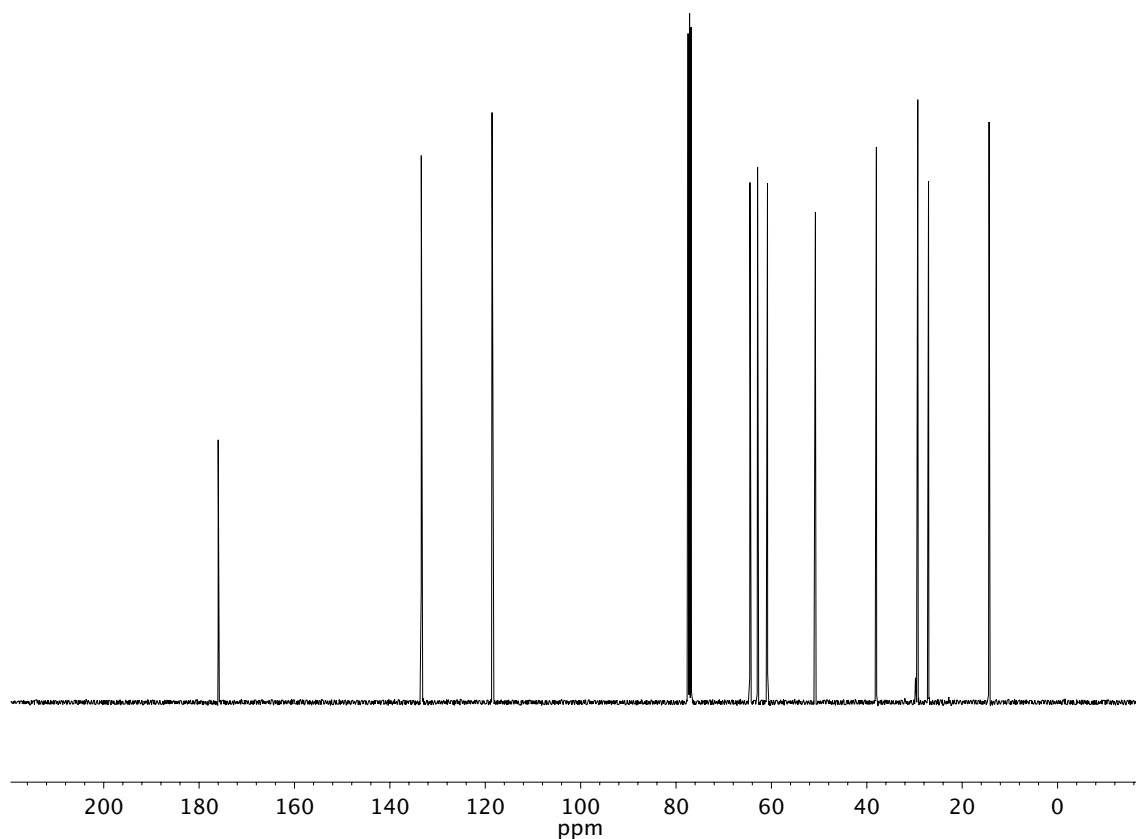


Figure A1.77 ¹³C NMR (100 MHz, CDCl₃) of compound **6**.

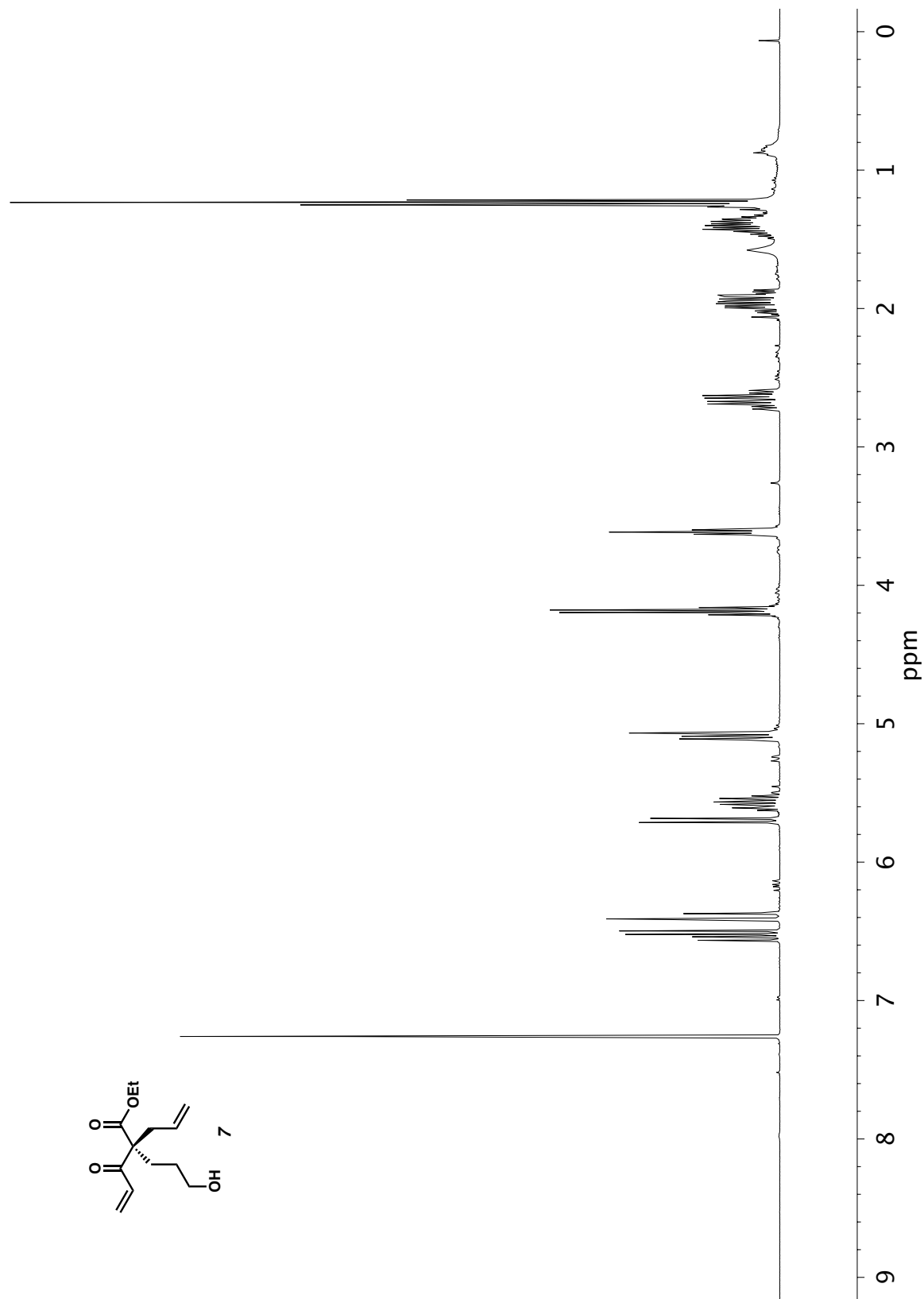


Figure A1.78 ^1H NMR (400 MHz, CDCl_3) of compound **7**.

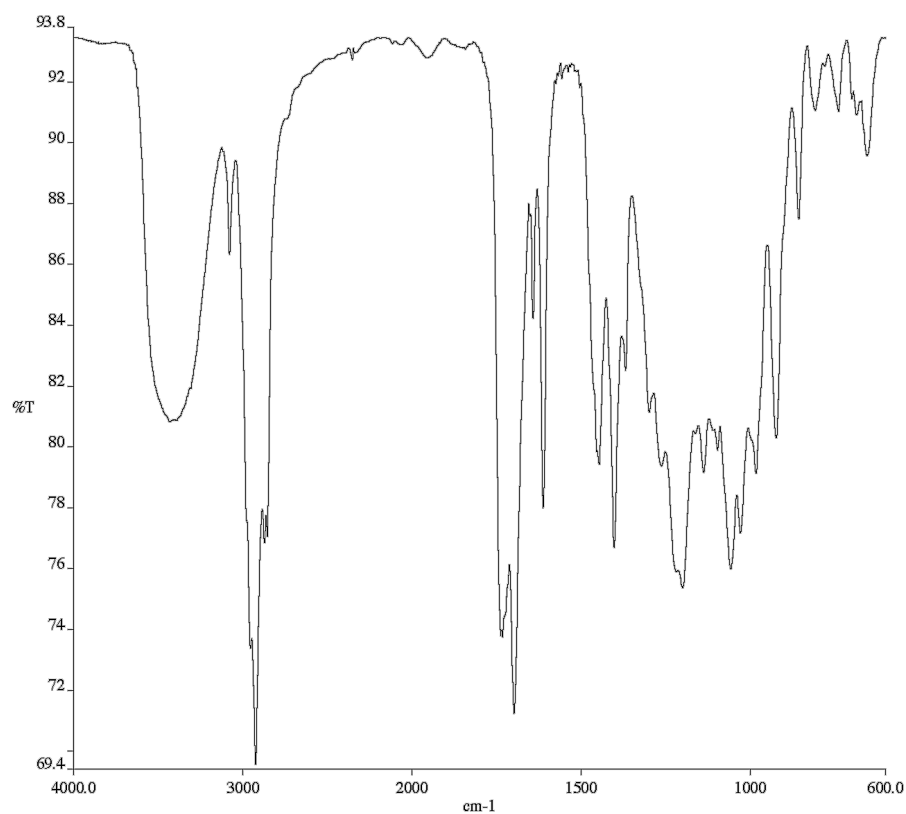


Figure A1.79 Infrared spectrum (Thin Film, NaCl) of compound 7.

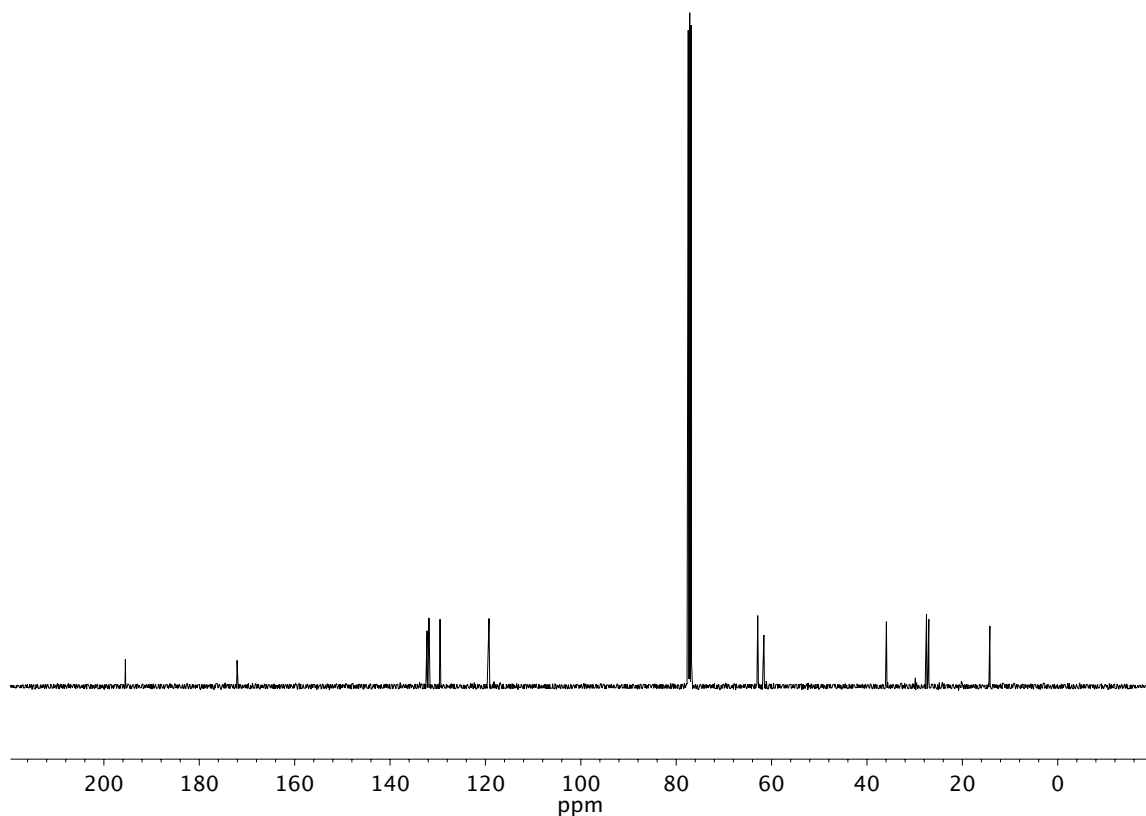


Figure A1.80 ¹³C NMR (100 MHz, CDCl₃) of compound 7.

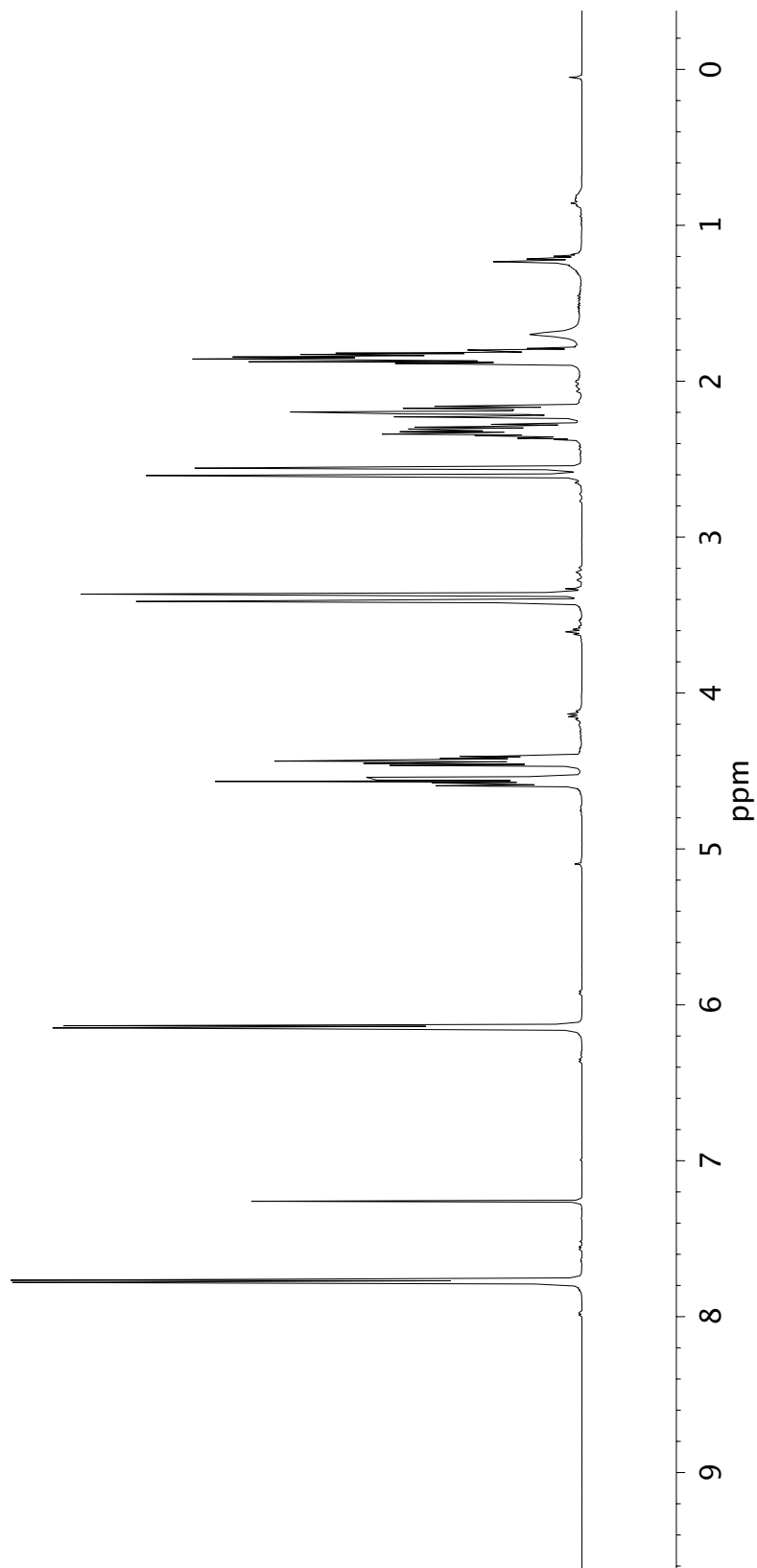
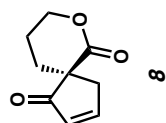


Figure A1.81 ^1H NMR (400 MHz, CDCl_3) of compound **8**.

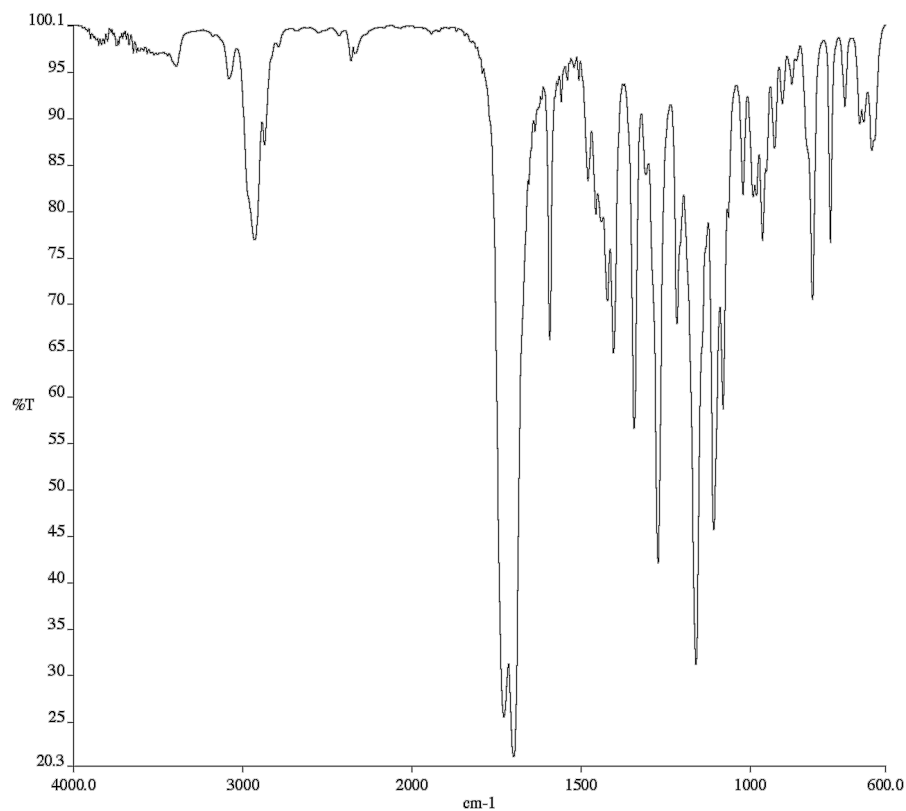


Figure A1.82 Infrared spectrum (Thin Film, NaCl) of compound **8**.

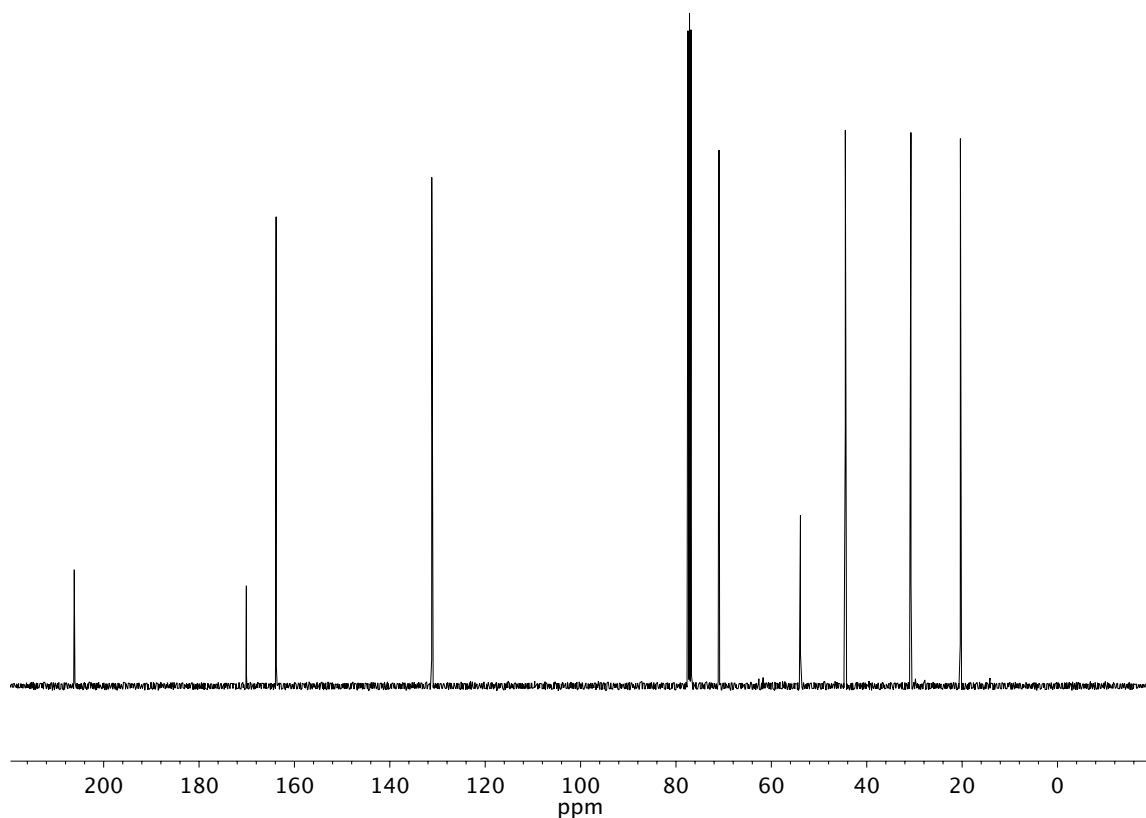


Figure A1.83 ¹³C NMR (100 MHz, CDCl₃) of compound **8**.

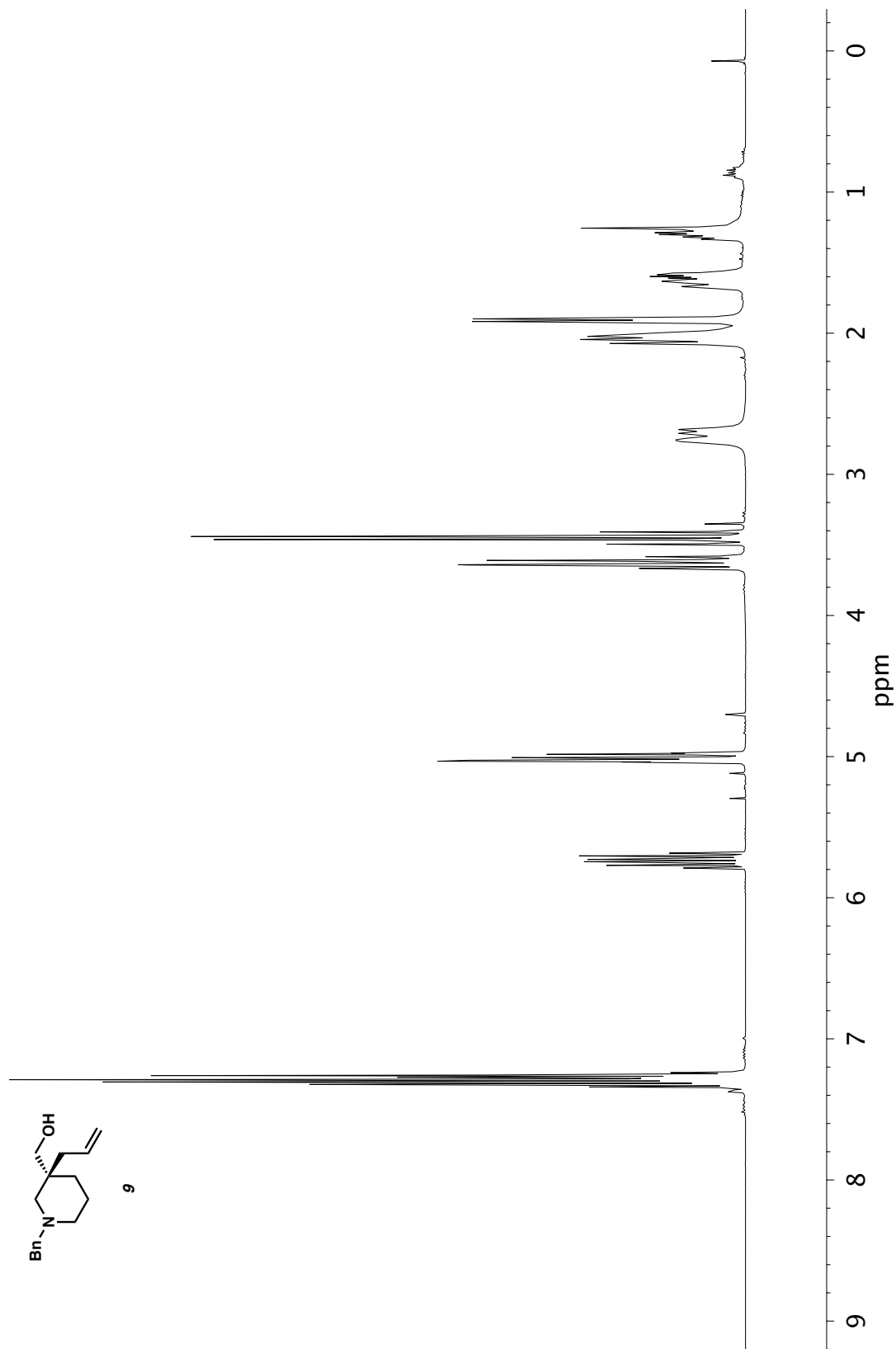


Figure A1.84 ¹H NMR (400 MHz, CDCl₃) of compound **9**.

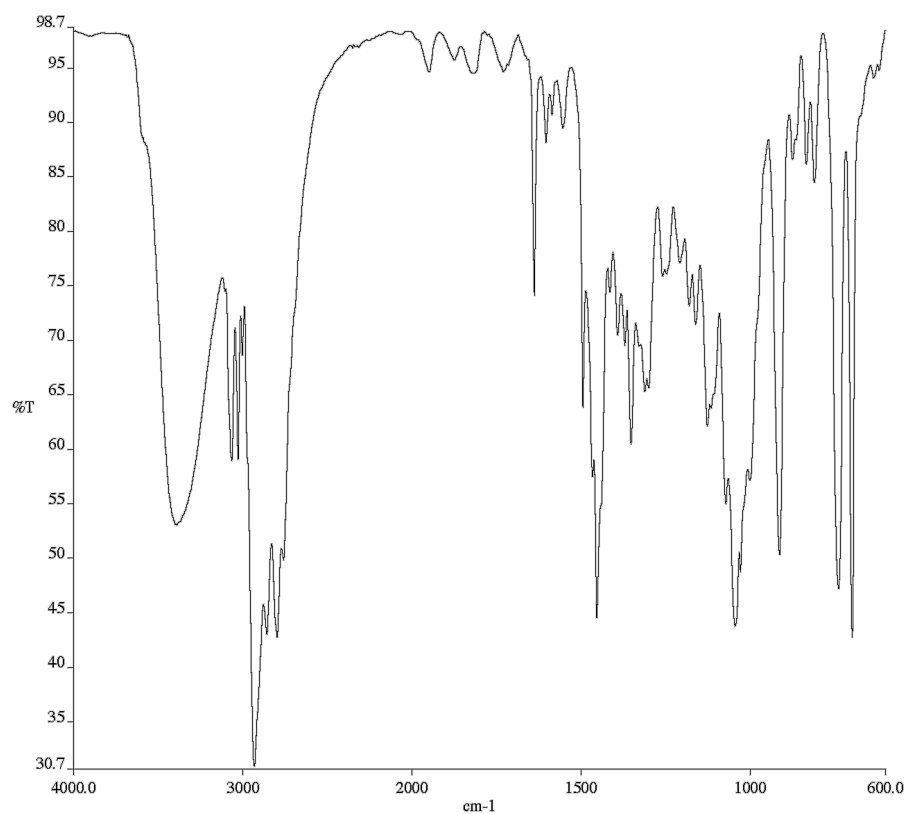


Figure A1.85 Infrared spectrum (Thin Film, NaCl) of compound **9**.

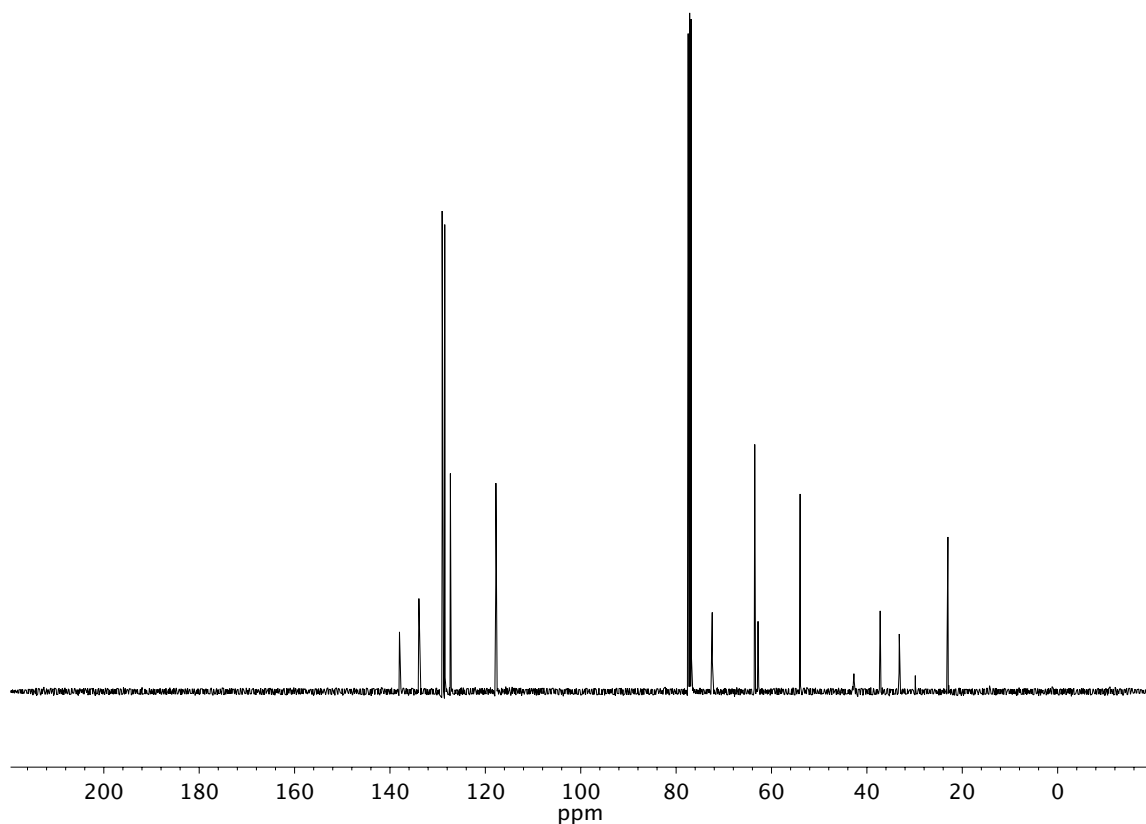


Figure A1.86 ¹³C NMR (100 MHz, CDCl₃) of compound **9**.

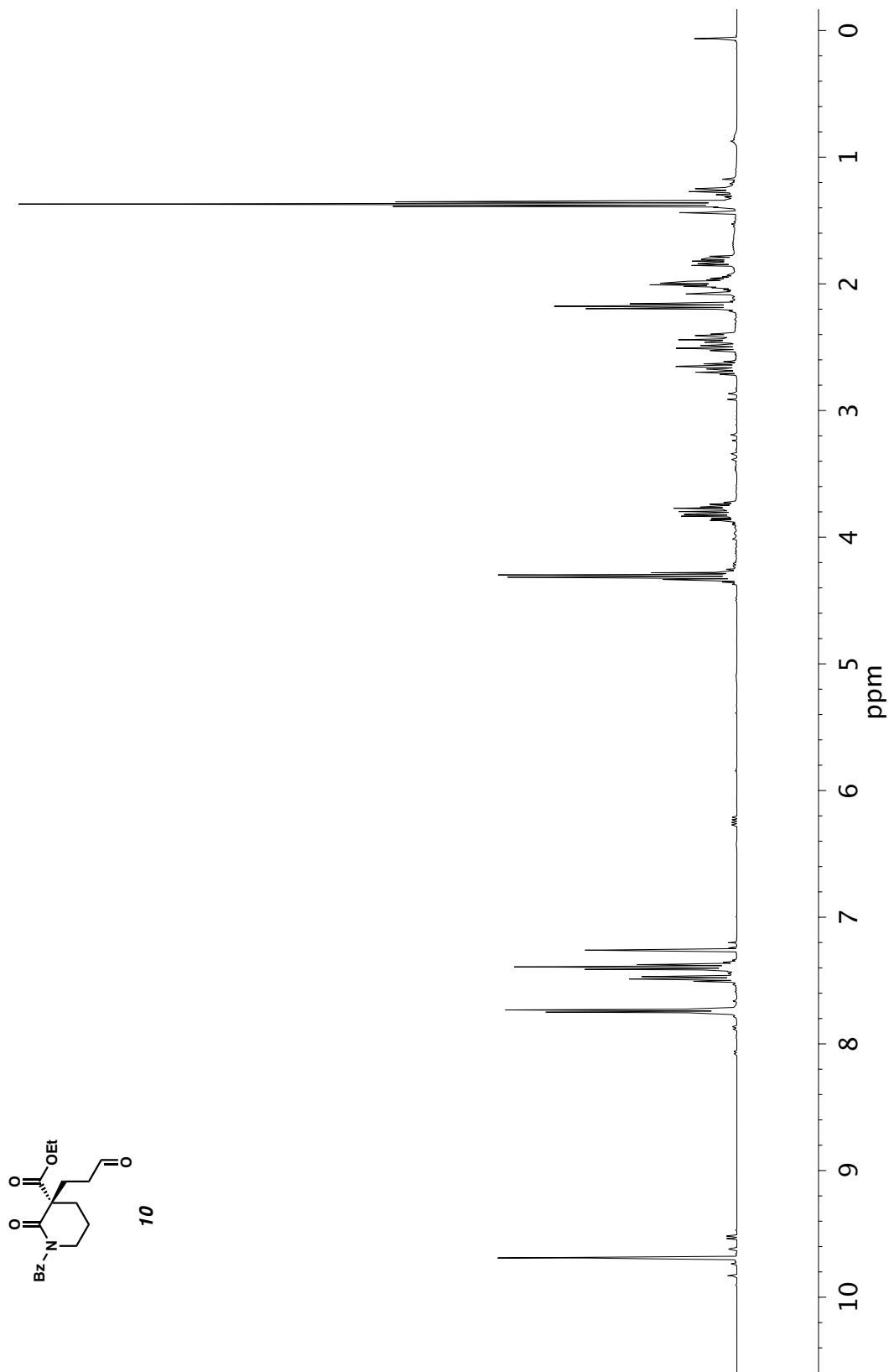


Figure A1.86 ¹H NMR (400 MHz, CDCl₃) of compound **10**.

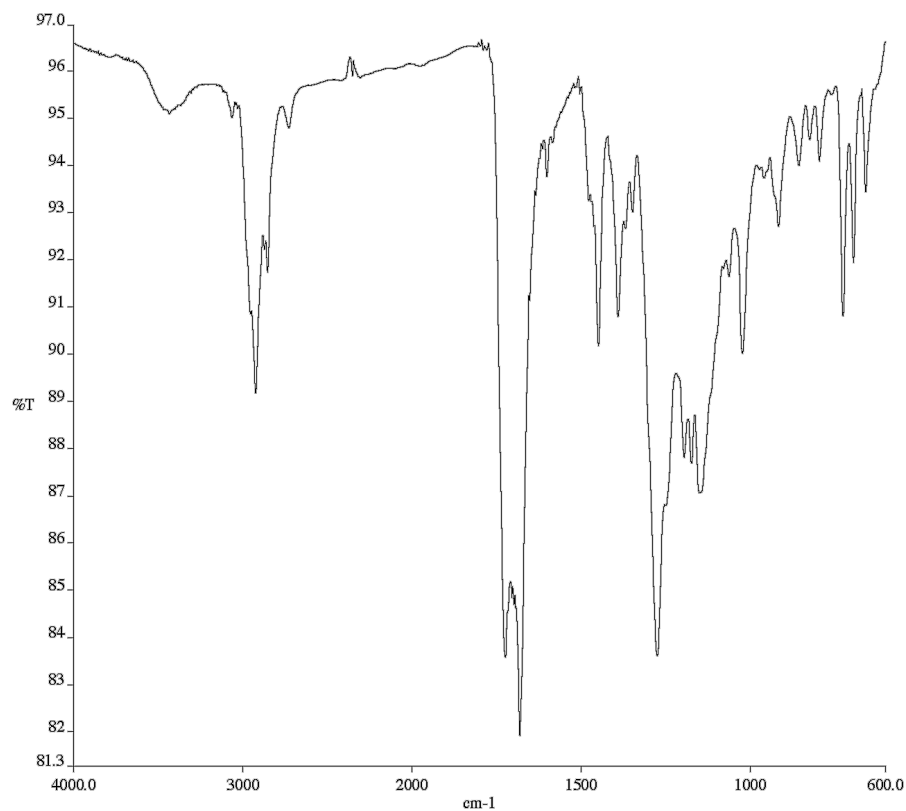


Figure A1.87 Infrared spectrum (Thin Film, NaCl) of compound **10**.

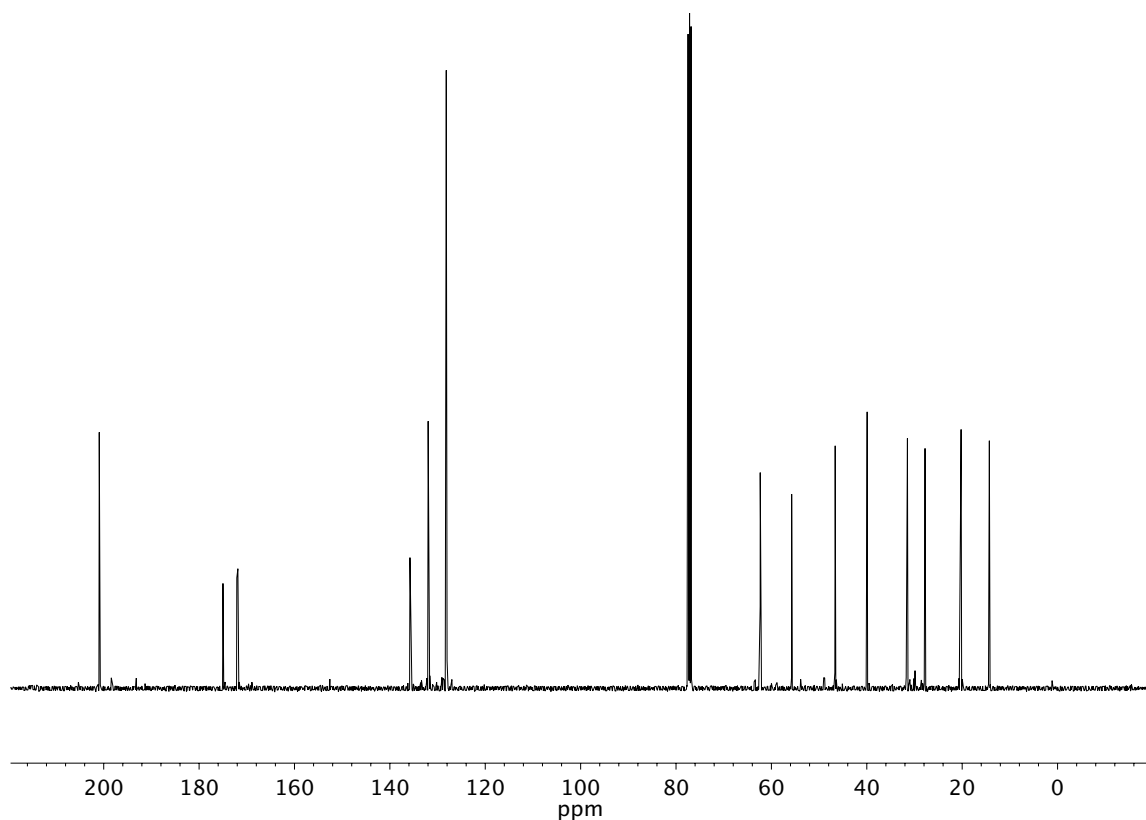


Figure A1.88 ¹³C NMR (100 MHz, CDCl₃) of compound **10**.

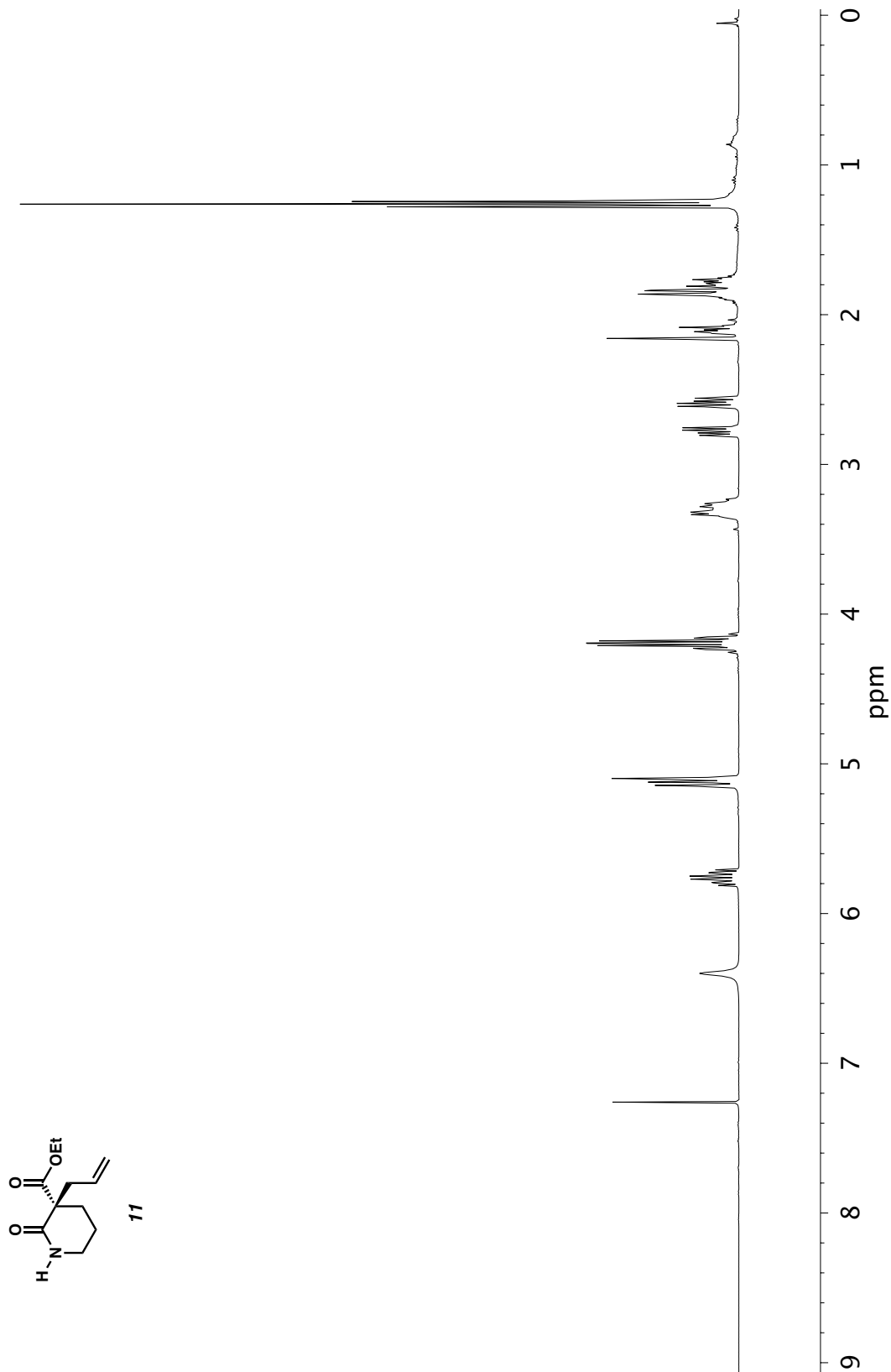


Figure A1.90 ^1H NMR (400 MHz, CDCl_3) of compound **11**.

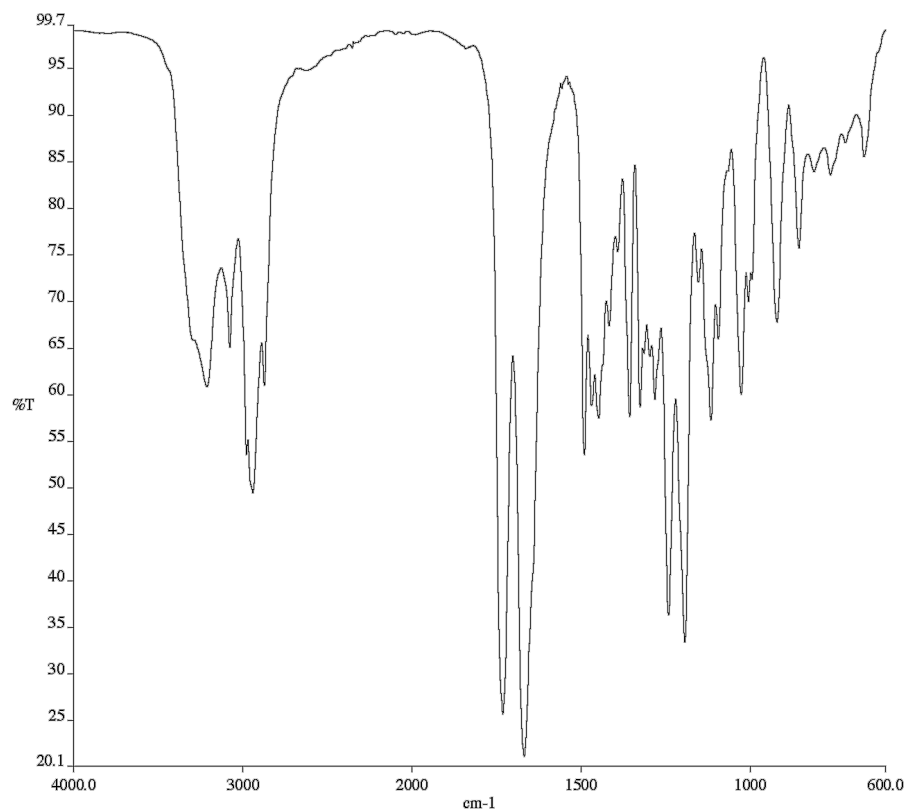


Figure A1.91 Infrared spectrum (Thin Film, NaCl) of compound **11**.

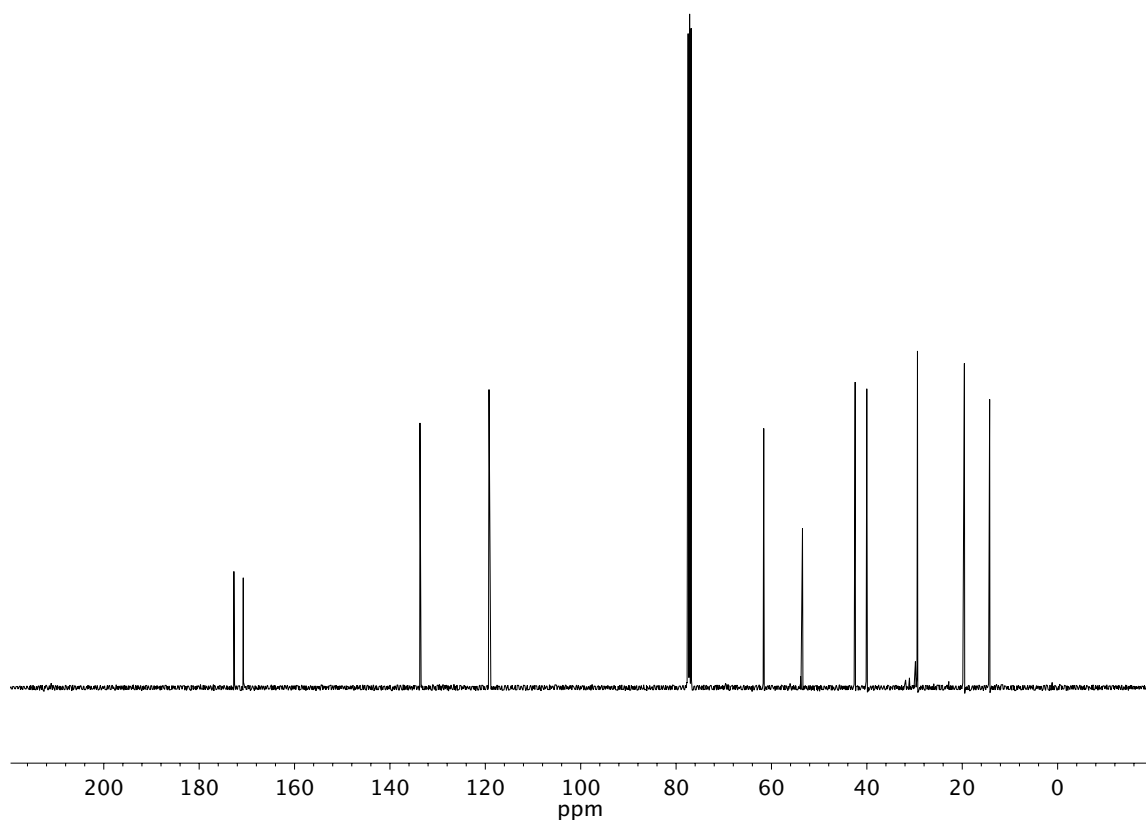


Figure A1.92 ¹³C NMR (100 MHz, CDCl₃) of compound **11**.

APPENDIX 2

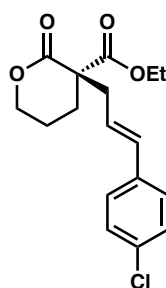
X-Ray Crystallography Reports Relevant to Chapter 1:

*Nickel-Catalyzed Enantioselective Allylic Alkylation of Lactones and
Lactams with Unactivated Allylic Alcohols*

A2.1 GENERAL EXPERIMENTAL

X-ray crystallographic analysis was obtained from the Caltech X-Ray Crystallography Facility using a Bruker D8 Venture Kappa Duo Photon 100 CMOS diffractometer.

A2.2 X-RAY CRYSTAL STRUCTURE ANALYSIS OF ALLYLIC ALKYLATION PRODUCT **3af**



The alkylation product **3af** (87% ee) was recrystallized from chloroform at $-30\text{ }^{\circ}\text{C}$ to provide crystals suitable for X-ray analysis.

Figure A2.1 X-ray crystal structure of allylic alkylation product **3af**.

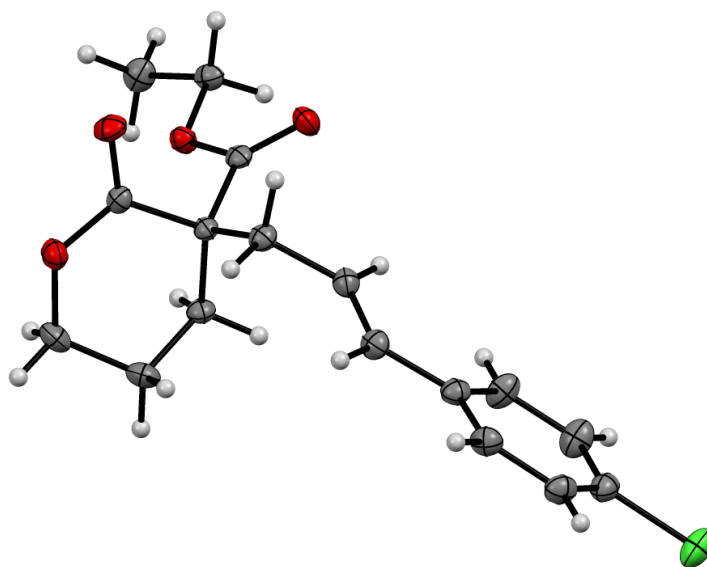


Table A2.1 Crystal data and structure refinement for allylic alkylation product **3af**.

Identification code	P17471	
Empirical formula	C ₁₇ H ₁₉ Cl O ₄	
Formula weight	322.77	
Temperature	100(2) K	
Wavelength	1.54178 Å	
Crystal system	Orthorhombic	
Space group	P2 ₁ 2 ₁ 2 ₁	
Unit cell dimensions	a = 6.9832(6) Å	α = 90°.
	b = 8.5007(7) Å	β = 90°.
	c = 26.483(2) Å	γ = 90°.
Volume	1572.1(2) Å ³	
Z	4	
Density (calculated)	1.364 Mg/m ³	
Absorption coefficient	2.289 mm ⁻¹	
F(000)	680	
Crystal size	0.300 x 0.150 x 0.050 mm ³	
Theta range for data collection	3.337 to 74.260°.	
Index ranges	-8 ≤ h ≤ 8, -10 ≤ k ≤ 10, -32 ≤ l ≤ 32	
Reflections collected	25120	
Independent reflections	3188 [R(int) = 0.0489]	
Completeness to theta = 67.679°	100.0 %	
Absorption correction	Semi-empirical from equivalents	
Max. and min. transmission	0.7538 and 0.6272	
Refinement method	Full-matrix least-squares on F ²	
Data / restraints / parameters	3188 / 0 / 200	
Goodness-of-fit on F ²	1.060	
Final R indices [I > 2σ(I)]	R1 = 0.0260, wR2 = 0.0656	
R indices (all data)	R1 = 0.0278, wR2 = 0.0664	
Absolute structure parameter	0.061(4)	

Extinction coefficient	n/a
Largest diff. peak and hole	0.227 and -0.175 e.Å ⁻³

Table A2.2 Atomic coordinates ($\times 10^4$) and equivalent isotropic displacement parameters ($\text{\AA}^2 \times 10^3$) for **3af**. $U(\text{eq})$ is defined as one third of the trace of the orthogonalized U^{ij} tensor.

	x	y	z	U(eq)
O(1)	928(2)	7806(2)	4419(1)	23(1)
C(1)	835(2)	6277(2)	4310(1)	17(1)
O(2)	-713(2)	5637(2)	4313(1)	24(1)
C(2)	2622(2)	5380(2)	4140(1)	16(1)
C(3)	4511(2)	6200(2)	4290(1)	19(1)
C(4)	4363(3)	7952(2)	4186(1)	24(1)
C(5)	2756(3)	8620(2)	4498(1)	26(1)
C(6)	2541(2)	3772(2)	4398(1)	17(1)
O(3)	2596(2)	2523(1)	4186(1)	24(1)
C(7)	2528(3)	2501(2)	5202(1)	20(1)
O(4)	2462(2)	3939(1)	4901(1)	19(1)
C(8)	2567(3)	3008(2)	5747(1)	27(1)
C(9)	2380(3)	5189(2)	3561(1)	20(1)
C(10)	4143(3)	4629(2)	3291(1)	21(1)
C(11)	4812(3)	5296(2)	2874(1)	22(1)
C(12)	6521(2)	4825(2)	2586(1)	21(1)
C(13)	7937(3)	3834(3)	2784(1)	27(1)
C(14)	9558(3)	3457(3)	2508(1)	29(1)
C(15)	9789(3)	4068(2)	2030(1)	24(1)
Cl(1)	11856(1)	3606(1)	1692(1)	34(1)
C(16)	8423(3)	5039(2)	1816(1)	24(1)
C(17)	6799(3)	5404(2)	2097(1)	24(1)

Table A2.3 Bond lengths [\AA] and angles [$^\circ$] for **3af**.

O(1)-C(1)	1.333(2)
O(1)-C(5)	1.467(2)
C(1)-O(2)	1.210(2)
C(1)-C(2)	1.530(2)
C(2)-C(6)	1.530(2)
C(2)-C(3)	1.543(2)
C(2)-C(9)	1.551(2)
C(3)-C(4)	1.518(3)
C(3)-H(3A)	0.9900
C(3)-H(3B)	0.9900
C(4)-C(5)	1.505(3)
C(4)-H(4A)	0.9900
C(4)-H(4B)	0.9900
C(5)-H(5A)	0.9900
C(5)-H(5B)	0.9900
C(6)-O(3)	1.202(2)
C(6)-O(4)	1.340(2)
C(7)-O(4)	1.459(2)
C(7)-C(8)	1.508(3)
C(7)-H(7A)	0.9900
C(7)-H(7B)	0.9900
C(8)-H(8A)	0.9800
C(8)-H(8B)	0.9800
C(8)-H(8C)	0.9800
C(9)-C(10)	1.502(2)
C(9)-H(9A)	0.9900
C(9)-H(9B)	0.9900
C(10)-C(11)	1.326(3)
C(10)-H(10)	0.9500
C(11)-C(12)	1.472(3)

C(11)-H(11)	0.9500
C(12)-C(17)	1.397(3)
C(12)-C(13)	1.401(3)
C(13)-C(14)	1.384(3)
C(13)-H(13)	0.9500
C(14)-C(15)	1.379(3)
C(14)-H(14)	0.9500
C(15)-C(16)	1.382(3)
C(15)-Cl(1)	1.7431(19)
C(16)-C(17)	1.392(3)
C(16)-H(16)	0.9500
C(17)-H(17)	0.9500

C(1)-O(1)-C(5)	122.26(14)
O(2)-C(1)-O(1)	118.72(16)
O(2)-C(1)-C(2)	120.46(16)
O(1)-C(1)-C(2)	120.61(15)
C(1)-C(2)-C(6)	106.47(13)
C(1)-C(2)-C(3)	113.40(14)
C(6)-C(2)-C(3)	108.67(14)
C(1)-C(2)-C(9)	104.69(14)
C(6)-C(2)-C(9)	110.14(14)
C(3)-C(2)-C(9)	113.22(14)
C(4)-C(3)-C(2)	109.75(14)
C(4)-C(3)-H(3A)	109.7
C(2)-C(3)-H(3A)	109.7
C(4)-C(3)-H(3B)	109.7
C(2)-C(3)-H(3B)	109.7
H(3A)-C(3)-H(3B)	108.2
C(5)-C(4)-C(3)	108.75(16)
C(5)-C(4)-H(4A)	109.9

C(3)-C(4)-H(4A)	109.9
C(5)-C(4)-H(4B)	109.9
C(3)-C(4)-H(4B)	109.9
H(4A)-C(4)-H(4B)	108.3
O(1)-C(5)-C(4)	113.07(15)
O(1)-C(5)-H(5A)	109.0
C(4)-C(5)-H(5A)	109.0
O(1)-C(5)-H(5B)	109.0
C(4)-C(5)-H(5B)	109.0
H(5A)-C(5)-H(5B)	107.8
O(3)-C(6)-O(4)	124.08(16)
O(3)-C(6)-C(2)	125.33(16)
O(4)-C(6)-C(2)	110.55(14)
O(4)-C(7)-C(8)	106.47(14)
O(4)-C(7)-H(7A)	110.4
C(8)-C(7)-H(7A)	110.4
O(4)-C(7)-H(7B)	110.4
C(8)-C(7)-H(7B)	110.4
H(7A)-C(7)-H(7B)	108.6
C(6)-O(4)-C(7)	116.84(13)
C(7)-C(8)-H(8A)	109.5
C(7)-C(8)-H(8B)	109.5
H(8A)-C(8)-H(8B)	109.5
C(7)-C(8)-H(8C)	109.5
H(8A)-C(8)-H(8C)	109.5
H(8B)-C(8)-H(8C)	109.5
C(10)-C(9)-C(2)	114.54(15)
C(10)-C(9)-H(9A)	108.6
C(2)-C(9)-H(9A)	108.6
C(10)-C(9)-H(9B)	108.6
C(2)-C(9)-H(9B)	108.6

H(9A)-C(9)-H(9B)	107.6
C(11)-C(10)-C(9)	123.40(17)
C(11)-C(10)-H(10)	118.3
C(9)-C(10)-H(10)	118.3
C(10)-C(11)-C(12)	126.94(18)
C(10)-C(11)-H(11)	116.5
C(12)-C(11)-H(11)	116.5
C(17)-C(12)-C(13)	117.39(17)
C(17)-C(12)-C(11)	119.79(17)
C(13)-C(12)-C(11)	122.81(17)
C(14)-C(13)-C(12)	121.30(18)
C(14)-C(13)-H(13)	119.3
C(12)-C(13)-H(13)	119.3
C(15)-C(14)-C(13)	119.48(18)
C(15)-C(14)-H(14)	120.3
C(13)-C(14)-H(14)	120.3
C(14)-C(15)-C(16)	121.37(18)
C(14)-C(15)-Cl(1)	118.91(15)
C(16)-C(15)-Cl(1)	119.72(15)
C(15)-C(16)-C(17)	118.44(17)
C(15)-C(16)-H(16)	120.8
C(17)-C(16)-H(16)	120.8
C(16)-C(17)-C(12)	122.01(18)
C(16)-C(17)-H(17)	119.0
C(12)-C(17)-H(17)	119.0

Table A2.4 Anisotropic displacement parameters ($\text{\AA}^2 \times 10^3$) for **3af**. The anisotropic displacement factor exponent takes the form: $-2\pi^2 [h^2 a^{*2} U^{11} + \dots + 2 h k a^* b^* U^{12}]$.

U11	U22	U33	U23	U13	U12
-----	-----	-----	-----	-----	-----

O(1)	22(1)	19(1)	28(1)	-3(1)	0(1)	4(1)
C(1)	16(1)	19(1)	17(1)	2(1)	0(1)	2(1)
O(2)	15(1)	27(1)	32(1)	4(1)	1(1)	0(1)
C(2)	13(1)	16(1)	19(1)	-1(1)	-1(1)	0(1)
C(3)	15(1)	21(1)	22(1)	-1(1)	-1(1)	-2(1)
C(4)	25(1)	19(1)	29(1)	2(1)	-2(1)	-7(1)
C(5)	31(1)	16(1)	30(1)	-4(1)	-2(1)	-4(1)
C(6)	11(1)	18(1)	23(1)	0(1)	-1(1)	-1(1)
O(3)	31(1)	16(1)	27(1)	-3(1)	2(1)	-1(1)
C(7)	17(1)	17(1)	26(1)	6(1)	0(1)	2(1)
O(4)	22(1)	16(1)	20(1)	2(1)	0(1)	0(1)
C(8)	28(1)	28(1)	24(1)	6(1)	1(1)	6(1)
C(9)	17(1)	22(1)	21(1)	0(1)	-1(1)	0(1)
C(10)	20(1)	21(1)	22(1)	-3(1)	-1(1)	2(1)
C(11)	20(1)	22(1)	24(1)	1(1)	-2(1)	2(1)
C(12)	20(1)	22(1)	21(1)	-1(1)	-1(1)	-3(1)
C(13)	24(1)	38(1)	18(1)	4(1)	0(1)	3(1)
C(14)	24(1)	40(1)	24(1)	2(1)	-3(1)	7(1)
C(15)	21(1)	27(1)	23(1)	-4(1)	1(1)	-3(1)
Cl(1)	27(1)	48(1)	28(1)	-1(1)	8(1)	5(1)
C(16)	27(1)	27(1)	19(1)	2(1)	1(1)	-4(1)
C(17)	24(1)	24(1)	24(1)	4(1)	-2(1)	0(1)

Table A2.5 Hydrogen coordinates ($\times 10^4$) and isotropic displacement parameters ($\text{\AA}^2 \times 10^3$) for **3af**.

	x	y	z	U(eq)
H(3A)	4771	6023	4653	23
H(3B)	5585	5747	4093	23

H(4A)	5583	8477	4274	29
H(4B)	4108	8133	3822	29
H(5A)	3106	8551	4859	31
H(5B)	2594	9746	4413	31
H(7A)	3689	1884	5119	24
H(7B)	1387	1843	5134	24
H(8A)	3645	3726	5802	40
H(8B)	2714	2082	5964	40
H(8C)	1367	3547	5830	40
H(9A)	1329	4433	3497	24
H(9B)	1991	6214	3417	24
H(10)	4813	3751	3425	25
H(11)	4115	6171	2748	26
H(13)	7782	3413	3113	32
H(14)	10505	2782	2648	35
H(16)	8589	5447	1485	29
H(17)	5851	6067	1953	28

Table A2.6 Torsion angles [°] for **3af**.

C(5)-O(1)-C(1)-O(2)	170.67(16)
C(5)-O(1)-C(1)-C(2)	-14.5(2)
O(2)-C(1)-C(2)-C(6)	-45.3(2)
O(1)-C(1)-C(2)-C(6)	139.99(16)
O(2)-C(1)-C(2)-C(3)	-164.76(17)
O(1)-C(1)-C(2)-C(3)	20.5(2)
O(2)-C(1)-C(2)-C(9)	71.34(19)
O(1)-C(1)-C(2)-C(9)	-103.36(18)
C(1)-C(2)-C(3)-C(4)	-43.6(2)
C(6)-C(2)-C(3)-C(4)	-161.81(15)

C(9)-C(2)-C(3)-C(4)	75.47(19)
C(2)-C(3)-C(4)-C(5)	60.8(2)
C(1)-O(1)-C(5)-C(4)	32.0(2)
C(3)-C(4)-C(5)-O(1)	-54.7(2)
C(1)-C(2)-C(6)-O(3)	124.19(18)
C(3)-C(2)-C(6)-O(3)	-113.33(19)
C(9)-C(2)-C(6)-O(3)	11.2(2)
C(1)-C(2)-C(6)-O(4)	-57.84(17)
C(3)-C(2)-C(6)-O(4)	64.64(18)
C(9)-C(2)-C(6)-O(4)	-170.80(13)
O(3)-C(6)-O(4)-C(7)	2.6(2)
C(2)-C(6)-O(4)-C(7)	-175.38(13)
C(8)-C(7)-O(4)-C(6)	175.89(14)
C(1)-C(2)-C(9)-C(10)	168.24(15)
C(6)-C(2)-C(9)-C(10)	-77.66(18)
C(3)-C(2)-C(9)-C(10)	44.2(2)
C(2)-C(9)-C(10)-C(11)	-132.25(19)
C(9)-C(10)-C(11)-C(12)	-179.98(17)
C(10)-C(11)-C(12)-C(17)	165.5(2)
C(10)-C(11)-C(12)-C(13)	-16.1(3)
C(17)-C(12)-C(13)-C(14)	0.7(3)
C(11)-C(12)-C(13)-C(14)	-177.81(19)
C(12)-C(13)-C(14)-C(15)	0.1(3)
C(13)-C(14)-C(15)-C(16)	-0.7(3)
C(13)-C(14)-C(15)-Cl(1)	179.04(16)
C(14)-C(15)-C(16)-C(17)	0.6(3)
Cl(1)-C(15)-C(16)-C(17)	-179.20(15)
C(15)-C(16)-C(17)-C(12)	0.2(3)
C(13)-C(12)-C(17)-C(16)	-0.8(3)
C(11)-C(12)-C(17)-C(16)	177.69(18)

CHAPTER 2

Palladium-Catalyzed Enantioselective

Decarboxylative Allylic Alkylation of Cyclic Siloxyketones[†]

2.1 INTRODUCTION

Silicon-containing heterocycles are an important class of organic molecules often used in the context of temporary functional groups in the synthesis of natural products and drug molecules.¹ In particular, oxasilacycles or cyclic siloxanes are frequently employed in various stages of total syntheses.² These moieties are characterized not only by their high tolerance to a range of reaction conditions, but also for their ability to be selectively and easily utilized in a variety of useful transformations.

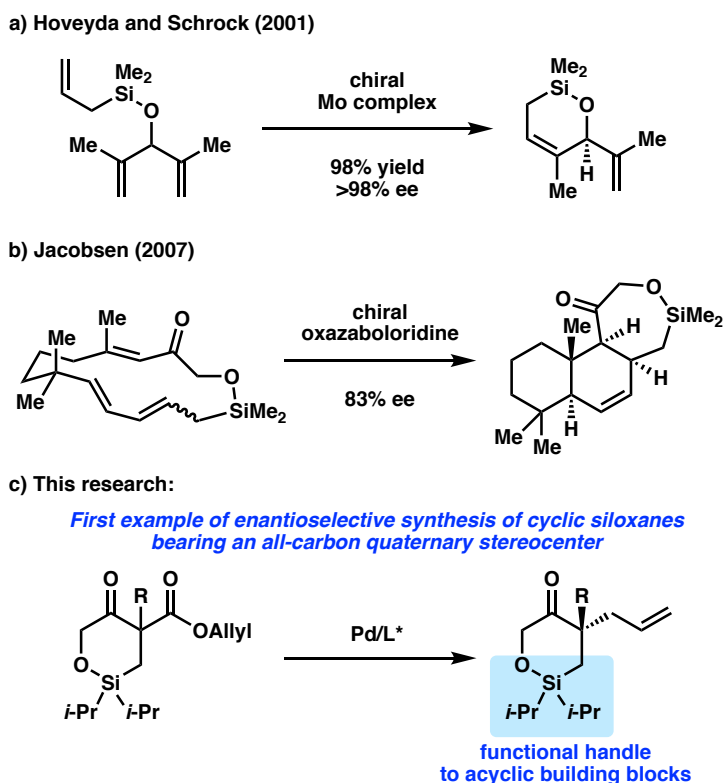
[†] This research was performed in collaboration with Dr. Toshihiko Iwayama and Dr. Michael D. Bartberger. Portions of this chapter have been reproduced with permission from Ngamnithiporn, A.; Iwayama, T.; Bartberger, M. D.; Stoltz, B. M. *Chemical Science*. **2020**, *11*, 11068–11071. © 2020 Royal Society of Chemistry.

While a number of non-asymmetric methods have been reported for the preparation of cyclic siloxanes,³ methods to access enantioenriched cyclic siloxanes are limited, with a majority of examples requiring the use of enantioenriched starting materials.⁴ To the best of our knowledge, there are only two existing reports detailing the enantioselective synthesis of cyclic siloxanes.⁵ In 2001, Hoveyda, Schrock and coworkers reported an enantioselective desymmetrization of trienes via asymmetric ring-closing metathesis utilizing their developed Mo-catalyst (Scheme 2.1a).^{5a} An enantioenriched cyclic siloxane could be obtained in 98% yield with excellent enantioselectivity. Jacobsen later disclosed a method for asymmetric transannular Diels–Alder reactions (Scheme 2.1b).^{5b} In the presence of a chiral oxazaborolidine catalyst, the fused cyclic siloxane was obtained with good enantioselectivity. Subsequent oxidative cleavage of this siloxane provided a precursor to a number of sesquiterpine natural products. Although these two reports showcase unique synthetic strategies to access cyclic siloxanes in an enantioselective fashion, the substrate scope in each report only contains a single example of a cyclic siloxane. Furthermore, an enantioselective method to access cyclic siloxanes bearing all-carbon quaternary stereocenters has not been reported to date.

To this end, we sought to target the synthesis of this useful motif as part of our on-going research interest in the development of asymmetric allylic alkylation methodologies.^{6,7} Namely, we envisioned performing an enantioselective decarboxylative allylic alkylation of a cyclic siloxy- β -ketoester to access a siloxyketone bearing a quaternary stereocenter (Scheme 2.1c).⁸ Furthermore, we believe that utilization of the silicon functionality in the alkylation products would

allow for the synthesis of enantioenriched acyclic quaternary stereocenters, a motif that still poses a significant challenge in organic synthesis.⁹ Herein, we report our efforts toward the realization of these goals.

Scheme 2.1 Enantioselective synthesis of cyclic siloxanes.

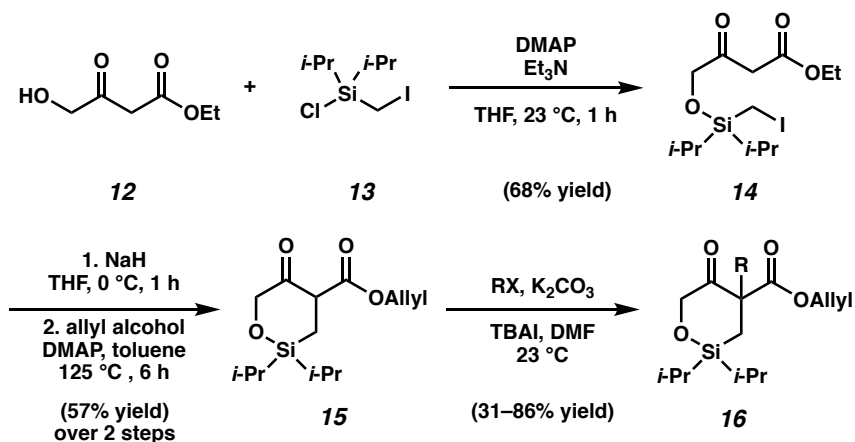


2.2 SUBSTRATE SYNTHESIS

As the synthesis of cyclic siloxy- β -ketoester substrates had not been previously reported, we initiated our study by first establishing a synthetic route to access the cyclic siloxy- β -ketoester substrates (Scheme 2). Our developed process began with intermolecular O-silylation of alcohol **12** with silyl chloride **13**, affording β -ketoester **14**. Cyclization via intramolecular nucleophilic substitution and subsequent transesterification with allyl alcohol provided allyl β -ketoester **15**

in 57% yield over 2 steps. Lastly, functionalization of **15** with various electrophiles delivered a variety of siloxy- β -ketoester substrates **16**.¹⁰

Scheme 2.2 Siloxy- β -ketoester substrate synthesis.



2.3 REACTION OPTIMIZATION

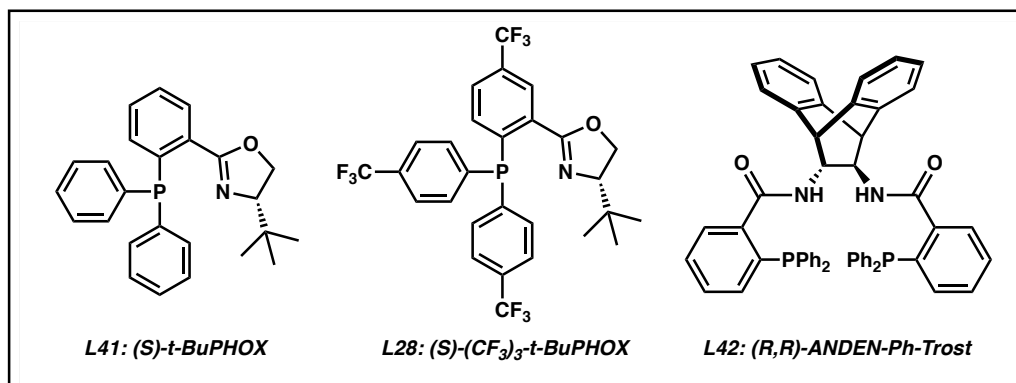
With the substrates in hand, our studies continued with an investigation of the palladium-catalyzed decarboxylative allylic alkylation (Table 2.1). We were pleased to find that treatment of **16a** to commonly employed allylic alkylation conditions¹¹ using Pd₂(dba)₃ and (*S*)-*t*-BuPHOX ligand (**L41**) in toluene proceeded smoothly with >95% conversion and provided the desired cyclic siloxane **17a** in a moderate 75% ee (Table 2.1, entry 1). An examination of additional ligands revealed that switching to the more electron-deficient PHOX ligand **L28** delivered the product in an excellent 91% ee (entry 2), while the use of Trost-type bisphosphine ligand **L42**¹² provided **17a** in a slightly diminished 89% ee (entry 3). Continuing with the optimal ligand **L28**, a survey of different solvents revealed that while consistently high levels of enantioselectivity could be achieved (entries

4–7), toluene remained the optimal solvent. Finally, by performing the reaction at 0 °C, the highest ee of 94% was obtained with no loss in reactivity.

Table 2.1 Optimization of reaction parameters.^a

16a **17a**

entry	ligand	solvent	% conversion ^b	% ee ^c
1	<i>L41</i>	toluene	>95	75
2	<i>L28</i>	toluene	>95	91
3	<i>L42</i>	toluene	>95	–89
4	<i>L28</i>	THF	>95	87
5	<i>L28</i>	MTBE	>95	87
6	<i>L28</i>	1,4-dioxane	>95	89
7	<i>L28</i>	2:1 hexane/toluene	>95	89
8 ^d	<i>L28</i>	toluene	>95	94



[a] Conditions: **16a** (0.1 mmol), Pd₂(dba)₃ (5 mol %), ligand (12.5 mol %) in solvent (3 mL). [b] Conversion determined by ¹H NMR of crude reaction mixture using 1,3,5-trimethoxybenzene as a standard. [c] % ee determined by chiral SFC analysis of the isolated product. [d] Reaction performed at 0 °C.

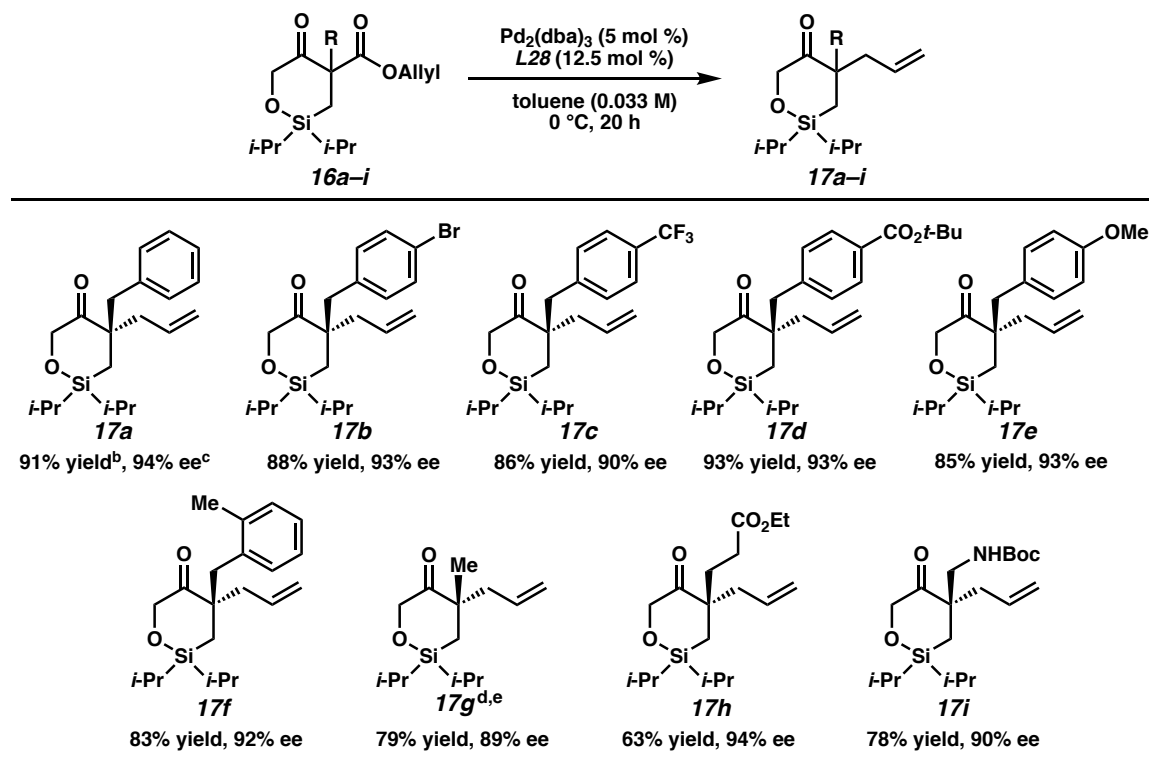
2.4 SUBSTRATE SCOPE EXPLORATION

Having identified the optimal reaction conditions, we next explored the substrate scope of this transformation (Table 2.2). With the benzyl group at the α-quaternary position, the enantioenriched cyclic siloxane product (**17a**) was isolated

in 91% yield with 94% ee. An investigation of the electronic nature of this benzyl group demonstrated that both electron-withdrawing and electron-donating groups (**17b–17e**) were well tolerated (90–93% ee). A sterically hindered *ortho*-substituted benzyl substrate fared well under our optimized reaction conditions, providing product **17f** in 83% yield with 92% ee. A significant loss of reactivity, however, was observed when a methyl-substituted substrate was employed (**17g**, ca. 30% conversion). Pleasingly, we were able to improve the reactivity of this substrate by increasing the temperature to 23 °C, delivering product **17g** in 79% yield with 89% ee. Additionally, cyclic siloxane starting materials bearing ester (**16h**) and Boc-protected alkyl amine (**16i**) functionalities delivered products **17h** and **17g** in 94% ee and 90% ee, respectively.

Despite several attempts at procuring x-ray quality crystals for determination of the absolute stereochemistry of the products, these efforts proved fruitless, presumably due to the non-polar nature and flexibility of these molecules. Thus, vibrational circular dichroism (VCD) was utilized for the determination of absolute configuration of products **17a** and **17g**. Sufficient agreement between the computed and measured VCD spectra were achieved such that the absolute configurations of **17a** and **17g** could be assigned with confidence as (*R*) and (*S*), respectively, as depicted in Table 2.2.¹³ Additionally, the measured optical rotation of **17g** was found to be consistent with that computed for the Boltzmann-weighted conformational ensemble of the (*S*) enantiomer. With these configurations assigned, the absolute configurations for all other products have been inferred by analogy.

Table 2.2 Substrate scope.^a



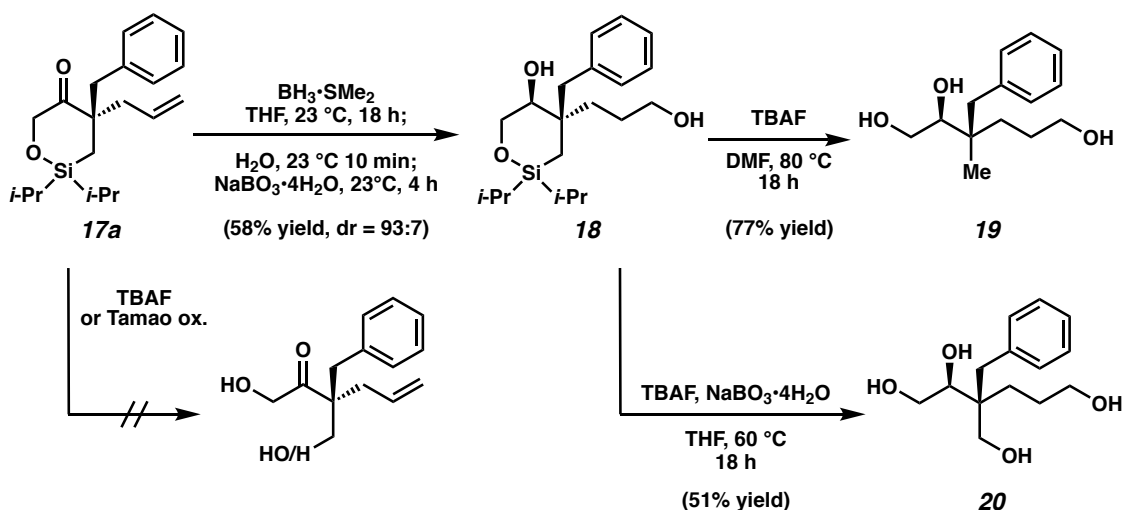
[a] Reactions performed on 0.2 mmol scale. [b] Yield of isolated product. [c] %ee determined by chiral SFC analysis. [d] Reaction performed at 23 °C. [e] Absolute configuration determined by experimental and computed VCD and optical rotation, see text.

2.5 PRODUCT TRANSFORMATIONS

In order to demonstrate the utility of this transformation, the final stage of our study involved the utilization of the silyl fragment as a functional handle to access acyclic chiral building blocks (Scheme 2.3). Unfortunately, the direct ring-opening of cyclic siloxane **17a** proved to be challenging as both neutral (TBAF) and oxidative (Tamao oxidation) conditions failed to deliver the desired acyclic products. However, we were pleased to find that with prior hydroboration/oxidation and concomitant ketone reduction, facile ring opening could be achieved. The diol **18** was isolated in 58% yield as a 93:7 mixture of diastereomers.¹⁴ Siloxane ring

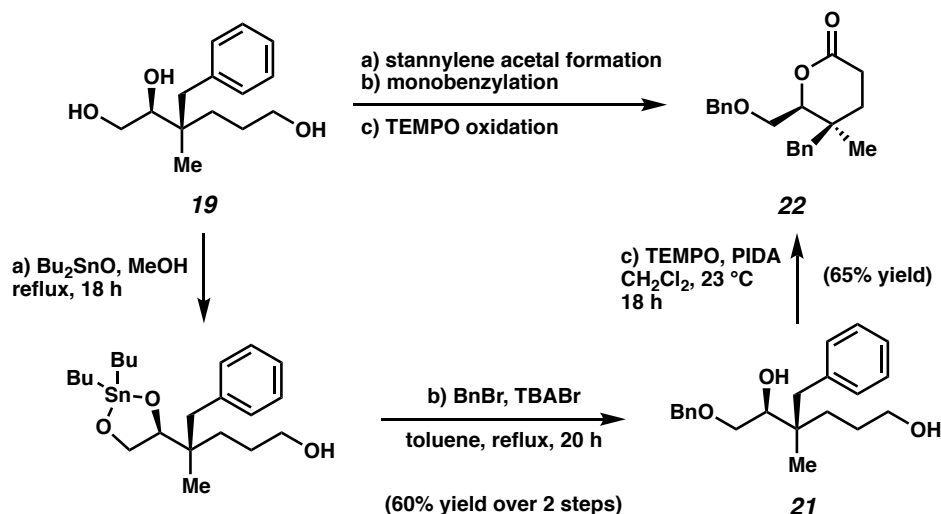
opening was then achieved with TBAF either in the absence or presence of NaBO₃ as an oxidant to deliver triol **19** or tetraol **20** in 77% yield and 51% yield, respectively.

Scheme 2.3 Synthesis of highly oxygenated, chiral, acyclic quaternary stereocenters.



We also sought to further demonstrate the utility of these highly oxygenated acyclic building blocks by preparing a densely functionalized lactone (**22**, Scheme 2.4). First, selective monobenzylation of triol **19** provided **21** via a stannylene acetal intermediate.¹⁵ Subsequently, δ -lactone **22**, bearing vicinal quaternary-trisubstituted stereocenters, could be generated from TEMPO oxidation in 39% yield over 3 steps.

Scheme 2.4 Synthesis of lactone bearing vicinal quaternary-trisubstituted stereocenters.



2.6 CONCLUSIONS

In summary, we have developed the first enantioselective synthesis of cyclic siloxanes bearing an all-carbon quaternary stereocenter. Through Pd-catalyzed decarboxylative allylic alkylation, enantioenriched cyclic siloxanes can be constructed in good yield (up to 91% yield) and with high enantiomeric excess (up to 94% ee). The reaction conditions exhibit a high tolerance toward a range of functional groups, and the alkylation products can be further derivatized to obtain stereochemically rich acyclic building blocks. Efforts to further extend the substrate scope of this transformation, as well as applications in natural product synthesis, are currently underway in our laboratory.

2.7 EXPERIMENTAL SECTION

2.7.1 MATERIALS AND METHODS

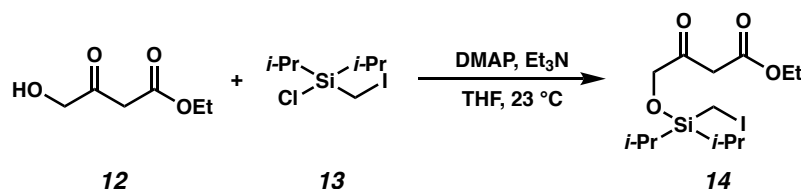
Unless otherwise stated, reactions were performed in flame-dried glassware under an argon or nitrogen atmosphere using dry, deoxygenated solvents. Solvents were dried by passage through an activated alumina column under argon. Reaction progress was monitored by thin-layer chromatography (TLC) or Agilent 1290 UHPLC-MS. TLC was performed using E. Merck silica gel 60 F254 precoated glass plates (0.25 mm) and visualized by UV fluorescence quenching, *p*-anisaldehyde, or KMnO₄ staining. Silicycle SiliaFlash® P60 Academic Silica gel (particle size 40–63 μm) was used for flash chromatography. ¹H NMR spectra were recorded on Bruker 400 MHz or Varian Mercury 300 MHz spectrometers and are reported relative to residual CHCl₃ (δ 7.26 ppm) or CH₃OH (δ 3.31 ppm). ¹³C NMR spectra were recorded on Bruker 400 MHz spectrometer (100 MHz) and are reported relative to CHCl₃ (δ 77.16 ppm) or CH₃OH (δ 49.00 ppm). ¹⁹F NMR spectra were recorded on Varian Mercury 300 MHz spectrometer (282 MHz). Data for ¹H NMR are reported as follows: chemical shift (δ ppm) (multiplicity, coupling constant (Hz), integration). Multiplicities are reported as follows: s = singlet, d = doublet, t = triplet, q = quartet, p = pentet, sept = septuplet, m = multiplet, br s = broad singlet, br d = broad doublet, app = apparent. Data for ¹³C NMR are reported in terms of chemical shifts (δ ppm). IR spectra were obtained using Perkin Elmer Spectrum BXII spectrometer or Nicolet 6700 FTIR spectrometer using thin films deposited on NaCl plates and reported in frequency of absorption (cm⁻¹). Optical rotations were measured with a Jasco P-2000 polarimeter operating on the sodium D-line (589 nm), using a 100 mm path-length cell and are reported as: $[\alpha]_{\text{D}}^{\text{T}}$ (concentration in 10 mg/1 mL, solvent).

Analytical SFC was performed with a Mettler SFC supercritical CO₂ analytical chromatography system utilizing Chiralpak (AD-H, AS-H or IC) or Chiralcel (OD-H, OJ-H, or OB-H) columns (4.6 mm x 25 cm) obtained from Daicel Chemical Industries, Ltd. Analytical chiral GC was performed with an Agilent 6850 GC utilizing a Chiraldex G-TA (30 m x 0.25cm) column (1.0 mL/min carrier gas flow). High resolution mass spectra (HRMS) were obtained from Agilent 6200 Series TOF with an Agilent G1978A Multimode source in electrospray ionization (ESI+), atmospheric pressure chemical ionization (APCI+), or mixed ionization mode (MM: ESI-APCI+), or obtained from the Caltech mass spectrometry laboratory.

Reagents were purchased from Sigma-Aldrich, Acros Organics, Strem, or Alfa Aesar, and used as received unless otherwise stated.

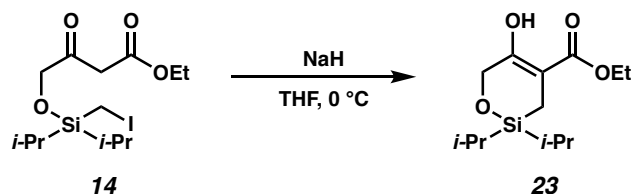
2.7.2 EXPERIMENTAL PROCEDURES AND SPECTROSCOPIC DATA

2.7.2.1 Synthesis of allyl β -ketoester starting materials



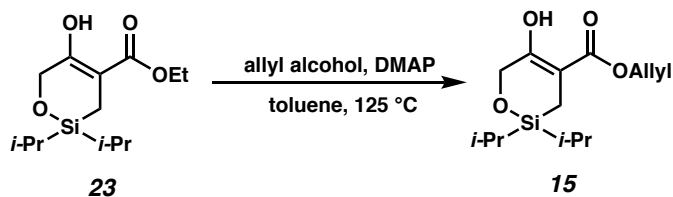
Ethyl 4-(((iodomethyl)diisopropylsilyl)oxy)-3-oxobutanoate (14): To a solution of alcohol **12**¹⁶ (3.14 g, 21.5 mmol, 1.00 equiv) in THF (72 mL) at 0 °C was added chlorosilane **13**¹⁷ (6.25 g, 21.5 mmol, 1.00 equiv), triethylamine (3.0 mL, 21.5 mmol, 1.00 equiv), and DMAP (0.14 g, 1.1 mmol, 0.05 equiv). The reaction mixture was warmed to room temperature and stirred for 1 hour. After complete consumption of the alcohol starting material, as observed by TLC, the reaction was cooled to 0 °C and

quenched with saturated aqueous NH_4Cl . The layers were separated and the aqueous layer was extracted with CH_2Cl_2 twice. The combined organic phases were dried over Na_2SO_4 , filtered, and concentrated under vacuum. The crude residue was purified by column chromatography (5% to 10% EtOAc in hexanes) to afford **14** as a colorless oil (5.89 g, 68% yield); ^1H NMR (400 MHz, CDCl_3) δ 4.40 (s, 2H), 4.20 (q, $J = 7.2$ Hz, 2H), 3.62 (s, 2H), 2.09 (s, 2H), 1.32 – 1.24 (m, 5H), 1.10 (d, $J = 4.0$ Hz, 6H), 1.08 (d, $J = 3.8$ Hz, 6H); ^{13}C NMR (100 MHz, CDCl_3) δ 203.6, 167.3, 69.6, 61.6, 45.8, 17.6, 17.5, 14.3, 12.3; IR (Neat Film, NaCl) 2944, 2867, 1743, 1726, 1464, 1369, 1320, 1227, 1134, 1109, 1035, 882, 810, 731 cm^{-1} ; HRMS (MM) m/z calc'd for $\text{C}_{13}\text{H}_{26}\text{IO}_4\text{Si}$ $[\text{M}+\text{H}]^+$: 401.0640, found 401.0625.

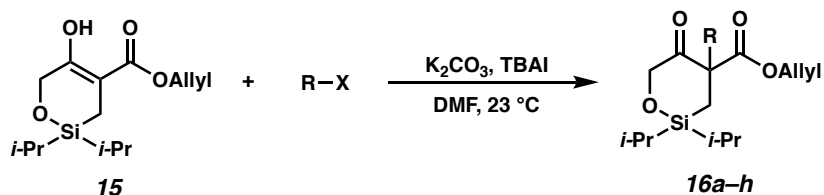


Ethyl 2,2-diisopropyl-5-oxo-1,2-oxasilinane-4-carboxylate (23): To a solution of **14** (2.95 g, 7.37 mmol, 1.00 equiv) in THF (74 mL) at 0 °C, NaH (60% in mineral oil, 0.34 g, 8.11 mmol, 1.10 equiv) was added. The reaction mixture was stirred for 1 hour at 0 °C, at which point complete consumption of the starting material was observed by TLC. The reaction was quenched with saturated aqueous NH_4Cl . The layers were separated and the aqueous layer was extracted with EtOAc twice. The combined organics were washed with brine, dried over Na_2SO_4 , filtered, and concentrated under vacuum. The crude residue was purified by column chromatography (10% EtOAc in hexanes) to afford **23** as a colorless oil (1.70 g, 85% yield); ^1H NMR (400 MHz, CDCl_3) δ 12.50 (s, 1H, OH), 4.44 (d, $J = 1.3$ Hz, 2H), 4.25 (q, $J = 7.1$ Hz, 2H), 1.43 (d, $J = 1.4$ Hz, 2H), 1.34 (t, $J = 7.1$ Hz,

3H), 1.01 (d, $J = 6.1$ Hz, 14H); ^{13}C NMR (100 MHz, CDCl_3) δ 173.7, 170.6, 95.3, 64.6, 61.0, 17.1, 17.1, 14.4, 12.8, 1.9; IR (Neat Film, NaCl) 2943, 2866, 1655, 1464, 1314, 1221, 1154, 1104, 1048, 882, 785 cm^{-1} ; HRMS (MM) m/z calc'd for $\text{C}_{13}\text{H}_{25}\text{O}_4\text{Si}$ $[\text{M}+\text{H}]^+$: 273.1517, found 273.1514.

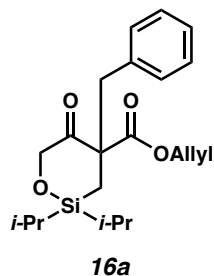


Allyl 2,2-diisopropyl-5-oxo-1,2-oxasilinane-4-carboxylate (15): To a solution of **23** (0.50 g, 1.84 mmol, 1.00 equiv) in toluene (6 mL) in a sealed tube, allyl alcohol (3.12 mL, 45.9 mmol, 25.0 equiv) and DMAP (22.4 mg, 0.18 mmol, 0.10 equiv) were added. The reaction mixture was heated to 125 $^\circ\text{C}$ and stirred for 6 hours. The reaction was allowed to cool to room temperature and concentrated under vacuum. The crude residue was purified by column chromatography (5% EtOAc in hexanes) to afford **15** as a colorless oil (0.38 g, 67% yield); ^1H NMR (400 MHz, CDCl_3) δ 12.40 (s, 1H, OH), 5.99 (ddt, $J = 17.2, 10.5, 5.6$ Hz, 1H), 5.36 (dq, $J = 17.2, 1.6$ Hz, 1H), 5.28 (dq, $J = 10.4, 1.3$ Hz, 1H), 4.71 (dt, $J = 5.5, 1.4$ Hz, 2H), 4.45 (t, $J = 1.4$ Hz, 2H), 1.47 (t, $J = 1.4$ Hz, 2H), 1.04 – 0.98 (m, 14H); ^{13}C NMR (100 MHz, CDCl_3) δ 173.2, 171.1, 132.2, 118.4, 95.2, 65.5, 64.6, 17.1, 17.1, 12.8, 1.9; IR (Neat Film, NaCl) 2943, 2892, 2866, 1656, 1463, 1313, 1216, 1153, 1108, 993, 882, 786, 736 cm^{-1} ; HRMS (MM) m/z calc'd for $\text{C}_{14}\text{H}_{25}\text{O}_4\text{Si}$ $[\text{M}+\text{H}]^+$: 285.1517, found 285.1519.



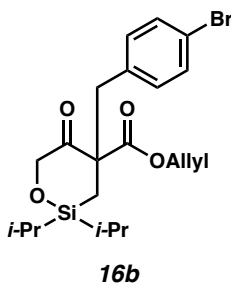
General Procedure 1:

To a solution of β -keto ester **15** (1.00 equiv) in DMF (0.10 M), alkyl halide (1.10 equiv), K_2CO_3 (1.10 equiv), and TBAI (1.10 equiv) were added sequentially. The reaction mixture was stirred at room temperature overnight, then quenched with saturated NH_4Cl . The layers were separated and the aqueous phase was extracted with Et_2O twice. The combined organic layers were dried over Na_2SO_4 , filtered, and concentrated. The crude residue was purified by column chromatography to afford alkylated product **16**.



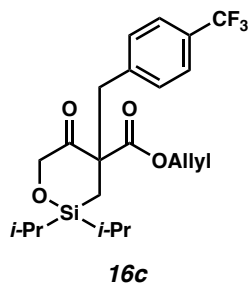
Allyl 4-benzyl-2,2-diisopropyl-5-oxo-1,2-oxasilinane-4-carboxylate (16a): Prepared according to General Procedure 1 using benzyl bromide and purified by column chromatography (10% Et_2O in hexanes) to afford **16a** as a colorless oil (378 mg, 83% yield). 1H NMR (400 MHz, $CDCl_3$) δ 7.19 – 7.12 (m, 3H), 7.10 – 7.03 (m, 2H), 5.66 (ddt, $J = 17.2, 10.4, 5.9$ Hz, 1H), 5.21 – 5.08 (m, 2H), 4.50 (ddt, $J = 13.0, 5.8, 1.3$ Hz, 1H), 4.44 (d, $J = 18.4$ Hz, 1H), 4.31 (ddt, $J = 13.0, 6.0, 1.3$ Hz, 1H), 4.20 (dd, $J = 18.4, 0.6$ Hz, 1H), 3.26 (d, $J = 13.6$ Hz, 1H), 2.88 (d, $J = 13.6$ Hz, 1H), 1.67 (d, $J = 15.2$ Hz, 1H), 1.10 – 0.87 (m, 14H), 0.65 (d, $J = 15.2$ Hz, 1H); ^{13}C NMR (100 MHz, $CDCl_3$) δ 208.8, 170.6,

136.5, 131.3, 130.7, 128.1, 126.9, 119.2, 70.3, 66.2, 59.9, 42.5, 17.7, 17.3, 17.1, 17.1, 15.3, 13.4, 12.7; IR (Neat Film, NaCl) 2944, 2867, 1718, 1462, 1269, 1245, 1192, 1093, 995, 883, 781, 743, 701 cm^{-1} ; HRMS (MM) m/z calc'd for $\text{C}_{21}\text{H}_{31}\text{O}_4\text{Si}$ $[\text{M}+\text{H}]^+$: 375.1986, found 375.1991.

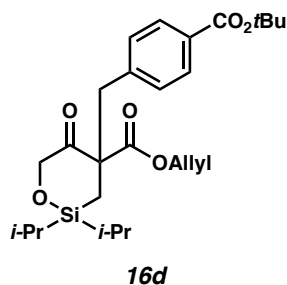


Allyl 4-(4-bromobenzyl)-2,2-diisopropyl-5-oxo-1,2-oxasilinane-4-carboxylate (16b):

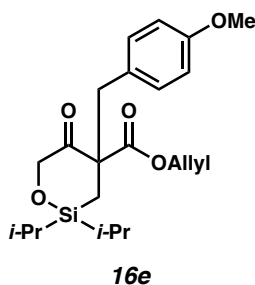
Prepared according to General Procedure 1 using 4-bromobenzyl bromide and purified by column chromatography (0 to 5% Et_2O in hexanes) to afford **5b** as a colorless oil (154 mg, 38% yield). ^1H NMR (400 MHz, CDCl_3) δ 7.36 (d, $J = 8.4$ Hz, 2H), 7.03 (d, $J = 8.4$ Hz, 2H), 5.73 (ddt, $J = 17.3, 10.4, 5.9$ Hz, 1H), 5.27 – 5.17 (m, 2H), 4.56 (ddt, $J = 13.0, 5.8, 1.4$ Hz, 1H), 4.50 (d, $J = 18.5$ Hz, 1H), 4.38 (ddt, $J = 13.0, 6.1, 1.3$ Hz, 1H), 4.26 (d, $J = 18.4$ Hz, 1H), 3.27 (d, $J = 13.6$ Hz, 1H), 2.89 (d, $J = 13.7$ Hz, 1H), 1.71 (d, $J = 15.2$ Hz, 1H), 1.07 – 0.97 (m, 14H), 0.71 (d, $J = 15.2$ Hz, 1H); ^{13}C NMR (100 MHz, CDCl_3) δ 208.7, 170.5, 135.5, 132.4, 131.2, 131.1, 121.0, 119.4, 70.2, 66.3, 59.7, 41.9, 17.6, 17.3, 17.1, 17.0, 15.5, 13.4, 12.7; IR (Neat Film, NaCl) 2944, 2895, 2867, 1719, 1488, 1463, 1192, 1094, 995, 883, 777 cm^{-1} ; HRMS (MM) m/z calc'd for $\text{C}_{21}\text{H}_{30}\text{BrO}_4\text{Si}$ $[\text{M}+\text{H}]^+$: 453.1091, found 453.1066.



Allyl 2,2-diisopropyl-5-oxo-4-(4-(trifluoromethyl)benzyl)-1,2-oxasilinane-4-carboxylate (16c): Prepared according to General Procedure 1 using 4-(trifluoromethyl)benzyl bromide and purified by column chromatography (0 to 3% Et₂O in hexanes) to afford **5c** as a colorless oil (215 mg, 42% yield). ¹H NMR (400 MHz, CDCl₃) δ 7.48 (d, *J* = 8.1 Hz, 2H), 7.26 (d, *J* = 8.0 Hz, 2H), 5.65 (ddt, *J* = 17.2, 10.4, 5.9 Hz, 1H), 5.21 – 5.11 (m, 2H), 4.56 – 4.44 (m, 2H), 4.39 – 4.21 (m, 2H), 3.37 (d, *J* = 13.5 Hz, 1H), 2.95 (d, *J* = 13.5 Hz, 1H), 1.72 (d, *J* = 15.1 Hz, 1H), 1.06 – 0.95 (m, 14H), 0.72 (d, *J* = 15.1 Hz, 1H); ¹³C NMR (100 MHz, CDCl₃) δ 208.6, 170.4, 140.8, 131.0, 131.0, 129.2 (q, *J* = 32.0 Hz), 125.0 (q, *J* = 3.8 Hz), 124.4 (q, *J* = 272.4 Hz), 119.5, 70.2, 66.4, 59.8, 42.3, 17.6, 17.3, 17.1, 17.0, 15.8, 13.4, 12.7; ¹⁹F NMR (282 MHz, CDCl₃) δ -62.50; IR (Neat Film, NaCl) 2945, 2868, 1719, 1463, 1325, 1192, 1165, 1126, 1113, 1068, 1019, 777, 714 cm⁻¹; HRMS (MM) *m/z* calc'd for C₂₂H₃₀F₃O₄Si [M+H]⁺: 443.1860, found 443.1863.

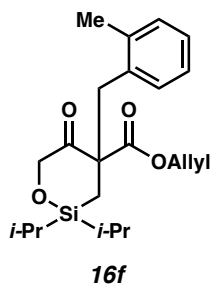


Allyl 4-(4-(*tert*-butoxycarbonyl)benzyl)-2,2-diisopropyl-5-oxo-1,2-oxasilinane-4-carboxylate (16d): Prepared according to General Procedure 1 using *tert*-butyl 4-(bromomethyl)benzoate and purified by column chromatography (5% Et₂O in hexanes) to afford **16d** as a white solid (282 mg, 54% yield). ¹H NMR (400 MHz, CDCl₃) δ 7.87 (d, *J* = 8.3 Hz, 2H), 7.18 (d, *J* = 8.3 Hz, 2H), 5.76 (ddt, *J* = 17.2, 10.4, 5.9 Hz, 1H), 5.31 – 5.16 (m, 2H), 4.59 (ddt, *J* = 13.0, 5.8, 1.3 Hz, 1H), 4.50 (d, *J* = 18.5 Hz, 1H), 4.40 (ddt, *J* = 13.0, 6.2, 1.3 Hz, 1H), 4.28 (d, *J* = 18.4 Hz, 1H), 3.35 (d, *J* = 13.5 Hz, 1H), 2.99 (d, *J* = 13.6 Hz, 1H), 1.71 (d, *J* = 15.2 Hz, 1H), 1.58 (s, 9H), 1.07 – 0.95 (m, 14H), 0.71 (d, *J* = 15.2 Hz, 1H); ¹³C NMR (100 MHz, CDCl₃) δ 208.5, 170.4, 165.9, 141.3, 131.2, 130.7, 130.5, 129.3, 119.5, 81.0, 70.2, 66.4, 59.8, 42.4, 28.4, 17.7, 17.3, 17.1, 17.1, 15.3, 13.4, 12.7; IR (Neat Film, NaCl) 2941, 2867, 1716, 1611.5, 1462, 1368, 1292, 1254, 1170, 1106, 1020, 778, 758, 706 cm⁻¹; HRMS (MM) *m/z* calc'd for C₂₆H₃₉O₆Si [M+H]⁺: 475.2510, found 475.2508.



Allyl 2,2-diisopropyl-4-(4-methoxybenzyl)-5-oxo-1,2-oxasilinane-4-carboxylate

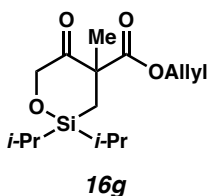
(16e): Prepared according to General Procedure 1 using 4-(methoxy)benzyl bromide and purified by column chromatography (5 to 15% Et₂O in hexanes) to afford **16e** as a colorless oil (153 mg, 31% yield). ¹H NMR (400 MHz, CDCl₃) δ 7.08 – 7.03 (m, 2H), 6.81 – 6.76 (m, 2H), 5.75 (ddt, *J* = 17.2, 10.4, 5.9 Hz, 1H), 5.27 – 5.16 (m, 2H), 4.58 (ddt, *J* = 13.0, 5.7, 1.4 Hz, 1H), 4.49 (d, *J* = 18.4 Hz, 1H), 4.39 (ddt, *J* = 13.0, 6.0, 1.3 Hz, 1H), 4.26 (d, *J* = 18.6 Hz, 1H), 3.77 (s, 3H), 3.26 (d, *J* = 13.7 Hz, 1H), 2.90 (d, *J* = 13.8 Hz, 1H), 1.72 (d, *J* = 15.2 Hz, 1H), 1.17 – 0.94 (m, 14H), 0.71 (d, *J* = 15.3 Hz, 1H); ¹³C NMR (100 MHz, CDCl₃) δ 208.9, 170.7, 158.6, 131.6, 131.4, 128.4, 119.1, 113.5, 70.3, 66.2, 59.8, 55.3, 41.7, 17.7, 17.3, 17.1, 17.1, 15.2, 13.4, 12.7; IR (Neat Film, NaCl) 2944, 2867, 1719, 1613, 1514, 1464, 1442, 1271, 1249, 1193, 1178, 1094, 1036, 884, 776, 727, 709 cm⁻¹; HRMS (MM) *m/z* calc'd for C₂₂H₃₃O₅Si [M+H]⁺: 405.2092, found 405.2093.



Allyl 2,2-diisopropyl-4-(2-methylbenzyl)-5-oxo-1,2-oxasilinane-4-carboxylate (16f):

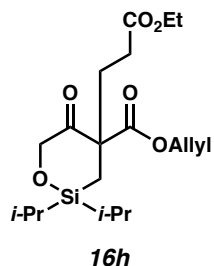
Prepared according to General Procedure 1 using 2-(methyl)benzyl bromide and purified

by column chromatography (5 to 15% Et₂O in hexanes) to afford **16f** as a colorless oil (157 mg, 35% yield). ¹H NMR (400 MHz, CDCl₃) δ 7.13 – 7.08 (m, 4H), 5.74 (ddt, *J* = 17.2, 10.4, 5.9 Hz, 1H), 5.24 (dq, *J* = 17.2, 1.5 Hz, 1H), 5.21 – 5.17 (m, 1H), 4.60 (ddt, *J* = 13.0, 5.7, 1.4 Hz, 1H), 4.54 (d, *J* = 18.4 Hz, 1H), 4.37 (ddt, *J* = 13.0, 6.2, 1.3 Hz, 1H), 4.31 (d, *J* = 18.5 Hz, 1H), 3.40 (d, *J* = 14.2 Hz, 1H), 3.07 (d, *J* = 14.3 Hz, 1H), 2.27 (s, 3H), 1.74 (d, *J* = 15.1 Hz, 1H), 1.21 – 0.91 (m, 14H), 0.74 (d, *J* = 15.2 Hz, 1H); ¹³C NMR (100 MHz, CDCl₃) δ 208.9, 170.8, 137.3, 134.8, 131.3, 131.3, 130.6, 126.9, 125.6, 119.2, 70.2, 66.3, 59.5, 37.8, 20.1, 17.7, 17.3, 17.1, 17.1, 15.1, 13.4, 12.7; IR (Neat Film, NaCl) 3021, 2944, 2894.4, 2867, 1719, 1463, 1270, 1220, 1191, 1093, 884, 779, 747, 710 cm⁻¹; HRMS (MM) *m/z* calc'd for C₂₂H₃₃O₄Si [M+H]⁺: 389.2143, found 389.2136.



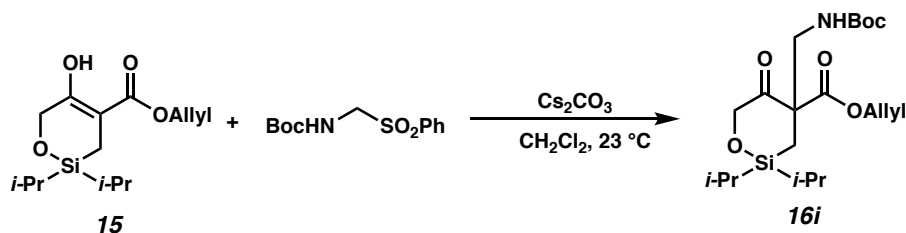
Allyl 2,2-diisopropyl-4-methyl-5-oxo-1,2-oxasilinane-4-carboxylate (16g): Prepared according to General Procedure 1 using methyl iodide, without TBAI, and purified by column chromatography (3 to 15% Et₂O in hexanes) to afford **16g** as a colorless oil (271 mg, 60% yield). ¹H NMR (400 MHz, CDCl₃) δ 5.88 (ddt, *J* = 17.2, 10.5, 5.7 Hz, 1H), 5.31 (dq, *J* = 17.2, 1.5 Hz, 1H), 5.24 (dq, *J* = 10.5, 1.3 Hz, 1H), 4.68 (ddt, *J* = 13.2, 5.6, 1.4 Hz, 1H), 4.56 (ddt, *J* = 13.2, 5.9, 1.4 Hz, 1H), 4.50 (d, *J* = 18.6 Hz, 1H), 4.30 (d, *J* = 18.6 Hz, 1H), 1.85 (d, *J* = 15.5 Hz, 1H), 1.43 (s, 3H), 1.18 – 0.99 (m, 14H), 0.77 (d, *J* = 15.5 Hz, 1H); ¹³C NMR (100 MHz, CDCl₃) δ 209.7, 172.6, 131.5, 118.9, 70.1, 66.3, 54.7, 24.0, 17.6, 17.3, 17.1, 17.1, 13.3, 12.8; IR (Neat Film, NaCl) 2942, 2896, 1720, 1464,

1262, 1195, 1162, 1124, 1095, 1067, 993, 883, 780, 733, 712 cm^{-1} ; HRMS (MM) m/z calc'd for $\text{C}_{15}\text{H}_{27}\text{O}_4\text{Si}$ $[\text{M}+\text{H}]^+$: 299.1673, found 299.1669.



Allyl 4-(3-ethoxy-3-oxopropyl)-2,2-diisopropyl-5-oxo-1,2-oxasilinane-4-carboxylate

(16h): Prepared according to General Procedure 1 using ethyl acrylate, without TBAI, and purified by column chromatography (10 to 15% Et_2O in hexanes) to afford **16h** as a colorless oil (150 mg, 32% yield). ^1H NMR (400 MHz, CDCl_3) δ 5.89 (ddt, $J = 17.2$, 10.5, 5.9 Hz, 1H), 5.33 (dq, $J = 17.2$, 1.5 Hz, 1H), 5.26 (dq, $J = 10.4$, 1.2 Hz, 1H), 4.71 (ddt, $J = 13.0$, 5.7, 1.4 Hz, 1H), 4.59 – 4.53 (m, 1H), 4.50 (d, $J = 18.5$ Hz, 1H), 4.29 – 4.22 (m, 1H), 4.12 (q, $J = 7.2$ Hz, 2H), 2.44–2.19 (m, 3H), 2.08–2.01 (m, 1H), 1.80 (d, $J = 15.2$ Hz, 1H), 1.25 (t, $J = 7.1$ Hz, 3H), 1.11 – 0.95 (m, 14H), 0.70 (d, $J = 15.2$ Hz, 1H); ^{13}C NMR (100 MHz, CDCl_3) δ 208.8, 173.1, 171.1, 131.3, 119.4, 70.1, 66.5, 60.7, 57.2, 31.8, 29.7, 17.6, 17.3, 17.1, 17.1, 14.9, 14.4, 13.4, 12.7; IR (Neat Film, NaCl) 2944, 2868, 1737, 1719, 1464, 1377, 1299, 1251, 1192, 1140, 1096, 883, 781, 733, 713 cm^{-1} ; HRMS (MM) m/z calc'd for $\text{C}_{19}\text{H}_{33}\text{O}_6\text{Si}$ $[\text{M}+\text{H}]^+$: 385.2041, found 385.2045.



Allyl 4-(((*tert*-butoxycarbonyl)amino)methyl)-2,2-diisopropyl-5-oxo-1,2-oxasilinane-

4-carboxylate (16i): To a solution of β -keto ester **15** (275 mg, 0.97 mmol, 1.00 equiv) in

CH_2Cl_2 (3.2 mL), sulfonylmethyl carbamate¹⁸ (315 mg, 1.16 mmol, 1.20 equiv) and

Cs_2CO_3 (792 mg, 2.43 mmol, 2.5 equiv) were added. The reaction mixture was stirred at

room temperature overnight. Upon complete consumption of the starting material, as

observed by TLC, the reaction was quenched with saturated NH_4Cl . The layers were

separated and the aqueous phase was extracted with DCM twice. The combined organic

layers were dried over Na_2SO_4 , filtered, and concentrated. The crude residue was purified

by column chromatography (5 to 10% EtOAc in hexanes) to afford alkylated product **16i**

as a colorless viscous oil (344 mg, 86% yield). ^1H NMR (400 MHz, CDCl_3) δ 5.89 (ddt, J

= 16.5, 10.4, 5.9 Hz, 1H), 5.32 (dq, J = 17.2, 1.5 Hz, 1H), 5.24 (dq, J = 10.5, 1.2 Hz, 1H),

5.16 – 5.07 (m, 1H), 4.68 (ddt, J = 12.9, 5.8, 1.4 Hz, 1H), 4.58 – 4.45 (m, 2H), 4.26 (d, J

= 18.8 Hz, 1H), 3.62 (dd, J = 13.9, 7.8 Hz, 1H), 3.39 (dd, J = 13.8, 5.7 Hz, 1H), 1.73 (d, J

= 15.5 Hz, 1H), 1.40 (s, 9H), 1.16 – 0.95 (m, 14H), 0.80 (d, J = 15.4 Hz, 1H); ^{13}C NMR

(100 MHz, CDCl_3) δ 210.4, 170.1, 155.9, 131.4, 119.3, 79.5, 70.2, 66.8, 59.3, 46.4, 28.4,

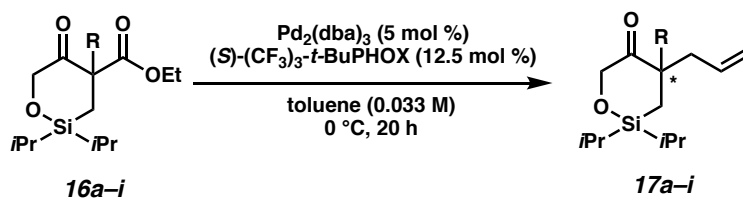
17.5, 17.2, 17.1, 17.0, 13.3, 12.7, 12.3; IR (Neat Film, NaCl) 3465, 2943, 2868, 1749,

1720, 1501, 1464, 366, 1248, 1167, 1106, 1068, 883, 779, 739 cm^{-1} ; HRMS (MM) m/z

calc'd for $\text{C}_{20}\text{H}_{36}\text{NO}_6\text{Si}$ $[\text{M}+\text{H}]^+$: 414.2306, found 414.2312.

2.7.2.2 General Procedure for the Palladium-Catalyzed Allylic Alkylation

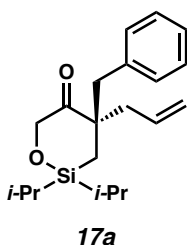
Please note that the absolute configuration was determined only for compounds **17a** and **17g** via vibrational circular dichroism (VCD) and optical rotation. The absolute configuration for all other products has been inferred by analogy. For respective HPLC, SFC, or GC conditions, please refer to Table 2.3.



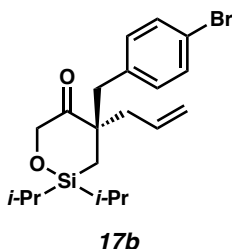
General procedure 2:

In a nitrogen-filled glovebox, to an oven-dried 4-mL vial equipped with a stir bar was added $\text{Pd}_2(\text{dba})_3$ (5 mol %), $(S)\text{-(CF}_3)_3\text{-}t\text{-BuPHOX}$ (12.5 mol %) and toluene (0.003 M based on Pd source). After stirring at room temperature for 30 min, the catalyst mixture was cooled to 0 °C and a solution of starting material **16** in toluene (0.066 M) was then added. The vial was sealed with a PTFE-lined septum cap and stirred at 0 °C. After 20 hours, the vial was removed from the glovebox. The crude reaction mixture was filtered through a silica plug with Et_2O , concentrated under vacuum, and purified by silica gel flash chromatography to furnish the product.

2.7.2.3 Spectroscopic Data for the Alkylation Products

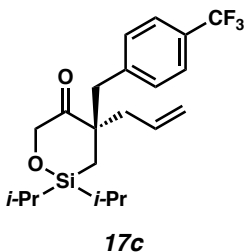


(R)-4-allyl-4-benzyl-2,2-diisopropyl-1,2-oxasilinan-5-one (17a): Product **17a** was prepared using General Procedure 2 and purified by column chromatography (5% Et₂O in hexanes) to provide a colorless oil (60.0 mg, 91% yield); 94% ee, $[\alpha]_{\text{D}}^{25} +3.47$ (*c* 0.92, CHCl₃); ¹H NMR (400 MHz, CDCl₃) δ 7.33 – 7.21 (m, 3H), 7.17 – 7.12 (m, 2H), 5.81 (dddd, *J* = 16.9, 10.3, 7.8, 6.5 Hz, 1H), 5.29 – 5.07 (m, 2H), 4.46 (d, *J* = 18.8 Hz, 1H), 4.42 (d, *J* = 18.8 Hz, 1H), 3.14 (d, *J* = 13.7 Hz, 1H), 2.93 (d, *J* = 13.8 Hz, 1H), 2.52 (ddt, *J* = 14.3, 7.8, 1.2 Hz, 1H), 2.34 (ddt, *J* = 14.4, 6.5, 1.4 Hz, 1H), 1.11 – 1.02 (m, 14H), 0.98 (d, *J* = 1.9 Hz, 2H); ¹³C NMR (100 MHz, CDCl₃) δ 213.8, 137.5, 134.0, 130.7, 128.2, 126.6, 118.9, 71.6, 52.5, 42.5, 41.0, 17.6, 17.5, 17.3, 15.0, 13.6, 13.4; IR (Neat Film, NaCl) 3064, 3029, 2943, 2893, 2866, 1710, 1496, 1464, 1438, 1146, 1100, 918, 883, 789, 736, 702; HRMS (MM) *m/z* calc'd for C₂₀H₃₄O₂NSi [M+NH₄]⁺: 348.2353, found 348.2353; SFC Conditions: 5% IPA, 2.5 mL/min, Chiralpak AD-H column, λ = 210 nm, *t_R* (min): major = 2.86, minor = 3.17.



(R)-4-allyl-4-(4-bromobenzyl)-2,2-diisopropyl-1,2-oxasilinan-5-one (17b): Product

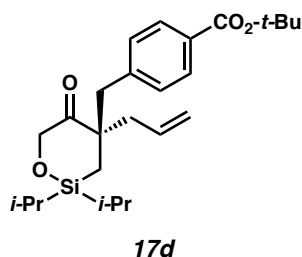
17b was prepared using General Procedure 2 and purified by column chromatography (3% Et₂O in hexanes) to provide a colorless oil (72.2 mg, 88% yield); 93% ee, [α]_D²⁵ +3.48 (*c* 1.00, CHCl₃); ¹H NMR (400 MHz, CDCl₃) δ 7.44 – 7.33 (m, 2H), 7.05 – 6.97 (m, 2H), 5.73 (dddd, *J* = 16.9, 10.2, 7.7, 6.7 Hz, 1H), 5.19 – 5.07 (m, 2H), 4.39 (s, 2H), 2.98 (d, *J* = 13.8 Hz, 1H), 2.88 (d, *J* = 13.8 Hz, 1H), 2.54 (ddt, *J* = 14.5, 7.7, 1.2 Hz, 1H), 2.27 (ddt, *J* = 14.4, 6.6, 1.4 Hz, 1H), 1.08 – 0.97 (m, 14H), 0.90 (s, 2H); ¹³C NMR (100 MHz, CDCl₃) δ 213.6, 136.6, 133.6, 132.5, 131.3, 120.6, 119.2, 71.5, 52.4, 41.7, 41.0, 17.5, 17.5, 17.3, 17.3, 14.8, 13.6, 13.4; IR (Neat Film, NaCl) 2943, 2866, 1711, 1488, 1463, 1101, 1074, 1012, 882, 785, 756; HRMS (FAB+) *m/z* calc'd for C₂₀H₃₀BrO₂Si [M+H]⁺: 409.1198, found 409.1187; SFC Conditions: 10% IPA, 2.5 mL/min, Chiralpak AD-H column, λ = 210 nm, *t*_R (min): major = 3.01, minor = 3.33.



(R)-4-allyl-2,2-diisopropyl-4-(4-(trifluoromethyl)benzyl)-1,2-oxasilinan-5-one (17c):

Product **6c** was prepared using General Procedure 2 and purified by column chromatography (0 to 5% Et₂O in hexanes) to provide a colorless oil (68.5 mg, 86%

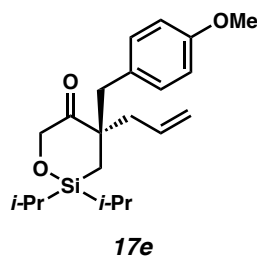
yield); 90% ee, $[\alpha]_D^{25} -6.05$ (c 0.99, CHCl_3); ^1H NMR (400 MHz, CDCl_3) δ 7.52 (d, J = 8.0 Hz, 2H), 7.31 – 7.13 (m, 2H), 5.75 (dddd, J = 17.0, 10.3, 7.6, 6.7 Hz, 1H), 5.25 – 5.08 (m, 2H), 4.41 (s, 2H), 3.06 (d, J = 13.7 Hz, 1H), 3.01 (d, J = 13.7 Hz, 1H), 2.58 (ddt, J = 14.5, 7.6, 1.3 Hz, 1H), 2.28 (ddt, J = 14.5, 6.7, 1.4 Hz, 1H), 1.11 – 0.95 (m, 14H), 0.91 (s, 2H); ^{13}C NMR (100 MHz, CDCl_3) δ 213.5, 142.0, 133.5, 131.1, 128.9 (q, J = 32.4 Hz), 125.1 (q, J = 3.8 Hz), 124.4 (q, J = 271.8 Hz), 119.3, 71.5, 52.5, 42.1, 41.2, 17.5, 17.5, 17.3, 17.3, 14.9, 13.6, 13.4; ^{19}F NMR (282 MHz, CDCl_3) δ -62.44; IR (Neat Film, NaCl) 2946, 2896, 2868, 1712, 1619, 1464, 1441, 1417, 1326, 1164, 1125, 1069, 1020, 788, 757; HRMS (FAB+) m/z calc'd for $\text{C}_{21}\text{H}_{30}\text{F}_3\text{O}_2\text{Si}$ $[\text{M}+\text{H}]^+$: 399.1967, found 399.1943; SFC Conditions: 3% IPA, 2.5 mL/min, Chiralpak AD-H column, λ = 210 nm, t_R (min): major = 2.38, minor = 2.96.



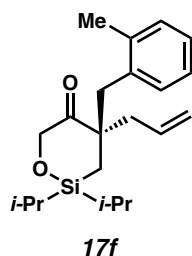
tert-butyl (R)-4-((4-allyl-2,2-diisopropyl-5-oxo-1,2-oxasilinan-4-yl)methyl)benzoate

(17d): Product **17d** was prepared using General Procedure 2 and purified by column chromatography (5% Et_2O in hexanes) to provide a colorless oil (80.4 mg, 93% yield); 93% ee, $[\alpha]_D^{25} +1.44$ (c 0.99, CHCl_3); ^1H NMR (400 MHz, CDCl_3) δ 7.88 (d, J = 8.3 Hz, 2H), 7.22 – 7.11 (m, 2H), 5.74 (dddd, J = 17.0, 10.3, 7.6, 6.7 Hz, 1H), 5.19 – 5.10 (m, 2H), 4.40 (s, 2H), 3.09 (d, J = 13.6 Hz, 1H), 2.95 (d, J = 13.6 Hz, 1H), 2.55 (ddt, J = 14.4, 7.6, 1.2 Hz, 1H), 2.26 (ddt, J = 14.4, 6.6, 1.3 Hz, 1H), 1.58 (s, 9H), 1.09 – 0.94 (m, 14H), 0.91 (s, 2H); ^{13}C NMR (100 MHz, CDCl_3) δ 213.5, 165.8, 142.6, 133.7, 130.6,

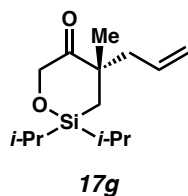
130.3, 130.3, 129.3, 119.2, 81.0, 71.5, 52.5, 42.2, 41.0, 28.3, 17.5, 17.5, 17.3, 15.0, 13.6, 13.4; IR (Neat Film, NaCl) 3402, 3077, 1944, 2895, 2867, 1713, 1611, 1463, 1367, 1293, 1255, 1169, 1117, 1108, 1020, 883, 790, 773, 744; HRMS (MM) m/z calc'd for $C_{25}H_{42}O_4NSi$ $[M+NH_4]^+$: 448.2878, found 448.2883; SFC Conditions: 10% IPA, 2.5 mL/min, Chiralpak AD-H column, λ = 210 nm, t_R (min): major = 2.72, minor = 3.12.



(R)-4-allyl-2,2-diisopropyl-4-(4-methoxybenzyl)-1,2-oxasilinan-5-one (6e): Product **6e** was prepared using General Procedure 2 and purified by column chromatography (10% Et₂O in hexanes) to provide a colorless oil (61.8 mg, 85% yield); 93% ee, $[\alpha]_D^{25} +3.12$ (c 0.96, CHCl₃); ¹H NMR (400 MHz, CDCl₃) δ 7.13 – 6.96 (m, 2H), 6.85 – 6.75 (m, 2H), 5.77 (dddd, J = 16.8, 10.3, 7.8, 6.5 Hz, 1H), 5.17 – 5.07 (m, 2H), 4.43 (d, J = 19.1 Hz, 1H), 4.38 (d, J = 19.1 Hz, 1H), 3.78 (s, 3H), 3.06 (d, J = 13.9 Hz, 1H), 2.83 (d, J = 13.9 Hz, 1H), 2.46 (ddt, J = 14.3, 7.8, 1.2 Hz, 1H), 2.31 (ddt, J = 14.3, 6.5, 1.4 Hz, 1H), 1.15 – 0.97 (m, 14H), 0.94 (s, 2H); ¹³C NMR (100 MHz, CDCl₃) δ 214.0, 158.3, 134.1, 131.6, 129.4, 118.8, 113.6, 71.6, 55.3, 52.6, 41.7, 41.0, 17.6, 17.5, 17.3, 17.3, 14.8, 13.5, 13.5; IR (Neat Film, NaCl) 3075, 2944, 2866, 1710, 1612, 1514, 1464, 1441, 1301, 1250, 1179, 1146, 1111, 1099, 1038, 994, 918, 883, 788, 772, 751; HRMS (MM) m/z calc'd for $C_{21}H_{36}O_3NSi$ $[M+NH_4]^+$: 378.2459, found 378.2457; SFC Conditions: 5% IPA, 2.5 mL/min, Chiralpak AD-H column, λ = 210 nm, t_R (min): major = 5.04, minor = 5.96.

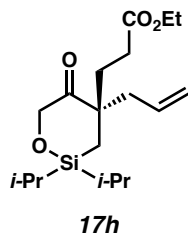


(R)-4-allyl-2,2-diisopropyl-4-(2-methylbenzyl)-1,2-oxasilinan-5-one (6f): Product **6f** was prepared using General Procedure 2 and purified by column chromatography (0 to 3% Et₂O in hexanes) to provide a colorless oil (57.0 mg, 83% yield); 92% ee, $[\alpha]_D^{25} = 0.73$ (*c* 0.95, CHCl₃); ¹H NMR (400 MHz, CDCl₃) δ 7.20 – 7.00 (m, 4H), 5.74 (dddd, *J* = 16.9, 10.3, 7.6, 6.7 Hz, 1H), 5.19 – 5.03 (m, 2H), 4.44 (d, *J* = 18.6 Hz, 1H), 4.38 (d, *J* = 16.9 Hz, 1H), 3.10 (d, *J* = 14.5 Hz, 1H), 3.06 (d, *J* = 14.6 Hz, 1H), 2.51 – 2.43 (m, 2H), 2.31 (s, 3H), 1.13 – 0.93 (m, 16H); ¹³C NMR (100 MHz, CDCl₃) δ 214.0, 137.3, 136.4, 134.1, 130.7, 130.6, 126.5, 125.8, 118.9, 71.7, 53.1, 42.0, 38.5, 20.7, 17.6, 17.5, 17.4, 17.3, 14.2, 13.6, 13.5; IR (Neat Film, NaCl) 3076, 3020, 2943, 2894, 2866, 1710, 1463, 1146, 1098, 994, 918, 883, 791, 742; HRMS (MM) *m/z* calc'd for C₂₁H₃₆O₂NSi [M+NH₄]⁺: 362.2510, found 362.2514; SFC Conditions: 1% IPA, 2.5 mL/min, Chiralcel OJ-H column, λ = 210 nm, *t_R* (min): major = 3.96, minor = 4.51.



(S)-4-allyl-2,2-diisopropyl-4-methyl-1,2-oxasilinan-5-one (17g): Product **17g** was prepared using General Procedure 2 at 23 °C instead of 0 °C and purified by column chromatography (5% Et₂O in hexanes) to provide a pale yellow oil (40.0 mg, 79% yield); 89% ee, $[\alpha]_D^{25} = -34.54$ (*c* 0.95, CHCl₃); ¹H NMR (400 MHz, CDCl₃) δ 5.72 (dddd, *J* =

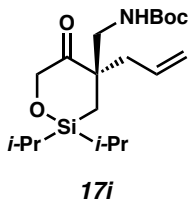
16.9, 10.4, 7.8, 6.9 Hz, 1H), 5.14 – 5.02 (m, 2H), 4.40 (d, $J = 18.6$ Hz, 1H), 4.32 (d, $J = 18.6$ Hz, 1H), 2.45 (ddt, $J = 13.8, 7.7, 1.2$ Hz, 1H), 2.33 (ddt, $J = 13.8, 7.0, 1.3$ Hz, 1H), 1.23 (s, 3H), 1.07 – 1.01 (m, 15H), 0.89 (d, $J = 15.5$ Hz, 1H); ^{13}C NMR (100 MHz, CDCl_3) δ 215.2, 134.2, 118.5, 70.9, 47.9, 44.2, 25.0, 17.5, 17.5, 17.3, 17.2, 13.5, 13.4; IR (Neat Film, NaCl) 3076, 2943, 2894, 2867, 1713, 1463, 1249, 1164, 1114, 994, 916, 883, 787, 753, 738; HRMS (MM) m/z calc'd for $\text{C}_{14}\text{H}_{27}\text{O}_2\text{Si}$ $[\text{M}+\text{H}]^+$: 255.1775, found 255.1768; GC Conditions: G-TA column, 100 °C, isotherm, t_R (min): minor = 98.83, major = 100.76.



Ethyl (S)-3-(4-allyl-2,2-diisopropyl-5-oxo-1,2-oxasilinan-4-yl)propanoate (17h):

Product **17h** was prepared using General Procedure 2 and purified by column chromatography (10 to 15% Et_2O in hexanes) to provide a pale yellow oil (43.0 mg, 63% yield); 94% ee, $[\alpha]_D^{25} -3.67$ (c 0.93, CHCl_3); ^1H NMR (400 MHz, CDCl_3) δ 5.67 (dddd, $J = 16.2, 10.8, 7.7, 6.8$ Hz, 1H), 5.15 – 5.03 (m, 2H), 4.36 (d, $J = 0.7$ Hz, 2H), 4.12 (q, $J = 7.1$ Hz, 2H), 2.53 (ddt, $J = 14.3, 7.8, 1.2$ Hz, 1H), 2.38 – 2.26 (m, 2H), 2.20 – 2.07 (m, 2H), 1.91 (ddd, $J = 13.9, 11.4, 5.4$ Hz, 1H), 1.25 (t, $J = 7.1$ Hz, 3H), 1.11 – 1.01 (m, 14H), 0.97 (d, $J = 4.4$ Hz, 2H). ^{13}C NMR (100 MHz, CDCl_3) δ 214.1, 173.5, 133.2, 119.0, 71.2, 60.7, 50.7, 40.7, 31.4, 29.4, 17.5, 17.5, 17.3, 14.9, 14.3, 13.5, 13.5; IR (Neat Film, NaCl) 2943, 2867, 1738, 1710, 1464, 1376, 1303, 1250, 1177, 1104, 918, 883, 788, 749; HRMS (MM) m/z calc'd for $\text{C}_{18}\text{H}_{33}\text{O}_4\text{Si}$ $[\text{M}+\text{H}]^+$: 341.2143, found 341.2144; SFC

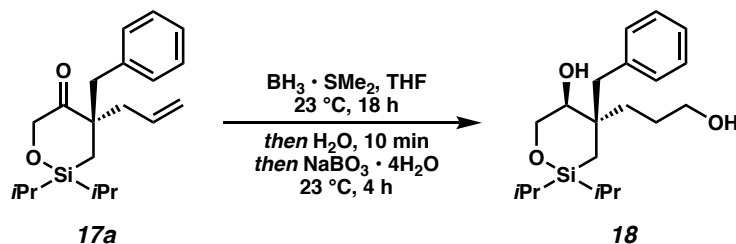
Conditions: 3% IPA, 2.5 mL/min, Chiralpak IC column, λ = 210 nm, t_R (min): minor = 9.30, major = 9.86.



tert-butyl (R)-((4-allyl-2,2-diisopropyl-5-oxo-1,2-oxasilinan-4-yl)methyl)carbamate

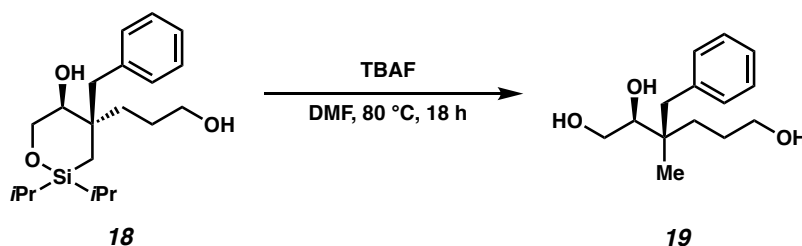
(17i): Product **17i** was prepared using General Procedure 2 and purified by column chromatography (5% EtOAc in hexanes, then 5% acetone in hexanes) to provide a colorless oil (57.9 mg, 78% yield); 90% ee, $[\alpha]_D^{25} +29.83$ (c 0.94, CHCl_3); ^1H NMR (400 MHz, CDCl_3) δ 5.67 (ddt, J = 19.2, 9.4, 7.4 Hz, 1H), 5.12 (s, 1H), 5.10 – 5.05 (m, 1H), 4.92 (t, J = 6.7 Hz, 1H), 4.34 (d, J = 1.2 Hz, 2H), 3.29 (d, J = 6.7 Hz, 2H), 2.62 (ddt, J = 14.3, 7.5, 1.3 Hz, 1H), 2.45 – 2.33 (m, 1H), 1.40 (s, 9H), 1.13 – 0.91 (m, 16H). ^{13}C NMR (100 MHz, CDCl_3) δ 215.6, 156.5, 132.4, 119.5, 79.3, 71.0, 53.1, 46.3, 39.9, 28.5, 17.5, 17.4, 17.2, 13.6, 13.3, 12.1; IR (Neat Film, NaCl) 3465, 3369, 3078, 2943, 2896, 2867, 1708, 1504, 1464, 1366, 1247, 1169, 1109, 883, 787, 751; HRMS (MM) m/z calc'd for $\text{C}_{19}\text{H}_{36}\text{NO}_4\text{Si}$ $[\text{M}+\text{H}]^+$: 370.2408, found 370.2409; SFC Conditions: 5% IPA, 2.5 mL/min, Chiralpak AD-H column, λ = 210 nm, t_R (min): minor = 2.80, major = 3.06.

2.7.2.4 Experimental Procedures and Characterization Data for Product Transformation

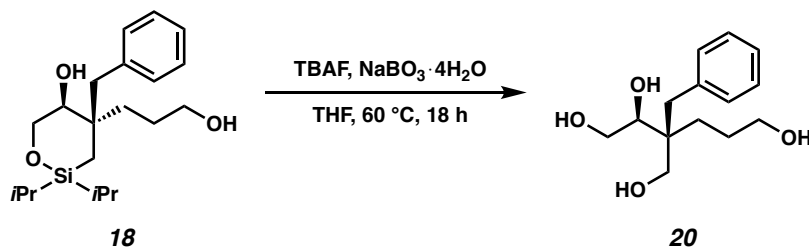


4*R*,5*S*-4-benzyl-4-(3-hydroxypropyl)-2,2-diisopropyl-1,2-oxasilinan-5-ol (**18**): To a solution of **17a** (257 mg, 0.78 mmol) in THF (3.8 mL) in a 10 mL round-bottom flask was added 2.0 M solution of $\text{BH}_3 \cdot \text{SMe}_2$ in THF (0.78 mL, 1.56 M) at room temperature and stirred for 18 hours. Upon complete consumption of starting material **17a** as observed by TLC, H_2O (1 mL) was added dropwise. After stirring for 10 minutes, $\text{NaBO}_3 \cdot 4\text{H}_2\text{O}$ (840 mg, 5.45 mmol) was added and the mixture was stirred for an additional 4 hours. The reaction mixture was quenched with 2 M HCl, the organic layer was collected, and the aqueous phase was extracted with EtOAc twice. The organic phases were combined, dried over Na_2SO_4 , and concentrated. The crude material was purified by column chromatography (40 to 50% EtOAc in hexanes) to furnish product **18** as a viscous, colorless oil (158 mg, 58% yield) as a 93:7 mixture of diastereomers; $[\alpha]_{\text{D}}^{25} -16.53$ (c 0.38, CHCl_3). Major diastereomer: ^1H NMR (400 MHz, CDCl_3) δ 7.33 – 7.17 (m, 5H), 4.09 (dd, $J = 12.3, 1.7$ Hz, 1H), 3.89 (dd, $J = 12.3, 3.9$ Hz, 1H), 3.63 (t, $J = 6.6$ Hz, 2H), 3.39 (dd, $J = 3.5, 1.8$ Hz, 1H), 2.92 (d, $J = 13.3$ Hz, 1H), 2.75 (d, $J = 13.3$ Hz, 1H), 1.72 (ddt, $J = 12.8, 8.3, 4.3$ Hz, 2H), 1.42 – 1.15 (m, 2H), 1.15 – 0.97 (m, 14H), 0.83 (d, $J = 15.2$ Hz, 1H), 0.56 (d, $J = 15.1$ Hz, 1H); ^{13}C NMR (100 MHz, CDCl_3) δ 138.4, 130.7, 130.7, 128.1, 128.1, 126.2, 72.4, 65.2, 63.3, 43.3, 41.3, 30.9, 26.9, 17.5, 17.5, 17.4, 17.4,

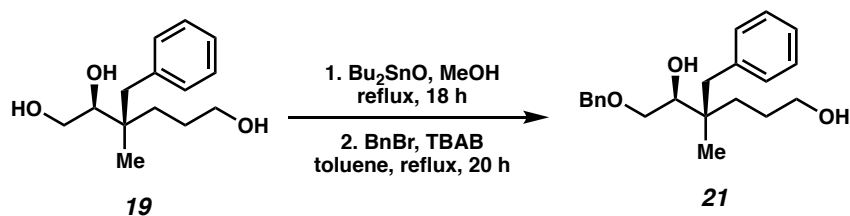
14.2, 13.2, 12.7; IR (Neat Film, NaCl) 3387, 2941, 2865, 1462, 1130, 1054, 882, 828, 733, 703 cm^{-1} ; HRMS (MM) m/z calc'd for $\text{C}_{20}\text{H}_{35}\text{O}_3\text{Si}$ $[\text{M}+\text{H}]^+$: 351.2350, found 351.2353.



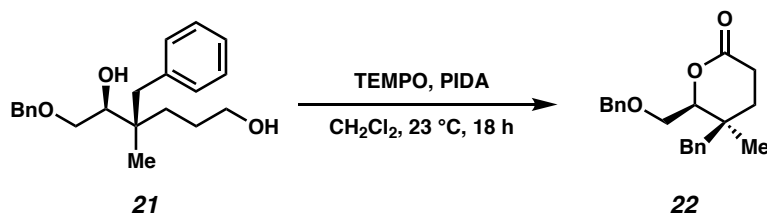
(2*S*,3*S*)-3-benzyl-3-methylhexane-1,2,6-triol (19): To a solution of **18** (45.5 mg, 0.13 mmol) in DMF (1.3 mL) in a 1-dram vial was added 1.0 M solution of TBAF in THF (0.52 mL, 0.52 mmol) at room temperature and sealed with a Teflon-lined cap. The solution was stirred at 80 °C for 18 hours, then 5% aqueous LiCl was added and the organic phase was collected. The aqueous was extracted with EtOAc three times. The organic phases were combined, washed with water, then brine, dried over Na_2SO_4 , and concentrated. The crude residue was purified by column chromatography (100% EtOAc) to furnish product **19** as a white solid (23.9 mg, 77% yield); $[\alpha]_{\text{D}}^{25} -5.10$ (c 0.18, CH_3OH); ^1H NMR (400 MHz, CD_3OD) δ 7.27 – 7.13 (m, 5H), 3.78 (dd, $J = 10.0, 1.3$ Hz, 1H), 3.55 – 3.44 (m, 4H), 2.76 (d, $J = 13.2$ Hz, 1H), 2.62 (d, $J = 13.2$ Hz, 1H), 1.72 – 1.59 (m, 1H), 1.59–1.47 (m, 1H), 1.39 (ddd, $J = 13.6, 12.5, 4.3$ Hz, 1H), 1.11 – 1.00 (m, 1H), 0.86 (s, 3H); ^{13}C NMR (100 MHz, CDCl_3) δ 140.0, 131.9, 128.7, 126.9, 77.6, 64.0, 63.7, 42.6, 40.9, 32.8, 27.7, 21.1; IR (Neat Film, NaCl) 3363, 2924, 2854, 1660, 1450, 1056, 1016, 830, 702, 683 cm^{-1} ; HRMS (ES $^+$) m/z calc'd for $\text{C}_{14}\text{H}_{23}\text{O}_3$ $[\text{M}+\text{H}]^+$: 239.1647, found 239.1633.



(2*S*,3*S*)-3-benzyl-3-(hydroxymethyl)hexane-1,2,6-triol (20): To a solution of **18** (13.8 mg, 0.039 mmol) in THF (0.4 mL) in a 1-dram vial was added a 1.0 M solution of TBAF in THF (0.16 mL, 0.16 mmol) and NaBO₃•4H₂O (24.2 mg, 0.16 mmol) at room temperature. The vial was sealed with a Teflon-lined cap and the reaction mixture was heated to 60 °C and stirred for 18 hours. Upon complete consumption of the starting material as judged by TLC, the reaction mixture was quenched with 2 M HCl. The organic layer was collected and the aqueous phase was extracted with EtOAc twice. The organic phases were combined, washed with brine, dried over Na₂SO₄, and concentrated under vacuum. The crude residue was purified by preparative-TLC (10% MeOH in CH₂Cl₂) to furnish product **20** as a colorless solid (5.0 mg, 51% yield); [α]_D²⁵ −0.94 (*c* 0.26, CH₃OH); ¹H NMR (400 MHz, CD₃OD) δ 7.31 – 7.21 (m, 4H), 7.21 – 7.15 (m, 1H), 3.75 (dd, *J* = 11.5, 3.2 Hz, 1H), 3.65 (dd, *J* = 11.5, 7.0 Hz, 1H), 3.55 – 3.43 (m, 5H), 2.86 (d, *J* = 13.4 Hz, 1H), 2.72 (d, *J* = 13.4 Hz, 1H), 1.77 – 1.65 (m, 1H), 1.65 – 1.53 (m, 1H), 1.30 (ddd, *J* = 13.8, 12.3, 4.4 Hz, 1H, overlapped with an OH proton), 1.14 – 1.05 (m, 1H); ¹³C NMR (100 MHz, CD₃OD) δ 139.3, 131.9, 128.9, 127.1, 77.2, 65.5, 63.9, 63.7, 45.0, 37.9, 28.0, 27.4 ; IR (Neat Film, NaCl) 3339, 2926, 2874, 2860, 1455, 1052, 753, 732, 705, 682cm^{−1}; HRMS (ES⁺) *m/z* calc'd for C₁₄H₂₃O₄ [M+H]⁺: 255.1596, found 255.1577.

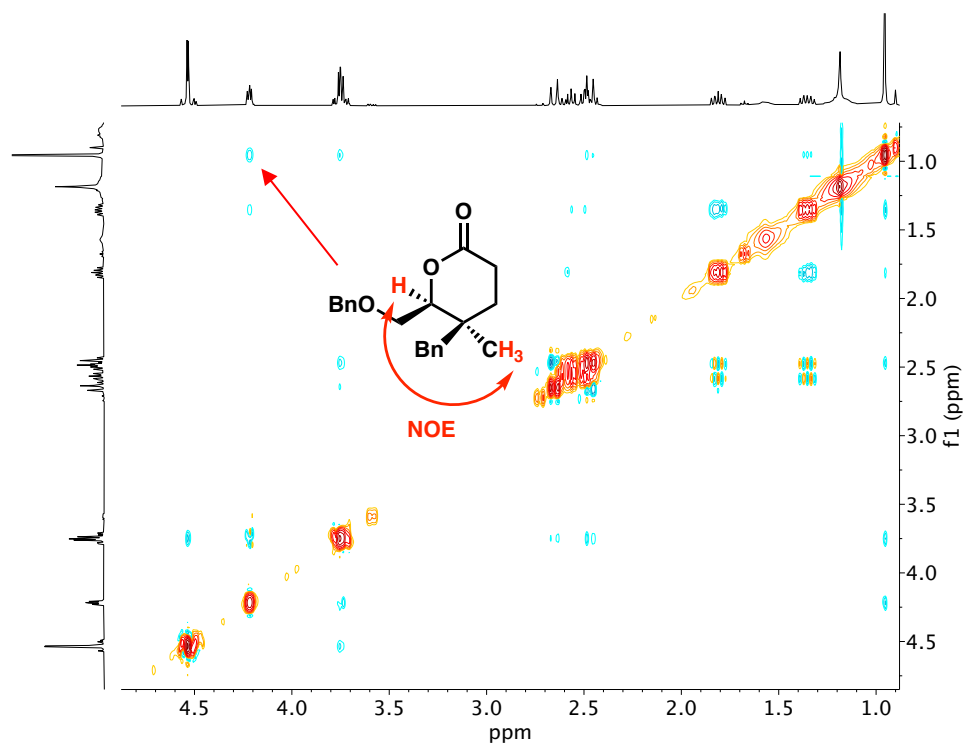


(4*S*,5*S*)-4-benzyl-6-(benzyloxy)-4-methylhexane-1,5-diol (21): To a solution of **19** (10 mg, 0.042 mmol) in MeOH (0.4 mL) in a 1-dram vial was added Bu₂SnO (11 mg, 0.044 mmol) at room temperature. The vial was sealed with a Teflon-lined cap and stirred at 70 °C. After 18 hours, the reaction mixture was concentrated, then redissolved in toluene (0.4 mL). Benzyl bromide (6 μ L, 0.05 mmol) and TBAB (16 mg, 0.05 mmol) were added and the reaction was heated to reflux in a sealed vial. After refluxing overnight, the reaction was cooled to room temperature. EtOAc and H₂O were added. The organic layer was collected and the aqueous phase was extracted with EtOAc three times. The organic phases were combined, washed with brine, dried over Na₂SO₄, and concentrated under vacuum. The crude residue was purified by preparative-TLC (50% EtOAc in hexanes) to furnish product **21** as a colorless solid (8.3 mg, 60% yield); [α]_D²⁵ 3.29 (*c* 0.23, CHCl₃); ¹H NMR (400 MHz, CDCl₃) δ 7.40 – 7.29 (m, 5H), 7.28 – 7.22 (m, 2H), 7.22 – 7.15 (m, 3H), 4.56 (d, *J* = 3.6 Hz, 2H), 3.72 – 3.63 (m, 2H), 3.58 (t, *J* = 6.5 Hz, 2H), 3.49 (td, *J* = 9.7, 9.1, 1.9 Hz, 1H), 2.83 (d, *J* = 13.3 Hz, 1H), 2.57 (d, *J* = 13.2 Hz, 1H), 1.73 – 1.46 (m, 2H), 1.39 (ddd, *J* = 13.6, 12.0, 4.6 Hz, 1H), 1.06 (ddd, *J* = 13.6, 12.1, 4.6 Hz, 1H), 0.89 (s, 3H); ¹³C NMR (100 MHz, CDCl₃) δ 138.6, 138.0, 131.0, 128.7, 128.0, 128.0, 127.9, 126.1, 74.0, 73.6, 71.24, 63.7, 41.6, 39.5, 31.5, 26.9, 20.7; IR (Neat Film, NaCl) 3427, 2926, 2870, 1455, 1372, 1256, 1064, 908, 732, 702, 666, 634 cm⁻¹; HRMS (ES⁺) *m/z* calc'd for C₂₁H₂₉O₃ [M+H]⁺: 329.2117, found 329.2117.



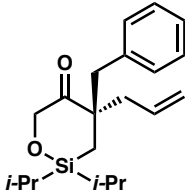
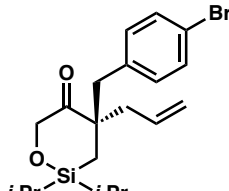
(5*S*,6*S*)-5-benzyl-6-((benzyloxy)methyl)-5-methyltetrahydro-2*H*-pyran-2-one (22):

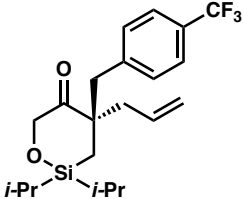
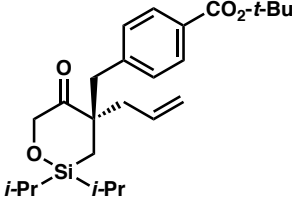
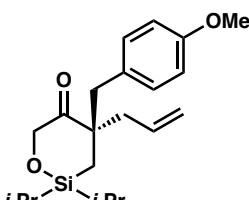
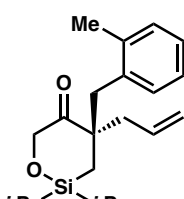
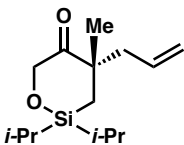
To a solution of **21** (8.3 mg, 0.025 mmol) in CH₂Cl₂ (0.3 mL) in a 1-dram vial was added (diacetoxyiodo)benzene (PIDA) (25.7 mg, 0.08 mmol) and TEMPO (1.0 mg, 0.005 mmol) at room temperature. The vial was sealed with a Teflon-lined cap and the solution was stirred for 18 hours. At this point, complete consumption of the starting material was observed by TLC, and the reaction was quenched with saturated aqueous Na₂S₂O₃. Additional Et₂O was added, the organic phase was collected, and the aqueous phase was extracted with Et₂O three times. The organic phases were combined, washed with brine, dried over Na₂SO₄, and concentrated under vacuum. The crude residue was purified by preparative-TLC (50% EtOAc in hexanes) to furnish product **22** as a colorless solid (5.3 mg, 65% yield); [α]_D²⁵ 14.81 (*c* 0.51, CHCl₃); ¹H NMR (300 MHz, CDCl₃) δ 7.42 – 7.19 (m, 8H), 7.16 – 7.06 (m, 2H), 4.61 (d, *J* = 1.6 Hz, 2H), 4.29 (dd, *J* = 5.0, 3.6 Hz, 1H), 3.82 (dd, *J* = 4.3, 3.3 Hz, 2H), 2.78 – 2.47 (m, 4H), 1.88 (ddd, *J* = 14.1, 7.9, 6.4 Hz, 1H), 1.42 (dt, *J* = 14.4, 7.6 Hz, 1H), 1.03 (s, 3H); ¹³C NMR (100 MHz, CDCl₃) δ 171.5, 137.8, 136.7, 130.6, 128.6, 128.3, 128.0, 127.9, 126.8, 68.9, 73.9, 69.4, 39.7, 35.3, 29.9, 27.2, 23.7; IR (Neat Film, NaCl) 2927, 1732, 1454, 1354, 1256, 1202, 1166, 1074, 730, 700, 636 cm⁻¹; HRMS (ES⁺) *m/z* calc'd for C₂₁H₂₅O₃ [M+H]⁺: 325.1804, found 325.1801.

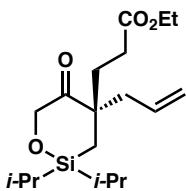
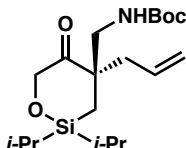


2.7.3 DETERMINATION OF ENANTIOMERIC EXCESS

Table 2.3 Determination of enantiomeric excess.

entry	compound	analytic conditions	ee (%)
1	 <p>17a</p>	SFC, Chiralpak AD-H, $\lambda = 210$ nm 5% IPA/CO ₂ , 2.5 mL/min tr (min) major 2.86, minor 3.17	94
2	 <p>17b</p>	SFC, Chiralpak AD-H, $\lambda = 210$ nm 10% IPA/CO ₂ , 2.5 mL/min tr (min) major 3.01, minor 3.33	93

entry	compound	analytic conditions	ee (%)
3	 <p>17c</p>	SFC, Chiralpak AD-H, $\lambda = 210$ nm 3% IPA/CO ₂ , 2.5 mL/min tr (min) major 2.38, minor 2.96	90
4	 <p>17d</p>	SFC, Chiralpak AD-H, $\lambda = 210$ nm 10% IPA/CO ₂ , 2.5 mL/min tr (min) major 2.72, minor 3.12	93
5	 <p>17e</p>	SFC, Chiralpak AD-H, $\lambda = 210$ nm 5% IPA/CO ₂ , 2.5 mL/min tr (min) major 5.04, minor 5.96	93
6	 <p>17f</p>	SFC, Chiralcel OJ-H, $\lambda = 210$ nm 10% IPA/CO ₂ , 2.5 mL/min tr (min) major 3.96, minor 4.51	92
7	 <p>17g</p>	GC, G-TA column 100 °C, isotherm tr (min) minor 98.83, major 100.76	89

entry	compound	analytic conditions	ee (%)
8	 <p>17h</p>	SFC, Chiralpak IC, λ = 210 nm 3% IPA/CO ₂ , 2.5 mL/min tr (min) minor 9.30, major 9.86	94
9	 <p>17i</p>	SFC, Chiralpak AD-H, λ = 210 nm 5% IPA/CO ₂ , 2.5 mL/min tr (min) minor 2.80, major 3.06	90

2.7.4 DETERMINATION OF ABSOLUTE CONFIGURATION

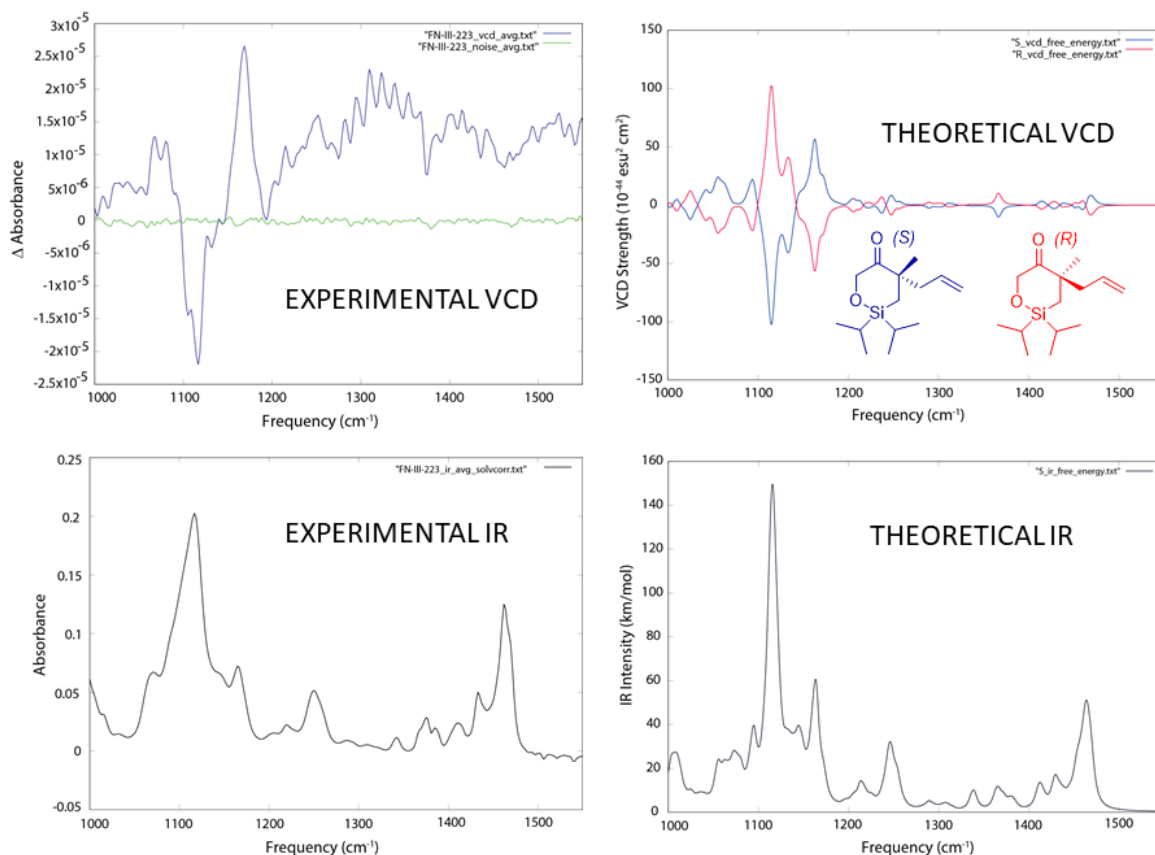
2.7.4.1 Determination of Absolute Configuration of 17g via VCD and OR

Method 1 – Vibrational Circular Dichroism (VCD):

Experimental Protocol. A solution of **17g** (30 mg/mL) was prepared in CDCl₃ and loaded into a front-loading SL-4 cell (International Crystal Laboratories) possessing BaF₂ windows and 100 μ m path length. Infrared (IR) and VCD spectra were acquired on a BioTools ChiralIR-2X VCD spectrometer as a set of 30 one-hour blocks (30 blocks, 3120 scans per block) in dual PEM mode. A 15-minute acquisition of neat (+)- α -pinene control (separate 75 μ m BaF₂ cell) yielded a VCD spectrum in agreement with literature spectra. IR and VCD spectra were background-corrected using a 30-minute block IR acquisition of the empty instrument chamber under gentle N₂ purge, and were solvent corrected using a 4-hour (4 blocks, 3120 scans per block) IR/VCD acquisition of CDCl₃ in the same 100 μ m BaF₂ cell. The reported spectra represent the result of block averaging.

Computational Protocol. The arbitrarily chosen (*S*) enantiomer of compound **17g** was subjected to an exhaustive initial molecular mechanics-based conformational search (MMFF94 force field, 0.08 Å geometric RMSD cutoff, and 30 kcal/mol energy window) as implemented in MOE 2019.0102 (Chemical Computing Group, Montreal, CA). All conformers retained the (*S*) configuration. All MMFF94 conformers under a 10 kcal/mol energy window were then subjected to geometry optimization, harmonic frequency calculation, and VCD rotational strength evaluation using density functional theory. All quantum mechanical calculations first utilized the B3LYP functional, small 6-31G* basis, and IEFPCM model (chloroform solvent) as an initial filter, followed by subsequent optimization using B3PW91 functional, cc-pVTZ basis, and implicit IEFPCM chloroform solvation model on all IEFPCM-B3LYP/6-31G* conformers below 5 kcal/mol. All calculations were performed with the *Gaussian 16* program system (Rev. C.01; Frisch *et al.*, Gaussian, Inc., Wallingford, CT). Resultant IEFPCM-B3PW91/cc-pVTZ harmonic frequencies were scaled by 0.98. All structurally unique conformers possessing all positive Hessian eigenvalues were Boltzmann weighted by relative free energy at 298.15 K. The predicted IR and VCD frequencies and intensities of the retained conformers were convolved using Lorentzian line shapes ($\gamma = 4\text{ cm}^{-1}$) and summed using the respective Boltzmann weights to yield the final predicted IR and VCD spectra of the (*S*) enantiomer of **17g**. The predicted VCD of the corresponding (*R*) enantiomer was generated by inversion of sign. From the reasonable agreement between the predicted and measured IR and VCD spectra in the useful range (1000-1400 cm^{-1} ; see below) supported by a separate, optical rotation-based assignment (see Method 2), the absolute configuration of **17g** was established as (*S*).

Figure 2.1 Experimental (left) and computed (right) IR and VCD spectra for **17g**.



Method 2 – Optical Rotation (OR):

Computational Protocol. The ensemble of unique IEFPCM-B3PW91/cc-pVTZ conformers of the (*S*)-enantiomer of **17g** generated in Method 1 above were subjected to optical rotation calculation at 589.0 nm using the B3LYP hybrid density functional, the large and diffuse 6-311++G(2df,2pd) basis set, and the IEFPCM implicit chloroform solvent model. From the computed IEFPCM-B3PW91/cc-pVTZ free energies at 298.15 K and IEFPCM-B3LYP/6-31++G(2df,2pd) optical rotations, a Boltzmann-weighted OR value of -34.7° was determined for the (*S*)-configuration **17g**. (Weighted OR values instead of using IEFPCM-B3PW91/cc-pVTZ total energies or IEFPCM-B3LYP/6-

31++G(2df,2pd)//IEFPCM-B3PW91/cc-pVTZ total energies were found to be -42.5° and -39.2° , respectively).

As the measured optical rotation of **17g** was found to be -34.54° (CHCl_3 solvent, 25°C , $c = 0.95$), the absolute configuration of **17g** is therefore assigned as (*S*), consistent with the configuration assigned using the VCD method.

2.7.4.2 Determination of Absolute Configuration of **17a** via VCD and OR

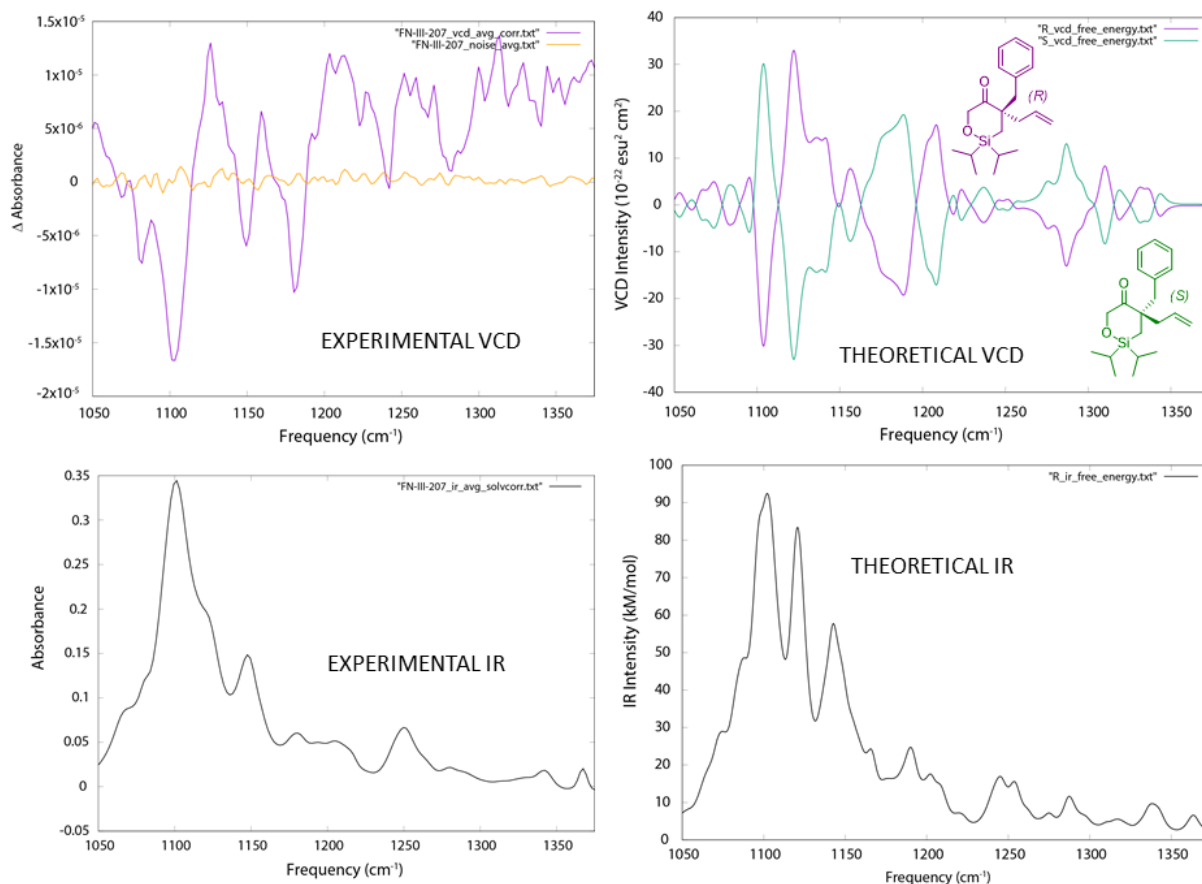
Method 1 – Vibrational Circular Dichroism (VCD):

Experimental Protocol. A solution of **17a** (55 mg/mL) was prepared in CDCl_3 and loaded into a front-loading SL-4 cell (International Crystal Laboratories) possessing BaF_2 windows and 100 μm path length. Infrared (IR) and VCD spectra were acquired on a BioTools ChiralIR-2X VCD spectrometer as a set of 30 one-hour blocks (30 blocks, 3120 scans per block) in dual PEM mode. A 15-minute acquisition of neat (*-*)- α -pinene control (separate 75 μm BaF_2 cell) yielded a VCD spectrum in agreement with literature spectra. IR and VCD spectra were background-corrected using a 30-minute block IR acquisition of the empty instrument chamber under gentle N_2 purge, and were solvent corrected using a 4-hour (4 blocks, 3120 scans per block) IR/VCD acquisition of CDCl_3 in the same 100 μm BaF_2 cell as that used for sample acquisition. The reported spectra represent the result of block averaging.

Computational Protocol. The arbitrarily chosen (*R*) enantiomer of compound **17a** was subjected to an exhaustive initial molecular mechanics-based conformational search (MMFF94 force field, 0.08 Å geometric RMSD cutoff, and 30 kcal/mol energy window) as implemented in MOE 2019.0102 (Chemical Computing Group, Montreal, CA). All conformers retained the (*R*) configuration. All MMFF94 conformers under a 10 kcal/mol

energy window were then subjected to geometry optimization, harmonic frequency calculation, and VCD rotational strength evaluation using density functional theory. All quantum mechanical calculations first utilized the B3LYP functional, small 6-31G* basis, and IEFPCM model (chloroform solvent) as an initial filter, followed by subsequent optimization using B3PW91 functional, cc-pVTZ basis, and implicit IEFPCM chloroform solvation model on all IEFPCM-B3LYP/6-31G* conformers below 3 kcal/mol. All calculations were performed with the *Gaussian 16* program system (Rev. C.01; Frisch *et al.*, Gaussian, Inc., Wallingford, CT). Resultant IEFPCM-B3PW91/cc-pVTZ harmonic frequencies were scaled by 0.98. All structurally unique conformers possessing all positive Hessian eigenvalues were Boltzmann weighted by relative free energy at 298.15 K. The predicted IR and VCD frequencies and intensities of the retained conformers were convolved using Lorentzian line shapes ($\gamma = 4 \text{ cm}^{-1}$) and summed using the respective Boltzmann weights to yield the final predicted IR and VCD spectra of the (*R*) enantiomer of **17a**. The predicted VCD of the corresponding (*S*) enantiomer was generated by inversion of sign. From the reasonable agreement between the predicted and measured IR and VCD spectra in the useful range (1050-1375 cm^{-1} ; see below), the absolute configuration of **17a** is proposed, with moderate confidence, to likely be (*R*).

Figure 2.2 Experimental (left) and computed (right) IR and VCD spectra for **17a**.



(Attempted) Method 2 – Optical Rotation (OR):

Computational Protocol. The ensemble of unique IEFPCM-B3PW91/cc-pVTZ conformers of the (*R*) enantiomer of **17a** generated in Method 1 above were subjected to optical rotation calculation at 589.0 nm using the B3LYP hybrid density functional, the large and diffuse 6-311++G(2df,2pd) basis set, and the IEFPCM implicit chloroform solvent model. Unlike the case of **17g**, the geometric and energetic characteristics of **17a** (including a preponderance of boat-like structures among the lowest energy conformers) give rise to individual, per-conformer optical rotations which fluctuate too greatly in sign to be confidently weighted and summed in order to compare with the experiment (for

which the measured value of $+3.47^\circ$ is also too close to zero to be compared to theory with any degree of confidence). The individual relative energies, free energies, and optical rotational signatures of each conformer of **17a** (again, *not* used for assignment of **17a**, but provided for transparency) are provided in the accompanying Microsoft Excel file.

2.8 REFERENCES AND NOTES

- (1) a) Bols, M.; Skrydstrup, T. *Chem. Rev.* **1995**, *95*, 1253–1277; b) Bracegirdle, S.; Anderson, E. A. *Chem. Soc. Rev.* **2010**, *39*, 4114–4129.
- (2) For selected examples, see a) Shvartsbart, A.; Smith, A. B., III. *J. Am. Chem. Soc.* **2015**, *137*, 3510–3519; b) Lu, P.; Mailyan, A.; Gu, Z.; Guptill, D. M.; Wang, H.; Davies, H. M. L.; Zakarian, A. *J. Am. Chem. Soc.* **2014**, *136*, 17738–17749; c) Lee, E.; Song, H. Y.; Kang, J. W.; Kim, D.-S.; Jung, C.-K.; Joo, J. M. *J. Am. Chem. Soc.* **2002**, *124*, 384–385.
- (3) For a C–H oxygenation approach, see a) Huang, C.; Ghavtadze, N.; Godoi, B.; Gevorgyan, V. *Chem. Eur. J.* **2012**, *18*, 9789–9792. For a Heck reaction approach, see b) Parasram, M.; Iaroshenko, V. O.; Gevorgyan, V. *J. Am. Chem. Soc.* **2014**, *136*, 17926–17929. For other approaches such as cycloaddition and hydrosilylation, see ref. 1a and 1b.
- (4) For examples of enantiospecific methods to access chiral siloxanes, see a) Trost, B. M.; Ball, Z. T.; Laemmerhold, K. M. *J. Am. Chem. Soc.* **2005**, *127*, 10028–10038; b) Gallagher, A. G.; Tian, H.; Torres-Herrera, O. A.; Yin, S.; Xie, A.;

- Lange, D. M.; Wilson, J. K.; Mueller, L. G.; Gau, M. R.; Carroll, P. J.; Martinez-Solorio, D. *Org. Lett.* **2019**, *21*, 8646–8651.
- (5) a) Aeilts, S. L.; Cefalo, D. R.; Bonitatebus, P. J. Jr.; Houser, J. H.; Hoveyda, A. H.; Schrock, R. R. *Angew. Chem. Int. Ed.* **2001**, *40*, 1452–1456; b) Balskus, E. P.; Jacobsen, E. N. *Science* **2007**, *317*, 1736–1740.
- (6) For our recent examples, see a) Jette, C. I.; Tong, Z. J.; Hadt, R. G.; Stoltz, B. M. *Angew. Chem. Int. Ed.* **2020**, *59*, 2033–2038; b) Sercel, Z. P.; Sun, A. W.; Stoltz, B. M. *Org. Lett.* **2019**, *21*, 9158–9161; c) Alexy, E. J.; Fulton, T. J.; Zhang, H.; Stoltz, B. M. *Chem. Sci.* **2019**, *10*, 5996–6000; d) Sun, A. W.; Hess, S. N.; Stoltz, B. M. *Chem. Sci.* **2019**, *10*, 788–792; e) Ngamnithiporn, A.; Jette, C. I.; Bachman, S.; Virgil, S. C.; Stoltz, B. M. *Chem. Sci.* **2018**, *9*, 2547–2551; f) Alexy, E. J.; Zhang, H.; Stoltz, B. M. *J. Am. Chem. Soc.* **2018**, *140*, 10109–10112; For a review, see g) Liu, Y.; Han, S.-J.; Liu, W.-B.; Stoltz, B. M. *Acc. Chem. Res.* **2015**, *48*, 740–751.
- (7) For reviews on the development of Pd-catalyzed decarboxylative allylic alkylation, see a) Weaver, J. D.; Recio, A.; Grenning, A. J.; Tunge, J. A. *Chem. Rev.* **2011**, *68*, 1846–1913; b) James, J.; Jackson, M.; Guiry, P. J. *Adv. Synth. Catal.* **2019**, *361*, 3016–3049. c) Tunge, J. A. *Isr. J. Chem.* **2020**, *60*, 351–359.
- (8) For asymmetric allylic alkylation of silicon-containing starting materials, see a) Chen, J.-P.; Ding, C.-H.; Liu, W.; Hou, X.-L.; Dai, L.-X. *J. Am. Chem. Soc.* **2010**, *132*, 15493–15495; b) Yamano, M. M.; Knapp, R. R.; Ngamnithiporn, A.;

- Ramirez, M.; Houk, K. N.; Stoltz, B. M.; Garg, N. K. *Angew. Chem. Int. Ed.* **2019**, *58*, 5653–5657.
- (9) For recent reviews, see a) Trost, B.; Schultz, J. E. *Synthesis* **2019**, *51*, 1–30; b) Feng, J.; Holmes, M.; Krische, M. J. *Chem. Rev.* **2017**, *117*, 12564–12580.
- (10) Attempts to access 5- and 7-membered siloxyketones via this synthetic route proved challenging. No reaction was observed in the α -alkylation of 5-membered allyl- β -ketoester substrate.
- (11) Behenna, D. C.; Mohr, J. T.; Sherden, N. H.; Marinescu, S. C.; Harned, A. M.; Tani, K.; Seto, M.; Ma, S.; Novák, Z.; Krout, M. R.; McFadden, R. M.; Roizen, J. L.; Enquist, J. A. Jr.; White, D. E.; Levine, S. R.; Petrova, K. V.; Iwashita, A.; Virgil, S. C.; Stoltz, B. M. *Chem. Eur. J.* **2011**, *17*, 14199–14223.
- (12) a) Alexy, E. J.; Virgil, S. C.; Bartberger, M. D.; Stoltz, B. M. *Org. Lett.* **2017**, *19*, 5007–5009; b) Trost, B. M.; Xu, J.; Schmidt, T. *J. Am. Chem. Soc.* **2009**, *131*, 18343–18357.
- (13) See sections 2.7.2.6 and 2.7.2.7 for the computational protocols, computed and measured VCD spectra.
- (14) Diastereoselective reduction has been previously observed in similar systems, see a) Trost, B. M.; Radinov, R.; Grenzer, E. M. *J. Am. Chem. Soc.* **1997**, *119*, 7879–7880; b) Sha, C.-K.; Chiu, R.-T.; Yang, C.-F.; Yao, N.-T.; Tseng, W.-H.; Liao, F.-L.; Wang, S.-L. *J. Am. Chem. Soc.* **1997**, *119*, 4130–4135.

- (15) Simas, A. B. C.; Pais, K. C.; da Silva, A. A. T. *J. Org. Chem.* **2003**, *68*, 5426–5428.
- (16) Miller, D. J.; Yu, F.; Knight, D. W.; Allemann, R. K. *Org. Biomol. Chem.* **2009**, *7*, 962–975.
- (17) Parasram, M.; Iaroshenko, V. O.; Gevorgyan, V. *J. Am. Chem. Soc.* **2014**, *52*, 17926–17929.
- (18) a) Klepacz, A.; Zwierzak, A. *Tetrahedron Lett.* **2002**, *43*, 1079–1080; b) Sikriwal, D.; Kant, R.; Maulik, P. R.; Dikshit, D. K. *Tetrahedron* **2010**, *66*, 6167–6173.

APPENDIX 3

Spectra Relevant to Chapter 2:

*Enantioselective Synthesis of Highly Oxygenated Acyclic Quaternary
Center-Containing Building Blocks via Palladium-Catalyzed
Decarboxylative Allylic Alkylation of Cyclic Siloxyketones*

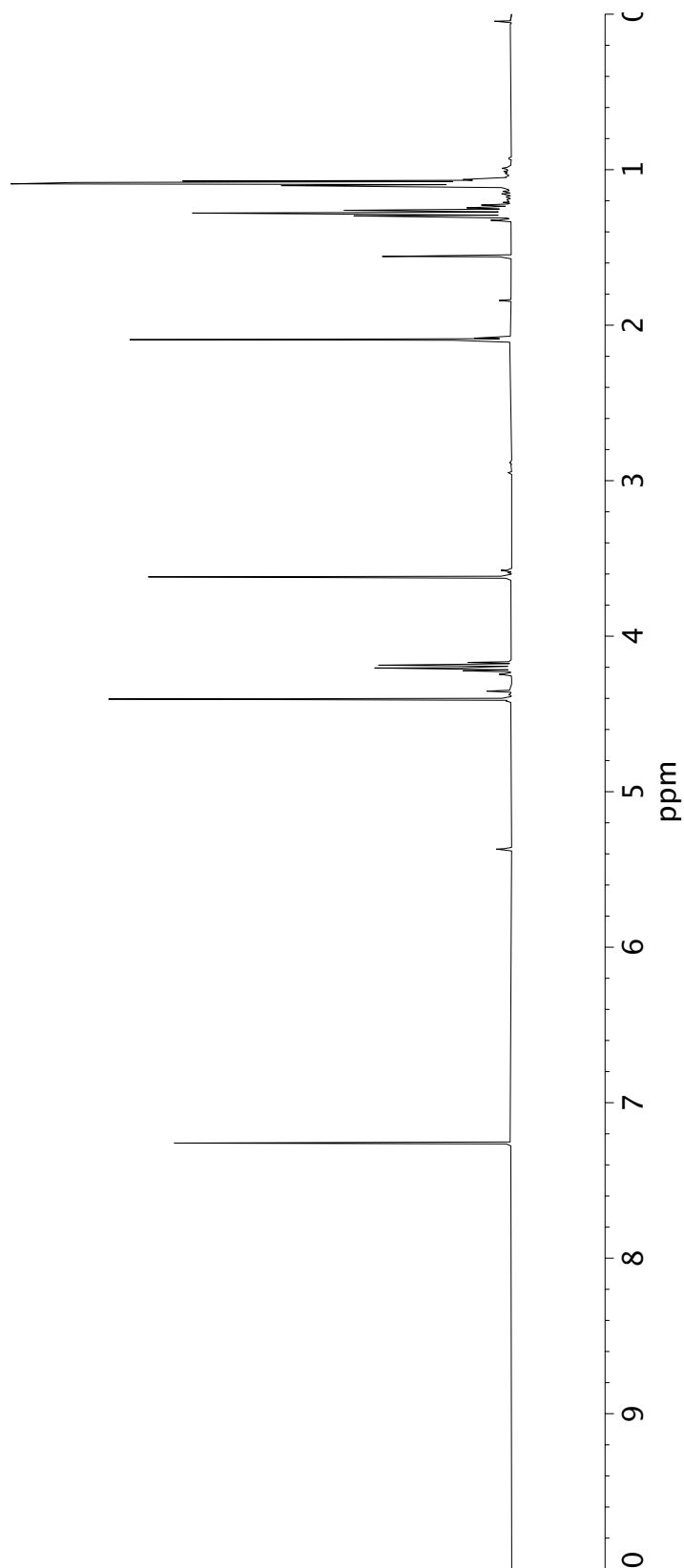
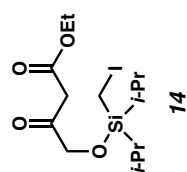


Figure A3.1 ^1H NMR (500 MHz, CDCl_3) of compound **14**.

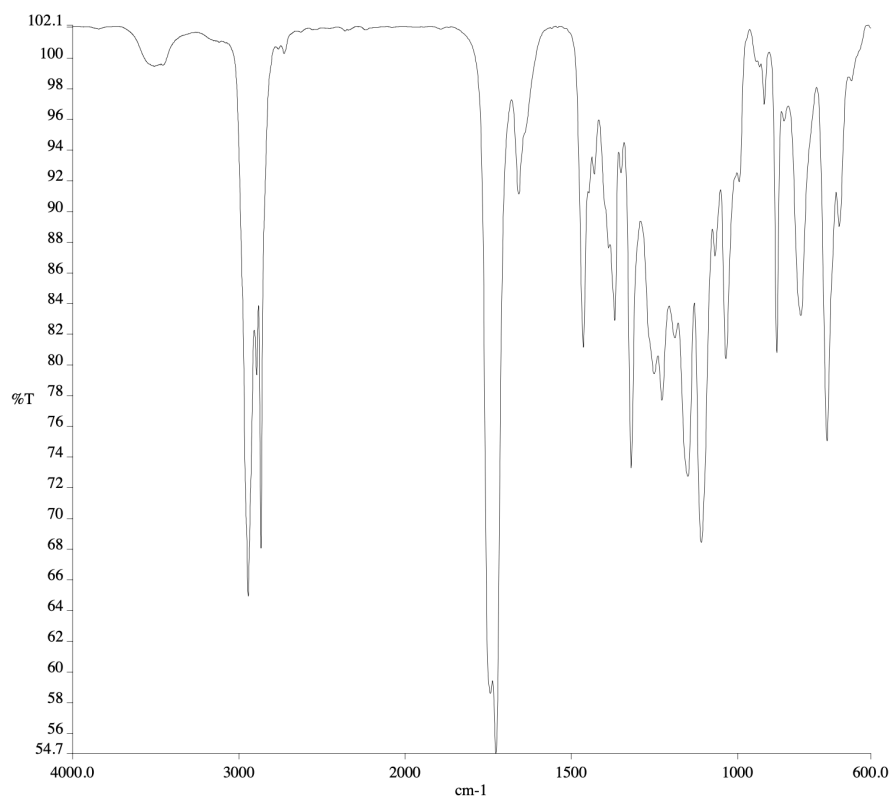


Figure A3.2 Infrared spectrum (Thin Film, NaCl) of compound **14**.

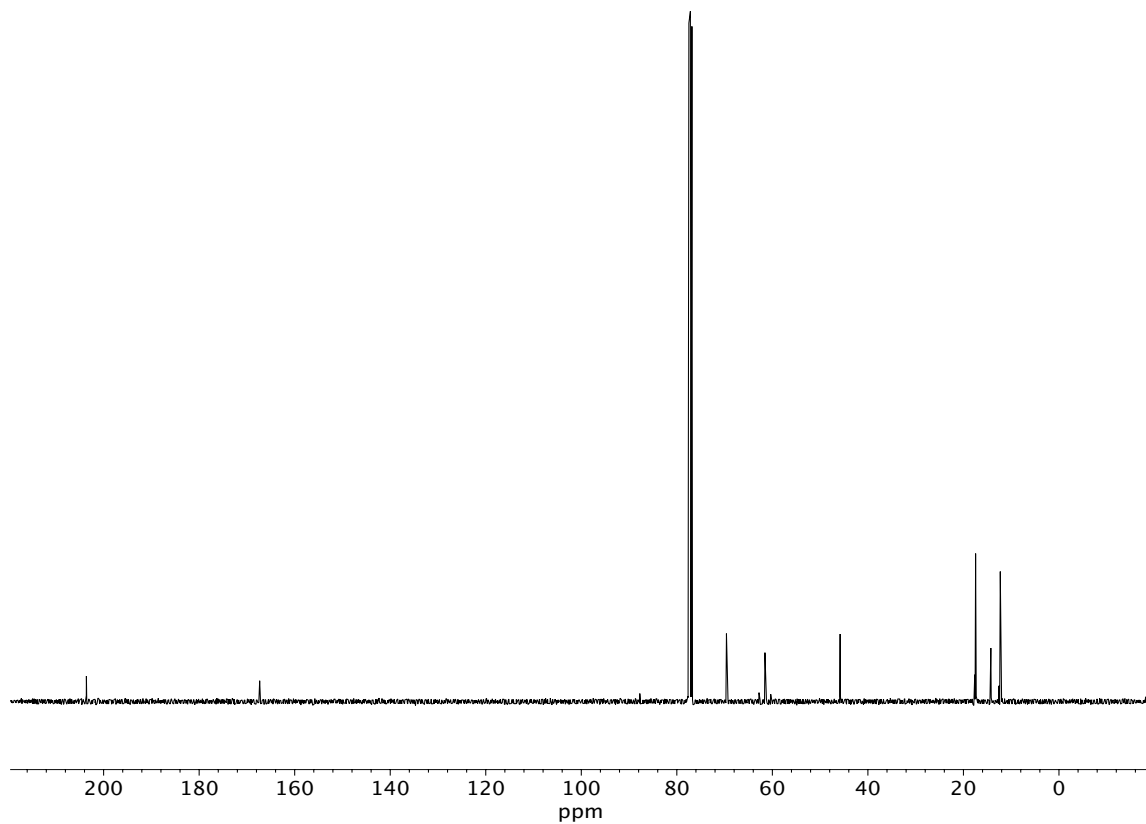


Figure A3.3 ¹³C NMR (125 MHz, CDCl₃) of compound **14**.

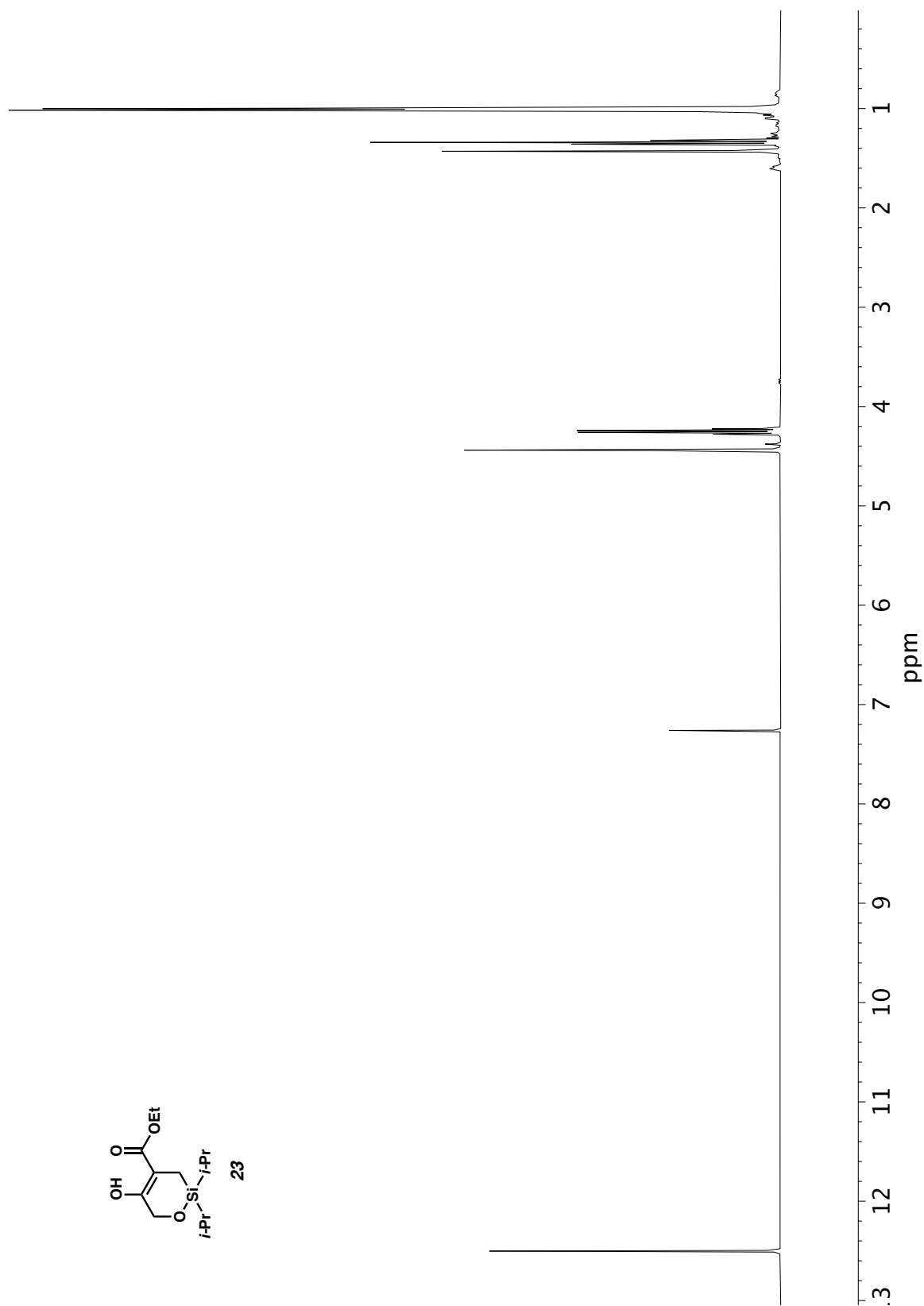


Figure A3.4 ^1H NMR (400 MHz, CDCl_3) of compound **23**.

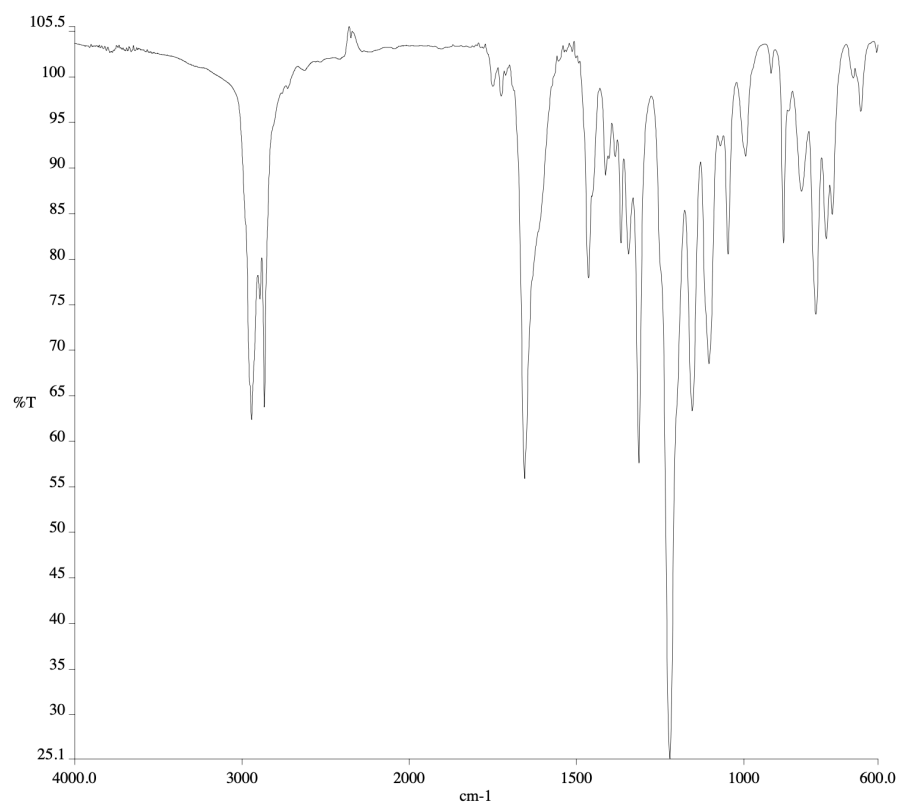


Figure A3.5 Infrared spectrum (Thin Film, NaCl) of compound **23**.

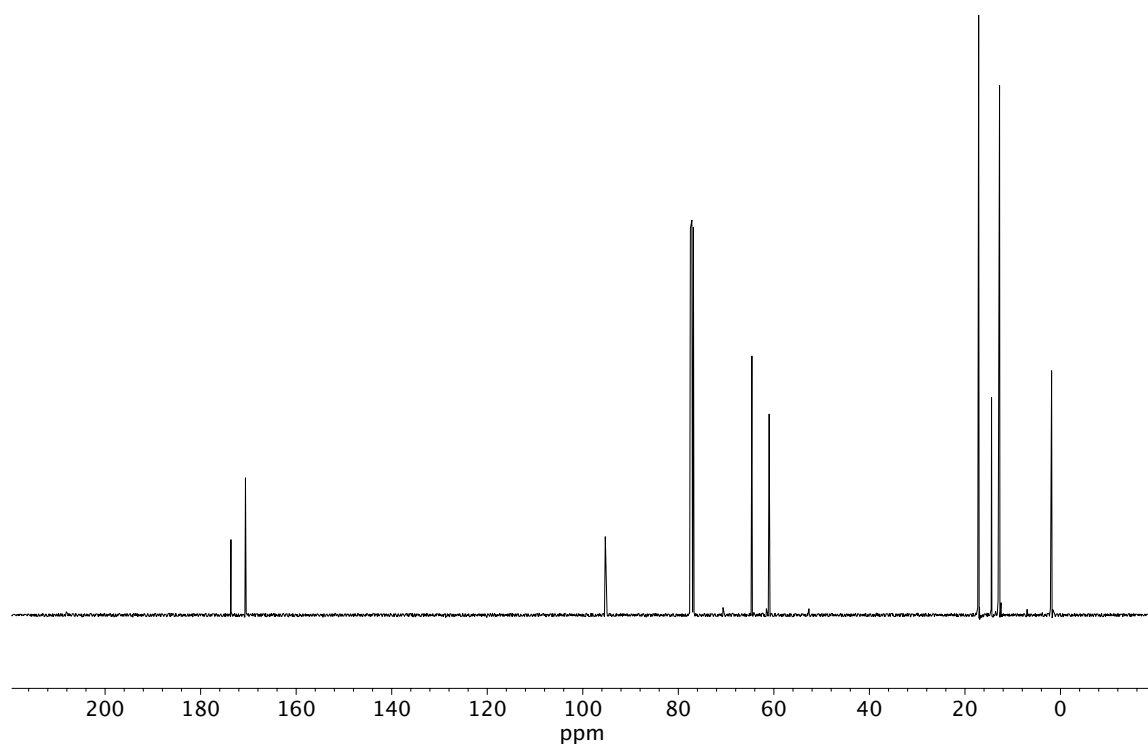


Figure A3.6 ¹³C NMR (100 MHz, CDCl₃) of compound **23**.

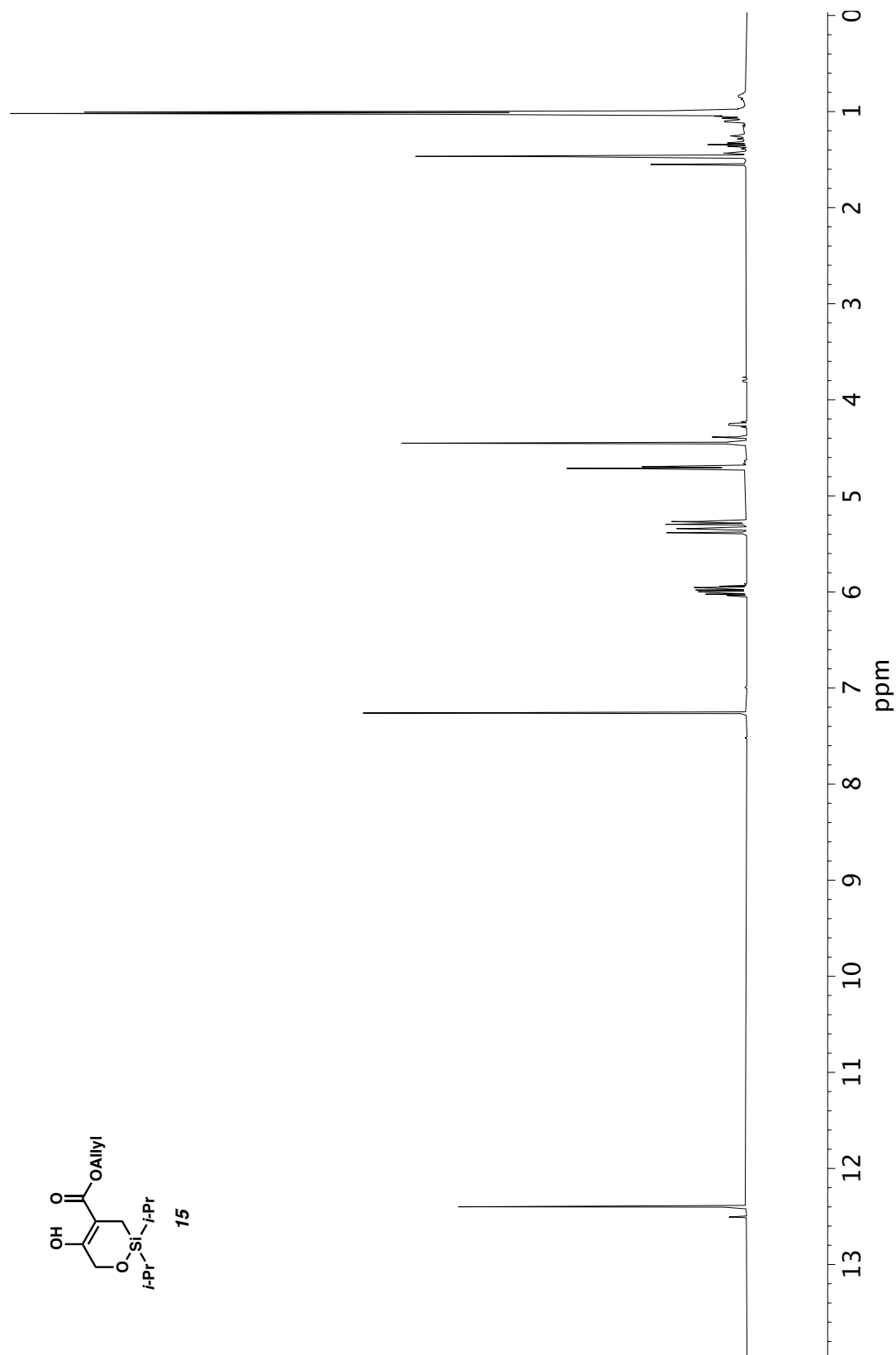


Figure A3.7 ¹H NMR (400 MHz, CDCl₃) of compound **15**.

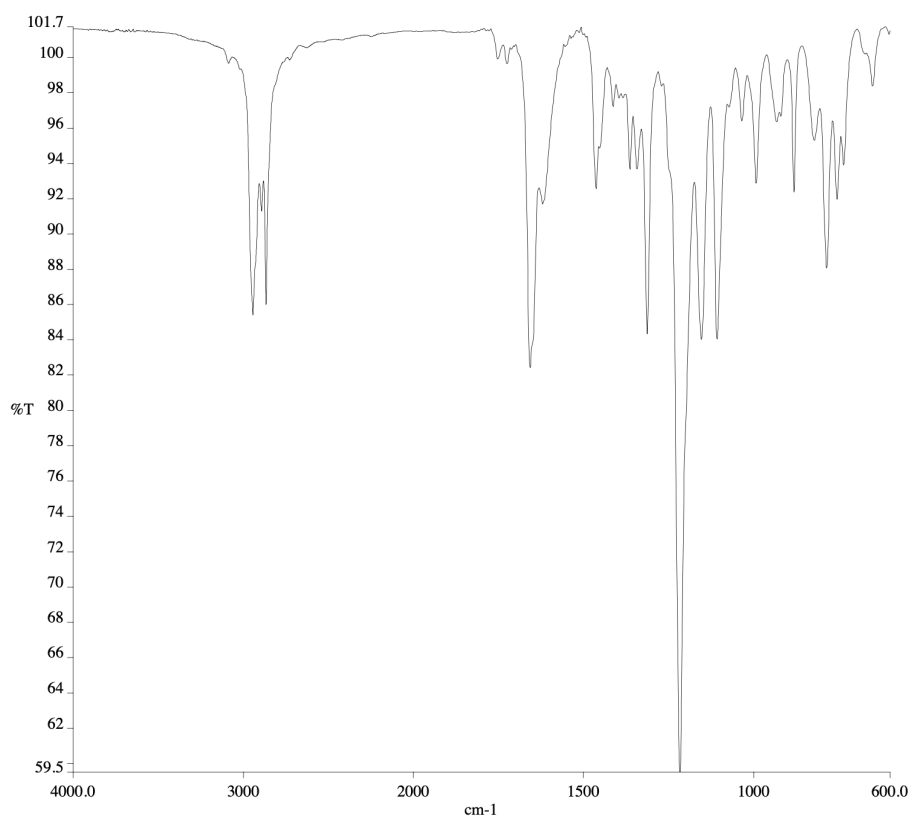


Figure A3.8 Infrared spectrum (Thin Film, NaCl) of compound **15**.

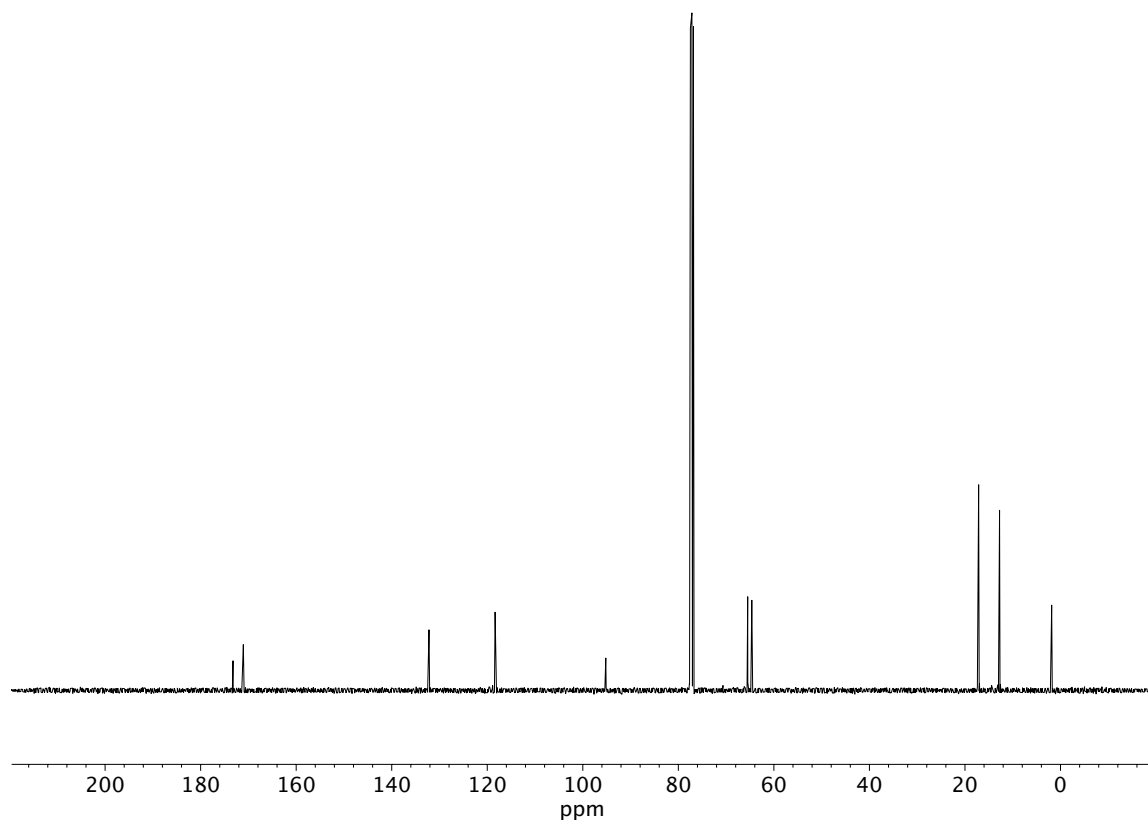


Figure A3.9 ¹³C NMR (100 MHz, CDCl₃) of compound **15**.

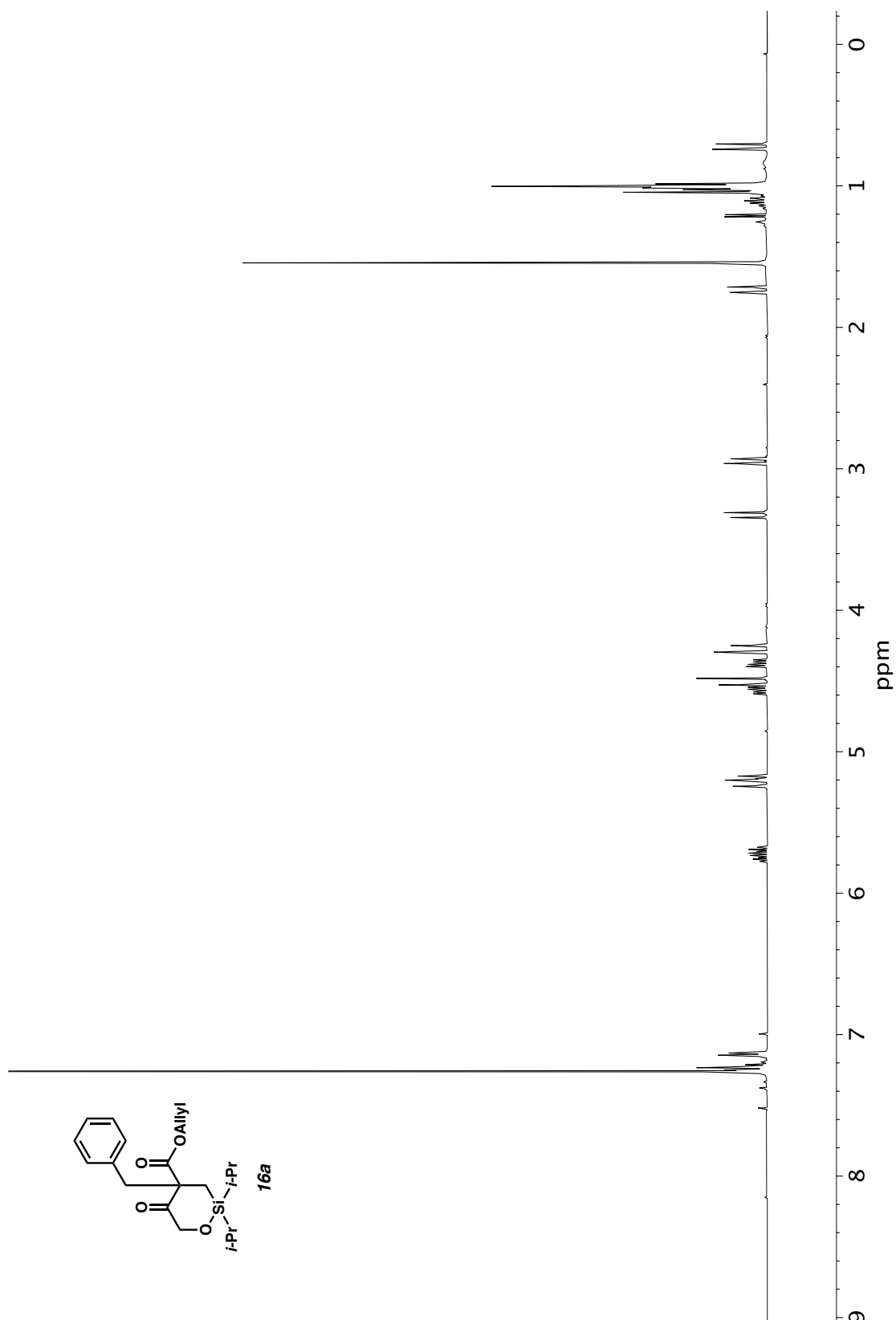


Figure A3.10 ^1H NMR (400 MHz, CDCl_3) of compound **16a**.

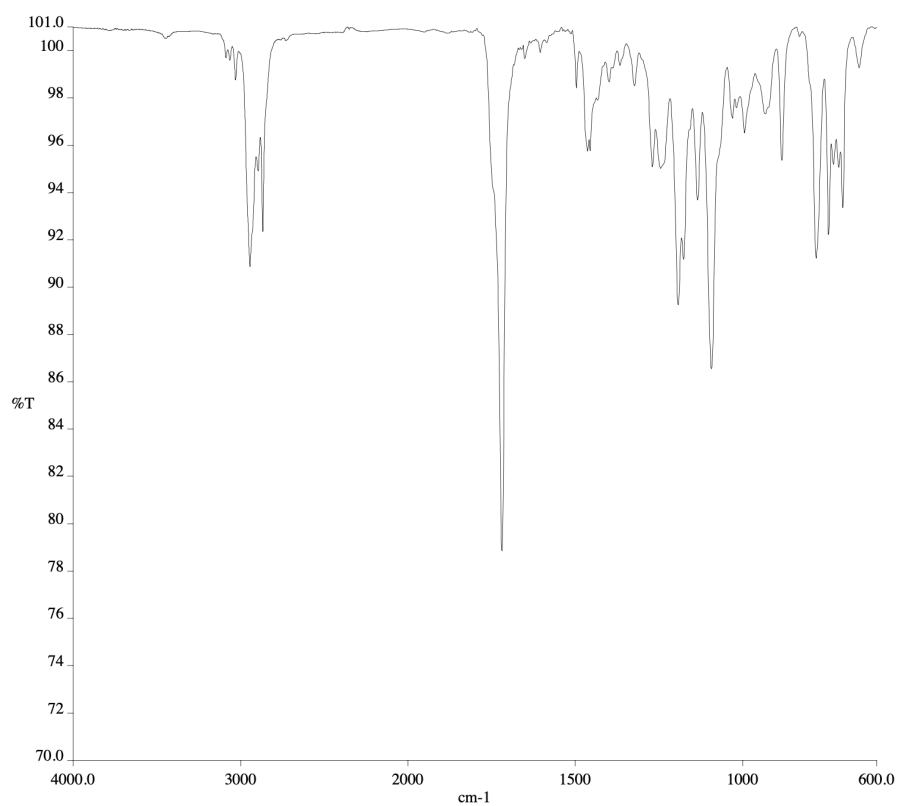


Figure A3.11 Infrared spectrum (Thin Film, NaCl) of compound **16a**.

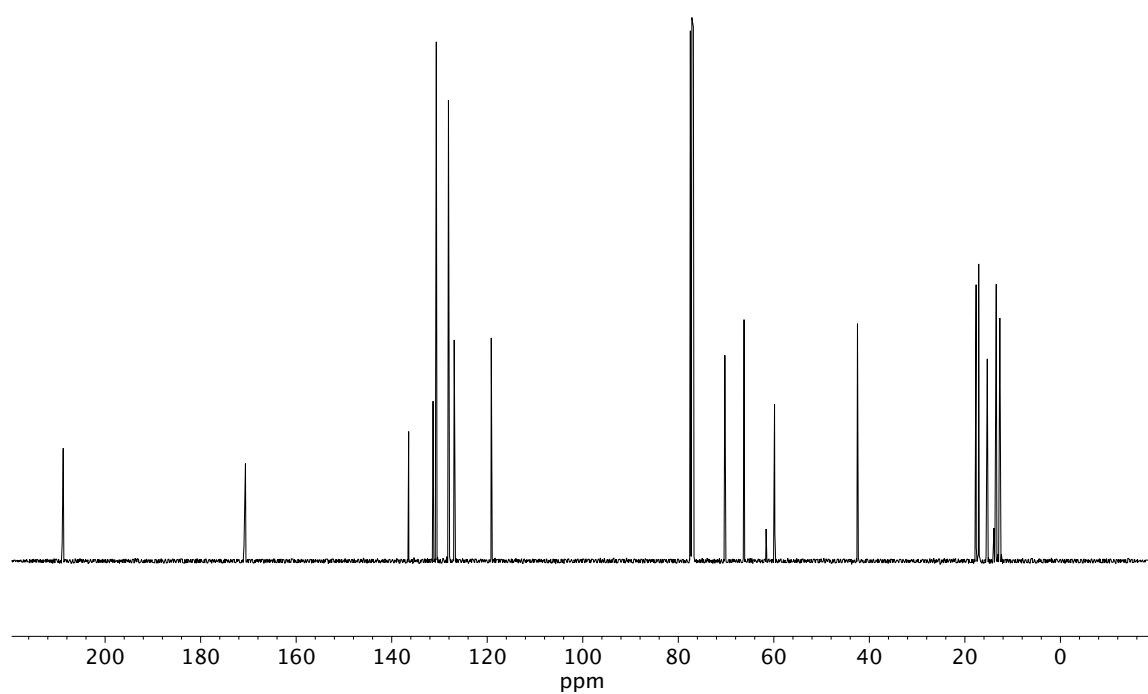


Figure A3.12 ¹³C NMR (100 MHz, CDCl₃) of compound **16a**.

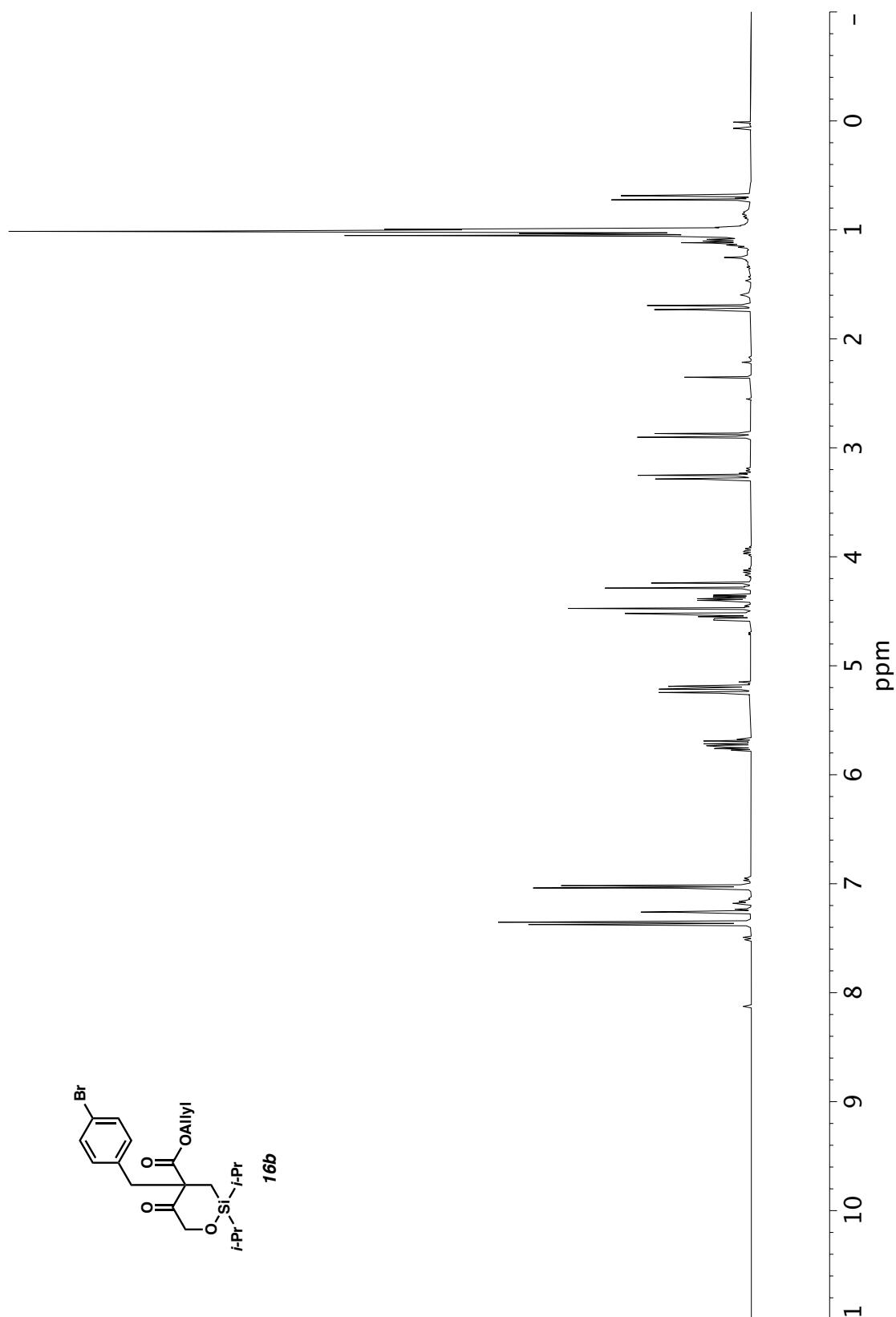


Figure A3.13 ^1H NMR (400 MHz, CDCl_3) of compound **16b**.

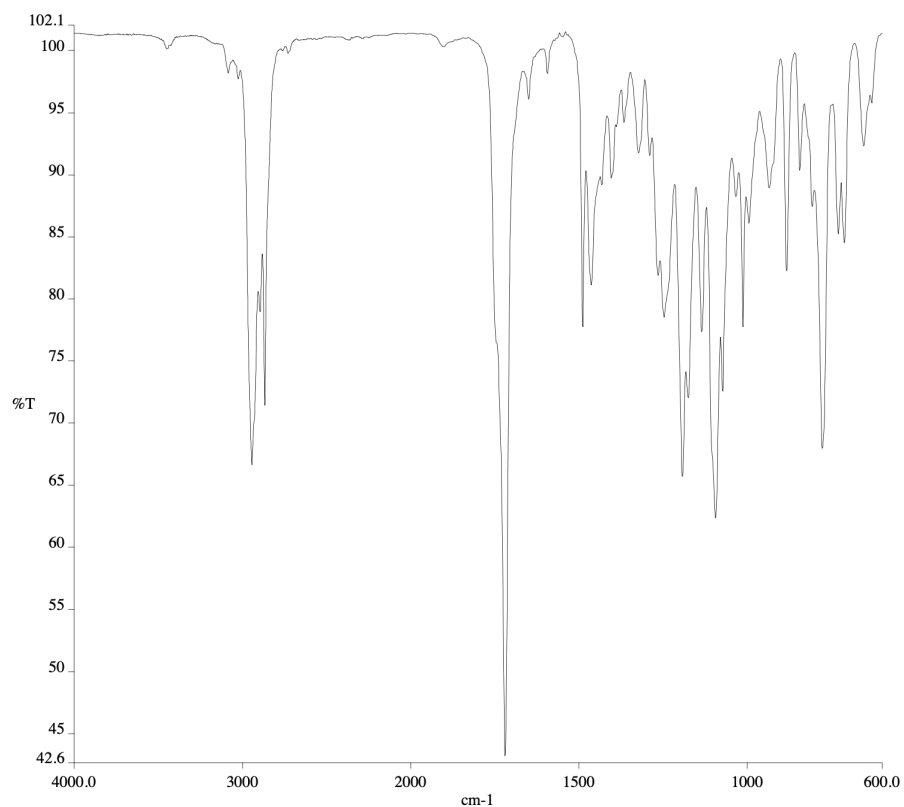


Figure A3.14 Infrared spectrum (Thin Film, NaCl) of compound **16b**.

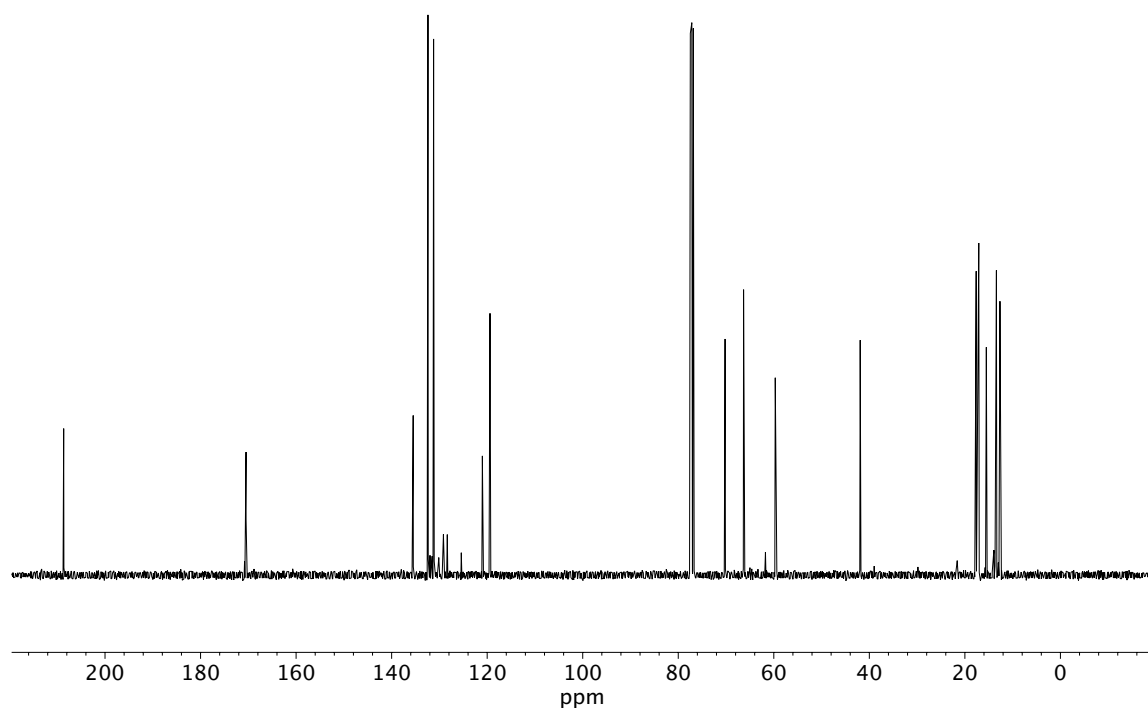


Figure A3.15 ¹³C NMR (100 MHz, CDCl₃) of compound **16b**.

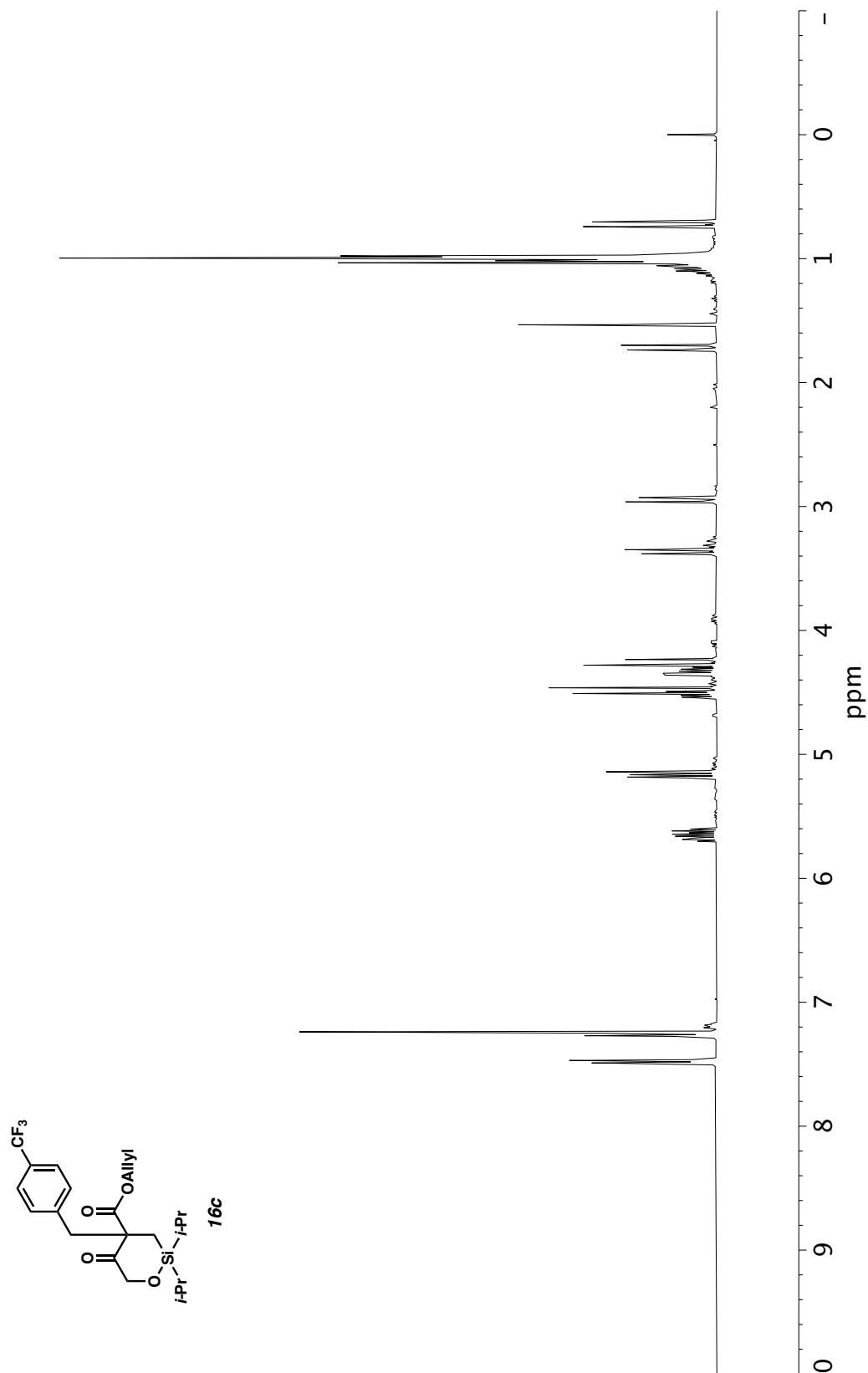


Figure A3.16 ^1H NMR (400 MHz, CDCl_3) of compound **16c**.

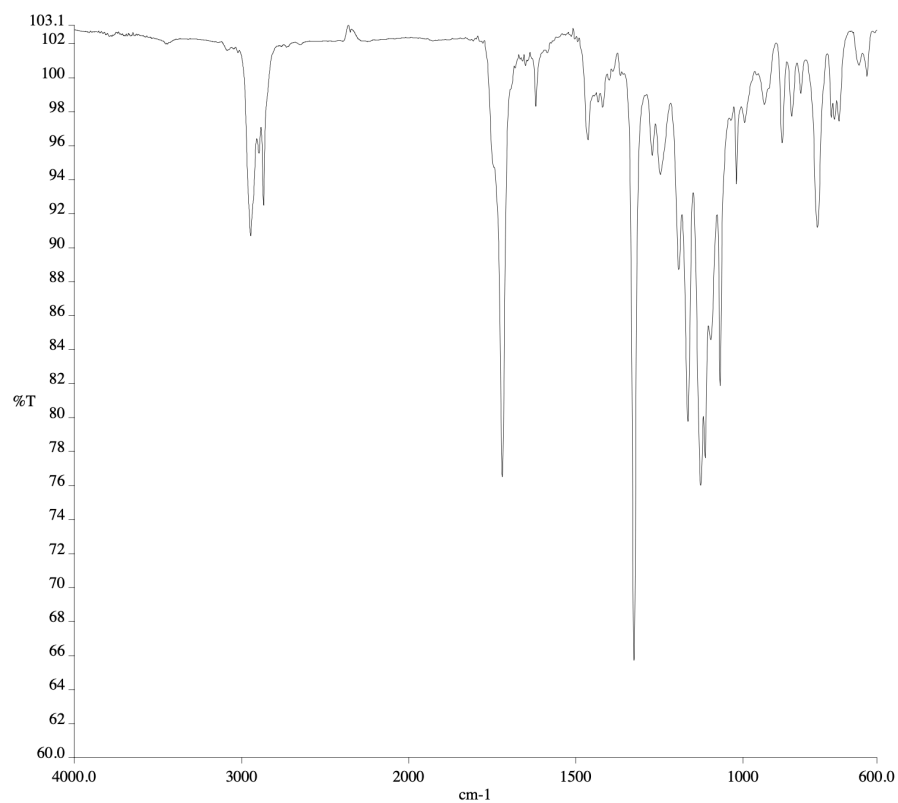


Figure A3.17 Infrared spectrum (Thin Film, NaCl) of compound **16c**.

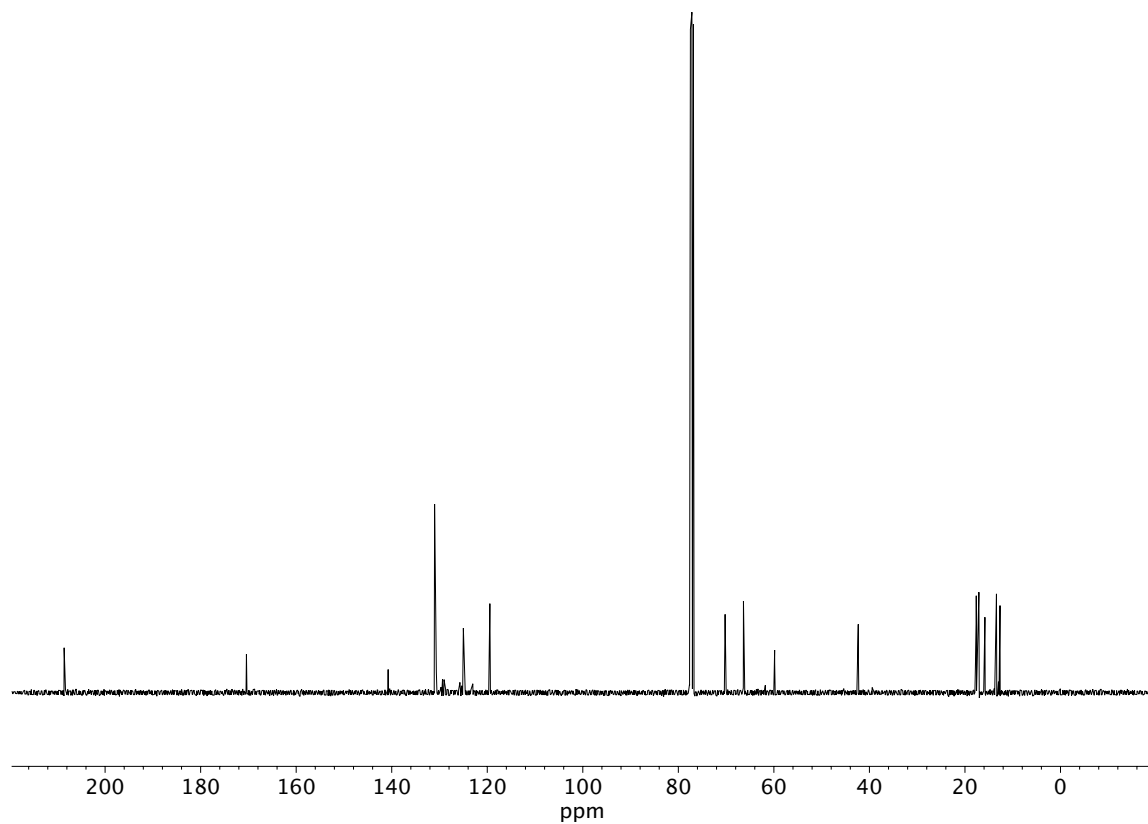


Figure A3.18 ¹³C NMR (100 MHz, CDCl₃) of compound **16c**.

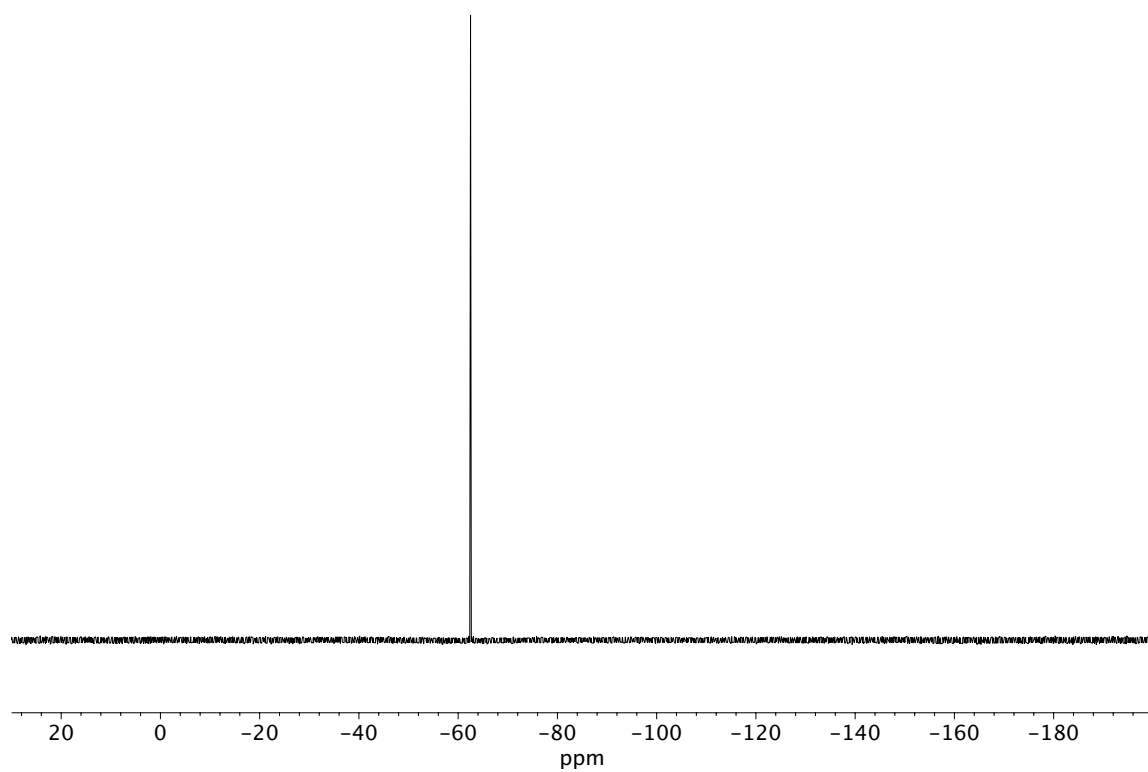


Figure A3.19 ^{19}F NMR (282 MHz, CDCl_3) of compound **16c**.

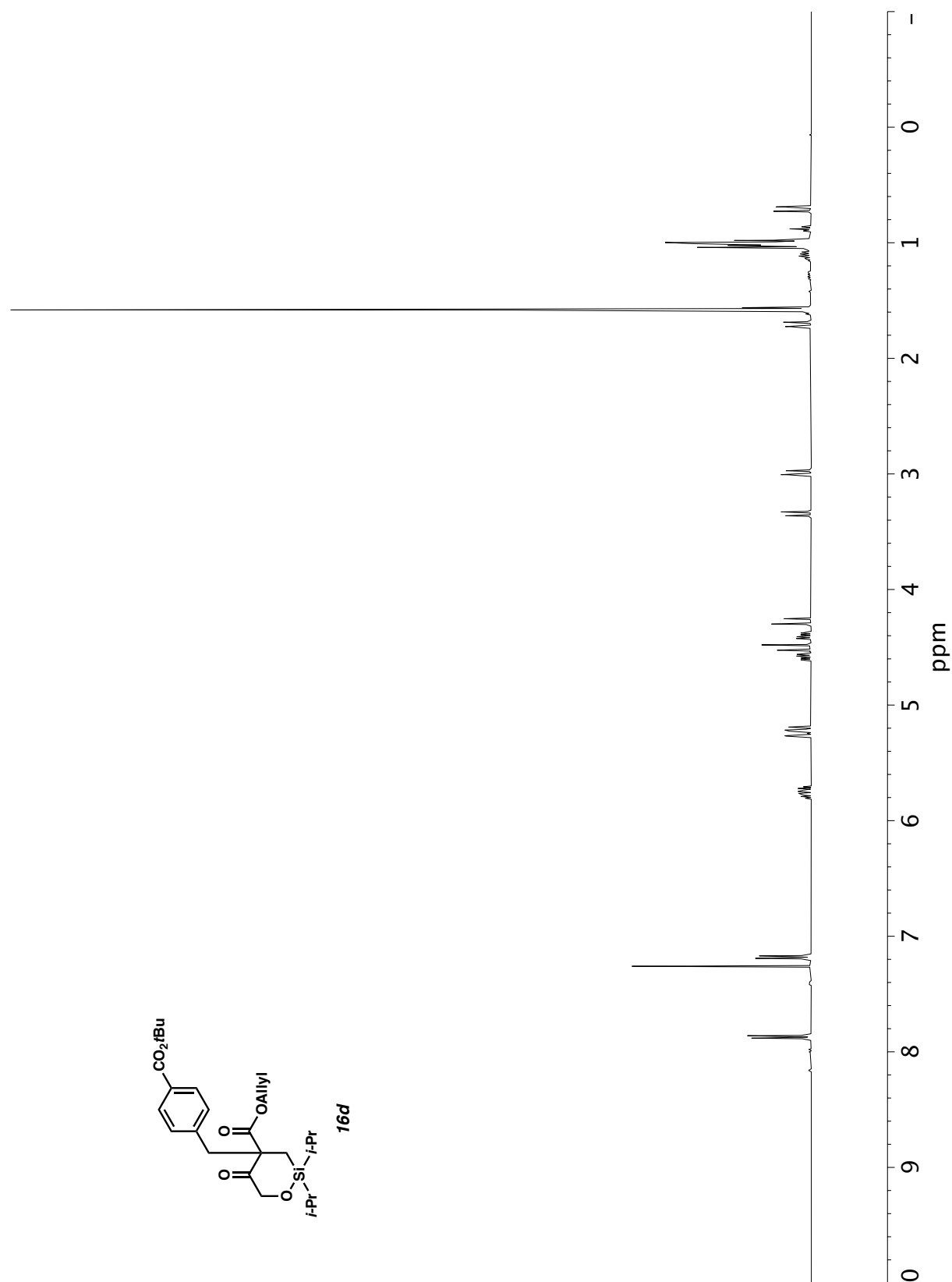


Figure A3.20 ^1H NMR (400 MHz, CDCl_3) of compound **16d**.

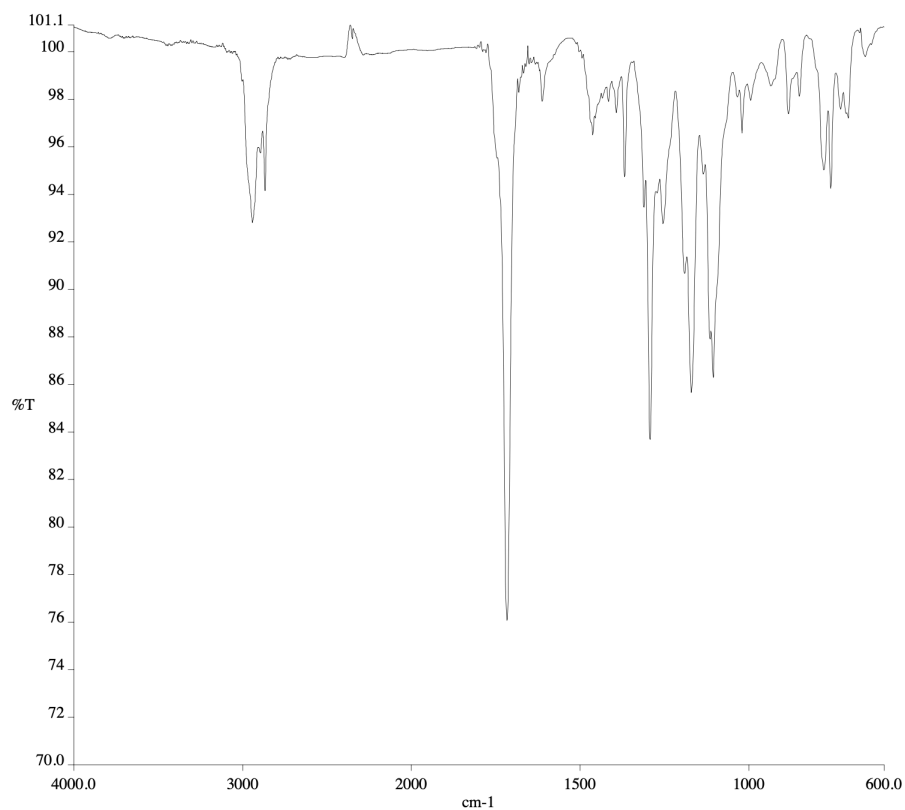


Figure A3.21 Infrared spectrum (Thin Film, NaCl) of compound **16d**.

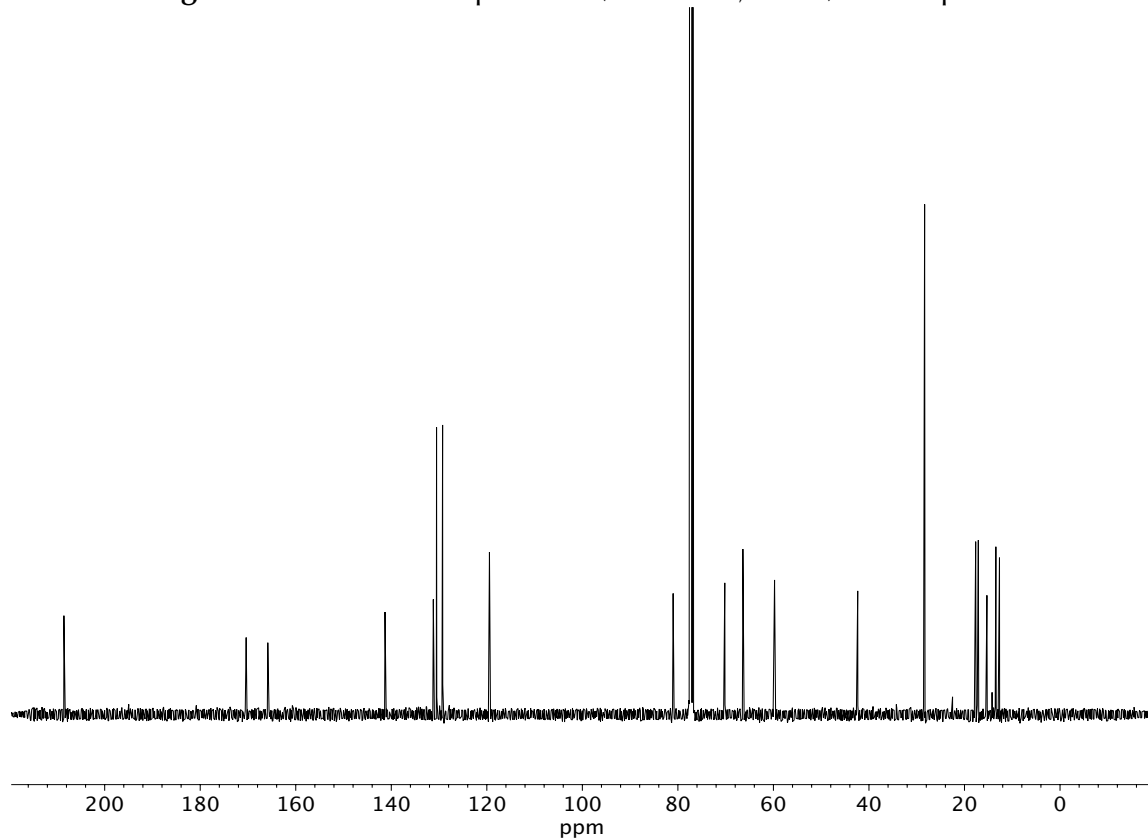


Figure A3.22 ^{13}C NMR (100 MHz, CDCl_3) of compound **16d**.

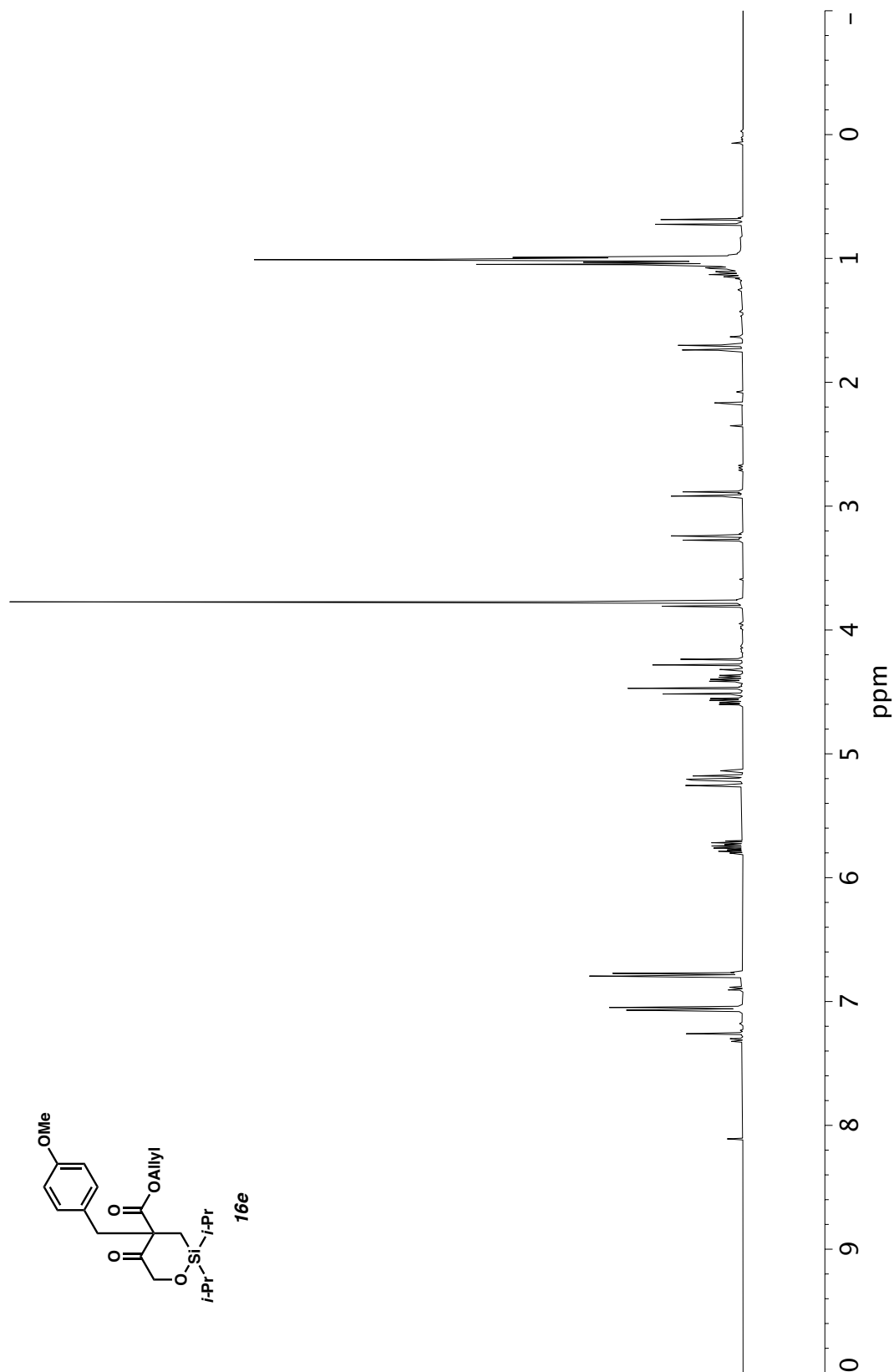


Figure A3.23 ^1H NMR (400 MHz, CDCl_3) of compound **16e**.

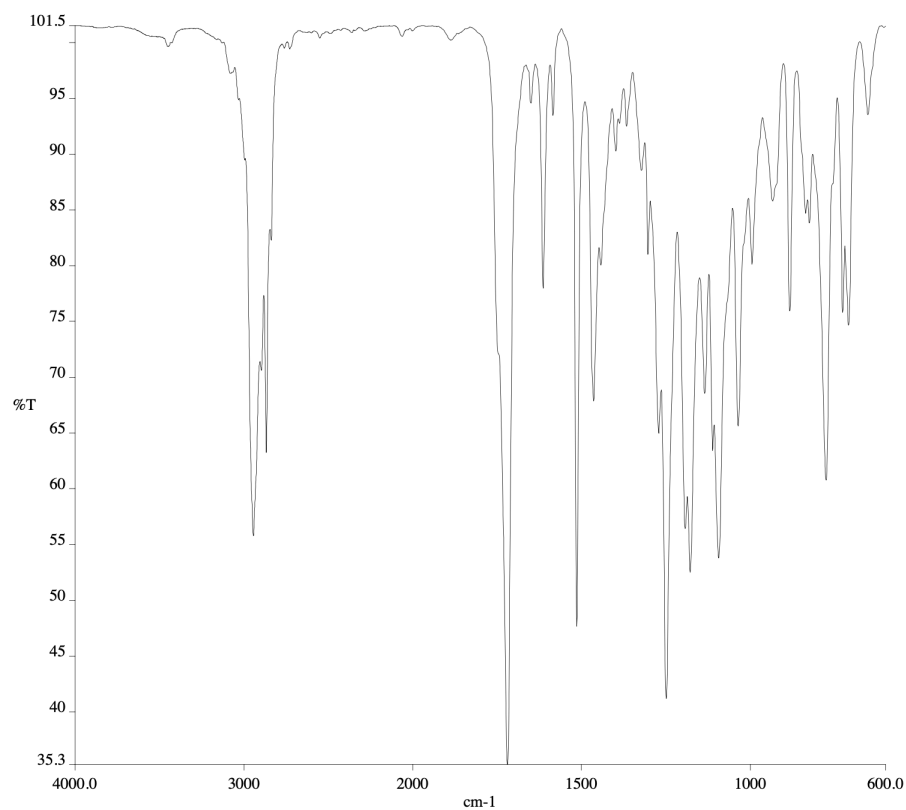


Figure A3.24 Infrared spectrum (Thin Film, NaCl) of compound **16e**.

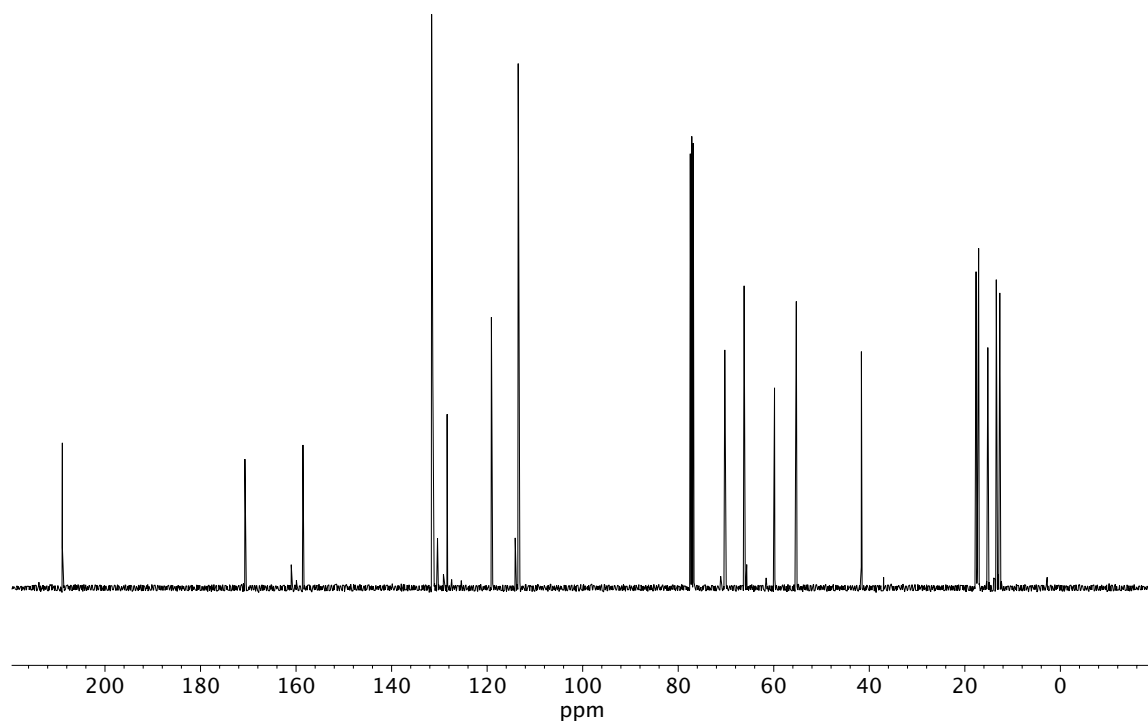


Figure A3.25 ¹³C NMR (100 MHz, CDCl₃) of compound **16e**.

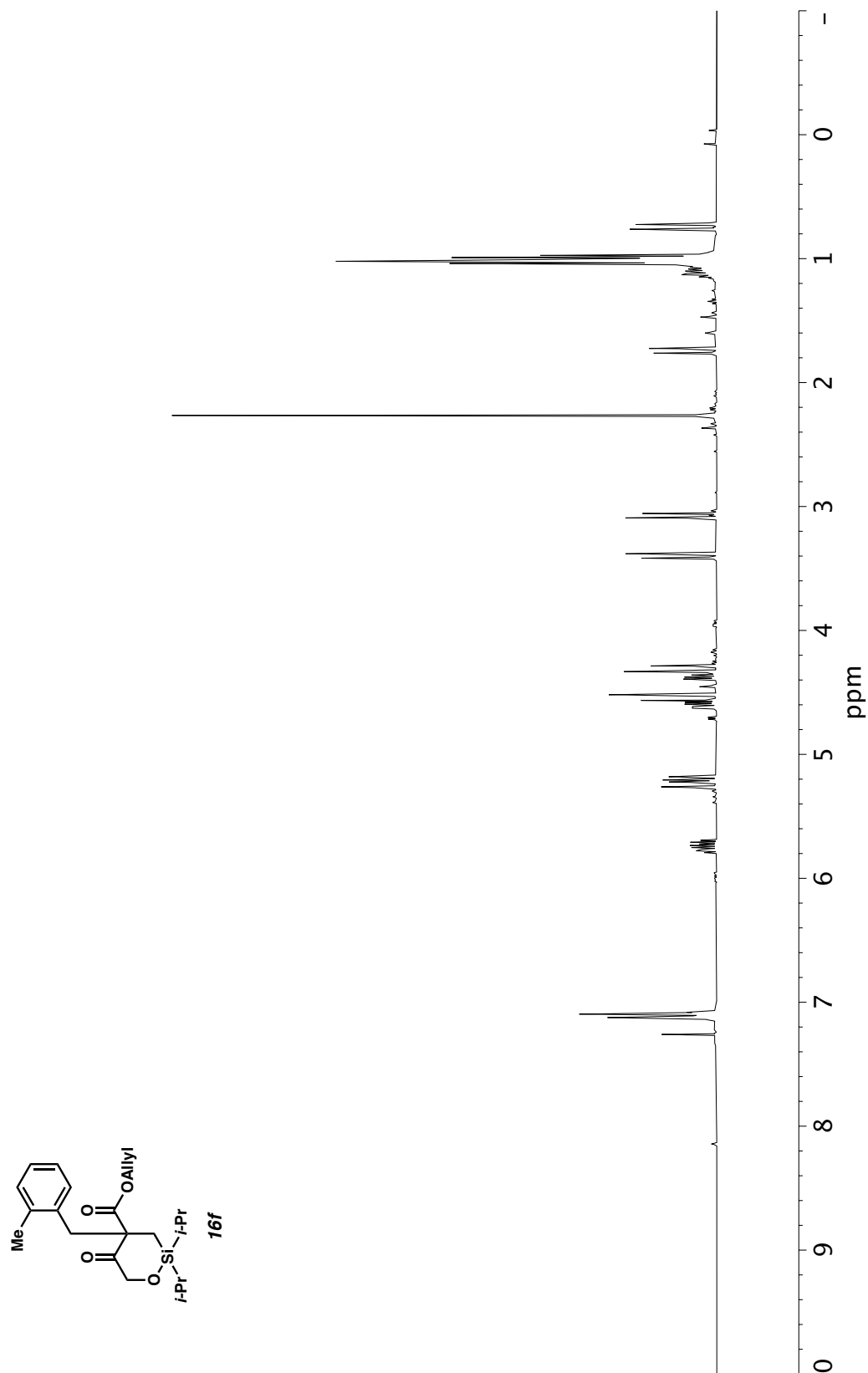


Figure A3.26 ^1H NMR (400 MHz, CDCl_3) of compound **16f**.

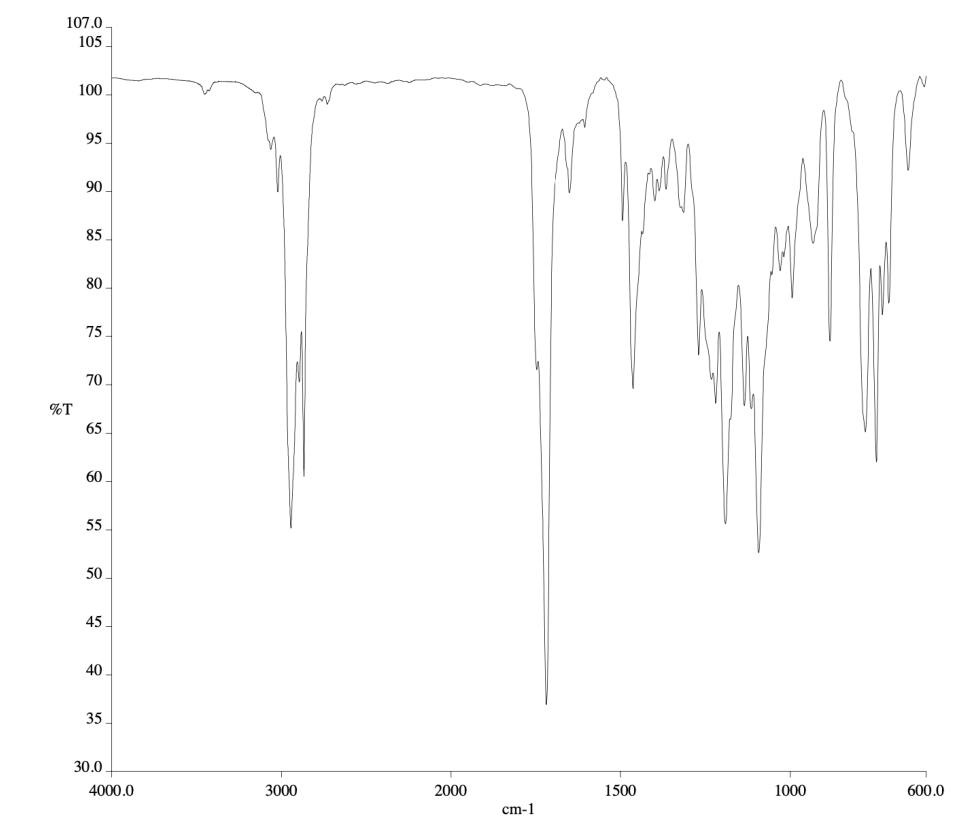


Figure A3.27 Infrared spectrum (Thin Film, NaCl) of compound **16f**.

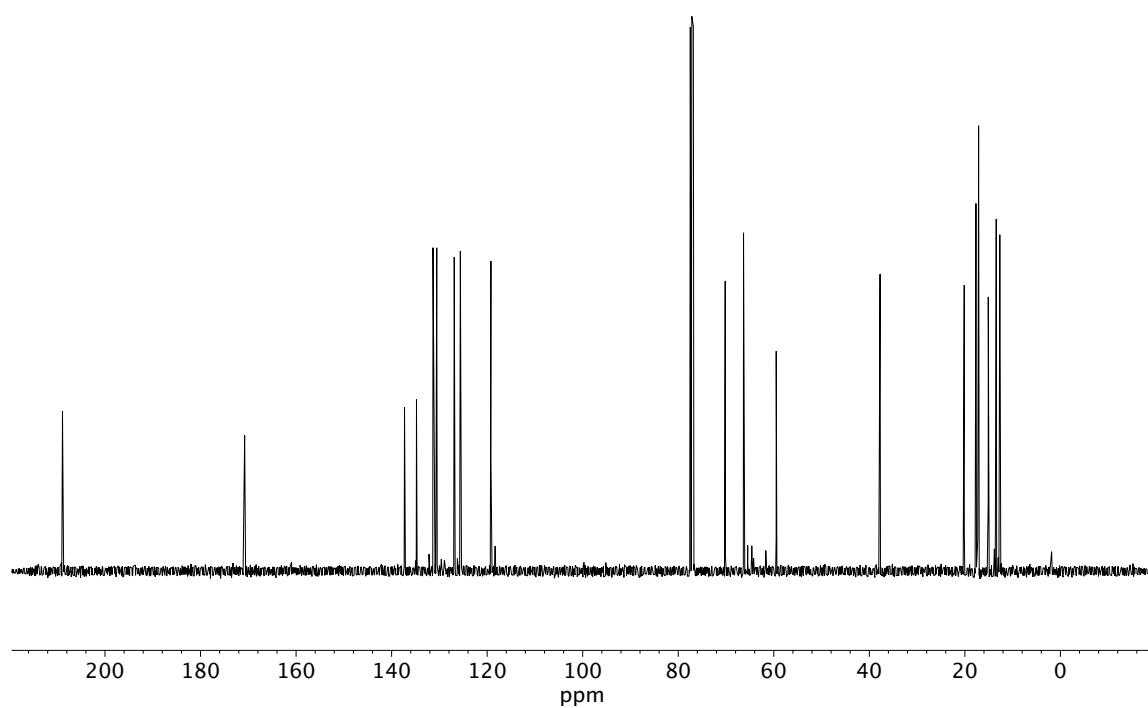


Figure A3.28 ¹³C NMR (100 MHz, CDCl₃) of compound **16f**.

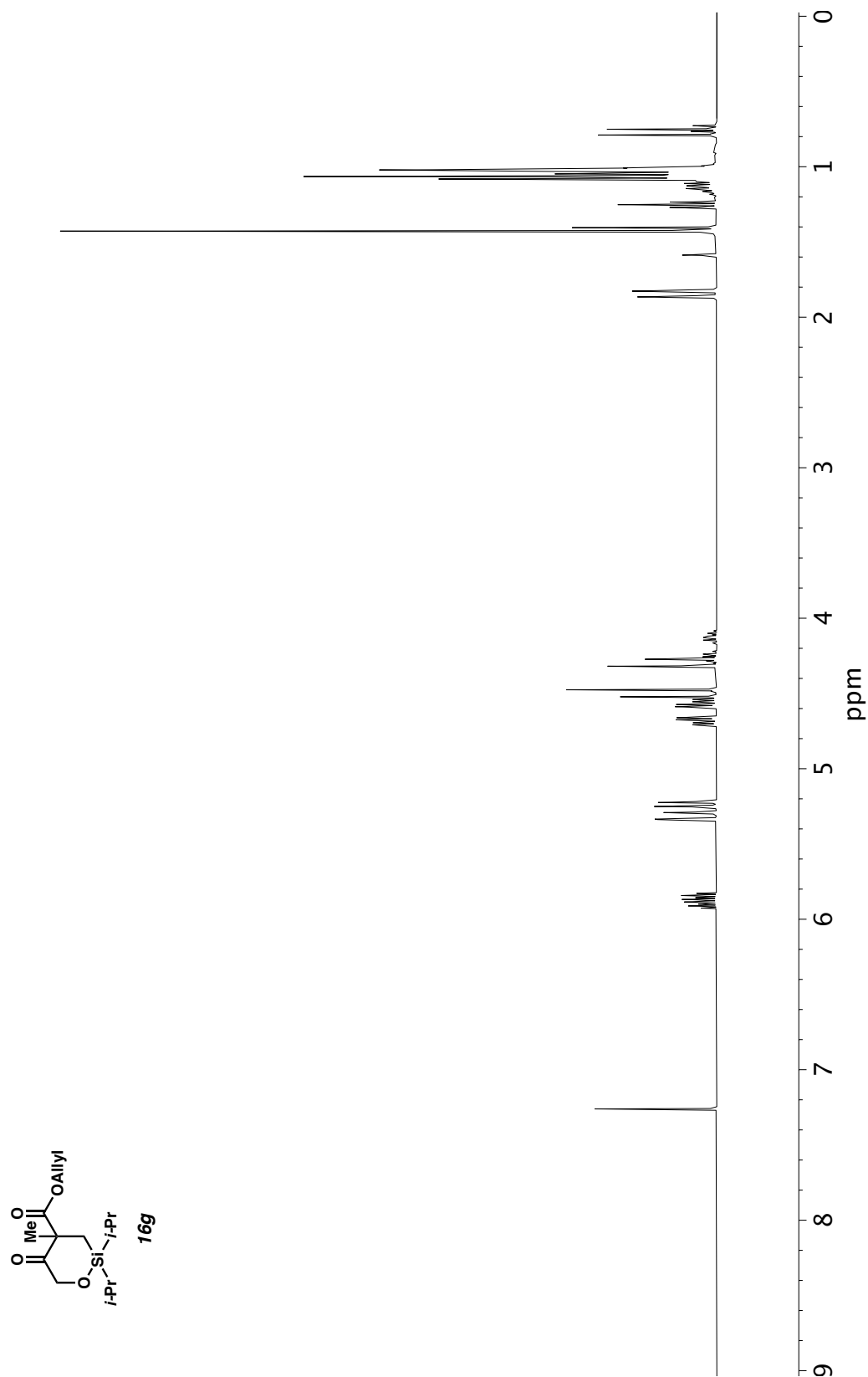


Figure A3.29 ^1H NMR (400 MHz, CDCl_3) of compound **16g**:

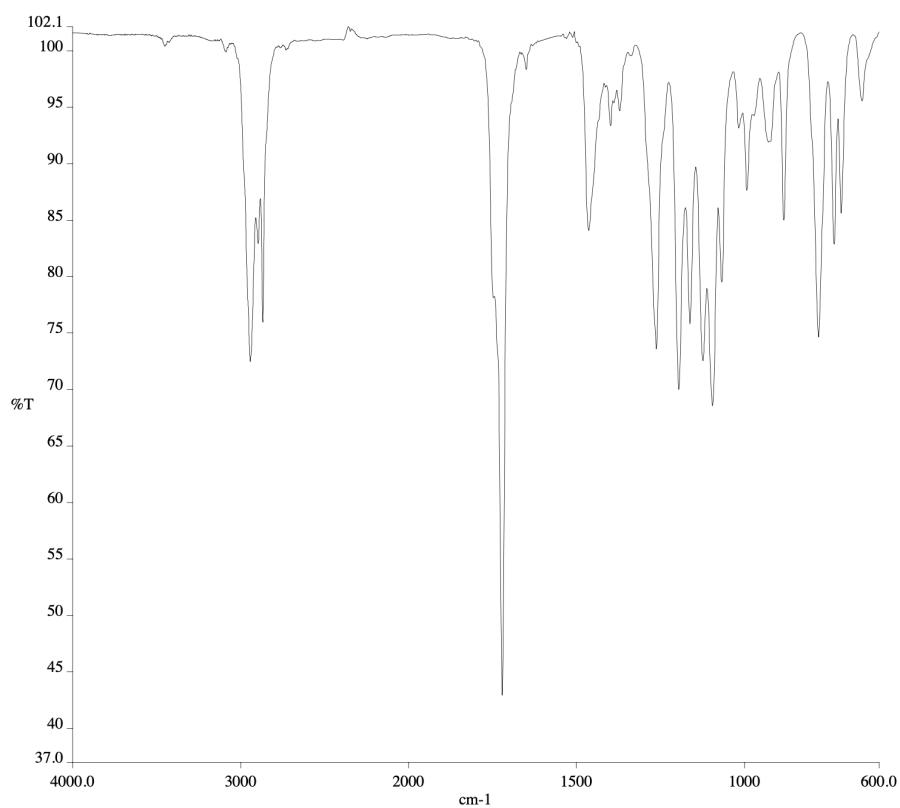


Figure A3.30 Infrared spectrum (Thin Film, NaCl) of compound **16g**.

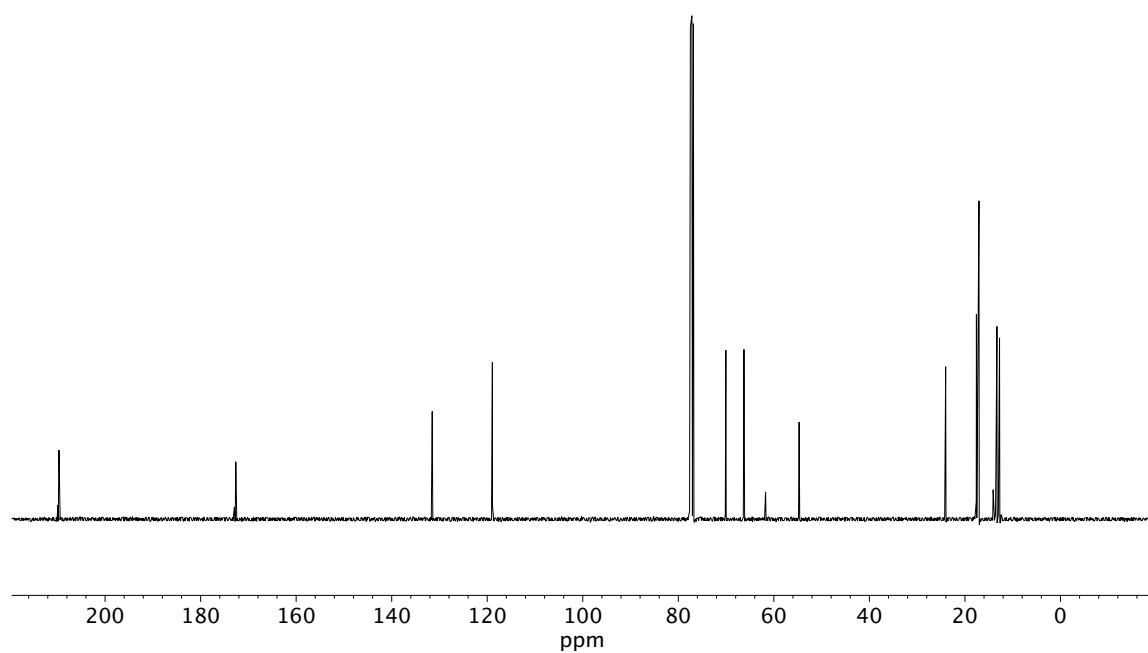


Figure A3.31 ¹³C NMR (100 MHz, CDCl₃) of compound **16g**.

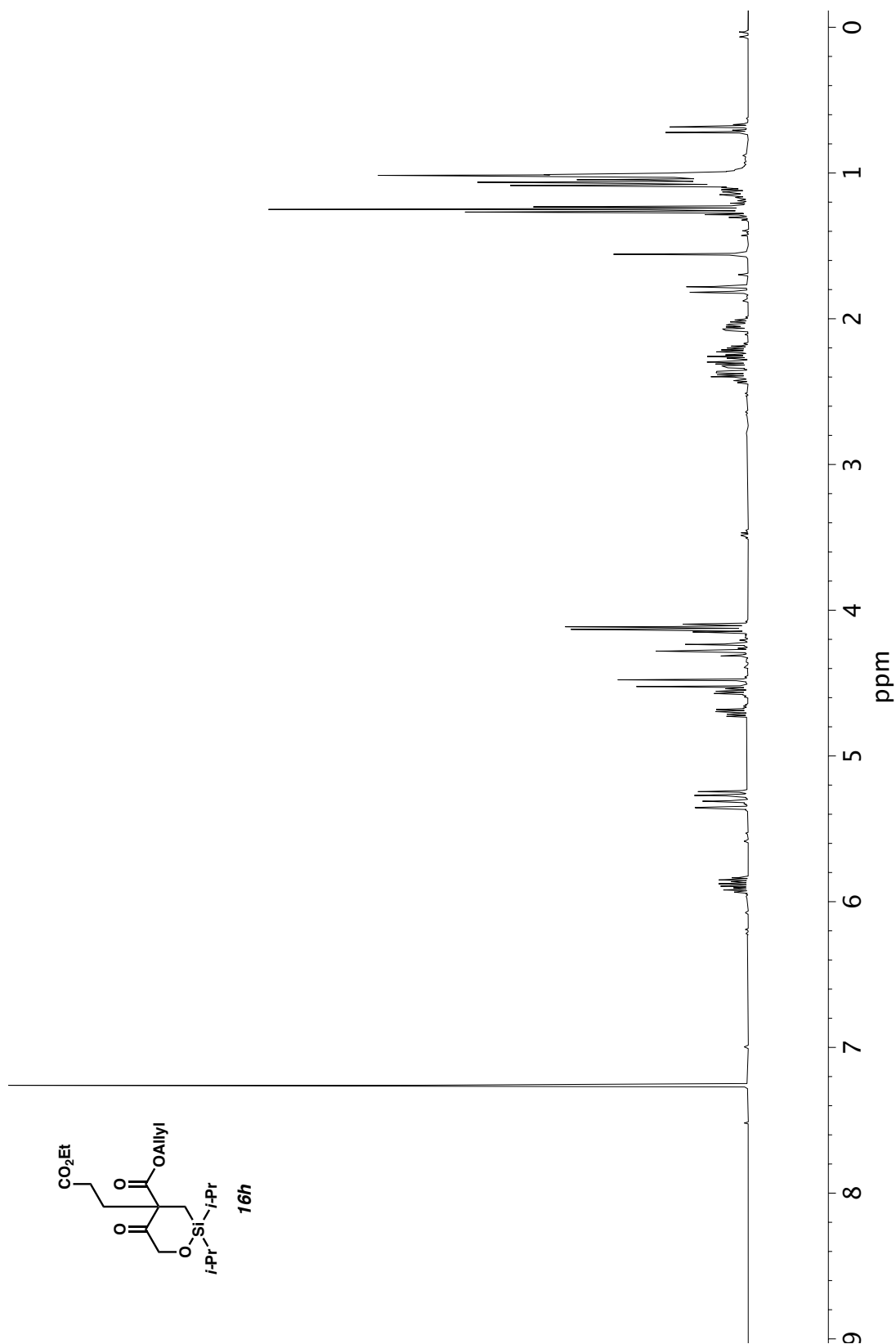


Figure A3.32 ^1H NMR (400 MHz, CDCl_3) of compound **16h**.

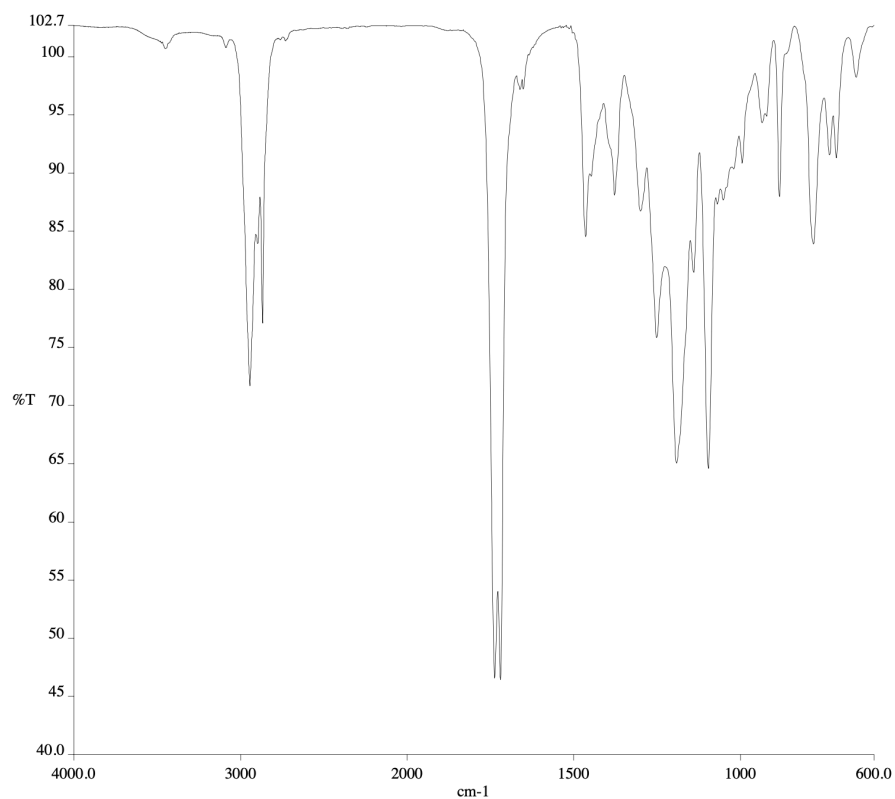


Figure A3.33 Infrared spectrum (Thin Film, NaCl) of compound **16h**.

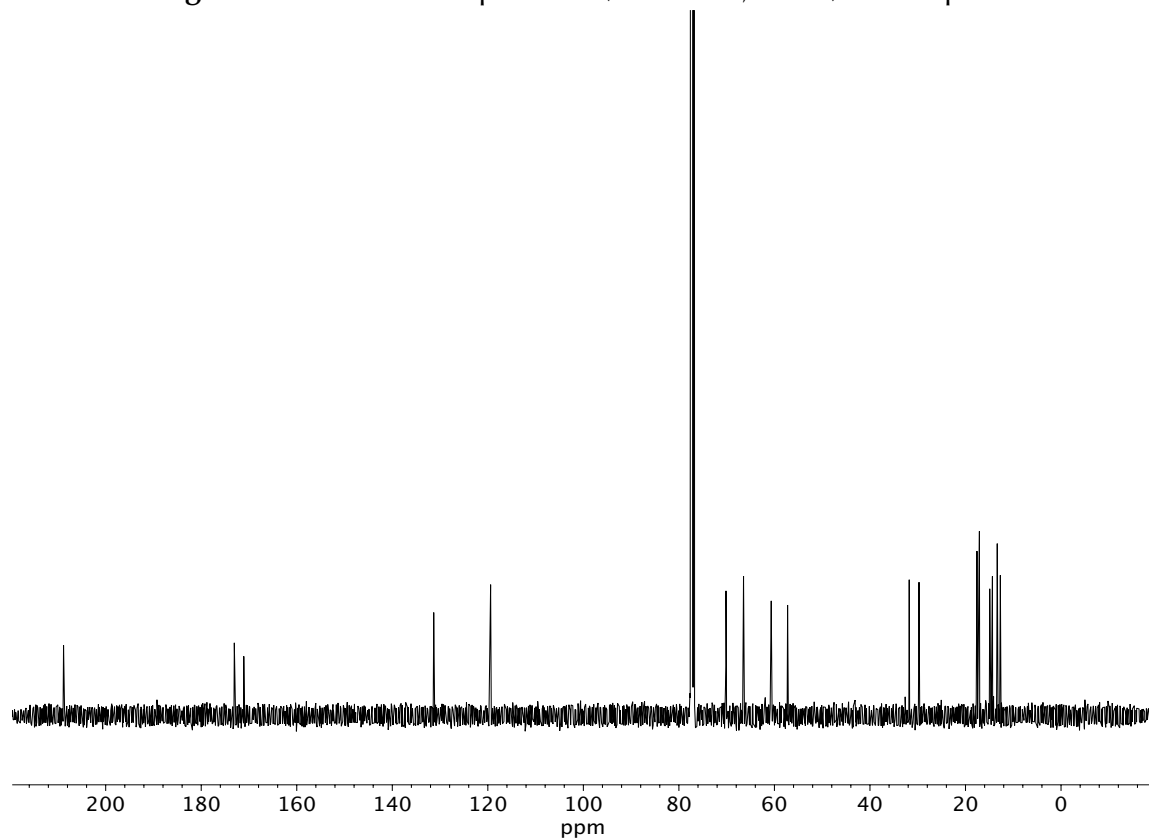


Figure A3.34 ¹³C NMR (100 MHz, CDCl₃) of compound **16h**.

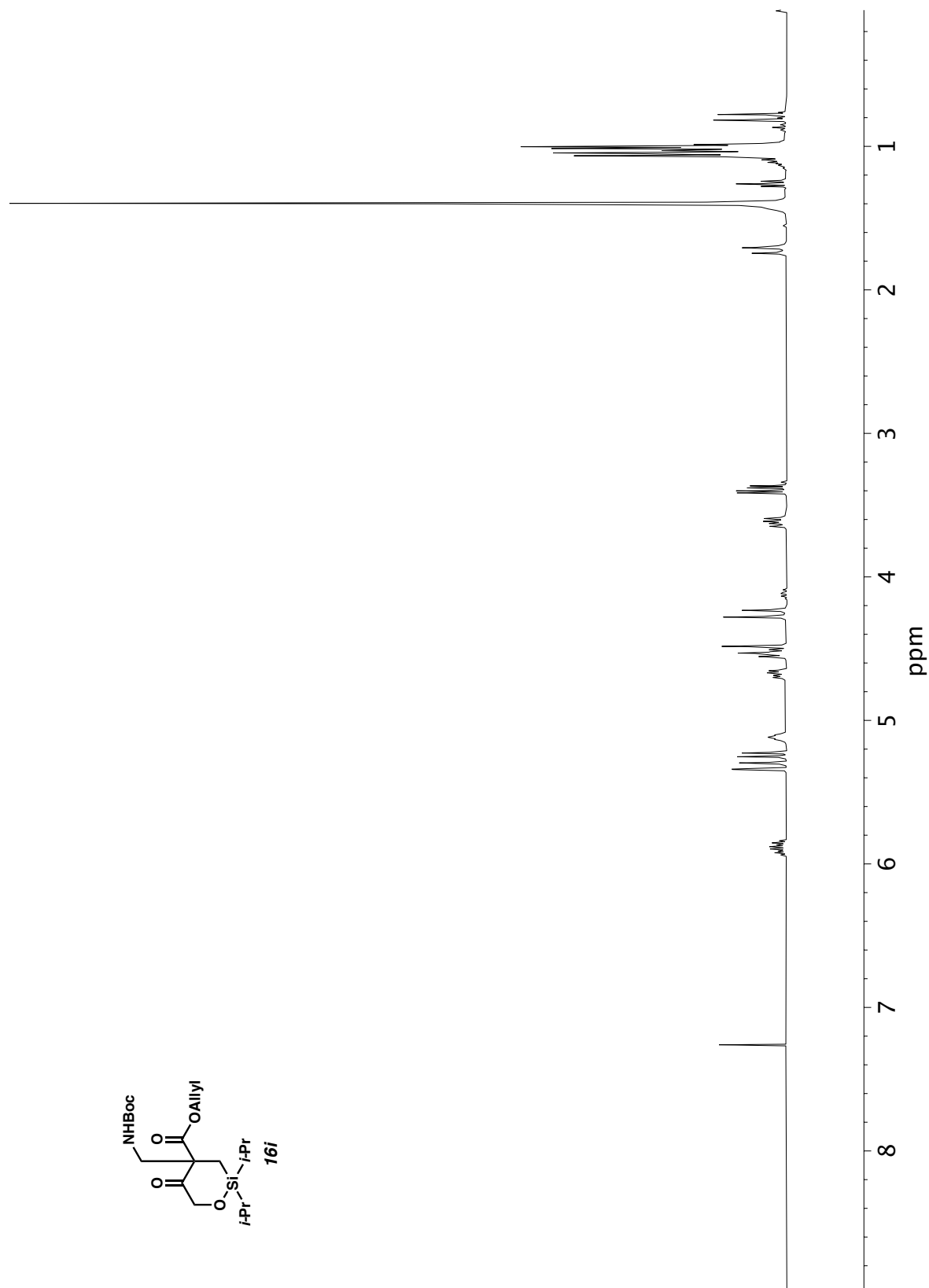


Figure A3.35 ^1H NMR (400 MHz, CDCl_3) of compound **16i**.

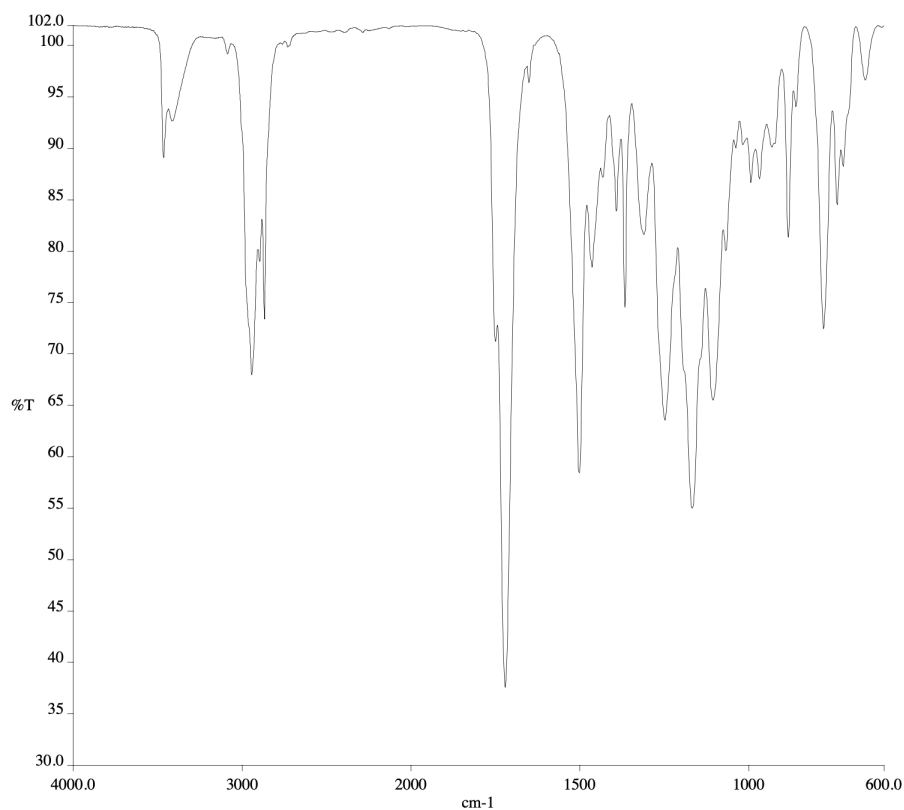


Figure A3.36 Infrared spectrum (Thin Film, NaCl) of compound **16i**.

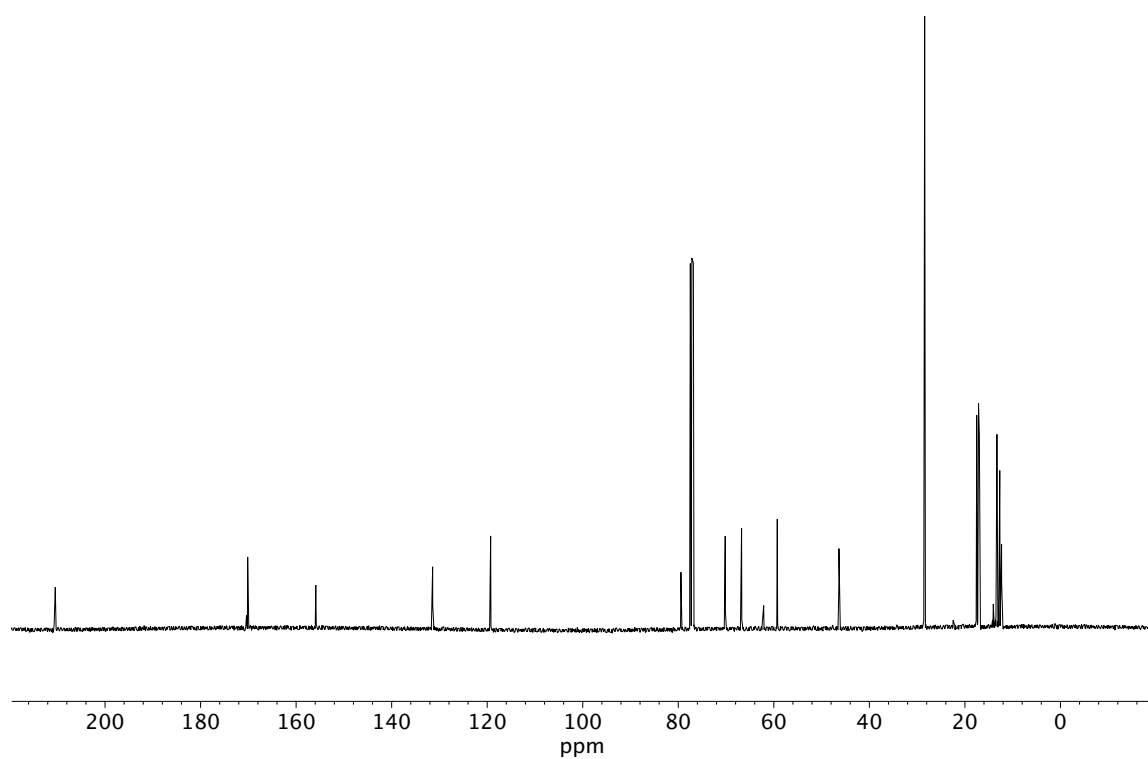


Figure A3.37 ^{13}C NMR (100 MHz, CDCl_3) of compound **16i**.

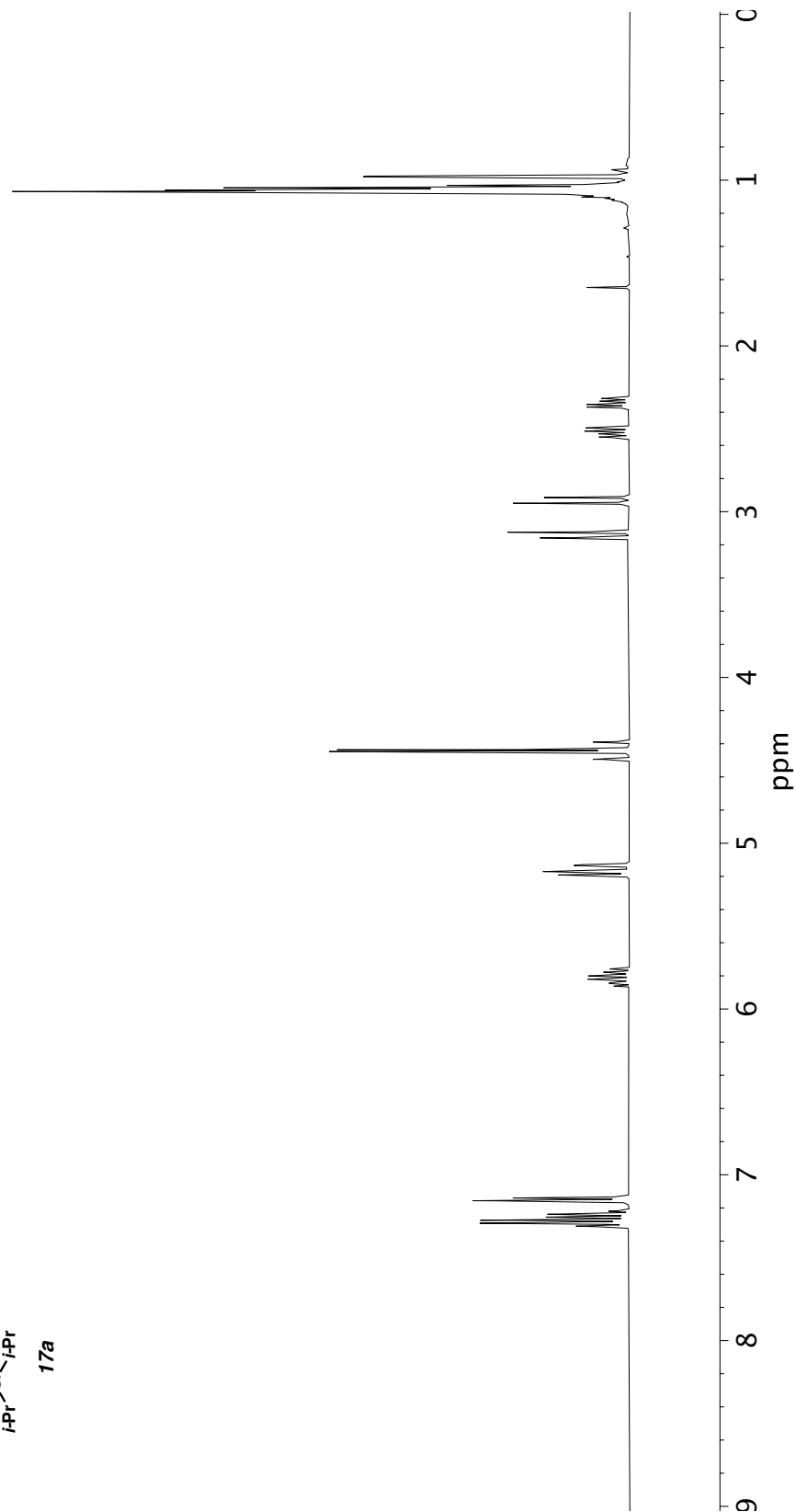
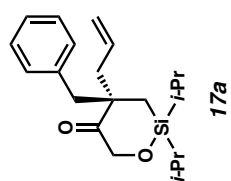


Figure A3.38 ^1H NMR (400 MHz, CDCl_3) of compound **17a**.

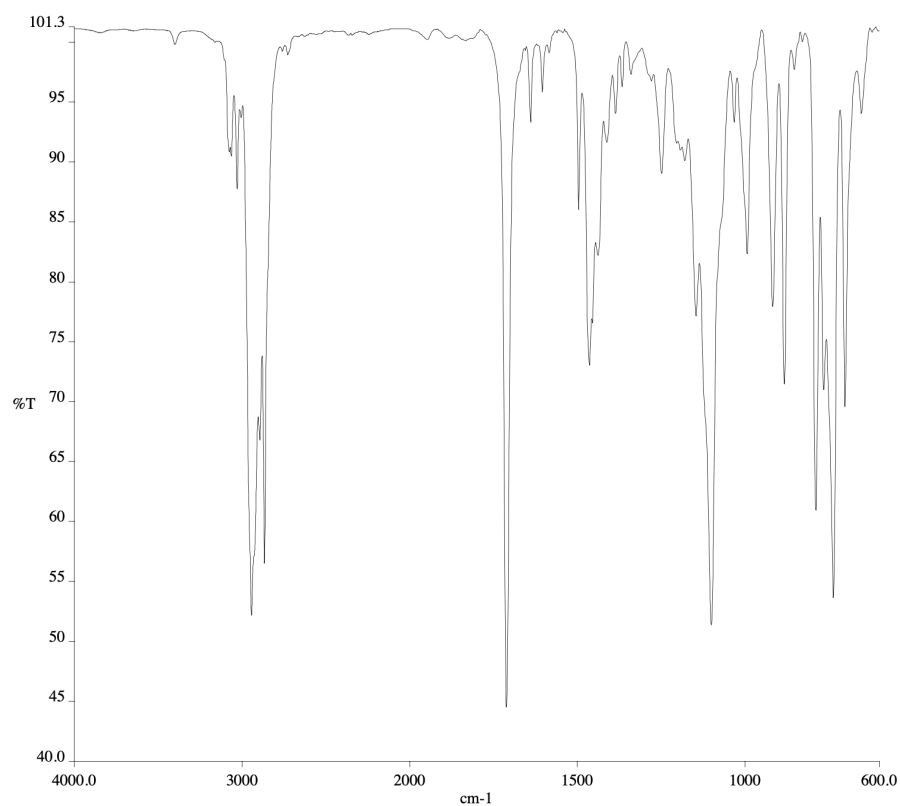


Figure A3.39 Infrared spectrum (Thin Film, NaCl) of compound **17a**.

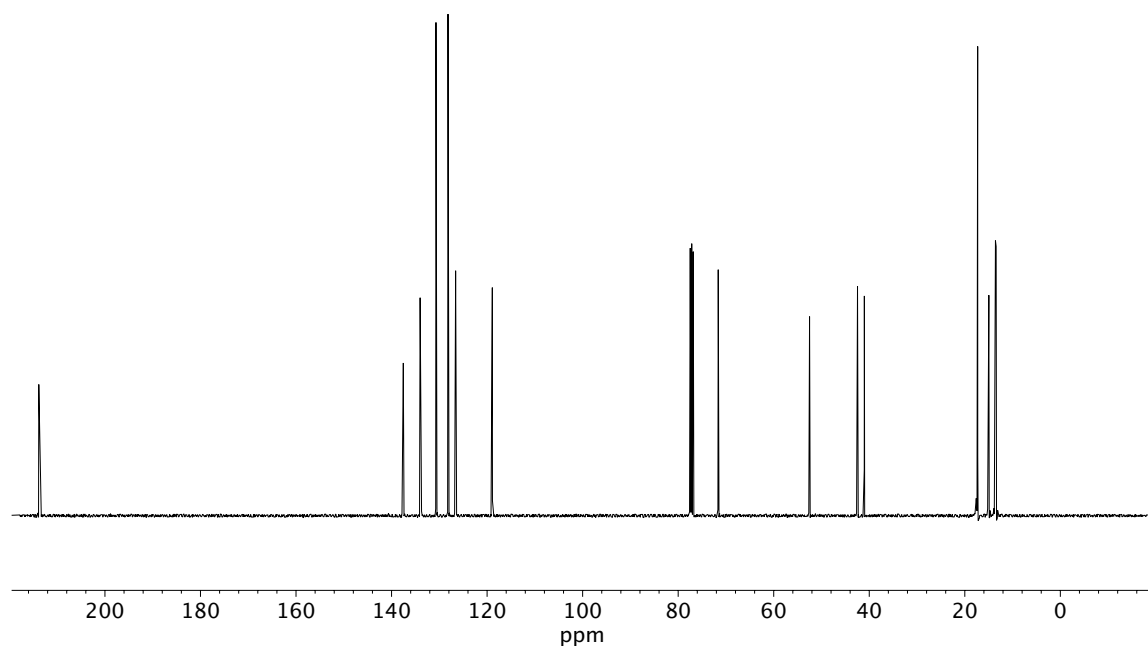


Figure A3.40 ¹³C NMR (100 MHz, CDCl₃) of compound **17a**.

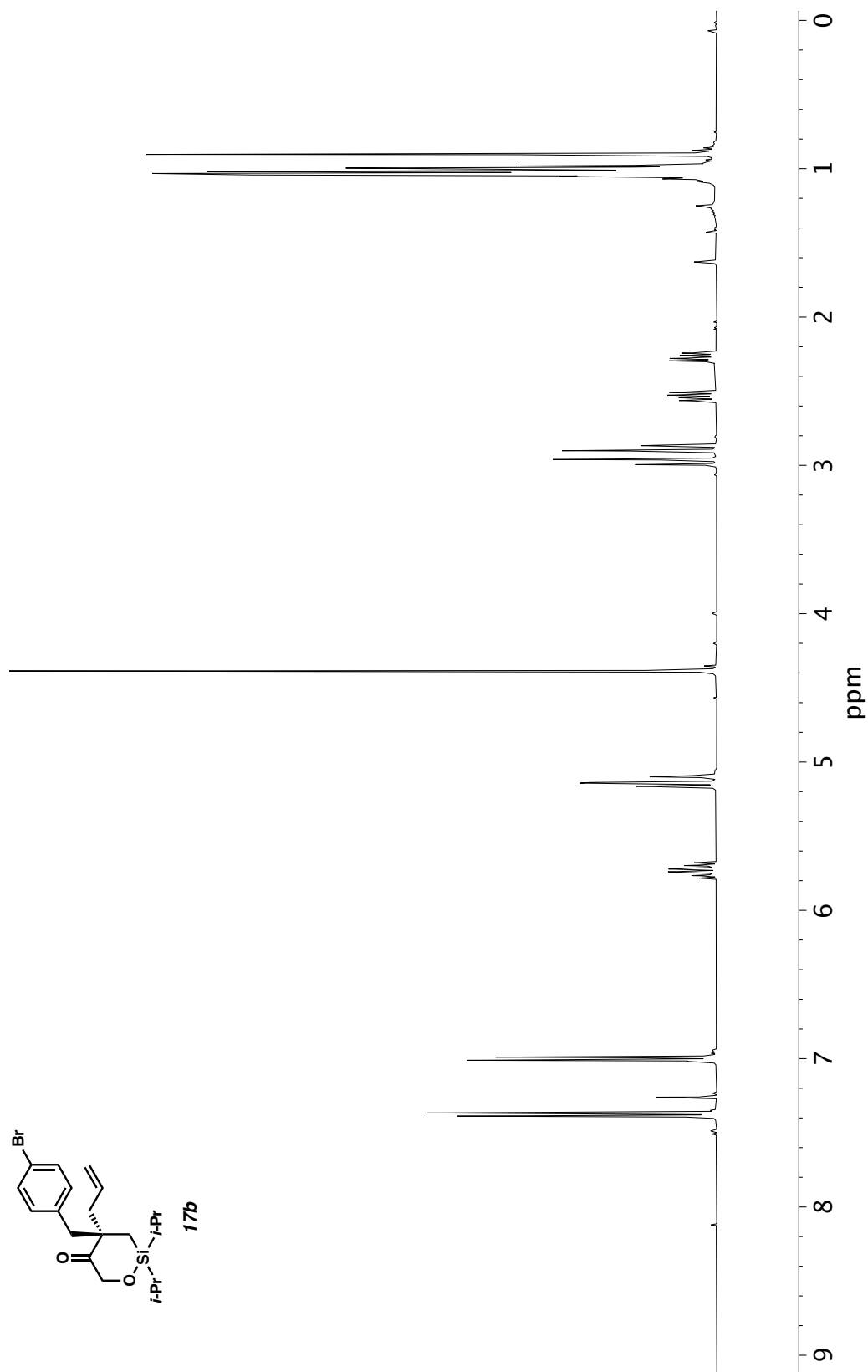


Figure A3.41 ^1H NMR (400 MHz, CDCl_3) of compound **17b**.

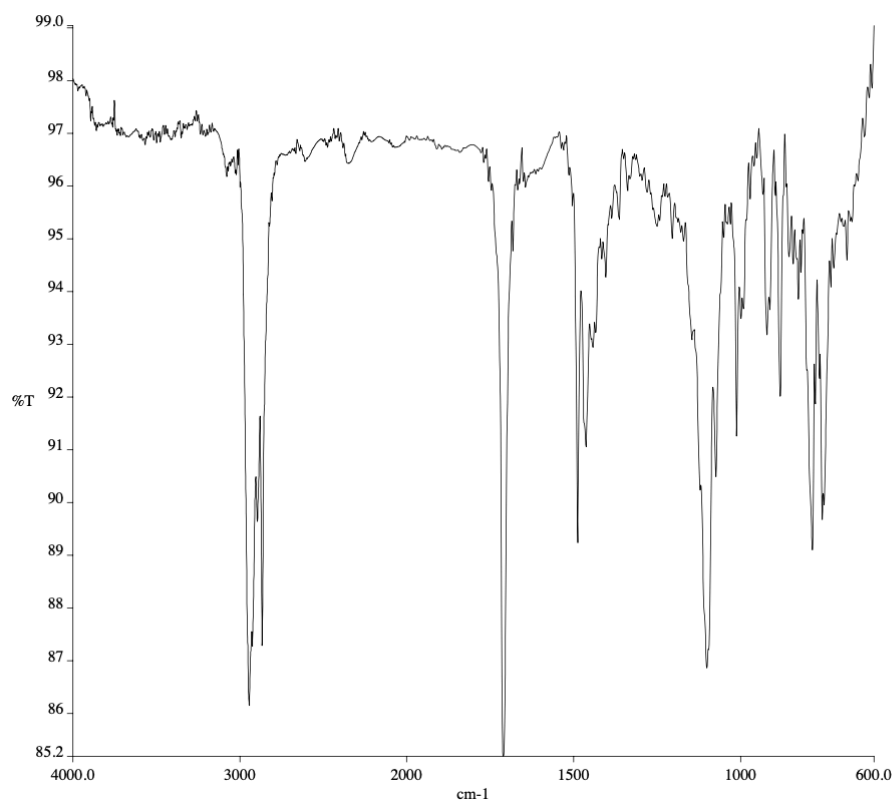


Figure A3.42 Infrared spectrum (Thin Film, NaCl) of compound **17b**.

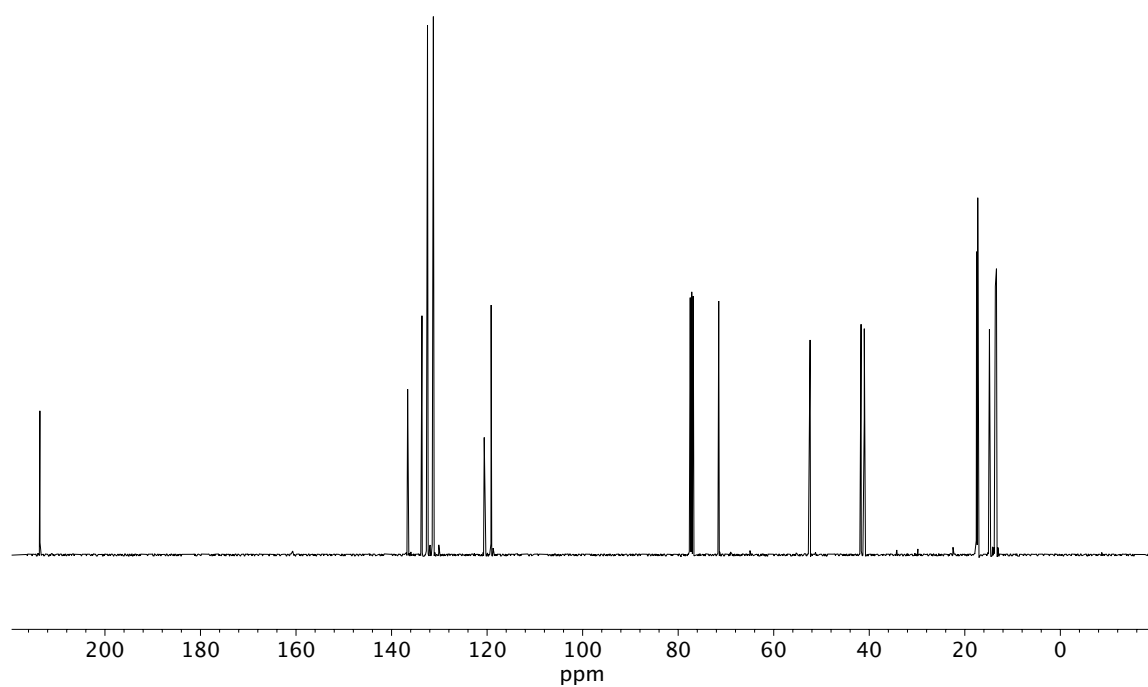


Figure A3.43 ¹³C NMR (100 MHz, CDCl₃) of compound **17b**.

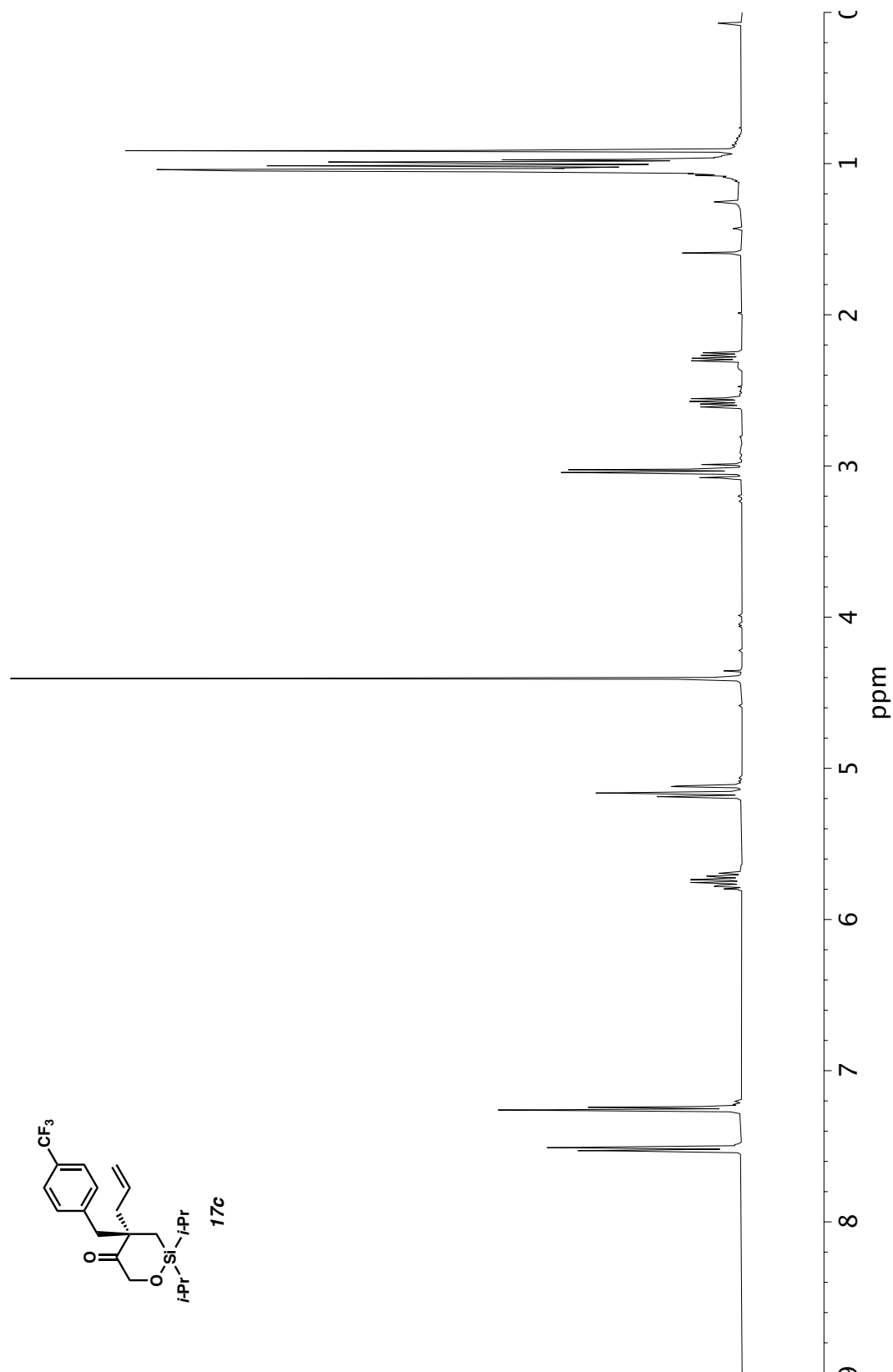


Figure A3.44 ^1H NMR (400 MHz, CDCl_3) of compound **17c**.

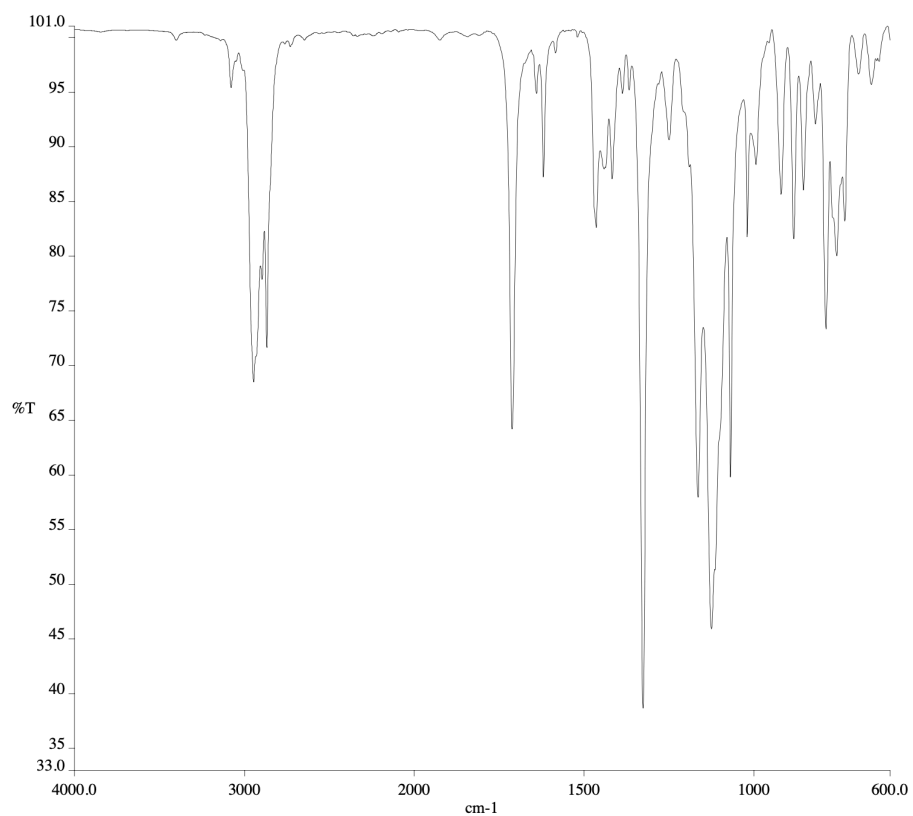


Figure A3.45 Infrared spectrum (Thin Film, NaCl) of compound **17c**.

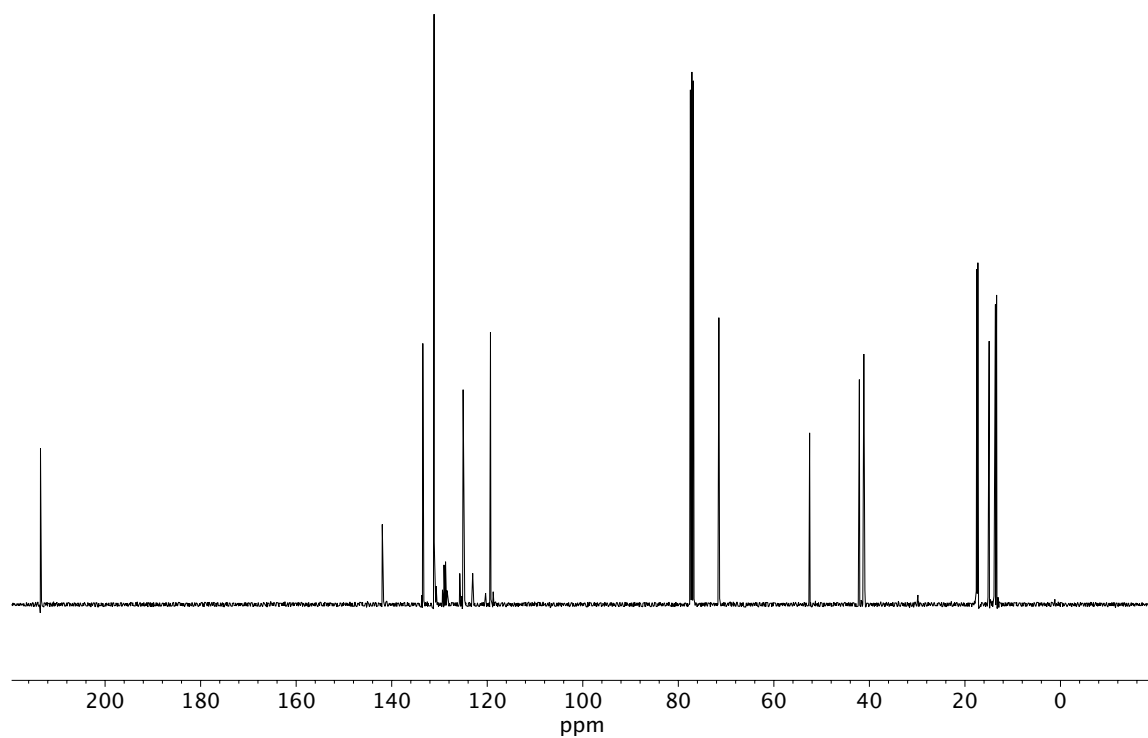


Figure A3.46 ¹³C NMR (100 MHz, CDCl₃) of compound **17c**.

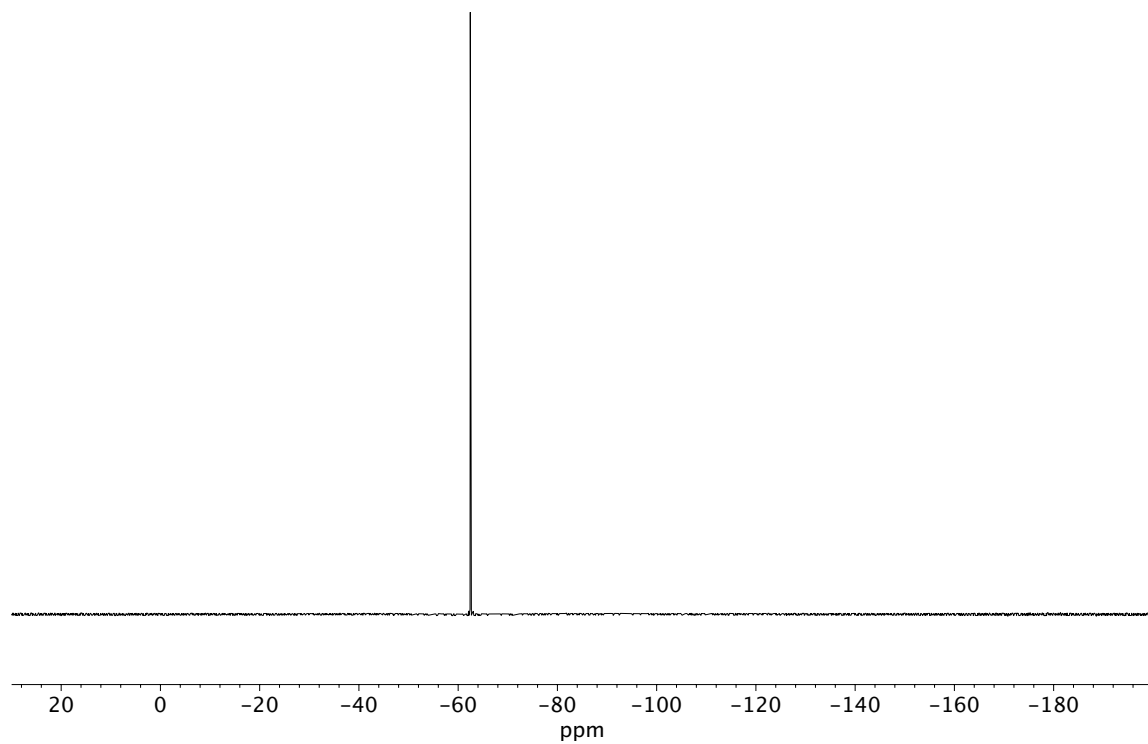


Figure A3.47 ^{19}F NMR (282 MHz, CDCl_3) of compound **17c**.

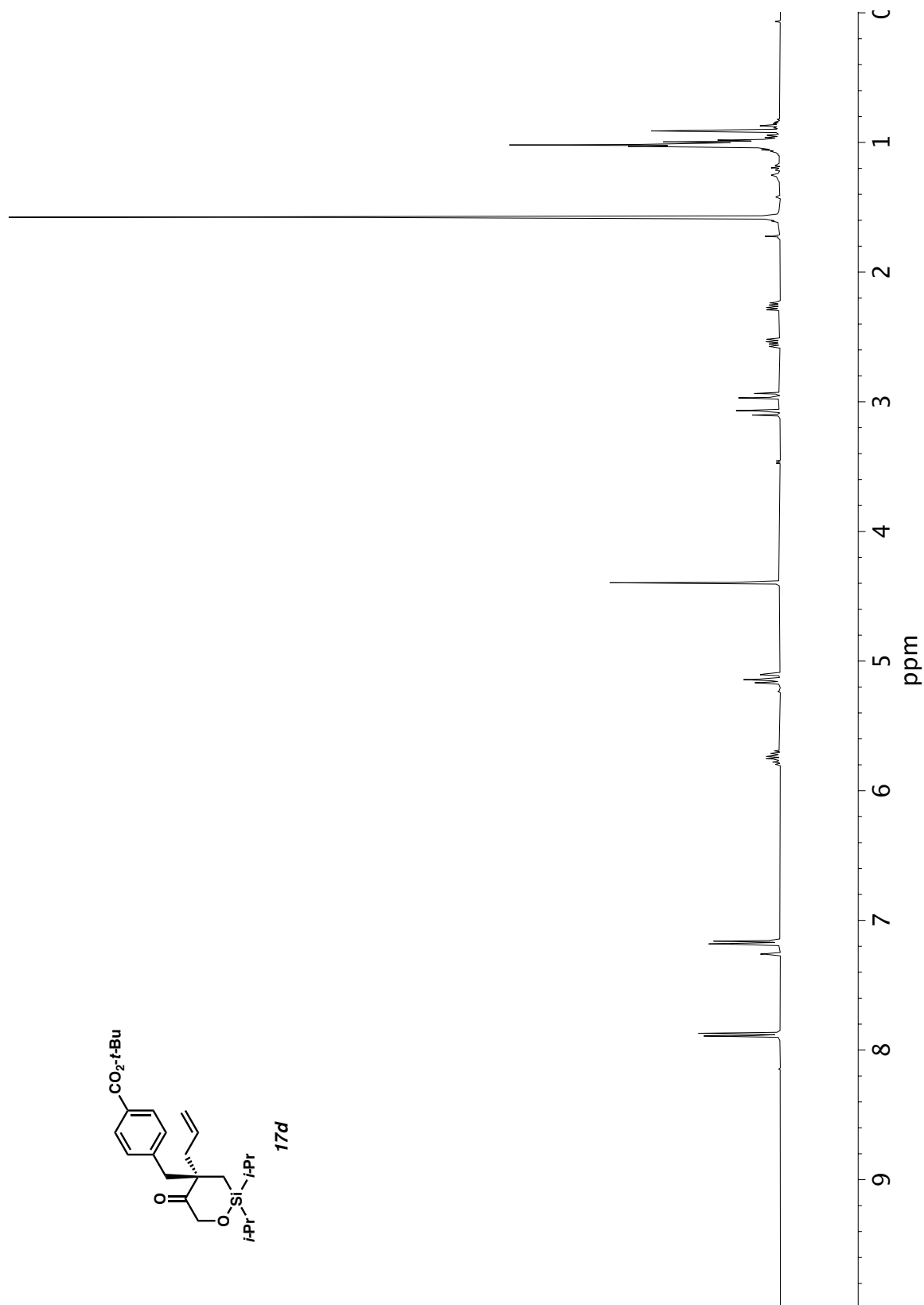


Figure A3.48 ¹H NMR (400 MHz, CDCl₃) of compound **17d**.

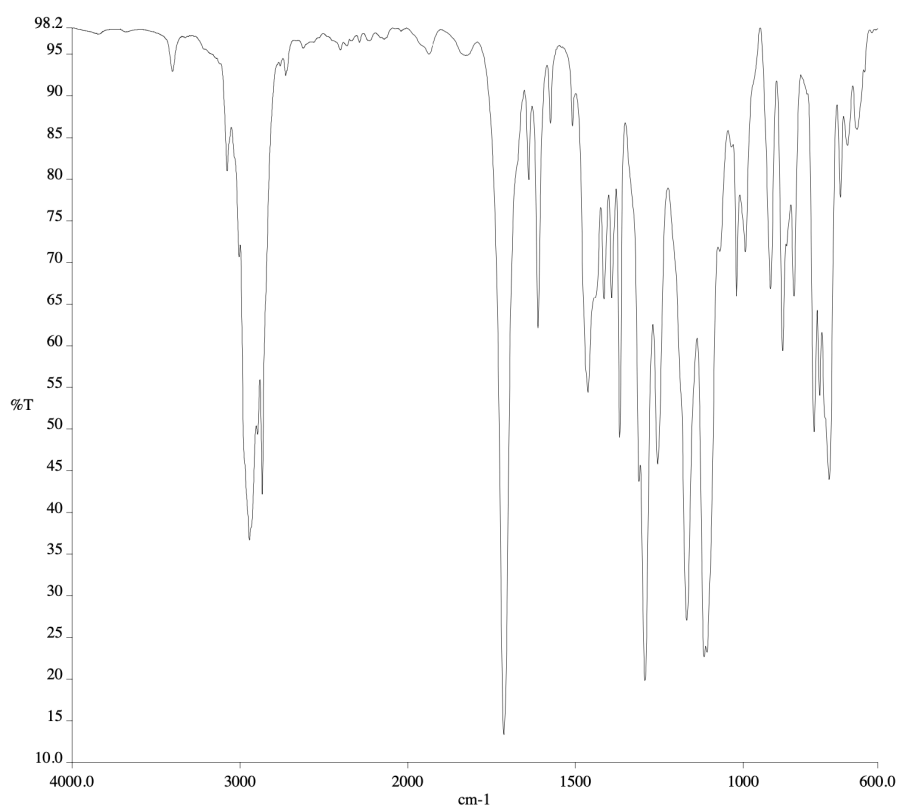


Figure A3.49 Infrared spectrum (Thin Film, NaCl) of compound **17d**.

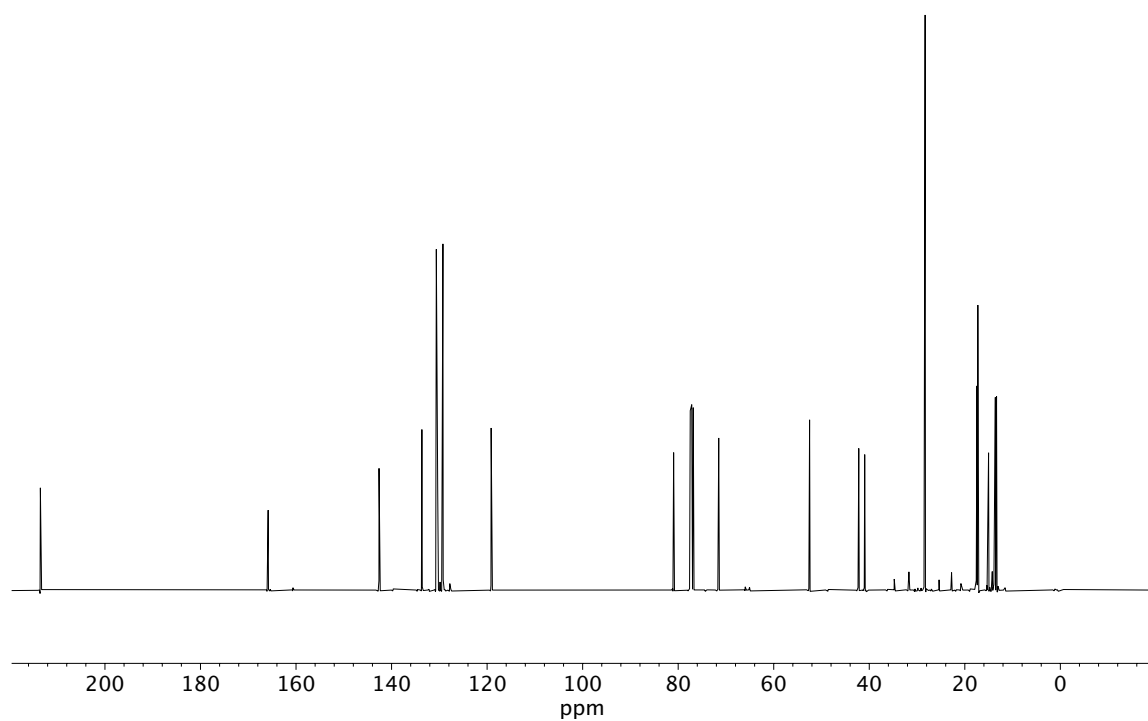


Figure A3.50 ¹³C NMR (100 MHz, CDCl₃) of compound **17d**.

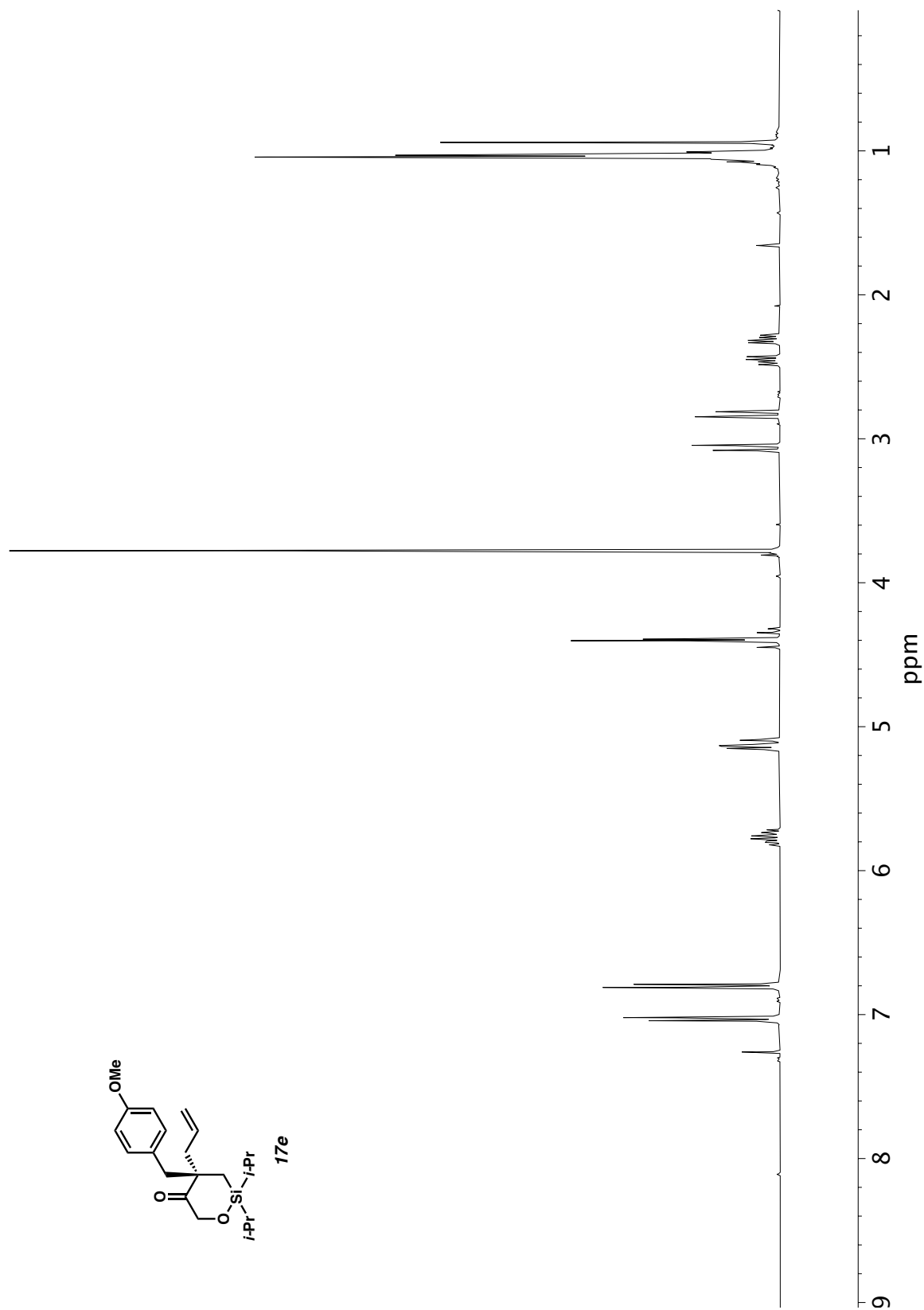


Figure A3.51 ^1H NMR (400 MHz, CDCl_3) of compound **17e**.

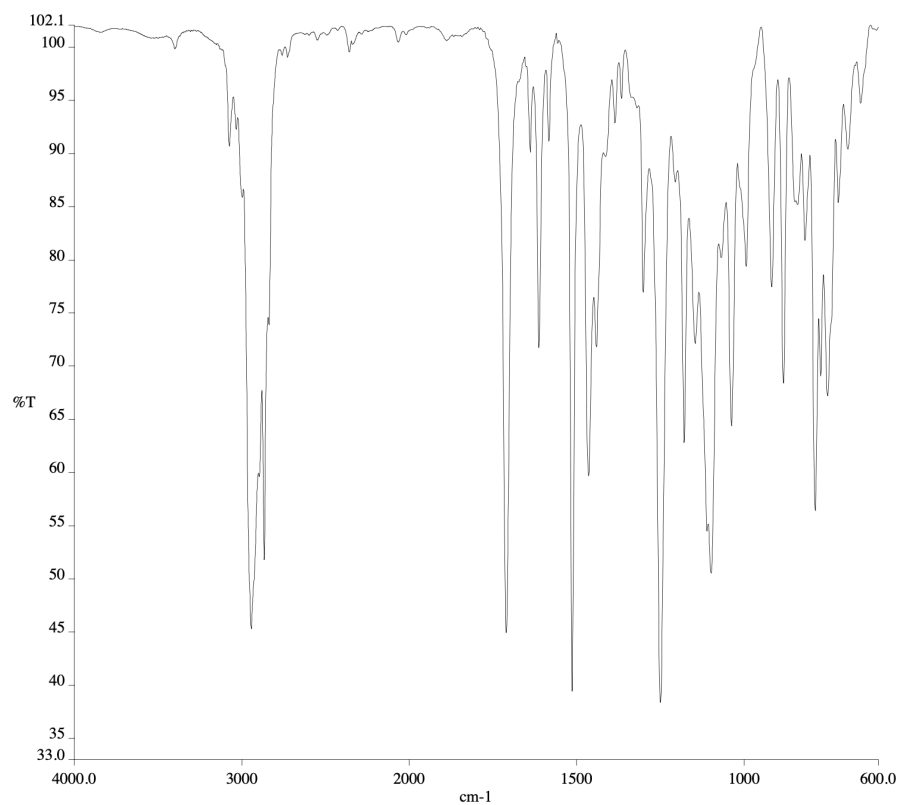


Figure A3.52 Infrared spectrum (Thin Film, NaCl) of compound **17e**.

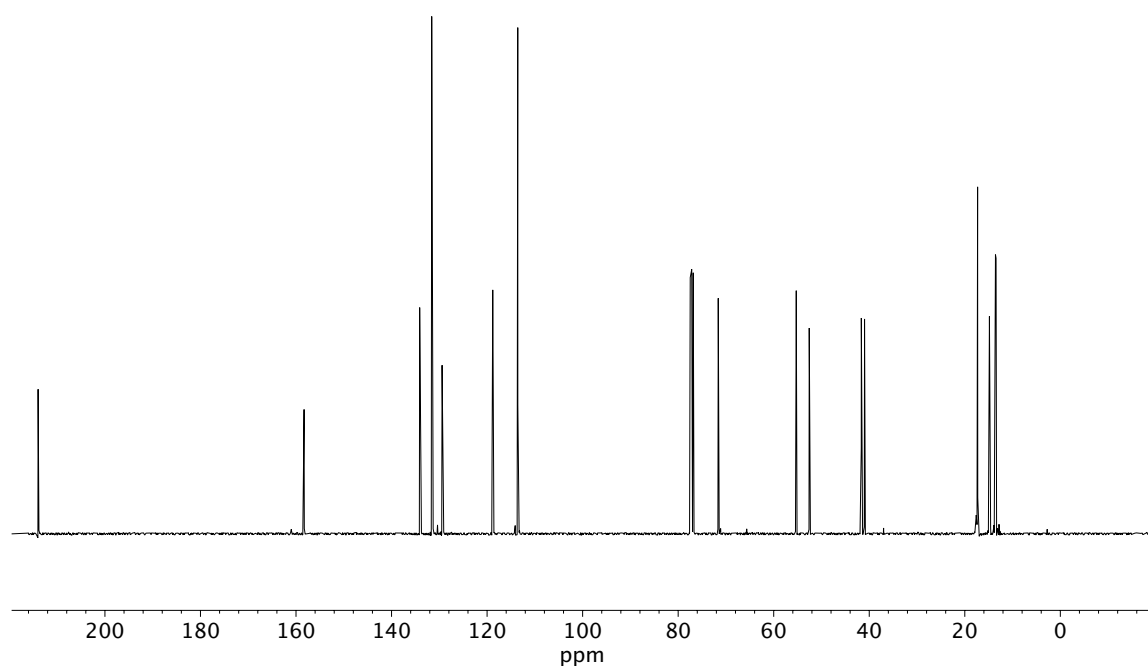


Figure A3.53 ¹³C NMR (100 MHz, CDCl₃) of compound **17e**.

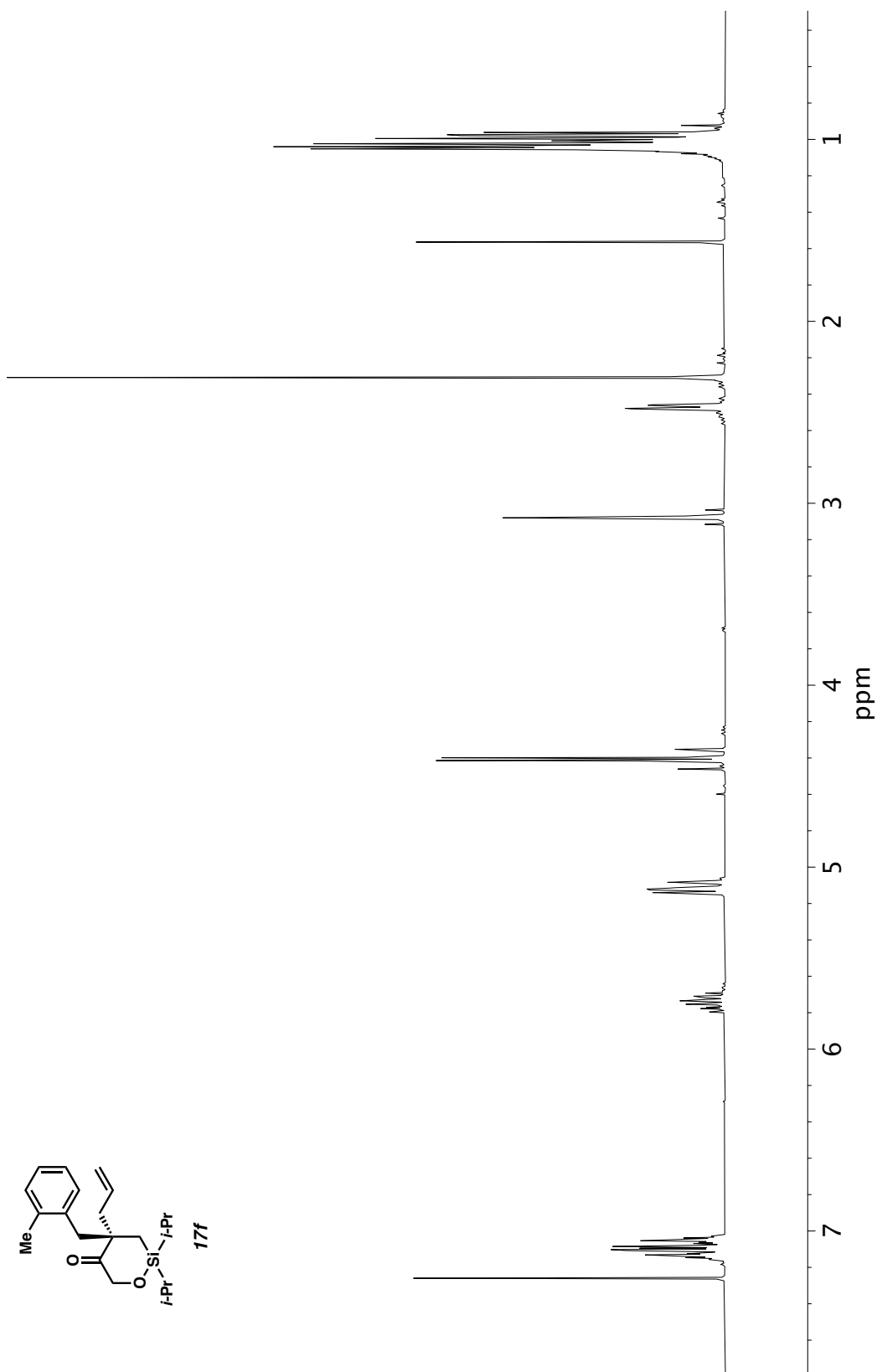


Figure A3.54 ^1H NMR (400 MHz, CDCl_3) of compound **17f**.

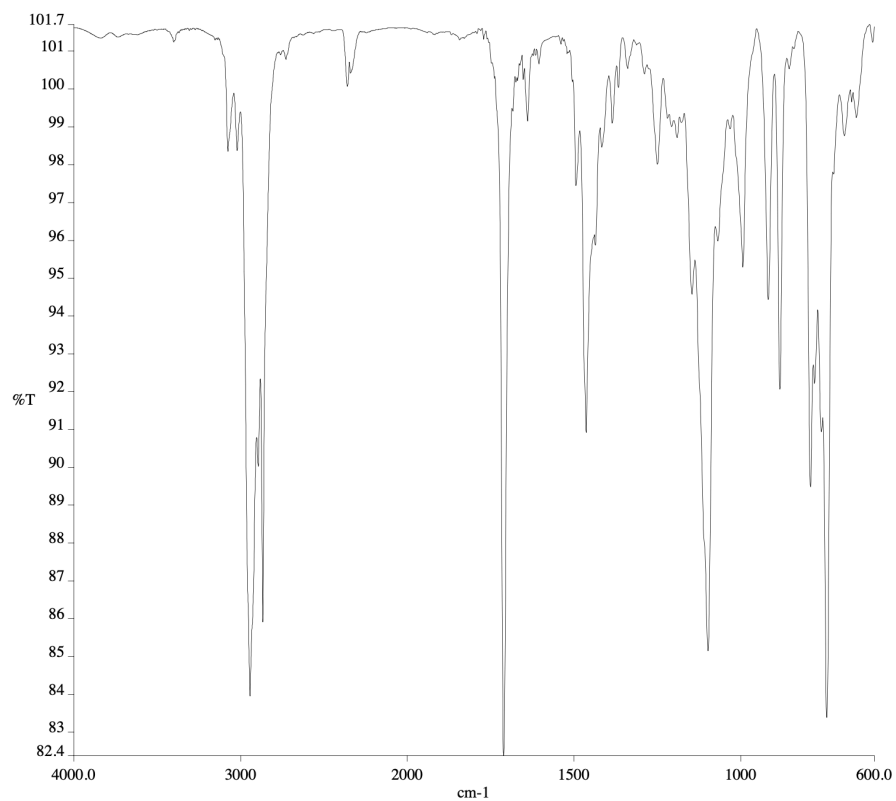


Figure A3.55 Infrared spectrum (Thin Film, NaCl) of compound **17f**.

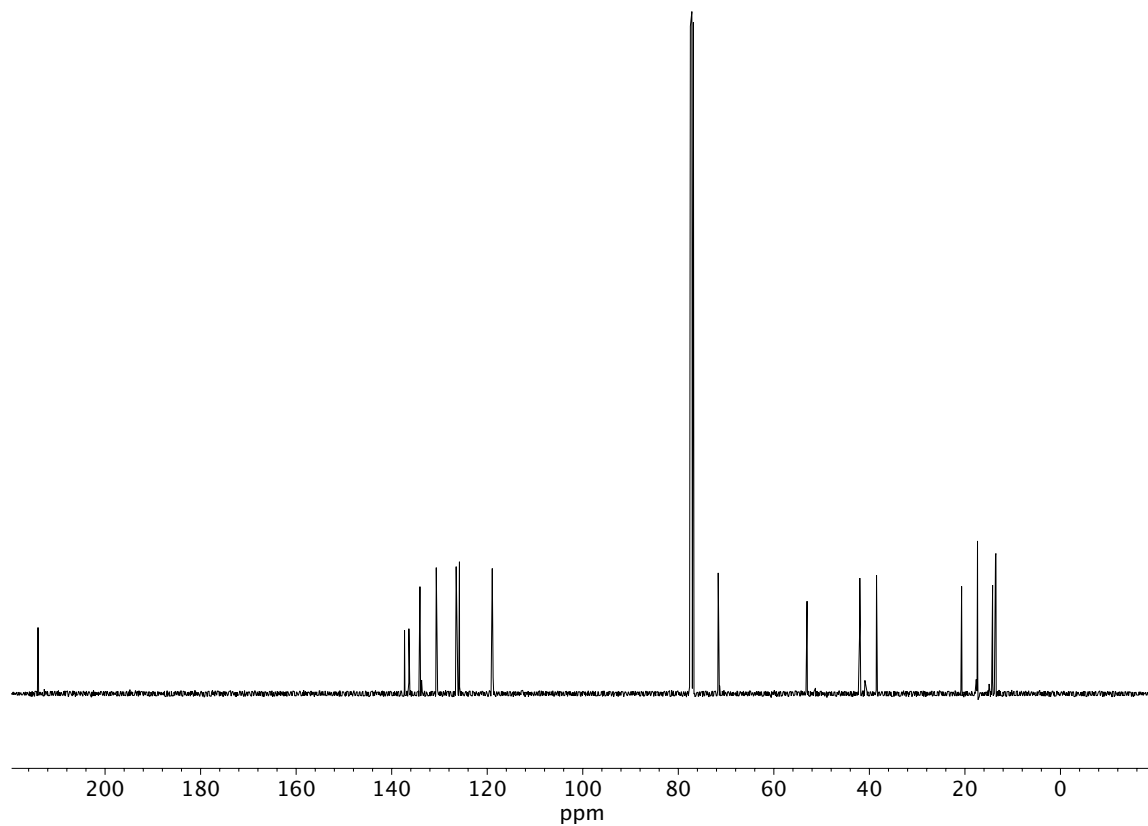


Figure A3.56 ¹³C NMR (100 MHz, CDCl₃) of compound **17f**.

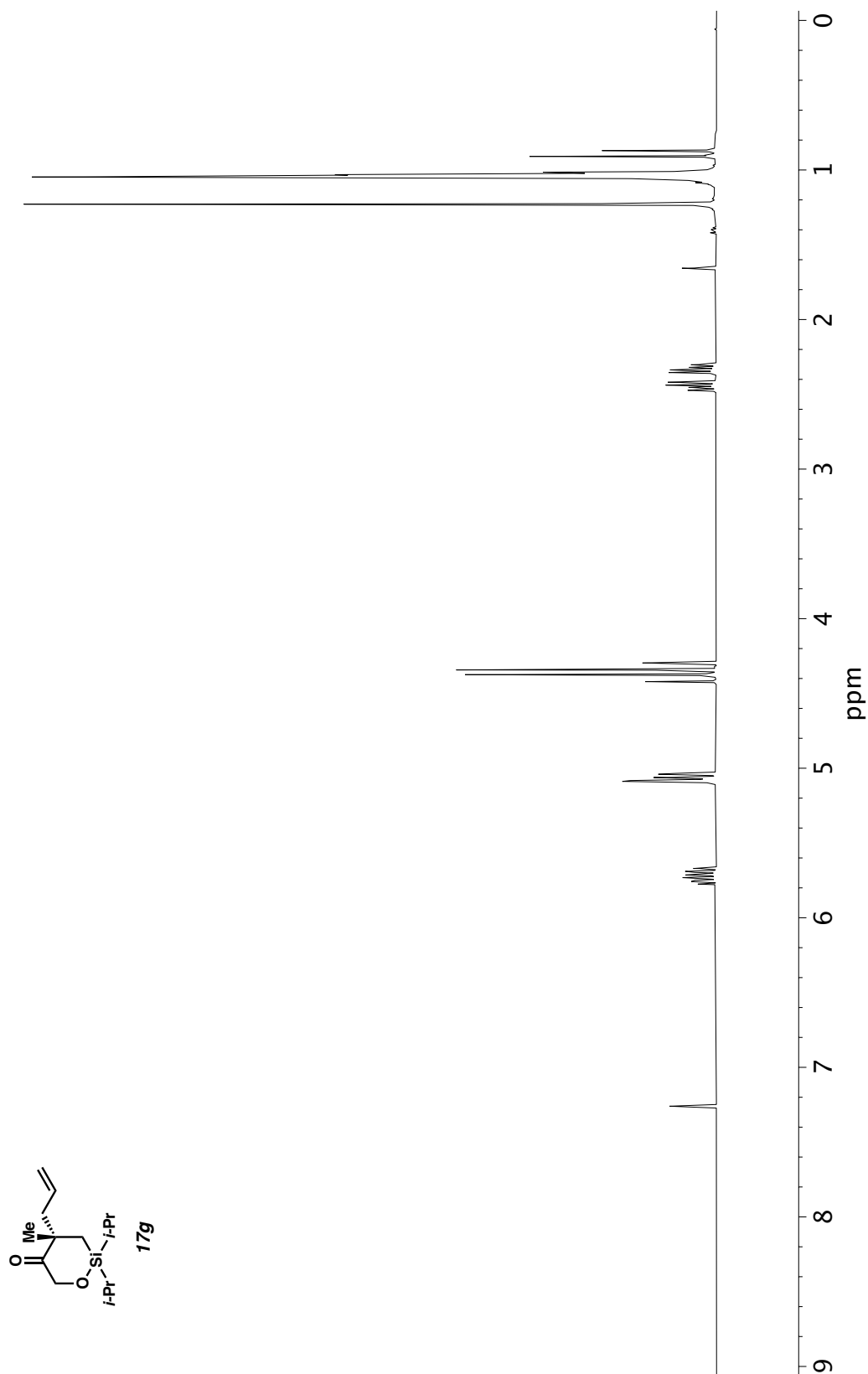


Figure A3.57 ^1H NMR (400 MHz, CDCl_3) of compound **17g**.

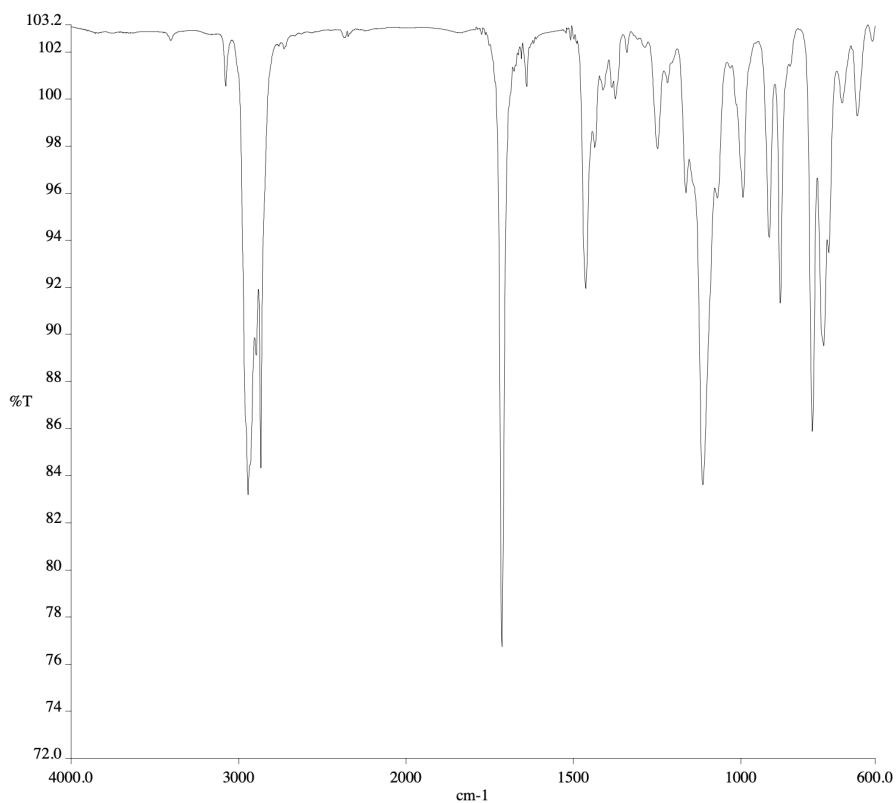


Figure A3.58 Infrared spectrum (Thin Film, NaCl) of compound **17g**.

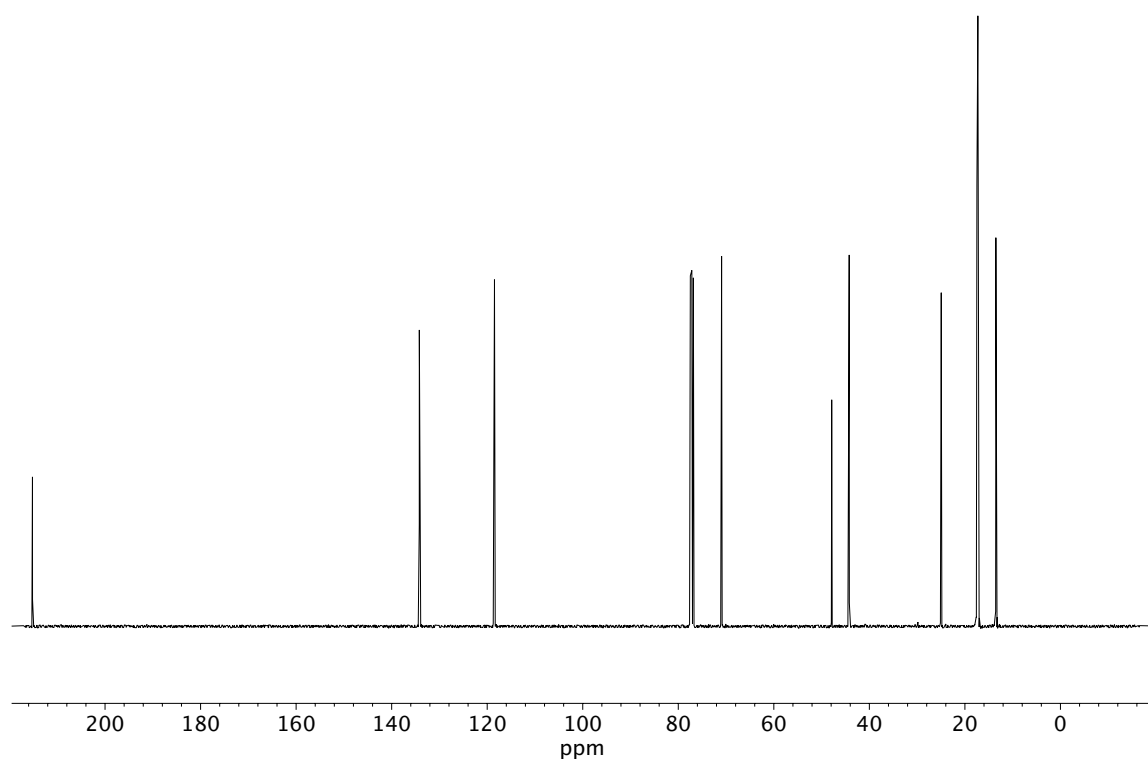


Figure A3.59 ¹³C NMR (100 MHz, CDCl₃) of compound **17g**.

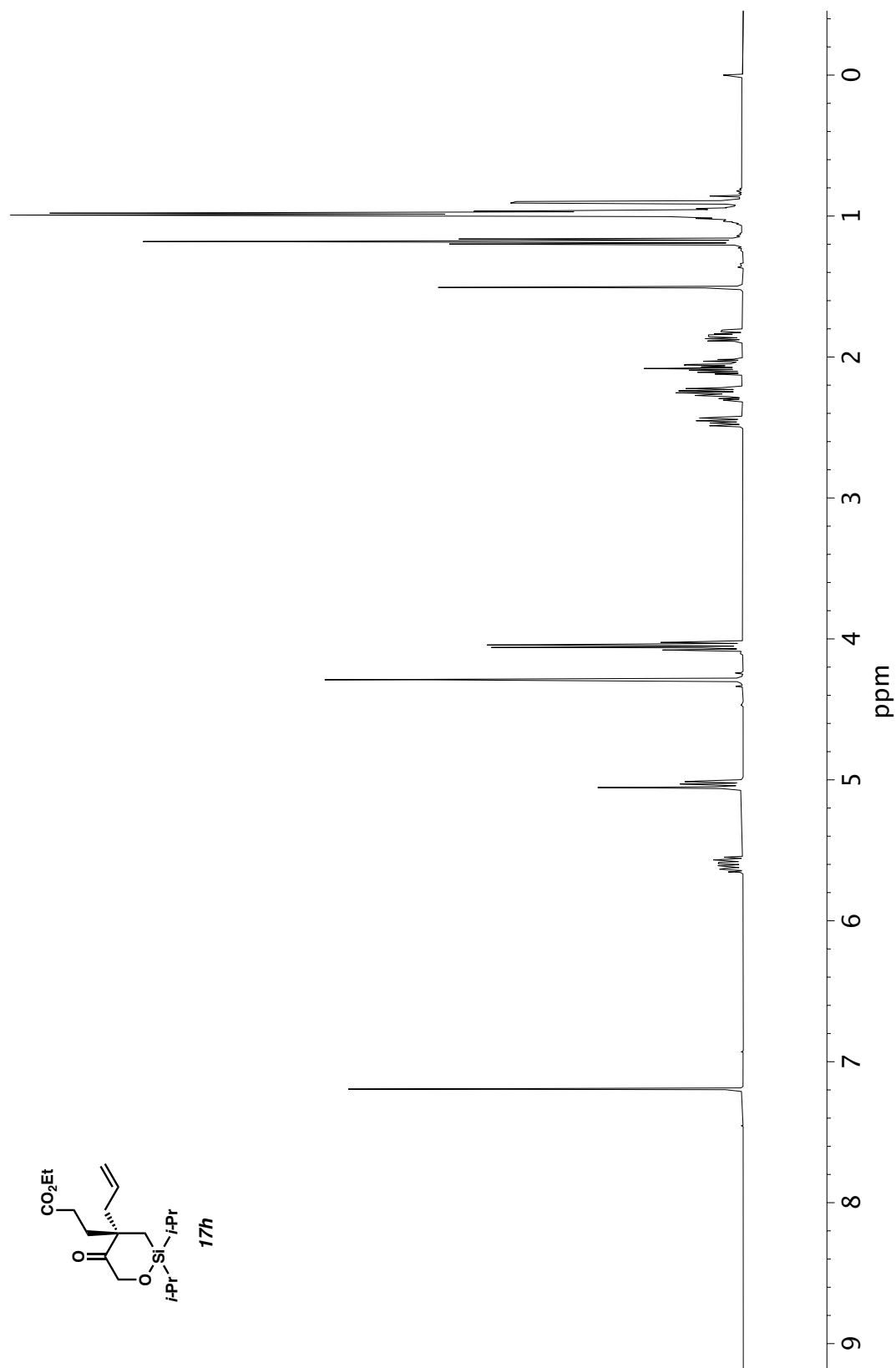


Figure A3.60 ^1H NMR (400 MHz, CDCl_3) of compound **17h**.

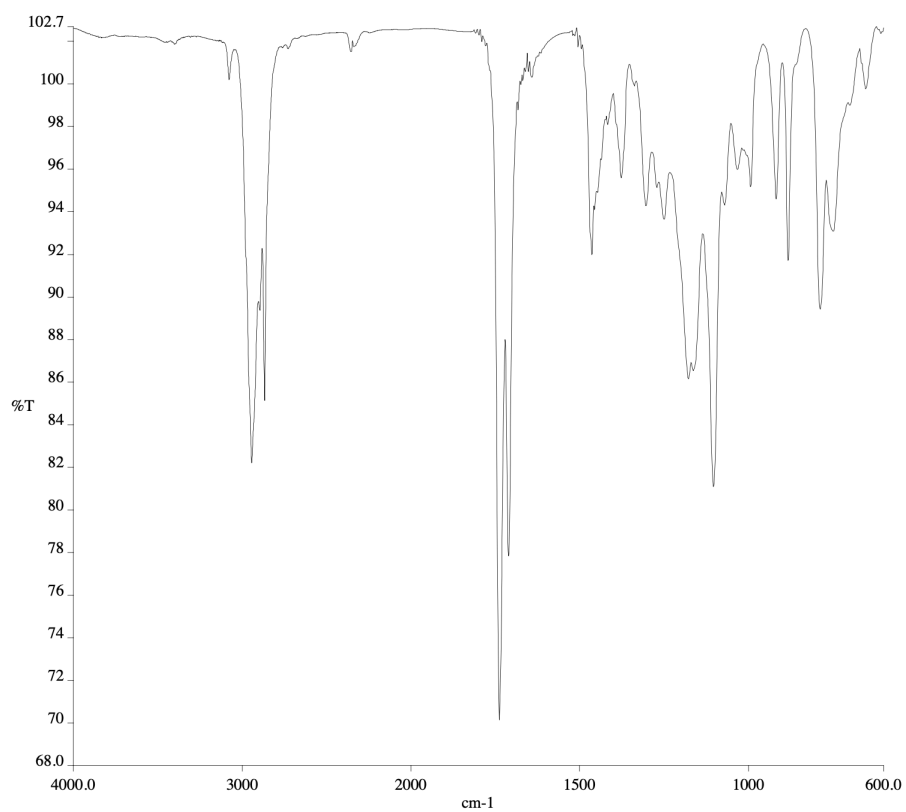


Figure A3.61 Infrared spectrum (Thin Film, NaCl) of compound **17h**.

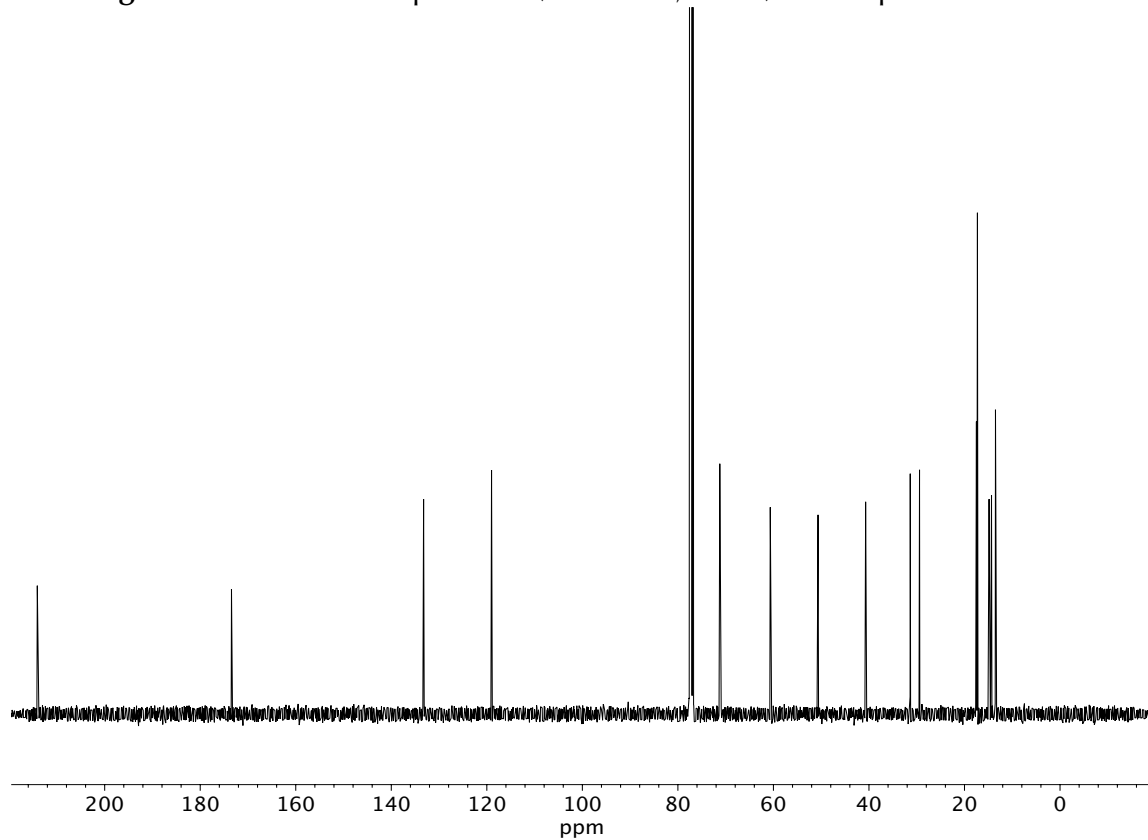


Figure A3.62 ^{13}C NMR (100 MHz, CDCl_3) of compound **17h**.

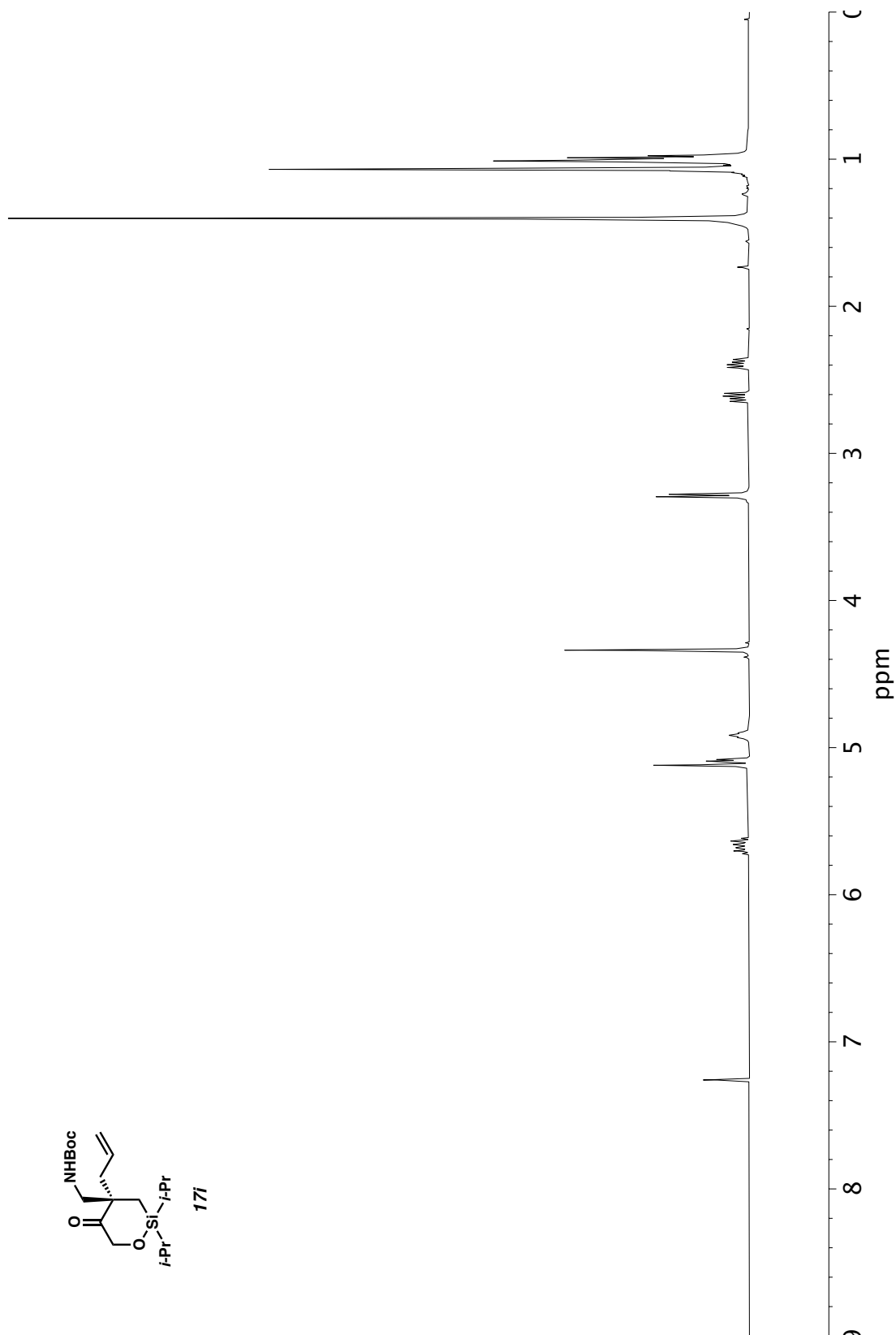


Figure A3.63 ^1H NMR (400 MHz, CDCl_3) of compound **17i**.

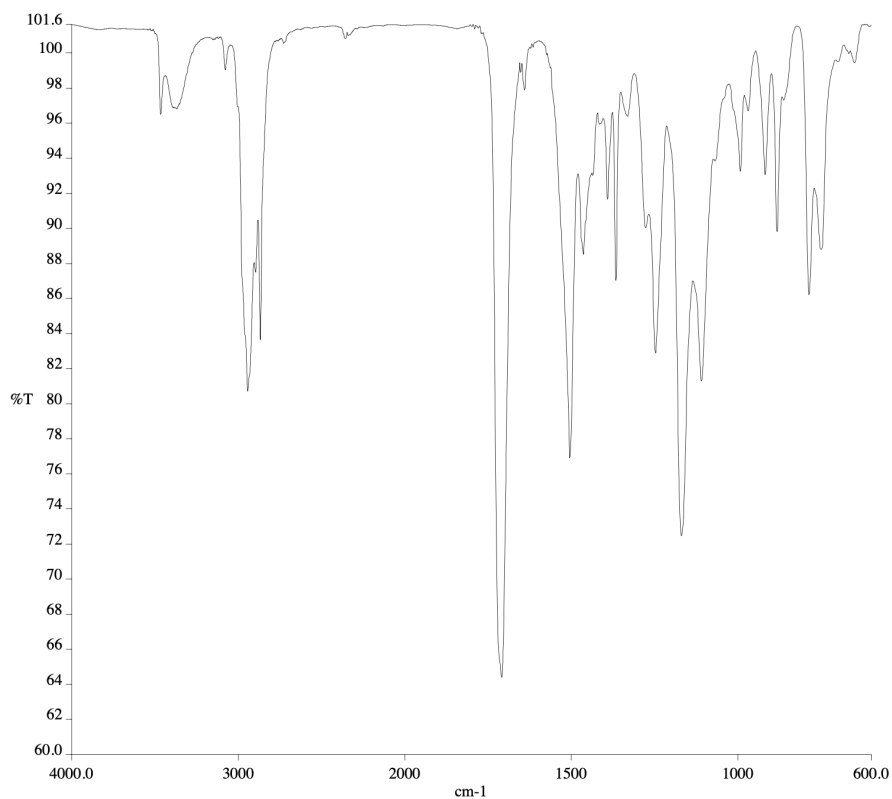


Figure A3.64 Infrared spectrum (Thin Film, NaCl) of compound **17i**.

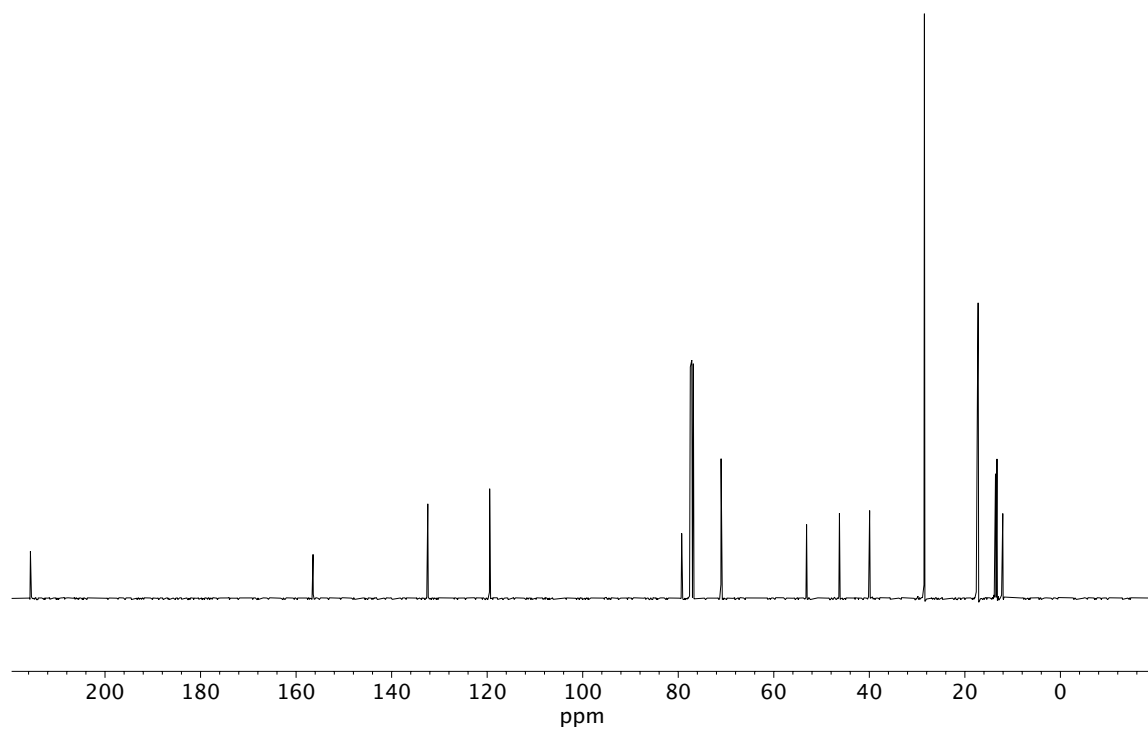


Figure A3.65 ¹³C NMR (100 MHz, CDCl₃) of compound **17i**.

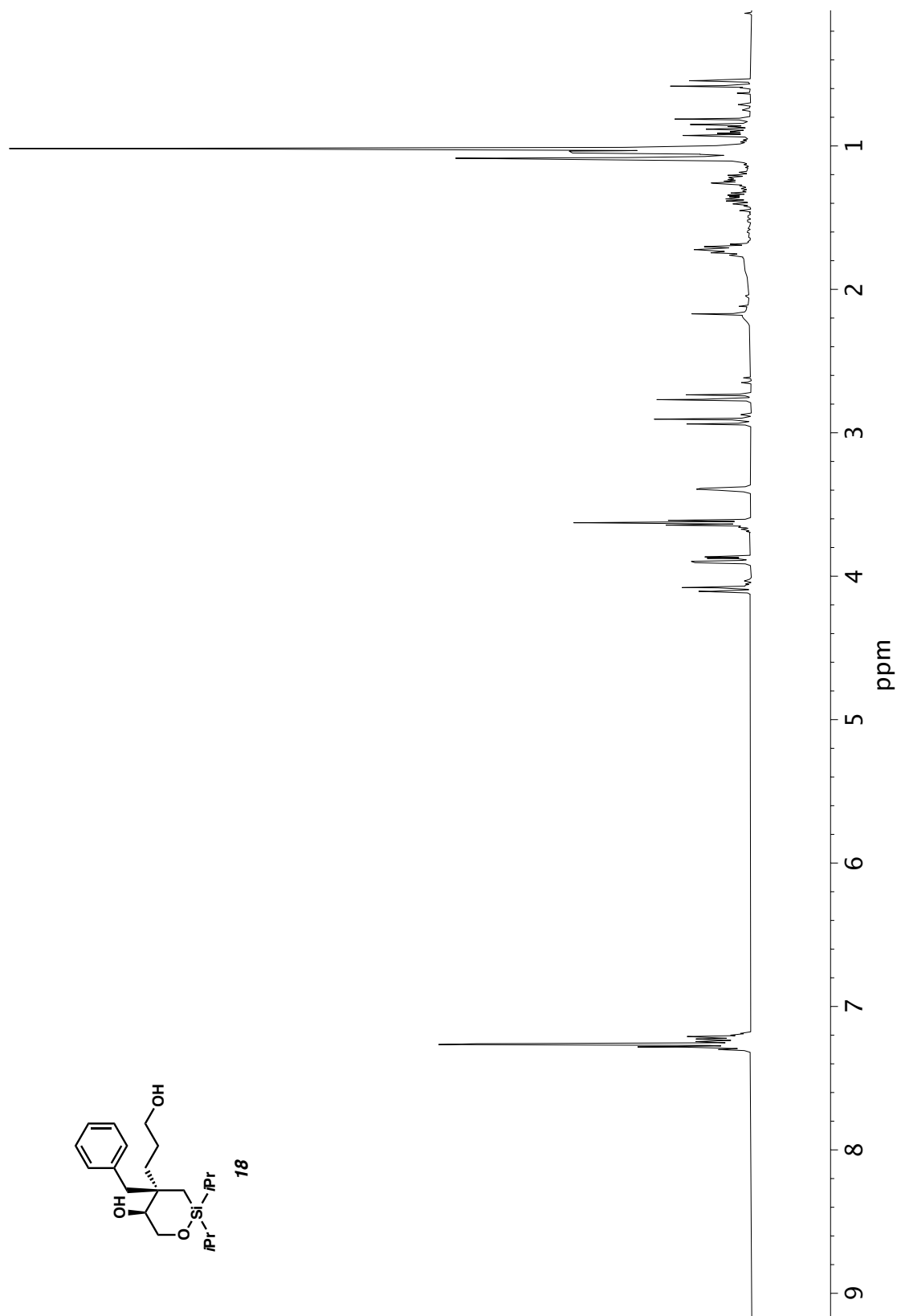


Figure A3.66 ^1H NMR (400 MHz, CDCl_3) of compound **18**.

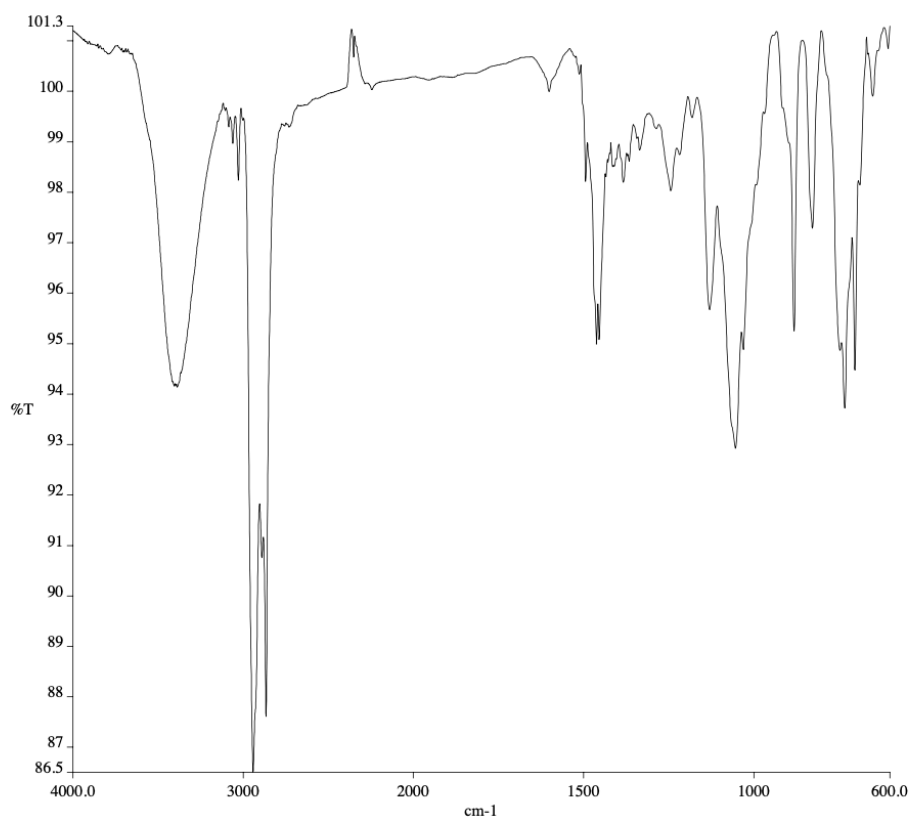


Figure A3.67 Infrared spectrum (Thin Film, NaCl) of compound **18**.

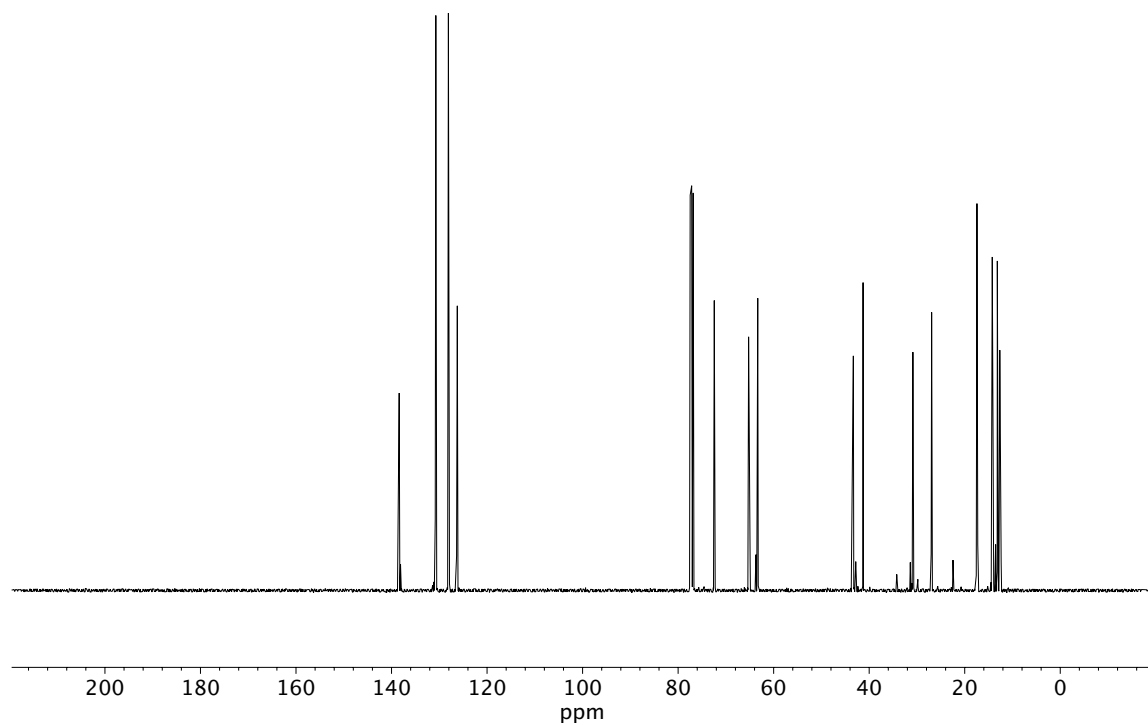


Figure A3.68 ¹³C NMR (100 MHz, CDCl₃) of compound **18**.

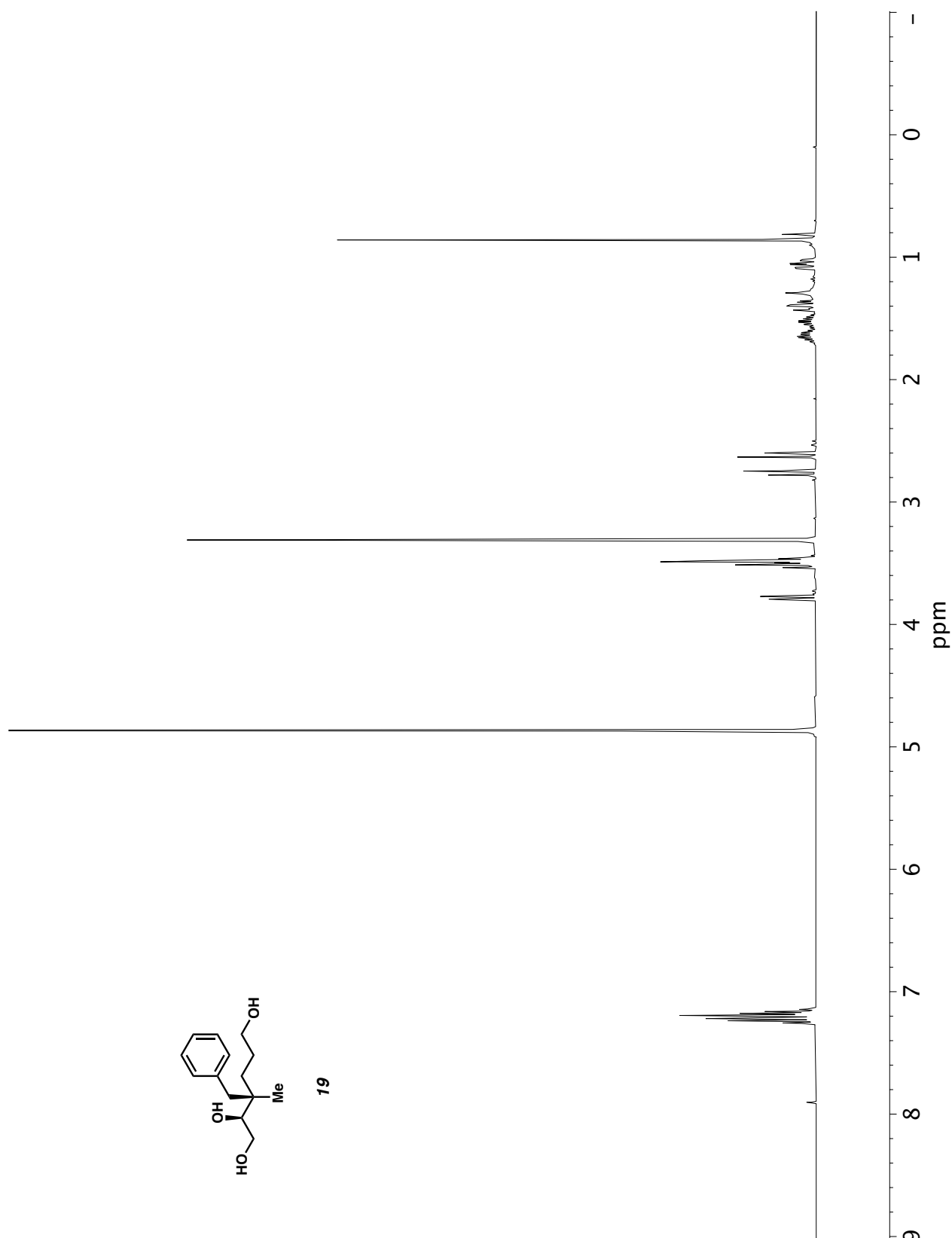


Figure A3.69 ¹H NMR (400 MHz, CD₃OD) of compound **19**.

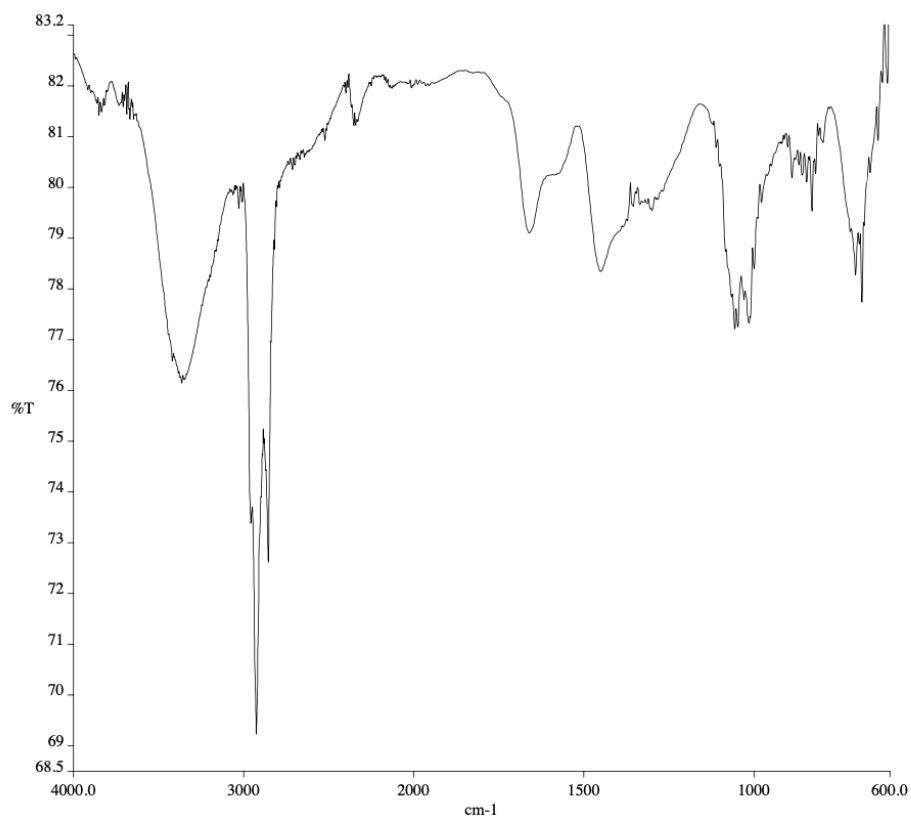


Figure A3.70 Infrared spectrum (Thin Film, NaCl) of compound **19**.

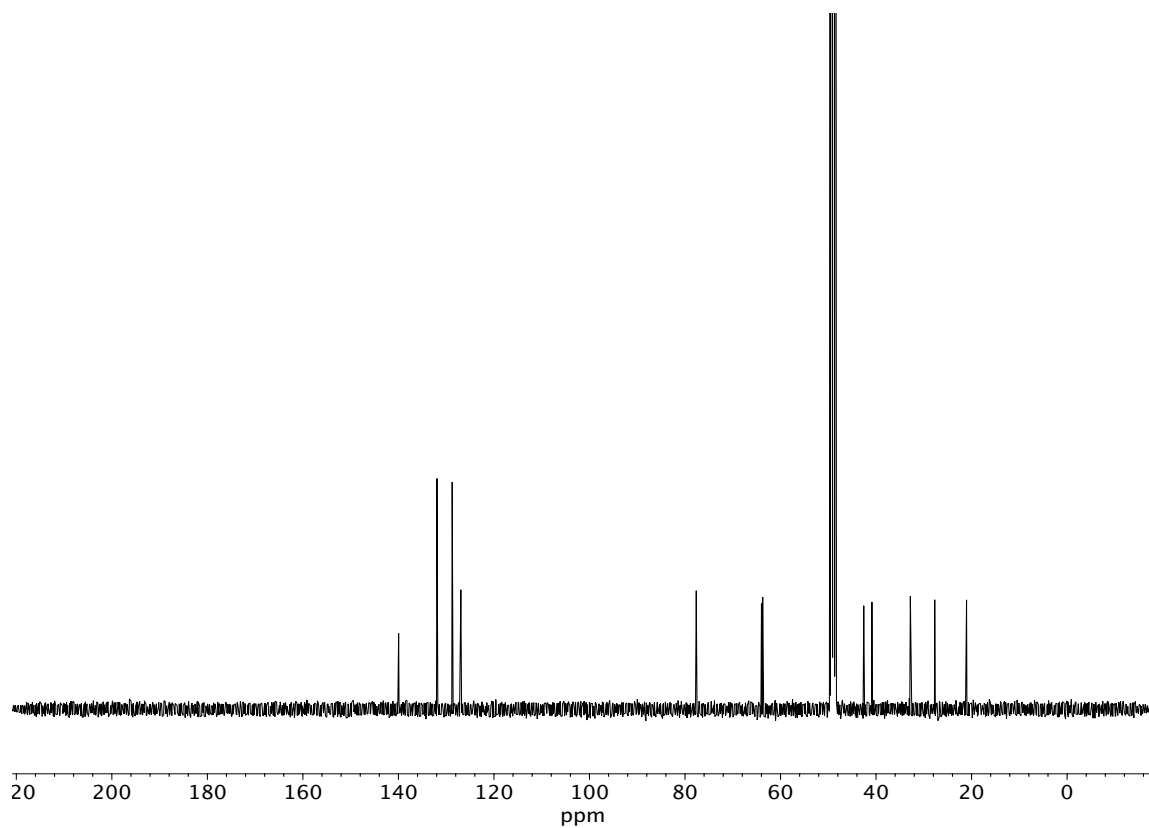


Figure A3.71 ¹³C NMR (100 MHz, CD₃OD) of compound **19**.

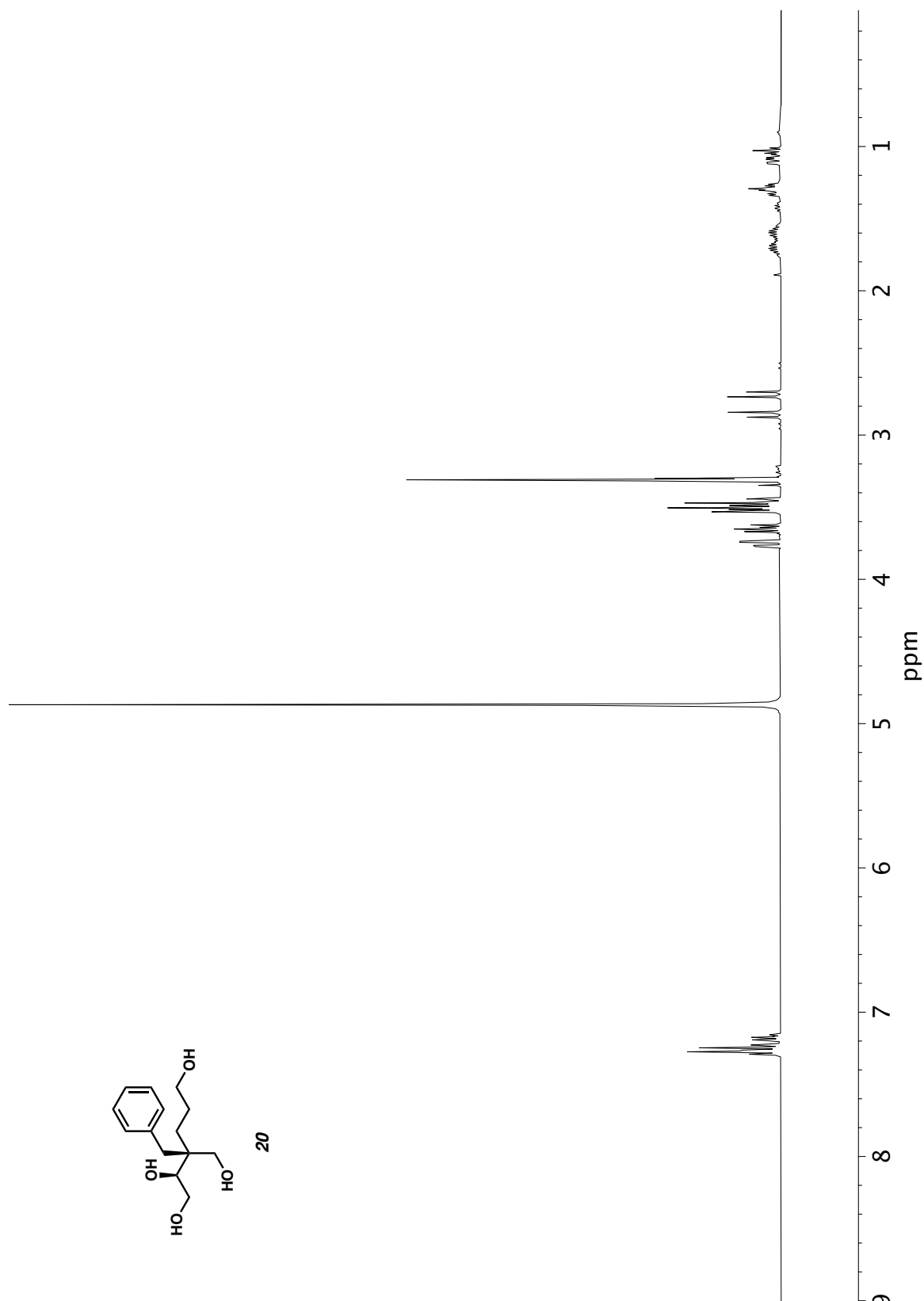


Figure A3.72 ¹H NMR (400 MHz, CD₃OD) of compound **20**.

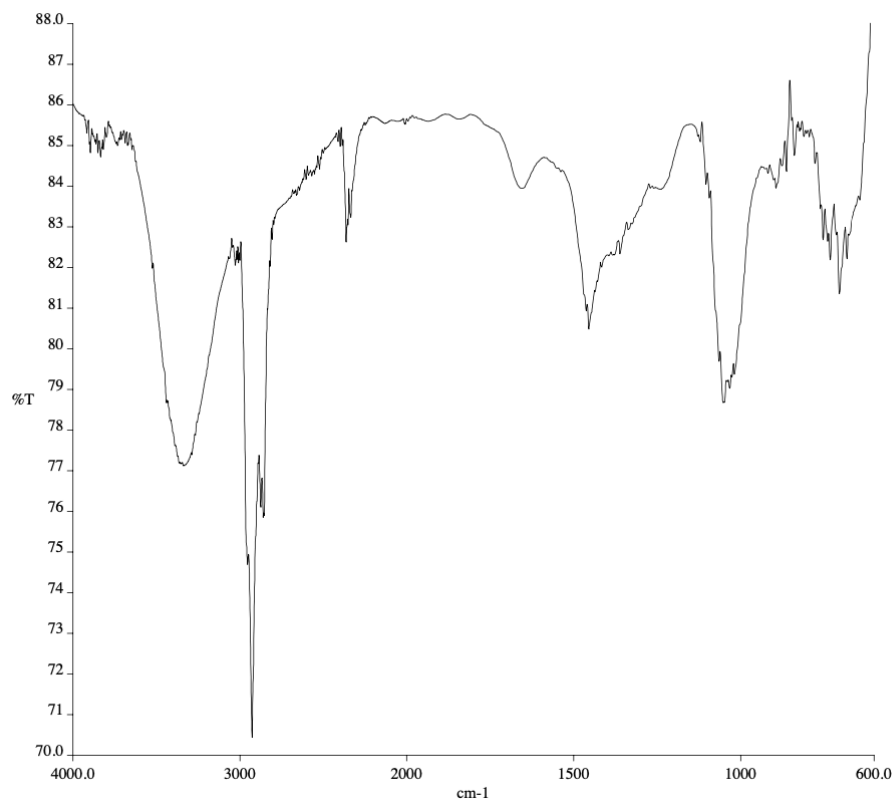


Figure A3.73 Infrared spectrum (Thin Film, NaCl) of compound **20**.

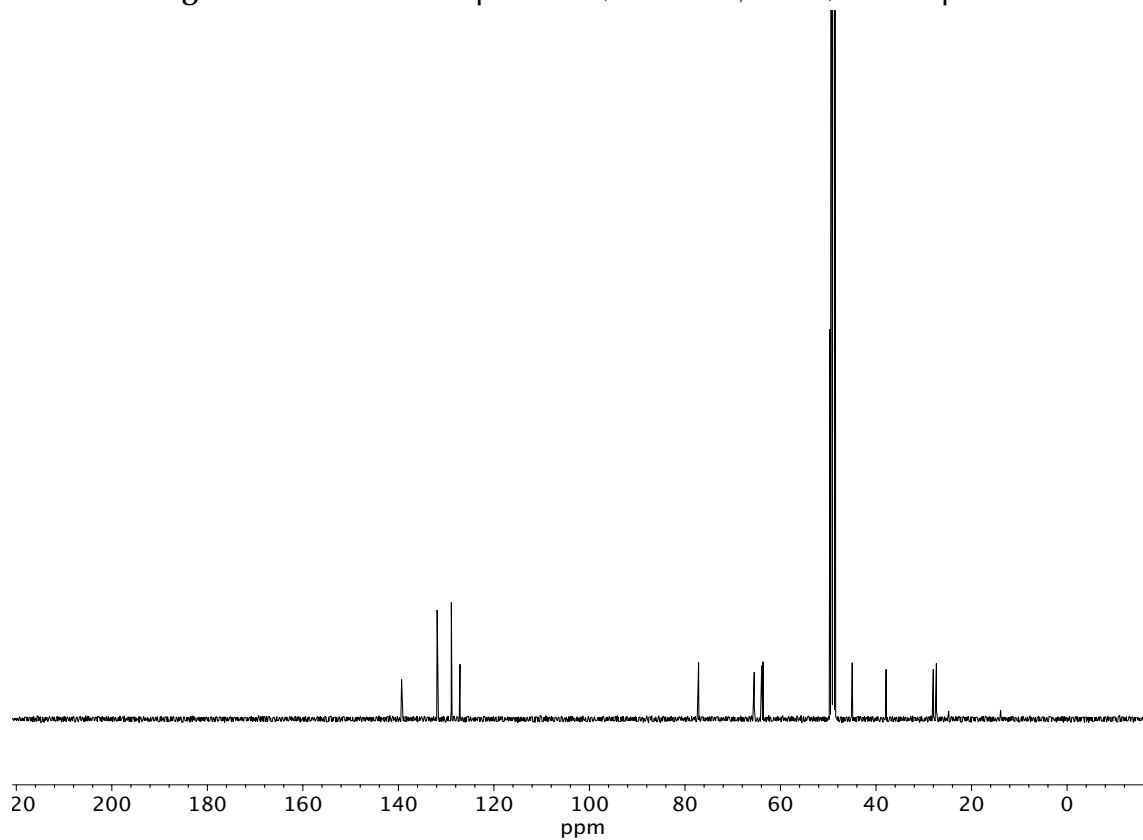


Figure A3.74 ¹³C NMR (100 MHz, CD₃OD) of compound **20**.

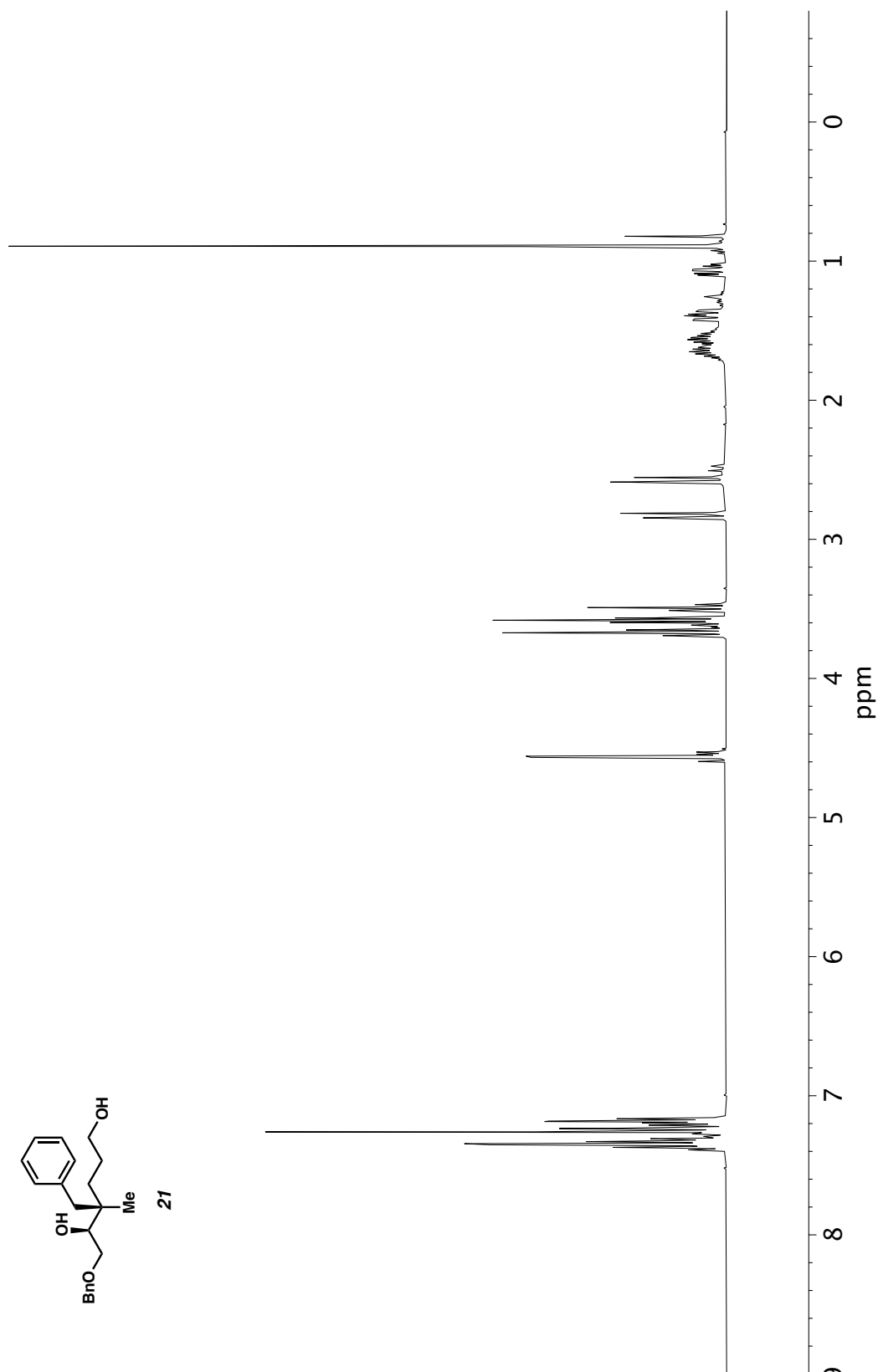


Figure A3.75 ^1H NMR (400 MHz, CDCl_3) of compound **21**.

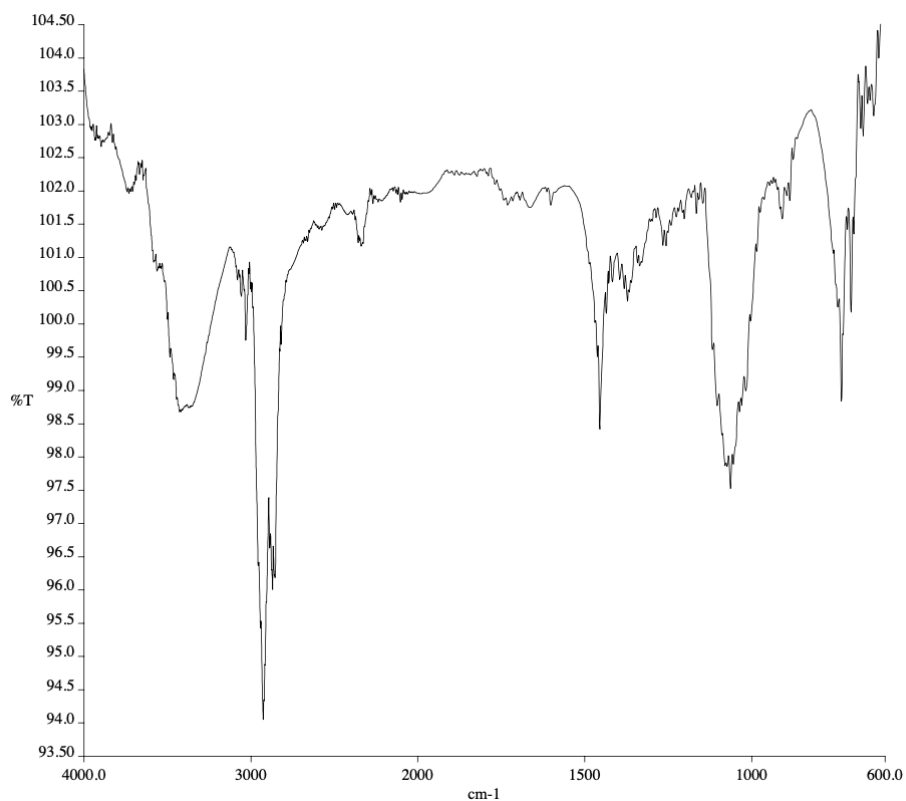


Figure A3.76 Infrared spectrum (Thin Film, NaCl) of compound **21**.

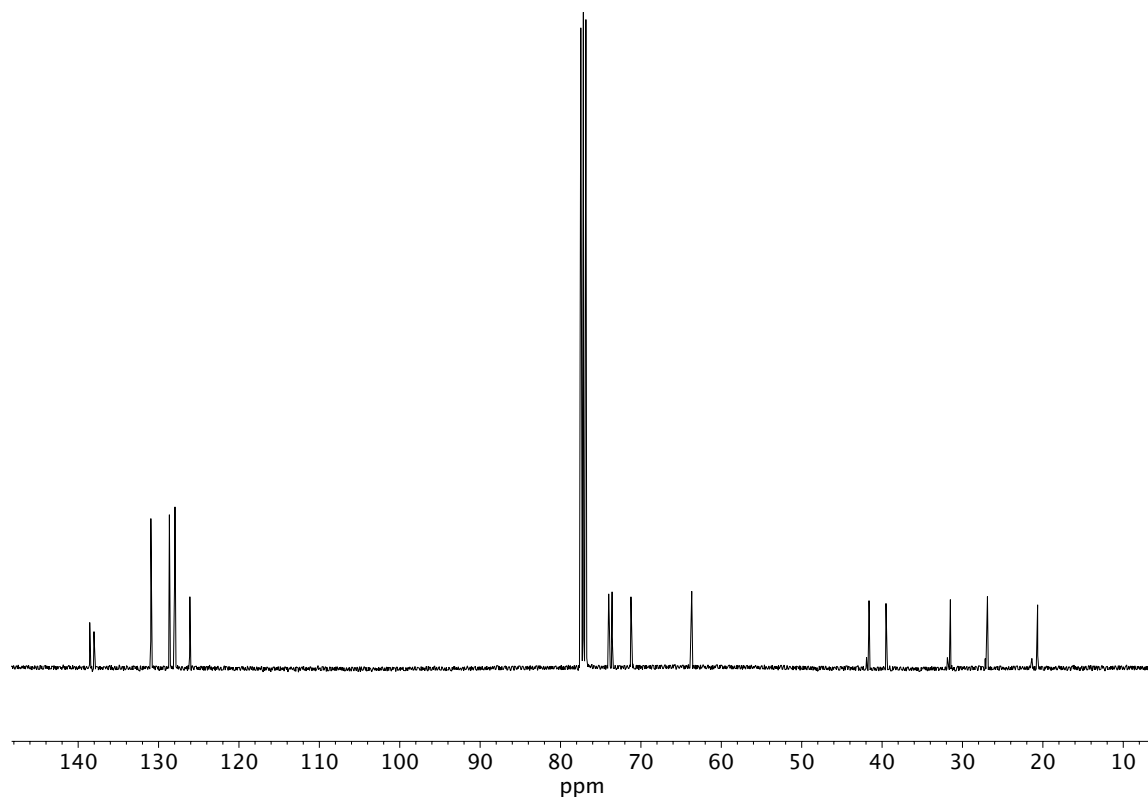


Figure A3.77 ¹³C NMR (100 MHz, CDCl₃) of compound **21**.

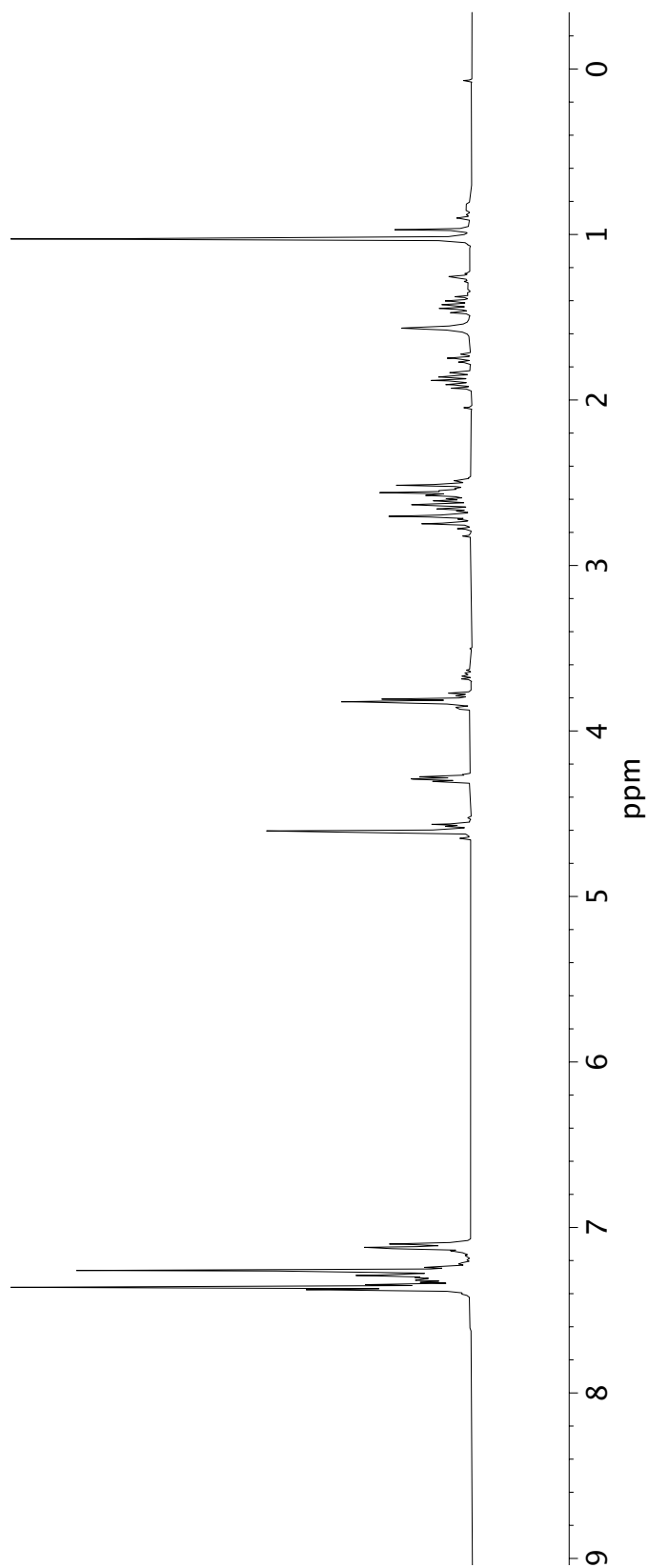
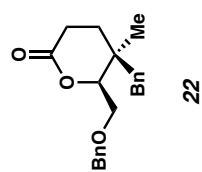


Figure A3.78 ^1H NMR (400 MHz, CDCl_3) of compound **22**.

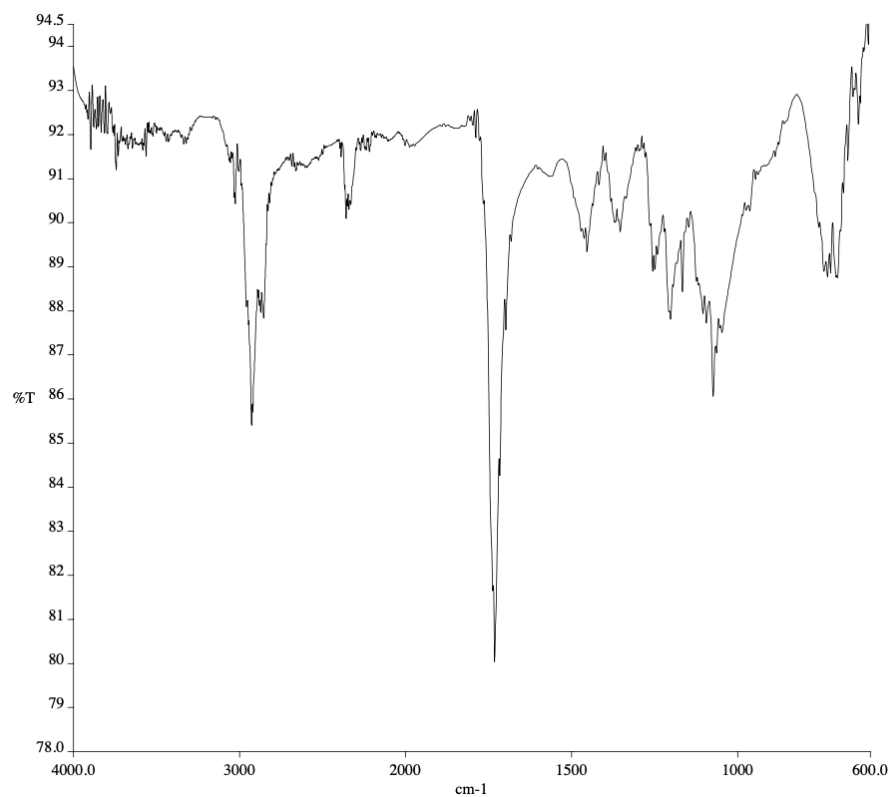


Figure A3.79 Infrared spectrum (Thin Film, NaCl) of compound **22**.

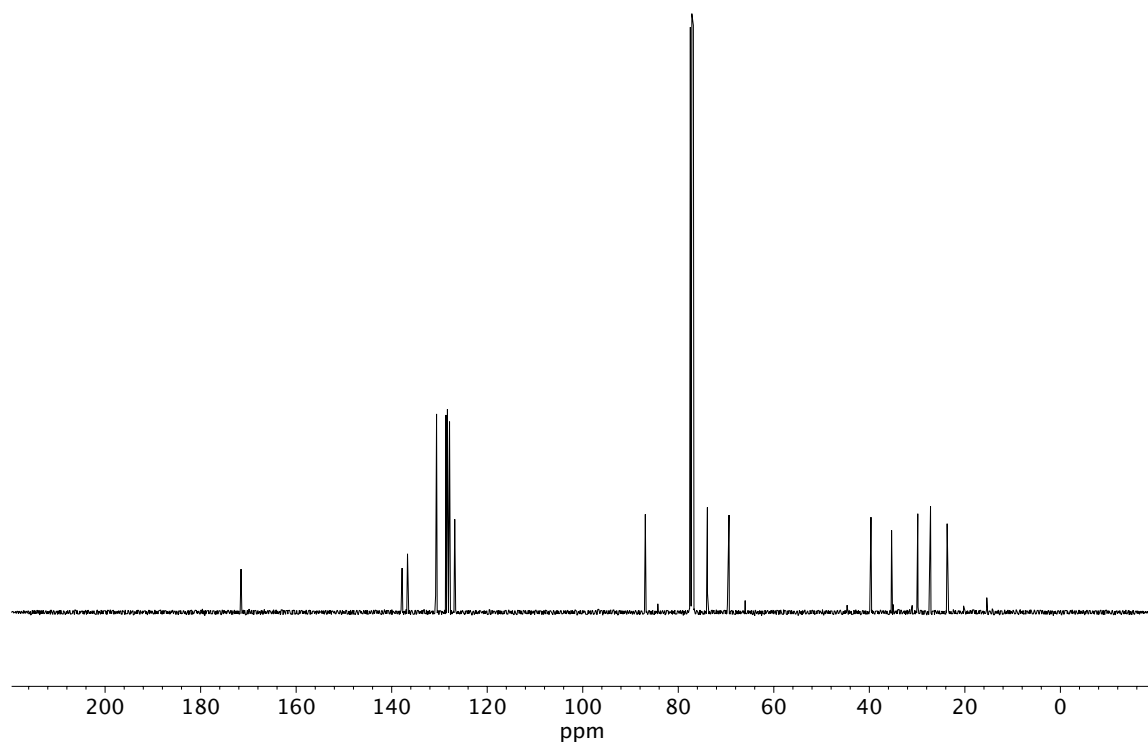


Figure A3.80 ¹³C NMR (100 MHz, CDCl₃) of compound **22**.

APPENDIX 4

Cycloadditions of Oxacyclic Allenes and a Catalytic Asymmetric Entryway to Enantioenriched Cyclic Allenes[†]

A4.1 INTRODUCTION

As shown in Chapter 2, we have successfully developed the Pd-catalyzed enantioselective decarboxylative allylic alkylation of cyclic siloxyketones and demonstrated the utility of the resulting silicon-containing heterocycles for the synthesis of highly oxygenated acyclic quaternary building blocks. Along with these β -silylated substrates, we have also initiated the development of a Pd-catalyzed allylic alkylation of α -silylated oxacyclic ketones in collaboration with

[†] This research was performed in collaboration with Michael M. Yamano, Rachel R. Knapp, and Melissa Ramirez. Portions of this chapter have been reproduced with permission from Yamano, M. M.; Knapp, R. R.; Ngamnithiporn, A.; Ramirez, M.; Houk, K. N.; Stoltz, B. M.; Garg, N. K. *Angew. Chem. Int. Ed.* **2019**, 58, 5653–5657. © 2019 Wiley-VCH.

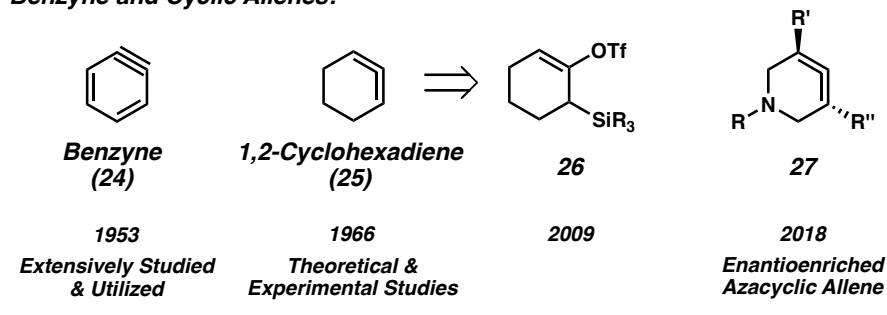
the Garg lab at UCLA. We envisioned this motif to provide an entryway to enantioenriched cyclic allenes which could be subsequently employed in (4+2), (3+2), and (2+2) cycloaddition reactions, providing enantioselective access to a wide variety of complex heterocyclic scaffolds.

Despite once being mere scientific curiosities, strained cyclic intermediates have become a popular arena for chemical discoveries. A notable breakthrough in the field was the discovery of benzyne (**24**), initially proposed by Wittig in 1942 and validated by Roberts in 1953 (Figure A4.1).¹ In the modern era, benzyne (**24**) and other cyclic alkynes are readily used to make natural products,² medicinal agents,³ agrochemicals,⁴ materials,⁵ tools for chemical biology,⁶ and ligands for catalysis.^{7,8} The related intermediate 1,2-cyclohexadiene (**25**) has generally received less attention, despite being validated not long after benzyne (**24**) in 1966.⁹ Historically, theoretical studies of **25** and its derivatives have been popular.¹⁰ However, only recently has **25** seen synthetic use in cycloadditions.¹¹ This is largely due to its ability to be accessed under mild fluoride-mediated conditions from silyl triflate **26**.^{12,13}

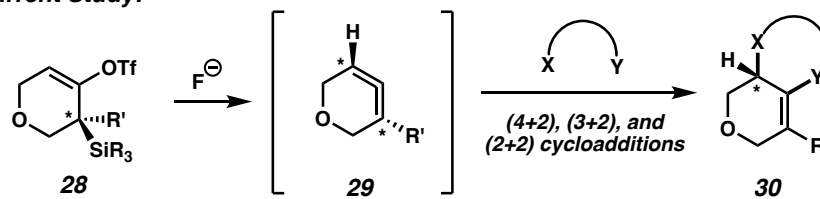
One exciting opportunity in the field of strained cyclic intermediates is the ability to access heterocyclic allenes. Early efforts in this field relied on harsh reaction conditions;^{14,15} however, we recently demonstrated that azacyclic allenes **27** (Figure A4.1) can be accessed using mild reaction conditions. Moreover, using chiral separation technology, enantioenriched **27** was intercepted (R=Cbz, R'=H, R''=Me), and its stereospecific trapping allowed for a unique approach to access enantioenriched cycloadducts.¹⁶

Figure A4.1 Highlights of benzyne and cyclic allene chemistry and cycloadditions of oxacyclic allenes described in this study.

Benzyne and Cyclic Allenes:



Current Study:



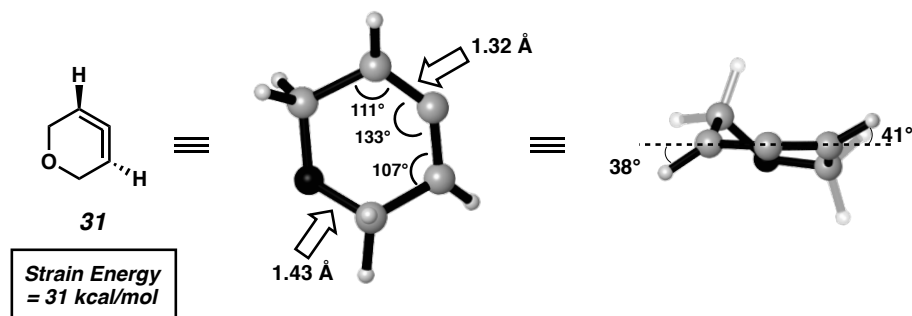
Given the potential for heterocyclic allenes to provide a facile means to rapidly assemble stereochemically-rich scaffolds,¹⁶ we questioned whether oxacyclic allenes **29** could be employed efficiently in cycloadditions to access oxygen-containing heterocycles.¹⁷ Oxygenated heterocycles are often seen in natural products and drugs^{18, 19, 20, 21} and are known bioisosteres for their nitrogen and sulfur-containing counterparts.²² A single report by Christl demonstrated that **29** ($R'=H$) could be generated using the Doering–Moore–Skattebøl rearrangement, however, this required harsh organolithium-based conditions.¹⁴ If **29** could be generated under mild conditions from silyl triflates **28**, the untapped synthetic utility of this species could be unlocked. Additionally, we sought to establish a catalytic, asymmetric method to access **29** in enantioenriched form, ideally by preparing an enantioenriched precursor to the desired allene **29**. By accessing enantioenriched **28**, we could explore the possibility of transferring stereochemical information from allene precursor **28** to cycloadduct **30**, via a

point chirality/axial chirality/point chirality transfer process. The results presented herein not only demonstrate the scope and utility of oxacyclic allene cycloadditions, but also showcase an exciting strategy that merges asymmetric catalysis with cyclic allene chemistry as a means to access enantioenriched scaffolds.

A4.2 COMPUTATIONAL ANALYSIS OF OXACYCLIC ALLENE **31**

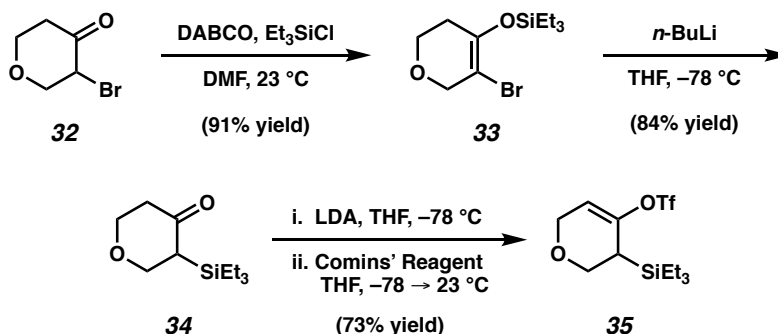
Density functional theory (DFT) calculations on the structure of heterocyclic allene **31** were performed using ω B97XD/6-31G(d) (Figure A4.2).^{10a,10c,10d,23} The C=C bond length of the allene is 1.32 Å, which is only slightly longer than the C=C bond length in a linear allene.¹⁶ Furthermore, the internal angle at the central allene carbon is 133°, which is a significant deviation from the typical internal angle of 180° seen in linear allenes. The allene π orbitals in **31** are not perfectly orthogonal, resulting in the C–H bonds being twisted out-of-plane (i.e., 38° and 41°). Thus, **31** is inherently chiral, analogous to linear allenes. The ground state geometry deviates from C₂ symmetry because the molecule adopts an envelope shape; inversion of the envelope requires only 0.8 kcal/mol. Interestingly, oxacyclic allene **31** is calculated to possess 31.0 kcal/mol of strain energy, which is nearly 4 kcal/mol more than the azacyclic variant we previously reported.¹⁶ This difference can be attributed to the smaller atomic radius of oxygen and the shorter C–O bond length relative to the C–N bond length in the azacyclic variant. The significant strain associated with oxacyclic allene **31** was expected to promote rapid cycloadditions.

Figure A4.2 Ground state structure of oxacyclic allene **31**. The structure was computed using ω B97XD/6-31G(d).



A4.3 SUBSTRATE SYNTHESIS

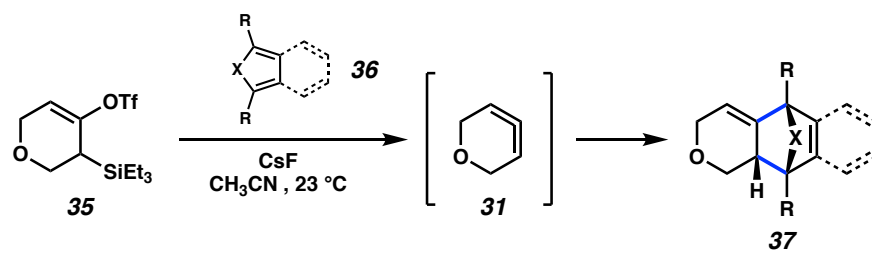
With the aim of accessing oxacyclic allene **31**, we first targeted silyl triflate **35** (Scheme A4.1), given the wide synthetic utility of silyl triflates as precursors to strained alkyne and allene intermediates.^{12,24} Bromoketone **32** (commercially available or readily synthesized from tetrahydro-4-pyranone) was converted to triethylsilyl enol ether **33** upon treatment with DABCO and TESC1.²⁵ Subsequent retro-Brook rearrangement furnished the desired α -silyl ketone **34**. Lastly, triflation afforded silyl triflate **35**.¹⁶ Our scalable,²⁶ three step synthesis of **35** provides a new strategy to synthesize α -silyl ketones en route to cyclic allene precursors. Currently, α -silyl ketones are most commonly prepared by 1,4-reduction of the corresponding α,β -unsaturated ketones.^{11a,12,16,27}

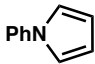
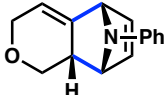
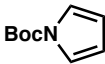
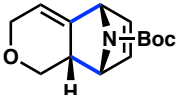
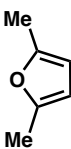
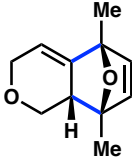
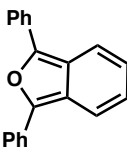
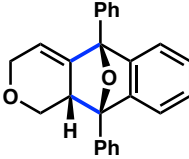
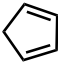
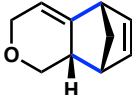
Scheme A4.1 Synthesis of silyl triflate.

A4.4 CYCLOADDITIONS OF OXACYCLIC ALLENE

With silyl triflate **35** in hand, we generated and trapped **31** in Diels–Alder, (3+2), and (2+2) cycloadditions. By simply employing a variety of dienes, a number of cycloadducts were prepared in good to excellent yields (Table A4.1, entries 1–5).²⁸ In almost all cases, the reactions were performed at $23\text{ }^\circ\text{C}$, thus highlighting the mildness of the reaction conditions. Although the range of diastereoselectivities is variable, in all examples, the major diastereomer observed is the endo product. Furthermore, the observed selectivities are supported by computations as the endo transition states were found to be more energetically favorable compared to the exo transition states.²⁶ It should be noted that in each case, the products formed are considerably complex from a structural perspective, each bearing three stereocenters, a bridged [2.2.1]-bicyclic framework, and 1 or 2 heteroatoms.

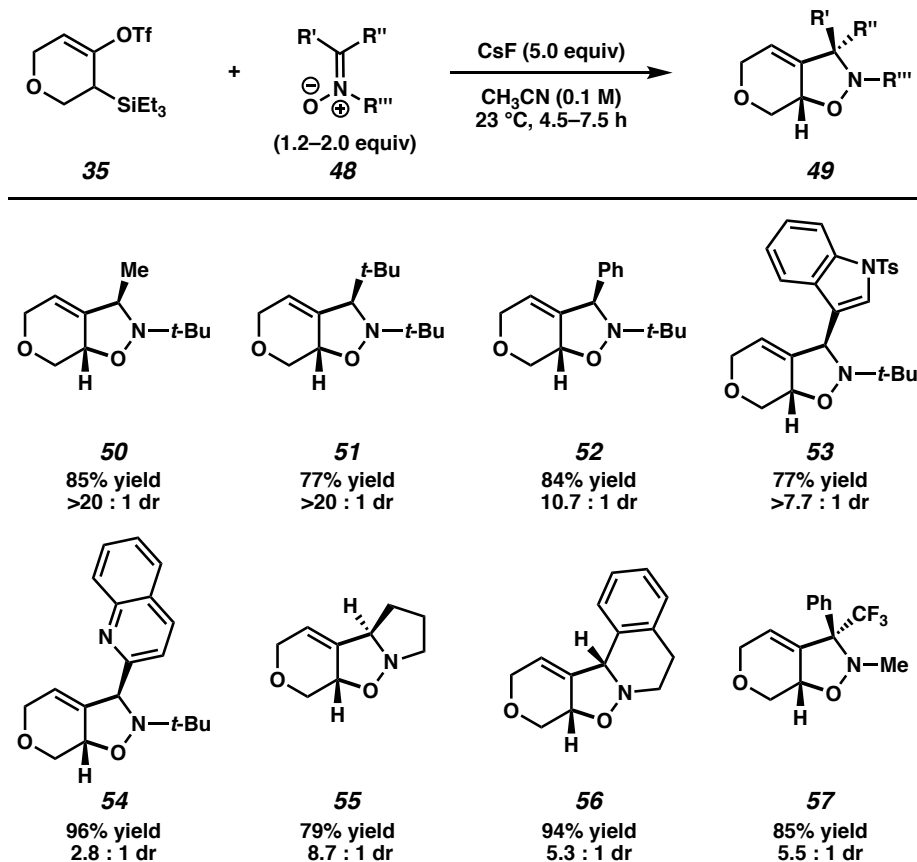
Table A4.1 Mild generation of oxacyclic allene **31** and its trapping in Diels–Alder cycloadditions.^a


Reaction scheme: Oxacyclic allene **31** is generated from **35** (a 2-(triethylsilyl)-4-(trifluoromethanesulfonyl)-2,3-dihydro-1,4-dioxole) and **36** (a substituted cyclopentadiene with substituents R and X) using CsF in CH₃CN at 23 °C. The intermediate **31** then undergoes Diels–Alder cycloaddition with **36** to form the bicyclic product **37**.

Entry	Diene	Cycloadduct ^b	Yield ^c Diastereoselectivity ^d
1	 38	 39	91% 3.8 : 1 dr
2	 40	 41	74% 6.2 : 1 dr
3	 42	 43	86% 9.2 : 1 dr
4	 44	 45	97% ^e 2.0 : 1 dr
5	 46	 47	83% 1.6 : 1 dr

[a] The major diastereomer is shown. [b] Yields reflect an average of two isolation experiments. [c] Diastereomeric ratios were determined by ¹H NMR analysis of the crude reaction mixture. [d] The reaction was performed at 60 °C for 2.5 h using 2.0 equiv of diene **44**.

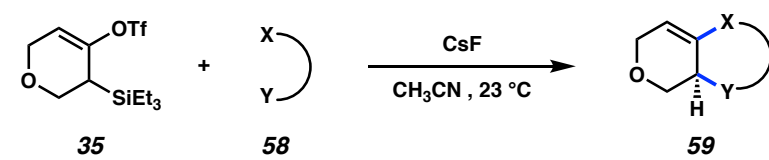
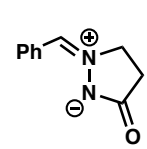
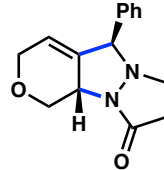
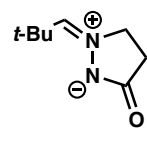
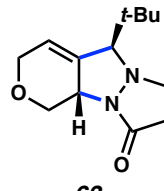
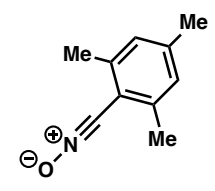
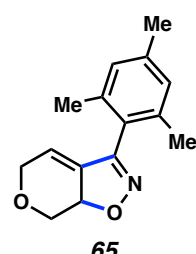
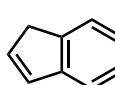
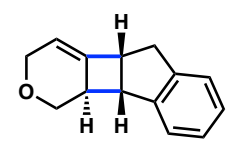
Figure A4.3 (3+2) cycloadditions with nitrones. The major diastereomeric product is shown. Yields reflect an average of two isolation experiments. Diastereomeric ratios were determined by ^1H NMR analysis of the crude reaction mixture.



The results of the (3+2) and (2+2) cycloadditions are shown in Figure A4.3 and Table A4.2, respectively. The use of simple nitrones gave high yields of isoxazolidine products **50**–**52**, whereas nitrones bearing either an indole or quinoline unit delivered cycloadducts **53** and **54**. We also evaluated two cyclic nitrones where R'' and R''' of **48** were tethered, which furnished fused tri- and tetracyclic products **55** and **56**. Additionally, a ketone-derived nitrone was utilized, ultimately giving rise to the heteroatom-rich trifluoromethylated product **57**. Azomethine imines **60** and **62** were tested, giving rise to the corresponding pyrazolidines **61** and **63** in good to excellent diastereoselectivities (Table A4.2, entries 1 and 2). The use of nitrile oxide **64** led to the

formation of isoxazoline **65** in 91% yield (entry 3). With regard to a (2+2) cycloaddition, the use of indene gave cyclobutane **67** in excellent yield and with high regioselectivity (entry 4).

Table A4.2 Additional (3+2) and (2+2) cycloadditions.^a

			
Entry	Trapping Agent	Cycloadduct ^b	Yield ^c Diastereoselectivity ^d
1	 60	 61	76% 7.6 : 1 dr
2	 62	 63	83% >20 : 1 dr
3	 64	 65	91% N/A
4	 66	 67	96% 5.2 : 1 dr

[a] The major diastereomer is shown. [b] Yields reflect an average of two isolation experiments. [c] Diastereomeric ratios were determined by ¹H NMR analysis of the crude reaction mixture.

Overall, silyl triflate **35** was elaborated to 17 different sp^3 -rich heterocyclic cycloadducts. Several of these bear a multitude of rings, stereocenters, and heteroatoms, thus showcasing the value of oxacyclic allenes for the rapid generation of complex scaffolds. Accordingly, this methodology should be especially valuable to those pursuing modern drug discovery efforts.¹⁷

A4.5 CATALYTIC ASYMMETRIC APPROACH TO OXACYCLIC ALLENES AND EVALUATION OF ENANTIOSPECIFICITY

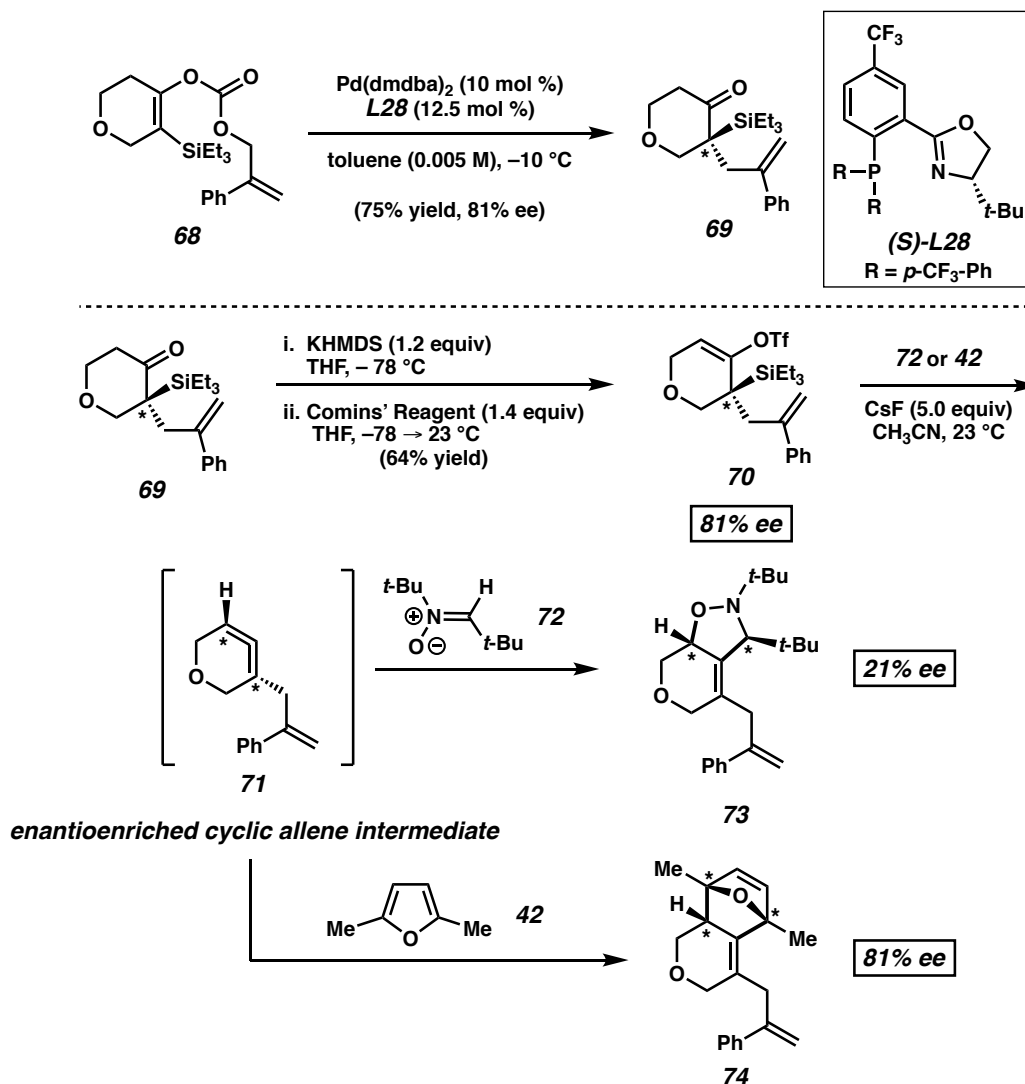
As noted earlier, one of the most exciting opportunities regarding cyclic allene chemistry is the possibility of intercepting enantioenriched allenes for the synthesis of enantioenriched cycloadducts. In a seminal study, Christl and Engels generated 1-phenyl-1,2-cyclohexadiene in enantioenriched form, as judged by the formation of an enantioenriched cycloadduct, albeit in low yield, likely owing to the necessary use of organolithium reagents.²⁹ Our laboratory recently disclosed a mild, alternative strategy whereby silyl triflate precursors to the desired cyclic allenes could be employed in enantioenriched form.¹⁶ However, in both cases, the key substrates were only accessible via chiral separation technologies. A catalytic asymmetric strategy to access enantioenriched cyclic allene precursors has not yet been disclosed.

Our efforts in this area are highlighted in Scheme A4.2. Enol carbonate **68** was formed by intercepting the enolate intermediate generated during the retro-Brook rearrangement of **33** (see Scheme A4.1). This set the stage for a Pd-catalyzed decarboxylative asymmetric allylic alkylation. Allylation was attractive, given that allyl groups serve as versatile handles for further manipulation.³⁰ After extensive

experimentation,²⁶ it was found that treatment of **68** with Pd(dmdba)₂ and (*S*)-(CF₃)₃-*t*Bu-PHOX ligand (**L28**) in toluene at –10 °C gave the desired ketone **69** in 81% ee and 75% yield. This is the first example of a decarboxylative asymmetric allylic alkylation reaction being performed on an α -silyl-substituted enol carbonate. In fact, decarboxylative asymmetric allylic alkylations on substrates bearing α -heteroatoms are significantly underdeveloped.^{30,31} Ketone **69** was converted to silyl triflate **70** in one-step, thus establishing the first catalytic asymmetric strategy for the synthesis of enantioenriched cyclic allene precursors.

Silylated enol triflate **70** was treated with trapping agent **72** or **42** in the presence of CsF in acetonitrile at 23 °C. Interestingly, the nitron cycloadduct, isoxazolidine **73**, was obtained in only 21% ee. On the other hand, the Diels–Alder cycloadduct, oxabicycle **74**, was obtained in 81% ee (>20:1 dr), reflective of complete transfer of stereochemical information. Given this latter result, we surmise that enantioenriched **71** is formed under the mild reaction conditions with complete transfer of stereochemical information. In the case of the nitron trapping, previous computational studies have demonstrated that trapping may occur through either a stepwise or concerted pathway,^{11a} which accounts for the partial loss of stereochemical information.³² However, in the case of the Diels–Alder reaction, it is likely that a concerted pathway is operative, based on our recent computational investigation of azacyclic allenes,¹⁶ thus leading to complete transfer of stereochemical information in this case.

Scheme A4.2 Catalytic asymmetric approach and cycloaddition results.



The overall conversion of **70** to **71** to **74** deserves special attention. This is a scenario wherein the silyl-bearing stereocenter in **70** was ultimately accessed by asymmetric catalysis. The point chirality in **70** is then transferred to the axially chiral transient intermediate **71**, which is then relayed to product **74**, which possesses point chirality. Enantioenriched cycloadduct **74** contains three stereocenters, none of which were present in the starting material that bears only one stereocenter. The transformation occurs preferentially with the olefin more distal to the 2-phenyl allyl group undergoing

cycloaddition. This is presumably because of favorable electronic interactions in the transition state based on our prior studies,¹⁶ however, we cannot rule out the steric impact of the 2-Ph allyl chain as a contributor to the observed regioselectivity.

A4.6 CONCLUSIONS

We have discovered an efficient synthetic route to prepare a silyl triflate precursor to 3,4-oxacyclohexadiene, the first generation of an oxacyclic allene under mild conditions, and the in situ trapping of the oxacyclic allene in diastereo- and regioselective cycloadditions. These efforts collectively establish the synthetic utility of oxacyclic allenenes for the rapid generation of complex heterocyclic scaffolds. In addition, we have uncovered the first catalytic, asymmetric approach to access an enantioenriched cyclic allene precursor. This relies on a Pd-catalyzed allylic allylation, performed for the first time on an α -silyl substituted substrate, ultimately permitting access to the necessary enantioenriched silyl triflate precursor. We show that trapping of the enantioenriched oxacyclic allene in a Diels–Alder reaction occurs with complete transfer of stereochemical information via a point chirality/axial chirality/point chirality transfer process. These results showcase an exciting strategy that merges asymmetric catalysis with cyclic allene chemistry as a means to access densely functionalized, enantioenriched scaffolds.

A4.7 EXPERIMENTAL SECTION

Supporting information, which includes detailed experimental procedures, spectroscopic data, and computational methods can be found under: <https://onlinelibrary.wiley.com/doi/full/10.1002/anie.201900503>

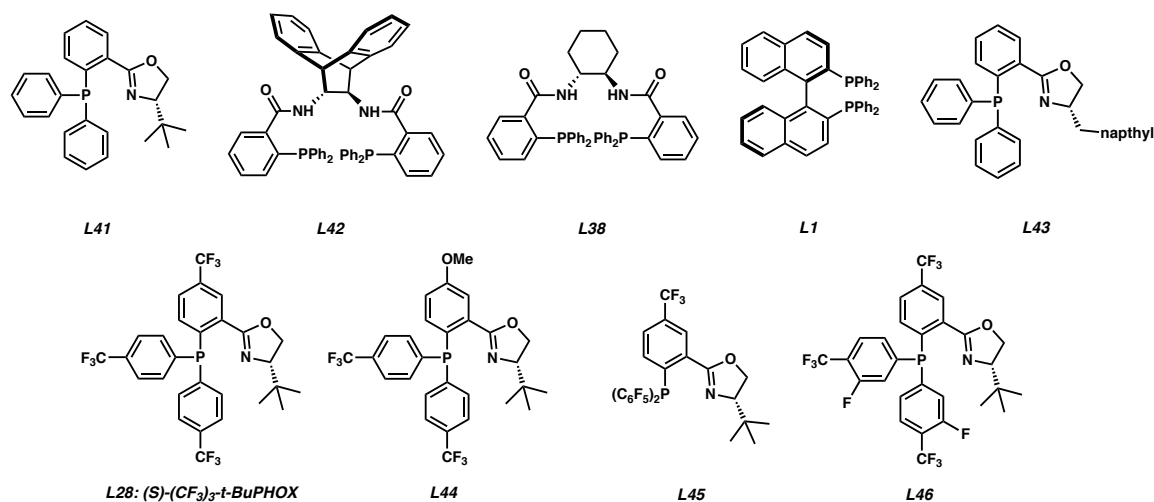
A4.7.1 Additional Optimization Results for Asymmetric Allylic Alkylation

Table A4.3 Effects of ligands, solvents, and temperatures.^a

Reaction scheme: Enol carbonate **75** reacts with $\text{Pd}_2(\text{dba})_3$ (5 mol %), ligand (12.5 mol %), in solvent (0.033 M) at temperature (temp.) for 20 h to yield product **76**.

entry	ligand	solvent	temp (°C)	% conversion ^b	% ee ^c
1	<i>L41</i>	toluene	23	>95	21
2	<i>L42</i>	toluene	23	>95	2
3	<i>L38</i>	toluene	23	>95	7
4	<i>L1</i>	toluene	23	>95	13
5	<i>L43</i>	toluene	23	>95	0
6	<i>L28</i>	toluene	23	>95	62
7	<i>L44</i>	toluene	23	>95	53
8	<i>L45</i>	toluene	23	47	61
9	<i>L46</i>	toluene	23	>95	58
10	<i>L28</i>	THF	23	>95	47
11	<i>L28</i>	1,4-dioxane	23	>95	57
12	<i>L28</i>	MTBE	23	>95	52
13	<i>L28</i>	benzene	23	>95	60
14	<i>L28</i>	2:1 hexane:toluene	23	>95	61
15	<i>L28</i>	toluene	0	>95	68
16	<i>L28</i>	toluene	−10	>95	70

[a] Conditions: enol carbonate **75** (0.05 mmol), $\text{Pd}_2(\text{dba})_3$ (5 mol %), and ligand (12.5 mol %). [b] Conversion determined by ^1H NMR of crude reaction mixture using trimethoxybenzene as a standard. [c] Determined by chiral SFC analysis of isolated product.

Ligand List:

Table A4.4 Substrate, temperature, and concentration optimization experiments.^a

entry	ligand	SiR ₃	R'	temperature	conc. (M)	%ee ^b	yield ^c
1	L41	SiEt ₃	H	23 °C	0.033	25	51%
2	L28	SiEt ₃	H	23 °C	0.033	62	85%
3	L28	SiMe ₂ Ph	H	23 °C	0.033	58	69%
4	L28	SiMe ₃	H	23 °C	0.033	70	88%
5	L28	SiMe ₃	H	−10 °C	0.005	75	85%
6	L28	SiEt ₃	H	−10 °C	0.005	74	95%
7	L28	SiEt ₃	Ph	−10 °C	0.005	81	75%

[a] Reactions performed at 23 °C utilized Pd₂(dba)₃ while reactions performed at −10 °C utilized Pd(dmdba)₂. [b] Determined by chiral SFC analysis. [c] Determined by chiral SFC analysis of isolated product. [c] Determined by ¹H NMR of crude reaction mixture using trimethoxybenzene as a standard.

A4.8 REFERENCES AND NOTES

- (1) a) Wittig, G. *Naturwissenschaften* **1942**, *30*, 696–703; b) Roberts, J. D.; Simmons, H. E.; Carlsmith, L. A.; Vaughn, C. W. *J. Am. Chem. Soc.* **1953**, *75*, 3290–3291.
- (2) For recent examples of arynes and related species in total synthesis, see: a) Kou, K. G. M.; Pflueger, J. J.; Kiho, T.; Morrill, L. C.; Fisher, E. L.; Clagg, K.; Lebold, T. P.; Kisunzu, J. K.; Sarpong, R. *J. Am. Chem. Soc.* **2018**, *140*, 8105–8109; b) Goetz, A. E.; Silberstein, A. L.; Corsello, M. A.; Garg, N. K. *J. Am. Chem. Soc.* **2014**, *136*, 3036–3039; c) Neog, K.; Borah, A.; Gogoi, P. *J. Org. Chem.* **2016**, *81*, 11971–11977; d) Neumeyer, M.; Kopp, J.; Brückner, R. *Eur. J. Org. Chem.* **2017**, 2883–2915; e) Corsello, M. A.; Kim, J.; Garg, N. K. *Nat. Chem.* **2017**, *9*, 944–949.
- (3) a) Carroll, F. I.; Robinson, T. P.; Brieady, L. E.; Atkinson, R. N.; Mascarella, S. W.; Damaj, M. I.; Martin, B. R.; Navarrio, H. A. *J. Med. Chem.* **2007**, *50*, 6383–6391; c) Willis, P. G.; Pavlova, O. A.; Chefer, S. I.; Vaupel, D. B.; Mukhin, A. G.; Horti, A. G. *J. Med. Chem.* **2005**, *48*, 5813–5822; d) Jacob, P. III. *J. Med. Chem.* **1981**, *24*, 1348–1353; e) Coe, J. W. et al., *Bioorg. Med. Chem. Lett.* **2005**, *15*, 4889–4897.
- (4) Schleth, F.; Vettiger, T.; Rommel, M.; Tobler, H. WO2011131544 A1, **2011**.
- (5) Lin, J. B.; Shah, T. J.; Goetz, A. E.; Garg, N. K.; Houk, K. N. *J. Am. Chem. Soc.* **2017**, *139*, 10447–10455.
- (6) Chupakhin, E. G.; Krasavin, M.Y. *Chem. Heterocycl. Compd.* **2018**, *54*, 483–501.

- (7) a) Surry, D. S.; Buchwald, S. L. *Angew. Chem. Int. Ed.* **2008**, *47*, 6338–6361; *Angew. Chem.* **2008**, *120*, 6438–6461; b) Mauger, C. C.; Mignani, G. A. *Org. Proc. Res. Dev.* **2004**, *8*, 1065–1071.
- (8) For recent reviews of arynes and related intermediates, see: a) Goetz, A. E.; Garg, N. K. *J. Org. Chem.* **2014**, *79*, 846–851; b) Yoshida, S.; Hosoya, T. *Chem. Lett.* **2015**, *44*, 1450–1460; c) Bhojgude, S. S.; Bhunia, A.; Biju, A. T. *Acc. Chem. Res.* **2016**, *49*, 1658–1670; d) Shi, J.; Li, Y.; Li, Y. *Chem. Soc. Rev.* **2017**, *46*, 1707–1719; e) Asamdi, M.; Chikhaliya, K. H. *Asian J. Org. Chem.* **2017**, *6*, 1331–1348; f) Idiris, F. I. M.; Jones, C. R. *Org. Biomol. Chem.* **2017**, *15*, 9044–9056; g) Takikawa, H.; Nishii, A.; Sakai, T.; Suzuki, K. *Chem. Soc. Rev.* **2018**, *47*, 8030–8056; h) Dhokale, R. A.; Mhaske, S. B. *Synthesis* **2018**, *50*, 1–16.
- (9) Wittig, G.; Fritze, P. *Angew. Chem. Int. Ed.* **1966**, *5*, 846; *Angew. Chem.* **1966**, *78*, 905.
- (10) a) Angus, R. O.; Schmidt, M. W.; Johnson, R. P.; *J. Am. Chem. Soc.* **1985**, *107*, 532–537; b) Engels, B.; Schöneboom, J. C.; Münster, A. F.; Geoetsch, S.; Christl, M. *J. Am. Chem. Soc.* **2002**, *124*, 287–297; c) Schmidt, M. W.; Angus, R. O.; Johnson, R. P. *J. Am. Chem. Soc.* **1982**, *104*, 6838–6839; d) Dillion, P. W.; Underwood, G. R.; *J. Am. Chem. Soc.* **1974**, *96*, 779–787; e) Daoust, K. J.; Hernandez, S. M.; Konrad, K. M.; Mackie, I.; Winstanley, J.; Johnson, R. P. *J. Org. Chem.* **2006**, *71*, 5708–5714.

- (11) a) Barber, J. S.; Styduhar, E. D.; Pham, H. W.; McMahon, T. C.; Houk, K. N.; Garg, N. K. *J. Am. Chem. Soc.* **2016**, *138*, 2512–2515; b) Lofstrand, V. A.; West, F. G. *Chem. Eur. J.* **2016**, *22*, 10763–10767.
- (12) Quintana, I.; Peña, D.; Pérez, D.; Guitián, E. *Eur. J. Org. Chem.* **2009**, 5519–5524.
- (13) Additionally, 1,2-cyclohexadiene has been generated through a similar silyl bromide elimination: Shakespeare, W. C.; Johnson, R. P. *J. Am. Chem. Soc.* **1990**, *112*, 8578–8579.
- (14) Schreck, M.; Christl, M. *Angew. Chem. Int. Ed.* **1987**, *26*, 690–692; *Angew. Chem.* **1987**, *99*, 720–721.
- (15) For heterocyclic allene generation under harsh conditions or utilizing highly basic reagents, see; a) Christl, M.; Braun, M.; Wolz, E.; Wagner, W. *Chem. Ber.* **1994**, *127*, 1137–1142; b) Ruzziconi, R.; Naruse, Y.; Schlosser, M. *Tetrahedron* **1991**, *47*, 4603–4610; c) Drinkuth, S.; Groetsch, S.; Peters, E.; Peters, K.; Christl, M. *Eur. J. Org. Chem.* **2001**, 2665–2670.
- (16) Barber, J. S.; Yamano, M. M.; Ramirez, M.; Darzi, E. R.; Knapp, R. R.; Liu, F.; Houk, K. N.; Garg, N. K. *Nat. Chem.* **2018**, *10*, 953–960.
- (17) Blakemore, D. C.; Castro, L.; Churcher, I.; Rees, D. C.; Thomas, A. W.; Wilson, D. M.; Wood, A. *Nat. Chem.* **2018**, *10*, 383–394.
- (18) a) Atul, G.; Amit, K.; Ashutosh, R. *Chem. Rev.* **2013**, *113*, 1614–1640; b) Radadiya, A.; Shah, A. *Eur. J. Med. Chem.* **2015**, *97*, 356–376.

- (19) a) Klayman, D. L. *Science* **1985**, 228, 1049–1055; b) Dondorp, A. M. et al., *N. Engl. J. Med.* **2009**, 361, 455–467.
- (20) Montgomery, C. T.; Cassels, B. K.; Shamma, M. *J. Nat. Prod.* **1983**, 46, 441–453.
- (21) Salaski, E. J. et al., *J. Med. Chem.* **2009**, 52, 2181–2184.
- (22) a) Tomaszewski, Z. et al., *J. Med. Chem.* **2005**, 48, 926–934; b) Nevagi, R. J.; Dighe, S. N. *Eur. J. Med. Chem.* **2015**, 97, 561–581; c) Zhang, S.; Zhen, J.; Reith, M. E. A.; Dutta, A. K. *Bioorg. Med. Chem.* **2004**, 12, 6301–6315; d) Zhang, S.; Reith, M. E. A.; Dutta, A. K. *Bioorg. Med. Chem. Lett.* **2003**, 13, 1591–1595.
- (23) The racemization barrier for 3,4-oxacyclohexadiene (**31**) was calculated to be 15.2 kcal/mol (ω B97XD/6-311+G(d,p)/SMD(MeCN)). In comparison, the racemization barrier for 3,4-azacyclohexadiene was found to be 14.7 kcal/mol.
- (24) Himeshima, Y.; Sonoda, T.; Kobayashi, H. *Chem. Lett.* **1983**, 12, 1211–1214.
- (25) Shah, T. K.; Medina, J. M.; Garg, N. K. *J. Am. Chem. Soc.* **2016**, 138, 4948–4954.
- (26) See section A4.7 for details.
- (27) Recently, an innovative approach to a 1,2-cyclohexadiene precursor was reported; see: Inoue, K.; Nakura, R.; Okano, K.; Mori, A. *Eur. J. Org. Chem.* **2018**, 3343–3347.
- (28) In the absence of a trapping partner, (2+2) dimerization of the allene is observed.
- (29) Christl, M.; Fischer, H.; Arnone, M.; Engels, B. *Chem. Eur. J.* **2009**, 15, 11266–11272.
- (30) Behenna, D. C. et. al., *Chem. Eur. J.* **2011**, 17, 14199–14223.

- (31) For recent examples, see: a) Vita, M. V.; Caramenti, P.; Waser, J. *Org. Lett.* **2015**, *17*, 5832–5835; b) Hong, A. Y.; Bennett, N. B.; Krout, M. R.; Jensen, T.; Harned, A. M.; Stoltz, B. M. *Tetrahedron* **2011**, *67*, 10234–10248; c) Kondo, H.; Maeno, M.; Hirano, K.; Shibata, N. *Chem. Commun.* **2018**, *54*, 5522–5525; d) Skardon-Duncan, J.; Sparenberg, M.; Bayle, A.; Alexander, S.; Stephen, C. J. *Org. Lett.* **2018**, *20*, 2782–2786; e) Zhang, Z.-W.; Wang, C.-C.; Xue, H.; Dong, Y.; Yang, J.-H.; Shouxin, L.; Wen-Qing, L.; Wei-Dong, Z. *Org. Lett.* **2018**, *20*, 1050–1053; f) Lian, W.-F.; Wang, C.-C.; Kang, H.-P.; Li, H.-L.; Feng, J.; Liu, S.; Zhang, Z.-W. *Tetrahedron Lett.* **2017**, *58*, 1399–1402.
- (32) Another plausible explanation for **73** being obtained in diminished ee is that racemization of **71** occurs more readily than the nitron cycloaddition. However, the kinetic barriers for nitron and Diels–Alder cycloadditions on related systems have been calculated to be roughly 14 kcal / mol and 19 kcal / mol, respectively (see references 11a and 16). Since the Diels–Alder cycloaddition appears to be a more challenging process, yet proceeds with complete enantiospecificity, we disfavor racemization of **71** as being the cause of partial loss of ee in the case of **73**.

CHAPTER 3

Concise Total Syntheses of (–)-Jorunnamycin A and (–)-Jorumycin

Enabled by Asymmetric Catalysis[†]

3.1 INTRODUCTION

The bis-tetrahydroisoquinoline (bis-THIQ) natural products have been studied intensively by chemists and biologists alike during the 40+ years since their initial discovery due to their intriguing chemical structures, potent biological

[†] This research was performed in collaboration with Dr. Eric R. Welin, Dr. Max Klatte, Dr. Guillaume Lapointe, Dr. Gerit M. Pototschnig, Dr. Martina S. J. McDermott, Dr. Dylan Conklin, Dr. Christopher D. Gilmore, Dr. Pamela M. Tadross, Dr. Christopher K. Haley, Dr. Kenji Negoro, Dr. Emil Glibstrup, Dr. Christian Grünanger, Dr. Kevin M. Allan, and Dr. Scott C. Virgil. Portions of this chapter have been reproduced with permission from Welin, E. R.; Ngamnithiporn, A.; Klatte, M.; Lapointe, G.; Pototschnig, G. M.; McDermott, M. S. J.; Conklin, D.; Gilmore, C. D.; Tadross, P. M.; Haley, C. K.; Negoro, K.; Glibstrup, E.; Grünanger, C. U.; Allan, K. M.; Virgil, S. C.; Slamon, D. J.; Stoltz, B. M. *Science*. **2019**, 363, 270–275 © 2019 The American Association for the Advancement of Science.

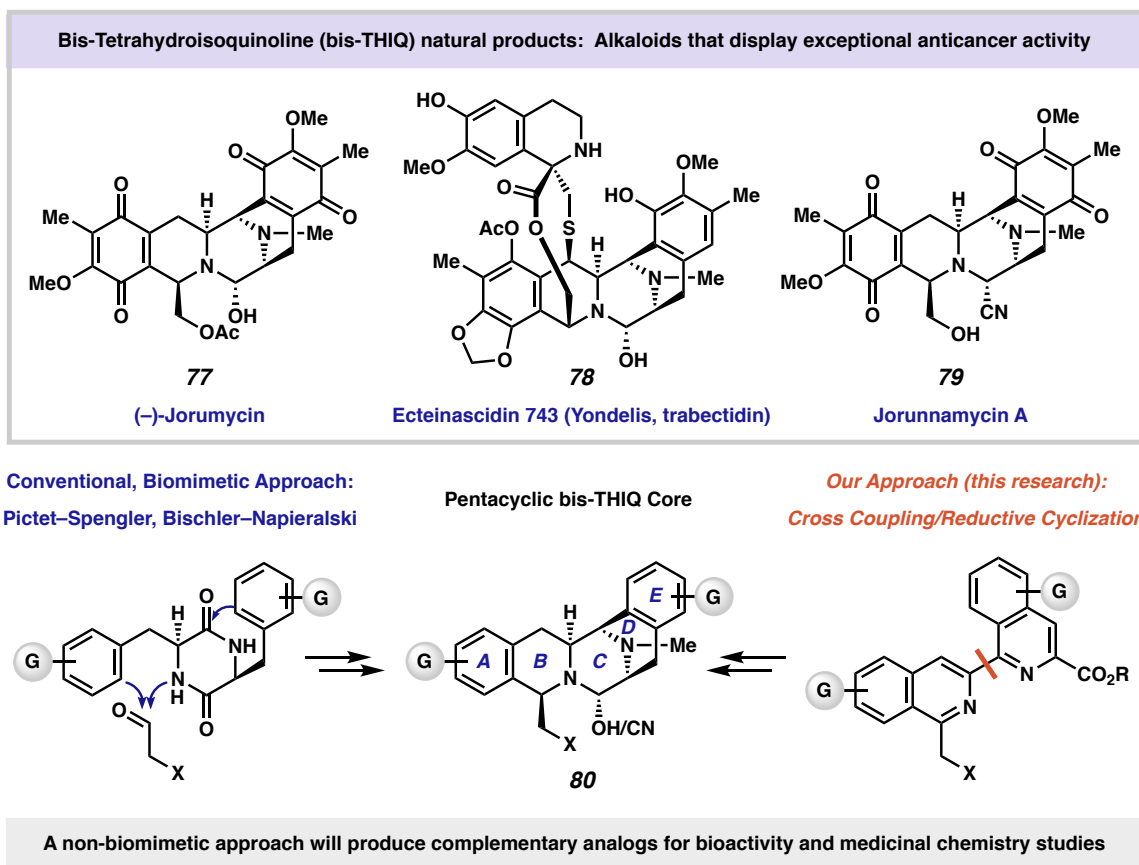
activities, and unique mechanisms of action.^{1,2} Jorumycin (**77**, Figure 3.1) and its congeners ecteinascidin 743 (Et 743, **78**) and jorunnamycin A (**79**) possess a pentacyclic carbon skeleton, highly oxygenated ring termini, and a central proiminium ion (manifested either as a carbinolamine or an α -aminonitrile motif). This latter functionality serves as an alkylating agent *in vivo*, resulting in covalent modification of DNA in a process that ultimately leads to cell death.³ The promise of these natural products as anticancer agents has been realized in the case of Et 743 (Yondelis[®], trabectedin), which has been approved in the United States, Europe, and elsewhere for the treatment of a variety of drug-resistant and unresectable soft-tissue sarcomas and ovarian cancer.³ Although **78** is available from nature, isolation of one gram of the drug would require more than one ton of biological material. For this reason, the successful application of **78** as an antitumor agent has necessitated its large-scale chemical synthesis, a 21-step process that begins with cyanosafracin A, a fermentable and fully functionalized bis-THIQ natural product.⁴ This has restricted medicinal chemistry endeavors through this route to the production of only compounds with a high degree of similarity to the natural products themselves.

Although **77** and **79** possess quinone rings, these moieties are rapidly reduced in cells to their hydroquinone oxidation states, more closely resembling those of **78**.⁵ These highly electron-rich functional groups are key components in the biosynthetic pathways of the bis-THIQ's, which are forged by the action of Pictet–Spenglerase enzymes.^{6,7} Previously reported chemical syntheses of bis-THIQ natural products feature elegant and creative application of electrophilic aromatic substitution (EAS) chemistry for the construction of one or more of the

THIQ motifs. Though highly enabling, this approach has also limited the synthesis of non-natural analogs to highly natural product-like derivatives. As a key example, despite the scores of analogs produced over the past few decades,^{8,9,10,11} the majority of the derivatives focus on substitution of the heteroatom moiety appended to the B-ring (cf. structure **80**, Figure 3.1), and only a select few possess significant structural and substitutional variation around the aromatic or quinone A- and E-rings.^{8–11} Furthermore, derivatives possessing electron-withdrawing groups on these rings are inaccessible using biomimetic approaches, as these would inhibit the EAS chemistry used to construct the THIQs. This latter point is significant, as studies have indicated that the smaller bis-THIQ natural products such as **77** and **79** are more susceptible to metabolic degradation than Et 743 and other larger bis-THIQs,^{12,13} and the installation of electron-withdrawing groups is a commonly employed strategy to improve a drug molecule's metabolic stability.¹⁴

Jorumycin has been the target of four total syntheses^{15,16,17,18} and two semisyntheses^{19,20} since its isolation in 2000,²¹ and jorunnamycin A has frequently been prepared en route. Jorumycin displays IC₅₀'s of 0.24 nM vs. A549 lung cancer, 0.49 nM vs. DU145 prostate cancer, and 0.57 nM vs. HCT116 colon cancer,^{17,19,21} among others, thus offering immense therapeutic potential. Furthermore, jorumycin and jorunnamycin A are appealing targets for further synthetic elaboration: the oxygen substitution appended to the B-ring (cf. structure **80**, X = OH, Figure 3.1) could allow rapid diversification to the ecteinascidin, saframycin, safracin, and renieramycin scaffolds.¹ To overcome the limitations of the current state of the art with respect to analog diversity, we sought an alternative, non-biomimetic route to these natural products.

Figure 3.1 Bis-tetrahydroisoquinoline natural products.

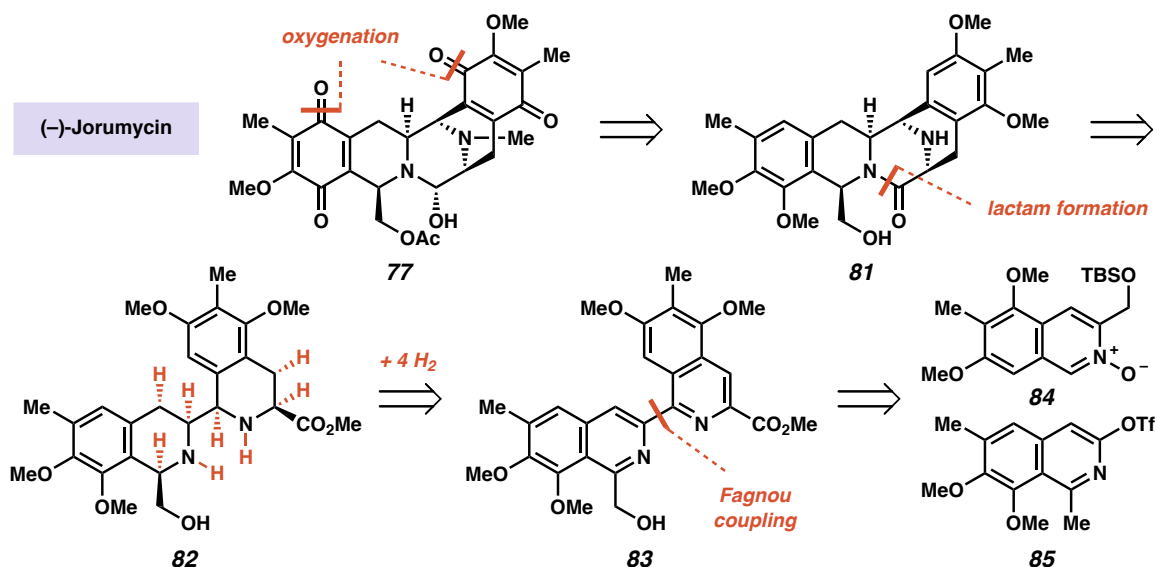


3.2 GENERAL SYNTHETIC STRATEGY

Specifically, we envisioned the retrosynthetic strategy shown in Scheme 3.1. We posited that a late stage oxygenation event to provide jorumycin (**77**) would greatly simplify the construction of the precursor, pentacycle **81**. We then considered disconnection of the central C-ring (cf. Figure 3.1) through cleavage of the lactam moiety in **81**, providing bis-THIQ compound **82**. Critically, bis-THIQ structure **82** was recognized as a potential product of an enantioselective hydrogenation of bis-isoquinoline **83**. The central biaryl bond of **83** could be formed through a C–H cross-coupling reaction, leading to isoquinoline monomers **84** and **85**, thus greatly simplifying the

synthetic challenge. As a key advantage, isoquinolines **84** and **85** could be prepared through the application of any known method, not limited only to those requiring highly electron-rich and π -nucleophilic species. Crucially, this approach would allow access to the natural products themselves, as well as derivatives featuring substantial structural and/or electronic variation.

Scheme 3.1 Retrosynthesis of (–)-jorumycin.

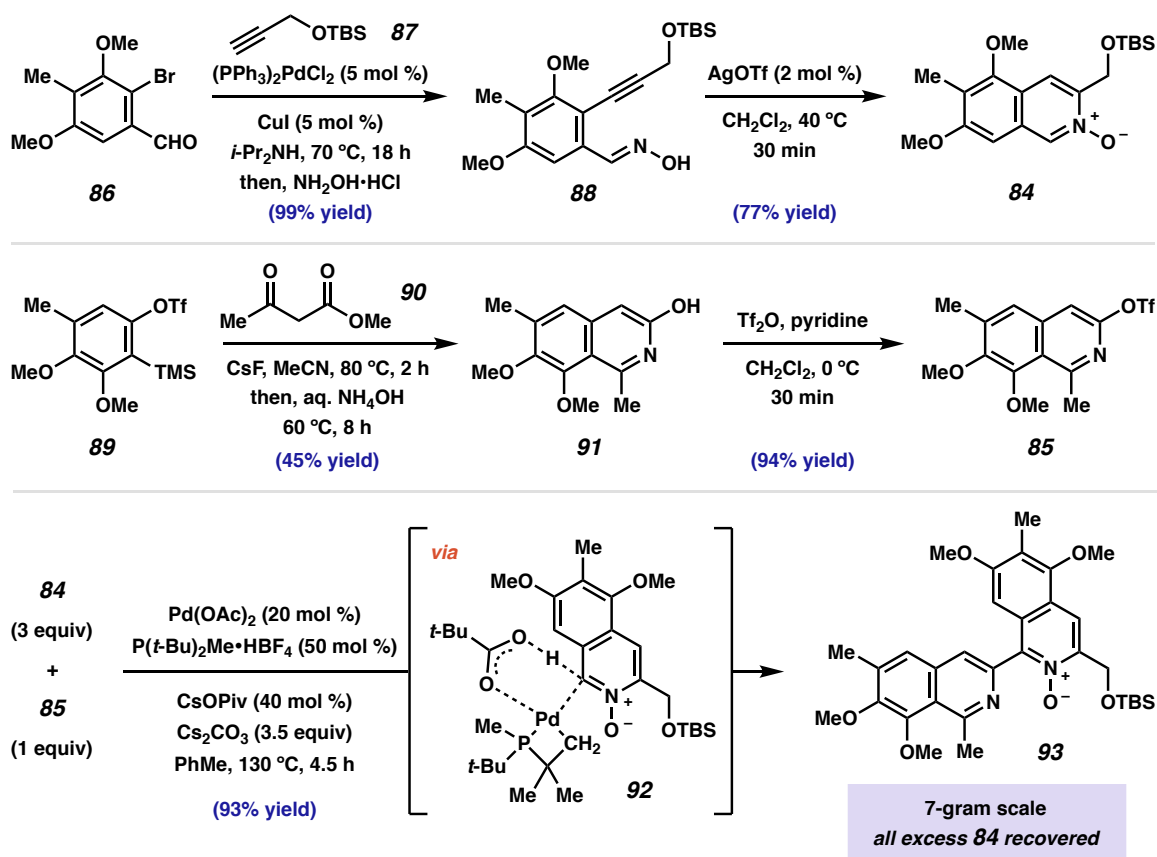


3.3 TOTAL SYNTHESIS OF JORUMYCIN

As shown in Scheme 3.2, we initiated our synthetic studies with the Sonogashira coupling of aryl bromide **86** (available in two steps from 3,5-dimethoxybenzaldehyde, see Experimental Section) with *tert*-butyldimethylsilyl propargyl ether (**87**); simply adding solid hydroxylamine hydrochloride to the reaction mixture after the coupling provided oxime-bearing alkyne **88** in 99% yield. Catalytic silver(I) triflate activated the alkyne toward nucleophilic attack by the oxime, directly generating isoquinoline *N*-oxide **84** in 77% yield on up to a 12-gram scale.²² Next, we began our synthesis of isoquinoline

triflate **85** by using aryne-based methodology developed in our laboratories.²³ Silyl aryl triflate **89** (available in 3 steps from 2,3-dimethoxytoluene, see Experimental Section) was treated with cesium fluoride to generate the corresponding aryne intermediate *in situ* (not shown), which underwent aryne acyl-alkylation with *in situ* condensation to provide 3-hydroxy-isoquinoline **91** in 45% yield. Reaction with trifluoromethanesulfonic anhydride provided electrophilic coupling partner **85** in 94% yield.

Scheme 3.2 Synthesis of isoquinoline monomers **84** and **85** and Fagnou coupling.



With working routes to both isoquinoline monomers in hand, we turned our attention to the palladium-catalyzed cross-coupling reaction which would be used to construct the carbon skeleton of jorumycin. We were pleased to find that isoquinolines **84** and **85** were efficiently coupled under modified conditions developed by Fagnou and co-

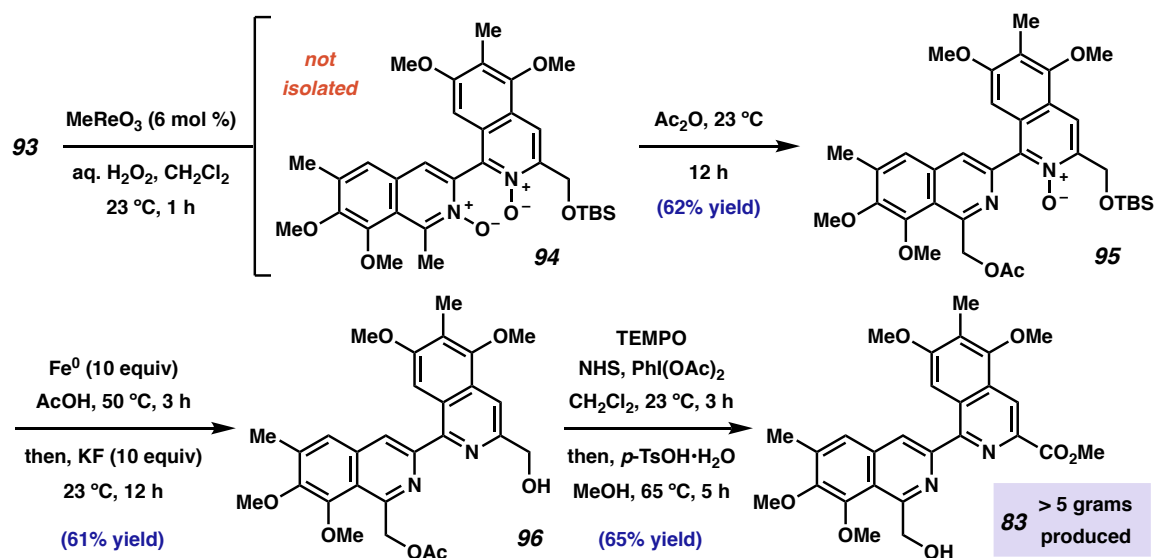
workers to provide bis-isoquinoline **93** in 94% yield on a 7-gram scale.²⁴ This large-scale application of C–H activation likely proceeds through a transition state similar to **92** and allows for the direct construction of **93** without the need for prefunctionalization.²⁵ The excess of *N*-oxide **84** required to achieve maximum levels of efficiency appears to be only a kinetic factor, as all excess **84** was recovered after the reaction.

At this stage, we sought to install the level of oxidation necessary to initiate our hydrogenation studies (Scheme 3.3). Specifically, this required selective oxidation of the nitrogen-adjacent methyl and methylene groups on the B- and D-rings, respectively. We attempted a double-Boekelheide rearrangement to transpose the *N*-oxidation to both *C*-positions simultaneously, effecting formal C–H oxidation reactions.²⁶ Unfortunately, after oxidation to intermediate bis-*N*-oxide **94**, only the B-ring azine underwent rearrangement. Despite this setback, we found that it was possible to parlay this reactivity into a one-pot protocol by adding acetic anhydride upon complete oxidation, providing differentially protected diol **95** in 62% yield. N–O bond cleavage and oxyl-mediated oxidation provided bis-isoquinoline **83** in two additional steps. To date, we have produced more than 5 grams of bisisoquinoline **83**.

With a scaleable route to isoquinoline **83** in hand, we turned our attention to the key hydrogenation event. If successful, this strategic disconnection would add four molar equivalents of hydrogen, create four new stereocenters, and form the central C-ring lactam. Although the enantioselective hydrogenation of nitrogen-based heterocycles is a well-studied reaction, isoquinolines are possibly the most challenging and least investigated substrates.²⁷ To our knowledge only four reports existed prior to our studies

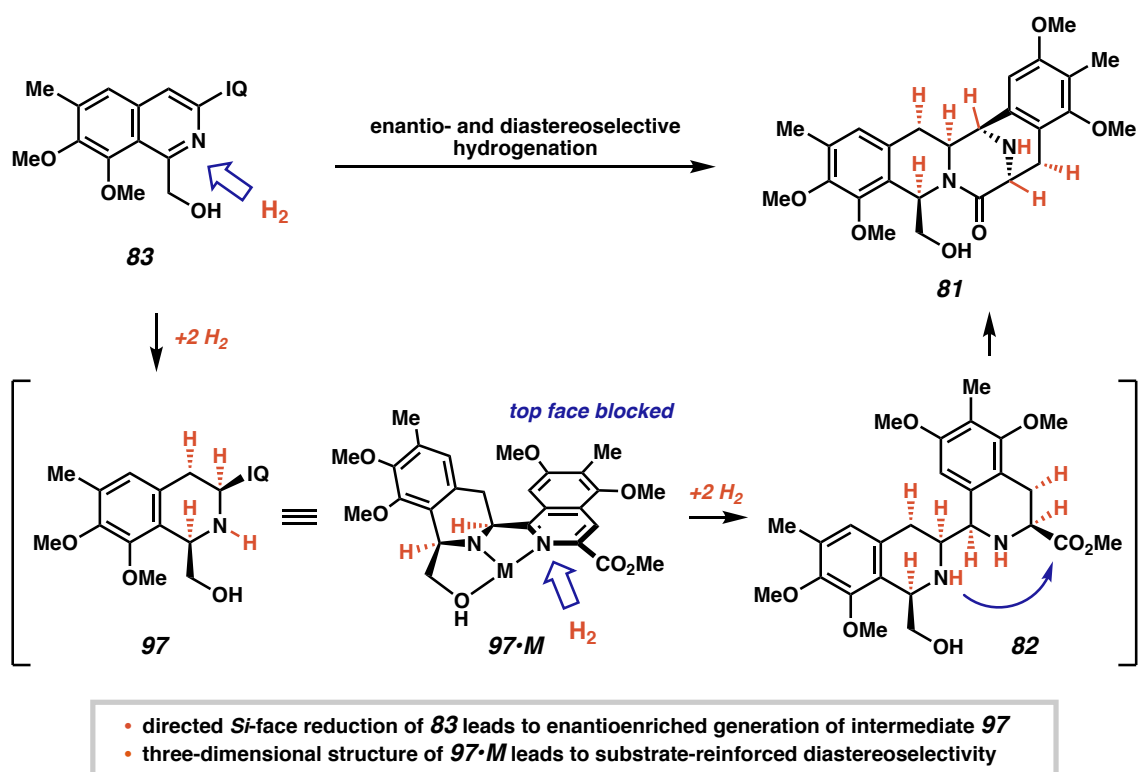
that describe asymmetric isoquinoline hydrogenation, and only one appears to tolerate 1,3-disubstitution patterns.^{28,29,30,31}

Scheme 3.3 Synthesis of hydrogenation precursor **83**.



We nonetheless noted that metal-catalyzed imine and carbonyl reduction is a comparatively successful and well-studied transformation.^{32,33} We were drawn to the iridium catalyst developed by scientists at Ciba-Geigy (now Syngenta) for asymmetric ether-directed imine reduction in the preparation of Metolachlor.³⁴ Considering the positioning of the hydroxymethyl group appended to the B-ring of **83** and the electronic similarity of the adjacent C1–N π -bond to that of an imine, we posited that a similar catalytic system might be used to direct the initial reduction to this position (Scheme 3.4). Furthermore, the chelation mode was attractive as a scaffolding element to enable enantioselective *Si*-face reduction. In keeping with previous observations,^{28–31} we anticipated that full B-ring reduction would provide *cis*-mono-THIQ **97** as the major product. We believed that **97** would then act as a tridentate ligand for a metal ion (although not necessarily the catalytically active species), and the three-dimensional

Scheme 3.4 Stereochemical rationale for the hydrogenation of bis-isoquinoline **83**.

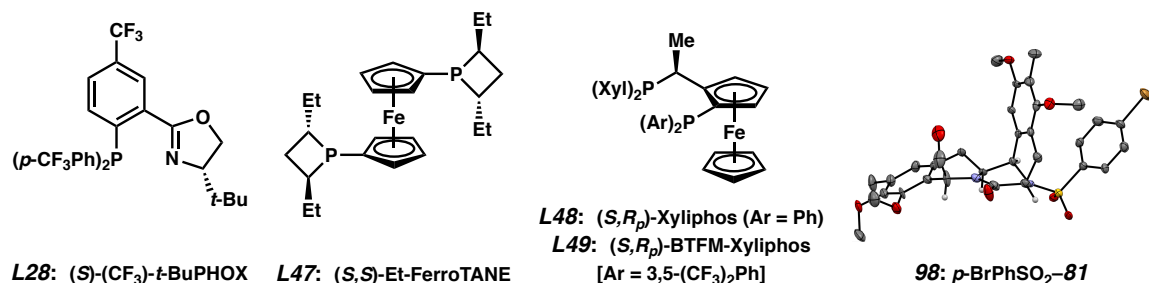


Upon beginning our enantioselective hydrogenation studies, we found that we could identify trace amounts of conversion to mono-THIQ product **97** by using the catalyst mixture developed at Ciba-Geigy,³⁴ thus confirming the accelerating effects of the pendent hydroxy directing group. Under these general conditions, we then performed a broad evaluation of more than 60 chiral ligands commonly used in enantioselective catalysis protocols (see section 3.6.4). From this survey, we identified three ligands that

provided **97** in at least 80% enantiomeric excess (ee) and with uniformly excellent diastereoselectivity (all >20:1 diastereomeric ratio, dr): (*S*)-(CF₃)-*t*-BuPHOX (**L28**, Table 3.1, Entry 2, 22% yield, –82% ee), (*S,S*)-Et-FerroTANE (**L47**, Entry 3, 26% yield, –87% ee), and (*S,R_P*)-Xyliphos (**L48**, Entry 4, 30% yield, 80% ee). After evaluating these ligand classes further, we identified (*S,R_P*)-BTfM-Xyliphos (**L49**)³⁵ as a strongly activating ligand that provided mono-THIQ **97** in 83% yield, >20:1 dr, and in a remarkable 94% ee (Entry 5). Moreover, we were elated to find that ligand **L49** formed a catalyst that provided pentacycle **81** as a single diastereomer in 10% yield. Further evaluation of the reaction parameters revealed that increasing temperature provided higher levels of reactivity, albeit at the expense of enantioselectivity (Entry 6, 31% yield of **97**, 87% ee, 43% yield of **81**). The best results were achieved by performing the reaction at 60 °C for 18 hours, and then increasing the temperature to 80 °C for 24 hours. Under these conditions, **81** was isolated in 59% yield with >20:1 dr and 88% ee (Entry 7).³⁶ In the end, doubling the catalyst loading allowed us to isolate **81** in 83% yield, also with >20:1 dr and 88% ee (Entry 8) on greater than 1 mmol scale. bis-THIQ **81** could be easily accessed in enantiopure form (>99% ee by HPLC) by crystallization from a slowly evaporating acetonitrile solution, and we were able to confirm the relative and absolute stereochemistry by obtaining an x-ray crystal structure on corresponding 4-bromophenyl sulfonamide **98**. In the context of this synthesis, the relatively high catalyst loading (20 mol % Ir) is mitigated by the substantial structural complexity generated in this single transformation.

Table 3.1 Optimization of the hydrogenation reaction.^a

entry	catalyst loading	ligand	temperature	yield 97 ^b	ee 97 ^c	yield 81 ^b	dr 81 ^d	ee 81 ^c
1	5 mol %	L48	23 °C	2%	ND	0%	--	--
2	5 mol %	L28	60 °C	22%	–82%	0%	--	--
3	5 mol %	L47	60 °C	26%	–87%	0%	--	--
4	5 mol %	L48	60 °C	30%	80%	0%	--	--
5	5 mol %	L49	60 °C	83%	94%	10%	>20:1	ND
6	5 mol %	L49	80 °C	31%	87%	43%	>20:1	ND
7	5 mol %	L49	60 °C → 80 °C ^e	7%	94%	59% ^f	>20:1	88%
8	10 mol %	L49	60 °C → 80 °C ^e	3%	94%	83% ^f	>20:1	88% (>99%) ^g

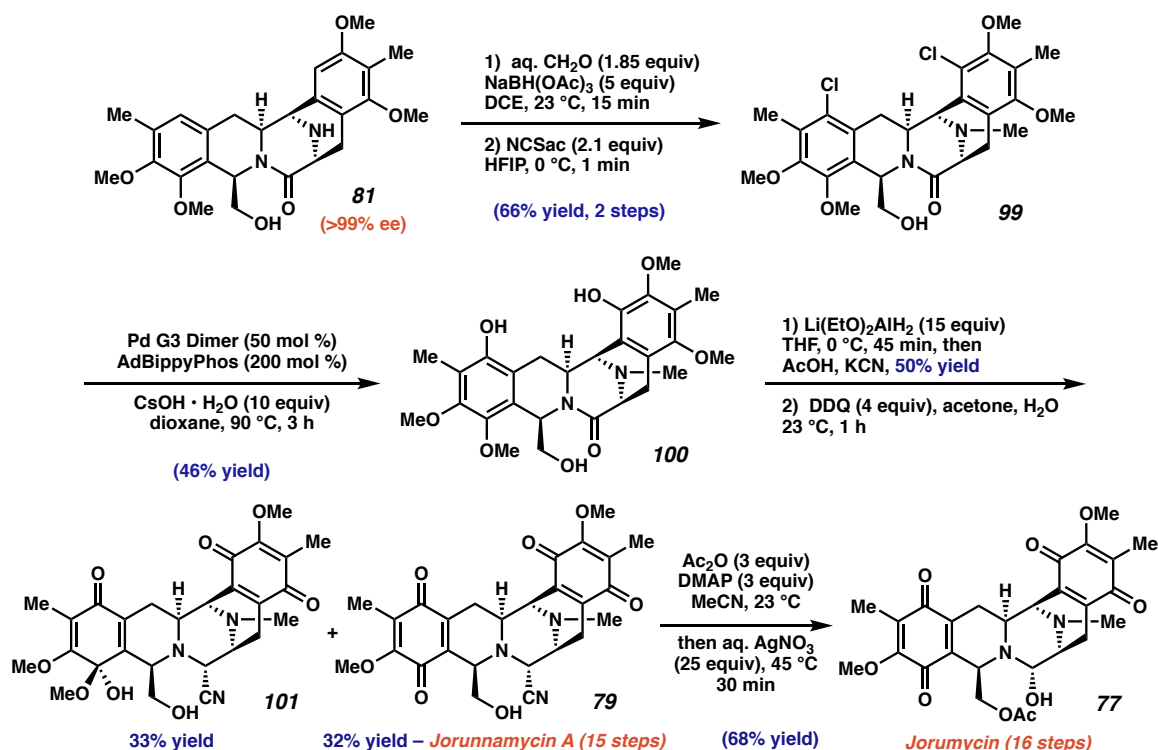


[a] Reactions performed in 9:1 toluene:acetic acid (0.02 M) using a 1.2:1 ligand:metal ratio and a 3:1 iodide:metal ratio under a hydrogen atmosphere (60 bar) for 18 h. [b] Measured by UHPLC-MS UV absorption vs. 1,3,5-trimethoxybenzene internal standard unless otherwise noted. [c] Measured by chiral HPLC analysis. [d] Measured by ¹H-NMR analysis of the crude reaction mixture. [e] Reaction performed at 60 °C for 18 h, then the temperature was raised to 80 °C and maintained at that temperature for 24 h. [f] Yield of isolated product after column chromatography using 10.5 mol % **L49** in entry 7 and 21 mol % **L49** in entry 8. [g] After one recrystallization.

At this stage, we were poised to investigate the third and final key disconnection from our retrosynthetic analysis, namely, late-stage C–H oxidation of the arenes (Scheme 3.5). To set up this chemistry the piperazinone N–H of **81** was methylated under reductive amination conditions in quantitative yield. Despite numerous attempts to effect catalytic C–H oxidation on this advanced intermediate, we found that a two-step procedure was necessary instead. We were able to chlorinate both of the remaining

aromatic positions, providing bis-THIQ **99** in 68% yield. From here, we once again turned to catalysis, this time for the oxygenation of aryl halides. After extensive investigation, we found that Stradiotto and coworkers' recently developed protocol for the hydroxylation of aryl halides was uniquely effective.³⁷ Further optimization revealed that the combination of adamantyl BippyPhos ligand with Buchwald's cyclometalated palladium(II) dimer was ideal,³⁸ providing dihydroxylated bis-THIQ **100** in 46% yield, an impressive result for such a challenging coupling reaction on a sterically large, electron-rich, and Lewis-basic substrate in the final stages of the synthesis. Partial lactam reduction with cyanide trapping proceeded in 50% yield, and oxidation of the phenols provided jorunnamycin A (**79**) in only 15 linear steps. We isolated hemiacetal **101** in 33% yield, which was surprising given the generally low stability of acyclic hemiacetals.

Scheme 3.5 Completion of jorunnamycin A and jorumycin.



Finally, we developed conditions for the conversion of jorunnamycin A into jorumycin in a single step, providing **77** in 68% yield in 16 linear steps (Scheme 3.4). Jorunnamycin A (**79**) and jorumycin (**77**) are produced in 0.24% and 0.17% yield, respectively, from commercially available materials, but key bis-THIQ **81**, the branching point for derivative synthesis, is accessed over 10 steps in 5.0% overall yield on greater than 500 mg scale. These efforts are similar to Zhu and coworkers' elegant synthesis of jorumycin with regard to brevity.¹⁶

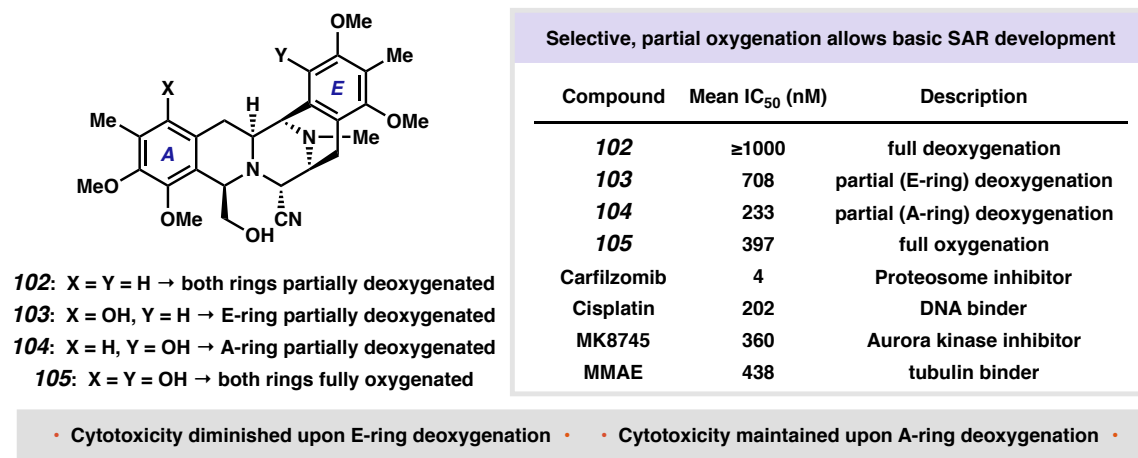
3.4 BIOLOGICAL EVALUATION OF BIS-THIQ ANALOGS

Central to the anticancer activity of the bis-THIQ natural products is the capacity to alkylate DNA upon loss of water or cyanide from the central carbinolamine or α -cyanoamine, respectively.³⁹ After alkylation, compelling evidence suggests that formation of reactive oxygen species⁵ or DNA-protein cross-links^{8,40} leads to cell-cycle arrest or cell death. We therefore synthesized analogs **102–105**, which feature the non-oxygenated framework as well as all permutations of partial and full oxygenation. The activity of this series would allow us to determine the relative importance of the location and degree of oxygenation on the A- and E-rings, the structure-activity relationships of which have not previously been explored.

With the backdrop that preclinical efficacy studies are complex and demanding, we conducted preliminary studies to probe the relative cytotoxicity of synthetic analogues **102–105** and established that modifying one site on the scaffold greatly diminishes cytotoxicity, whereas other modifications conserved cytotoxicity. The cytostatic and cytotoxic properties of **102–105** were determined using long-term, growth-maximizing

assay conditions against 29 cancer cell lines known to be responsive in vitro to other general cytotoxics (Figure 3.2, also see section 3.6.6).^{41,42} Cells were routinely assessed for mycoplasma contamination using a multiplex PCR method and STR profiling for cell-line authentication. This methodology differs markedly from the standard 72-hour, luminescence-based cytotoxicity assays employed most commonly for in vitro quantification of drug response. This approach was chosen as it is specifically well suited to determine the activity of compounds wherein anti-proliferative effects occur over a longer time period than standard cytotoxic agents. Perhaps not surprisingly, removal of both phenolic oxygens resulted in a complete loss in activity (i.e., **102**, all IC₅₀'s > 1 μM), while fully oxygenated bis-THIQ **105** showed cytotoxicity. The most notable results were provided by **103** and **104**, which possess A- and E-ring monohydroxylation, respectively. While compound **103**, which is devoid of E-ring oxygenation, showed diminished activity, we were surprised to find that compound **104** featuring only E-ring oxygenation maintained a similar activity profile to fully oxygenated **105** (see section 3.6.6). At the moment, we believe these data to be the result of general cytotoxicity, as opposed to cancer cell-specific activity. As a reference, three out of four previously known anticancer agents that function through general cytotoxicity showed similar levels of activity in our model. While more sophisticated studies are necessary to determine actual efficacy, the ability to delete one oxygen atom and retain activity is both intriguing and unexpected.

Figure 3.2 Biological evaluation of non-natural analogs.



3.5 CONCLUSIONS

In conclusion, we have developed a synthesis of (–)-jorumycin (**77**) that is orthogonal to existing bis-THIQ syntheses, obviating the need for highly electron-rich and π -nucleophilic aromatic rings. The synthesis relies on an unprecedented combination of C–H cross-coupling assembly followed by asymmetric hydrogenation with self-reinforcing diastereoselectivity to afford the skeleton of the bis-THIQ from relatively simple, achiral precursors. This will allow for the development of electron-deficient analogs that could be more metabolically stable than the natural products themselves. These analogs will have the potential to extend the still-largely untapped therapeutic potential of the bis-THIQ family of natural products.

3.6 EXPERIMENTAL SECTION

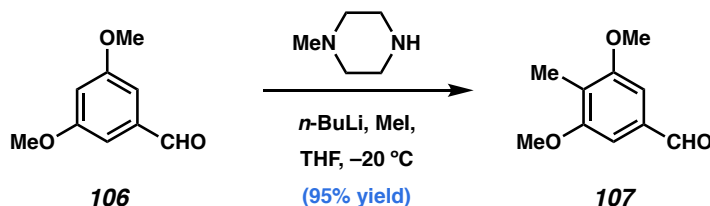
3.6.1 MATERIALS AND METHODS

Unless stated otherwise, reactions were performed at ambient temperature (23 °C) in flame-dried glassware under an argon atmosphere using dry, deoxygenated solvents (distilled or passed over a column of activated alumina).⁴³ Commercially available reagents were used as received. Reactions requiring external heat were modulated to the specified temperatures using an IKAmag temperature controller. Thin-layer chromatography (TLC) was performed using E. Merck silica gel 60 F254 pre-coated plates (0.25 mm) and visualized by UV fluorescence quenching or potassium permanganate staining. Silicycle SiliaFlash P60 Academic Silica gel (particle size 40–63 μm) was used for flash chromatography. Purified water was obtained using a Barnstead NANOpure Infinity UV/UF system. ^1H and ^{13}C NMR spectra were recorded on a Varian Inova 500 (500 MHz and 125 MHz, respectively) and a Bruker AV III HD spectrometer equipped with a Prodigy liquid nitrogen temperature cryoprobe (400 MHz and 100 MHz, respectively) and are reported in terms of chemical shift relative to CHCl_3 (δ 7.26 and 77.16, respectively). ^{19}F and ^{31}P NMR spectra were recorded on a Varian Inova 300 (282 MHz and 121 MHz, respectively). Data for ^1H NMR spectra are reported as follows: chemical shift (δ ppm) (multiplicity, coupling constant, integration). Infrared (IR) spectra were recorded on a Perkin Elmer Paragon 1000 Spectrometer and are reported in frequency of absorption (cm^{-1}). Analytical chiral SFC was performed with a Mettler SFC supercritical CO_2 analytical chromatography system with Chiralpak (AD-H) or Chiracel (OD-H) columns obtained from Daicel Chemical Industries, Ltd. High resolution mass spectra (HRMS) were obtained from the Caltech Center for Catalysis and Chemical

Synthesis using an Agilent 6200 series TOF with an Agilent G1978A Multimode source in mixed (Multimode ESI/APCI) ionization mode. Optical rotations were measured on a Jasco P-2000 polarimeter using a 100 mm path-length cell at 589 nm. For X-Ray structure determination (see Appendix 6), low-temperature diffraction data were collected on a Bruker AXS D8 VENTURE KAPPA diffractometer coupled to a PHOTON 100 CMOS detector with *K* radiation ($\lambda = 1.54178 \text{ \AA}$) from an I μ S micro-source for the structure of compound P17208. The structure was solved by direct methods using SHELXS⁴⁴ and refined against F^2 on all data by full-matrix least squares with SHELXL-2014⁴⁵ using established refinement techniques.⁴⁶ All non-hydrogen atoms were refined anisotropically. All hydrogen atoms were included into the model at geometrically calculated positions and refined using a riding model. The isotropic displacement parameters of all hydrogen atoms were fixed to 1.2 times the *U* value of the atoms they are linked to (1.5 times for methyl groups). Unless otherwise noted, all disordered atoms were refined with the help of similarity restraints on the 1,2- and 1,3-distances and displacement parameters as well as rigid bond restraints for anisotropic displacement parameters. Compound P17208 crystallizes in the orthorhombic space group $P2_12_12$ with one molecule in the asymmetric unit along with two molecules of isopropanol. The hydroxide group and both isopropanol molecules were disordered over two positions. The Flack parameter refines to be 0.138(9).

3.6.2 EXPERIMENTAL PROCEDURES AND SPECTROSCOPIC DATA

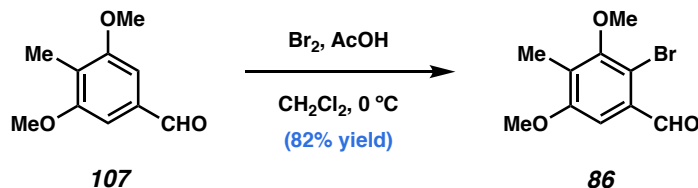
3.6.2.1 Synthesis of isoquinoline N-oxide



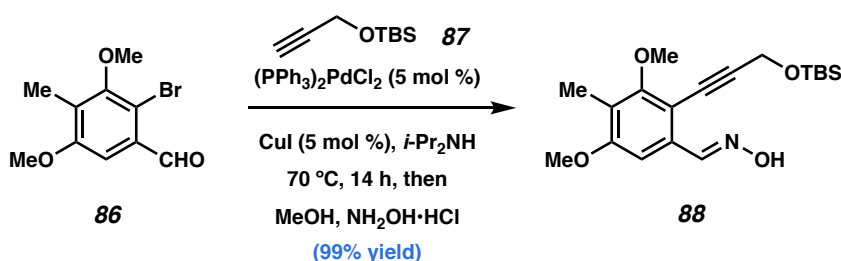
Note: This procedure could be readily increased to 10 g scale with minimal loss in yield.

3,5-dimethoxy-4-methylbenzaldehyde (107): The procedure was adapted from the method of Comins *et al.*⁴⁷ *N*-methylpiperazine (670 μ L, 6.6 mmol, 1.1 equiv) was dissolved in 20 mL THF and cooled to -20 °C. *n*-Butyllithium (2.4 M, 2.65 mL, 6.3 mmol, 1.05 equiv) was added in a dropwise fashion, resulting in an orange solution. The solution was stirred at this temperature 15 min before a solution of 3,5-dimethoxybenzaldehyde (**106**, 1.00 g, 6.0 mmol, 1 equiv) in 3 mL THF was added in a dropwise fashion, causing a color change to yellow. The solution was stirred at this temperature 30 min before a second portion of *n*-butyllithium (2.4 M, 7.5 mL, 18.1 mmol, 3 equiv) was added in a dropwise fashion. At this point, the flask was stored in a -20 °C freezer for 24 h. The flask was re-submerged in a -20 °C bath, and freshly distilled methyl iodide (2.25 mL, 36.1 mmol, 6 equiv) was added in a dropwise fashion, resulting in a mild exotherm. The solution was stirred 30 min at -20 °C and was removed from its bath, warming to room temperature. After 30 min, the reaction was quenched by the addition of 20 mL 0.5 M HCl, and the solution was stirred 30 min open to air. The layers were separated and the aqueous phase was saturated with sodium chloride. The aqueous phase was extracted with Et₂O, dried over MgSO₄, and concentrated. The

product was purified by column chromatography (10% EtOAc/hex). Colorless solid, 1.03 g, 5.72 mmol, 95% yield. NMR spectra were identical to the previously reported compound.⁴⁷ ¹H NMR (400 MHz, CDCl₃) δ 9.88 (s, 1H), 7.03 (s, 2H), 3.87 (s, 6H), 2.14 (s, 3H); ¹³C NMR (100 MHz, CDCl₃) δ 192.0, 158.7, 135.1, 122.5, 104.7, 55.9, 9.0.

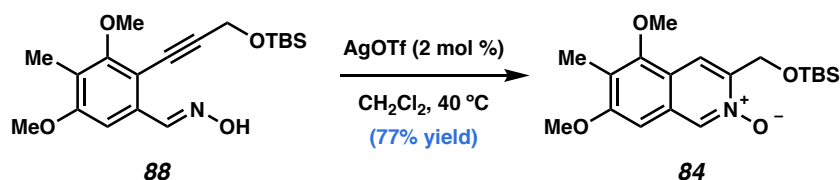


2-Bromo-3,5-dimethoxy-4-methylbenzaldehyde (86): Aldehyde **107** (8.62 g, 47.8 mmol, 1 equiv) was dissolved in CH₂Cl₂ (100 mL, 0.5 M) and acetic acid (30 μL, 0.5 mmol, 0.01 equiv) was added. The solution was cooled to 0 °C before bromine was added in a slow, dropwise fashion. The solution was stirred 30 min after complete addition at 0 °C, at which time TLC (10% EtOAc/hex) showed complete conversion. The reaction was quenched by the addition of 10% aqueous sodium thiosulfate and saturated NaHCO₃ solution. The layers were separated and the aqueous phase was extracted with CHCl₃. The combined organic phases were washed with water, dried over MgSO₄ and concentrated. The product was purified by dissolving in ~50 mL boiling hexanes, under which conditions the trace amounts of dibromide are insoluble. The solution was filtered while boiling, providing the pure product. Colorless solid, 10.13 g, 39.1 mmol, 82% yield. NMR spectra were identical to the previously reported compound.⁴⁸ ¹H NMR (400 MHz, CDCl₃) δ 10.33 (s, 1H), 7.21 (s, 1H), 3.87 (s, 3H), 3.81 (s, 3H), 2.25 (s, 3H); ¹³C NMR (100 MHz, CDCl₃) δ 191.8, 158.2, 156.2, 132.2, 129.5, 114.9, 106.0, 60.8, 56.1, 10.6.



(E)-2-(3-((tert-butyldimethylsilyl)oxy)prop-1-yn-1-yl)-3,5-dimethoxy-4-methylbenzaldehyde oxime (88): Bromide **86** (19.4 g, 74.9 mmol, 1 equiv), $(PPh_3)_2PdCl_2$ (2.6 g, 3.70 mmol, 0.05 equiv), and CuI (714 mg, 3.75 mmol, 0.05 equiv) were slurried in diisopropylamine (300 mL, 0.25 M, freshly distilled from CaH_2) in a 2 liter 3-necked roundbottom flask, and the orange suspension was sparged with N_2 for 10 min. *O*-tert-butyldimethylsilyl propargyl alcohol (**87**, 17.3 g, 101 mmol, 1.35 equiv)⁴⁹ was added in one portion, causing the suspension to darken as the palladium catalyst was reduced. The suspension was sparged with N_2 for a further 1 min, then heated to $70\text{ }^\circ C$ for 24 h. At this stage, TLC and LCMS indicated complete conversion of bromide **86**, so the suspension was cooled to $50\text{ }^\circ C$ and 200 mL $MeOH$ was added. Hydroxylamine hydrochloride (6.24 g, 89.8 mmol, 1.2 equiv) was added in one portion and the solution was heated to reflux ($85\text{ }^\circ C$) for 2 h. At this stage, TLC and LCMS indicated complete conversion to the product. The solution was cooled to room temperature and celite (~100 g) was added. The suspension was filtered through a pad of celite, topped with sand, eluting with ethyl acetate. The filtrate was concentrated and purified by column chromatography (15% EtOAc/hex). Colorless solid, 26.9 g, 74.1 mmol, 99% yield. 1H NMR (500 MHz, $CDCl_3$) δ 8.60 (s, 1H), 7.46 (s, 1H), 7.10 (s, 1H), 4.62 (s, 2H), 3.86 (s, 6H), 2.15 (s, 3H), 0.95 (s, 9H), 0.18 (s, 6H); ^{13}C NMR (125 MHz, $CDCl_3$) δ 160.5, 158.8, 149.5, 132.8, 122.5, 110.3, 101.9, 96.2, 78.2, 61.0, 55.9, 52.6, 26.0, 18.5, 9.3, –5.0; IR (thin film, NaCl):

3270, 3093, 2997, 1954, 2932, 2896, 2857, 2221, 1611, 1592, 1560, 1464, 1403, 1384, 1331, 1282, 1255, 1218, 1192, 1164, 1137, 1121, 110, 1080, 1035, 977, 904, 838, 780, 722, 704; HRMS (ESI-TOF) calc'd for $[M^+]$ $C_{19}H_{29}NO_4Si$ = 363.1866, found 363.1939.

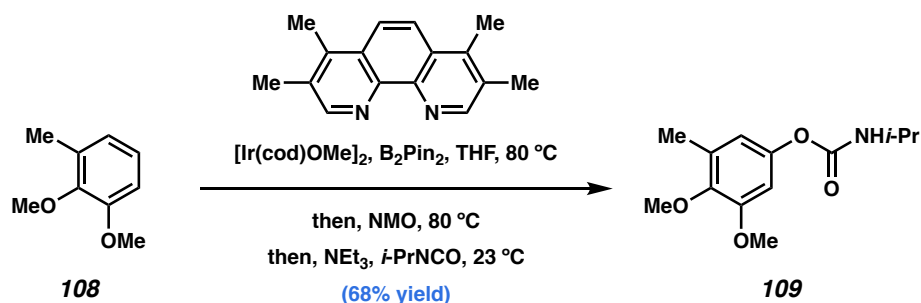


3-(((tert-butyldimethylsilyl)oxy)methyl)-5,7-dimethoxy-6-methylisoquinoline-N-

oxide (84): Oxime **88** (15.92 g, 45.7 mmol, 1 equiv) was dissolved in CH_2Cl_2 (460 mL, 0.1 M) and the flask was vacuum purged and refilled with nitrogen five times, then heated to reflux. AgOTf (235 mg, 0.91 mmol, 0.02 equiv) was added in one portion to the refluxing solution, resulting in a rapid and mildly exothermic reaction. The reaction flask was shielded from light and maintained at reflux for 15 min, at which time LCMS indicated full conversion to the product. The solution was filtered through a 1 inch pad of silica with 500 mL CH_2Cl_2 and 1 L 10% MeOH/EtOAc. Silica gel (40 mL) was added to the second portion of filtrate, which was then concentrated. The product was purified by column chromatography using a 6 inch pad of silica (30–50–100% EtOAc/ CH_2Cl_2 ; then 2–5–10–20% MeOH/EtOAc + 1% NEt_3). Colorless solid, 12.27 g, 33.8 mmol, 77% yield. The product is initially isolated as a black solid that is spectroscopically pure, and can be recrystallized to a colorless solid from minimal boiling heptanes. Very little mass is lost during this process (less than 50 mg from a 12 g batch), indicating the presence of very minor yet highly colored impurities. ^1H NMR (400 MHz, CDCl_3) δ 8.65 (s, 1H), 8.02 (s, 1H), 6.71 (s, 1H), 5.01 (d, J = 1.4 Hz, 2H), 3.92 (s, 3H), 3.87 (s, 3H), 2.27 (s, 3H), 1.00 (s, 9H), 0.15 (s, 6H); ^{13}C NMR (100 MHz, CDCl_3) δ 159.4, 153.7, 145.9, 135.2, 128.4,

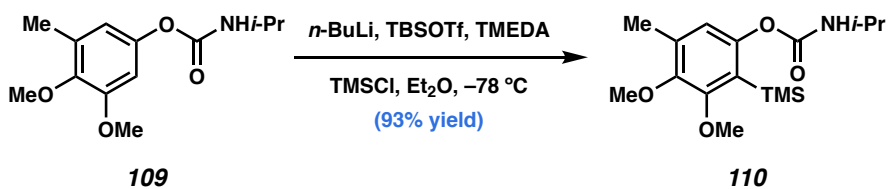
123.6, 120.1, 115.0, 97.4, 61.7, 60.1, 55.9, 26.0, 18.4, 9.8, -5.3; IR (thin film, NaCl): 3390, 3074, 2998, 2954, 2892, 2857, 1637, 1613, 1568, 1471, 1391, 1372, 1341, 1308, 1254, 1210, 1185, 1148, 1116, 1021, 1007, 957, 900, 839, 808, 778, 702, 670, 638; HRMS (ESI-TOF) calc'd for $[M^+]$ $C_{19}H_{29}NO_4Si$ = 363.1866, found 363.1863.

3.6.2.2 Synthesis of isoquinoline triflate



3,4-Dimethoxy-5-methylphenyl isopropylcarbamate (109): In a nitrogen-filled glovebox, $[Ir(cod)OMe]_2$ (22.3 mg, 0.034 mmol, 0.005 equiv) and 3,4,7,8-tetramethyl-1,10-phenanthroline (15.9 mg, 0.067 mmol, 0.01 equiv) were dissolved in 5 mL THF and stirred 30 min. In the meantime, 2,3-dimethoxytoluene (**108**, 1.00 mL, 6.73 mmol, 1 equiv) and B_2Pin_2 (1.28 g, 5.05 mmol, 0.75 equiv) were weighed into a 20 mL sealable microwave vial (also in the glovebox) with a teflon-coated stir bar and 5 mL THF was added. Upon complete dissolution, the catalyst solution was transferred to the microwave vial, which was sealed prior to removal from the glovebox. The vial was then placed in a preheated 80 °C oil-bath and stirred for 48 h, at which time TLC (20% EtOAc/hex) revealed complete conversion to a single borylated product. The vial was cooled to room temperature and the cap was removed. *N*-methylmorpholine-*N*-oxide (2.37 g, 20.2 mmol, 3 equiv) was added in a few small portions and the vial was resealed and returned to the 80 °C oil-bath for 3 h, at which time TLC (20% EtOAc/hex) indicated complete oxidation

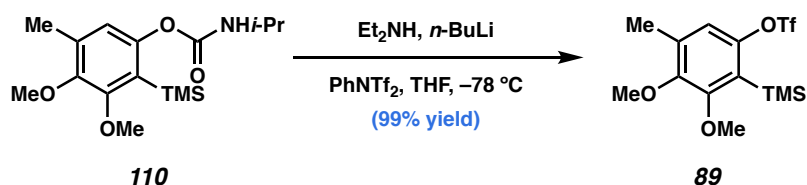
to the intermediate phenol. Triethylamine (4.7 mL, 33.7 mmol, 5 equiv) and isopropyl isocyanate (2.6 mL, 26.9 mmol, 4 equiv) were added at 23 °C and the solution was stirred for 16 h, at which time TLC (50% EtOAc/hex) indicated complete conversion to carbamate **109**. The contents of the vial were transferred to a 100 mL roundbottom flask and 10% aq. Na₂S₂O₃ was added to quench the remaining oxidant, and citric acid hydrate (4.5 g, >3 equiv) was added to chelate the boron. This solution was stirred for 1 h, and concentrated HCl was added 1 mL at a time until an acidic pH was achieved. The layers were separated and the aqueous phase was extracted with EtOAc. The combined organic phases were then washed with aqueous K₂CO₃, dried over MgSO₄ and concentrated. The product was purified by column chromatography (25% EtOAc/hex). Colorless solid, 1.16 g, 4.6 mmol, 68% yield. NMR spectra were identical to the previously reported compound.⁵⁰ ¹H NMR (400 MHz, CDCl₃) δ 6.55 (d, *J* = 2.6 Hz, 1H), 6.52 (d, *J* = 2.8 Hz, 1H), 4.84 (d, *J* = 7.8 Hz, 1H), 3.88 (ddd, *J* = 16.1, 13.9, 7.6 Hz, 1H), 3.82 (s, 3H) 3.76 (s, 3H), 2.24 (s, 3H), 1.23 (s, 3H), 1.21 (s, 3H); ¹³C NMR (100 MHz, CDCl₃) δ 154.0, 153.0, 146.8, 144.7, 132.3, 115.4, 104.3, 60.3, 55.9, 43.6, 23.0, 16.0.



3,4-Dimethoxy-5-methyl-2-(trimethylsilyl)phenyl isopropylcarbamate (**110**):

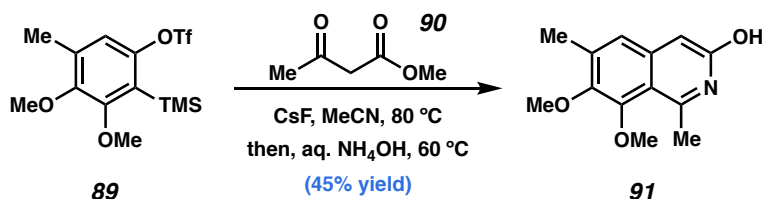
Note: Vigorous stirring was required throughout the course of the reaction due to the formation of insoluble triflate salts. Carbamate **109** (17.30 g, 68.2 mmol, 1 equiv) was dissolved in Et₂O (340 mL, 0.2 M), *N,N,N',N'*-tetramethylethylenediamine (TMEDA, 11.3 mL, 75.1 mmol, 1.1 equiv) was added, and the solution was cooled to 0 °C before

tert-butyldimethylsilyl triflate (TBSOTf, 17.25 mL, 75.1 mmol, 1.1 equiv) was added in a slow stream. The solution was stirred 10 min at 0 °C, removed from the ice bath and stirred at 23 °C for 30 min. A second portion of TMEDA (41 mL, 273 mmol, 4 equiv) was added and the solution was cooled to –78 °C. *n*-Butyllithium (2.4 M, 114 mL, 274 mmol, 4 equiv) was added in a dropwise fashion through a flame-dried addition funnel over the course of 1 h, being sure to not let the temperature rise significantly. The resulting yellow suspension was stirred vigorously for 4 h at –78 °C, taking care not to let the temperature rise. Trimethylsilyl chloride (61 mL, 478 mmol, 7 equiv) was then added dropwise via the addition funnel over the course of 30 min and the suspension was stirred at –78 °C for 30 min, then was removed from the dry ice bath and stirred at 23 °C for 16 h. The reaction was quenched by the addition of 300 mL aqueous NH₄Cl (30 mL saturated solution diluted to 300 mL) through an addition funnel, the first 50 mL of which were added dropwise, followed by the addition of the remainder in a slow stream. The aqueous phase was then further acidified by the addition of small portions of concentrated HCl until an acidic pH was achieved (~30 mL required). The layers were separated and the aqueous phase was extracted twice with Et₂O. The combined organic phases were washed with saturated aqueous NH₄Cl, dried over MgSO₄ and concentrated. The product was purified by column chromatography (20–30% Et₂O/hex). Colorless solid, 20.61 g, 63.3 mmol, 93% yield. NMR spectra were identical to the previously reported compound.⁵⁰ ¹H NMR (300 MHz, CDCl₃) δ 6.63 (s, 1H), 4.69 (d, *J* = 8.1 Hz, 1H), 3.96–3.85 (m, 1H), 3.83 (s, 3H), 3.76 (s, 3H), 2.23 (s, 3H), 1.24 (s, 3H), 1.22 (s, 3H), 0.30 (s, 9H); 157.9, ¹³C NMR (125 MHz, CDCl₃) δ 157.9, 154.2, 150.5, 148.5, 134.6, 123.0, 120.1, 60.5, 59.8, 43.5, 23.1, 16.1, 1.3.



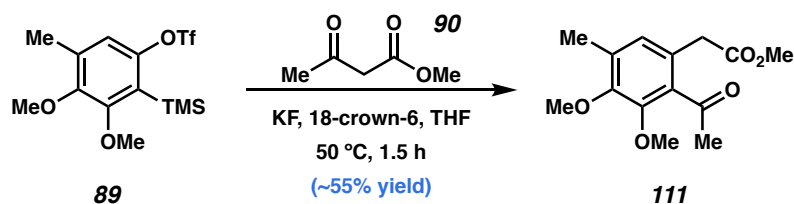
3,4-Dimethoxy-5-methyl-2-(trimethylsilyl)phenyl trifluoromethanesulfonate (89):

Note: Arene 89 can be isolated as a colorless oil, but undergoes decomposition and should be used within the day of its isolation. Carbamate **110** (8.08 g, 24.8 mmol, 1 equiv) was dissolved in THF (100 mL, 0.25 M) and diethylamine (3.85 mL, 37.2 mmol, 1.5 equiv) was added and the solution was cooled to -78°C . *n*-Butyllithium (2.5 M, 15 mL, 37.5 mmol, 1.5 equiv) was added slowly over the course of 15 min. The solution was stirred at that temperature for 30 min, then removed from its bath and stirred at 23°C for 30 min. *N*-Phenyl triflimide (10.6 g, 29.8 mmol, 1.2 equiv) was added in one portion and the solution was stirred 30 min. A second portion of diethylamine (4.6 mL, 44.7 mmol, 1.8 equiv) was added and the solution was stirred 2 h. The solution was filtered through a 1 inch pad of silica gel with 50% Et₂O/hex and concentrated. The product was purified by column chromatography (10% Et₂O/hex). Colorless oil, 9.15 g, 24.6 mmol, 99% yield. NMR spectra were identical to the previously reported compound.⁵⁰ ¹H NMR (400 MHz, CDCl₃) δ 6.87 (s, 1H), 3.87 (s, 3H), 3.78 (s, 3H), 2.28 (d, $J = 0.7$ Hz, 3H), 0.38 (s, 9H); ¹³C NMR (100 MHz, CDCl₃) δ 158.5, 150.4, 149.0, 135.6, 124.2, 118.7 (q, $J = 320.6$ Hz), 117.7, 60.6, 59.8, 16.3, 1.2; ¹⁹F NMR (282 MHz, CDCl₃) δ -73.1 (s, 3F).



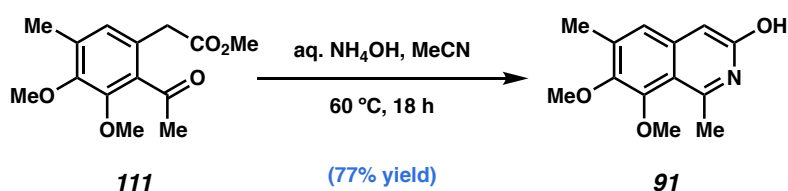
7,8-Dimethoxy-1,6-dimethyl-3-hydroxyisoquinoline (91): Cesium fluoride (204 mg, 1.34 mmol, 2.5 equiv) was dissolved in acetonitrile (5.4 mL, 0.1 M) in a 20 mL microwave vial and water (9.7 μ L, 0.537 mmol, 1.0 equiv) and methyl acetoacetate (58 μ L, 0.537 mmol, 1.0 equiv) were added. Aryne precursor **89** (250 mg, 0.671 mmol, 1.25 equiv) was added neat via syringe, and the vial was placed in a preheated 80 °C oil bath. After 2 h, TLC revealed complete consumption of **89**, so NH_4OH (28–30%, 5.4 mL) was added in one portion. The vial was moved to a preheated 60 °C oil bath and stirred for 8 h. The solution was poured into brine inside a separatory funnel and the solution was extracted with EtOAc (2x 30 mL). The aqueous phase was brought to pH 7 by the addition of concentrated HCl and was extracted with EtOAc (2x 30 mL). The aqueous phase was discarded. The organic phase was then extracted with 2M HCl (5x 20 mL). The organic phase was checked by LCMS to confirm that all of product **91** had transferred to the aqueous phase and was subsequently discarded. The aqueous phase was then brought back to pH 7 by the addition of 100 mL 2M NaOH and was extracted with EtOAc (5x 20 mL). The combined organic phases were washed with brine, dried over Na_2SO_4 and concentrated, providing the product. Yellow solid, 56.9 mg, 0.243 mmol, 45% yield. ^1H NMR (300 MHz, CDCl_3) δ 6.92 (d, J = 0.7 Hz, 1H), 6.51 (s, 1H), 3.90 (s, 3H), 3.81 (s, 3H), 3.03 (d, J = 0.7 Hz, 3H), 2.28 (d, J = 1.0 Hz, 3H); ^{13}C NMR (125 MHz, CDCl_3) δ 161.8, 149.5, 145.9, 142.6, 140.4, 121.4, 113.1, 104.8, 60.5, 60.2, 21.1, 17.3; IR (thin film, NaCl): 3327, 2938, 2609, 1652, 1455, 1324, 1227, 1178, 1147, 1090, 1062, 1035, 1001, 960, 938, 892, 862, 813, 724, 683, 662; HRMS (ESI-TOF) calc'd for $[\text{M}^+]$ $\text{C}_{13}\text{H}_{15}\text{NO}_3$ = 233.1052, found 233.1057.

*Note: When performed on multi-gram scale, this reaction proved highly variable due to unknown factors. Yields typically dropped into the 20–30% range. We have therefore developed the two-step procedure below that requires extensive column chromatography and generates significantly more organic waste, but that does provide **91** in higher overall yield.*



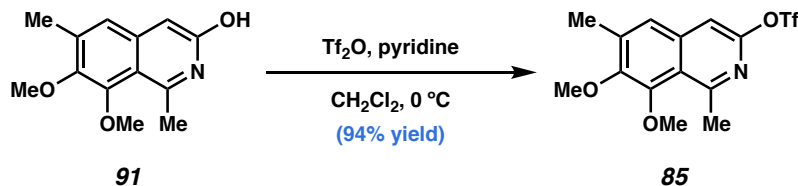
Methyl 2-(2-acetyl-3,4-dimethoxy-5-methylphenyl)acetate (111): Anhydrous potassium fluoride (7.0 g, 120.5 mmol, 3.3 equiv) and 18-crown-6 (31.0 g, 117.3 mmol, 3.2 equiv) were weighed into a flame-dried 1L recovery flask inside a nitrogen-filled glovebox to minimize exposure to atmospheric water. The flask was removed from the glovebox, anhydrous THF (370 mL, 0.1 M in **89**) was added, and the resulting slurry was heated to 50 °C in an oil bath. Aryne precursor **89** (13.67 g, 36.7 mmol, 1.0 equiv) was dissolved in anhydrous THF (30 mL) and added to the warm fluoride solution in a slow, dropwise fashion via cannula over 1 h, followed by a 10 mL rinse of the flask and cannula, added rapidly. After stirring 1 h at 50 °C, TLC revealed complete consumption of **89** and the appearance of at least five new products (the product has an $R_f = 0.35$ in 20% EtOAc/hex, major middle spot). The crude reaction was filtered through a 1" pad of SiO₂ using 1L of 30% EtOAc/hex and the filtrate was concentrated. The product was purified by column chromatography [4x10" SiO₂, 2L 5% EtOAc/hex (collected in Erlenmeyer flasks)–1.5L 10%–1.5L 20%–1L 30%–600 mL 50% EtOAc/hex]. The product could not be completely purified from the reaction mixture, but using the above

conditions **111** could be obtained in roughly 80% purity as estimated by ^1H NMR. Colorless oil, 6.70 g isolated, ~5.36 g **111** adjusted for purity, ~20.1 mmol, ~55% yield. NMR spectra were identical to the previously reported compound.⁵⁰ Because of the low purity, only ^1H NMR spectra were recorded for this compound. ^1H NMR (500 MHz, CDCl_3) δ 6.78 (q, $J = 0.7$ Hz, 1H), 3.87 (s, 3H), 3.82 (s, 4H), 3.68 (s, 3H), 3.62 (s, 2H), 2.55 (s, 3H), 2.24 (d, $J = 0.7$ Hz, 3H).



7,8-Dimethoxy-1,6-dimethyl-3-hydroxyisoquinoline (91): In a 250 mL flask equipped with a Kontes valve, arene **111** was dissolved in MeCN (15 mL) and NH_4OH (28–30%, 30 mL), the flask was sealed to prevent loss of gaseous ammonia, and was placed in a preheated 60 $^\circ\text{C}$ oil bath. Within 1 h, yellow **91** began to precipitate from the reaction solution. After stirring at 60 $^\circ\text{C}$ for 18 h, the flask was cooled to room temperature, then placed in a -25 $^\circ\text{C}$ freezer for 3 h, after which time the suspension was filtered. The yellow filter cake was washed with cold (-25 $^\circ\text{C}$) MeCN until the filtrate was no longer yellow. The filter cake was allowed to dry on the filter paper for 15 min, then was transferred to a vial and dried at high vacuum for 24 h to provide the analytically pure product. Yellow solid, 3.61 g, 15.5 mmol, 77% yield. ^1H NMR (300 MHz, CDCl_3) δ 6.92 (d, $J = 0.7$ Hz, 1H), 6.51 (s, 1H), 3.90 (s, 3H), 3.81 (s, 3H), 3.03 (d, $J = 0.7$ Hz, 3H), 2.28 (d, $J = 1.0$ Hz, 3H); ^{13}C NMR (156 MHz, CDCl_3) δ 161.8, 149.5, 145.9, 142.6, 140.4, 121.4, 113.1, 104.8, 60.5, 60.2, 21.1, 17.3; IR (thin film, NaCl): 3327, 2938, 2609, 1652,

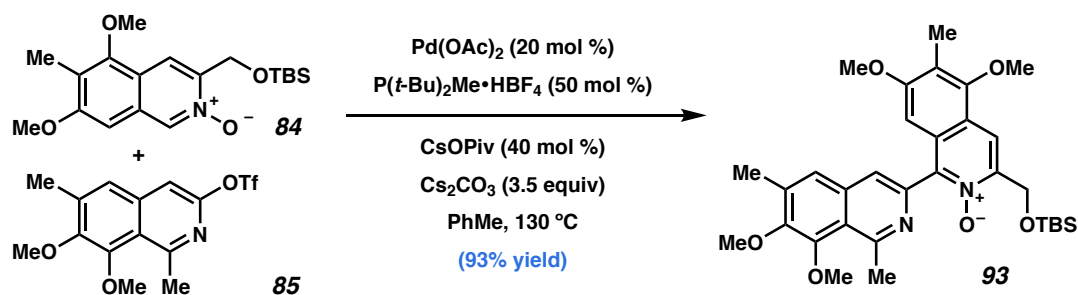
1455, 1324, 1227, 1178, 1147, 1090, 1062, 1035, 1001, 960, 938, 892, 862, 813, 724, 683, 662; HRMS (ESI-TOF) calc'd for $[M^+]$ $C_{13}H_{15}NO_3 = 233.1052$, found 233.1057.



7,8-Dimethoxy-1,6-dimethyl-3-(trifluoromethanesulfonyloxy)isoquinoline (10):

Hydroxyisoquinoline **91** (2.60 g, 11.1 mmol, 1 equiv) was dissolved in CH_2Cl_2 (70 mL, 0.16 M) and pyridine (11.4 mL, 140.6 mmol, 12.7 equiv) was added and the solution was cooled to 0 °C. Trifluoromethanesulfonic anhydride (Tf_2O , 3.00 mL, 17.8 mmol, 1.6 equiv) was added dropwise, causing the yellow solution to turn dark red. After 30 min, TLC (10% EtOAc/hex) revealed complete conversion, so the reaction was quenched by the addition of saturated aqueous NaHCO_3 (70 mL). The solution was stirred vigorously until bubbling ceased, at which time the layers were separated. The organic phase was extracted with CH_2Cl_2 and the combined organic phases were dried over Na_2SO_4 and concentrated. The product was purified by column chromatography (10% Et₂O/hex). Yellow oil, 3.82 g, 10.5 mmol, 94% yield. ^1H NMR (400 MHz, CDCl_3) δ 7.39 (d, $J = 1.0$ Hz, 1H), 7.21 (s, 1H), 3.98 (s, 3H), 3.93 (s, 3H), 3.07 (d, $J = 0.7$ Hz, 3H), 2.44 (d, $J = 1.0$ Hz, 3H); ^{13}C NMR (100 MHz, CDCl_3) δ 158.6, 151.0, 150.5, 149.9, 139.2, 136.8, 123.6, 122.9, 118.8 (q, $J = 320.5$ Hz), 107.6, 60.8, 60.2, 26.7, 17.0; ^{19}F NMR (282 MHz, CDCl_3) δ -72.99; IR (thin film, NaCl): 3436, 2939, 1606, 1554, 1494, 1416, 1381, 1352, 1333, 1249, 1209, 1134, 1097, 1060, 1010, 983, 966, 941, 892, 835, 768, 695, 649, 608; HRMS (ESI-TOF) calc'd for $[M^+]$ $C_{14}H_{14}F_3NO_5S = 365.0545$, found 365.0547.

3.6.2.3 Fagnou cross-coupling reaction

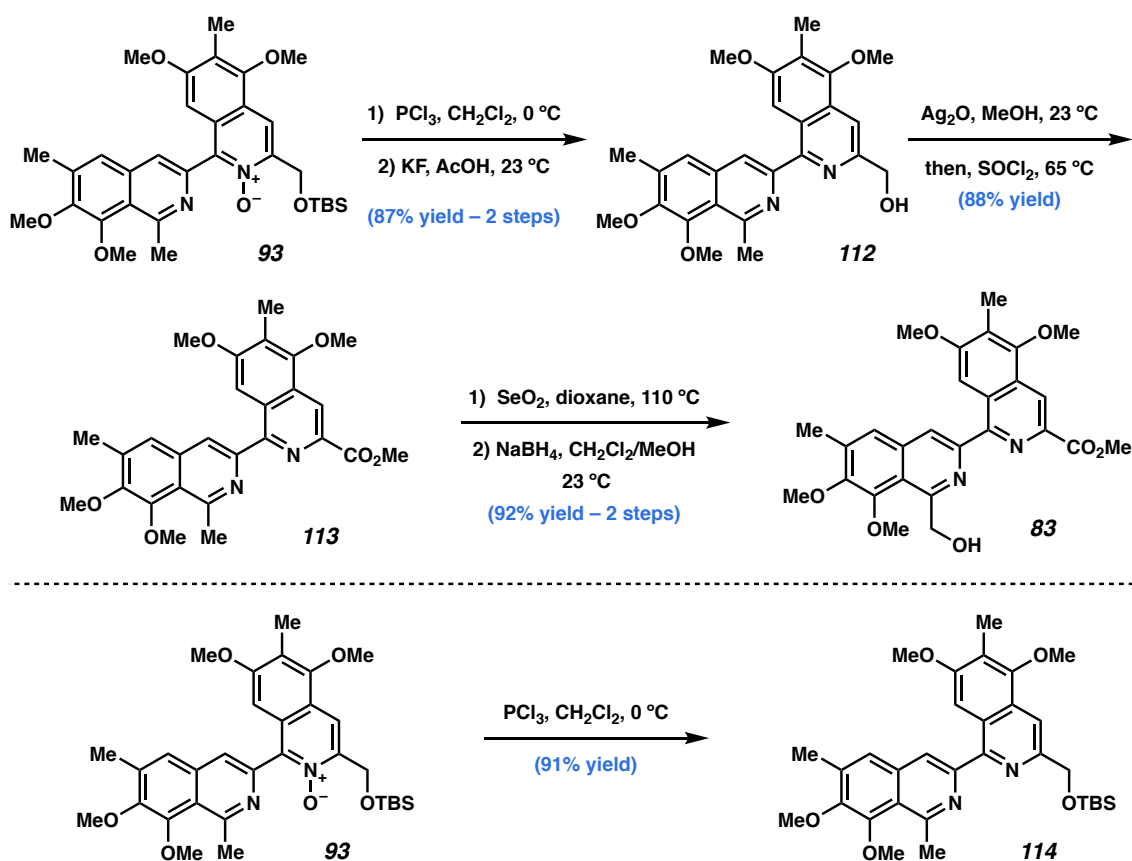


3-(((tert-butyldimethylsilyl)oxy)methyl)-5,7,7',8'-tetramethoxy-1',6,6'-trimethyl-

[1,3'-biisoquinoline] 2-oxide (93): Palladium acetate (347 mg, 1.54 mmol, 0.20 equiv), di-*tert*-butyl (methyl)phosphonium tetrafluoroborate (957 mg, 3.86 mmol, 0.50 equiv), and cesium carbonate (1.26 g, 3.41 mmol, 0.50 equiv) were weighed into a 100 mL pear-shaped flask and brought into a nitrogen-filled glovebox and cesium pivalate (CsOPiv , 722 mg, 3.09 mmol, 0.40 equiv) was added to the flask. In the glovebox, degassed toluene (80 mL) was added, the flask was sealed with a rubber septum and removed from the glovebox, to be placed in a 60°C preheated oil bath, where it was stirred for 30 min and allowed to cool to room temperature. In the meantime, *N*-oxide **84** (8.42 g, 23.1 mmol, 3 equiv) and cesium carbonate (7.54 g, 23.1 mmol, 3 equiv) were weighed into a 250 mL sealable flask equipped with a Kontes valve, to which 50 mL toluene was added, and this suspension was sparge-degassed with nitrogen for 10 min. Isoquinoline triflate **85** (2.77 g, 6.82 mmol, 1.00 equiv) was dissolved in 10 mL toluene, which was sparge-degassed with nitrogen for 10 min. The solution of isoquinoline triflate **85** was then added via cannula to the cooled catalyst solution, rinsing the flask with 5 mL degassed toluene. The catalyst/triflate solution was then added via cannula to the 250 mL sealable flask, rinsing with 10 mL degassed toluene. The flask was sealed and placed in a 130°C

preheated oil bath for 4.5 h. The flask was then allowed to cool to room temperature and Celite (10 g) was added. This suspension was then filtered through a 1 inch pad of Celite that was topped with sand, rinsing with CH₂Cl₂ and acetone (500 mL each). The solution was concentrated, providing the crude product. ¹H NMR of the crude reaction mixture showed a 2:1 mixture of bis-isoquinoline **93** and *N*-oxide **84** at this point, indicating complete conversion to product. The product was purified by column chromatography (10–20% EtOAc/hex, then 20–50–100% EtOAc/hex + 1% NEt₃, then 10–20% MeOH/EtOAc + 1% NEt₃. bis-Isoquinoline **93** elutes during the 50–100% EtOAc/hex portion, and the remaining *N*-oxide **84** elutes during the 10–20% MeOH/EtOAc portion). Colorless foam, 3.88 g, 6.70 mmol, 98% yield. An analogous coupling performed with 2.39 g isoquinoline triflate **85** provided 3.30 g of product (87% yield), together providing 7.18 g bis-isoquinoline **93** in 93% average yield. ¹H NMR (400 MHz, CDCl₃) δ 8.13 (d, *J* = 0.9 Hz, 1H), 7.81 (s, 1H), 7.42 (d, *J* = 1.1 Hz, 1H), 6.60 (s, 1H), 5.06 (d, *J* = 1.4 Hz, 2H), 4.01 (s, 3H), 3.97 (s, 3H), 3.90 (s, 3H), 3.65 (s, 3H), 3.17 (s, 3H), 2.45 (d, *J* = 0.9 Hz, 3H), 2.28 (s, 3H), 1.03 (s, 9H), 0.17 (s, 6H); ¹³C NMR (100 MHz, CDCl₃) δ 158.9, 157.8, 153.8, 151.3, 149.6, 146.0, 143.7, 142.0, 137.6, 134.8, 128.2, 124.3, 122.7, 122.5, 121.5, 120.4, 114.5, 98.6, 61.8, 60.9, 60.4, 60.3, 55.7, 27.2, 26.1, 18.5, 17.1, 9.7, –5.2; IR (thin film, NaCl): 3418, 2954, 2857, 1615, 1567, 1463, 1393, 1329, 1255, 1213, 1190, 1139, 1118, 1089, 1057, 1008, 961, 937, 897, 839, 816, 778, 734, 702, 634; HRMS (ESI-TOF) calc'd for [M⁺] C₃₂H₄₂N₂O₆Si = 578.2812, found 578.2796.

3.6.2.4 First-generation synthesis of bis-isoquinoline 83

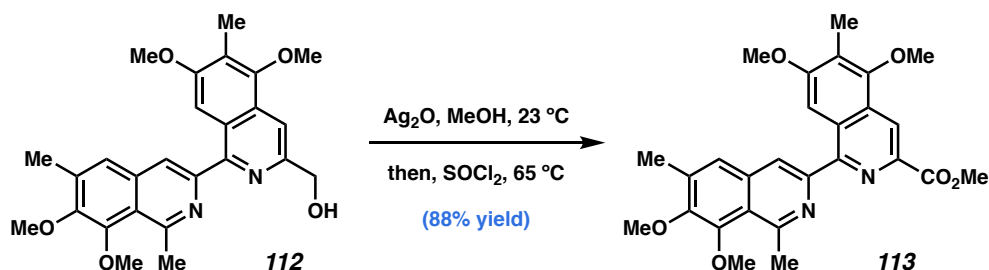


3-(((Tert-butyl dimethylsilyl)oxy)methyl)-5,7,7',8'-tetramethoxy-1',6,6'-trimethyl-

1,3'-biisoquinoline (114): Bis-isoquinoline-*N*-oxide **93** (6.16 g, 10.6 mmol, 1.00 equiv) was dissolved in CH_2Cl_2 (210 mL, 0.05 M) and the solution was cooled to 0°C . Neat phosphorus trichloride (1.86 mL, 21.3 mmol, 2.00 equiv) was added at a dropwise pace over 5 minutes, causing the solution to immediately turn dark purple. After 30 min, TLC revealed complete conversion to the product, so the reaction was quenched with saturated aqueous K_2CO_3 and diluted with water. The layers were separated and the aqueous phase was extracted with EtOAc. The combined organic phases were dried over Na_2SO_4 and concentrated (note: a brine wash caused a significant emulsion regardless of extraction solvent, and was avoided). The product was purified by column chromatography (10%

Bis-isoquinoline **114** (5.44 g, 9.7 mmol, 1.00 equiv) was dissolved in acetic acid (40 mL, 0.25 M) and solid potassium fluoride (2.81 g, 48.0 mmol, 5.00 equiv) was added in one portion. The solution was stirred 30 min at room temperature, at which time LCMS showed complete conversion to the product. The solution was diluted with CH₂Cl₂ and ice and the solution was stirred vigorously as a solution of sodium hydroxide (25 g, 0.625 mol, 0.9 equiv relative to 40 mL AcOH) in 70 mL water was added slowly. The rest of the acetic acid was quenched by the addition of saturated aqueous K₂CO₃. The layers were separated and the aqueous phase was extracted with CH₂Cl₂. The combined organic phases were washed with brine, dried over Na₂SO₄, and concentrated. The product was purified by column chromatography (1–2–3–4–5% MeOH/CH₂Cl₂ + 1% NEt₃). Colorless solid, 4.17 g, 9.31 mmol, 96% yield. ¹H NMR (400 MHz, CDCl₃) δ 8.09 (s, 1H), 8.03 (s,

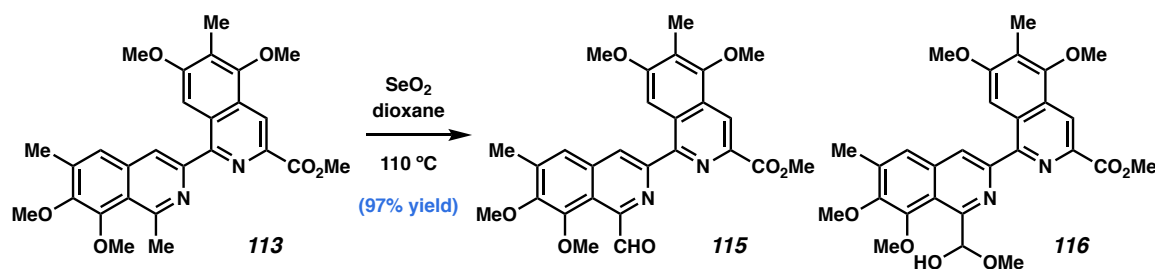
1H), 7.79 (d, $J = 0.9$ Hz, 1H), 7.49 (d, $J = 1.1$ Hz, 1H), 4.94 (s, 2H), 4.03 (s, 3H), 3.97 (s, 3H), 3.89 (s, 3H), 3.87 (s, 3H), 3.22 (s, 3H), 2.47 (d, $J = 1.0$ Hz, 3H), 2.35 (s, 4H); ^{13}C NMR (100 MHz, CDCl_3) δ 157.8, 156.0, 155.2, 153.5, 151.1, 150.3, 149.7, 149.6, 137.6, 135.4, 129.0, 126.2, 124.7, 124.6, 122.2, 119.9, 111.3, 101.3, 65.0, 61.7, 60.9, 60.3, 55.6, 27.2, 17.1, 9.9; IR (thin film, NaCl): 3352, 3129, 2937, 2855, 1620, 1594, 1557, 1484, 1462, 1455, 1416, 1392, 1355, 1331, 1303, 1243, 1218, 1196, 1133, 1117, 1091, 1060, 1008, 964, 906, 885, 841, 796, 733, 646; HRMS (ESI-TOF) calc'd for $[\text{M}^+]$ $\text{C}_{26}\text{H}_{28}\text{N}_2\text{O}_5$ = 448.1998, found 448.1992.



Methyl 5,7,7',8'-tetramethoxy-1',6,6'-trimethyl-[1,3'-biisoquinoline]-3-carboxylate

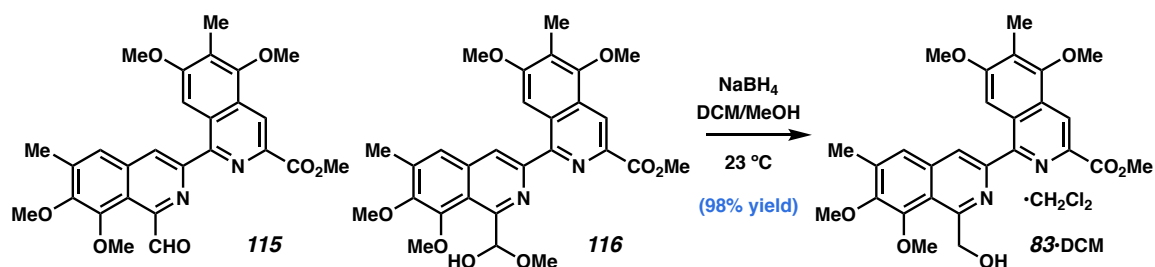
(113): bis-Isoquinoline **112** (1.50 g, 3.34 mmol, 1.00 equiv) and silver(I) oxide (3.88 g, 16.7 mmol, 5.00 equiv) were slurried in MeOH (35 mL, 0.1 M). After 30 min, the solution appeared to be fully homogeneous and deep red in color. After 4 h, LCMS showed full conversion to a mixture of methyl ester **113** and the corresponding carboxylic acid. Thionyl chloride (1.21 mL, 16.7 mmol, 5.00 equiv) was added through the top of a reflux condenser, and following the complete addition, the solution was heated to reflux. After 1.5 h, LCMS showed complete conversion to methyl ester **113**. The solution was cooled to room temperature and celite was added, and the solution was filtered through more celite, rinsing with EtOAc. The solution was concentrated, then redissolved in CH_2Cl_2 and washed with dilute aqueous K_2CO_3 and brine. The layers were

separated and the aqueous phase was extracted with CH₂Cl₂. The combined organic phases were washed with brine, dried over Na₂SO₄, and concentrated. The product was purified by column chromatography (25% EtOAc/hex + 1% NEt₃). White solid, 1.40 g, 2.94 mmol, 88% yield. ¹H NMR (400 MHz, CDCl₃) δ 8.75 (d, *J* = 0.9 Hz, 1H), 8.19 (s, 1H), 8.13 (s, 1H), 7.52 (d, *J* = 1.1 Hz, 1H), 4.05 (s, 3H), 4.01 (s, 3H), 3.97 (s, 3H), 3.94 (s, 3H), 3.90 (s, 3H), 3.20 (s, 3H), 2.46 (d, *J* = 1.0 Hz, 3H), 2.36 (s, 3H); ¹³C NMR (100 MHz, CDCl₃) δ 167.0, 160.0, 156.0, 155.8, 154.9, 151.1, 149.9, 149.5, 139.0, 137.5, 135.6, 128.6, 128.0, 125.0, 124.7, 122.3, 120.5, 118.6, 101.9, 62.3, 60.9, 60.3, 55.8, 52.8, 27.1, 17.1, 9.9; IR (thin film, NaCl): 3443, 2949, 1714, 1615, 1454, 1407, 1384, 1330, 1305, 1270, 1226, 1137, 1089, 1057, 1008, 871, 786, 733; HRMS (ESI-TOF) calc'd for [M⁺] C₂₇H₂₈N₂O₆ = 476.1947, found 476.1952.



Bis-isoquinoline aldehyde (115) hemiacetal (116). bis-Isoquinoline **113** (1.40 g, 2.94 mmol, 1.00 equiv) and selenium dioxide (652 mg, 5.88 mmol, 2.00 equiv) were slurried in dioxane and the flask was fitted with a reflux condenser. The flask was vacuum purged/refilled with N₂ five times, then heated to reflux. At about 80 °C, the solution became fully homogeneous. After 1 h at reflux, the flask was cooled to room temperature and LCMS showed full conversion to aldehyde **115**. Celite was added to the crude reaction and the resulting slurry was filtered through more celite, rinsing with EtOAc. SiO₂ was added to the filtrate and the solution was concentrated. Due to the insolubility

of the products, a mixture of MeOH and CH₂Cl₂ was required during purification by column chromatography (10% MeOH/DCM + 1% NEt₃). During this process, the highly electrophilic aldehyde moiety is converted to the hemiacetal in a thermodynamic 85:15 mixture favoring the hemiacetal. The two products can neither be interconverted nor separated, and as such, were characterized as a mixture. White solid, total mass = 1.47 g, 85:15 molar ratio of **116:115** by ¹H NMR, corresponding to 1.25 g hemiacetal **116** (2.39 mmol, 82% yield) and 220 mg **115** (0.45 mmol, 15% yield), 2.84 mmol total, 97% combined yield. *Aldehyde 115*: ¹H NMR (400 MHz, CDCl₃) δ 10.92 (s, 1H), 8.78 (s, 1H), 8.72 (s, 1H), 8.56 (s, 1H), 7.68 (d, *J* = 1.2 Hz, 1H), 4.07 (s, 3H), 4.04 (s, 3H), 4.02 (s, 3H), 3.95 (s, 3H), 3.70 (s, 3H), 2.51 (d, *J* = 1.0 Hz, 3H), 2.37 (s, 3H); ¹³C NMR (101 MHz, CDCl₃) δ 193.4, 160.6, 154.8, 154.1, 151.8, 151.3, 151.0, 147.1, 139.2, 135.8, 128.7, 128.1, 125.3, 125.0, 124.1, 121.6, 119.1, 102.0, 67.2, 60.7, 60.6, 56.3, 46.1, 17.4. *Hemiacetal 116*: ¹H NMR (400 MHz, CDCl₃) δ 8.78 (d, *J* = 0.8 Hz, 1H), 8.44 (s, 1H), 7.97 (s, 1H), 7.61 (d, *J* = 1.1 Hz, 1H), 6.52 (d, *J* = 10.6 Hz, 1H), 6.41 (d, *J* = 10.6 Hz, 1H), 4.10 (s, 3H), 4.06 (s, 3H), 3.98 (s, 3H), 3.98 (s, 3H), 3.92 (s, 3H), 3.63 (s, 3H), 2.48 (d, *J* = 1.0 Hz, 3H), 2.37 (s, 3H); ¹³C NMR (100 MHz, CDCl₃) δ 166.8, 160.3, 155.2, 154.9, 152.9, 151.5, 148.6, 148.2, 138.9, 138.6, 136.5, 128.5, 127.9, 125.2, 124.9, 123.4, 120.1, 118.9, 101.5, 95.2, 62.3, 60.8, 60.3, 56.0, 55.2, 52.8, 17.3, 10.0. IR (thin film, NaCl): 3437, 2949, 2847, 1738, 1711, 1620, 1462, 1387, 1304, 1272, 1229, 1136, 1086.2, 1002, 901, 734; HRMS (ESI-TOF) for aldehyde **115** calc'd for [M⁺] C₂₇H₂₆N₂O₇ = 490.1740, found 490.1742; HRMS (ESI-TOF) for hemiacetal **116** calc'd for [M⁺] C₂₈H₃₀N₂O₈ = 522.2002, found 522.2005.



Bis-isoquinoline methyl ester dichloromethane solvate (83•CH₂Cl₂). *Note: Aldehyde*

115 and hemiacetal 116 appear to be in thermal equilibrium at 23 °C in a 4:1 v/v mixture

of CH₂Cl₂:MeOH in a 1:3 ratio of 115:116. When excess NaBH₄ was utilized,

competitive reduction of the methyl ester was observed; however, when NaBH₄ was

employed in substoichiometric fashion, selective reduction of the aldehyde was observed.

Presumably the reaction proceeds to completion as a manifestation of Le Châtelier's

principle. A mixture of bis-isoquinolines 115 and 116 (2.84 mmol in total, 1.00 equiv)

was dissolved in CH₂Cl₂ (24 mL) and MeOH (6 mL, 0.1 M) and NaBH₄ (36.0 mg, 0.946

mmol, 0.33 equiv) was added. Gas evolution was observed for ~1 minute, then stopped. 5

minutes after the addition of NaBH₄, LCMS showed complete and selective reduction to

product 83. The reaction was quenched by the addition of citric acid monohydrate (594

mg, 2.84 mmol, 1.00 equiv) and water, and the solution was stirred at 1500 rpm for 10

min, then was basified by the addition of saturated aqueous NaHCO₃. The layers were

separated and the aqueous phase was extracted with CH₂Cl₂. The combined organic

phases were dried over Na₂SO₄ and concentrated. The product was purified by column

chromatography using a 1:1 mixture of CH₂Cl₂:EtOAc as the polar solvent (20–30–40–

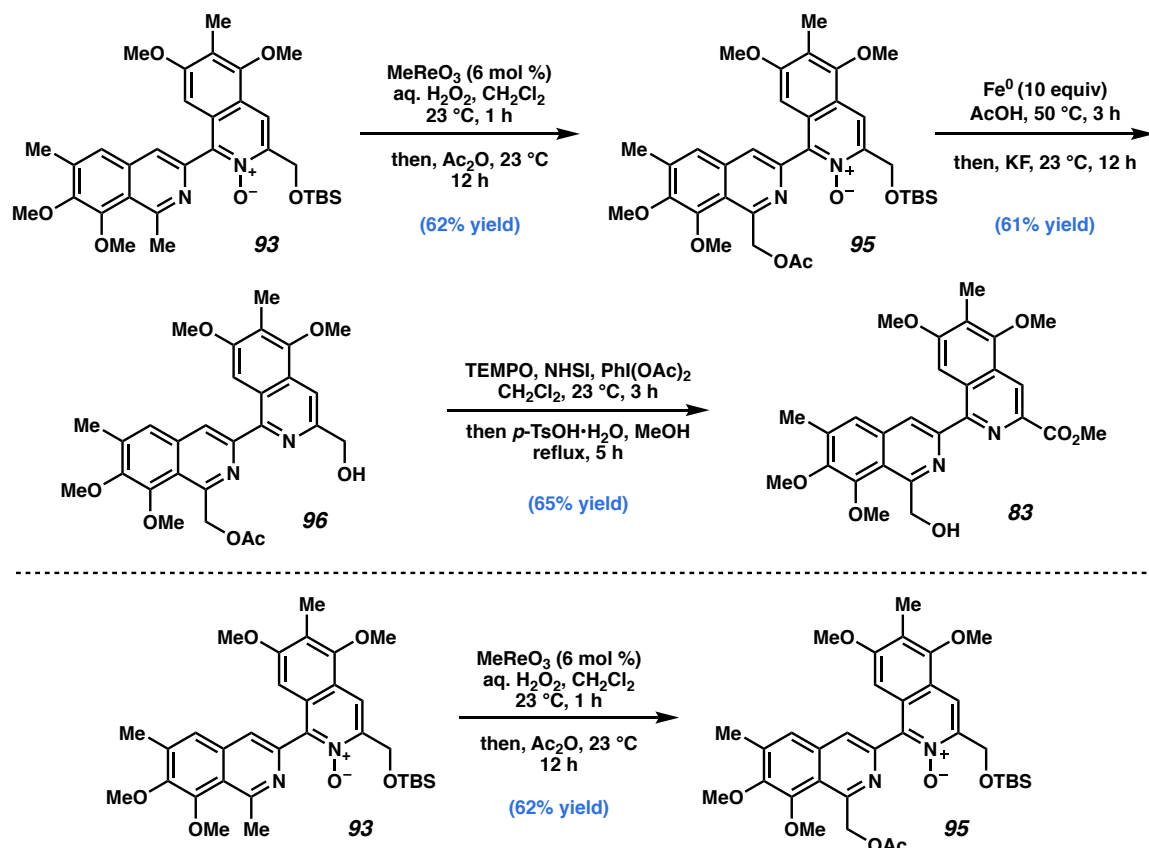
50–60–100% polar solvent/hex + 1% NEt₃). Colorless solid, 1.55 g, 2.68 mmol, 98%

yield. Note: A stoichiometric amount of dichloromethane could not be removed from the

product despite extensive time on high vacuum (10 mTorr), leading to the conclusion that

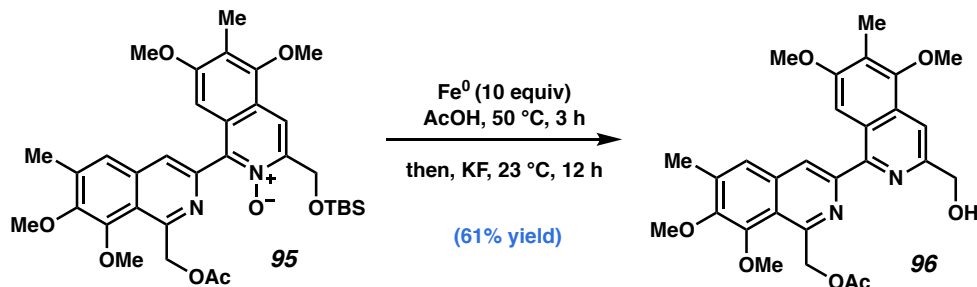
the product is isolated as a stoichiometric dichloromethane monosolvate. ^1H NMR (400 MHz, CDCl_3) δ 8.79 (d, J = 0.8 Hz, 1H), 8.30 (s, 1H), 7.90 (s, 1H), 7.59 (d, J = 0.5 Hz, 1H), 5.55 (t, J = 3.5 Hz, 1H), 5.39 (d, J = 3.5 Hz, 2H), 5.30 [s, 2H (CH_2Cl_2)], 4.06 (s, 3H), 4.06 (s, 3H), 3.99 (s, 3H), 3.96 (s, 3H), 3.90 (s, 3H), 2.49 (d, J = 0.9 Hz, 3H), 2.38 (s, 3H); ^{13}C NMR (100 MHz, CDCl_3) δ 166.9, 160.2, 155.8, 155.6, 155.0, 151.1, 149.1, 148.5, 139.0, 138.4, 135.5, 128.5, 127.9, 125.3, 124.8, 121.6, 120.3, 118.8, 101.3, 64.7, 62.4, 60.9, 60.3, 56.1, 53.4, 52.9, 17.2, 10.0; IR (thin film, NaCl): 3365, 3130, 2930, 2856, 1691, 1621, 1594, 1557, 1462, 1413, 1392, 1357, 1331, 1302, 1259, 1196, 1130, 1089, 1059, 1010, 964, 886, 838, 802, 777; HRMS (ESI-TOF) calc'd for $[\text{M}^+]$ $\text{C}_{27}\text{H}_{28}\text{N}_2\text{O}_7$ = 492.1897, found 492.1894.

3.6.2.5 Second-generation synthesis of bis-isoquinoline 83



1'-(acetoxymethyl)-3-(((*tert*-butyldimethylsilyl)oxy)methyl)-5,7,7',8'-tetramethoxy-6,6'-dimethyl-[1,3'-biisoquinoline] 2-oxide (95): *Note: Addition of the catalyst in a single portion resulted in rapid over-oxidation, but addition in 3 portions, at least 20 minutes apart resulted in clean conversion. Furthermore, bis-N-oxide 94 was not stable to Na₂SO₄, MgSO₄, or SiO₂, and as such it was neither dried nor purified by column chromatography, but the clean reaction profile did not necessitate purification.* Bis-isoquinoline-*N*-oxide **93** (150 mg, 0.259 mmol, 1 equiv) and methyl trioxorhenium (1.3 mg, 0.0052 mmol, 0.02 equiv) were dissolved in CH₂Cl₂ (2.6 mL, 0.1 M) and 35% aqueous hydrogen peroxide (40 μL, 0.454 mmol, 1.75 equiv) was added. The solution was stirred at 1300 rpm for 30 min, at which point a second portion of MeReO₃ (1.3 mg, 0.0052 mmol, 0.02 equiv) was added. After 30 min, a third and final portion of MeReO₃ (1.3 mg, 0.0052 mmol, 0.02 equiv) was added. After a further 30 min, LCMS showed complete consumption of the bis-isoquinoline-*N*-oxide, so acetic anhydride (0.122 mL, 1.30 mmol, 5 equiv) was then added, and the reaction mixture was stirred at 23 °C. After 12 hours, LCMS showed complete consumption of the bis-*N*-oxide. The reaction was quenched with water and basified with aqueous K₂CO₃. The layers were separated and the aqueous phase was extracted with CH₂Cl₂. The combined organic layers were dried over Na₂SO₄, filtered, concentrated, and azeotroped with benzene twice. The crude product was purified by column chromatography (35% EtOAc/hex + 1% NEt₃). Yellow foam, 102.0 mg, 0.160 mmol, 62% yield. ¹H NMR (400 MHz, CDCl₃) δ 8.15 (s, 1H), 8.05 (s, 1H), 7.49 (s, 1H), 6.64 (s, 1H), 5.85 (s, 2H), 5.05 (s, 2H), 4.04 (s, 3H), 3.96 (s, 3H), 3.92 (s, 3H), 3.73 (s, 3H), 2.46 (s, 3H), 2.29 (s, 3H), 1.99 (s, 3H), 1.04 (s, 9H), 0.18 (s, 6H); ¹³C NMR (100 MHz, CDCl₃) δ 171.2, 159.1, 153.2, 145.8, 138.2, 134.9, 128.3,

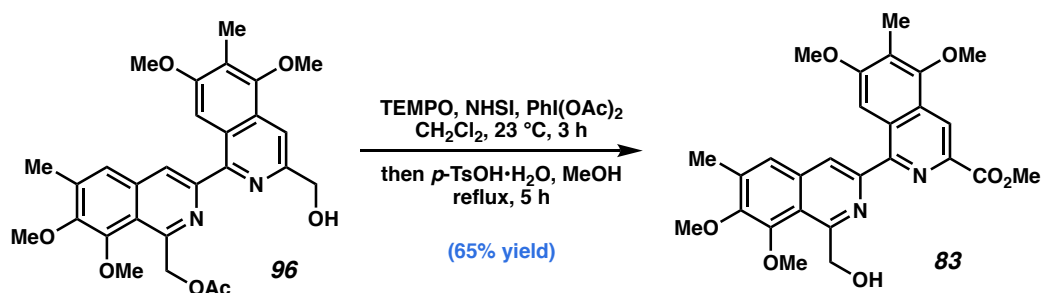
124.4, 123.8, 122.9, 114.7, 98.8, 68.1, 61.8, 60.9, 60.4, 60.2, 55.8, 26.1, 21.1, 18.5, 17.1, 9.8, –5.2. IR (thin film, NaCl): 2932, 2856, 1742, 1614, 1557, 1463, 1454, 1360, 1316, 1236, 1137, 1090, 1006, 897, 839, 754; HRMS (ESI-TOF) calc'd for $[M+H]^+$ $C_{34}H_{45}N_2O_8Si$ = 637.2940, found 637.2944.



(3-(hydroxymethyl)-5,7,7',8'-tetramethoxy-6,6'-dimethyl-[1,3'-biisoquinolin]-1'-

yl)methyl acetate (96): To a solution of bis-isoquinoline-N-oxide **95** (99.0 mg, 0.155 mmol, 1 equiv) in acetic acid (1.6 mL), Fe powder (86.8 mg, 1.55 mmol, 10 equiv) was added at 23 °C. The reaction mixture was stirred at 50 °C for 3 hours, at which point the LCMS showed complete consumption of the starting material. The reaction mixture was then cooled to room temperature and KF (90.1 mg, 1.55 mmol, 10 equiv) was added. After 12 hours, LCMS showed complete consumption of the TBS-protected alcohol intermediate, so the reaction was diluted with CH_2Cl_2 and washed with aqueous K_2CO_3 . The aqueous layer was separated and extracted with EtOAc twice. The combined organic layers were washed with brine, dried over Na_2SO_4 , and concentrated. The crude was purified by column chromatography (50% EtOAc/ CH_2Cl_2 + 1% Et_3N). Pale yellow solid, 48.1 mg, 0.095 mmol, 61% yield. ^1H NMR (400 MHz, CDCl_3) δ 8.13 (s, 1H), 7.85 (s, 1H), 7.74 (d, J = 0.9 Hz, 1H), 7.47 (d, J = 1.1 Hz, 1H), 5.84 (s, 2H), 4.87 (d, J = 0.9 Hz, 2H), 3.99 (s, 3H), 3.88 (s, 3H), 3.84 (s, 3H), 3.83 (s, 3H), 2.41 (d, J = 1.0 Hz, 3H), 2.29

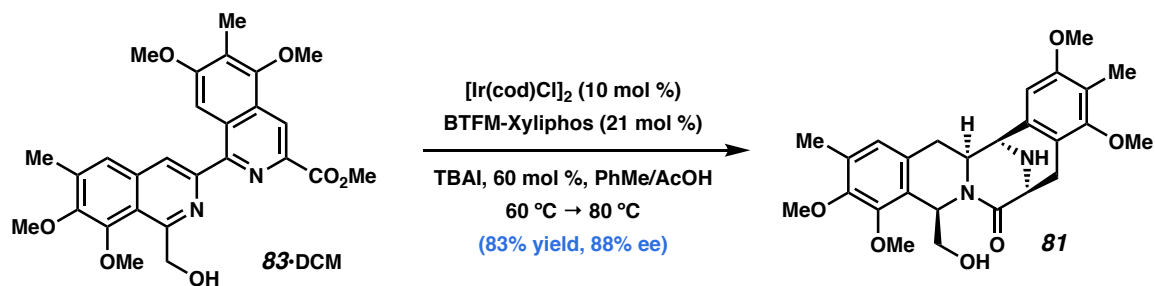
(s, 3H), 1.98 (s, 3H); ^{13}C NMR (100 MHz, CDCl_3) δ 171.2, 157.9, 155.1, 153.5, 151.6, 151.0, 150.5, 149.5, 148.6, 138.1, 135.7, 129.0, 126.3, 124.8, 124.6, 121.5, 121.1, 111.5, 101.3, 68.3, 64.9, 61.8, 60.9, 60.2, 55.8, 21.2, 17.1, 10.0; IR (thin film, NaCl): 3418, 2939, 1738, 1595, 1557, 1455, 1418, 1303, 1238, 1131, 1091, 1006, 888, 755; HRMS (ESI-TOF) calc'd for $[\text{M}+\text{H}]^+$ $\text{C}_{28}\text{H}_{31}\text{N}_2\text{O}_7$ = 507.2126, found 507.2130.



Hydrogenation precursor (83): Alcohol **96** (29.5 mg, 0.058 mmol, 1 equiv), TEMPO (4.5 mg, 0.029 mmol, 0.5 equiv), N-hydroxysuccinimide (7.4 mg, 0.064 mmol, 1.1 equiv), and (diacetoxyiodo)benzene (75.0 mg, 0.233 mmol, 4 equiv) were dissolved in CH_2Cl_2 (1.2 mL, 0.05 M) and stirred at room temperature. After 3 hours, LCMS showed complete consumption of the alcohol. Methanol (1.2 mL) and *p*-toluenesulfonic acid monohydrate (110.7 mg, 0.582 mmol, 10 equiv) were added and the reaction heated at reflux for 5 hours. The solution was concentrated, then redissolved in CH_2Cl_2 and was washed with dilute aqueous K_2CO_3 and brine. The layers were separated and the aqueous phase was extracted with CH_2Cl_2 . The combined organic phases were dried over Na_2SO_4 and concentrated. The product was purified by column chromatography using a 1:1 mixture of CH_2Cl_2 :EtOAc as the polar solvent (20–30–40–50–60–100% polar solvent/hex + 1% NEt_3). Pale yellow solid, 18.6 mg, 0.038 mmol, 65% yield. ^1H NMR (400 MHz, CDCl_3) δ 8.79 (d, J = 0.8 Hz, 1H), 8.30 (s, 1H), 7.90 (s, 1H), 7.59 (d, J = 0.5

Hz, 1H), 5.55 (t, $J = 3.5$ Hz, 1H), 5.39 (d, $J = 3.5$ Hz, 2H), 4.06 (s, 3H), 4.06 (s, 3H), 3.99 (s, 3H), 3.96 (s, 3H), 3.90 (s, 3H), 2.49 (d, $J = 0.9$ Hz, 3H), 2.38 (s, 3H); ^{13}C NMR (100 MHz, CDCl_3) δ 166.9, 160.2, 155.8, 155.6, 155.0, 151.1, 149.1, 148.5, 139.0, 138.4, 135.5, 128.5, 127.9, 125.3, 124.8, 121.6, 120.3, 118.8, 101.3, 64.7, 62.4, 60.9, 60.3, 56.1, 53.4, 52.9, 17.2, 10.0; IR (thin film, NaCl): 3365, 3130, 2930, 2856, 1691, 1621, 1594, 1557, 1462, 1413, 1392, 1357, 1331, 1302, 1259, 1196, 1131, 1089, 1059, 1010, 964, 890, 838, 802, 777, 734; HRMS (ESI-TOF) calc'd for $[\text{M}^+]$ $\text{C}_{27}\text{H}_{28}\text{N}_2\text{O}_7 = 492.1897$, found 492.1894.

3.6.2.6 Asymmetric hydrogenation of bis-isoquinoline **83**



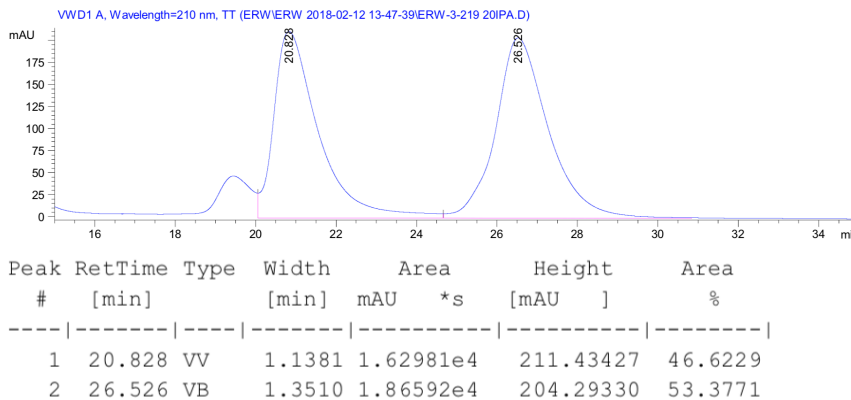
Bis-THIQ pentacycle (81): *Note: Due to the air-sensitivity of the phosphine ligand and the low-valent iridium complex, the preparation of the catalyst and the reaction mixture was performed inside a nitrogen-filled glovebox. The reaction was performed in a 100 mL roundbottom flask with a teflon-coated, egg-shaped stir bar, which was placed inside a Parr bomb. Said bomb was also brought into the glovebox for reaction setup, with the exception of the pressure gauge. A piece of electrical tape was used to seal the bomb immediately upon its removal via the large antechamber, and care was taken to minimize the time between the removal of the tape and the replacement of the gauge.* bis-Isoquinoline **83** (620 mg, 1.07 mmol, 1 equiv) was weighed in air into a 100 mL

roundbottom flask with a teflon-coated stir bar and the flask was brought into a nitrogen-filled glovebox. Solid tetra-*n*-butylammonium iodide (238 mg, 0.644 mmol, 0.6 equiv, 3 equiv relative to Ir) was added to the flask. [Ir(cod)Cl]₂ (72.1 mg, 0.107 mmol, 0.1 equiv, 20 mol% Ir) and BTfM-Xyliphos (a.k.a. SL-J008-2, 205 mg, 0.225 mmol, 0.21 equiv) were dissolved in 10 mL toluene in a scintillation vial and the resulting solution was allowed to stand for 10 min. 28.3 mL of toluene was added to the flask containing bis-isoquinoline **83**, followed by the addition of 5.4 mL AcOH, resulting in a yellow solution of protonated **83**. The iridium-ligand solution was then added to the flask with two 5 mL rinses, bringing the final volume to 53.7 mL of 9:1 PhMe:AcOH (0.02 M in **83**). The flask was sealed with a rubber septum that was then pierced with three 16 gauge (purple) needles, each bent at a 90° angle. The flask was placed inside the bomb, which was then sealed prior to removal from the glovebox via the large antechamber. At this stage, the tape was removed from the top of the bomb and the pressure gauge was quickly screwed in place and tightened. With 200 rpm stirring, the bomb was charged to 10 bar of H₂ and slowly released. This process was repeated twice, before charging the bomb to 60 bar of H₂, at which time it was placed in a preheated 60 °C oil bath. The bath was maintained at this temperature for 18 h, then raised to 80 °C for 24 h. At this time, the bomb was removed from the oil bath and the hydrogen pressure was vented. The flask was removed from the bomb and the solution was transferred to a 250 mL roundbottom flask and basified by the careful addition of saturated aqueous K₂CO₃ and water until pH > 7. The solution was transferred to a separatory funnel and the layers were separated. The aqueous phase was extracted 5x with EtOAc, and the combined organic phases were washed twice with water and once with brine, dried over Na₂SO₄, and concentrated. The

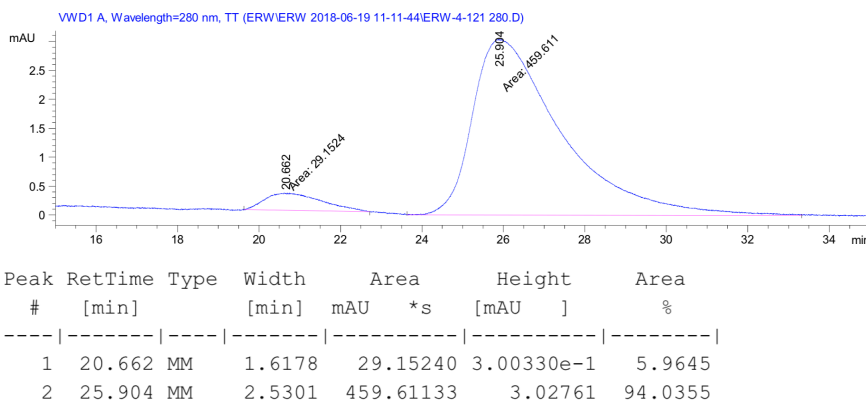
product was purified by column chromatography (15x1", 1% MeOH/DCM + 1% NEt₃). At this stage, ¹H NMR determined the purity of the product to be 90% as a brown foam. 469 mg, 422 mg adjusted for purity, 0.899 mmol, 83% yield, 88% ee. Enantiomeric excess was determined by chiral HPLC analysis [AD, 20% IPA, 280 nm, 1.0 mL/min: t_R(minor) = 21.6 min, t_R(minor) = 26.9 min]. The product could then be crystallized to analytical and optical purity (>99% ee) by dissolving the brown foam in acetonitrile and allowing the solution to slowly evaporate under a stream of N₂. The crystals were washed 3x with 500 μL portions of –40 °C acetonitrile. The resulting crystals were dried *in vacuo*, providing 203 mg of enantiopure (>99% ee) bis-tetrahydroisoquinoline **81**. The mother liquor could be purified by preparative SFC (AD-H, 20% IPA/CO₂, 210 nm, flow rate = 40 mL/min, t_R(minor) = 25.0 min, t_R(major) = 30.0 min) to provide the remaining material in enantiopure fashion. The crystals isolated above were used to collect the following characterization data. ¹H NMR (500 MHz, CDCl₃) δ 6.73 (s, 1H), 6.35 (s, 1H), 5.79 (dd, *J* = 6.7, 3.8 Hz, 1H), 4.12 – 4.10 (m, 2H), 3.93 (dt, *J* = 12.7, 2.9 Hz, 1H), 3.91 (s, 3H), 3.83 (s, 3H), 3.78 (s, 3H), 3.70 (s, 3H), 3.43 (d, *J* = 10.6 Hz, 1H), 3.22 – 3.10 (m, 3H), 3.03 (dd, *J* = 17.2, 6.6 Hz, 1H), 2.74 (dd, *J* = 14.5, 2.6 Hz, 1H), 2.67 – 2.60 (m, 1H), 2.25 (s, 3H), 2.15 (s, 3H); ¹³C NMR (125 MHz, CDCl₃) δ 172.9, 157.7, 156.6, 150.0, 149.7, 131.8, 131.2, 130.9, 125.0, 124.4, 119.8, 119.7, 106.1, 69.0, 61.7, 60.7, 60.4, 60.0, 55.9, 55.0, 54.4, 52.8, 33.2, 30.1, 15.9, 9.2; IR (thin film, NaCl): 3302, 3053, 2940, 2859, 2836, 1622, 1614, 1486, 1463, 1455, 1410, 1353, 1324, 1274, 1233, 1191, 1124, 1082.0, 1001, 958, 926, 894, 849, 817, 789, 735, 703.; HRMS (ESI-TOF) calc'd for [M⁺] C₂₆H₃₂N₂O₆ = 468.2260, found 468.2255; [α]_D = –56.9° (c = 0.5, CHCl₃).

HPLC traces of racemic, enantioenriched, and enantiopure **81**:

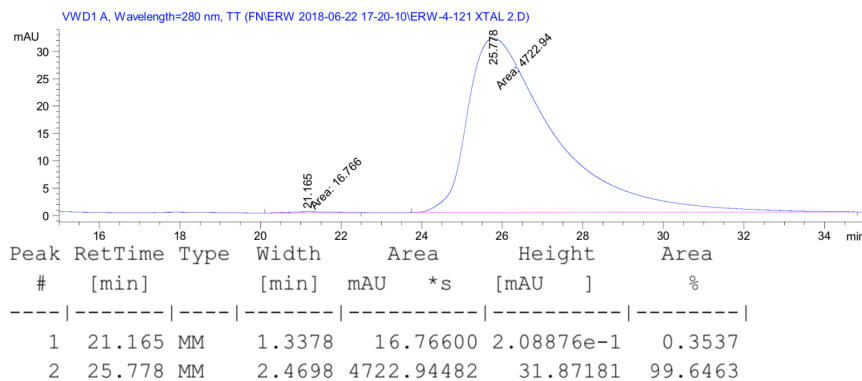
Racemic **81**:



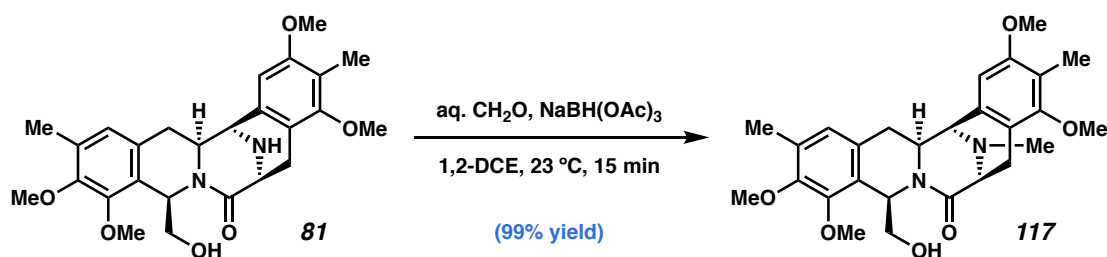
Enantioenriched **81**:



Enantiopure **81**:

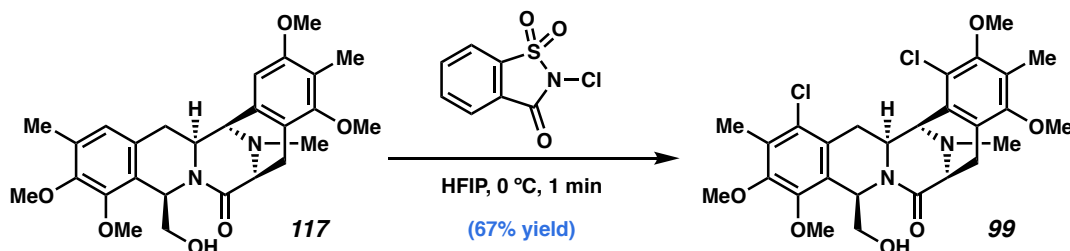


3.6.2.7 Endgame synthesis of Jorumycin



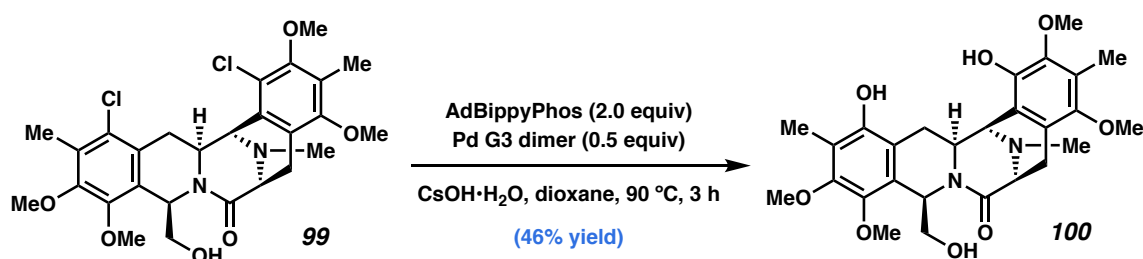
N-methyl bis-THIQ pentacycle (117): Enantiopure bis-tetrahydroisoquinoline **81** (120 mg, 0.256 mmol, 1 equiv) was dissolved in 1,2-dichloroethane (1,2-DCE, 5.1 mL, 0.05 M) and 37% aqueous formaldehyde (35 μ L, 0.474 mmol, 1.85 equiv) was added. The solution was stirred at 800 rpm for 10 min before sodium triacetoxyborohydride (307 mg, 1.45 mmol, 5 equiv) was added. This solution was stirred at 23 °C for 15 min, at which time LCMS showed full conversion to the product. Citric acid monohydrate (404 mg, 1.92 mmol, 7.5 equiv) was added to the solution, followed by 20 mL water. This solution was stirred for 10 min before the slow addition of saturated aqueous K₂CO₃ until pH > 7. The layers were separated and the aqueous phase was extracted with CH₂Cl₂. The combined organic phases were washed with brine, dried over Na₂SO₄ and concentrated. The product was purified by column chromatography (1% MeOH/DCM + 1% NEt₃). Colorless solid, 123 mg, 0.255 mmol, quantitative yield. ¹H NMR (500 MHz, CDCl₃) δ 6.72 (s, 1H), 6.34 (s, 1H), 5.77 (dd, *J* = 6.5, 3.8 Hz, 1H), 4.00 (dt, *J* = 12.4, 3.0 Hz, 1H), 3.90 (s, 3H), 3.83 (s, 3H), 3.80 – 3.76 (m, 2H), 3.78 (s, 3H), 3.70 (s, 3H), 3.44 (ddd, *J* = 8.6, 7.1, 6.0 Hz, 1H), 3.22 – 3.15 (m, 2H), 3.14 (dd, *J* = 17.6, 6.5 Hz, 1H), 2.96 (br s, 1H), 2.94 (dd, *J* = 17.6, 1.2 Hz, 1H), 2.67 (dd, *J* = 14.5, 2.6 Hz, 1H), 2.62 – 2.53 (m, 1H), 2.47 (s, 3H), 2.24 (s, 3H), 2.15 (s, 3H); ¹³C NMR (125 MHz, CDCl₃) δ 173.4, 157.4, 156.7, 150.0, 149.7, 131.7, 131.5, 128.8, 125.0, 124.4, 119.7, 119.0, 106.9, 69.1, 61.4,

60.7, 60.4, 60.3, 60.0, 58.4, 55.9, 52.8, 40.1, 33.0, 24.2, 15.9, 9.1; IR (thin film, NaCl): 3383, 2938, 2862, 1633, 1608, 1485, 1463, 1446, 1410, 1360, 1325, 1272, 1233, 1190, 1124, 1080, 1015, 1001, 963, 910, 848, 804, 646; HRMS (ESI-TOF) calc'd for $[M^+]$ $C_{27}H_{34}N_2O_6$ = 482.2417, found 482.2414; $[\alpha]_D = -76.2^\circ$ ($c = 0.5$, $CHCl_3$).



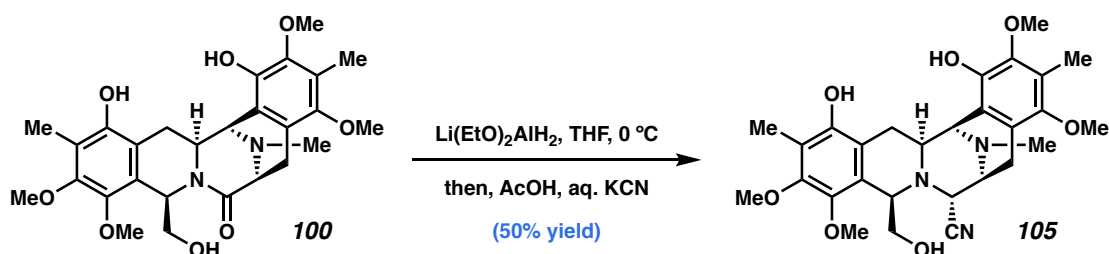
Dichlorinated bis-THIQ (99): bis-Tetrahydroisoquinoline **117** (179.9 mg, 0.372 mmol, 1.0 equiv) was dissolved in HFIP (16.6 mL, 0.02 M after complete addition) and the solution was cooled to 0 °C. *N*-Chlorosaccharine (170 mg, 0.782 mmol, 2.1 equiv) was dissolved in 2 mL HFIP and this solution was added at a slow dropwise pace, allowing the orange color to dispel after each addition, and the resulting yellow solution was stirred at 0 °C. An LCMS sample taken 1 min after complete addition showed full conversion to the dichloride product, so the reaction was quenched by the addition of saturated aqueous $Na_2S_2O_3$. The resulting mixture was transferred to a separatory funnel and diluted with CH_2Cl_2 and water, creating a triphasic system with HFIP on bottom, CH_2Cl_2 in the middle, and the aqueous phase on top. The bottom two phases were collected directly in a 250 mL roundbottom flask. The aqueous phase was basified with K_2CO_3 and extracted with CH_2Cl_2 , draining the organic phase directly into the flask. The flask was concentrated and azeotropically dried twice with toluene. The product was then purified by column chromatography (1% MeOH/ CH_2Cl_2 + 1% NEt_3). White solid, 138.3 mg, 0.251 mmol, 67% yield. 1H NMR (500 MHz, $CDCl_3$) δ 5.85 (dd, $J = 7.2, 4.1$ Hz,

1H), 4.47 (dd, $J = 3.7, 1.1$ Hz, 1H), 4.04 (ddd, $J = 12.8, 3.7, 2.6$ Hz, 1H), 3.90 (s, 3H), 3.82 (dd, $J = 15.6, 2.6$ Hz, 1H), 3.82 (s, 3H), 3.78 – 3.76 (m, 1H), 3.77 (s, 3H), 3.72 (s, 3H), 3.42 (dt, $J = 10.8, 4.8$ Hz, 1H), 3.18 (dd, $J = 7.0, 4.8$ Hz, 1H), 3.13 (dd, $J = 18.2, 6.7$ Hz, 1H), 3.13 – 3.08 (m, 1H), 3.00 (dd, $J = 18.1, 1.3$ Hz, 1H), 2.45 (s, 3H), 2.31 (s, 3H), 2.27 (s, 3H), 2.17 (dd, $J = 15.6, 12.8$ Hz, 1H); ^{13}C NMR (125 MHz, CDCl_3) 173.3, 156.1, 153.8, 150.4, 148.3, 130.7, 129.8, 128.0, 127.9, 126.2, 125.6, 124.5, 123.9, 69.1, 60.9, 60.5, 60.4, 59.5, 58.8, 57.6, 52.1, 40.3, 29.5, 24.7, 13.8, 10.1; IR (thin film, NaCl): 3418, 2940, 1644, 1634, 1462, 1455, 1404, 1361, 1330, 1272, 1236, 1224, 1191.6, 1147, 1106, 1082, 1005, 951, 932, 833, 794; HRMS (ESI-TOF) calc'd for $[\text{M}^+]$ $\text{C}_{27}\text{H}_{32}\text{N}_2\text{O}_6\text{Cl}_2$ = 550.1637, found 550.1637; $[\alpha]_{\text{D}} = -119.0^\circ$ ($c = 0.5$, CHCl_3).



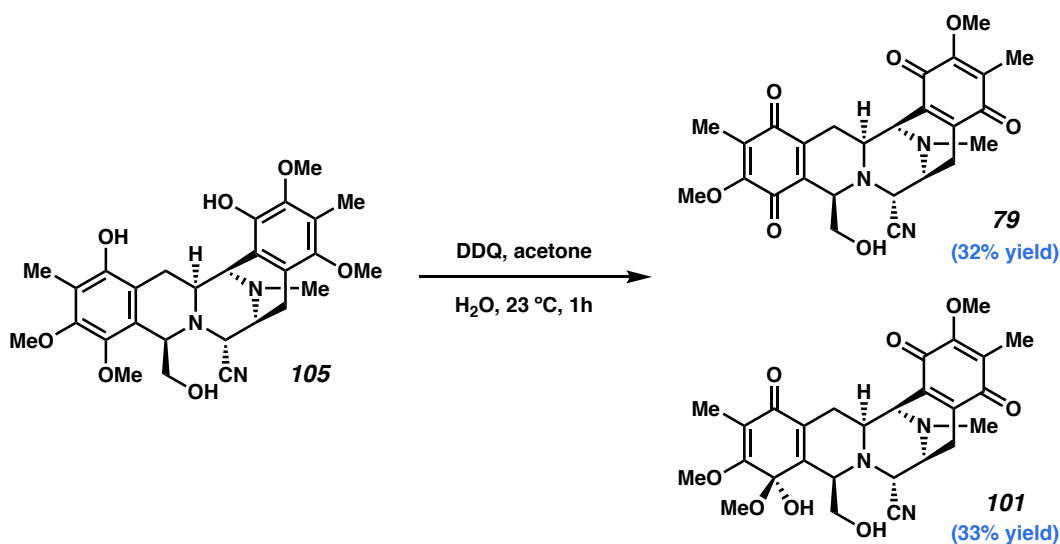
Dihydroxylated bis-THIQ (100). *Note: If the reaction vessel is prematurely exposed to air at elevated temperatures, aerobic oxidation leads to the formation of quinones, which undergo hydrolysis of the vinylogous ester in the presence of CsOH. The solution must be fully cooled to room temperature prior to breaking the seal. The bisphenol product is otherwise not sensitive to aerobic oxidation, in the solid state or in solution.* In a nitrogen-filled glovebox, (2'-Amino-1,1'-biphenyl-2-yl)methanesulfonatopalladium(II) dimer (Buchwald's dimer, 33.5 mg, 0.0453 mmol, 0.500 equiv) and 5-[di(1-adamantyl)phosphino]-1',3',5'-triphenyl-1'H-[1,4']bipyrazole (AdBippyPhos, 120.2 mg, 0.181 mmol, 2.00 equiv) were weighed into a scintillation vial and dioxane (8.1 mL) was

added. The vial was sealed with electrical tape and removed from the glovebox, sonicated briefly, and returned to the glovebox. The resulting tan solution was then transferred to a 20 mL microwave vial containing bis-THIQ **99** (50.0 mg, 0.0907 mmol, 1.00 equiv) and CsOH•H₂O (152.3 mg, 0.907 mmol, 10.0 equiv), followed by a 1 mL rinse (9.1 mL total volume, 0.01 M in **99**). The vial was sealed, removed from the glovebox, and placed in a preheated 90 °C oil bath. After 3 h, the vial was removed and allowed to cool fully to room temperature prior to removing the seal. Acetic acid (46.5 µL, 0.813 mmol, 9 equiv) was added to quench the remaining CsOH and the contents of the vial were transferred to a roundbottom flask, to which silica gel and solid KHCO₃ (to quench excess acetic acid) were added directly to dry load the crude mixture onto a silica gel column. The solution was concentrated, and the product was purified by column chromatography (2–4–6–8–10% MeOH + CH₂Cl₂; 200 mL portions, no NEt₃ added, product elutes in the 6% portion). Tan solid, 21.4 mg, 0.0416 mmol, 46% yield. ¹H NMR (500 MHz, CDCl₃) δ 5.80 (dd, *J* = 7.2, 4.2 Hz, 1H), 4.34 (d, *J* = 2.0 Hz, 1H), 3.96 (dt, *J* = 12.3, 2.5 Hz, 1H), 3.81 (s, 3H), 3.80 (dd, *J* = 6.0, 1.0 Hz, 1H), 3.77 (s, 3H), 3.75 (s, 3H), 3.65 (s, 3H), 3.52 (br s, 1H), 3.47 – 3.40 (m, 2H), 3.23 (dd, *J* = 10.8, 7.2 Hz, 1H), 3.14 (dd, *J* = 18.1, 6.7 Hz, 1H), 3.02 (d, *J* = 18.0 Hz, 1H), 2.45 (s, 3H), 2.21 (s, 3H), 2.14 (s, 3H), 2.09 (dd, *J* = 15.2, 12.2 Hz, 1H); ¹³C NMR (125 MHz, CDCl₃) δ 173.6, 150.0, 149.7, 146.8, 144.1, 143.5, 143.4, 124.6, 123.7, 122.6, 118.6, 118.3, 115.9, 69.2, 61.0, 60.9, 60.4, 60.3, 59.6, 59.0, 55.3, 52.5, 40.1, 25.2, 24.5, 9.7, 9.3; IR (thin film, NaCl): 3332, 2937, 1613, 1462, 1453, 1414, 1353, 1302, 1191, 1109, 1068, 1006, 910, 836, 806, 731; HRMS (ESI-TOF) calc'd for [M⁺] C₂₇H₃₄N₂O₈ = 514.2315, found 514.2311; [α]_D = –91.6° (c = 0.5, CHCl₃).



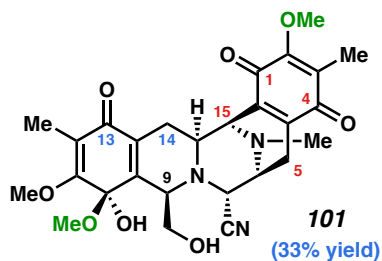
Dihydroxylated bis-THIQ aminonitrile (105): In an oven-dried vial, LiAlH_4 solution (1.0 M in THF, 2 mL, 2.0 mmol) was cooled to $0\text{ }^\circ\text{C}$. A solution of ethyl acetate (230 μL , 2.35 mmol) in 2 mL THF was added slowly, and the resulting solution was stirred 30 min at $0\text{ }^\circ\text{C}$, providing a 0.47 M solution of $\text{Li(EtO)}_2\text{AlH}_2$ in THF. bis-THIQ **100** (49.0 mg, 0.095 mmol, 1.0 equiv) was dissolved in THF (4.8 mL, 0.02 M) and the resulting solution was cooled to $0\text{ }^\circ\text{C}$. A solution of $\text{Li(EtO)}_2\text{AlH}_2$ (0.47 M in THF, 3.0 mL, 1.43 mmol, 15.0 equiv) was added slowly, resulting in extensive evolution of H_2 . After stirring 50 min, the reaction was quenched with acetic acid (115 μL , 2.00 mmol, 21 equiv) and aqueous potassium cyanide (4.8 M, 120 μL , 0.571 mmol, 6.0 equiv) was added, followed by celite and anhydrous Na_2SO_4 (roughly 1 g each). The solution was diluted with 8 mL THF and stirred 10 h, warming to room temperature. More celite was added, and the suspension was filtered through celite, rinsing with EtOAc. The filtrate was transferred to a roundbottom flask and was concentrated. At this stage, LCMS revealed a ~4:1 mixture of product **105** and starting material **100**, so the crude mixture was resubjected to the reduction conditions, using 3 mL THF as the reaction solvent and 1 mL of freshly prepared $\text{Li(EtO)}_2\text{AlH}_2$ solution. After 10 min, LCMS showed minimal conversion of the remaining starting material, with some over-reduced product ($m/z = 501$). The reaction mixture was quenched and worked up as described above. The product was purified by column chromatography (50–75–100% EtOAc/hex, 200 mL each; product elutes in the

75% portion). Colorless solid, 25.2 mg, 47.9 μmol , 50% yield. ^1H NMR (400 MHz, CDCl_3) δ 4.19 (dD, $J = 2.7, 1.1$ Hz, 1H), 4.00 – 4.05 (m, 2H), 3.81 (s, 3H), 3.751 (s, 3H), 3.749 (s, 3H), 3.70 (s, 3H), 3.56 (dd, $J = 10.9, 4.4$ Hz, 1H), 3.40 (ddd, $J = 7.5, 2.5, 1.2$ Hz, 1H), 3.31 (dt, $J = 12.1, 2.7$ Hz, 1H), 3.18 (d, $J = 9.4$ Hz, 1H), 3.13 (dd, $J = 15.6, 2.7$ Hz, 1H), 3.10 (dd, $J = 18.6, 7.8$ Hz, 1H), 2.51 (d, $J = 18.6$ Hz, 1H), 2.34 (s, 3H), 2.22 (s, 3H), 2.09 (s, 3H), 1.85 (dd, $J = 15.6, 12.0$ Hz, 1H); ^{13}C NMR (100 MHz, CDCl_3) δ 149.6, 148.7, 146.6, 143.7, 143.4, 143.1, 125.4, 123.5, 122.7, 118.1, 118.0, 117.1, 116.7, 66.2, 61.2, 61.0, 60.8, 60.4, 60.2, 58.5, 57.1, 56.7, 55.2, 41.9, 25.4, 21.7, 9.8, 9.0; IR (thin film, NaCl): 3428, 2936, 2833, 2228, 1607, 1463, 1412, 1385, 1350, 1320, 1301, 1251, 1218.1, 1191, 1151, 1108, 1070, 1002, 982, 908, 875, 830, 754; HRMS (ESI-TOF) calc'd for $[\text{M}^+]$ $\text{C}_{28}\text{H}_{35}\text{N}_3\text{O}_7 = 525.2475$, found 525.2471; $[\alpha]_{\text{D}} = +22.9^\circ$ ($c = 0.5$, CHCl_3).



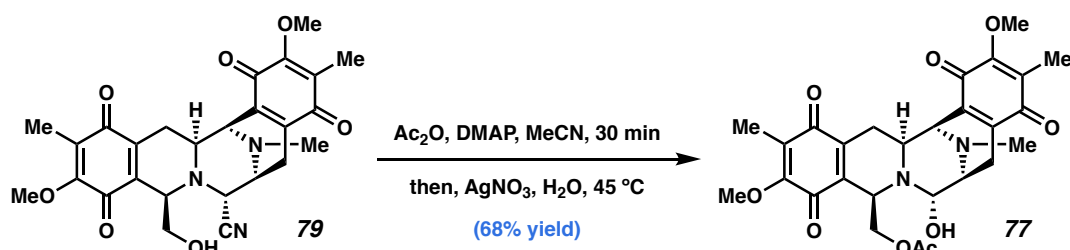
(–)-Jorunnamycin A (79): bis-Tetrahydroisoquinoline **105** (22.0 mg, 41.9 μmol , 1.0 equiv) and DDQ (38.0 mg, 167 μmol , 4.0 equiv) were weighed into a roundbottom flask and 8.4 mL of a 9:1 mixture of acetone and water was added (0.005 M). The purple solution gradually turned blood red. After 1 h, the reaction was quenched with saturated

aqueous NaHCO₃. The phases were separated and the aqueous phase was extracted with ethyl acetate. The combined organic phases were washed with brine, dried over Na₂SO₄, and concentrated. The product was purified using reverse-phase (C₁₈) preparative HPLC (MeCN/0.4% acetic acid in water, 5.0 mL/min, monitor wavelength = 254 nm, 20–70% MeCN over 5 min, hold at 70% for 3 min, hold at 95% for 3 min. Product **3** has *t*_R = 7.2 min). Yellow film, 6.6 mg, 13.4 μmol, 32% yield. ¹H NMR (500 MHz, CDCl₃) δ 4.11 (d, *J* = 2.6 Hz, 1H), 4.08 (dd, *J* = 3.0, 1.0 Hz, 1H), 4.03 (s, 3H), 3.99 (s, 3H), 3.90 (app q, *J* = 3.1 Hz, 1H), 3.71 (dd, *J* = 11.3, 3.4 Hz, 1H), 3.50 (br s, 1H), 3.42 (ddd, *J* = 7.4, 2.6, 1.5 Hz, 1H), 3.18 (dt, *J* = 11.4, 2.9 Hz, 1H), 2.93 (ddd, *J* = 17.4, 2.8, 0.9 Hz, 1H), 2.83 (dd, *J* = 21.0, 7.5 Hz, 1H), 2.31 (s, 3H), 2.26 (d, *J* = 21.0 Hz, 1H), 1.95 (s, 3H), 1.94 (s, 3H), 1.41 (ddd, *J* = 17.5, 11.5, 2.7 Hz, 1H); ¹³C NMR (125 MHz, CDCl₃) δ 186.4, 185.6, 182.4, 181.5, 155.6, 155.5, 141.8, 141.5, 136.2, 135.8, 129.1, 128.8, 117.0, 64., 61.3, 61.3, 59.1, 58.1, 54.6, 54.4, 54.4, 41.8, 25.5, 21.6, 9.0, 8.9; IR (thin film, NaCl): 3508.5, 2943.0, 2226.8, 1651.8, 1620.8, 1447.2, 1373.6, 1310.6, 1277.4, 1236.0, 1190.6, 1151.1, 1098.1, 1077.8, 963.7, 886.8, 775.3; HRMS (ESI-TOF) calc'd for [M⁺] C₂₆H₂₇N₃O₇ = 493.1849, found 493.1848; [α]_D = –94.3° (c = 0.35, CHCl₃).



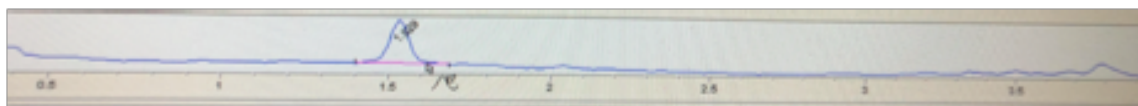
Hemiactal (101): Product **101** was also isolated from the preparative HPLC method described above, with *t*_R = 9.3 min. Yellow film, 7.3 mg, 13.9 μmol, 33% yield. The structure was assigned using diagnostic nOe correlations (highlighted methoxy groups)

and HMBC correlations (C13 to C14 but not C9, C1 to C15 and C5, C4 to C15 and C5). ^1H NMR (400 MHz, CDCl_3) δ 4.54 (t, $J = 7.7$ Hz, 1H), 4.16 (dd, $J = 3.8, 1.5$ Hz, 1H), 4.08 (s, 3H), 4.00 (s, 3H), 3.74 (dd, $J = 7.8, 5.8$ Hz, 1H), 3.66 (d, $J = 2.6$ Hz, 1H), 3.43 (ddd, $J = 7.8, 2.8, 1.7$ Hz, 1H), 3.29 (dt, $J = 10.8, 4.2$ Hz, 1H), 3.13 (s, 3H), 2.82 (dd, $J = 20.9, 7.8$ Hz, 1H), 2.62 (ddd, $J = 18.6, 4.6, 3.0$ Hz, 1H), 2.28 (s, 3H), 2.13 (d, $J = 20.9$ Hz, 1H), 1.93 (s, 3H), 1.75 (s, 3H), 1.68 (br s, 1H, OH), 1.52 (ddd, $J = 18.5, 10.7, 3.1$ Hz, 1H); ^{13}C NMR (400 MHz, CDCl_3) δ 186.6, 185.2, 182.7, 160.4, 155.9, 143.2, 141.2, 136.2, 128.5, 127.7, 117.9, 116.0, 99.0, 74.2, 61.2, 60.5, 59.1, 56.0, 55.6, 54.6, 53.9, 51.8, 41.9, 26.0, 21.5, 8.8, 7.9; IR (thin film, NaCl): 3446, 3014, 2953, 2854, 2226, 1644, 1615, 1455, 1413, 1373, 1318, 1272, 1248, 1189, 1154, 1092, 1061, 1026, 991, 973, 950, 896, 878, 759, 721; HRMS (ESI-TOF) calc'd for $[\text{M}-\text{OH}]^+$ $\text{C}_{27}\text{H}_{29}\text{N}_3\text{O}_7 = 493.1849$, found 493.1848; $[\alpha]_{\text{D}} = -94.3^\circ$ ($c = 0.35$, CHCl_3).



(–)-Jorumycin (77): In a 1-dram vial, Jorunnamycin A (**79**, 6.6 mg, 13.4 μmol , 1.0 equiv) and DMAP (4.9 mg, 40.1 μmol , 3.0 equiv) were dissolved in acetonitrile (400 μL , 0.03 M) and acetic anhydride (3.8 μL , 40.1 μmol , 3.0 equiv) was added neat. The brown solution immediately turned yellow. After 30 minutes, LCMS showed complete conversion to the acetylated intermediate. At this stage, silver nitrate (57.0 mg, 334 μmol , 25.0 equiv) and water (260 μL) were added in rapid succession. The vial was resealed and placed in a preheated 45°C heating block, then protected from light with aluminum

foil. After 30 minutes, LCMS showed complete conversion to (–)-jorumycin (**77**), so the solution was filtered to remove AgCN and silver black, and the crude reaction mixture was purified directly using preparative HPLC (MeCN/0.4% acetic acid in water, 5.0 mL/min, monitor wavelength = 265 nm, 10–55% MeCN over 7 min, ramp to 95% MeCN over 0.2 min, hold at 95% for 1.8 min for a total run time of 9 min. Product has t_R = 6.6 min). Yellow film, 4.8 mg, 9.12 μ mol, 68% yield. ^1H NMR (500 MHz, CDCl_3) δ 4.44 (dd, J = 11.2, 3.5 Hz, 1H), 4.44 (br s, 1H), 4.37 (d, J = 3.1 Hz, 1H), 4.01 (s, 3H), 3.99 (s, 3H), 3.92 (br s, 1H), 3.82 (dd, J = 11.3, 3.4 Hz, 1H), 3.21 – 3.16 (m, 1H), 3.14 (dd, J = 7.3, 4.7 Hz, 1H), 2.84 (dd, J = 16.6, 2.4 Hz, 1H), 2.66 (dd, J = 21.1, 7.6 Hz, 1H), 2.27 (s, 3H), 2.23 (d, J = 21.0 Hz, 1H), 1.96 (s, 3H), 1.94 (s, 3H), 1.76 (s, 3H), 1.24 (ddd, J = 16.6, 11.3, 2.6 Hz, 1H); ^{13}C NMR (125 MHz, CDCl_3) δ 186.0, 181.4, 170.2, 155.8, 155.4, 142.1, 142.0, 137.4, 128.9, 128.5, 83.1, 64.4, 61.19, 61.17, 57.6, 54.4, 52.9, 51.1, 41.6, 25.7, 20.74, 20.69, 8.9, 8.8; IR (thin film, NaCl): 3478, 2924, 2850, 1738, 1652, 1621, 1449, 1374, 1309, 1260, 1234, 1189, 1150, 1096, 1083, 1013, 902, 872, 840, 801, 730; HRMS (ESI-TOF) calc'd for $[\text{M}^+]$ $\text{C}_{27}\text{H}_{30}\text{N}_2\text{O}_9$ = 526.1951, found 526.1956; $[\alpha]_D = -86.8^\circ$ (c = 0.1, CHCl_3). *Note: After purification via the method described above (preparative HPLC using MeCN and 0.4% AcOH in H_2O with lyophilization of the product-containing fractions), we obtained jorumycin as a yellow solid in high purity as determined from the following LCMS trace (TIC):*



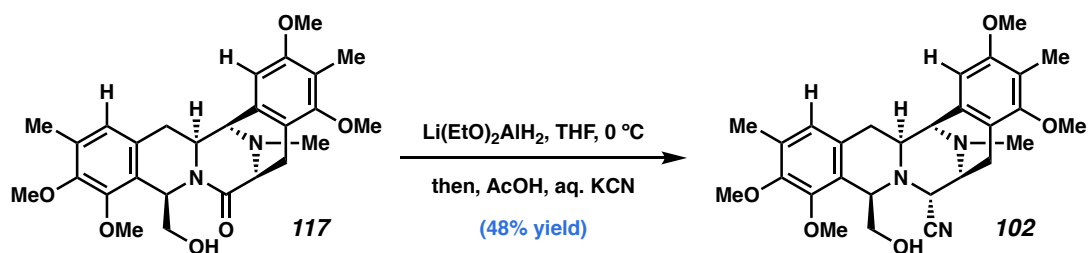
Following this method of purification, a sample was prepared for NMR spectroscopy using CDCl_3 that had been freshly distilled from flame-dried K_2CO_3 , and a ^1H spectrum

was recorded within minutes of preparing the sample. Despite all of our precautions, significant impurities were present in the spectrum at 1.25 ppm, 2–2.25 ppm, and 5–6 ppm. The sample was immediately tested for purity using the same LCMS method as above and provided the following chromatogram (TIC):



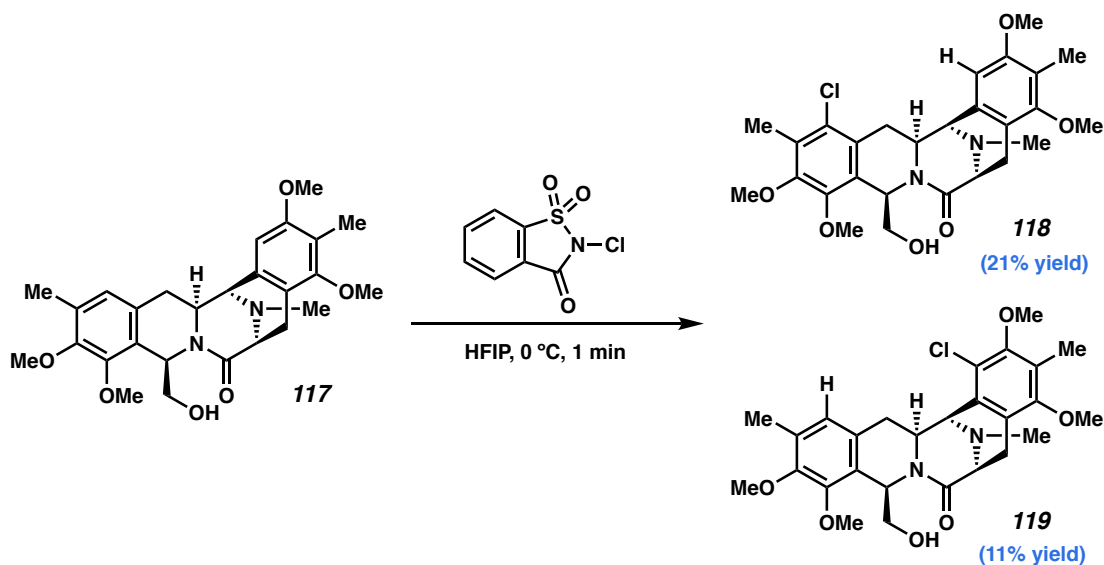
Many attempts to repurify our samples were made, including repurification via the method described above, preparative HPLC with MeCN and H₂O in the absence of AcOH, column chromatography with 1% MeOH in CH₂Cl₂ in the presence or absence of NEt₃, and column chromatography on SiO₂ or basic alumina with EtOAc in the absence of NEt₃. In all cases, spectra containing the impurities described above were obtained, independent of the method of purification. This leads us to conclude that jorumycin is not stable in chloroform; this is also consistent to observations made in the isolation report.²¹ The optical rotation listed above was measured by repurifying the product as originally described and dissolving the sample in CHCl₃ that had been freshly distilled from flame-dried K₂CO₃ immediately prior to recording its optical rotation to minimize decomposition, and this method provided a value in good agreement with previous literature;^{15–20} however, a ¹H NMR spectrum of this sample showed the same impurities described above. We therefore conclude that future synthetic endeavors should avoid the use of chloroform as a solvent for analytical characterization.^{51,52} We are currently working to obtain the requisite data in a solvent such as benzene or acetonitrile.

3.6.2.8 Synthesis of derivatives 102–105



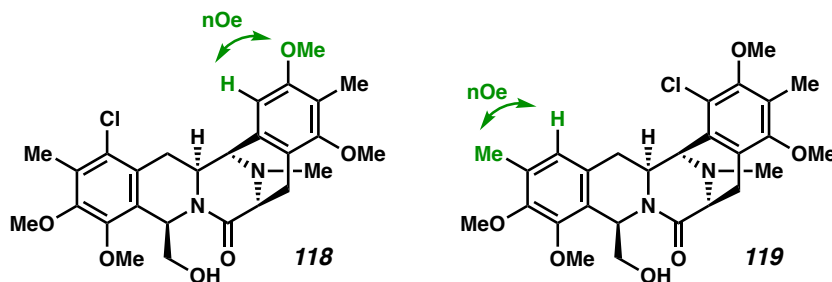
(6*S*,7*R*,9*R*,14*aS*,15*R*)-9-(hydroxymethyl)-2,4,10,11-tetramethoxy-3,12,16-trimethyl-6,7,9,14,14*a*,15-hexahydro-5*H*-6,15-epiminobenzo[4,5]azocino[1,2-*b*]isoquinoline-7-carbonitrile (102). In an oven-dried vial, LiAlH_4 solution (1.0 M in THF, 2 mL, 2.0 mmol) was cooled to 0 °C. A solution of ethyl acetate (230 μL , 2.35 mmol) in 2 mL THF was added slowly, and the resulting solution was stirred 30 min at 0 °C, providing a 0.47 M solution of $\text{Li(EtO)}_2\text{AlH}_2$ in THF. bis-Tetrahydroisoquinoline **117** (8.0 mg, 16.6 μmol , 1.0 equiv) was dissolved in THF (0.75 mL, 0.02 M) and the resulting solution was cooled to 0 °C. A solution of $\text{Li(EtO)}_2\text{AlH}_2$ (0.47 M in THF, 0.47 mL, 0.21 mmol, 15.0 equiv) was added slowly, resulting in extensive evolution of H_2 . After stirring for 45 min, the reaction was quenched with acetic acid (17.7 μL , 0.31 mmol, 21 equiv) and aqueous potassium cyanide (4.8 M, 18.4 μL , 88.4 μmol , 6.0 equiv) was added, followed by celite and anhydrous Na_2SO_4 (roughly 300 mg each). The solution was diluted with 1 mL THF and stirred 10 h, warming to room temperature. More celite was added, and the suspension was filtered through celite, rinsed with EtOAc, and concentrated. The product was purified by preparative HPLC (MeCN/0.4% acetic acid in water, 5.0 mL/min, monitor wavelength = 230 nm, 35–95% MeCN over 8 min, hold at 95% for 1 min for a total run time of 9 min. Product **102** has t_R = 6.5 min). Colorless solid, 3.9 mg, 7.9 μmol , 48% yield. ^1H NMR (400 MHz, CDCl_3) δ 6.57 (s, 1H), 6.23 (s, 1H), 4.02 (d, J = 2.4 Hz,

1H), 3.99 (t, $J = 4.4$ Hz, 1H), 3.80 (s, 3H), 3.75 (s, 3H), 3.69 (s, 3H), 3.66 (s, 3H), 3.55 – 3.51 (m, 1H), 3.48 (d, $J = 10.4$ Hz, 1H), 3.36 (d, $J = 7.7$ Hz, 1H), 3.25 (dt, $J = 12.1, 2.6$ Hz, 1H), 3.13 – 3.07 (m, 1H), 3.05 (dd, $J = 18.4, 7.8$ Hz, 1H), 2.49 – 2.39 (m, 2H), 2.31 (s, 3H), 2.25 – 2.16 (m, 1H), 2.13 (s, 3H), 2.06 (s, 3H); ^{13}C NMR (100 MHz, CDCl_3) δ 155.4, 148.5, 148.1, 130.0, 129.2, 124.9, 124.2, 123.5, 118.1, 117.7, 116.9, 107.3, 106.2, 64.9, 62.4, 61.3, 60.1, 59.3, 58.9, 57.5, 55.5, 54.8, 54.6, 40.7, 31.8, 20.6, 14.7, 8.0; IR (thin film, NaCl): 3441, 2961, 2928, 2855, 1607, 1456, 1410, 1326, 1261, 1190, 1123, 1082, 1030, 912, 865, 801, 734; HRMS (ESI-TOF) calc'd for $[\text{M}^+]$ $\text{C}_{28}\text{H}_{35}\text{N}_3\text{O}_5 = 493.2577$, found 493.2579; $[\alpha]_{\text{D}} = -43.3^\circ$ ($c = 0.05$, CHCl_3).



Monochlorinated bis-THIQ pentacycles (118 and 119): bis-THIQ **117** (112.0 mg, 0.232 mmol, 1.0 equiv) was dissolved in HFIP (11.6 mL, 0.02 M after complete addition) and the solution was cooled to 0 °C. *N*-Chlorosaccharine (55.6 mg, 0.255 mmol, 1.1 equiv) was dissolved in 1.6 mL HFIP and this solution was added at a slow dropwise pace, allowing the orange color to dispel after each addition, and the resulting yellow

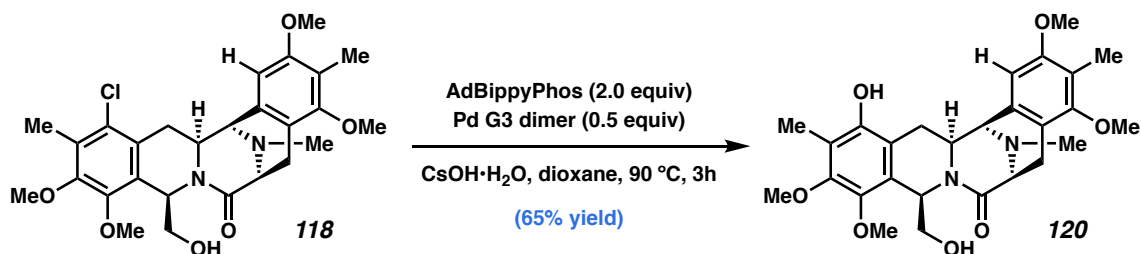
solution was stirred at 0 °C. An LCMS sample taken 1 min after complete addition showed a 2.5:1.7:1.0:1.5 mixture of starting material **117**:**118**:**119**:product **99**. The reaction was quenched by the addition of saturated aqueous Na₂S₂O₃ and transferred to a separatory funnel with CH₂Cl₂ and water, creating a triphasic system with HFIP on bottom, CH₂Cl₂ in the middle, and the aqueous phase on top. The bottom two phases were collected. The aqueous phase was basified with K₂CO₃ and extracted with CH₂Cl₂. The combined organic phases were concentrated and azeotropically dried twice with benzene. Products **118** and **119** were isolated using preparative HPLC (MeCN/0.4% acetic acid in water, 5.0 mL/min, monitor wavelength = 235 nm, 50–80% MeCN over 10 min, ramp to 95% MeCN over 0.5 min, hold at 95% for 2.5 min for a total run time of 13 min. Starting material **117**, product **118**, and **119** has *t*_R = 3.1, 5.1, and 6.7 min, respectively). Starting material **117** was recovered as a colorless solid, 24.3 mg, 0.050 mmol, 22% yield. **118** was isolated as a white solid, 25.2 mg, 0.049 mmol, 21% yield, and 27% yield based on recovered starting material. **119** is a white solid, 13.7 mg, 0.026 mmol, 11% yield, 15% yield based on recovered starting material. The structures of **118** and **119** were assigned using diagnostic nOe correlations (highlighted -OMe or -Me).



Product **118**: ¹H NMR (400 MHz, CDCl₃) δ 6.42 (s, 1H), 5.75 (dd, *J* = 6.4, 4.0 Hz, 1H), 3.95 (ddd, *J* = 12.6, 3.6, 2.5 Hz, 1H), 3.89 (s, 3H), 3.85 (s, 3H), 3.84 – 3.78 (m, 2H), 3.77

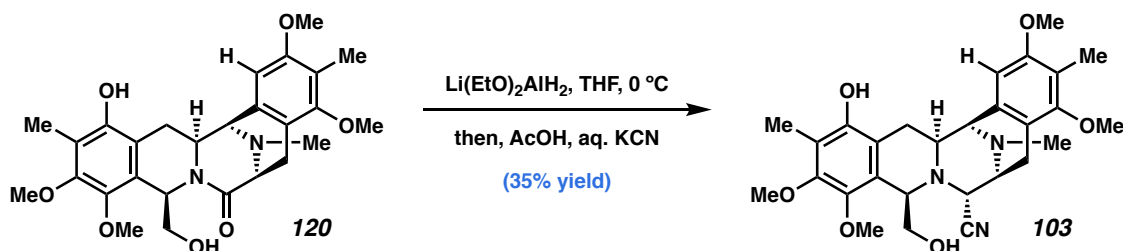
(s, 3H), 3.69 (s, 3H), 3.40 (dd, $J = 11.0, 4.0$ Hz, 1H), 3.26 (dd, $J = 15.2, 2.5$ Hz, 1H), 3.18 (dd, $J = 10.9, 6.4$ Hz, 2H), 3.12 (d, $J = 6.6$ Hz, 1H), 2.94 (dd, $J = 17.7, 1.3$ Hz, 1H), 2.47 (s, 3H), 2.41 (dd, $J = 15.2, 12.6$ Hz, 1H), 2.31 (s, 3H), 2.14 (s, 3H); ^{13}C NMR (100 MHz, CDCl_3) δ 173.1, 157.4, 156.8, 150.4, 148.5, 130.6, 129.7, 128.5, 127.5, 126.2, 119.8, 118.7, 107.0, 68.8, 61.1, 60.9, 60.4, 60.4, 60.1, 57.6, 55.9, 52.7, 40.0, 30.6, 24.0, 13.8, 9.1; IR (thin film, NaCl): 3388, 2938, 1634, 1456, 1407, 1330, 1123, 1081, 1013, 754; HRMS (ESI-TOF) calc'd for $[\text{M}+\text{H}]^+$ $\text{C}_{27}\text{H}_{34}\text{ClN}_2\text{O}_6 = 517.2100$, found 517.2082; $[\alpha]_{\text{D}} = -73.6^\circ$ ($c = 0.89$, CHCl_3).

Product **119**: ^1H NMR (400 MHz, CDCl_3) δ 6.73 (s, 1H), 5.85 (dd, $J = 7.5, 4.2$ Hz, 1H), 4.46 – 4.39 (m, 1H), 4.08 (dt, $J = 12.9, 2.9$ Hz, 1H), 3.90 (s, 3H), 3.80 (s, 3H), 3.77 (s, 4H), 3.71 (s, 4H), 3.44 (dd, $J = 10.8, 4.2$ Hz, 1H), 3.22 – 3.06 (m, 3H), 3.00 (dd, $J = 18.1, 1.3$ Hz, 1H), 2.43 (s, 3H), 2.39 – 2.29 (m, 1H), 2.26 (s, 3H), 2.23 (s, 3H); ^{13}C NMR (100 MHz, CDCl_3) δ 173.3, 156.0, 153.6, 149.8, 149.4, 131.7, 131.3, 127.8, 126.1, 124.8, 124.4, 124.2, 123.5, 69.0, 60.6, 60.4, 60.3, 59.9, 59.3, 59.2, 57.6, 52.0, 40.1, 31.7, 24.8, 15.7, 10.0; IR (thin film, NaCl): 3418, 2939, 2870, 1644, 1634, 1455, 1446, 1326, 1224, 1106, 1081, 1005, 932, 755; HRMS (ESI-TOF) calc'd for $[\text{M}+\text{H}]^+$ $\text{C}_{27}\text{H}_{34}\text{ClN}_2\text{O}_6 = 517.2100$, found 517.2101; $[\alpha]_{\text{D}} = -114.0^\circ$ ($c = 0.86$, CHCl_3).



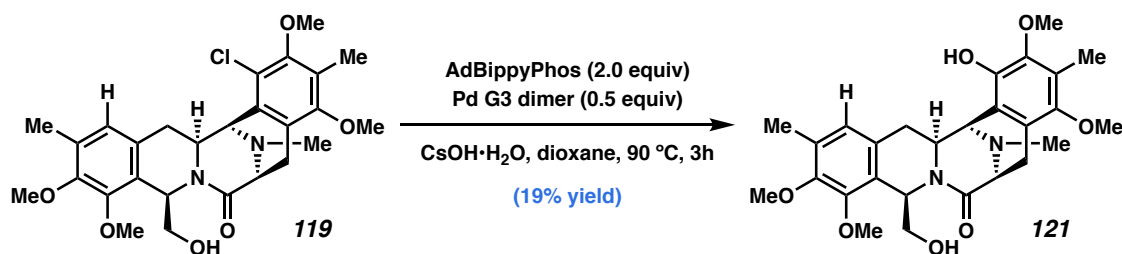
Monohydroxy(A-ring) bis-THIQ (120): In a nitrogen-filled glovebox, Buchwald's dimer (16.4 mg, 0.022 mmol, 0.50 equiv) and 5-[di(1-adamantyl)phosphino]-1',3',5'-

triphenyl-1'-H-[1,4']bipyrazole (AdBippyPhos, 58.9 mg, 0.089 mmol, 2.00 equiv) were weighed into a scintillation vial and dioxane (4.0 mL) was added. The vial was sealed with electrical tape and removed from the glovebox, sonicated briefly, and returned to the glovebox. The resulting tan solution was then transferred to a scintillation vial containing bis-tetrahydroisoquinoline **118** (23.0 mg, 0.045 mmol, 1.00 equiv) and CsOH•H₂O (74.7 mg, 0.045 mmol, 10.0 equiv), followed by a 0.5 mL rinse (4.5 mL total volume, 0.01 M). The vial was sealed, removed from the glovebox, and placed in a preheated 90 °C oil bath. After 3 h, the vial was removed and allowed to cool fully to room temperature prior to removing the seal. Acetic acid (23 µL, 0.401 mmol, 9 equiv) was added to quench the remaining CsOH and the contents of the vial were transferred to a roundbottom flask, to which silica gel was added directly to dry load the crude mixture onto a silica gel column. The solution was concentrated, and the product was purified by column chromatography (2–4–6–8% MeOH + CH₂Cl₂: no NEt₃ added). Colorless solid, 14.4 mg, 0.029 mmol, 65% yield. *Note: Based on the ¹H NMR spectrum of the isolated product, there is approximately 20% of an additional side product.* ¹H NMR (500 MHz, CDCl₃) δ 6.55 (s, 1H), 5.85 (dd, *J* = 6.7, 4.1 Hz, 1H), 4.15 – 3.98 (m, 2H), 3.94 (d, *J* = 2.5 Hz, 7H), 3.89 (s, 4H), 3.81 (s, 4H), 3.50 (dd, *J* = 11.0, 4.2 Hz, 1H), 3.34 – 3.22 (m, 3H), 3.07 (dd, *J* = 17.6, 1.2 Hz, 1H), 2.60 (s, 3H), 2.37 (dd, *J* = 14.9, 12.6 Hz, 1H), 2.28 (s, 3H), 2.26 (s, 3H); ¹³C NMR (100 MHz, CDCl₃) δ 173.3, 157.3, 156.8, 150.0, 146.3, 143.7, 128.7, 125.3, 119.8, 118.8, 118.3, 117.4, 107.2, 69.1, 61.3, 60.9, 60.4, 60.2, 60.2, 58.1, 56.0, 52.6, 40.0, 29.8, 26.1, 24.0, 9.1; IR (thin film, NaCl): 3318, 2935, 1622, 1608, 1587, 1463, 1456, 1355, 1272, 1123, 1069, 755; HRMS (ESI-TOF) calc'd for [M+H]⁺ C₂₇H₃₅N₂O₇ = 499.2439, found 499.2449; [α]_D = –87.2° (c = 1.03, CHCl₃).



Monohydroxy(A-ring) bis-THIQ aminonitrile (103): In an oven-dried 1-dram vial, LiAlH_4 solution (1.0 M in THF, 1 mL, 1.0 mmol) was cooled to 0 °C. A solution of ethyl acetate (115 μL , 1.18 mmol) in 1 mL THF was added slowly, and the resulting solution was stirred 30 min at 0 °C, providing a 0.47 M solution of $\text{Li}(\text{EtO})_2\text{AlH}_2$ in THF. bis-THIQ **120** (14.4 mg, 28.9 μmol , 1.0 equiv) was dissolved in THF (1.5 mL, 0.02 M) and the resulting solution was cooled to 0 °C. A solution of $\text{Li}(\text{EtO})_2\text{AlH}_2$ (0.47 M in THF, 0.92 mL, 0.43 mmol, 15.0 equiv) was added slowly, resulting in extensive evolution of H_2 . After stirring 20 min, LCMS showed complete consumption of **120**, so the reaction was quenched with acetic acid (34.7 μL , 0.607 mmol, 21 equiv) and aqueous potassium cyanide (4.8 M, 36.1 μL , 0.173 mmol, 6.0 equiv) was added, followed by celite and anhydrous Na_2SO_4 (roughly 500 mg each). The solution was diluted with 3 mL THF and stirred for 12 h, warming to room temperature. At this stage, LCMS revealed some unreacted starting material, so the reaction was stirred at 50 °C for an additional 3 hours. ~1 g of K_2CO_3 was added, followed by celite. The suspension was filtered through celite, rinsed with EtOAc, and concentrated. The product was purified by preparative HPLC (MeCN/0.4% acetic acid in water, 5.0 mL/min, monitor wavelength = 230 nm, 40–60% MeCN over 7 min, ramp to 95% MeCN over 0.5 min, hold at 95% for 2.5 min for a total run time of 10 min. Product **103** has t_R = 5.1 min). Colorless solid, 5.1 mg, 10.0 μmol , 35% yield. ^1H NMR (600 MHz, CDCl_3) δ 6.37 (s, 1H), 4.09 (d, J = 2.4 Hz, 1H), 4.07 (t, J

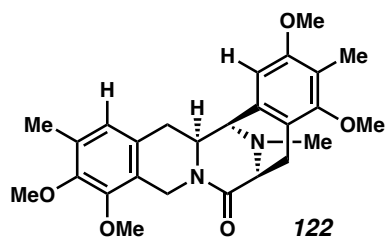
= 4.6 Hz, 1H), 3.83 (s, 3H), 3.81 (s, 3H), 3.77 (s, 3H), 3.73 (s, 3H), 3.65 – 3.62 (m, 1H), 3.53 (dd, $J = 10.9, 4.5$ Hz, 1H), 3.43 (dt, $J = 7.8, 1.5$ Hz, 1H), 3.27 (dt, $J = 12.0, 2.7$ Hz, 1H), 3.16 – 3.09 (m, 2H), 2.94 (dd, $J = 15.1, 2.7$ Hz, 1H), 2.50 (d, $J = 18.2$ Hz, 1H), 2.39 (s, 3H), 2.13 (s, 3H), 2.12 (s, 3H), 2.10 (d, $J = 12.3$ Hz, 1H), 1.99 (dd, $J = 15.1, 12.1$ Hz, 1H); ^{13}C NMR (101 MHz, CDCl_3) δ 156.6, 156.1, 149.6, 146.3, 143.3, 130.4, 125.8, 119.3, 118.9, 118.1, 117.8, 116.1, 107.6, 66.2, 63.6, 61.4, 60.8, 60.5, 60.1, 58.5, 56.4, 55.9, 55.8, 41.9, 26.1, 21.8, 9.2, 8.9; IR (thin film, NaCl): 3444, 2937, 2359, 1606, 1463, 1418, 1354, 1263, 1191, 1122, 1070, 983, 911, 733; HRMS (ESI-TOF) calc'd for $[\text{M}^+]$ $\text{C}_{28}\text{H}_{36}\text{N}_3\text{O}_6 = 510.2599$, found 510.2589; $[\alpha]_{\text{D}} = +36.4^\circ$ ($c = 0.36$, CHCl_3).



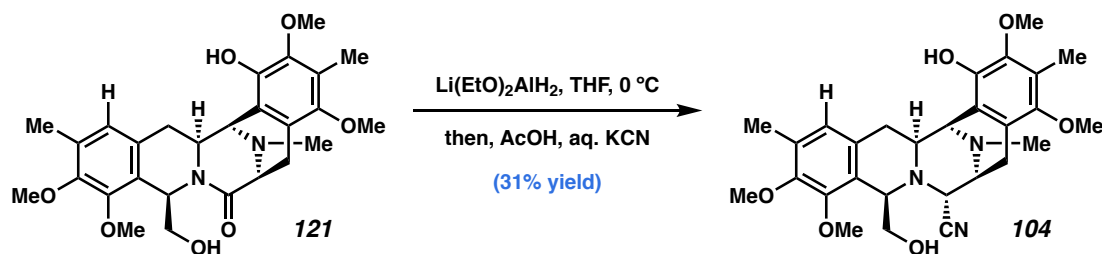
Monohydroxy(E-ring) bis-THIQ (121). In a nitrogen-filled glovebox, Buchwald's dimer (6.8 mg, 9.2 μmol , 0.50 equiv) and 5-[di(1-adamantyl)phosphino]-1',3',5'-triphenyl-1'H-[1,4']bipyrazole (AdBippyPhos, 24.4 mg, 0.037 mmol, 2.00 equiv) were weighed into a scintillation vial and dioxane (1.6 mL) was added. The vial was sealed with electrical tape and removed from the glovebox, sonicated briefly, and returned to the glovebox. The resulting tan solution was then transferred to a 1-dram vial containing bis-tetrahydroisoquinoline **119** (9.5 mg, 0.018 mmol, 1.00 equiv) and $\text{CsOH}\cdot\text{H}_2\text{O}$ (30.9 mg, 0.184 mmol, 10.0 equiv), followed by a 0.2 mL rinse (1.8 mL total volume, 0.01 M). The vial was sealed, removed from the glovebox, and placed in a preheated 90 $^\circ\text{C}$ oil bath. After 3 h, the vial was removed and allowed to cool fully to room temperature prior to

removing the seal. Acetic acid (9.5 μ L, 0.166 mmol, 9 equiv) was added to quench the remaining CsOH and the contents of the vial were transferred to a scintillation vial, to which silica gel was added directly to dry load the crude mixture onto a silica gel column. The solution was concentrated, and the product was purified by column chromatography (2–4–6–8% MeOH + CH₂Cl₂: no NEt₃ added). Due to a significant amount of impurities present in the sample, the isolated product was repurified using preparative HPLC (MeCN/0.4% acetic acid in water, 5.0 mL/min, monitor wavelength = 235 nm, 25–55% MeCN over 10 min, ramp to 95% MeCN over 0.5 min, hold at 95% for 2.5 min for a total run time of 13 min. Product **121** has t_R = 5.1 min). White solid, 1.7 mg, 3.41 μ mol, 19% yield. ¹H NMR (400 MHz, CDCl₃) δ 6.72 (s, 1H), 5.81 (dd, J = 7.2, 3.6 Hz, 1H), 5.65 (s, 1H), 4.27 (dd, J = 3.7, 1.3 Hz, 1H), 4.02 (dt, J = 12.7, 2.9 Hz, 1H), 3.90 (s, 3H), 3.78 (s, 3H), 3.77 (s, 3H), 3.76–3.73 (m, 1H), 3.68 (s, 3H), 3.45 (dd, J = 11.0, 4.1 Hz, 1H), 3.22 (dd, J = 10.6, 7.2 Hz, 1H), 3.13 (dd, J = 18.0, 6.7 Hz, 1H), 3.07 – 2.93 (m, 2H), 2.47 – 2.32 (m, 4H), 2.24 (s, 3H), 2.23 – 2.20 (m, 4H); ¹³C NMR (100 MHz, CDCl₃) δ 173.6, 149.9, 149.8, 149.6, 143.7, 143.0, 132.2, 131.7, 124.8, 124.7, 123.4, 123.0, 115.9, 69.4, 61.1, 60.7, 60.5, 60.0, 59.7, 59.2, 55.2, 52.7, 40.2, 31.8, 24.8, 15.9, 9.8; IR (thin film, NaCl): 3424, 2936, 1628, 1439, 1412, 1326, 1260, 1236, 1109, 1080, 1052, 1006, 731; HRMS (ESI-TOF) calc'd for [M+H]⁺ C₂₇H₃₅N₂O₇ = 499.2439, found 499.2439; [α]_D = –45.8° (c = 0.10, CHCl₃).

*Note: In addition to the desired product **121**, we were also able to isolate and assign the structure of side product **122**. **122** presumably arises from palladium-mediate oxidative deformylation. Similar byproducts have been identified by LCMS in other runs, but have neither been isolated nor quantified.*



Oxidative deformylated byproduct (122). Isolated from preparative HPLC as described above. Product **122** has $t_R = 11.3$ min. Colorless solid, 0.9 mg, 1.99 μmol , 11% yield. ^1H NMR (400 MHz, CDCl_3) δ 6.67 (s, 1H), 6.38 (s, 1H), 4.66 (d, $J = 18.7$ Hz, 1H), 4.55 (d, $J = 18.7$ Hz, 1H), 4.05 (ddd, $J = 12.2, 4.8, 2.7$ Hz, 1H), 3.87 (dd, $J = 4.7, 1.2$ Hz, 1H), 3.85 (s, 3H), 3.82 (s, 4H), 3.78 (s, 3H), 3.70 (s, 3H), 3.10 (dd, $J = 17.9, 7.1$ Hz, 1H), 2.97 – 2.88 (m, 1H), 2.69 (dd, $J = 15.0, 2.7$ Hz, 1H), 2.48 (s, 3H), 2.45 – 2.34 (m, 1H), 2.21 (s, 3H), 2.13 (s, 3H); ^{13}C NMR (100 MHz, CDCl_3) δ 171.0, 157.3, 156.6, 149.7, 130.6, 129.5, 129.1, 124.7, 123.4, 119.6, 119.1, 107.0, 60.7, 60.2, 59.5, 55.9, 55.8, 40.6, 40.1, 33.7, 22.8, 15.8, 9.1; IR (thin film, NaCl): 2935, 2858, 2362, 2344, 1654, 1638, 1610, 1458, 1448, 1413, 1327, 1124, 1078, 1001, 731; HRMS (ESI-TOF) calc'd for $[\text{M}+\text{H}]^+$ $\text{C}_{26}\text{H}_{33}\text{N}_2\text{O}_5 = 453.2384$, found 453.2379; $[\alpha]_D = -123.4^\circ$ ($c = 0.06$, CHCl_3).

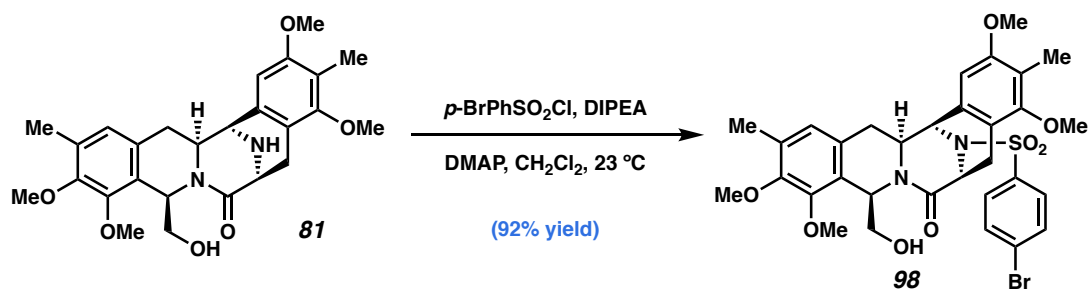


Monohydroxy(E-ring) bis-THIQ aminonitrile (104). In an oven-dried 1-dram vial, LiAlH_4 solution (1.0 M in THF, 1 mL, 1.0 mmol) was cooled to 0 °C. A solution of ethyl acetate (115 μL , 1.18 mmol) in 1 mL THF was added slowly, and the resulting solution was stirred 30 min at 0 °C, providing a 0.47 M solution of $\text{Li}(\text{EtO})_2\text{AlH}_2$ in THF. bis-

THIQ **121** (2.2 mg, 4.41 μmol , 1.0 equiv) was dissolved in THF (0.2 mL, 0.02 M) and the resulting solution was cooled to 0 °C. A solution of $\text{Li}(\text{EtO})_2\text{AlH}_2$ (0.47 M in THF, 141 μL , 66.2 μmol , 15.0 equiv) was added slowly, resulting in extensive evolution of H_2 . After stirring for 20 min, LCMS showed complete consumption of **121**, so the reaction was quenched with acetic acid (5.3 μL , 92.7 μmol , 21 equiv). Aqueous KCN (4.8 M, 5.5 μL , 26.5 μmol , 6.0 equiv) was added, followed by celite, anhydrous Na_2SO_4 (ca. 100 mg each), and 0.4 mL of THF. The reaction was warmed to room temperature and stirred for 12 h. ~150 mg of K_2CO_3 and celite were added. The suspension was filtered through celite, rinsed with EtOAc, and concentrated. The product was purified by preparative HPLC (MeCN/0.4% acetic acid in water, 5.0 mL/min, monitor wavelength = 230 nm, 40–70% MeCN over 10 min, ramp to 95% MeCN over 0.5 min, hold at 95% for 2.5 min for a total run time of 13 min. Product **104** has t_R = 4.7 min). Colorless solid, 0.7 mg, 1.4 μmol , 31% yield. ^1H NMR (400 MHz, CDCl_3) δ 6.65 (s, 1H), 5.52 (s, 1H), 4.15 (s, 1H), 4.07 (d, J = 3.0 Hz, 2H), 3.87 (s, 3H), 3.75 (t, J = 0.9 Hz, 7H), 3.70 (s, 3H), 3.56 (d, J = 8.6 Hz, 2H), 3.43 – 3.31 (m, 2H), 3.10 (dd, J = 18.5, 7.8 Hz, 1H), 2.80 (dd, J = 15.4, 2.5 Hz, 1H), 2.50 (d, J = 18.5 Hz, 1H), 2.34 (s, 3H), 2.23 (s, 3H), 2.20 (s, 4H); ^{13}C NMR (100 MHz, CDCl_3) δ 155.5, 149.2, 148.7, 143.6, 143.3, 142.1, 131.8, 131.2, 125.2, 124.9, 123.5, 118.1, 116.9, 66.0, 61.1, 61.1, 60.5, 60.2, 60.1, 58.7, 57.5, 56.6, 55.3, 41.9, 32.0, 21.8, 15.8, 9.8; IR (thin film, NaCl): 3400, 2930, 2859, 2351, 2250, 1664, 1458, 1412, 1327, 1308, 1261, 1106, 1080, 1057, 1010, 911, 801, 733; HRMS (ESI-TOF) calc'd for $[\text{M}^+]$ $\text{C}_{28}\text{H}_{36}\text{N}_3\text{O}_6$ = 510.2599, found 510.2596; $[\alpha]_D$ = -21.8° (c = 0.05, CHCl_3).

Dihydroxylated bis-THIQ aminonitrile (105): See page 298 for experimental procedure and characterization data.

3.6.2.9 Preparation of **98** for crystal structure analysis



Sulfonamide (98): Bis-THIQ **81** (45 mg, 0.096 mmol, 1.0 equiv, 88% ee), 4-dimethylaminopyridine (DMAP, 1.2 mg, 0.0096 mmol, 0.10 equiv), and p -bromophenylsulfonyl chloride (27 mg, 0.105 mmol, 1.10 equiv) were dissolved in CH_2Cl_2 (2 mL, 0.05 M) and diisopropylethylamine (DIPEA, 33 μL , 0.192 mmol, 2.0 equiv) was added. The solution was stirred 2 h, at which time LCMS revealed full conversion to product **98**. The reaction was quenched by the addition of 1M HCl. The layers were separated and the aqueous phase was extracted with CH_2Cl_2 . The combined organic phases were washed with brine, dried over Na_2SO_4 , and concentrated. The product was purified by column chromatography (1% MeOH/ CH_2Cl_2 + 1% NEt_3). Colorless solid, 61.0 mg, 0.089 mmol, 92% yield. ^1H NMR (400 MHz, CDCl_3) δ 7.55 (d, $J = 8.7$ Hz, 2H), 7.47 (d, $J = 8.8$ Hz, 2H), 6.73 (s, 1H), 6.35 (s, 1H), 5.70 (dd, $J = 6.3, 4.3$ Hz, 1H), 5.07 (dd, $J = 3.5, 1.6$ Hz, 1H), 4.74 (dt, $J = 7.0, 1.3$ Hz, 1H), 4.01 (dt, $J = 12.7, 2.9$ Hz, 1H), 3.90 (s, 3H), 3.84 (s, 3H), 3.77 (s, 3H), 3.49 (s, 3H), 3.41 (dt, $J = 10.4, 4.9$ Hz, 1H), 3.19 (dt, $J = 11.2, 5.6$ Hz, 1H), 3.03 (dd, $J = 17.6, 1.3$ Hz, 1H), 2.77 (dd, $J = 14.4, 2.6$ Hz, 1H), 2.71 (dd, $J = 17.6, 6.9$ Hz, 1H), 2.62 (t, $J = 13.4$ Hz, 1H), 2.49 (t, $J = 5.6$ Hz, 1H), 2.24 (s, 3H), 2.09 (s, 3H).

3.6.3 COMPARISON OF NMR DATA TO KNOWN SAMPLES

Table 3.2 Tabulated NMR data for (–)-jorunnamycin A (**79**).

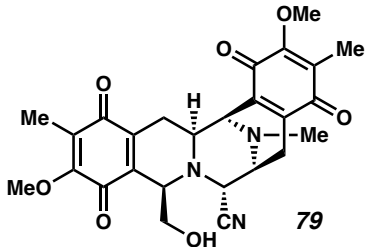
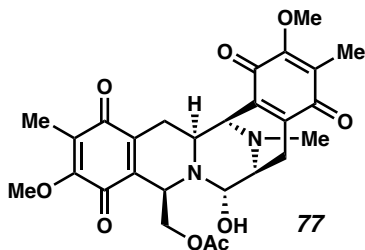
Synthetic Jorunnamycin A (79) ¹ H NMR	Authentic Jorunnamycin A (79) ¹ H NMR ¹⁵	Synthetic 79 ¹³ C NMR	Authentic 79 ¹³ C NMR ¹⁵
4.11 (d, <i>J</i> = 2.6 Hz, 1H)	4.08 (d, <i>J</i> = 2.3 Hz, 1H)	186.4	186.5
4.08 (dd, <i>J</i> = 3.0, 1.0 Hz, 1H)	4.06 (app d, <i>J</i> = 2.1 Hz, 1H)	185.6	185.7
4.03 (s, 3H)	4.01 (s, 3H)	182.4	182.5
3.99 (s, 3H)	3.97 (s, 3H)	181.5	181.6
3.90 (app q, <i>J</i> = 3.1 Hz, 1H)	3.87 (ddd, <i>J</i> = 5.8, 3.0, 3.0 Hz, 1H)	155.6	155.7
3.71 (dd, <i>J</i> = 11.3, 3.4 Hz, 1H)	3.69 (dt, <i>J</i> = 11.5, 2.8 Hz, 1H)	155.5	155.6
3.50 (br s, 1H)	3.48 (m, 1H)	141.8	141.8
3.42 (ddd, <i>J</i> = 7.4, 2.6, 1.5 Hz, 1H)	3.39 (app d, <i>J</i> = 7.5 Hz, 1H)	141.5	141.6
3.18 (dt, <i>J</i> = 11.4, 2.9 Hz, 1H)	3.15 (dt, <i>J</i> = 11.5, 2.8 Hz, 1H)	136.2	136.3
2.93 (ddd, <i>J</i> = 17.4, 2.8, 0.9 Hz, 1H)	2.91 (dd, <i>J</i> = 17.5, 2.6 Hz, 1H)	135.8	135.8
2.83 (dd, <i>J</i> = 21.0, 7.5 Hz, 1H)	2.81 (dd, <i>J</i> = 20.9, 7.5 Hz, 1H)	129.1	129.1
2.31 (s, 3H)	2.28 (s, 3H)	128.8	128.8
2.26 (d, <i>J</i> = 21.0 Hz, 1H)	2.23 (d, <i>J</i> = 21.1 Hz, 1H)	117.0	117.0
1.95 (s, 3H)	1.93 (s, 3H)	64.1	64.2
1.94 (s, 3H)	1.92 (s, 3H)	61.3	61.3
1.41 (ddd, <i>J</i> = 17.5, 11.5, 2.7 Hz, 1H)	1.38 (ddd, <i>J</i> = 17.3, 11.5, 2.6 Hz, 1H)	61.3	61.3
		59.1	59.2
		58.1	58.2
		54.6	54.7
		54.4	54.5
		54.4	54.4
		41.8	41.8
		25.5	25.6
		21.6	21.7
		9.0	9.0
		8.9	8.9

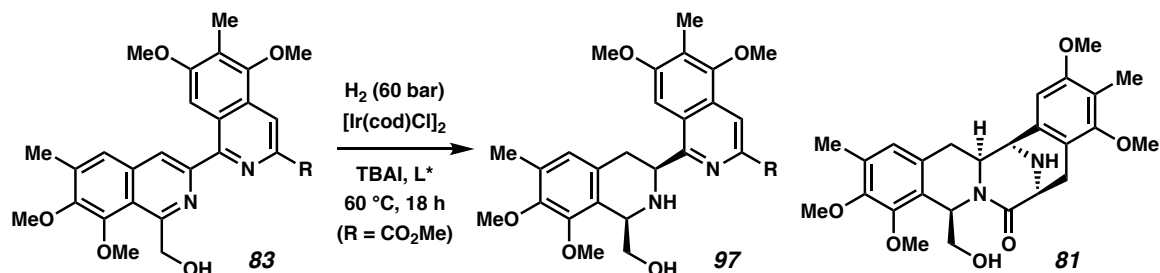
Table 3.3 Tabulated NMR data for (–)-jorunnamycin (**77**).

Synthetic Jorumycin (77) ¹ H NMR	Authentic Jorumycin (77) ¹ H NMR ¹⁵	Synthetic 77 ¹³ C NMR	Authentic 77 ¹³ C NMR ¹⁵
4.47 – 4.41 (m, 1H)	4.41 (dd, <i>J</i> = 11.1, 3.4 Hz, 1H),	186.7	186.8
4.44 (dd, <i>J</i> = 11.2, 3.5 Hz, 1H)	4.41 (d, <i>J</i> = 11.1 Hz, 1H),	186.0	186.1
4.36 (q, <i>J</i> = 3.6, 3.2 Hz, 1H)	4.35 (ddd, <i>J</i> = 5.5, 2.8, 2.8 Hz, 1H),	186.7	182.8
4.00 (s, 3H)	3.98 (s, 3H),	181.5	181.6
3.98 (s, 3H)	3.96 (s, 3H),	170.2	170.3
3.90 (app d, <i>J</i> = 2.5 Hz, 1H)	3.88 (app d, <i>J</i> = 2.7 Hz, 1H),	155.8	155.9
3.88 (br s, 1H, C21-OH)	3.86 (d, <i>J</i> = 10.9 Hz, 1H, C21-OH),	155.4	155.5
3.81 (dd, <i>J</i> = 11.2, 3.3 Hz, 1H)	3.80 (dd, <i>J</i> = 11.1, 3.2 Hz, 1H),	142.1	142.2
3.20 – 3.12 (m, 2H)	3.16 (m, 1H),	142.0	142.1
	3.14 (m, 1H),	137.4	137.5
2.84 (dd, <i>J</i> = 16.7, 2.2 Hz, 1H)	2.82 (dd, <i>J</i> = 16.8, 2.3 Hz, 1H),	134.6	134.7
2.65 (dd, <i>J</i> = 21.0, 7.5 Hz, 1H)	2.63 (dd, <i>J</i> = 21.1, 7.5 Hz, 1H),	128.9	129.0
2.26 (s, 3H)	2.24 (s, 3H),	128.5	128.6
2.23 (d, <i>J</i> = 18.8 Hz, 1H)	2.22 (d, <i>J</i> = 20.0 Hz, 1H),	83.2	83.2
1.96 (s, 3H)	1.94 (s, 3H),	64.3	64.4
1.93 (s, 3H)	1.91 (s, 3H),	61.2	61.2
1.76 (s, 3H)	1.74 (s, 3H),	61.2	61.2
1.28 (dd, <i>J</i> = 11.5, 2.6 Hz, 1H)	1.24 (ddd, <i>J</i> = 16.6, 11.3, 2.6 Hz, 1H)	57.6	57.7
		54.3	54.4
		52.9	52.9
		51.2	51.3
		41.6	41.7
		25.8	25.8
		20.7	20.8
		20.6	20.7
		9.0	9.0
		8.8	8.9

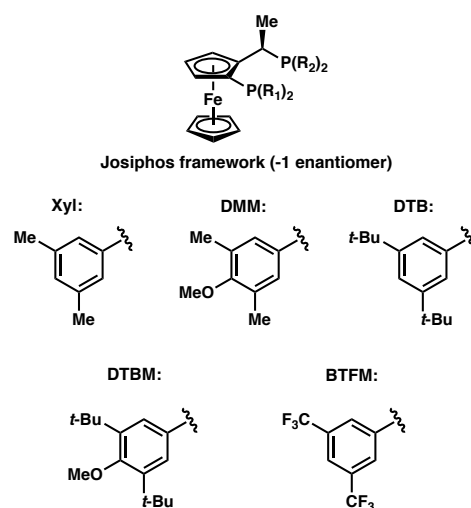


3.6.4 OPTIMIZATION OF THE ENANTIOSELECTIVE HYDROGENATION

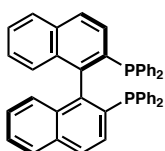
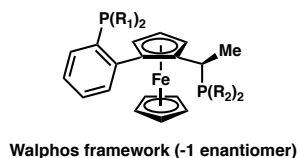
Table 3.4 Optimization of the enantioselective hydrogenation.



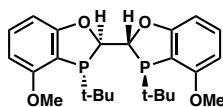
Josiphos lig.	R ₁	R ₂	yield and ee of 97
L50: SL-J001-1	Ph	Cy	--
L51: SL-J002-1	Ph	<i>t</i> -Bu	--
L48: SL-J005-2	Ph	Xyl	26%, 80% ee
L52: SL-J216-1	1-Nap	<i>t</i> -Bu	--
L53: SL-J404-1	1-Nap	Xyl	68%, –15% ee
L54: SL-J006-1	BTfM	Cy	--
L49: SL-J008-1	BTfM	Xyl	83%, 94% ee
L55: SL-J007-1	DMM-Ph	Cy	--
L56: SL-J013-1	DMM-Ph	<i>t</i> -Bu	--
L57: SL-J418-1	DMM-Ph	Xyl	30%, –77% ee
L58: SL-J212-1	2-fur	<i>t</i> -Bu	--
L59: SL-J015-1	2-fur	Xyl	22%, –16% ee
L60: SL-J003-2	Cy	Cy	--
L61: SL-J009-1	Cy	<i>t</i> -Bu	--
L62: SL-J004-1	Cy	Ph	--
L63: SL-J502-1	<i>t</i> -Bu	Ph	--
L64: SL-J505-1	<i>t</i> -Bu	<i>o</i> -Tol	--



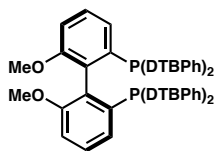
Walphos lig.	R ₁	R ₂	yield and ee of 22
L31: SL-W002-1	Ph	Ph	--
L65: SL-W006-1	Ph	Xyl	--
L66: SL-W001-1	Ph	BTfM	2%, ee ND
L67: SL-W005-1	DMM-Ph	BTfM	6%, ee ND
L68: SL-W003-1	Ph	Cy	4%, ee ND
L69: SL-W008-1	Cy	BTfM	2%, ee ND
L70: SL-W009-1	Xyl	Xyl	--
L71: SL-W022-1	Ph	norbornyl	--



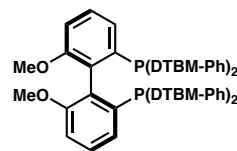
L1: BINAP
--



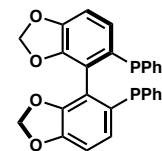
L72: MeO-BIBOP
<1 %, ee ND



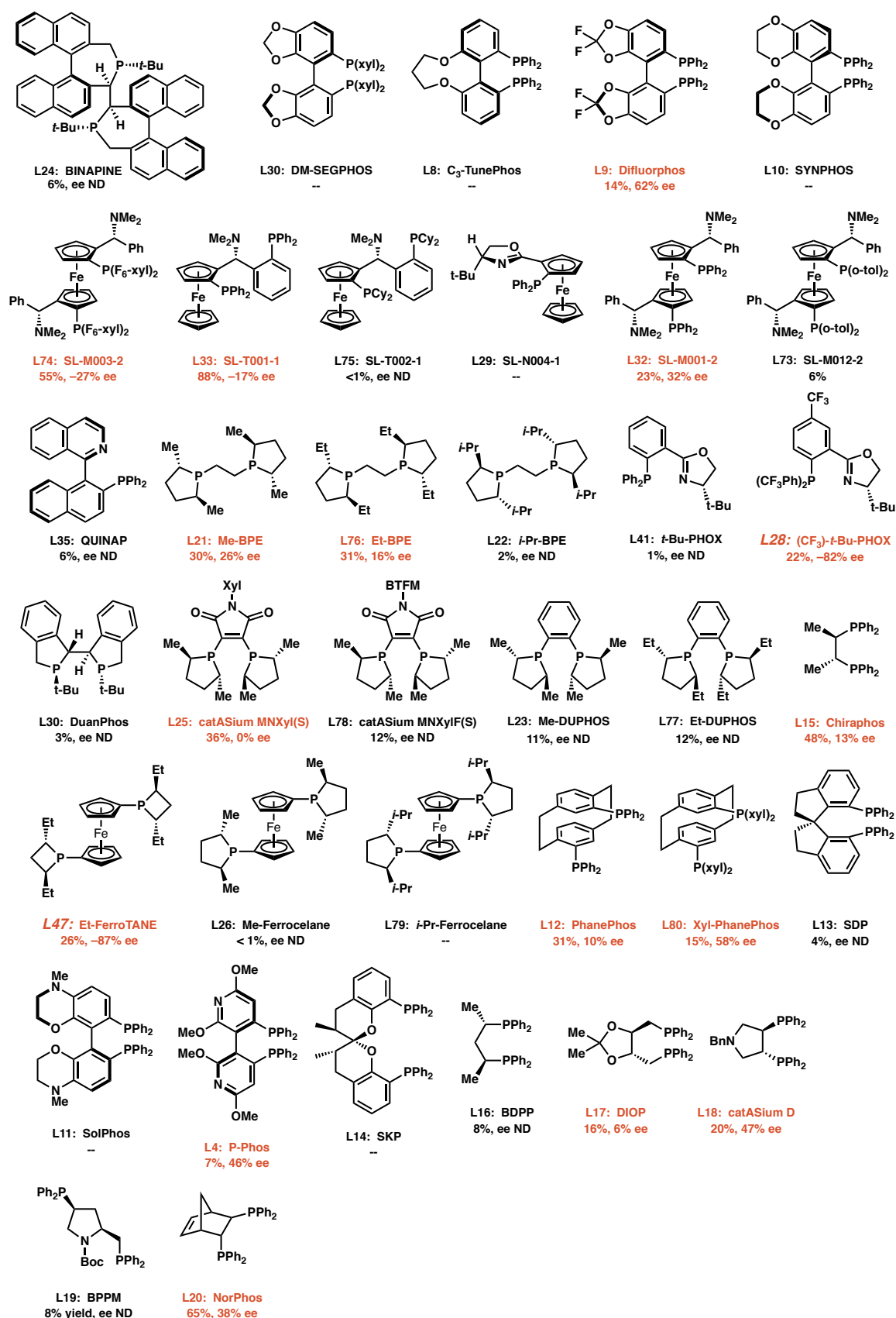
L5: DTB-MeOBIPHEP
--



L6: DTBM-MeOBIPHEP
--



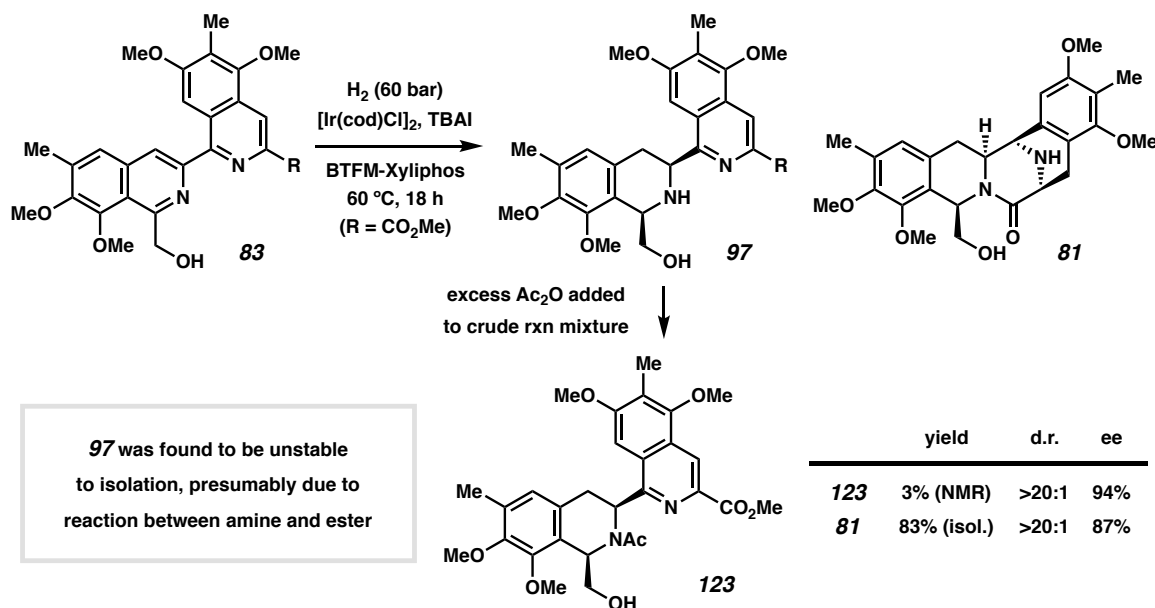
L3: SEGPHOS
<1 %, ee ND



3.6.5 EXPLANATION OF SELECTIVITY DIFFERENCES

Of all the ligands tested, only BTFM-Xyliphos (**L49**) enables the further reduction of **97** to **81** following lactamization. Intriguingly, the product **97** shows a 94% ee, while product **81** only shows 87% ee (Scheme 3.6). We propose that the discrepancy in enantioenrichment of the products is due to competitive D-ring reduction with lower enantioselectivity than that observed when the B-ring is reduced first. Because no other diastereomers are observed, global reduction via this route also appears to be fully diastereoselective.

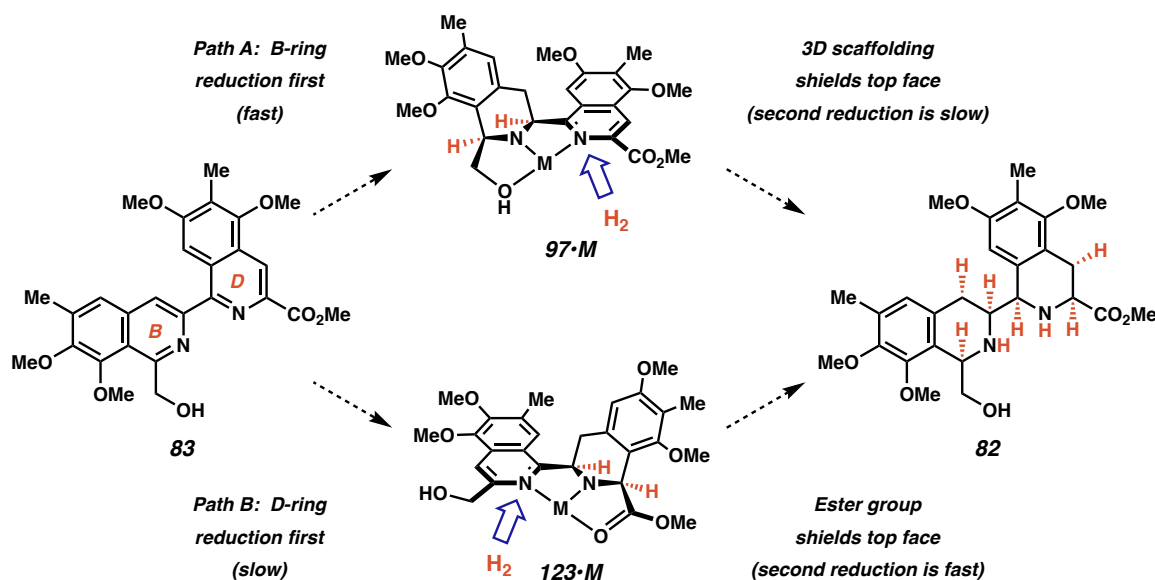
Scheme 3.6 Observed discrepancy in enantioenrichment of products **97** and **81**.



We believe that Path A is faster than Path B for all ligands to such an extent that Path B is only observed when the most activating ligand, BTFM-Xyliphos, is used. Both partially reduced intermediates are expected to form tridentate chelates to the metal to form **97•M** and **123•M** (with **M** not necessarily being the catalytically active metal), with the three dimensional structures of each leading to the all-*syn* product as the major

diastereomer (Scheme 3.7). Furthermore, because B-ring reduction appears to be faster than D-ring reduction in all cases, intermediate **97** can be isolated (after *N*-protection) while intermediate **123** has never been directly observed. The discrepancy in enantiomeric excess between intermediate **97** and fully hydrogenated intermediate **82** (as manifested by the enantiomeric excess of **123** and bis-THIQ **81**, respectively) can be explained if the enantioselectivity of Path B is significantly lower than that of Path A. As the two paths converge onto the same product, the enantiopurity of **81** would be expected to be less than that of **97**.

Scheme 3.7 Possible reaction pathways to generate pentacycle **81**.



3.6.6 BIOLOGICAL EVALUATION OF NON-NATURAL ANALOGS

3.6.6.1 Cell Culture and Proliferation Assays

Cell lines, cell culture, and reagents: A panel of 29 cell lines, representing 4 major cancer types (lung, colon, breast, and ovarian), was assayed for response to THIQ agents. Cells were cultured in appropriate culture media (e.g., RPMI 1640, DMEM, L-15) supplemented with 10% to 15% heat-inactivated fetal bovine serum (FBS), 2 mmol/L

glutamine, and 1% penicillin G-streptomycin-fungizone solution (PSF, Irvine Scientific) as previously described.⁴¹ Cells were routinely assessed for mycoplasma contamination using a multiplex PCR method, and STR profiling by the GenePrint 10 System (Promega) was used for cell-line authentication.

In vitro proliferation assays: Response to THIQ agents was measured by a six-day proliferation assay. Stock solutions of THIQ agents were prepared at 10 mM in DMSO. Cells were seeded in 48-well plates at a seeding density previously determined to maximize growth over a 6-day treatment window. After 24 h, the cells were treated with six 1:10 (**105**) or 1:5 (**101–104**) dilutions of inhibitor starting at 1 μ M. Control wells were imaged at this time for baseline cell counts. After 6 days of treatment, cells were counted on a custom automation platform designed by Tecan. This robotic system trypsinizes adherent cells, centrifuges cells to the bottom of the wells, and counts cells via brightfield image segmentation on a Synentec Cellavista imaging system. IC₅₀ values for each molecule were calculated by fitting curves to data points from each dose–response assay using the Proc NLIN function in SAS for Windows version 9.2 (SAS Institute, Inc.).

3.6.6.2 Biological Activity of Non-Natural Analogs

Table 3.5 Geometric mean of IC₅₀ values and their statistics.

Compound	IC ₅₀ Statistics (all numbers in μ M)			
	Geometric Mean	Median	Maximum	Minimum
Carfilzomib	.004	.005	.020	.001
Cisplatin	.202	.199	.799	.028
MK8745	.360	.380	1.000	0.079
MMAE	.438	.405	3.978	.077
101	.807	1.000	1.000	.225
102	1.000	1.000	1.000	1.000
103	.708	.891	1.000	.256
104	.233	.213	.787	.120
105	.397	.516	.812	.109

Table 3.6 IC₅₀'s (nM) of compounds **101–105** (data listed as 1000 nM are ≥1000 nM).

		101	102	103	104	105
H810	Lung	260	ND	260	210	110
A427	Lung	660	1000	880	210	340
H1836	Lung	470	1000	700	280	490
H226	Lung	1000	ND	770	210	660
H441	Lung	1000	ND	980	270	740
H1437	Lung	1000	ND	1000	740	760
H647	Lung	1000	1000	1000	540	770
NCIH747	Colon	1000	1000	290	150	120
SW837	Colon	910	1000	890	140	230
SW480	Colon	1000	ND	720	190	370
LS174t	Colon	1000	1000	1000	260	610
SNUC1	Colon	1000	ND	820	500	730
SKCO1	Colon	1000	1000	1000	790	780
SW48	Colon	1000	1000	720	120	810
OVCAR3	Ovarian	1000	1000	1000	150	120
ES2	Ovarian	1000	1000	410	200	170
OV207	Ovarian	1000	1000	970	250	170
OVTOKO	Ovarian	1000	1000	860	210	420
RMG1	Ovarian	1000	1000	990	200	520
RMUGS	Ovarian	1000	1000	1000	300	550
OVCAR5	Ovarian	1000	ND	310	220	650
EFO21	Ovarian	1000	1000	1000	240	780
MB468	Breast	1000	ND	470	140	210
ZR751	Breast	1000	ND	330	180	230
EFM19	Breast	460	ND	1000	140	230
MB453	Breast	260	ND	1000	250	350
HCC1806	Breast	1000	ND	560	190	380
T47D	Breast	1000	ND	1000	210	540
COLO824	Breast	230	ND	260	200	790

3.7 REFERENCES AND NOTES

- (1) Chrzanowska, M.; Grajewska, A.; Rozwadowska, M. D. *Chem. Rev.* **2016**, *116*, 12369–12465.
- (2) Newman, D. J.; Cragg, G. M. *J. Nat. Prod.* **2016**, *79*, 629–661.
- (3) Cuevas, C.; Francesch, A. *Nat. Prod. Rep.* **2009**, *26*, 322–337.
- (4) Cuevas, C. *et al.*, *Org. Lett.* **2000**, *2*, 2545–2548.
- (5) Lown, J. W.; Joshua, A. V.; Lee, J. S. *Biochemistry* **1982**, *21*, 419–428.
- (6) Rath, C. M. *et al.*, *ACS Chem. Biol.* **2011**, *6*, 1244–1256.
- (7) Song, L.-Q.; Zhang, Y.-Y.; Pu, J.-Y.; Tang, M.-C.; Peng, C.; Tang, G.-L. *Angew. Chem., Int. Ed.* **2017**, *56*, 9116–9120.
- (8) Martinez, E. J.; Owa, T.; Schreiber, S. L.; Corey, E. J. *Proc. Natl. Acad. Sci. USA* **1999**, *96*, 3496–3501.
- (9) Myers, A. G.; Plowright, A. T. *J. Am. Chem. Soc.* **2001**, *123*, 5114–5115.
- (10) Myers, A. G.; Lanman, B. A. *J. Am. Chem. Soc.* **2002**, *124*, 12969–12971.
- (11) Ocio, E. M. *et al.*, *Blood* **2009**, *113*, 3781–3791.
- (12) Carter, N. J.; Keam, S. J. *Drugs* **2010**, *70*, 355–376.
- (13) Spencer, J. R. *et al.*, *Bioorg. Med. Chem. Lett.* **2006**, *16*, 4884–4888.
- (14) Gunaydin, H.; Altman, M. D.; Ellis, J. M.; Fuller, P.; Johnson, S. A.; Lahue, B.; Lapointe, B. *ACS Med. Chem. Lett.* **2018**, *9*, 528–533.
- (15) Lane, J. W.; Chen, Y.; Williams, R. M. *J. Am. Chem. Soc.* **2005**, *127*, 12684–12690.
- (16) Wu, Y.-C.; Zhu, J. *Org. Lett.* **2009**, *11*, 5558–5561.

- (17) Liu, W.; Liao, X.; Dong, W.; Yan, Z.; Wang, N.; Liu, Z. *Tetrahedron* **2012**, *68*, 2759–2764.
- (18) Chen, R.; Liu, H.; Chen, X. *J. Nat. Prod.* **2013**, *76*, 1789–1795.
- (19) Saito, N.; Tanaka, C.; Koizumi, Y.-i.; Suwanborirux, K.; Amnuoypol, S.; Pummangura, S.; Kubo, A. *Tetrahedron* **2004**, *60*, 3873–3881.
- (20) Xu, S. *et al.*, *Eur. J. Org. Chem.* **2017**, *2017*, 975–983.
- (21) Fontana, A.; Cavaliere, P.; Wahidulla, S.; Naik, C. G.; Cimino, G. *Tetrahedron* **2000**, *56*, 7305–7308.
- (22) Yeom, H.-S.; Kim, S.; Shin, S. *Synlett* **2008**, *2008*, 924–928.
- (23) Allan, K. M.; Hong, B. D.; Stoltz, B. M. *Org. Biomol. Chem.* **2009**, *7*, 4960–4964.
- (24) Campeau, L.-C.; Schipper, D. J.; Fagnou, K. *J. Am. Chem. Soc.* **2008**, *130*, 3266–3267.
- (25) Tan, Y.; Barrios-Landeros, F.; Hartwig, J. F. *J. Am. Chem. Soc.* **2012**, *134*, 3683–3686.
- (26) Boekelheide, V.; Linn, W. J.; *J. Am. Chem. Soc.* **1954**, *76*, 1286–1291.
- (27) Wang, D.-S.; Chen, Q.-A.; Lu, S.-M.; Zhou, Y.-G. *Chem. Rev.* **2012**, *112*, 2557–2590.
- (28) Lu, S.-M.; Wang, Y.-Q.; Han, X.-W.; Zhou, Y.-G. *Angew. Chem., Int. Ed.* **2006**, *45*, 2260–2263.
- (29) Shi, L.; Ye, Z.-S.; Cao, L.-L.; Guo, R.-N.; Hu, Y.; Zhou, Y.-G. *Angew. Chem., Int. Ed.* **2012**, *51*, 8286–8289.

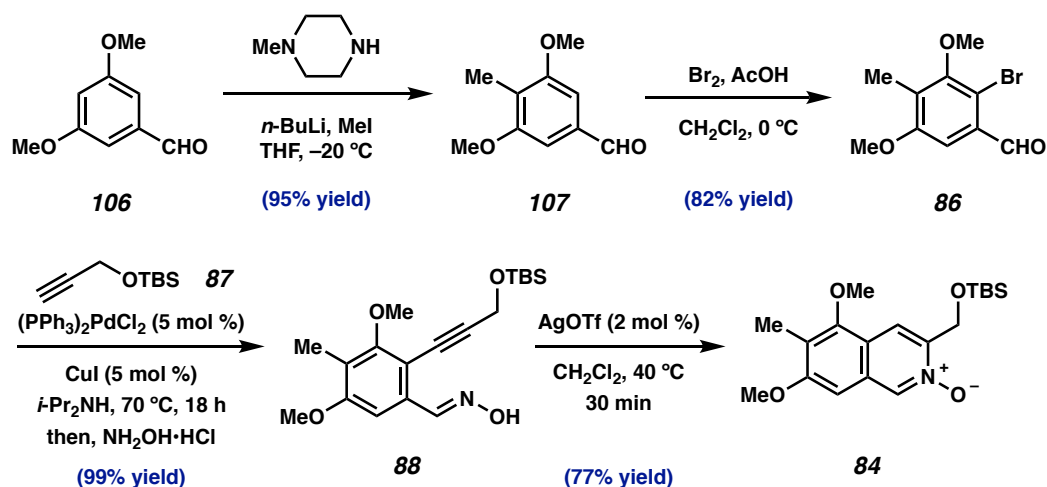
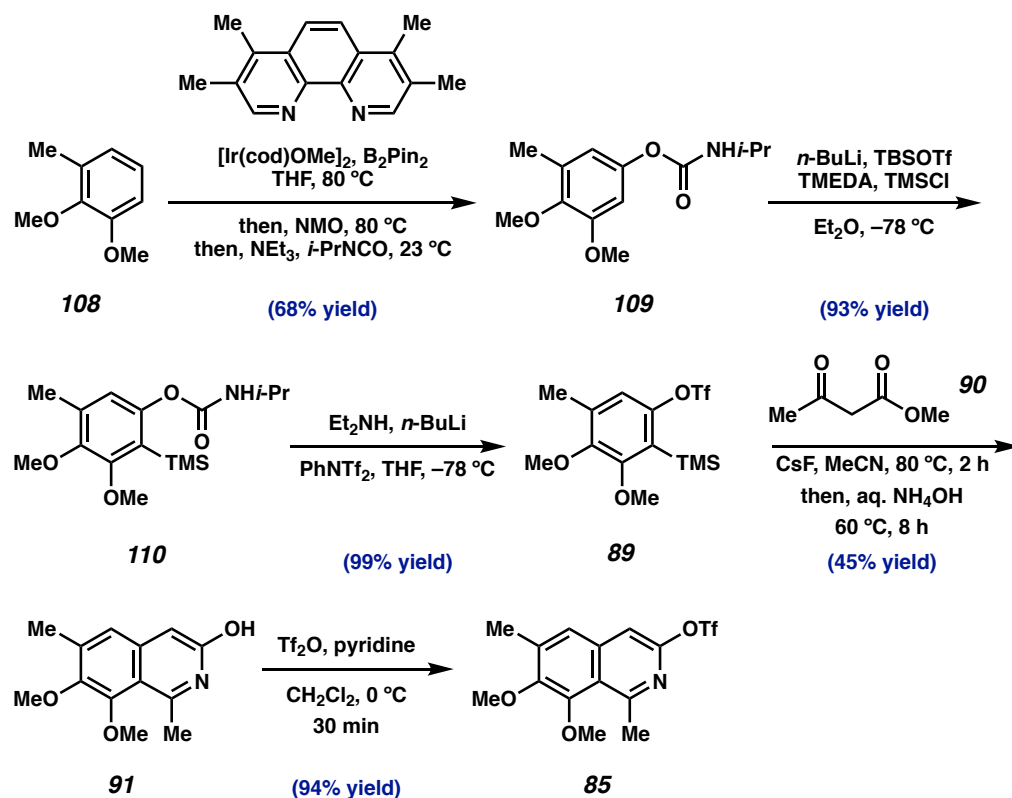
- (30) Kita, Y.; Yamaji, K.; Higashida, K.; Sathaiah, K.; Iimuro, A.; Mashima, K. *Angew. Chem., Int. Ed.* **2013**, *52*, 2046–2050.
- (31) Wen, J.; Tan, R.; Liu, S.; Zhao, Q.; Zhang, X. *Chem. Sci.* **2016**, *7*, 3047–3051.
- (32) Noyori, R.; Hashiguchi, S. *Acc. Chem. Res.* **1997**, *20*, 97–102.
- (33) Xie, J.-H.; Zhu, S.-F.; Zhou, Q.-L. *Chem. Rev.* **2011**, *111*, 1713–1760.
- (34) Dorta, R.; Broggini, D.; Stoop, R.; Rüegger, H.; Spindler, F.; Togni, A. *Chem. Eur. J.* **2014**, *10*, 267–278.
- (35) (*S,R_P*)-BTfM-Xyliphos (**L49**) is produced and sold by Solvias AG and is licensed to Sigma-Aldrich Co. and Strem Chemicals under the name SL-J008-2.
- (36) The lower ee measured on isolated **81** as compared to isolated **97** can be rationalized by competitive (although minor), non-selective D-ring reduction leading to the same major diastereomer, see section 3.6.5.
- (37) Lavery, C. B.; Rotta-Loria, N. L.; McDonald, R.; Stradiotto, M. *Adv. Synth. Catal.* **2013**, *335*, 981–987.
- (38) Bruno, N. C.; Tudge, M. T.; Buchwald, S. L. *Chem. Sci.* **2013**, *4*, 916–920.
- (39) Pommier, Y.; Kohlhaagen, G.; Bailly, C.; Waring, M.; Mazumder, A.; Kohn, K. W. *Biochemistry* **1996**, *35*, 13303–13309.
- (40) Xing, C.; LaPorte, J. R.; Barbay, J. K.; Myers, A. G. *Proc. Natl. Acad. Sci. USA* **2004**, *101*, 5862–5866.
- (41) O'Brien, N. A.; McDonald, K.; Luo, T.; Euw, E.; Kalous, O.; Conklin, D.; Hurvitz, S. A.; Tomaso, E. D.; Schnell, C.; Linnartz, R.; Finn, R. S.; Hirawat, S.; Slamon, D. J. *Clin. Cancer Res.* **2014**, *20*, 3507–2510.

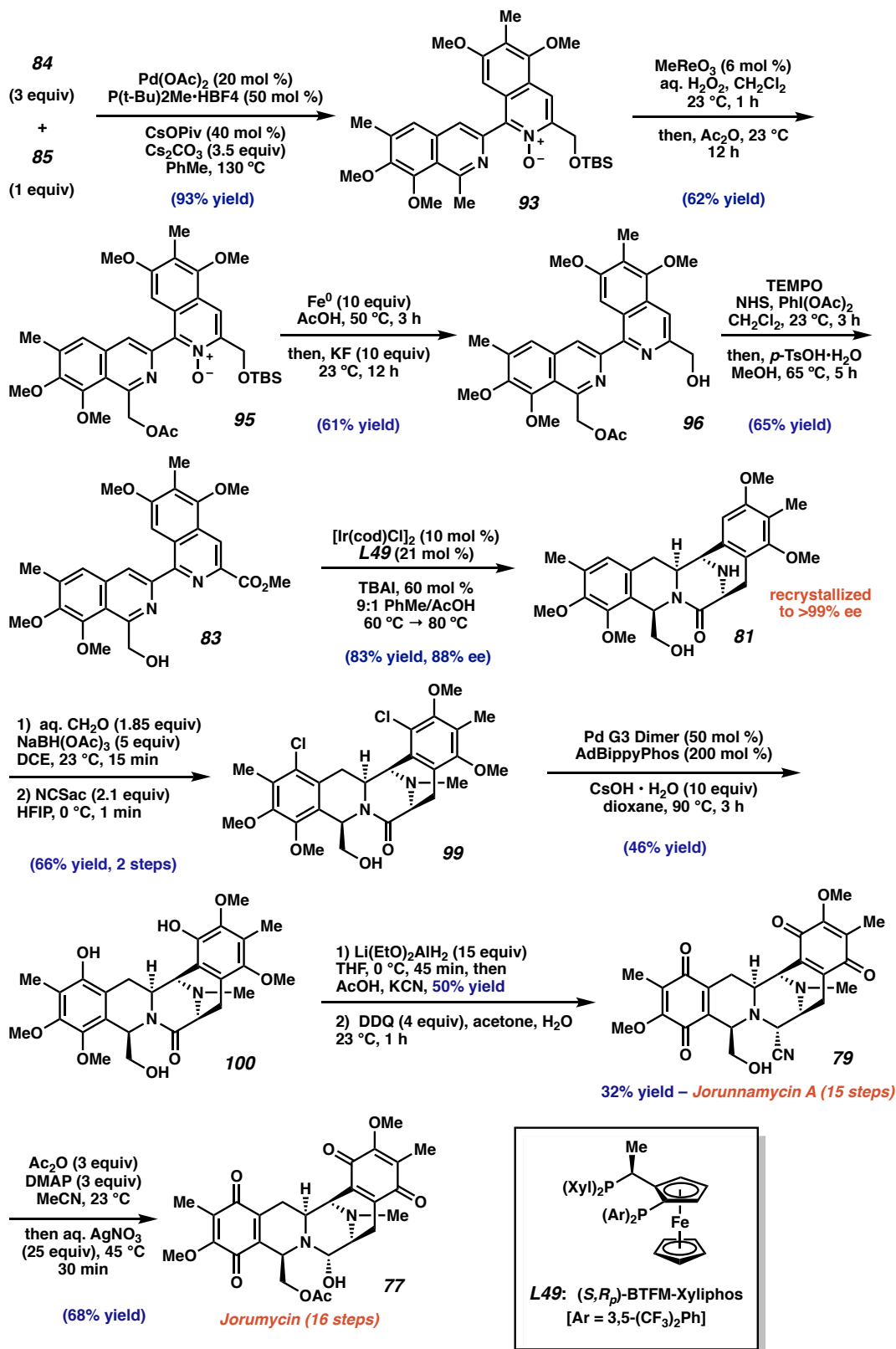
- (42) Finn, R. S.; Dering, J.; Conklin, D.; Kalous, O.; Cohen, D. J.; Desai, A. J.; Ginther, C.; Atefi, M.; Chen, I.; Fowst, C.; Los, G.; Slamon, D. J. *Breast Cancer Res.* **2009**, *11*, R77–R89.
- (43) Pangborn, A. B.; Giardello, M. A.; Grubbs, R. H.; Rosen, R. K.; Timmers, F. J. *Organometallics*, **1996**, *15*, 1518–1520.
- (44) Sheldrick, G. M. *Acta Cryst.* **1990**, *A46*, 467–473.
- (45) Sheldrick, G. M. *Acta Cryst.* **2008**, *A64*, 112–122.
- (46) Müller, P. *Crystallography Reviews*, **2009**, *15*, 57–83.
- (47) Comins, D. L.; Brown, J. D.; *J. Org. Chem.* **1984**, *49*, 1078–1083.
- (48) Harmata, M.; Yang, W.; Barnes, C. L. *Tetrahedron Lett.* **2009**, *50*, 2326–2328.
- (49) Nicolaou, K. C.; Rhoades, D.; Lamani, M.; Pattanayak, M. R.; Kumar, S. M. *J. Am. Chem. Soc.* **2016**, *138*, 7532–7535.
- (50) Tadross, P. M.; Gilmore, C. D.; Bugga, P.; Virgil, S. C.; Stoltz, B. M. *Org. Lett.* **2010**, *12*, 1224–1227.
- (51) A similar compound (carbinolamine analog of jorunnamycin C) has been previously reported to also decompose in CDCl₃, see ref. 52.
- (52) Charupant, K.; Suwanborirux, K.; Amnuaypol, S.; Saito, E.; Kubo, A.; Saito, N. *Chem. Pharm. Bull.* **2007**, *55*, 81–86.

APPENDIX 5

Synthetic Summary of Chapter 3:

Concise Total Syntheses of (–)-Jorunnamycin A and (–)-Jorumycin

Scheme A5.1 Synthesis of isoquinoline *N*-oxide **84**.**Scheme A5.2** Synthesis of isoquinoline triflate **85**.

Scheme A5.3 Total syntheses of jorunnamycin A and jorumycin.

APPENDIX 6

Spectra Relevant to Chapter 3:

Concise Total Syntheses of (–)-Jorunnamycin A and (–)-Jorumycin

Enabled by Asymmetric Catalysis

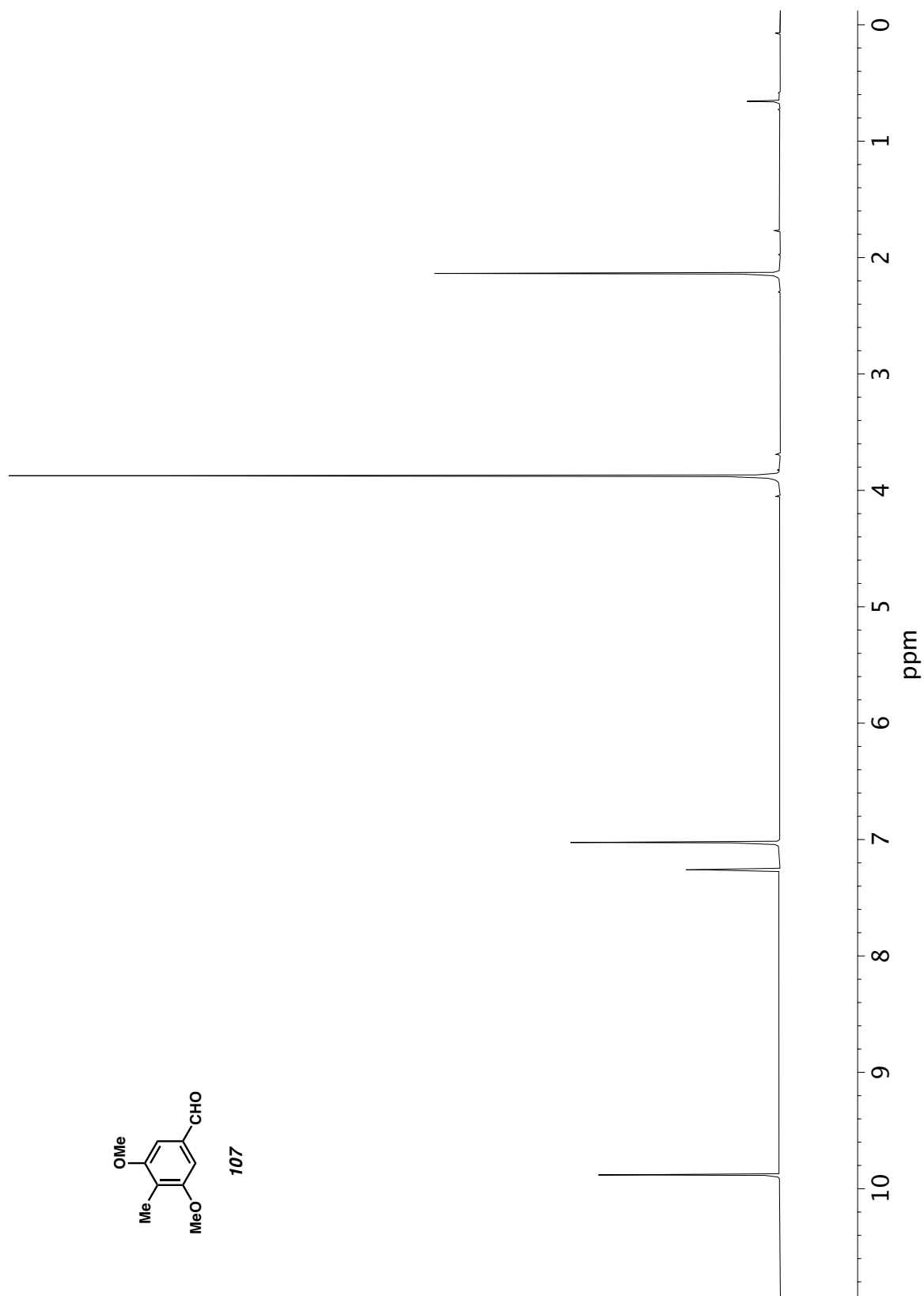


Figure A6.1 ¹H NMR (400 MHz, CDCl₃) of compound **107**.

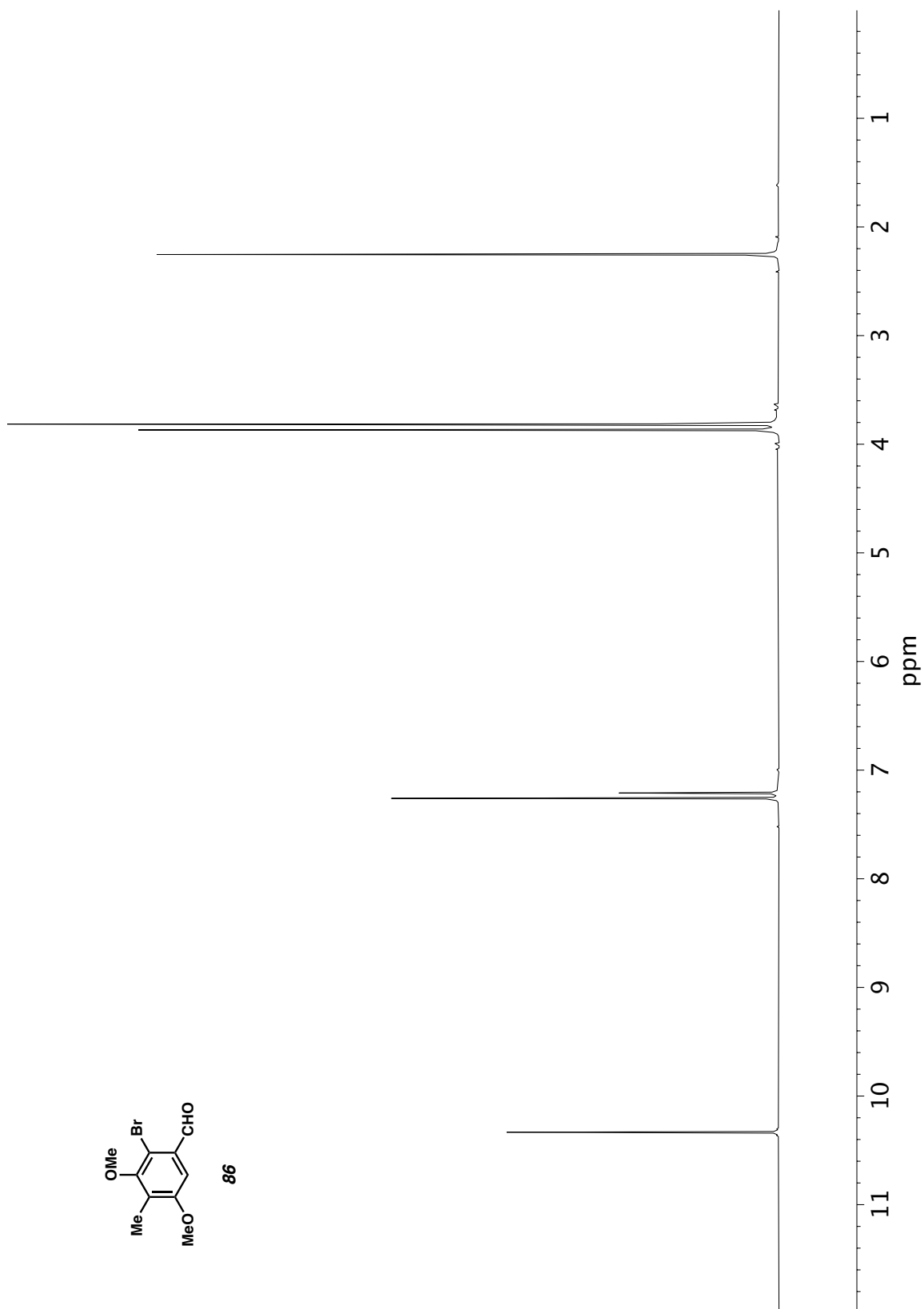


Figure A6.2 ¹H NMR (400 MHz, CDCl₃) of compound **86**.



Figure A6.3 ^1H NMR (500 MHz, CDCl_3) of compound **88**.

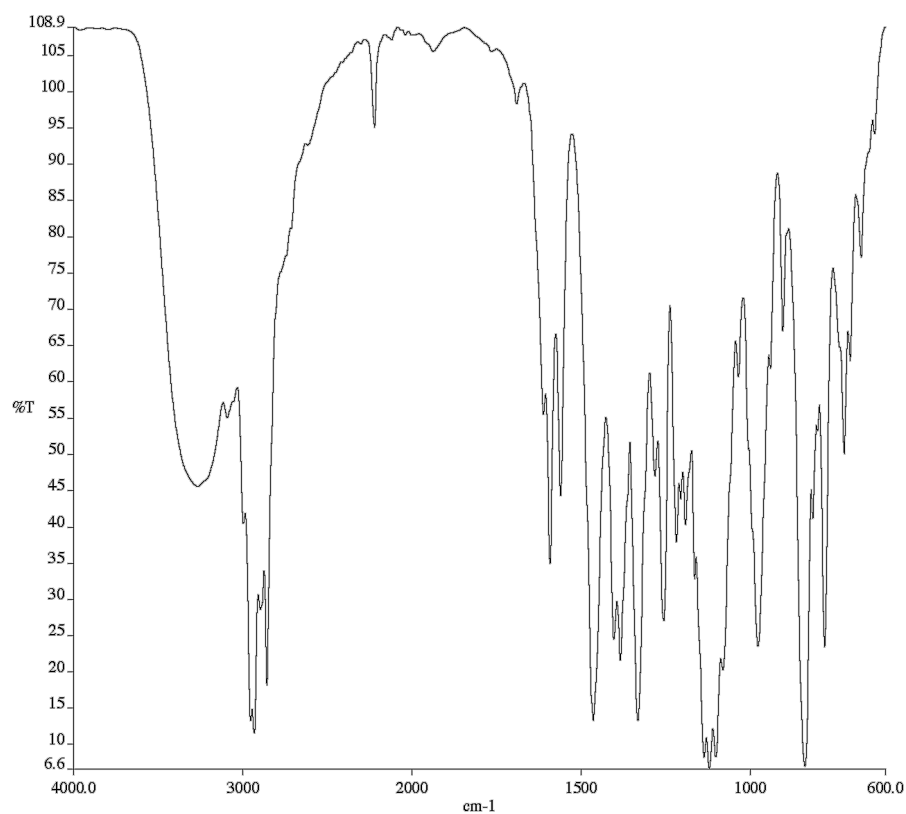


Figure A6.4 Infrared spectrum (Thin Film, NaCl) of compound **88**.

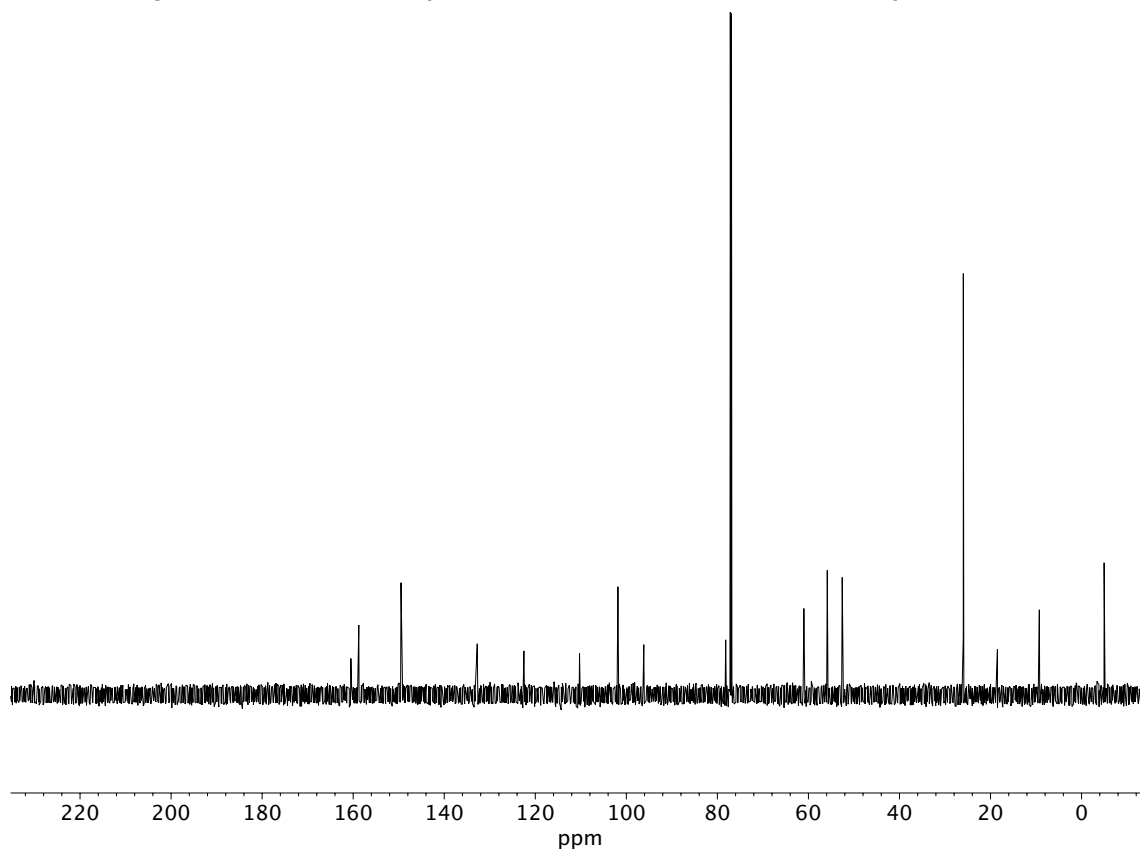


Figure A6.5 ¹³C NMR (125 MHz, CDCl₃) of compound **88**.

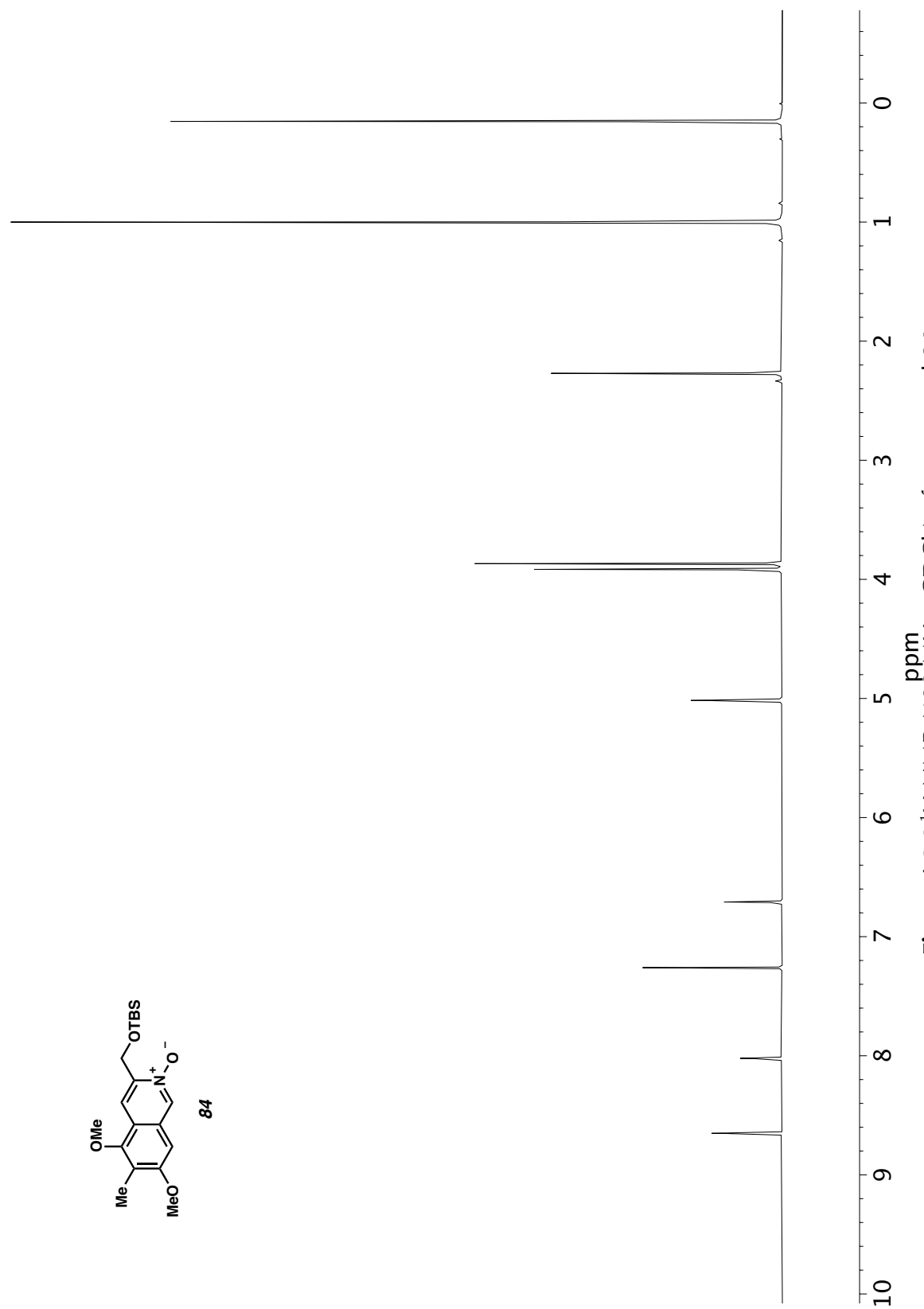


Figure A6.6 ¹H NMR (400 MHz, CDCl₃) of compound **84**.

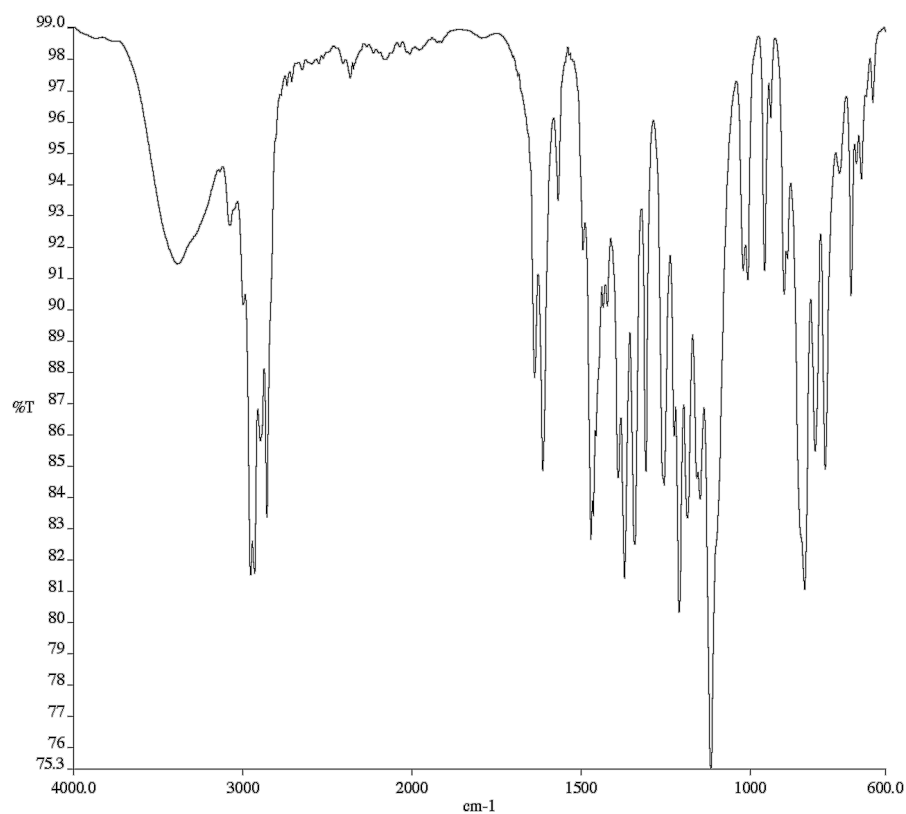


Figure A6.7 Infrared spectrum (Thin Film, NaCl) of compound **84**.

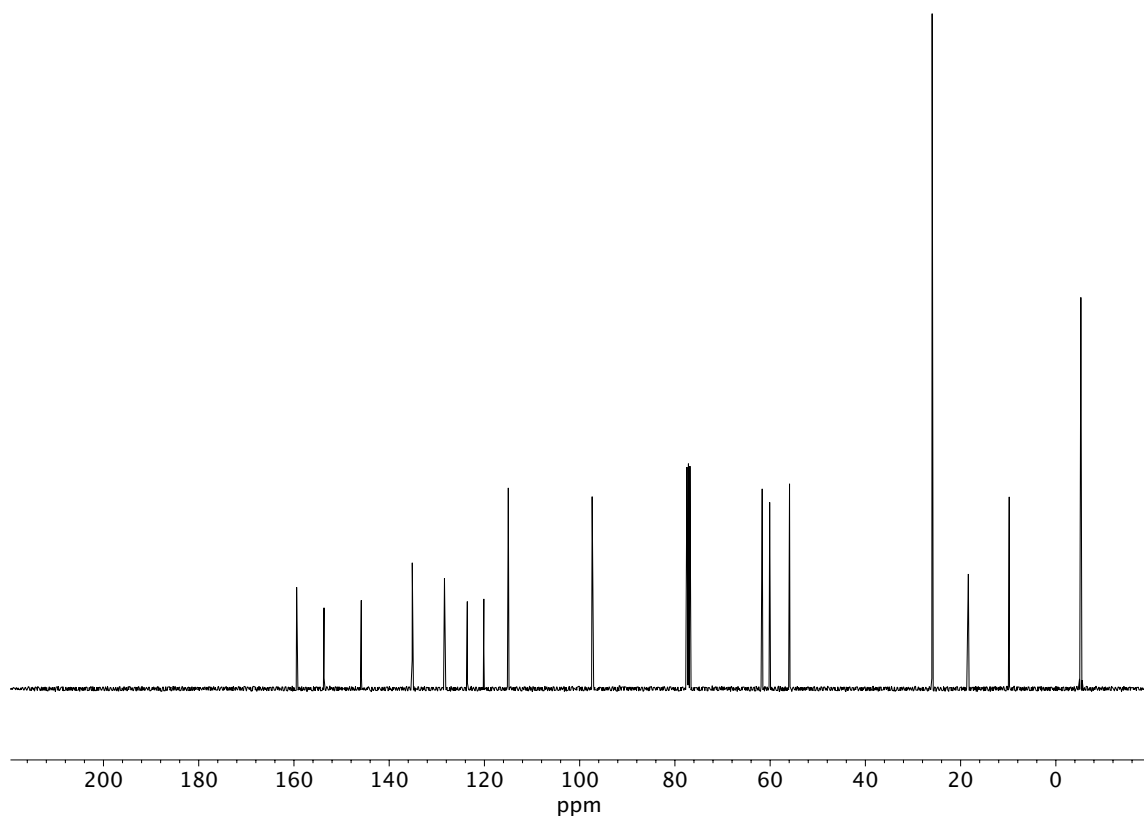


Figure A6.8 ¹³C NMR (100 MHz, CDCl₃) of compound **84**.

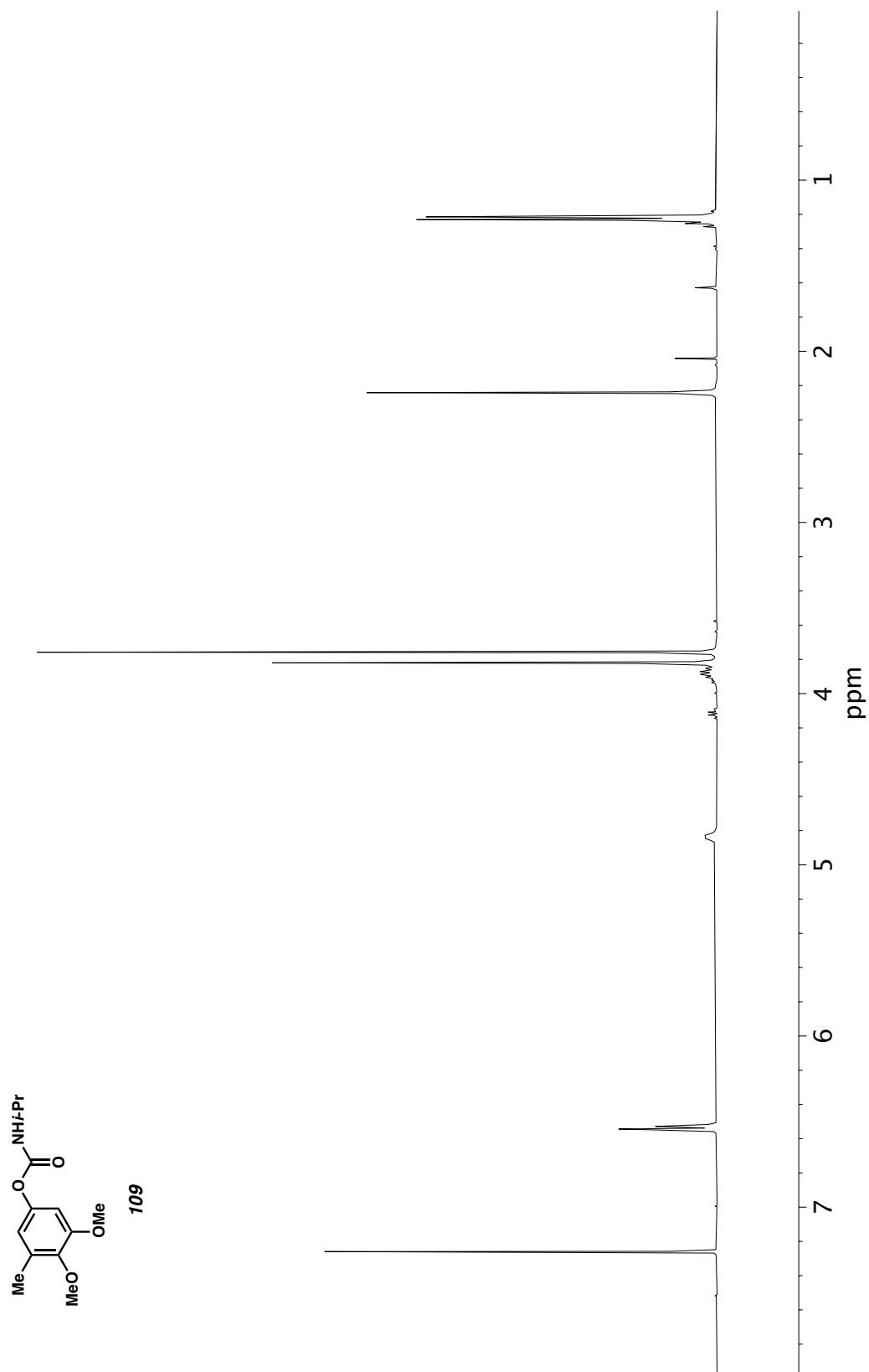


Figure A6.9 ^1H NMR (400 MHz, CDCl_3) of compound **109**.

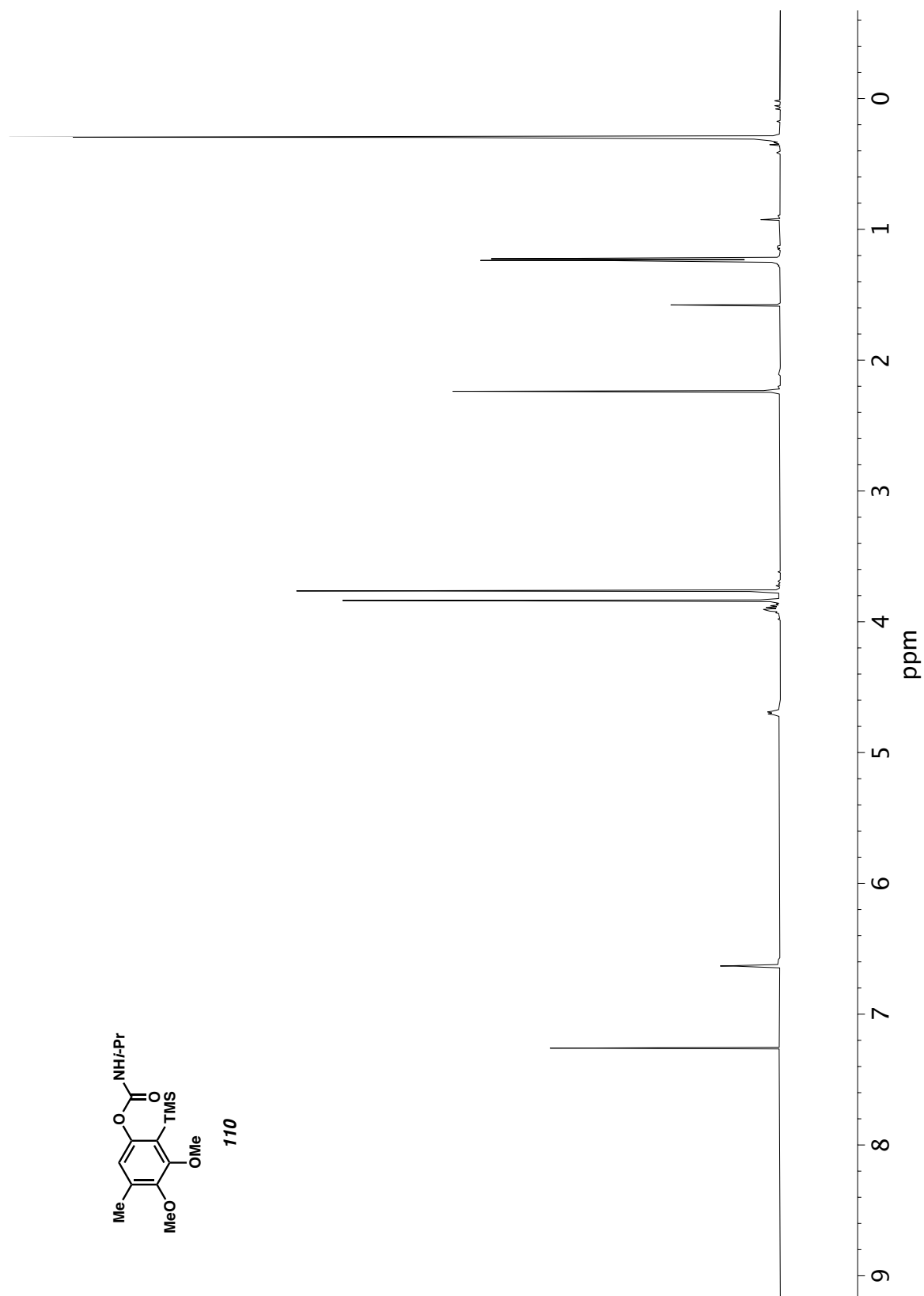


Figure A6.10 ^1H NMR (400 MHz, CDCl_3) of compound **110**.

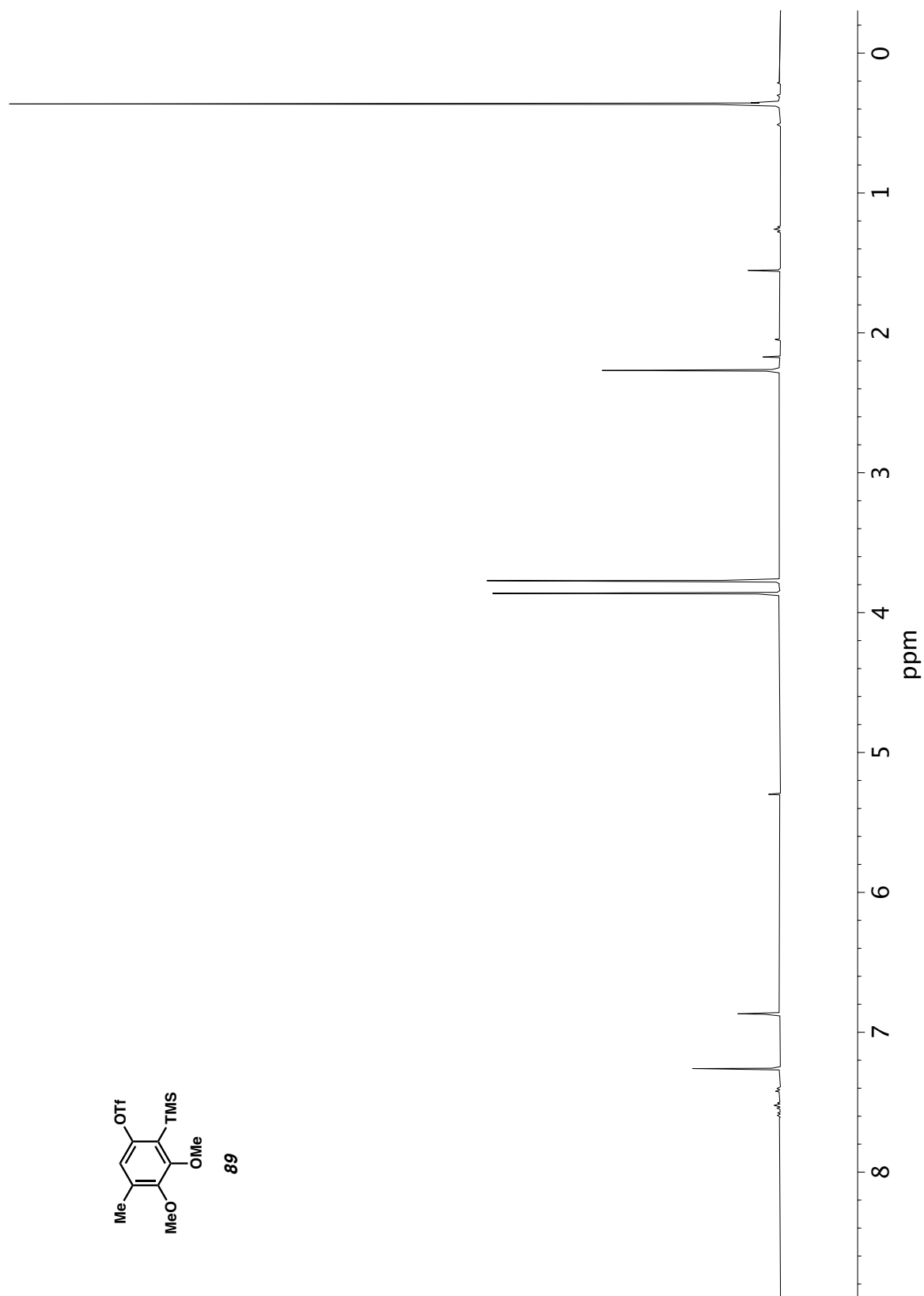


Figure A6.11 ^1H NMR (400 MHz, CDCl_3) of compound **89**.

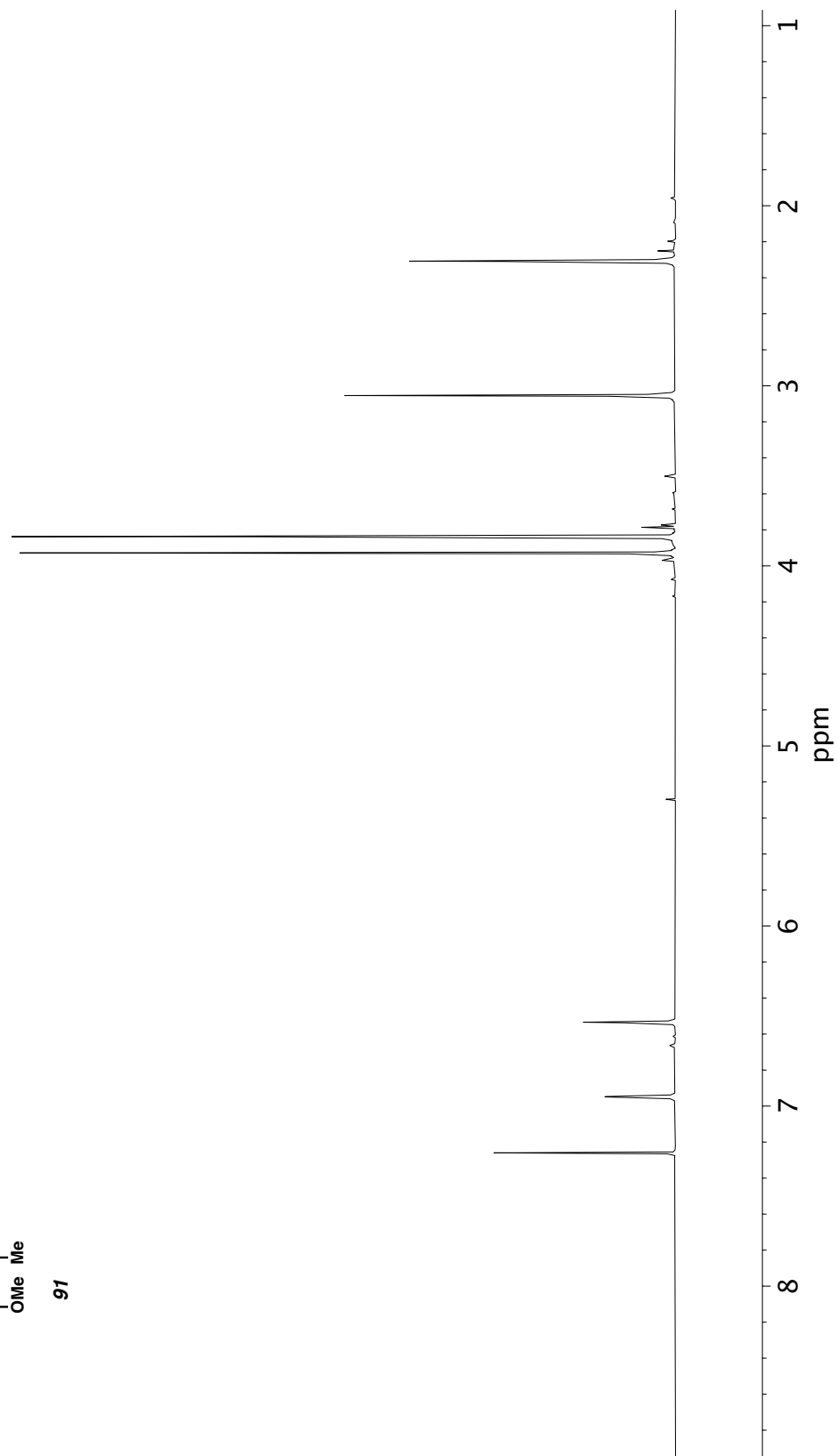
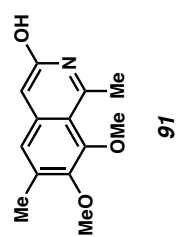


Figure A6.12 ¹H NMR (300 MHz, CDCl₃) of compound **91**.

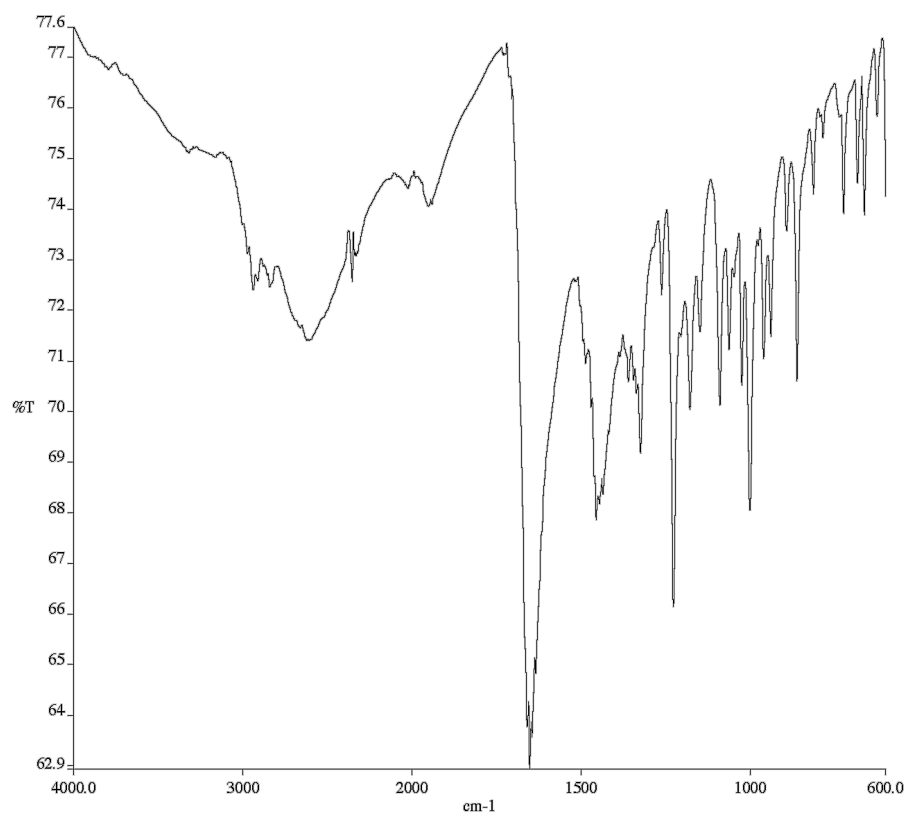


Figure A6.13 Infrared spectrum (Thin Film, NaCl) of compound **91**.

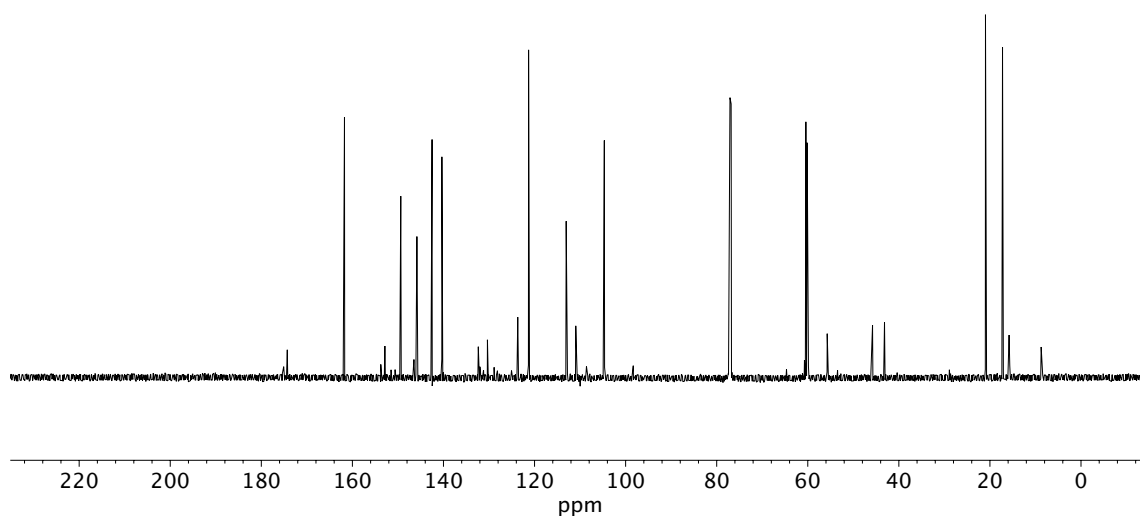


Figure A6.14 ¹³C NMR (125 MHz, CDCl₃) of compound **91**.

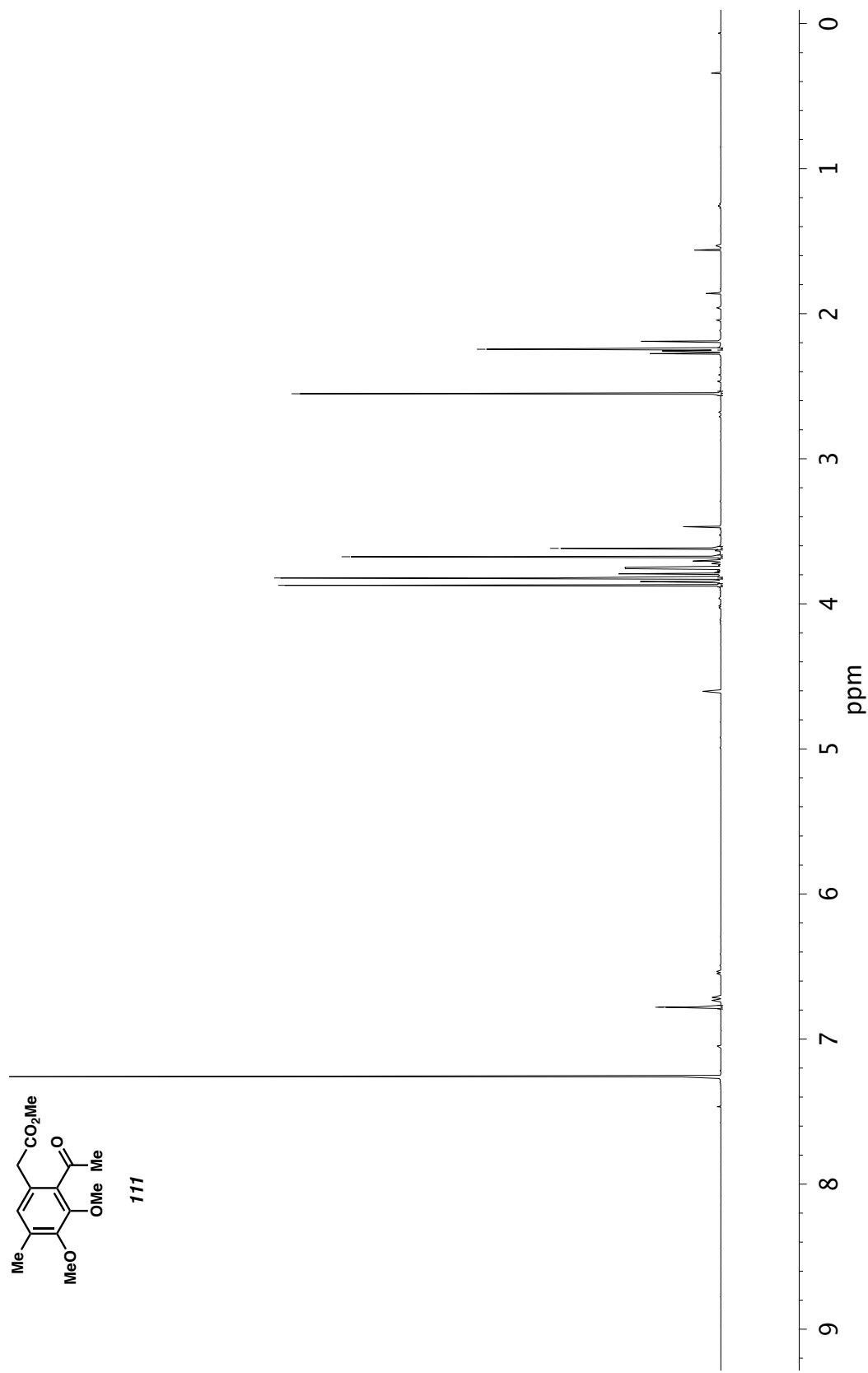


Figure A6.15 ¹H NMR (400 MHz, CDCl₃) of compound **111**.

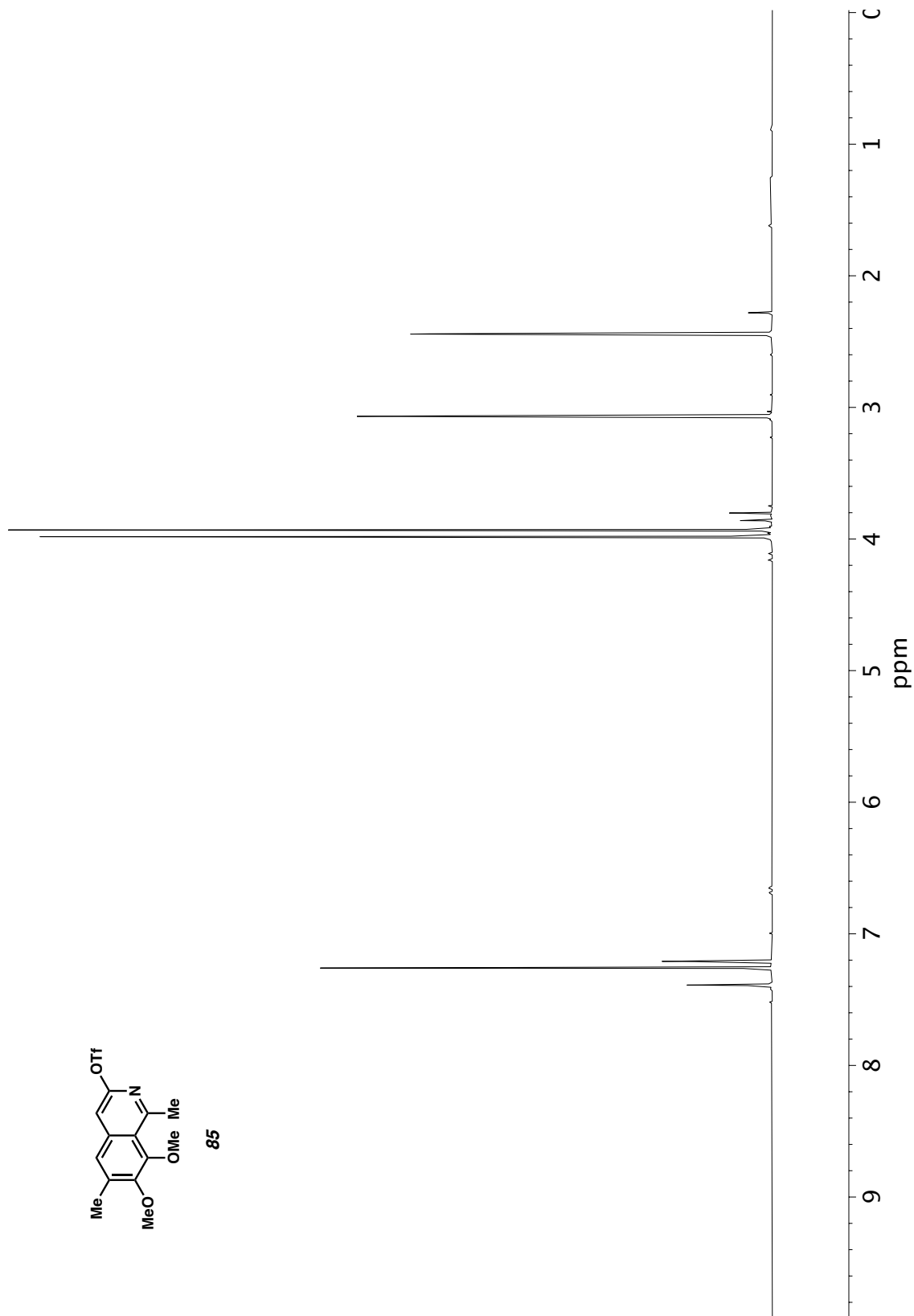


Figure A6.16 ¹H NMR (400 MHz, CDCl₃) of compound **85**.

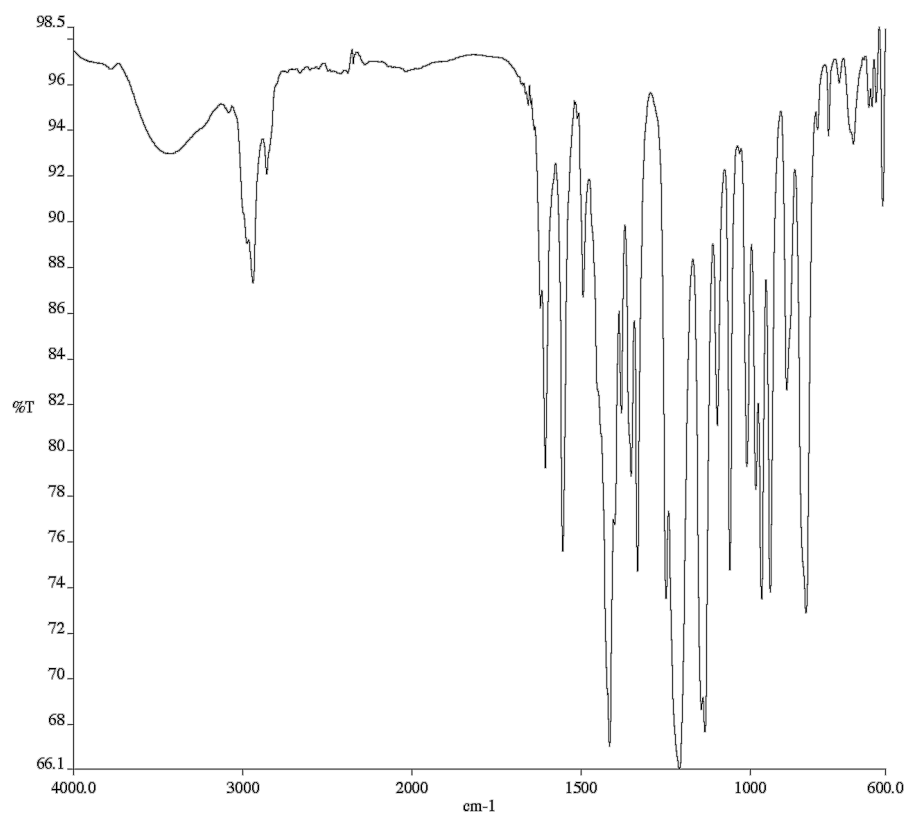


Figure A6.17 Infrared spectrum (Thin Film, NaCl) of compound **85**.

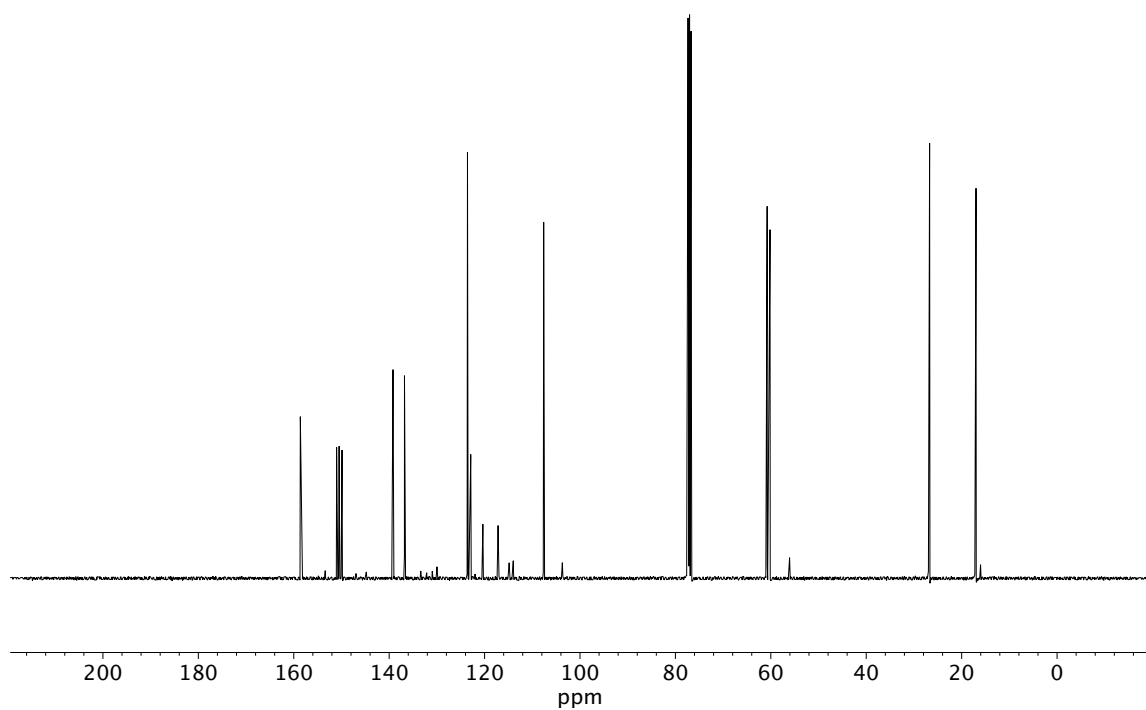


Figure A6.18 ¹³C NMR (100 MHz, CDCl₃) of compound **85**.

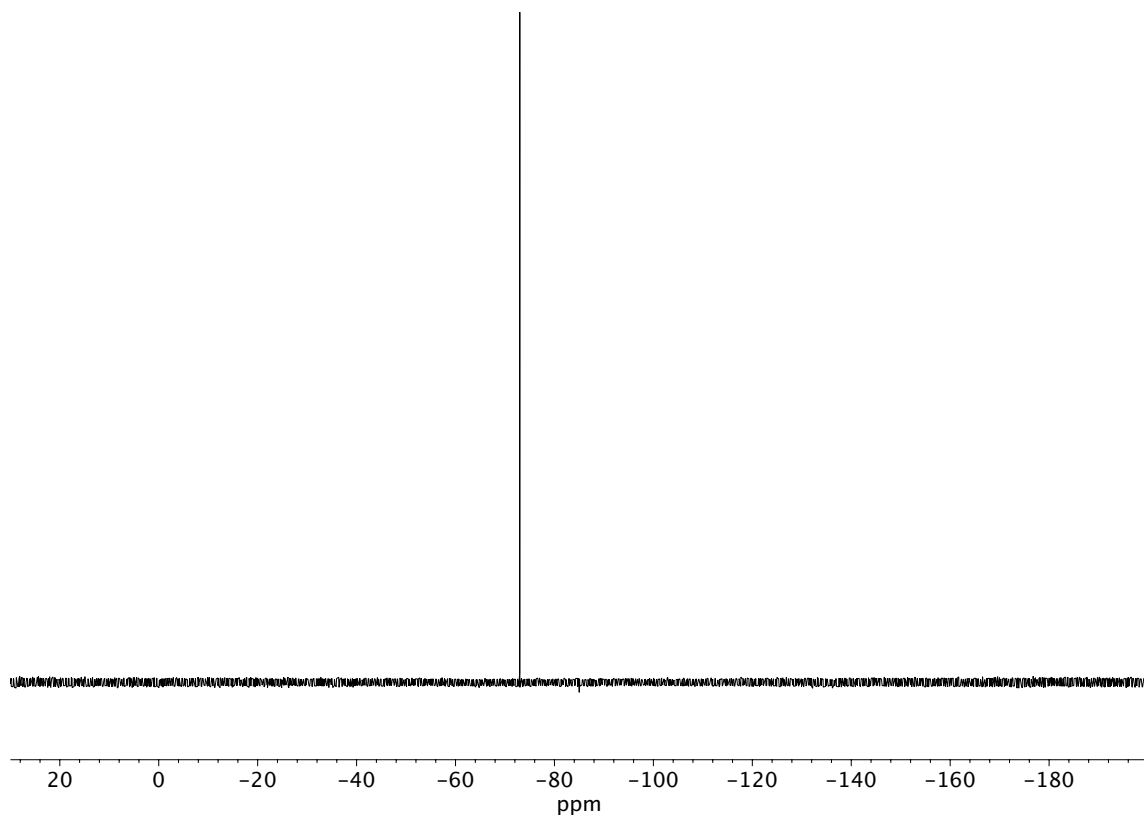


Figure A6.19 ^{19}F NMR (282 MHz, CDCl_3) of compound **85**.

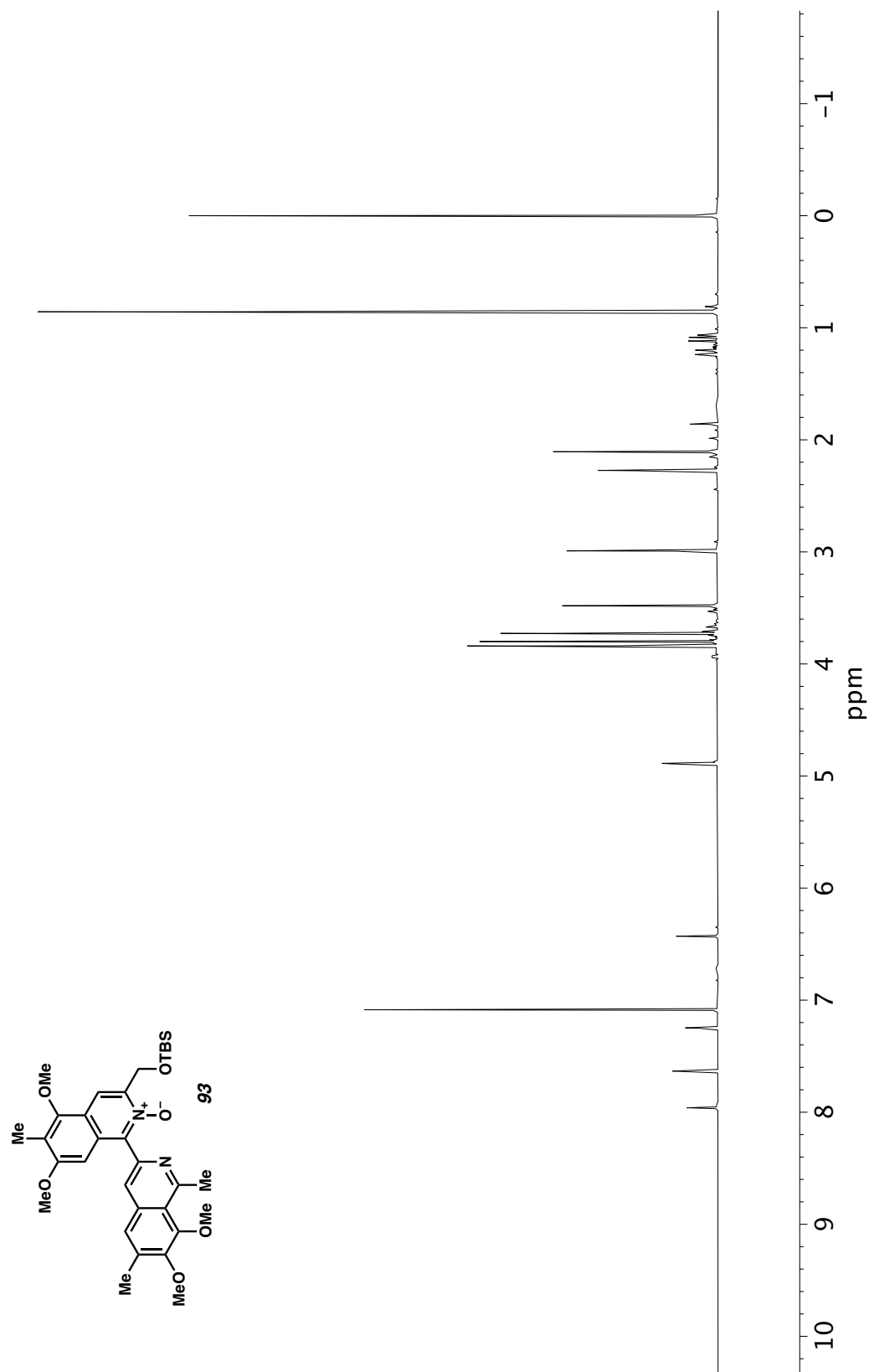


Figure A6.20 ^1H NMR (400 MHz, CDCl_3) of compound **93**.

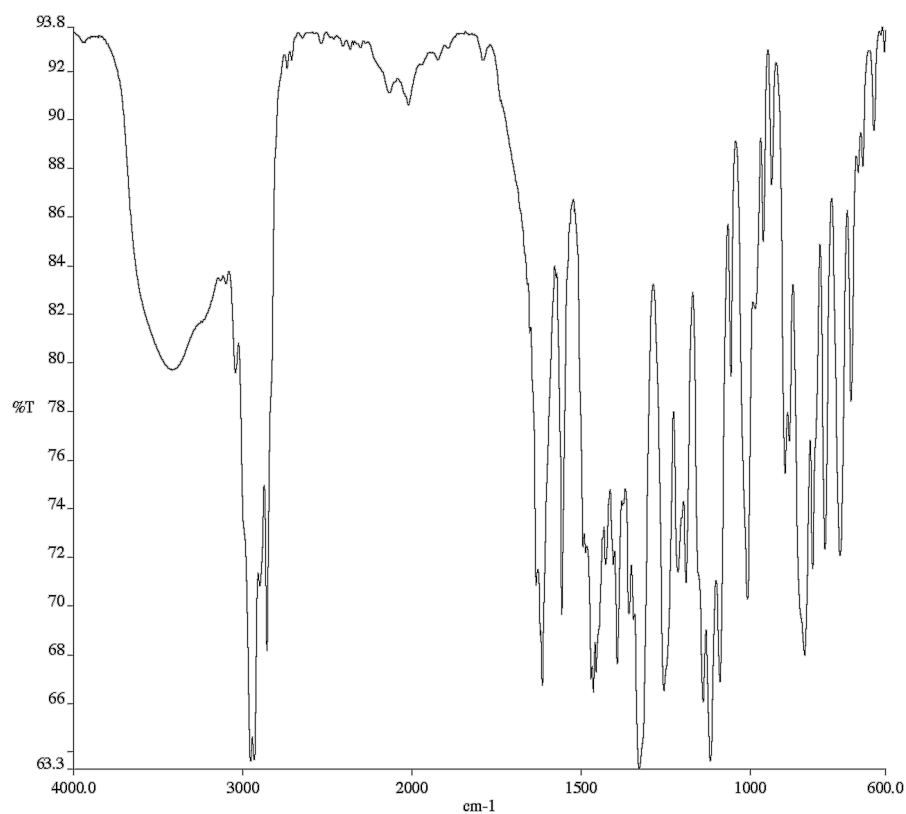


Figure A6.21 Infrared spectrum (Thin Film, NaCl) of compound **93**.

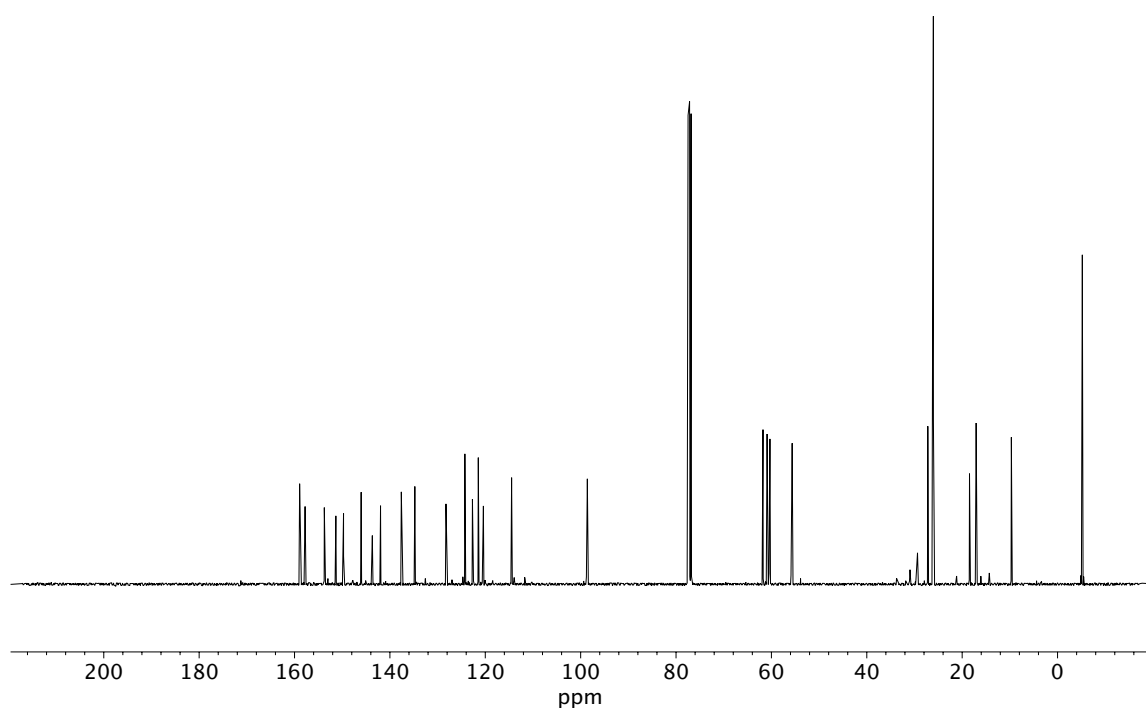


Figure A6.22 ¹³C NMR (100 MHz, CDCl₃) of compound **93**.

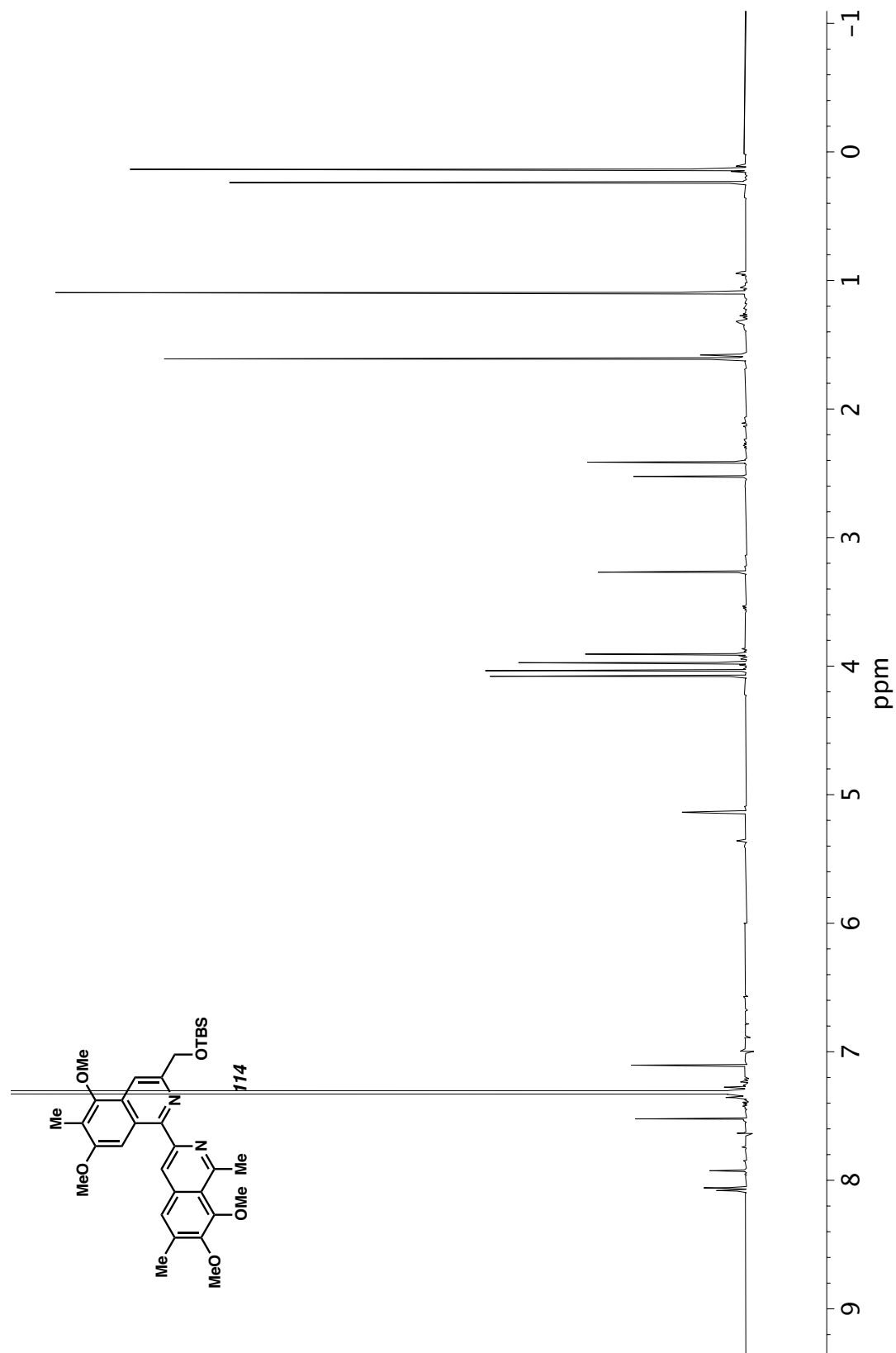


Figure A6.23 ^1H NMR (400 MHz, CDCl_3) of compound **114**.

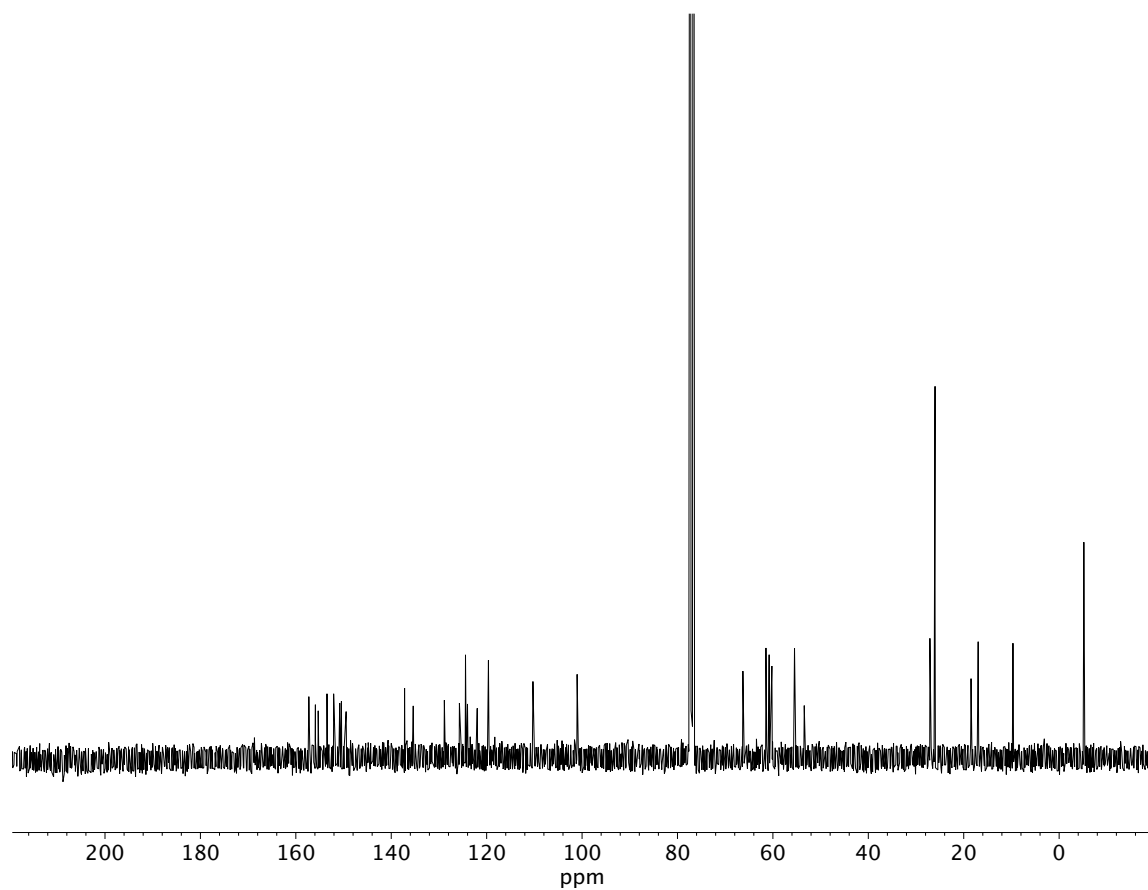


Figure A6.24 ^{13}C NMR (100 MHz, CDCl_3) of compound **114**.

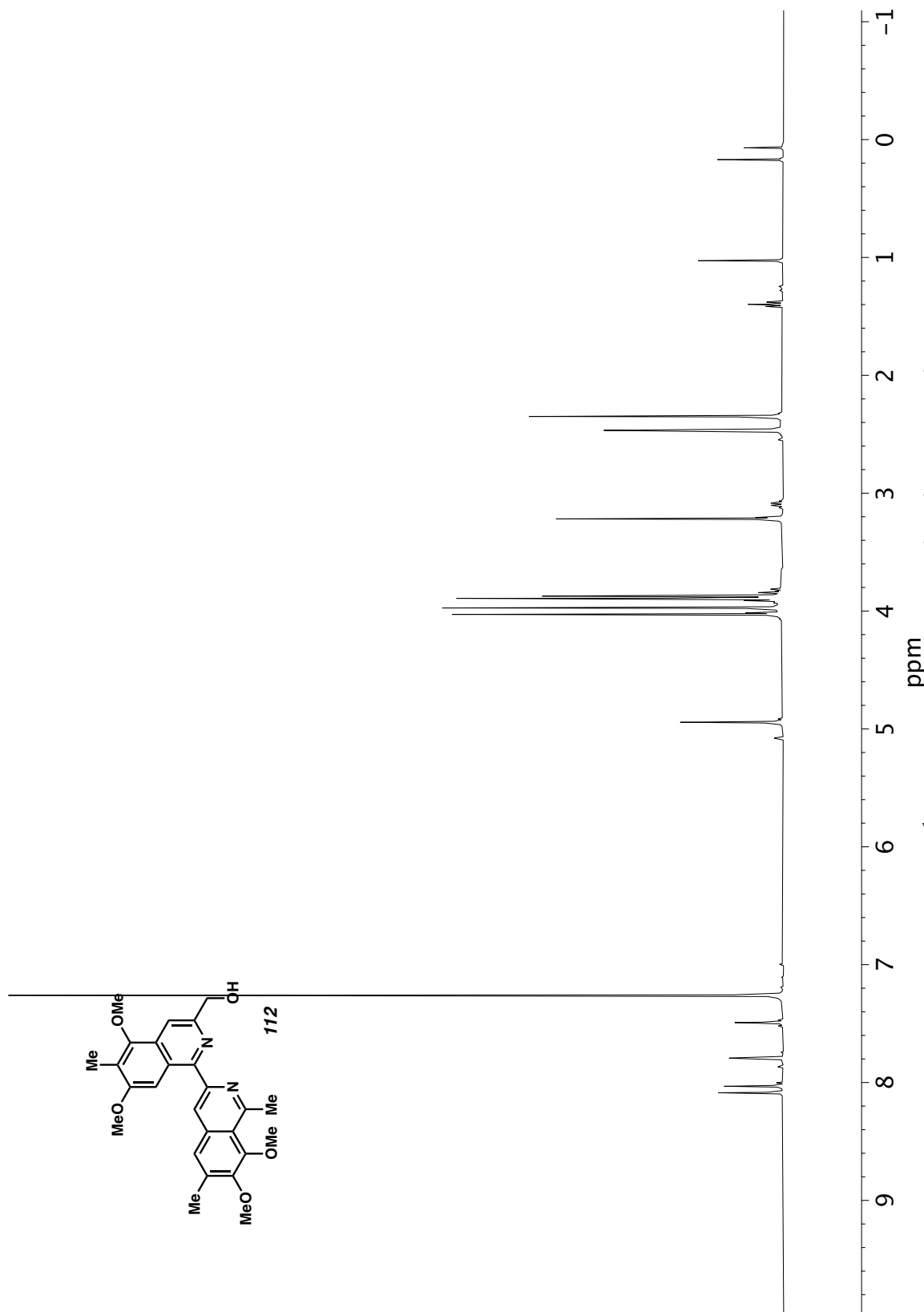


Figure A6.25 ^1H NMR (400 MHz, CDCl_3) of compound **112**.

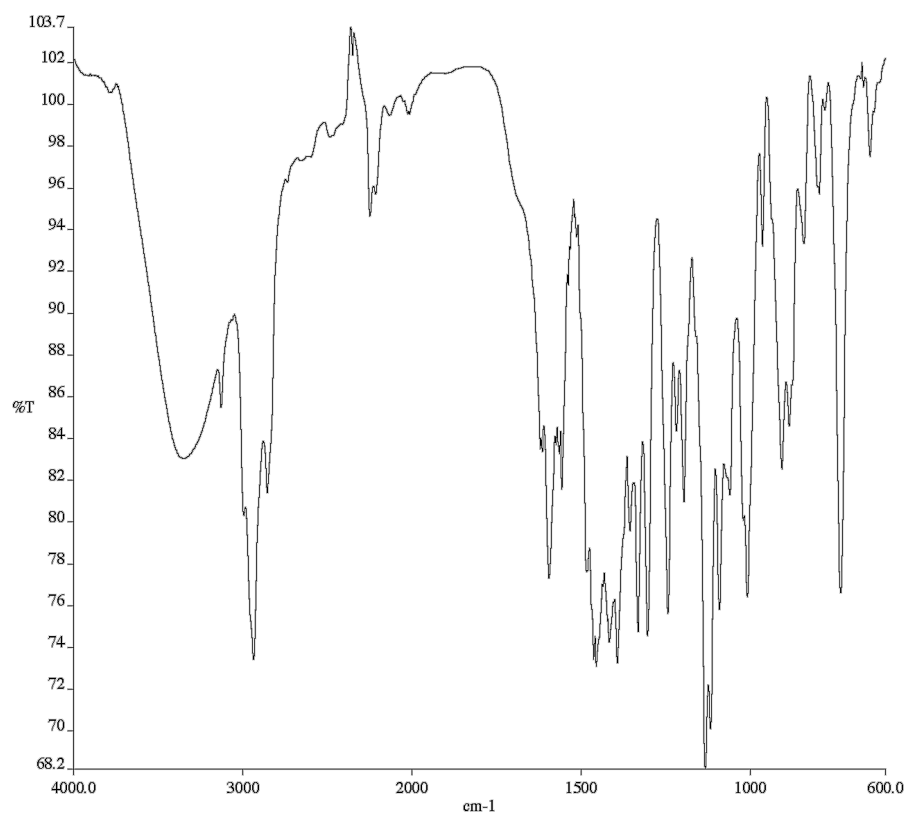


Figure A6.26 Infrared spectrum (Thin Film, NaCl) of compound **112**.

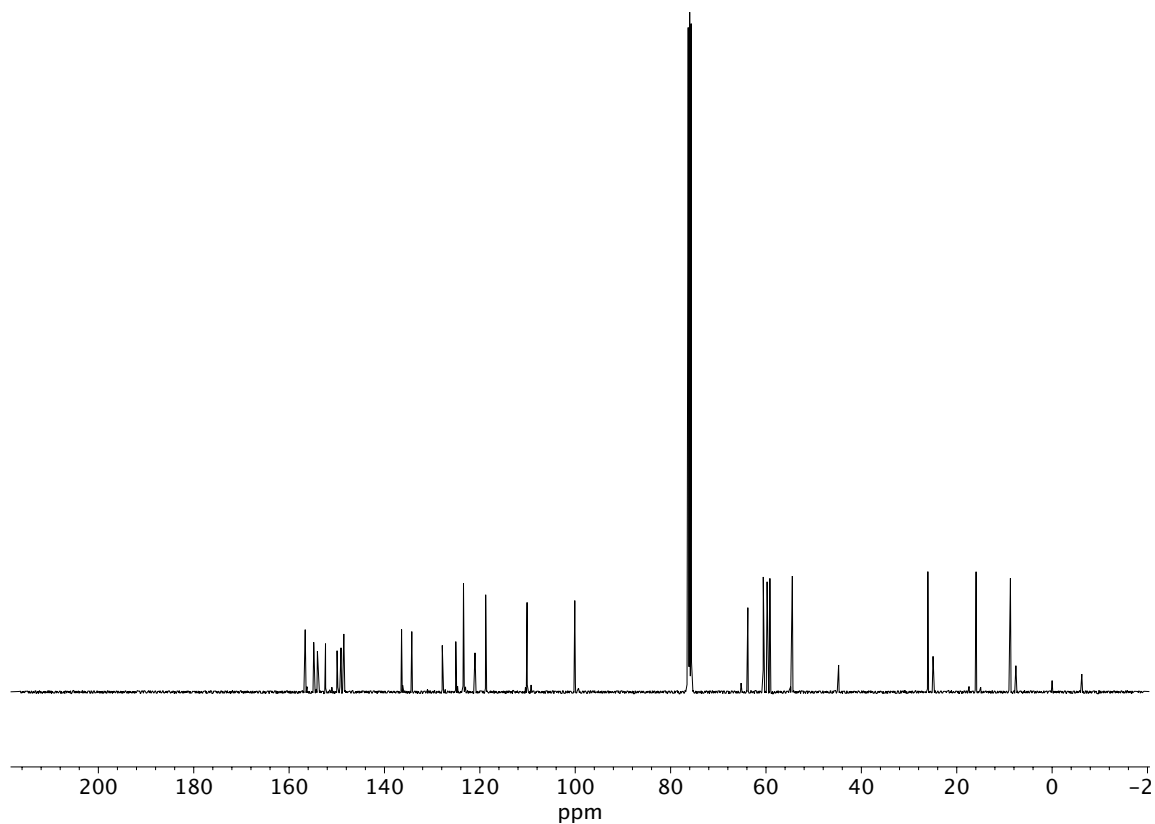


Figure A6.27 ¹³C NMR (100 MHz, CDCl₃) of compound **112**.

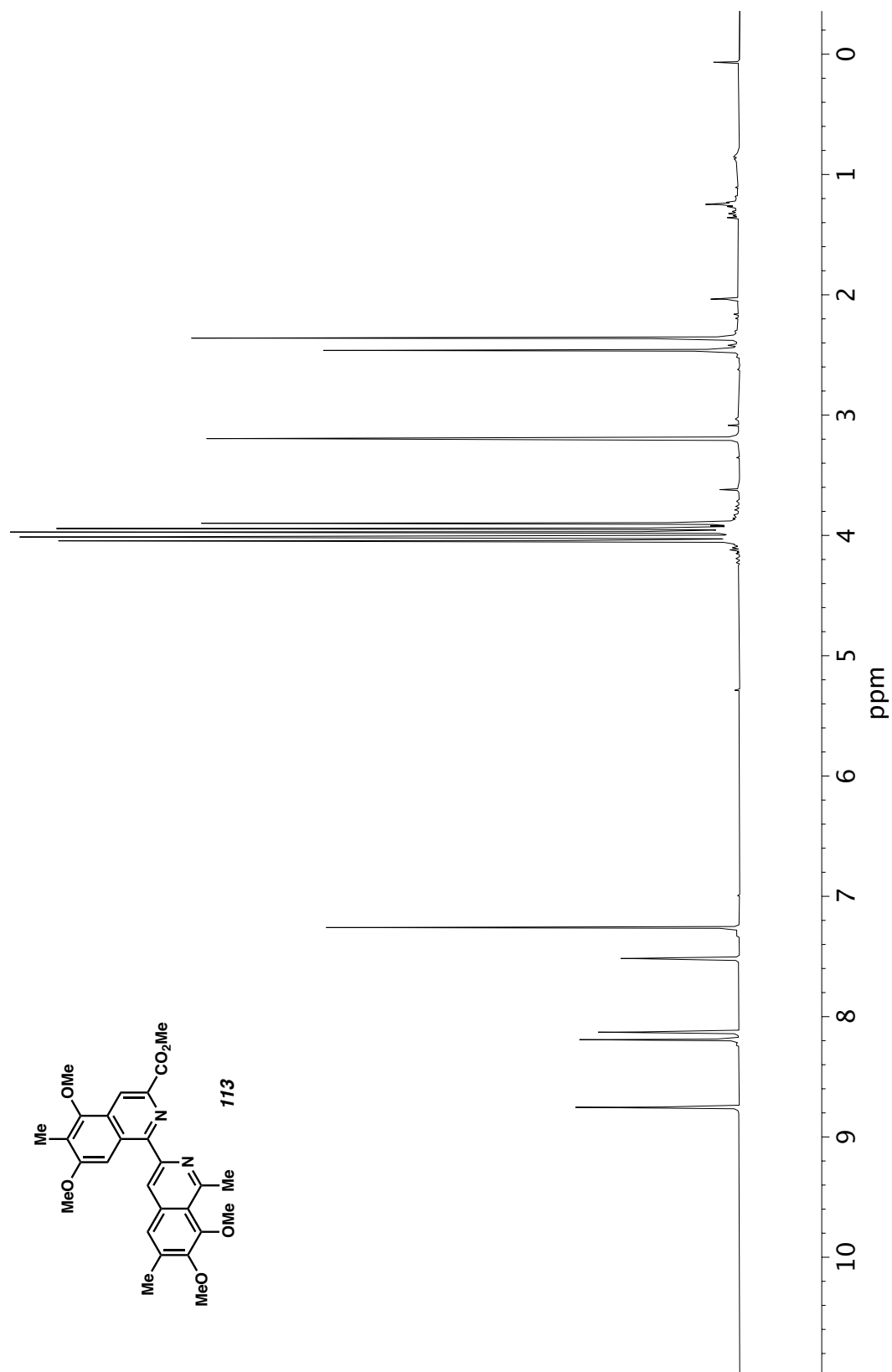


Figure A6.28 ^1H NMR (400 MHz, CDCl_3) of compound **113**.

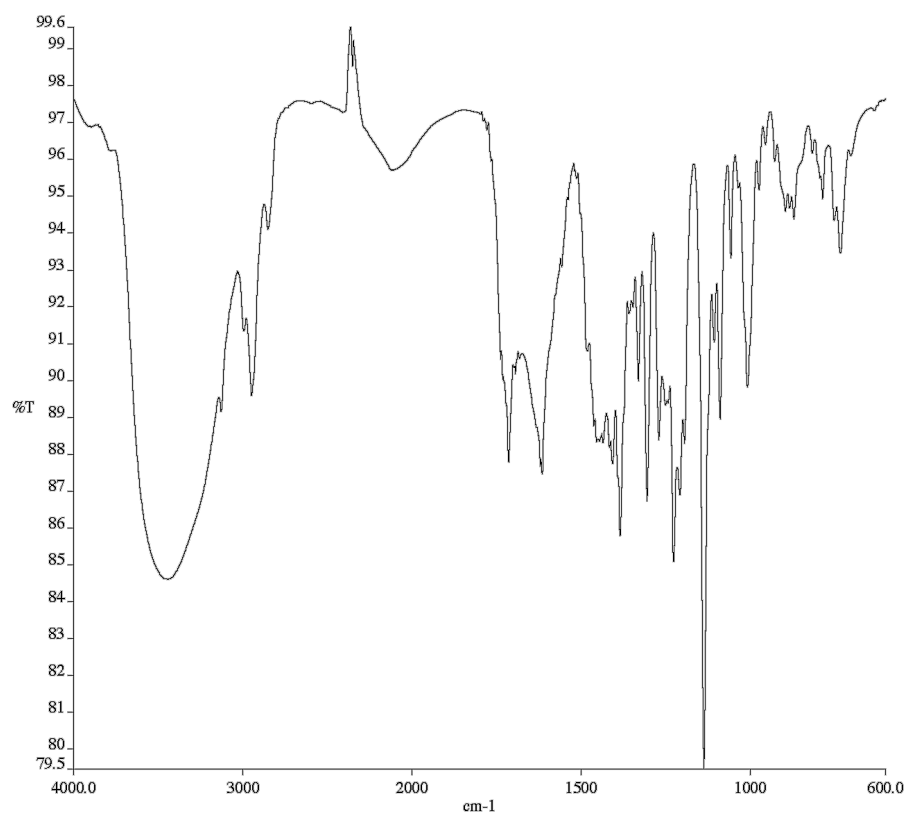


Figure A6.29 Infrared spectrum (Thin Film, NaCl) of compound **113**.

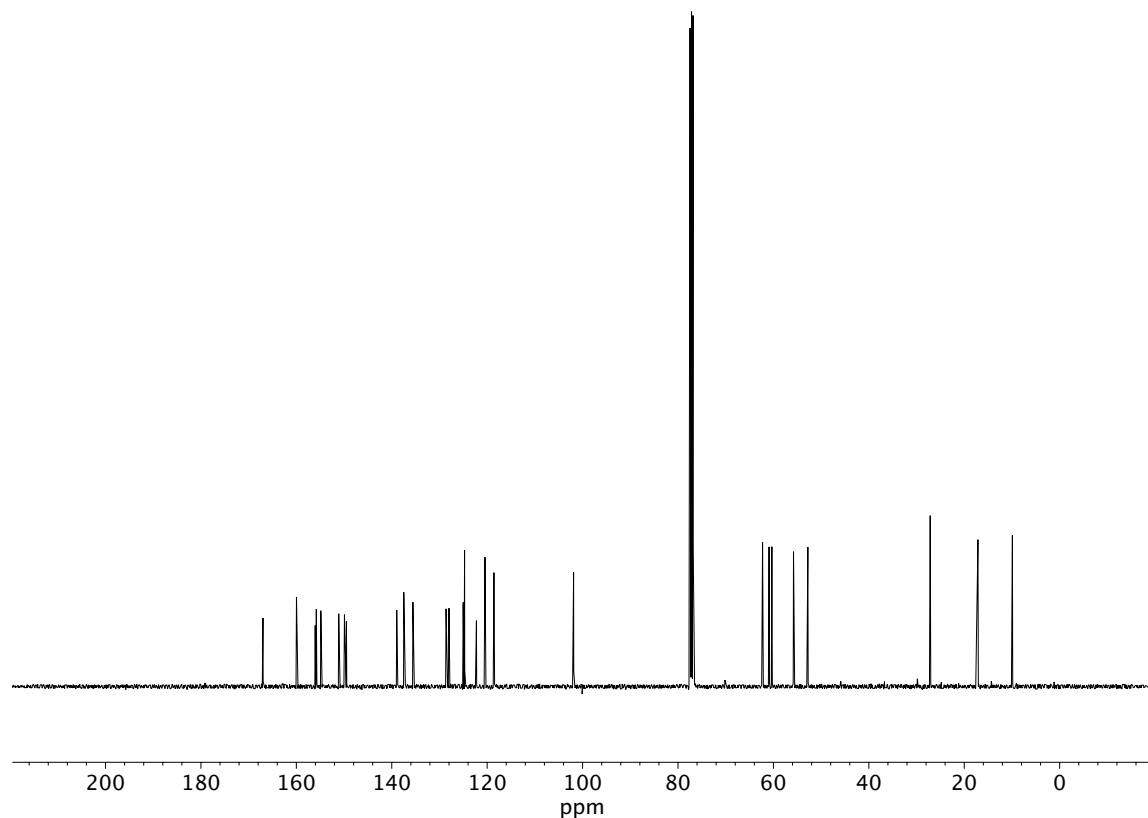


Figure A6.30 ¹³C NMR (100 MHz, CDCl₃) of compound **113**.

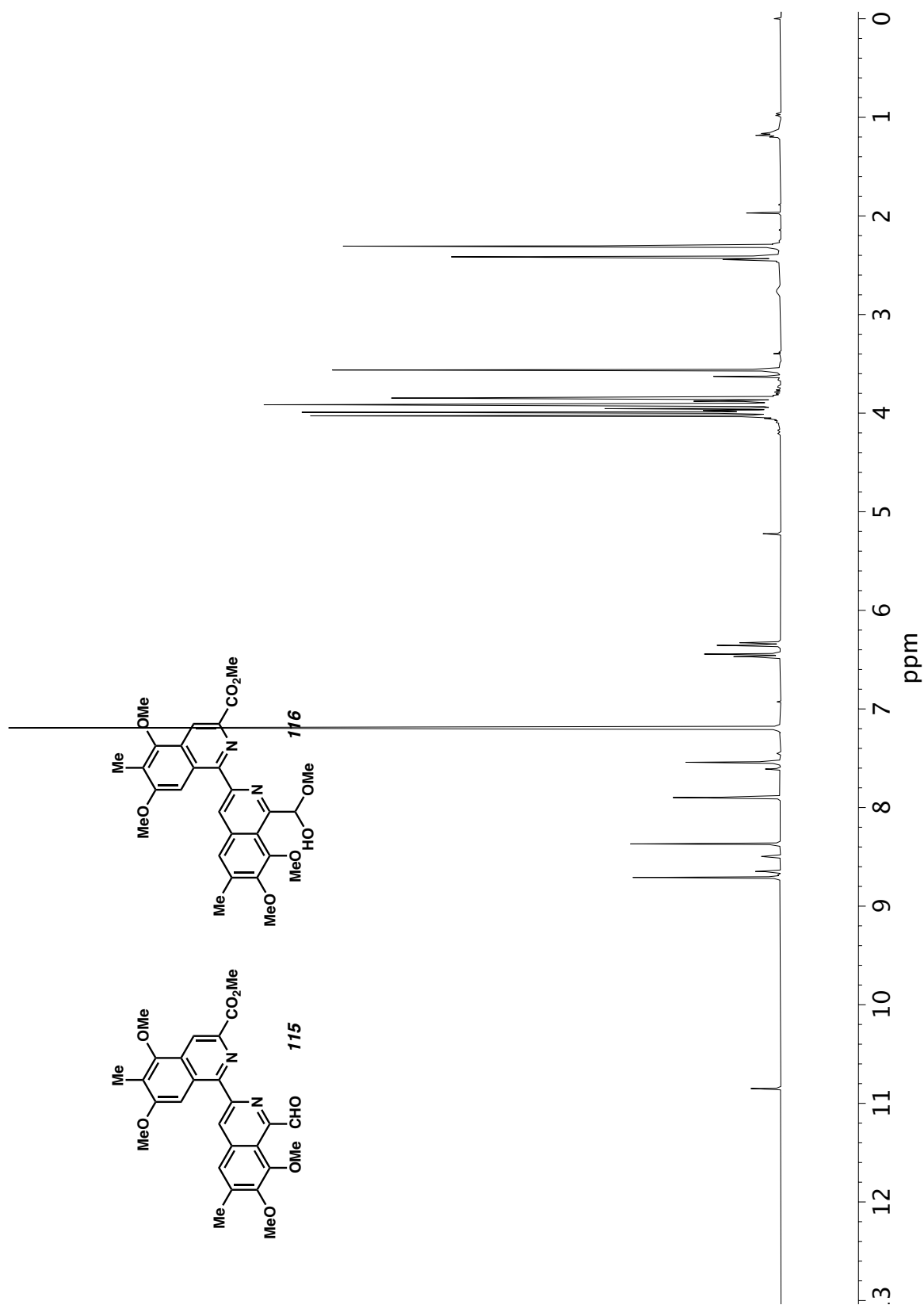


Figure A6.31 ^1H NMR (400 MHz, CDCl_3) of compounds **115** and **116**.

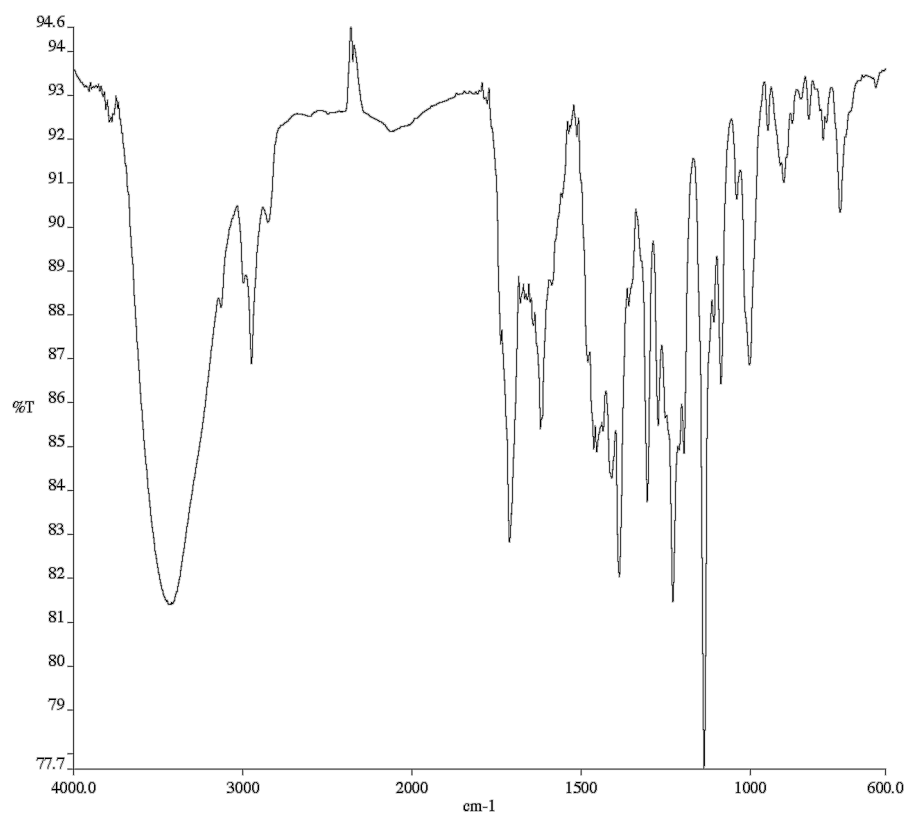


Figure A6.32 Infrared spectrum (Thin Film, NaCl) of compounds **115** and **116**.

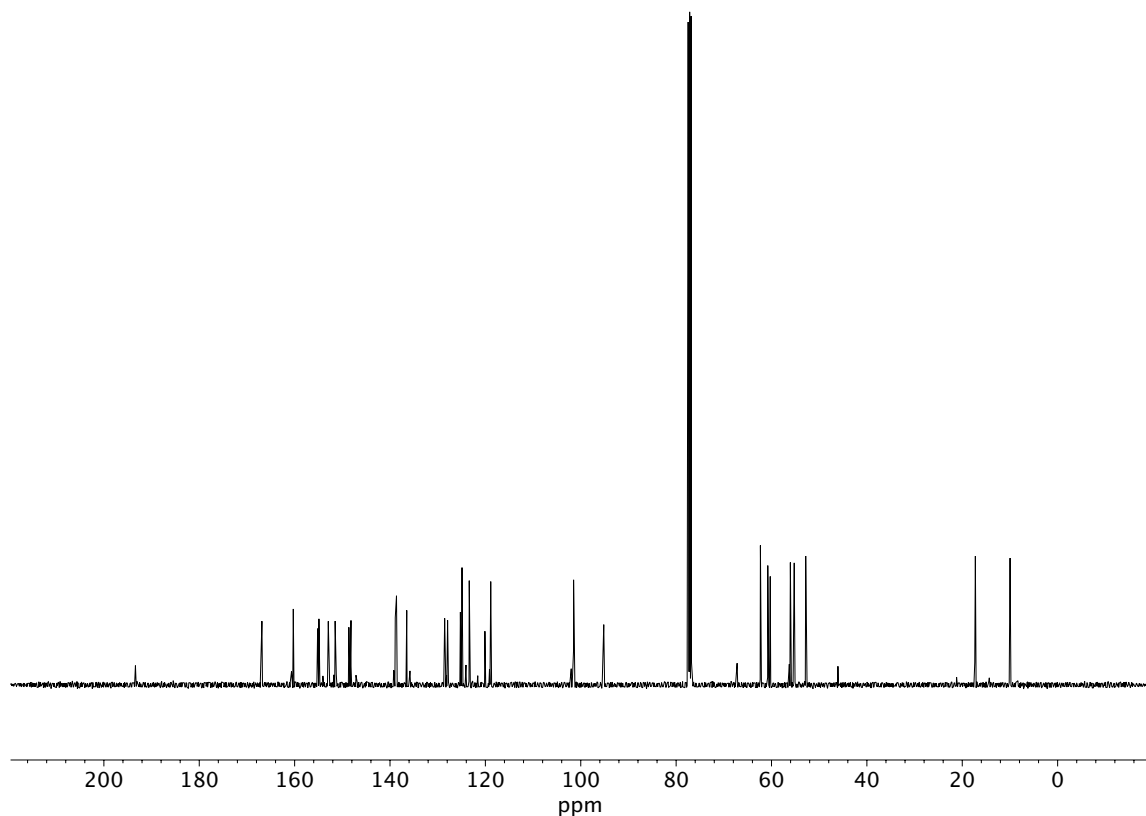


Figure A6.33 ¹³C NMR (100 MHz, CDCl₃) of compounds **115** and **116**.

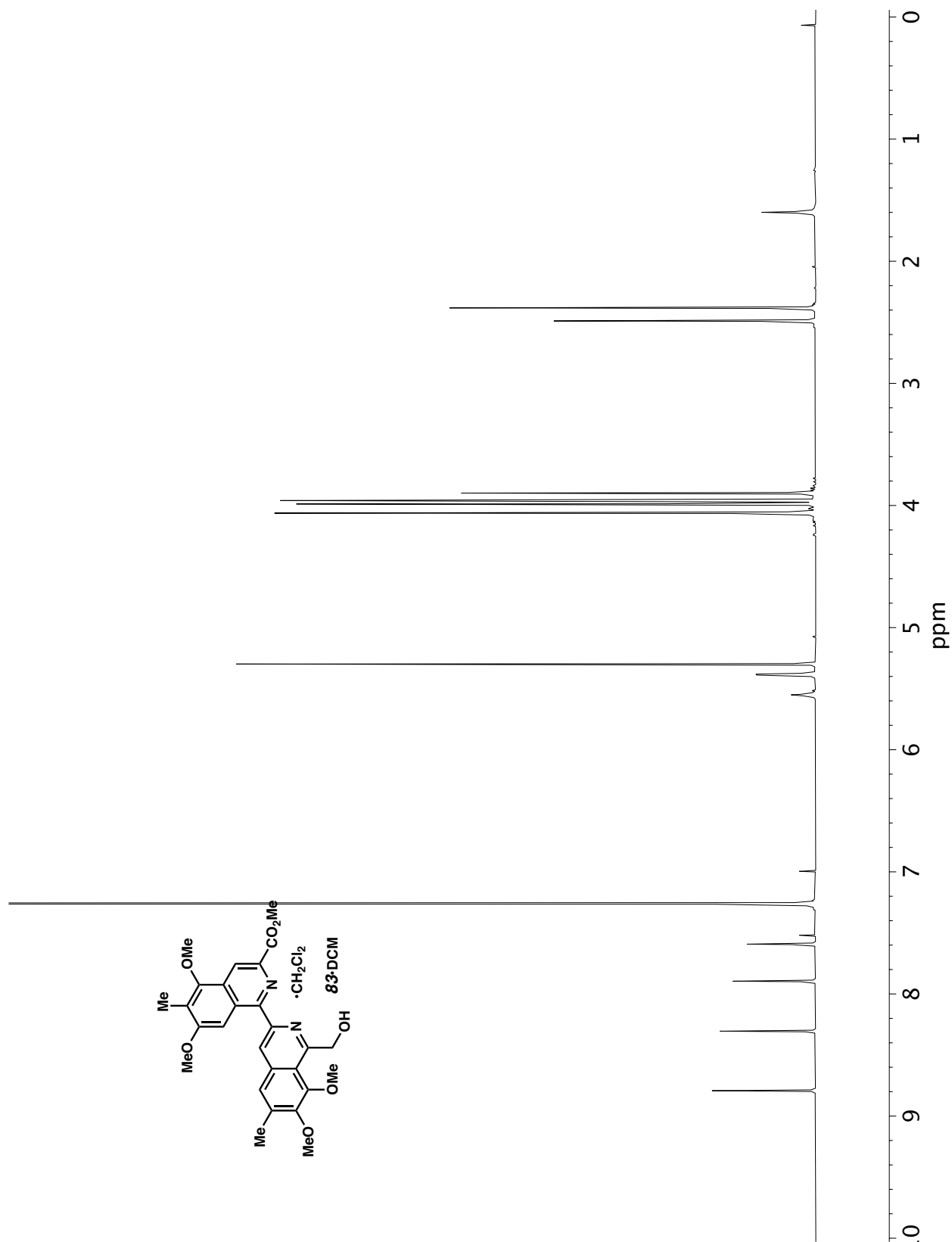


Figure A6.34 ¹H NMR (400 MHz, CDCl₃) of compound 83 • DCM.

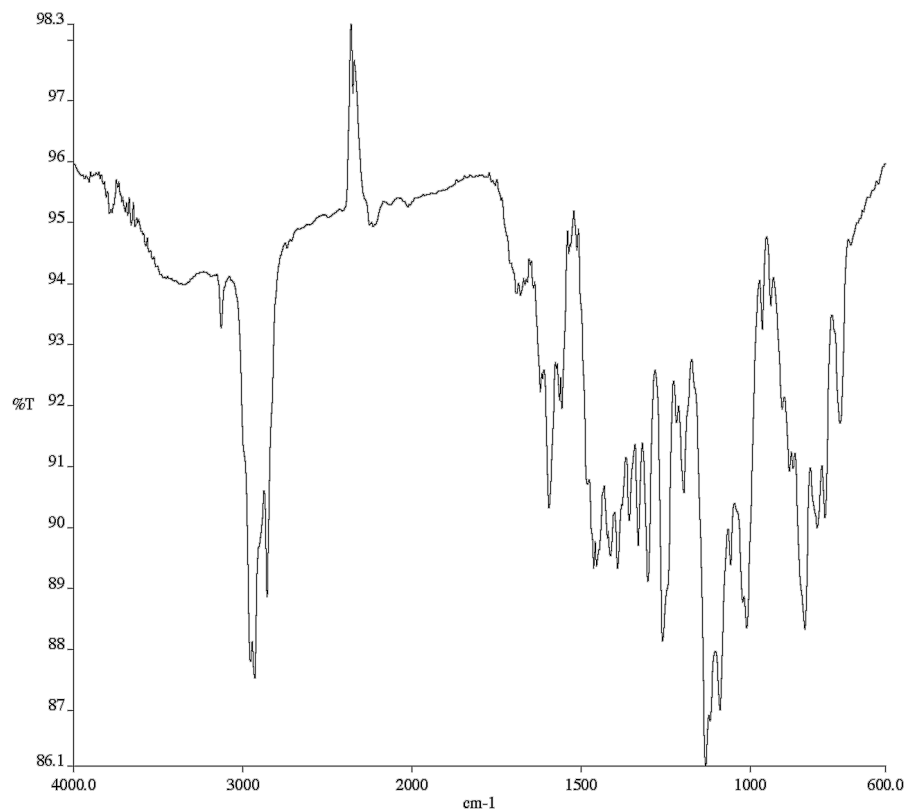


Figure A6.35 Infrared spectrum (Thin Film, NaCl) of compound **83 • DCM**.

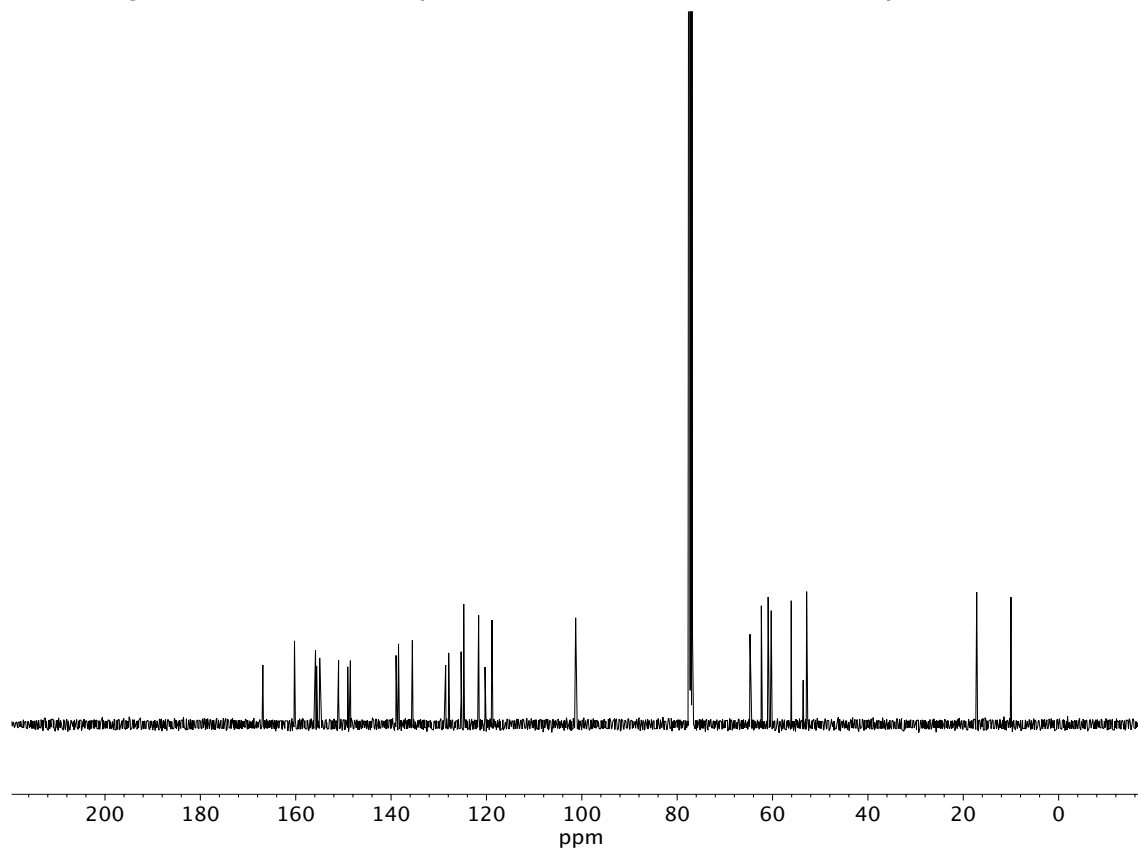


Figure A6.36 ¹³C NMR (100 MHz, CDCl₃) of compound **83 • DCM**.

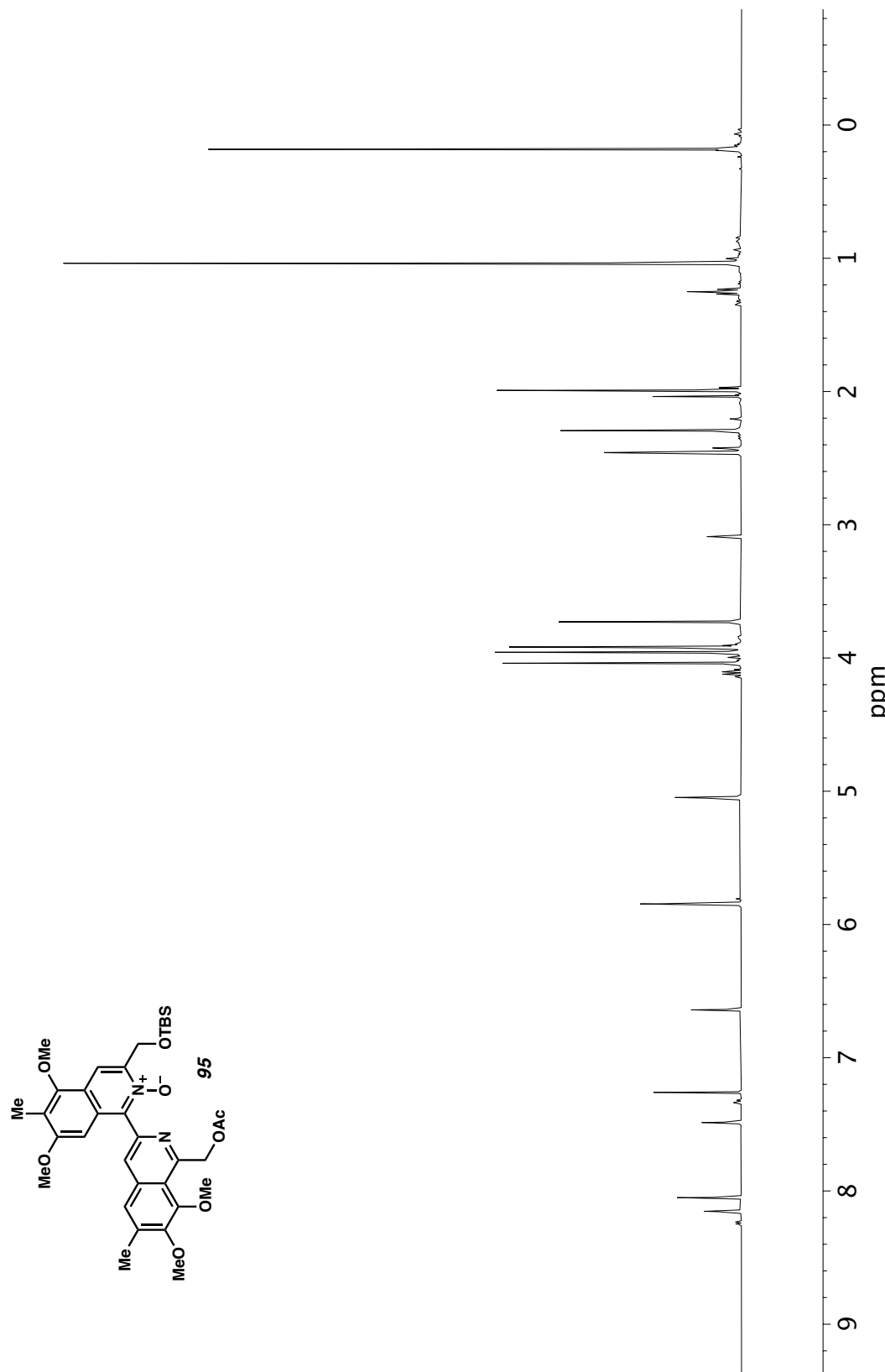


Figure A6.37 ^1H NMR (400 MHz, CDCl_3) of compound **95**.

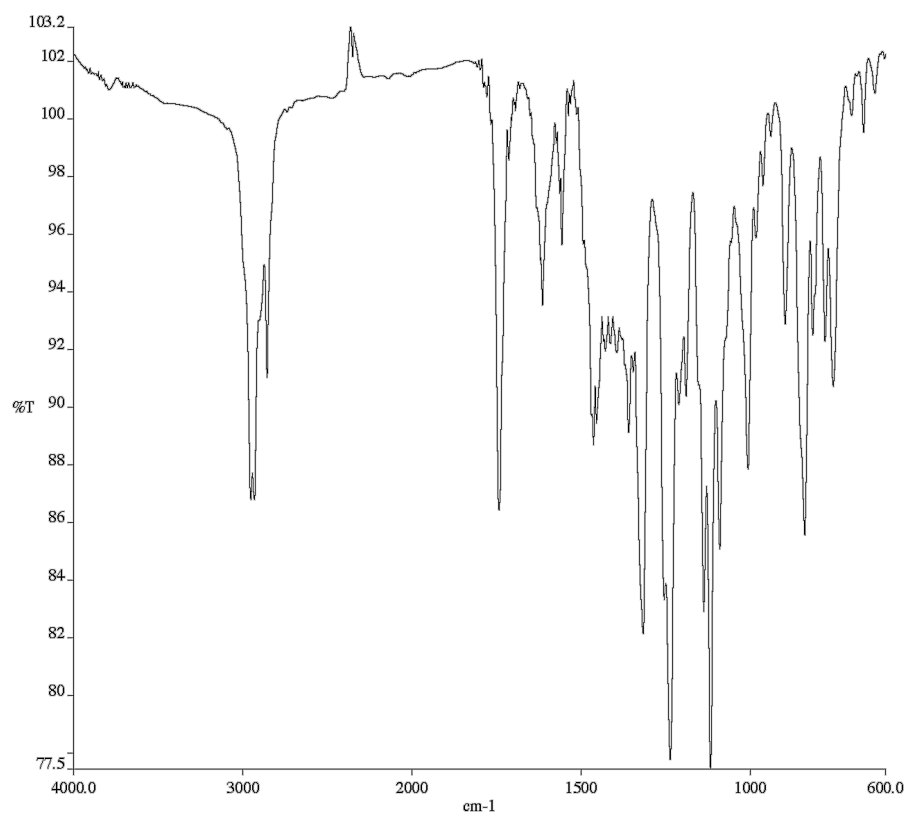


Figure A6.38 Infrared spectrum (Thin Film, NaCl) of compound **95**.

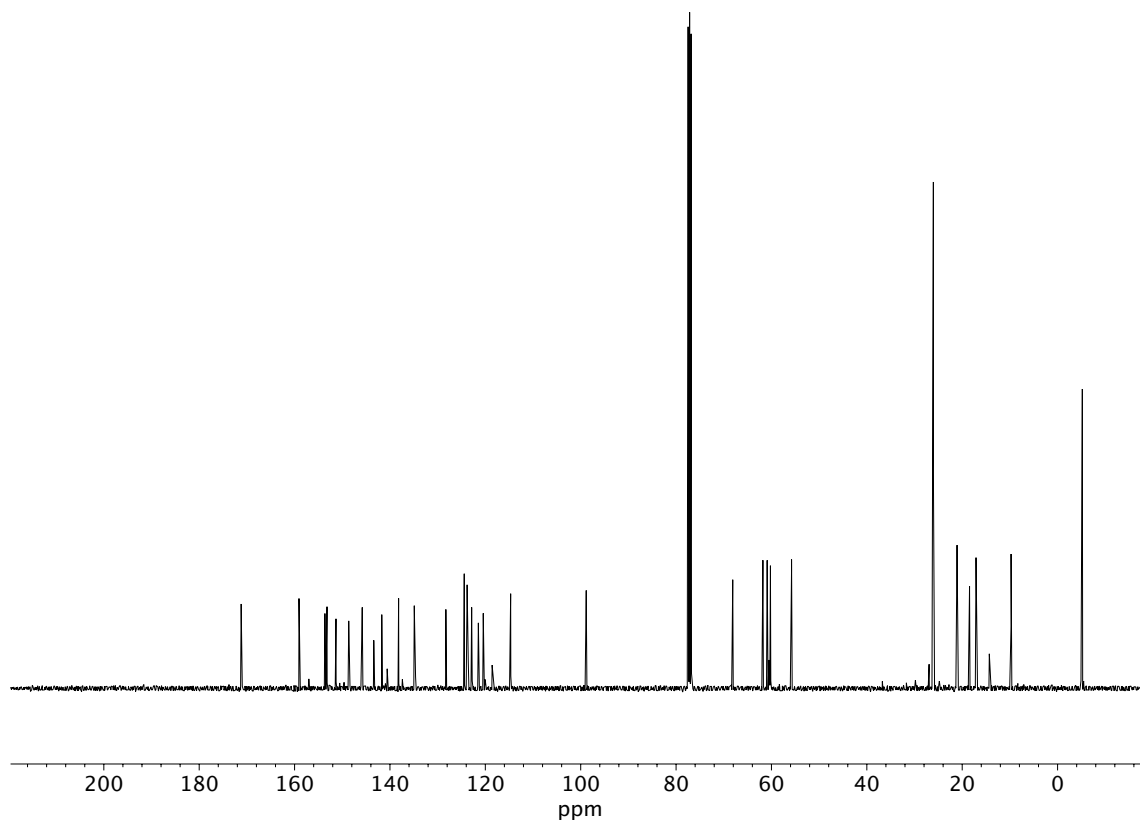


Figure A6.39 ¹³C NMR (100 MHz, CDCl₃) of compound **95**.

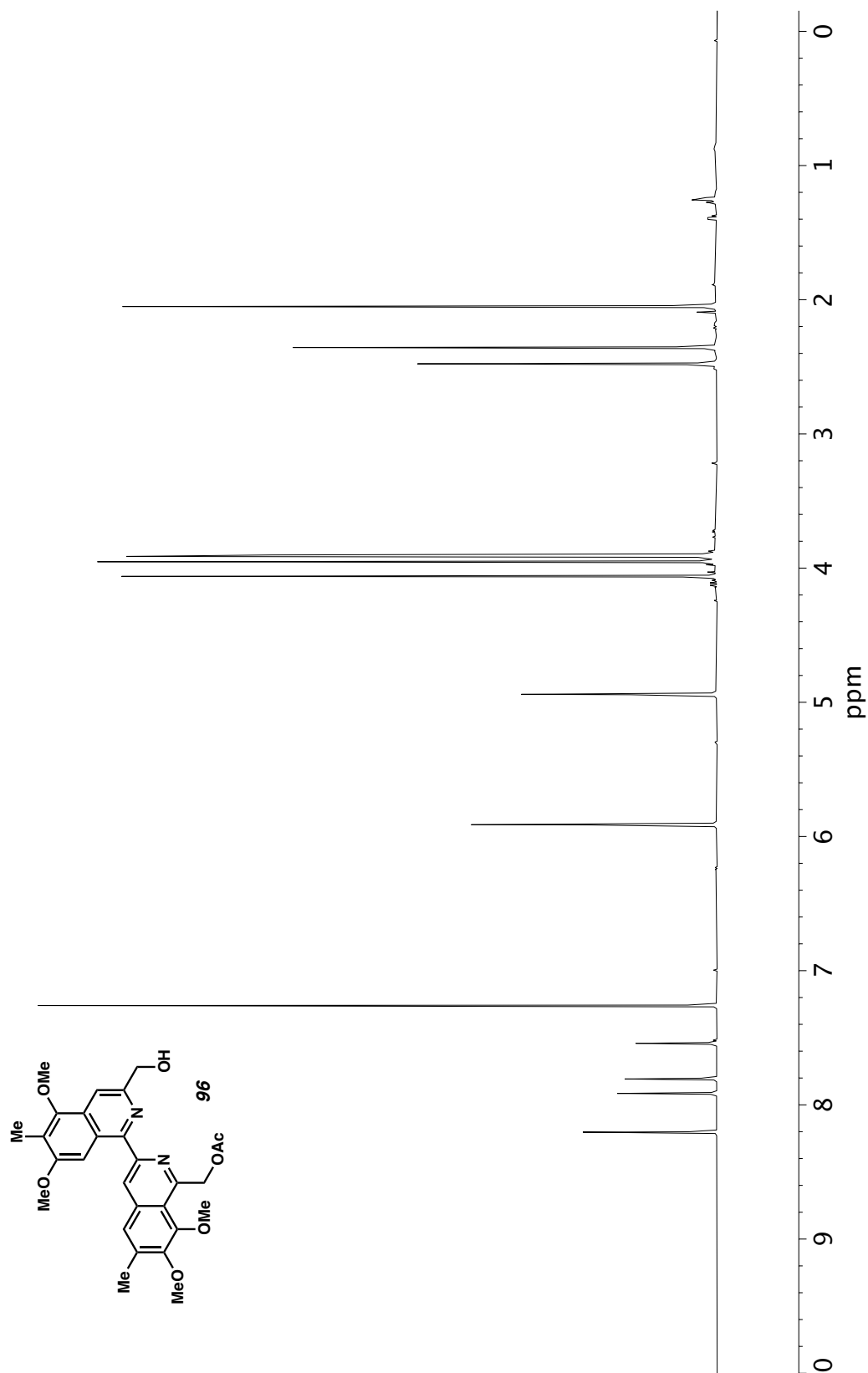


Figure A6.40 ¹H NMR (400 MHz, CDCl₃) of compound **96**.

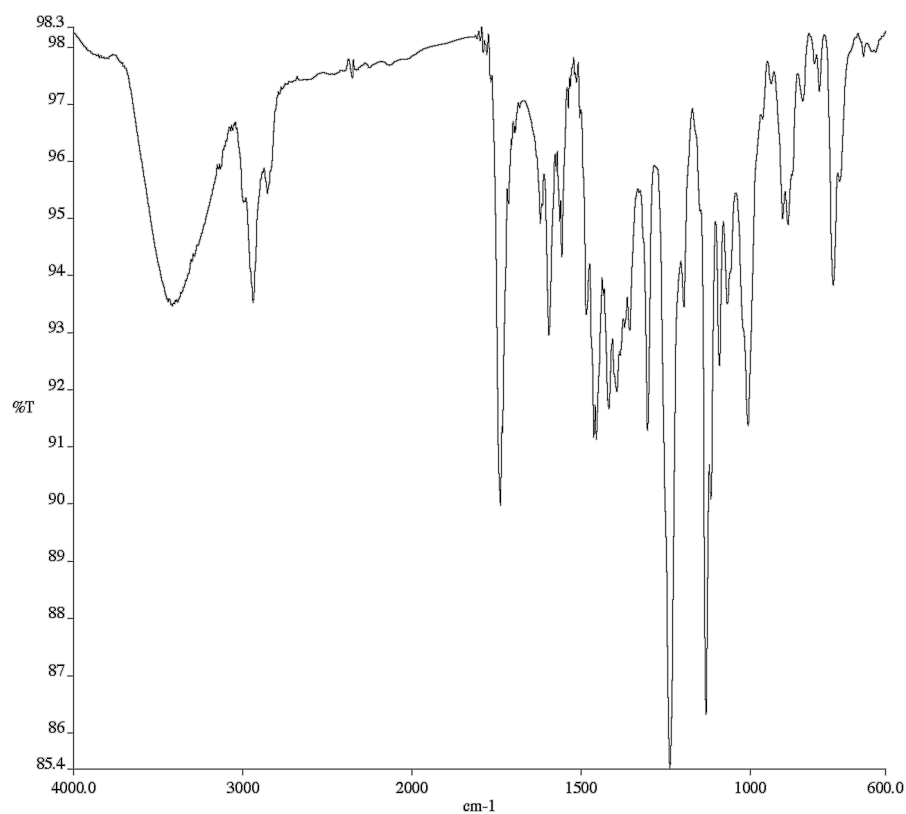


Figure A6.41 Infrared spectrum (Thin Film, NaCl) of compound **96**.

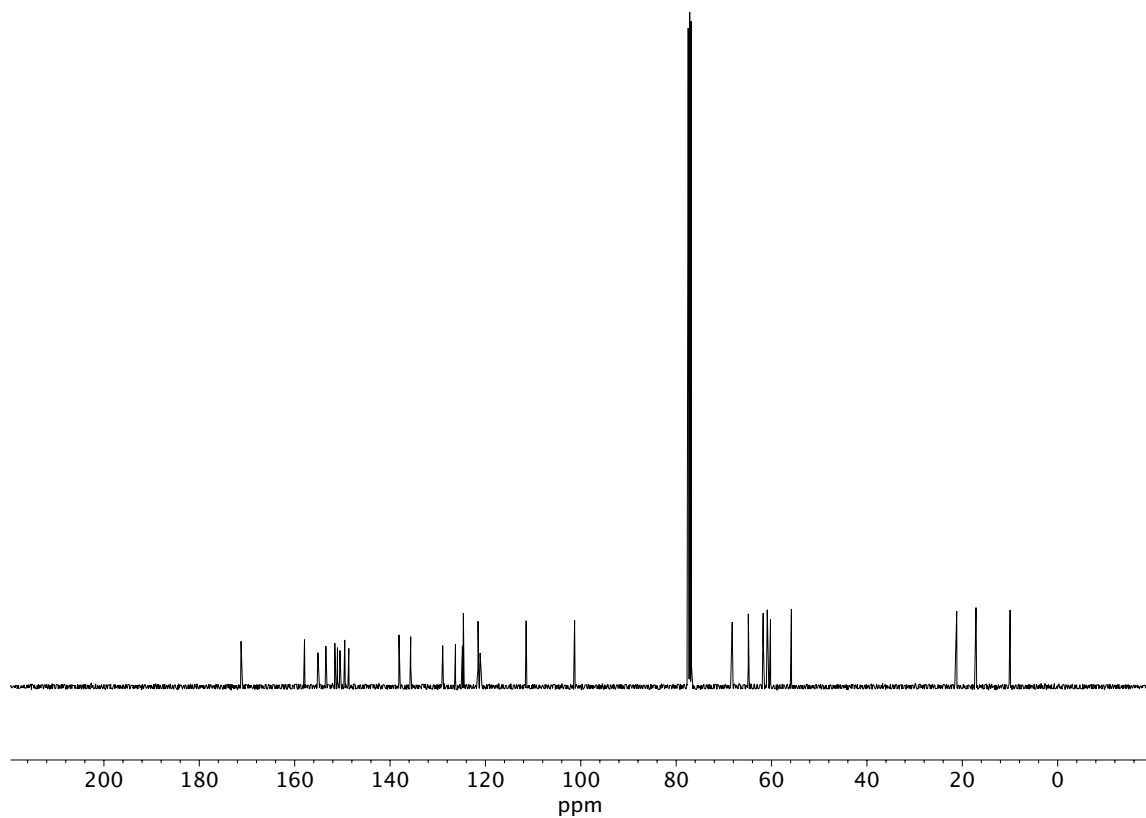


Figure A6.42 ¹³C NMR (100 MHz, CDCl₃) of compound **96**.

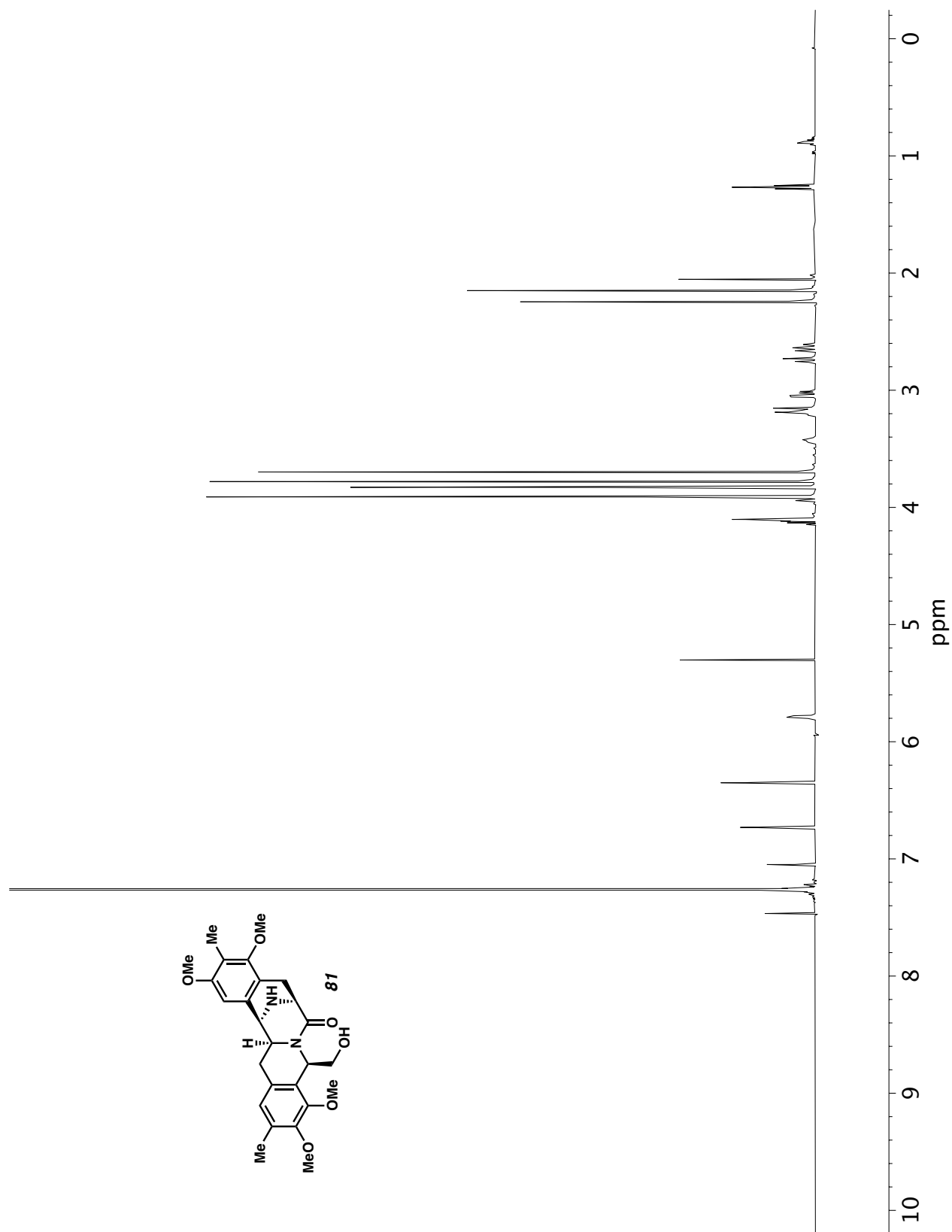


Figure A6.43 ^1H NMR (500 MHz, CDCl_3) of compound **81**.

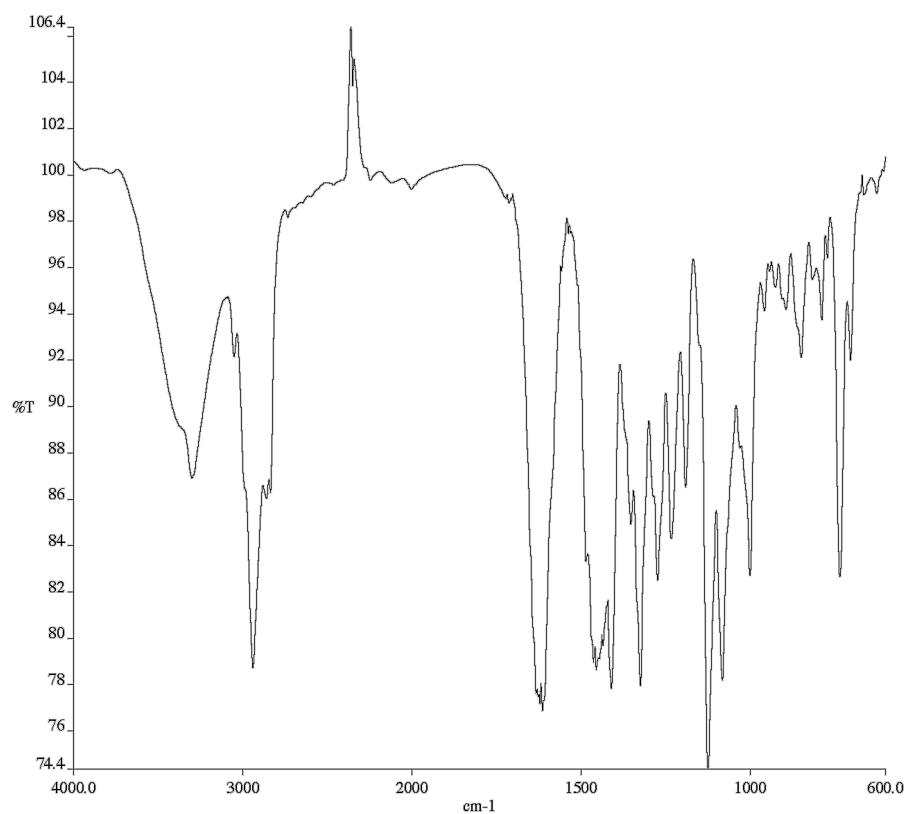


Figure A6.44 Infrared spectrum (Thin Film, NaCl) of compound **81**.

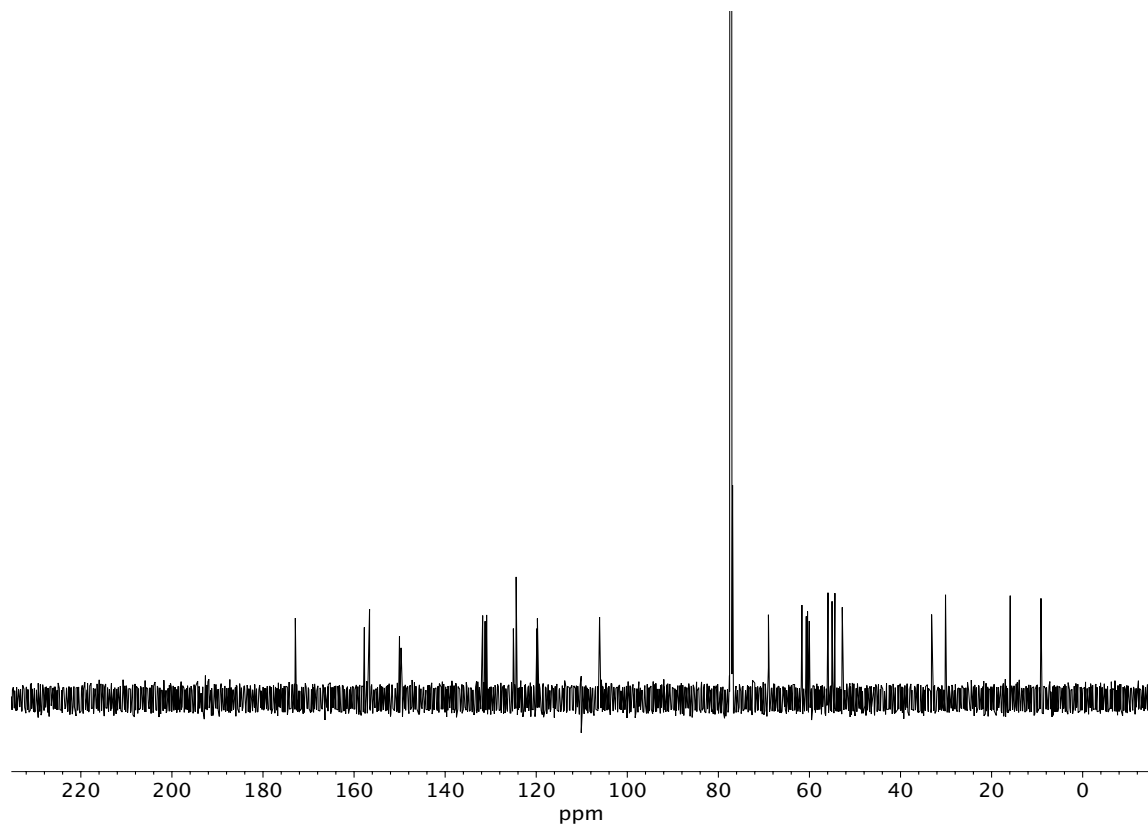


Figure A6.45 ¹³C NMR (125 MHz, CDCl₃) of compound **81**.

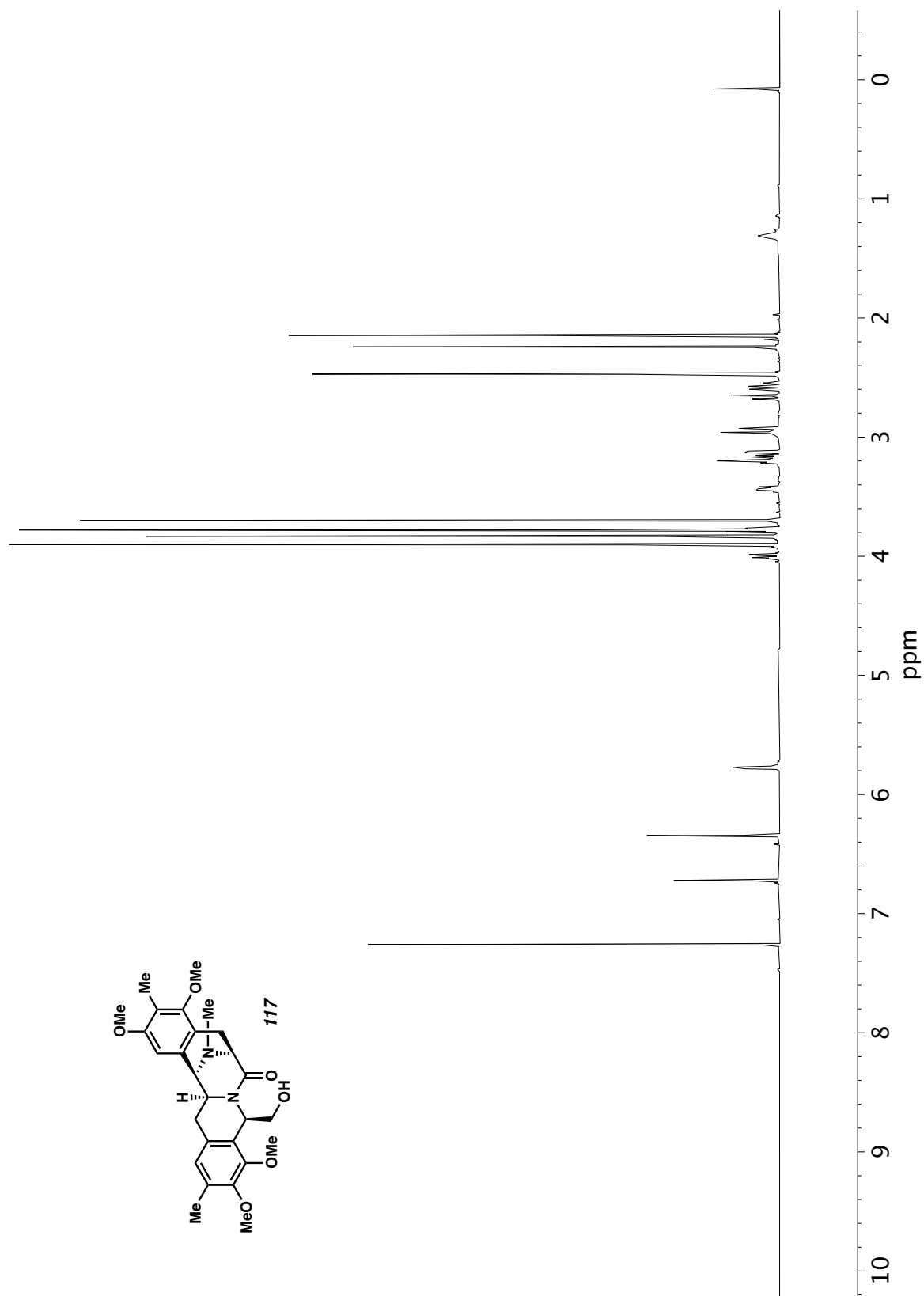


Figure A6.46 ^1H NMR (500 MHz, CDCl_3) of compound **117**.

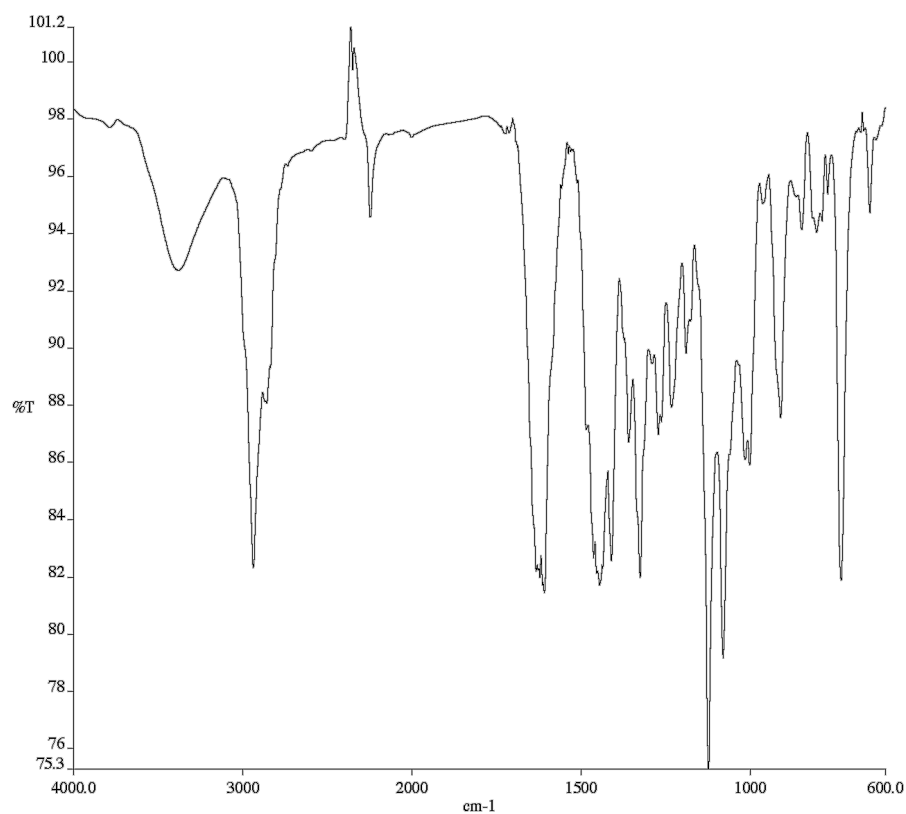


Figure A6.47 Infrared spectrum (Thin Film, NaCl) of compound **117**.

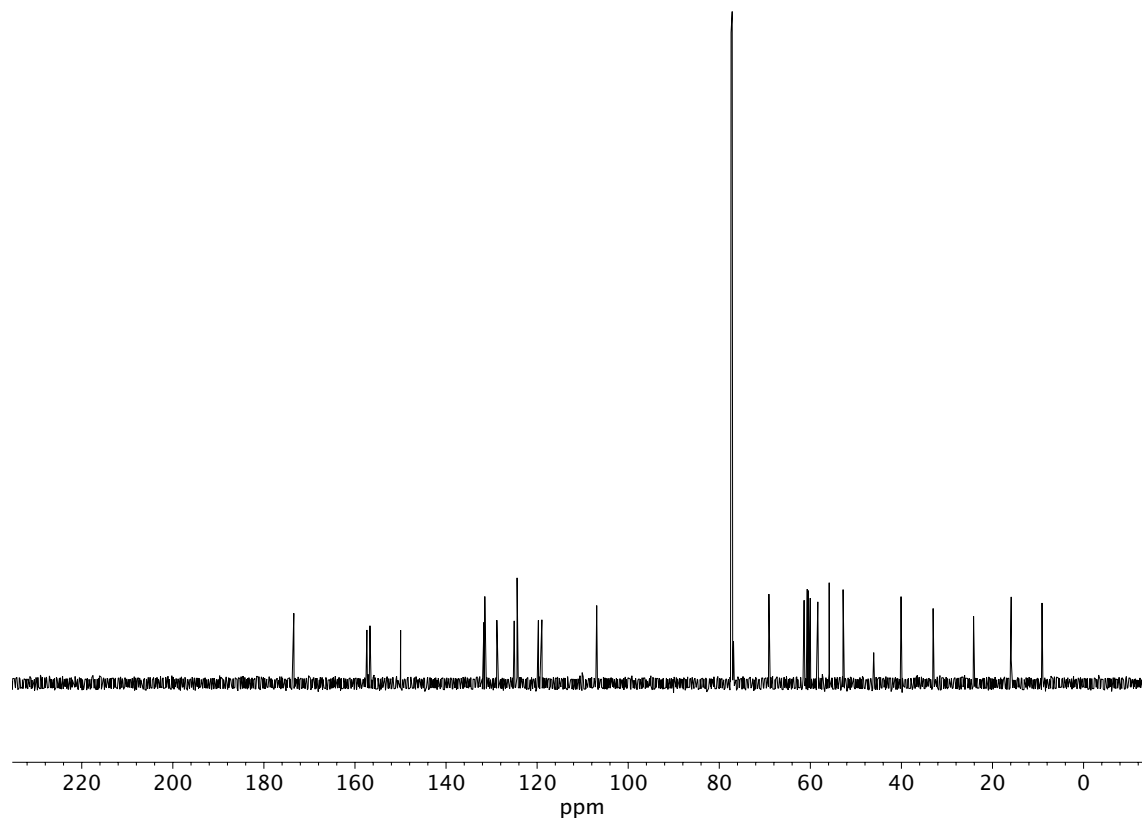


Figure A6.48 ¹³C NMR (125 MHz, CDCl₃) of compound **117**.

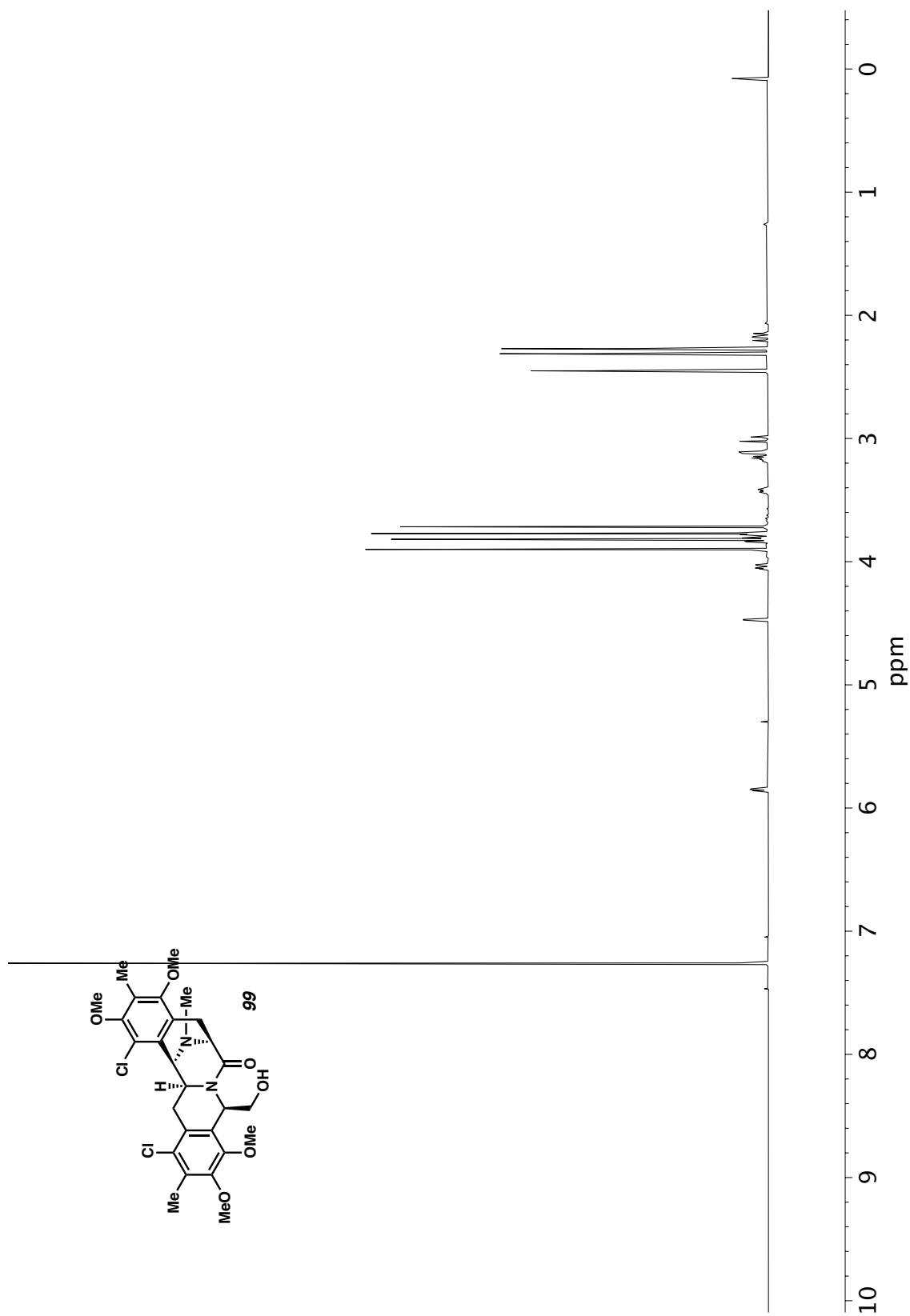


Figure A6.49 ^1H NMR (500 MHz, CDCl_3) of compound **99**.

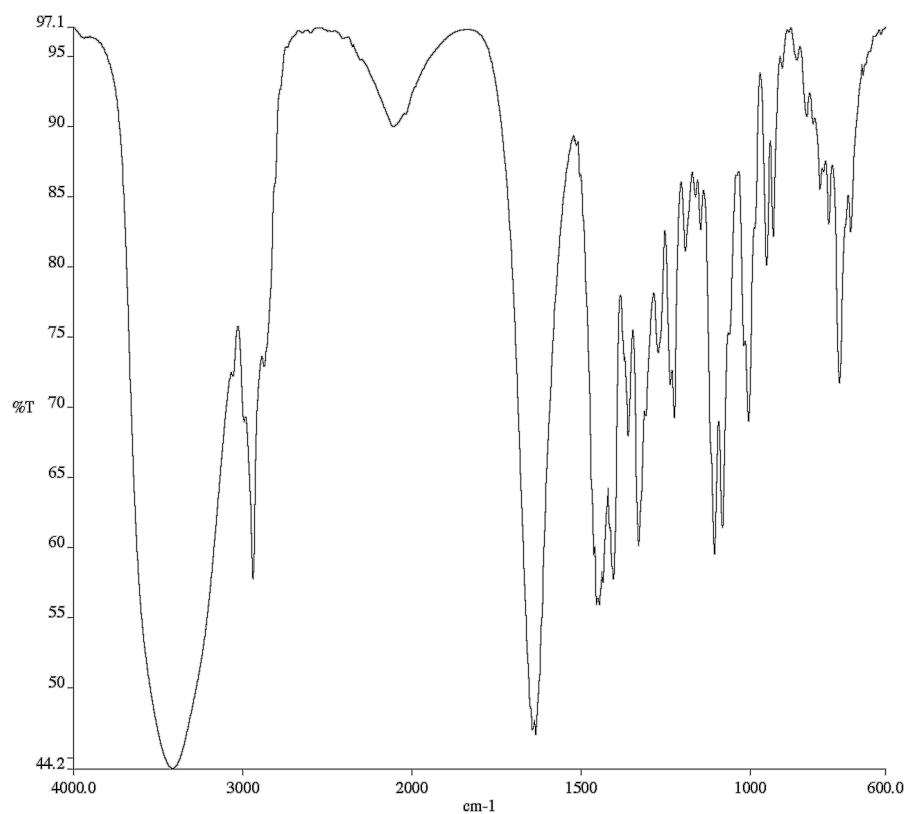


Figure A6.50 Infrared spectrum (Thin Film, NaCl) of compound **99**.

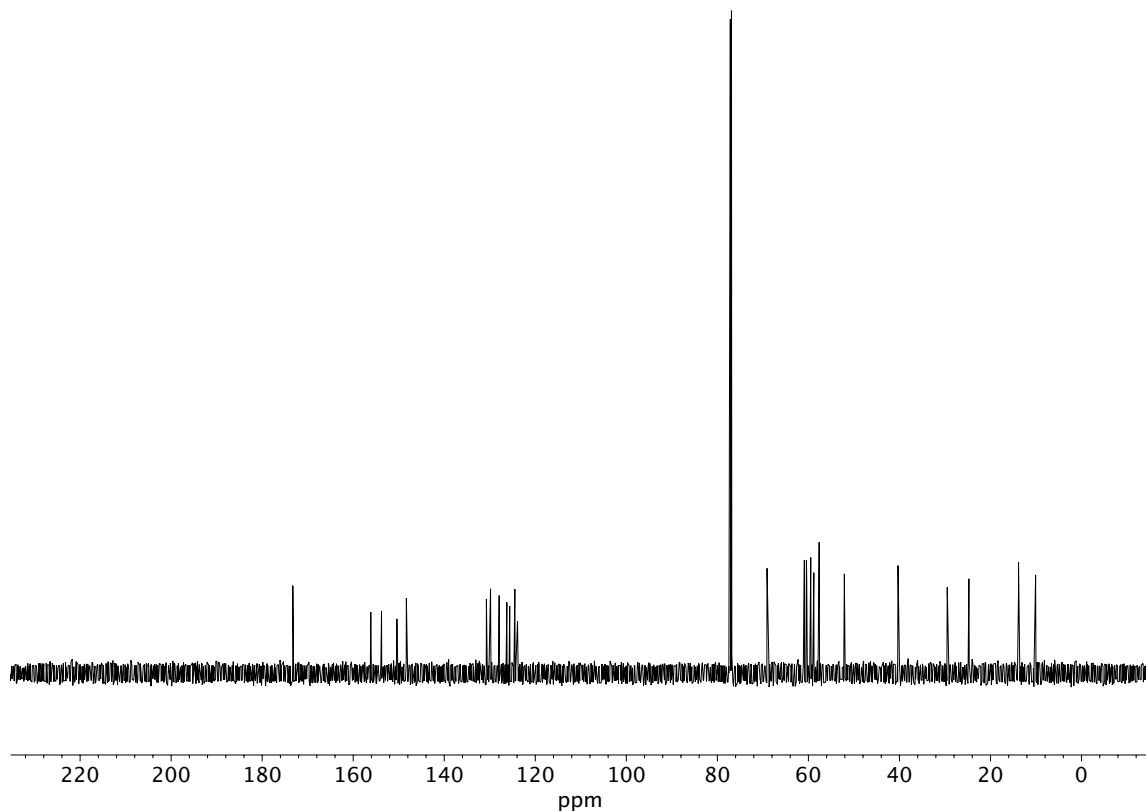


Figure A6.51 ¹³C NMR (125 MHz, CDCl₃) of compound **99**.

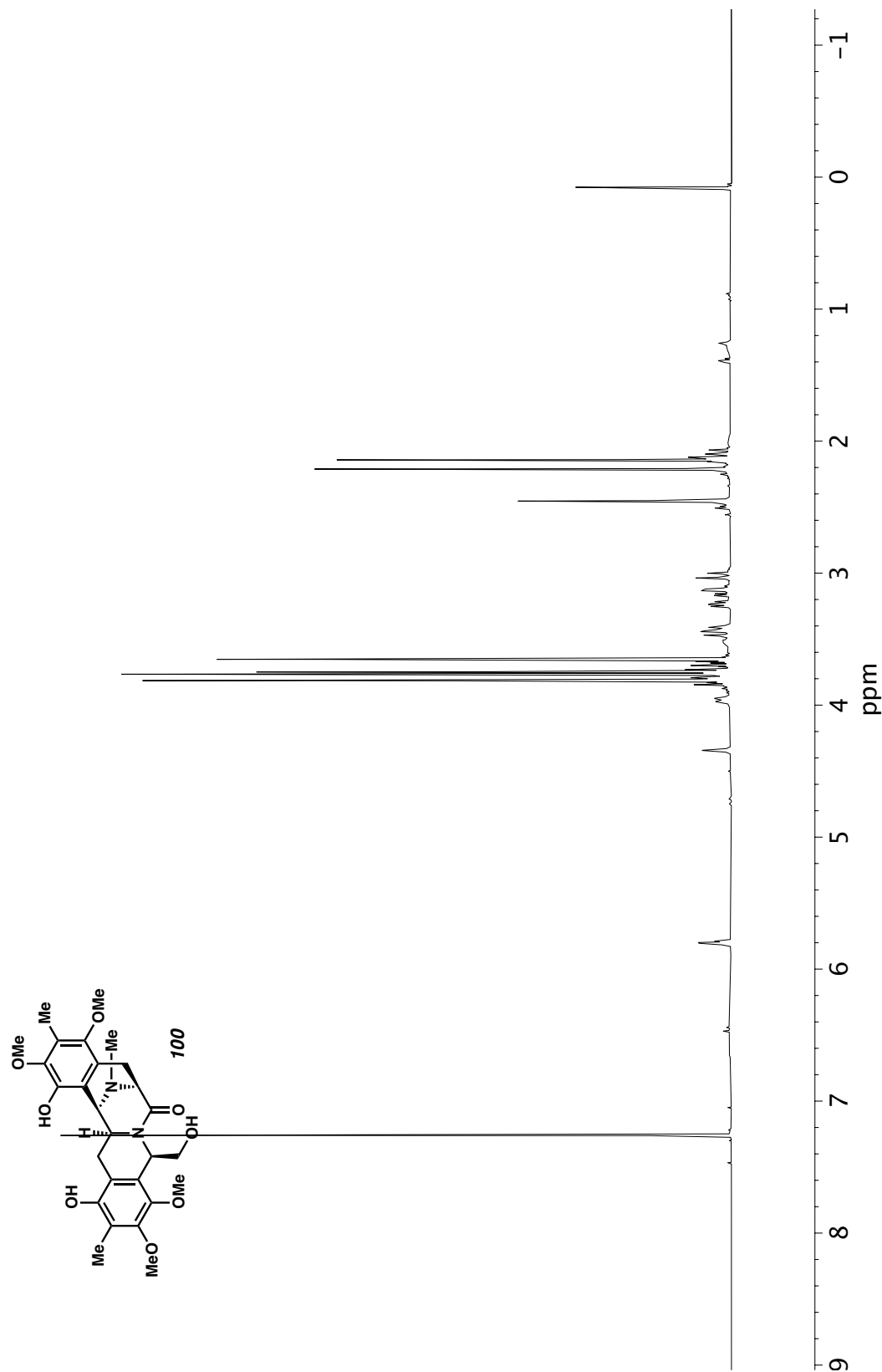


Figure A6.52 ^1H NMR (500 MHz, CDCl_3) of compound **100**.

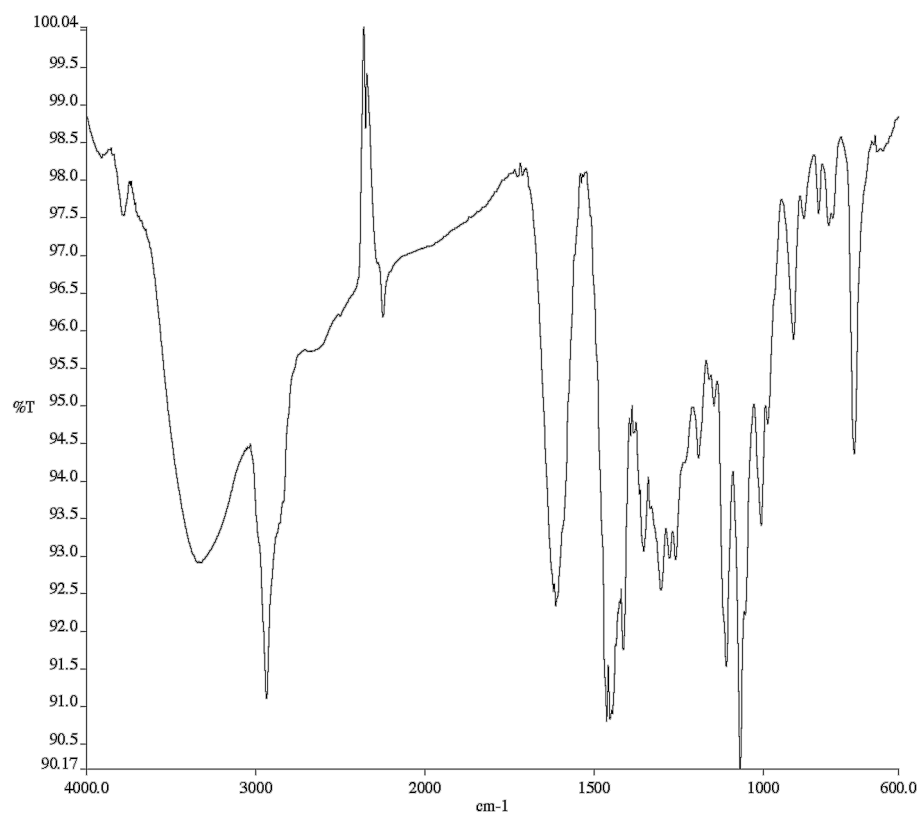


Figure A6.53 Infrared spectrum (Thin Film, NaCl) of compound **100**.

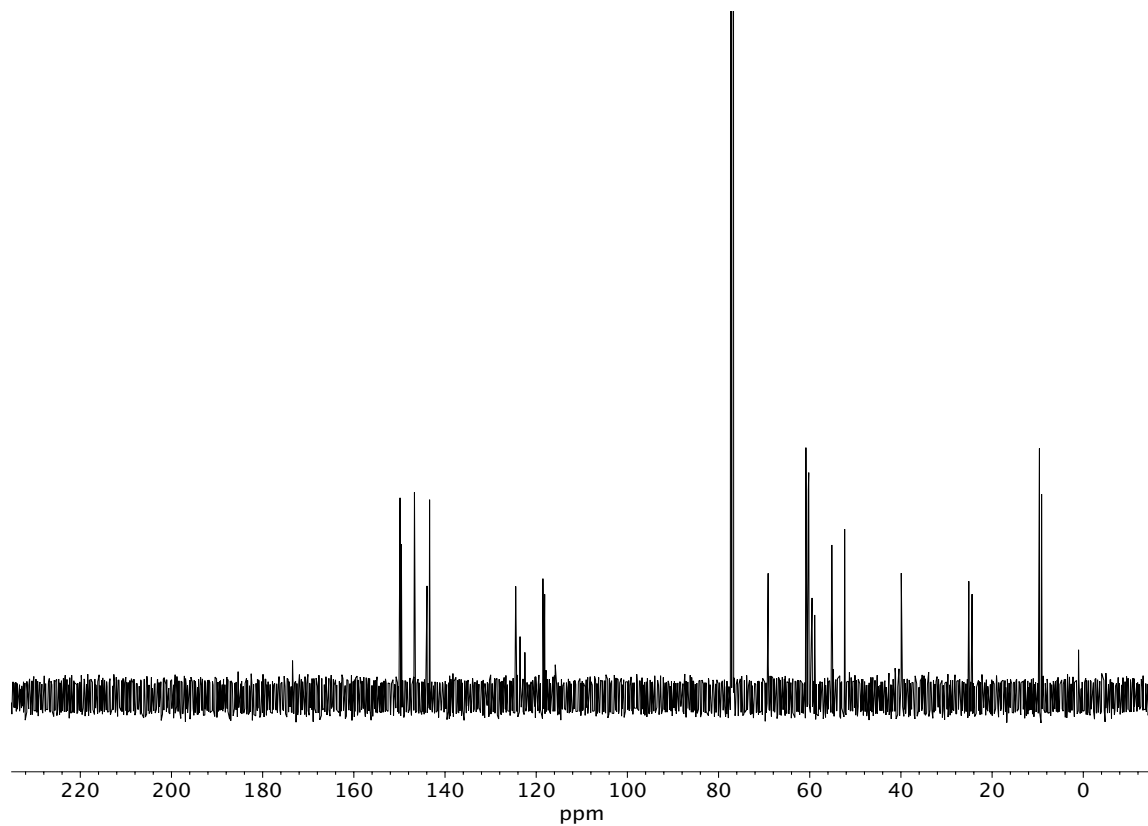


Figure A6.54 ¹³C NMR (125 MHz, CDCl₃) of compound **100**.

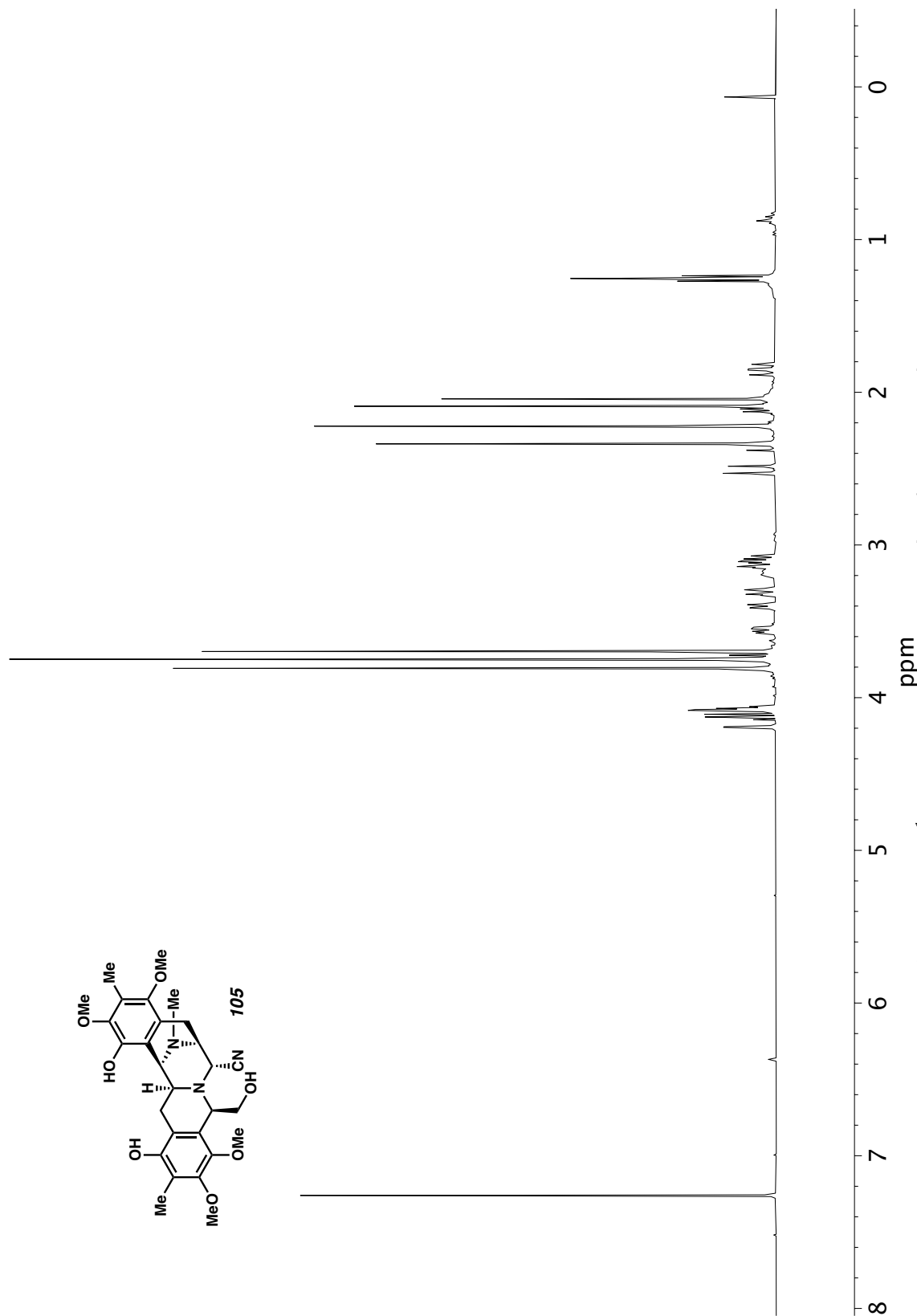


Figure A6.55 ^1H NMR (400 MHz, CDCl_3) of compound **105**.

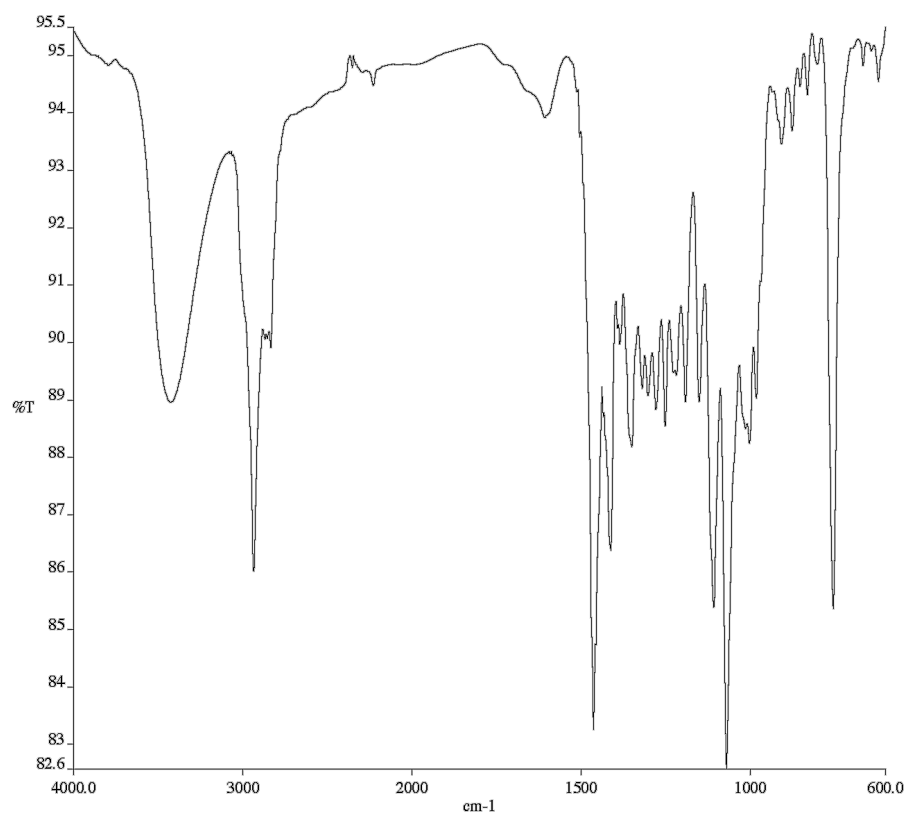


Figure A6.56 Infrared spectrum (Thin Film, NaCl) of compound **105**.

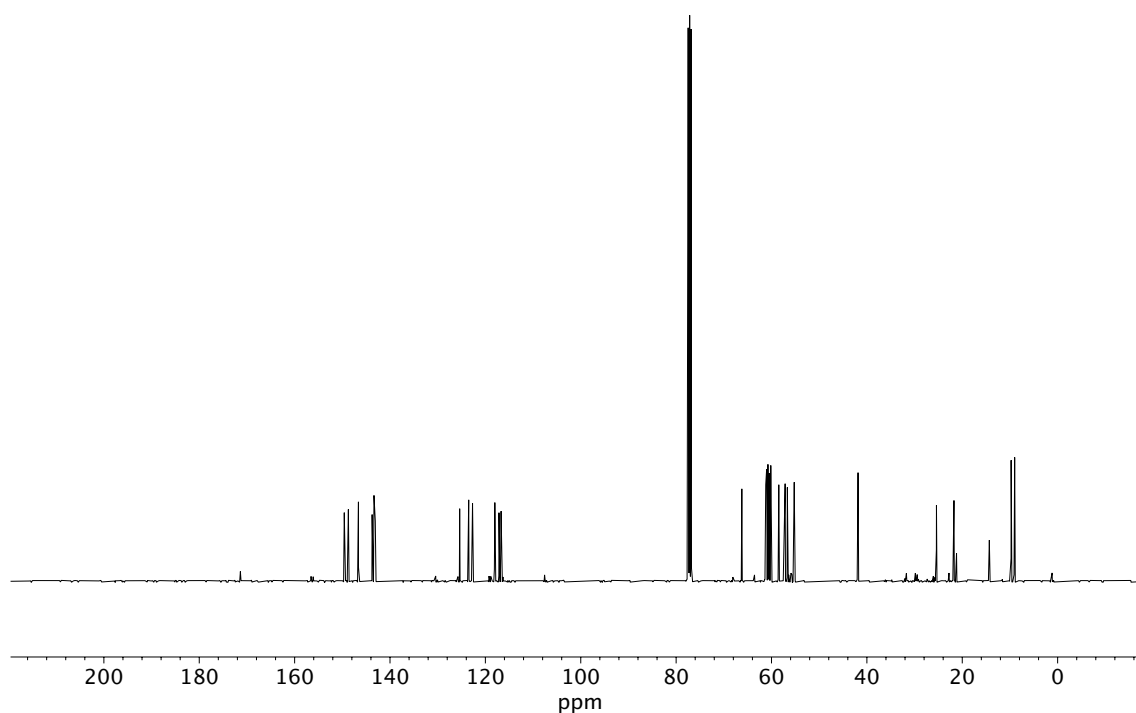


Figure A6.57 ¹³C NMR (100 MHz, CDCl₃) of compound **105**.

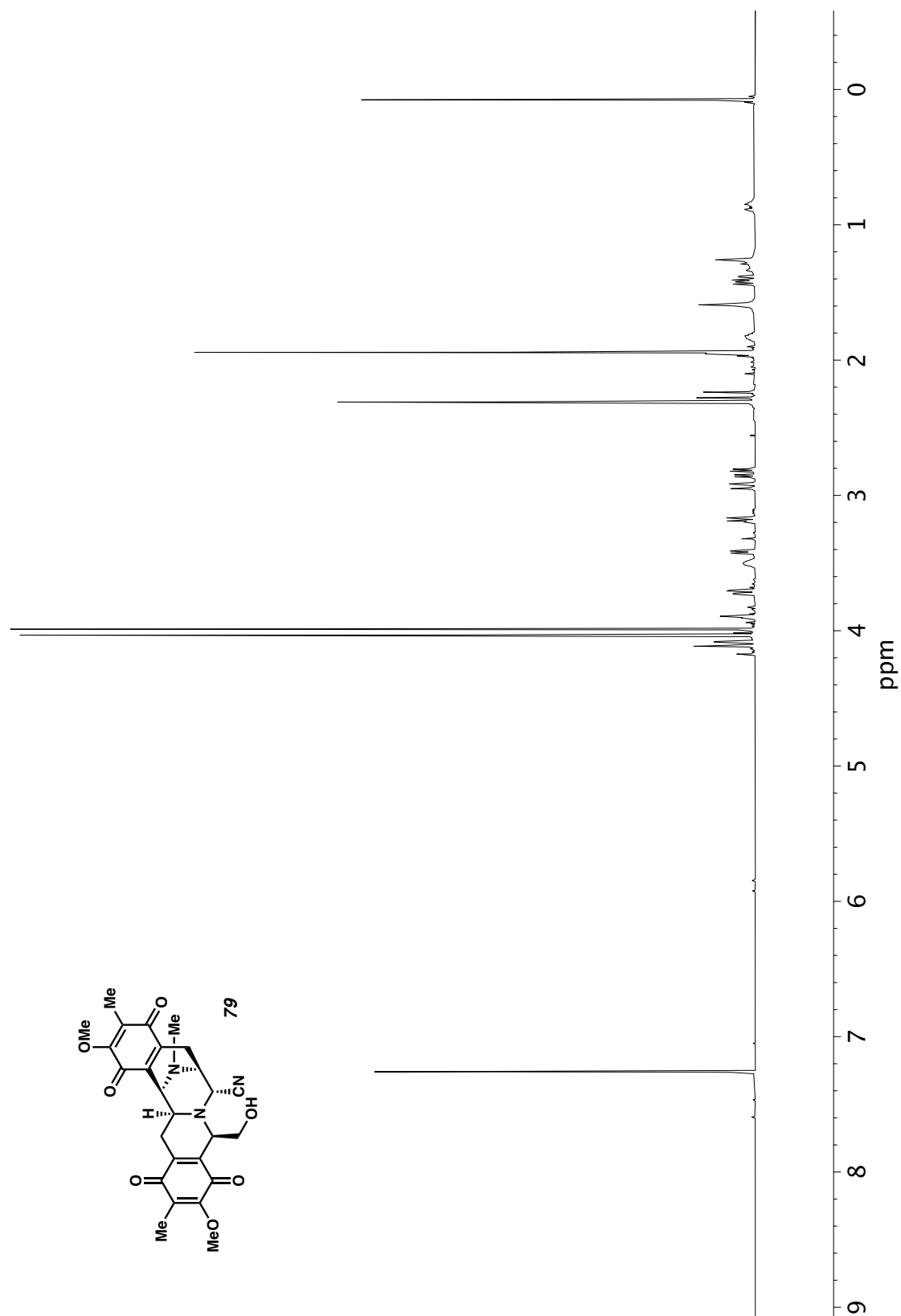


Figure A6.58 ^1H NMR (500 MHz, CDCl_3) of compound 79.

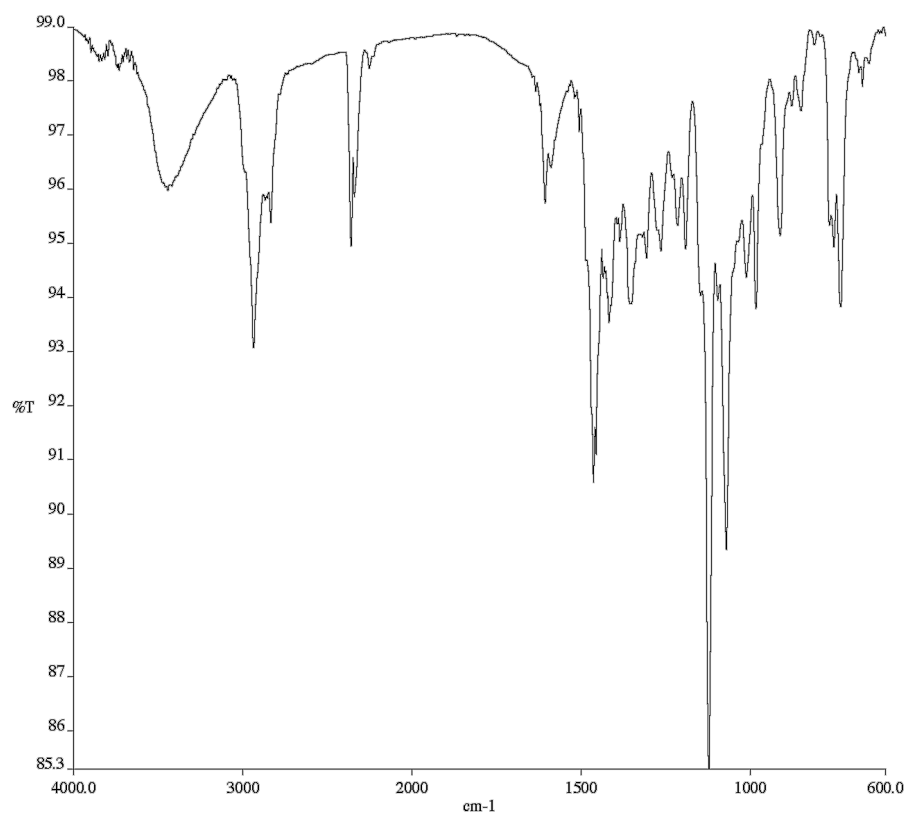


Figure A6.59 Infrared spectrum (Thin Film, NaCl) of compound **79**.

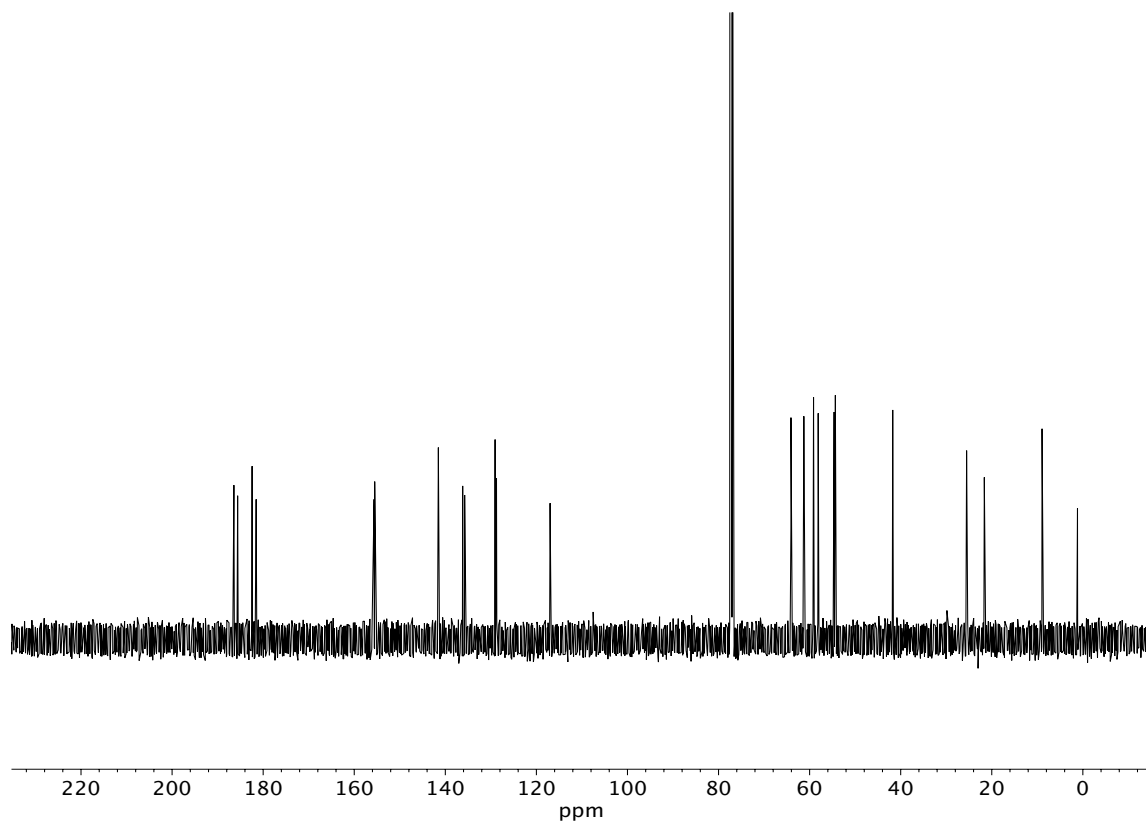


Figure A6.60 ¹³C NMR (125 MHz, CDCl₃) of compound **79**.

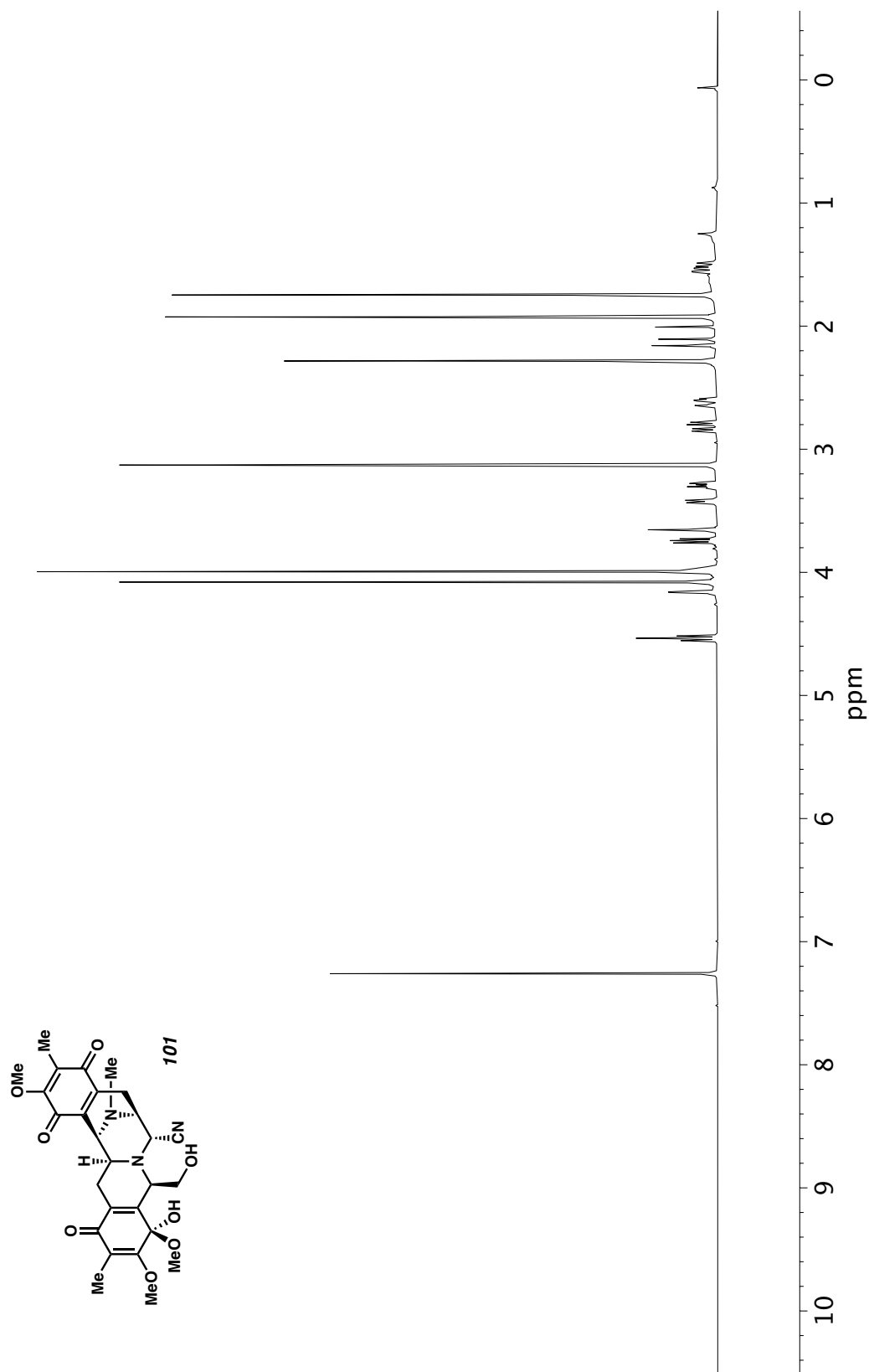


Figure A6.61 ^1H NMR (400 MHz, CDCl_3) of compound **101**.

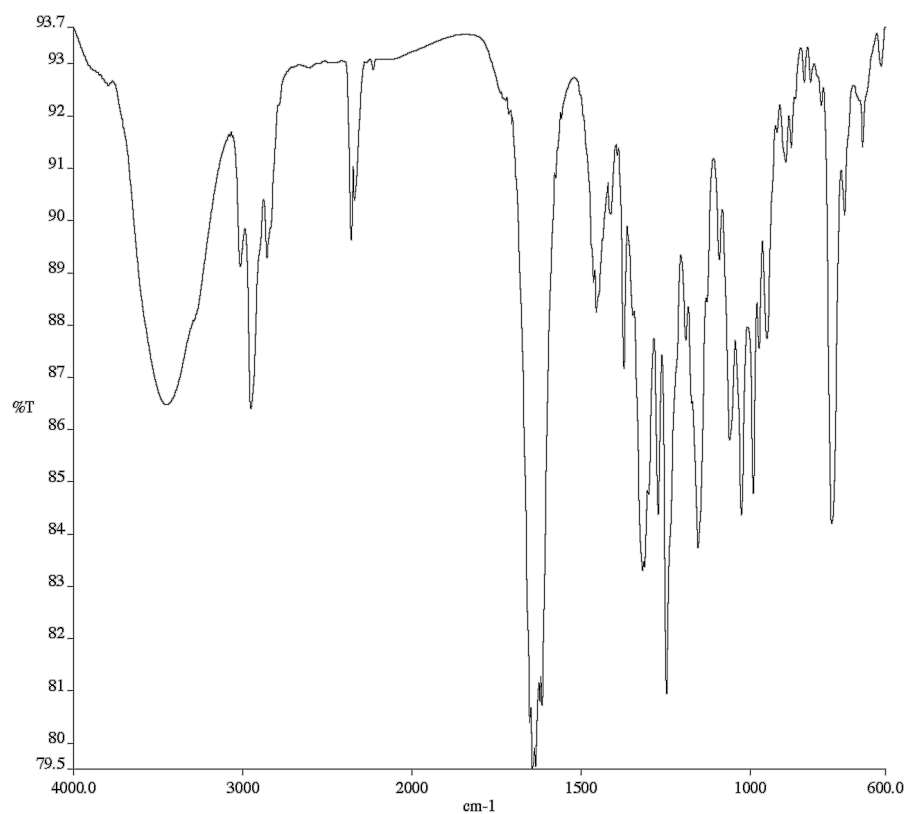


Figure A6.62 Infrared spectrum (Thin Film, NaCl) of compound **101**.

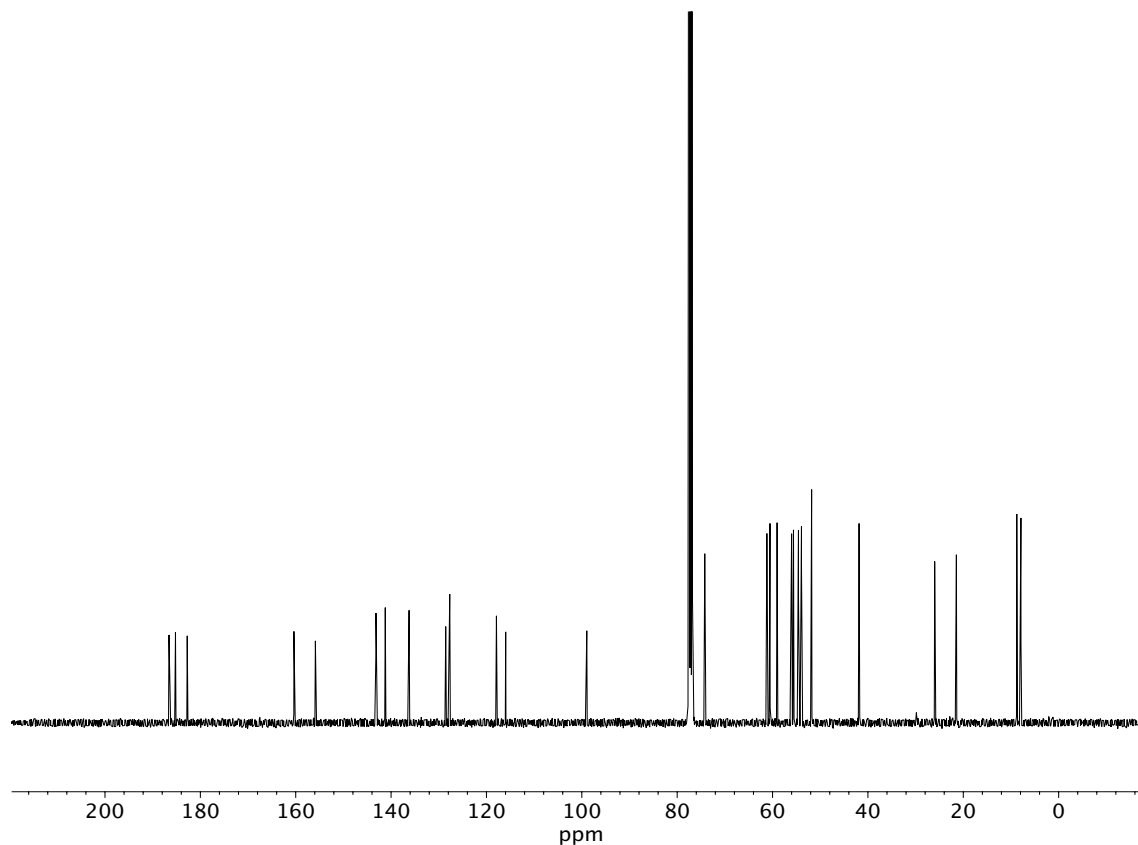


Figure A6.63 ¹³C NMR (100 MHz, CDCl₃) of compound **101**.

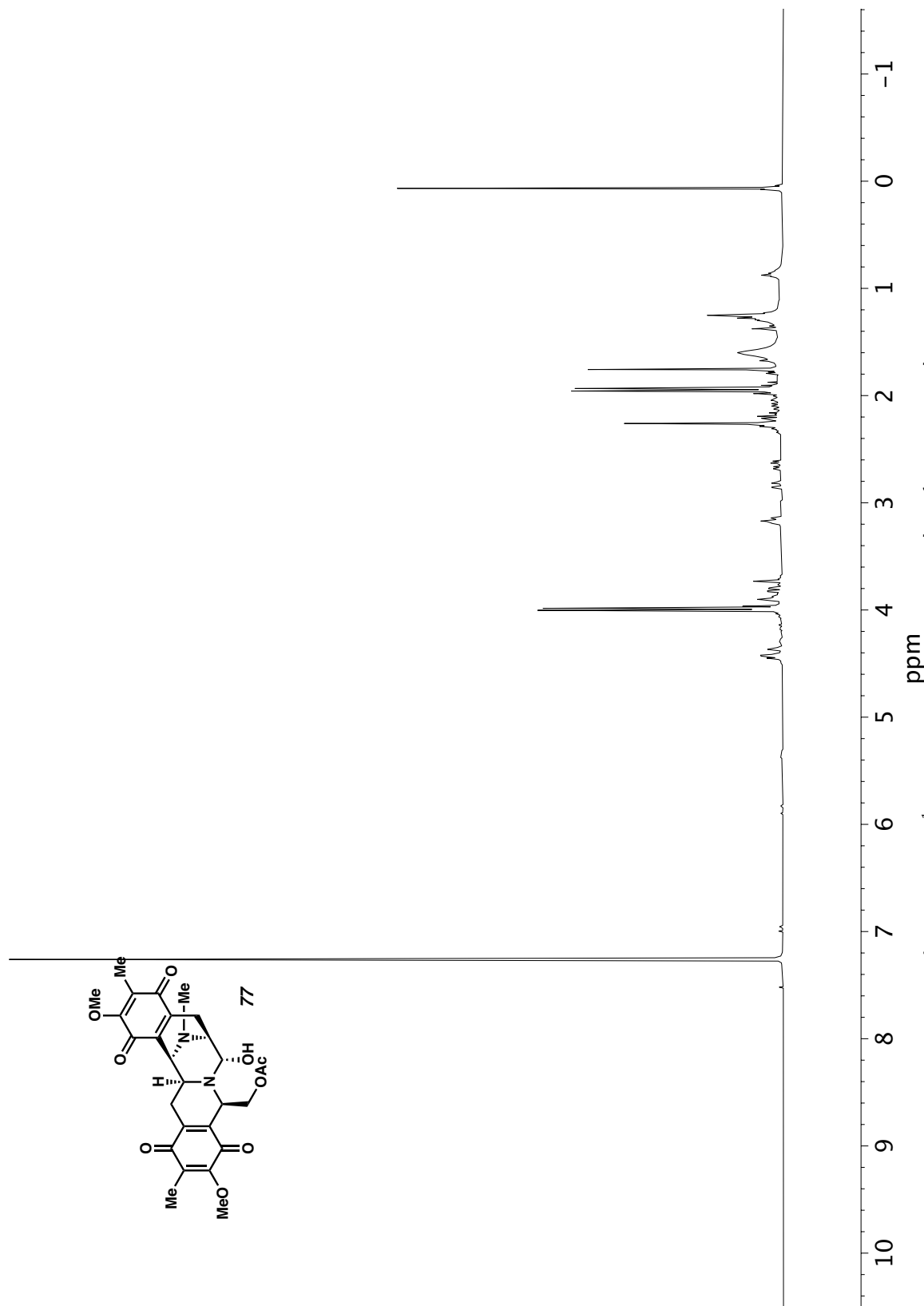


Figure A6.64 ^1H NMR (400 MHz, CDCl_3) of compound 77.

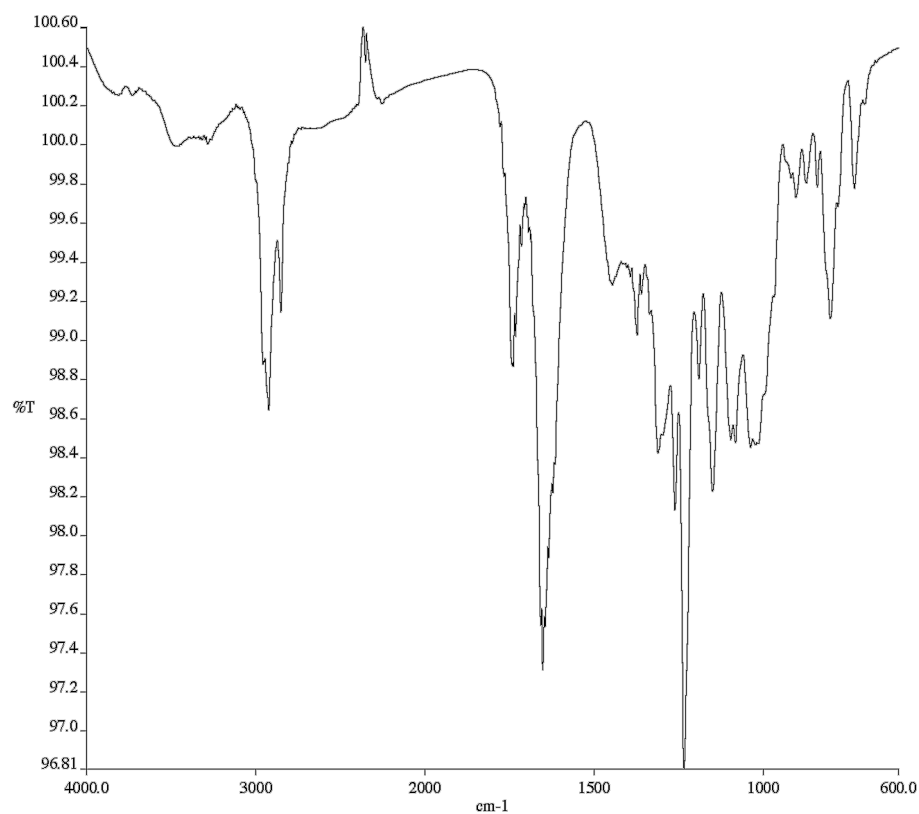


Figure A6.65 Infrared spectrum (Thin Film, NaCl) of compound 77.

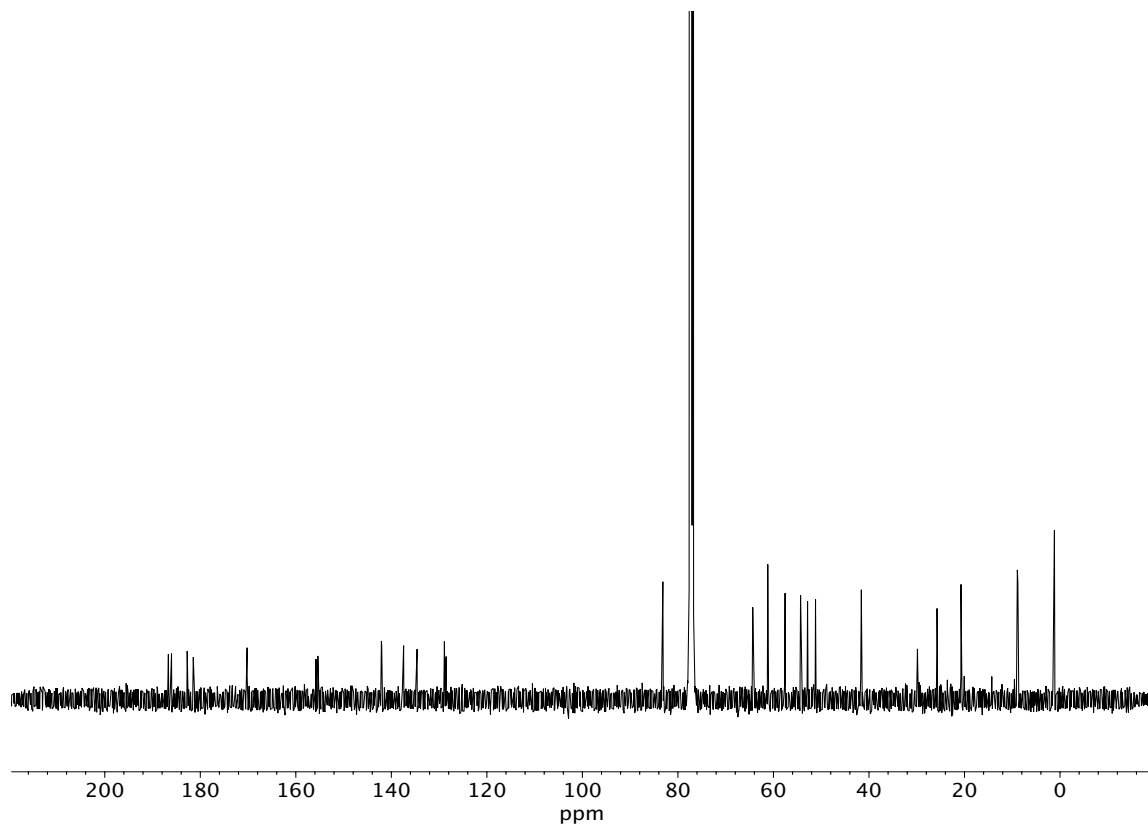


Figure A6.66 ¹³C NMR (100 MHz, CDCl₃) of compound 77.

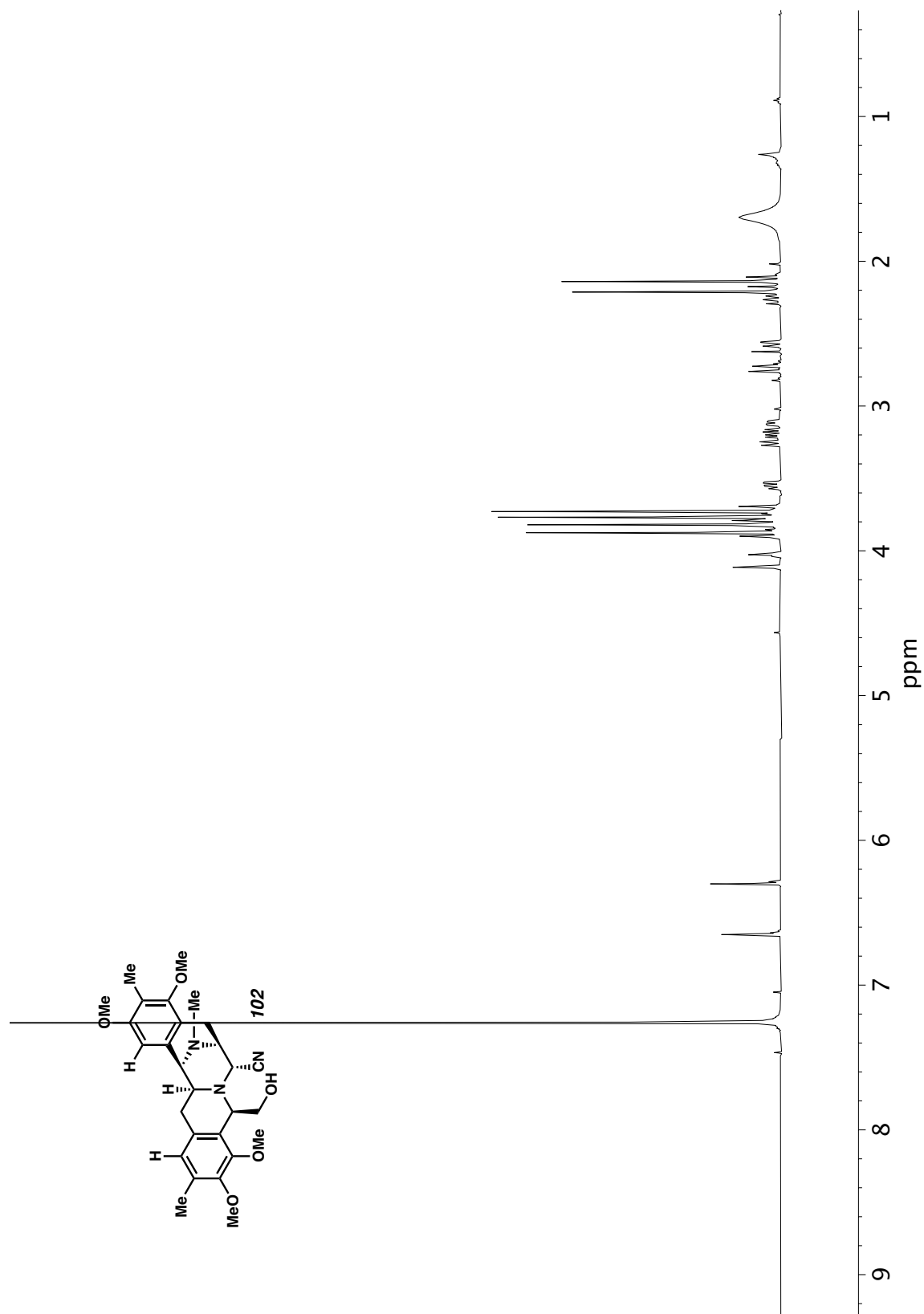


Figure A6.67 ^1H NMR (400 MHz, CDCl_3) of compound **102**.

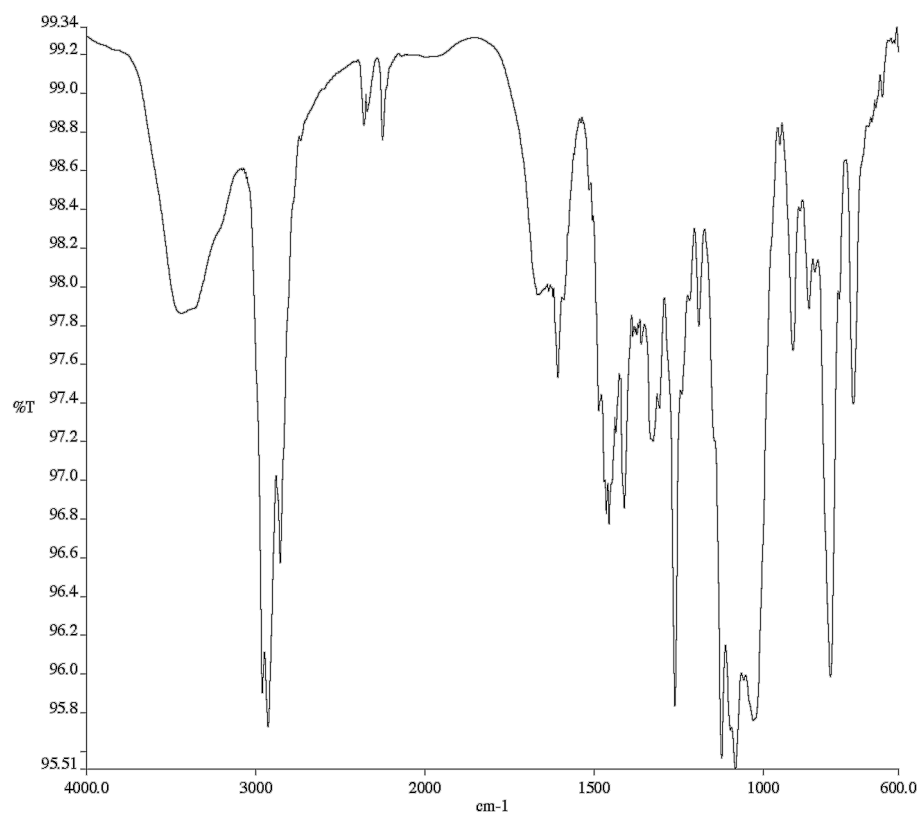


Figure A6.68 Infrared spectrum (Thin Film, NaCl) of compound **102**.

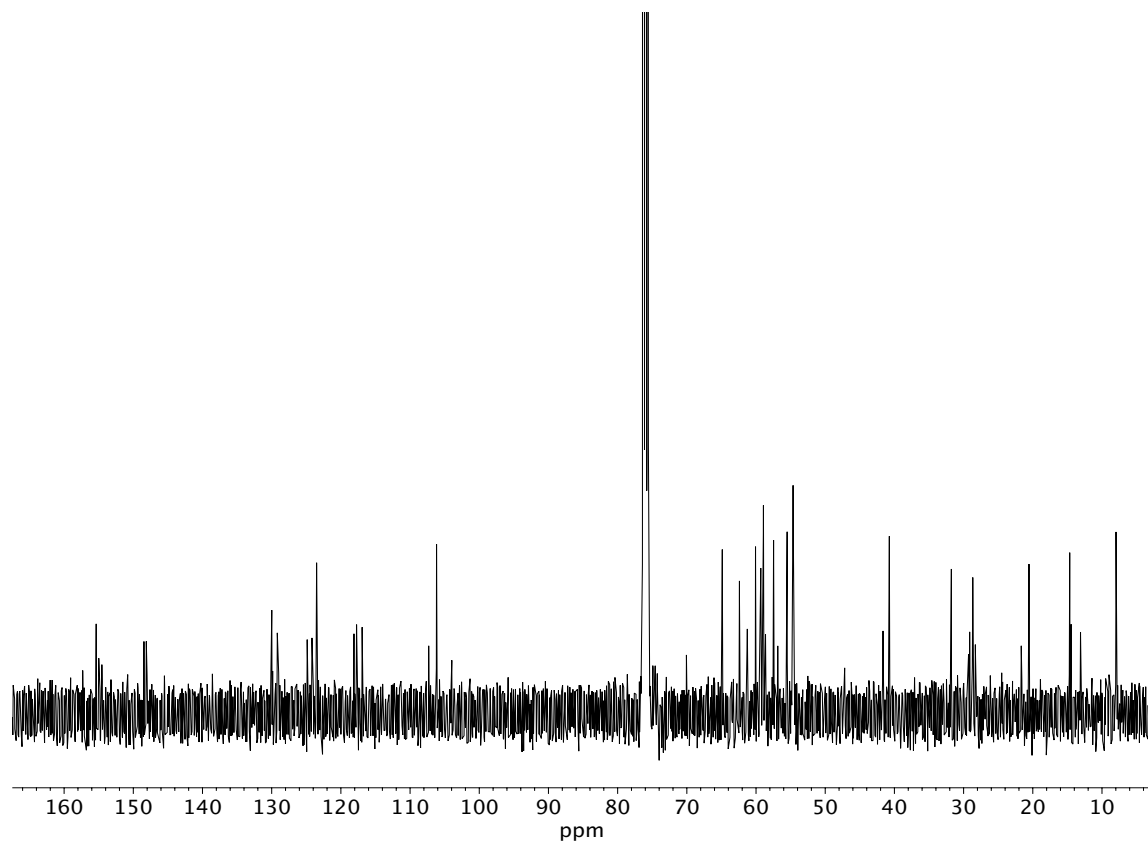


Figure A6.69 ¹³C NMR (100 MHz, CDCl₃) of compound **102**.

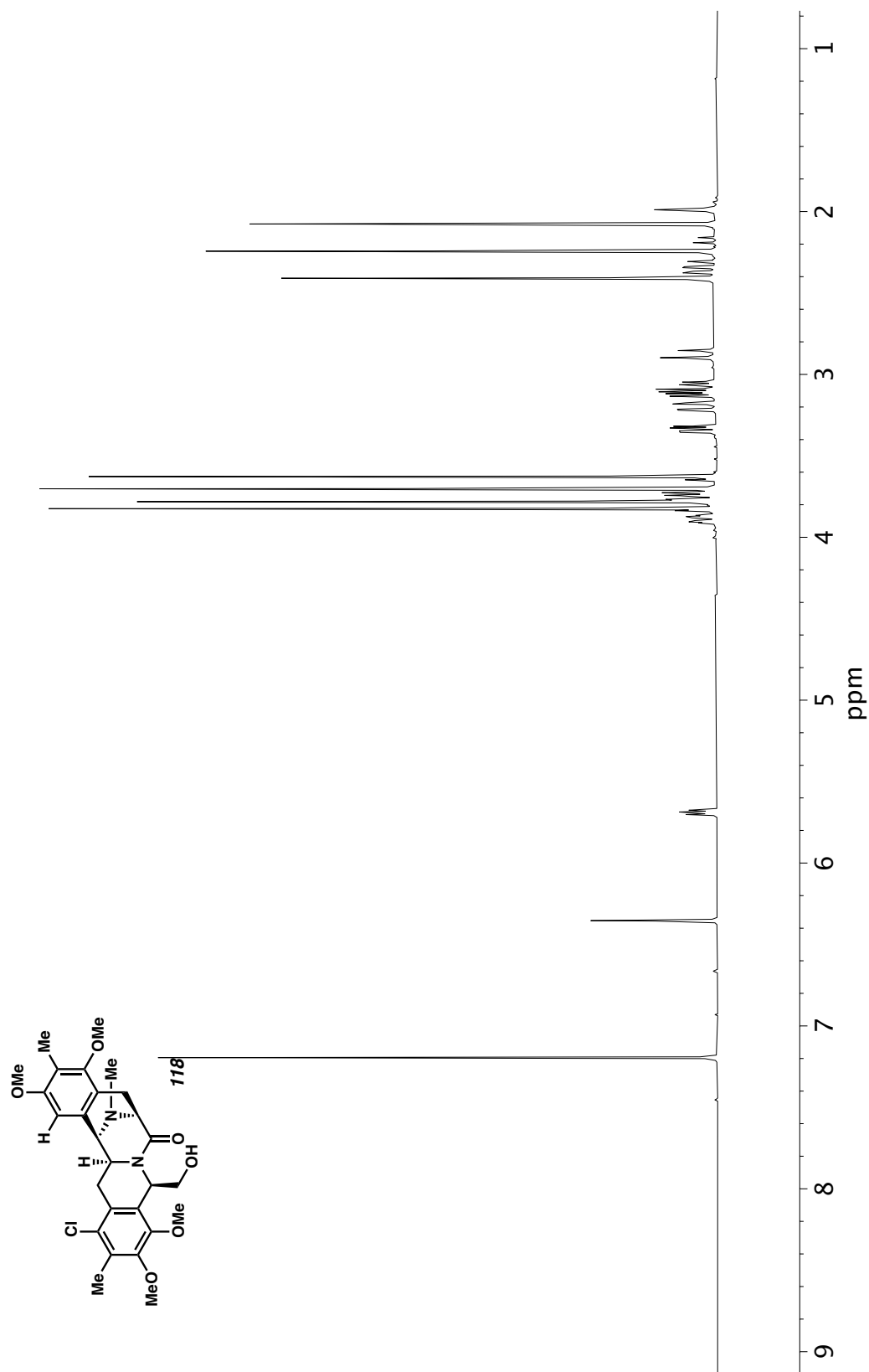


Figure A6.70 ^1H NMR (400 MHz, CDCl_3) of compound **118**.

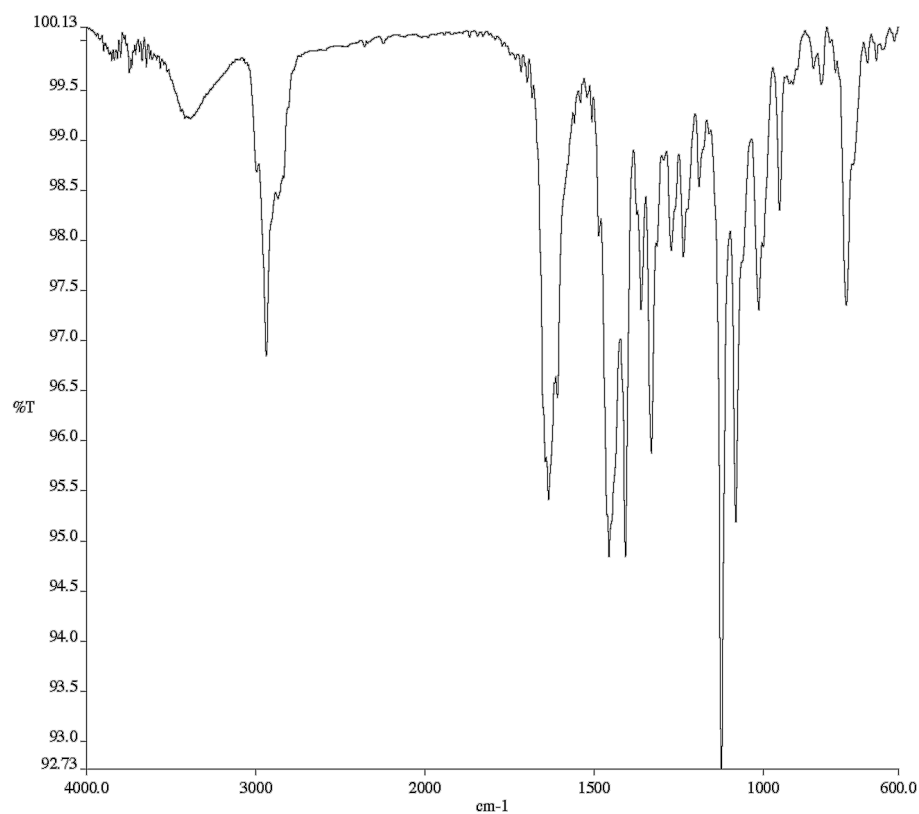


Figure A6.71 Infrared spectrum (Thin Film, NaCl) of compound **118**.

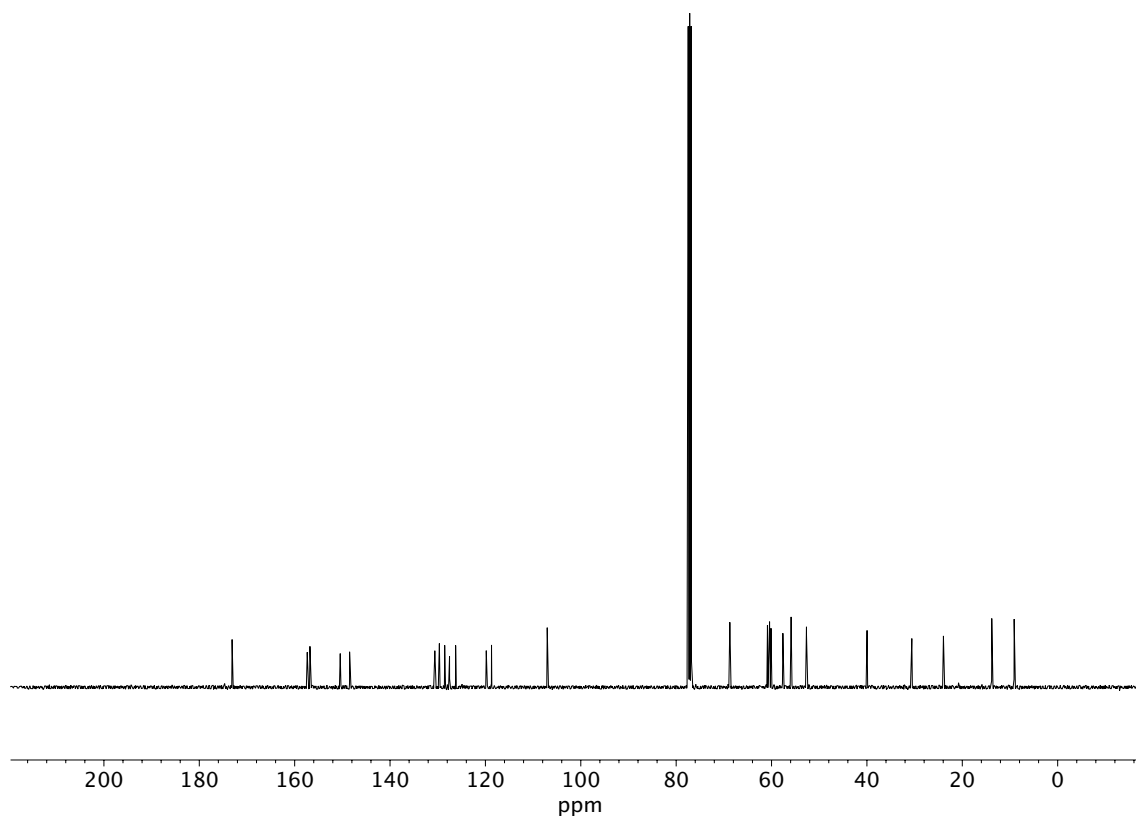


Figure A6.72 ¹³C NMR (100 MHz, CDCl₃) of compound **118**.

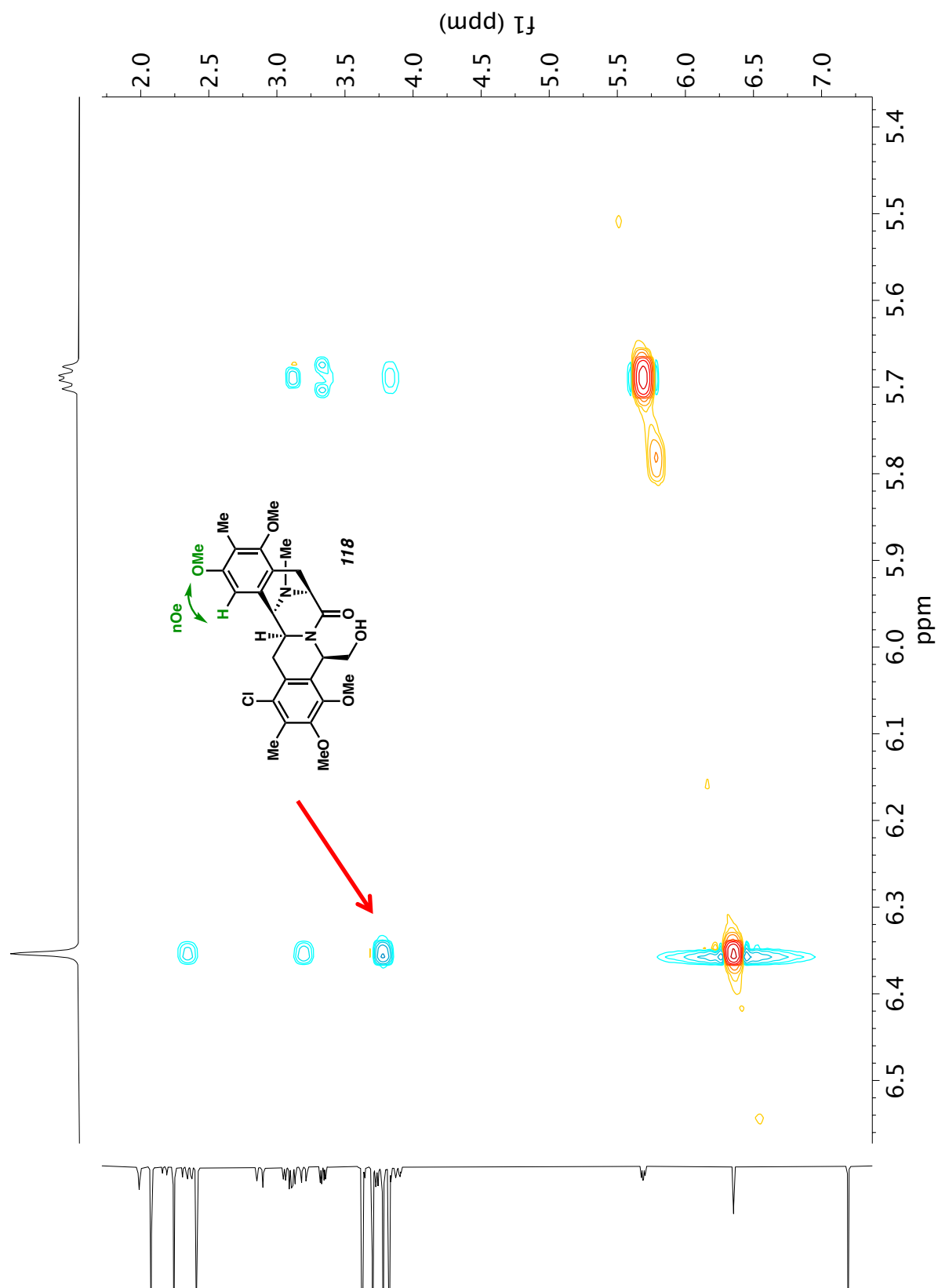


Figure A6.73 2D NOESY NMR of compound **118**.

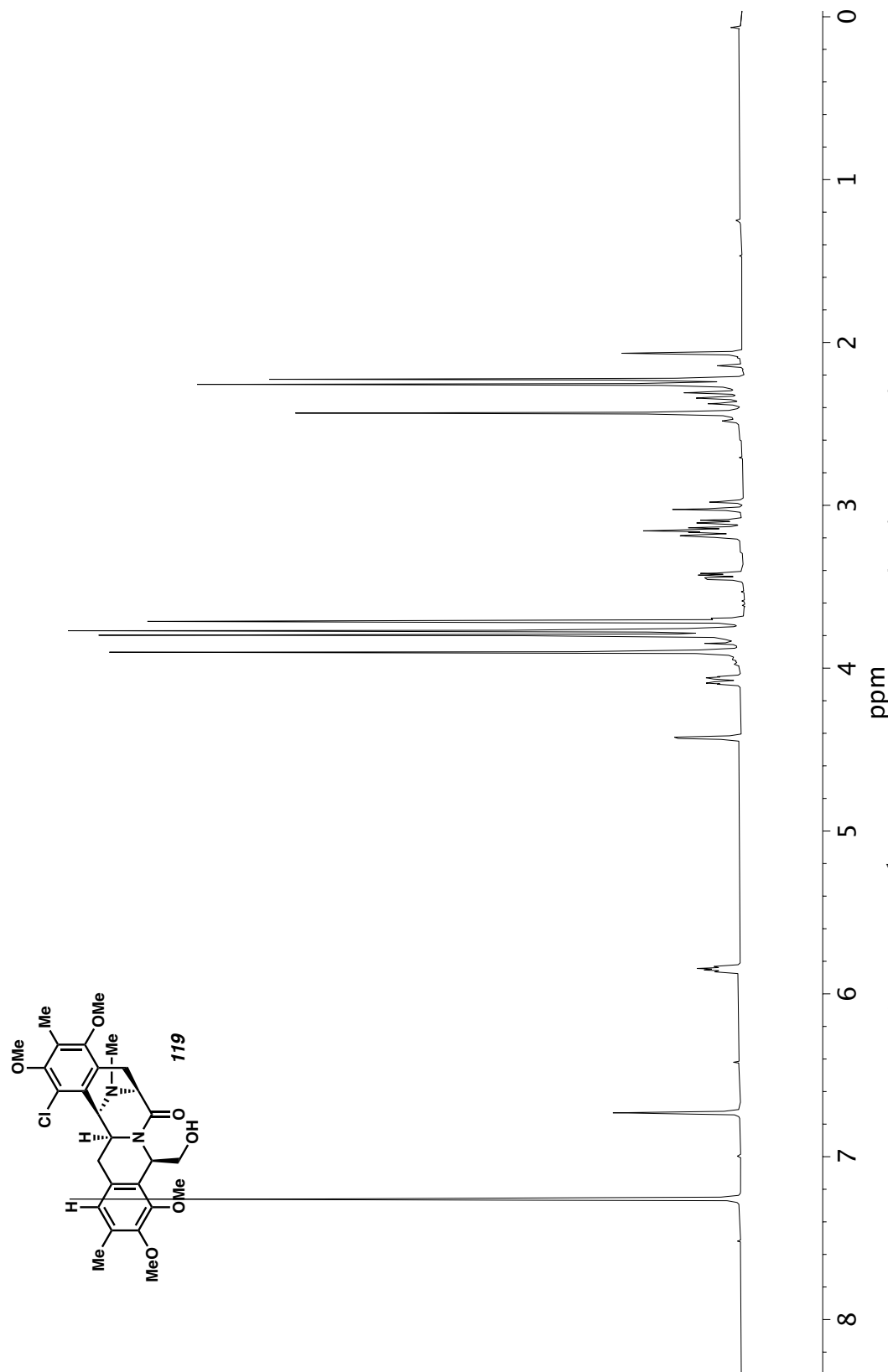


Figure A6.74 ^1H NMR (400 MHz, CDCl_3) of compound **119**.

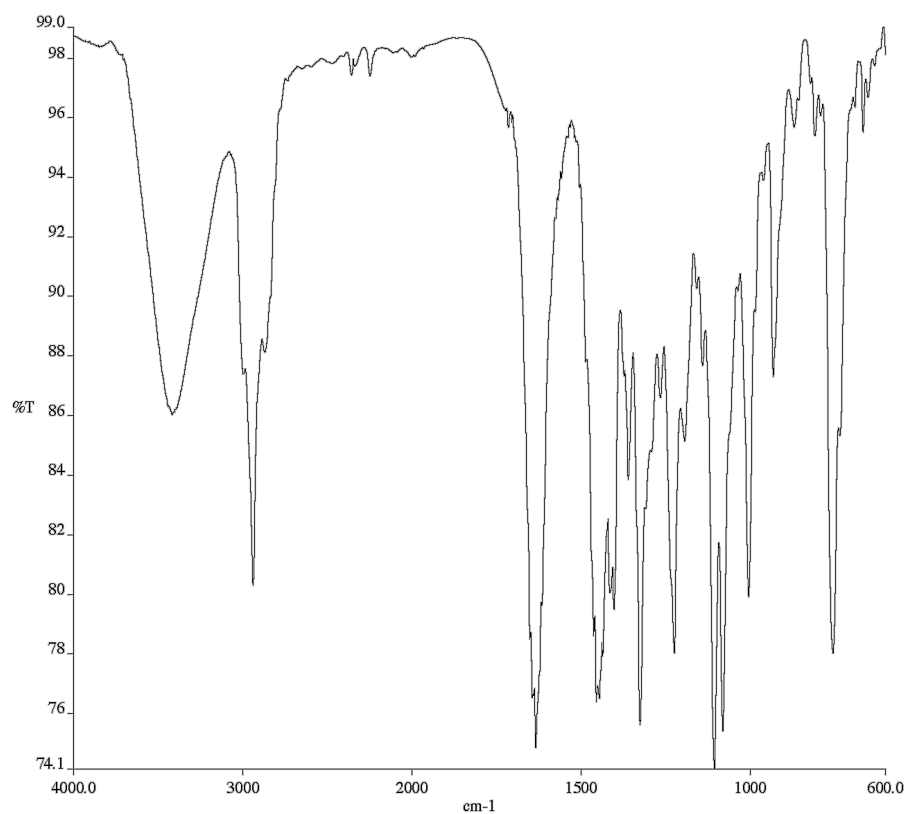


Figure A6.75 Infrared spectrum (Thin Film, NaCl) of compound **119**.

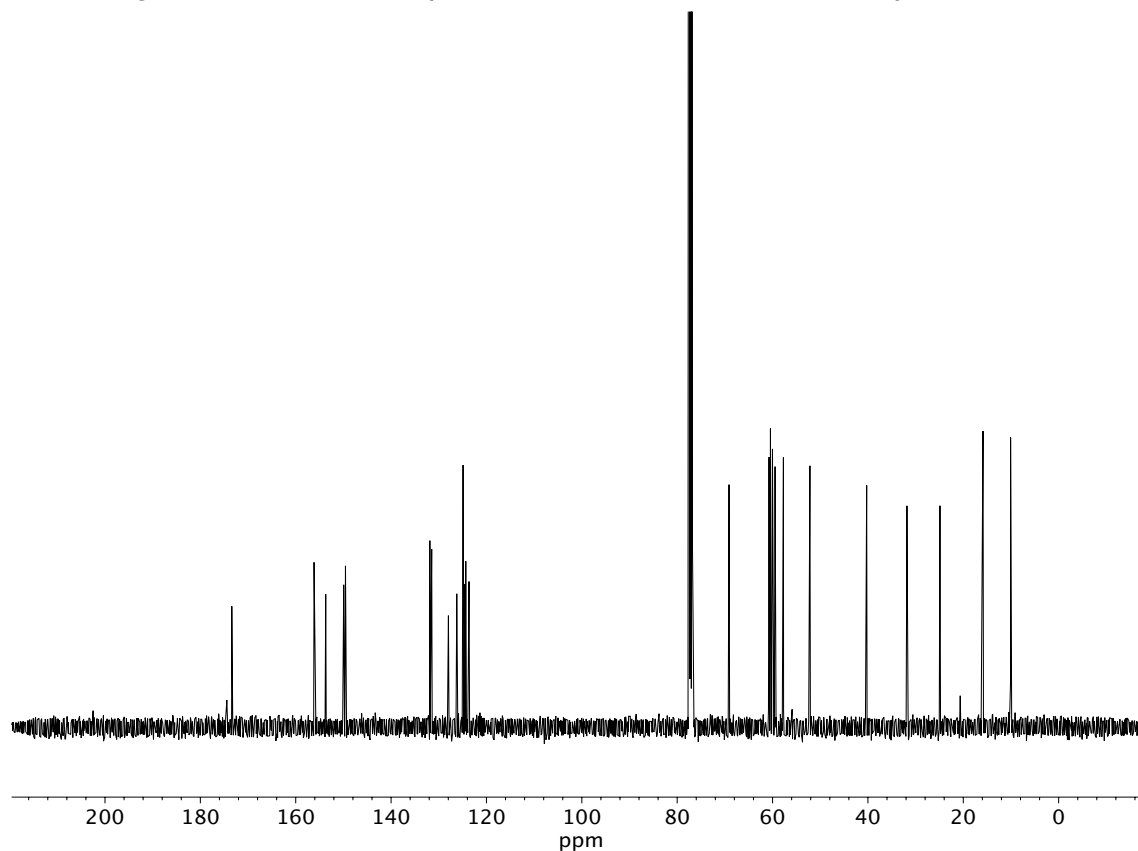


Figure A6.76 ¹³C NMR (100 MHz, CDCl₃) of compound **119**.

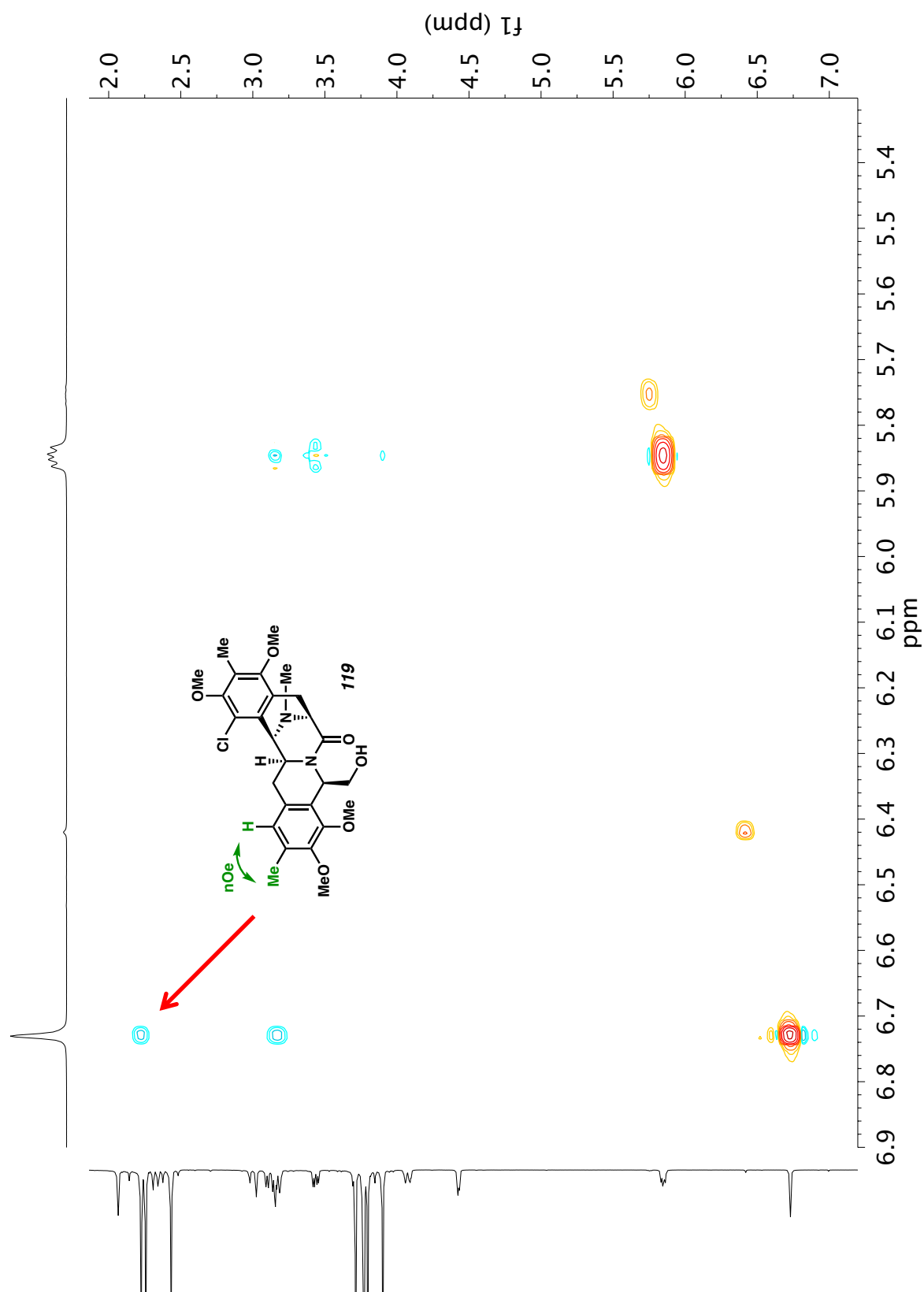


Figure A6.77 2D NOESY NMR of compound **119**.

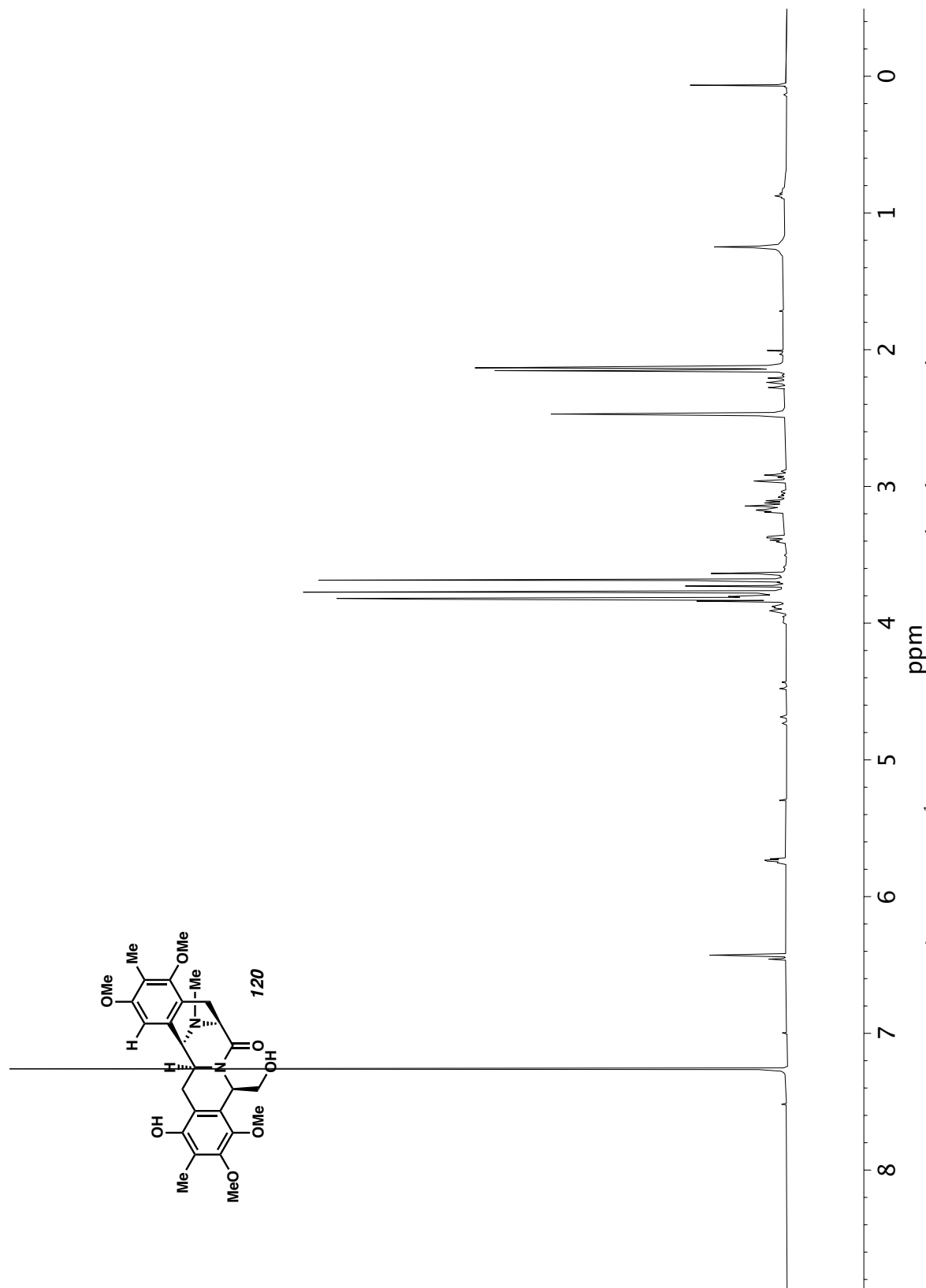


Figure A6.78 ^1H NMR (500 MHz, CDCl_3) of compound **120**.

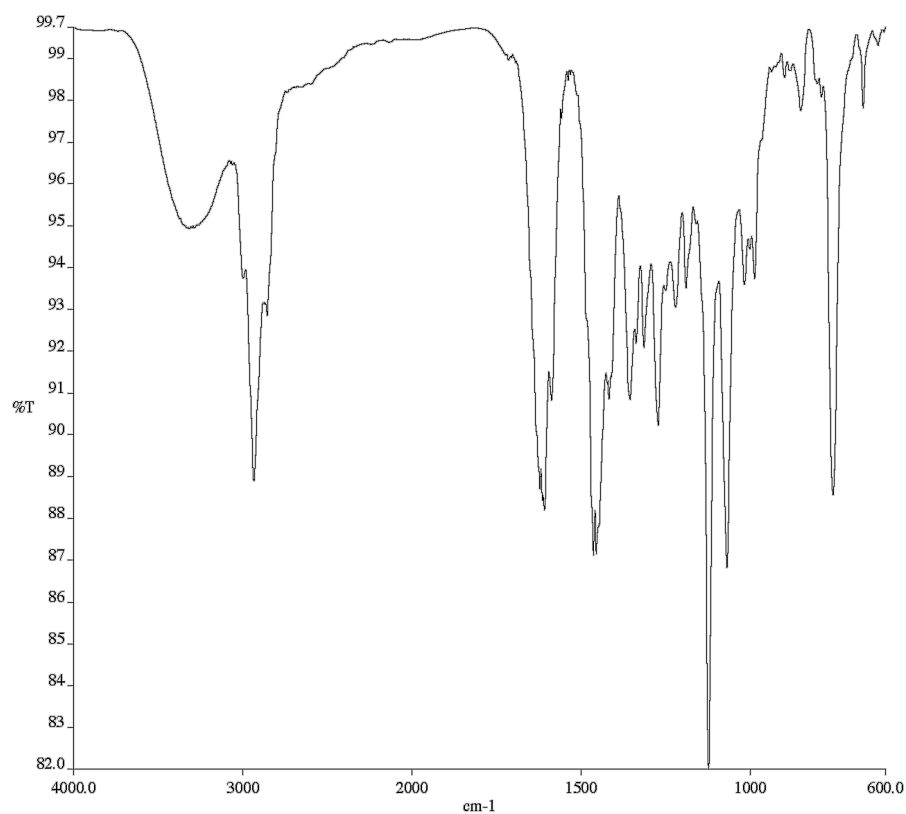


Figure A6.79 Infrared spectrum (Thin Film, NaCl) of compound **120**.

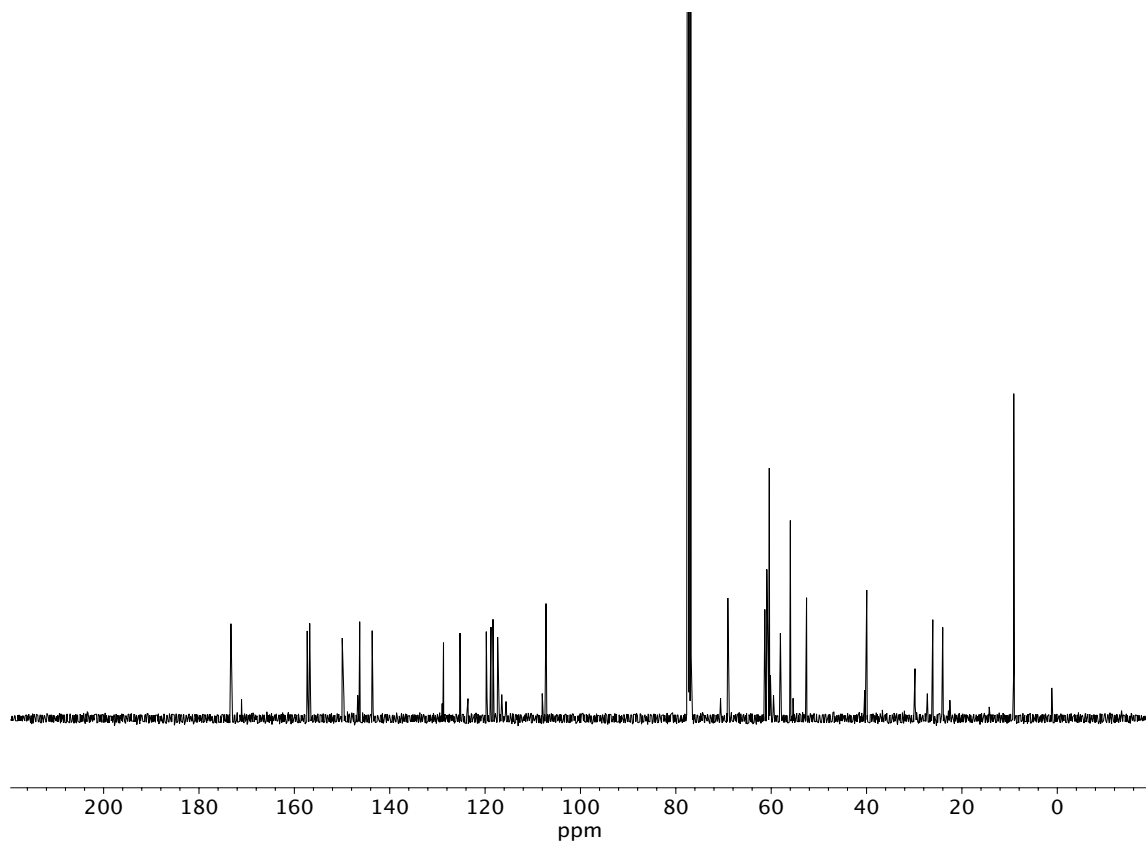


Figure A6.80 ¹³C NMR (100 MHz, CDCl₃) of compound **120**.

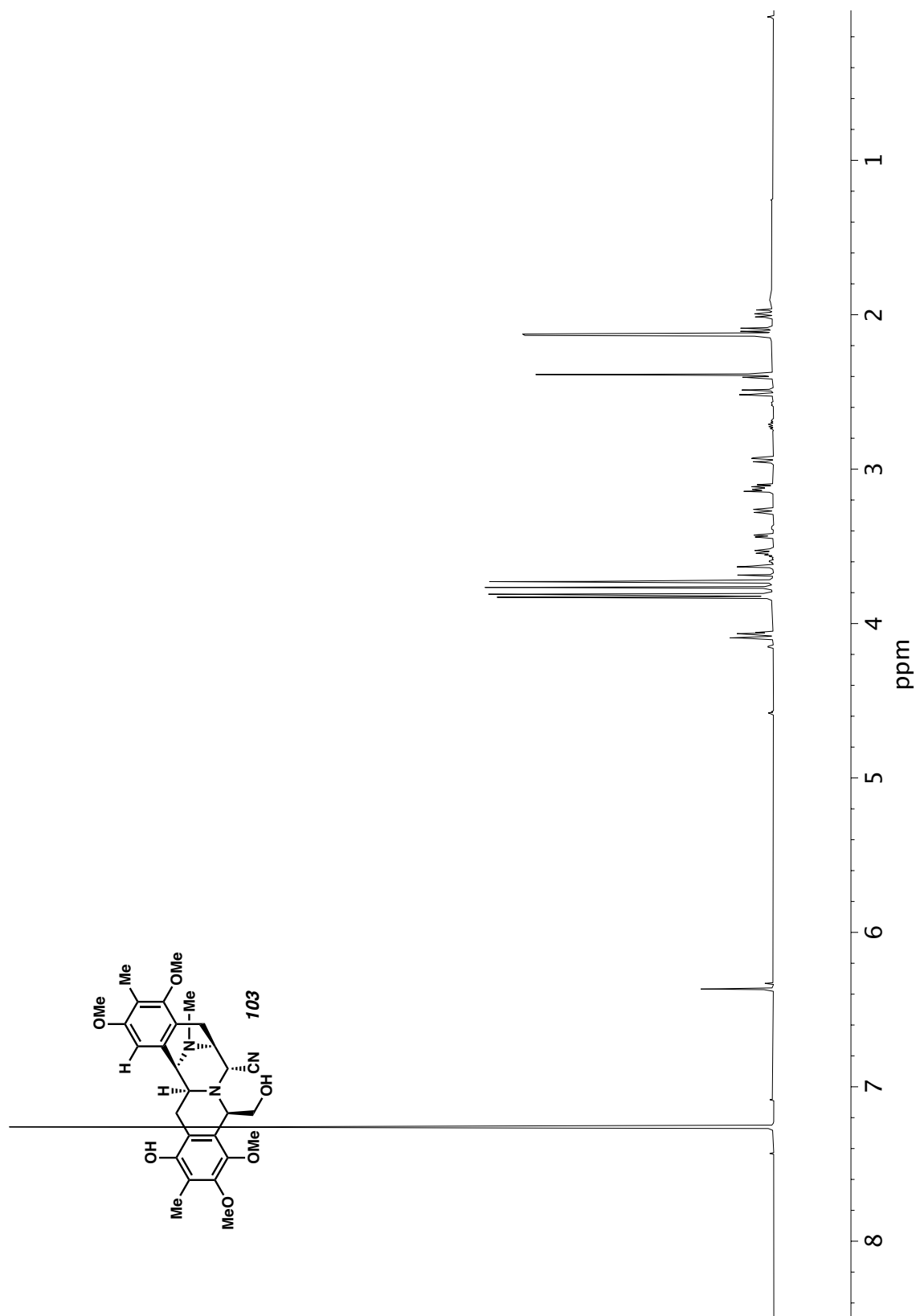


Figure A6.81 ^1H NMR (600 MHz, CDCl_3) of compound **103**.

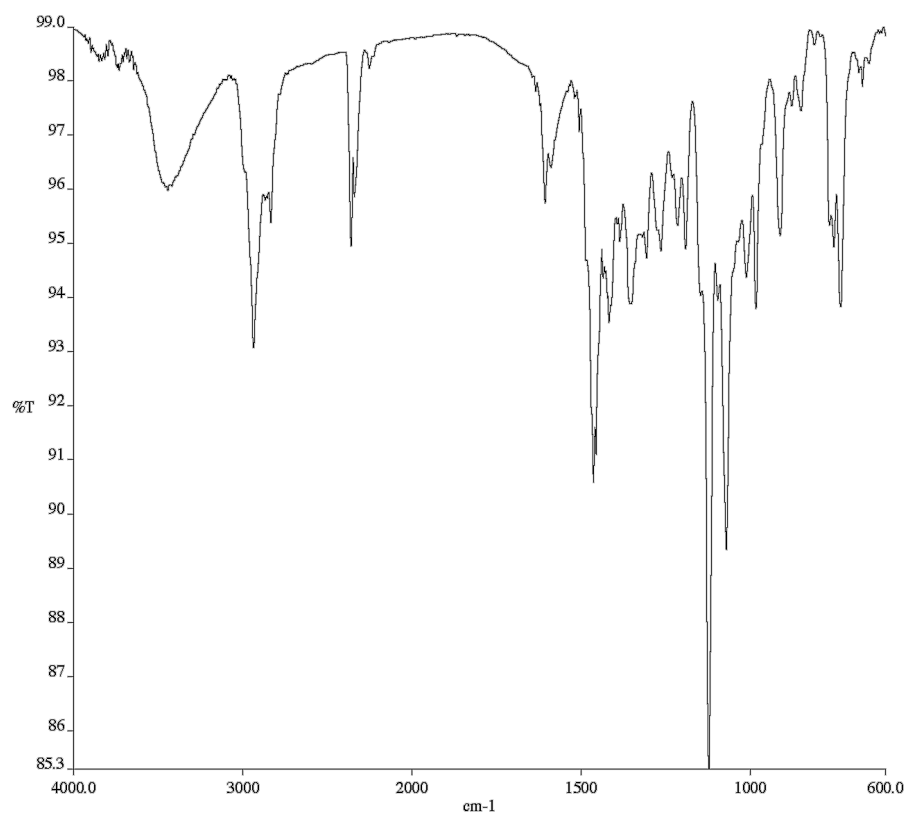


Figure A6.82 Infrared spectrum (Thin Film, NaCl) of compound **103**.

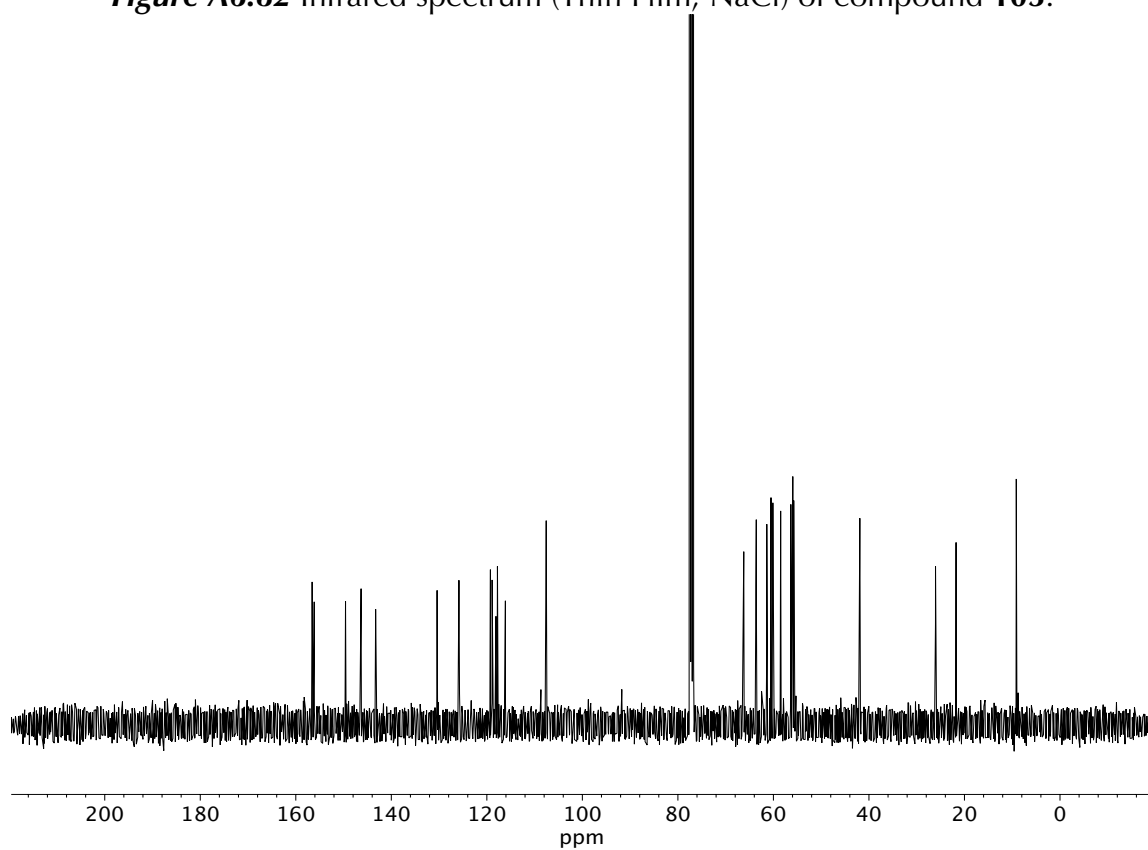


Figure A6.83 ¹³C NMR (100 MHz, CDCl₃) of compound **103**.

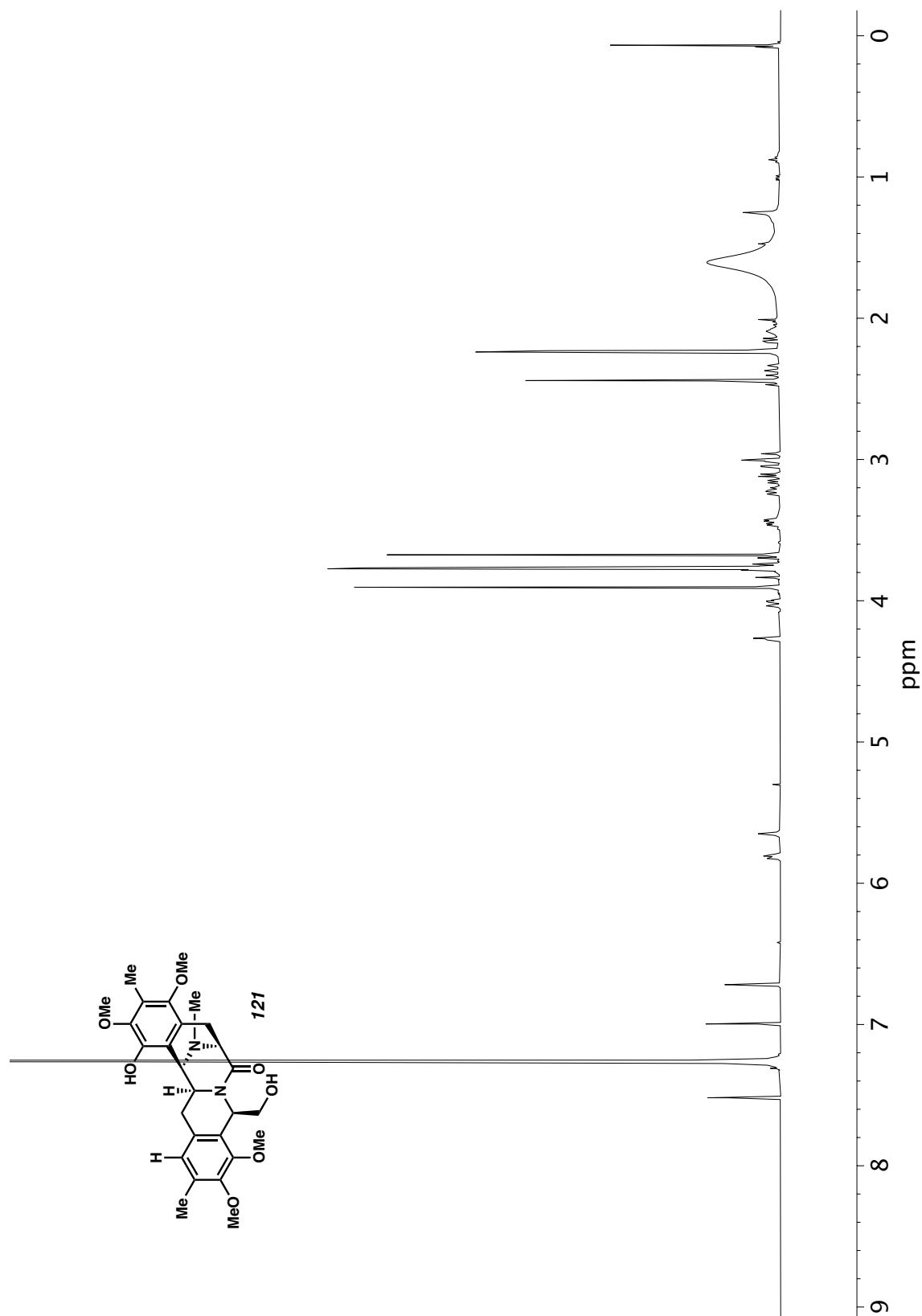


Figure A6.84 ^1H NMR (400 MHz, CDCl_3) of compound **121**.

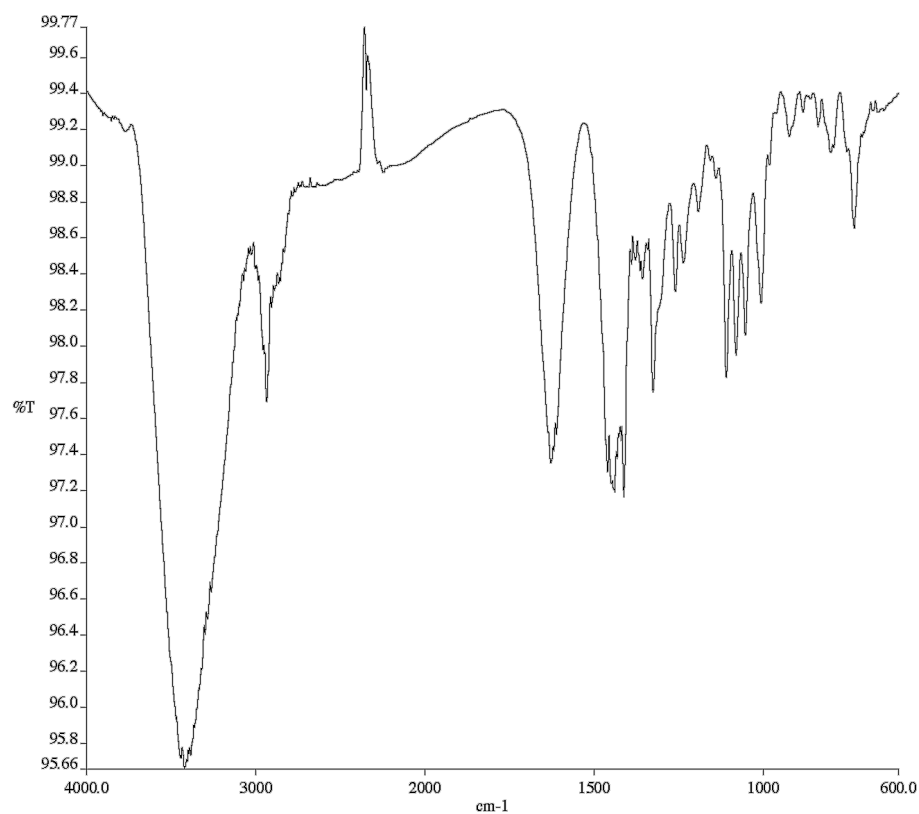


Figure A6.85 Infrared spectrum (Thin Film, NaCl) of compound **121**.

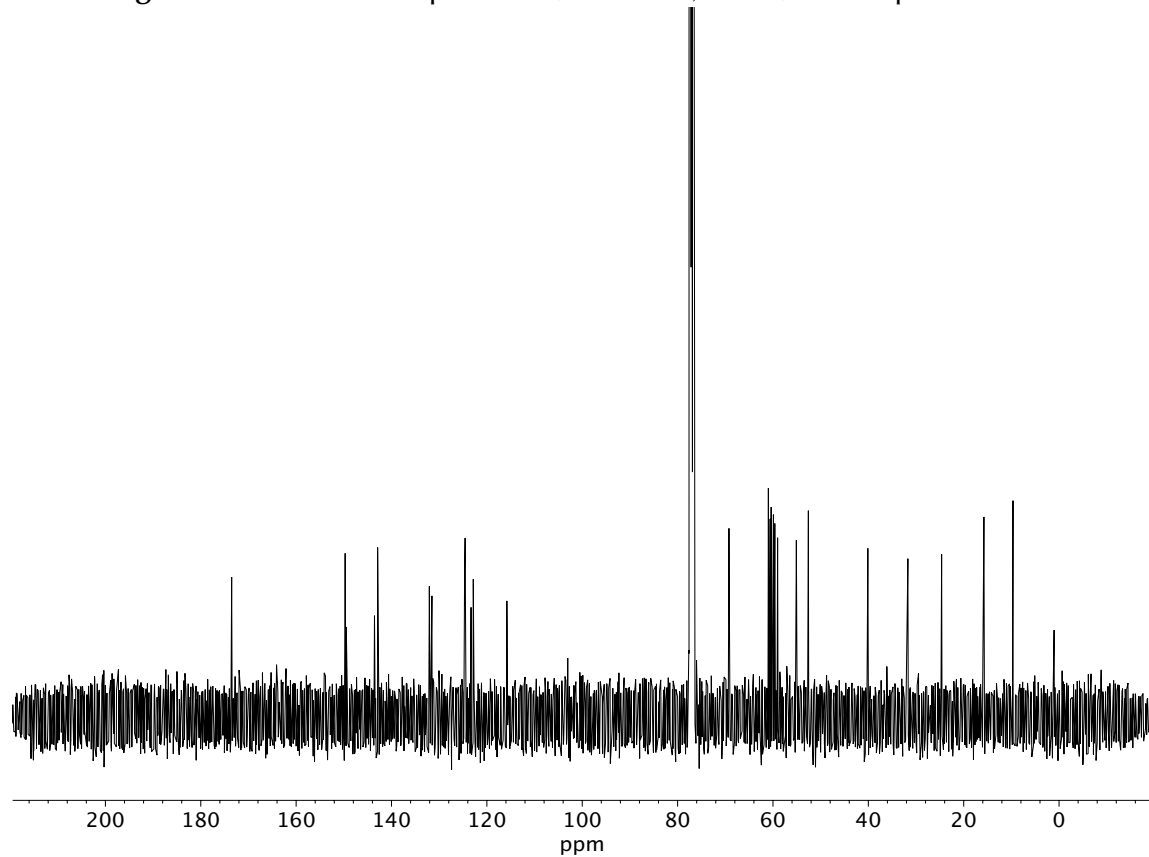


Figure A6.86 ¹³C NMR (100 MHz, CDCl₃) of compound **121**.

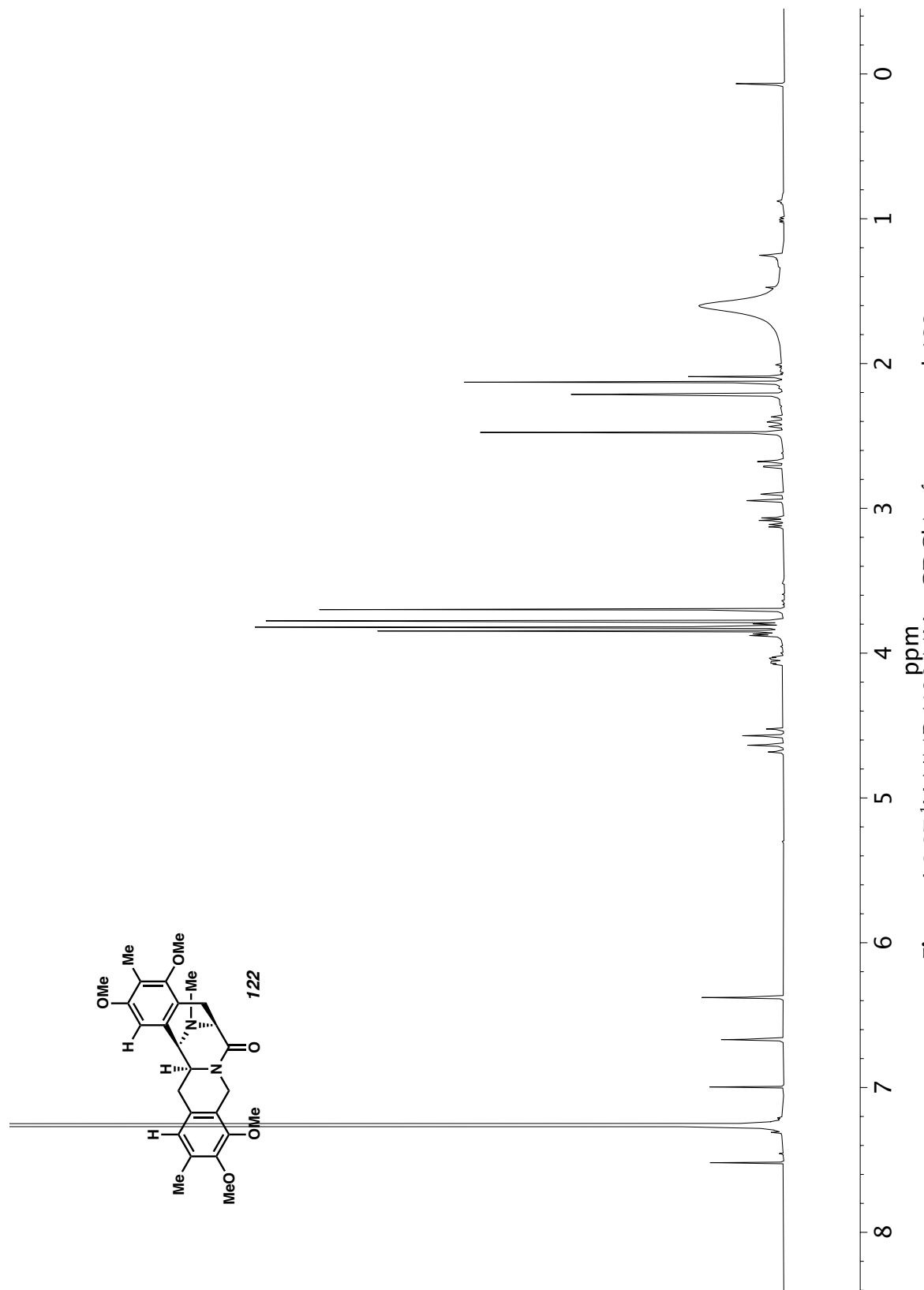


Figure A6.87 ^1H NMR (400 MHz, CDCl_3) of compound **122**.

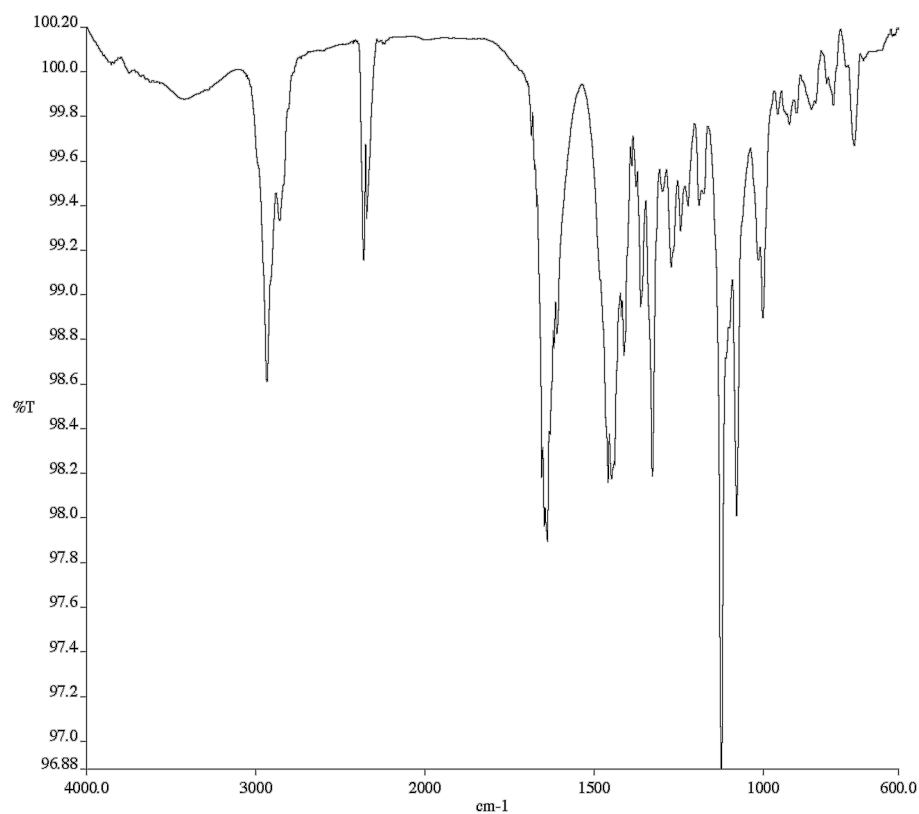


Figure A6.88 Infrared spectrum (Thin Film, NaCl) of compound **122**.

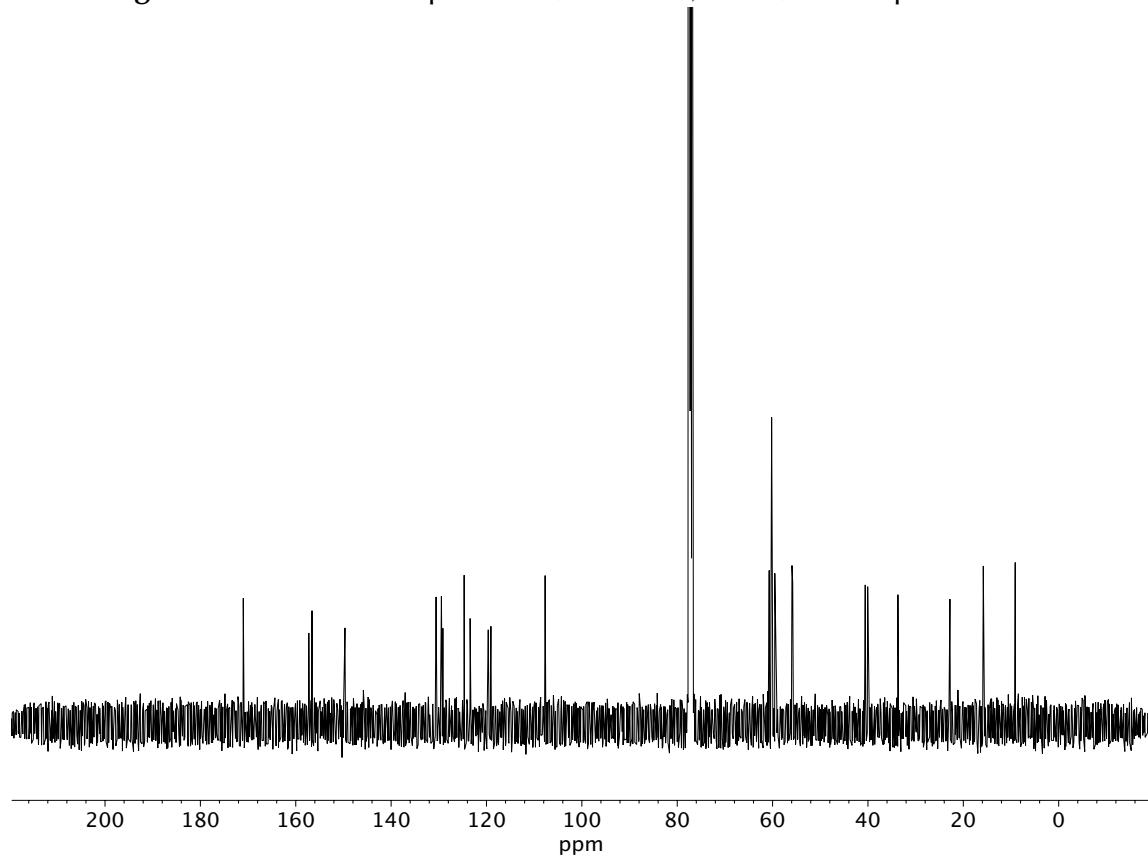


Figure A6.89 ¹³C NMR (100 MHz, CDCl₃) of compound **122**.

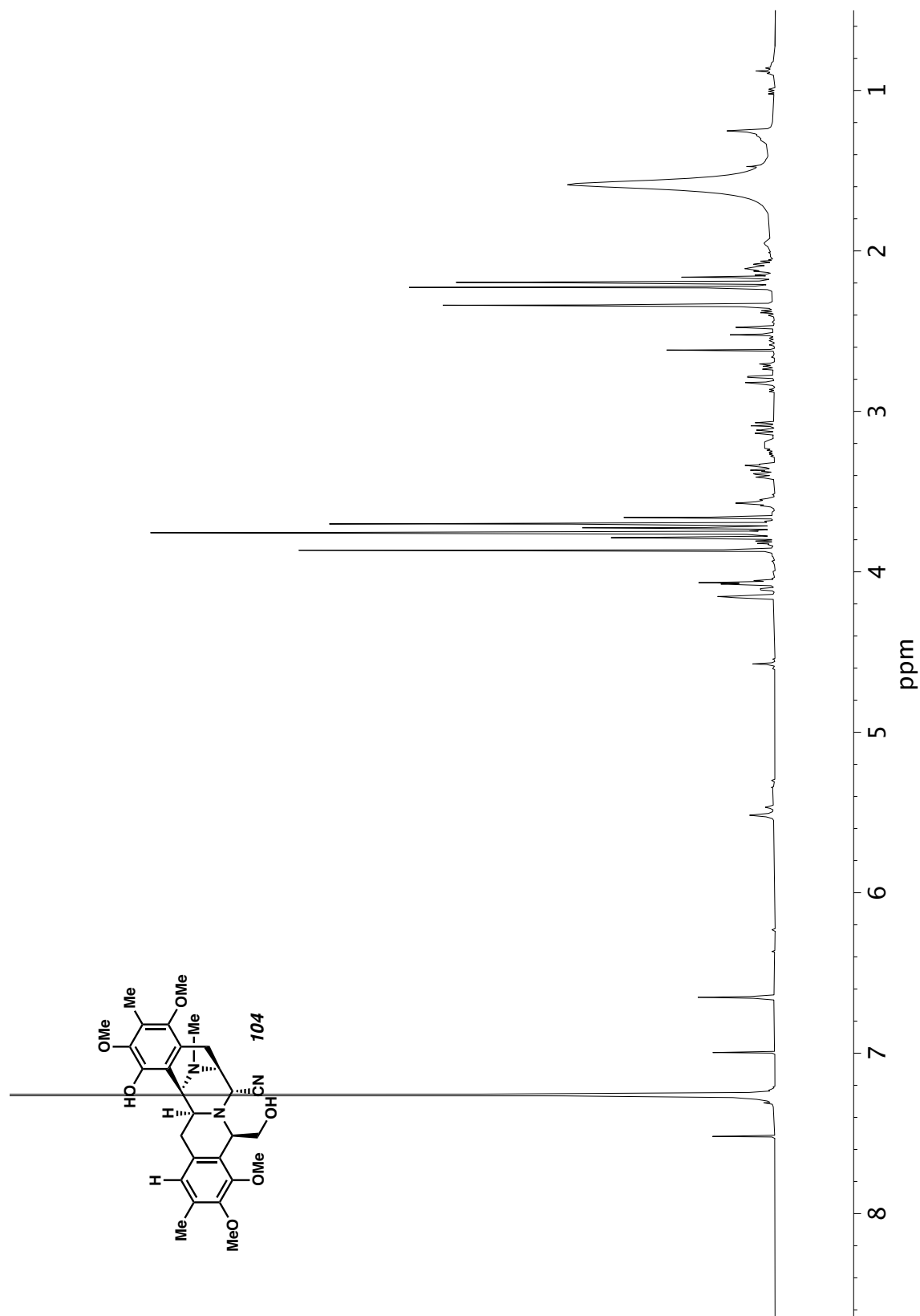


Figure A6.90 ^1H NMR (400 MHz, CDCl_3) of compound **104**.

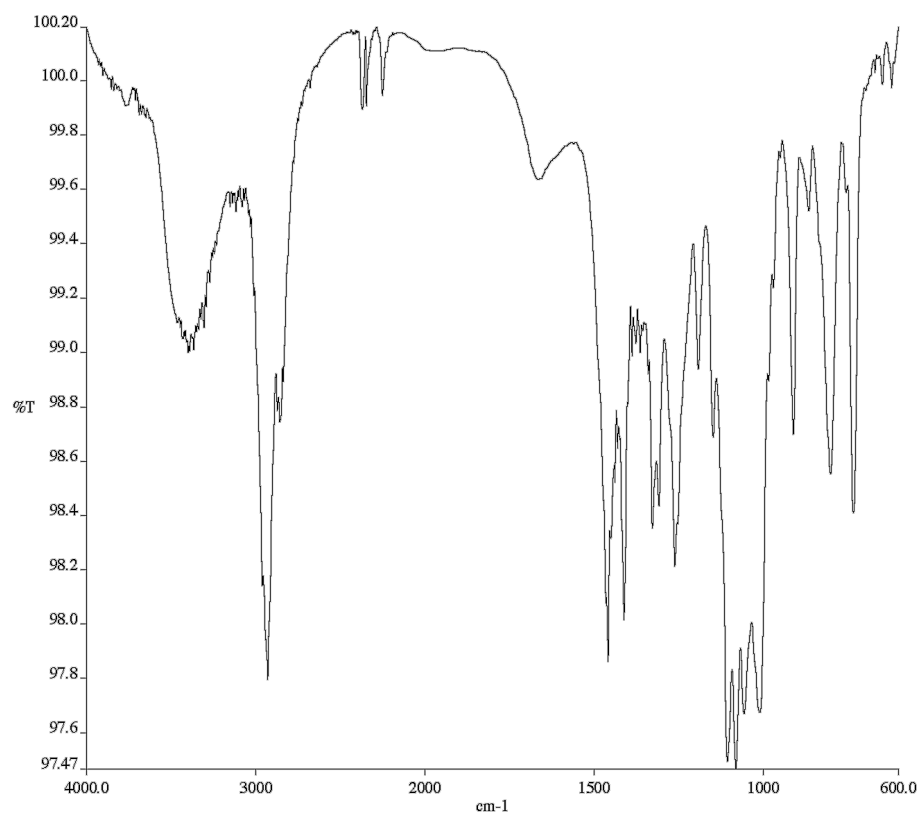


Figure A6.91 Infrared spectrum (Thin Film, NaCl) of compound **104**.

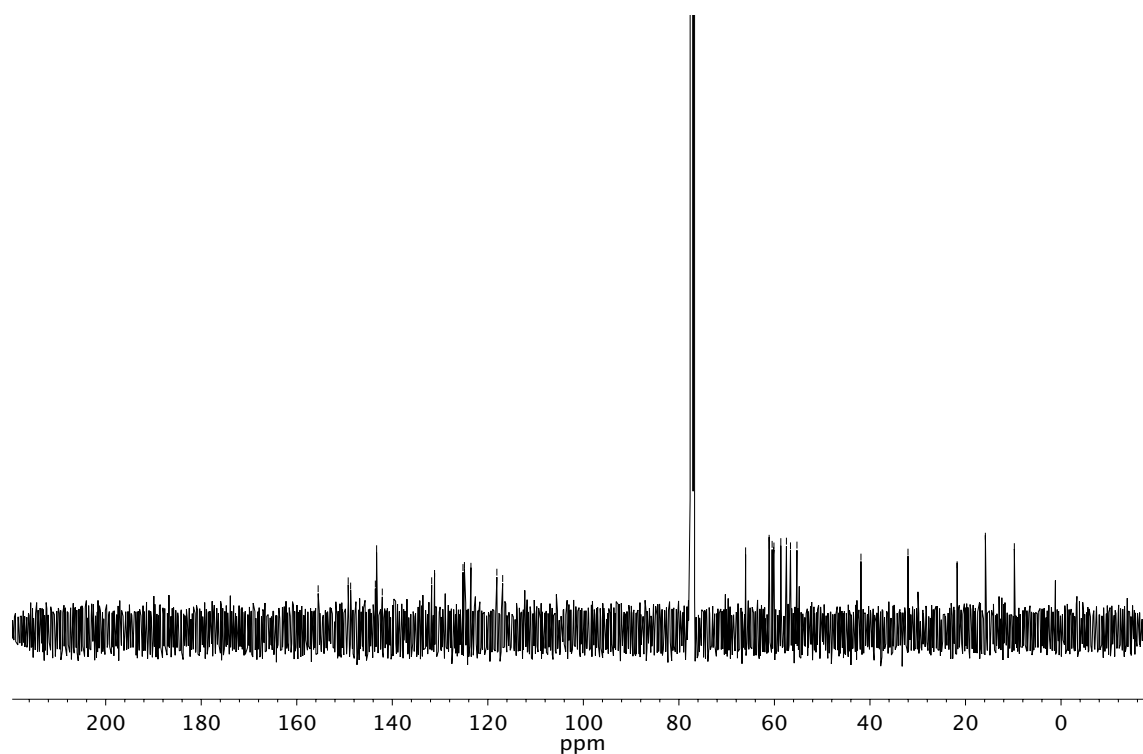


Figure A6.92 ¹³C NMR (100 MHz, CDCl₃) of compound **104**.

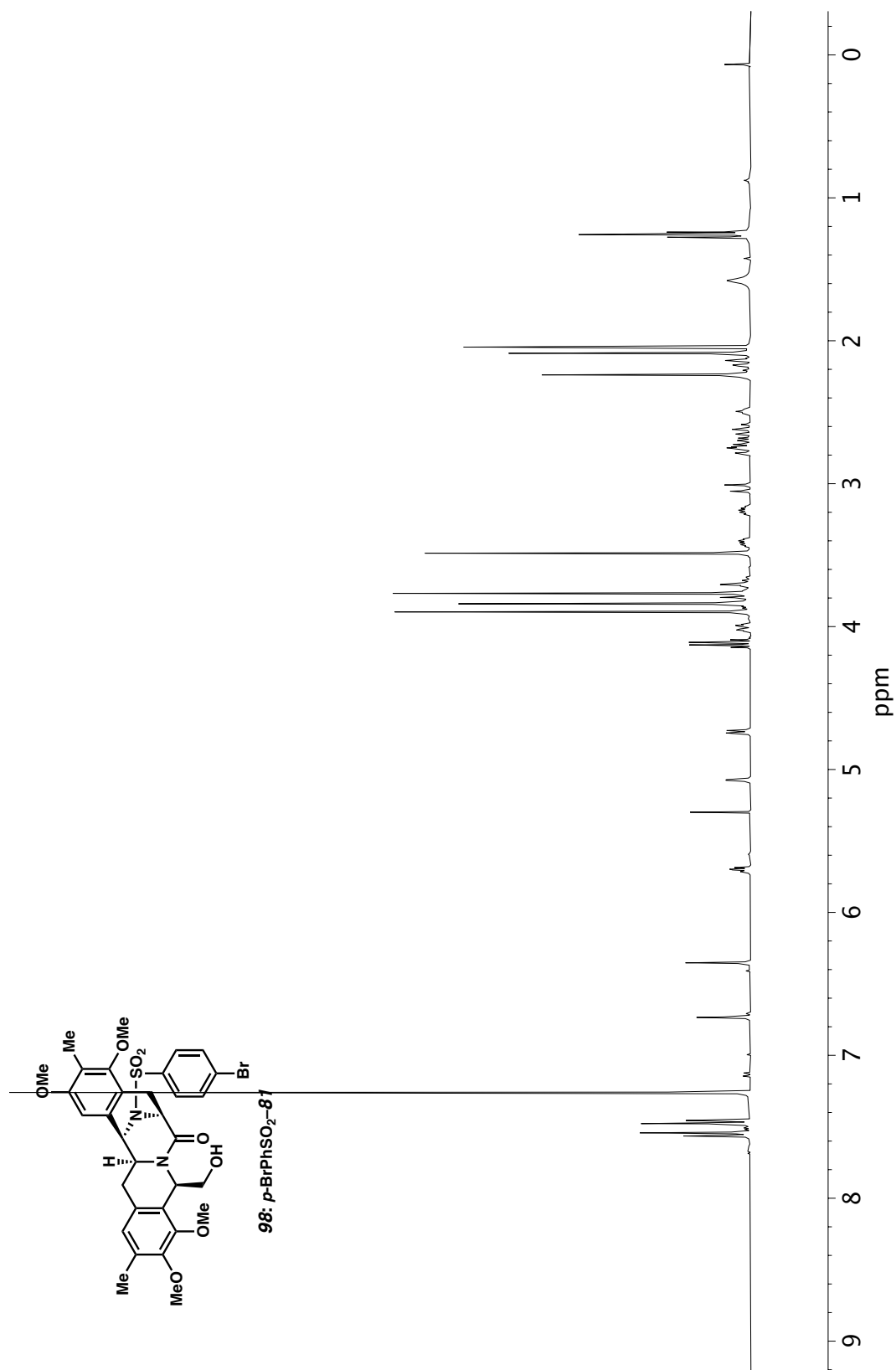


Figure A6.93 ¹H NMR (400 MHz, CDCl₃) of compound **98**.

APPENDIX 7

X-Ray Crystallography Reports Relevant to Chapter 3:

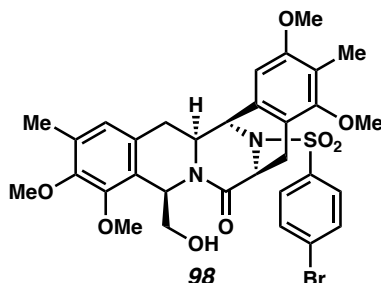
Concise Total Syntheses of (–)-Jorunnamycin A and (–)-Jorumycin

Enabled by Asymmetric Catalysis

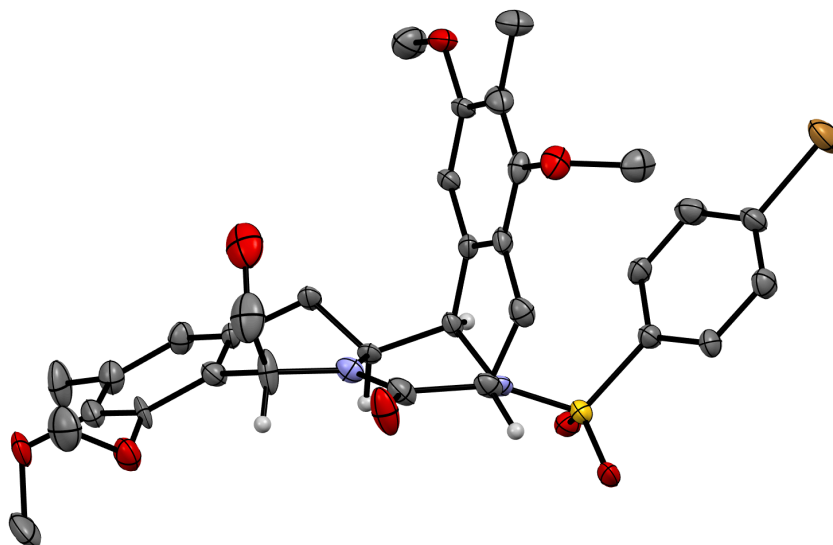
A7.1 GENERAL EXPERIMENTAL

Low-temperature diffraction data were collected on a Bruker AXS D8 VENTURE KAPPA diffractometer coupled to a PHOTON 100 CMOS detector with K radiation ($= 1.54178 \text{ \AA}$) from an $I\mu\text{S}$ micro-source for the structure of compound P17208 (**98**). The structure was solved by direct methods using SHELXS and refined against F^2 on all data by full-matrix least squares with SHELXL-2014 using established refinement techniques. All non-hydrogen atoms were refined anisotropically. All hydrogen atoms were included into the model at geometrically calculated positions and refined using a riding model. The isotropic displacement parameters of all hydrogen atoms were fixed to 1.2 times the U value of the atoms they are linked to (1.5 times for methyl groups). Unless otherwise noted, all disordered atoms were refined with the help of similarity restraints on the 1,2- and 1,3-distances and displacement parameters as well as rigid bond restraints for anisotropic displacement parameters. Compound P17208 crystallizes in the orthorhombic space group $P2_12_12$ with one molecule in the asymmetric unit along with two molecules of isopropanol. The hydroxide group and both isopropanol molecules were disordered over two positions. The Flack parameter refines to be 0.138(9).

A7.2 X-RAY CRYSTAL STRUCTURE ANALYSIS OF SULFONAMIDE **98**



X-ray quality crystals were obtained by allowing the slow evaporation of an isopropanol solution of **98**. The major enantiomer of the mixture is shown below.

Figure A7.1 X-ray crystal structure of sulfonamide **98**.**Table A7.1** Crystal data and structure refinement for product **98**.

Identification code	P17208
Empirical formula	C ₃₈ H ₅₁ Br N ₂ O ₁₀ S
Formula weight	807.77
Temperature	100(2) K
Wavelength	1.54178 Å
Crystal system	Orthorhombic
Space group	P2 ₁ 2 ₁ 2
Unit cell dimensions	a = 29.7321(15) Å a = 90°. b = 10.3172(5) Å b = 90°. c = 12.6857(5) Å g = 90°.
Volume	3891.4(3) Å ³
Z	4
Density (calculated)	1.379 Mg/m ³
Absorption coefficient	2.426 mm ⁻¹
F(000)	1696
Crystal size	0.250 x 0.150 x 0.050 mm ³
Theta range for data collection	2.972 to 74.895°.
Index ranges	-37 ≤ h ≤ 37, -12 ≤ k ≤ 12, -15 ≤ l ≤ 13
Reflections collected	45084
Independent reflections	7959 [R(int) = 0.0739]

Completeness to theta = 67.679°	100.0 %
Absorption correction	Semi-empirical from equivalents
Max. and min. transmission	0.7538 and 0.5857
Refinement method	Full-matrix least-squares on F ²
Data / restraints / parameters	7959 / 402 / 569
Goodness-of-fit on F ²	1.115
Final R indices [I>2sigma(I)]	R1 = 0.0767, wR2 = 0.1896
R indices (all data)	R1 = 0.0827, wR2 = 0.1932
Absolute structure parameter	0.138(9)
Extinction coefficient	n/a
Largest diff. peak and hole	1.066 and -0.843 e.Å ⁻³

Table A7.2 Atomic coordinates ($\times 10^4$) and equivalent isotropic displacement parameters ($\text{\AA}^2 \times 10^3$) for **98**. $U(\text{eq})$ is defined as one third of the trace of the orthogonalized U_{ij} tensor.

	x	y	z	U(eq)
S(1)	7330(1)	9529(2)	5282(1)	21(1)
O(1)	7382(2)	10830(5)	5676(4)	26(1)
O(2)	7712(2)	8714(5)	5193(5)	25(1)
C(1)	7091(3)	9659(7)	4003(6)	20(2)
C(2)	7040(3)	8533(8)	3407(6)	24(2)
C(3)	6848(3)	8611(9)	2430(7)	30(2)
C(4)	6721(3)	9829(8)	2046(6)	27(2)
Br(1)	6463(1)	9894(1)	672(1)	44(1)
C(5)	6777(3)	10919(8)	2608(7)	26(2)
C(6)	6959(3)	10842(8)	3625(6)	23(2)
N(1)	6986(2)	8806(6)	6076(5)	19(1)
N(2)	6545(2)	7601(7)	7718(5)	23(1)
C(7)	6601(3)	9510(8)	6531(6)	23(2)
C(8)	6441(3)	8857(8)	7564(6)	27(2)
O(3)	6207(3)	9498(7)	8157(5)	43(2)
C(9)	6354(3)	7011(9)	8688(7)	34(2)

C(26)	5842(6)	6970(30)	8740(20)	51(5)
O(4)	5736(5)	5946(19)	8061(14)	52(4)
C(26A)	5876(5)	6590(20)	8358(17)	41(5)
O(4A)	5608(5)	5980(20)	9140(14)	65(5)
C(10)	6605(3)	5795(8)	8993(6)	24(2)
C(11)	6654(3)	5434(8)	10053(6)	25(2)
O(5)	6497(2)	6289(6)	10816(5)	33(1)
C(27)	6132(4)	5865(12)	11453(9)	49(3)
C(12)	6877(3)	4311(9)	10335(6)	27(2)
O(6)	6899(2)	3954(6)	11394(5)	34(1)
C(28)	7254(4)	4587(12)	11946(7)	45(3)
C(13)	7070(3)	3513(8)	9578(7)	30(2)
C(29)	7346(4)	2355(10)	9889(8)	45(3)
C(14)	7012(3)	3866(8)	8530(7)	26(2)
C(15)	6786(3)	4969(8)	8237(5)	21(1)
C(16)	6749(3)	5418(7)	7107(6)	22(2)
C(17)	6862(3)	6871(7)	7060(5)	18(1)
C(18)	6872(3)	7419(7)	5938(6)	18(2)
C(19)	6439(3)	7261(7)	5311(6)	20(1)
C(20)	6360(3)	6056(7)	4816(6)	20(2)
C(21)	5970(3)	5890(7)	4228(6)	20(2)
O(7)	5852(2)	4737(6)	3772(4)	26(1)
C(30)	6156(4)	3681(9)	3839(9)	40(2)
C(22)	5658(3)	6909(9)	4089(7)	28(2)
C(31)	5241(3)	6720(10)	3457(8)	35(2)
C(23)	5756(3)	8094(8)	4567(6)	23(2)
O(8)	5462(2)	9120(6)	4435(5)	31(1)
C(32)	5585(3)	9946(9)	3576(7)	34(2)
C(24)	6140(3)	8272(7)	5196(6)	21(2)
C(25)	6208(3)	9569(8)	5748(6)	24(2)
O(1S)	5417(12)	4360(30)	9650(30)	149(9)

C(11S)	5442(14)	2970(30)	9740(30)	160(9)
C(12S)	5879(16)	2530(40)	9240(40)	146(12)
C(13S)	5430(20)	2650(50)	10910(40)	160(10)
O(2S)	5258(14)	3230(30)	9460(30)	167(9)
C(21S)	5190(13)	2300(40)	10310(30)	169(9)
C(22S)	5170(20)	960(30)	9810(40)	189(14)
C(23S)	5592(19)	2450(50)	11050(40)	163(11)
O(3S)	5234(9)	3630(30)	7350(30)	164(9)
C(31S)	5499(8)	3070(30)	6520(30)	131(7)
C(32S)	5967(7)	2713(15)	6970(20)	60(6)
C(33S)	5231(9)	1900(30)	6140(30)	98(7)
O(4S)	4896(10)	3880(30)	6440(30)	141(8)
C(41S)	5176(10)	2810(30)	6170(30)	128(7)
C(42S)	5669(10)	3150(40)	6160(40)	117(8)
C(43S)	5065(12)	1590(30)	6760(30)	106(9)

Table A7.3 Bond lengths [\AA] and angles [$^\circ$] for **98**.

S(1)-O(2)	1.418(6)
S(1)-O(1)	1.440(6)
S(1)-N(1)	1.618(7)
S(1)-C(1)	1.777(7)
C(1)-C(6)	1.368(11)
C(1)-C(2)	1.394(11)
C(2)-C(3)	1.365(12)
C(2)-H(2)	0.9500
C(3)-C(4)	1.400(13)
C(3)-H(3)	0.9500
C(4)-C(5)	1.343(12)
C(4)-Br(1)	1.906(7)

C(5)-C(6)	1.401(11)
C(5)-H(5)	0.9500
C(6)-H(6)	0.9500
N(1)-C(7)	1.473(10)
N(1)-C(18)	1.481(9)
N(2)-C(8)	1.347(10)
N(2)-C(17)	1.466(10)
N(2)-C(9)	1.486(10)
C(7)-C(25)	1.535(11)
C(7)-C(8)	1.549(11)
C(7)-H(7)	1.0000
C(8)-O(3)	1.220(11)
C(9)-C(10)	1.511(11)
C(9)-C(26)	1.523(19)
C(9)-C(26A)	1.544(19)
C(9)-H(9A)	1.0000
C(9)-H(9B)	1.0000
C(26)-O(4)	1.40(2)
C(26)-H(26A)	0.9900
C(26)-H(26B)	0.9900
O(4)-H(4)	0.8400
C(26A)-O(4A)	1.42(2)
C(26A)-H(26C)	0.9900
C(26A)-H(26D)	0.9900
O(4A)-H(4A)	0.8400
C(10)-C(15)	1.390(11)
C(10)-C(11)	1.404(10)
C(11)-C(12)	1.383(12)
C(11)-O(5)	1.390(10)
O(5)-C(27)	1.422(12)
C(27)-H(27A)	0.9800

C(27)-H(27B)	0.9800
C(27)-H(27C)	0.9800
C(12)-C(13)	1.389(13)
C(12)-O(6)	1.395(10)
O(6)-C(28)	1.423(12)
C(28)-H(28A)	0.9800
C(28)-H(28B)	0.9800
C(28)-H(28C)	0.9800
C(13)-C(14)	1.389(12)
C(13)-C(29)	1.500(12)
C(29)-H(29A)	0.9800
C(29)-H(29B)	0.9800
C(29)-H(29C)	0.9800
C(14)-C(15)	1.374(11)
C(14)-H(14)	0.9500
C(15)-C(16)	1.511(10)
C(16)-C(17)	1.537(10)
C(16)-H(16A)	0.9900
C(16)-H(16B)	0.9900
C(17)-C(18)	1.531(10)
C(17)-H(17)	1.0000
C(18)-C(19)	1.523(11)
C(18)-H(18)	1.0000
C(19)-C(24)	1.379(11)
C(19)-C(20)	1.412(10)
C(20)-C(21)	1.390(10)
C(20)-H(20)	0.9500
C(21)-O(7)	1.368(9)
C(21)-C(22)	1.413(12)
O(7)-C(30)	1.417(12)
C(30)-H(30A)	0.9800

C(30)-H(30B)	0.9800
C(30)-H(30C)	0.9800
C(22)-C(23)	1.396(12)
C(22)-C(31)	1.489(11)
C(31)-H(31A)	0.9800
C(31)-H(31B)	0.9800
C(31)-H(31C)	0.9800
C(23)-O(8)	1.382(9)
C(23)-C(24)	1.405(11)
O(8)-C(32)	1.431(11)
C(32)-H(32A)	0.9800
C(32)-H(32B)	0.9800
C(32)-H(32C)	0.9800
C(24)-C(25)	1.523(11)
C(25)-H(25A)	0.9900
C(25)-H(25B)	0.9900
O(1S)-C(11S)	1.442(19)
O(1S)-H(1S)	0.8400
C(11S)-C(12S)	1.516(17)
C(11S)-C(13S)	1.521(17)
C(11S)-H(11S)	1.0000
C(12S)-H(12A)	0.9800
C(12S)-H(12B)	0.9800
C(12S)-H(12C)	0.9800
C(13S)-H(13A)	0.9800
C(13S)-H(13B)	0.9800
C(13S)-H(13C)	0.9800
O(2S)-C(21S)	1.450(19)
O(2S)-H(2S)	0.8400
C(21S)-C(22S)	1.520(17)
C(21S)-C(23S)	1.529(17)

C(21S)-H(21S)	1.0000
C(22S)-H(22A)	0.9800
C(22S)-H(22B)	0.9800
C(22S)-H(22C)	0.9800
C(23S)-H(23A)	0.9800
C(23S)-H(23B)	0.9800
C(23S)-H(23C)	0.9800
O(3S)-C(31S)	1.438(19)
O(3S)-H(3S)	0.8400
C(31S)-C(33S)	1.525(17)
C(31S)-C(32S)	1.547(17)
C(31S)-H(31S)	1.0000
C(32S)-H(32D)	0.9800
C(32S)-H(32E)	0.9800
C(32S)-H(32F)	0.9800
C(33S)-H(33A)	0.9800
C(33S)-H(33B)	0.9800
C(33S)-H(33C)	0.9800
O(4S)-C(41S)	1.426(18)
O(4S)-H(4S)	0.8400
C(41S)-C(43S)	1.494(17)
C(41S)-C(42S)	1.511(17)
C(41S)-H(41S)	1.0000
C(42S)-H(42A)	0.9800
C(42S)-H(42B)	0.9800
C(42S)-H(42C)	0.9800
C(43S)-H(43A)	0.9800
C(43S)-H(43B)	0.9800
C(43S)-H(43C)	0.9800

O(2)-S(1)-O(1)	119.7(4)
O(2)-S(1)-N(1)	106.4(3)
O(1)-S(1)-N(1)	106.3(3)
O(2)-S(1)-C(1)	107.0(4)
O(1)-S(1)-C(1)	106.8(3)
N(1)-S(1)-C(1)	110.5(3)
C(6)-C(1)-C(2)	121.5(7)
C(6)-C(1)-S(1)	120.1(6)
C(2)-C(1)-S(1)	118.4(6)
C(3)-C(2)-C(1)	119.3(8)
C(3)-C(2)-H(2)	120.4
C(1)-C(2)-H(2)	120.4
C(2)-C(3)-C(4)	118.7(8)
C(2)-C(3)-H(3)	120.6
C(4)-C(3)-H(3)	120.6
C(5)-C(4)-C(3)	122.2(7)
C(5)-C(4)-Br(1)	120.4(6)
C(3)-C(4)-Br(1)	117.3(6)
C(4)-C(5)-C(6)	119.3(8)
C(4)-C(5)-H(5)	120.4
C(6)-C(5)-H(5)	120.4
C(1)-C(6)-C(5)	118.9(8)
C(1)-C(6)-H(6)	120.5
C(5)-C(6)-H(6)	120.5
C(7)-N(1)-C(18)	110.1(6)
C(7)-N(1)-S(1)	120.5(5)
C(18)-N(1)-S(1)	121.1(5)
C(8)-N(2)-C(17)	124.0(7)
C(8)-N(2)-C(9)	115.2(7)
C(17)-N(2)-C(9)	120.5(6)
N(1)-C(7)-C(25)	111.0(6)

N(1)-C(7)-C(8)	110.9(6)
C(25)-C(7)-C(8)	109.3(7)
N(1)-C(7)-H(7)	108.5
C(25)-C(7)-H(7)	108.5
C(8)-C(7)-H(7)	108.5
O(3)-C(8)-N(2)	124.3(8)
O(3)-C(8)-C(7)	117.6(7)
N(2)-C(8)-C(7)	118.0(7)
N(2)-C(9)-C(10)	111.2(7)
N(2)-C(9)-C(26)	115.4(13)
C(10)-C(9)-C(26)	117.5(12)
N(2)-C(9)-C(26A)	104.2(9)
C(10)-C(9)-C(26A)	106.8(11)
N(2)-C(9)-H(9A)	103.5
C(10)-C(9)-H(9A)	103.5
C(26)-C(9)-H(9A)	103.5
N(2)-C(9)-H(9B)	111.4
C(10)-C(9)-H(9B)	111.4
C(26A)-C(9)-H(9B)	111.4
O(4)-C(26)-C(9)	102.7(15)
O(4)-C(26)-H(26A)	111.2
C(9)-C(26)-H(26A)	111.2
O(4)-C(26)-H(26B)	111.2
C(9)-C(26)-H(26B)	111.2
H(26A)-C(26)-H(26B)	109.1
C(26)-O(4)-H(4)	109.5
O(4A)-C(26A)-C(9)	116.9(15)
O(4A)-C(26A)-H(26C)	108.1
C(9)-C(26A)-H(26C)	108.1
O(4A)-C(26A)-H(26D)	108.1
C(9)-C(26A)-H(26D)	108.1

H(26C)-C(26A)-H(26D)	107.3
C(26A)-O(4A)-H(4A)	109.5
C(15)-C(10)-C(11)	117.3(7)
C(15)-C(10)-C(9)	121.6(7)
C(11)-C(10)-C(9)	121.1(7)
C(12)-C(11)-O(5)	120.9(7)
C(12)-C(11)-C(10)	121.3(8)
O(5)-C(11)-C(10)	117.7(7)
C(11)-O(5)-C(27)	117.1(7)
O(5)-C(27)-H(27A)	109.5
O(5)-C(27)-H(27B)	109.5
H(27A)-C(27)-H(27B)	109.5
O(5)-C(27)-H(27C)	109.5
H(27A)-C(27)-H(27C)	109.5
H(27B)-C(27)-H(27C)	109.5
C(11)-C(12)-C(13)	121.1(7)
C(11)-C(12)-O(6)	119.5(8)
C(13)-C(12)-O(6)	119.4(8)
C(12)-O(6)-C(28)	112.8(7)
O(6)-C(28)-H(28A)	109.5
O(6)-C(28)-H(28B)	109.5
H(28A)-C(28)-H(28B)	109.5
O(6)-C(28)-H(28C)	109.5
H(28A)-C(28)-H(28C)	109.5
H(28B)-C(28)-H(28C)	109.5
C(12)-C(13)-C(14)	117.0(8)
C(12)-C(13)-C(29)	121.0(8)
C(14)-C(13)-C(29)	121.9(8)
C(13)-C(29)-H(29A)	109.5
C(13)-C(29)-H(29B)	109.5
H(29A)-C(29)-H(29B)	109.5

C(13)-C(29)-H(29C)	109.5
H(29A)-C(29)-H(29C)	109.5
H(29B)-C(29)-H(29C)	109.5
C(15)-C(14)-C(13)	122.5(8)
C(15)-C(14)-H(14)	118.7
C(13)-C(14)-H(14)	118.7
C(14)-C(15)-C(10)	120.7(7)
C(14)-C(15)-C(16)	123.1(7)
C(10)-C(15)-C(16)	116.0(7)
C(15)-C(16)-C(17)	108.7(6)
C(15)-C(16)-H(16A)	110.0
C(17)-C(16)-H(16A)	110.0
C(15)-C(16)-H(16B)	110.0
C(17)-C(16)-H(16B)	110.0
H(16A)-C(16)-H(16B)	108.3
N(2)-C(17)-C(18)	110.7(6)
N(2)-C(17)-C(16)	109.9(6)
C(18)-C(17)-C(16)	113.7(6)
N(2)-C(17)-H(17)	107.5
C(18)-C(17)-H(17)	107.5
C(16)-C(17)-H(17)	107.5
N(1)-C(18)-C(19)	111.1(6)
N(1)-C(18)-C(17)	104.6(6)
C(19)-C(18)-C(17)	115.3(6)
N(1)-C(18)-H(18)	108.5
C(19)-C(18)-H(18)	108.5
C(17)-C(18)-H(18)	108.5
C(24)-C(19)-C(20)	120.8(7)
C(24)-C(19)-C(18)	121.3(6)
C(20)-C(19)-C(18)	117.9(7)
C(21)-C(20)-C(19)	119.1(7)

C(21)-C(20)-H(20)	120.4
C(19)-C(20)-H(20)	120.4
O(7)-C(21)-C(20)	123.2(7)
O(7)-C(21)-C(22)	115.2(7)
C(20)-C(21)-C(22)	121.5(7)
C(21)-O(7)-C(30)	118.6(6)
O(7)-C(30)-H(30A)	109.5
O(7)-C(30)-H(30B)	109.5
H(30A)-C(30)-H(30B)	109.5
O(7)-C(30)-H(30C)	109.5
H(30A)-C(30)-H(30C)	109.5
H(30B)-C(30)-H(30C)	109.5
C(23)-C(22)-C(21)	117.5(7)
C(23)-C(22)-C(31)	121.5(8)
C(21)-C(22)-C(31)	121.1(8)
C(22)-C(31)-H(31A)	109.5
C(22)-C(31)-H(31B)	109.5
H(31A)-C(31)-H(31B)	109.5
C(22)-C(31)-H(31C)	109.5
H(31A)-C(31)-H(31C)	109.5
H(31B)-C(31)-H(31C)	109.5
O(8)-C(23)-C(22)	119.1(7)
O(8)-C(23)-C(24)	118.8(7)
C(22)-C(23)-C(24)	122.1(7)
C(23)-O(8)-C(32)	112.9(6)
O(8)-C(32)-H(32A)	109.5
O(8)-C(32)-H(32B)	109.5
H(32A)-C(32)-H(32B)	109.5
O(8)-C(32)-H(32C)	109.5
H(32A)-C(32)-H(32C)	109.5
H(32B)-C(32)-H(32C)	109.5

C(19)-C(24)-C(23)	119.0(7)
C(19)-C(24)-C(25)	122.0(7)
C(23)-C(24)-C(25)	118.9(7)
C(24)-C(25)-C(7)	111.3(6)
C(24)-C(25)-H(25A)	109.4
C(7)-C(25)-H(25A)	109.4
C(24)-C(25)-H(25B)	109.4
C(7)-C(25)-H(25B)	109.4
H(25A)-C(25)-H(25B)	108.0
C(11S)-O(1S)-H(1S)	109.5
O(1S)-C(11S)-C(12S)	108(2)
O(1S)-C(11S)-C(13S)	107(2)
C(12S)-C(11S)-C(13S)	112(2)
O(1S)-C(11S)-H(11S)	109.9
C(12S)-C(11S)-H(11S)	109.9
C(13S)-C(11S)-H(11S)	109.9
C(11S)-C(12S)-H(12A)	109.5
C(11S)-C(12S)-H(12B)	109.5
H(12A)-C(12S)-H(12B)	109.5
C(11S)-C(12S)-H(12C)	109.5
H(12A)-C(12S)-H(12C)	109.5
H(12B)-C(12S)-H(12C)	109.5
C(11S)-C(13S)-H(13A)	109.5
C(11S)-C(13S)-H(13B)	109.5
H(13A)-C(13S)-H(13B)	109.5
C(11S)-C(13S)-H(13C)	109.5
H(13A)-C(13S)-H(13C)	109.5
H(13B)-C(13S)-H(13C)	109.5
C(21S)-O(2S)-H(2S)	109.5
O(2S)-C(21S)-C(22S)	107.5(19)
O(2S)-C(21S)-C(23S)	106.3(19)

C(22S)-C(21S)-C(23S)	112(2)
O(2S)-C(21S)-H(21S)	110.2
C(22S)-C(21S)-H(21S)	110.2
C(23S)-C(21S)-H(21S)	110.2
C(21S)-C(22S)-H(22A)	109.5
C(21S)-C(22S)-H(22B)	109.5
H(22A)-C(22S)-H(22B)	109.5
C(21S)-C(22S)-H(22C)	109.5
H(22A)-C(22S)-H(22C)	109.5
H(22B)-C(22S)-H(22C)	109.5
C(21S)-C(23S)-H(23A)	109.5
C(21S)-C(23S)-H(23B)	109.5
H(23A)-C(23S)-H(23B)	109.5
C(21S)-C(23S)-H(23C)	109.5
H(23A)-C(23S)-H(23C)	109.5
H(23B)-C(23S)-H(23C)	109.5
C(31S)-O(3S)-H(3S)	109.5
O(3S)-C(31S)-C(33S)	105.4(18)
O(3S)-C(31S)-C(32S)	108.7(19)
C(33S)-C(31S)-C(32S)	113.5(19)
O(3S)-C(31S)-H(31S)	109.7
C(33S)-C(31S)-H(31S)	109.7
C(32S)-C(31S)-H(31S)	109.7
C(31S)-C(32S)-H(32D)	109.5
C(31S)-C(32S)-H(32E)	109.5
H(32D)-C(32S)-H(32E)	109.5
C(31S)-C(32S)-H(32F)	109.5
H(32D)-C(32S)-H(32F)	109.5
H(32E)-C(32S)-H(32F)	109.5
C(31S)-C(33S)-H(33A)	109.5
C(31S)-C(33S)-H(33B)	109.5

H(33A)-C(33S)-H(33B)	109.5
C(31S)-C(33S)-H(33C)	109.5
H(33A)-C(33S)-H(33C)	109.5
H(33B)-C(33S)-H(33C)	109.5
C(41S)-O(4S)-H(4S)	109.5
O(4S)-C(41S)-C(43S)	114(2)
O(4S)-C(41S)-C(42S)	113(2)
C(43S)-C(41S)-C(42S)	115(2)
O(4S)-C(41S)-H(41S)	104.9
C(43S)-C(41S)-H(41S)	104.9
C(42S)-C(41S)-H(41S)	104.9
C(41S)-C(42S)-H(42A)	109.5
C(41S)-C(42S)-H(42B)	109.5
H(42A)-C(42S)-H(42B)	109.5
C(41S)-C(42S)-H(42C)	109.5
H(42A)-C(42S)-H(42C)	109.5
H(42B)-C(42S)-H(42C)	109.5
C(41S)-C(43S)-H(43A)	109.5
C(41S)-C(43S)-H(43B)	109.5
H(43A)-C(43S)-H(43B)	109.5
C(41S)-C(43S)-H(43C)	109.5
H(43A)-C(43S)-H(43C)	109.5
H(43B)-C(43S)-H(43C)	109.5

Table A7.4 Anisotropic displacement parameters ($\text{\AA}^2 \times 10^3$) for **98**. The anisotropic displacement factor exponent takes the form: $-2\pi^2 [h^2 a^{*2} U^{11} + \dots + 2 h k a^* b^* U^{12}]$

	U ¹¹	U ²²	U ³³	U ²³	U ¹³	U ¹²
S(1)	27(1)	21(1)	16(1)	3(1)	-5(1)	-3(1)
O(1)	42(3)	23(3)	13(2)	1(2)	-3(2)	-8(2)

O(2)	28(3)	19(3)	28(3)	2(2)	-7(2)	-3(2)
C(1)	26(4)	17(4)	18(3)	0(3)	-3(3)	0(3)
C(2)	33(4)	15(4)	23(4)	2(3)	-1(3)	-2(3)
C(3)	35(5)	28(4)	27(4)	-6(4)	-5(4)	-1(4)
C(4)	37(4)	26(4)	18(3)	-1(3)	-9(3)	-1(4)
Br(1)	66(1)	39(1)	26(1)	3(1)	-18(1)	6(1)
C(5)	34(4)	21(4)	24(4)	4(3)	-3(3)	3(3)
C(6)	28(4)	21(4)	21(4)	6(3)	-5(3)	0(3)
N(1)	26(3)	13(3)	18(3)	-5(2)	-4(3)	0(2)
N(2)	26(4)	25(3)	18(3)	-5(3)	1(3)	2(3)
C(7)	32(4)	18(3)	19(4)	-5(3)	-4(3)	4(3)
C(8)	35(4)	27(4)	20(4)	-1(3)	-7(3)	6(4)
O(3)	68(5)	38(4)	22(3)	4(3)	14(3)	23(3)
C(9)	43(5)	34(4)	25(4)	17(3)	12(3)	17(4)
C(26)	41(8)	58(11)	52(11)	15(9)	17(7)	13(7)
O(4)	31(8)	71(10)	52(9)	13(8)	11(6)	4(7)
C(26A)	37(7)	41(11)	44(10)	20(8)	19(7)	19(7)
O(4A)	40(7)	102(13)	53(9)	41(9)	2(6)	-11(8)
C(10)	27(4)	24(4)	19(4)	0(3)	-5(3)	1(3)
C(11)	34(4)	32(4)	9(3)	10(3)	-1(3)	2(3)
O(5)	45(4)	34(3)	19(3)	1(2)	2(3)	1(3)
C(27)	55(6)	58(7)	33(5)	3(5)	16(5)	4(5)
C(12)	29(4)	33(4)	19(4)	7(3)	-3(3)	-4(3)
O(6)	49(4)	35(3)	17(3)	13(3)	-5(3)	0(3)
C(28)	49(6)	62(7)	26(5)	13(5)	-15(4)	-1(5)
C(13)	36(5)	27(4)	25(4)	6(3)	3(3)	2(3)
C(29)	65(7)	35(5)	34(5)	19(4)	4(5)	16(5)
C(14)	35(5)	19(4)	25(4)	1(3)	5(3)	3(3)
C(15)	31(4)	17(3)	14(3)	4(3)	-2(3)	-3(3)
C(16)	36(4)	14(3)	15(3)	-2(3)	-3(3)	-2(3)
C(17)	27(4)	16(3)	12(3)	-4(3)	-1(3)	-3(3)

C(18)	29(4)	14(3)	12(3)	1(3)	-2(3)	3(3)
C(19)	28(4)	17(3)	14(3)	3(3)	1(3)	-4(3)
C(20)	26(4)	20(3)	14(3)	0(3)	-5(3)	-2(3)
C(21)	28(4)	19(3)	14(3)	-2(3)	-6(3)	-3(3)
O(7)	28(3)	30(3)	22(3)	-4(2)	-4(2)	-8(2)
C(30)	50(6)	25(5)	45(6)	-1(4)	-10(5)	-1(4)
C(22)	21(4)	35(4)	26(4)	4(3)	-2(3)	-2(3)
C(31)	31(5)	38(5)	36(5)	-7(4)	-10(4)	-3(4)
C(23)	23(4)	19(4)	27(4)	7(3)	3(3)	4(3)
O(8)	23(3)	29(3)	40(4)	7(3)	-2(2)	6(2)
C(32)	35(4)	22(4)	45(5)	0(4)	-7(4)	7(4)
C(24)	24(4)	21(4)	18(4)	8(3)	-2(3)	1(3)
C(25)	29(4)	25(4)	19(3)	-1(3)	1(3)	4(3)
O(1S)	140(20)	126(16)	180(20)	60(15)	22(18)	-2(15)
C(11S)	150(20)	134(15)	190(20)	52(15)	7(16)	-3(15)
C(12S)	140(20)	120(20)	180(30)	47(19)	-10(20)	1(18)
C(13S)	160(20)	130(18)	190(20)	50(15)	13(17)	-2(17)
O(2S)	160(20)	141(17)	200(20)	38(16)	7(17)	-2(16)
C(21S)	160(20)	145(16)	200(20)	49(15)	4(16)	-2(16)
C(22S)	180(30)	152(19)	230(30)	38(18)	-20(20)	3(18)
C(23S)	150(20)	137(19)	200(20)	40(17)	10(18)	5(18)
O(3S)	156(16)	154(15)	183(18)	-26(14)	-10(13)	32(12)
C(31S)	122(13)	122(12)	149(15)	-14(11)	-34(11)	24(10)
C(32S)	95(13)	2(7)	82(14)	2(8)	-20(10)	-7(7)
C(33S)	71(13)	96(13)	128(17)	-19(13)	-42(12)	49(10)
O(4S)	132(15)	143(14)	147(18)	-21(14)	-23(14)	44(12)
C(41S)	111(13)	126(12)	147(16)	-14(12)	-25(12)	28(10)
C(42S)	112(14)	110(14)	129(18)	-14(14)	-11(12)	25(11)
C(43S)	67(15)	115(14)	140(20)	-21(14)	-35(15)	35(12)

Table A7.5 Hydrogen coordinates ($\times 10^4$) and isotropic displacement parameters ($\text{\AA}^2 \times 10^3$) for **98**.

	x	y	z	U(eq)
H(2)	7137	7722	3677	28
H(3)	6803	7852	2020	36
H(5)	6695	11735	2320	31
H(6)	6991	11598	4046	28
H(7)	6698	10416	6695	28
H(9A)	6437	7642	9254	41
H(9B)	6345	7648	9282	41
H(26A)	5736	6798	9464	61
H(26B)	5709	7796	8486	61
H(4)	5940	5386	8087	77
H(26C)	5713	7361	8100	49
H(26D)	5904	5980	7757	49
H(4A)	5335	6139	9021	98
H(27A)	5865	5742	11011	73
H(27B)	6069	6519	11993	73
H(27C)	6211	5043	11793	73
H(28A)	7542	4365	11620	68
H(28B)	7254	4304	12684	68
H(28C)	7209	5527	11915	68
H(29A)	7320	1685	9345	67
H(29B)	7236	2014	10562	67
H(29C)	7662	2611	9963	67
H(14)	7133	3323	7996	32
H(16A)	6441	5267	6841	26
H(16B)	6961	4924	6659	26
H(17)	7168	6987	7368	22
H(18)	7122	6989	5542	22

H(20)	6570	5369	4884	24
H(30A)	6440	3916	3499	60
H(30B)	6026	2925	3483	60
H(30C)	6211	3473	4581	60
H(31A)	5089	7555	3363	52
H(31B)	5040	6120	3827	52
H(31C)	5319	6360	2766	52
H(32A)	5892	10264	3681	51
H(32B)	5378	10683	3544	51
H(32C)	5569	9458	2915	51
H(25A)	5929	9808	6128	29
H(25B)	6268	10247	5214	29
H(1S)	5541	4593	9081	224
H(11S)	5181	2560	9376	192
H(12A)	5905	1590	9293	219
H(12B)	5880	2787	8493	219
H(12C)	6133	2944	9599	219
H(13A)	5444	1710	11008	240
H(13B)	5682	3063	11270	240
H(13C)	5145	2975	11216	240
H(2S)	5363	3915	9711	250
H(21S)	4904	2491	10689	203
H(22A)	5123	307	10363	283
H(22B)	4918	924	9309	283
H(22C)	5451	780	9440	283
H(23A)	5561	1835	11637	244
H(23B)	5870	2262	10663	244
H(23C)	5601	3333	11322	244
H(3S)	5021	4060	7084	246
H(31S)	5534	3702	5931	157
H(32D)	6151	2325	6413	89

H(32E)	6115	3498	7234	89
H(32F)	5931	2091	7548	89
H(33A)	5395	1464	5572	148
H(33B)	5188	1291	6728	148
H(33C)	4937	2185	5881	148
H(4S)	5029	4573	6291	211
H(41S)	5101	2610	5419	154
H(42A)	5847	2388	5971	176
H(42B)	5722	3843	5643	176
H(42C)	5759	3457	6862	176
H(43A)	5268	898	6537	159
H(43B)	5100	1746	7517	159
H(43C)	4753	1343	6609	159

Table A7.6 Torsion angles [°] for **98**.

O(2)-S(1)-C(1)-C(6)	-134.9(7)
O(1)-S(1)-C(1)-C(6)	-5.5(8)
N(1)-S(1)-C(1)-C(6)	109.7(7)
O(2)-S(1)-C(1)-C(2)	45.4(7)
O(1)-S(1)-C(1)-C(2)	174.8(6)
N(1)-S(1)-C(1)-C(2)	-70.0(7)
C(6)-C(1)-C(2)-C(3)	-0.9(13)
S(1)-C(1)-C(2)-C(3)	178.8(7)
C(1)-C(2)-C(3)-C(4)	1.8(13)
C(2)-C(3)-C(4)-C(5)	-0.6(14)
C(2)-C(3)-C(4)-Br(1)	179.2(7)
C(3)-C(4)-C(5)-C(6)	-1.5(14)
Br(1)-C(4)-C(5)-C(6)	178.6(6)
C(2)-C(1)-C(6)-C(5)	-1.2(13)
S(1)-C(1)-C(6)-C(5)	179.1(6)

C(4)-C(5)-C(6)-C(1)	2.4(13)
O(2)-S(1)-N(1)-C(7)	166.3(5)
O(1)-S(1)-N(1)-C(7)	37.7(6)
C(1)-S(1)-N(1)-C(7)	-77.9(6)
O(2)-S(1)-N(1)-C(18)	-48.4(6)
O(1)-S(1)-N(1)-C(18)	-177.0(5)
C(1)-S(1)-N(1)-C(18)	67.4(6)
C(18)-N(1)-C(7)-C(25)	-67.5(8)
S(1)-N(1)-C(7)-C(25)	81.3(7)
C(18)-N(1)-C(7)-C(8)	54.2(8)
S(1)-N(1)-C(7)-C(8)	-157.1(5)
C(17)-N(2)-C(8)-O(3)	-173.8(8)
C(9)-N(2)-C(8)-O(3)	0.0(13)
C(17)-N(2)-C(8)-C(7)	10.4(11)
C(9)-N(2)-C(8)-C(7)	-175.8(7)
N(1)-C(7)-C(8)-O(3)	161.8(8)
C(25)-C(7)-C(8)-O(3)	-75.6(10)
N(1)-C(7)-C(8)-N(2)	-22.1(10)
C(25)-C(7)-C(8)-N(2)	100.6(8)
C(8)-N(2)-C(9)-C(10)	-160.7(8)
C(17)-N(2)-C(9)-C(10)	13.3(11)
C(8)-N(2)-C(9)-C(26)	62.2(14)
C(17)-N(2)-C(9)-C(26)	-123.8(13)
C(8)-N(2)-C(9)-C(26A)	84.6(12)
C(17)-N(2)-C(9)-C(26A)	-101.4(12)
N(2)-C(9)-C(26)-O(4)	76.5(19)
C(10)-C(9)-C(26)-O(4)	-58(2)
N(2)-C(9)-C(26A)-O(4A)	-179.8(18)
C(10)-C(9)-C(26A)-O(4A)	62(2)
N(2)-C(9)-C(10)-C(15)	-34.2(12)
C(26)-C(9)-C(10)-C(15)	101.9(15)

C(26A)-C(9)-C(10)-C(15)	78.9(12)
N(2)-C(9)-C(10)-C(11)	147.9(8)
C(26)-C(9)-C(10)-C(11)	-76.0(16)
C(26A)-C(9)-C(10)-C(11)	-99.1(12)
C(15)-C(10)-C(11)-C(12)	0.9(12)
C(9)-C(10)-C(11)-C(12)	178.9(8)
C(15)-C(10)-C(11)-O(5)	176.4(7)
C(9)-C(10)-C(11)-O(5)	-5.6(12)
C(12)-C(11)-O(5)-C(27)	-69.2(11)
C(10)-C(11)-O(5)-C(27)	115.2(9)
O(5)-C(11)-C(12)-C(13)	-174.1(8)
C(10)-C(11)-C(12)-C(13)	1.3(13)
O(5)-C(11)-C(12)-O(6)	7.7(12)
C(10)-C(11)-C(12)-O(6)	-176.9(8)
C(11)-C(12)-O(6)-C(28)	-83.4(10)
C(13)-C(12)-O(6)-C(28)	98.3(10)
C(11)-C(12)-C(13)-C(14)	-2.6(13)
O(6)-C(12)-C(13)-C(14)	175.6(8)
C(11)-C(12)-C(13)-C(29)	174.9(9)
O(6)-C(12)-C(13)-C(29)	-6.9(14)
C(12)-C(13)-C(14)-C(15)	1.8(13)
C(29)-C(13)-C(14)-C(15)	-175.7(9)
C(13)-C(14)-C(15)-C(10)	0.4(13)
C(13)-C(14)-C(15)-C(16)	175.3(8)
C(11)-C(10)-C(15)-C(14)	-1.7(12)
C(9)-C(10)-C(15)-C(14)	-179.8(8)
C(11)-C(10)-C(15)-C(16)	-177.0(7)
C(9)-C(10)-C(15)-C(16)	5.0(11)
C(14)-C(15)-C(16)-C(17)	-132.6(8)
C(10)-C(15)-C(16)-C(17)	42.4(9)
C(8)-N(2)-C(17)-C(18)	-28.2(10)

C(9)-N(2)-C(17)-C(18)	158.3(7)
C(8)-N(2)-C(17)-C(16)	-154.5(7)
C(9)-N(2)-C(17)-C(16)	32.0(10)
C(15)-C(16)-C(17)-N(2)	-59.9(8)
C(15)-C(16)-C(17)-C(18)	175.5(6)
C(7)-N(1)-C(18)-C(19)	53.3(8)
S(1)-N(1)-C(18)-C(19)	-95.2(7)
C(7)-N(1)-C(18)-C(17)	-71.8(7)
S(1)-N(1)-C(18)-C(17)	139.7(6)
N(2)-C(17)-C(18)-N(1)	56.0(8)
C(16)-C(17)-C(18)-N(1)	-179.8(6)
N(2)-C(17)-C(18)-C(19)	-66.3(8)
C(16)-C(17)-C(18)-C(19)	57.9(9)
N(1)-C(18)-C(19)-C(24)	-18.1(10)
C(17)-C(18)-C(19)-C(24)	100.6(8)
N(1)-C(18)-C(19)-C(20)	159.6(6)
C(17)-C(18)-C(19)-C(20)	-81.7(8)
C(24)-C(19)-C(20)-C(21)	-1.5(11)
C(18)-C(19)-C(20)-C(21)	-179.2(7)
C(19)-C(20)-C(21)-O(7)	-176.1(7)
C(19)-C(20)-C(21)-C(22)	1.9(11)
C(20)-C(21)-O(7)-C(30)	-4.4(12)
C(22)-C(21)-O(7)-C(30)	177.5(8)
O(7)-C(21)-C(22)-C(23)	178.0(7)
C(20)-C(21)-C(22)-C(23)	-0.1(12)
O(7)-C(21)-C(22)-C(31)	-1.9(12)
C(20)-C(21)-C(22)-C(31)	180.0(8)
C(21)-C(22)-C(23)-O(8)	178.9(7)
C(31)-C(22)-C(23)-O(8)	-1.2(12)
C(21)-C(22)-C(23)-C(24)	-2.2(12)
C(31)-C(22)-C(23)-C(24)	177.7(8)

C(22)-C(23)-O(8)-C(32)	-93.9(9)
C(24)-C(23)-O(8)-C(32)	87.2(9)
C(20)-C(19)-C(24)-C(23)	-0.7(11)
C(18)-C(19)-C(24)-C(23)	176.9(7)
C(20)-C(19)-C(24)-C(25)	178.1(7)
C(18)-C(19)-C(24)-C(25)	-4.3(11)
O(8)-C(23)-C(24)-C(19)	-178.5(7)
C(22)-C(23)-C(24)-C(19)	2.6(12)
O(8)-C(23)-C(24)-C(25)	2.7(11)
C(22)-C(23)-C(24)-C(25)	-176.2(7)
C(19)-C(24)-C(25)-C(7)	-7.8(10)
C(23)-C(24)-C(25)-C(7)	170.9(7)
N(1)-C(7)-C(25)-C(24)	42.7(9)
C(8)-C(7)-C(25)-C(24)	-79.9(8)

Table A7.7 Hydrogen bonds for **98** [Å and °].

D-H...A	d(D-H)	d(H...A)	d(D...A)	<(DHA)
C(2)-H(2)...O(1)#1	0.95	2.56	3.477(10)	163.6
C(3)-H(3)...O(5)#2	0.95	2.40	3.320(11)	163.2
C(5)-H(5)...O(6)#3	0.95	2.64	3.508(10)	151.5
C(6)-H(6)...O(2)#4	0.95	2.55	3.462(10)	162.2
C(9)-H(9B)...Br(1)#5	1.00	2.93	3.910(10)	165.6
C(26)-H(26B)...O(3)	0.99	2.33	2.92(3)	116.8
C(26A)-H(26C)...O(3)	0.99	2.65	3.17(2)	113.0
O(4A)-H(4A)...O(2S)#6	0.84	1.96	2.73(4)	151.5
C(27)-H(27A)...O(4A)	0.98	2.51	3.32(2)	140.9
C(27)-H(27A)...O(1S)	0.98	2.61	3.49(4)	149.8
C(27)-H(27C)...O(6)	0.98	2.39	3.016(14)	121.3
C(28)-H(28B)...S(1)#7	0.98	2.87	3.729(9)	146.5

C(28)-H(28C)...O(5)	0.98	2.65	3.193(12)	115.0
C(18)-H(18)...O(1)#1	1.00	2.45	3.435(9)	168.8
O(1S)-H(1S)...O(4)	0.84	1.99	2.76(4)	151.8
O(1S)-H(1S)...O(3S)	0.84	2.58	3.06(5)	117.6
C(12S)-H(12A)...Br(1)#8	0.98	2.98	3.71(4)	132.1
C(12S)-H(12B)...O(3S)	0.98	2.56	3.27(6)	129.3
O(2S)-H(2S)...O(4A)	0.84	2.37	3.06(4)	139.8
C(23S)-H(23B)...Br(1)#8	0.98	3.01	3.72(6)	130.4
O(3S)-H(3S)...O(4)#6	0.84	2.57	3.05(3)	117.7
O(3S)-H(3S)...O(3S)#6	0.84	2.52	3.14(6)	131.9
C(33S)-H(33C)...O(8)#6	0.98	2.57	3.17(2)	119.6
C(42S)-H(42B)...O(7)	0.98	2.58	3.48(5)	154.3

Symmetry transformations used to generate equivalent atoms:

#1 $-x+3/2, y-1/2, -z+1$ #2 $x, y, z-1$ #3 $x, y+1, z-1$
 #4 $-x+3/2, y+1/2, -z+1$ #5 $x, y, z+1$ #6 $-x+1, -y+1, z$
 #7 $-x+3/2, y-1/2, -z+2$ #8 $x, y-1, z+1$

APPENDIX 8

Progress Toward the Syntheses of bis-Tetrahydroisoquinoline Analogs[†]

A8.1 INTRODUCTION

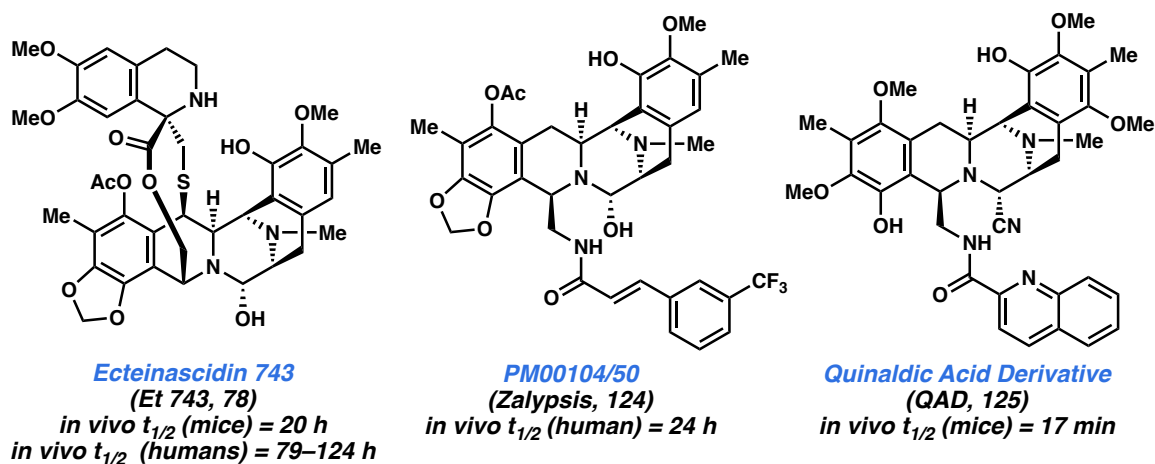
As shown in Chapter 3, we have successfully developed a modular synthesis of (–)-jorumycin (**77**) and (–)-jorunamycin A (**79**). With the remarkable biological activity conserved across the bis-tetrahydroisoquinoline (bis-THIQ) family of natural products,¹ we aim to further utilize the general synthetic strategy developed for the total synthesis of jorumycin to prepare non-natural bis-THIQ analogs for biological evaluation.

Of particular interest is the syntheses of electron-deficient bis-THIQ analogs. Since previous synthetic efforts have focused on the use of electrophilic aromatic substitution chemistry to access the core THIQ structure,² electron-deficient analogs have thus far been inaccessible, and consequently, their cytotoxic

[†] This research was performed in collaboration with Dr. Eric Welin and Dr. Gerit Pototschnig.

activities are not known. Additionally, studies have shown that metabolic stability (as measured by *in vivo* half-lives) varies greatly with different bis-THIQ molecules (Figure A8.1),³ and oxidative degradation is reported to be a major metabolic pathway.⁴ As a result, we believe that incorporation of electron-withdrawing atoms, particularly fluorine,⁵ might be able to improve the metabolic stability of these non-natural analogs (**124** and **125**). Our synthetic strategy, which exploits the tandem cross-coupling/hydrogenation approach outlined in Chapter 3, should allow for the introduction of a wide range of functionality regardless of their electronic nature. Overall, this research aims to generate bis-THIQ analog with simplified structure, while maintaining or improving both potency and metabolic stability.

Figure A8.1 Non-natural bis-THIQ analogs with their corresponding *in vivo* half-lives.

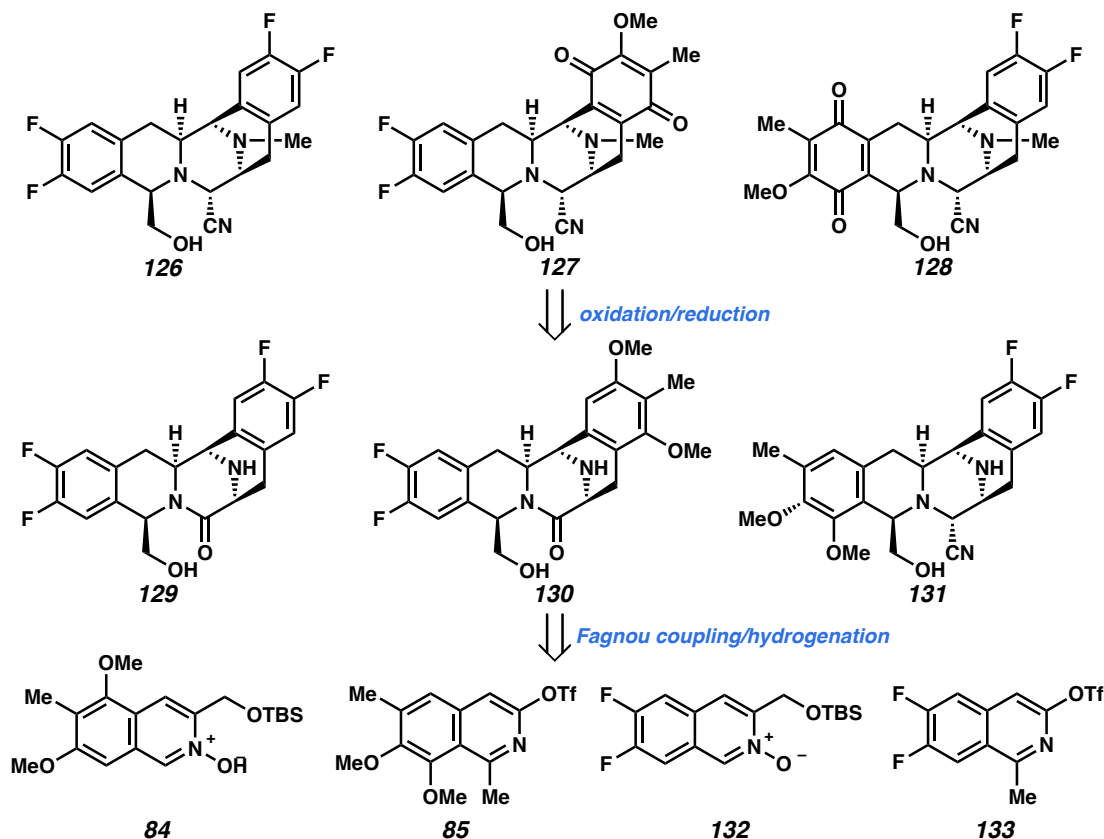


A8.2 APPROACH

Our initial efforts focused on the syntheses of polyfluorinated bis-THIQ analogs **126–128** (Scheme A8.1). These included all possible combinations of “natural” (**84** and **85**) and “fluorinated” (**132** and **133**) isoquinoline fragments that could be coupled via a

Fagnou reaction. Subsequently, we envisioned accessing the bis-THIQ pentacyclic cores **129–131** via the enantioselective hydrogenation developed in Chapter 3. At this stage, we hoped to probe the substrate tolerance of the previously established hydrogenation technology.

Scheme A8.1 Targeted polyfluorinated bis-THIQ analogs **126–128**.



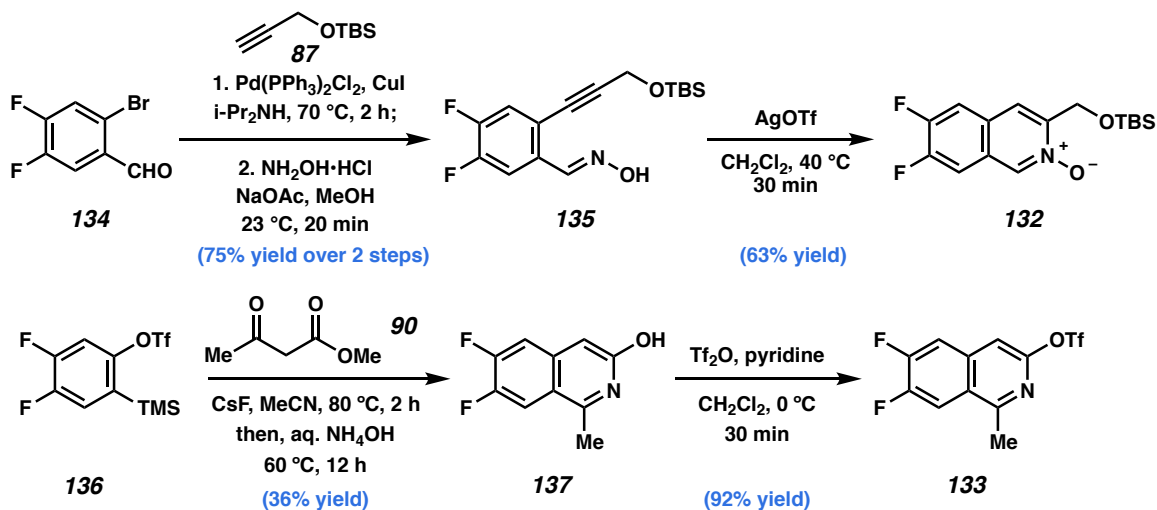
With the pentacyclic cores in hand, we planned to oxidize one of the termini (i.e., A- or E-rings) to the quinone oxidation state. We envisioned that the electronic differentiation between the A- and E-rings in bis-THIQs **130** and **131** should allow for the selective functionalization of the more electron-rich ring, leaving the difluorinated arene intact. This sequence would produce analogs **127–128**, which will allow us to systematically investigate whether reducing the electron density of the A-ring, E-ring, or

both rings improves metabolic stability. The general cytotoxicity of these analogs will also be evaluated against a range of cancer cell lines.

A8.2.1 Synthesis of Difluorinated isoquinolines **132** and **133**

We commenced our synthetic studies with the preparation of isoquinoline *N*-oxide **132** and isoquinoline triflate **133**. *N*-oxide **132** was synthesized via a 3-step protocol from commercially available 4,5-difluoro-2-bromobenzaldehyde (**134**). Sonogashira coupling of aryl bromide **134** with TBS-protected propargyl alcohol (**87**) provided an alkyne intermediate (not shown) in 89% yield. Condensation with hydroxylamine afforded oxime-bearing alkyne **135** in 84% yield, which was subsequently subjected to a silver-catalyzed 6-*endo-dig* cyclization to furnish 6,7-difluoroisoquinoline *N*-oxide **132** in 63% yield.

Scheme A8.2 Synthesis of isoquinoline *N*-oxide **132** and isoquinoline triflate **133**.



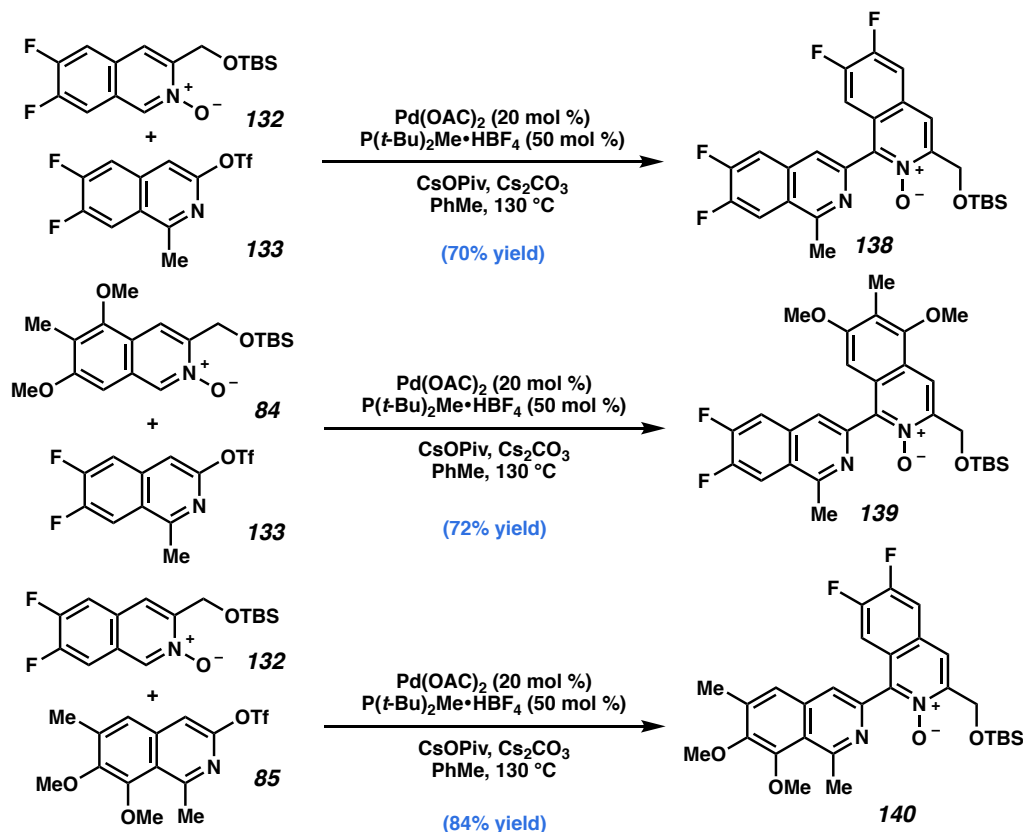
For the preparation of the isoquinoline triflate (**133**), we performed the aryne acyl-alkylation of *ortho*-silyl triflate **136**⁶ with in situ condensation to deliver 3-hydroxyisoquinoline **137** in 36% yield (Scheme A8.2). Attempt to further improve the yield via a 2-step procedure analogous to those performed in the synthesis of jorumycin

(see section 3.6.2.2) proved unsuccessful, providing isoquinoline **137** in only 15–25% yield over 2 steps. Finally, triflation of the resulting hydroxyisoquinoline **137** with triflic anhydride provided isoquinoline triflate **133** in 92% yield.

A8.2.2 Fagnou Coupling

As shown in Scheme A8.1, we envisioned employing the Fagnou coupling for the preparation of the bis-isoquinolines (bis-IQs). To our delight, we found that the developed reaction conditions (see Chapter 3) were amenable to the production of **138**–**140** (Scheme A8.3). Tetrafluorinated bis-IQ **138** was synthesized in 70% yield, and the excess *N*-oxide **132** could be recovered quantitatively. Furthermore, difluorinated bis-IQs **139** and **140** were also prepared in 72% yield and 84% yield, respectively, thus highlighting the modularity and flexibility of our developed synthetic strategy.

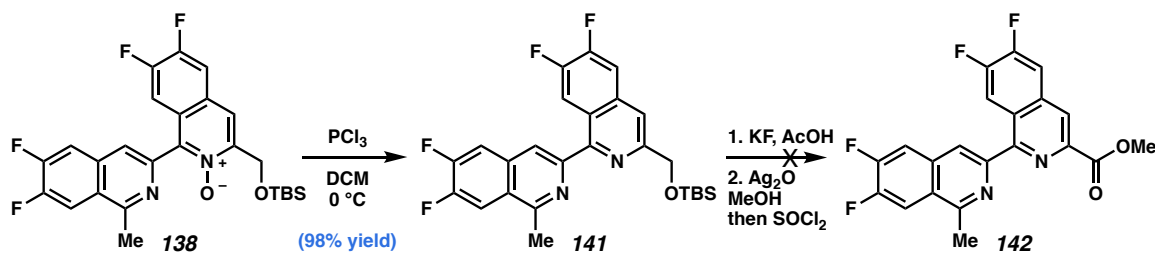
Scheme A8.3 Syntheses of bis-isoquinolines **138**–**140**.



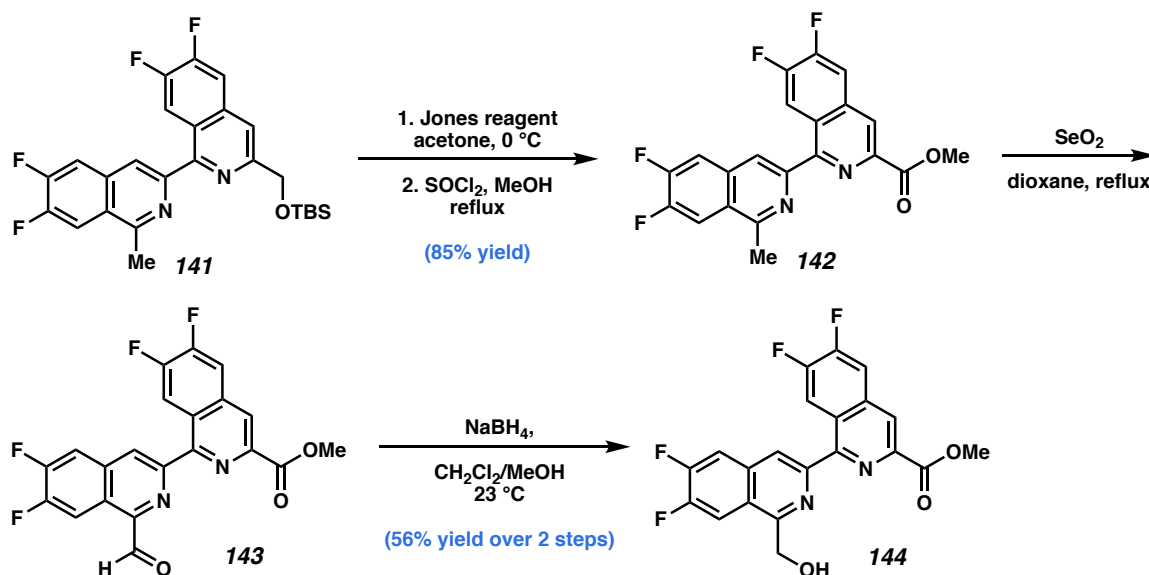
A8.2.3 Preparation of the Hydrogenation Precursors

The general sequence to access the hydrogenation precursors consists of deoxygenation, alcohol deprotection, oxidation of the benzyl alcohol to the methyl ester, and installation of the hydroxy group at the benzylic position of the western isoquinoline fragment. Tetrafluorinated bis-IQ *N*-oxide **138** smoothly underwent deoxygenation with phosphorus trichloride to provide bis-IQ **141** in 98% yield (Scheme A8.4). Unfortunately, upon the removal of the TBS group, the desired alcohol was only slightly soluble in organic solvents, resulting in difficulties in product purification. The subsequent oxidation using silver(I) oxide previously utilized in the total synthesis of jorumycin also failed to deliver the desired bis-IQ ester **142** in a synthetically useful yield.

Scheme A8.4 Attempt to prepare bis-IQ methylester **142**.



To circumvent these problems, we elected to exploit Jones reagent for the in situ cleavage of the TBS ether and oxidation of the resulting alcohol to the carboxylic acid oxidation state. Attempts to simultaneously esterify the carboxylic acid via Fischer esterification in the same pot proved unsuccessful, thus the crude carboxylic acid was converted to the methyl ester through the acid chloride intermediate (Scheme A8.5). With the bis-IQ ester **142** in hand, we next performed a selenium dioxide-mediated oxidation, followed by NaBH_4 reduction to install the hydroxy group in hydrogenation precursor **144**.

Scheme A8.5 Synthetic route to access tetrafluorinated bis-IQ hydrogenation precursor **144**.

We took a similar approach to prepare the difluorinated hydrogenation precursors. From difluorinated bis-IQ **139**, we were able to reduce the N-oxide, affording bis-IQ **145** in quantitative yield (Scheme A8.6). However, unexpectedly, the deprotection-oxidation of bis-IQ **145** via Jones reagent was sluggish, and increasing the temperature with prolonged reaction time did not improve the results (Table A8.1, entry 1). After 2 days, we still observed a mixture of deprotected alcohol, aldehyde, and carboxylic acid.

We next elected to remove the TBS protecting group and survey different oxidation conditions on alcohol **146**. Silver(I) oxidation afforded trace amounts of desired ester **149**, with the majority of the mass balance being unreacted starting material **146** (Table A8.1, entry 2). TEMPO oxidation, which was successfully employed in the total synthesis of jorumycin, resulted only in aldehyde **147** (entry 3). Lastly, N-heterocyclic carbene-catalyzed oxidation in methanol⁷ provided 2:1 mixture of aldehyde **147** and methyl ester **149** (entry 4).

The clean reaction profile from TEMPO oxidation (Table A8.1, entry 3) prompted us to subject the aldehyde product (**147**) to a subsequent Corey-Gillman-Ganem oxidation⁸ (entry 5). We were pleased to find that the desired methyl ester **149** was formed in 85% yield. Attempt to perform MnO₂ double oxidation directly on alcohol **146**, however, resulted in only 50% yield of the desired ester (entry 6).

Table A8.1 Optimization of the alcohol oxidation to access bis-IQ **149**.

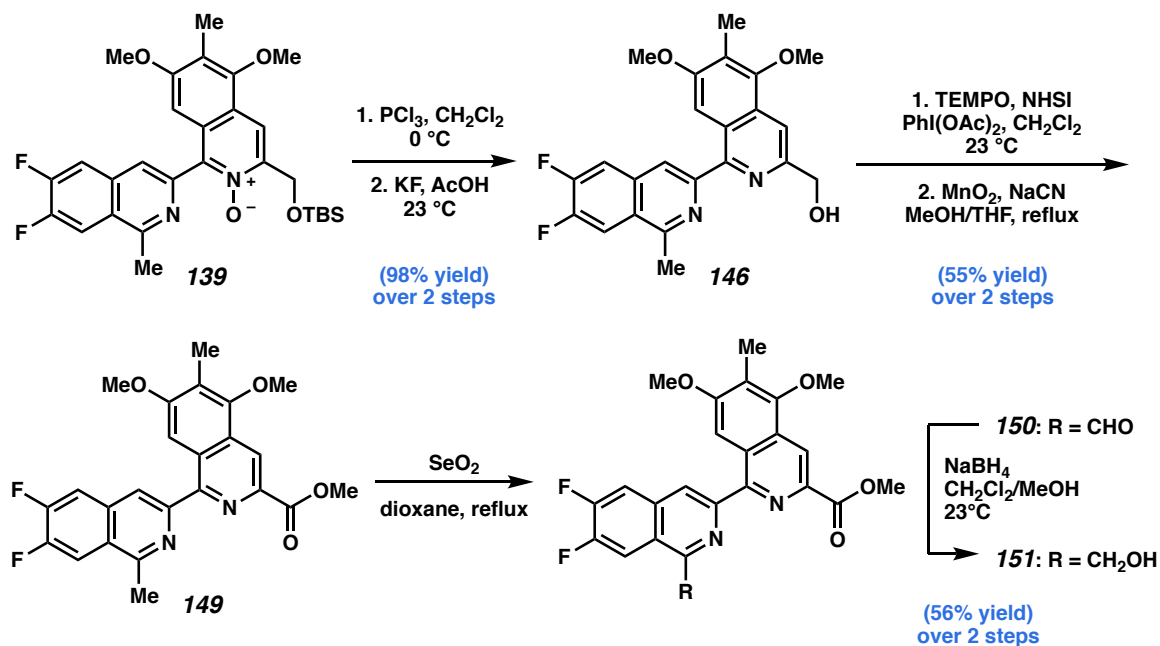
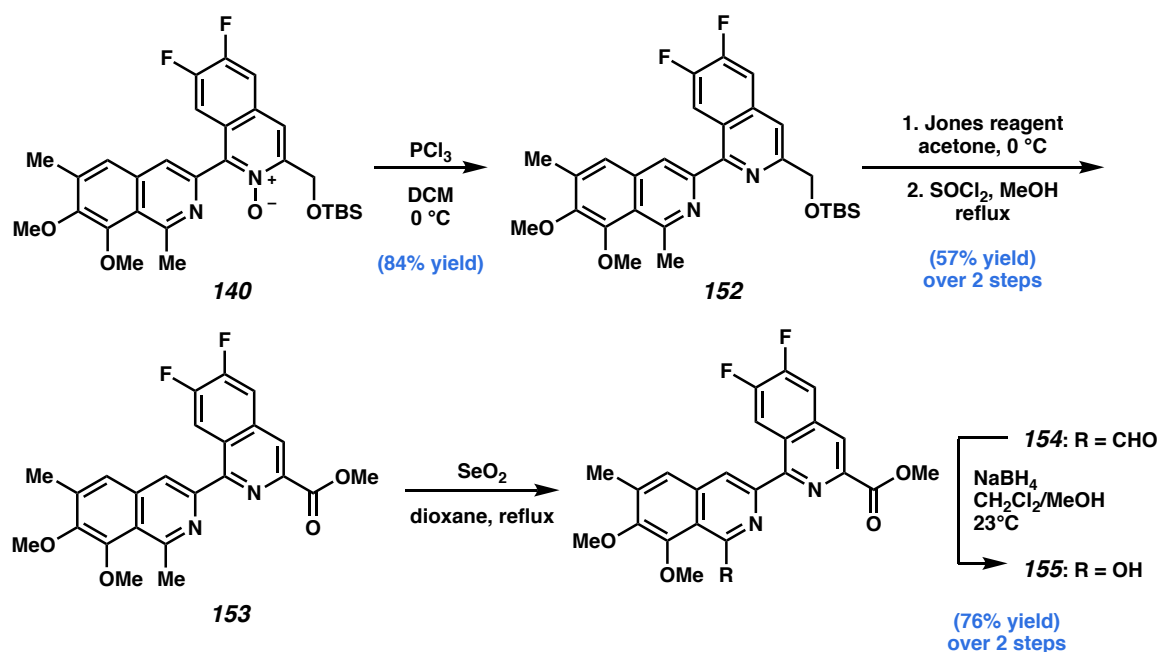
145: R = TBS
 146: R = H

147: X = H
 148: X = OH
 149: X = OMe

entry	conditions	146	147	148	149	note
1	Jones reagent, acetone 0 to 23 °C	some	some	some	–	used 145 instead of 146 as SM side pdt m/z = 431 (≈ 35%)
2	Ag ₂ O, MeOH, 23 °C	major	–	trace	trace	no change at 60 °C
3	TEMPO, PhI(OAc) ₂ NHSI ^a , DCM, 23 °C	–	major	–	–	no change after adding more equiv of NHSI/ TEMPO, no change with longer reaction time
4	MnO ₂ , NHC cat ^b DBU, MeOH, reflux	–	major ≈ 65%	–	minor ≈ 35%	low conversion at 23 °C
5	MnO ₂ , NaCN MeOH/THF, reflux	–	minor ≈ 15%	–	major ≈ 85%	aldehyde 147 was used as SM
6	MnO ₂ , NaCN MeOH/THF, reflux	–	≈ 50 %	–	≈ 50 %	reaction stalled after 18 hours

^aNHSI =
^bNHC cat =

With the oxidation conditions identified, we subsequently installed the hydroxyl group at the benzylic position in bis-IQ **149** by performing selenium dioxide-mediated oxidation, followed by NaBH₄ reduction of the resulting aldehyde to the corresponding alcohol. The modified sequence to access difluorinated hydrogenation precursor **151** is summarized in Scheme A8.6.

Scheme A8.6 Synthetic route to access difluorinated bis-IQ hydrogenation precursor **151**.**Scheme A8.7** Synthetic route to access difluorinated bis-IQ hydrogenation precursor **155**.

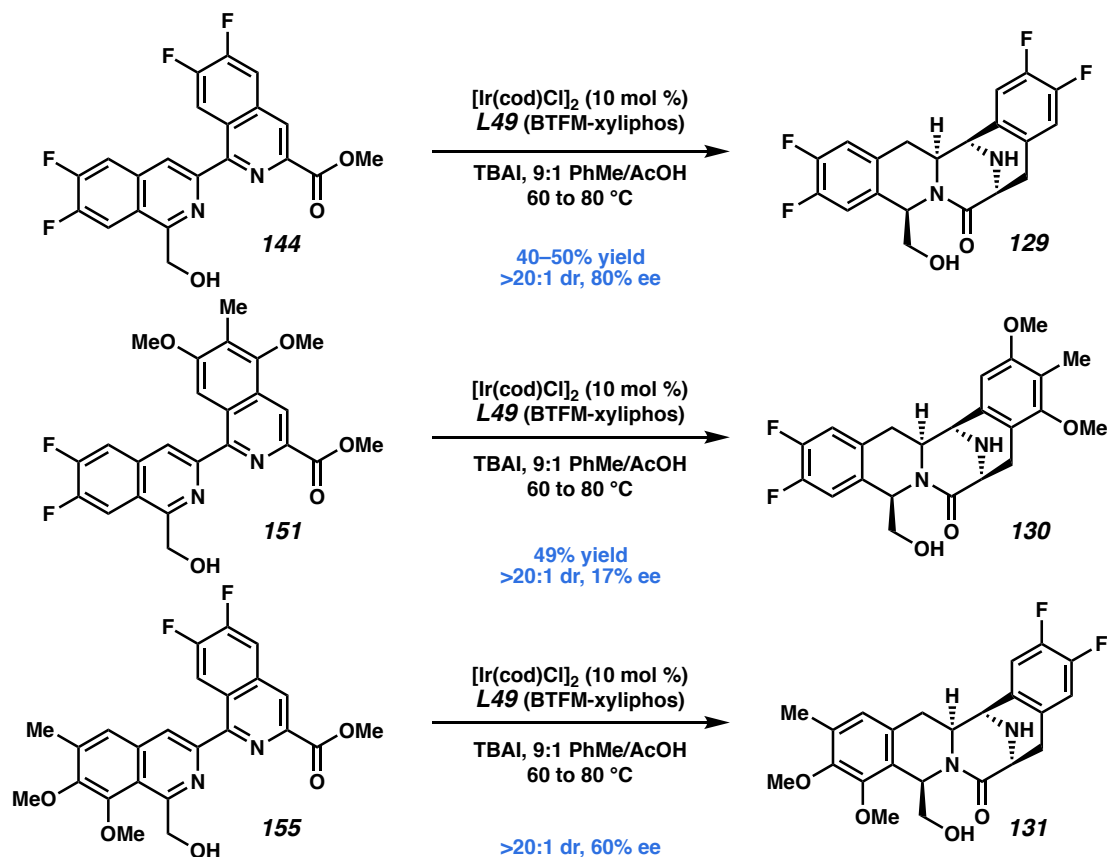
Difluorinated hydrogenation precursor **155**, having the difluorinated isoquinoline on the eastern side of the molecule, was prepared via the same sequence developed for tetrafluorinated bis-IQ **144**. Intermediates in this series behaved similarly to those in the

tetrafluorinated system, and difluorinated hydrogenation precursor **155** was obtained in 36% yield over 5 steps from bis-IQ **140** (Scheme A8.7).

A8.2.4 Ir-Catalyzed Enantioselective Hydrogenation

With polyfluorinated hydrogenation precursors **144**, **151**, and **155** in hand, we were able to examine the substrate tolerance of the developed enantioselective hydrogenation (Scheme A8.8). To our delight, tetrafluorinated bis-IQ **144** was hydrogenated, and in situ lactamization proceeded to deliver tetrafluorinated pentacycle **129** in 40–50% yield,⁹ with >20:1 dr and 80% ee. These results highlight the versatility of our key asymmetric hydrogenation as electronic variations have little impact on the reduction efficiency.

Scheme A8.8 Ir-catalyzed diastereo- and enantioselective hydrogenation.

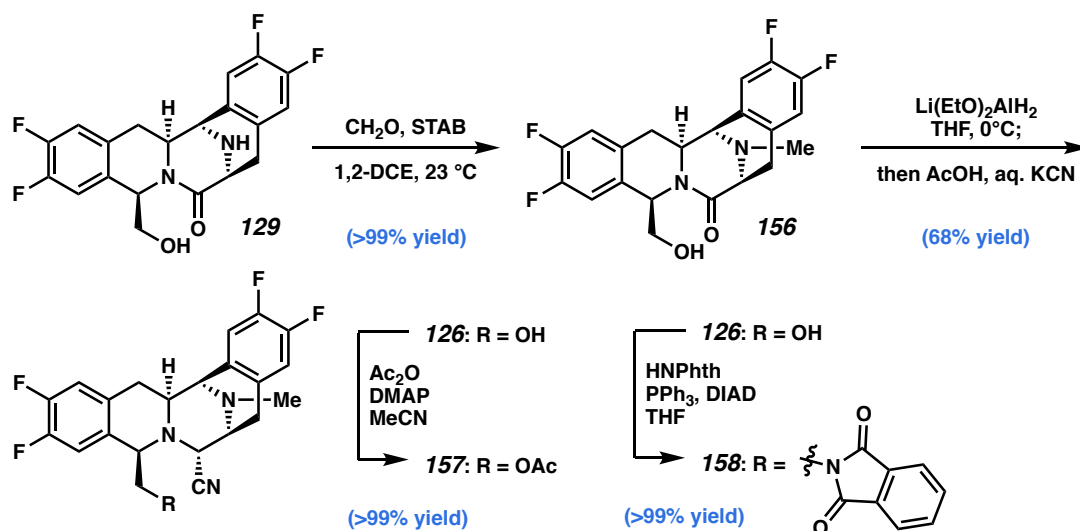


Intriguingly, however, isolated difluorinated pentacycles **130** and **131** were obtained in only 17% ee and 60% ee, respectively. Although additional experiments are required to fully understand the mode of enantioinduction, we currently attribute the observed loss in enantioselectivity to the less selective, competitive D-ring reduction (see Chapter 3, Scheme 3.7, Path B).

A8.2.5 End-route toward bis-THIQ analogs 126-128

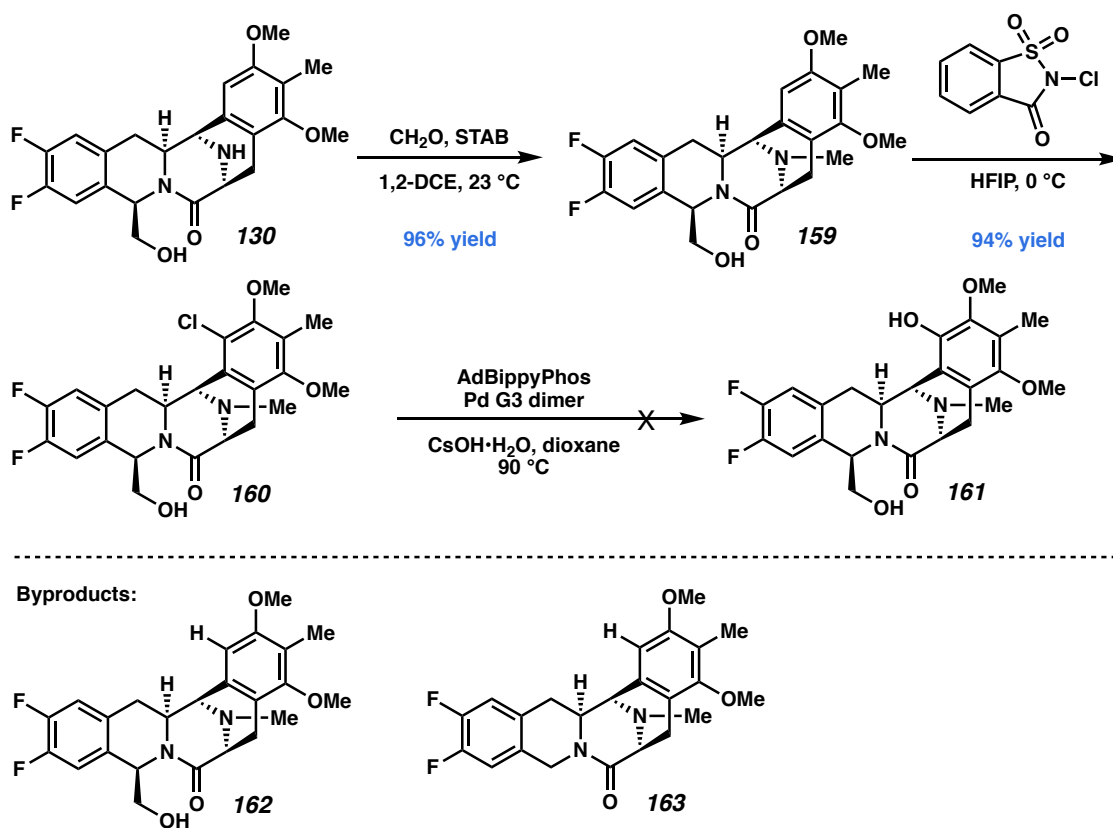
The final sequence in the synthesis of bis-THIQ analog **126** includes reductive amination and partial lactam reduction with cyanide trapping (Scheme A8.9). Reductive amination of **129** with aqueous formaldehyde and sodium triacetoxyborohydride (STAB) proceeded with quantitative yield. Finally, the partial reduction of lactam, followed by cyanide trapping provided the desired tetrafluorinated bis-THIQ analog (**126**) in 68% yield. We also synthesized two additional analogs in the tetrafluorinated series by 1) acylating the free alcohol in **126** to generate analog **157**, and 2) performing the Mitsunobu reaction to replace the alcohol with phthalimide (**158**).¹⁰

Scheme A8.9 Syntheses of tetrafluorinated bis-THIQ analog **126** and its derivatives.



Along the synthetic route to access difluorinated bis-THIQ **127** with fluorines in the western fragment (Scheme A8.10), we found that the electronic differentiation between the A- and E-rings was sufficient to selectively chlorinate only the more electron-rich E-ring, providing monochlorinated bis-THIQ **160** in 94% yield. Unfortunately, the Pd-catalyzed hydroxylation from the jorumycin synthesis failed to deliver the desired hydroxylated product **161**; we only observed protodechlorinated product **162** and oxidative deformylated-protodechlorinated product **163**.¹¹

Scheme A8.10 End-route toward difluorinated bis-THIQ analog **127**.



A8.3 CONCLUSIONS AND FUTURE DIRECTIONS

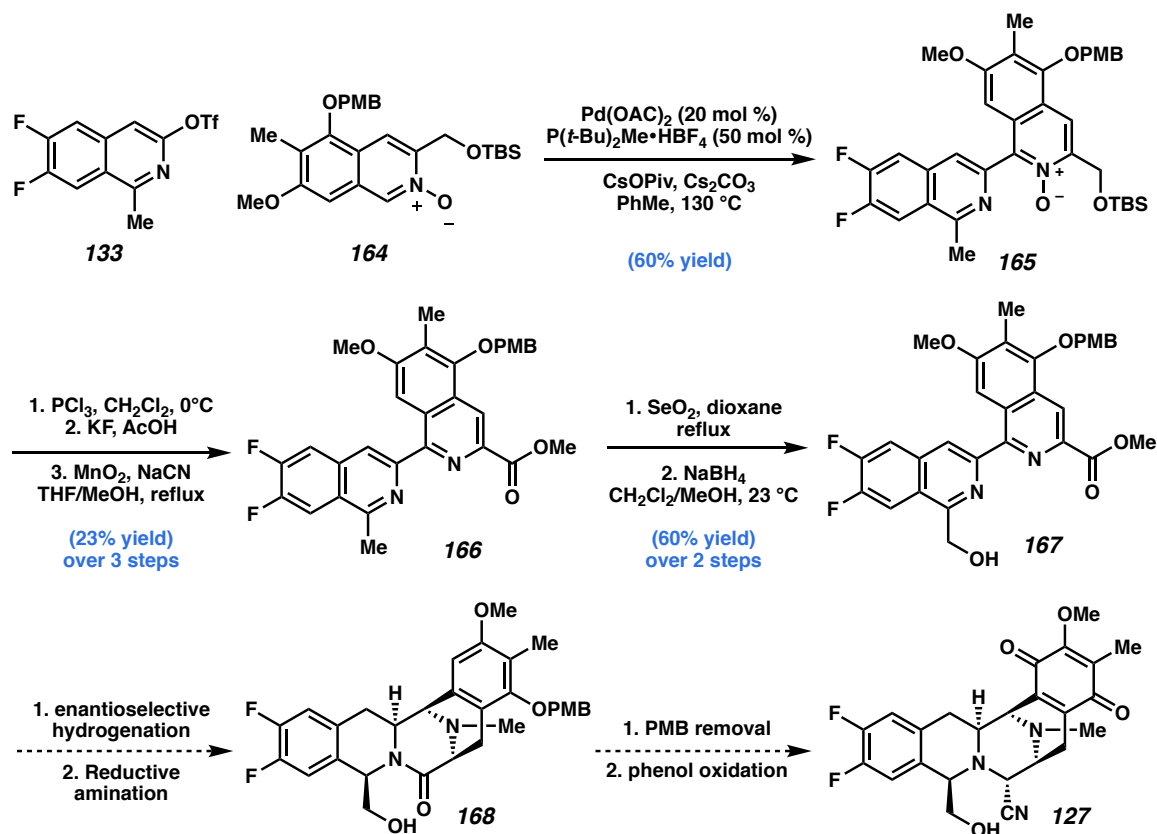
In conclusion, we have completed the syntheses of tetrafluorinated bis-THIQ analogs **126**, **157**, and **158** by exploiting the Fagnou coupling/hydrogenation strategy developed for the total synthesis of jorumycin. These non-natural analogs, which can be obtained in reasonable yields and with good enantioselectivity, highlight the flexibility of our developed synthetic strategy and represent the first set of electron-deficient bis-THIQ analogs produced to date. Studies to evaluate their biological activity by our collaborators at the UCLA Translational Oncology Research Laboratories are currently underway.

Given the difficulty in the Pd-catalyzed hydroxylation reaction encountered en route to difluorinated bis-THIQ **127**, one strategy moving forward is the use of different phenol protecting group such as *p*-methoxybenzyl, instead of methyl, on the eastern isoquinoline fragment (cf. **164**, Scheme A8.11). Upon removal of the PMB group in **168**, we envisioned that phenol oxidation by salcomine/O₂¹² should directly provide analog **127**, thus bypassing the requirement of the challenging C–O coupling reaction. Initial efforts to access bis-IQ **167** demonstrated that the Fagnou coupling between IQ-triflate **133** and IQ *N*-oxide **164**¹³ delivered bis-IQ product **165** in 60% yield. Deoxygenation, desilylation, followed by oxidation of **165** generated **166** in 23% yield over 3 steps. Lastly, PMB-protected bis-IQ hydrogenation precursor **167** was prepared in 60% yield from the selenium oxidation-sodium borohydride reduction sequence.

Should the subsequent steps in this strategy fail to deliver the desired bis-IQ analog **127**, future directions of this research will focus on exploring different conditions for late-stage hydroxylation. The lithiation/borylation/oxidation

sequence¹⁴ and the direct aromatic C–H oxygenation developed by Ritter¹⁵ are of interest. Furthermore, a collaboration with the Arnold lab, exploiting the power of biocatalysis for this oxidation, also represents an alternative strategy.

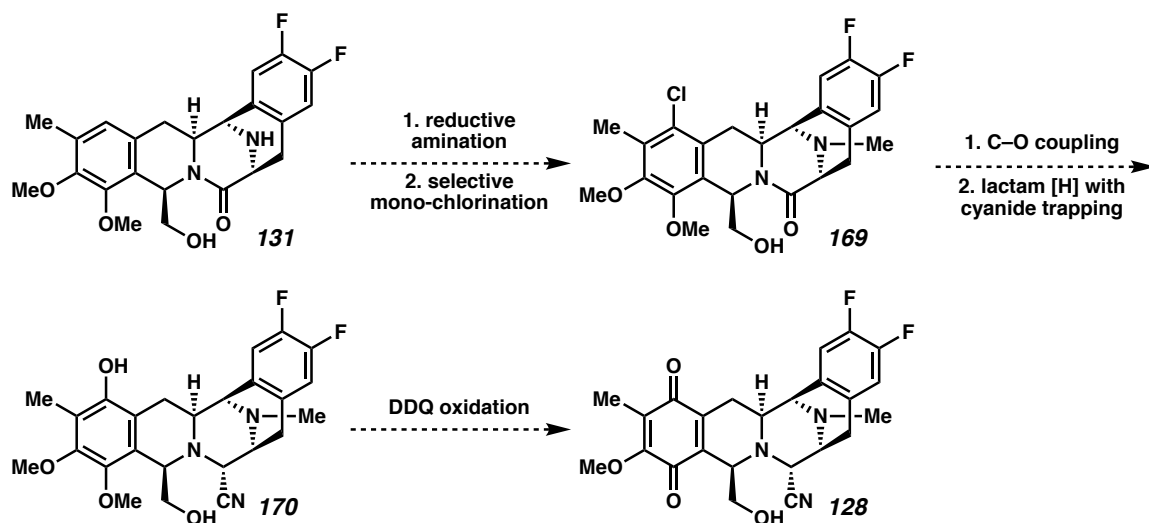
Scheme A8.11 Alternative strategy to access difluorinated bis-THIQ analog **127**.



Finally, we still have not yet been successful in obtaining difluorinated bis-IQ analog **128**. However, based on the results observed in the preparation of mono-hydroxylated analogs **103** and **104** (see Chapter 3), we expect the Pd-catalyzed C–O coupling to be more facile on the A-ring. The remaining steps to access this analog (**128**) is shown in A8.12. Once we have these additional difluorinated bis-THIQ analogs in hand, a systematic investigation into the effects of electronic variations of the A- and E-rings can be achieved. Using data from the toxicity screening and drug metabolism-

pharmacokinetic (DMPK) studies, we aim to design the next generation of bis-THIQ analogs with improved biological properties and metabolic stability.

Scheme A8.12 End-route toward difluorinated bis-THIQ analog **128**.



A8.4 EXPERIMENTAL SECTION

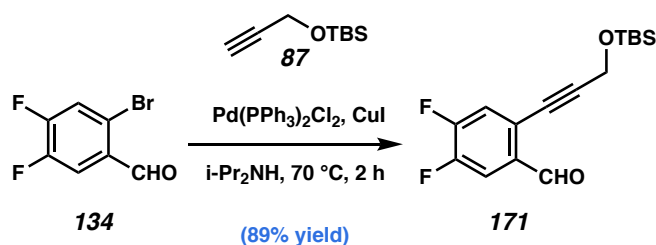
A8.4.1 MATERIALS AND METHODS

Unless stated otherwise, reactions were performed at ambient temperature (23 °C) in flame-dried glassware under an argon atmosphere using dry, deoxygenated solvents (distilled or passed over a column of activated alumina).¹⁶ Commercially available reagents were used as received. Reactions requiring external heat were modulated to the specified temperatures using an IKAmag temperature controller. Thin-layer chromatography (TLC) was performed using E. Merck silica gel 60 F254 pre-coated plates (0.25 mm) and visualized by UV fluorescence quenching or potassium permanganate staining. Silicycle SiliaFlash P60 Academic Silica gel (particle size 40–63 μm) was used for flash chromatography. Purified water was obtained using a Barnstead NANOpure Infinity UV/UF system. ¹H and ¹³C NMR spectra were recorded on a Varian

Inova 500 (500 MHz and 125 MHz, respectively) and a Bruker AV III HD spectrometer equipped with a Prodigy liquid nitrogen temperature cryoprobe (400 MHz and 100 MHz, respectively), and are reported in terms of chemical shift relative to CHCl_3 (δ 7.26 and 77.16, respectively). ^{19}F and ^{31}P NMR spectra were recorded on a Varian Inova 300 (282 MHz and 121 MHz, respectively). Data for ^1H NMR spectra are reported as follows: chemical shift (δ ppm) (multiplicity, coupling constant, integration). Infrared (IR) spectra were recorded on a Perkin Elmer Paragon 1000 Spectrometer and are reported in frequency of absorption (cm^{-1}). Analytical chiral HPLC was performed with an Agilent 1100 Series HPLC utilizing Chiralpak (AD) or Chiralcel (OJ) columns (4.6 mm x 25 cm) obtained from Daicel Chemical Industries, Ltd. High resolution mass spectra (HRMS) were obtained from the Caltech Center for Catalysis and Chemical Synthesis using an Agilent 6200 series TOF with an Agilent G1978A Multimode source in mixed (Multimode ESI/APCI) ionization mode. Optical rotations were measured on a Jasco P-2000 polarimeter using a 100 mm path-length cell at 589 nm.

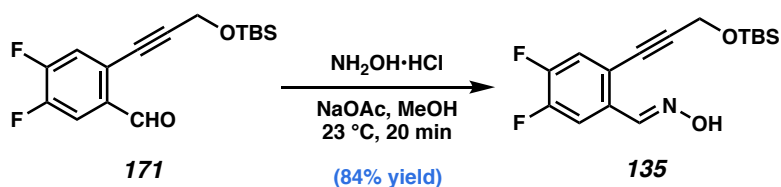
A8.4.2 EXPERIMENTAL PROCEDURES AND SPECTROSCOPIC DATA

A8.4.2.1 Synthesis of difluorinated isoquinoline *N*-oxide **132**



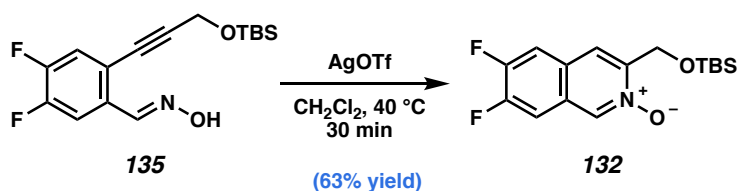
Sonogashira product 171: 2-bromide-4,5-difluorobenzaldehyde (**134**) (9.00 g, 40.7 mmol, 1 equiv), $(\text{PPh}_3)_2\text{PdCl}_2$ (1.43 g, 2.04 mmol, 0.05 equiv), and CuI (388 mg, 2.04 mmol, 0.05 equiv) were slurried in diisopropylamine (160 mL, 0.25 M, freshly distilled

from CaH_2), and the suspension was sparged with N_2 for 10 min. *O*-tert-butyltrimethylsilyl propargyl alcohol (**87**, 8.32 g, 48.9 mmol, 1.35 equiv)¹⁷ was added in one portion, causing the suspension to darken as the palladium catalyst was reduced, and the reaction mixture was heated to 70 °C. After 2 hours, TLC indicated complete conversion of bromide **134**, so the suspension was cooled to room temperature and celite was added. The mixture was filtered through a pad of celite and eluted with Et_2O . The filtrate was concentrated and purified by column chromatography (5% Et_2O /hexanes) to afford **171** as a colorless solid (11.30 g, 89% yield); ^1H NMR (500 MHz, CDCl_3) δ 10.38 (d, $J = 3.2$ Hz, 1H), 7.72 (dd, $J = 10.0, 8.2$ Hz, 1H), 7.34 (dd, $J = 10.1, 7.1$ Hz, 1H), 4.58 (s, 2H), 0.94 (s, 9H), 0.16 (s, 6H); ^{13}C NMR (100 MHz, CDCl_3) δ 189.3, 153.8 (dd, $J = 259.6, 13.8$ Hz), 151.0 (dd, $J = 255.6, 13.1$ Hz), 133.7 (dd, $J = 4.5, 3.3$ Hz), 124.0 (dd, $J = 8.9, 3.8$ Hz), 122.1 (d, $J = 19.3$ Hz), 116.3 (dd, $J = 18.5, 2.4$ Hz), 96.1 (d, $J = 2.0$ Hz), 78.4 (t, $J = 1.9$ Hz), 52.19, 25.91, 18.47, -5.00 .



Difluorinated oxime 135: Aldehyde **171** (11.30 g, 36.4 mmol, 1.0 equiv) was dissolved in MeOH (75 mL, 0.5 M), and to the solution was added NaOAc (6.57 g, 80.1 mmol, 2.2 equiv). The solution was then stirred at room temperature for 5 minutes. Hydroxylamine hydrochloride (2.78 g, 40.0 mmol, 1.1 equiv) was added in one portion and NaCl began to precipitate immediately. After 20 minutes, TLC revealed complete consumption of the starting material, so the reaction was quenched with saturated aqueous NaHCO_3 and diluted with H_2O . The layers were separated and the aqueous phase was extracted with

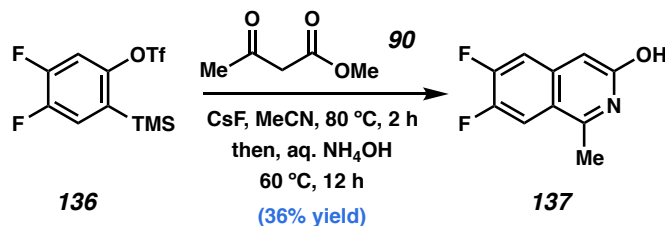
CH₂Cl₂ three times. The combined organic phases were washed with brine, dried over Na₂SO₄, and concentrated. The crude material was purified by column chromatography (10% Et₂O/hexanes) to provide **135** (10.00 g, 84% yield) as a colorless solid. ¹H NMR indicates 10:1 mixture of E:Z isomers; ¹H NMR of (*E*)-isomer (300 MHz, CDCl₃) δ 8.51 (d, *J* = 1.7 Hz, 1H), 7.63 (dd, *J* = 11.1, 8.2 Hz, 1H), 7.25 – 7.18 (m, 1H), 4.56 (s, 2H), 0.94 (s, 9H), 0.17 (s, 6H).



Difluorinated isoquinoline *N*-oxide 132: Oxime **135** (10.0 g, 30.7 mmol, 1 equiv) was dissolved in CH₂Cl₂ (300 mL, 0.1 M) and the flask was vacuum purged and refilled with nitrogen five times, then heated to reflux. AgOTf (158 mg, 0.61 mmol, 0.02 equiv) was added in one portion to the refluxing solution, resulting in a rapid and mildly exothermic reaction. The reaction flask was shielded from light and maintained at reflux for 15 min, at which time LCMS indicated full consumption of the starting material. The solution was filtered through a pad of silica with CH₂Cl₂ and 10% MeOH/EtOAc, then concentrated. The crude material was purified by column chromatography (20–50–100% EtOAc/hexanes + 1% NEt₃ ; then 10% MeOH/EtOAc + 1% NEt₃) to afford *N*-oxide **132** (6.30g, 63% yield) as a colorless solid.; ¹H NMR (300 MHz, CDCl₃) δ 8.72 (s, 1H), 7.84 (s, 1H), 7.59 (dd, *J* = 10.0, 7.5 Hz, 1H), 7.47 (dd, *J* = 9.8, 7.7 Hz, 1H), 5.00 (s, 2H), 1.00 (s, 9H), 0.19 (s, 6H); ¹³C NMR (100 MHz, CDCl₃) δ 151.9 (dd, *J* = 256.2, 15.8 Hz), 151.8 (dd, *J* = 255.0, 16.0 Hz), 149.2–149.3 (m), 135.4 – 135.3 (m), 126.5 (dd, *J* = 8.0, 1.4 Hz), 125.7 – 125.5 (m), 119.9 (dd, *J* = 5.4, 1.7 Hz), 113.6 (dd, *J* = 18.1, 1.2 Hz),

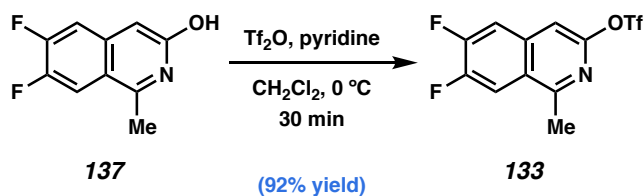
111.0 (d, $J = 18.7$ Hz), 60.2, 26.2, 18.6, -5.1 ; ^{19}F NMR (282 MHz, CDCl_3) δ -131.01 – -131.19 (m), -131.73 – -131.92 (m).

A8.4.2.2 Synthesis of difluorinated isoquinoline triflate **133**



6,7-Difluoro-1-methyl-3-hydroxyisoquinoline (137**):**¹⁸ Cesium fluoride (2.64 g, 17.4 mmol, 2.5 equiv) was dissolved in acetonitrile (35 mL, 0.2 M based on methyl acetoacetate) in a Schlenk flask and methyl acetoacetate (0.75 mL, 6.94 mmol, 1.0 equiv) was added. Aryne precursor **136**⁶ (2.90 g, 8.67 mmol, 1.25 equiv) was added neat via syringe dropwise, and the flask was placed in a preheated 80 °C oil bath. After 2 h, TLC revealed complete consumption of **136**, so aqueous NH₄OH (28–30%, 35 mL) was added in one portion. The flask was then capped, moved to a preheated 60 °C oil bath and stirred for 12 h. The solution was poured into brine inside a separatory funnel and the solution was extracted with EtOAc three times. The aqueous phase was brought to pH 7 by the addition of 2M HCl and was extracted with EtOAc twice. The aqueous phase was discarded. The organic phase was then extracted with 2M HCl three times. The organic phase was analyzed by LCMS to confirm that all of product **137** had transferred to the aqueous phase, and was subsequently discarded. The aqueous phase was then brought back to pH 7 by the addition of 5M NaOH and was extracted with EtOAc (5x 20 mL). The combined organic phases were washed with brine, dried over MgSO₄ and concentrated, providing the product (488 mg, 36% yield) as a yellow solid. *Note: The*

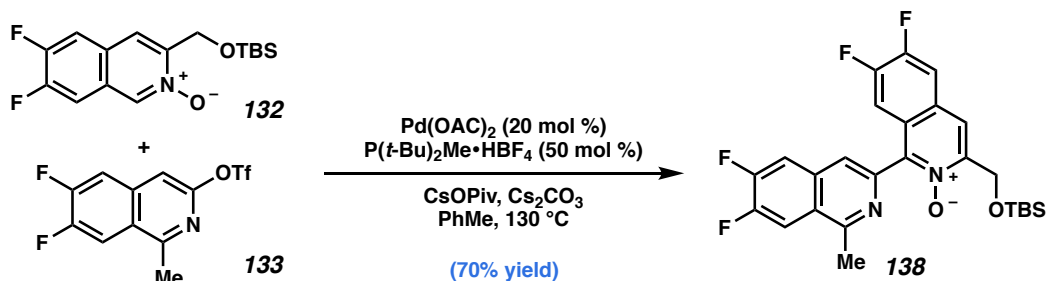
product is not soluble in CDCl_3 . Characterization data match those reported in the literature.¹⁸



Difluoroisoquinoline triflate 133: Hydroxyisoquinoline **137** (43.6 mg, 0.223 mmol, 1.0 equiv) was dissolved in CH_2Cl_2 (1.1 mL, 0.2 M) and pyridine (0.18 mL, 2.23 mmol, 10 equiv) was added and the solution was cooled to 0 °C. Trifluoromethanesulfonic anhydride (Tf_2O , 75 μL , 0.446 mmol, 2.0 equiv) was added dropwise, causing the yellow solution to turn dark red. After 30 minutes, TLC (30% EtOAc/hexanes) revealed complete consumption of **137**, so the reaction was quenched by the addition of saturated aqueous NaHCO_3 . The solution was stirred vigorously until bubbling ceased, at which time the layers were separated. The organic phase was extracted with CH_2Cl_2 and the combined organic phases were washed with brine, dried over Na_2SO_4 , and concentrated. The crude product was purified by column chromatography (15% EtOAc/hexanes) to provide **133** (70.1 mg, 96% yield) as a pale yellow oil; ^1H NMR (500 MHz, CDCl_3) δ 7.94 – 7.86 (m, 1H), 7.63 (dd, $J = 9.9, 7.5$ Hz, 1H), 7.37 (s, 1H), 2.92 (s, 3H).

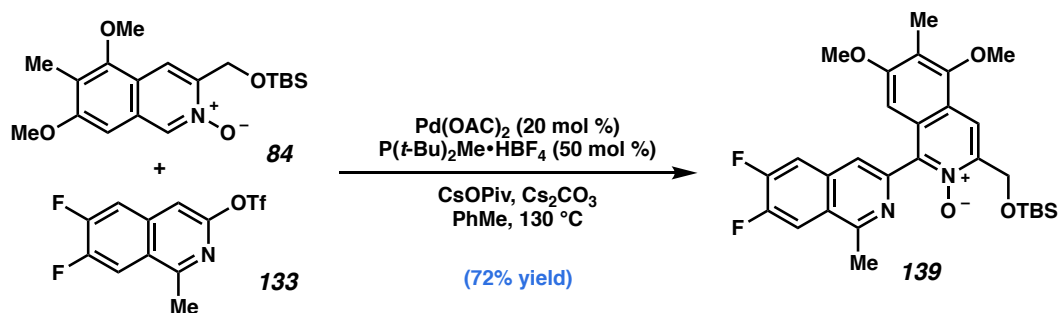
A8.4.2.3 Fagnou coupling

General Procedure 1: Fagnou coupling

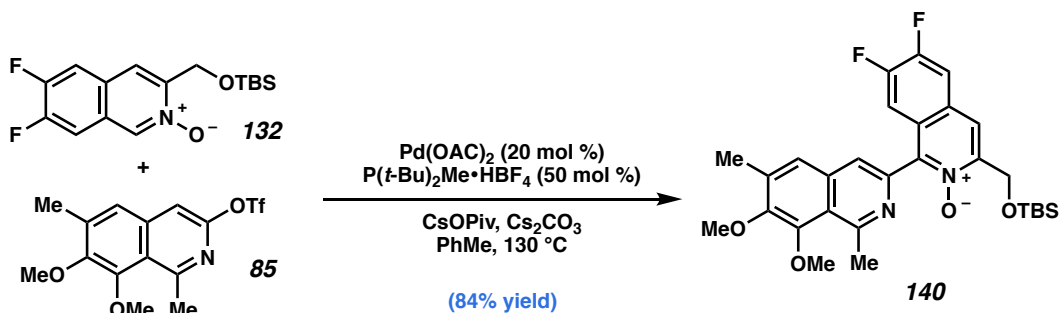


Tetrafluorinated bis-isoquinoline N-oxide 138: Palladium acetate (48.7 mg, 0.217 mmol, 0.2 equiv), di-*tert*-butyl (methyl)phosphonium tetrafluoroborate (135 mg, 0.543 mmol, 0.5 equiv), and cesium carbonate (141 mg, 0.434 mmol, 0.4 equiv) were weighed into a pear-shaped flask and brought into a nitrogen-filled glovebox. Cesium pivalate (CsOPiv, 102 mg, 0.434 mmol, 0.4 equiv) was added to the flask. In the glovebox, degassed toluene (5 mL) was added to the flask, and it was sealed with a rubber septum and removed from the glovebox. The flask was placed in a 60 °C preheated oil bath, where it was stirred for 30 min after which the reaction mixture turned from orange to golden yellow. In the meantime, *N*-oxide **132** (1.06 g, 3.26 mmol, 3 equiv) and cesium carbonate (0.92 g, 2.82 mmol, 2.6 equiv) were weighed into a sealable flask equipped with a Kontes valve, to which 15 mL toluene was added, and this suspension was sparge-degassed with nitrogen for 10 min. Isoquinoline triflate **133** (355 mg, 1.09 mmol, 1.0 equiv) was dissolved in 2.5 mL toluene, which was sparge-degassed with nitrogen for 10 min. The solution of isoquinoline triflate **85** was then added via cannula to the catalyst solution while at 60 °C, and the flask was rinsed with 2 mL degassed toluene. The catalyst/triflate solution was then added via cannula to the *N*-oxide solution and rinsed with 2 mL degassed toluene. The flask was sealed and placed in a 130 °C preheated oil bath. After 12 h, TLC and LCMS indicated full consumption of isoquinoline triflate **133**, so the flask was allowed to cool to room temperature and Celite (2 g) was added. This suspension was then filtered through a pad of Celite that was topped with sand and rinsed with CH₂Cl₂ and acetone. The solution was concentrated and subsequently purified by column chromatography (20–50–100% EtOAc/hex, then 10–20% MeOH/EtOAc + Et₃N) to afford bis-Isoquinoline **138** as a colorless foam (382 mg, 70% yield). Excess

isoquinoline *N*-oxide **132** was obtained after 10–20% MeOH/EtOAc flush, and recovered quantitatively (706 mg, 2.17 mmol); ^1H NMR (300 MHz, CDCl_3) δ 8.02 – 7.89 (m, 3H), 7.63 (dd, J = 10.0, 7.7 Hz, 2H), 7.25 (dd, J = 11.4, 7.7 Hz, 1H), 5.03 (s, 2H), 3.00 (s, 3H), 1.01 (s, 9H), 0.19 (s, 6H); ^{19}F NMR (282 MHz, CDCl_3) δ –129.11 – –129.66 (m), –130.73 – –131.26 (m), –131.66 – –132.03 (m), –132.17 – –132.68 (m). Due to an overlap of a product peak with a residual CHCl_3 solvent peak, we also obtained ^1H spectra in CD_2Cl_2 ; ^1H NMR (400 MHz, CD_2Cl_2) δ 8.00 (dd, J = 11.0, 7.8 Hz, 1H), 7.96 – 7.89 (m, 2H), 7.67 (ddd, J = 12.9, 10.3, 7.8 Hz, 2H), 7.23 (dd, J = 11.7, 7.9 Hz, 1H), 4.98 (s, 2H), 2.97 (s, 3H), 1.03 (s, 9H), 0.21 (s, 6H). Multiple ^{13}C – ^{19}F couplings in product **138** resulted in complicated ^{13}C spectra. The multiplicities and coupling constants of the following signals have not been assigned: ^{13}C NMR (100 MHz, CD_2Cl_2) δ 154.7, 154.5, 152.7, 152.7, 152.6, 152.5, 152.4, 152.1, 152.0, 150.2, 150.2, 150.1, 150.0, 150.0, 149.9. We expect these signals to correspond to the four carbons adjacent to the four fluorine atoms. The rest of the ^{13}C signals are assigned as follows: ^{13}C NMR (100 MHz, CD_2Cl_2) δ 159.4 (dd, J = 5.4, 1.6 Hz), 149.7 – 149.5 (m), 143.7 (dd, J = 5.8, 2.9 Hz), 143.3 (d, J = 2.7 Hz), 134.2 (dd, J = 8.8, 1.3 Hz), 126.6 (dd, J = 8.1, 1.3 Hz), 126.0 (dd, J = 8.3, 1.3 Hz), 124.8 (d, J = 5.4 Hz), 122.8 – 120.7 (m), 120.2 – 118.4 (m), 114.3 (d, J = 17.0 Hz), 113.7 (d, J = 17.2 Hz), 113.0 (dd, J = 17.4, 1.3 Hz), 112.0 (d, J = 20.0 Hz), 60.6, 26.1, 22.9, 18.7, –5.2. *Note: Future characterization efforts should focus on simplifying the data by obtaining ^{13}C spectrum with simultaneous ^1H and ^{19}F decoupled (^{13}C – $\{^1\text{H}, ^{19}\text{F}\}$).*

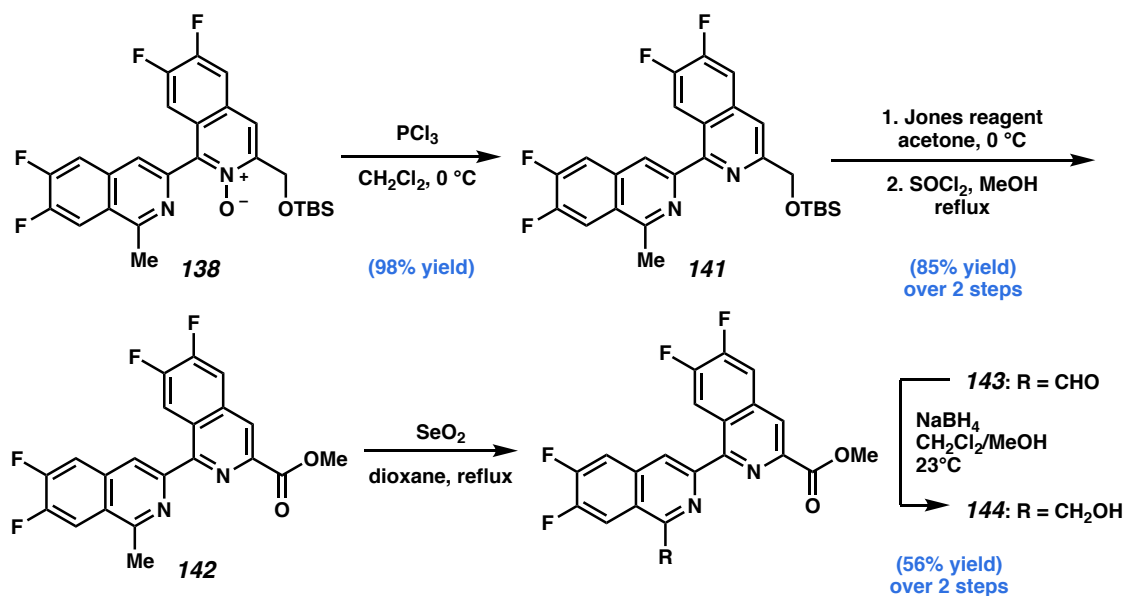


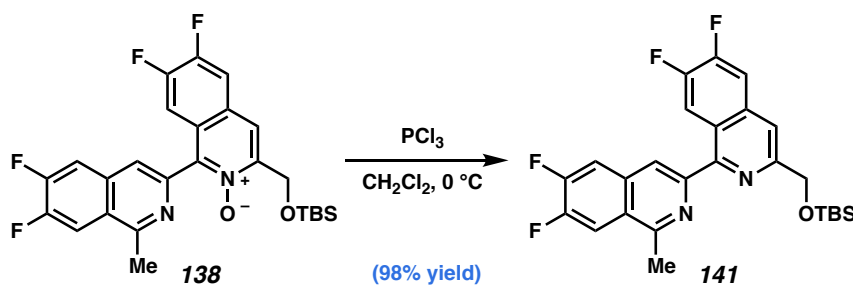
Difluorinated bis-isoquinoline *N*-oxide 139: Prepared according to General Procedure 1 using *N*-Oxide **84** (1.82 g, 5.00 mmol, 3.0 equiv) and isoquinoline triflate **133** (545 mg, 1.65 mmol, 1.0 equiv). Reaction completed after 5 hours. The crude material was purified by column chromatography (30–40–50–60–70–100% EtOAc/hex, then 10% MeOH/EtOAc + 1% Et₃N) to afford bis-Isoquinoline **139** as a white solid (647 mg, 72% yield); ¹H NMR (400 MHz, CDCl₃) δ 8.17 – 8.05 (m, 1H), 8.00 – 7.89 (m, 2H), 7.62 (dd, $J = 10.2, 7.8$ Hz, 1H), 6.49 (s, 1H), 5.06 (d, $J = 1.3$ Hz, 2H), 3.91 (s, 3H), 3.64 (s, 3H), 2.99 (s, 3H), 2.29 (s, 3H), 1.03 (s, 9H), 0.18 (s, 6H); ¹³C NMR (100 MHz, CDCl₃) δ 159.17, 158.75 (dd, $J = 5.4, 1.5$ Hz), 153.87, 153.20 (dd, $J = 219.2, 15.6$ Hz), 150.66 (dd, $J = 216.6, 15.7$ Hz), 146.06, 143.94 (d, $J = 2.7$ Hz), 143.11, 134.05 (dd, $J = 8.6, 1.1$ Hz), 128.08, 124.33 (dd, $J = 6.3, 1.3$ Hz), 123.02, 120.50, 114.88, 113.94 (d, $J = 16.8$ Hz), 112.60 (dd, $J = 17.4, 1.3$ Hz), 98.07, 61.81, 60.33, 55.62, 26.03, 22.76, 18.46, 9.72, – 5.21; ¹⁹F NMR (282 MHz, CDCl₃) δ –129.98 (dt, $J = 23.4, 8.8$ Hz), –131.28 – –132.39 (m); IR (thin film, NaCl): 2952, 2856, 161, 1516, 1464, 1430, 1326, 1250, 1188, 1136, 1117, 858, 838, 845, 777, 756; HRMS (ESI-TOF) calc'd for $[\text{M}+\text{H}^+]$ C₂₉H₃₅F₂N₂O₄Si = 541.2329, found 541.2326.



Difluorinated bis-isoquinoline *N*-oxide 140: Prepared according to General Procedure 1 using *N*-Oxide **132** (2.44 g, 7.50 mmol, 3.0 equiv) and isoquinoline triflate **85** (913 mg, 2.50 mmol, 1.0 equiv). Reaction completed after 5 hours. The crude material was purified by column chromatography (20–30–50% EtOAc/hex, then 10% MeOH/EtOAc + 1% Et_3N) to afford bis-Isoquinoline **140** as a colorless solid (1.14 g, 84% yield); ^1H NMR (300 MHz, CDCl_3) δ 7.88 (s, 1H), 7.80 (s, 1H), 7.60 (dd, $J = 10.0, 7.7$ Hz, 1H), 7.42 (s, 1H), 7.31 (dd, $J = 11.5, 7.8$ Hz, 1H), 5.03 (s, 2H), 4.02 (s, 3H), 3.98 (s, 3H), 3.17 (s, 3H), 2.46 (s, 3H), 1.01 (s, 9H), 0.18 (s, 6H); ^{19}F NMR (282 MHz, CDCl_3) δ –132.48 (ddd, $J = 19.5, 11.5, 7.7$ Hz), –132.99 (ddd, $J = 20.6, 10.0, 7.9$ Hz).

A8.4.2.4 Syntheses of hydrogenation precursors 144, 151, and 155

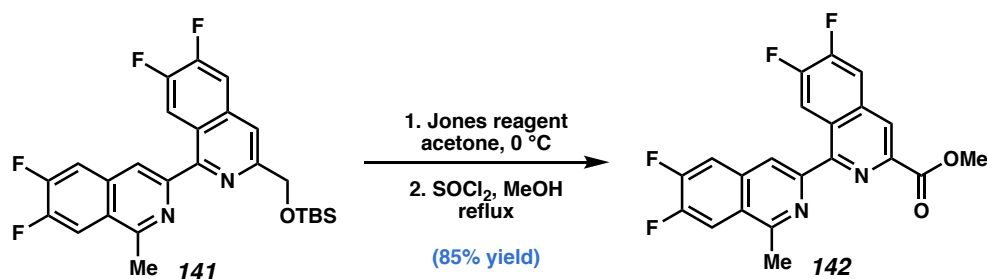


General Procedure 2: Deoxygenation

Tetrafluoro bis-isoquinoline alcohol 141: Bis-isoquinoline-*N*-oxide **138** (79 mg, 0.157 mmol, 1.0 equiv) was dissolved in CH_2Cl_2 (3.0 mL, 0.05 M) and the solution was cooled to $0\text{ }^\circ\text{C}$. Neat phosphorus trichloride (28 μL , 0.314 mmol, 2.0 equiv) was added dropwise. After 15 min, TLC revealed complete consumption of **138**, so the reaction was quenched with saturated aqueous K_2CO_3 at $0\text{ }^\circ\text{C}$ and diluted with water. The biphasic mixture was allowed to warm to room temperature, and the layers were separated. The aqueous phase was extracted with EtOAc. The combined organic phases were dried over Na_2SO_4 and concentrated (note: a brine wash caused a significant emulsion regardless of extraction solvent, and was avoided). The crude material (75 mg, 98% yield) was obtained as a colorless solid and crude ^1H NMR showed >95% purity. *Note: Attempt to perform this reaction on a larger scale (382 mg, 0.76 mmol) led to a formation of byproducts, thus requiring column purification (7% EtOAc/hexanes + 1% Et_3N). On larger scale, after purification, the product was obtained as a colorless solid (188 mg, 51% yield);* ^1H NMR (400 MHz, CDCl_3) δ 8.55 (dd, $J = 12.1, 8.3$ Hz, 1H), 8.17 (s, 1H), 7.94 (dd, $J = 10.4, 7.8$ Hz, 1H), 7.85 – 7.75 (m, 1H), 7.65 (ddd, $J = 19.9, 10.4, 7.8$ Hz, 2H), 5.07 (s, 2H), 3.04 (s, 3H), 1.02 (s, 9H), 0.19 (s, 6H); ^{13}C NMR (100 MHz, CDCl_3) δ 157.38 (dd, $J = 5.5, 1.7$ Hz), 155.91 (dd, $J = 5.7, 1.8$ Hz), 154.85 (d, $J = 2.2$ Hz), 153.18 (dd, $J = 238.2, 15.7$ Hz), 153.05 (dd, $J = 248.4, 16.0$ Hz), 151.36 – 151.22 (m), 150.60 (dd, $J = 227.0, 16.0$ Hz),

150.10 (dd, $J = 250.4, 15.2$ Hz), 136.69 – 135.19 (m), 134.56 (dd, $J = 8.6, 1.3$ Hz), 124.18 (dd, $J = 6.4, 1.3$ Hz), 122.88 (dd, $J = 7.3, 1.1$ Hz), 120.13 (dd, $J = 4.9, 2.3$ Hz), 115.71 (dd, $J = 4.9, 2.0$ Hz), 115.15 – 114.53 (m), 114.48 – 113.66 (m), 112.92 (d, $J = 16.9$ Hz), 112.52 (dd, $J = 17.3, 1.6$ Hz), 66.08, 26.16, 22.90, 18.65, –5.12; ^{19}F NMR (282 MHz, CDCl_3) δ –129.97 (ddd, $J = 20.3, 10.3, 7.8$ Hz), –130.63 (ddd, $J = 20.9, 10.5, 8.3$ Hz), –131.80 (ddd, $J = 20.3, 10.8, 7.8$ Hz), –134.20 (ddd, $J = 20.4, 12.1, 7.9$ Hz); IR (thin film, NaCl): 2954, 2930, 2886, 2858, 1511, 1432, 1247, 1125, 1101, 894, 858, 838, 776; HRMS (ESI-TOF) calc'd for $[\text{M}+\text{H}^+]$ $\text{C}_{26}\text{H}_{27}\text{F}_4\text{N}_2\text{OSi} = 487.1823$, found 487.1805.

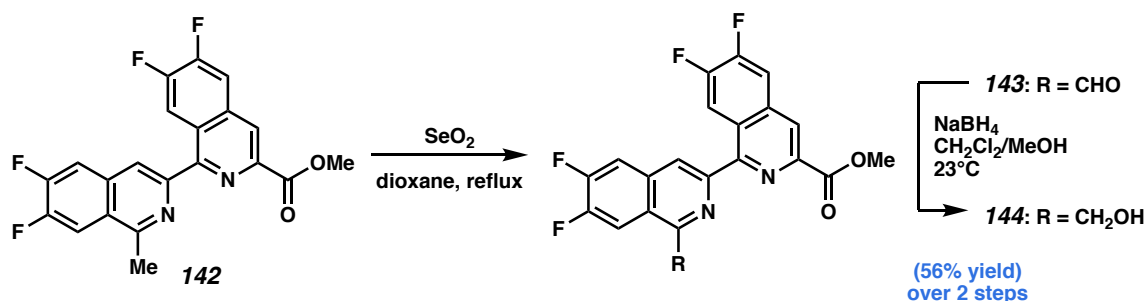
General Procedure 3: Jones oxidation/esterification



Tetrafluoro bis-isoquinoline ester 142: Bis-isoquinoline TBS-protected alcohol **141** (68 mg, 0.14 mmol, 1.0 equiv) was dissolved in acetone (2.2 mL, 0.065 M) and cooled to 0 °C. Jones reagent (25 g CrO_3 in 25 mL conc. HCl and 75 mL H_2O , ca. 0.12 mL) was added. After 1 hour, LCMS showed complete conversion to the carboxylic acid, so the reaction mixture was filtered through celite and rinsed with MeOH. The filtrate was concentrated, redissolved in distilled MeOH (2.2 mL, 0.065 M), and SOCl_2 (0.1 mL, 1.40 mmol, 10 equiv) was added dropwise at room temperature. The solution was heated to reflux and stirred for 1 hour, at which time the LCMS revealed complete consumption of the carboxylic acid. The solution was cooled to room temperature, concentrated, and purified by column chromatography (20% EtOAc/ CH_2Cl_2 + 1% Et_3N) to afford bis-IQ

ester **142** as a colorless solid (48 mg, 85% yield); ^1H NMR (300 MHz, CDCl_3) δ 8.82 (dd, $J = 12.0, 8.1$ Hz, 1H), 8.57 (s, 1H), 8.37 (s, 1H), 7.94 (dd, $J = 10.7, 7.7$ Hz, 1H), 7.75 (ddd, $J = 12.6, 10.1, 7.8$ Hz, 2H), 4.07 (s, 3H), 3.04 (s, 3H).

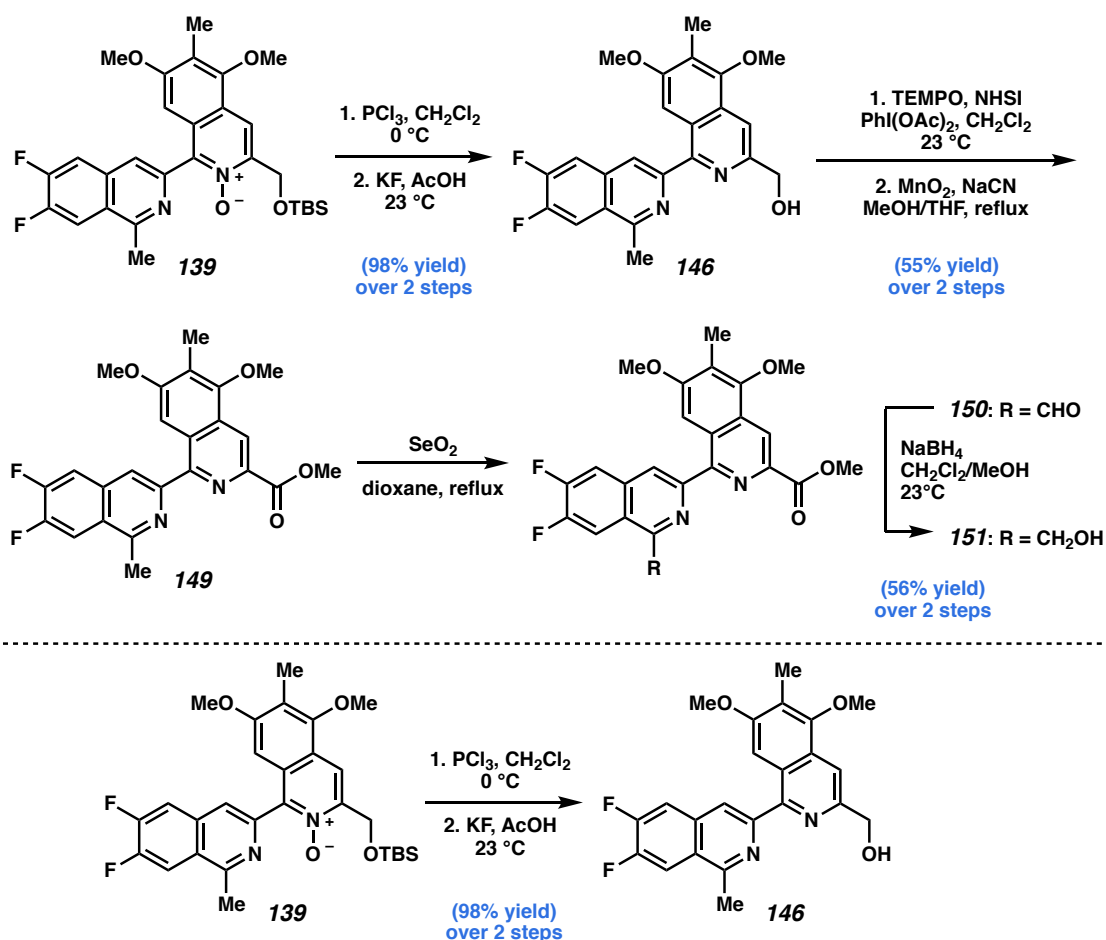
General Procedure 4: SeO_2 oxidation/ NaBH_4 reduction



Tetrafluorinated hydrogenation precursor 144: To bis-isoquinoline ester **142** (290 mg, 0.724 mmol, 1.0 equiv) in a pressure tube was added dioxane (14 mL, 0.05 M) and SeO_2 (161 mg, 1.449 mmol, 2.0 equiv) at room temperature. After heating the reaction mixture to reflux, the reaction became homogeneous. The solution was kept at reflux for an additional 4 hours, at which point LCMS revealed complete consumption of starting material **142**, so the reaction was cooled to room temperature. Celite was added and the resulting slurry was filtered through more celite, rinsing with EtOAc and CH_2Cl_2 . The filtrate was concentrated to afford aldehyde **143**. Attempt to purify this crude material resulted in poor mass recovery, thus we elected to use the crude product in the subsequent step without further purification.

To a scintillation vial containing aldehyde **143** was added CH_2Cl_2 , MeOH (4:1 $\text{CH}_2\text{Cl}_2/\text{MeOH}$, 7.5 mL, 0.1 M), and NaBH_4 (9.0 mg, 0.239 mmol, 0.33 equiv). Gas evolution was observed for ~1 minute, then stopped. After stirring at room temperature for 10 minutes, LCMS indicated the presence of aldehyde **143**, so additional NaBH_4 (9.0 mg, 0.239 mmol, 0.33 equiv) was added. After another 10 minutes, LCMS showed

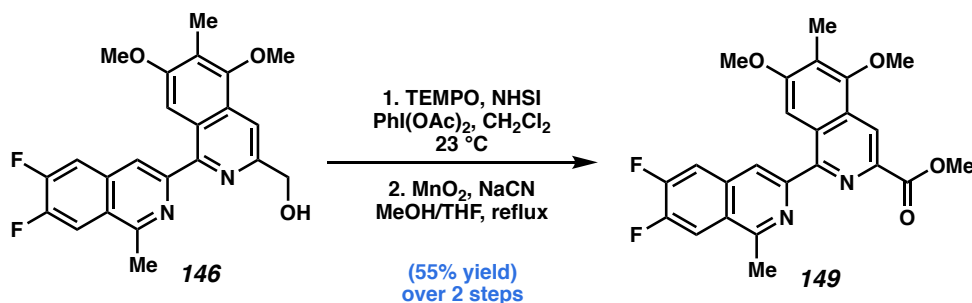
complete consumption of aldehyde **143**. The reaction was quenched by the addition of citric acid monohydrate (300 mg) and water, and the solution was stirred for 5 min, then was basified by the addition of saturated aqueous NaHCO_3 . The layers were separated and the aqueous phase was extracted with CH_2Cl_2 . The combined organic phases were dried over Na_2SO_4 and concentrated. The product was purified by column chromatography (20–30–40–50% EtOAc/ CH_2Cl_2 + 1% NEt_3) to afford hydrogenation precursor **144** as a colorless solid (170 mg, 56% yield); ^1H NMR (300 MHz, CDCl_3) δ 8.61 (s, 1H), 8.49 (dd, $J = 11.2, 8.2$ Hz, 1H), 8.41 (s, 1H), 7.86 – 7.75 (m, 3H), 5.29 (s, 2H), 4.08 (s, 3H).



Diffuorinated bis-isoquinoline alcohol 146: Deoxygenation of **139** (647 mg, 1.20 mmol) was performed according to General Procedure 2 to quantitatively provide deoxygenated product **145** as a tan solid. The crude material was >95% pure by ^1H NMR and can be used in the next step without further purification; ^1H NMR (500 MHz, CDCl_3) δ 8.15 (s, 1H), 8.10 – 8.02 (m, 1H), 7.92 (dd, $J = 10.7, 7.7$ Hz, 1H), 7.78 (s, 1H), 7.67 (dd, $J = 10.3, 7.8$ Hz, 1H), 5.08 (d, $J = 1.0$ Hz, 2H), 3.92 (s, 3H), 3.84 (s, 3H), 3.03 (s, 3H), 2.35 (s, 3H), 1.03 (s, 9H), 0.17 (s, 6H); IR (thin film, NaCl): 2930, 2856, 1596, 1513, 1462, 1429, 1393, 1300, 1250, 1200, 1127, 1023, 891, 857, 838, 776; HRMS (ESI-TOF) calc'd for $[\text{M}+\text{H}^+]$ $\text{C}_{29}\text{H}_{35}\text{F}_2\text{N}_2\text{O}_3\text{Si} = 525.2380$, found 525.2383. *Note: In some experiments where byproducts were detected in >10%, the crude material could be purified by column chromatography (15% EtOAc/hexanes + 1% Et₃N), albeit with modest mass recovery (ca. 70%).*

The deoxygenated bis-isoquinoline intermediate (**145**, 113.5 mg, 0.216 mmol, 1.0 equiv) was dissolved in acetic acid (0.9 mL, 0.25 M), and solid potassium fluoride (25.2 mg, 0.433 mmol, 2.0 equiv) was added in one portion. The solution was stirred for 4 h at room temperature, at which time LCMS showed complete consumption of **145**. The solution was diluted with CH_2Cl_2 and ice, then stirred vigorously as a solution of sodium hydroxide (565 mg, 14.1 mmol, 0.9 equiv relative to 0.9 mL AcOH) in 1.5 mL water was added slowly. The rest of the acetic acid was quenched by the addition of saturated aqueous K_2CO_3 . The layers were separated and the aqueous phase was extracted with CH_2Cl_2 . The combined organic phases were washed with brine, dried over Na_2SO_4 , and concentrated to afford **146** as a colorless solid (86.7 mg, 98% yield). The crude ^1H NMR showed >95% purity; ^1H NMR (300 MHz, CDCl_3) δ 8.22 (s, 1H), 8.01 – 7.87 (m, 2H),

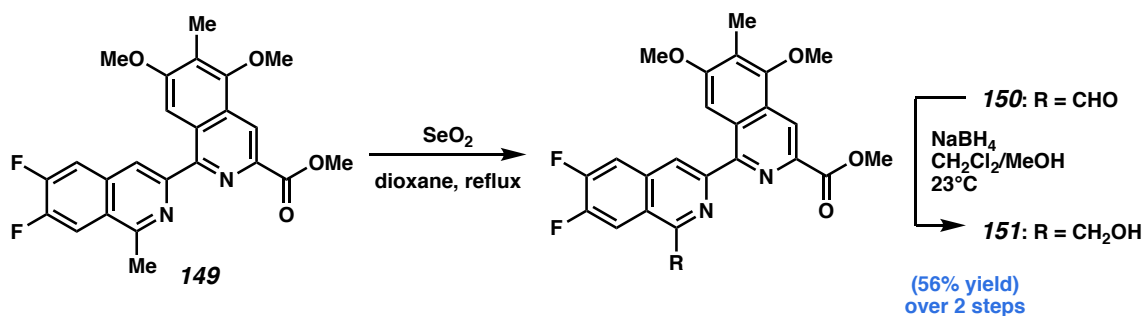
7.87 – 7.80 (m, 1H), 7.69 (dd, $J = 10.3, 7.8$ Hz, 1H), 4.97 (d, $J = 4.8$ Hz, 2H), 3.91 (s, 3H), 3.87 (s, 3H), 3.04 (s, 3H), 2.36 (s, 3H); ^{19}F NMR (282 MHz, CDCl_3) δ –130.27 (ddd, $J = 20.4, 10.2, 7.8$ Hz), –132.29 (ddd, $J = 20.3, 10.9, 7.8$ Hz); IR (thin film, NaCl): 3196, 2926, 1594, 1511, 1453, 1433, 1399, 1308, 1248, 1133, 1118, 1024, 886, 858, 839, 726; HRMS (ESI-TOF) calc'd for $[\text{M}+\text{H}^+]$ $\text{C}_{23}\text{H}_{21}\text{F}_2\text{N}_2\text{O}_3 = 411.1515$, found 411.1500.



Difluoro bis-isoquinoline ester 149: Alcohol **146** (261 mg, 0.64 mmol, 1.00 equiv), TEMPO (79.7 mg, 0.51 mmol, 0.80 equiv), N-hydroxysuccinimide (NHSI, 127.7 mg, 1.11 mmol, 1.75 equiv), and (diacetoxyiodo)benzene (1.30 g, 4.04 mmol, 6.35 equiv) were dissolved in CH_2Cl_2 (20 mL, 0.032 M) and stirred at room temperature. The white heterogeneous mixture gradually turned to a homogeneous orange solution. After 3 hours, LCMS showed complete consumption of the alcohol, affording the aldehyde as the major product, so the reaction was quenched with saturated aqueous K_2CO_3 . The aqueous layer was extracted with CH_2Cl_2 three times. The combined organic phases were dried over Na_2SO_4 and concentrated. *Note: Oxidation to the carboxylic acid was not observed even with higher temperature and prolonged reaction time. Since the oxidation stops at the aldehyde oxidation state, this experiment can be performed without NHSI.*

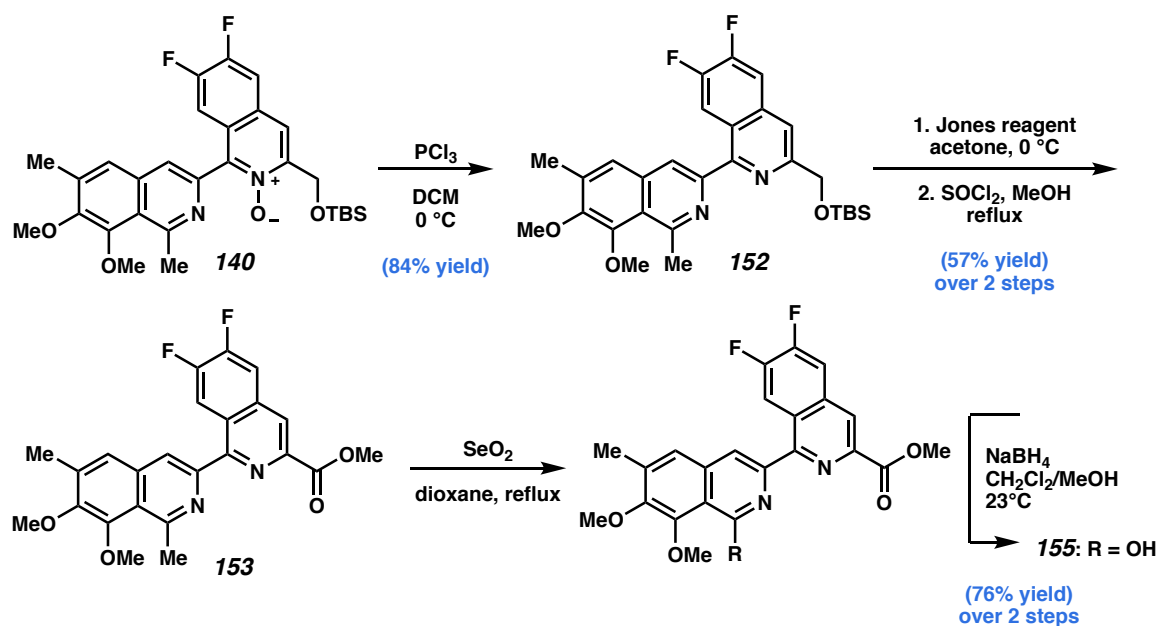
To the aldehyde intermediate (**147**, 0.636 mmol) was added MnO_2 (1.32 g, 15.2 mmol, 24 equiv), NaCN (49.5 mg, 1.01 mmol, 1.6 equiv), and THF (10 mL, 0.06 M), respectively, at room temperature. MeOH (0.2 mL, 5.05 mmol, 7.9 equiv) was added and

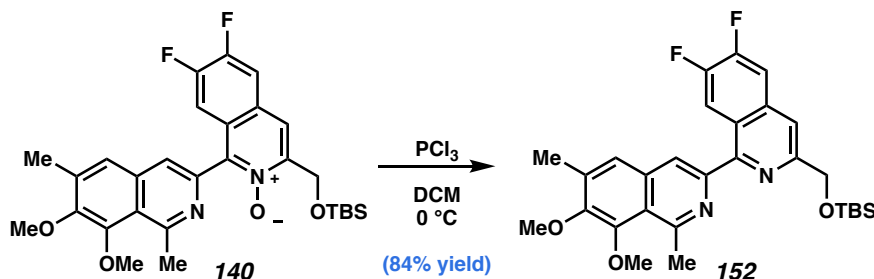
the reaction was heated to reflux. After 12 hours, the reaction mixture was cooled to room temperature and filtered through celite, before rinsing with CH_2Cl_2 , and concentrated. The filtrate was redissolved in CH_2Cl_2 , washed with water, and back-extracted with CH_2Cl_2 twice. The combined organic phases were dried over MgSO_4 , concentrated, and purified by column chromatography (10–20% EtOAc/ CH_2Cl_2 + 1% NEt_3) to provide **149** as a colorless solid (153 mg, 55% yield over 2 steps); ^1H NMR (400 MHz, CDCl_3) δ 8.78 (d, J = 0.7 Hz, 1H), 8.33 (s, 1H), 8.03 (s, 1H), 7.92 (dd, J = 10.6, 7.6 Hz, 1H), 7.70 (dd, J = 10.3, 7.8 Hz, 1H), 4.05 (s, 3H), 3.95 (s, 3H), 3.90 (s, 3H), 3.01 (s, 3H), 2.37 (s, 3H); ^{13}C NMR (100 MHz, CDCl_3) δ 166.8, 160.2, 156.7 (dd, J = 5.5, 1.6 Hz), 155.4, 155.0, 153.4 (ddd, J = 256.7, 15.7, 0.0 Hz), 151.8 (d, J = 2.8 Hz), 150.7 (dd, J = 254.1, 15.6 Hz), 139.0, 134.8 (dd, J = 8.6, 1.2 Hz), 128.5, 128.1, 125.3, 124.1 (dd, J = 6.3, 1.3 Hz), 120.6 (dd, J = 4.9, 2.3 Hz), 119.0, 114.3 (d, J = 16.4 Hz), 112.4 (dd, J = 17.3, 1.5 Hz), 101.4, 62.3, 55.8, 52.9, 22.7, 9.9; ^{19}F NMR (282 MHz, CDCl_3) δ –130.23 (ddd, J = 20.3, 10.3, 7.8 Hz), –132.14 (ddd, J = 20.3, 10.9, 7.8 Hz); IR (thin film, NaCl): 2926, 1708, 1620, 1515, 1455, 1434, 1396, 1311, 1278, 1248, 1233, 1217, 1140, 1118, 996, 893, 858; HRMS (ESI-TOF) calc'd for $[\text{M}+\text{H}^+]$ $\text{C}_{24}\text{H}_{21}\text{F}_2\text{N}_2\text{O}_4$ = 439.1464, found 439.1463.



Diffluorinated hydrogenation precursor 151: Compound **151** was prepared from bis-isoquinoline **149** (180 mg, 0.411 mmol) using General Procedure 4. The reduction

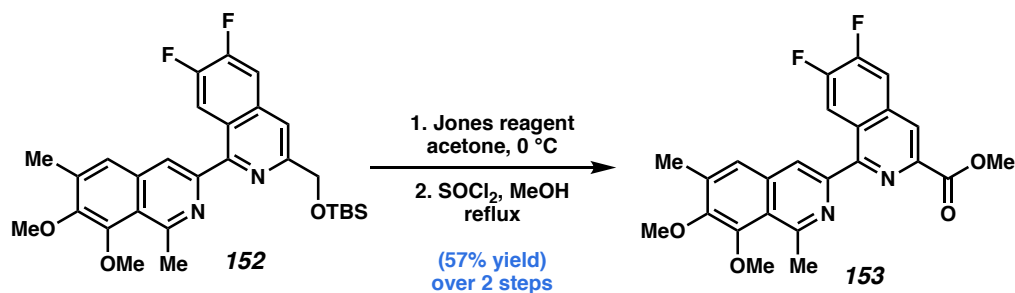
required only 0.33 equiv of NaBH₄. The crude product was purified by column chromatography (20–40–50% EtOAc/CH₂Cl₂ + 1% NEt₃) to afford **151** as a colorless solid (105 mg, 56% yield); ¹H NMR (400 MHz, CDCl₃) δ 8.82 (d, *J* = 0.7 Hz, 1H), 8.46 (s, 1H), 7.87 (s, 1H), 7.77 (ddd, *J* = 21.1, 10.2, 7.7 Hz, 2H), 5.26 (s, 2H), 4.07 (s, 3H), 3.99 (s, 3H), 3.89 (s, 3H), 2.39 (s, 3H); ¹³C NMR (100 MHz, CDCl₃) δ 166.7, 160.5, 155.8 (dd, *J* = 5.7, 1.6 Hz), 155.1, 154.9, 150.7 (d, *J* = 2.3 Hz), 139.0, 135.2 (dd, *J* = 8.7, 1.2 Hz), 128.5, 128.1, 125.6, 121.8 (dd, *J* = 4.8, 2.1 Hz), 121.6 (d, *J* = 6.5 Hz), 119.3, 114.8 (d, *J* = 16.4 Hz), 110.2 (dd, *J* = 17.6, 1.4 Hz), 100.9, 62.4, 61.9, 56.1, 52.9, 10.0; ¹⁹F NMR (282 MHz, CDCl₃) δ –128.41 (ddd, *J* = 20.3, 10.2, 7.7 Hz), –130.36 (ddd, *J* = 20.1, 10.3, 7.7 Hz). *Note:* Due to the poor signal-to-noise ratio in ¹³C spectrum, we were not able to confidently pick peaks that correspond to the two carbons adjacent to the fluorine atoms. The splitting pattern of these signals is expected to be a doublet of doublets.





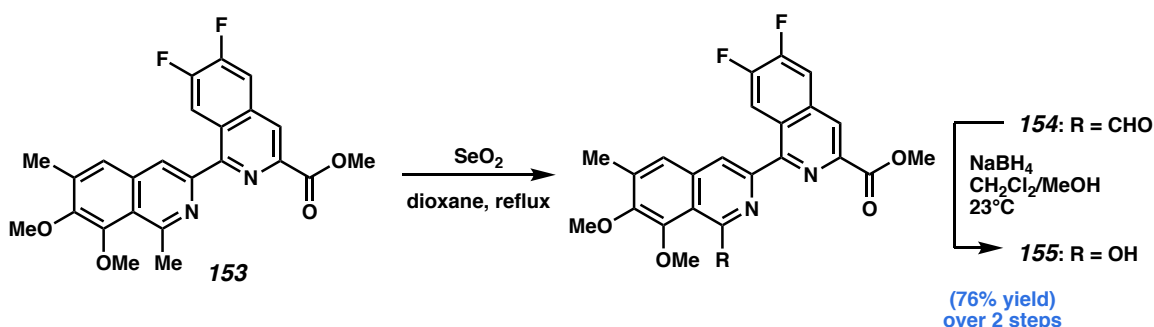
Difluorinated bis-isoquinoline TBS-protected alcohol 152: Deoxygenation of **140**

(1.14 g, 2.11 mmol) was performed according to General Procedure 2. The crude material was purified by column chromatography (10% EtOAc/hexanes) to afford the desired product (**152**) as a colorless solid (932 mg, 84% yield); ^1H NMR (500 MHz, CDCl_3) δ 8.58 (dd, $J = 12.2, 8.3$ Hz, 1H), 8.00 (s, 1H), 7.78 (d, $J = 0.9$ Hz, 1H), 7.60 (dd, $J = 10.6, 7.9$ Hz, 1H), 7.51 – 7.44 (m, 1H), 5.07 (s, 2H), 4.02 (s, 3H), 3.98 (s, 3H), 3.30 – 3.10 (m, 3H), 2.46 (d, $J = 0.9$ Hz, 3H), 1.02 (s, 9H), 0.18 (s, 3H); ^{13}C NMR (100 MHz, CDCl_3) δ 156.6, 156.6 (dd, $J = 5.6, 1.7$ Hz), 154.8 (d, $J = 2.1$ Hz), 152.9 (dd, $J = 256.4, 16.2$ Hz), 151.3, 149.9 (dd, $J = 250.2, 15.5$ Hz), 149.6, 149.3, 137.7, 136.0 (d, $J = 7.9$ Hz), 135.3, 124.6, 123.0 (dd, $J = 7.3, 1.1$ Hz), 122.4, 120.1, 115.2 (d, $J = 17.7$ Hz), 115.2 (dd, $J = 4.8, 1.8$ Hz), 112.7 (d, $J = 16.7$ Hz), 66.1, 60.9, 60.4, 27.4, 26.2, 18.6, 17.1, –5.1.



Difluorinated bis-isoquinoline ester 153: Compound **153** was prepared according to General Procedure 3 from **152** (900 mg, 1.72 mmol). The crude material was purified by column chromatography using a 1:1 mixture of CH_2Cl_2 :EtOAc as the polar solvent (40% polar solvent/hexanes + 1% NEt_3) to afford the desired product (**153**) as a colorless solid

(437 mg, 57% yield); ^1H NMR (400 MHz, CDCl_3) δ 8.89 (dd, $J = 12.1, 8.3$ Hz, 1H), 8.53 – 8.43 (m, 1H), 8.20 (s, 1H), 7.72 (dd, $J = 10.0, 7.9$ Hz, 1H), 7.59 – 7.45 (m, 1H), 4.06 (s, 3H), 4.02 (s, 3H), 3.98 (s, 3H), 3.20 (s, 3H), 2.46 (d, $J = 0.8$ Hz, 3H); ^{13}C NMR (100 MHz, CDCl_3) δ 166.3, 157.3 (dd, $J = 5.5, 1.7$ Hz), 156.5, 153.1 (dd, $J = 265.2, 21.6$ Hz), 151.6 (dd, $J = 252.0, 12.7$ Hz), 151.5, 149.6, 148.7, 141.4 (d, $J = 2.5$ Hz), 137.8, 135.3, 135.2 (dd, $J = 8.7, 1.0$ Hz), 125.8 (dd, $J = 7.9, 1.4$ Hz), 124.8, 123.0 (dd, $J = 4.8, 2.1$ Hz), 122.5, 120.8, 116.2 (dd, $J = 19.4, 1.2$ Hz), 114.2 (d, $J = 17.2$ Hz), 60.9, 60.3, 53.1, 27.3, 17.1; ^{19}F NMR (282 MHz, CDCl_3) δ –129.10 (ddd, $J = 20.9, 9.9, 8.5$ Hz), –129.50 (ddd, $J = 20.7, 12.1, 7.8$ Hz).

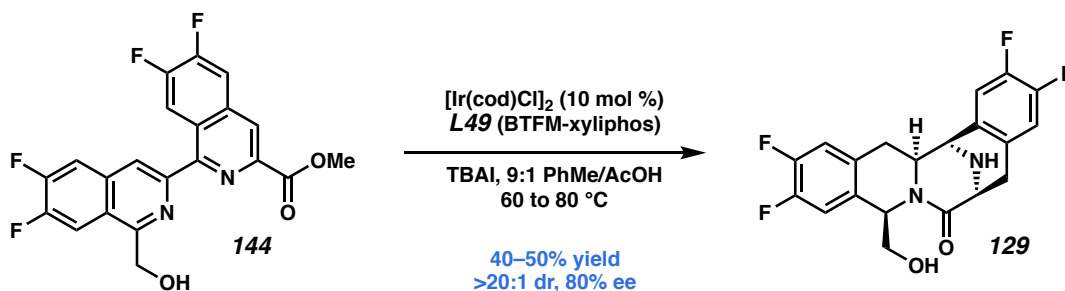


Diffluorinated hydrogenation precursor 155: Compound **155** was prepared according to General Procedure 4 from **153** (415 mg, 0.95 mmol). The crude material was purified by column chromatography using a 1:1 mixture of CH_2Cl_2 :EtOAc as the polar solvent (40% polar solvent/hexanes + 1% NEt_3) to afford the desired product (**155**) as a white solid (376 mg, 76% yield over 2 steps); ^1H NMR (400 MHz, CDCl_3) δ 8.56 – 8.53 (m, 1H), 8.51 – 8.43 (m, 1H), 8.22 (s, 1H), 7.76 (t, $J = 8.8$ Hz, 1H), 7.62 – 7.53 (m, 1H), 5.38 (d, $J = 4.2$ Hz, 2H), 5.27 (t, $J = 4.4$ Hz, 1H, OH), 4.06 (s, 3H), 4.05 (s, 3H), 3.96 (s, 3H), 2.48 (d, $J = 0.8$ Hz, 3H); ^{13}C NMR (100 MHz, CDCl_3) δ 166.1, 157.3 (d, $J = 3.4$ Hz), 156.7, 153.2 (dd, $J = 260.9, 17.6$ Hz), 151.8 (dd, $J = 257.9, 16.9$ Hz), 151.4, 149.1, 147.2,

141.4 (d, $J = 1.6$ Hz), 138.8, 135.1, 134.9 (dd, $J = 6.5, 3.6$ Hz), 125.7 (dd, $J = 6.0, 3.1$ Hz), 124.7, 123.2 (d, $J = 2.8$ Hz), 121.9, 120.5, 115.3 (dd, $J = 16.3, 4.5$ Hz), 114.4 (t, $J = 9.2$ Hz), 64.7, 60.92, 60.3, 53.1, 17.2; ^{19}F NMR (282 MHz, CDCl_3) δ -128.44 – -128.58 (m).

A8.4.2.5 Ir-catalyzed enantioselective hydrogenation

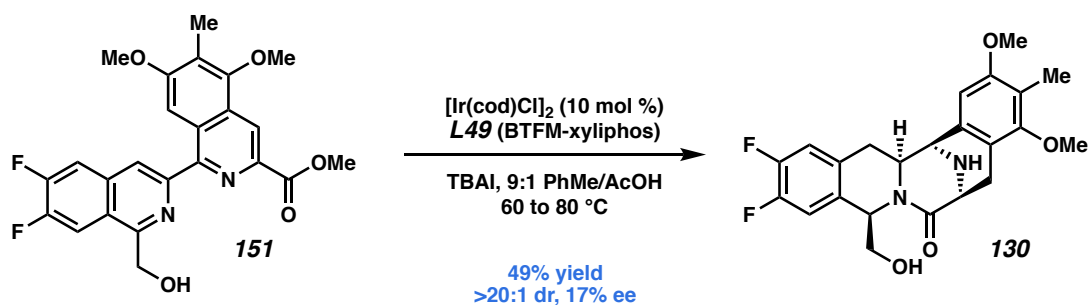
General Procedure 5: Hydrogenation



Tetrafluorinated bis-THIQ pentacycle (129): A flame-dried 100-mL roundbottom flask with a teflon-coated stir bar and bis-IQ hydrogenation precursor **144** (169 mg, 0.407 mmol, 1.00 equiv) was placed into a Parr bomb and brought in to a nitrogen-filled glovebox, with the exception of the pressure gauge. A layer of plastic wrap and a rubber band were also brought in to seal the top of the bomb. In a nitrogen-filled glovebox, a solution of **L49** (BTfM-xylyphos) (89.0 mg, 0.098 mmol, 0.24 equiv) and $[\text{Ir}(\text{cod})\text{Cl}]_2$ (27.34 mg, 0.041 mmol, 0.10 equiv) in toluene (10 mL) was prepared and allowed to stand for 10 minutes. Meanwhile, TBAI (90.2 mg, 0.244 mmol, 0.60 equiv) and AcOH (2 mL) were added to the flask containing bis-isoquinoline **144**. Afterwards, the homogeneous iridium-ligand solution was transferred to the flask with two 4 mL toluene rinses, bringing the final volume to 20 mL of 9:1 PhMe:AcOH (0.02 M of **129**). After sealing the flask with a rubber septum that was pierced with three 16 gauge (purple) needles, each bent at a 90° angle, the flask was placed inside the bomb, and the top was

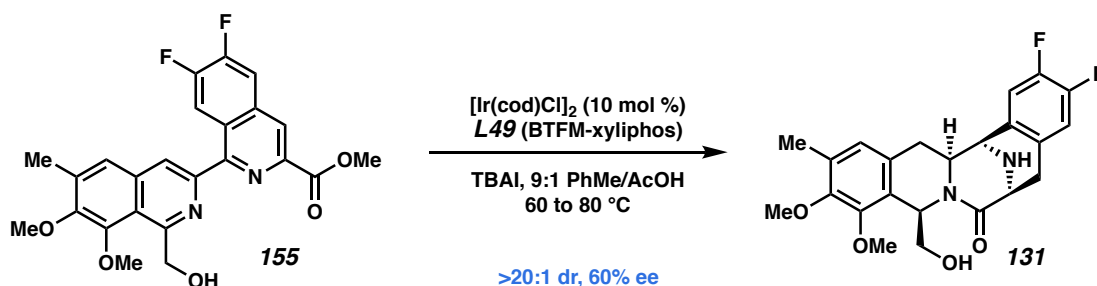
covered tightly with plastic wrap secured by a rubber band. The bomb was then removed from the glovebox, and the pressure gauge was quickly screwed in place and tightened. The bomb was charged to 5-10 bar H₂ and slowly released. This process was repeated twice, before charging the bomb to 60 bar of H₂, at which time it was placed in a preheated 60 °C oil bath. The bath was maintained at this temperature for 18 h, then raised to 80 °C. After 24 h, the bomb was removed from the oil bath and the hydrogen pressure was vented. The flask was removed from the bomb and the solution was transferred to a 250 mL roundbottom flask and basified by the careful addition of saturated aqueous K₂CO₃ and water until pH > 7. The solution was transferred to a separatory funnel and the layers were separated. The aqueous phase was extracted with EtOAc, and the combined organic phases were washed with water, then brine, dried over Na₂SO₄, and concentrated. The product was purified using reverse-phase (C₁₈) preparative HPLC (MeCN/0.05% TFA in water, 35.0 mL/min, monitor wavelength = 210 nm, 20–38% MeCN over 6.2 min, ramp to 100% for 0.1 min, hold at 100% for 2 min; t_R = 5.7 min) to furnish pentacycle **129** as a white solid (63 mg, 40% yield); 78% ee; [α]_D²⁵ –26.4 (c 0.97, CHCl₃); ¹H NMR (400 MHz, CDCl₃) δ 7.06 – 6.93 (m, 3H), 6.89 (dd, *J* = 10.4, 7.8 Hz, 1H), 5.17 (t, *J* = 5.6 Hz, 1H), 4.12 (d, *J* = 3.0 Hz, 1H), 3.99 (d, *J* = 6.1 Hz, 1H), 3.90 (dt, *J* = 12.6, 2.6 Hz, 1H), 3.31 (dd, *J* = 10.8, 5.2 Hz, 1H), 3.20 – 3.10 (m, 1H), 3.08 (dd, *J* = 10.8, 6.2 Hz, 1H), 3.00 (d, *J* = 17.1 Hz, 1H), 2.82 – 2.74 (m, 2H, overlapped with NH), 2.53 (t, *J* = 13.5 Hz, 1H); ¹³C NMR (100 MHz, CDCl₃) δ 171.1, 149.9 (dd, *J* = 249.6, 12.7 Hz), 149.5 (dd, *J* = 247.9, 11.6 Hz), 149.3 (dd, *J* = 247.0, 12.1 Hz), 148.2 (dd, *J* = 248.1, 13.1 Hz), 131.5 (dd, *J* = 6.1, 3.8 Hz), 130.8 (dd, *J* = 5.9, 3.8 Hz), 130.3 (dd, *J* = 5.9, 3.8 Hz), 128.4 (t, *J* = 4.1 Hz), 118.1 (d, *J* = 16.9 Hz), 117.2 (d, *J* = 18.0 Hz),

116.7 (d, $J = 17.1$ Hz), 116.5 (d, $J = 17.6$ Hz), 66.8, 60.6, 57.2, 53.8, 53.6, 33.9, 32.6; ^{19}F NMR (282 MHz, CDCl_3) δ -137.75 (ddd, $J = 21.6, 10.7, 7.8$ Hz), -138.85 (ddd, $J = 21.4, 10.2, 7.6$ Hz), -139.29 – -139.71 (m), -139.99 – -140.57 (m); IR (Neat Film, NaCl) 3288, 2928, 1633, 1514, 1433, 1413, 1312, 1296, 1214, 1120, 1052, 879, 807, 755 cm^{-1} ; HRMS (MM:ESI-APCI+) m/z calc'd for $\text{C}_{20}\text{H}_{17}\text{F}_4\text{N}_2\text{O}_2$ $[\text{M}+\text{H}]^+$: 393.1221, found 393.1204; HPLC conditions: 40% IPA/hexanes, 1.0 mL/min, Chiralpak AD-H column, $\lambda = 210$ nm, t_R (min): minor = 8.3, major = 10.4.



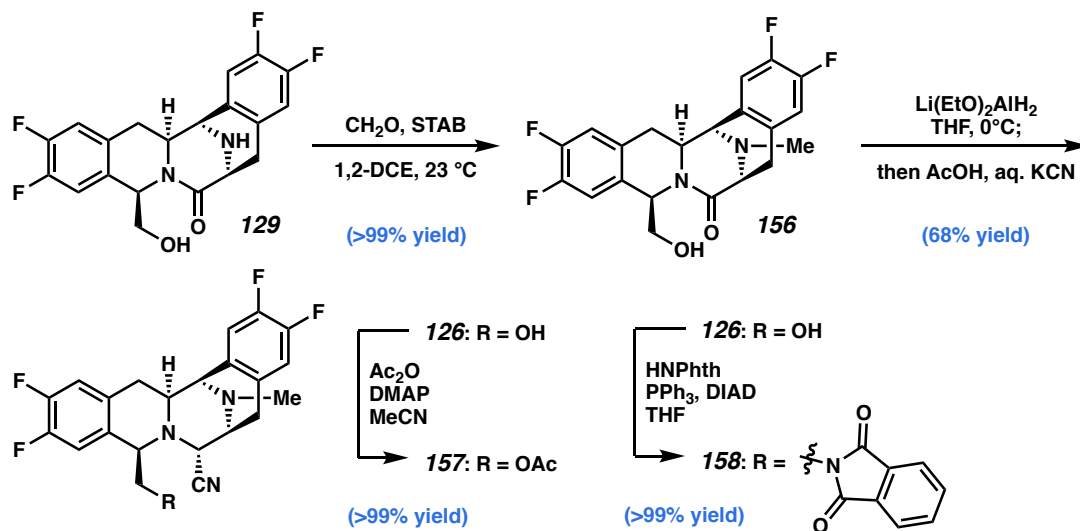
Difluorinated bis-THIQ pentacycle 130: Prepared according to General Procedure 5 using bis-IQ **151** (25.0 mg, 0.055 mmol) as the starting material. The product was purified using reverse-phase (C_{18}) preparative HPLC (MeCN/0.4% acetic acid in water, 5.0 mL/min, monitor wavelength = 225 nm, 15.0–40.5% MeCN over 8.50 min, ramp to 95% MeCN over 0.5 min, and hold at 95% for 4 min; $t_R = 6.9$ min) to furnish pentacycle **130** as a white solid (11.5 mg, 49% yield); 17% ee; ^1H NMR (400 MHz, CDCl_3) δ 7.02 (ddd, $J = 10.9, 7.6, 3.3$ Hz, 2H), 6.33 (s, 1H), 5.31 (t, $J = 5.5$ Hz, 1H), 4.13 (d, $J = 3.3$ Hz, 1H), 4.10 (d, $J = 5.6$ Hz, 1H), 3.95 (dt, $J = 12.5, 2.9$ Hz, 1H), 3.83 (s, 3H), 3.68 (s, 3H), 3.29 (d, $J = 5.5$ Hz, 2H), 3.13 (dd, $J = 17.4, 1.5$ Hz, 1H), 3.02 (dd, $J = 17.4, 6.4$ Hz, 1H), 2.80 (dd, $J = 14.7, 2.6$ Hz, 1H), 2.73 – 2.54 (m, 3H, overlapped with OH and NH), 2.14 (s, 3H); ^{13}C NMR (100 MHz, CDCl_3) δ 172.3, 157.8, 156.8, 149.6 (dd, $J = 243.6, 7.3$ Hz), 149.5 (dd, $J = 246.3, 11.2$ Hz), 132.1 (dd, $J = 6.1, 3.9$ Hz), 130.6, 130.70 – 130.48

(m), 120.1, 119.7, 117.1 (d, $J = 17.8$ Hz), 116.6 (d, $J = 17.4$ Hz), 106.1, 68.2, 61.0, 60.5, 57.5, 56.0, 54.9, 54.3, 33.0, 30.0, 9.3; ^{19}F NMR (282 MHz, CDCl_3) δ -138.67 – -139.26 (m), -139.30 – -139.75 (m); IR (Neat Film, NaCl) 3288, 2941, 1634, 1608, 1513, 1455, 1407, 1371, 1335, 1310, 1296, 1274, 1214, 1125, 1061, 753 cm^{-1} ; HRMS (MM:ESI-APCI+) m/z calc'd for $\text{C}_{23}\text{H}_{25}\text{F}_2\text{N}_2\text{O}_2$ $[\text{M}+\text{H}]^+$: 431.1777, found 431.1774; HPLC conditions: 10% IPA/hexanes, 1.0 mL/min, Chiralcel OD-H column, $\lambda = 220$ nm, t_R (min): major = 67.3, minor = 77.7.

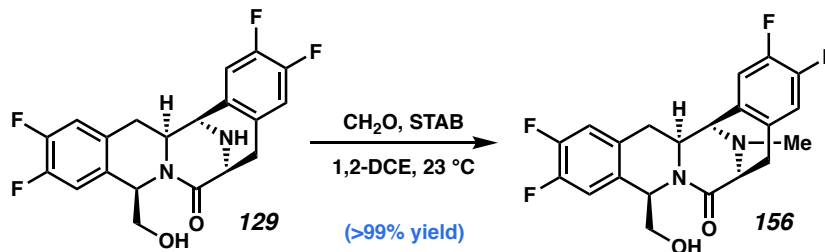


Difluorinated bis-THIQ pentacycle 131: Prepared according to General Procedure 5 using bis-IQ **155** (10.0 mg, 0.022 mmol) as the starting material to furnish pentacycle **131**; 60% ee; ^1H NMR (400 MHz, CDCl_3) δ 7.01 (dd, $J = 10.7, 7.8$ Hz, 1H), 6.92 (dd, $J = 10.6, 7.7$ Hz, 1H), 6.72 (s, 1H), 5.77 (dd, $J = 6.8, 3.9$ Hz, 1H), 4.12 (d, $J = 3.4$ Hz, 1H), 4.05 (dd, $J = 6.2, 1.8$ Hz, 1H), 3.95 – 3.87 (m, 1H), 3.91 (s, 3H), 3.7 (s, 3H), 3.44 (dd, $J = 11.0, 4.0$ Hz, 1H), 3.20 (dd, $J = 11.0, 6.8$ Hz, 1H), 3.17 – 3.05 (m, 2H), 2.71 (dd, $J = 14.4, 2.4$ Hz, 1H), 2.60 – 2.47 (m, 1H), 2.24 (s, 4H, overlapped with NH proton); ^{13}C NMR (100 MHz, CDCl_3) δ 172.2, 150.1, 149.9 (dd, $J = 249.4, 12.7$ Hz), 149.7, 148.3 (dd, $J = 247.7, 13.1$ Hz), 132.0, 131.0 – 130.9 (m), 130.8, 128.8 (t, $J = 4.2$ Hz), 124.7, 124.5, 118.2 (d, $J = 17.0$ Hz), 116.8 (d, $J = 17.0$ Hz), 68.9, 61.5, 60.7, 60.0, 54.1, 53.9, 52.9, 34.3, 33.0, 15.9; HPLC conditions: 20% IPA, 1.0 mL/min, Chiralcel OD-H column, $\lambda = 210$ nm, t_R (min): minor = 15.8, major = 36.0.

A8.4.2.6 Completion of bis-THIQ analogs

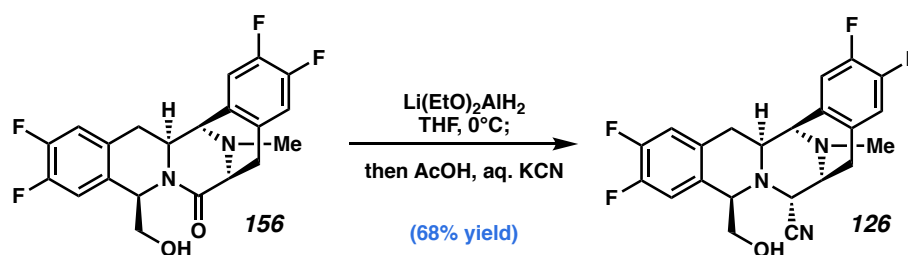


General Procedure 6: Reductive amination



N-methyl tetrafluorinated bis-THIQ 156: bis-tetrahydroisoquinoline **129** (48 mg, 0.122 mmol, 1.00 equiv) was dissolved in 1,2-dichloroethane (1,2-DCE, 2.5 mL, 0.05 M) and 37% aqueous formaldehyde (17 μL , 0.226 mmol, 1.85 equiv) was added. The solution was stirred for 10 min before sodium triacetoxyborohydride (130 mg, 0.612 mmol, 5 equiv) was added. This solution was stirred at 23 °C for 30 min, at which time LCMS showed complete consumption of **129**. Citric acid monohydrate (193 mg, 0.917 mmol, 7.5 equiv) was added to the solution, followed by 5 mL water. This solution was stirred for 10 min before the slow addition of saturated aqueous K_2CO_3 until $\text{pH} > 7$. The layers were separated and the aqueous phase was extracted with CH_2Cl_2 . The combined organic phases were dried over Na_2SO_4 and concentrated to furnish **156** as a colorless solid (50

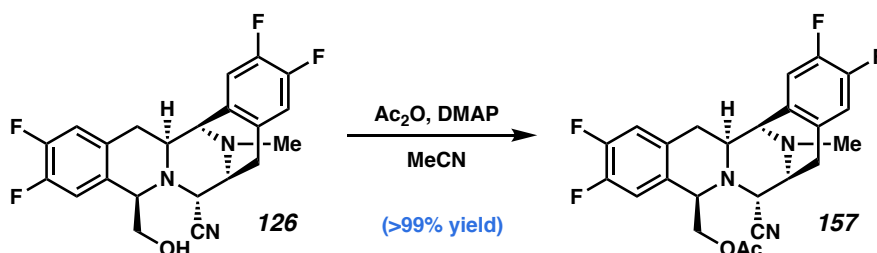
mg, quantitative yield) with >95% purity; $[\alpha]_{\text{D}}^{25} -53.3$ (c 1.203, CHCl_3); ^1H NMR (400 MHz, CDCl_3) δ 7.09 – 6.95 (m, 3H), 6.91 (dd, J = 10.3, 7.8 Hz, 1H), 5.27 (t, J = 4.6 Hz, 1H), 4.01 (dt, J = 12.6, 2.8 Hz, 1H), 3.79 (d, J = 3.3 Hz, 1H), 3.73 (d, J = 6.5 Hz, 1H), 3.34 – 3.21 (m, 3H), 2.86 (d, J = 17.5 Hz, 1H), 2.72 (dd, J = 14.6, 2.4 Hz, 1H), 2.54 (t, J = 13.6 Hz, 1H), 2.46 (s, 3H); ^{13}C NMR (100 MHz, CDCl_3) δ 171.9, 149.9 (dd, J = 249.6, 12.7 Hz), 149.6 (dd, J = 246.3, 9.8 Hz), 149.4 (dd, J = 246.8, 11.7 Hz), 148.5 (dd, J = 248.4, 12.9 Hz), 131.9 (dd, J = 6.0, 3.8 Hz), 130.4 – 130.2 (m), 130.3 – 130.1 (m), 126.6 (t, J = 4.1 Hz), 117.8 (d, J = 17.0 Hz), 117.6 (d, J = 17.4 Hz), 117.1 (d, J = 17.9 Hz), 116.6 (d, J = 17.6 Hz), 68.2 – 65.7 (m), 60.3, 59.7, 57.6, 57.4, 40.0, 32.6, 28.1; ^{19}F NMR (282 MHz, CDCl_3) δ -137.47 – -137.89 (m), -138.68 (ddd, J = 21.3, 10.1, 7.6 Hz), -138.93 – -139.28 (m), -139.58 – -139.93 (m); IR (Neat Film, NaCl) 3288, 2930, 1639, 1513, 1438, 1419, 1364, 1338, 1312, 1213, 1178, 1140, 1109, 1059, 909, 880, 794, 733 cm^{-1} ; HRMS (MM:ESI-APCI+) m/z calc'd for $\text{C}_{21}\text{H}_{19}\text{F}_4\text{N}_2\text{O}_2$ $[\text{M}+\text{H}]^+$: 407.1377, found 407.1386.



Tetrafluorinated bis-THIQ aminonitrile 126: In an oven-dried vial, LiAlH_4 solution (1.0 M in THF, 2 mL, 2.0 mmol) was cooled to 0°C . A solution of ethyl acetate (230 μL , 2.35 mmol) in 2 mL THF was added slowly, and the resulting solution was stirred 30 min at 0°C , providing a 0.47 M solution of $\text{Li}(\text{EtO})_2\text{AlH}_2$ in THF. bis-THIQ **156** (49.7 mg, 0.122 mmol, 1.0 equiv) was dissolved in THF (6.1 mL, 0.02 M) and the resulting solution

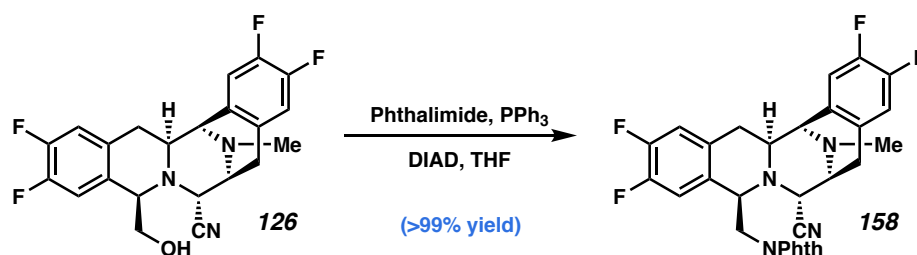
was cooled to 0 °C. A solution of $\text{Li}(\text{EtO})_2\text{AlH}_2$ (0.47 M in THF, 3.9 mL, 1.83 mmol, 15.0 equiv) was added slowly, resulting in extensive evolution of H_2 . After stirring for 30 min, the LCMS indicated full consumption of the starting material, so the reaction was quenched with acetic acid (150 μL , 2.56 mmol, 21 equiv) and aqueous potassium cyanide (4.8 M, 153 μL , 0.732 mmol, 6.0 equiv) was added, followed by celite and anhydrous Na_2SO_4 (roughly 1 g each). The solution was diluted with 12 mL THF and stirred at 50 °C for 16 h. At this stage, LCMS revealed full consumption of the iminium, thus celite and K_2CO_3 (4 g) were added, and the suspension was filtered through celite, rinsing with EtOAc and CH_2Cl_2 . The filtrate was transferred to a roundbottom flask and was concentrated. The product was purified using reverse-phase (C_{18}) preparative HPLC (MeCN/0.4% acetic acid in water, 5.0 mL/min, monitor wavelength = 270 nm, 50–80% MeCN over 10 min, ramp to 95% over 0.5 min, hold at 95% for 2.4 min; t_{R} = 7.3 min) to furnish amino nitrile **126** as a white powder (34.4 mg, 68% yield); $[\alpha]_{\text{D}}^{25}$ -57.3 (c 1.012, CHCl_3); ^1H NMR (400 MHz, CDCl_3) δ 7.00 – 6.81 (m, 4H), 4.11 (d, J = 2.5 Hz, 1H), 3.82 (t, J = 4.7 Hz, 1H), 3.62 (dd, J = 2.8, 1.2 Hz, 1H), 3.55 (dd, J = 11.2, 4.2 Hz, 1H), 3.41 (ddd, J = 7.5, 2.6, 1.3 Hz, 1H), 3.35 (dt, J = 12.1, 2.7 Hz, 1H), 3.20 (dd, J = 11.2, 5.2 Hz, 1H), 3.18 – 3.10 (m, 1H), 2.63 – 2.52 (m, 2H), 2.36 (s, 3H), 2.28 – 2.17 (m, 1H); ^{13}C NMR (100 MHz, CDCl_3) δ 149.6 (dd, J = 248.6, 12.7 Hz), 149.2 (dd, J = 252.8, 16.9 Hz), 149.2 (dd, J = 241.9, 7.6 Hz), 148.2 (dd, J = 248.3, 12.9 Hz), 131.2 (dd, J = 6.0, 3.6 Hz), 130.9 (dd, J = 5.7, 3.8 Hz), 129.9 (dd, J = 5.4, 3.7 Hz), 128.0 (t, J = 3.9 Hz), 117.9 (d, J = 16.5 Hz), 117.5, 116.5 (d, J = 9.3 Hz), 116.3 (d, J = 9.1 Hz), 116.0 (d, J = 17.7 Hz), 67.4, 62.5 (d, J = 1.5 Hz), 62.4, 60.7, 56.0, 55.2, 41.7, 32.4, 25.7; ^{19}F NMR (282 MHz, CDCl_3) δ -138.81 (ddd, J = 21.3, 10.9, 7.9 Hz), -139.65 (ddd, J = 21.5, 10.4, 7.6

Hz), $-139.84 - -140.35$ (m), -140.64 (ddd, $J = 21.3, 10.0, 7.8$ Hz); IR (Neat Film, NaCl) $3477, 2938, 1614, 1515, 1435, 1354, 1320, 1268, 1216, 1144, 1100, 1054, 912, 890, 762$ cm^{-1} ; HRMS (MM:ESI-APCI+) m/z calc'd for $\text{C}_{22}\text{H}_{20}\text{F}_4\text{N}_3\text{O}$ $[\text{M}+\text{H}]^+$: 418.1537, found 418.1544.



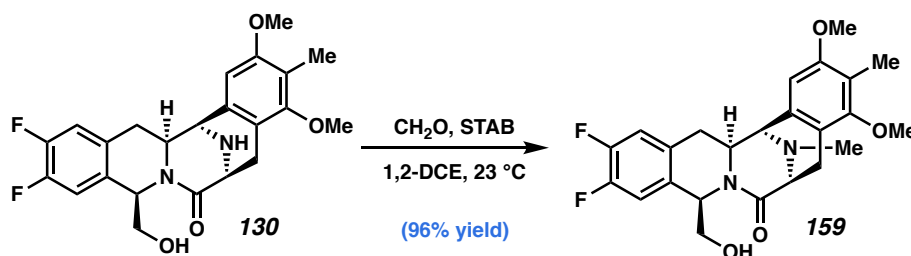
Tetrafluorinated Acylated bis-THIQ aminonitrile 157: In a 1-dram vial, bis-THIQ **126** (6.0 mg, 0.015 mmol, 1.0 equiv) and DMAP (4.8 mg, 0.043 mmol, 3.0 equiv) were dissolved in acetonitrile (300 μL , 0.05 M), and acetic anhydride (4.1 μL , 0.043 μmol , 3.0 equiv) was added neat. After 30 minutes, LCMS showed complete consumption of **126**. The reaction was concentrated and the crude material was purified using reverse-phase (C_{18}) preparative HPLC (MeCN/0.4% acetic acid in water, 5.0 mL/min, monitor wavelength = 260 nm, 60–84% MeCN over 8 min, ramp to 95 over 0.5 min, hold at 95% for 1.5 min; $t_{\text{R}} = 7.2$ min) to afford acylated bis-THIQ analog **157** as a colorless solid (6.0 mg, >99% yield); $[\alpha]_{\text{D}}^{25} +55.3$ (c 0.400, CHCl_3); ^1H NMR (400 MHz, CDCl_3) δ 6.98 – 6.87 (m, 3H), 6.83 (dd, $J = 10.2, 7.8$ Hz, 1H), 4.28 (dd, $J = 11.3, 4.6$ Hz, 1H), 4.07 (d, $J = 2.5$ Hz, 1H), 3.89 (t, $J = 4.4$ Hz, 1H), 3.61 (dd, $J = 11.3, 4.1$ Hz, 1H), 3.58 – 3.56 (m, 1H), 3.39 (ddd, $J = 7.6, 2.6, 1.3$ Hz, 1H), 3.28 (dt, $J = 11.9, 2.6$ Hz, 1H), 3.08 (dd, $J = 18.1, 8.0$ Hz, 1H), 2.67 – 2.51 (m, 2H), 2.34 (s, 3H), 2.25 – 2.13 (m, 1H), 1.70 (s, 3H); ^{13}C NMR (100 MHz, CDCl_3) δ 170.3, 149.6 (dd, $J = 247.9, 12.6$ Hz), 149.4 (dd, $J = 247.5, 11.2$ Hz), 149.2 (dd, $J = 246.5, 12.2$ Hz), 148.0 (dd, $J = 247.7, 12.9$ Hz), 131.6

(dd, $J = 6.1, 3.6$ Hz), 131.5 (dd, $J = 5.9, 3.8$ Hz), 129.4 (dd, $J = 5.5, 3.8$ Hz), 127.99 – 127.71 (m), 117.7 (d, $J = 16.2$ Hz), 117.6, 116.7 – 116.3 (m, 2 carbons), 116.1 (d, $J = 17.9$ Hz), 66.7, 62.3, 60.7, 60.4, 56.0, 55.2, 41.8, 32.7, 25.3, 20.6; ^{19}F NMR (282 MHz, CDCl_3) δ –139.32 (ddd, $J = 21.4, 10.3, 7.8$ Hz), –139.51 – –140.17 (m), –141.34 – –141.90 (m); HRMS (MM:ESI-APCI+) m/z calc'd for $\text{C}_{24}\text{H}_{22}\text{F}_4\text{N}_3\text{O}_2$ $[\text{M}+\text{H}]^+$: 460.1643, found 460.1627.

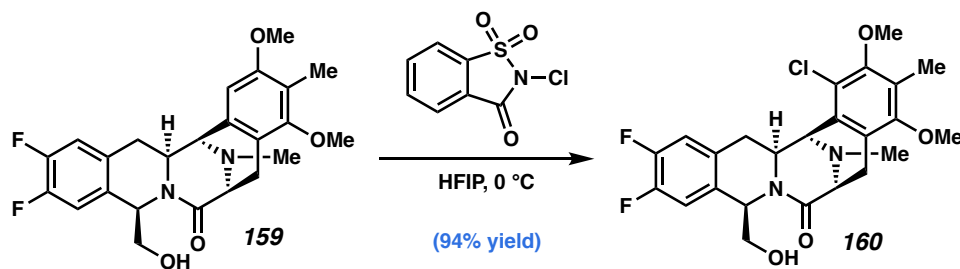


Tetrafluorinated Phthalimido bis-THIQ aminonitrile 158: In a 1-dram vial, bis-THIQ **126** (6.0 mg, 0.015 mmol, 1.0 equiv), phthalimide (4.2 mg, 0.029 mmol, 2.0 equiv), and triphenylphosphine (7.5 mg, 0.029 mmol, 2.0 equiv) were dissolved in THF (300 μL , 0.05 M). DIAD (5.7 μL , 0.029 mmol, 2.0 equiv) was added. After 2 hours, LCMS showed complete consumption of starting material **126**, so the reaction was quenched with H_2O . The layers were separated, and the aqueous phase was extracted with CH_2Cl_2 . The organic phases were combined, concentrated, and the crude material was purified using reverse-phase (C_{18}) preparative HPLC (MeCN/0.4% acetic acid in water, 5.0 mL/min, monitor wavelength = 230 nm, 65–95% MeCN over 10 min, hold at 95% for 2 min; $t_{\text{R}} = 6.7$ min) to afford phthalimide analog **158** as a colorless solid (6.4 mg, quantitative yield); $[\alpha]_{\text{D}}^{25} +48.6$ (c 0.367, CHCl_3); ^1H NMR (400 MHz, CDCl_3) δ 7.73 (s, 4H), 6.88 (ddd, $J = 23.1, 10.0, 7.6$ Hz, 2H), 6.71 (dd, $J = 10.5, 7.8$ Hz, 2H), 4.16 – 4.08 (m, 2H), 3.60 (dd, $J = 14.1, 6.7$ Hz, 1H), 3.52 (dd, $J = 2.9, 1.2$ Hz, 1H), 3.45 (dd, $J =$

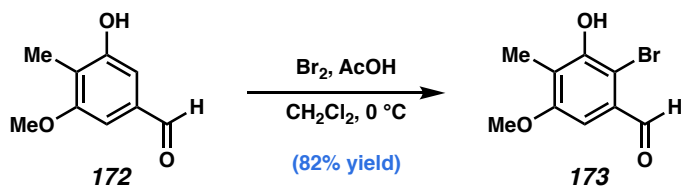
14.1, 4.7 Hz, 1H), 3.36 (dt, $J = 8.0, 1.6$ Hz, 1H), 3.22 (dt, $J = 12.0, 2.5$ Hz, 1H), 3.10 – 2.93 (m, 1H), 2.62 – 2.49 (m, 2H), 2.31 (s, 3H), 2.20 – 2.06 (m, 1H); ^{13}C NMR (100 MHz, CDCl_3) δ 167.7, [signals for 4 carbons adjacent to fluorines: 150.7, 150.6, 150.5, 150.4, 149.2, 149.1, 148.3, 148.1, 148.1, 148.0, 146.7, 146.6], 134.3, 131.8 (dd, $J = 6.0, 3.7$ Hz), 131.5, 131.1 (dd, $J = 5.8, 3.8$ Hz), 130.6 (dd, $J = 5.4, 3.9$ Hz), 127.7 (t, $J = 3.9$ Hz), 123.6, 117.7, 117.3 (d, $J = 16.5$ Hz), 116.6 (d, $J = 17.1$ Hz, 2 carbons), 116.3 (d, $J = 18.1$ Hz), 62.2, 60.5, 60.5, 57.3, 55.3, 43.9, 41.6, 32.8, 25.3; ^{19}F NMR (282 MHz, cdcl_3) δ –139.13 (dd, $J = 20.0, 9.9$ Hz), –139.49 (dt, $J = 19.6, 9.4$ Hz), –139.84 – –140.56 (m), –141.13 – –142.10 (m); HRMS (MM:ESI-APCI+) m/z calc'd for $\text{C}_{30}\text{H}_{23}\text{F}_4\text{N}_4\text{O}_2$ $[\text{M}+\text{H}]^+$: 547.1752, found 547.1740.



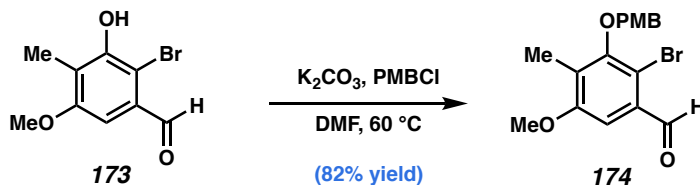
N-methyl tetrafluorinated bis-THIQ 159: Prepared according to General Procedure 6 using pentacycle **130** as the starting material (11.5 mg, 0.027 mmol). The crude product of **159** was obtained as a colorless solid (11.4 mg, 96% yield) and ^1H NMR indicated >95% purity; ^1H NMR (400 MHz, CDCl_3) δ 7.02 (dt, $J = 10.1, 7.4$ Hz, 2H), 6.33 (s, 1H), 5.32 (t, $J = 5.5$ Hz, 1H), 4.01 (dt, $J = 12.4, 3.0$ Hz, 1H), 3.84 (s, 3H), 3.79 (dd, $J = 6.5, 1.5$ Hz, 2H), 3.69 (s, 3H), 3.33 (dd, $J = 11.1, 5.0$ Hz, 1H), 3.27 (dd, $J = 11.1, 6.0$ Hz, 1H), 3.13 (dd, $J = 17.8, 6.7$ Hz, 1H), 2.96 – 2.84 (m, 1H), 2.73 (dd, $J = 14.7, 2.7$ Hz, 1H), 2.61 (t, $J = 13.5$ Hz, 1H), 2.46 (s, 3H), 2.14 (s, 3H); ^{19}F NMR (282 MHz, CDCl_3) δ –139.12 (ddd, $J = 21.3, 10.2, 7.7$ Hz), –139.40 – –139.78 (m).



Difluorinated monochlorinated bis-THIQ 160: bis-THIQ **159** (5.9 mg, 0.013 mmol, 1.0 equiv) was dissolved in HFIP (0.65 mL, 0.02 M) and the solution was cooled to 0 °C. *N*-Chlorosaccharine (3.0 mg, 0.014 mmol, 1.05 equiv) was added, after which the cloudy white mixture turned yellow and became homogeneous. After complete addition, the LCMS showed complete consumption of **159**, so the reaction was quenched by the addition of saturated aqueous Na₂S₂O₃. The resulting mixture was transferred to a separatory funnel and diluted with CH₂Cl₂ and water, creating a triphasic system with HFIP on the bottom, CH₂Cl₂ in the middle, and the aqueous phase on top. The bottom two phases were collected. The aqueous phase was basified with saturated aqueous K₂CO₃ solution and extracted with CH₂Cl₂. The organic phases were combined, concentrated, and azeotropically dried twice with benzene to afford the crude material with >95% purity as a yellow solid (6.0 mg, 94% yield); ¹H NMR (500 MHz, CDCl₃) δ 7.01 (ddd, *J* = 10.4, 7.6, 4.3 Hz, 2H), 5.37 (t, *J* = 5.9 Hz, 1H), 4.44 (d, *J* = 3.7 Hz, 1H), 4.35 (br s, 1H, OH), 4.09 (dt, *J* = 12.7, 3.0 Hz, 1H), 3.82 (s, 3H), 3.76 (d, *J* = 6.8 Hz, 1H), 3.71 (s, 3H), 3.43 – 3.19 (m, 3H), 3.12 (dd, *J* = 18.1, 6.9 Hz, 1H), 2.96 (d, *J* = 18.1 Hz, 1H), 2.44 (s, 3H), 2.38 (t, *J* = 14.0 Hz, 1H), 2.27 (s, 3H).

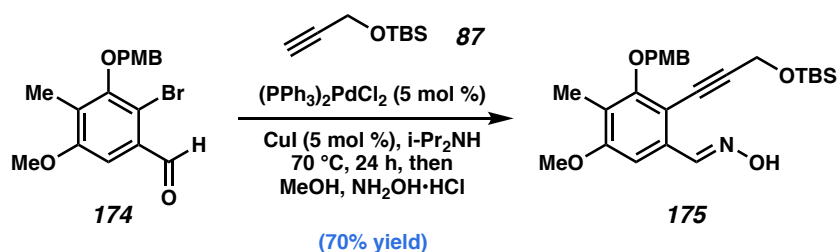
A8.4.2.7 Preparation of PMB-protected bis-isoquinoline

2-bromo-3-hydroxy-5-methoxy-4-methylbenzaldehyde (173): Aldehyde **172**¹⁹ (3.97 g, 23.9 mmol, 1.00 equiv) was dissolved in CH₂Cl₂ (48 mL, 0.5 M), and acetic acid (14 μ L, 0.24 mmol, 0.01 equiv) was added. The solution was cooled to 0 °C before bromine (1.35 mL, 26.3 mmol, 1.10 equiv) was added in a slow, dropwise fashion. The solution was stirred 30 min after complete addition at 0 °C, at which time TLC (20% EtOAc/hex) showed complete consumption of starting material **172**. The reaction was quenched by the addition of saturated aqueous sodium thiosulfate and saturated NaHCO₃ solution. The layers were separated and the aqueous phase was extracted with CH₂Cl₂ and EtOAc. The combined organic phases were washed with water, dried over MgSO₄ and concentrated. The crude residue (brown solid, 5.17 mg, 88% yield) was sufficiently pure by ¹H NMR and was used in the subsequent step without further purification; ¹H NMR (500 MHz, CDCl₃) δ 10.24 (s, 1H), 7.08 (s, 1H), 5.88 (s, 1H), 3.88 (s, 3H), 2.25 (s, 3H).



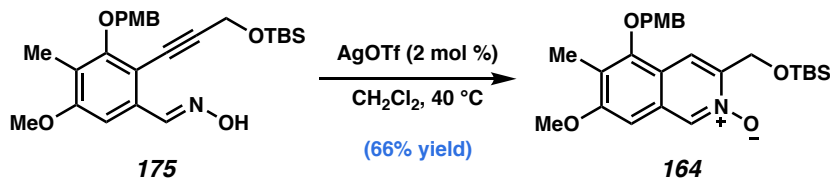
2-bromo-5-methoxy-3-((4-methoxybenzyl)oxy)-4-methylbenzaldehyde (174): To a solution of alcohol **173** (245 mg, 1.0 mmol, 1.0 equiv) in DMF (5 mL, 0.2 M) was added 4-methoxybenzyl chloride (PMBCl, 0.15 mL, 1.1 mmol, 1.1 equiv) and K₂CO₃ (166 mg, 1.2 mmol, 1.2 equiv). After heating at 60 °C for 15 h, the reaction mixture was cooled to

ambient temperature, and quenched with ice and water. The layers were separated, and the aqueous phase was extracted with EtOAc. The combined organic phases were washed with brine, dried over Na₂SO₄, and concentrated. The crude residue was purified by column chromatography (10% EtOAc/hexanes) to furnish PMB-protected alcohol **174** as a white solid (298 mg, 82% yield); ¹H NMR (400 MHz, CDCl₃) δ 10.37 (s, 1H), 7.47 (d, *J* = 8.6 Hz, 2H), 7.25 (s, 1H), 6.94 (d, *J* = 8.7 Hz, 2H), 4.87 (s, 2H), 3.88 (s, 3H), 3.84 (s, 3H), 2.23 (s, 3H).

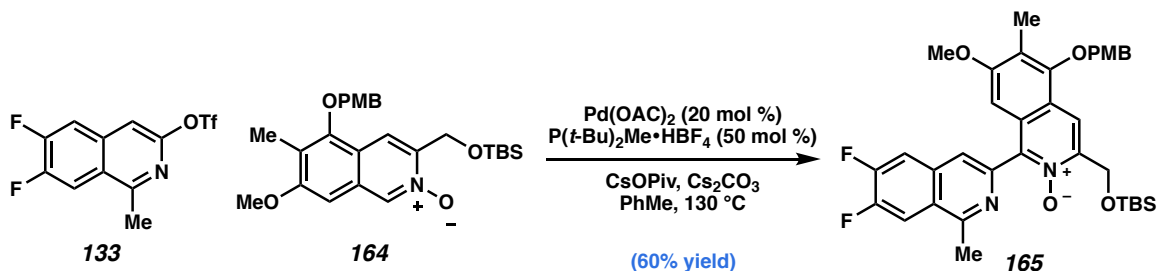


Oxime 175: Bromide **174** (5.73 g, 15.69 mmol, 1 equiv), (PPh₃)₂PdCl₂ (550 mg, 0.784 mmol, 0.05 equiv), and CuI (149 mg, 0.784 mmol, 0.05 equiv) were slurried in diisopropylamine (60 mL, 0.25 M, freshly distilled from CaH₂), and the yellow suspension was sparged with N₂ for 10 min. *O*-*tert*-butyldimethylsilyl propargyl alcohol²⁰ (**87**, 3.61 g, 21.18 mmol, 4.35 equiv) was added in one portion, causing the suspension to darken. The suspension was sparged with N₂ for a further 1 min, then heated to 70 °C for 24 h. At this stage, TLC and LCMS indicated complete consumption of bromide **86**, so the brown suspension was cooled to 50 °C and 40 mL of distilled MeOH was added. Hydroxylamine hydrochloride (1.31 g, 18.85 mmol, 1.2 equiv) was added in one portion and the solution was heated to reflux (85 °C). After 2 h, TLC and LCMS indicated complete consumption of the intermediate aldehyde. The solution was cooled to room temperature and celite (~20 g) was added. The suspension was filtered through a pad of

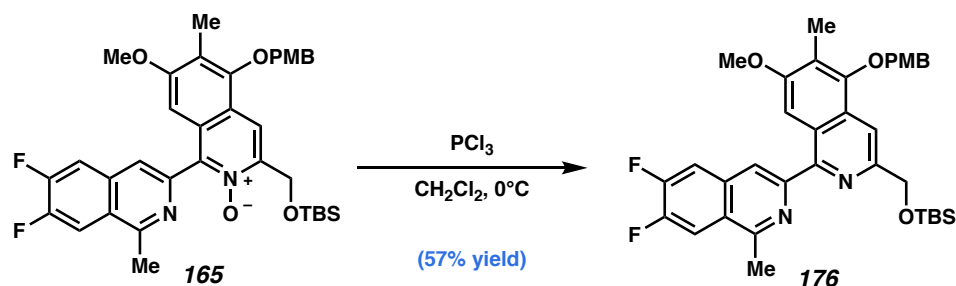
celite, topped with sand, eluting with ethyl acetate. The filtrate was concentrated and purified by column chromatography (20–25–50–100% EtOAc/hexanes) to afford **175** as a brown solid (5.19 g, 70% yield); ^1H NMR (300 MHz, CDCl_3) δ 8.64 (s, 1H), 7.42 (d, J = 8.7 Hz, 2H), 7.12 (s, 1H), 6.90 (d, J = 8.7 Hz, 2H), 4.96 (s, 2H), 4.61 (s, 2H), 3.85 (s, 3H), 3.82 (s, 3H), 2.07 (s, 3H), 0.93 (s, 9H), 0.15 (s, 6H).



Isoquinoline N-oxide 164: Oxime **175** (5.19 g, 11.05 mmol, 1 equiv) was dissolved in CH_2Cl_2 (110 mL, 0.1 M) and the flask was vacuum purged and refilled with nitrogen five times, then heated to reflux. AgOTf (57 mg, 0.22 mmol, 0.02 equiv) was added in one portion to the refluxing solution, resulting in a rapid and mildly exothermic reaction. The reaction flask was shielded from light and maintained at reflux for 15 min, at which time TLC indicated partial conversion to the product. No significant change was observed after another 25 minutes at reflux, so additional AgOTf (57 mg, 0.22 mmol, 0.0 equiv) was added to the reaction. After 15 minutes, complete consumption of the oxime was observed by LCMS, so the solution was filtered through a pad of silica with CH_2Cl_2 and 5–10% MeOH/EtOAc + 1% Et_3N . The crude residue was purified by column chromatography (50–100% EtOAc/hexanes + 1% Et_3N ; then 5–10–20% MeOH/EtOAc + 1% NEt_3) to afford N-oxide **164** as a colorless solid (3.43 g, 66% yield); ^1H NMR (300 MHz, CDCl_3) δ 8.69 (s, 1H), 8.09 (s, 1H), 7.41 (d, J = 8.5 Hz, 2H), 6.93 (d, J = 8.7 Hz, 2H), 6.76 (s, 1H), 5.03 (s, 2H), 4.91 (s, 2H), 3.95 (s, 3H), 3.84 (s, 3H), 2.27 (s, 3H), 0.97 (s, 9H), 0.17 (s, 6H).

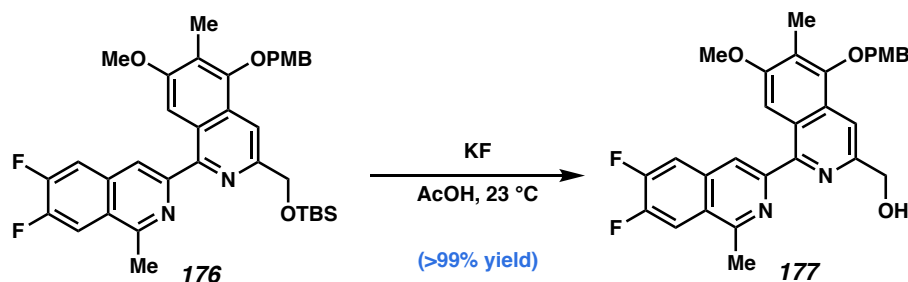


Difluorinated PMB bis-IQ *N*-oxide 165: Prepared according to General Procedure 1 using isoquinoline triflate **133** (424 mg, 1.295 mmol) and isoquinoline *N*-oxide **164** (1.83 g, 3.886 mmol). Reaction completed after 17 hours. The crude material was purified by column chromatography (30–50–100% EtOAc/hex + 1% Et_3N , then 10–20% MeOH/EtOAc + 1% Et_3N) to afford bis-isoquinoline **165** as a white solid (388 mg, 60% yield). This isolated product is ca. 90% pure by NMR; ^1H NMR (400 MHz, CDCl_3) δ 8.23 (s, 1H), 8.01 – 7.91 (m, 2H), 7.63 (dd, $J = 10.2, 7.8$ Hz, 1H), 7.45 (d, $J = 8.7$ Hz, 2H), 6.95 (d, $J = 8.7$ Hz, 2H), 6.51 (s, 1H), 5.06 (d, $J = 1.2$ Hz, 2H), 4.93 (s, 2H), 3.85 (s, 3H), 3.66 (s, 3H), 3.01 (s, 3H), 2.26 (s, 3H), 0.98 (s, 9H), 0.17 (s, 6H).



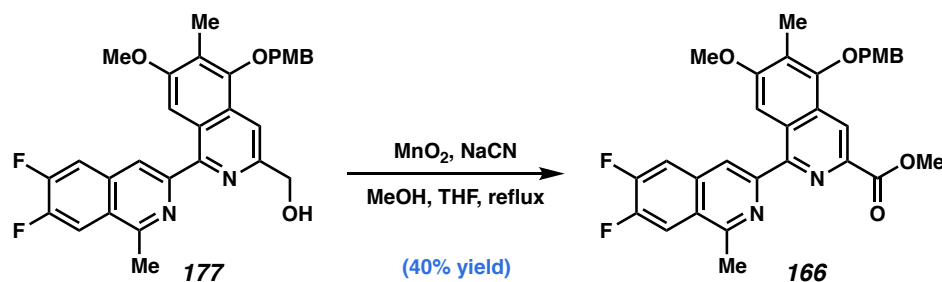
Difluorinated PMB bis-IQ 176: Prepared according to General Procedure 2 using *N*-oxide **165** (388 mg, 0.60 mmol) as the starting material. Reaction stalled after 1 h, so additional PCl_3 (0.1 mL, 1.2 mmol, 2.0 equiv) was added and stirred at 0°C for another 30 minutes. The crude material was purified by column chromatography (10% EtOAc/hex + 1% Et_3N) to afford bis-isoquinoline **176** as a white solid (218 mg, 57% yield); ^1H NMR (500 MHz, CDCl_3) δ 8.15 (s, 2H), 7.93 (dd, $J = 10.8, 7.8$ Hz, 1H), 7.78

(s, 1H), 7.67 (dd, $J = 10.2, 7.9$ Hz, 1H), 7.49 (d, $J = 8.6$ Hz, 2H), 6.96 (d, $J = 8.6$ Hz, 2H), 5.09 (s, 2H), 4.94 (s, 2H), 3.86 (s, 3H), 3.85 (s, 3H), 3.04 (s, 3H), 2.32 (s, 3H), 1.00 (s, 9H), 0.18 (s, 6H). *Note:* The reaction profile was very clean according to TLC and LCMS, but low yield was obtained as a result of poor mass recovery after column purification. This is consistent with what was observed in previous deoxygenation reactions.

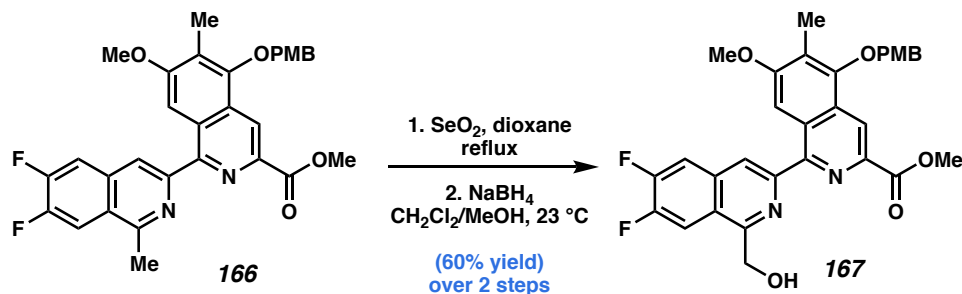


Difluorinated PMB bis-IQ 177: Bis-isoquinoline **176** (218 mg, 0.345 mmol, 1.0 equiv) was dissolved in acetic acid (7.0 mL, 0.05 M) and solid potassium fluoride (40.1 mg, 0.689 mmol, 2.0 equiv) was added in one portion. The solution was stirred for 2 h at room temperature, at which point TLC showed complete conversion to the product. The reaction mixture was dilute with CH_2Cl_2 , and ice and the solution was stirred vigorously as a solution of sodium hydroxide (4.4 g, 0.11 mol, 0.9 equiv relative to 7 mL AcOH) in 12 mL water was added slowly. The rest of the acetic acid was quenched by the addition of saturated aqueous K_2CO_3 . The layers were separated and the aqueous phase was extracted with CH_2Cl_2 . The combined organic phases were washed with brine, dried over Na_2SO_4 , and concentrated to afford crude **177** as a white solid (208 mg, >99 yield). Crude ^1H NMR (500 MHz, CDCl_3) δ 8.25 (d, $J = 2.7$ Hz, 1H), 7.98 – 7.90 (m, 2H), 7.82 (s, 1H), 7.76 – 7.67 (m, 1H), 7.44 (d, $J = 8.3$ Hz, 2H), 6.97 (d, $J = 8.0$ Hz, 2H), 4.94 (s, 2H), 4.93 (s, 2H), 3.88 (s, 3H), 3.86 (s, 3H), 3.05 (s, 3H), 2.34 (s, 3H). *Note:* We elected to use the

crude material in the subsequent step without further purification due to its poor solubility in organic solvents.



Diffuorinated PMB bis-IQ ester 166: To a solution of desilylated bis-isoquinoline **177** (167 mg, 0.325 mmol, 1.0 equiv) in THF (7.6 mL, 0.04 M) was added MnO_2 (988 mg, 11.4 mmol, 35 equiv), NaCN (18.6 mg, 0.379 mmol, 1.2 equiv), and MeOH (77 μL , 1.895 mmol, 5.8 equiv). The reaction mixture was stirred for 18 hours at reflux, after which time a ca. 1:1 mixture of aldehyde/ester was observed by LCMS. At this stage, additional NaCN (18.6 mg, 0.379 mmol, 1.2 equiv) and MeOH (77 μL , 1.895 mmol, 5.8 equiv) were added, and the reaction mixture was stirred at reflux for another 18 hours. The reaction mixture was cooled to room temperature and filtered through celite, rinsing with CH_2Cl_2 and MeOH . The filtrate was concentrated, then redissolved in CH_2Cl_2 , washed with water, dried over Na_2SO_4 , and concentrated. The crude residue was purified by column chromatography using a 1:1 mixture of CH_2Cl_2 :EtOAc as the polar solvent (30–50% polar solvent/hexanes + 1% NEt_3) to provide **166** as a colorless solid (71 mg, 40% yield). *Note:* The R_f difference between the aldehyde and the ester is very small. The isolated product still contains ca. 10% aldehyde; ^1H NMR (500 MHz, CDCl_3) δ 8.80 (s, 1H), 8.34 (s, 1H), 8.02 (s, 1H), 7.94 (dd, $J = 10.5, 7.8$ Hz, 1H), 7.77 – 7.65 (m, 1H), 7.47 (d, $J = 8.5$ Hz, 2H), 6.97 (d, $J = 8.5$ Hz, 2H), 4.99 (s, 2H), 4.05 (s, 3H), 3.91 (s, 3H), 3.86 (s, 3H), 3.05 (s, 3H), 2.34 (s, 3H).



Difluorinated PMB bis-IQ hydrogenation precursor 167: Prepared according to General Procedure 4 using bis-isoquinoline ester **166** (9.3 mg, 0.017 mmol) as the starting material. The reduction required only 0.33 mmol of NaBH_4 . The crude material was purified by preparative TLC (50% EtOAc/hexanes) to afford hydrogenation precursor **167** as a white solid (5.8 mg, 60% yield over 2 steps); ^1H NMR (500 MHz, CDCl_3) δ 8.81 (s, 1H), 8.46 (s, 1H), 7.88 (s, 1H), 7.84 – 7.64 (m, 2H), 7.47 (d, $J = 8.5$ Hz, 2H), 6.98 (d, $J = 8.5$ Hz, 2H), 5.27 (s, 2H), 5.02 (s, 2H), 4.06 (s, 3H), 3.90 (s, 3H), 3.86 (s, 3H), 2.36 (s, 3H).

A8.5 REFERENCES AND NOTES

- (1) Scott, J. D.; Williams, R. M. *Chem. Rev.* **2002**, *102*, 1669–1730.
- (2) a) Chrzanowska, M.; Grajewska, A.; Rozwadowska, M. D. *Chem. Rev.* **2016**, *116*, 12369–12465; b) Chrzanowska, M.; Rozwadowska, M. D. *Chem. Rev.* **2004**, *104*, 3341–3370.
- (3) a) Perez-Ruixo, J. J.; Zannikos, P.; Hirankam, S.; Stuyckens, K.; Ludwig, E. A.; Soto-Matos, A.; Lopez-Lazaro, L.; Owen, J. S. *Clin. Pharmacokinet.* **2007**, *46*, 867–884; b) Pérez-Ruixo, C.; Valenzuela, B.; Fernández Teruel, C.; González-Sales, M.; Miguel-Lillo, B.; Soto-Matos, A.; Pérez-Ruixo, J. J. *Cancer*

- Chemother. Pharmacol.* **2012**, *69*, 15–24; c) Spencer, J. R.; Sendzik, M.; Oeh, J.; Sabbatini, P.; Dalrymple, S. A.; Magill, C.; Kim, H. M.; Zhang, P.; Squires, N.; Moss, K. G.; Sukbuntherng, J.; Graupe, D.; Eksterowicz, J.; Young, P. R.; Myers, A. G.; Green, M. J. *Bioorg. Med. Chem. Lett.* **2006**, *16*, 4884–4888; d) U.S. Food and Drug Administration, Center for Drug Evaluation and Research. ID No. 207953Orig1s000, Pharmacology Reviews.
- (4) a) Reid, J. M.; Kuffel, M. J.; Ruben, S. L.; Morales, J. J.; Rinehart, K. L.; Squillace, D. P.; Ames, M. M. *Clin Cancer Res* **2002**, *8*, 2952–2962; b) Beumer, J. H.; Rademaker-Lakhai, J. M.; Rosing, H.; Hillebrand, M. J. X.; Bosch, T. M.; Lopez-Lazaro, L.; Schellens, J. H. M.; Beijnen, J. H. *Cancer Chemother. Pharmacol.* **2007**, *59*, 825–837; c) Saito, N.; Tanaka, C.; Koizumi, Y.; Suwanborirux, K.; Amnuoypol, S.; Pummangura, S.; Kubo, A. *Tetrahedron* **2004**, *60*, 3873–3881.
- (5) Shah, P.; Westwell, A. D. *J. Enzyme Inhib. Med.* **2007**, *22*, 527–540.
- (6) *Ortho*-silyl triflate **136** is a known compound and can be prepared according to the procedure reported in Li, X.; Sun, Y.; Huang, X.; Zhang, L.; Kong, L.; Peng, B. *Org. Lett.* **2017**, *19*, 838–841.
- (7) Maki, B. E.; Chan, A.; Phillips, E. M.; Scheidt, K. A. *Org. Lett.* **2007**, *9*, 371–374.
- (8) Foot, J. S.; Kanno, H.; Giblin, G. M. P.; Taylor, R. J. K. *Synthesis* **2003**, *2003*, 1055–1064.
- (9) This product can only be purified by preparative HPLC. Attempt to monitor the product on TLC, both via UV and different stains, failed (see GMP-III-233).

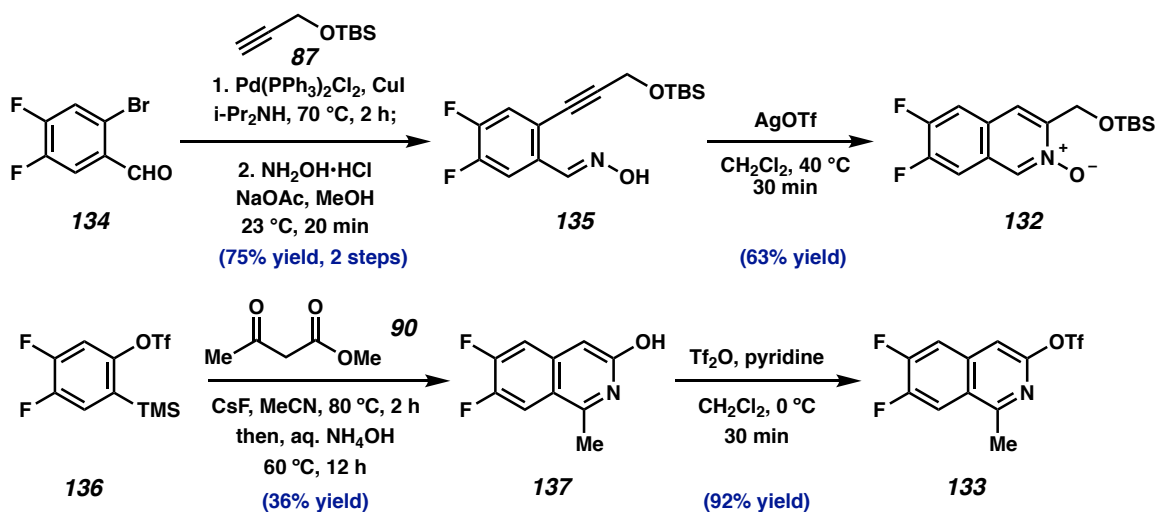
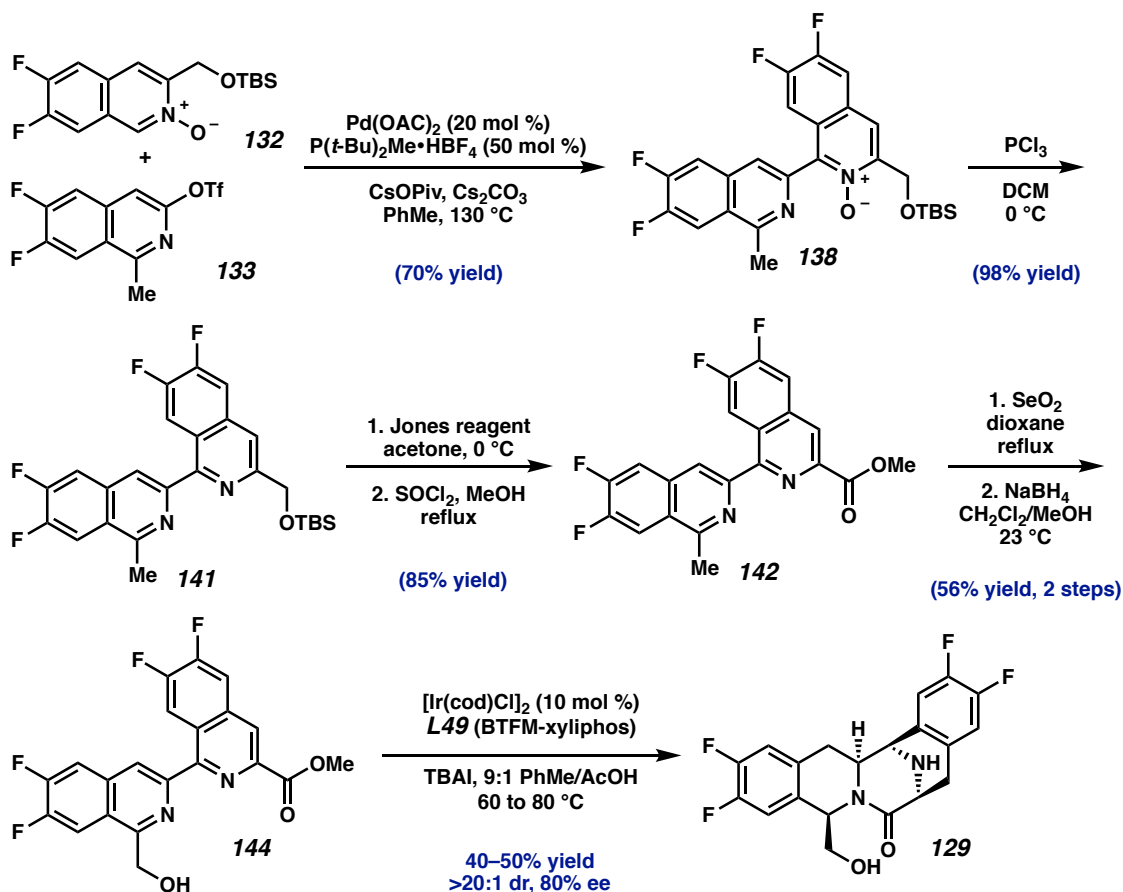
- (10) Previous studies have shown that acetyl-protected alcohol resulted in improved cytotoxic activities, see Charupant, K.; Daikuhara, N.; Saito, E.; Amnuoypol, S.; Suwanborirux, K.; Owa, T.; Saito, N. *Bioorg. Med. Chem.* **2009**, *17*, 4548–4558.
- (11) We have previously isolated and fully characterized the oxidative deformylated byproduct over the course of the synthesis of monohydrodxylylated bis-THIQ analog **121** (see section 3.6.2.9).
- (12) Xu, S.; Wang, G.; Zhu, J.; Shen, C.; Yang, Z.; Yu, J.; Li, Z.; Lin, T.; Sun, X.; Zhang, F. A *Eur. J. Org. Chem.* **2017**, *2017*, 975–983.
- (13) Isoquinolin *N*-oxide **164** can be prepared in 4 steps from a known compound in 33% overall yield, see Section A8.4.2.7.
- (14) During the course of our synthetic studies toward jorumycin, we observed approximately 30% of bis-borylated product through this sequence. See ERW's subgroup 6-6-17 and ERW-II-129 (notebook) for more details.
- (15) Börgel, J.; Tanwar, L.; Berger, F.; Ritter, T. *J. Am. Chem. Soc.* **2018**, *140*, 16026–16031.
- (16) Pangborn, A. B.; Giardello, M. A.; Grubbs, R. H.; Rosen, R. K.; Timmers, F. J. *Organometallics*, **1996**, *15*, 1518–1520.
- (17) Nicolaou, K. C.; Rhoades, D.; Lamani, M.; Pattanayak, M. R.; Kumar, S. M. *J. Am. Chem. Soc.* **2016**, *138*, 7532–7535.
- (18) Allan, K. M.; Hong, B. D.; Stoltz, B. M. *Org. Biomol. Chem.* **2009**, *7*, 4960–4964.
- (19) Crowley, B. M.; Mori, Y.; McComas, C. C.; Tang, D.; Boger, D. L. *J. Am. Chem. Soc.* **2004**, *126*, 4310–4317.

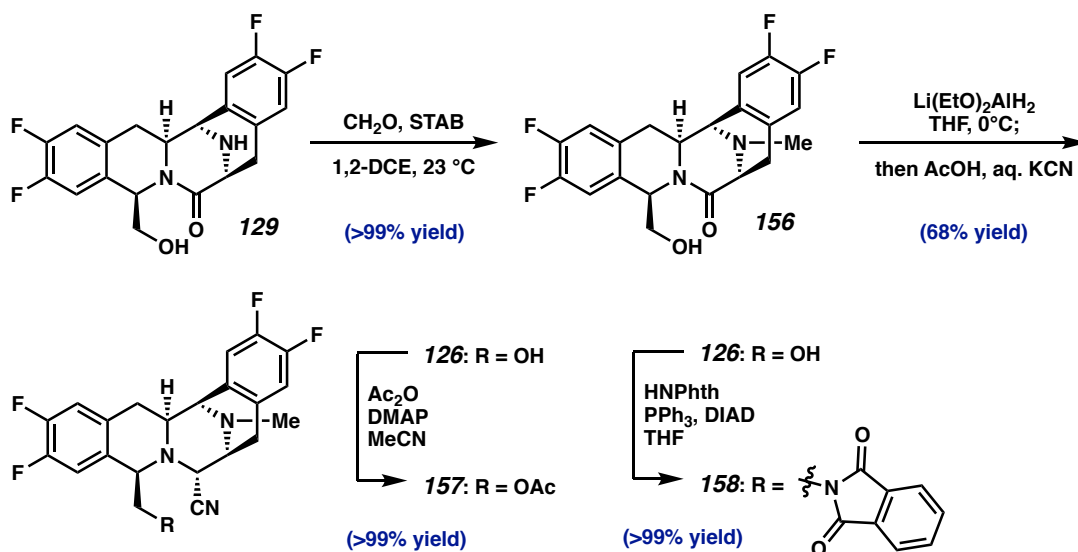
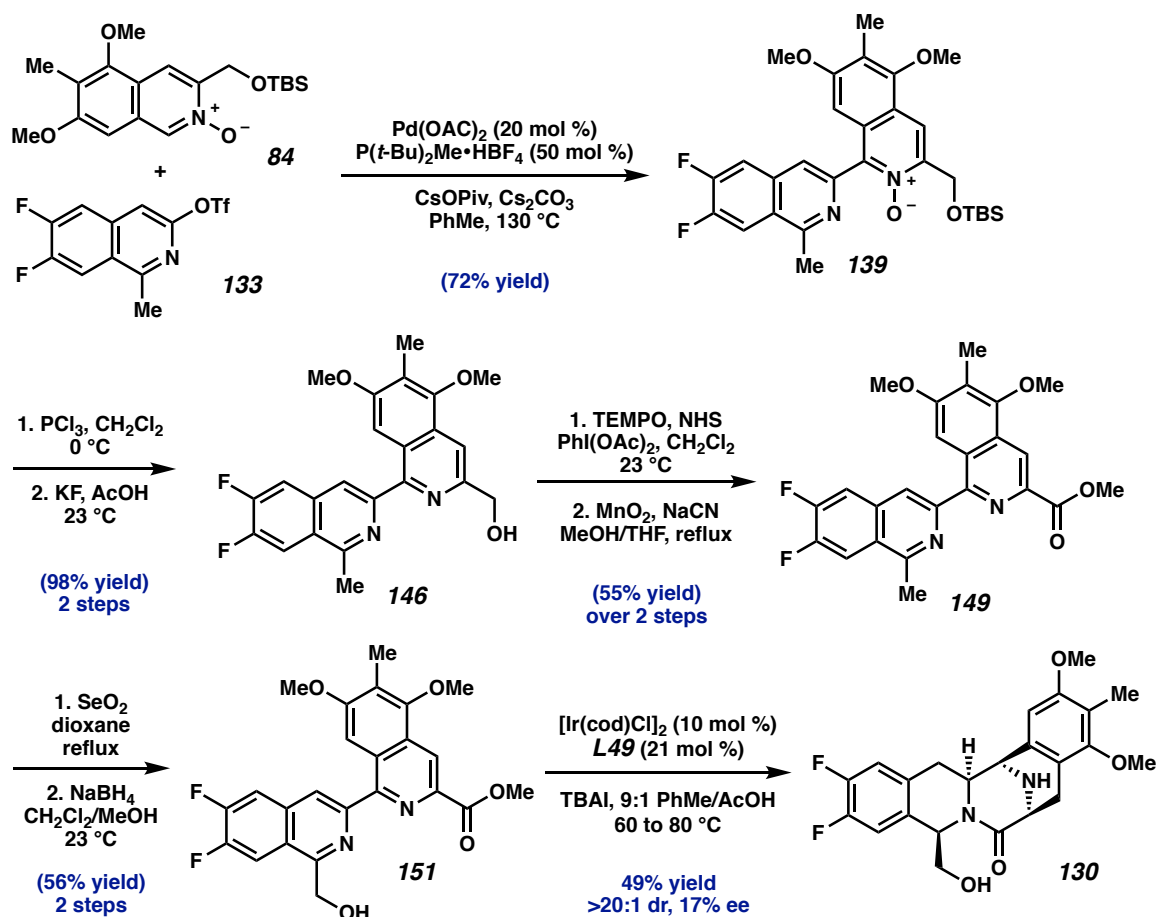
- (20) Nicolaou, K. C.; Rhoades, D.; Lamani, M.; Pattanayak, M. R.; Kumar, S. M. *J. Am. Chem. Soc.* **2016**, *138*, 7532–7535.

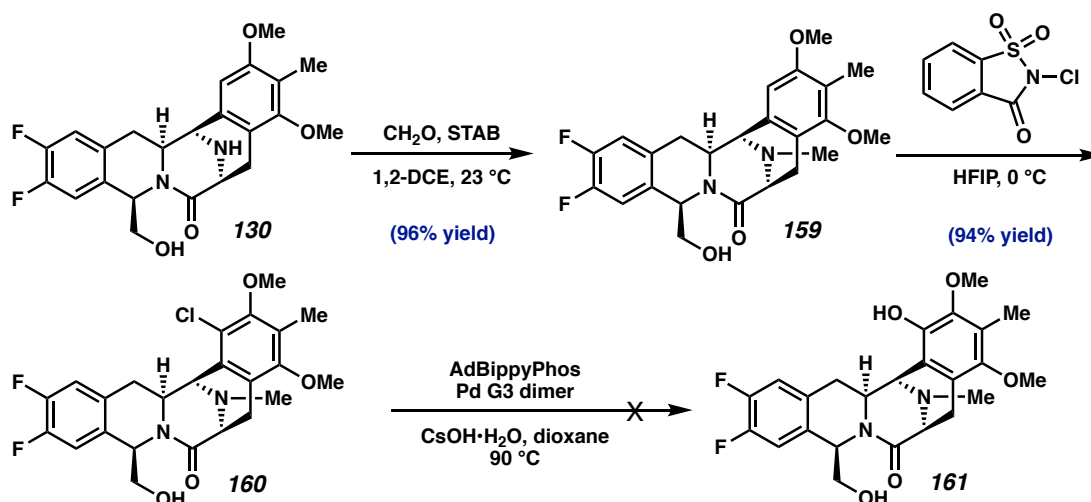
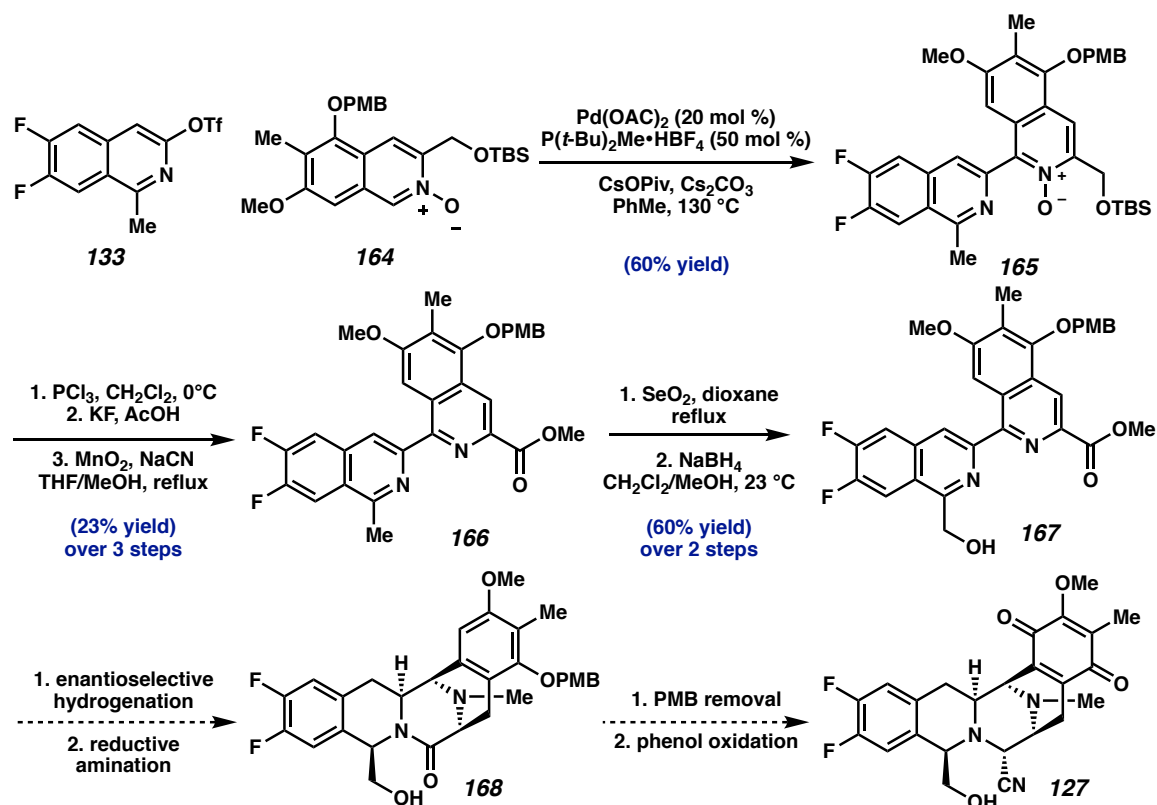
APPENDIX 9

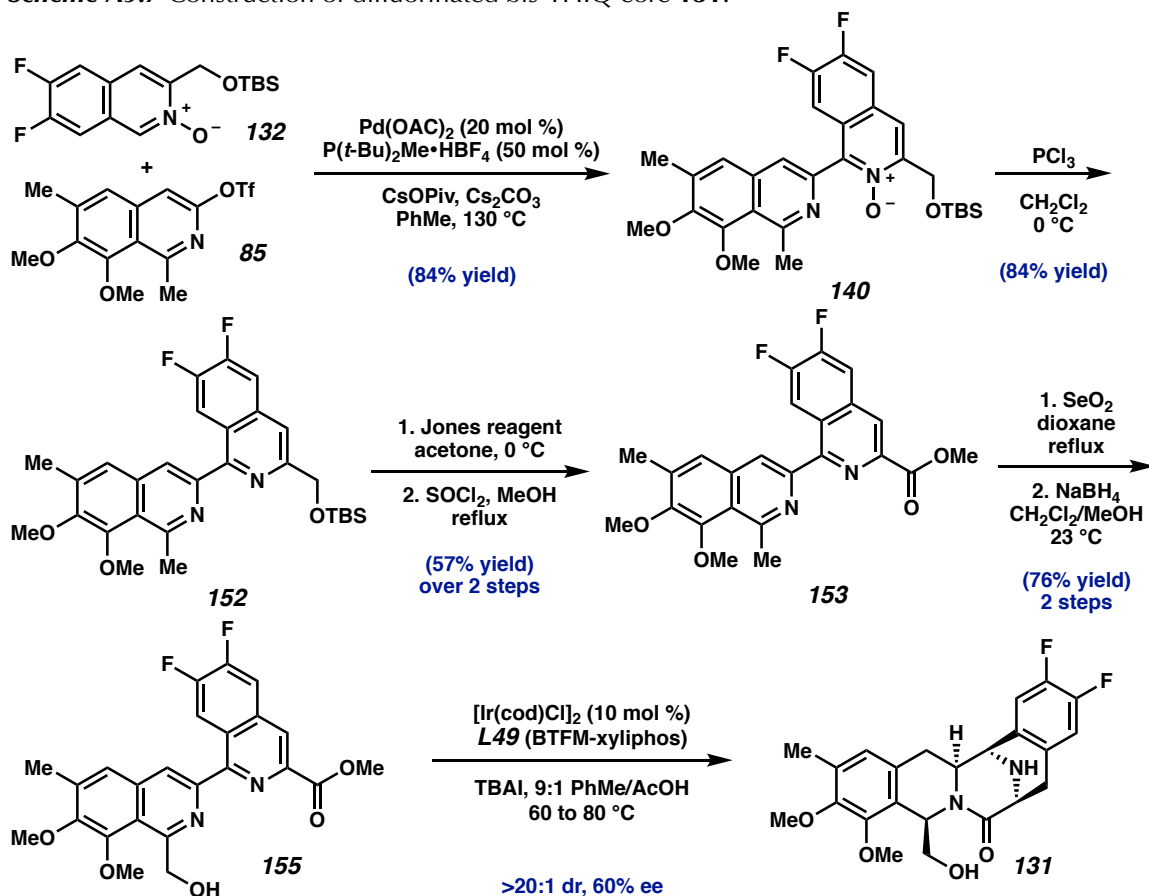
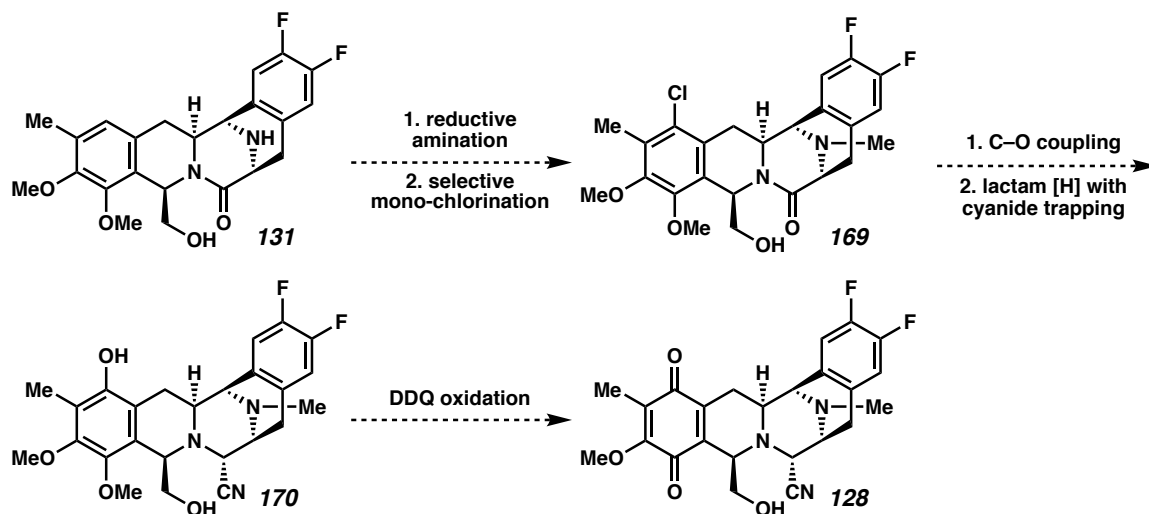
Synthetic Summary of Appendix 8:

Progress Toward the Syntheses of bis-Tetrahydroisoquinoline Analogs

Scheme A9.1 Syntheses of isoquinoline *N*-oxide **132** and isoquinoline triflate **133**.**Scheme A9.2** Construction of tetrafluorinated bis-THIQ core **129**.

Scheme A9.3 Syntheses of tetrafluorinated analog **126** and its derivatives **157**–**158**.**Scheme A9.4** Construction of difluorinated bis-THIQ core **130**.

Scheme A9.5 Synthetic route toward analog **127**.**Scheme A9.6** Alternative strategy to access difluorinated bis-THIQ analog **127**.

Scheme A9.7 Construction of difluorinated bis-THIQ core **131**.**Scheme A9.8** Proposed endgame toward difluorinated analog **128**.

APPENDIX 10

Spectra Relevant to Appendix 8:

Progress Toward

the Syntheses of bis-Tetrahydroisoquinoline Analogs

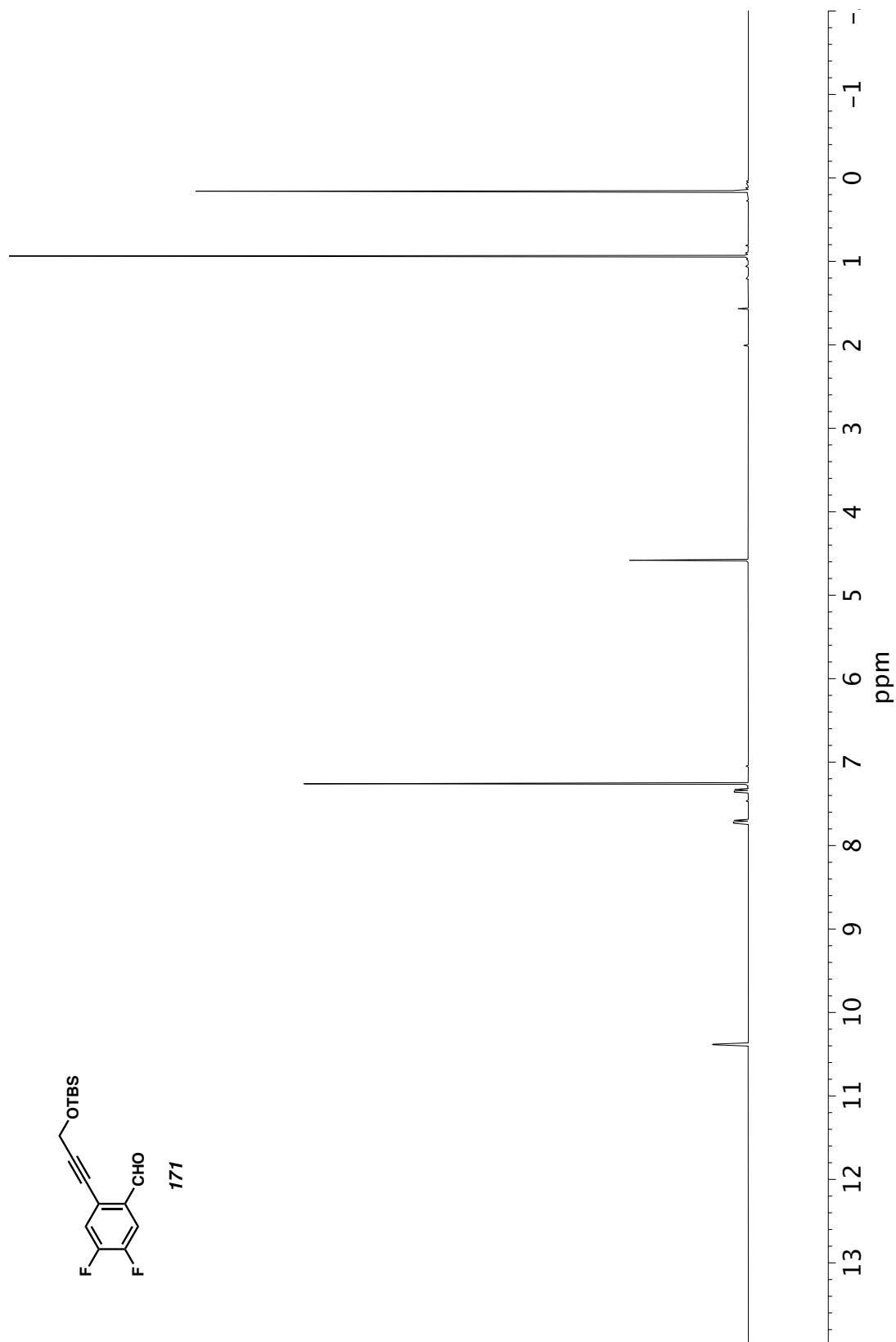


Figure A10.1 ¹H NMR (500 MHz, CDCl₃) of compound **171**.

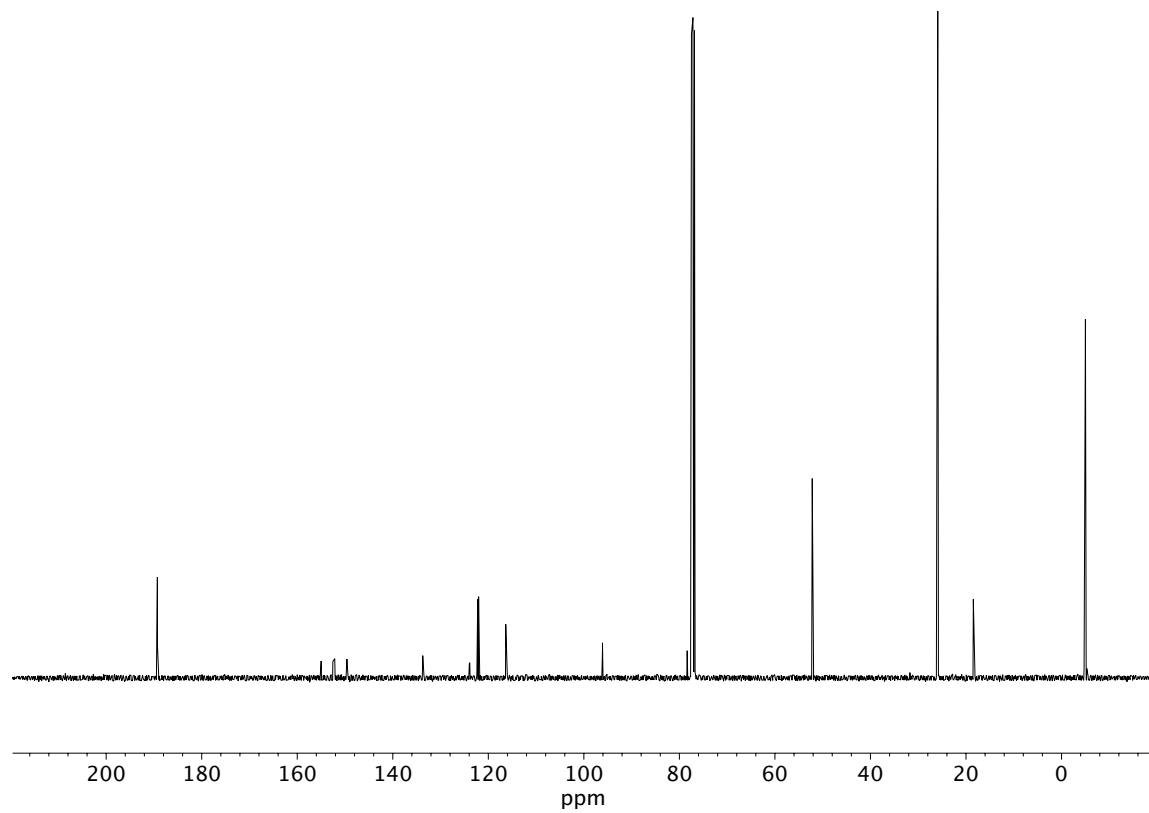


Figure A10.2 ^{13}C NMR (100 MHz, CDCl_3) of compound **171**.

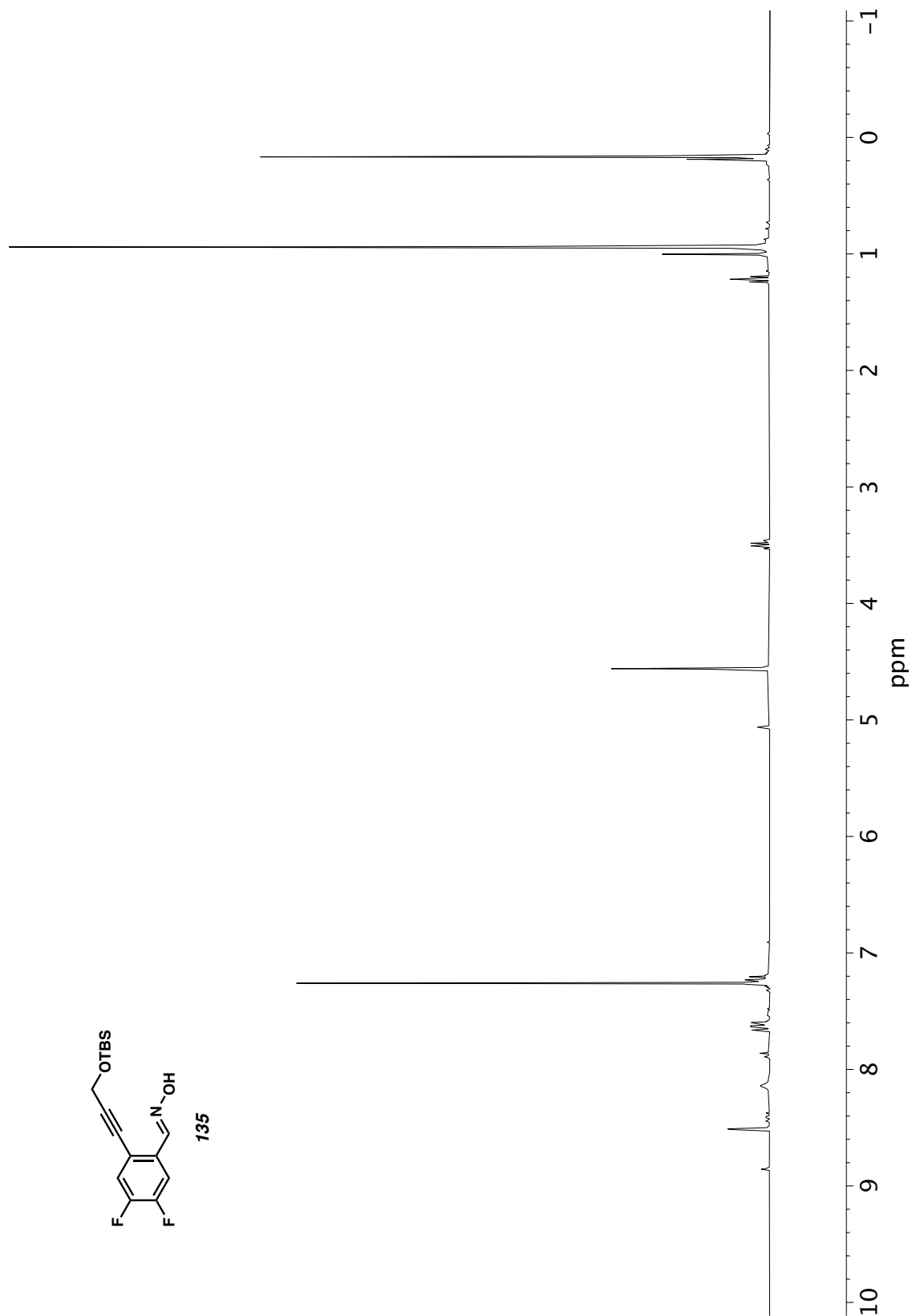


Figure A10.3 ¹H NMR (300 MHz, CDCl₃) of compound **135**.

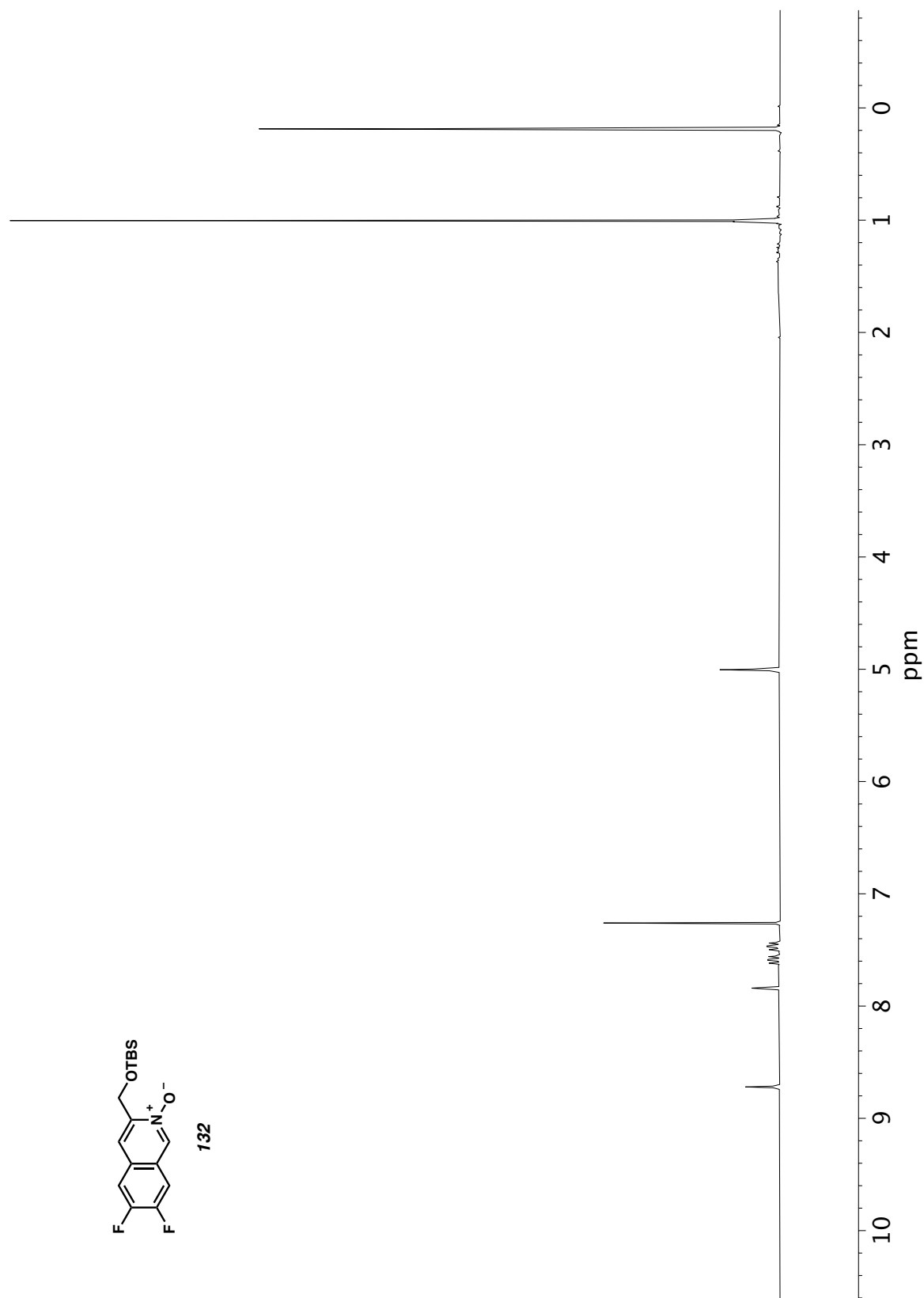


Figure A10.4 ^1H NMR (300 MHz, CDCl_3) of compound **132**.

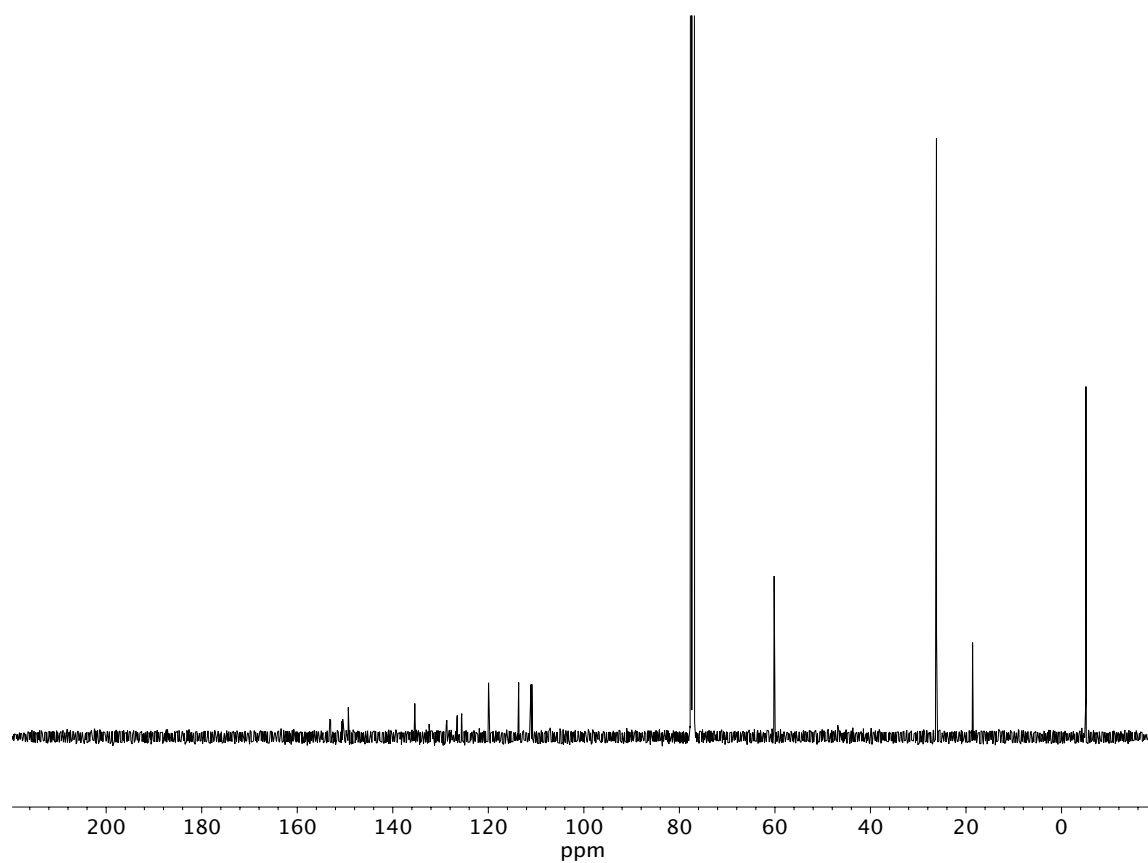


Figure A10.5 ^{13}C NMR (100 MHz, CDCl_3) of compound **132**.

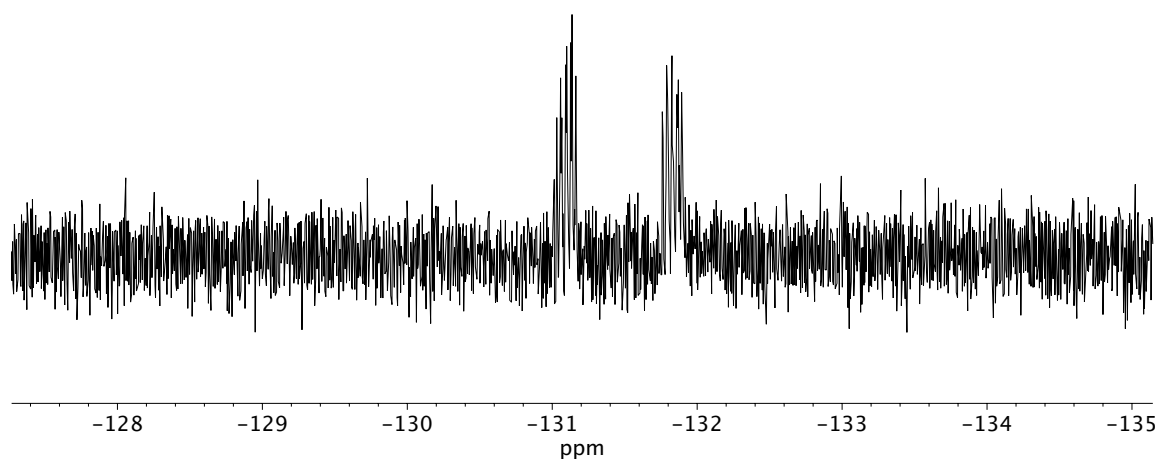


Figure A10.6 ^{19}F NMR (282 MHz, CDCl_3) of compound **132**.

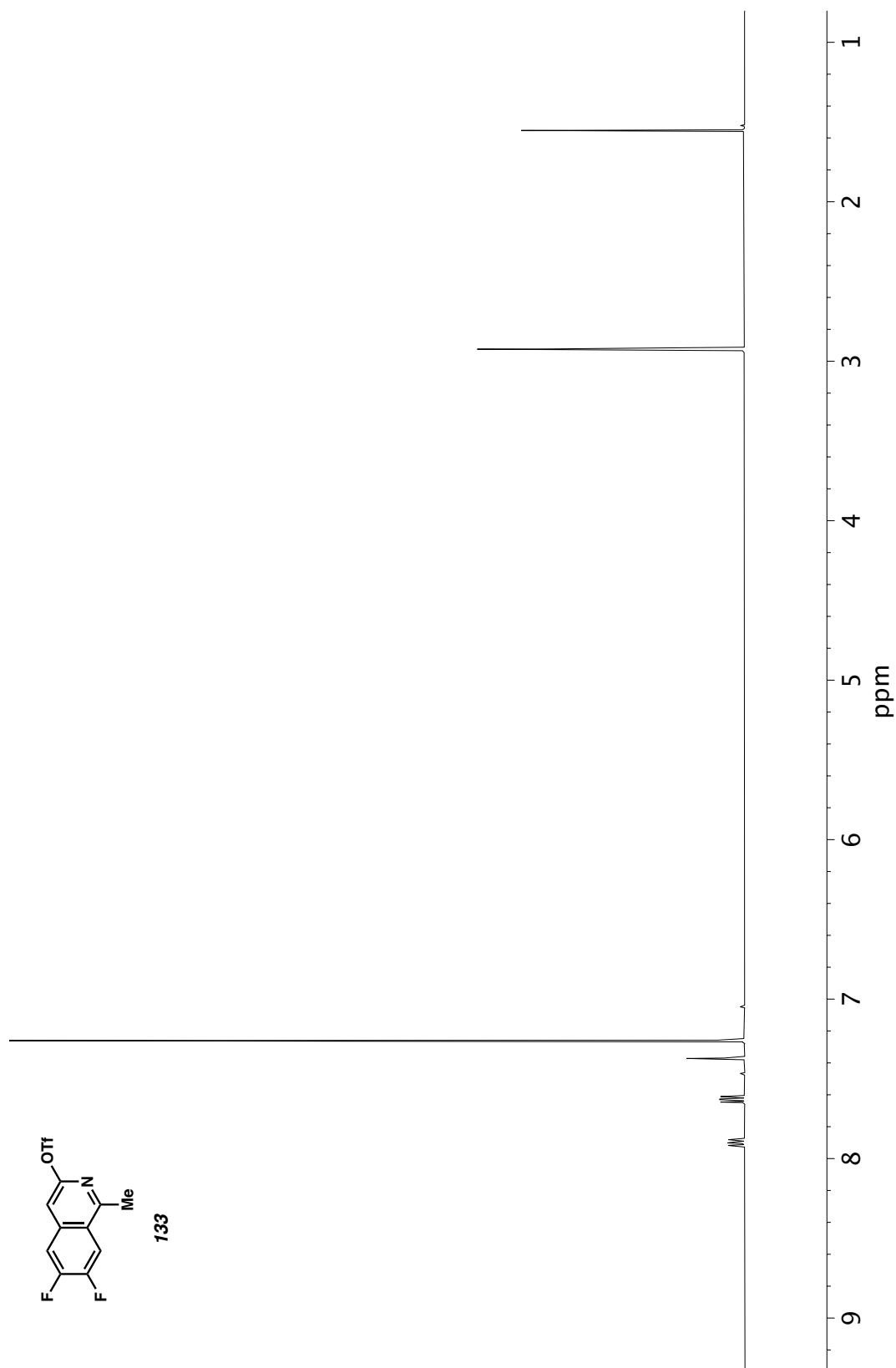


Figure A10.7 ^1H NMR (500 MHz, CDCl_3) of compound **133**.

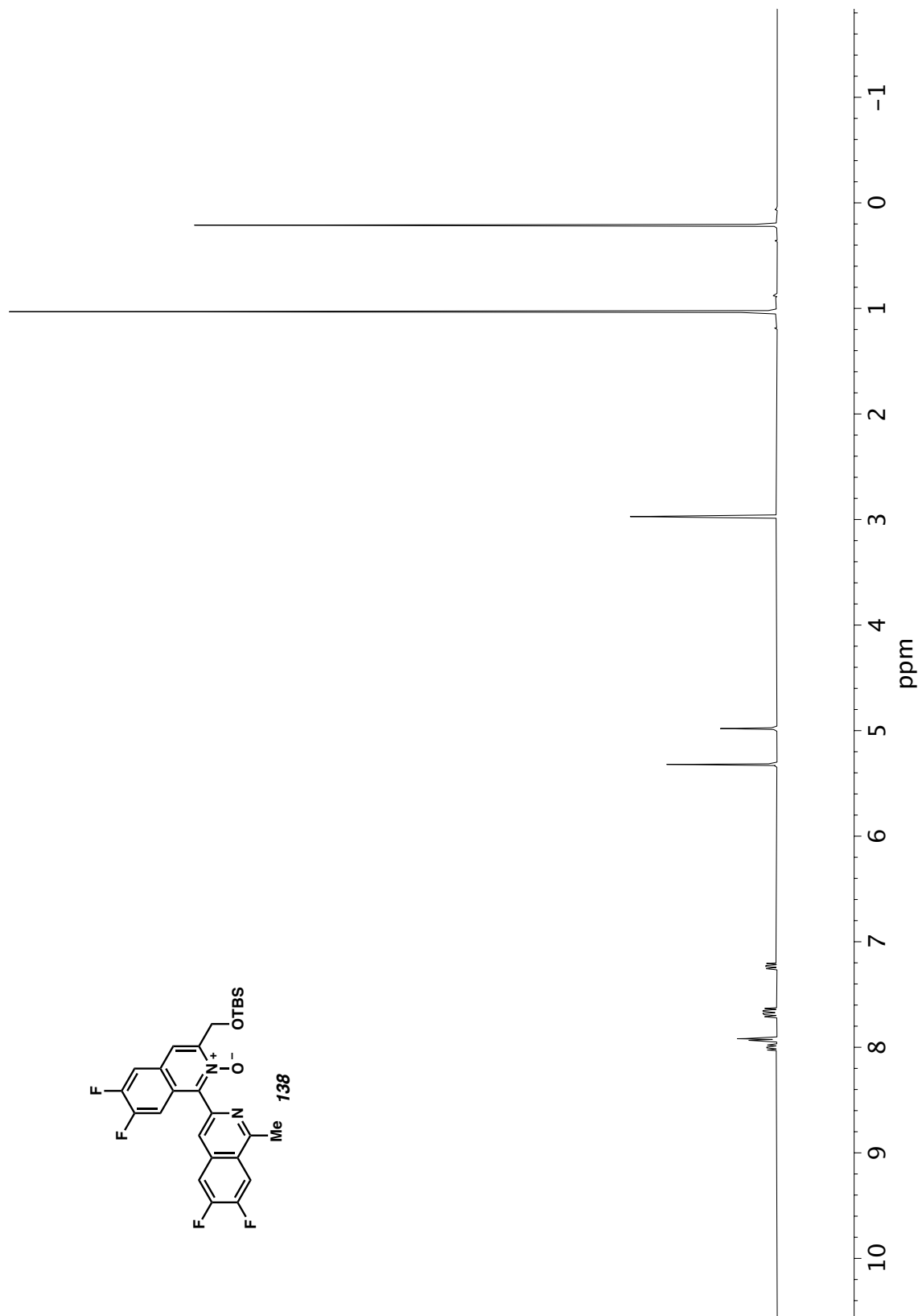


Figure A10.8 ^1H NMR (400 MHz, CD_2Cl_2) of compound **138**.

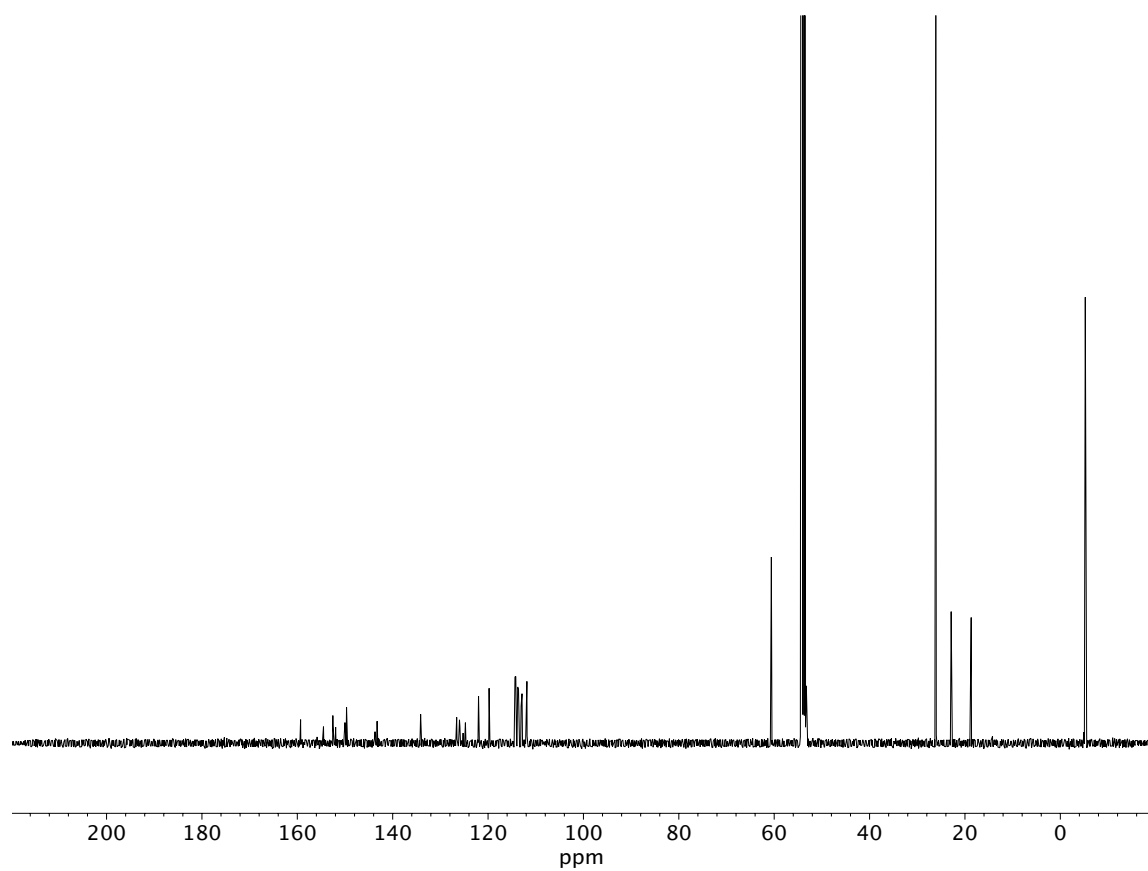


Figure A10.9 ^{13}C NMR (100 MHz, CD_2Cl_2) of compound **138**.

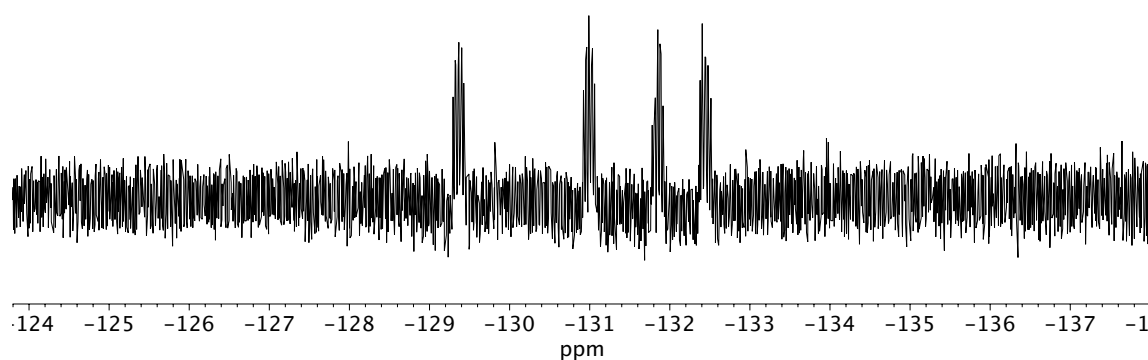


Figure A10.10 ^{19}F NMR (282 MHz, CDCl_3) of compound **138**.

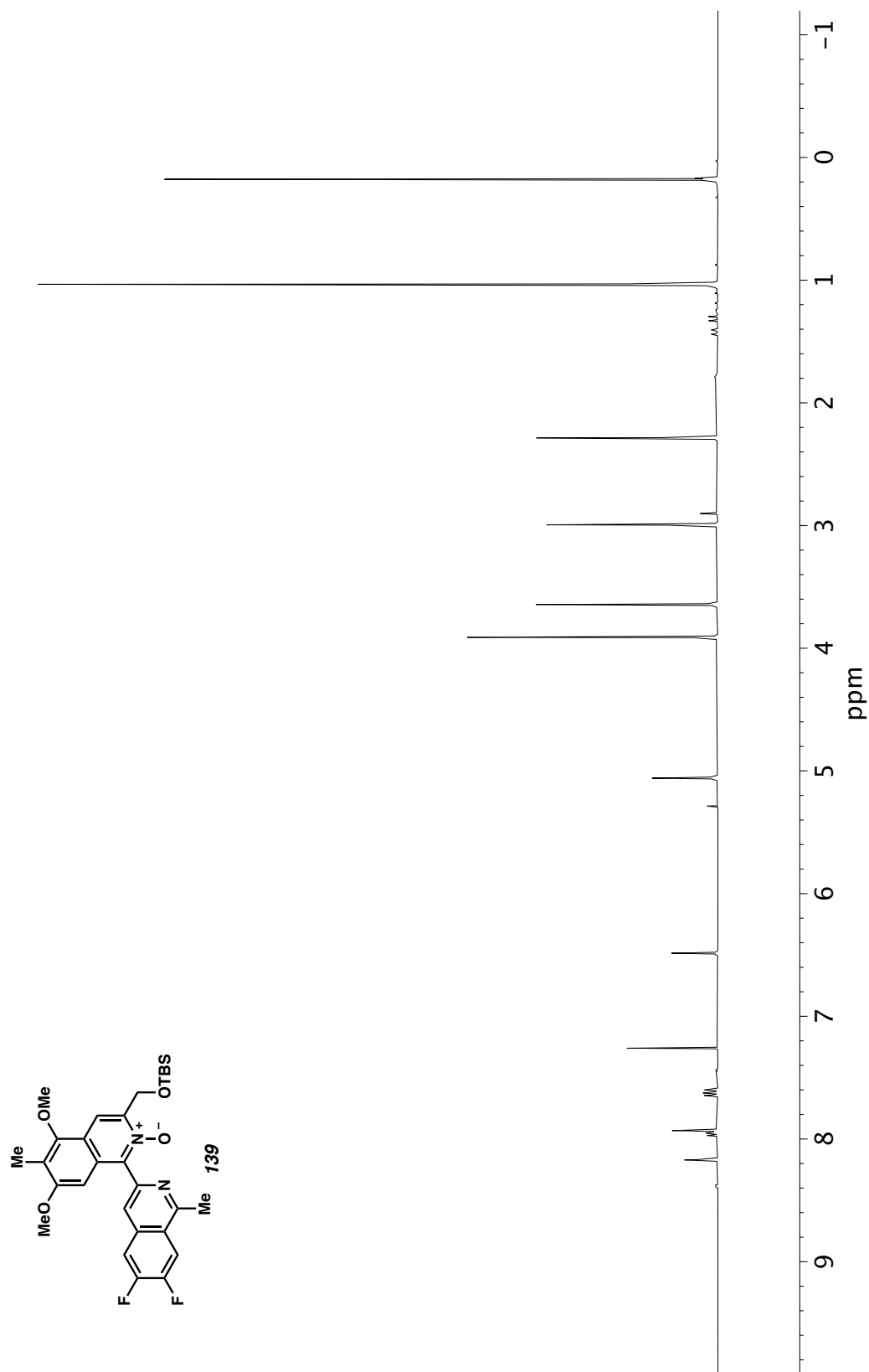


Figure A10.11 ^1H NMR (400 MHz, CDCl_3) of compound **139**.

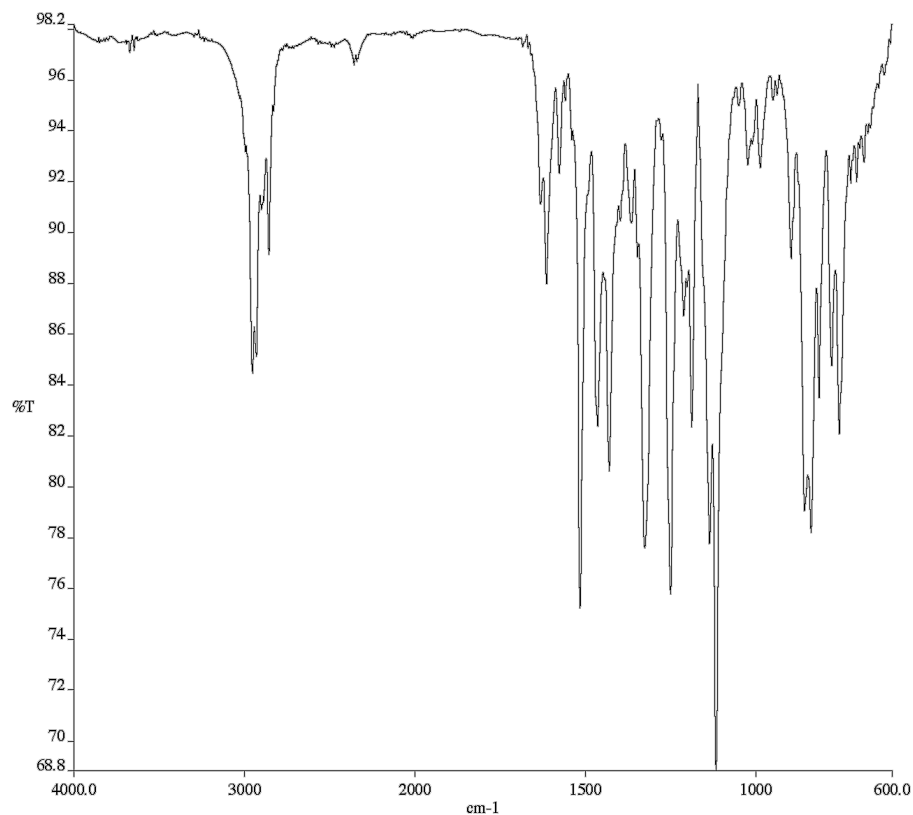


Figure A10.12 Infrared spectrum (Thin Film, NaCl) of compound **139**.

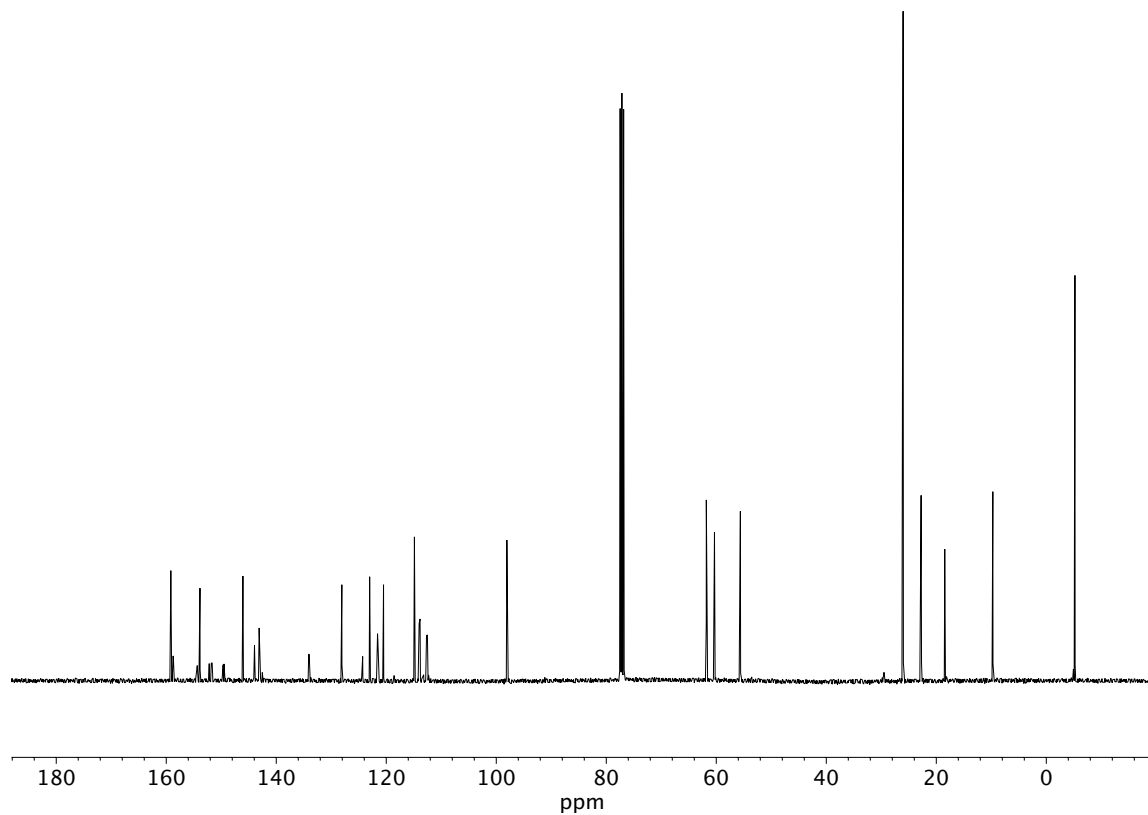


Figure A10.13 ¹³C NMR (100 MHz, CDCl₃) of compound **139**.

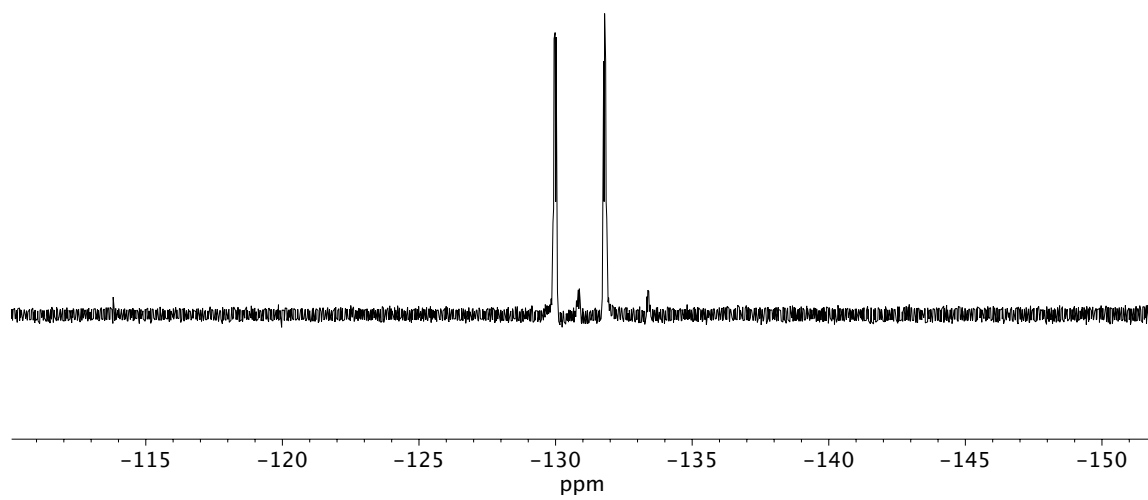


Figure A10.14 ^{19}F NMR (282 MHz, CDCl_3) of compound **139**.

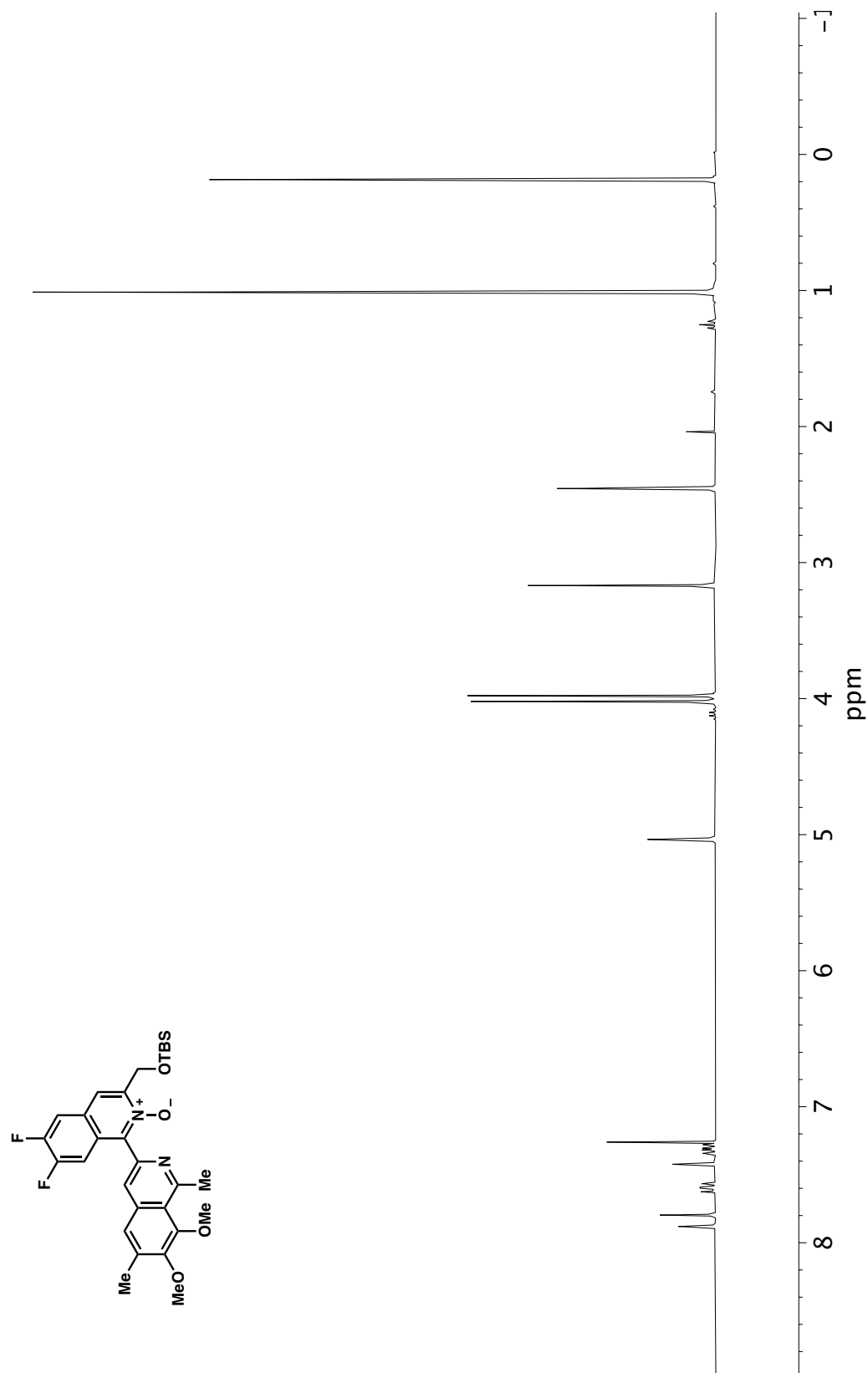


Figure A10.15 ^1H NMR (300 MHz, CDCl_3) of compound **140**.

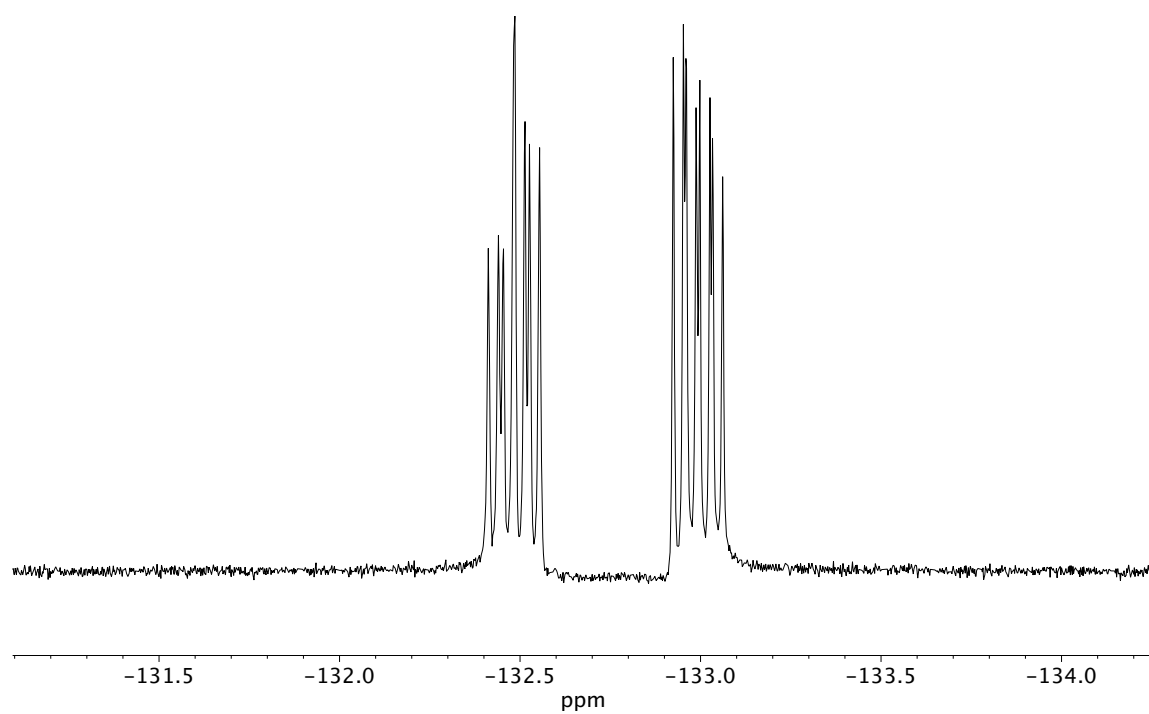


Figure A10.16 ^{19}F NMR (282 MHz, CDCl_3) of compound **140**.

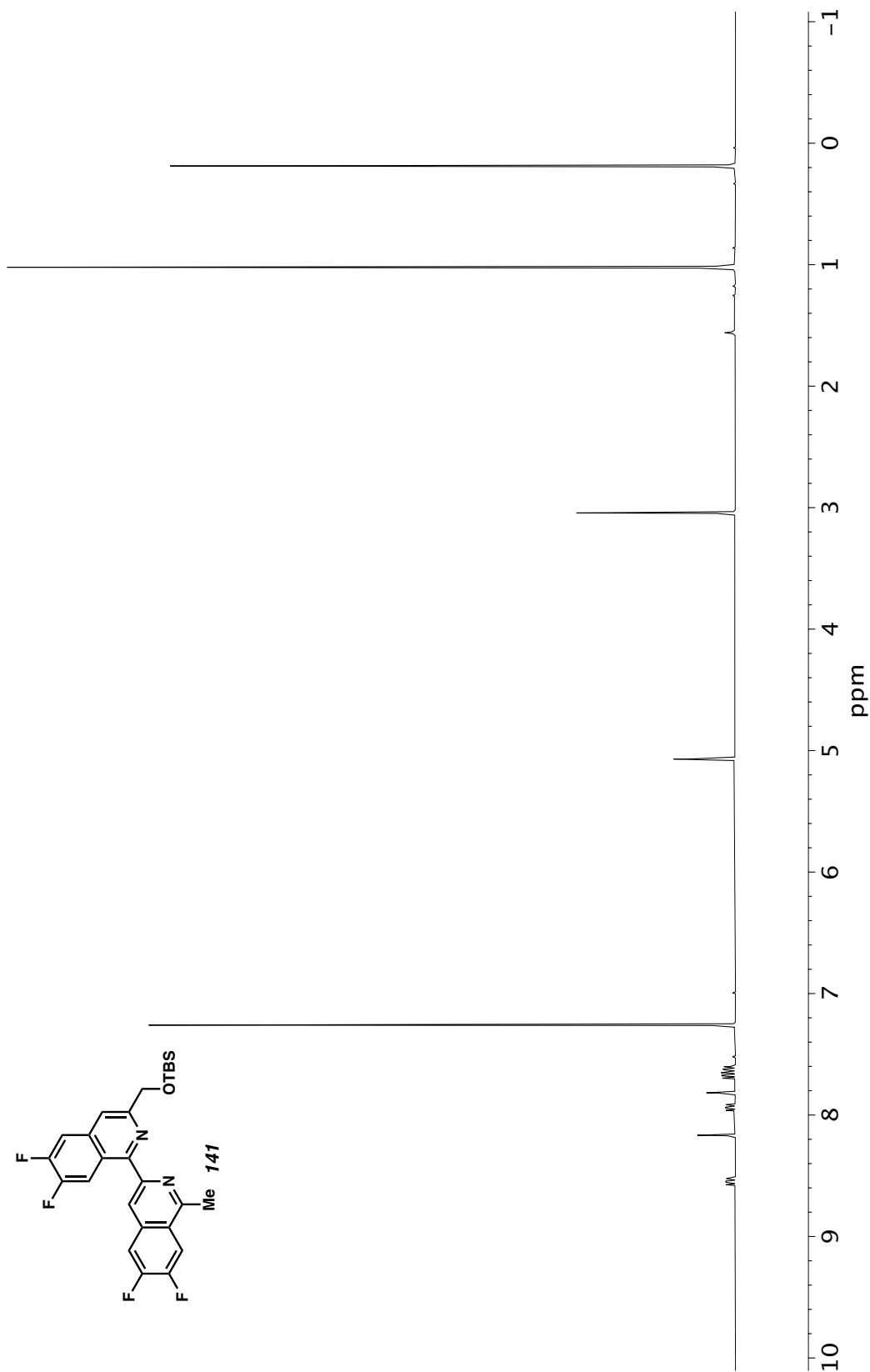


Figure A10.17 ^1H NMR (400 MHz, CDCl_3) of compound **141**.

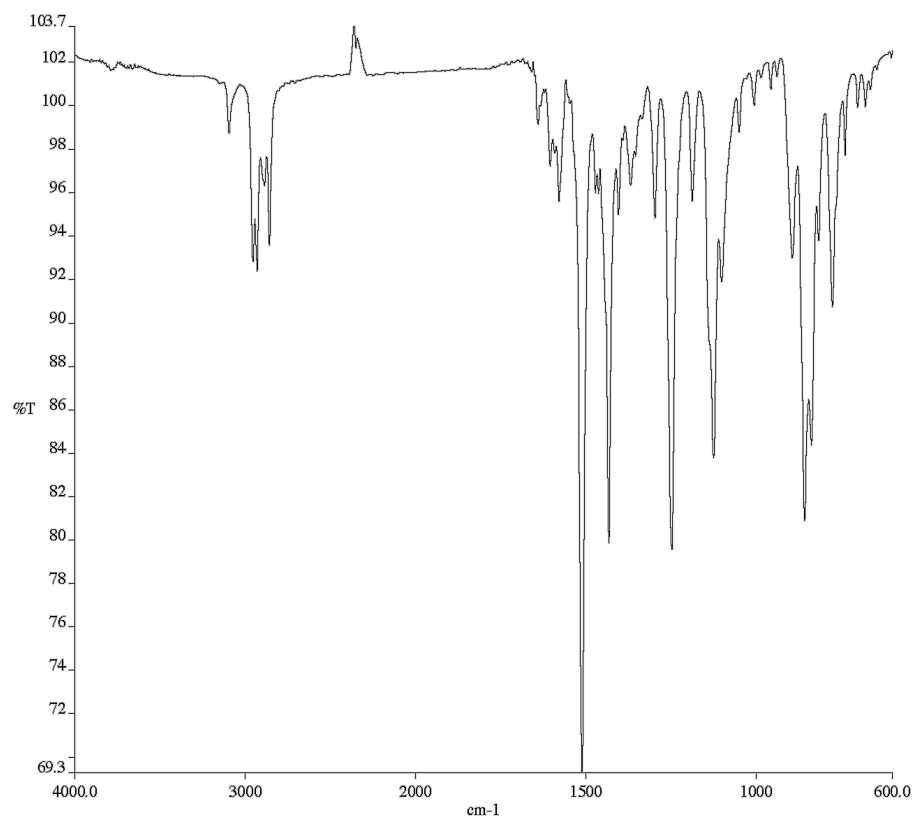


Figure A10.18 Infrared spectrum (Thin Film, NaCl) of compound **141**.

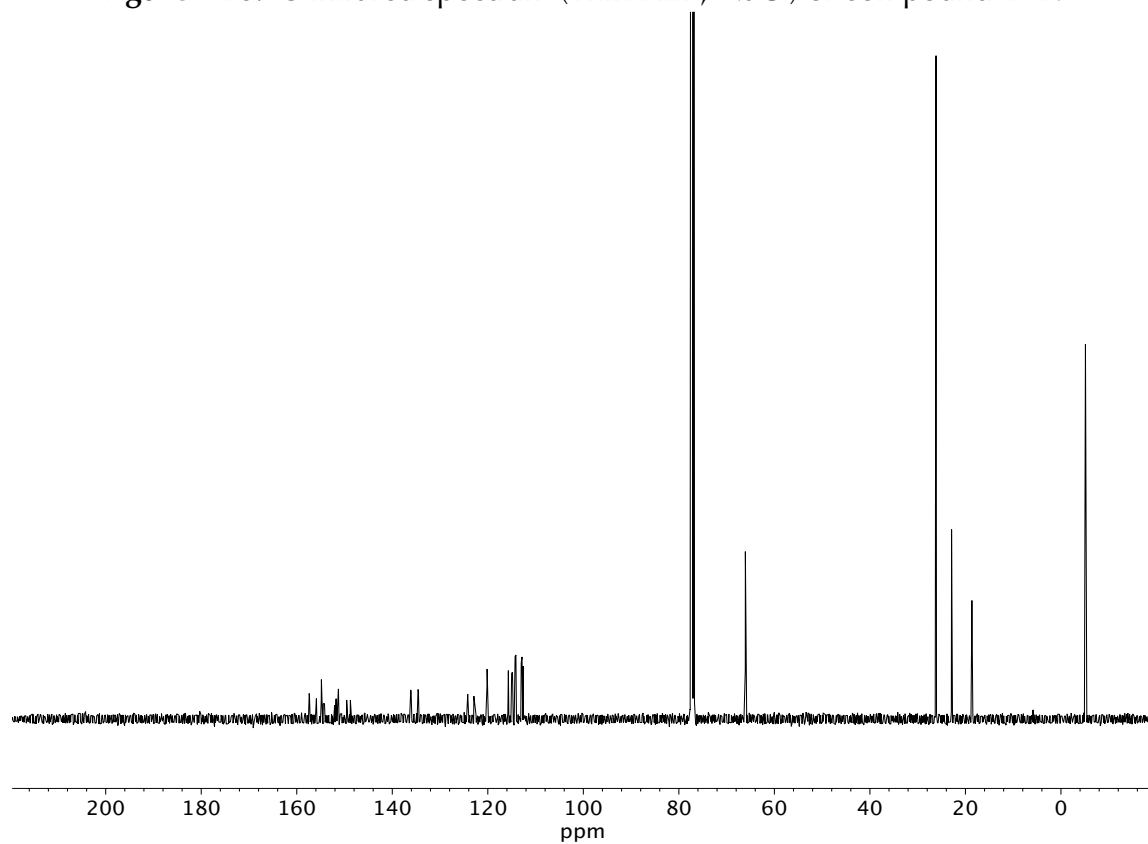


Figure A10.19 ¹³C NMR (100 MHz, CDCl₃) of compound **141**.

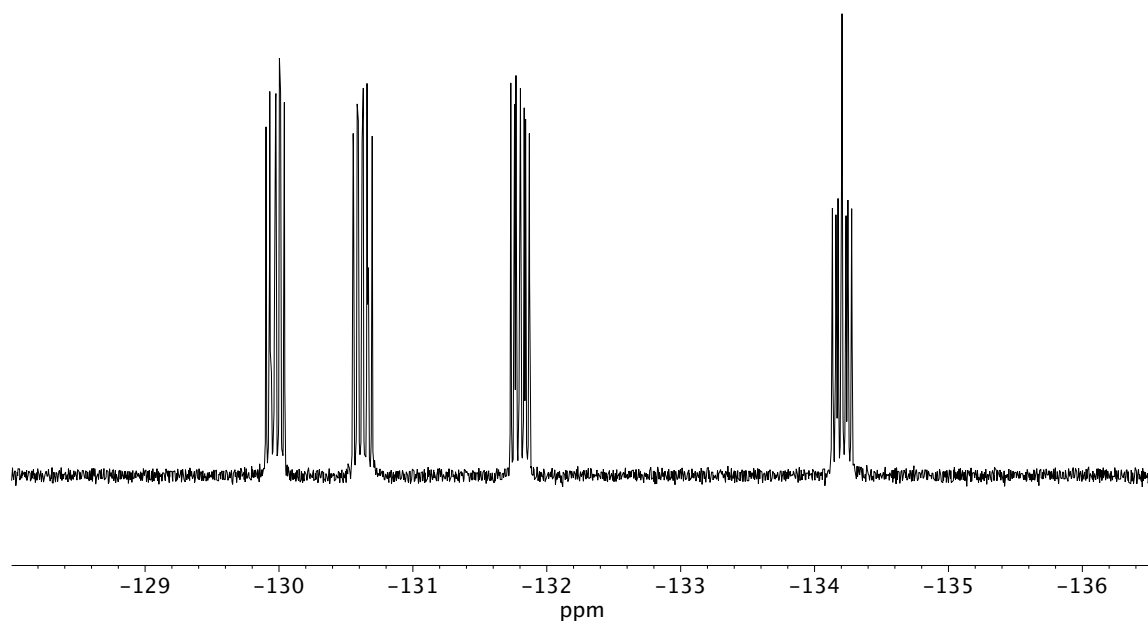


Figure A10.20 ^{19}F NMR (282 MHz, CDCl_3) of compound **141**.

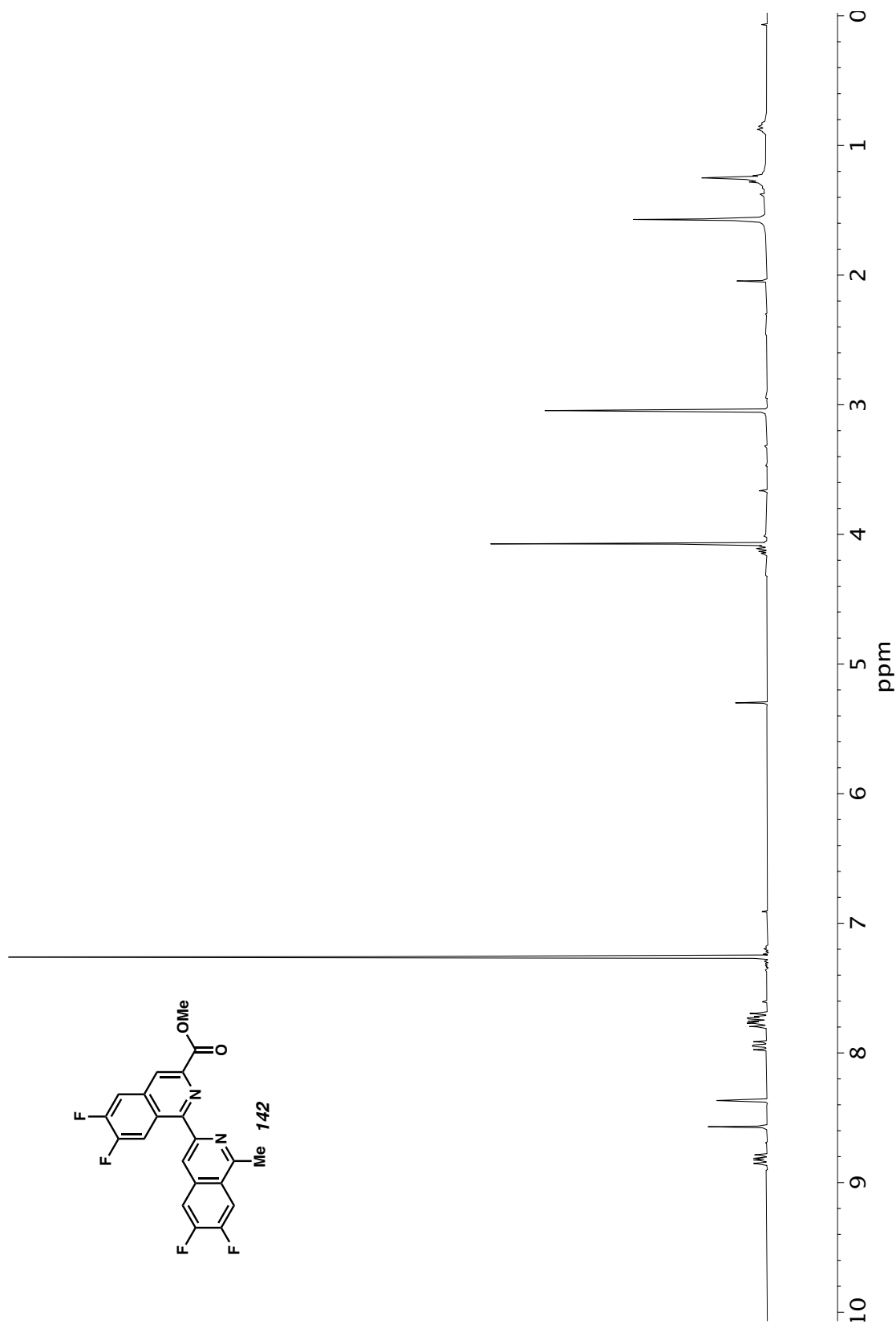


Figure A10.21 ^1H NMR (300 MHz, CDCl_3) of compound **142**.

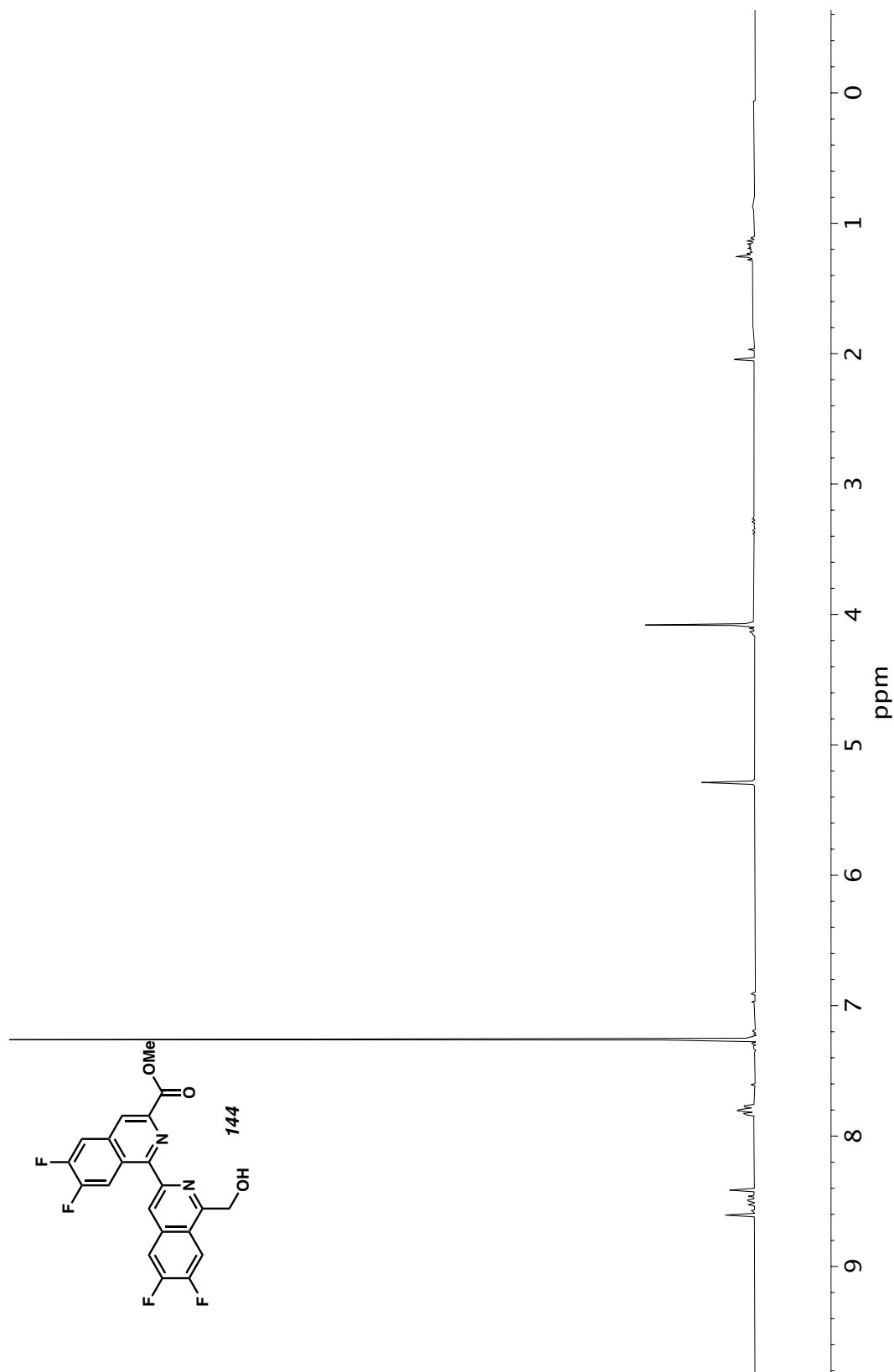


Figure A10.22 ^1H NMR (300 MHz, CDCl_3) of compound **144**.

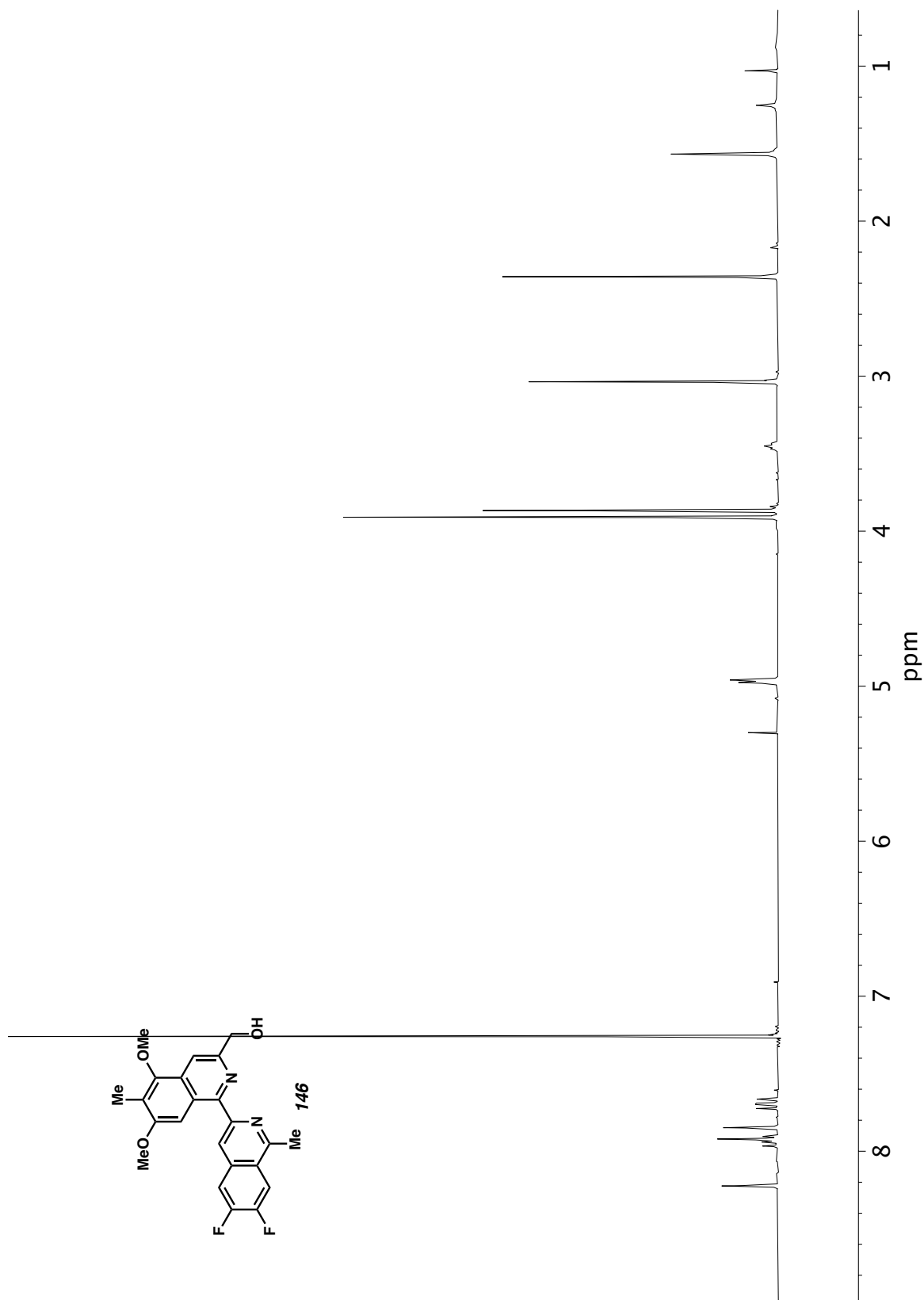


Figure A10.23 ¹H NMR (300 MHz, CDCl₃) of compound **146**.

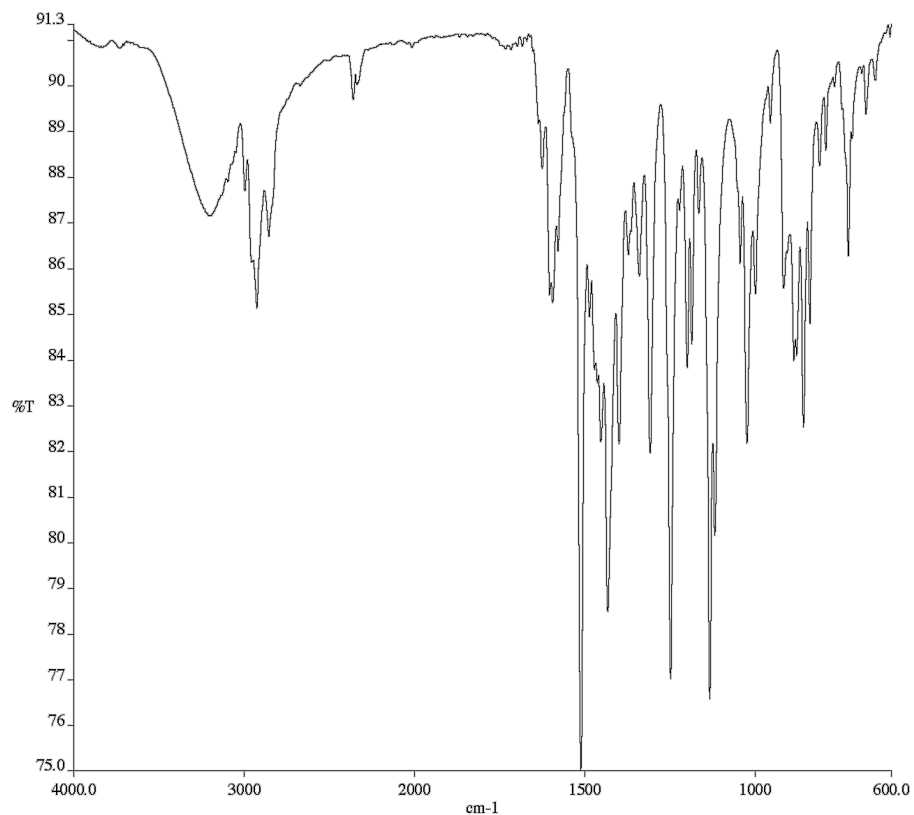


Figure A10.24 Infrared spectrum (Thin Film, NaCl) of compound **146**.

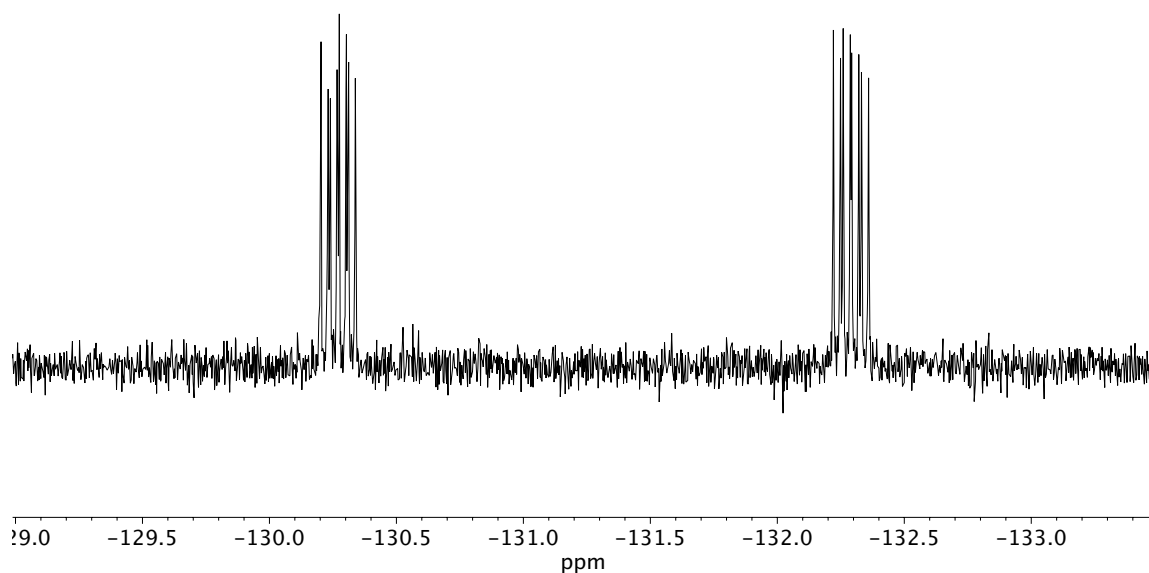


Figure A10.25 ¹⁹F NMR (282 MHz, CDCl₃) of compound **146**.

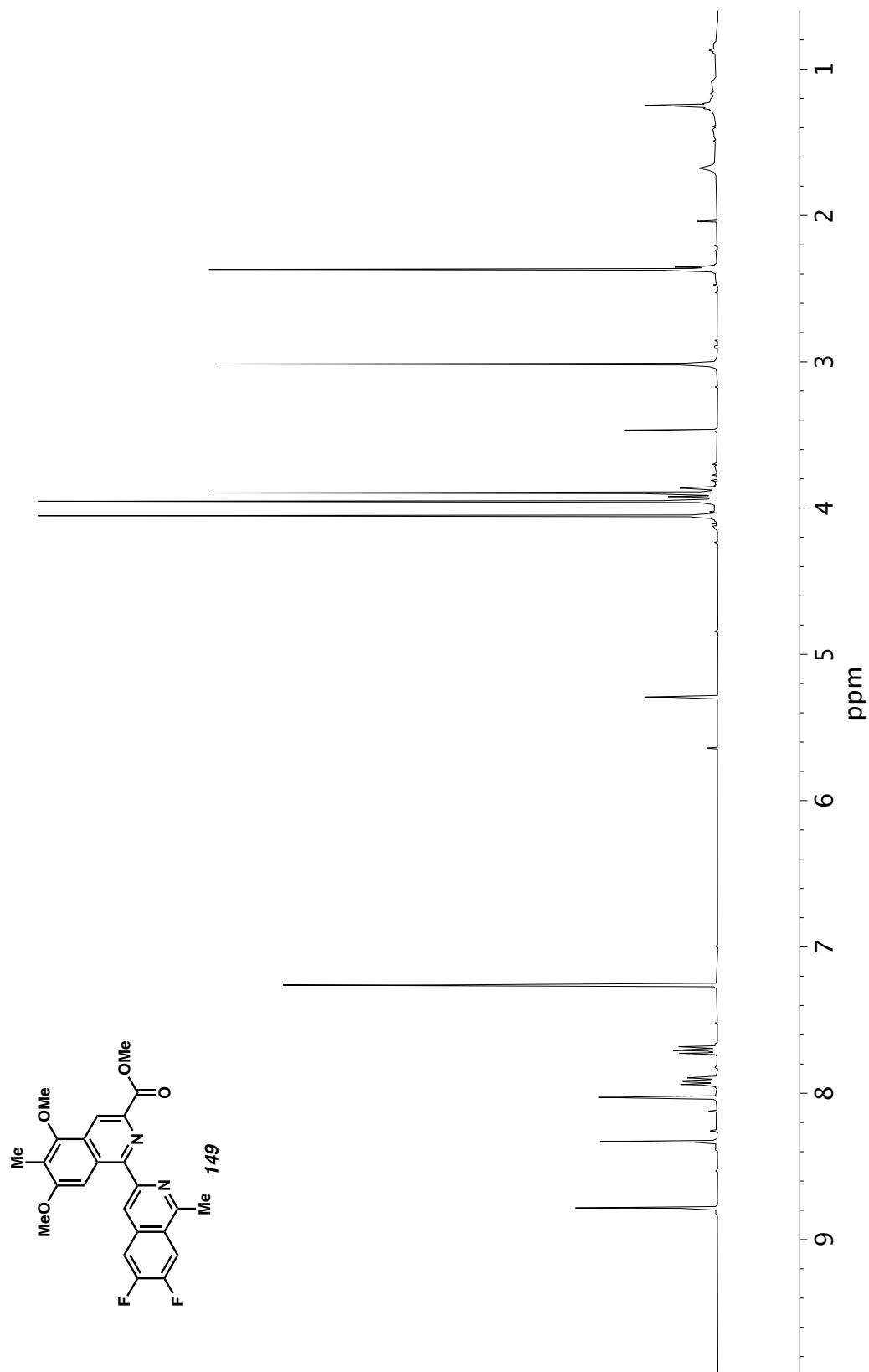


Figure A10.26 ^1H NMR (400 MHz, CDCl_3) of compound **149**.

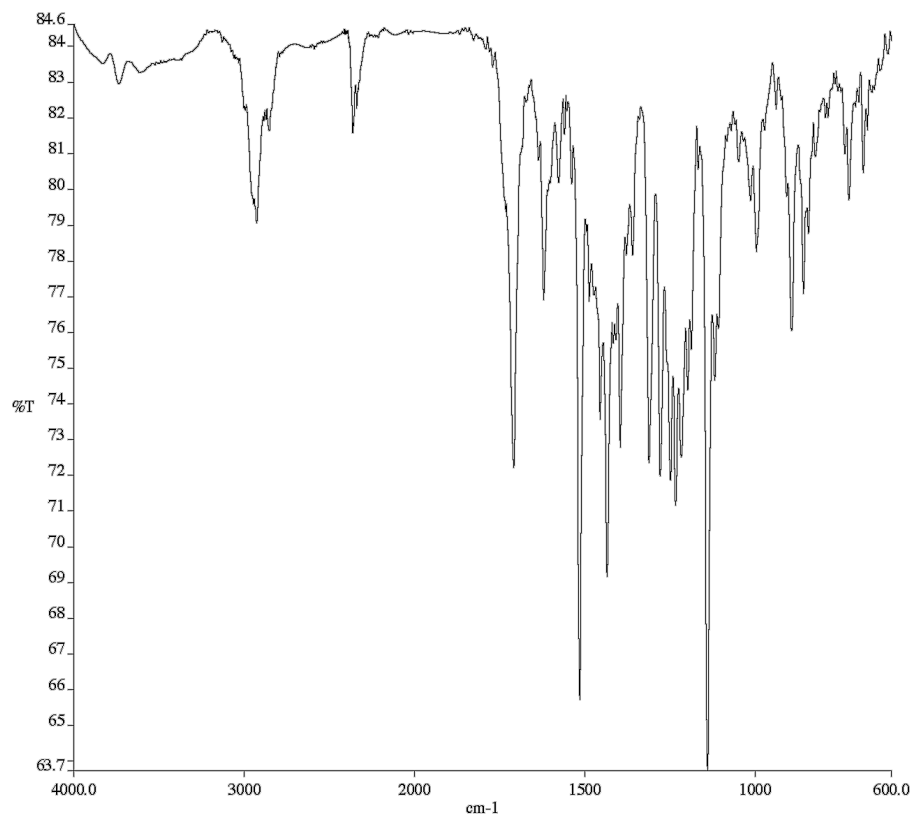


Figure A10.27 Infrared spectrum (Thin Film, NaCl) of compound **149**.

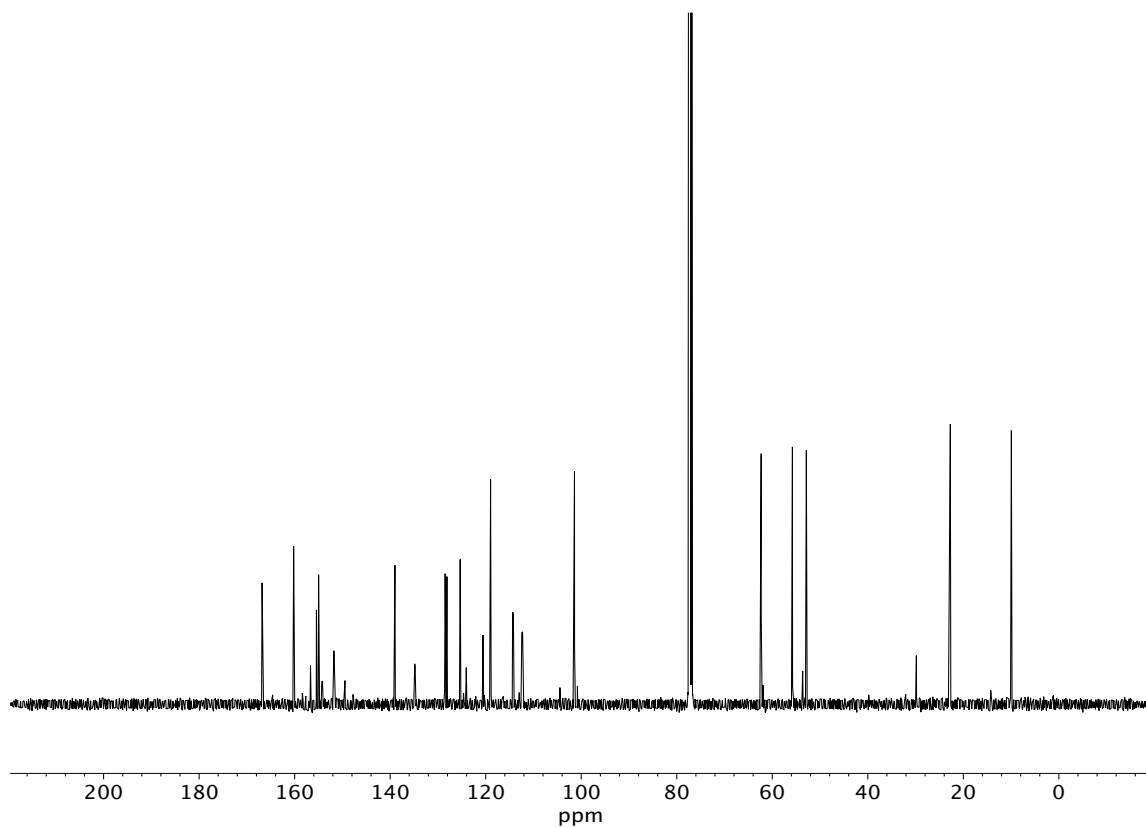


Figure A10.28 ¹³C NMR (100 MHz, CDCl₃) of compound **149**.

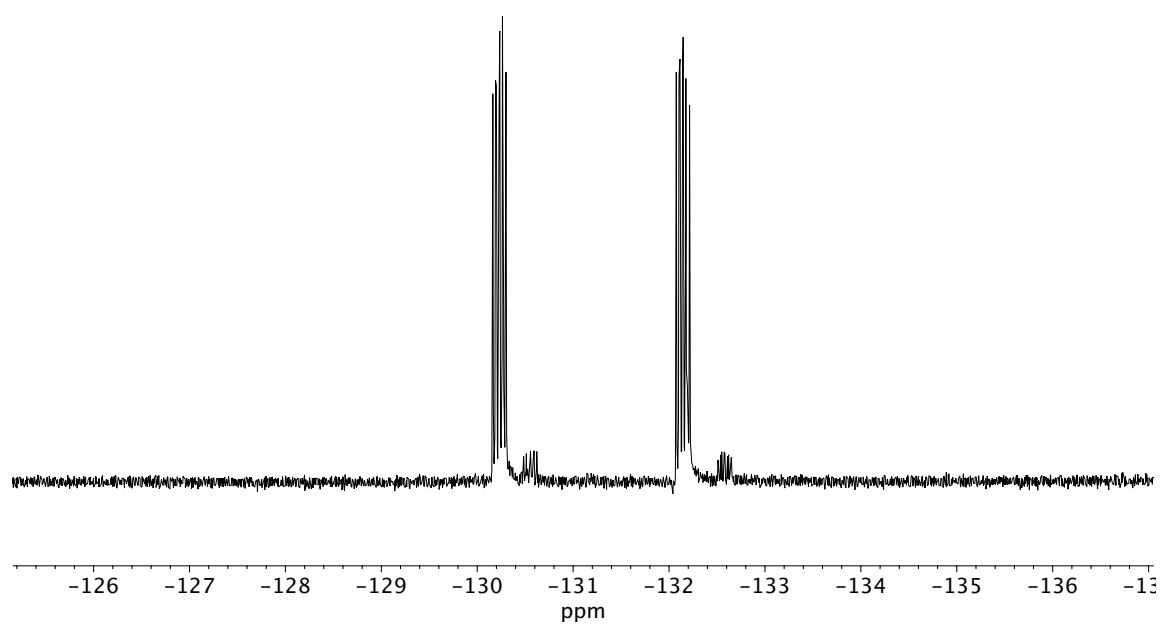


Figure A10.29 ^{19}F NMR (282 MHz, CDCl_3) of compound **149**.

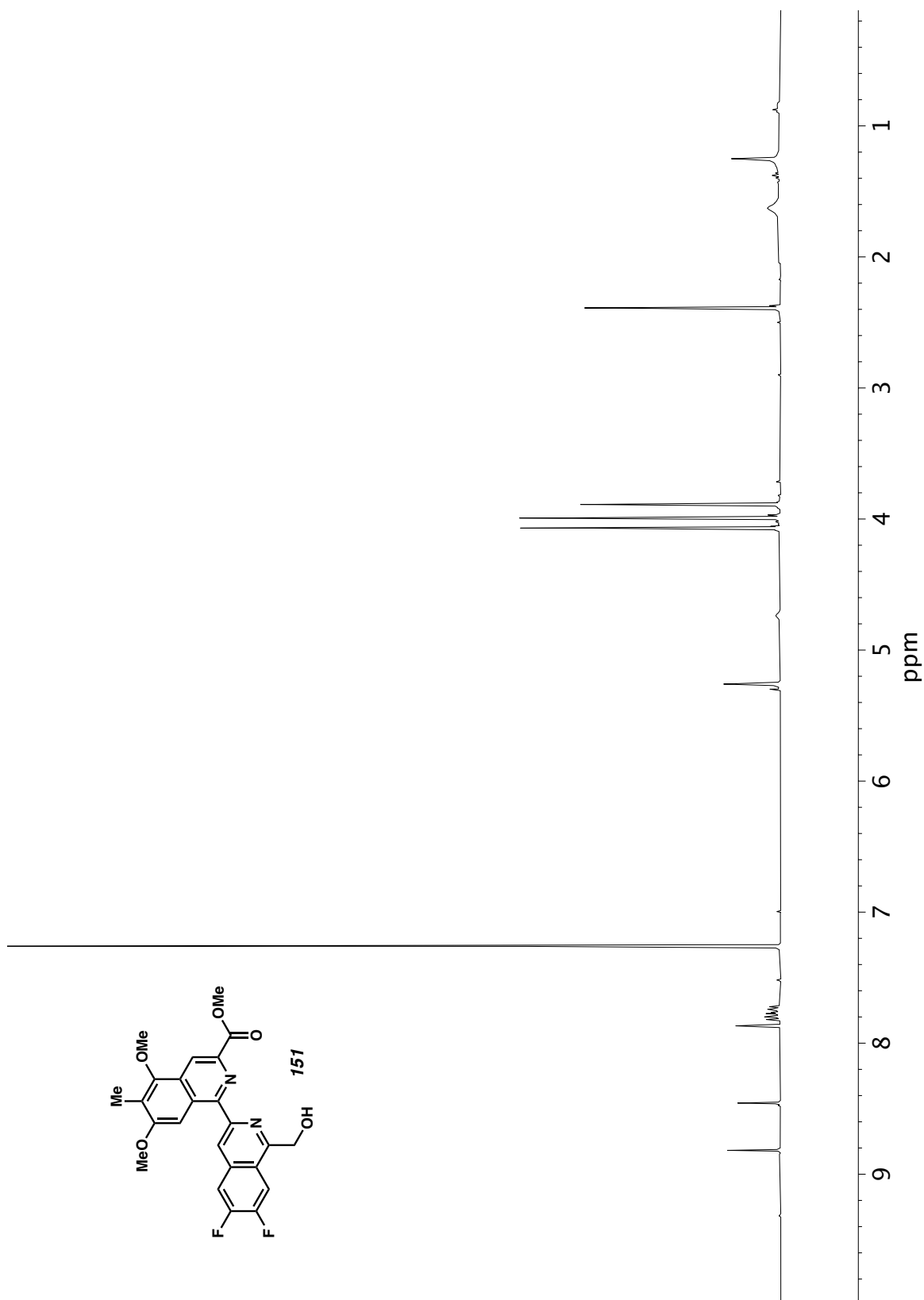


Figure A10.30 ¹H NMR (400 MHz, CDCl₃) of compound **151**.

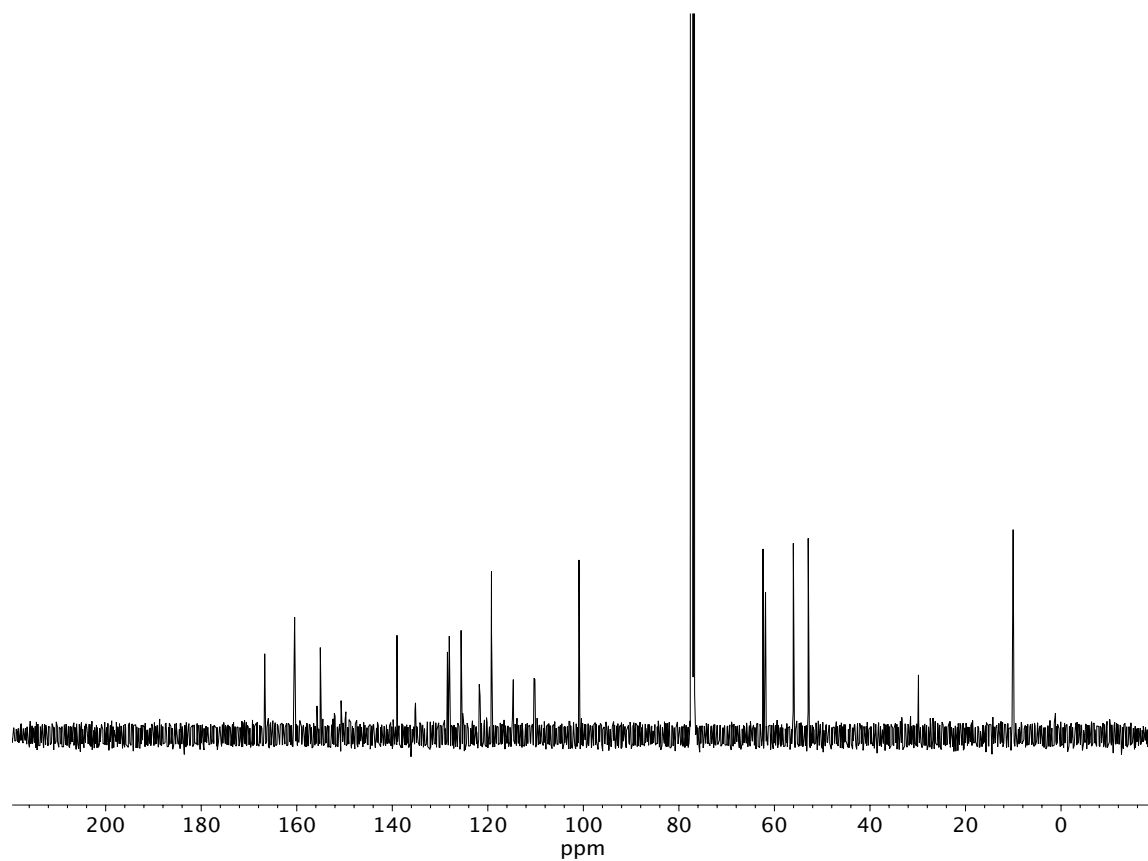


Figure A10.31 ^{13}C NMR (100 MHz, CDCl_3) of compound **151**.

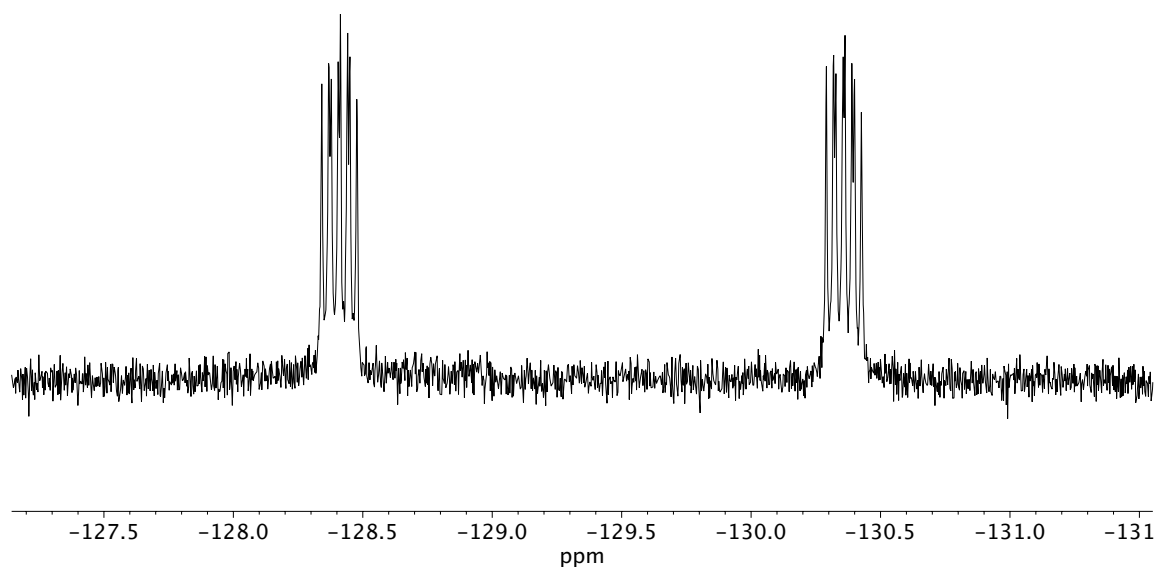


Figure A10.32 ^{19}F NMR (282 MHz, CDCl_3) of compound **151**.

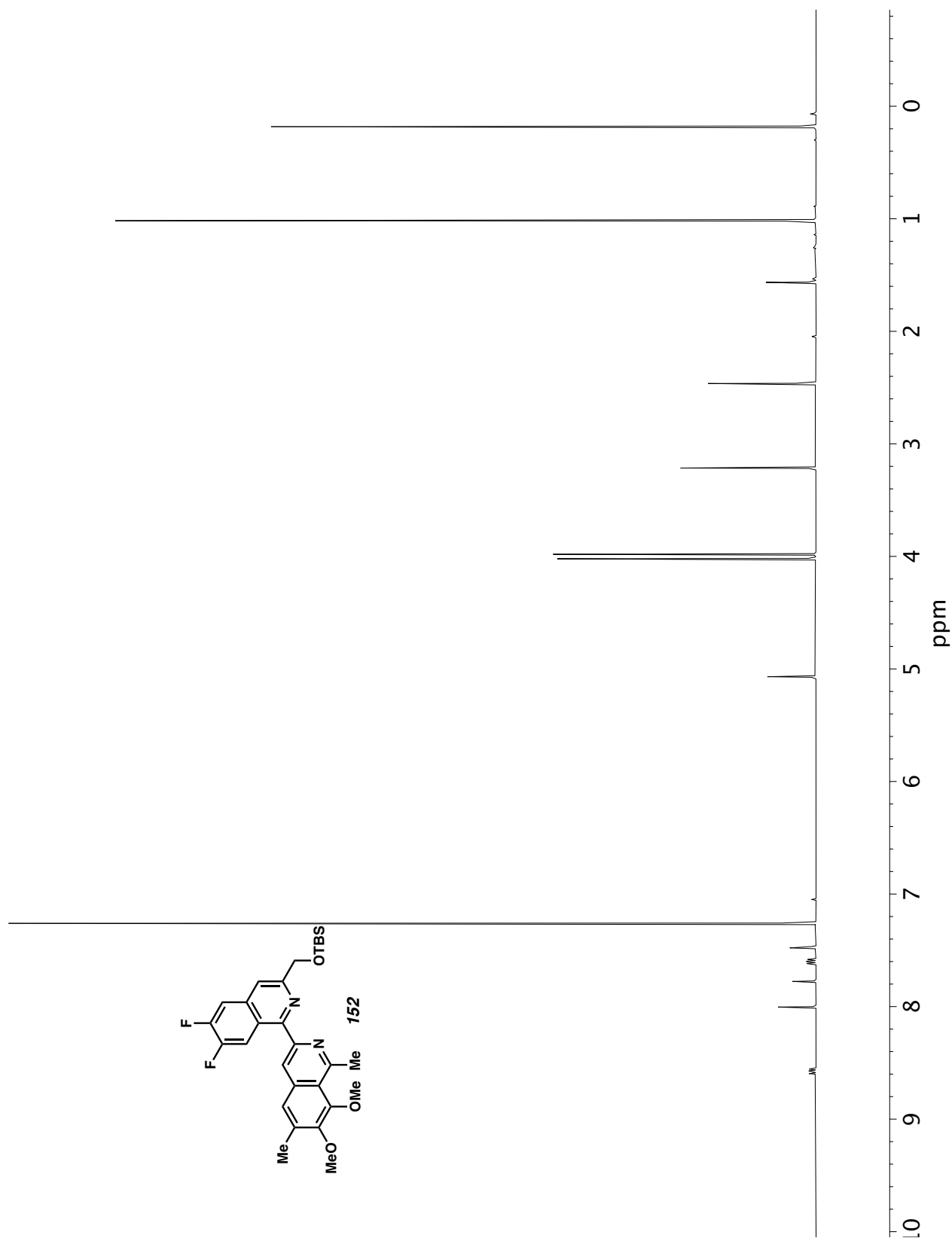


Figure A10.33 ^1H NMR (500 MHz, CDCl_3) of compound **152**.

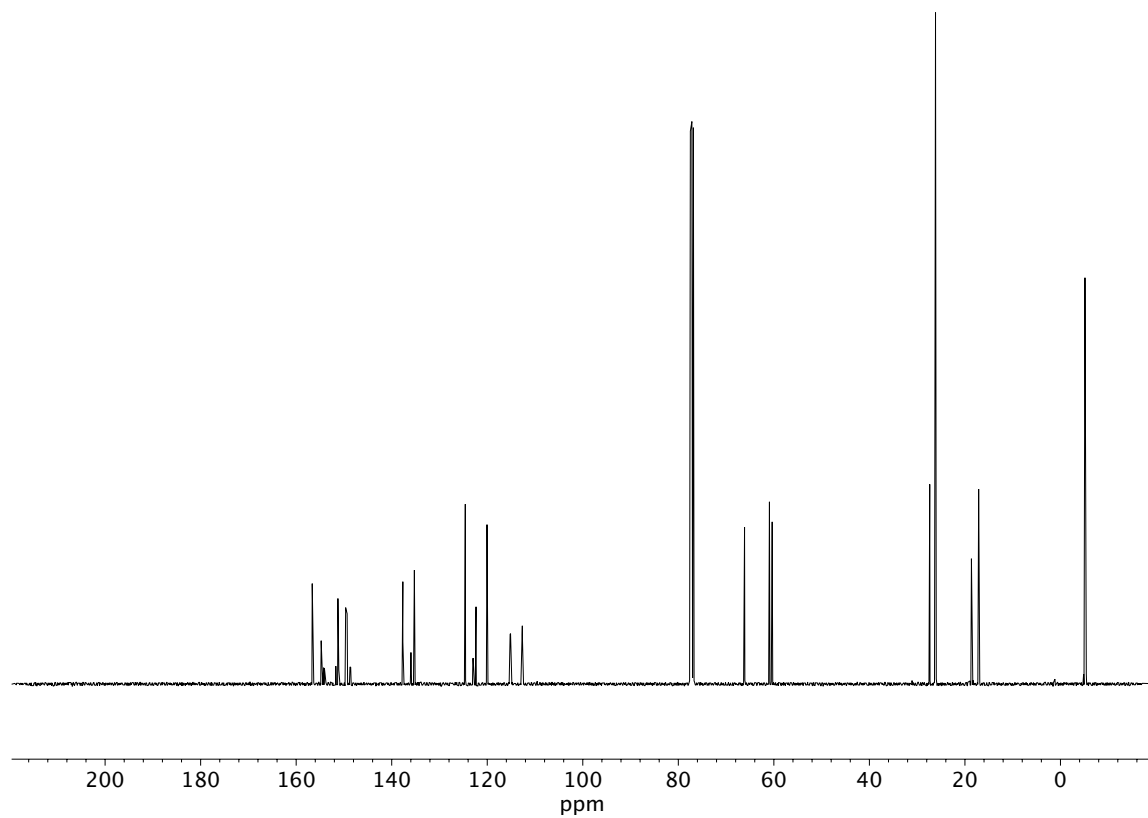


Figure A10.34 ^{13}C NMR (100 MHz, CDCl_3) of compound **152**.

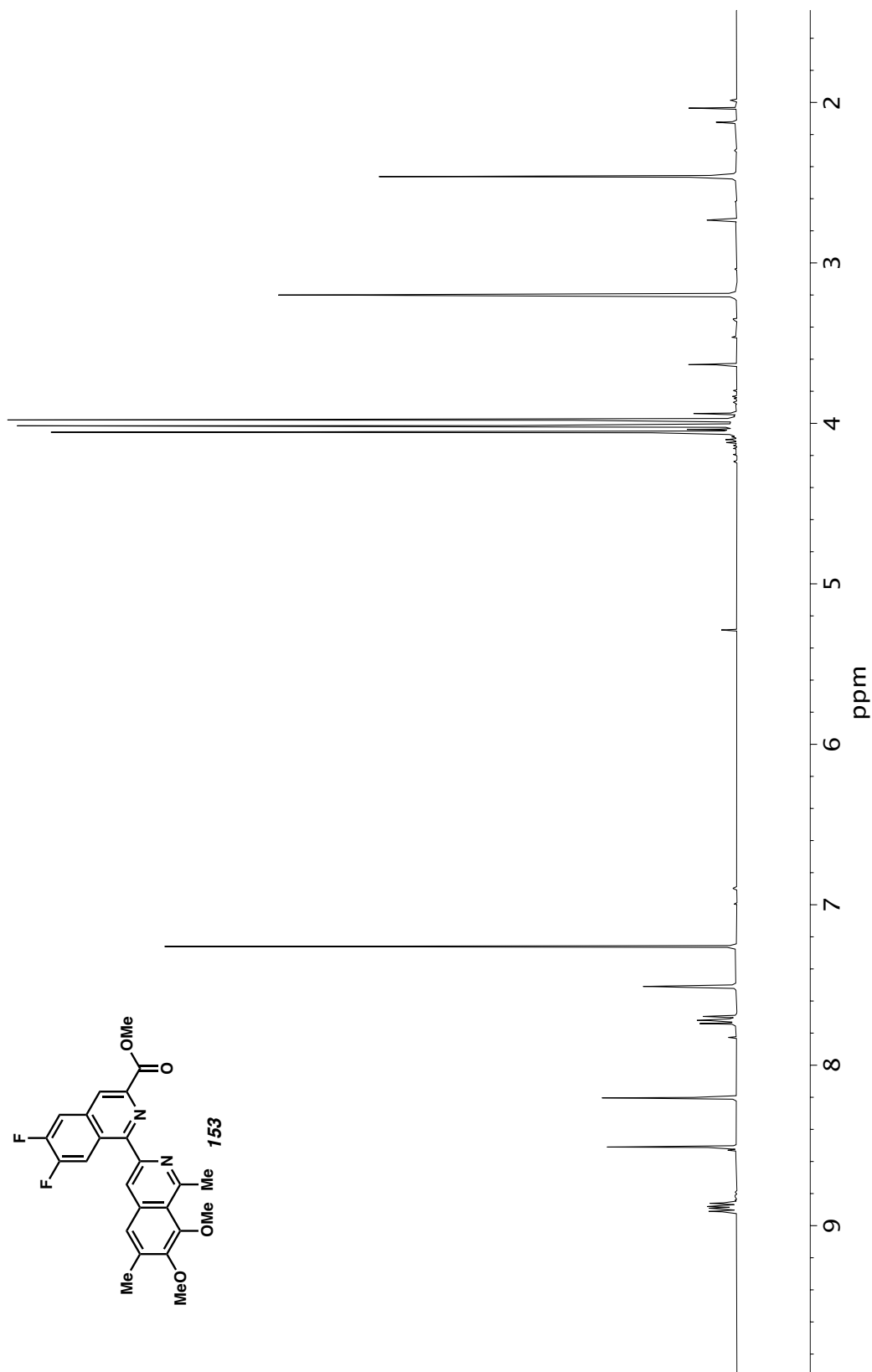


Figure A10.35 ^1H NMR (400 MHz, CDCl_3) of compound **153**.

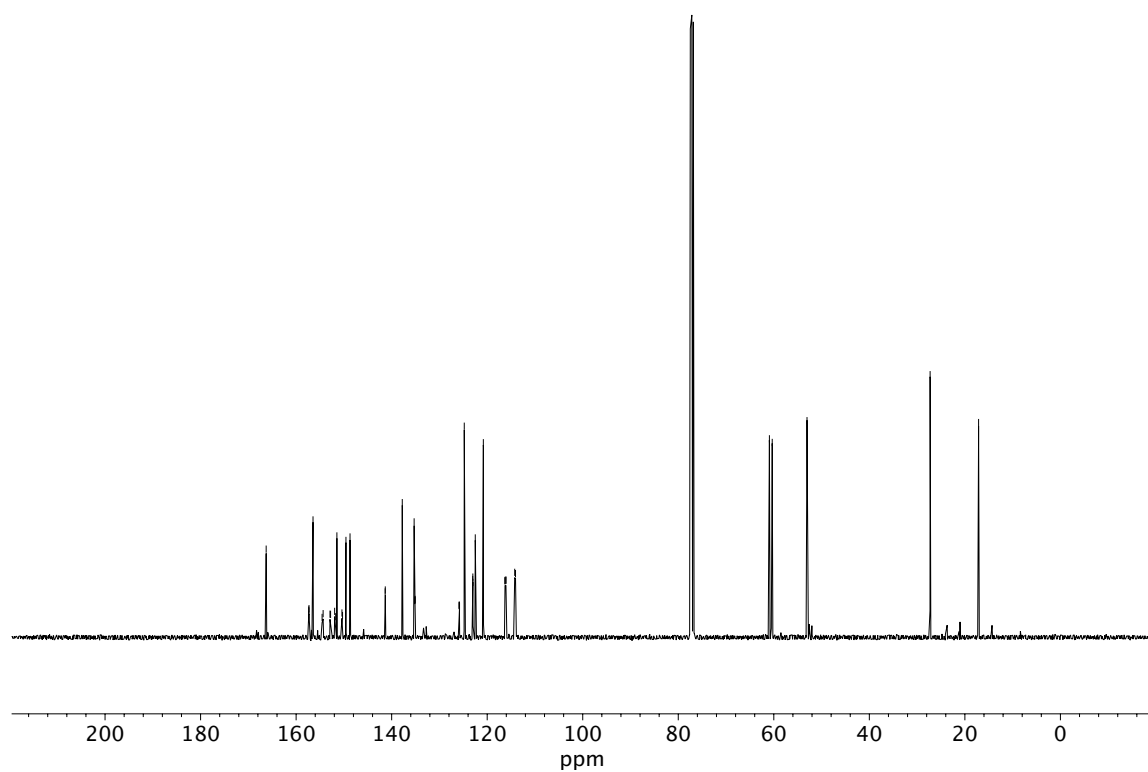


Figure A10.36 ^{13}C NMR (100 MHz, CDCl_3) of compound **153**.

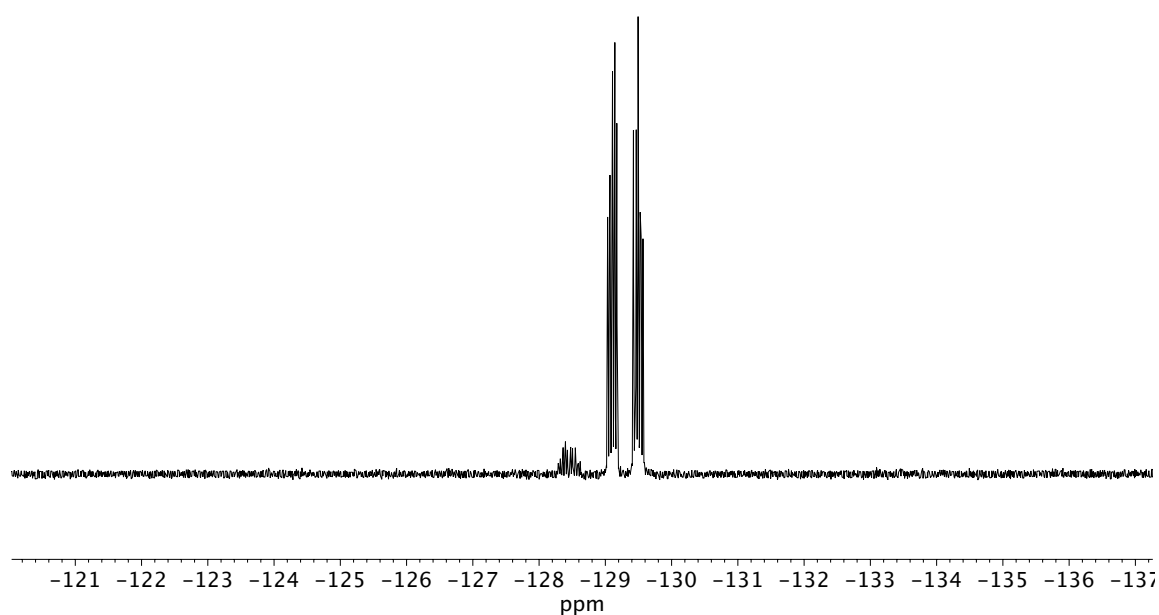
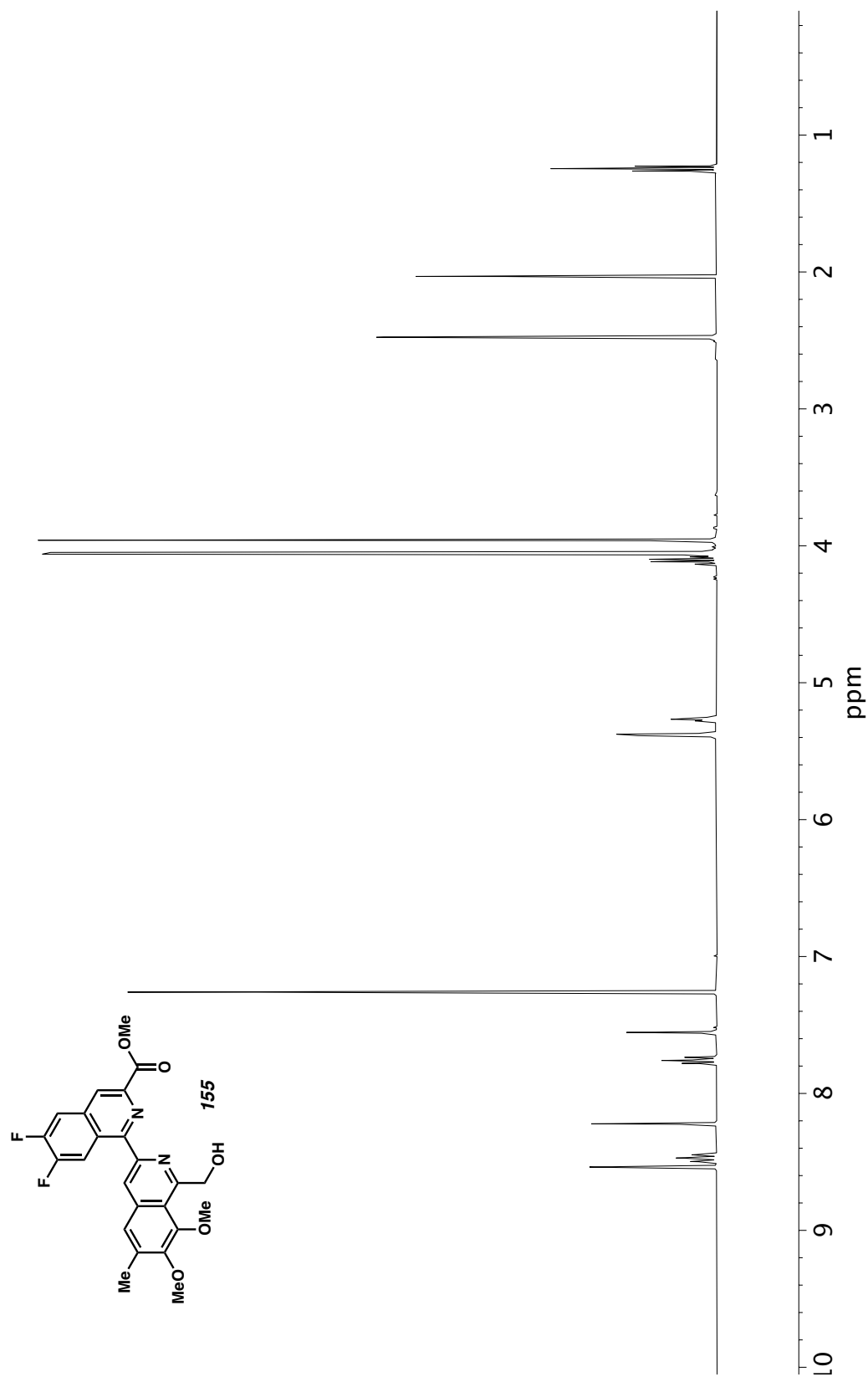


Figure A10.37 ^{19}F NMR (282 MHz, CDCl_3) of compound **153**.



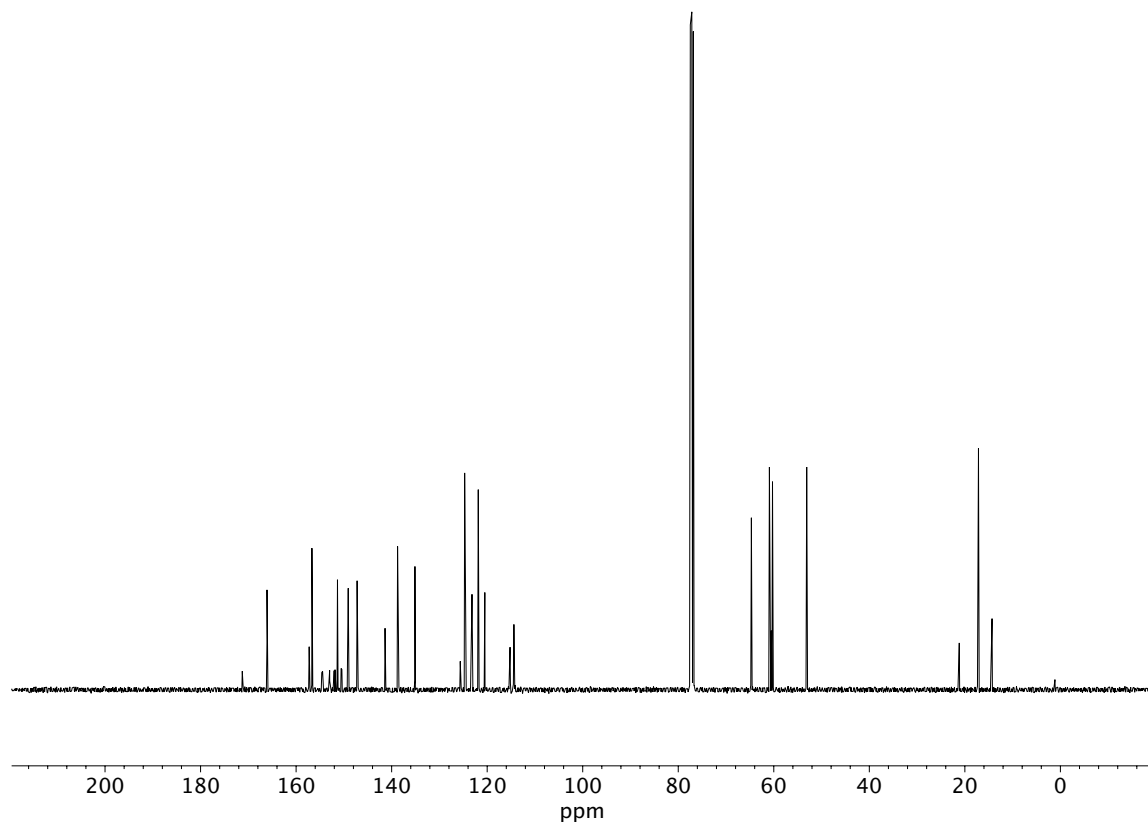


Figure A10.39 ^{13}C NMR (100 MHz, CDCl_3) of compound **155**.

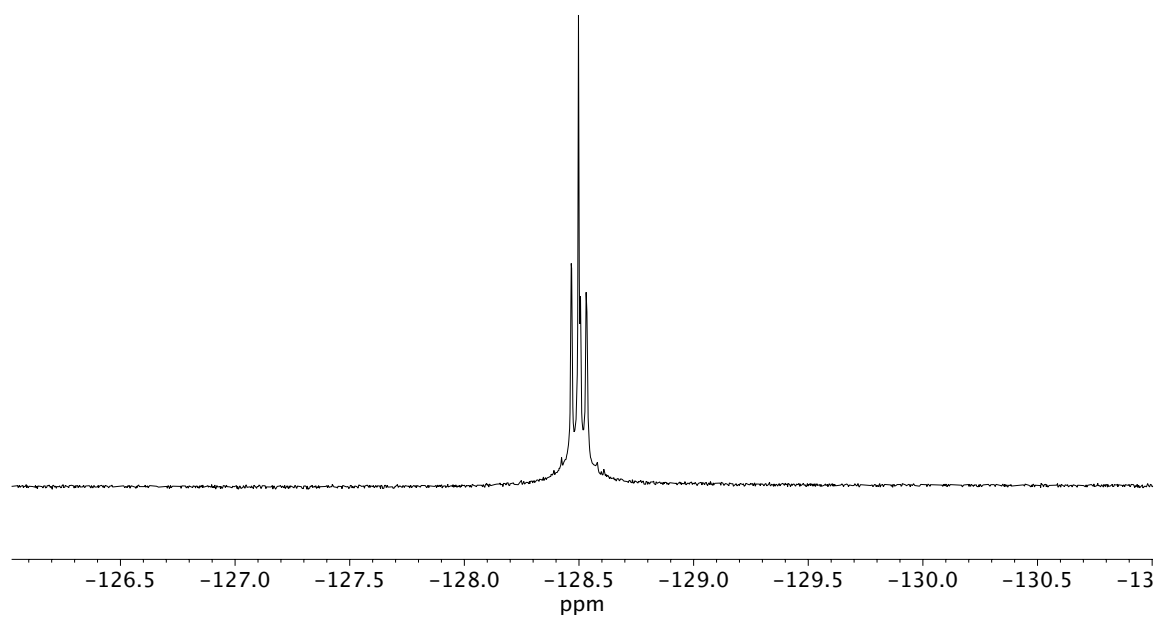


Figure A10.40 ^{19}F NMR (282 MHz, CDCl_3) of compound **155**.

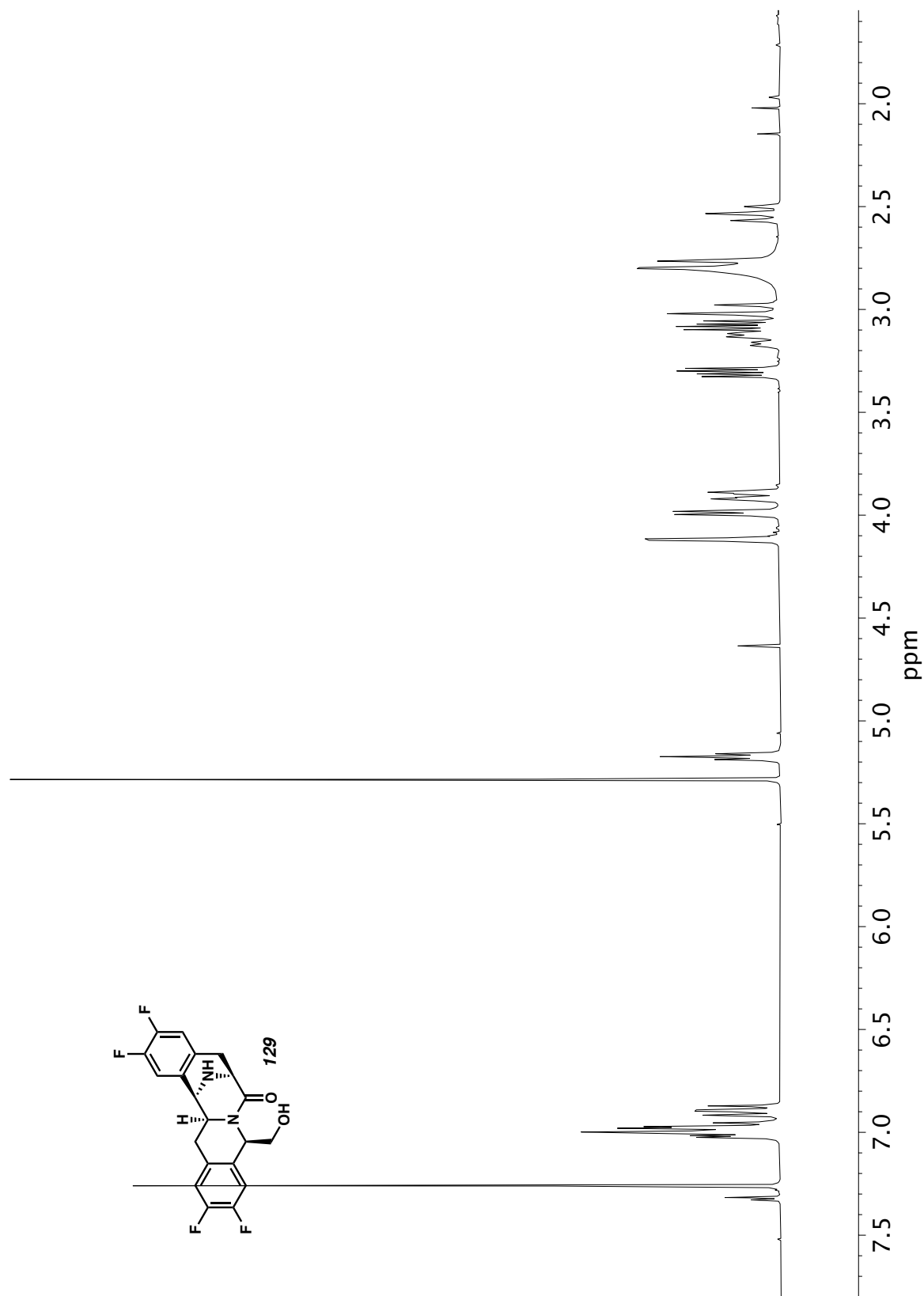


Figure A10.41 ^1H NMR (400 MHz, CDCl_3) of compound **129**.

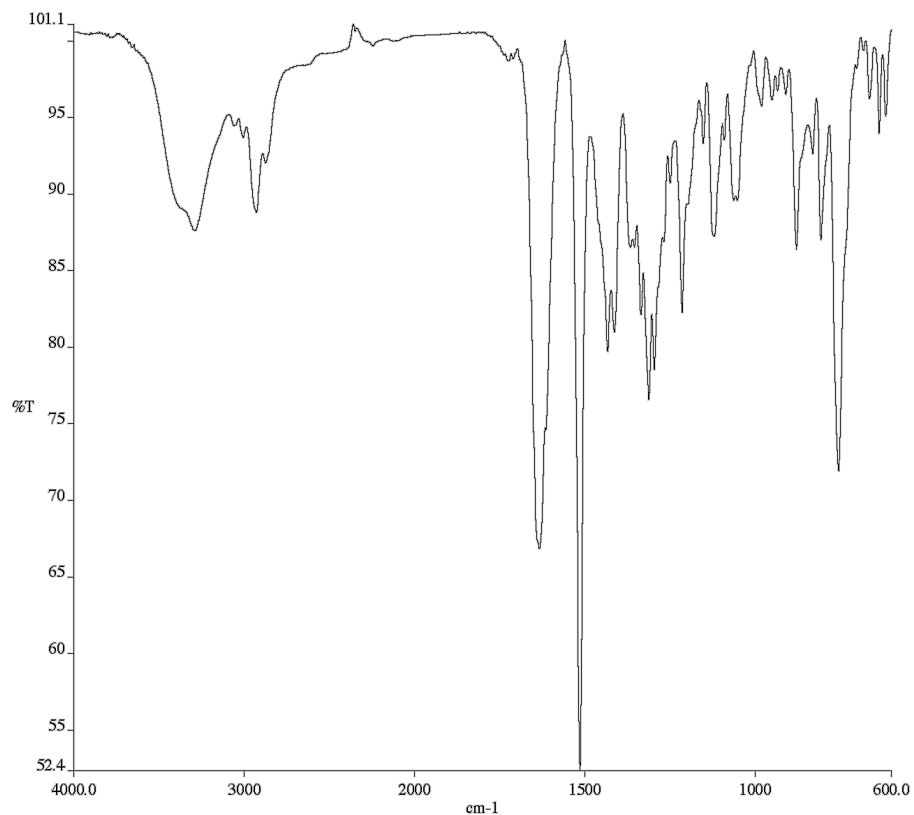


Figure A10.42 Infrared spectrum (Thin Film, NaCl) of compound **129**.

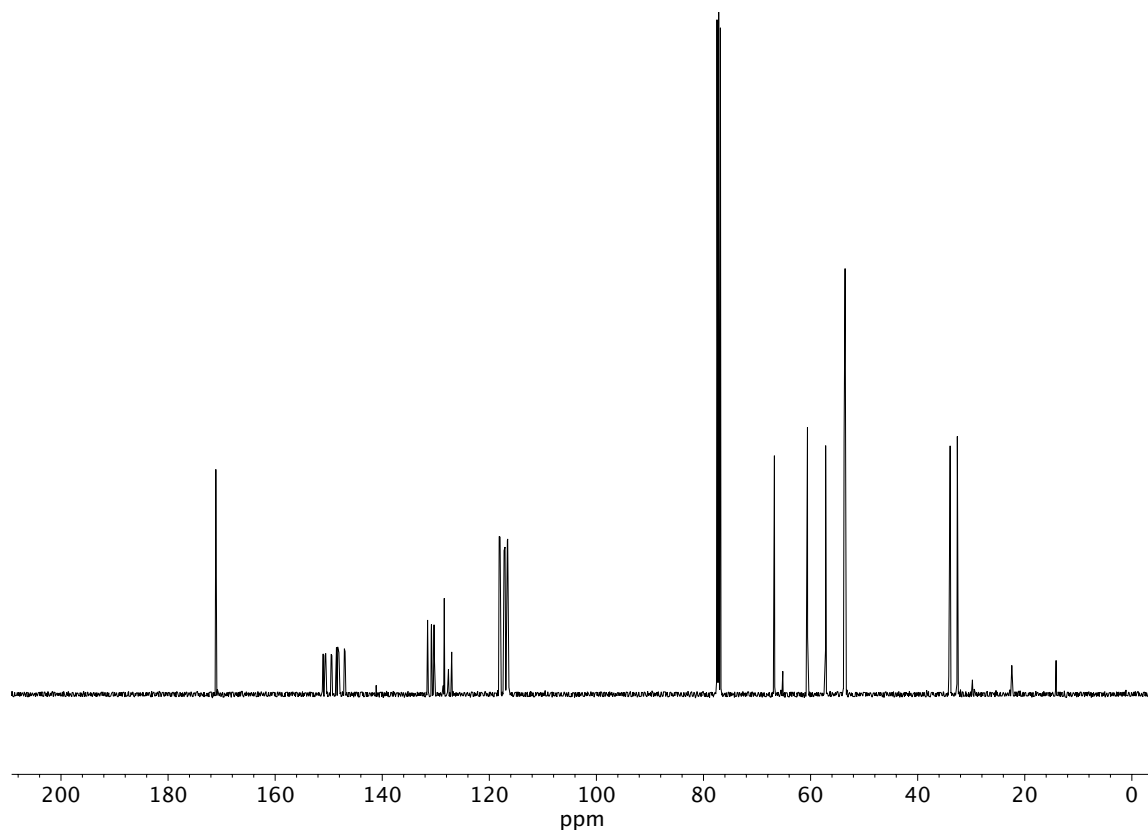


Figure A10.43 ¹³C NMR (100 MHz, CDCl₃) of compound **129**.

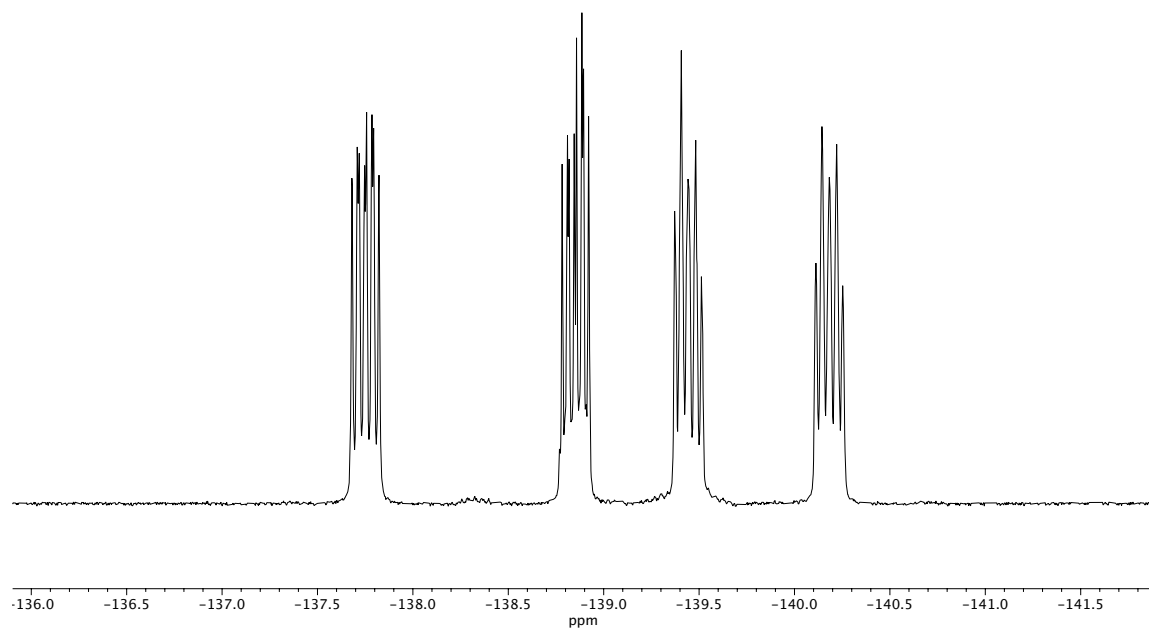


Figure A10.44 ^{19}F NMR (282 MHz, CDCl_3) of compound **129**.

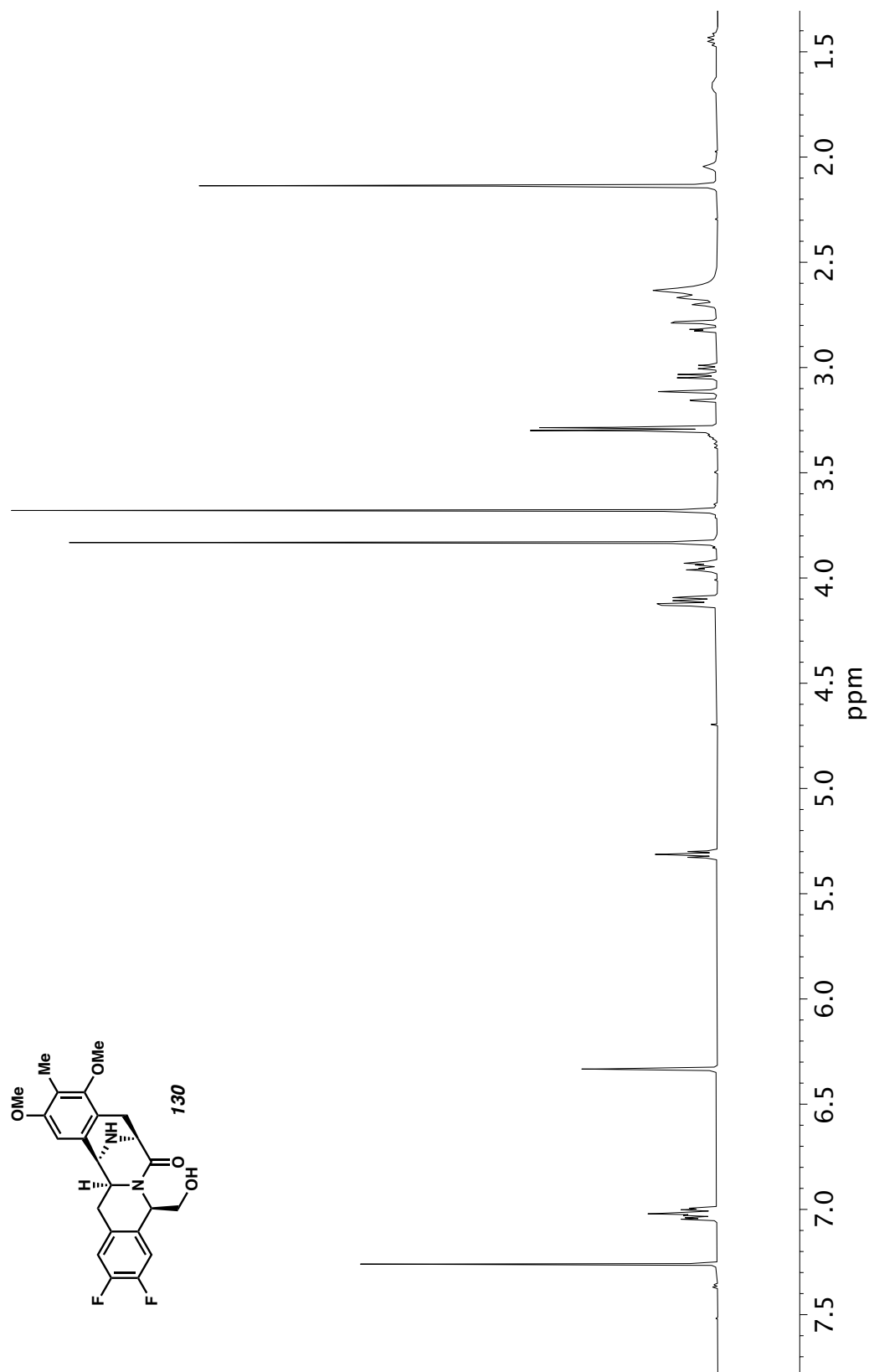


Figure A10.45 ^1H NMR (400 MHz, CDCl_3) of compound **130**.

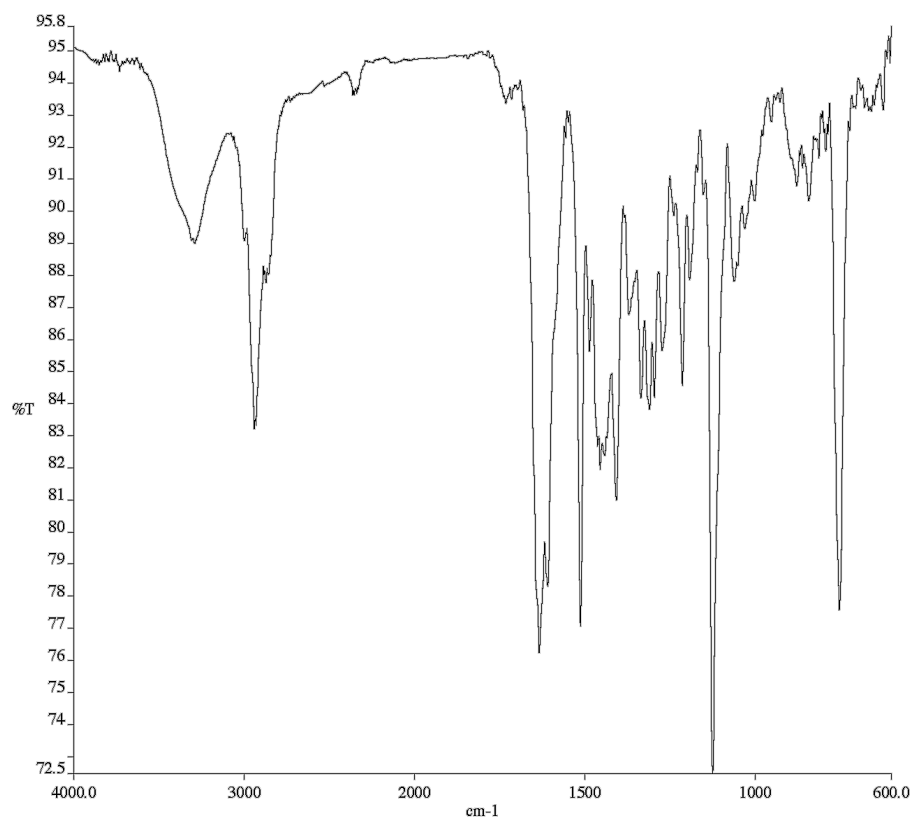


Figure A10.46 Infrared spectrum (Thin Film, NaCl) of compound **130**.

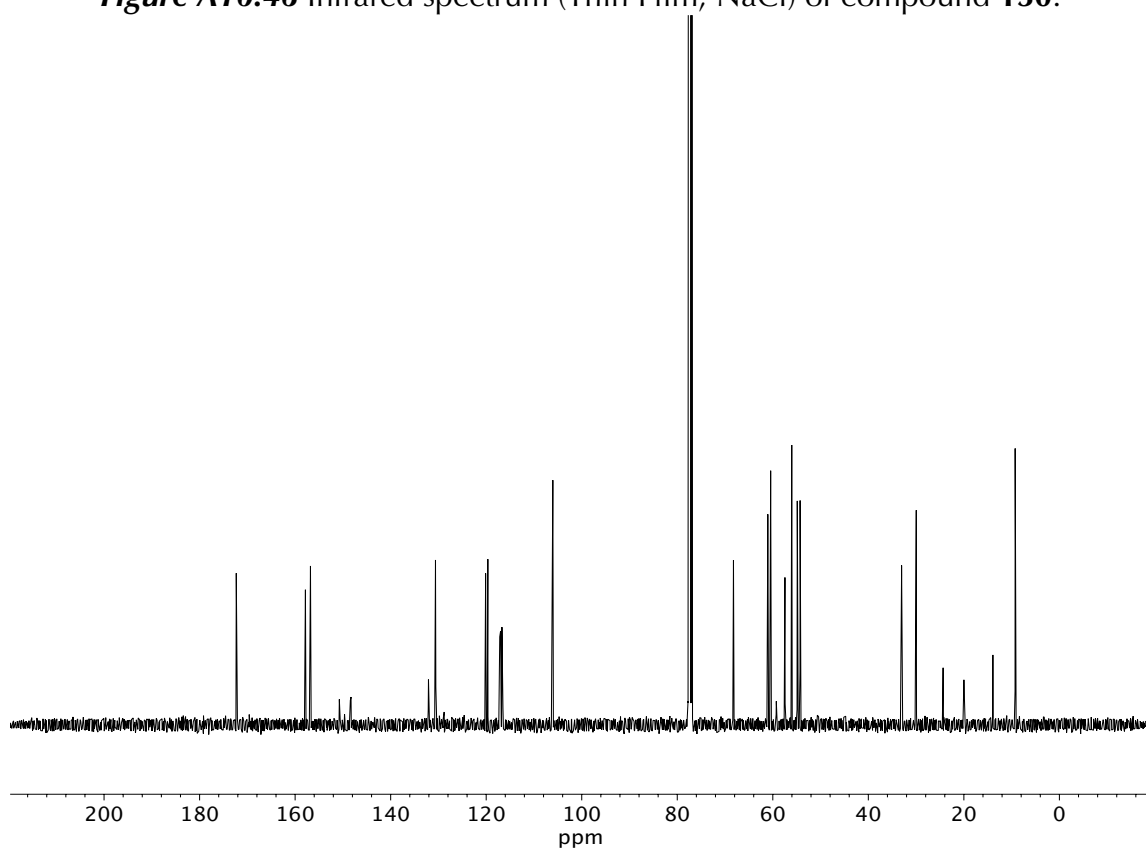


Figure A10.47 ¹³C NMR (100 MHz, CDCl₃) of compound **130**.

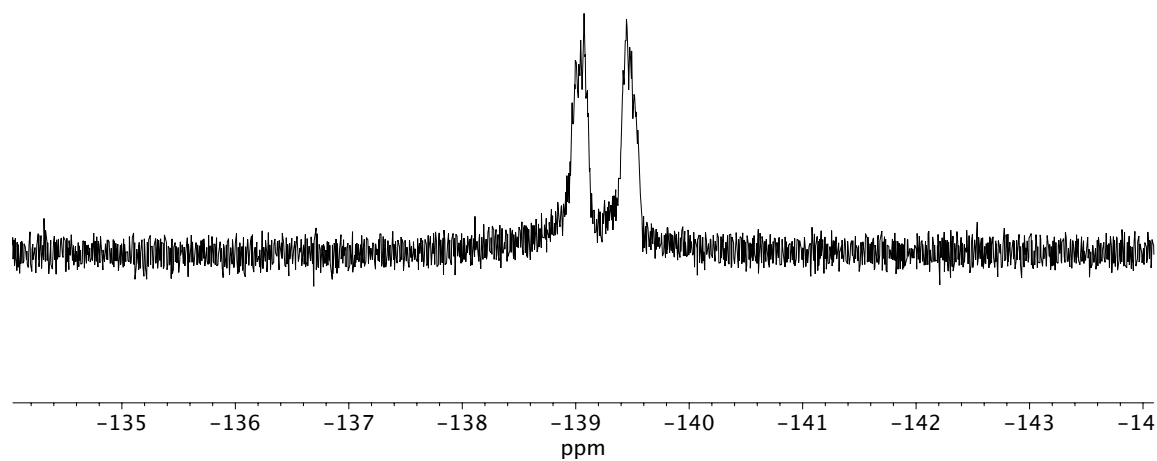


Figure A10.48 ^{19}F NMR (282 MHz, CDCl_3) of compound **130**.

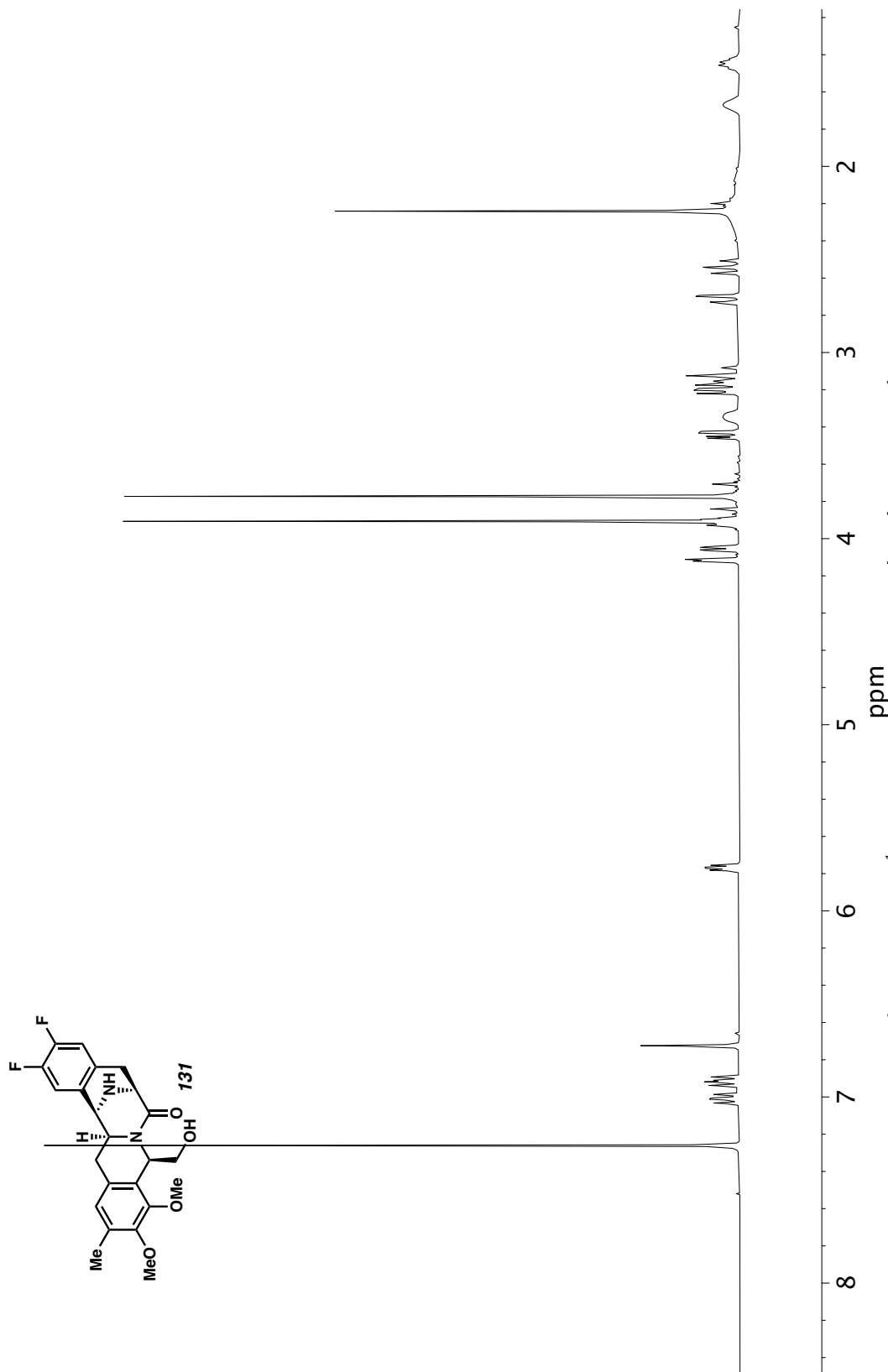


Figure A10.49 ^1H NMR (400 MHz, CDCl_3) of compound **131**.

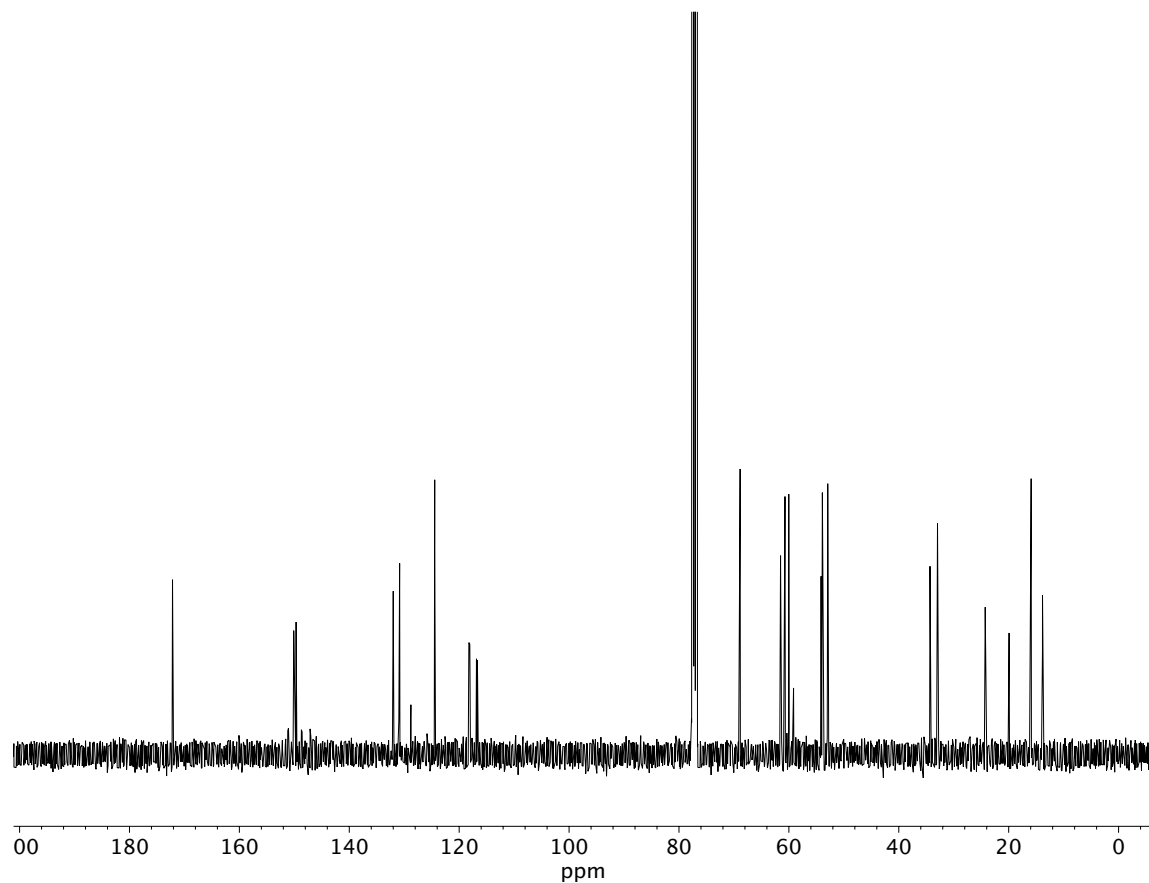


Figure A10.50 ^{13}C NMR (100 MHz, CDCl_3) of compound **131**.

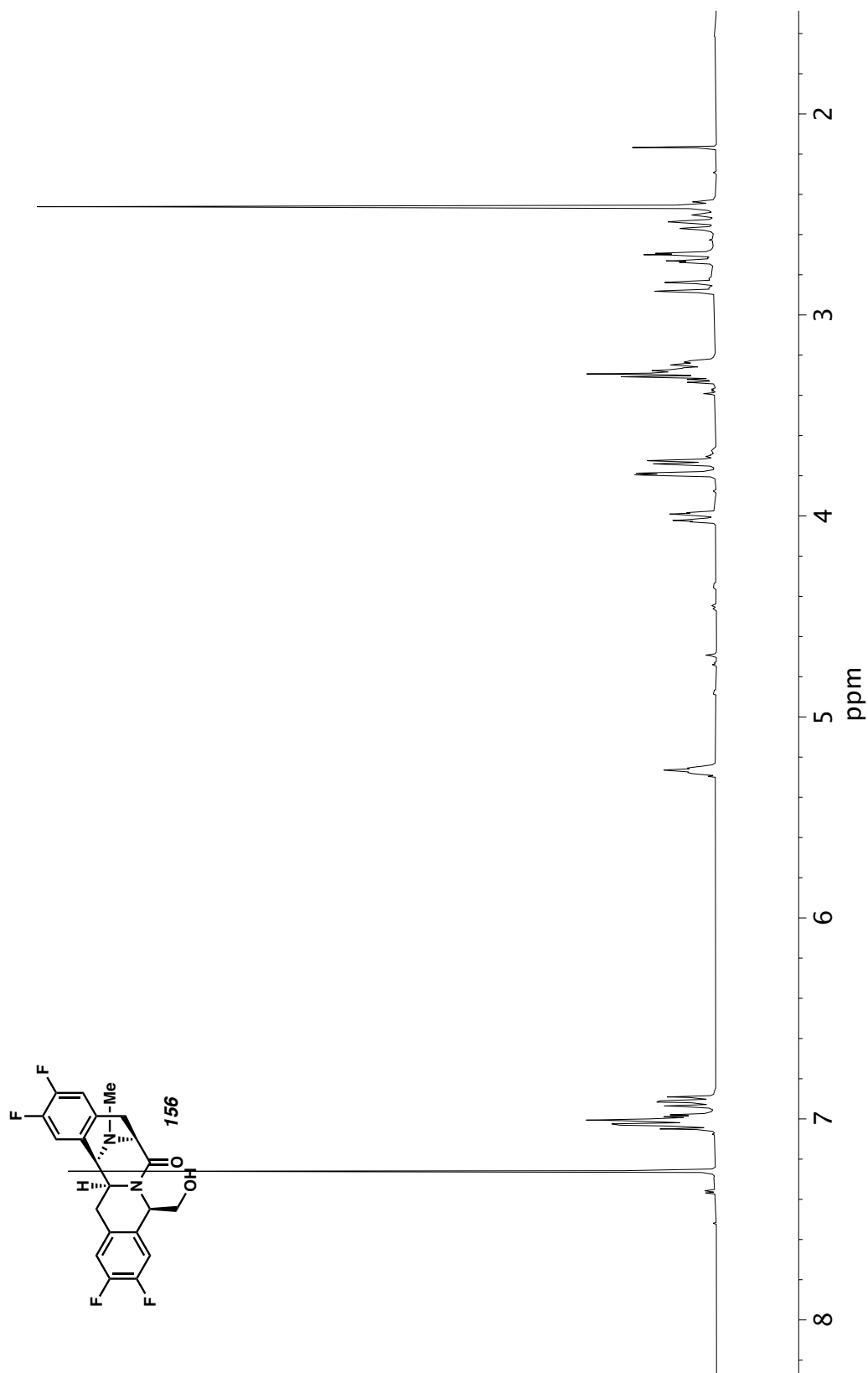


Figure A10.51 ^1H NMR (400 MHz, CDCl_3) of compound **156**.

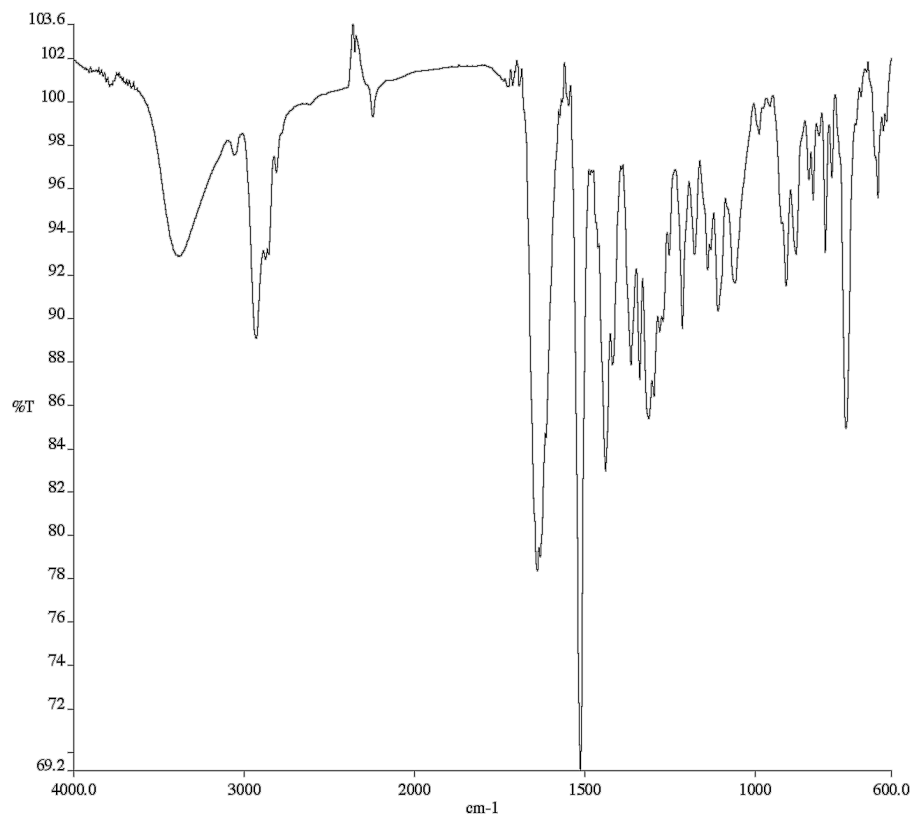


Figure A10.52 Infrared spectrum (Thin Film, NaCl) of compound **156**.

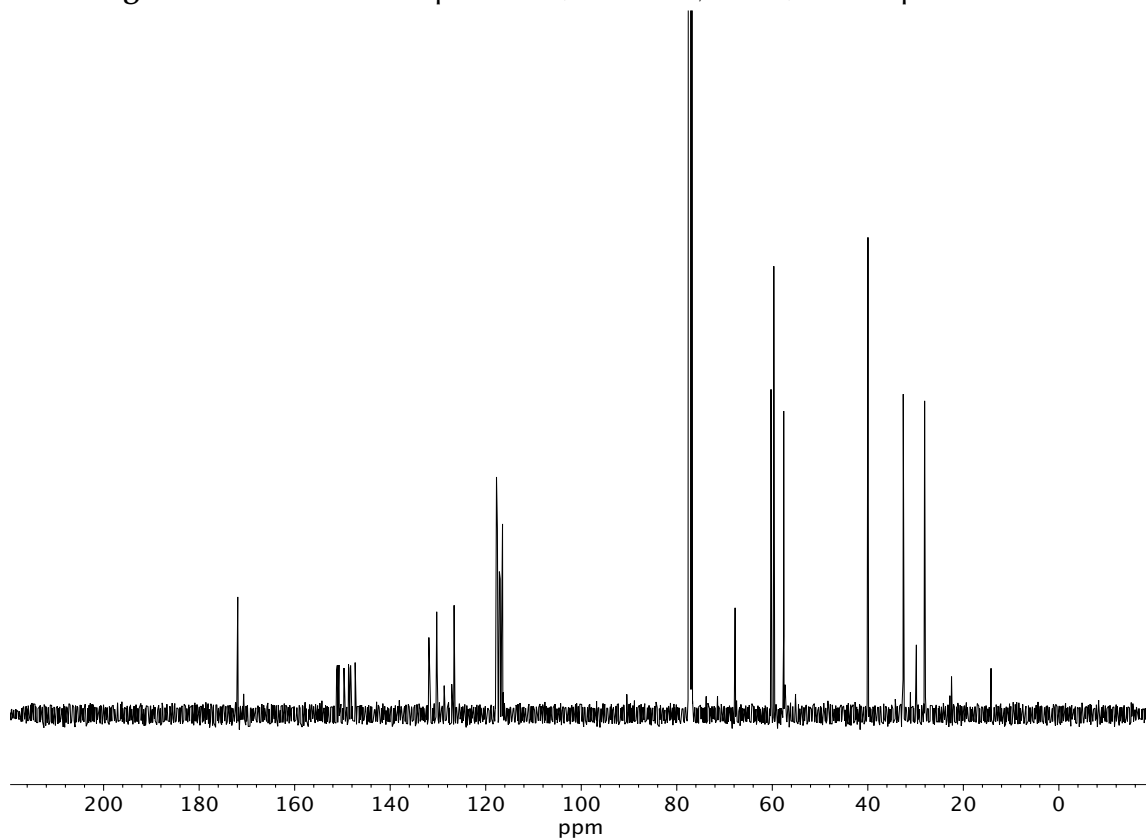


Figure A10.53 ¹³C NMR (100 MHz, CDCl₃) of compound **156**.

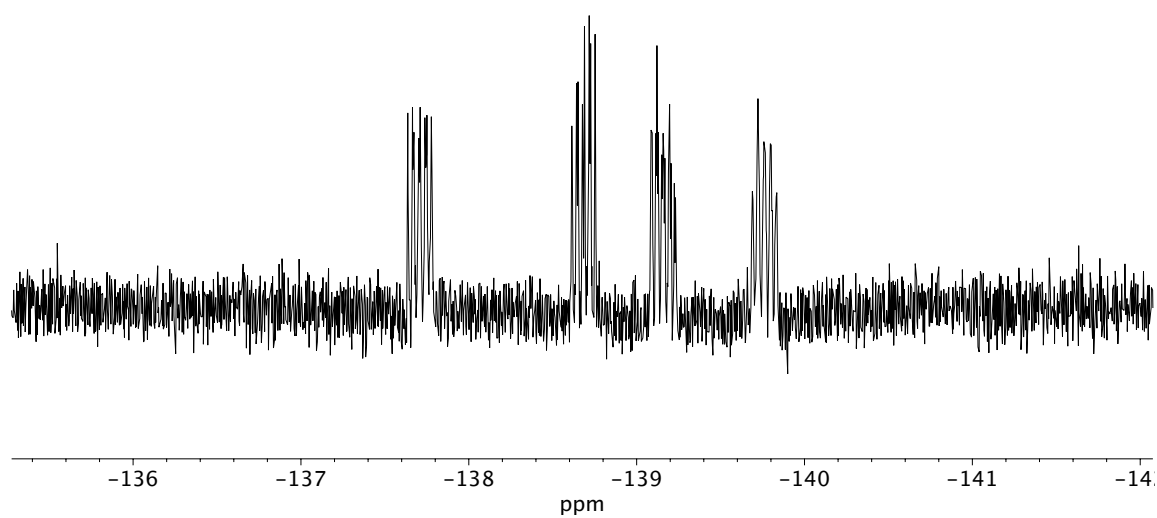


Figure A10.54 ^{19}F NMR (282 MHz, CDCl_3) of compound **156**.

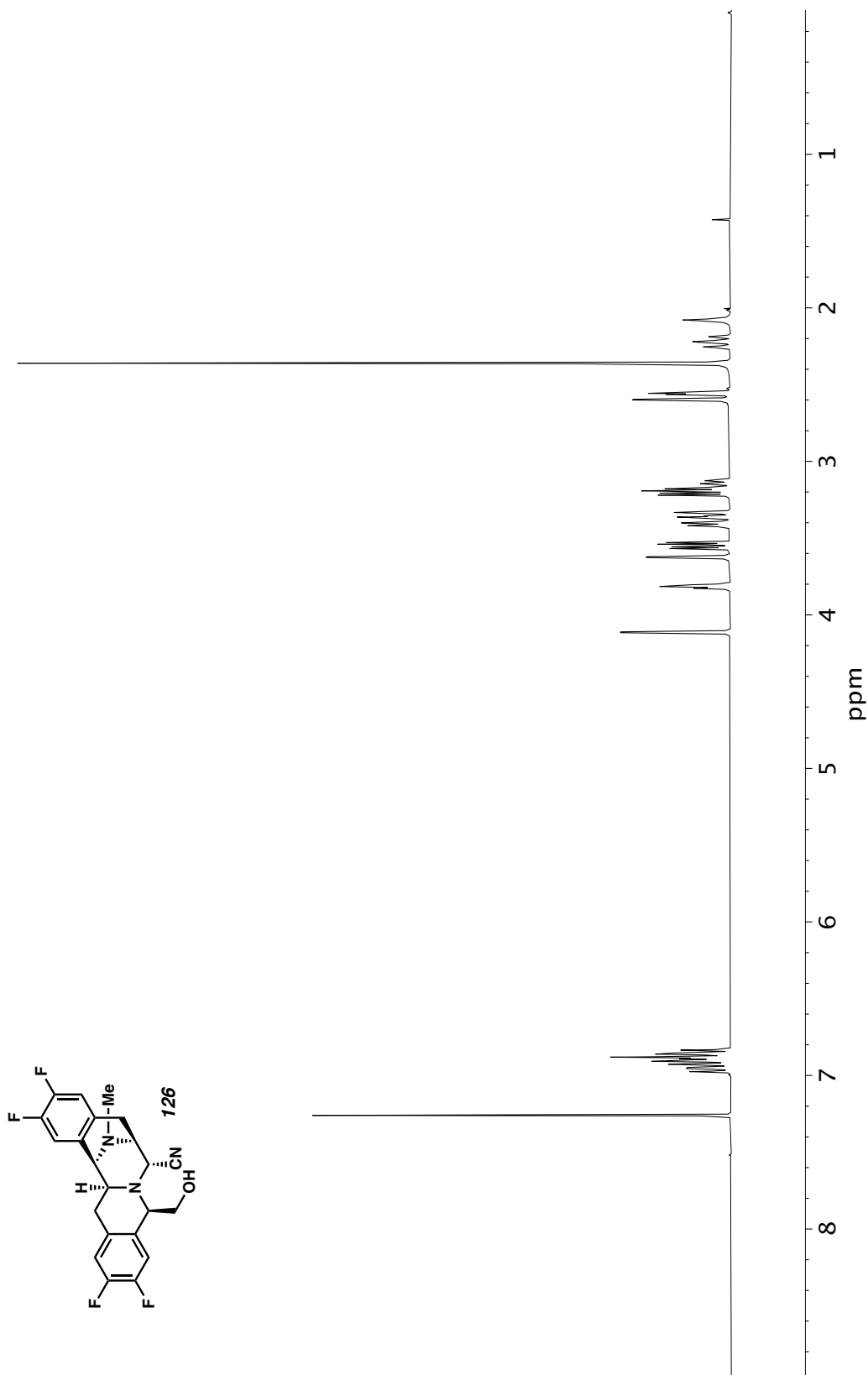


Figure A10.55 ^1H NMR (400 MHz, CDCl_3) of compound **126**.

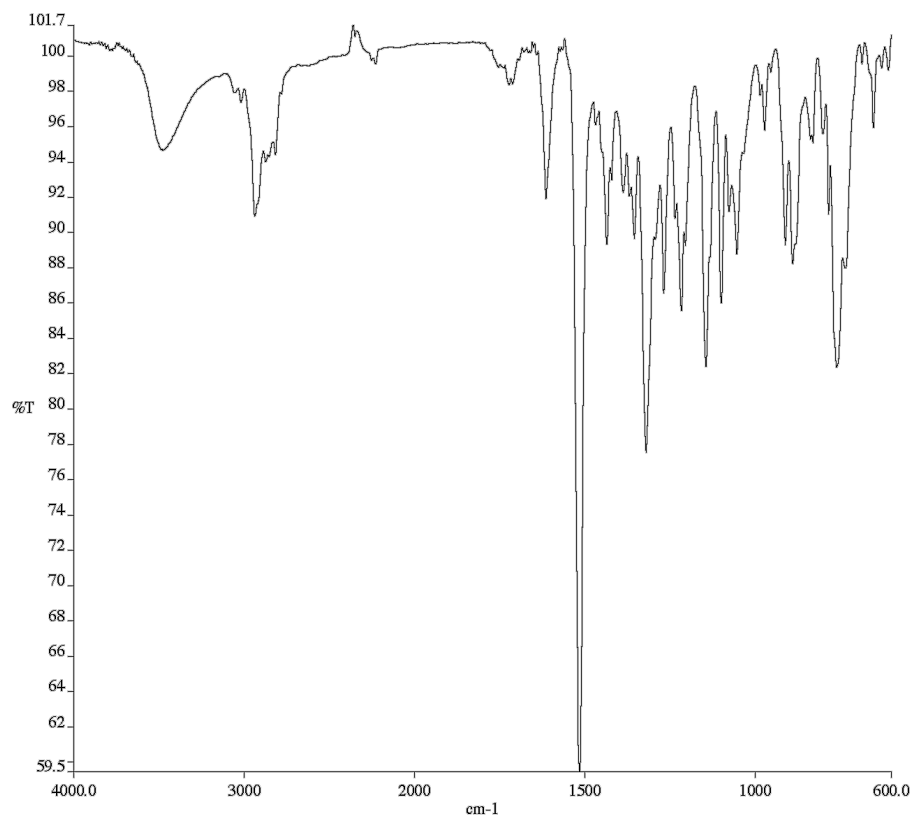


Figure A10.56 Infrared spectrum (Thin Film, NaCl) of compound **126**.

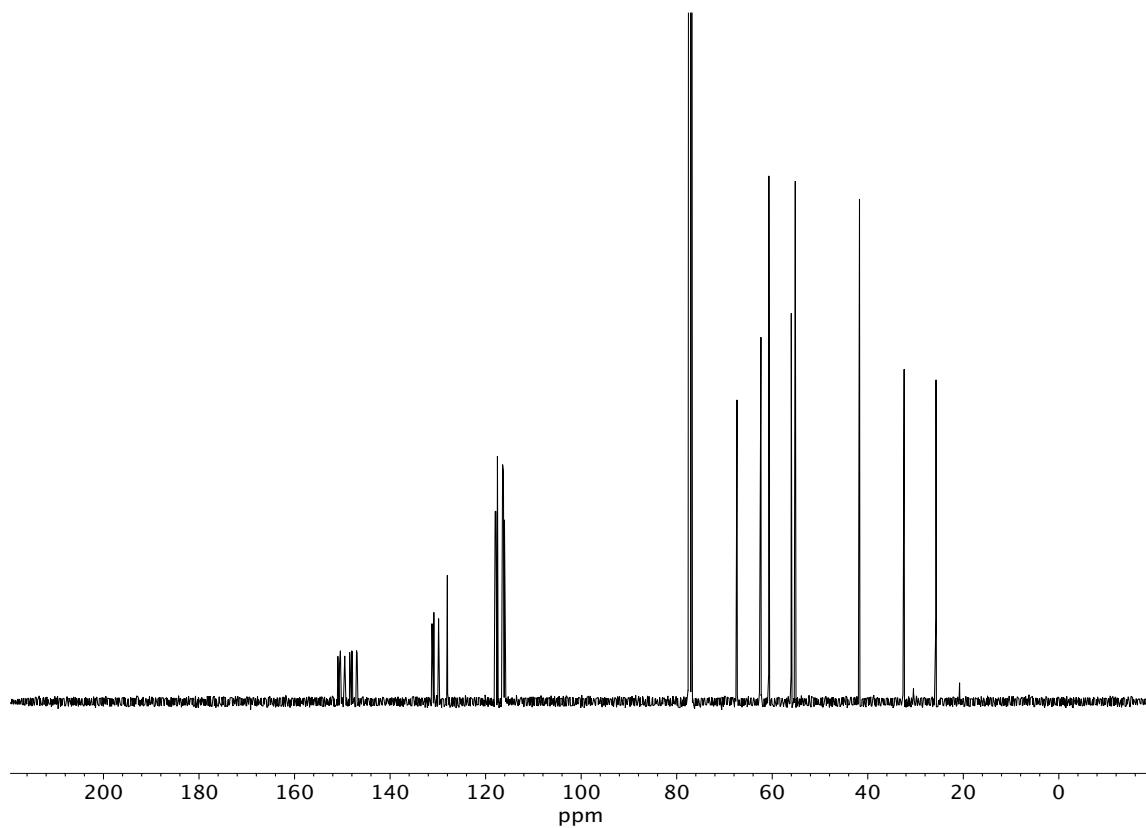


Figure A10.57 ¹³C NMR (100 MHz, CDCl₃) of compound **126**.

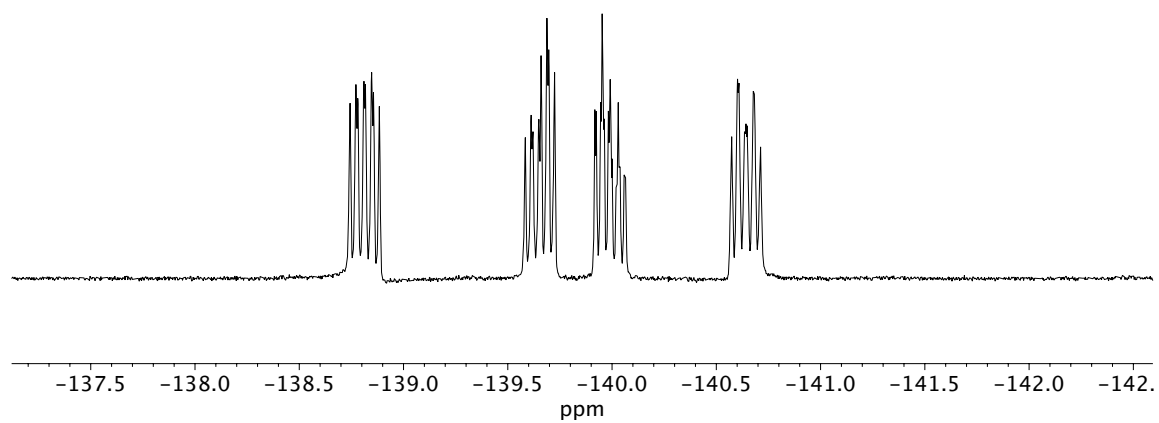


Figure A10.58 ^{19}F NMR (282 MHz, CDCl_3) of compound **126**.

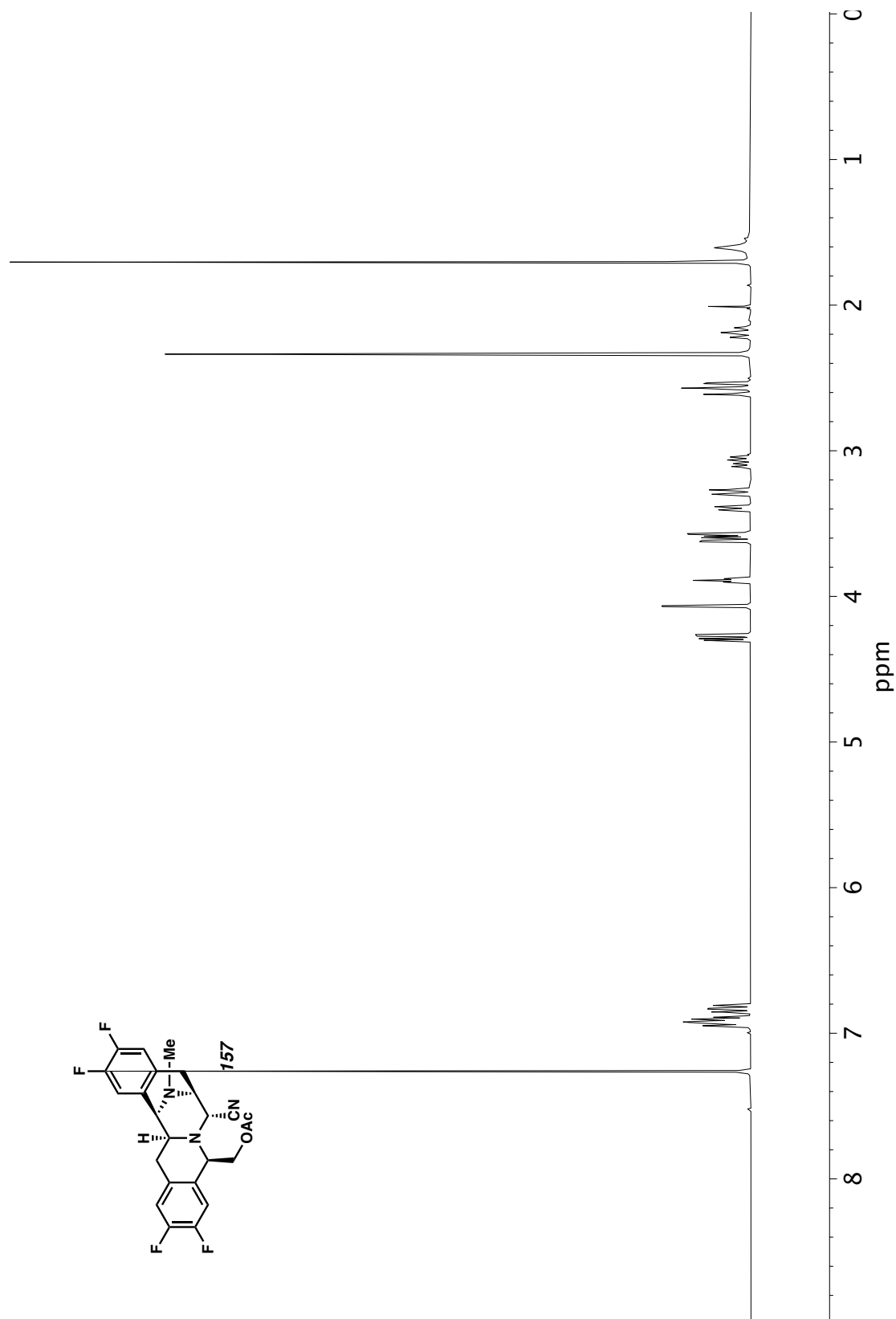


Figure A10.59 ^1H NMR (400 MHz, CDCl_3) of compound **157**.

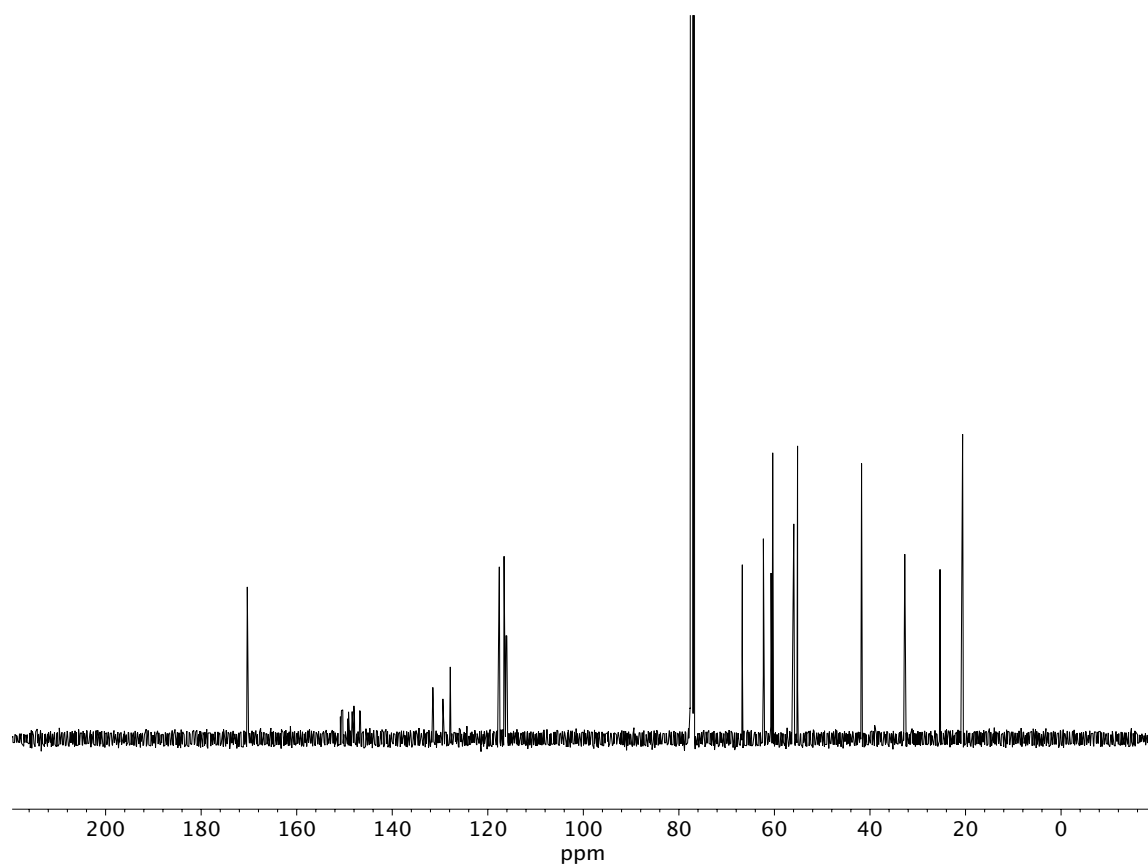


Figure A10.60 ^{13}C NMR (100 MHz, CDCl_3) of compound **157**.

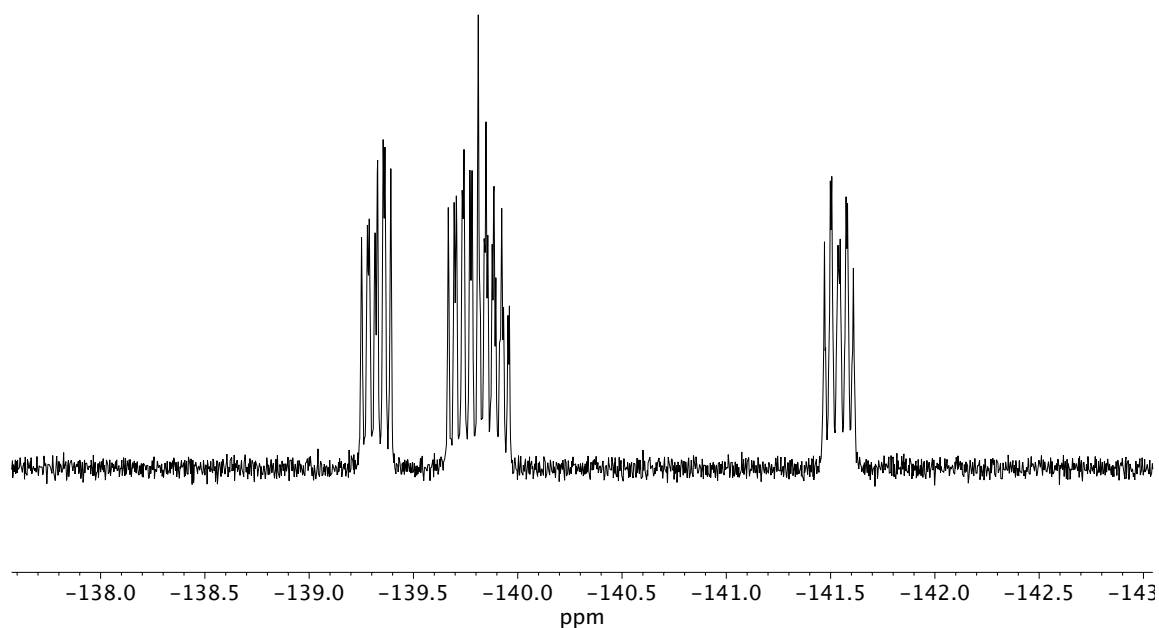


Figure A10.61 ^{19}F NMR (100 MHz, CDCl_3) of compound **157**.

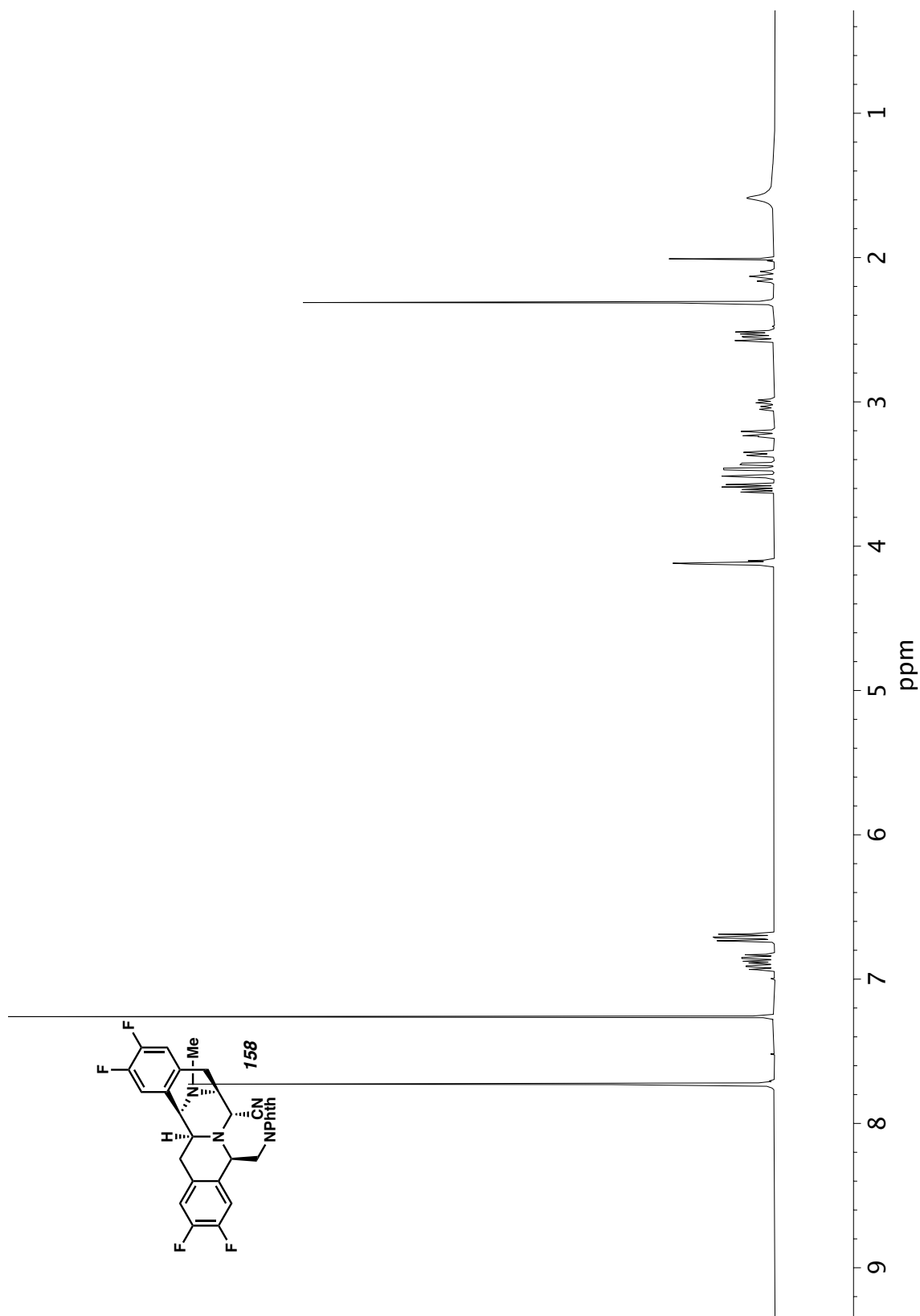


Figure A10.62 ^1H NMR (400 MHz, CDCl_3) of compound **158**.

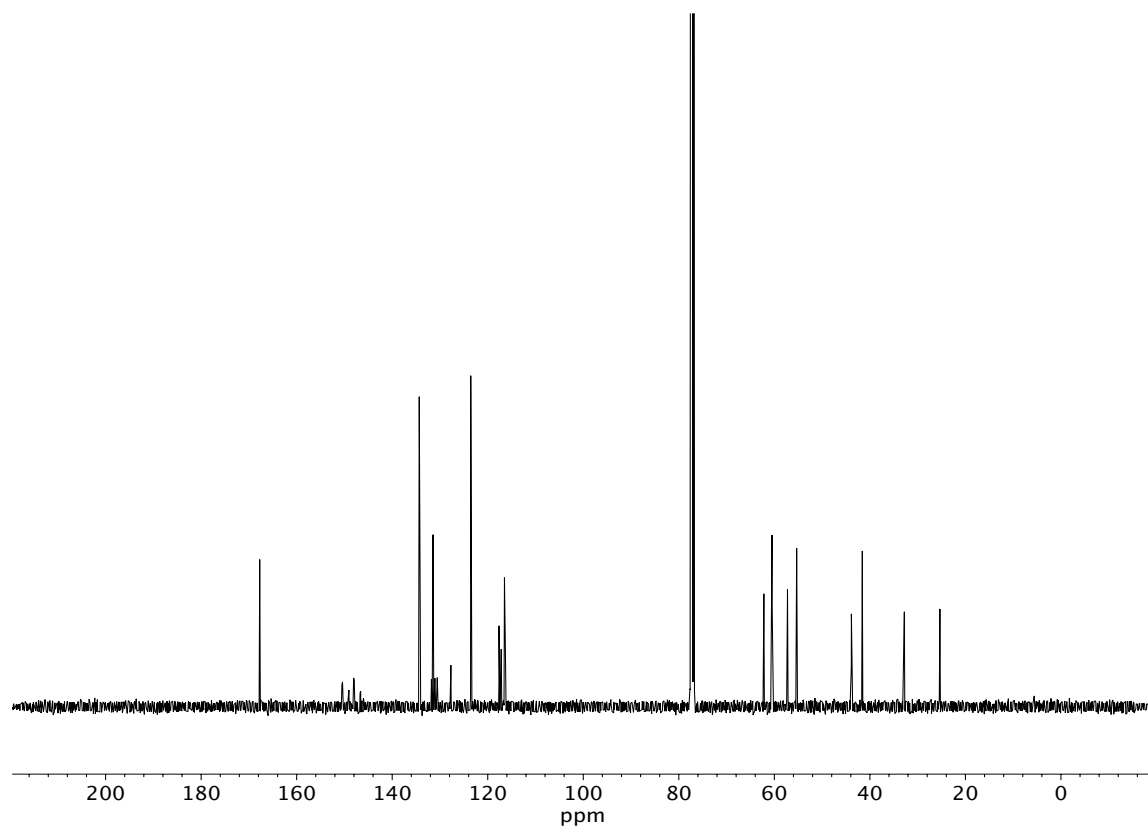


Figure A10.63 ^{13}C NMR (100 MHz, CDCl_3) of compound **158**.

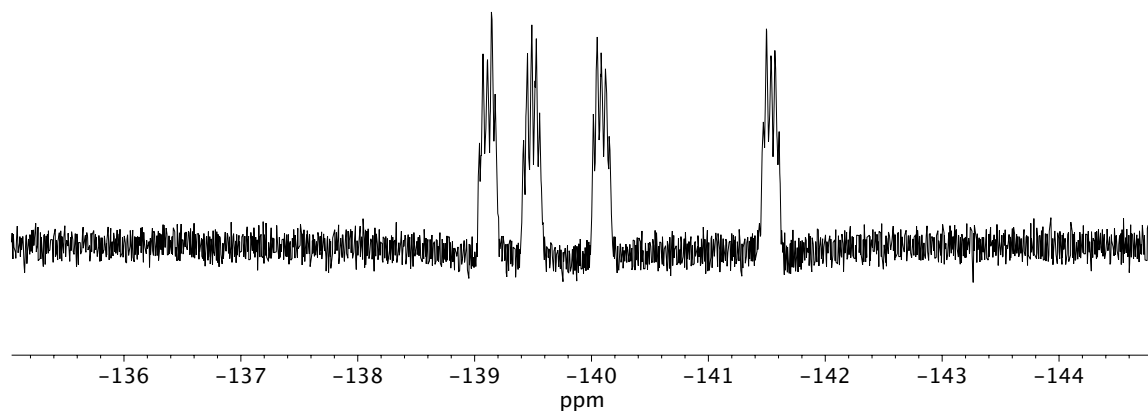


Figure A10.64 ^{19}F NMR (100 MHz, CDCl_3) of compound **158**.

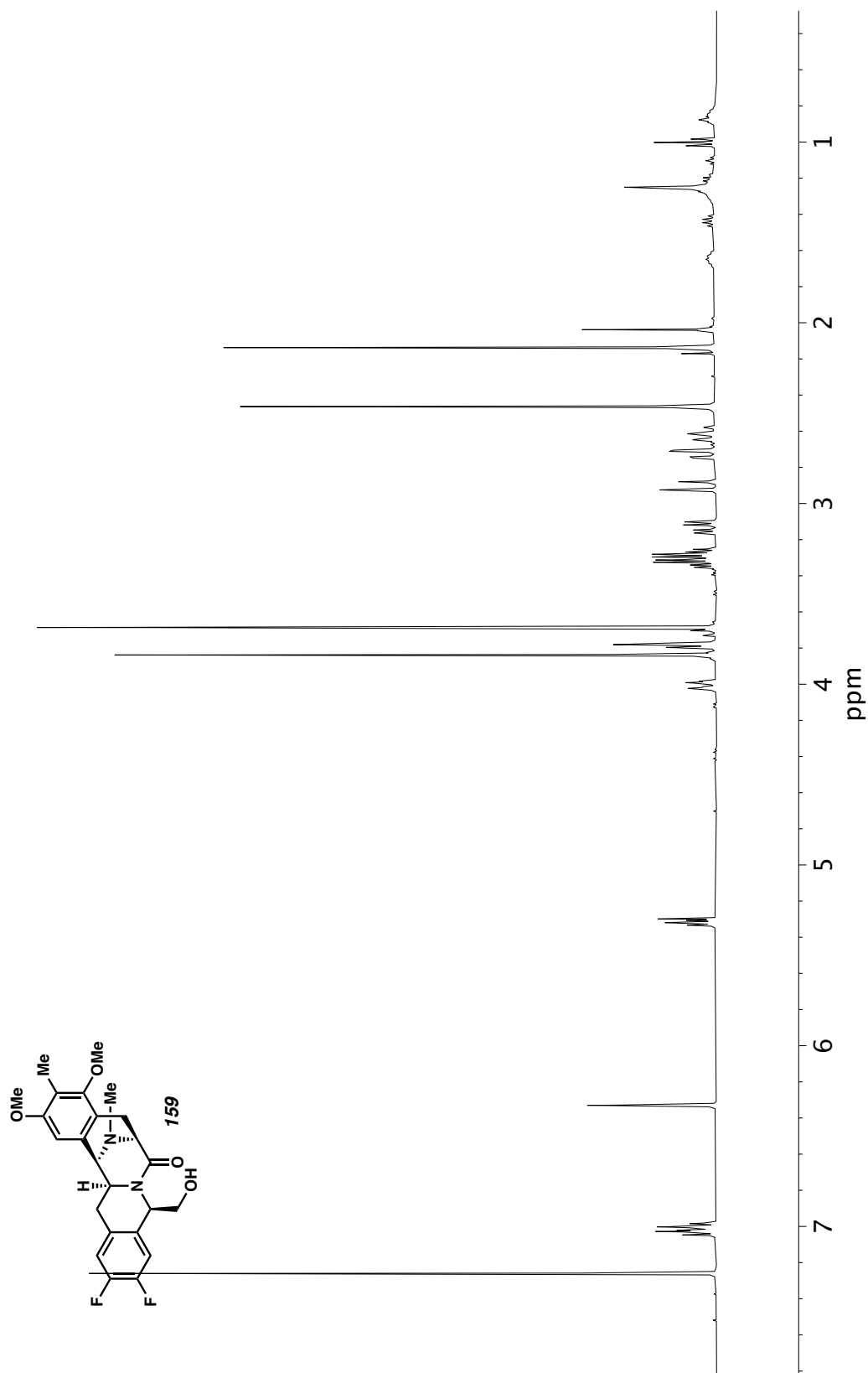


Figure A10.65 ¹H NMR (400 MHz, CDCl₃) of compound **159**.

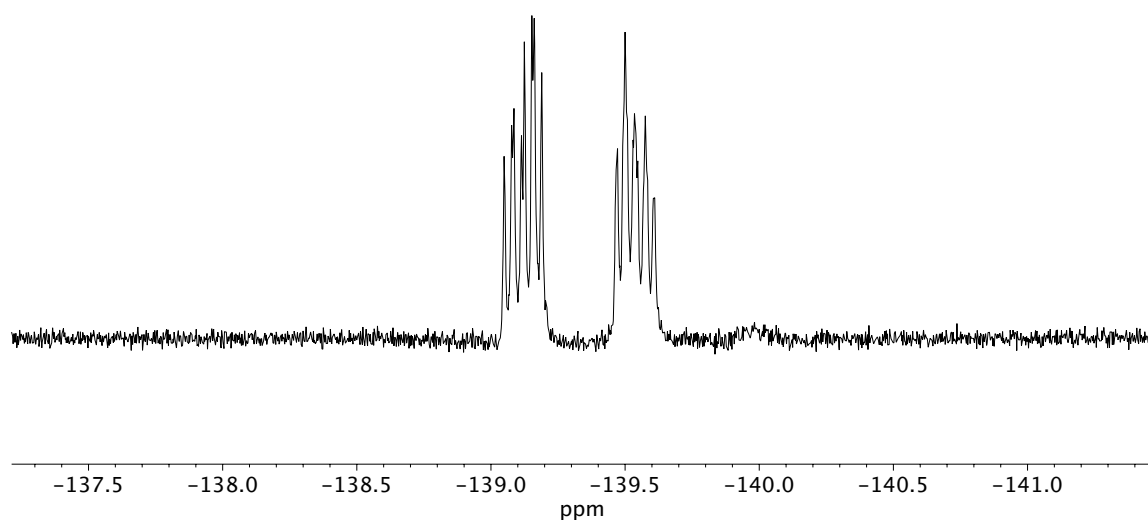


Figure A10.66 ^{19}F NMR (100 MHz, CDCl_3) of compound **159**.

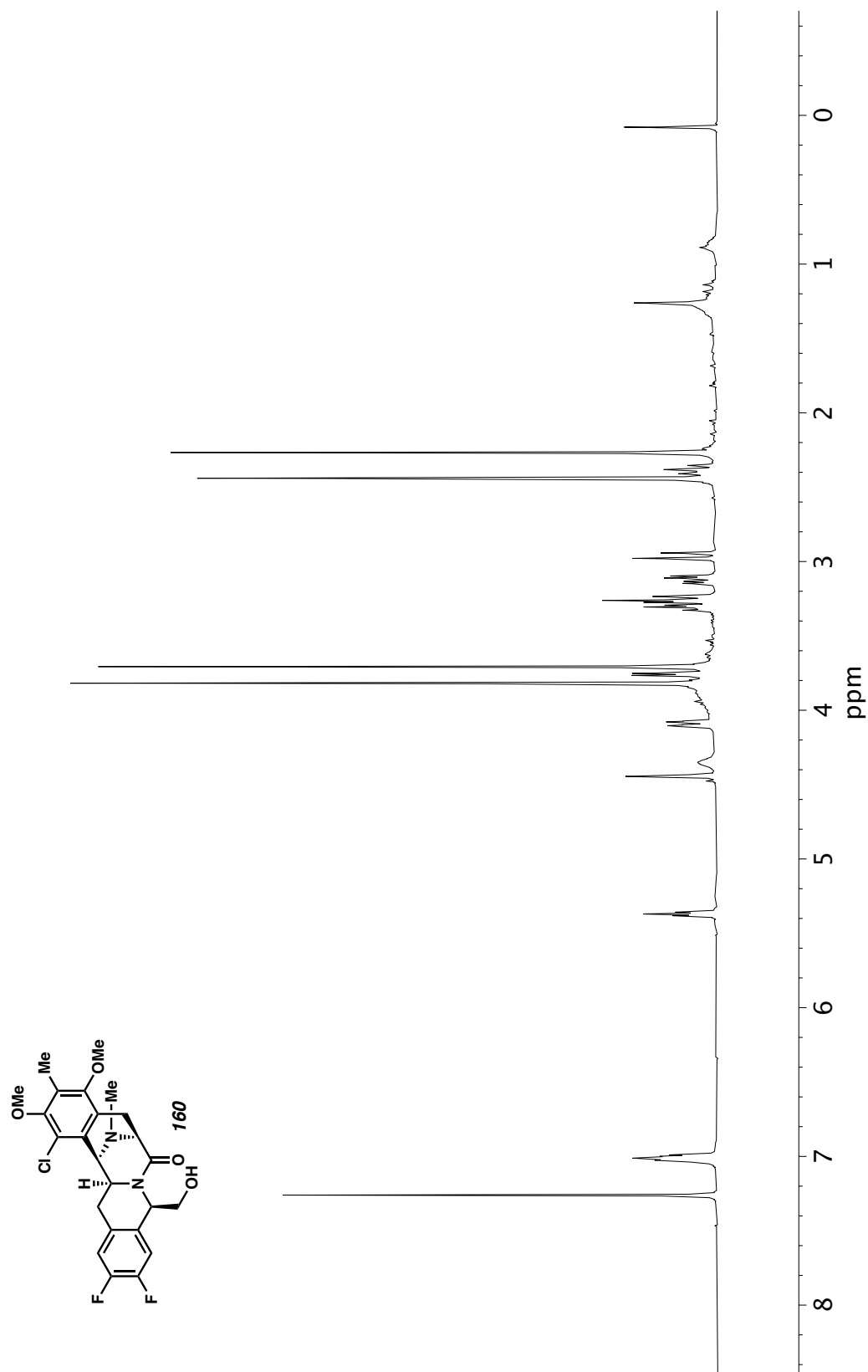


Figure A10.67 ^1H NMR (500 MHz, CDCl_3) of compound **160**.

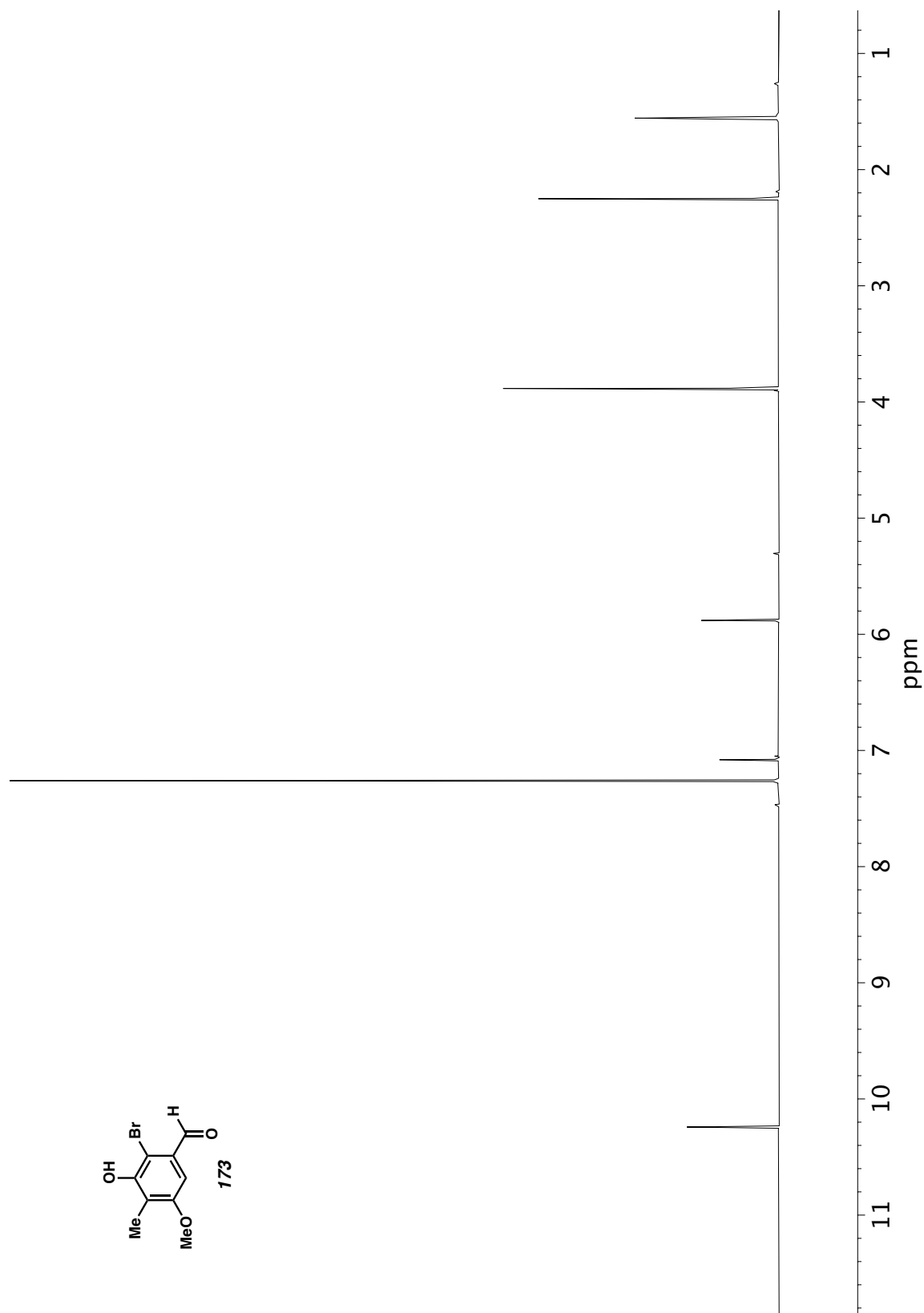


Figure A10.68 ^1H NMR (400 MHz, CDCl_3) of compound **173**.

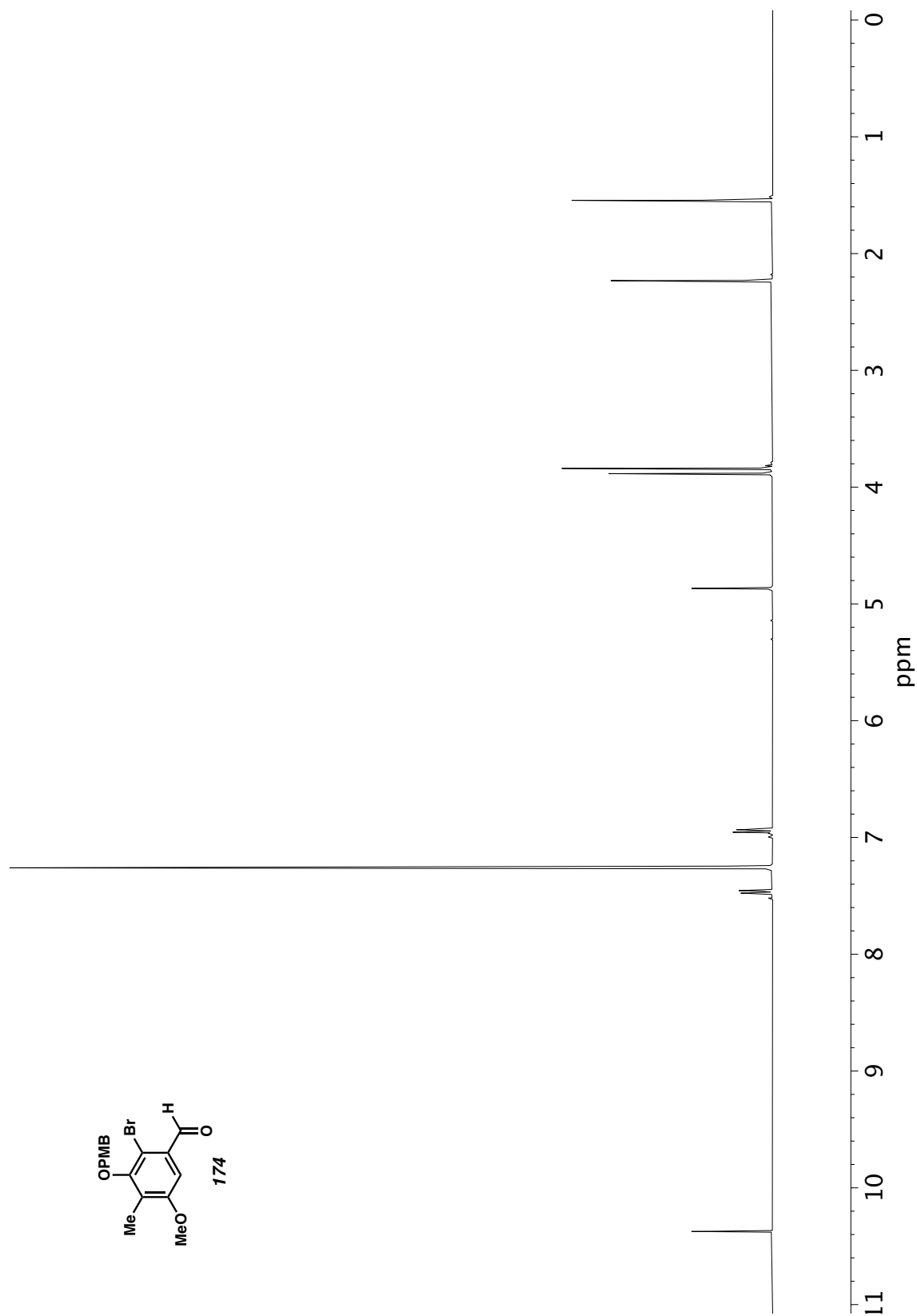


Figure A10.69 ¹H NMR (400 MHz, CDCl₃) of compound **174**.

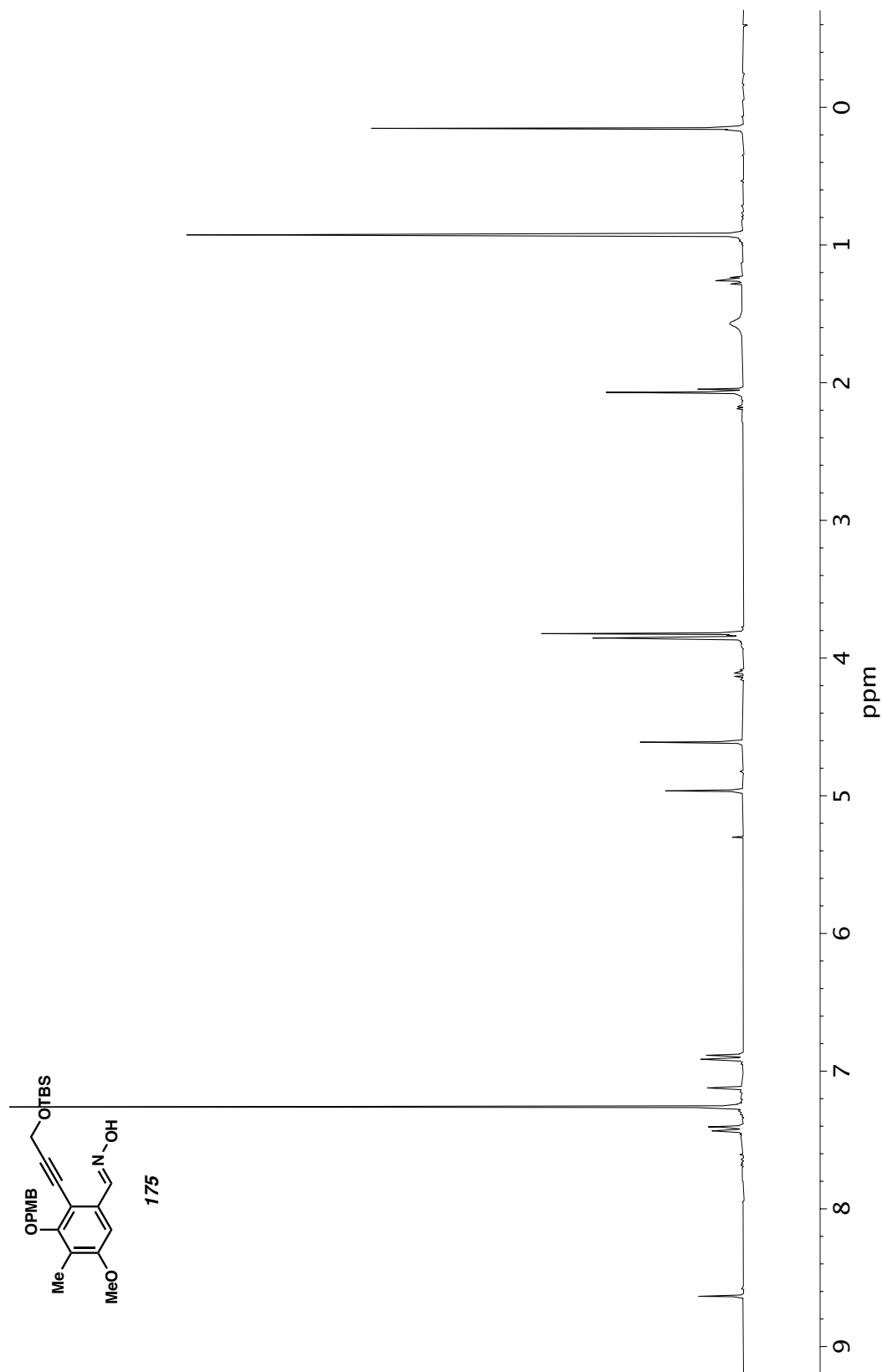


Figure A10.70 ^1H NMR (300 MHz, CDCl_3) of compound **175**.

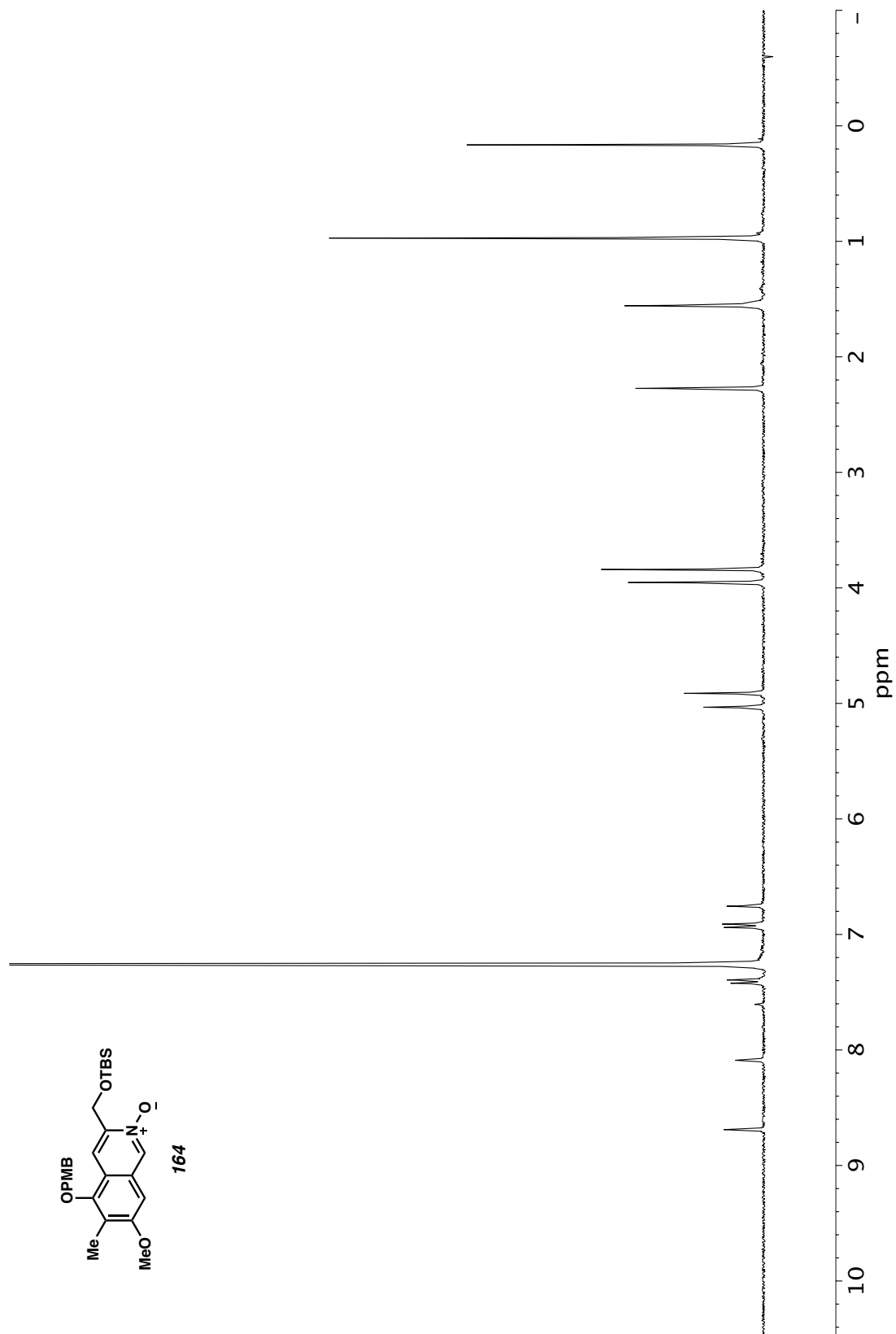


Figure A10.71 ^1H NMR (300 MHz, CDCl_3) of compound **164**.

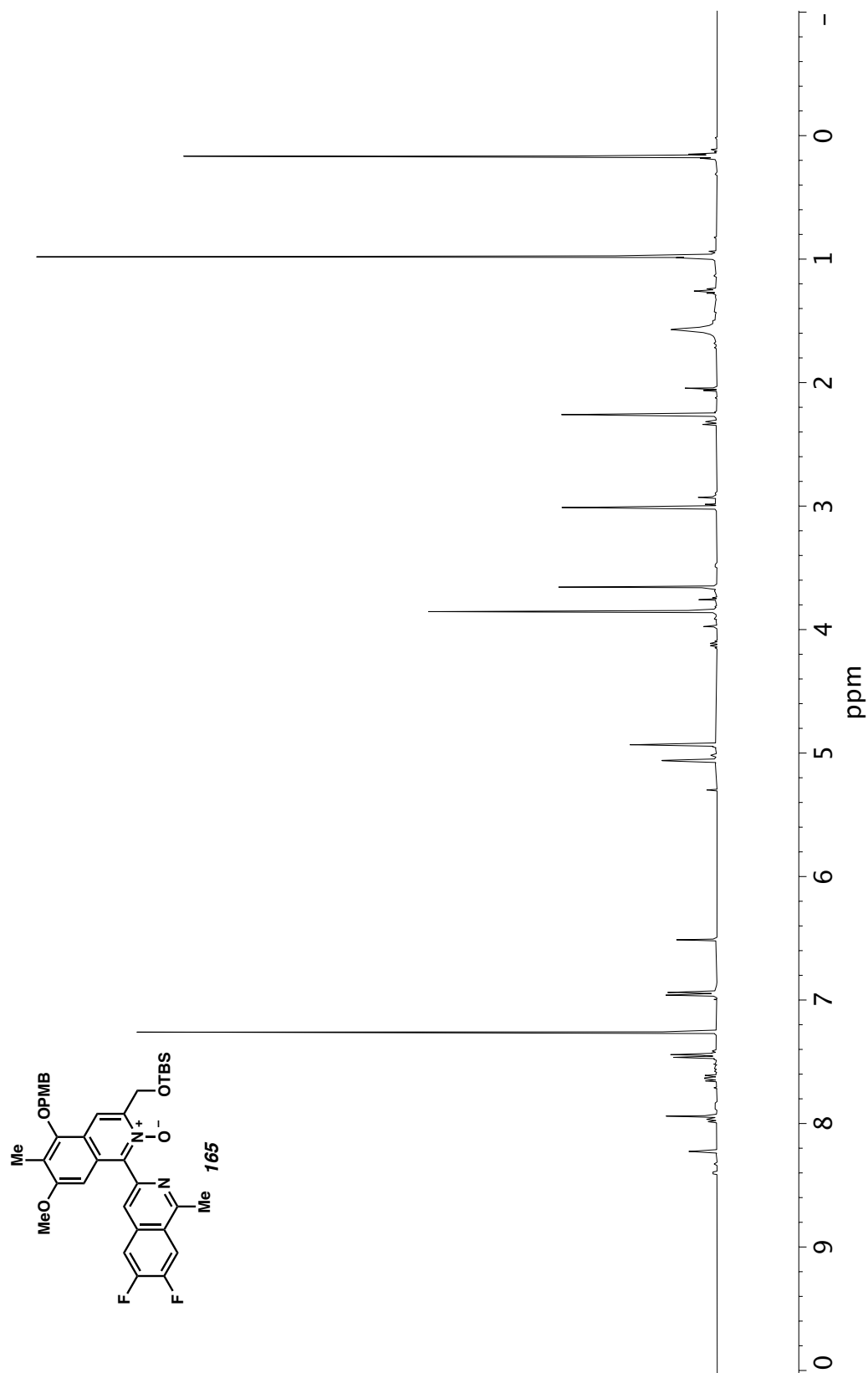


Figure A10.72 ^1H NMR (400 MHz, CDCl_3) of compound **165**.

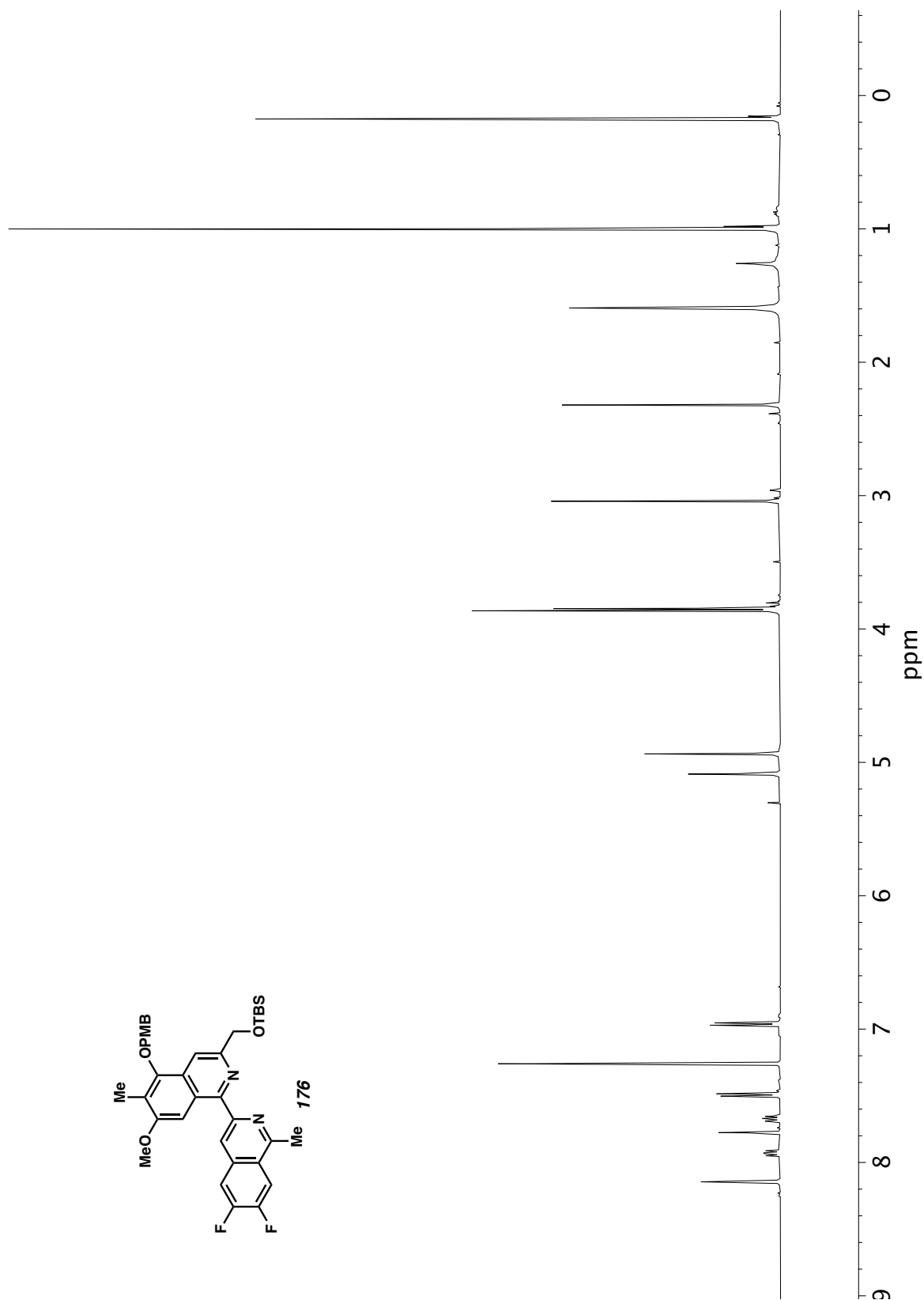


Figure A10.73 ^1H NMR (500 MHz, CDCl_3) of compound **176**.

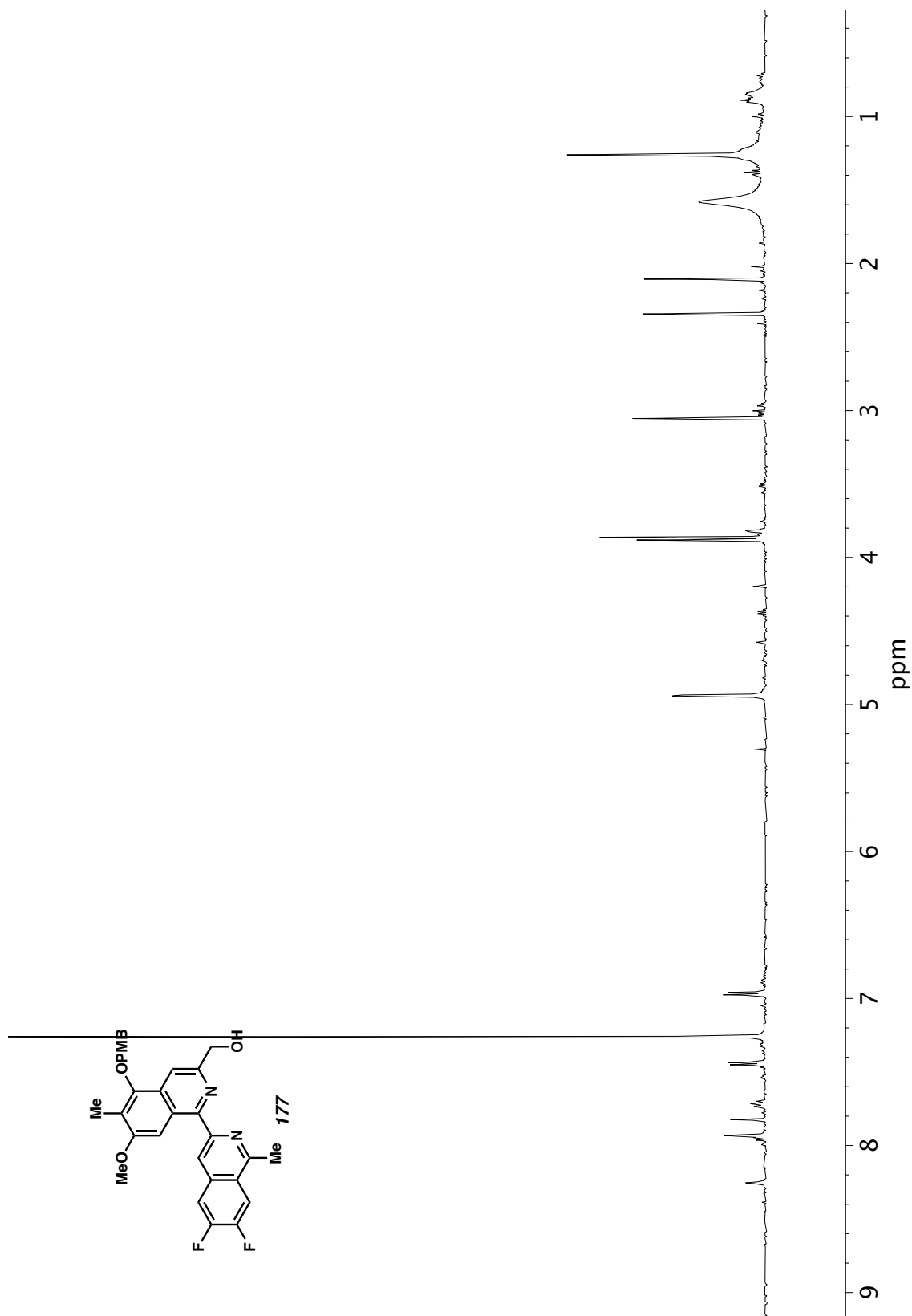


Figure A10.74 ^1H NMR (500 MHz, CDCl_3) of compound **177**.

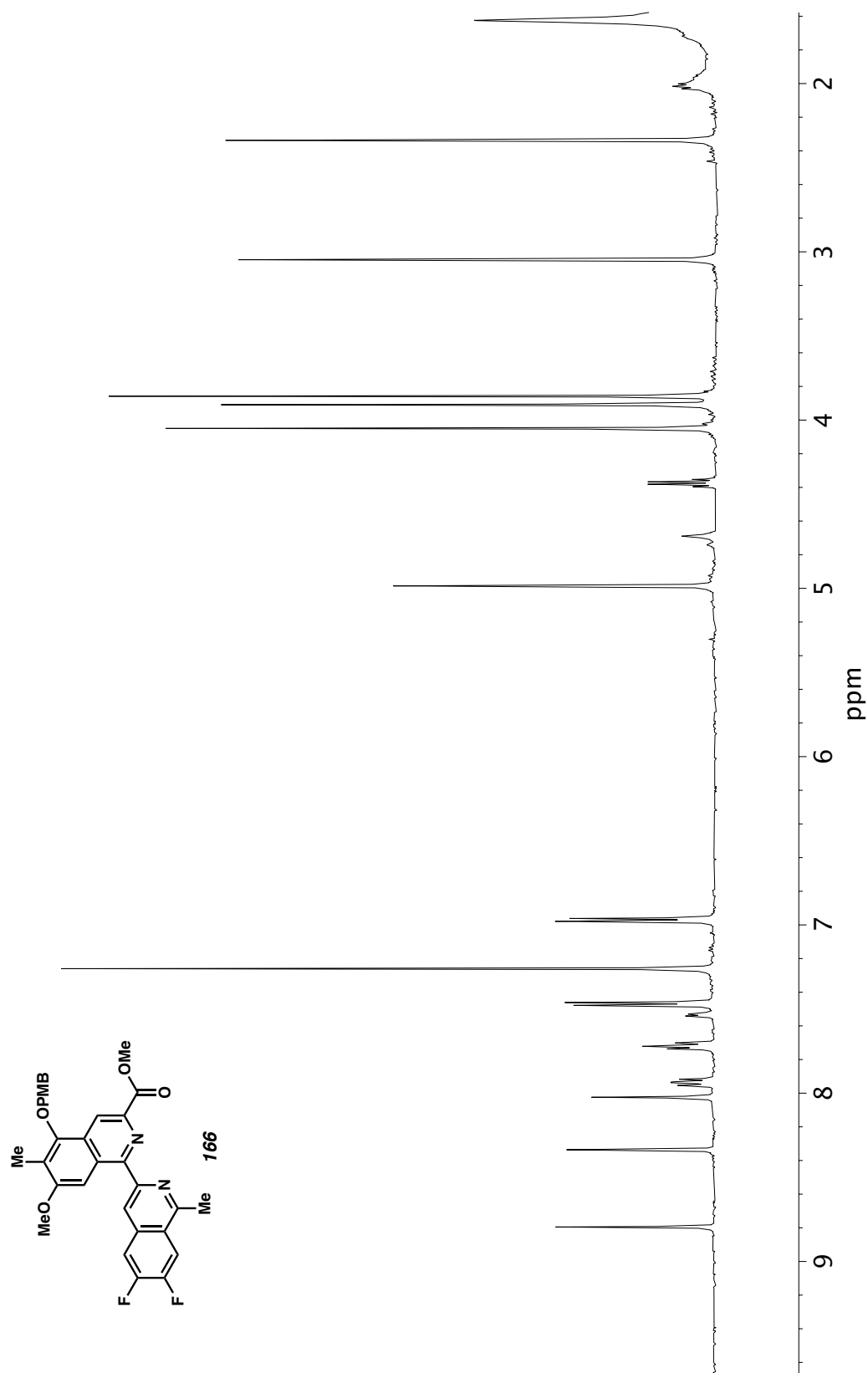


Figure A10.75 ¹H NMR (500 MHz, CDCl₃) of compound **166**.

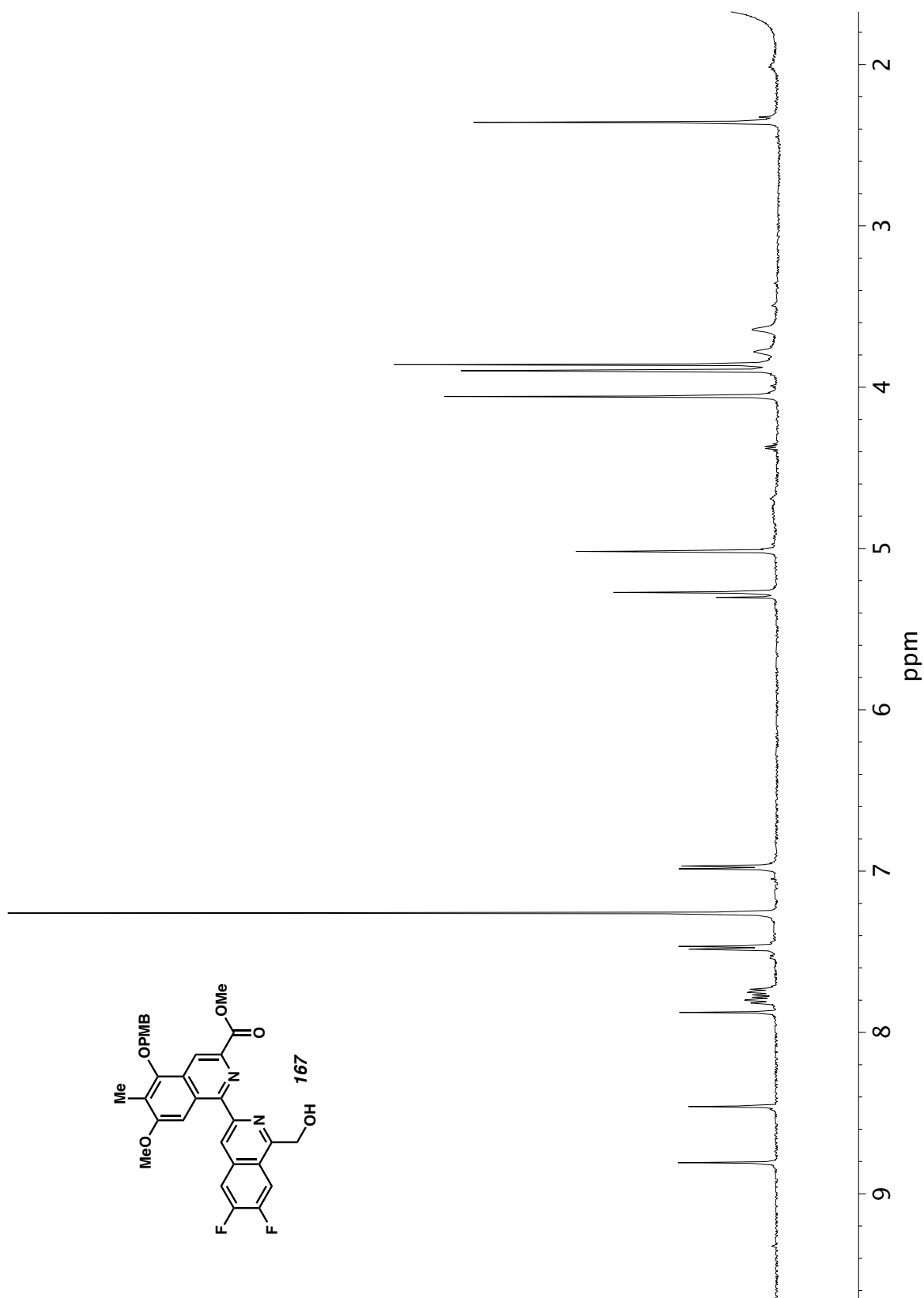


Figure A10.76 ^1H NMR (500 MHz, CDCl_3) of compound **167**.

CHAPTER 4

Iridium-Catalyzed Enantioselective and Diastereoselective Hydrogenation of 1,3-Disubstituted Isoquinolines[†]

4.1 INTRODUCTION

The stereocontrolled synthesis of nitrogen-containing heterocycles remains a challenge of great importance, as it provides direct access to chiral compounds that are prevalent structural motifs in many biologically active molecules.¹ As a result, the asymmetric hydrogenation of various hetero-aromatic compounds has been extensively explored as a direct, efficient synthesis of enantiopure cyclic amines.² Despite recent progress made toward the asymmetric hydrogenation of *N*-heterocycles such as

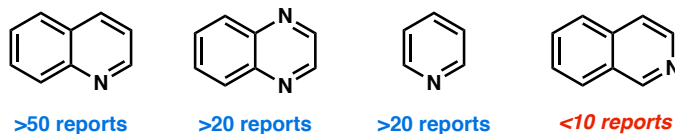
[†] This research was performed in collaboration with Alexia N. Kim, Dr. Eric Welin, Martin T. Daiger, Christian U. Grünanger, Dr. Michael D. Bartberger, and Dr. Scott C. Virgil. Portions of this chapter have been reproduced with permission from Kim, A. N.; Ngamnithiporn, A.; Welin, E. R.; Daiger, M. T.; Grünanger, C. U.; Bartberger, M. D.; Virgil, S. C.; Stoltz, B. M. *ACS Catal.* **2020**, *10*, 3241–3248 © 2020 American Chemical Society.

quinolines, quinoxalines, and pyridines, the synthesis of 1,2,3,4-tetrahydroisoquinolines (THIQs) from isoquinolines remains significantly under-developed (Figure 4.1A).² This is due in part to the stronger basicity and coordinating ability of the THIQ products compared to those of other heterocycles (e.g., quinolines), leading to catalyst deactivation, as well as the overall lower reactivity of isoquinoline substrates.³ Although a few effective strategies toward the asymmetric hydrogenation of substituted isoquinolines have been reported, these typically require preparation of the isoquinolinium salt, substrate activation with halogenides, and harsher hydrogenation reaction conditions (Figure 4.1B).⁴ Furthermore, previous to our research, there were only two catalytic systems describing efficient methods to access chiral 1,3-disubstituted tetrahydroisoquinolines,^{4c,e,g} a more complex and sterically challenging system that generates two stereogenic centers. In addition, the limited substrate scope from these reports demonstrates the low tolerance of additional Lewis basic functionalities, such as alcohols or heteroaryl-substituted isoquinolines, which limit the applicability of these methodologies in synthesis. Since 1,3-disubstituted tetrahydroisoquinolines with Lewis basic moieties are ubiquitous motifs present in a wide range of natural products, such as the saframycin, naphthyridinomycin, and quinocarcin families,⁵ a general method for highly enantioselective and diastereoselective hydrogenation of neutral disubstituted isoquinolines under mild reaction conditions would be a significant advancement toward the preparation of chiral amine-containing cyclic molecules.

Figure 4.1 A) Limitations in enantioselective hydrogenation of *N*-heterocycles. B) Previous examples of iridium-catalyzed enantioselective and diastereoselective hydrogenation of mono- and di-substituted isoquinolines.

A. Asymmetric Hydrogenation of *N*-Heterocycles:

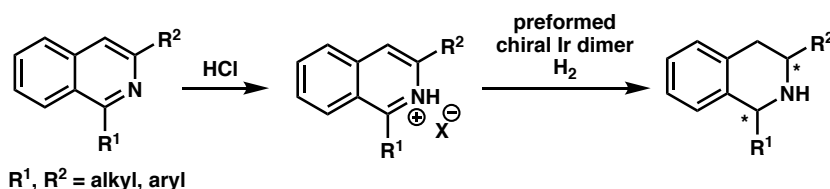
Substrates:



B. Prior Art in Ir-Catalyzed Asymmetric Hydrogenation of Isoquinolines:

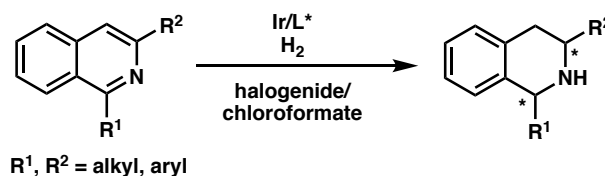
a) Substrate Activation via Isoquinolinium Salts

- 4 reports with only 1 report describing 1,3-disubstituted isoquinolines
- Requires prior formation of the salt for activation
- No example of substrate with additional Lewis basic functionalities



b) in situ and Transient Activation

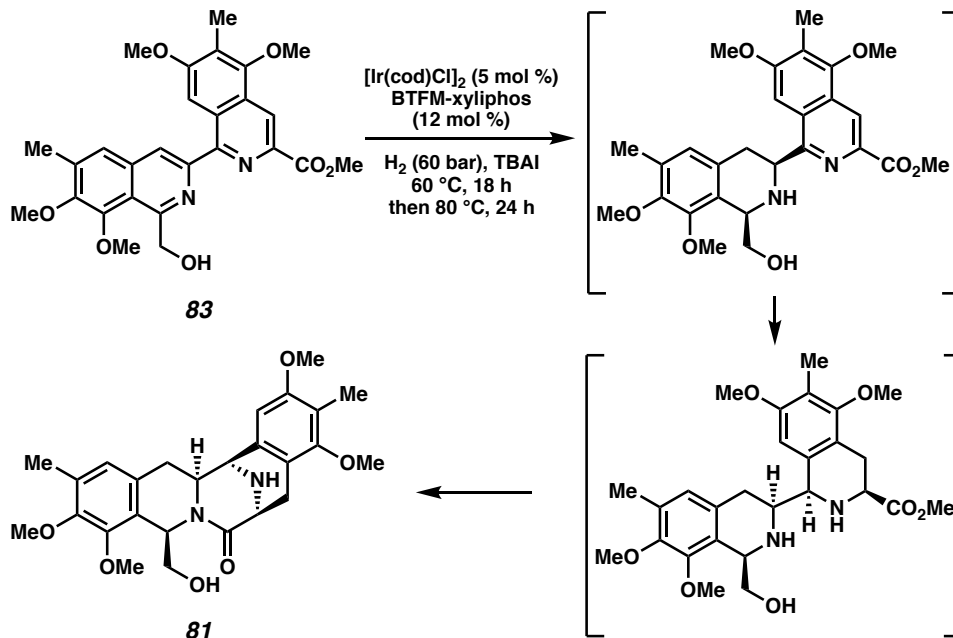
- 3 reports with only 1 report describing 1,3-disubstituted isoquinolines
- Requires high temperature & pressure
- No example of substrate with additional Lewis basic functionalities



Recently, our group has successfully completed the total synthesis of jorumycin (77) and jorunnamycin A (79), two bis-tetrahydroisoquinoline natural products that exhibit potent antiproliferative activity, as well as strong Gram-positive and Gram-negative antibiotic character (see Chapter 3).⁶ Through an unprecedented, nonbiomimetic synthetic route, we were successful in harnessing catalysis to allow expedient access to these natural products, as well as a diverse range of non-natural analogs that are otherwise inaccessible using prior biomimetic synthetic approaches. One of the key steps

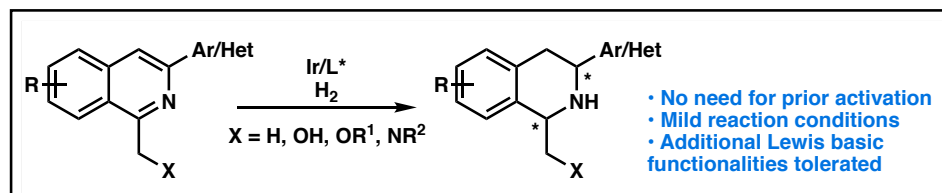
Figure 4.2 Our research on iridium-catalyzed enantioselective and diastereoselective hydrogenation of 1,3-disubstituted isoquinolines.

Jorumycin Synthesis: A Key Enantioselective Hydrogenation Step



This Research:

- 30 examples of 1,3-disubstituted isoquinolines
- General method for a variety of substitution patterns



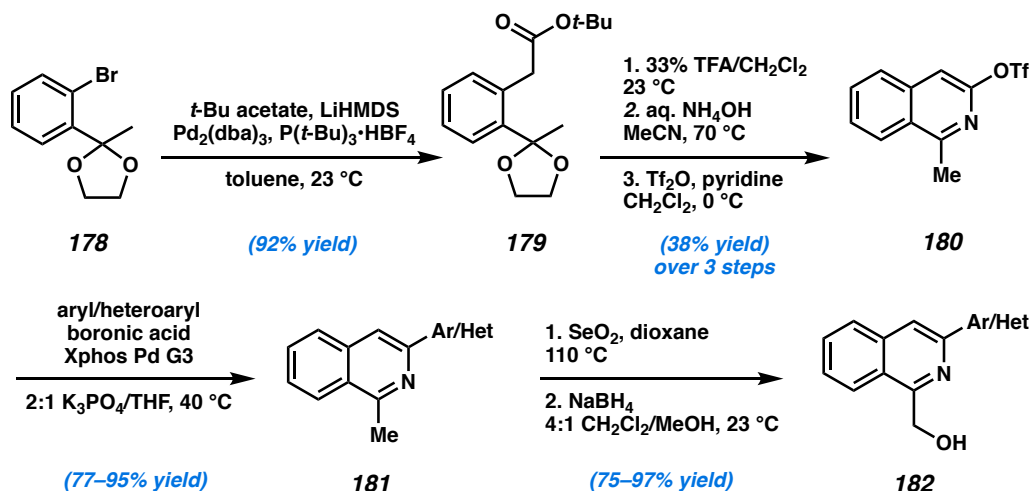
of this synthesis involves a catalytic enantioselective hydrogenation of bis-isoquinoline **83** to afford the THIQ motif, a crucial intermediate that forms the pentacyclic carbon skeleton **81** in one step by further hydrogenation of the second isoquinoline and eventual amide ring closure (Figure 4.2). Considering the ubiquity of the hydroxymethyl group at the C1 position, and the amino alcohol functionality in a large number of natural products, we envision that this synthetic method could access a wide variety of THIQs as well as chiral amino alcohols, both highly valuable pharmacophores. Following the

successful development of our asymmetric hydrogenation technology for bis-isoquinolines, herein we disclose a mild, general method for the enantioselective and diastereoselective hydrogenation of 1,3-disubstituted isoquinolines.

4.2 SUBSTRATE SYNTHESSES

Due to a limited number of methods for the syntheses of 1,3-disubstituted isoquinolines,⁷ we first established a simple and divergent sequence to access a wide variety of 1 (hydroxymethyl)-3-arylisoquinoline substrates (i.e., **182**, Scheme 4.1). Utilizing Pd-catalyzed arylation of ester enolates reported by Donohoe and coworkers,⁸ monoarylated *tert*-butyl acetate **179** was isolated in an excellent 92% yield. Cyclization to isoquinoline triflate **180** was then achieved via hydrolysis of the ketal, followed by isoquinoline annulation with aqueous ammonium hydroxide, and alcohol triflation.⁹ At this stage, different aryl or heteroaryl groups could be coupled with intermediate **180** using Suzuki coupling conditions to deliver a wide range of 1,3-disubstituted isoquinolines (i.e., **181**), highlighting the divergency of our synthetic route. Finally, SeO₂ oxidation to the aldehyde and subsequent NaBH₄ reduction provided our desired isoquinoline starting materials **182a–r**. It is worth noting that this sequence allows for an introduction of various aryl and heteroaryl groups at the C3-position of isoquinolines, as well as different substituents with varied electronics on the isoquinoline carbocycle (e.g., **184a–f**, *vide infra*, Scheme 4.4). Currently in the literature, the 1,3-disubstituted isoquinoline motif is typically accessed via transition-metal-catalyzed tandem C–H activation/annulation of arenes with alkynes.¹⁰ These methods have shown limited success in producing C3-heteroaryl isoquinolines.¹¹

Scheme 4.1 Syntheses of 1-(hydroxymethyl)-3-aryl isoquinoline substrates.



4.3 REACTION OPTIMIZATION

With a divergent sequence to access 1,3-disubstituted isoquinolines, we began our hydrogenation studies with 1-(hydroxymethyl)-3-phenylisoquinoline (**182a**) as our model substrate, using slightly modified conditions from our previously reported hydrogenation on the bis-isoquinoline system (Table 4.1). An initial experiment, employing 1.25 mol % $[\text{Ir}(\text{cod})\text{Cl}]_2$ and 3 mol % of the BTfM-xylylphos ligand (**L1**), gave high conversion of the substrate but surprisingly modest enantioselectivity (49% ee, entry 1). Seeking to improve the ee, we surveyed a wide variety of chiral ligand scaffolds (see Table 4.2, Section 4.7.3) and found the xylylphos ligand framework to be optimal. By exploring different electronics of this ligand scaffold, we observed that replacing the 3,5-bis(trifluoromethyl)phenyl (BTfM) with more electron-rich aryl groups provided the product with both excellent conversion and higher enantio-selectivity (entries 1–5). Ligand **L57**, which features 4-methoxy-3,5-dimethylphenyl (DMM) substituted phosphine delivers the product with the highest ee of 89%, albeit with a low 2:1

diastereoselectivity (entry 5). Interestingly, a background reaction was observed in the absence of the chiral ligand, providing the product in excellent conversion and diastereoselectivity (entry 6). From this finding, we obtained all racemic hydrogenated products by simply performing the hydrogenation in the absence of ligand, affording the *cis*-product as a single diastereomer.

Table 4.1 Optimization of the enantioselective hydrogenation of isoquinolines to afford THIQs.^a

entry	ligand	solvent	% conversion ^b	cis:trans ^b	% ee of cis ^c
1	L49	PhMe:AcOH	>95	>20:1	–49 ^d
2	L48	PhMe:AcOH	>95	3.2:1	84
3	L53	PhMe:AcOH	66	4.5:1	63
4	L59	PhMe:AcOH	92	4.9:1	3
5	L57	PhMe:AcOH	>95	2.0:1	89
6	–	PhMe:AcOH	>95	>20:1	0
7	L57	CH ₂ Cl ₂ :AcOH	>95	1.5:1	84
8	L57	dioxane:AcOH	66	5.5:1	87
9	L57	THF:AcOH	>95	9.7:1	90
10	L57	CPME:AcOH	38	>20:1	88
11	L57	2-MeTHF:AcOH	>95	9.5:1	90
12 ^e	L57	THF:AcOH	>95	15.7:1	92

L49: Ar = BTFM^d

L48: Ar = Ph

L53: Ar = 1-naphthyl

L59: Ar = furyl

L57: Ar = DMM

[a] Reactions conditions: 0.04 mmol of **182a**, 1.25 mol % [Ir(cod)Cl]₂, 3 mol % ligand, 7.5 mol % TBAI, 60 bar H₂ in 2.0 mL 9:1 solvent:AcOH. [b] Determined from crude ¹H NMR using 1,3,5-trimethoxybenzene as a standard. [c] Determined by chiral SFC analysis of Cbz-protected product. [d] Opposite enantiomer of ligand used. [e] Reaction performed on a 0.2 mmol scale at 23 °C, 20 bar H₂, and 0.1 M concentration of **182a**.

Investigation of different solvents with **L57** as the optimal ligand reveals that while the use of CH₂Cl₂ provided similar results to toluene (entry 7), the

diastereoselectivity could be improved with the use of ethereal solvents (entries 8–11). Although bulkier ethereal solvents proved to worsen conversion (entries 8 and 10), we were delighted to find that THF and the more sustainable solvent 2-MeTHF delivered the product in excellent conversion with high levels of diastereoselectivity and enantioselectivity (entries 9 and 11). The absence of AcOH resulted in low conversion,¹² while further exploration of different additives (e.g., LiI, NaI, KI, etc.) demonstrated that TBAI is the optimal additive (see Table 4.3, Section 4.7.3). Finally, we were excited to observe that lowering the temperature to 23 °C and H₂ pressure to 20 bar maintained excellent levels of conversion, diastereo-selectivity, and enantioselectivity (entry 12). To the best of our knowledge, these are the mildest reaction conditions reported for isoquinoline hydrogenation to afford chiral THIQs to date.⁴

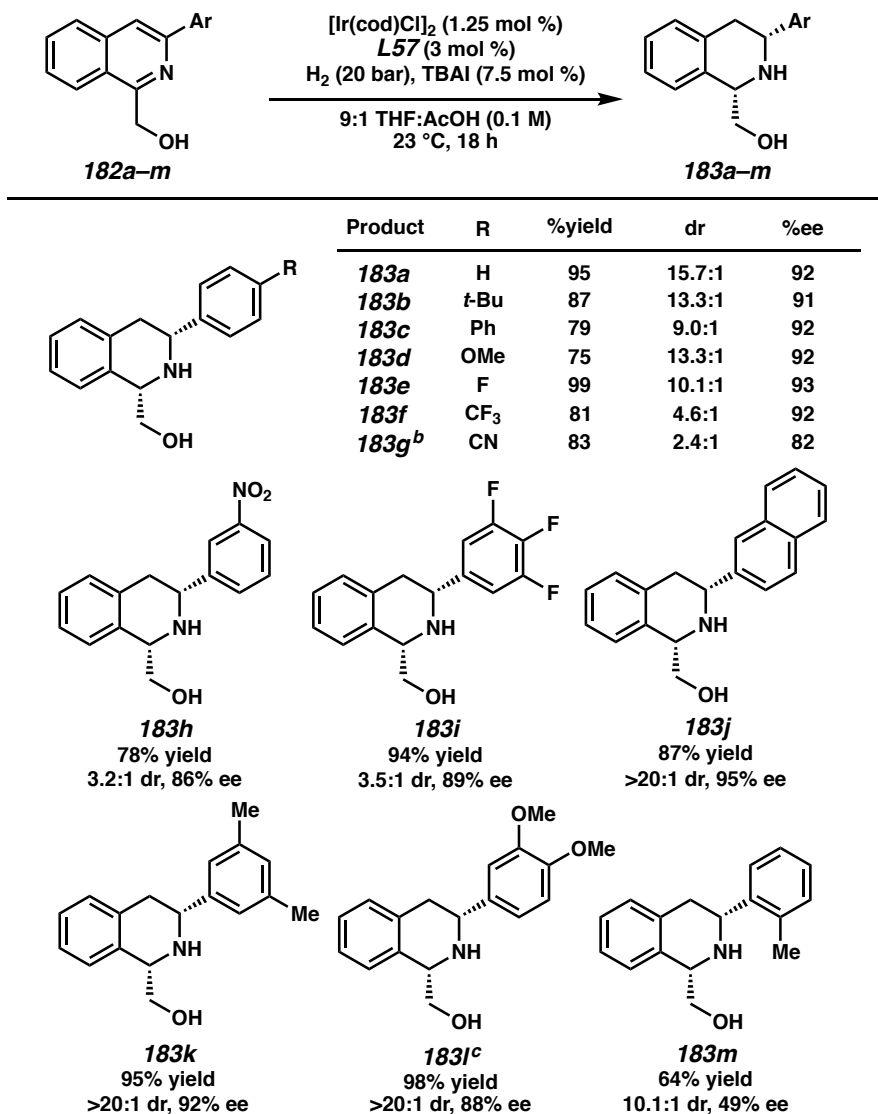
4.4 SUBSTRATE SCOPE

With optimized reaction conditions identified, we explored the general substrate scope for this transformation (Scheme 4.2). Gratifyingly, a wide variety of aryl substituents at the 3-position of the isoquinoline are well tolerated under the mild reaction conditions of 20 bar H₂ at ambient temperature. Substitution at the *para*-position of the 3-aryl ring delivered the hydrogenated products **183a–g** in consistently high yields and enantioselectivity. Electron-rich substrates such as the 3-(*p*-*tert*-butylphenyl)isoquinoline (**182b**) and the *p*-methoxyphenyl (**182d**) afforded chiral THIQs with excellent yields, diastereoselectivity, and enantioselectivity, similarly to **182a**. Interestingly, however, a general trend of lower diastereoselectivity was observed with electron-withdrawing substituents both at the *para*- and *meta*- positions (**182f–i**). We envision that the observed

lower diastereoselectivity arises from the weaker coordinating ability of the nitrogen to the iridium catalyst in electron-poor substrates, discouraging coordination to the catalyst in a bidentate fashion,¹³ and thus resulting in poorer facial selectivity in the second hydride addition step. However, at this time, we still cannot rule out the possibility that epimerization in situ also influences the trend seen in diastereoselectivity.¹⁴ Investigation of steric effects revealed that more sterically encumbered isoquinolines such as the 3-naphthyl and 3-xylyl substrates furnished the products (**183j–k**) in excellent isolated yields with similarly high enantioselectivity (95% and 92% ee, respectively) as a single diastereomer. The most sterically demanding substrate **182m**, bearing an *ortho*-tolyl substituent, provided product **183m** in a modest 64% yield with lower enantioselectivity (49% ee), albeit still with a high 10.1:1 diastereoselectivity. Additionally, we were pleased to find that the nitrile and nitro functional groups as well as the naphthyl substituent were not reduced (**183g**, **183h**, and **183j**), highlighting the chemoselectivity of this catalytic process.

Pleased to find the reaction tolerable to a range of 3-aryl substituted isoquinolines, we sought to further extend the scope of the transformation by exploring heteroaryl-substituted isoquinolines (Scheme 4.3). Although performing the hydrogenation at 23 °C and 20 bar H₂ resulted in lower conversion, partially due to solubility issues, we found that heterocyclic substituents including furan, thiophene, pyrazole, and pyridine were well tolerated at 60 °C and under higher pressure of 60 bar H₂, producing THIQs **183n–r**. We also observed that the substitution pattern on the heteroaryl groups strongly affects the reaction conversion. For instance, an isoquinoline with a 3-substituted thiophene proceeded with a significantly lower conversion than the 2-thiophene substrate (**183o** and

Scheme 4.2 Substrate scope of different aryl substituents.^a

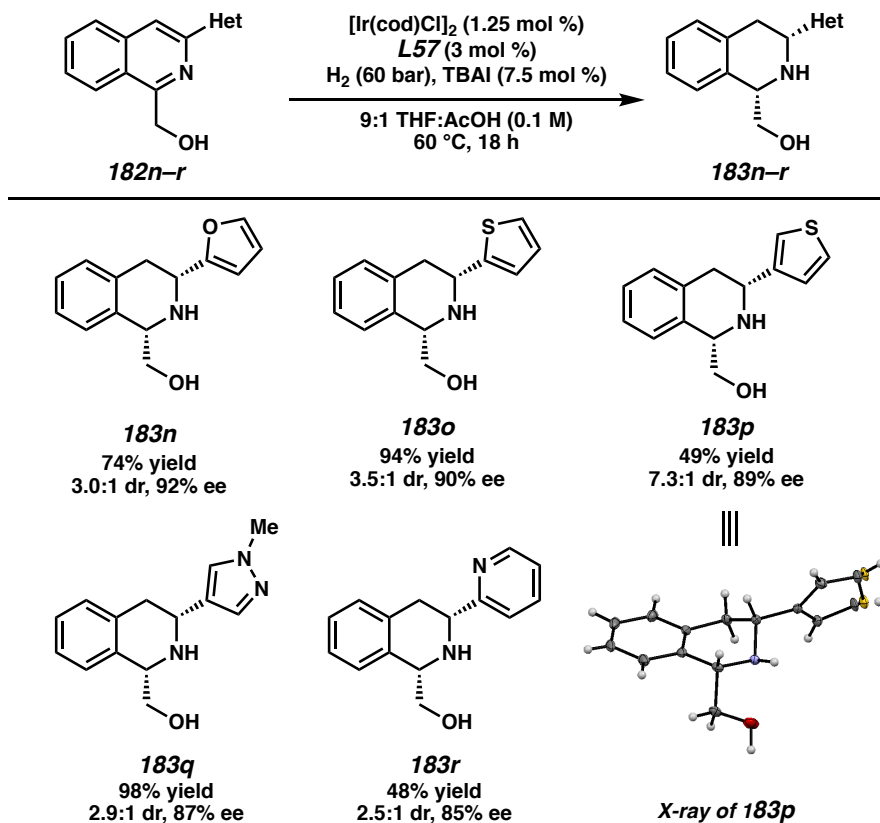


[a] Reactions performed on a 0.2 mmol scale. [b] Reaction performed at 60 °C and 60 bar H₂. [c] CH₂Cl₂ cosolvent used to improve substrate solubility.

183p). Similarly, no conversion was observed with 3- and 4-pyridyl substrates, whereas 2-pyridyl THIQ **183r** was isolated in 48% yield under the same reaction conditions. We speculate that this may be due to the competitive binding of the catalyst by the more distal heteroatom of 3- and 4-substituted heterocycles that inhibits directed hydrogenation of the isoquinoline ring. From product **183p**, we were successful in obtaining an X-ray

crystal structure to confirm the relative and absolute stereochemistry of our hydrogenation product.

Scheme 4.3 Substrate scope of heteroaryl substituents.^a



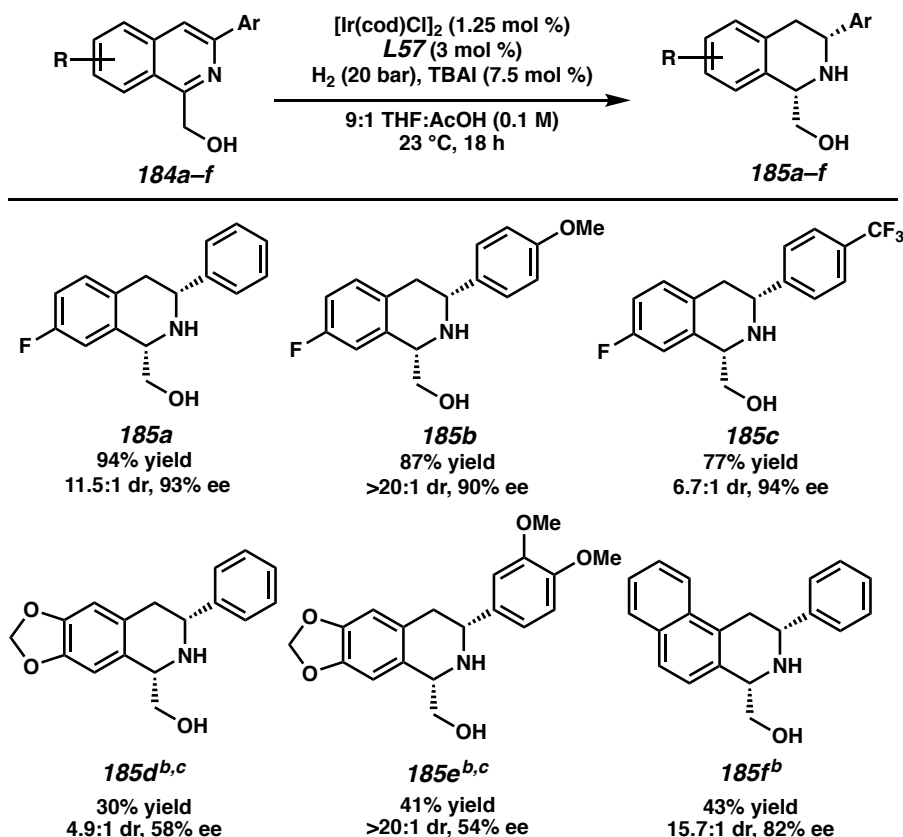
[a] Reactions performed on a 0.2 mmol scale.

Furthermore, we were interested in exploring the substrate scope of isoquinolines with different electronics and substitution patterns on the isoquinoline carbocycle (Scheme 4.4). Electron-poor fluorinated isoquinolines with varied electronics at the 3-position provided THIQs in high yields (77–94%) with high diastereoselectivity and enantioselectivity under our standard conditions (**185a–c**). It should be noted that these electron-poor THIQs would be difficult to access utilizing electrophilic aromatic substitution strategies, a classical method for the syntheses of THIQs. On the other hand,

the electron-rich dioxolane-appended isoquinolines (**184d–e**) afforded lowered conversion under the same reaction conditions, due in part to the poor solubility of the substrates in THF. Nevertheless, executing the reaction at 60 °C and 60 bar H₂ with CH₂Cl₂ as cosolvent improved the solubility and conversion to yield products **185d–e** with high diastereoselectivity.¹⁵ Interestingly, we observed significantly lower enantioselectivity for the dioxolane THIQs, which is observed in other reports as well.^{4a,g} Finally, the naphthyl-fused THIQ (**185f**) was obtained with high diastereoselectivity and enantioselectivity, despite its extended aromatic system and larger steric hindrance. Although we observed modest conversion for these highly decorated isoquinolines, we were pleased to see that we were able to isolate unreacted starting material after column chromatography to obtain 80%, 99%, and 79% yield, respectively, of **185d–f** based on recovered starting material. Consistent with our results for THIQs **183j** and **183r**, only the ring with the least degree of aromatic stabilization was reduced for **185f**.

Having demonstrated that this transformation is general for a wide variety of 1,3-disubstituted isoquinolines, we then turned our attention to investigate the effects of different “directing” groups at the C1-position (Scheme 4.5). Isoquinolines bearing other polar groups such as an ester (**186a**), ethers (**186b–c**), and a Boc-protected amine (**186d**) delivered the products in lower yields than the hydroxy-directed substrate at 23 °C and 20 bar H₂. However, to our delight, by increasing the temperature and H₂ pressure, these yields could be improved with no erosion of enantioselectivity and diastereoselectivity.

Scheme 4.4 Substrate scope of IQ backbone substituents.^a

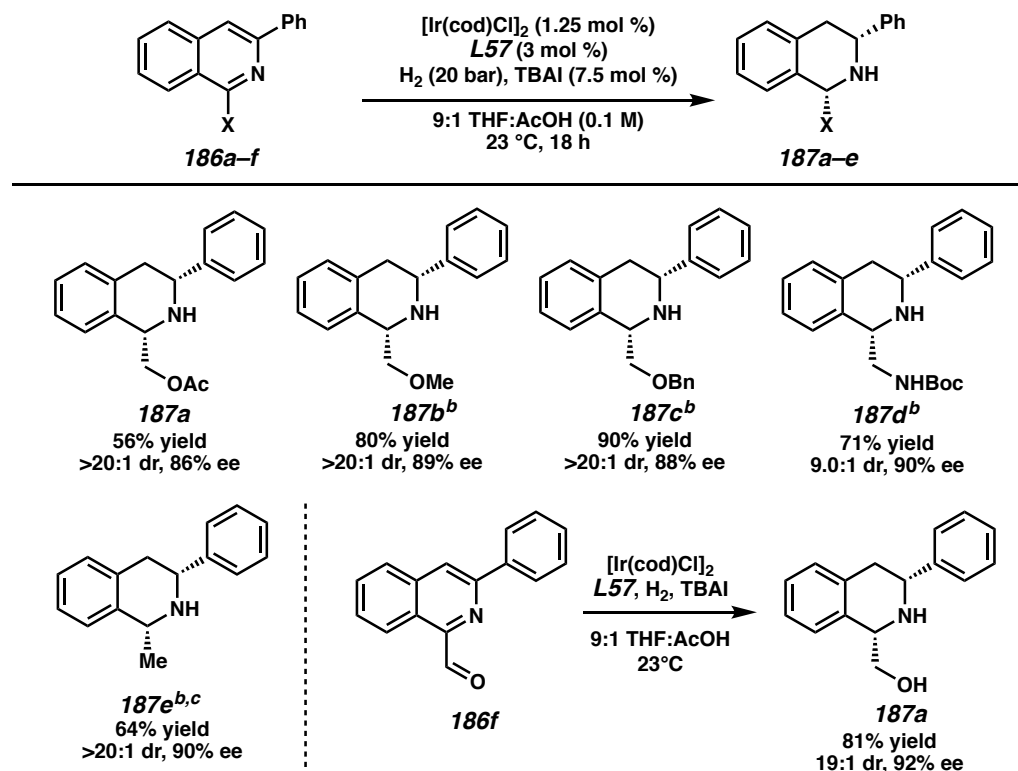


[a] Reactions performed on a 0.2 mmol scale. [b] Reaction performed at 60 °C and 60 bar H_2 . [c] CH_2Cl_2 cosolvent used to improve substrate solubility.

Additionally, we found that aldehyde **186f** was reduced to the alcohol in situ, affording the hydroxymethyl THIQ **187a** in comparable yield, enantioselectivity, and diastereoselectivity to that of the hydroxy-directing substrate **183a** (*vide supra*). Interestingly, an isoquinoline lacking a potential directing group (**187e**) also afforded chiral THIQs with no erosion of enantioselectivity (90% ee),¹⁶ although elevated temperature and pressure are needed to obtain a synthetically useful yield (64%). While the hydroxy-directing aspect is the enabling feature in the context of our total synthesis of jorumycin, we are pleased to find that we can obviate this requirement in our developed hydrogenation technology. Nevertheless, surveying a variety of different directing groups

demonstrates the importance of a functional group for directed hydrogenation, with the hydroxy functionality acting as the best directing group for mild and efficient asymmetric hydrogenation. Notably, this is the first asymmetric hydrogenation method of isoquinolines in which additional Lewis basic functionalities are tolerated. It is also the first report investigating the effects of different directing groups in enantioselective hydrogenation of isoquinolines.

Scheme 4.5 Substrate scope of different directing groups.^a

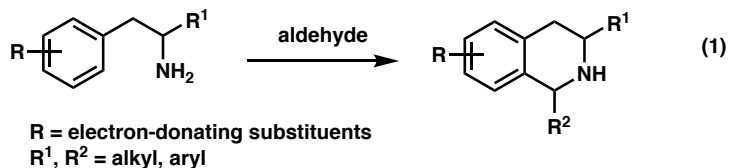


[a] Reactions performed on a 0.2 mmol scale. [b] Reaction performed at 60 °C and 60 bar H_2 . [c] Relative and absolute stereochemistry determined by experimental and computed VCD and optical rotation, see Supporting Information.¹⁶

4.5 SYNTHETIC UTILITY

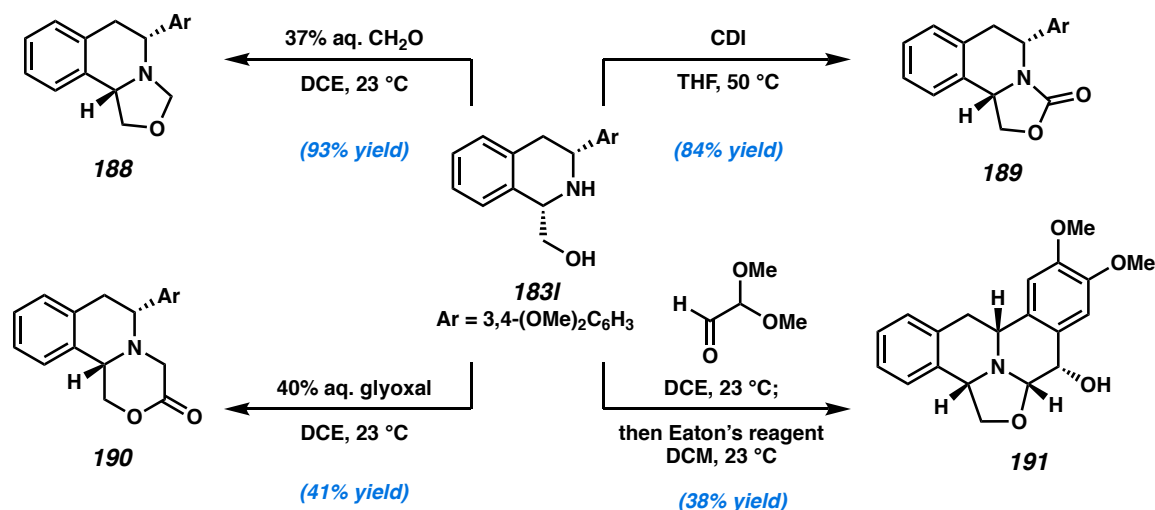
Overall, the broad application of our hydrogenation technology to afford chiral THIQs provides access to a range of decorated analogs that are difficult to synthesize via

biomimetic approaches (e.g., Pictet-Spengler, Bischler-Napieralski). These often require electron-rich substrates to undergo cyclization (eq 1).¹⁷



With the scope of the transformation established, we sought to demonstrate the synthetic utility of the produced chiral THIQs toward more complex scaffolds that could be applicable to natural products. Additionally, we envisioned taking advantage of the chiral β -amino alcohol that is generated in our product as a building block to forge more complex enantioenriched heterocyclic scaffolds (Scheme 4.6).¹⁸

Scheme 4.6 Derivatization of a hydrogenated product.



Prior to our investigation into the synthetic utility of THIQ products, we performed the hydrogenation of isoquinoline **182I** on a larger scale (1 mmol). We were pleased to find that the hydrogenated product **183I** was still obtained in good yield (91% isolated yield) with excellent selectivity (>20:1 dr, 88% ee). With an ample amount of **183I** in hand, we subjected THIQ **183I** to aqueous formaldehyde solution and found that

the tricyclic 1,2-fused oxazolidine THIQ **188** was formed rapidly via the cyclization of the alcohol onto the iminium generated in situ. Furthermore, the reaction of amino alcohol **183I** with carbonyldiimidazole (CDI) afforded oxazolidinone-fused THIQ **189** in 84% yield.¹⁹ To our delight, we found that these 6,6,5-tricyclic systems are conserved structural motifs in a number of natural products such as quinocarcin, tetrazomine, and bioxalomycin.⁵ Lastly, a different tricyclic scaffold containing fused morpholinone (**190**) can be isolated in 41% yield by the addition of excess glyoxal to **183I** at room temperature.²⁰ Being able to access a variety of complex heterocyclic scaffolds in one step from our hydrogenated THIQs further highlights the advantages of the hydroxymethyl functionality at the C1 position, beyond directing hydrogenation.

In addition to the tricyclic scaffold, we were pleased to find that an analog of tetrahydroprotoberberine alkaloids, a family of natural products with a tetracyclic bis-THIQ core,²¹ can be synthesized via a 2-step sequence. First, reaction of **183I** with glyoxal dimethyl acetal delivered the oxazolidine-fused intermediate with a dimethoxy acetal substituent at the carbinol-amine carbon. Subsequently, exploration of both Brønsted and Lewis acid-mediated Pomeranz-Fritsch reaction revealed that the use of Eaton's reagent²² delivered pentacyclic THIQ **191** in 38% yield as a single diastereomer. This complex scaffold could be of medicinal interest, as previous studies have shown that tetrahydroprotoberberine derivatives possess a wide array of interesting biological activities.^{17,23}

4.6 CONCLUSIONS

We have developed a general, efficient enantioselective hydrogenation reaction of 1,3-disubstituted isoquinolines toward the syntheses of chiral THIQs. Key to the success of this reaction is the installation of a directing group at the C1-position that facilitates hydrogenation to reduce a variety of isoquinolines under mild reaction conditions. The developed method affords chiral THIQs in good yields, with high levels of diastereoselectivity and enantioselectivity. The reaction conditions tolerate a wide range of substitution on the 1-, 3-, 6-, 7-, and 8-position of the isoquinoline core. To date, this report represents the broadest scope and highest tolerance of Lewis-basic functionality of any asymmetric isoquinoline reduction technology currently known. Furthermore, this method is amenable to the production of electron-deficient THIQs that are difficult to obtain through the classical Pictet-Spengler approach. In order to demonstrate the synthetic utility of the hydrogenated products, we utilize the hydroxyl directing group as a functional handle for further synthetic manipulations. As a result, we have completed the syntheses of various tricyclic and pentacyclic skeletons that are of potential medicinal interest. Further exploration of the mechanism and other applications of this technology are currently underway.

4.7 EXPERIMENTAL SECTION

4.7.1 MATERIALS AND METHODS

Unless otherwise stated, reactions were performed in flame-dried glassware under an argon or nitrogen atmosphere using dry, deoxygenated solvents.²⁴ Solvents were dried

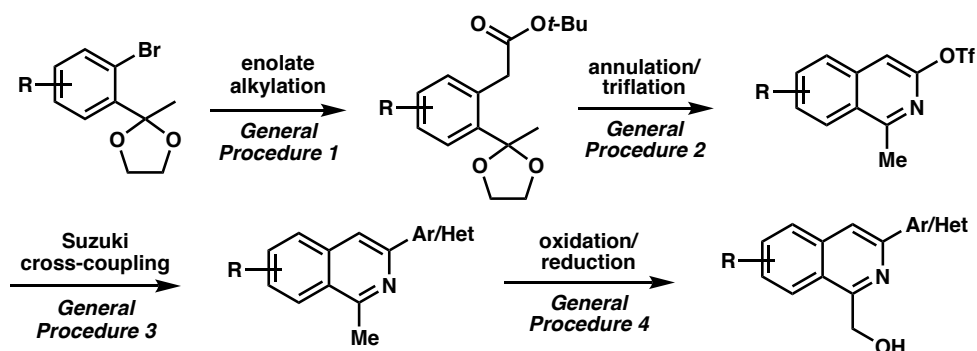
by passage through an activated alumina column under argon. Reaction progress was monitored by thin-layer chromatography (TLC) or Agilent 1290 UHPLC-MS. TLC was performed using E. Merck silica gel 60 F254 precoated glass plates (0.25 mm) and visualized by UV fluorescence quenching, *p*-anisaldehyde, or KMnO₄ staining. Silicycle SiliaFlash® P60 Academic Silica gel (particle size 40–63 nm) was used for flash chromatography. ¹H NMR spectra were recorded on Bruker 400 MHz or Varian Mercury 300 MHz spectrometers and are reported relative to residual CHCl₃ (δ 7.26 ppm). ¹³C NMR spectra were recorded on Bruker 400 MHz spectrometer (100 MHz) and are reported relative to CHCl₃ (δ 77.16 ppm). ¹⁹F NMR spectra were recorded on Varian Mercury 300 MHz spectrometer (282 MHz). Data for ¹H NMR are reported as follows: chemical shift (δ ppm) (multiplicity, coupling constant (Hz), integration). Multiplicities are reported as follows: s = singlet, d = doublet, t = triplet, q = quartet, p = pentet, sept = septuplet, m = multiplet, br s = broad singlet, br d = broad doublet, app = apparent. Data for ¹³C NMR are reported in terms of chemical shifts (δ ppm). IR spectra were obtained using Perkin Elmer Spectrum BXII spectrometer or Nicolet 6700 FTIR spectrometer using thin films deposited on NaCl plates and reported in frequency of absorption (cm⁻¹). Optical rotations were measured with a Jasco P-2000 polarimeter operating on the sodium D-line (589 nm), using a 100 mm path-length cell and are reported as: [α]_D^T (concentration in 10 mg/1 mL, solvent). Analytical SFC was performed with a Mettler SFC supercritical CO₂ analytical chromatography system utilizing Chiralpak (AD-H, AS-H or IC) or Chiralcel (OD-H, OJ-H, or OB-H) columns (4.6 mm x 25 cm) obtained from Daicel Chemical Industries, Ltd. High resolution mass spectra (HRMS) were obtained from Agilent 6200 Series TOF with an Agilent G1978A Multimode source in

electrospray ionization (ESI+), atmospheric pressure chemical ionization (APCI+), or mixed ionization mode (MM: ESI-APCI+), or obtained from Caltech mass spectrometry laboratory.

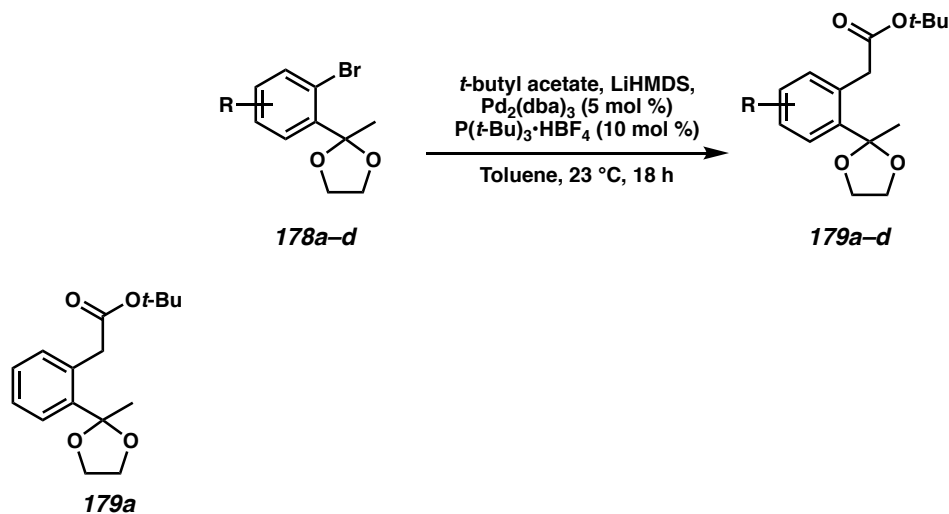
4.7.2 EXPERIMENTAL PROCEDURES AND SPECTROSCOPIC DATA

4.7.2.1 Syntheses of hydroxymethyl 1,3-disubstituted isoquinolines

General sequence:

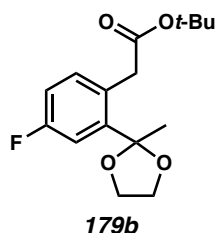


General procedure 1: Enolate alkylation of aryl bromide



***tert*-butyl 2-(2-(2-methyl-1,3-dioxolan-2-yl)phenyl)acetate (179a):** This procedure has been adapted from a previous report.⁸ In a Schlenk flask was added $P(t\text{-Bu})_3 \cdot \text{HBF}_4$ (119 mg, 0.41 mmol), $\text{Pd}_2(\text{dba})_3$ (188 mg, 0.21 mmol), a solution of 2-(2-bromophenyl)-2-

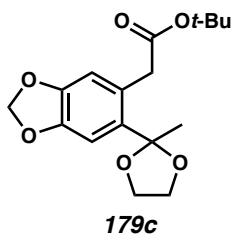
methyl-1,3-dioxolane (**178a**) (1.0 g, 4.1 mmol, 0.42 M), and *tert*-Butyl acetate (0.95 g, 8.2 mmol), respectively. The reaction mixture was cooled to $-78\text{ }^{\circ}\text{C}$ and sparged with nitrogen for 15 minutes. A degassed solution of LiHMDS (1.72 g, 10.25 mmol, 1 M in toluene) was then added via syringe. The reaction mixture was degassed for an additional 15 minutes at $-78\text{ }^{\circ}\text{C}$, and allowed to slowly warm to room temperature. The reaction was stirred at room temperature for 18 hours, and then quenched with saturated aqueous NaHCO_3 . The aqueous layer was extracted with Et_2O twice. The combined organic phases were dried over MgSO_4 , filtered, and the solvent was removed in vacuo. The crude product was purified by silica gel flash chromatography (5% EtOAc in hexanes) to afford **179a** as a yellow oil (1.05 g, 92% yield): ^1H NMR (400 MHz, CDCl_3) δ 7.53 – 7.45 (m, 1H), 7.20 – 7.06 (m, 3H), 3.96 – 3.83 (m, 2H), 3.71 (s, 2H), 3.68 – 3.55 (m, 2H), 1.60 (s, 3H), 1.39 (s, 9H); ^{13}C NMR (100 MHz, CDCl_3) δ 171.6, 141.1, 132.6, 132.3, 128.2, 127.1, 126.4, 109.2, 80.4, 64.3, 40.4, 28.2, 28.2, 27.6; IR (Neat Film, NaCl) 3454, 3062, 2977, 2936, 2893, 1731, 1484, 1455, 1392, 1368, 1218, 1196, 1168, 1037, 952, 869, 763, 706 cm^{-1} ; HRMS (MM:ESI-APCI+) m/z calc'd for $\text{C}_{16}\text{H}_{23}\text{O}_4$ $[\text{M}+\text{H}]^+$: 279.1591, found 279.1589.



tert-butyl 2-(4-fluoro-2-(2-methyl-1,3-dioxolan-2-yl)phenyl)acetate (**179b**):

Compound **179b** was prepared from aryl bromide (2-(2-bromo-5-fluorophenyl)-2-methyl-1,3-dioxolane) (**178b**) using general procedure 1, and purified by column

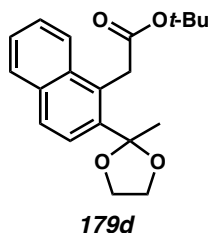
chromatography (10% EtOAc in hexanes) to afford **179b** with impurities. The compound was then subjected to the second column chromatography (15% Et₂O in hexanes) to obtain **179b** as a colorless solid (74 mg, 61% yield); ¹H NMR (400 MHz, CDCl₃) δ 7.28 (dd, *J* = 10.3, 2.8 Hz, 1H), 7.15 (dd, *J* = 8.4, 5.7 Hz, 1H), 6.94 (td, *J* = 8.2, 2.9 Hz, 1H), 4.06 – 3.90 (m, 2H), 3.74 (s, 2H), 3.72 – 3.69 (m, 2H), 1.65 (s, 3H), 1.45 (s, 9H); ¹³C NMR (100 MHz, CDCl₃) δ 171.5, 161.9 (d, *J* = 245.1 Hz), 143.9 (d, *J* = 6.2 Hz), 134.2 (d, *J* = 7.8 Hz), 127.9 (d, *J* = 3.3 Hz), 114.9 (d, *J* = 21.1 Hz), 113.5 (d, *J* = 23.0 Hz), 108.6, 80.6, 64.4, 39.6, 28.2, 27.3; ¹⁹F NMR (282 MHz, CDCl₃) δ –115.6 (ddd, *J* = 10.3, 8.0, 5.8 Hz); IR (Neat Film, NaCl) 2980, 1732, 1613, 1493, 1412, 1392, 1368, 1340, 1256, 1200, 1179, 1147, 1037, 947, 878 cm⁻¹; HRMS (MM:ESI-APCI+) *m/z* calc'd for C₁₆H₂₂FO₄ [M+H]⁺: 297.1497, found 297.1494.



tert-butyl 2-(6-(2-methyl-1,3-dioxolan-2-yl)benzo[d][1,3]dioxol-5-yl)acetate (179c):

Compound **179c** was prepared from aryl bromide (5-bromo-6-(2-methyl-1,3-dioxolan-2-yl)benzo[d][1,3]dioxole) (**178c**) using general procedure 1, and purified by column chromatography (5% to 15% EtOAc in hexanes) to afford **179c** as a pale yellow oil (83.4 mg, 63% yield): ¹H NMR (400 MHz, CDCl₃) δ 7.07 (s, 1H), 6.66 (s, 1H), 5.93 (s, 2H), 3.95 – 3.93 (m, 2H), 3.72 – 3.69 (m, 2H), 3.62 (s, 2H), 1.64 (s, 3H), 1.46 (s, 9H); ¹³C NMR (100 MHz, CDCl₃) δ 171.7, 147.2, 146.7, 135.2, 125.9, 112.3, 109.1, 107.0, 101.3, 80.6, 64.3, 40.0, 28.3, 27.6; IR (Neat Film, NaCl) 2978, 2897, 1732, 1504, 1486, 1369,

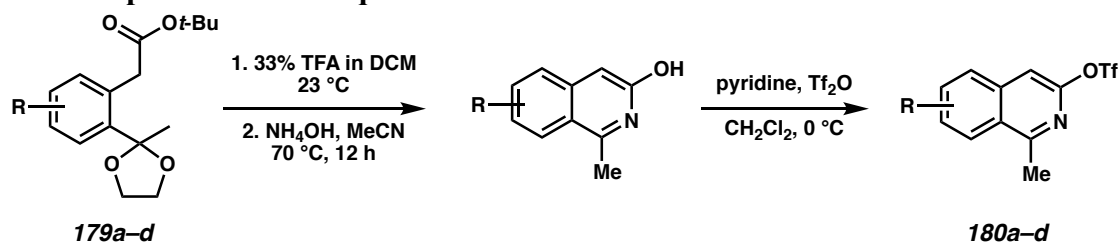
1332, 1259, 1197, 1166, 1142, 1041, 929, 869, 935 cm^{-1} ; HRMS (MM:ESI-APCI+) m/z calc'd for $\text{C}_{17}\text{H}_{23}\text{O}_6$ $[\text{M}+\text{H}]^+$: 323.1489, found 323.1501.

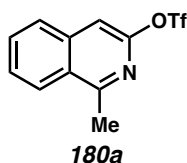


tert-butyl 2-(2-(2-methyl-1,3-dioxolan-2-yl)naphthalen-1-yl)acetate (179d):

Compound **179d** was prepared from aryl bromide (2-(1-bromonaphthalen-2-yl)-2-methyl-1,3-dioxolane) (**178d**) using general procedure 1, and purified by column chromatography (0% to 5% EtOAc in hexanes) to afford **179d** as a pale yellow oil (2.15 g, 98% yield): ^1H NMR (400 MHz, CDCl_3) δ 7.93 (d, $J = 8.0$ Hz, 1H), 7.82 (d, $J = 8.0$ Hz, 1H), 7.76 (s, 2H), 7.48 (ddd, $J = 7.9, 6.7, 1.4$ Hz, 2H), 4.38 (s, 2H), 4.04 – 4.00 (m, 2H), 3.79 – 3.73 (m, 2H), 1.78 (s, 3H), 1.45 (s, 9H); ^{13}C NMR (100 MHz, CDCl_3) δ 171.4, 139.3, 133.6, 128.7, 128.6, 127.8, 126.5, 125.8, 124.3, 124.1, 109.7, 80.7, 64.4, 36.2, 28.2, 27.8. IR (Neat Film, NaCl) 2980, 2890, 1732, 1454, 1368, 1336, 1142, 1100, 1037, 951, 884, 870, 822, 750 cm^{-1} ; HRMS (MM:ESI-APCI+) m/z calc'd for $\text{C}_{20}\text{H}_{25}\text{O}_4$ $[\text{M}+\text{H}]^+$: 329.1747, found 329.1739.

General procedure 2: Isoquinoline annulation and triflation

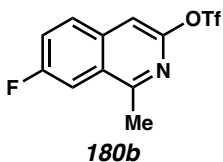




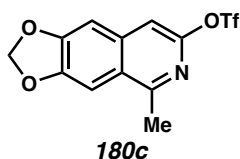
1-methyloisoquinolin-3-yl trifluoromethanesulfonate (180a): This procedure has been adapted from a previous report.⁹ In a RBF were added ester **179a** (2.78 g, 10.0 mmol), anhydrous CH_2Cl_2 (75 mL, 0.13 M), and TFA (25 mL, 33% volume of CH_2Cl_2), respectively. The reaction was stirred at room temperature for 2 hours, and then concentrated in vacuo. The crude was transferred to a Schlenk tube, dissolved in MeCN (10 mL, 1 M), and aqueous NH_4OH (28–30%, 20 mL, 200% volume of MeCN). The tube was sealed with Kontes valve to prevent loss of gaseous ammonia and stirred at 70 °C. Within 1 hour, the yellow solid of the 3-hydroxyisoquinoline began to precipitate from the reaction solution. After stirring for 18 hours at 70 °C, the reaction was cooled to room temperature, then placed in a –20 °C freezer, and the yellow solid was collected via vacuum filtration. This yellow powder was then washed with cold MeCN and dried under high vacuum to provide 3-hydroxyisoquinoline intermediate (0.70 g, 4.39 mmol). If any starting material remains, the filtrate could be transferred to a flask and concentrated in vacuo to undergo a second condensation reaction.

To a separate flame-dried RBF containing CH_2Cl_2 (22 mL, 0.2 M) and distilled pyridine (3.6 mL, 44 mmol), the collected yellow powder (0.70 g, 4.39 mmol) was added, and the resulting mixture was cooled to 0 °C. Trifluoromethanesulfonic anhydride (1.5 mL, 8.8 mmol) was then added dropwise at 0 °C, and the reaction was stirred at 0 °C for 1 hour. The reaction was then quenched with saturated aqueous NaHCO_3 at 0 °C, and then slowly warmed to room temperature. The reaction was extracted with CH_2Cl_2 , dried

over Na₂SO₄, and concentrated in vacuo. The crude product was purified by column chromatography (10% EtOAc in hexanes) to afford **180a** as a pale yellow oil (1.11 g, 38% yield over 3 steps): ¹H NMR (400 MHz, CDCl₃) δ 8.17 (dd, *J* = 8.5, 1.0 Hz, 1H), 7.88 (dt, *J* = 8.3, 1.0 Hz, 1H), 7.76 (ddd, *J* = 8.2, 6.9, 1.2 Hz, 1H), 7.67 (ddd, *J* = 8.3, 6.9, 1.3 Hz, 1H), 7.42 (s, 1H), 2.97 (s, 3H); ¹³C NMR (100 MHz, CDCl₃) δ 160.3, 151.3, 138.6, 131.5, 128.1, 127.8, 127.6, 126.1, 118.9 (q, *J* = 320.5 Hz), 109.0, 22.1; ¹⁹F NMR (282 MHz, CDCl₃) δ –73.0 IR (Neat Film, NaCl) 1624, 1600, 1563, 1422, 1327, 1213, 1138, 1116, 987, 958, 891, 832, 742, 616 cm^{–1}; HRMS (MM:ESI-APCI+) *m/z* calc'd for C₁₁H₉F₃NO₃S [M+H]⁺: 292.0250, found 292.0253.

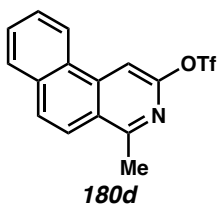


7-fluoro-1-methyloisoquinolin-3-yl trifluoromethanesulfonate (180b): Compound **180b** was prepared from ester **179b** using general procedure 2 and purified by column chromatography (10% EtOAc in hexanes) to provide a pale brown oil (384 mg, 31% yield over 3 steps): ¹H NMR (400 MHz, CDCl₃) δ 7.90 (dd, *J* = 9.0, 5.3 Hz, 1H), 7.76 (dd, *J* = 9.6, 2.5 Hz, 1H), 7.56 (ddd, *J* = 8.9, 8.0, 2.5 Hz, 1H), 7.43 (s, 1H), 2.92 (s, 3H); ¹³C NMR (100 MHz, CDCl₃) δ 161.4 (d, *J* = 251.1 Hz), 159.4 (d, *J* = 6.1 Hz), 151.1 (d, *J* = 3.3 Hz), 135.5, 130.3 (d, *J* = 8.7 Hz), 128.5 (d, *J* = 8.3 Hz), 122.2 (d, *J* = 25.6 Hz), 118.9 (q, *J* = 320.5 Hz), 109.8 (d, *J* = 21.8 Hz), 108.9, 22.1; ¹⁹F NMR (282 MHz, CDCl₃) δ –73.0, –109.0 (ddd, *J* = 9.5, 8.0, 5.4 Hz); IR (Neat Film, NaCl) 1598, 1573, 1516, 1416, 1209, 1136, 1114, 986, 960, 933, 875, 805, 764 cm^{–1}; HRMS (MM:ESI-APCI+) *m/z* calc'd for C₁₁H₈F₄NO₃S [M+H]⁺: 310.0156, found 310.0149.



5-methyl-[1,3]dioxolo[4,5-g]isoquinolin-7-yl trifluoromethanesulfonate (180c):

Compound **180c** was prepared from ester **179c** using general procedure 2 and purified by column chromatography (10 to 20% EtOAc in hexanes) to provide a white solid (608 mg, 58% yield over 3 steps): ^1H NMR (400 MHz, CDCl_3) δ 7.35 (s, 1H), 7.23 (s, 1H), 7.10 (s, 1H), 6.15 (s, 2H), 2.82 (s, 3H); ^{13}C NMR (100 MHz, CDCl_3) δ 156.9, 151.9, 150.9, 149.2, 137.3, 124.8, 118.8 (q, $J = 321.2$ Hz), 108.4, 103.3, 102.2, 101.8, 22.2; ^{19}F NMR (282 MHz, CDCl_3) δ -73.0; IR (Neat Film, NaCl) 2918, 1584, 1504, 1464, 1416, 1223, 1134, 1038, 964, 940, 873, 840 cm^{-1} ; HRMS (MM:ESI-APCI+) m/z calc'd for $\text{C}_{12}\text{H}_9\text{F}_3\text{NO}_5\text{S}$ $[\text{M}+\text{H}]^+$: 336.0148, found 336.0146.

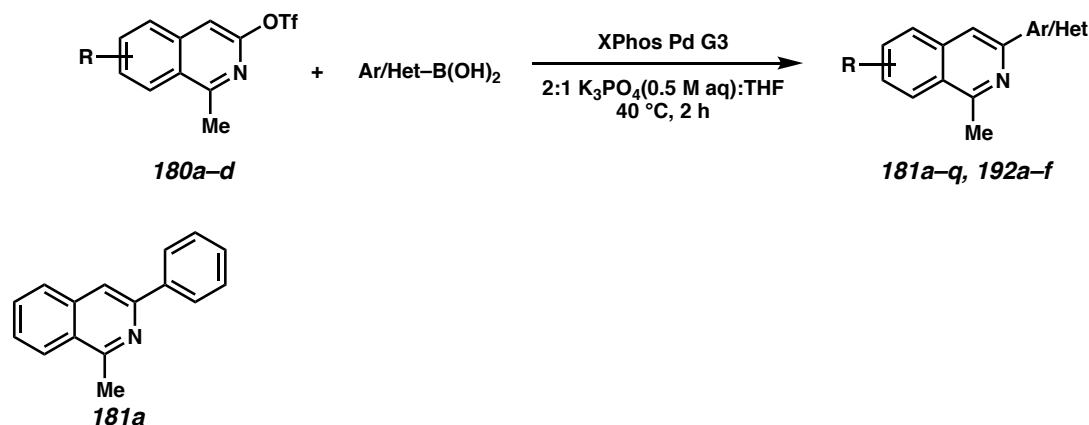


4-methylbenzo[f]isoquinolin-2-yl trifluoromethanesulfonate (180d):

Compound **180d** was prepared from ester **179d** using general procedure 2 and purified by column chromatography (5 to 10% EtOAc in hexanes) to provide a white solid (497 mg, 65% yield over 3 steps): ^1H NMR (400 MHz, CDCl_3) δ 8.63 – 8.57 (m, 1H), 8.15 (s, 1H), 8.01 – 7.95 (m, 2H), 7.90 (d, $J = 9.2$ Hz, 1H), 7.81 – 7.73 (m, 2H), 3.01 (s, 3H); ^{13}C NMR (100 MHz, CDCl_3) δ 158.8, 152.5, 138.6, 133.3, 129.6, 129.1, 128.9, 128.6, 127.8, 125.8, 123.6, 122.2, 118.8 (q, $J = 321.2$ Hz), 105.1, 22.4; ^{19}F NMR (282 MHz, CDCl_3) δ -78.3; IR (Neat Film, NaCl) 1588, 1416, 1377, 1207, 1180, 1138, 972, 878, 846, 817, 754 cm^{-1} ;

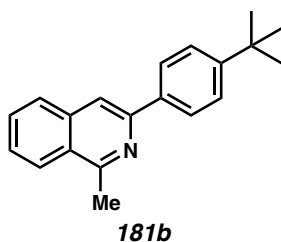
HRMS (MM:ESI-APCI+) m/z calc'd for $C_{15}H_{11}F_3NO_3S$ $[M+H]^+$: 342.0406, found 342.0399.

General procedure 3: Suzuki cross-coupling

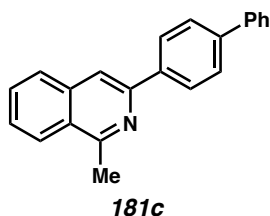


1-methyl-3-phenylisoquinoline (181a): This procedure has been adapted from a previous report.²⁵ To a flame-dried 20-mL scintillation vial capped with a PTFE-lined septum was added XPhos Pd G3 (11.63 mg, 0.014 mmol) and phenyl boronic acid (126 mg, 1.03 mmol). The reaction vial was then evacuated and backfilled with N_2 three times. The isoquinoline triflate **180a** (200 mg, 0.687 mmol) in degassed THF (2 mL, 0.3 M) was then added to the vial, followed by degassed 0.5 M K_3PO_4 solution (4 mL, 0.2 M). The reaction was then stirred at 40 °C for 2 hours. Afterwards, the reaction was diluted with water and the aqueous layer was extracted with Et_2O . The combined organic phases were dried over Na_2SO_4 , concentrated in vacuo, and purified by column chromatography (5% EtOAc in hexanes) to afford **181a** as a white solid (138 mg, 92% yield): 1H NMR (400 MHz, $CDCl_3$) δ 8.15 – 8.13 (m, 3H), 7.93 (s, 1H), 7.86 (dt, J = 8.3, 1.0 Hz, 1H), 7.67 (ddd, J = 8.2, 6.9, 1.2 Hz, 1H), 7.57 (ddd, J = 8.2, 6.8, 1.3 Hz, 1H), 7.52 – 7.48 (m, 2H), 7.42 – 7.38 (m, 1H), 3.05 (s, 3H); ^{13}C NMR (100 MHz, $CDCl_3$) δ 158.7, 150.2, 140.0, 136.9, 130.2, 128.9, 128.4, 127.8, 127.1, 126.9, 126.7, 125.8, 115.4, 22.9; IR (Neat Film,

NaCl) 3060, 1621, 1589, 1571, 1501, 1440, 1390, 1332, 1030, 902, 880, 786, 765, 692 cm^{-1} ; HRMS (MM:ESI-APCI+) m/z calc'd for $\text{C}_{16}\text{H}_{14}\text{N}$ $[\text{M}+\text{H}]^+$: 220.1121, found 220.1129.

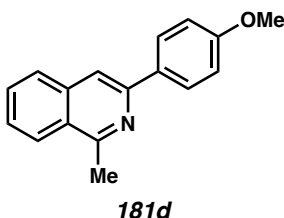


3-(4-(*tert*-butyl)phenyl)-1-methylisoquinoline (181b): Compound **181b** was prepared from triflate **180a** using general procedure 3 and purified by column chromatography (5% EtOAc in hexanes) to provide a pale yellow oil (177 mg, 93% yield); ^1H NMR (400 MHz, CDCl_3) δ 8.12 (d, $J = 8.4$ Hz, 1H) 8.06 (d, $J = 8.5$ Hz, 2H), 7.90 (s, 1H), 7.85 (d, $J = 8.2$ Hz, 1H), 7.66 (ddd, $J = 8.1, 6.8, 1.2$ Hz, 1H), 7.57 – 7.52 (m, 3H), 3.04 (s, 3H), 1.38 (s, 9H); ^{13}C NMR (100 MHz, CDCl_3) δ 158.6, 151.5, 150.3, 137.3, 136.9, 130.1, 127.7, 126.8, 126.7, 126.6, 125.8, 125.8, 115.0, 34.8, 31.5, 22.8; IR (Neat Film, NaCl) 2961, 1622, 1591, 1568, 1515, 1442, 1390, 1362, 1333, 1268, 1112, 1017, 837, 754, 743, 685 cm^{-1} ; HRMS (MM:ESI-APCI+) m/z calc'd for $\text{C}_{20}\text{H}_{22}\text{N}$ $[\text{M}+\text{H}]^+$: 276.1747, found 276.1749.

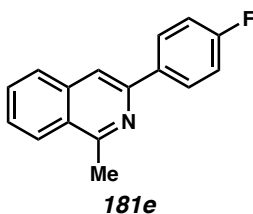


3-([1,1'-biphenyl]-4-yl)-1-methylisoquinoline (181c): Compound **181c** was prepared from triflate **180a** using general procedure 3 and purified by column chromatography (5% EtOAc in hexanes) to provide a colorless solid (191 mg, 94% yield); ^1H NMR (400

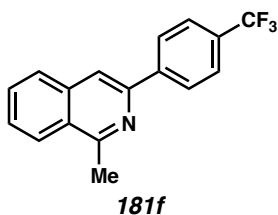
MHz, CDCl₃) δ 8.24 – 8.22 (m, 2H), 8.14 (d, J = 8.4 Hz, 1H), 7.98 (s, 1H), 7.88 (d, J = 8.1 Hz, 1H), 7.75 – 7.73 (m, 2H), 7.70 – 7.67 (m, 3H), 7.58 (ddd, J = 8.3, 6.9, 1.3 Hz, 1H), 7.50 – 7.46 (m, 2H), 7.39 – 7.37 (m, 1H), 3.06 (s, 3H); ¹³C NMR (100 MHz, CDCl₃) δ 158.8, 149.7, 141.2, 141.0, 138.9, 136.9, 130.2, 128.9, 127.8, 127.6, 127.5, 127.5, 127.2, 126.9, 126.8, 125.8, 115.2, 22.9; IR (Neat Film, NaCl) 3028, 1621, 1568, 1488, 1440, 1389, 1334, 842, 766, 730, 696 cm⁻¹; HRMS (MM:ESI-APCI+) m/z calc'd for C₂₂H₁₈N [M+H]⁺: 296.1434, found 296.1426.



3-(4-methoxyphenyl)-1-methylisoquinoline (181d): Compound **181d** was prepared from triflate **180a** using general procedure 3 and purified by column chromatography (5% EtOAc in hexanes) to afford a white solid (79 mg, 93% yield): ¹H NMR (400 MHz, CDCl₃) ¹H NMR (400 MHz, CDCl₃) δ 8.14 – 8.07 (m, 3H), 7.84 (s, 1H), 7.81 (d, J = 8.5, 1H), 7.64 (ddd, J = 8.2, 6.8, 1.2 Hz, 1H), 7.53 (ddd, J = 8.2, 6.8, 1.3 Hz, 1H), 7.06 – 7.01 (m, 2H), 3.88 (s, 3H), 3.03 (s, 3H); ¹³C NMR (100 MHz, CDCl₃) δ 160.0, 158.4, 149.8, 136.9, 132.6, 130.0, 128.2, 127.5, 126.4, 126.3, 125.7, 114.1, 114.1, 55.4, 22.7; IR (Neat Film, NaCl) 3060, 2955, 2835, 1608, 1568, 1514, 1439, 1390, 1290, 1249, 1174, 1034, 833, 751, 730 cm⁻¹; HRMS (MM:ESI-APCI+) m/z calc'd for C₁₇H₁₆NO [M+H]⁺: 250.1226, found 250.1220.

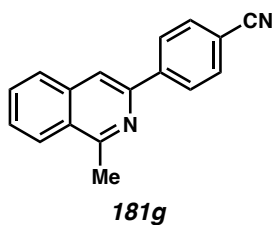


3-(4-fluorophenyl)-1-methylisoquinoline (181e): Compound **181e** was prepared from triflate **180a** using general procedure 3 and purified by column chromatography (10% EtOAc in hexanes) to provide a white solid (155 mg, 95% yield); ^1H NMR (400 MHz, CDCl_3) δ 8.17 – 8.07 (m, 3H), 7.89 – 7.81 (m, 2H), 7.68 (ddd, $J = 8.2, 6.9, 1.2$ Hz, 1H), 7.58 (ddd, $J = 8.2, 6.8, 1.3$ Hz, 1H), 7.20 – 7.16 (m, 2H), 3.04 (s, 3H); ^{13}C NMR (100 MHz, CDCl_3) δ 163.3 (d, $J = 247.3$ Hz), 158.8, 149.1, 136.9, 136.0 (d, $J = 3.3$ Hz), 130.3, 128.8 (d, $J = 8.2$ Hz), 127.7, 127.0, 126.6, 125.8, 115.7 (d, $J = 21.4$ Hz), 115.1, 22.8; ^{19}F NMR (282 MHz, CDCl_3) δ -114.2; IR (Neat Film, NaCl) 1605, 1570, 1510, 1440, 1390, 1332, 1231, 1156, 836, 749, 723 cm^{-1} ; HRMS (MM:ESI-APCI+) m/z calc'd for $\text{C}_{16}\text{H}_{13}\text{FN}$ $[\text{M}+\text{H}]^+$: 238.1027, found 238.1030.

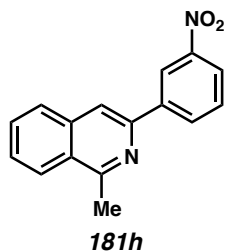


1-methyl-3-(4-(trifluoromethyl)phenyl)isoquinoline (181f): Compound **181f** was prepared from triflate **180a** using general procedure 3 and purified by column chromatography (2% to 3% EtOAc in hexanes) to afford a white solid (89 mg, 91% yield); ^1H NMR (400 MHz, CDCl_3) δ 8.26 (d, $J = 8.1$ Hz, 2H), 8.15 (d, $J = 8.4$, 1H), 7.96 (s, 1H), 7.88 (d, $J = 8.2$ Hz, 1H), 7.78 – 7.73 (m, 2H), 7.73 – 7.67 (m, 1H), 7.63 – 7.59 (m, 1H), 3.05 (s, 3H); ^{13}C NMR (100 MHz, CDCl_3) δ 159.1, 148.5, 143.3, 136.7, 130.4,

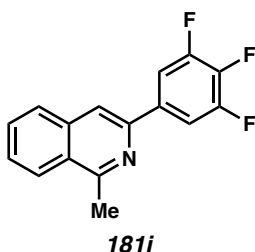
130.2 (q, $J = 32.5$ Hz), 127.9, 127.5, 127.3, 127.1, 125.8, 125.7 (q, $J = 3.8$ Hz), 124.4 (q, $J = 271.9$ Hz), 116.1, 22.8; ^{19}F NMR (282 MHz, CDCl_3) δ -62.4; IR (Neat Film, NaCl) 3070, 2357, 1622, 1573, 1418, 1390, 1324, 1162, 1122, 1066, 1015, 842, 754, 742, 682 cm^{-1} ; HRMS (MM:ESI-APCI+) m/z calc'd for $\text{C}_{17}\text{H}_{13}\text{F}_3\text{N}$ $[\text{M}+\text{H}]^+$: 288.0995, found 288.0988.



4-(1-methylisoquinolin-3-yl)benzonitrile (181g): Compound **181g** was prepared from triflate **180a** using general procedure 3 and purified by column chromatography (10% to 20% EtOAc in hexanes) to provide a white solid (144 mg, 86% yield); ^1H NMR (400 MHz, CDCl_3) δ 8.38 – 8.22 (m, 2H), 8.16 (d, $J = 8.3$ Hz, 1H), 7.99 (s, 1H), 7.89 (d, $J = 8.3$, 1H), 7.82 – 7.75 (m, 2H), 7.73 (ddd, $J = 8.1, 6.9, 1.2$ Hz, 1H), 7.64 (ddd, $J = 8.2, 6.9, 1.3$ Hz, 1H), 3.05 (s, 3H); ^{13}C NMR (100 MHz, CDCl_3) δ 159.3, 147.6, 144.0, 136.6, 132.7, 130.7, 128.0, 127.9, 127.6, 127.3, 125.9, 119.3, 116.6, 111.8, 22.8; IR (Neat Film, NaCl) 2224, 1618, 1570, 1508, 1441, 1390, 1334, 878, 844, 748, 731 cm^{-1} ; HRMS (MM:ESI-APCI+) m/z calc'd for $\text{C}_{17}\text{H}_{13}\text{N}_2$ $[\text{M}+\text{H}]^+$: 245.1073, found 245.1070.

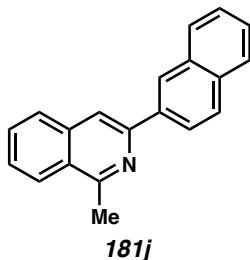


1-methyl-3-(3-nitrophenyl)isoquinoline (181h): Compound **181h** was prepared from triflate **180a** using general procedure 3 and purified by column chromatography (10% EtOAc in hexanes) to provide a white solid (139 mg, 77% yield); ^1H NMR (400 MHz, CDCl_3) δ 9.01 (t, $J = 2.0$ Hz, 1H), 8.51 (ddd, $J = 7.8, 1.8, 1.1$ Hz, 1H), 8.24 (ddd, $J = 8.2, 2.3, 1.1$ Hz, 1H), 8.16 (dd, $J = 8.3, 1.0$ Hz, 1H), 8.01 (s, 1H), 7.90 (dd, $J = 8.1, 0.7$ Hz, 1H), 7.72 (ddd, $J = 8.1, 6.9, 1.2$ Hz, 1H), 7.72 – 7.59 (m, 2H), 3.05 (s, 3H); ^{13}C NMR (100 MHz, CDCl_3) δ 159.3, 149.0, 147.3, 141.7, 136.6, 132.8, 130.6, 129.7, 127.9, 127.8, 127.2, 125.9, 123.0, 121.9, 116.0, 22.8; IR (Neat Film, NaCl) 1619, 1568, 1524, 1442, 1390, 1350, 880, 806, 749, 692 cm^{-1} ; HRMS (MM:ESI-APCI+) m/z calc'd for $\text{C}_{16}\text{H}_{13}\text{N}_2\text{O}_2$ $[\text{M}+\text{H}]^+$: 265.0972, found 265.0974.

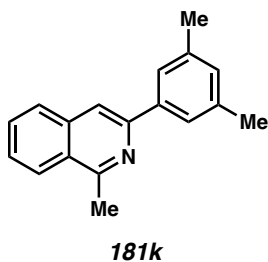


1-methyl-3-(3,4,5-trifluorophenyl)isoquinoline (181i): Compound **181i** was prepared from triflate **180a** using general procedure 3 and purified by column chromatography (5% EtOAc in hexanes) to afford a white solid (103 mg, 87% yield); ^1H NMR (400 MHz, CDCl_3) δ 8.13 (d, $J = 8.4$, 1H), 7.86 – 7.78 (m, 4H), 7.72 – 7.68 (m, 1H), 7.65 – 7.58 (m, 1H), 3.02 (s, 3H); ^{13}C NMR (100 MHz, CDCl_3) δ 159.1, 151.6 (ddd, $J = 248.4, 10.1, 4.1$ Hz), 146.5, 140.0 (dt, $J = 252.6, 15.7$ Hz), 136.6, 136.0 (td, $J = 7.5, 4.5$ Hz), 130.6, 127.8, 127.7, 127.1, 125.8, 115.4, 110.9 – 110.7 (m), 22.7; ^{19}F NMR (282 MHz, CDCl_3) δ – 134.4 (dd, $J = 20.5, 9.2$ Hz), –161.1 – –161.3 (m); IR (Neat Film, NaCl) 1619, 1570,

1526, 1446, 1392, 1352, 1237, 1034, 879, 847, 753 cm^{-1} ; HRMS (MM:ESI-APCI+) m/z
calc'd for $\text{C}_{16}\text{H}_{11}\text{F}_3\text{N}$ $[\text{M}+\text{H}]^+$: 274.0838, found 274.0841.

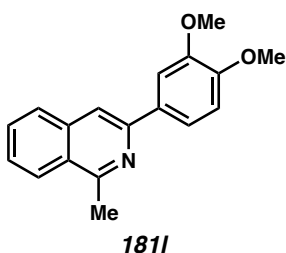


1-methyl-3-(naphthalen-2-yl)isoquinoline (181j): Compound **181j** was prepared from triflate **180a** using general procedure 3 and purified by column chromatography (5% EtOAc in hexanes) to provide a white solid (159 mg, 86% yield); ^1H NMR (400 MHz, CDCl_3) δ 8.68 (s, 1H), 8.27 (dd, $J = 8.6, 1.8$ Hz, 1H), 8.16 (dq, $J = 8.3, 1.0$ Hz, 1H), 8.07 (s, 1H), 8.00 – 7.96 (m, 2H), 7.91 – 7.86 (m, 2H), 7.70 (ddd, $J = 8.2, 6.8, 1.2$ Hz, 1H), 7.59 (ddd, $J = 8.2, 6.8, 1.3$ Hz, 1H), 7.56 – 7.46 (m, 2H), 3.09 (s, 3H); ^{13}C NMR (100 MHz, CDCl_3) δ 158.9, 149.9, 137.2, 137.0, 133.9, 133.5, 130.2, 128.9, 128.5, 127.8, 127.8, 127.0, 126.8, 126.3, 126.3, 125.8, 124.9, 115.7, 22.9; IR (Neat Film, NaCl) 3059, 1621, 1585, 1567, 1508, 1439, 1390, 879, 848, 816, 744 cm^{-1} ; HRMS (MM:ESI-APCI+) m/z calc'd for $\text{C}_{20}\text{H}_{16}\text{N}$ $[\text{M}+\text{H}]^+$: 270.1277, found 270.1270.

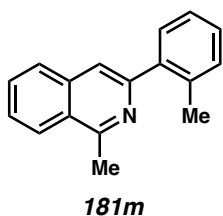


3-(3,5-dimethylphenyl)-1-methylisoquinoline (181k): Compound **181k** was prepared from triflate **180a** using general procedure 3 and purified by column chromatography to provide a white solid (156 mg, 92% yield); ^1H NMR (400 MHz, CDCl_3) δ 8.13 (dd, $J =$

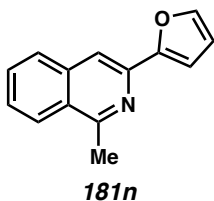
8.4, 1.1 Hz, 1H), 7.90 (s, 1H), 7.85 (dd, $J = 8.2, 0.7$ Hz, 1H), 7.75 (s, 2H), 7.66 (ddd, $J = 8.2, 6.8, 1.2$ Hz, 1H), 7.56 (ddd, $J = 8.2, 6.9, 1.3$ Hz, 1H), 7.05 (s, 1H), 3.05 (s, 3H), 2.43 (s, 6H); ^{13}C NMR (100 MHz, CDCl_3) δ 158.6, 150.5, 139.9, 138.3, 136.9, 130.2, 130.1, 127.7, 126.8, 126.7, 125.8, 125.0, 115.4, 22.8, 21.7; IR (Neat Film, NaCl) 2919, 2358, 1622, 1582, 1568, 1443, 1391, 1335, 874, 846, 786, 750, 711 cm^{-1} ; HRMS (MM:ESI-APCI+) m/z calc'd for $\text{C}_{18}\text{H}_{18}\text{N}$ $[\text{M}+\text{H}]^+$: 248.1434, found 248.1434.



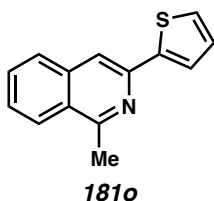
3-(3,4-dimethoxyphenyl)-1-methylisoquinoline (181l): Compound **181l** was prepared from triflate **180a** using general procedure 3 and purified by column chromatography (20% EtOAc in hexanes) to provide a white solid (195 mg, 99% yield); ^1H NMR (400 MHz, CDCl_3) δ 8.11 (d, $J = 8.4$, 1H), 7.89 – 7.81 (m, 2H), 7.77 (d, $J = 2.1$ Hz, 1H), 7.71 – 7.61 (m, 2H), 7.55 (ddd, $J = 8.3, 6.9, 1.3$ Hz, 1H), 6.99 (d, $J = 8.4$ Hz, 1H), 4.04 (s, 3H), 3.95 (s, 3H), 3.04 (s, 3H); ^{13}C NMR (100 MHz, CDCl_3) δ 158.6, 149.8, 149.6, 149.3, 137.0, 132.9, 130.2, 127.6, 126.7, 126.5, 125.8, 119.5, 114.5, 111.4, 110.3, 56.1, 22.8; IR (Neat Film, NaCl) 2936, 2833, 1568, 1516, 1454, 1436, 1317, 1259, 1236, 1170, 1026, 874, 817, 751 cm^{-1} ; HRMS (MM:ESI-APCI+) m/z calc'd for $\text{C}_{18}\text{H}_{18}\text{NO}_2$ $[\text{M}+\text{H}]^+$: 280.1332, found 280.1337.



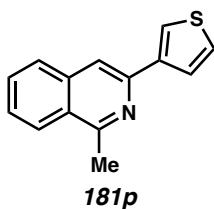
1-methyl-3-(*o*-tolyl)isoquinoline (181m): Compound **181m** was prepared from triflate **180a** using general procedure 3 and purified by column chromatography (10% EtOAc in hexanes) to provide a white solid (153 mg, 96% yield); ^1H NMR (400 MHz, CDCl_3) δ 8.17 (d, $J = 8.4$, 1H), 7.84 (d, $J = 8.3$, 1H), 7.70 (ddd, $J = 8.2$, 6.8, 1.3 Hz, 1H), 7.65 – 7.57 (m, 2H), 7.53 – 7.45 (m, 1H), 7.32 – 7.30 (m, 3H), 3.04 (s, 3H), 2.43 (s, 3H); ^{13}C NMR (100 MHz, CDCl_3) δ 158.1, 152.7, 140.9, 136.5, 136.3, 130.9, 130.1, 130.1, 128.1, 127.5, 127.0, 126.2, 126.0, 125.7, 118.9, 22.6, 20.6; IR (Neat Film, NaCl) 3053, 2950, 2920, 2355, 1622, 1584, 1567, 1498, 1446, 1392, 1360, 1330, 1144, 1033, 969, 906, 884, 763, 752, 726 cm^{-1} ; HRMS (MM:ESI-APCI+) m/z calc'd for $\text{C}_{17}\text{H}_{16}\text{N}$ $[\text{M}+\text{H}]^+$: 234.1277, found 234.1286.



3-(furan-2-yl)-1-methylisoquinoline (181n): Compound **181n** was prepared from triflate **180a** using general procedure 3 and purified by column chromatography (5% EtOAc in hexanes) to provide a white solid (106 mg, 99% yield): ^1H NMR (400 MHz, CDCl_3) δ 8.06 (d, $J = 8.4$ Hz, 1H), 7.86 (s, 1H), 7.80 (dd, $J = 8.4$ Hz, 1H), 7.67 – 7.59 (m, 1H), 7.57 – 7.49 (m, 2H), 7.13 (dd, $J = 3.4$, 0.8 Hz, 1H), 6.56 (dd, $J = 3.4$, 1.8 Hz, 1H), 2.99 (s, 3H); ^{13}C NMR (100 MHz, CDCl_3) δ 159.0, 154.4, 142.9, 142.3, 136.5, 130.2, 127.6, 126.7, 126.6, 125.8, 113.0, 112.0, 108.1, 22.6; IR (Neat Film, NaCl) 3067, 1622, 1568, 1488, 1447, 1390, 1325, 1288, 1216, 1157, 1007, 970, 883, 814, 736 cm^{-1} ; HRMS (MM:ESI-APCI+) m/z calc'd for $\text{C}_{14}\text{H}_{12}\text{NO}$ $[\text{M}+\text{H}]^+$: 210.0913, found 210.0910.

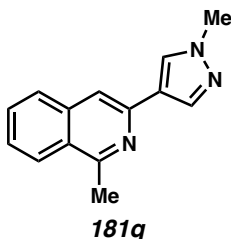


1-methyl-3-(thiophen-2-yl)isoquinoline (181o): Compound **181o** was prepared from triflate **180a** using general procedure 3 and purified by column chromatography (3% EtOAc in hexanes) to provide a white solid (103 mg, 92% yield): ^1H NMR (400 MHz, CDCl_3) δ 8.07 (dt, $J = 8.4$ Hz, 1H), 7.82 (s, 1H), 7.79 (dd, $J = 8.2$ Hz, 1H), 7.69 (dd, $J = 3.6, 1.1$ Hz, 1H), 7.64 (ddd, $J = 8.1, 6.8, 1.2$ Hz, 1H), 7.52 (ddd, $J = 8.2, 6.8, 1.2$ Hz, 1H), 7.38 (dd, $J = 5.1, 1.1$ Hz, 1H), 7.14 (dd, $J = 5.0, 3.6$ Hz, 1H), 2.99 (s, 3H); ^{13}C NMR (100 MHz, CDCl_3) δ 158.8, 145.5, 145.4, 136.6, 130.2, 128.1, 127.4, 126.7, 126.6, 125.8, 123.8, 113.1, 22.5; IR (Neat Film, NaCl) 3068, 1620, 1586, 1568, 1446, 1387, 1330, 1238, 1194, 1036, 876, 820, 748, 704 cm^{-1} ; HRMS (MM:ESI-APCI+) m/z calc'd for $\text{C}_{14}\text{H}_{12}\text{NS}$ $[\text{M}+\text{H}]^+$: 226.0685, found 226.0680.

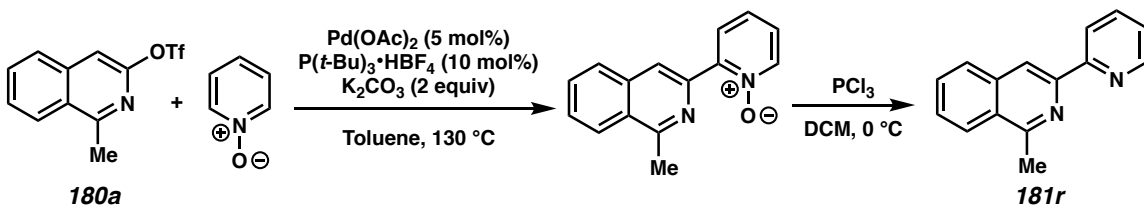


1-methyl-3-(thiophen-3-yl)isoquinoline (181p): Compound **181p** was prepared from triflate **180a** using general procedure 3 and purified by column chromatography (5% EtOAc in hexanes) to provide a white solid (148 mg, 95% yield); ^1H NMR (400 MHz, CDCl_3) δ 8.10 (dd, $J = 8.4, 1.0$ Hz, 1H), 8.04 (dd, $J = 3.1, 1.3$ Hz, 1H), 7.81 (dt, $J = 8.2, 0.9$ Hz, 1H), 7.79 (s, 1H), 7.73 (dd, $J = 5.0, 1.3$ Hz, 1H), 7.65 (ddd, $J = 8.2, 6.8, 1.2$ Hz, 1H), 7.54 (ddd, $J = 8.3, 6.9, 1.3$ Hz, 1H), 7.42 (dd, $J = 5.0, 3.1$ Hz, 1H), 3.01 (s, 3H); ^{13}C

NMR (100 MHz, CDCl₃) δ 158.8, 146.4, 142.7, 136.9, 130.2, 127.6, 126.7, 126.6, 126.3, 126.2, 125.8, 123.2, 114.7, 22.8; IR (Neat Film, NaCl) 3056, 2920, 1622, 1591, 1568, 1496, 1446, 1388, 1317, 874, 842, 795, 749, 696 cm⁻¹; HRMS (MM:ESI-APCI+) m/z calc'd for C₁₄H₁₂NS [M+H]⁺: 226.0685, found 226.0687.

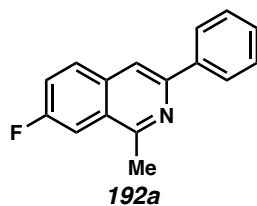


1-methyl-3-(1-methyl-1H-pyrazol-4-yl)isoquinoline (181q): Compound **181q** was prepared from triflate **180a** using general procedure 3 and purified by column chromatography (50% to 60% EtOAc in hexanes) to provide a white solid (112 mg, 99% yield): ¹H NMR (400 MHz, CDCl₃) δ 8.07 (d, J = 8.4 Hz, 1H), 8.04 – 8.00 (m, 2H), 7.77 (dd, J = 8.2, 1.1 Hz, 1H), 7.67 – 7.60 (m, 2H), 7.54 – 7.47 (m, 1H), 3.98 (s, 3H), 2.97 (s, 3H); ¹³C NMR (100 MHz, CDCl₃) δ 158.8, 137.4, 136.8, 130.1, 128.9, 127.1, 126.2, 126.1, 125.7, 113.3, 39.1, 22.6; IR (Neat Film, NaCl) 2940, 2351, 1620, 1601, 1568, 1556, 1493, 1416, 1182, 983, 840, 750, 702 cm⁻¹; HRMS (MM:ESI-APCI+) m/z calc'd for C₁₄H₁₄N₃ [M+H]⁺: 224.1182, found 224.1176.



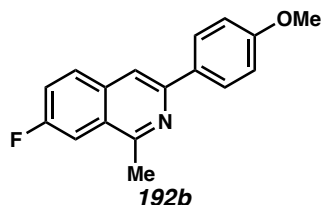
1-methyl-3-(pyridin-2-yl)isoquinoline (181r): Compound **181r** was prepared from triflate **180a** using a procedure adapted from a previous report.⁶ To a microwave vial was added flame-dried K₂CO₃ (142 mg, 1.03 mmol), Pd(OAc)₂ (5.8 mg, 0.026 mmol), P(*t*-

Bu_3HBF_4 (15 mg, 0.052 mmol), and the *N*-oxide (147 mg, 1.55 mmol). The vial was then evacuated and backfilled with argon three times. A solution of **180a** (150 mg, 0.52 mmol) in toluene (2 mL, 0.3 M) was then added, and the reaction was stirred at 130 °C overnight. The reaction was then cooled to room temperature, filtered through celite, and dissolved in CH_2Cl_2 (10 mL, 0.05 M). The reaction flask was then cooled to 0 °C and PCl_3 (0.27 mL, 3.1 mmol) was added dropwise, then the reaction stirred for 30 minutes at 0 °C. The reaction was then quenched with saturated aqueous K_2CO_3 , extracted with EtOAc, and dried over Na_2SO_4 . The crude product was purified by column chromatography (30% EtOAc in hexanes + 1% NEt_3) to provide a pale yellow solid (56 mg, 50% yield over 2 steps); ^1H NMR (400 MHz, CDCl_3) δ 8.72 (dd, J = 4.8, 1.9 Hz, 1H), 8.62 (s, 1H), 8.56 (dd, J = 8.0, 1.1 Hz, 1H), 8.14 (dd, J = 8.3, 1.0 Hz, 1H), 7.95 (dt, J = 8.2, 1.0 Hz, 1H), 7.84 (td, J = 7.7, 1.8 Hz, 1H), 7.68 (ddd, J = 8.1, 6.8, 1.2 Hz, 1H), 7.60 (ddd, J = 8.2, 6.9, 1.4 Hz, 1H), 7.29 (ddd, J = 7.5, 4.8, 1.2 Hz, 1H), 3.05 (s, 3H); ^{13}C NMR (100 MHz, CDCl_3) δ 158.5, 156.9, 149.4, 148.7, 137.1, 136.9, 130.2, 128.6, 127.7, 127.5, 125.8, 123.3, 121.4, 116.5, 22.9; IR (Neat Film, NaCl) 3053, 3004, 2916, 1621, 1580, 1568, 1474, 1443, 1426, 1391, 1335, 1142, 891, 796, 742, 681, 624 cm^{-1} ; HRMS (MM:ESI-APCI+) m/z calc'd for $\text{C}_{15}\text{H}_{13}\text{N}_2$ $[\text{M}+\text{H}]^+$: 221.1073, found 221.1076.

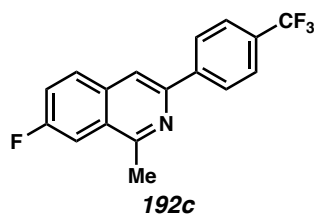


7-fluoro-1-methyl-3-phenylisoquinoline (192a): Compound **192a** was prepared from triflate **180b** using general procedure 3 and purified by column chromatography (5% EtOAc in hexanes) to provide a white solid (110 mg, 93% yield): ^1H NMR (400 MHz,

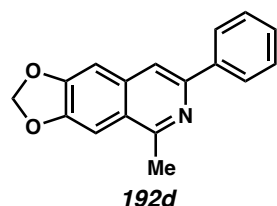
CDCl_3) δ 8.14 – 8.11 (m, 2H), 7.90 (s, 1H), 7.85 (dd, $J = 9.2, 5.7$ Hz, 1H), 7.73 – 7.68 (m, 1H), 7.54 – 7.48 (m, 2H), 7.48 – 7.38 (m, 2H), 2.99 (s, 3H); ^{13}C NMR (100 MHz, CDCl_3) δ 160.7 (d, $J = 248.3$ Hz), 158.0 (d, $J = 5.8$ Hz), 149.8 (d, $J = 2.8$ Hz), 139.7, 133.9, 130.3 (d, $J = 8.5$ Hz), 128.9, 128.5, 127.3 (d, $J = 7.8$ Hz), 127.0, 120.6 (d, $J = 25.3$ Hz), 114.9 (d, $J = 1.7$ Hz), 109.4 (d, $J = 21.0$ Hz), 22.8; ^{19}F NMR (282 MHz, CDCl_3) δ –109.7 – –111.8 (m); IR (Neat Film, NaCl) 3031, 2358, 1576, 1506, 1446, 1393, 1372, 1313, 1230, 1183, 1028, 972, 922, 904, 881, 822, 777, 764, 704 cm^{-1} ; HRMS (MM:ESI-APCI+) m/z calc'd for $\text{C}_{16}\text{H}_{13}\text{FN}$ $[\text{M}+\text{H}]^+$: 238.1027, found 238.1027.



7-fluoro-3-(4-methoxyphenyl)-1-methylisoquinoline (192b): Compound **192b** was prepared from triflate **180b** using general procedure 3 and purified by column chromatography (5% EtOAc in hexanes) to provide a white solid (110 mg, 99% yield): ^1H NMR (400 MHz, CDCl_3) δ 8.10 – 8.04 (m, 2H), 7.87 – 7.81 (m, 2H), 7.70 (dd, $J = 9.9, 2.6$ Hz, 1H), 7.44 (ddd, $J = 9.0, 8.3, 2.5$ Hz, 1H), 7.06 – 6.99 (m, 2H), 3.88 (s, 3H), 2.98 (s, 3H); ^{13}C NMR (100 MHz, CDCl_3) δ 160.4 (d, $J = 248.5$ Hz), 160.1, 157.7 (d, $J = 5.7$ Hz), 149.4 (d, $J = 2.8$ Hz), 133.9, 132.2, 130.0 (d, $J = 8.5$ Hz), 128.1, 126.7 (d, $J = 7.7$ Hz), 120.5 (d, $J = 25.3$ Hz), 114.2, 113.7 (d, $J = 1.8$ Hz), 109.3 (d, $J = 20.9$ Hz), 55.4, 22.7; ^{19}F NMR (282 MHz, CDCl_3) δ –111.9 (ddd, $J = 9.3, 9.1, 5.7$ Hz); IR (Neat Film, NaCl) 1608, 1514, 1443, 1393, 1288, 1252, 1186, 1029, 878, 863, 836, 821 cm^{-1} ; HRMS (MM:ESI-APCI+) m/z calc'd for $\text{C}_{17}\text{H}_{15}\text{FNO}$ $[\text{M}+\text{H}]^+$: 268.1132, found 268.1133.

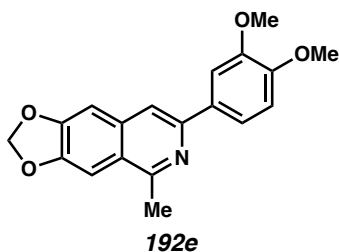


7-fluoro-1-methyl-3-(4-(trifluoromethyl)phenyl)isoquinoline (192c): Compound **192c** was prepared from triflate **180b** using general procedure 3 and purified by column chromatography (5% EtOAc in hexanes) to provide a white solid (150 mg, 98% yield): ^1H NMR (400 MHz, CDCl_3) δ 8.22 (d, $J = 8.0$ Hz, 2H), 7.94 (s, 1H), 7.90 – 7.85 (m, 1H), 7.74 (d, $J = 8.0$ Hz, 2H), 7.71 – 7.69 (m, 1H), 7.53 – 7.43 (m, 1H), 2.99 (s, 3H); ^{13}C NMR (100 MHz, CDCl_3) δ 161.1 (d, $J = 249.4$ Hz), 158.4 (d, $J = 6.2$ Hz), 148.1, 143.0, 133.7, 130.4 (d, $J = 8.5$ Hz), 130.2 (q, $J = 32.4$ Hz), 127.8 (d, $J = 8.1$ Hz), 127.2, 125.8 (q, $J = 3.8$ Hz), 124.5 (q, $J = 272.7$ Hz), 120.9 (d, $J = 24.9$ Hz), 115.6, 109.5 (d, $J = 21.4$ Hz), 22.8 ; ^{19}F NMR (282 MHz, CDCl_3) δ -62.5, -110.2 (ddd, $J = 9.9, 8.2, 5.5$ Hz); IR (Neat Film, NaCl) 1592, 1418, 1393, 1330, 1157, 1126, 1107, 1067, 880, 868, 847, 816 cm^{-1} ; HRMS (MM:ESI-APCI+) m/z calc'd for $\text{C}_{17}\text{H}_{12}\text{NF}_4$ $[\text{M}+\text{H}]^+$: 306.0900, found 306.0895.

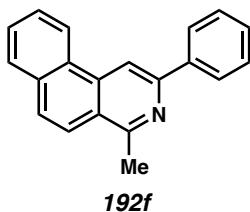


5-methyl-7-phenyl-[1,3]dioxolo[4,5-g]isoquinoline (192d): Compound **192d** was prepared from triflate **180c** using general procedure 3 and purified by column chromatography (10% EtOAc in hexanes) to provide a white solid (153 mg, 97% yield): ^1H NMR (400 MHz, CDCl_3) δ 8.08 (d, $J = 7.2$ Hz, 2H), 7.77 (s, 1H), 7.52 – 7.44 (m, 2H),

7.41 – 7.32 (m, 2H), 7.11 (s, 1H), 6.10 (s, 2H), 2.92 (s, 3H); ^{13}C NMR (100 MHz, CDCl_3) δ 156.4, 150.5, 149.5, 148.1, 140.0, 135.1, 128.7, 128.1, 126.8, 123.5, 115.1, 103.4, 101.9, 101.6, 23.0; IR (Neat Film, NaCl) 2914, 1591, 1486, 1462, 1232, 1189, 1039, 945, 878, 846, 695, 684 cm^{-1} ; HRMS (MM:ESI-APCI+) m/z calc'd for $\text{C}_{17}\text{H}_{14}\text{NO}_2$ $[\text{M}+\text{H}]^+$: 264.1019, found 264.1021.

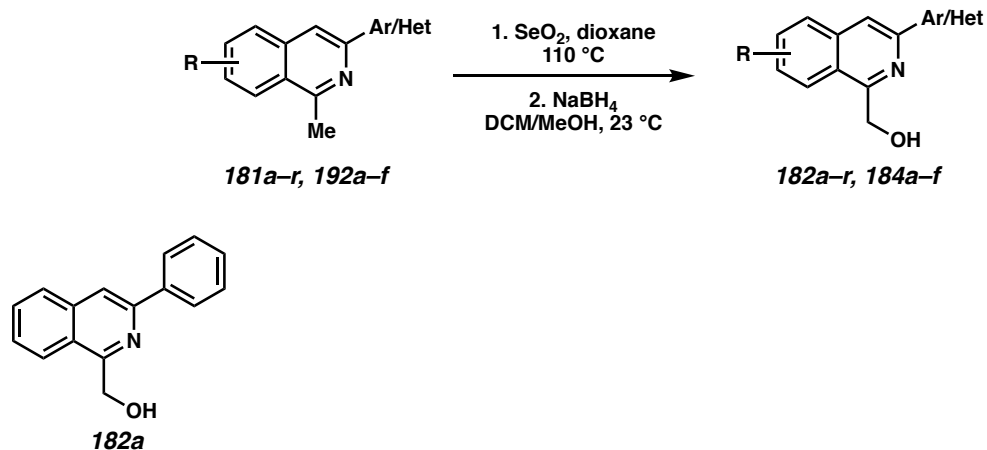


7-(3,4-dimethoxyphenyl)-5-methyl-[1,3]dioxolo[4,5-g]isoquinoline (192e): Compound **192e** was prepared from triflate **180c** using general procedure 3 at 65 °C and purified by column chromatography via dry loading (40% EtOAc in hexanes) to provide a white solid (202 mg, 82% yield); ^1H NMR (400 MHz, CDCl_3) δ 7.72 (d, J = 2.1 Hz, 1H), 7.69 (s, 1H), 7.60 (dd, J = 8.3, 2.0 Hz, 1H), 7.34 (s, 1H), 7.09 (s, 1H), 6.96 (d, J = 8.4 Hz, 1H), 6.09 (s, 2H), 4.02 (s, 3H), 3.94 (s, 3H), 2.91 (s, 3H); ^{13}C NMR (100 MHz, CDCl_3) δ 156.2, 150.5, 149.3, 149.2, 147.9, 135.2, 134.3, 133.0, 123.2, 119.1, 114.3, 111.2, 110.0, 103.3, 101.8, 101.5, 56.0, 56.0, 23.0; IR (Neat Film, NaCl) 2935, 1591, 1517, 1462, 1267, 1230, 1165, 1143, 1024, 872, 731 cm^{-1} ; HRMS (MM:ESI-APCI+) m/z calc'd for $\text{C}_{19}\text{H}_{18}\text{NO}_4$ $[\text{M}+\text{H}]^+$: 324.1230, found 324.1229.



4-methyl-2-phenylbenzo[*f*]isoquinoline (192f): Compound **192f** was prepared from triflate **180d** using general procedure 3 and the product was collected via vacuum filtration to provide a white solid (246 mg, 63% yield); ^1H NMR (400 MHz, CDCl_3) δ 8.55 – 8.40 (m, 2H), 7.96 – 7.88 (m, 2H), 7.73 (t, $J = 8.7$ Hz, 1H), 7.69 – 7.61 (m, 1H), 7.54 (t, $J = 8.3$ Hz, 1H), 7.45 – 7.42 (m, 2H), 7.26 (td, $J = 7.6, 1.7$ Hz, 2H), 7.16 (td, $J = 7.3, 1.7$ Hz, 1H), 2.81 (s, 3H); ^{13}C NMR (100 MHz, CDCl_3) δ 157.9, 152.0, 140.3, 135.6, 133.4, 129.3, 128.8, 128.7, 128.5, 128.4, 127.7, 127.2, 127.1, 124.4, 123.4, 122.9, 111.0, 23.1; IR (Neat Film, NaCl) 2342, 1574, 1506, 1483, 1444, 1386, 1242, 1028, 876, 824, 760, 725, 692 cm^{-1} ; HRMS (MM:ESI-APCI+) m/z calc'd for $\text{C}_{20}\text{H}_{16}\text{N}$ $[\text{M}+\text{H}]^+$: 270.1277, found 270.1289.

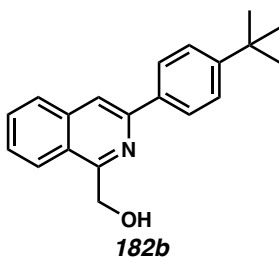
General procedure 4: Oxidation and reduction to hydroxymethyl isoquinoline



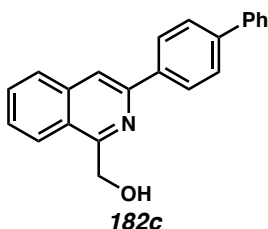
(3-phenylisoquinolin-1-yl)methanol (182a): This procedure has been adapted from a previous report.⁴ To a 20-mL microwave vial containing a stir bar was added SeO_2 (140 mg, 1.26 mmol), isoquinoline **181a** (138 mg, 0.63 mmol), and 1,4-dioxane (13 mL, 0.05 M). The reaction vial was then sealed and heated to 110 $^\circ\text{C}$ while stirring for 2 hours. The reaction was then cooled to room temperature, filtered through celite, and rinsed with

EtOAc. The filtrate was then concentrated in vacuo to afford the aldehyde intermediate, which was used in the next step without further purification.

A scintillation vial containing the crude in 4:1 DCM:MeOH (0.1 M) was added sodium borohydride (24 mg, 0.63 mmol) at room temperature. The reaction was stirred until no starting material remained by TLC, and then quenched by the addition of citric acid monohydrate (132 mg, 0.63 mmol). The reaction was stirred for an additional 10 minutes, then basified by the addition of saturated aqueous NaHCO₃. The layers were separated and the aqueous phase was extracted with CH₂Cl₂. The combined organic phases were dried over Na₂SO₄ and concentrated in vacuo. The crude product was purified by column chromatography (20% acetone in hexanes) to afford **182a** as a white solid (100 mg, 68% yield over 2 steps): ¹H NMR (400 MHz, CDCl₃) δ 8.18 – 8.15 (d, *J* = 7.0 Hz, 2H), 8.03 (s, 1H), 7.94 – 7.92 (m, 2H), 7.73 (ddd, *J* = 8.3, 6.9, 1.1 Hz, 1H), 7.61 (ddd, *J* = 8.1, 6.9, 1.2 Hz, 1H), 7.53 (t, *J* = 7.6 Hz, 2H), 7.46 – 7.42 (m, 1H), 5.31 (s, 2H), 5.26 (br s, 1H, OH); ¹³C NMR (100 MHz, CDCl₃) δ 157.4, 148.7, 138.9, 137.1, 130.9, 129.0, 128.9, 128.0, 127.5, 127.0, 124.2, 123.3, 116.3, 61.6; IR (Neat Film, NaCl) 3378, 3060, 2867, 1624, 1574, 1502, 1461, 1443, 1370, 1331, 1304, 1088, 1072, 1024, 1009, 882, 782, 766, 693 cm⁻¹; HRMS (MM:ESI-APCI+) *m/z* calc'd for C₁₆H₁₄NO [M+H]⁺: 236.1070, found 236.1078.

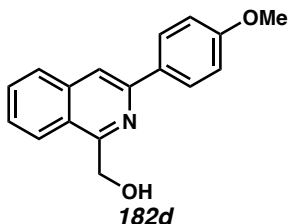


((3-(4-(*tert*-butyl)phenyl)isoquinolin-1-yl)methanol (182b): Compound **182b** was prepared from isoquinoline **181b** using general procedure 4 and purified by column chromatography (20% EtOAc in hexanes) to provide a white solid (162 mg, 95% yield); ^1H NMR (400 MHz, CDCl_3) δ 8.20 – 8.06 (m, 2H), 8.00 (s, 1H), 7.97 – 7.85 (m, 2H), 7.72 (ddd, $J = 8.4, 6.9, 1.2$ Hz, 1H), 7.62 – 7.58 (m, 1H), 7.58 – 7.52 (m, 2H), 5.30 (s, 3H), 1.40 (s, 9H); ^{13}C NMR (100 MHz, CDCl_3) δ 157.2, 152.1, 148.7, 137.1, 136.2, 130.8, 127.9, 127.3, 126.7, 125.9, 124.1, 123.3, 115.9, 61.5, 34.9, 31.5; IR (Neat Film, NaCl) 3385, 2958, 1626, 1574, 1514, 1446, 1416, 1360, 1333, 1265, 1088, 1014, 841, 744, 680 cm^{-1} ; HRMS (MM:ESI-APCI+) m/z calc'd for $\text{C}_{20}\text{H}_{22}\text{NO}$ $[\text{M}+\text{H}]^+$: 292.1696, found 292.1696.

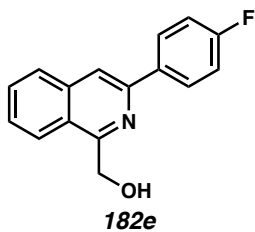


(3-([1,1'-biphenyl]-4-yl)isoquinolin-1-yl)methanol (182c): Compound **182c** was prepared from isoquinoline **181c** using general procedure 4 and purified by column chromatography (20% EtOAc in hexanes) to provide a colorless solid (181 mg, 92% yield); ^1H NMR (400 MHz, CDCl_3) δ 8.30 – 8.20 (m, 2H), 8.07 (s, 1H), 7.98 – 7.88 (m, 2H), 7.81 – 7.66 (m, 5H), 7.62 (ddd, $J = 8.4, 6.9, 1.2$ Hz, 1H), 7.49 (dd, $J = 8.2, 6.8$ Hz, 2H), 7.43 – 7.34 (m, 1H), 5.32 (s, 3H); ^{13}C NMR (100 MHz, CDCl_3) δ 157.4, 148.3, 141.7, 140.7, 137.8, 137.1, 130.9, 129.0, 128.0, 127.7, 127.7, 127.6, 127.3, 127.2, 124.2, 123.3, 116.2, 61.6; IR (Neat Film, NaCl) 3382, 3060, 2359, 1623, 1574, 1488, 1445,

1412, 1374, 1334, 1088, 1006, 840, 766, 729, 697 cm^{-1} ; HRMS (MM:ESI-APCI+) m/z calc'd for $\text{C}_{22}\text{H}_{18}\text{NO}$ $[\text{M}+\text{H}]^+$: 312.1382, found 312.1383.

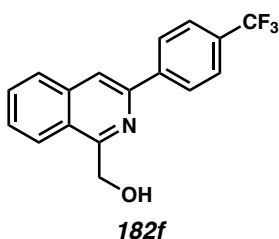


(3-(4-methoxyphenyl)isoquinolin-1-yl)methanol (182d): Compound **182d** was prepared from isoquinoline **181d** using general procedure 4 and purified by column chromatography (20% EtOAc in hexanes) to provide a white solid (48 mg, 73% yield): ^1H NMR (400 MHz, CDCl_3) δ 8.14 – 8.07 (m, 2H), 7.93 (s, 1H), 7.91 – 7.85 (m, 2H), 7.69 (ddd, $J = 8.2, 6.9, 1.1$ Hz, 1H), 7.56 (ddd, $J = 8.2, 6.9, 1.2$ Hz, 1H), 7.06 – 7.03 (m, 2H), 5.28 (s, 3H), 3.89 (s, 3H); ^{13}C NMR (100 MHz, CDCl_3) δ 160.3, 157.0, 148.3, 137.1, 131.4, 130.7, 128.1, 127.7, 127.0, 123.7, 123.1, 115.0, 114.2, 61.4, 55.4; IR (Neat Film, NaCl) 3376, 2928, 2836, 1608, 1573, 1515, 1442, 1372, 1334, 1287, 1250, 1175, 1087, 1032, 1010, 832, 750, 730 cm^{-1} ; HRMS (MM:ESI-APCI+) m/z calc'd for $\text{C}_{17}\text{H}_{16}\text{NO}_2$ $[\text{M}+\text{H}]^+$: 266.1176, found 266.1185.

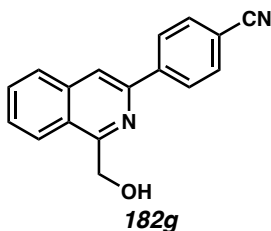


(3-(4-fluorophenyl)isoquinolin-1-yl)methanol (182e): Compound **182e** was prepared from isoquinoline **181e** using general procedure 4 and purified by column chromatography (20% EtOAc in hexanes) to provide a colorless solid (149 mg, 95% yield); ^1H NMR (400 MHz, CDCl_3) δ 8.13 (dd, $J = 8.9, 5.4$ Hz, 2H), 7.96 (s, 1H), 7.95 –

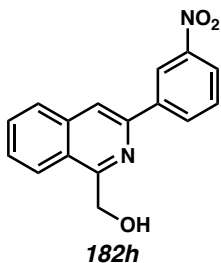
7.89 (m, 2H), 7.73 (ddd, $J = 8.3, 6.9, 1.1$ Hz, 1H), 7.61 (ddd, $J = 8.1, 6.9, 1.2$ Hz, 1H), 7.21 (dd, $J = 8.9, 8.5$ Hz, 2H), 5.30 (s, 2H), 5.17 (br s, 1H, OH); ^{13}C NMR (100 MHz, CDCl_3) δ 163.5 (d, $J = 248.3$ Hz), 157.5, 147.8, 137.0, 135.1 (d, $J = 3.2$ Hz), 131.0, 128.7 (d, $J = 8.2$ Hz), 127.9, 127.6, 124.1, 123.3, 116.0, 115.8, 61.6; ^{19}F NMR (282 MHz, CDCl_3) δ -113.3 – -113.4 (m); IR (Neat Film, NaCl) 3382, 3059, 2354, 1622, 1604, 1574, 1512, 1446, 1331, 1230, 1157, 1087, 1011, 837, 750, 725 cm^{-1} ; HRMS (MM:ESI-APCI+) m/z calc'd for $\text{C}_{16}\text{H}_{13}\text{FNO}$ $[\text{M}+\text{H}]^+$: 254.0974, found 254.0976.



(3-(4-(trifluoromethyl)phenyl)isoquinolin-1-yl)methanol (182f): Compound **182f** was prepared from isoquinoline **181f** using general procedure 4 and purified by column chromatography (10% to 20% EtOAc in hexanes) to provide a white solid (23 mg, 25% yield); ^1H NMR (400 MHz, CDCl_3) δ 8.26 (d, $J = 7.8$ Hz, 2H), 8.07 (s, 1H), 8.00 – 7.92 (m, 2H), 7.82 – 7.73 (m, 3H), 7.70 – 7.61 (m, 1H), 5.32 (s, 2H), 5.10 (br s, 1H, OH); ^{13}C NMR (100 MHz, CDCl_3) δ 157.9, 147.1, 142.3, 136.8, 131.2, 130.7 (q, $J = 32.5$ Hz), 128.2, 128.1, 127.2, 125.9 (q, $J = 3.8$ Hz), 124.6, 124.4 (q, $J = 273.7$ Hz), 123.4, 117.2, 61.6; ^{19}F NMR (282 MHz, CDCl_3) δ -62.5; IR (Neat Film, NaCl) 3408, 1623, 1574, 1418, 1324, 1166, 1111, 1075, 1014, 842, 753, 682 cm^{-1} ; HRMS (MM:ESI-APCI+) m/z calc'd for $\text{C}_{17}\text{H}_{13}\text{F}_3\text{NO}$ $[\text{M}+\text{H}]^+$: 304.0944, found 304.0934.

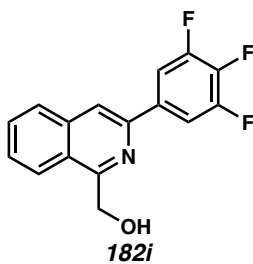


4-(1-(hydroxymethyl)isoquinolin-3-yl)benzonitrile (182g): Compound **182g** was prepared from isoquinoline **181g** using general procedure 4 and purified by column chromatography (30% EtOAc in hexanes) to provide a white solid (138 mg, 92% yield); ^1H NMR (400 MHz, CDCl_3) δ 8.31 – 8.18 (m, 2H), 8.09 (s, 1H), 7.97 (m, 2H), 7.86 – 7.74 (m, 3H), 7.68 (ddd, J = 8.2, 6.9, 1.2 Hz, 1H), 5.32 (s, 2H), 4.99 (s, 1H); ^{13}C NMR (100 MHz, CDCl_3) δ 158.2, 146.5, 143.2, 136.7, 132.8, 131.4, 128.5, 128.2, 127.4, 124.7, 123.5, 119.0, 117.7, 112.3, 61.7; IR (Neat Film, NaCl) 3404, 2895, 2358, 2224, 1416, 1332, 1303, 1085, 1006, 840, 764, 682 cm^{-1} ; HRMS (MM:ESI-APCI+) m/z calc'd for $\text{C}_{17}\text{H}_{13}\text{N}_2\text{O}$ $[\text{M}+\text{H}]^+$: 261.1022, found 261.1032.

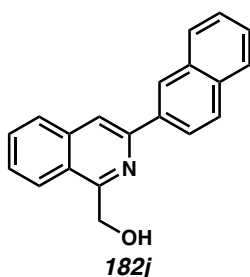


(3-(3-nitrophenyl)isoquinolin-1-yl)methanol (182h): Compound **182h** was prepared from isoquinoline **181h** using general procedure 4 and purified by column chromatography (20% EtOAc in CH_2Cl_2) to provide a white solid (67 mg, 38% yield); ^1H NMR (400 MHz, CDCl_3) δ 8.95 (t, J = 2.0 Hz, 1H), 8.52 (dt, J = 7.9, 1.3 Hz, 1H), 8.27 (ddd, J = 8.2, 2.3, 1.1 Hz, 1H), 8.11 (s, 1H), 8.04 – 7.90 (m, 2H), 7.78 (ddd, J = 8.0, 6.9, 1.2 Hz, 1H), 7.73 – 7.60 (m, 2H), 5.33 (s, 2H), 4.96 (br s, 1H, OH); ^{13}C NMR (100 MHz,

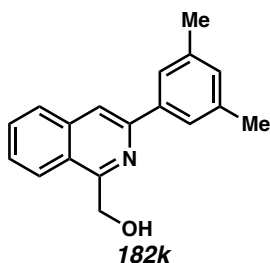
CDCl_3) δ 158.2, 149.0, 146.1, 140.7, 136.8, 132.7, 131.4, 129.9, 128.4, 128.2, 124.7, 123.5, 123.4, 121.6, 117.2, 61.7; IR (Neat Film, NaCl) 3389, 2614, 1538, 1520, 1505, 1353, 1333, 1088, 1007, 892, 751, 690 cm^{-1} ; HRMS (MM:ESI-APCI+) m/z calc'd for $\text{C}_{16}\text{H}_{13}\text{N}_2\text{O}_3$ $[\text{M}+\text{H}]^+$: 281.0921, found 281.0930.



(3-(3,4,5-trifluorophenyl)isoquinolin-1-yl)methanol (182i): Compound **182i** was prepared from isoquinoline **181i** using general procedure 4 and purified by column chromatography (20% EtOAc in hexanes) to provide a white solid (90 mg, 82% yield); ^1H NMR (400 MHz, CDCl_3) δ 7.99 – 7.89 (m, 3H), 7.84 – 7.71 (m, 3H), 7.65 (ddd, J = 8.2, 6.9, 1.3 Hz, 1H), 5.30 (s, 2H), 4.89 (br s, 1H, OH); ^{13}C NMR (100 MHz, CDCl_3) δ 158.0, 151.7 (ddd, J = 249.3, 10.2, 4.1 Hz), 145.4 (d, J = 2.5 Hz), 140.2 (dt, J = 253.9, 15.7 Hz), 136.7, 135.1 (td, J = 7.6, 4.5 Hz), 131.4, 128.3, 128.0, 124.5, 123.4, 116.6 (d, J = 1.4 Hz), 110.9 – 110.7 (m), 61.7; ^{19}F NMR (282 MHz, CDCl_3) δ –133.8 – –133.9 (m), –160.1 – –160.3 (m); IR (Neat Film, NaCl) 3351, 2882, 1557, 1531, 1451, 1350, 1326, 1080, 1039, 1008, 864, 848, 778, 747, 706 cm^{-1} ; HRMS (MM:ESI-APCI+) m/z calc'd for $\text{C}_{16}\text{H}_{11}\text{F}_3\text{NO}$ $[\text{M}+\text{H}]^+$: 290.0787, found 290.0795.

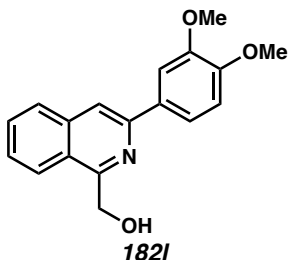


(3-(naphthalen-2-yl)isoquinolin-1-yl)methanol (182j): Compound **182j** was prepared from isoquinoline **181j** using general procedure 4 and purified by column chromatography (20% EtOAc in hexanes) to provide a white solid (158 mg, 97% yield); ^1H NMR (400 MHz, CDCl_3) δ 8.67 (s, 1H), 8.27 (dd, $J = 8.6, 1.8$ Hz, 1H), 8.16 (s, 1H), 8.05 – 7.93 (m, 4H), 7.91 – 7.89 (m, 1H), 7.75 (ddd, $J = 8.2, 6.9, 1.1$ Hz, 1H), 7.62 (ddd, $J = 8.2, 6.9, 1.2$ Hz, 1H), 7.58 – 7.47 (m, 2H), 5.34 (s, 3H); ^{13}C NMR (100 MHz, CDCl_3) δ 157.5, 148.5, 137.1, 136.2, 133.7, 133.7, 130.9, 128.8, 128.6, 128.0, 127.8, 127.6, 126.7, 126.6, 126.3, 124.6, 124.2, 123.3, 116.6, 61.6; IR (Neat Film, NaCl) 3393, 3056, 1622, 1573, 1506, 1445, 1410, 1375, 1344, 1314, 1086, 1008, 856, 817, 744 cm^{-1} ; HRMS (MM:ESI-APCI+) m/z calc'd for $\text{C}_{20}\text{H}_{16}\text{NO}$ $[\text{M}+\text{H}]^+$: 286.1231, found 286.1226.

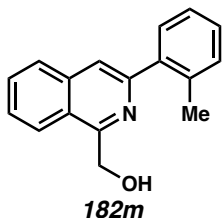


(3-(3,5-dimethylphenyl)isoquinolin-1-yl)methanol (182k): Compound **182k** was prepared from isoquinoline **181k** using general procedure 4 and purified by column chromatography (20% EtOAc in hexanes) to provide a white solid (155 mg, 95% yield); ^1H NMR (400 MHz, CDCl_3) δ 8.00 (s, 1H), 7.94 – 7.91 (m, 2H), 7.78 – 7.76 (m, 2H), 7.72 (ddd, $J = 8.3, 6.9, 1.2$ Hz, 1H), 7.60 (ddd, $J = 8.2, 6.9, 1.2$ Hz, 1H), 7.09 (s, 1H), 5.30 (s, 3H), 2.44 (s, 6H); ^{13}C NMR (100 MHz, CDCl_3) δ 157.2, 149.0, 138.9, 138.5, 137.1, 130.8, 130.6, 127.9, 127.4, 124.8, 124.1, 123.3, 116.3, 61.6, 21.7; IR (Neat Film, NaCl) 3382, 2913, 2338, 1622, 1574, 1503, 1444, 1379, 1332, 1084, 1011, 882, 849, 824,

750, 709 cm^{-1} ; HRMS (MM:ESI-APCI+) m/z calc'd for $\text{C}_{18}\text{H}_{18}\text{NO}$ $[\text{M}+\text{H}]^+$: 264.1382, found 264.1383.

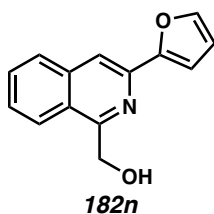


(3-(3,4-dimethoxyphenyl)isoquinolin-1-yl)methanol (182l): Compound **182l** was prepared from isoquinoline **181l** using general procedure 4 and purified by column chromatography (40% EtOAc in hexanes) to provide a white solid (180 mg, 91% yield); ^1H NMR (400 MHz, CDCl_3) δ 7.95 (s, 1H), 7.93 – 7.90 (m, 2H), 7.77 – 7.67 (m, 3H), 7.58 (ddd, J = 8.2, 6.9, 1.2 Hz, 1H), 7.03 – 7.01 (m, 1H), 5.30 (s, 2H), 5.26 (br s, 1H, OH), 4.03 (s, 3H), 3.97 (s, 3H); ^{13}C NMR (100 MHz, CDCl_3) δ 157.0, 149.8, 149.3, 148.3, 137.0, 131.8, 130.7, 127.7, 127.1, 123.8, 123.2, 119.5, 115.3, 111.3, 110.0, 61.4, 56.1, 56.0; IR (Neat Film, NaCl) 3372, 2936, 2838, 1623, 1604, 1573, 1518, 1456, 1438, 1314, 1260, 1237, 1134, 1027, 1008 cm^{-1} ; HRMS (MM:ESI-APCI+) m/z calc'd for $\text{C}_{18}\text{H}_{18}\text{NO}_3$ $[\text{M}+\text{H}]^+$: 296.1284, found 296.1283.

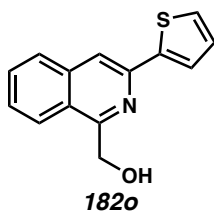


(3-(o-tolyl)isoquinolin-1-yl)methanol (182m): Compound **182m** was prepared from isoquinoline **181m** using general procedure 4 and purified by column chromatography (15% EtOAc in hexanes) to provide a white solid (130 mg, 79% yield); ^1H NMR (400

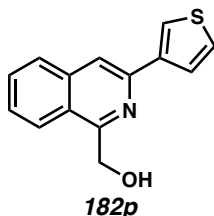
MHz, CDCl₃) δ 7.96 (dd, J = 8.4, 1.1 Hz, 1H), 7.91 (dd, J = 8.2, 1.2 Hz, 1H), 7.75 (ddd, J = 8.3, 6.9, 1.2 Hz, 1H), 7.71 (s, 1H), 7.64 (ddd, J = 8.3, 6.8, 1.3 Hz, 1H), 7.53 (d, J = 6.6 Hz, 1H), 7.39 – 7.29 (m, 3H), 5.30 (s, 2H), 5.14 (s, 1H), 2.45 (s, 3H); ¹³C NMR (100 MHz, CDCl₃) δ 156.8, 151.4, 140.1, 136.7, 136.5, 131.0, 130.8, 130.2, 128.4, 127.8, 127.6, 126.1, 123.7, 123.3, 120.0, 61.6, 20.9; IR (Neat Film, NaCl) 3389, 3057, 2932, 1626, 1573, 1502, 1455, 1402, 1377, 1330, 1087, 1069, 1008, 884, 786, 757, 727 cm⁻¹; HRMS (MM:ESI-APCI+) m/z calc'd for C₁₇H₁₆NO [M+H]⁺: 250.1226, found 250.1232.



(3-(furan-2-yl)isoquinolin-1-yl)methanol (182n): Compound **182n** was prepared from isoquinoline **181n** using general procedure 4 and purified by column chromatography (20% EtOAc in hexanes) to provide a white solid (56 mg, 52% yield): ¹H NMR (400 MHz, CDCl₃) δ 7.94 – 7.92 (m, 1H), 7.90 – 7.82 (m, 2H), 7.70 – 7.66 (m, 1H), 7.60 – 7.50 (m, 2H), 7.16 – 7.14 (m, 1H), 6.58 – 6.56 (m, 1H), 5.23 (s, 2H), 5.05 (br s, 1H, OH); ¹³C NMR (100 MHz, CDCl₃) δ 157.5, 153.7, 143.1, 140.9, 136.6, 130.9, 127.8, 127.2, 124.0, 123.3, 113.6, 112.1, 108.6, 61.3; IR (Neat Film, NaCl) 3390, 3118, 2886, 1624, 1574, 1492, 1372, 1323, 1306, 1157, 1092, 1079, 1006, 884, 836, 743 cm⁻¹; HRMS (MM:ESI-APCI+) m/z calc'd for C₁₄H₁₂NO₂ [M+H]⁺: 226.0863, found 226.0871.

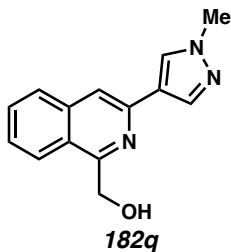


(3-(thiophen-2-yl)isoquinolin-1-yl)methanol (182o): Compound **182o** was prepared from isoquinoline **182o** (0.5 mmol) using general procedure 4 and purified by column chromatography (10% to 20% EtOAc in hexanes) to provide a white solid (46 mg, 38% yield): ^1H NMR (400 MHz, CDCl_3) δ 7.89 (s, 1H), 7.88 – 7.83 (m, 2H), 7.75 – 7.65 (m, 2H), 7.55 (ddd, $J = 8.2, 6.9, 1.2$ Hz, 1H), 7.41 (dd, $J = 5.0, 1.2$ Hz, 1H), 7.16 (dd, $J = 5.0, 3.6$ Hz, 1H), 5.25 (s, 2H), 5.02 (br s, 1H, OH); ^{13}C NMR (100 MHz, CDCl_3) δ 157.4, 144.4, 144.1, 136.8, 131.0, 128.2, 127.6, 127.2, 127.0, 124.1, 124.0, 123.3, 114.0, 61.3; IR (Neat Film, NaCl) 3382, 3066, 2868, 1621, 1589, 1573, 1501, 1452, 1402, 1329, 1084, 1006, 878, 822, 748, 701 cm^{-1} ; HRMS (MM:ESI-APCI+) m/z calc'd for $\text{C}_{14}\text{H}_{12}\text{NOS}$ $[\text{M}+\text{H}]^+$: 242.0634, found 242.0637.

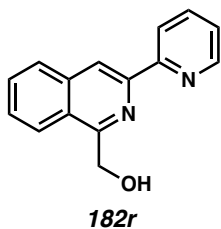


(3-(thiophen-3-yl)isoquinolin-1-yl)methanol (182p): Compound **182p** was prepared from isoquinoline **181p** (0.58 mmol) using general procedure 4 and purified by column chromatography (20% EtOAc in hexanes) to provide a white solid (127 mg, 91% yield); ^1H NMR (400 MHz, CDCl_3) δ 8.06 (dd, $J = 3.1, 1.3$ Hz, 1H), 7.94 – 7.84 (m, 3H), 7.76 (dd, $J = 5.1, 1.3$ Hz, 1H), 7.71 (ddd, $J = 8.2, 6.9, 1.1$ Hz, 1H), 7.58 (ddd, $J = 8.2, 6.9, 1.1$ Hz, 1H), 7.45 (dd, $J = 5.1, 3.0$ Hz, 1H), 5.27 (s, 2H), 5.19 (br s, 1H); ^{13}C NMR (100 MHz, CDCl_3) δ 157.4, 145.0, 141.7, 137.0, 130.9, 127.8, 127.3, 126.6, 126.0, 124.1, 123.4, 123.4, 115.6, 61.5; IR (Neat Film, NaCl) 3372, 3098, 2888, 2363, 1622, 1594,

1573, 1456, 1350, 1318, 1299, 1086, 1008, 880, 842, 793, 748, 697 cm^{-1} ; HRMS (MM:ESI-APCI+) m/z calc'd for $\text{C}_{14}\text{H}_{12}\text{NOS}$ $[\text{M}+\text{H}]^+$: 242.0634, found 242.0631.

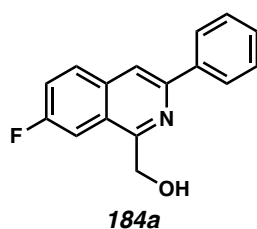


(3-(1-methyl-1H-pyrazol-4-yl)isoquinolin-1-yl)methanol (182q): Compound **182q** was prepared from isoquinoline **181q** using general procedure 4 and purified by column chromatography (70% to 80% EtOAc in hexanes + 1% NEt_3) to provide a pale beige solid (72 mg, 62% yield): ^1H NMR (400 MHz, CDCl_3) δ 8.08 – 7.95 (m, 2H), 7.85 – 7.79 (m, 2H), 7.71 – 7.59 (m, 2H), 7.53 – 7.49 (m, 1H), 5.21 (s, 2H), 3.98 (s, 3H); ^{13}C NMR (100 MHz, CDCl_3) δ 157.3, 143.2, 137.3, 136.9, 130.8, 128.8, 127.2, 126.7, 123.5, 123.2, 114.1, 61.2, 39.2; IR (Neat Film, NaCl) 3370, 3068, 2937, 1626, 1603, 1573, 1503, 1416, 1321, 1278, 1186, 1092, 1011, 845, 753, 702 cm^{-1} ; HRMS (MM:ESI-APCI+) m/z calc'd for $\text{C}_{14}\text{H}_{14}\text{N}_3\text{O}$ $[\text{M}+\text{H}]^+$: 240.1131, found 240.1123.

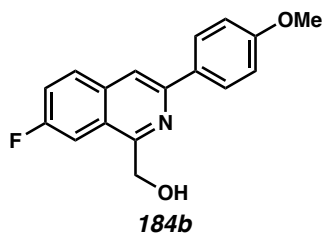


(3-(pyridin-2-yl)isoquinolin-1-yl)methanol (182r): Compound **182r** was prepared from isoquinoline **181r** using general procedure 4 and purified by column chromatography (10% to 20% acetone in CH_2Cl_2 + 1% NEt_3) to provide a pale cream solid (52 mg, 86% yield); ^1H NMR (400 MHz, CDCl_3) δ 8.74 – 8.72 (m, 2H), 8.52 (d, J = 8.2 Hz, 1H), 8.00

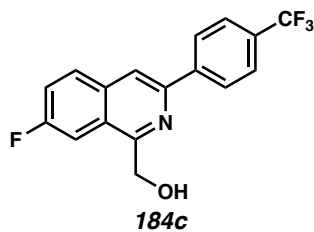
(d, $J = 8.3$ Hz, 1H), 7.94 (d, $J = 8.3$ Hz, 1H), 7.86 (td, $J = 7.8, 1.8$ Hz, 1H), 7.78 – 7.69 (m, 1H), 7.63 (ddd, $J = 8.1, 6.8, 1.2$ Hz, 1H), 7.33 (ddd, $J = 7.5, 4.8, 1.2$ Hz, 1H), 5.31 (s, 2H), 5.13 (br s, 1H, OH); ^{13}C NMR (100 MHz, CDCl_3) δ 157.2, 155.8, 149.5, 147.3, 137.2, 137.0, 130.9, 128.7, 128.1, 125.1, 123.6, 123.3, 121.1, 117.6, 61.6; IR (Neat Film, NaCl) 3390, 3048, 2359, 1622, 1583, 1474, 1428, 1333, 1309, 1166, 1087, 1009, 897, 793, 747, 681 cm^{-1} ; HRMS (MM:ESI-APCI+) m/z calc'd for $\text{C}_{15}\text{H}_{13}\text{N}_2\text{O}$ $[\text{M}+\text{H}]^+$: 237.1022, found 237.1020.



7-fluoro-3-phenylisoquinolin-1-yl)methanol (184a): Compound **184a** was prepared from isoquinoline **192a** using general procedure 4 and purified by column chromatography (10% EtOAc in hexanes) to provide a white solid (94 mg, 81% yield): ^1H NMR (400 MHz, CDCl_3) δ 8.13 (d, $J = 8.0$ Hz, 2H), 8.00 (s, 1H), 7.96 – 7.87 (m, 1H), 7.57 – 7.47 (m, 4H), 7.44 (td, $J = 6.9, 6.4, 1.4$ Hz, 1H), 5.21 (s, 2H), 5.11 (br s, 1H, OH); ^{13}C NMR (100 MHz, CDCl_3) δ 161.0 (d, $J = 250.3$ Hz), 156.8 (d, $J = 5.9$ Hz), 148.4, 138.6, 134.1, 130.5 (d, $J = 8.6$ Hz), 129.0, 126.8, 124.7 (d, $J = 8.5$ Hz), 121.4 (d, $J = 25.2$ Hz), 115.9 (d, $J = 2.0$ Hz), 107.2 (d, $J = 21.3$ Hz), 61.6; ^{19}F NMR (282 MHz, CDCl_3) δ –109.5 – –109.6 (m); IR (Neat Film, NaCl) 3393, 3063, 2878, 1594, 1579, 1506, 1417, 1392, 1321, 1232, 1185, 1085, 1015, 930, 777, 694 cm^{-1} ; HRMS (MM:ESI-APCI+) m/z calc'd for $\text{C}_{16}\text{H}_{13}\text{FNO}$ $[\text{M}+\text{H}]^+$: 254.0976, found 254.0968.

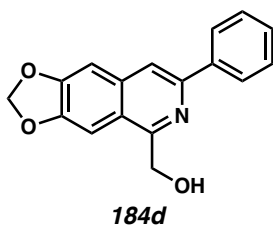


(7-fluoro-3-(4-methoxyphenyl)isoquinolin-1-yl)methanol (184b): Compound **184b** was prepared from isoquinoline **192b** using general procedure 4 and purified by column chromatography (20% EtOAc in hexanes) to provide a white solid (116 mg, 99% yield): ^1H NMR (400 MHz, CDCl_3) δ 8.10 – 8.08 (m, 2H), 7.93 (s, 1H), 7.92 – 7.88 (m, 1H), 7.52 – 7.45 (m, 2H), 7.07 – 7.02 (m, 2H), 5.21 (s, 2H), 5.14 (s, 1H), 3.90 (s, 3H); ^{13}C NMR (100 MHz, CDCl_3) δ 160.8 (d, $J = 249.0$ Hz), 160.5, 156.6 (d, $J = 5.9$ Hz), 148.3 (d, $J = 2.9$ Hz), 134.3, 131.3, 130.4 (d, $J = 8.6$ Hz), 128.1, 124.3 (d, $J = 8.2$ Hz), 121.4 (d, $J = 25.3$ Hz), 114.8 (d, $J = 1.7$ Hz), 114.4, 107.2 (d, $J = 21.3$ Hz), 61.6, 55.6; ^{19}F NMR (282 MHz, CDCl_3) δ -110.2 (ddd, $J = 8.9, 8.8, 5.5$ Hz); IR (Neat Film, NaCl) 3388, 2936, 1608, 1593, 1516, 1389, 1289, 1251, 1180, 1069, 1032, 1015, 929, 835 cm^{-1} ; HRMS (MM:ESI-APCI+) m/z calc'd for $\text{C}_{17}\text{H}_{15}\text{FNO}_2$ $[\text{M}+\text{H}]^+$: 284.1081, found 284.1074.

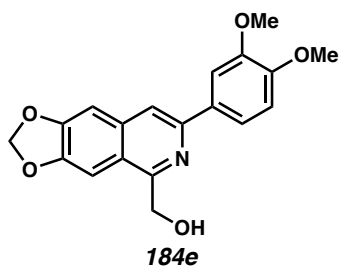


(7-fluoro-3-(4-(trifluoromethyl)phenyl)isoquinolin-1-yl)methanol (184c): Compound **184c** was prepared from isoquinoline **192c** using general procedure 4 and purified by column chromatography (10% EtOAc in hexanes) to provide a white solid (80 mg, 60% yield): ^1H NMR (400 MHz, CDCl_3) δ 8.20 (d, $J = 8.1$ Hz, 2H), 8.02 (s, 1H), 7.95 (dd, $J =$

9.8, 5.4 Hz, 1H), 7.74 (d, $J = 8.3$ Hz, 2H), 7.58 – 7.47 (m, 2H), 5.21 (s, 2H), 4.94 (br s, 1H, OH); ^{13}C NMR (100 MHz, CDCl_3) δ 161.3 (d, $J = 251.5$ Hz), 157.3 (d, $J = 5.9$ Hz), 146.8 (d, $J = 2.9$ Hz), 141.8 (d, $J = 1.5$ Hz), 133.8, 130.7 (d, $J = 8.7$ Hz), 130.7 (q, $J = 33.3$ Hz), 127.0, 125.9 (q, $J = 3.8$ Hz), 125.2 (d, $J = 8.4$ Hz), 124.3 (q, $J = 272.7$ Hz), 121.7 (d, $J = 25.3$ Hz), 116.8 (d, $J = 1.7$ Hz), 107.4 (d, $J = 21.5$ Hz), 61.7; ^{19}F NMR (282 MHz, CDCl_3) δ -62.5, -108.4 (ddd, $J = 8.7, 8.7, 5.4$ Hz); IR (Neat Film, NaCl) 3410, 2886, 1619, 1597, 1504, 1416, 1391, 1328, 1233, 1165, 1124, 1111, 1074, 1016, 931, 847, 680 cm^{-1} ; HRMS (MM:ESI-APCI+) m/z calc'd for $\text{C}_{17}\text{H}_{12}\text{F}_4\text{NO}$ $[\text{M}+\text{H}]^+$: 322.0850, found 322.0839.

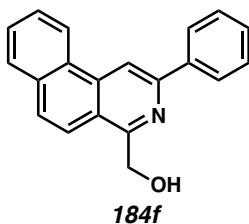


(7-phenyl-[1,3]dioxolo[4,5-g]isoquinolin-5-yl)methanol (184d): Compound **184d** was prepared from isoquinoline **192d** using general procedure 4 and purified by column chromatography (30% to 40% EtOAc in hexanes) to provide a white solid (135 mg, 83% yield): ^1H NMR (400 MHz, CDCl_3) δ 8.13 – 8.05 (m, 2H), 7.82 (s, 1H), 7.50 (m, 2H), 7.44 – 7.37 (m, 1H), 7.15 – 7.06 (m, 2H), 6.10 (s, 2H), 5.28 (br s, 1H, OH), 5.10 (s, 2H); ^{13}C NMR (100 MHz, CDCl_3) δ 154.9, 151.1, 148.6, 147.8, 138.9, 135.4, 128.8, 128.5, 126.6, 120.9, 115.9, 103.6, 101.9, 99.3, 61.4; IR (Neat Film, NaCl) 3324, 2914, 2355, 1597, 1497, 1463, 1436, 1422, 1236, 1066, 1036, 995, 940, 877, 775, 692 cm^{-1} ; HRMS (MM:ESI-APCI+) m/z calc'd for $\text{C}_{17}\text{H}_{14}\text{NO}_3$ $[\text{M}+\text{H}]^+$: 280.0968, found 280.0975.



(7-(3,4-dimethoxyphenyl)-[1,3]dioxolo[4,5-g]isoquinolin-5-yl)methanol (184e):

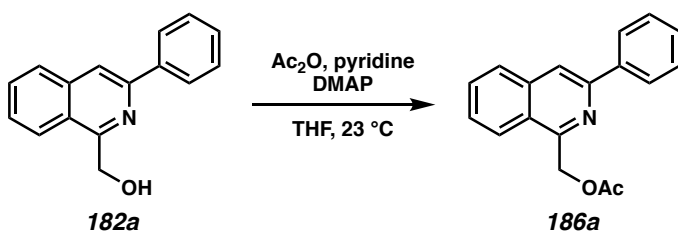
Compound **184e** was prepared from isoquinoline **192e** using general procedure 4 and purified by column chromatography (40% EtOAc in hexanes) via dry-loading to provide a pale pink solid (126 mg, 65% yield): ^1H NMR (400 MHz, CDCl_3) δ 7.77 (s, 1H), 7.69 – 7.60 (m, 2H), 7.16 – 7.07 (m, 2H), 6.99 (d, $J = 8.2$ Hz, 1H), 6.11 (s, 2H), 5.26 (br s, 1H, OH), 5.11 (s, 2H), 4.01 (s, 3H), 3.96 (s, 3H); ^{13}C NMR (100 MHz, CDCl_3) δ 154.7, 151.1, 149.7, 149.2, 148.4, 147.7, 135.5, 131.9, 120.6, 119.2, 115.1, 111.3, 109.7, 103.5, 101.8, 99.3, 61.4, 56.0, 56.0; IR (Neat Film, NaCl) 3378, 2912, 2353, 1595, 1519, 1496, 1463, 1456, 1435, 1258, 1234, 1034, 862, 730 cm^{-1} ; HRMS (MM:ESI-APCI+) m/z calc'd for $\text{C}_{19}\text{H}_{18}\text{NO}_5$ $[\text{M}+\text{H}]^+$: 340.1179, found 340.1172.



(2-phenylbenzo[1,3]isoquinolin-4-yl)methanol (184f): Compound **184f** was prepared from isoquinoline **192f** using general procedure 4 and purified by column chromatography (20% EtOAc in hexanes) to provide a white solid (51 mg, 62% yield): ^1H NMR (400 MHz, CDCl_3) δ 8.78 – 8.76 (m, 2H), 8.23 – 8.20 (m, 2H), 7.94 – 7.92 (m, 1H), 7.88 – 7.78 (m, 1H), 7.78 – 7.62 (m, 3H), 7.57 (t, $J = 7.5$ Hz, 2H), 7.48 (t, $J = 7.3$

Hz, 1H), 5.46 – 5.19 (m, 3H); ^{13}C NMR (100 MHz, CDCl_3) δ 156.3, 150.4, 139.2, 135.9, 133.5, 129.0, 129.0, 129.0, 128.8, 128.6, 127.5, 127.1, 123.5, 122.1, 120.0, 120.0, 111.7, 61.7; IR (Neat Film, NaCl) 3322, 3064, 2890, 1589, 1494, 1428, 1386, 1304, 1242, 1081, 1050, 814, 747 cm^{-1} ; HRMS (MM:ESI-APCI+) m/z calc'd for $\text{C}_{20}\text{H}_{16}\text{NO}$ $[\text{M}+\text{H}]^+$: 286.1226, found 286.1235.

4.7.2.2 Syntheses of isoquinolines with different directing groups



(3-phenylisoquinolin-1-yl)methyl acetate (186a): To a scintillation vial containing a stir bar and isoquinoline **182a** (165 mg, 0.70 mmol) in THF (7 mL, 0.1 M) was added DMAP (8.6 mg, 0.07 mmol) and pyridine (0.14 mL, 1.75 mmol). Acetic anhydride (0.1 mL, 1.05 mmol) was then added dropwise. The reaction was stirred overnight at room temperature, then diluted with Et_2O and washed with saturated aqueous NH_4Cl . The organic phase was collected, dried over Na_2SO_4 , and concentrated in vacuo. The crude product was purified by column chromatography (10% EtOAc in hexanes) to afford **186a** as a colorless viscous oil (194 mg, >99% yield): ^1H NMR (400 MHz, CDCl_3) δ 8.19 – 8.13 (m, 2H), 8.11 (dd, $J = 8.4, 1.0$ Hz, 1H), 8.07 (s, 1H), 7.92 (dt, $J = 8.3, 0.9$ Hz, 1H), 7.71 (ddd, $J = 8.2, 6.8, 1.2$ Hz, 1H), 7.61 (ddd, $J = 8.2, 6.8, 1.3$ Hz, 1H), 7.54 – 7.47 (m, 2H), 7.45 – 7.38 (m, 1H), 5.79 (s, 2H), 2.20 (s, 3H); ^{13}C NMR (100 MHz, CDCl_3) δ 170.9, 154.4, 150.2, 139.3, 137.5, 130.5, 128.9, 128.7, 128.0, 127.6, 127.1, 126.0, 124.8, 117.2, 66.1, 21.1; IR (Neat Film, NaCl) 2826, 2364, 1704, 1574, 1455, 1333, 1054, 904, 783, 764,

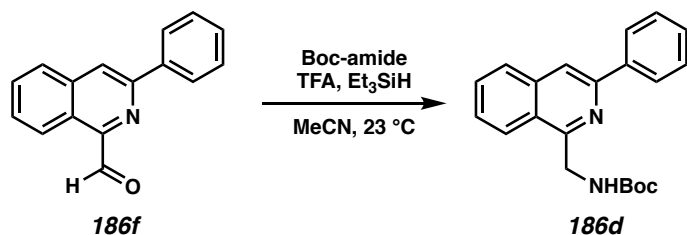
748, 719, 678 cm^{-1} ; HRMS (MM:ESI-APCI+) m/z calc'd for $\text{C}_{18}\text{H}_{16}\text{NO}_2$ $[\text{M}+\text{H}]^+$: 278.1176, found 278.1178.



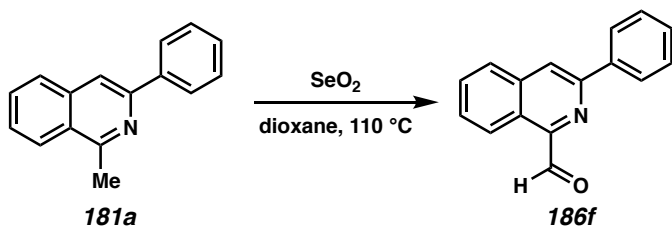
1-(methoxymethyl)-3-phenylisoquinoline (186b): To a scintillation vial containing a stir bar and isoquinoline **182a** (165 mg, 0.70 mmol) in THF (7 mL, 0.1 M) was added KO t -Bu (86 mg, 0.77 mmol) at room temperature. The resulting mixture was stirred for 5 minutes, then cooled to 0 $^\circ\text{C}$, and MeI (0.05 mL, 0.77 mmol) was added. The reaction was allowed to slowly warm to room temperature overnight, and then was quenched with saturated aqueous NH_4Cl . The organic phase was collected and the aqueous phase was extracted with EtOAc. The organic phases were combined, dried over MgSO_4 , and concentrated in vacuo. The crude product was purified by column chromatography (5% EtOAc in hexanes) to afford **186b** as a white solid (79 mg, 45% yield): ^1H NMR (400 MHz, CDCl_3) δ 8.36 (dd, $J = 8.4, 1.1$ Hz, 1H), 8.20 – 8.13 (m, 2H), 8.04 (s, 1H), 7.89 (d, $J = 8.3$ Hz, 1H), 7.69 (ddd, $J = 8.2, 6.8, 1.2$ Hz, 1H), 7.60 (ddd, $J = 8.2, 6.8, 1.3$ Hz, 1H), 7.51 (td, $J = 7.3, 6.5, 1.2$ Hz, 2H), 7.45 – 7.37 (m, 1H), 5.14 (s, 2H), 3.51 (s, 3H); ^{13}C NMR (100 MHz, CDCl_3) δ 157.1, 149.9, 139.7, 137.5, 130.4, 128.9, 128.6, 127.7, 127.3, 127.1, 126.5, 125.9, 117.1, 75.8, 58.7; IR (Neat Film, NaCl) 3058, 2918, 2817, 1622, 1590, 1500, 1455, 1338, 1188, 1104, 885, 770, 752, 695, 668 cm^{-1} ; HRMS (MM:ESI-APCI+) m/z calc'd for $\text{C}_{17}\text{H}_{16}\text{NO}$ $[\text{M}+\text{H}]^+$: 250.1226, found 250.1236.



1-((benzyloxy)methyl)-3-phenylisoquinoline (186c): This procedure has been adapted from a previous report.²⁶ To a flame-dried RBF equipped with a stir bar was added NaH (36.4 mg, 60% w/w in oil, 0.91 mmol) and THF (7 mL, 0.1 M). To this suspension, isoquinoline **182a** (165 mg, 0.70 mmol) was added. After 5 minutes of stirring at room temperature, the reaction mixture was cooled to 0 °C and BnBr (0.91 mL, 0.91 mmol) was added. The reaction was allowed to slowly warm to room temperature overnight. Silica (1 g) was then added and the solvent was evaporated under vacuum. The crude product was purified by column chromatography (5% EtOAc in hexanes) to afford **186c** as a colorless viscous oil (153 mg, 67% yield): ¹H NMR (400 MHz, CDCl₃) δ 8.39 (dd, *J* = 8.4, 1.1 Hz, 1H), 8.21 – 8.14 (m, 2H), 8.04 (s, 1H), 7.89 (d, *J* = 8.3 Hz, 1H), 7.69 (ddd, *J* = 8.2, 6.8, 1.2 Hz, 1H), 7.58 (ddd, *J* = 8.3, 6.8, 1.2 Hz, 1H), 7.51 (dd, *J* = 8.4, 6.9 Hz, 2H), 7.45 – 7.27 (m, 6H), 5.24 (s, 2H), 4.67 (s, 2H); ¹³C NMR (100 MHz, CDCl₃) δ 157.2, 149.9, 139.7, 138.2, 137.6, 130.4, 128.9, 128.6, 128.5, 128.3, 127.9, 127.7, 127.3, 127.1, 126.6, 126.1, 117.1, 73.6, 72.8; IR (Neat Film, NaCl) 3062, 2858, 1622, 1574, 1496, 1454, 1384, 1337, 1207, 1094, 1030, 885, 796, 768, 737, 696 cm⁻¹; HRMS (MM:ESI-APCI+) *m/z* calc'd for C₂₃H₂₀NO [M+H]⁺: 326.1539, found 326.1544.



***tert*-butyl ((3-phenylisoquinolin-1-yl)methyl)carbamate (186d):** This procedure has been adapted from a previous report.²⁷ To a solution of aldehyde **186f** (150 mg, 0.64 mmol) and *t*-butyl carbamate (150 mg, 1.28 mmol) in MeCN (6.5 mL, 0.1 M) were added trifluoroacetic acid (0.15 mL, 1.92 mmol) and triethylsilane (1.0 mL, 6.4 mmol). The reaction was stirred at room temperature overnight, and then quenched with saturated aqueous Na₂CO₃ and extracted with EtOAc. The combined organic phases were washed with brine, dried over Na₂SO₄, and concentrated in vacuo. The crude product was purified by column chromatography (15% EtOAc in hexanes) to afford **186d** as a white solid (160 mg, 75% yield): ¹H NMR (400 MHz, CDCl₃) δ 8.16 (d, *J* = 7.7 Hz, 2H), 8.10 (d, *J* = 8.4 Hz, 1H), 8.00 (s, 1H), 7.90 (d, *J* = 8.2 Hz, 1H), 7.70 (ddd, *J* = 8.1, 6.9, 1.1 Hz, 1H), 7.61 (ddd, *J* = 8.2, 6.9, 1.2 Hz, 1H), 7.53 (t, *J* = 7.6 Hz, 2H), 7.48 – 7.40 (m, 1H), 6.43 (br s, 1H), 5.03 (d, *J* = 4.4 Hz, 2H), 1.54 (s, 9H); ¹³C NMR (100 MHz, CDCl₃) δ 156.3, 155.0, 149.3, 139.4, 137.1, 130.6, 128.9, 128.8, 127.9, 127.6, 127.0, 125.1, 124.0, 116.3, 79.6, 43.5, 28.7; IR (Neat Film, NaCl) 3418, 2976, 1713, 1622, 1574, 1487, 1367, 1251, 1167, 1056, 882, 765, 695 cm⁻¹; HRMS (MM:ESI-APCI+) *m/z* calc'd for C₂₁H₂₃N₂O₂ [M+H]⁺: 335.1754, found 335.1760.

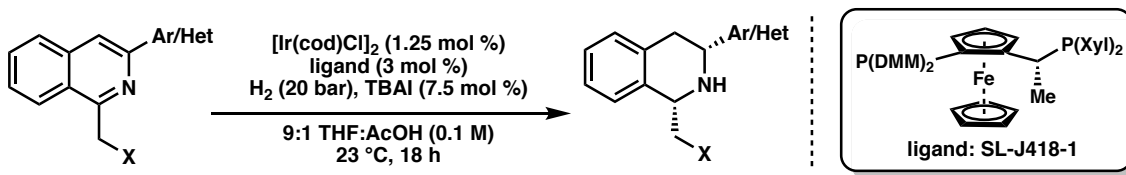


3-phenylisoquinoline-1-carbaldehyde (186f): To a Schlenk flask containing a stir bar was added SeO₂ (140 mg, 1.26 mmol) and isoquinoline **181a** (138 mg, 0.63 mmol) in 1,4-dioxane (13 mL, 0.05 M). The reaction vial was then sealed and heated to 110 °C

while stirring for 2 hours. The reaction was then cooled to room temperature and filtered through celite rinsing with EtOAc. The crude product was then purified by column chromatography (5% EtOAc in hexanes) to afford **186f** as a pale yellow solid (1.32 g, 96% yield): ^1H NMR (400 MHz, CDCl_3) δ 10.50 (s, 1H), 9.32 (d, J = 8.2 Hz, 1H), 8.31 (s, 1H), 8.24 (d, J = 8.1 Hz, 2H), 7.97 (d, J = 7.3 Hz, 1H), 7.84 – 7.67 (m, 2H), 7.56 (t, J = 7.5 Hz, 2H), 7.47 (t, J = 7.4 Hz, 1H); ^{13}C NMR (100 MHz, CDCl_3) δ 196.2, 150.8, 149.7, 138.5, 138.1, 131.0, 129.9, 129.3, 129.1, 127.5, 127.1, 125.9, 125.5, 121.3; IR (Neat Film, NaCl) 2826, 2364, 1704, 1574, 1455, 1333, 1054, 904, 783, 764, 678 cm^{-1} ; HRMS (MM:ESI-APCI+) m/z calc'd for $\text{C}_{16}\text{H}_{12}\text{NO}$ $[\text{M}+\text{H}]^+$: 234.0913, found 234.0914.

4.7.2.3 Hydrogenation reactions

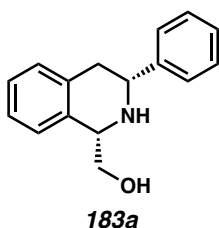
General Procedure 5: Hydrogenation Reactions



To an oven-dried 20-mL scintillation vial equipped with a stir bar and isoquinoline (0.2 mmol) was capped with a PTFE-lined septum and pierced with two 21-gauge green needles. The vials were then placed in a Parr bomb and brought into the glovebox, with the exception of the pressure gauge. A layer of plastic wrap and a rubber band were also brought in to seal the top of the bomb. In a nitrogen-filled glovebox, a solution of the ligand (SL-J418-1) (4.53 mg, 0.006 mmol per reaction) and $[\text{Ir}(\text{cod})\text{Cl}]_2$ (1.68 mg, 0.0025 mmol per reaction) in THF (1.8 mL per reaction) was prepared and allowed to stand for 10 minutes. Meanwhile, a solution of TBAI (5.54 mg, 0.015 mmol per reaction) in AcOH (0.2 mL per reaction) was prepared in a 1-dram vial, and 0.2 mL

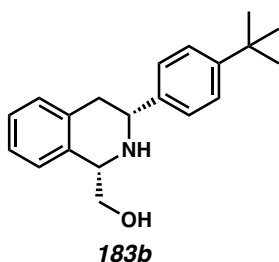
of the solution was added to each reaction vial via a syringe. Afterwards, 1.8 mL of the homogeneous iridium catalyst solution was added to each reaction vial via a syringe. After re-capping the vials with caps equipped with needles, the reactions were placed in the bomb and the top was covered tightly with plastic wrap secured by a rubber band. The bomb was then removed from the glovebox, and the pressure gauge was quickly screwed in place and tightened. The bomb was charged to 5-10 bar H₂ and slowly released. This process was repeated two more times, before charging the bomb to 20 bar of H₂ (or 60 bar H₂). The bomb was then left stirring at 200 rpm at room temperature (or placed in an oil bath and heated to 60 °C) for 18 hours. Then, the bomb was removed from the stir plate and the hydrogen pressure was vented. The reaction vials were removed from the bomb and each solution was basified by the addition of saturated aqueous K₂CO₃. The layers were separated, and the aqueous layer was extracted with EtOAc. The combined organics layers were then dried over Na₂SO₄, and concentrated in vacuo. The product was then purified by column chromatography to furnish the product as an inseparable mixture of diastereomers.

Please note that the NMR data listed is for the major diastereomer, and that the provided spectra for the following compounds reflect the inseparable mixture of *cis*- and *trans*-products. The enantiomeric excess was determined by chiral SFC analysis of the Cbz-protected amine (see Table 4.4, Section 4.7.4). The absolute configuration was determined for compound **183p** via x-ray crystallographic analysis. Absolute configuration of compound **187e** were determined using vibrational circular dichroism (VCD), *vide infra*. The absolute configuration for all other products has been inferred by analogy.



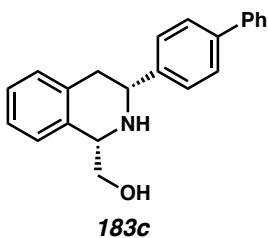
((1*S*,3*R*)-3-phenyl-1,2,3,4-tetrahydroisoquinolin-1-yl)methanol (183a): Compound **183a** was prepared from isoquinoline **182a** using general procedure 5 and purified by column chromatography (5% MeOH in CH₂Cl₂) to provide a tan solid as a mixture of diastereomers (47 mg, 98% yield) (dr = 15.7:1); 92% ee for major diastereomer; [α]_D²⁵ +110.2 (*c* 1.02, CHCl₃); *Cis*-diastereomer: ¹H NMR (400 MHz, CDCl₃) δ 7.50 – 7.43 (m, 2H), 7.41 – 7.34 (m, 2H), 7.34 – 7.28 (m, 1H), 7.25 – 7.17 (m, 3H), 7.15 – 7.10 (m, 1H), 4.43 – 4.41 (m, 1H), 4.10 (dd, *J* = 11.1, 3.5 Hz, 1H), 4.02 (dd, *J* = 10.8, 3.3 Hz, 1H), 3.90 (dd, *J* = 10.9, 5.4 Hz, 1H), 3.02 (ddt, *J* = 15.9, 11.1, 1.4 Hz, 1H), 2.90 (dd, *J* = 15.7, 3.5 Hz, 1H); ¹³C NMR (100 MHz, CDCl₃) δ 144.3, 136.7, 134.9, 129.3, 128.8, 127.7, 126.8, 126.7, 126.5, 125.5, 66.7, 58.7, 57.7, 39.0; IR (Neat Film, NaCl) 3296, 3060, 2910, 2360, 1494, 1455, 1314, 1116, 1036, 909, 742, 700 cm⁻¹; HRMS (MM:ESI-APCI+) *m/z* calc'd for C₁₆H₁₈NO [M+H]⁺: 240.1383, found 240.1385; SFC Conditions: 45% IPA, 3.5 mL/min, Chiralpak AD-H column, λ = 210 nm, *t*_R (min): major = 2.34, minor = 4.02.

Trans-diastereomer: ¹H NMR (400 MHz, CDCl₃) δ 7.49 – 7.43 (m, 2H), 7.42 – 7.38 (m, 2H), 7.36 – 7.27 (m, 1H), 7.26 – 7.10 (m, 4H), 4.23 (dd, *J* = 10.5, 4.8 Hz, 1H), 4.16 (dd, *J* = 11.2, 3.9 Hz, 1H), 3.80 (dd, *J* = 10.8, 4.8 Hz, 1H), 3.71 (t, *J* = 10.7 Hz, 1H), 3.07 (dd, *J* = 16.4, 3.9 Hz, 1H), 2.95 (dd, *J* = 15.9, 11.2 Hz, 1H); ¹³C NMR (100 MHz, CDCl₃) δ 143.5, 135.5, 134.7, 129.5, 128.8, 127.5, 127.0, 126.7, 126.6, 126.4, 63.8, 57.4, 50.7, 36.8.



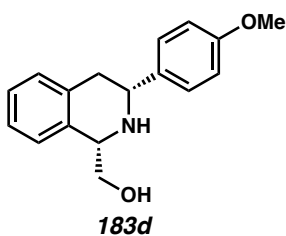
((1*S*,3*R*)-3-(4-(*tert*-butyl)phenyl)-1,2,3,4-tetrahydroisoquinolin-1-yl)methanol (183b):

Compound **183b** was prepared from isoquinoline **182b** using general procedure 5 and purified by column chromatography (50% EtOAc in hexanes) to provide a tan solid as a mixture of diastereomers (51 mg, 87% yield) (dr = 13.3:1); 91% ee for major diastereomer; $[\alpha]_D^{25} +78.8$ (c 1.03, CHCl_3); Major diastereomer: ^1H NMR (400 MHz, CDCl_3) δ 7.42 – 7.38 (m, 4H), 7.26 – 7.21 (m, 2H), 7.21 – 7.17 (m, 1H), 7.12 (d, J = 7.7 Hz, 1H), 4.42 – 4.40 (m, 1H), 4.08 (dd, J = 11.2, 3.4 Hz, 1H), 4.01 (dd, J = 10.8, 3.3 Hz, 1H), 3.89 (dd, J = 10.8, 5.4 Hz, 1H), 3.03 (dd, J = 15.8, 11.2 Hz, 1H), 2.89 (dd, J = 15.7, 3.4 Hz, 1H), 1.34 (s, 9H); ^{13}C NMR (100 MHz, CDCl_3) δ 150.7, 141.2, 136.7, 135.0, 129.3, 126.7, 126.5, 126.5, 125.7, 125.5, 66.6, 58.7, 57.3, 38.8, 34.7, 31.5; IR (Neat Film, NaCl) 3318, 2961, 2868, 1494, 1454, 1362, 1312, 1270, 1116, 1038, 820, 743 cm^{-1} ; HRMS (MM:ESI-APCI+) m/z calc'd for $\text{C}_{20}\text{H}_{26}\text{NO}$ $[\text{M}+\text{H}]^+$: 296.2009, found 296.2005; SFC Conditions: 45% IPA, 3.5 mL/min, Chiralpak AD-H column, λ = 210 nm, t_R (min): major = 1.81, minor = 2.73.



((1*S*,3*R*)-3-([1,1'-biphenyl]-4-yl)-1,2,3,4-tetrahydroisoquinolin-1-yl)methanol (183c):

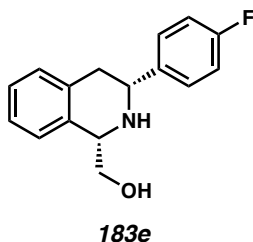
Compound **183c** was prepared from isoquinoline **182c** using general procedure 5 and purified by column chromatography (50% EtOAc in hexanes) to provide a tan solid as a mixture of diastereomers (50 mg, 79% yield) (dr = 9.0:1); 92% ee for major diastereomer; $[\alpha]_{\text{D}}^{25} +73.2$ (*c* 1.03, CHCl₃); Major diastereomer: ¹H NMR (400 MHz, CDCl₃) δ 7.65 – 7.58 (m, 4H), 7.55 – 7.53 (m, 2H), 7.47 – 7.44 (m, 2H), 7.39 – 7.32 (m, 1H), 7.28 – 7.16 (m, 3H), 7.15 (d, *J* = 6.2 Hz, 1H), 4.46 – 4.44 (m, 1H), 4.15 (dd, *J* = 11.2, 3.4 Hz, 1H), 4.04 (dd, *J* = 10.9, 3.3 Hz, 1H), 3.91 (dd, *J* = 10.9, 5.5 Hz, 1H), 3.12 – 3.00 (m, 1H), 2.94 (dd, *J* = 15.6, 3.4 Hz, 1H); ¹³C NMR (100 MHz, CDCl₃) δ 143.2, 141.0, 140.7, 136.5, 134.9, 129.3, 128.9, 127.5, 127.4, 127.3, 127.2, 126.8, 126.6, 125.5, 66.6, 58.7, 57.4, 38.9; IR (Neat Film, NaCl) 3318, 3029, 2924, 2365, 1487, 1455, 1312, 1218, 1112, 1038, 833, 763, 748, 699 cm⁻¹; HRMS (MM:ESI-APCI+) *m/z* calc'd for C₂₂H₂₂NO [M+H]⁺: 316.1696, found 316.1686; SFC Conditions: 45% IPA, 3.5 mL/min, Chiralpak AD-H column, λ = 210 nm, *t_R* (min): major = 4.08, minor = 5.18.



((1*S*,3*R*)-3-(4-methoxyphenyl)-1,2,3,4-tetrahydroisoquinolin-1-yl)methanol (183d):

Compound **183d** was prepared from isoquinoline **182d** using general procedure 5 and purified by column chromatography (50% to 60% EtOAc in hexanes + 1% NEt₃) to provide a pale yellow solid as a mixture of diastereomers (40 mg, 75% yield) (dr = 13.3:1); 92% ee for major diastereomer; $[\alpha]_{\text{D}}^{25} +69.3$ (*c* 1.01, CHCl₃); Major diastereomer: ¹H NMR (400 MHz, CDCl₃) δ 7.39 – 7.36 (m, 2H), 7.24 – 7.15 (m, 3H),

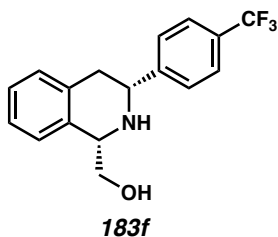
7.12 (d, $J = 7.6$ Hz, 1H), 6.94 – 6.90 (m, 2H), 4.41 – 4.39 (m, 1H), 4.07 – 3.97 (m, 2H), 3.86 (dd, $J = 10.9, 5.9$ Hz, 1H), 3.83 (s, 3H), 3.06 – 2.95 (m, 1H), 2.86 (dd, $J = 15.7, 3.4$ Hz, 1H); ^{13}C NMR (100 MHz, CDCl_3) δ 159.0, 136.6, 136.3, 134.8, 129.2, 127.8, 126.6, 126.3, 125.3, 114.0, 66.5, 58.6, 57.0, 55.4, 38.8; IR (Neat Film, NaCl) 3342, 2929, 2835, 1612, 1514, 1494, 1453, 1302, 1250, 1176, 1108, 1036, 824, 801, 743 cm^{-1} ; HRMS (MM:ESI-APCI+) m/z calc'd for $\text{C}_{17}\text{H}_{20}\text{NO}_2$ $[\text{M}+\text{H}]^+$: 270.1489, found 270.1486; SFC Conditions: 45% IPA, 2.5 mL/min, Chiralpak AD-H column, $\lambda = 210$ nm, t_{R} (min): major = 2.59, minor = 3.61.



((1*S*,3*R*)-3-(4-fluorophenyl)-1,2,3,4-tetrahydroisoquinolin-1-yl)methanol (183e):

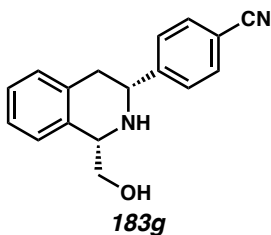
Compound **183e** was prepared from isoquinoline **182e** using general procedure 5 and purified by column chromatography (40% EtOAc in hexanes + 1% NEt_3) to provide a pale yellow solid as a mixture of diastereomers (51 mg, 99% yield) (dr = 10.1:1); 93% ee for major diastereomer; $[\alpha]_{\text{D}}^{25} +79.2$ (c 1.00, CHCl_3); Major diastereomer: ^1H NMR (400 MHz, CDCl_3) δ 7.45 – 7.41 (m, 2H), 7.24 – 7.18 (m, 3H), 7.12 (d, $J = 6.9$ Hz, 1H), 7.08 – 7.04 (m, 2H), 4.42 – 4.40 (m, 1H), 4.08 (dd, $J = 11.0, 3.5$ Hz, 1H), 4.02 (dd, $J = 10.8, 3.3$ Hz, 1H), 3.88 (dd, $J = 10.9, 5.5$ Hz, 1H), 3.03 – 2.91 (m, 1H), 2.87 (dd, $J = 15.7, 3.5$ Hz, 1H); ^{13}C NMR (100 MHz, CDCl_3) δ 162.3 (d, $J = 245.5$ Hz), 140.0 (d, $J = 3.0$ Hz), 136.4, 134.8, 129.3, 128.4 (d, $J = 7.9$ Hz), 126.8, 126.6, 125.5, 115.5 (d, $J = 21.2$ Hz), 66.7, 58.6, 57.1, 39.1; ^{19}F NMR (282 MHz, CDCl_3) δ –115.0 – –115.1 (m); IR (Neat Film,

NaCl) 3310, 3069, 2924, 2828, 1605, 1511, 1494, 1454, 1225, 1158, 1063, 1040, 844, 826, 744 cm^{-1} ; HRMS (MM:ESI-APCI+) m/z calc'd for $\text{C}_{16}\text{H}_{17}\text{FNO}$ $[\text{M}+\text{H}]^+$: 258.1289, found 258.1286; SFC Conditions: 45% IPA, 2.5 mL/min, Chiralpak AD-H column, λ = 210 nm, t_R (min): major = 1.93, minor = 2.87.



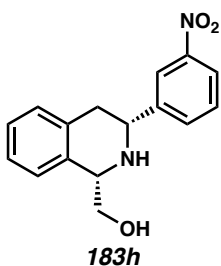
((1*S*,3*R*)-3-(4-(trifluoromethyl)phenyl)-1,2,3,4-tetrahydroisoquinolin-1-yl)methanol

(183f): Compound **183f** was prepared from isoquinoline **182f** using general procedure 5 and purified by column chromatography (30% EtOAc in hexanes + 1% NEt_3) to provide a yellow solid as a mixture of diastereomers (49 mg, 80% yield) (dr = 4.6:1); 92% ee for major diastereomer; $[\alpha]_D^{25}$ +35.5 (c 1.01, CHCl_3); Major diastereomer: ^1H NMR (400 MHz, CDCl_3) δ 7.57 – 7.55 (m, 2H, integration overlapped with minor diastereomer), 7.51 (d, J = 8.3 Hz, 2H), 7.18 – 7.10 (m, 3H), 7.10 – 7.03 (m, 1H), 4.36 – 4.34 (m, 1H), 4.08 (dd, J = 10.6, 4.0 Hz, 1H), 3.97 (dd, J = 10.8, 3.3 Hz, 1H), 3.81 (dd, J = 10.9, 5.8 Hz, 1H), 2.95 – 2.78 (m, 2H); ^{13}C NMR (100 MHz, CDCl_3) δ 148.3, 136.0, 134.7, 129.9 (q, J = 32.3 Hz), 129.3, 127.2, 126.9, 126.7, 125.7 (q, J = 3.8 Hz), 125.5, 124.3 (q, J = 272.2 Hz), 66.6, 58.4, 57.3, 38.8; ^{19}F NMR (282 MHz, CDCl_3) δ –115.1 (qd, J = 8.7, 5.6 Hz); IR (Neat Film, NaCl) 3304, 2917, 1621, 1418, 1325, 1166, 1123, 1068, 1018, 844, 745 cm^{-1} ; HRMS (MM:ESI-APCI+) m/z calc'd for $\text{C}_{17}\text{H}_{17}\text{F}_3\text{NO}$ $[\text{M}+\text{H}]^+$: 308.1257, found 308.1265; SFC Conditions: 25% IPA, 2.5 mL/min, Chiralpak AD-H column, λ = 210 nm, t_R (min): major = 3.11 minor = 5.54.



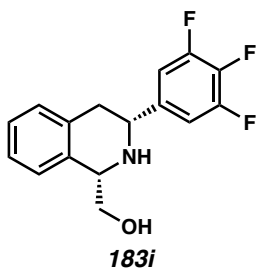
4-((1*S*,3*R*)-1-(hydroxymethyl)-1,2,3,4-tetrahydroisoquinolin-3-yl)benzonitrile

(183g): Compound **183g** was prepared from isoquinoline **182g** using general procedure 5 and purified by column chromatography (30% EtOAc in CH₂Cl₂ + 1% NEt₃) to provide a pale tan solid as a mixture of diastereomers (44 mg, 83% yield) (dr = 2.4:1); 82% ee for major diastereomer; $[\alpha]_{\text{D}}^{25} +57.4$ (*c* 1.00, CHCl₃); Major diastereomer: ¹H NMR (400 MHz, CDCl₃) δ 7.69 – 7.66 (m, 2H), 7.60 – 7.57 (m, 2H), 7.26 – 7.17 (m, 3H, integration overlapped with minor diastereomer), 7.16 – 7.12 (m, 1H), 4.43 – 4.41 (m, 1H), 4.16 (dd, *J* = 10.0, 4.6 Hz, 1H), 4.06 (dd, *J* = 10.9, 3.3 Hz, 1H), 3.89 (dd, *J* = 10.9, 5.8 Hz, 1H), 2.99 – 2.84 (m, 2H); ¹³C NMR (100 MHz, CDCl₃) δ 149.6, 135.7, 134.5, 132.6, 129.2, 127.6, 126.9, 126.8, 125.5, 118.9, 111.5, 66.7, 58.5, 57.4, 38.8; IR (Neat Film, NaCl) 3314, 3060, 2925, 2227, 1608, 1494, 1454, 1311, 1115, 1040, 910, 846, 826, 780, 740 cm⁻¹; HRMS (MM:ESI-APCI+) *m/z* calc'd for C₁₇H₁₇N₂O [M+H]⁺: 265.1335, found 265.1336; SFC Conditions: 45% IPA, 3.5 mL/min, Chiralpak AD-H column, λ = 210 nm, *t_R* (min): major = 2.03, minor = 3.33.



((1*S*,3*R*)-3-(3-nitrophenyl)-1,2,3,4-tetrahydroisoquinolin-1-yl)methanol (183h):

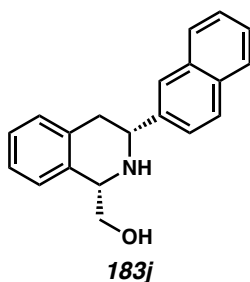
Compound **183h** was prepared from isoquinoline **182h** using general procedure 5 and purified by column chromatography (0% to 2% MeOH in CH₂Cl₂) to provide a pale yellow solid as a mixture of diastereomers (44 mg, 78% yield) (dr = 3.2:1); 86% ee for major diastereomer; $[\alpha]_{\text{D}}^{25} +54.4$ (*c* 1.02, CHCl₃); Major diastereomer: ¹H NMR (400 MHz, CDCl₃) δ 8.34 (s, 1H), 8.15 (d, *J* = 8.2 Hz, 1H), 7.81 (d, *J* = 8.1 Hz, 1H), 7.62 – 7.47 (m, 1H), 7.25 – 7.07 (m, 4H, integration overlapped with minor diastereomer), 4.43 – 4.41 (m, 1H), 4.20 (dd, *J* = 9.2, 5.4 Hz, 1H), 4.07 (dd, *J* = 10.9, 3.2 Hz, 1H), 3.91 – 3.83 (m, 1H), 3.15 – 3.02 (m, 1H), 2.98 – 2.91 (m, 2H); ¹³C NMR (100 MHz, CDCl₃) δ 148.7, 146.5, 135.7, 134.6, 133.2, 129.8, 129.4, 127.0, 126.9, 125.6, 122.9, 122.0, 66.8, 58.7, 57.2, 38.9; IR (Neat Film, NaCl) 3388, 2924, 1635, 1531, 1495, 1454, 1350, 1220, 1117, 1038, 802, 781, 748, 738, 682 cm⁻¹; HRMS (MM:ESI-APCI+) *m/z* calc'd for C₁₆H₁₇N₂O₃ [M+H]⁺: 285.1234, found 285.1234; SFC Conditions: 45% IPA, 3.5 mL/min, Chiralpak AD-H column, λ = 210 nm, *t_R* (min): major = 2.45, minor = 3.23.



((1*S*,3*R*)-3-(3,4,5-trifluorophenyl)-1,2,3,4-tetrahydroisoquinolin-1-yl)methanol

(183i): Compound **183i** was prepared from isoquinoline **182i** using general procedure 5 and purified by column chromatography (5% to 10% EtOAc in CH₂Cl₂ + 1% NEt₃) to provide a pale yellow solid as a mixture of diastereomers (55 mg, 94% yield) (dr = 3.5:1); 89% ee for major diastereomer; $[\alpha]_{\text{D}}^{25} +61.6$ (*c* 1.02, CHCl₃); Major diastereomer: ¹H

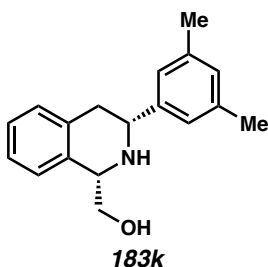
NMR (400 MHz, CDCl₃) δ 7.25 – 7.18 (m, 2H, integration overlapped with minor diastereomer), 7.16 – 7.08 (m, 4H), 4.40 – 4.38 (m, 1H), 4.09 – 4.00 (m, 2H), 3.87 (dd, J = 10.9, 5.9 Hz, 1H), 2.88 (d, J = 8.4 Hz, 2H); ¹³C NMR (100 MHz, CDCl₃), complicated spectrum due to mixture of diastereomers and C–F coupling, multiplicities listed to the best of our ability δ 151.4 (ddd, J = 250.1, 9.8, 3.6 Hz), 139.0 (dt, J = 251.0, 15.5 Hz), 135.5, 134.4, 129.4, 129.2, 126.9, 126.8, 125.5, 110.9 – 110.6 (m), 66.7, 58.5, 56.2, 38.8; ¹⁹F NMR (282 MHz, CDCl₃) δ –133.6 – –134.4 (m), –161.8 – –162.0 (m); IR (Neat Film, NaCl) 3307, 2928, 1621, 1532, 1454, 1372, 1340, 1235, 1043, 866, 804, 748, 698 cm^{–1}; HRMS (MM:ESI-APCI+) m/z calc'd for C₁₆H₁₅F₃NO [M+H]⁺: 294.1100, found 294.1095; SFC Conditions: 40% IPA, 2.5 mL/min, Chiralpak AD-H column, λ = 210 nm, t_R (min): major = 1.67, minor = 2.20.



((1*S*,3*R*)-3-(naphthalen-2-yl)-1,2,3,4-tetrahydroisoquinolin-1-yl)methanol (183j):

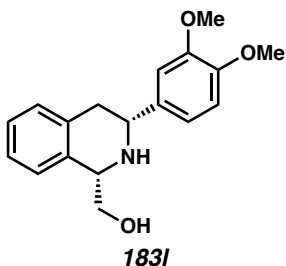
Compound **183j** was prepared from isoquinoline **182j** using general procedure 5 and purified by column chromatography (30% EtOAc in hexanes + 1% NEt₃) to provide a pale yellow solid as a single diastereomer (49 mg, 80% yield); 95% ee; [α]_D²⁵ +90.7 (c 1.00, CHCl₃); ¹H NMR (400 MHz, CDCl₃) δ 7.90 (s, 1H), 7.88 – 7.84 (m, 3H), 7.60 (dd, J = 8.5, 1.8 Hz, 1H), 7.53 – 7.45 (m, 2H), 7.28 – 7.20 (m, 3H), 7.15 (d, J = 6.8 Hz, 1H), 4.48 – 4.46 (m, 1H), 4.27 (dd, J = 11.1, 3.5 Hz, 1H), 4.06 (dd, J = 10.9, 3.3 Hz, 1H), 3.94

(dd, $J = 10.8, 5.4$ Hz, 1H), 3.14 – 3.07 (m, 1H), 2.98 (dd, $J = 15.7, 3.5$ Hz, 1H); ^{13}C NMR (100 MHz, CDCl_3) δ 141.8, 136.7, 135.1, 133.7, 133.2, 129.4, 128.6, 128.1, 127.9, 126.9, 126.7, 126.4, 126.1, 125.6, 125.3, 66.8, 58.8, 57.9, 39.1; IR (Neat Film, NaCl) 3056, 2917, 2356, 1602, 1494, 1454, 1425, 1366, 1314, 1276, 1112, 1047, 862, 820, 743 cm^{-1} ; HRMS (MM:ESI-APCI+) m/z calc'd for $\text{C}_{20}\text{H}_{20}\text{NO}$ $[\text{M}+\text{H}]^+$: 290.1539, found 290.1540; SFC Conditions: 45% IPA, 3.5 mL/min, Chiralpak AD-H column, $\lambda = 210$ nm, t_{R} (min): major = 3.61, minor = 5.81.



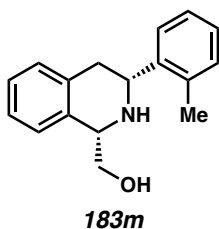
((1S,3R)-3-(3,5-dimethylphenyl)-1,2,3,4-tetrahydroisoquinolin-1-yl)methanol (183k):

Compound **183k** was prepared from isoquinoline **182k** using general procedure 5 and purified by column chromatography (30% EtOAc in hexanes + 1% NEt_3) to provide a pale yellow solid as a single diastereomer (49 mg, 80% yield); 92% ee; $[\alpha]_{\text{D}}^{25} +93.5$ (c 0.98, CHCl_3): ^1H NMR (400 MHz, CDCl_3) δ 7.25 – 7.16 (m, 3H), 7.12 (d, $J = 6.5$ Hz, 1H), 7.07 (s, 2H), 6.95 (s, 1H), 4.41 – 4.39 (m, 1H), 4.02 (dd, $J = 10.9, 3.3$ Hz, 2H), 3.90 (dd, $J = 10.8, 5.4$ Hz, 1H), 3.04 – 3.00 (m, 1H), 2.88 (dd, $J = 15.8, 3.4$ Hz, 1H), 2.34 (s, 6H); ^{13}C NMR (100 MHz, CDCl_3) δ 144.2, 138.3, 136.8, 135.0, 129.3, 126.7, 126.4, 125.4, 124.6, 66.6, 58.7, 57.6, 38.9, 21.5; IR (Neat Film, NaCl) 3318, 3014, 2916, 1607, 1494, 1454, 1313, 1117, 1038, 854, 782, 746, 725 cm^{-1} ; HRMS (MM:ESI-APCI+) m/z calc'd for $\text{C}_{18}\text{H}_{22}\text{NO}$ $[\text{M}+\text{H}]^+$: 268.1696, found 268.1702; SFC Conditions: 45% IPA, 3.5 mL/min, Chiralpak AD-H column, $\lambda = 210$ nm, t_{R} (min): major = 1.95, minor = 3.02.



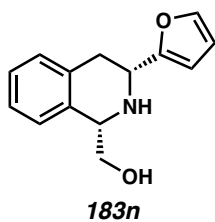
((1*S*,3*R*)-3-(3,4-dimethoxyphenyl)-1,2,3,4-tetrahydroisoquinolin-1-yl)methanol

(183l): Compound **183l** was prepared from isoquinoline **182l** using general procedure 5 and purified by column chromatography (1% MeOH in CH₂Cl₂ + 1% NEt₃) to provide a pale yellow solid as a single diastereomer (49 mg, 80% yield); 88% ee; [α]_D²⁵ +62.4 (*c* 1.00, CHCl₃); ¹H NMR (400 MHz, CDCl₃) δ 7.22 – 7.16 (m, 3H), 7.12 (d, *J* = 6.7 Hz, 1H), 7.04 – 6.94 (m, 2H), 6.87 – 6.84 (m, 1H), 4.38 – 4.36 (m, 1H), 4.01 (dt, *J* = 11.2, 4.0 Hz, 2H), 3.90 (s, 3H), 3.88 (s, 3H), 3.84 (dd, *J* = 11.0, 6.0 Hz, 1H), 3.08 – 3.00 (m, 1H), 2.87 (dd, *J* = 15.8, 3.3 Hz, 1H); ¹³C NMR (100 MHz, CDCl₃) δ 149.2, 148.5, 136.5, 136.4, 134.6, 129.3, 126.7, 126.4, 125.3, 119.0, 111.2, 110.0, 66.3, 58.8, 57.6, 56.1, 38.7; IR (Neat Film, NaCl) 3332, 2934, 2832, 1593, 1518, 1494, 1454, 1264, 1238, 1141, 1028, 745, 720 cm⁻¹; HRMS (MM:ESI-APCI+) *m/z* calc'd for C₁₈H₂₂NO₃ [M+H]⁺: 300.1594, found 300.1600; SFC Conditions: 45% IPA, 3.5 mL/min, Chiralpak AD-H column, λ = 210 nm, *t*_R (min): major = 2.28, minor = 2.93.



((1*S*,3*R*)-3-(*o*-tolyl)-1,2,3,4-tetrahydroisoquinolin-1-yl)methanol (183m): Compound **183m** was prepared from isoquinoline **182m** using general procedure 5 and purified by

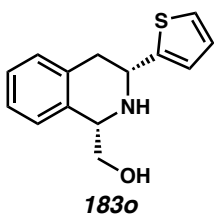
column chromatography (30% EtOAc in hexanes + 1% NEt₃) to provide a pale beige solid as a mixture of diastereomers (49 mg, 80% yield) (dr = 10.1:1); 49% ee from major diastereomer; $[\alpha]_D^{25} +53.7$ (*c* 1.01, CHCl₃): ¹H NMR (400 MHz, CDCl₃) δ 7.60 (d, *J* = 7.1 Hz, 1H), 7.29 – 7.26 (m, 1H), 7.26 – 7.17 (m, 5H), 7.14 (d, *J* = 7.3 Hz, 1H), 4.44 – 4.42 (m, 1H), 4.32 (dd, *J* = 10.9, 3.5 Hz, 1H), 4.04 (dd, *J* = 10.8, 3.2 Hz, 1H), 3.92 (dd, *J* = 10.8, 5.3 Hz, 1H), 3.03 – 2.92 (m, 1H), 2.88 (dd, *J* = 15.8, 3.5 Hz, 1H), 2.39 (s, 3H); ¹³C NMR (100 MHz, CDCl₃) δ 142.2, 136.9, 135.2, 135.0, 130.6, 129.4, 127.3, 126.7, 126.5, 125.6, 125.5, 66.6, 58.9, 53.4, 37.7, 19.5; IR (Neat Film, NaCl) 3318, 3022, 2925, 2354, 1492, 1454, 1316, 1117, 1037, 864, 751, 743, 727 cm⁻¹; HRMS (MM:ESI-APCI+) *m/z* calc'd for C₁₇H₂₀NO [M+H]⁺: 254.1539, found 254.1539; SFC Conditions: 30% IPA, 2.5 mL/min, Chiralpak AD-H column, λ = 210 nm, *t*_R (min): major = 5.91, minor = 6.39.



((1*S*,3*R*)-3-(furan-2-yl)-1,2,3,4-tetrahydroisoquinolin-1-yl)methanol (183n):

Compound **183n** was prepared from isoquinoline **182n** using general procedure 5 and purified by column chromatography (40% EtOAc in hexanes + 1% NEt₃) to provide a pale yellow solid as a mixture of diastereomers (34 mg, 74% yield) (dr = 3.3:1); 92% ee for major diastereomer; $[\alpha]_D^{25} +35.5$ (*c* 1.00, CHCl₃); Major diastereomer: ¹H NMR (400 MHz, CDCl₃) δ 7.41 – 7.39 (m, 1H), 7.24 – 7.14 (m, 4H, integration overlapped with minor diastereomer), 6.37 (dd, *J* = 3.3, 1.9 Hz, 1H), 6.28 (d, *J* = 3.2 Hz, 1H), 4.37 – 4.35 (m, 1H), 4.20 (dd, *J* = 11.0, 3.7 Hz, 1H), 4.03 (dd, *J* = 11.0, 3.3 Hz, 1H), 3.86 – 3.75 (m,

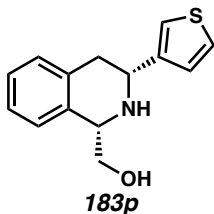
1H), 3.18 – 3.05 (m, 1H), 3.05 – 2.95 (m, 1H); ¹³C NMR (100 MHz, CDCl₃) δ 141.8, 135.5, 134.7, 129.4, 126.9, 126.7, 126.5, 125.3, 110.2, 105.3, 66.2, 57.9, 50.7, 34.5; IR (Neat Film, NaCl) 3304, 2920, 1495, 1454, 1316, 1146, 1114, 1062, 1037, 1009, 883, 740 cm⁻¹; HRMS (MM:ESI-APCI+) *m/z* calc'd for C₁₄H₁₆NO₂ [M+H]⁺: 230.1176, found 230.1181; SFC Conditions: 35% IPA, 2.5 mL/min, Chiralpak OJ-H column, λ = 210 nm, *t*_R (min): major = 1.52, minor = 1.82.



((1*S*,3*R*)-3-(thiophen-2-yl)-1,2,3,4-tetrahydroisoquinolin-1-yl)methanol (183o**):**

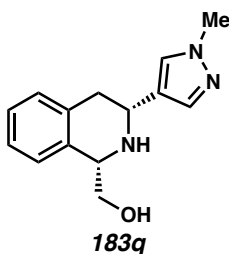
Compound **183o** was prepared from isoquinoline **182o** using general procedure 5 and purified by column chromatography (40% EtOAc in hexanes + 1% NEt₃) to provide a pale beige solid as a mixture of diastereomers (46 mg, 94% yield) (dr = 3.6:1); 90% ee for major diastereomer; [α]_D²⁵ +57.4 (*c* 1.04, CHCl₃); Major diastereomer: ¹H NMR (400 MHz, CDCl₃) δ 7.34 – 7.28 (m, 1H), 7.28 – 7.21 (m, 3H, integration overlapped with minor diastereomer), 7.19 – 7.15 (m, 1H), 7.11 – 7.09 (m, 1H), 7.07 – 7.04 (m, 1H), 4.47 – 4.42 (m, 2H), 4.06 (dd, *J* = 10.9, 3.4 Hz, 1H), 3.87 (dd, *J* = 11.0, 5.9 Hz, 1H), 3.19 – 2.98 (m, 2H); ¹³C NMR (100 MHz, CDCl₃) δ 148.1, 135.8, 134.7, 129.1, 126.7, 126.7, 126.6, 125.3, 124.2, 123.5, 66.4, 58.5, 53.1, 39.3; IR (Neat Film, NaCl) 3312, 2923, 2360, 1494, 1454, 1424, 1310, 1280, 1112, 1038, 850, 830, 744, 704 cm⁻¹; HRMS (MM:ESI-APCI+) *m/z* calc'd for C₁₄H₁₆NOS [M+H]⁺: 246.0947, found 246.0941; SFC

Conditions: 35% IPA, 2.5 mL/min, Chiralpak OJ-H column, $\lambda = 210$ nm, t_R (min): major = 2.86, minor = 6.02.



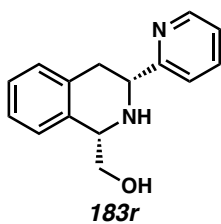
((1*S*,3*R*)-3-(thiophen-3-yl)-1,2,3,4-tetrahydroisoquinolin-1-yl)methanol (183p**):**

Compound **183p** was prepared from isoquinoline **182p** using general procedure 5 and purified by column chromatography (30% EtOAc in hexanes + 1% NEt₃) to provide a pale beige solid as a mixture of diastereomers (25.5 mg, 52% yield) (dr = 7.3:1). The isolated product contained long-chain hydrocarbon impurities, so it was repurified by partitioning between acetonitrile and hexanes. The acetonitrile layer was collected and concentrated to afford **183p** as a pale yellow solid (24.0 mg, 49% yield); 89% ee for major diastereomer; $[\alpha]_D^{25} +86.8$ (*c* 0.99, CHCl₃): ¹H NMR (400 MHz, CDCl₃) δ 7.24 (dd, *J* = 4.9, 3.0 Hz, 1H), 7.18 – 7.16 (m, 1H), 7.13 – 7.07 (m, 4H), 7.05 – 7.02 (m, 1H), 4.28 – 4.26 (m, 1H), 4.10 (dd, *J* = 10.8, 3.8 Hz, 1H), 3.93 (dd, *J* = 10.9, 3.4 Hz, 1H), 3.73 (dd, *J* = 11.0, 6.1 Hz, 1H), 2.99 – 2.90 (m, 1H), 2.86 (dd, *J* = 15.8, 3.8 Hz, 1H); ¹³C NMR (100 MHz, CDCl₃) δ 145.3, 136.2, 134.9, 129.3, 126.7, 126.5, 126.5, 126.2, 125.3, 120.9, 66.3, 58.5, 53.3, 38.1; IR (Neat Film, NaCl) 3318, 2924, 2366, 1494, 1454, 1424, 1313, 1279, 1218, 1116, 1038, 854, 782, 748 cm⁻¹; HRMS (MM:ESI-APCI+) *m/z* calc'd for C₁₄H₁₆NOS [M+H]⁺: 246.0947, found 246.0952; SFC Conditions: 35% IPA, 2.5 mL/min, Chiralpak AD-H column, $\lambda = 210$ nm, t_R (min): major = 3.19, minor = 4.05.



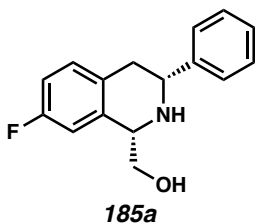
((1*S*,3*R*)-3-(1-methyl-1*H*-pyrazol-4-yl)-1,2,3,4-tetrahydroisoquinolin-1-yl)methanol

(183q): Compound **183q** was prepared from isoquinoline **182q** using general procedure 5 and purified by column chromatography (5% to 10% MeOH in EtOAc + 1% NEt₃) to provide a pale yellow solid as a mixture of diastereomers (48 mg, 98% yield) (dr = 2.9:1); 87% ee for major diastereomer; $[\alpha]_{\text{D}}^{25} +37.1$ (*c* 1.021, CHCl₃); Major diastereomer: ¹H NMR (400 MHz, CDCl₃) δ 7.63 – 7.61 (m, 2H), 7.26 – 7.16 (m, 2H, integration overlapped with minor diastereomer), 7.19 – 7.06 (m, 2H), 4.50 – 4.98 (m, 1H), 4.20 (dd, *J* = 11.8, 3.3 Hz, 1H), 4.02 (dd, *J* = 11.6, 3.3 Hz, 1H), 3.84 (s, 3H), 3.34 – 3.22 (m, 1H), 3.13 – 2.89 (m, 2H); ¹³C NMR (100 MHz, CDCl₃) δ 138.2, 134.7, 132.2, 129.3, 129.2, 127.2, 126.9, 125.4, 121.5, 64.6, 58.6, 49.1, 39.0, 36.1; IR (Neat Film, NaCl) 3315, 2931, 2371, 1560, 1494, 1455, 1408, 1295, 1169, 1031, 1008, 986, 748, 724 cm⁻¹; HRMS (MM:ESI-APCI+) *m/z* calc'd for C₁₄H₁₈N₃O [M+H]⁺: 244.1444, found 244.1448; SFC Conditions: 25% IPA, 2.5 mL/min, Chiralpak OJ-H column, λ = 210 nm, *t_R* (min): minor = 1.84, major = 2.60.



((1*S*,3*R*)-3-(pyridin-2-yl)-1,2,3,4-tetrahydroisoquinolin-1-yl)methanol (183r):

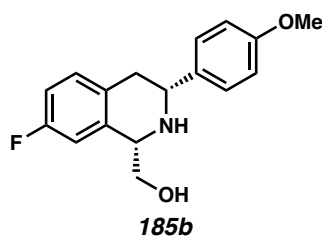
Compound **183r** was prepared from isoquinoline **182r** using general procedure 5 and purified using reverse-phase (C₁₈) preparative-HPLC (MeCN/0.4% acetic acid in water, 5.0 mL/min, monitor wavelength = 255 nm, 5–23% MeCN over 6 min, ramp to 95% MeCN over 0.5 min, and hold at 95% for 3.5 min) to provide a tan solid as a mixture of diastereomers (49 mg, 80% yield) (dr = 2.5:1). *Note:* This compound appears to be unstable and significant decomposition was observed under prolonged storage; 85% ee for major diastereomer; $[\alpha]_D^{25} +49.0$ (c 1.01, CHCl₃); Major diastereomer: ¹H NMR (400 MHz, CDCl₃) δ 8.60 – 8.57 (m, 1H), 7.72 – 7.67 (m, 2H), 7.43 (d, *J* = 7.8 Hz, 1H), 7.22 – 7.11 (m, 4H, integration overlapped with minor diastereomer), 4.41 – 4.39 (m, 1H), 4.23 – 4.20 (m, 1H, integration overlapped with minor diastereomer), 4.07 (dd, *J* = 11.1, 3.4 Hz, 1H), 3.85 (dd, *J* = 11.0, 6.4 Hz, 1H), 3.08 – 3.00 (m, 2H, integration overlapped with minor diastereomer); ¹³C NMR (100 MHz, CDCl₃) δ 162.2, 149.4, 137.0, 136.0, 135.3, 129.4, 126.7, 126.5, 125.4, 122.6, 121.1, 66.4, 58.6, 58.0, 36.5; IR (Neat Film, NaCl) 3300, 3056, 2934, 1592, 1574, 1473, 1454, 1435, 1316, 1142, 1060, 910, 744 cm⁻¹; HRMS (MM:ESI-APCI+) *m/z* calc'd for C₁₅H₁₇N₂O [M+H]⁺: 241.1335, found 241.1334; SFC Conditions: 30% IPA, 2.5 mL/min, Chiralpak OD-H column, λ = 210 nm, t_R (min): minor = 2.52, major = 2.79.



((1*S*,3*R*)-7-fluoro-3-phenyl-1,2,3,4-tetrahydroisoquinolin-1-yl)methanol (185a):

Compound **185a** was prepared from isoquinoline **184a** using general procedure 5 and

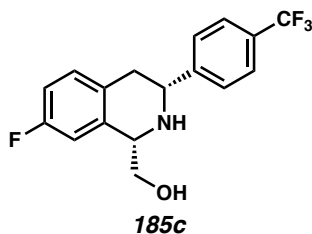
purified by column chromatography (30% EtOAc in hexanes + 1% NEt₃) to provide a pale yellow solid as a mixture of diastereomers (49 mg, 94% yield) (dr = 11.5:1); 93% ee for major diastereomer; $[\alpha]_D^{25} +76.9$ (*c* 1.04, CHCl₃); Major diastereomer: ¹H NMR (400 MHz, CDCl₃) δ 7.47 – 7.42 (m, 2H), 7.40 – 7.36 (m, 2H), 7.33 – 7.30 (m, 1H), 7.08 (dd, *J* = 8.4, 5.8 Hz, 1H), 6.97 – 6.87 (m, 2H), 4.38 – 4.36 (m, 1H), 4.06 (dd, *J* = 10.8, 3.7 Hz, 1H), 3.99 (dd, *J* = 10.9, 3.3 Hz, 1H), 3.86 (dd, *J* = 10.9, 5.2 Hz, 1H), 3.00 – 2.82 (m, 2H); ¹³C NMR (100 MHz, CDCl₃) δ 161.5 (d, *J* = 243.8 Hz), 144.0, 136.9 (d, *J* = 6.8 Hz), 132.2 (d, *J* = 3.0 Hz), 130.6 (d, *J* = 7.9 Hz), 128.8, 127.8, 126.8, 113.9 (d, *J* = 21.3 Hz), 112.1 (d, *J* = 21.8 Hz), 66.4, 58.6 (d, *J* = 2.1 Hz), 57.7, 38.2; ¹⁹F NMR (282 MHz, CDCl₃) δ –116.2 – –116.4 (m); IR (Neat Film, NaCl) 3309, 2918, 1614, 1498, 1455, 1428, 1255, 1221, 1031, 911, 868, 808, 758, 745 cm⁻¹; HRMS (MM:ESI-APCI+) *m/z* calc'd for C₁₆H₁₇FNO [M+H]⁺: 258.1289, found 258.1281; SFC Conditions: 40% IPA, 2.5 mL/min, Chiralpak AD-H column, λ = 210 nm, *t*_R (min): major = 2.56, minor = 3.04.



((1*S*,3*R*)-7-fluoro-3-(4-methoxyphenyl)-1,2,3,4-tetrahydroisoquinolin-1-yl)methanol

(185b): Compound **185b** was prepared from isoquinoline **184b** using general procedure 5 and purified by column chromatography (30% to 40% EtOAc in hexanes + 1% NEt₃) to provide a pale yellow solid as a single diastereomer (57 mg, 99% yield); 90% ee; $[\alpha]_D^{25} +57.8$ (*c* 0.99, CHCl₃); ¹H NMR (400 MHz, CDCl₃) δ 7.38 – 7.34 (m, 2H), 7.07 (dd, *J* = 8.4, 5.8 Hz, 1H), 6.97 – 6.84 (m, 4H), 4.36 – 4.34 (m, 1H), 3.99 (ddd, *J* = 12.3, 10.9, 3.4

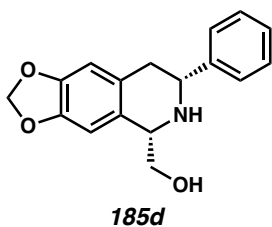
Hz, 2H), 3.86 – 3.84 (m, 1H), 3.82 (s, 3H), 2.99 – 2.87 (m, 1H), 2.83 (dd, $J = 15.6, 3.5$ Hz, 1H); ^{13}C NMR (100 MHz, CDCl_3) δ 161.5 (d, $J = 243.7$ Hz), 159.2, 136.9 (d, $J = 6.7$ Hz), 136.2, 132.3, 130.6 (d, $J = 7.9$ Hz), 127.9, 114.1, 113.8 (d, $J = 21.3$ Hz), 112.1 (d, $J = 21.8$ Hz), 66.4, 58.7 (d, $J = 2.0$ Hz), 57.1, 55.5, 38.3; ^{19}F NMR (282 MHz, CDCl_3) δ –116.3 – –116.4 (m); IR (Neat Film, NaCl) 3305, 2930, 2838, 1614, 1591, 1514, 1498, 1304, 1249, 1178, 1111, 1034, 912, 868, 830, 736 cm^{-1} ; HRMS (MM:ESI-APCI+) m/z calc'd for $\text{C}_{17}\text{H}_{19}\text{FNO}_2$ $[\text{M}+\text{H}]^+$: 288.1394, found 288.1404; SFC Conditions: 30% IPA, 2.5 mL/min, Chiralpak OJ-H column, $\lambda = 210$ nm, t_R (min): major = 1.93, minor = 2.42.



((1*S*,3*R*)-7-fluoro-3-(4-(trifluoromethyl)phenyl)-1,2,3,4-tetrahydroisoquinolin-1-

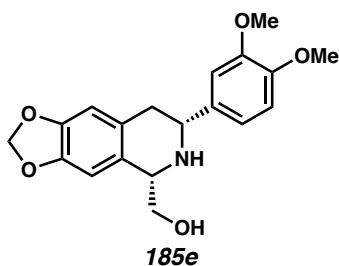
yl)methanol (185c): Compound **185c** was prepared from isoquinoline **184c** using general procedure 5 and purified by column chromatography (20% to 30% EtOAc in hexanes + 1% NEt_3) to provide a pale yellow solid as a mixture of diastereomers (50 mg, 77% yield) (dr = 6.7:1); 94% ee for major diastereomer; $[\alpha]_{\text{D}}^{25} +44.2$ (c 1.002, CHCl_3); Major diastereomer: ^1H NMR (400 MHz, CDCl_3) δ 7.64 (d, $J = 8.3$ Hz, 2H), 7.58 (d, $J = 8.1$ Hz, 2H), 7.09 (dd, $J = 8.4, 5.7$ Hz, 1H), 7.00 – 6.87 (m, 2H), 4.39 – 4.37 (m, 1H), 4.13 (dd, $J = 8.9, 5.7$ Hz, 1H), 4.02 (dd, $J = 10.9, 3.3$ Hz, 1H), 3.88 (dd, $J = 10.9, 5.4$ Hz, 1H), 2.94 – 2.84 (m, 2H); ^{13}C NMR (100 MHz, CDCl_3) δ 161.6 (d, $J = 244.2$ Hz), 148.0, 136.7 (d, $J = 6.7$ Hz), 131.5 (d, $J = 3.1$ Hz), 130.6 (d, $J = 7.9$ Hz), 130.1 (q, $J = 32.5$ Hz), 127.2, 125.7 (q, $J = 3.8$ Hz), 124.2 (q, $J = 272.1$ Hz), 114.0 (d, $J = 21.3$ Hz), 112.1 (d, $J = 21.9$

Hz) 66.4, 58.5 (d, $J = 2.0$ Hz), 57.4, 38.2; ^{19}F NMR (282 MHz, CDCl_3) δ -62.5, -115.8 – -115.9 (m); IR (Neat Film, NaCl) 3304, 2922, 1620, 1593, 1500, 1428, 1326, 1255, 1222, 1165, 1125, 1068, 1018, 868, 836, 816 cm^{-1} ; HRMS (MM:ESI-APCI+) m/z calc'd for $\text{C}_{17}\text{H}_{16}\text{F}_4\text{NO}$ $[\text{M}+\text{H}]^+$: 326.1163, found 326.1175; SFC Conditions: 20% IPA, 2.5 mL/min, Chiralpak AD-H column, $\lambda = 210$ nm, t_R (min): major = 3.93, minor = 4.46.

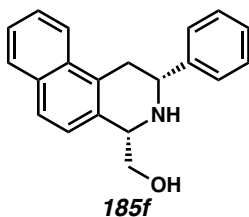


((5*S*,7*R*)-7-phenyl-5,6,7,8-tetrahydro-[1,3]dioxolo[4,5-*g*]isoquinolin-5-yl)methanol

(185d): Compound **185d** was prepared from isoquinoline **184d** using general procedure 5 and purified by column chromatography (75% EtOAc in hexanes + 1% NEt_3) to provide a pale beige solid as a mixture of diastereomers (17 mg, 30% yield) (dr = 4.9:1); 58% ee for major diastereomer; $[\alpha]_{\text{D}}^{25} +29.2$ (c 0.940, CHCl_3); Major diastereomer: ^1H NMR (400 MHz, CDCl_3) δ 7.47 – 7.41 (m, 2H), 7.39 – 7.37 (m, 2H), 7.33 – 7.27 (m, 1H), 6.71 (s, 1H), 6.60 – 6.58 (m, 1H), 5.95 – 5.89 (m, 2H), 4.32 – 4.30 (m, 1H), 4.04 (dd, $J = 11.1$, 3.4 Hz, 1H), 3.93 (dd, $J = 10.9$, 3.2 Hz, 1H), 3.82 (dd, $J = 10.9$, 5.1 Hz, 1H), 2.97 – 2.88 (m, 1H), 2.78 (dd, $J = 15.5$, 3.4 Hz, 1H); ^{13}C NMR (100 MHz, CDCl_3) δ 146.5, 146.4, 144.2, 130.0, 128.8, 127.9, 127.7, 126.8, 109.0, 105.5, 101.0, 66.7, 58.6, 57.7, 39.0; IR (Neat Film, NaCl) 3324, 3028, 2897, 1504, 1486, 1454, 1434, 1384, 1306, 1279, 1231, 1128, 1038, 936, 910, 858, 750, 733, 701 cm^{-1} ; HRMS (MM:ESI-APCI+) m/z calc'd for $\text{C}_{17}\text{H}_{18}\text{NO}_3$ $[\text{M}+\text{H}]^+$: 284.1281, found 284.1276; SFC Conditions: 45% IPA, 2.5 mL/min, Chiralpak AD-H column, $\lambda = 210$ nm, t_R (min): major = 5.00, minor = 7.22.

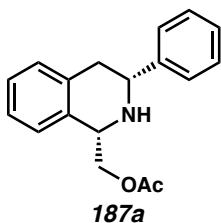


((5*S*,7*R*)-7-(3,4-dimethoxyphenyl)-5,6,7,8-tetrahydro-[1,3]dioxolo[4,5-*g*]isoquinolin-5-yl)methanol (185e): Compound **185e** was prepared from isoquinoline **184e** using general procedure 5 and purified by column chromatography (100% EtOAc to 10% MeOH in EtOAc + 1% NEt₃) to provide a pale yellow solid as a single diastereomer (28 mg, 41% yield); 54% ee; [α]_D²⁵ +25.5 (*c* 0.197, CH₃OH); ¹H NMR (400 MHz, CDCl₃) δ 6.99 – 6.96 (m, 2H), 6.87 – 6.85 (m, 1H), 6.71 (s, 1H), 6.60 – 6.58 (m, 1H), 5.94 – 5.91 (m, 2H), 4.32 – 4.30 (m, 1H), 3.99 (dd, *J* = 11.1, 3.4 Hz, 1H), 3.94 (dd, *J* = 11.1, 3.4 Hz, 1H), 3.91 (s, 3H), 3.89 (s, 3H), 3.83 (dd, *J* = 11.0, 5.0 Hz, 1H), 2.97 – 2.85 (m, 1H), 2.76 (dd, *J* = 15.6, 3.4 Hz, 1H); ¹³C NMR (100 MHz, CDCl₃) δ 149.3, 148.7, 146.7, 146.5, 136.9, 130.1, 127.8, 119.0, 111.4, 110.0, 109.1, 105.6, 101.1, 66.7, 58.8, 57.7, 56.2, 39.1; IR (Neat Film, NaCl) 3374, 2890, 2360, 1505, 1487, 1268, 1260, 1237, 1140, 1076, 1024, 971, 932, 918, 730 cm⁻¹; HRMS (MM:ESI-APCI+) *m/z* calc'd for C₁₉H₂₂NO₅ [M+H]⁺: 344.1492, found 344.1483; SFC Conditions: 45% IPA, 2.5 mL/min, Chiralpak AD-H column, λ = 210 nm, *t*_R (min): major = 3.89, minor = 5.16.



((2*R*,4*S*)-2-phenyl-1,2,3,4-tetrahydrobenzo[*f*]isoquinolin-4-yl)methanol (185f):

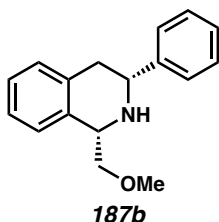
Compound **185f** was prepared from isoquinoline **184f** using general procedure 5 and purified by column chromatography (40% to 60% EtOAc in hexanes + 1% NEt₃) to provide a pale yellow solid as a mixture of diastereomers (25 mg, 43% yield) (dr = 15.7:1); 82% ee for major diastereomer; $[\alpha]_{\text{D}}^{25} +85.7$ (*c* 1.01, CHCl₃); Major diastereomer: ¹H NMR (400 MHz, CDCl₃) δ 7.93 – 7.91 (m, 1H), 7.85 – 7.82 (m, 1H), 7.75 (d, *J* = 8.6 Hz, 1H), 7.55 (d, *J* = 7.2 Hz, 2H), 7.50 – 7.47 (m, 2H), 7.45 – 7.34 (m, 4H), 4.61 – 4.59 (m, 1H), 4.20 (dd, *J* = 11.0, 3.4 Hz, 1H), 4.09 (dd, *J* = 10.9, 3.2 Hz, 1H), 4.01 (dd, *J* = 10.9, 4.8 Hz, 1H), 3.50 – 3.39 (m, 1H), 3.23 – 3.10 (m, 1H); ¹³C NMR (100 MHz, CDCl₃) δ 144.4, 132.2, 132.1, 132.0, 131.9, 128.8, 128.4, 127.7, 126.8, 126.7, 126.3, 125.5, 123.4, 122.9, 66.4, 59.1, 57.6, 35.4; IR (Neat Film, NaCl) 3306, 3056, 2918, 1417, 1308, 1034, 910, 884, 813, 762, 700, 736, 682 cm⁻¹; HRMS (MM:ESI-APCI+) *m/z* calc'd for C₂₀H₂₀NO [M+H]⁺: 290.1539, found 290.1534; SFC Conditions: 45% IPA, 2.5 mL/min, Chiralpak AD-H column, λ = 210 nm, *t_R* (min): major = 5.31, minor = 10.01.



((1*S*,3*R*)-3-phenyl-1,2,3,4-tetrahydroisoquinolin-1-yl)methyl acetate (187a):

Compound **187a** was prepared from isoquinoline **186a** using general procedure 5 and purified by column chromatography (5% EtOAc in CH₂Cl₂ + 1% NEt₃) to provide a yellow oil as a single diastereomer (32 mg, 56% yield); 86% ee; $[\alpha]_{\text{D}}^{25} +103.8$ (*c* 1.01,

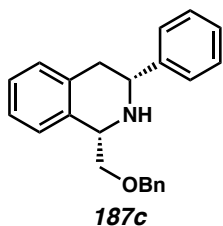
CHCl₃); ¹H NMR (400 MHz, CDCl₃) δ 7.51 – 7.45 (m, 2H), 7.41 – 7.37 (m, 2H), 7.34 – 7.30 (m, 1H), 7.27 – 7.24 (m, 1H), 7.23 – 7.18 (m, 2H), 7.16 – 7.10 (m, 1H), 4.78 (dd, *J* = 10.8, 3.5 Hz, 1H), 4.54 – 4.51 (m, 1H), 4.14 (dd, *J* = 10.8, 8.7 Hz, 1H), 4.05 (dd, *J* = 11.1, 3.4 Hz, 1H), 3.08 – 3.01 (m, 1H), 2.90 (dd, *J* = 15.5, 3.6 Hz, 1H), 2.08 (s, 3H); ¹³C NMR (100 MHz, CDCl₃) δ 171.1, 144.4, 136.3, 134.1, 129.5, 128.8, 127.7, 126.9, 126.9, 126.3, 125.3, 69.1, 57.9, 56.4, 39.2, 21.2; IR (Neat Film, NaCl) 3024, 2926, 2802, 1741, 1494, 1454, 1386, 1366, 1314, 1229, 1118, 1034, 754, 701 cm⁻¹; HRMS (MM:ESI-APCI+) *m/z* calc'd for C₁₈H₂₀NO₂ [M+H]⁺: 282.1489, found 282.1492; SFC Conditions: 20% IPA, 2.5 mL/min, Chiralpak OJ-H column, λ = 210 nm, *t*_R (min): major = 3.32, major = 3.93.



(1*S*,3*R*)-1-(methoxymethyl)-3-phenyl-1,2,3,4-tetrahydroisoquinoline (187b):

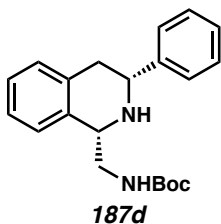
Compound **187b** was prepared from isoquinoline **186b** using general procedure 5 and purified by column chromatography (10% EtOAc in CH₂Cl₂+ 1% NEt₃) to provide a viscous yellow oil as a single diastereomer (40 mg, 80% yield); 89% ee; [*α*]_D²⁵ +94.3 (*c* 0.98, CHCl₃); ¹H NMR (400 MHz, CDCl₃) δ 7.48 – 7.46 (m, 2H), 7.39 – 7.35 (m, 2H), 7.32 – 7.27 (m, 1H), 7.25 – 7.20 (m, 1H), 7.20 – 7.15 (m, 2H), 7.16 – 7.10 (m, 1H), 4.45 – 4.42 (m, 1H), 4.07 – 3.94 (m, 2H), 3.59 (t, *J* = 8.7 Hz, 1H), 3.43 (s, 3H), 3.06 (dd, *J* = 16.0, 11.1 Hz, 1H), 2.92 (dd, *J* = 16.0, 3.6 Hz, 1H); ¹³C NMR (100 MHz, CDCl₃) δ 144.5, 136.3, 135.4, 129.5, 128.7, 127.5, 126.9, 126.6, 126.1, 124.8, 59.3, 58.1, 57.4,

39.0; IR (Neat Film, NaCl) 3028, 2895, 2812, 1604, 1494, 1454, 1313, 1194, 1112, 1072, 1030, 958, 923, 840, 744, 700 cm^{-1} ; HRMS (MM:ESI-APCI+) m/z calc'd for $\text{C}_{17}\text{H}_{20}\text{NO}$ $[\text{M}+\text{H}]^+$: 254.1539, found 254.1531; SFC Conditions: 20% IPA, 2.5 mL/min, Chiralpak OD-H column, $\lambda = 210$ nm, t_R (min): major = 4.82, major = 5.25.



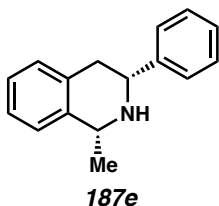
(1S,3R)-1-((benzyloxy)methyl)-3-phenyl-1,2,3,4-tetrahydroisoquinoline (187c):

Compound **187c** was prepared from isoquinoline **186c** using general procedure 5 and purified by column chromatography (5% EtOAc in CH_2Cl_2 + 1% NEt_3) to provide a pale yellow oil as a single diastereomer (60 mg, 90% yield); 88% ee; $[\alpha]_D^{25} +80.4$ (c 1.02, CHCl_3); ^1H NMR (400 MHz, CDCl_3) δ 7.48 – 7.46 (m, 2H), 7.40 – 7.34 (m, 6H), 7.32 – 7.28 (m, 2H), 7.22 – 7.16 (m, 3H), 7.14 – 7.11 (m, 1H), 4.61 (s, 2H), 4.48 (dd, $J = 8.7$, 3.4 Hz, 1H), 4.12 (dd, $J = 9.0$, 3.6 Hz, 1H), 4.04 (dd, $J = 11.1$, 3.5 Hz, 1H), 3.67 (t, $J = 8.7$ Hz, 1H), 3.05 (dd, $J = 15.9$, 11.1 Hz, 1H), 2.91 (dd, $J = 15.8$, 3.5 Hz, 1H); ^{13}C NMR (100 MHz, CDCl_3) δ 144.6, 138.3, 136.3, 135.3, 129.5, 128.7, 128.6, 127.9, 127.8, 127.5, 126.9, 126.6, 126.1, 124.9, 74.8, 73.6, 58.1, 57.5, 39.2; IR (Neat Film, NaCl) 3060, 3028, 2862, 1494, 1454, 1366, 1312, 1098, 1028, 742, 698 cm^{-1} ; HRMS (MM:ESI-APCI+) m/z calc'd for $\text{C}_{23}\text{H}_{24}\text{NO}$ $[\text{M}+\text{H}]^+$: 330.1852, found 330.1857; SFC Conditions: 25% IPA, 2.5 mL/min, Chiralpak OD-H column, $\lambda = 210$ nm, t_R (min): major = 5.66, major = 6.38.



tert-butyl (((1*S*,3*R*)-3-phenyl-1,2,3,4-tetrahydroisoquinolin-1-yl)methyl)carbamate

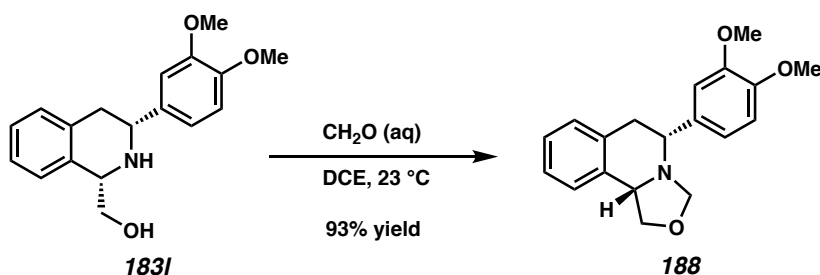
(187d): Compound **187d** was prepared from isoquinoline **186d** using general procedure 5 and purified by column chromatography (15% EtOAc in hexanes + 1% NEt₃) to provide a white solid as a mixture of diastereomers (44 mg, 71% yield) (dr = 9.0:1); 90% ee for major diastereomer; $[\alpha]_D^{25} +50.4$ (*c* 0.99, CHCl₃); Major diastereomer: ¹H NMR (400 MHz, CDCl₃) δ 7.46 (d, *J* = 7.1 Hz, 2H), 7.38 (t, *J* = 7.5 Hz, 2H), 7.36 – 7.26 (m, 2H), 7.26 – 7.14 (m, 2H), 7.11 (d, *J* = 6.7 Hz, 1H), 5.02 (s, 1H), 4.44 (s, 1H), 4.04 (dd, *J* = 11.0, 3.5 Hz, 1H), 3.77 – 3.72 (m, 1H), 3.49 (dt, *J* = 13.2, 6.3 Hz, 1H), 3.00 (dd, *J* = 15.8, 10.9 Hz, 1H), 2.89 (dd, *J* = 15.8, 3.5 Hz, 1H), 1.41 (s, 9H); ¹³C NMR (100 MHz, CDCl₃) δ 156.4, 144.4, 136.4, 135.2, 129.2, 128.7, 127.7, 126.8, 126.6, 126.4, 125.7, 79.4, 58.0, 57.1, 46.3, 39.1, 28.5; IR (Neat Film, NaCl) 3352, 2978, 2932, 1704, 1495, 1455, 1392, 1366, 1247, 1171, 752, 701 cm⁻¹; HRMS (MM:ESI-APCI+) *m/z* calc'd for C₂₁H₂₇N₂O₂ [M+H]⁺: 339.2067, found 339.2063; SFC Conditions: 40% IPA, 2.5 mL/min, Chiralpak AD-H column, λ = 210 nm, *t_R* (min): major = 1.41, major = 1.76.



(1*R*,3*R*)-1-methyl-3-phenyl-1,2,3,4-tetrahydroisoquinoline (187e): Compound **187e** was prepared from 1-methyl-3-phenylisoquinoline (**181a**) using general procedure 5 and

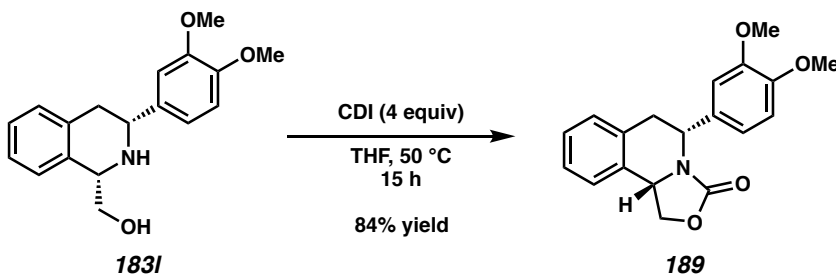
purified by column chromatography (10% to 20% EtOAc in hexanes + 1% NEt₃) to provide a colorless oil as a single diastereomer (29 mg, 64% yield); 90% ee; [α]_D²⁵ +133.3 (*c* 0.79, CHCl₃); ¹H NMR (400 MHz, CDCl₃) δ 7.49 – 7.46 (m, 2H), 7.41 – 7.37 (m, 2H), 7.33 – 7.29 (m, 1H), 7.28 – 7.23 (m, 1H), 7.23 – 7.14 (m, 2H), 7.11 (d, *J* = 6.9 Hz, 1H), 4.34 (q, *J* = 6.6 Hz, 1H), 4.08 (dd, *J* = 11.1, 3.9 Hz, 1H), 3.12 – 3.01 (m, 1H), 2.96 (dd, *J* = 16.2, 4.1 Hz, 1H), 1.55 (d, *J* = 6.5 Hz, 3H); ¹³C NMR (100 MHz, CDCl₃) δ 144.5, 139.9, 135.2, 129.1, 128.7, 127.5, 126.7, 126.2, 126.2, 125.4, 58.8, 53.6, 38.9, 22.4; IR (Neat Film, NaCl) 3024, 2962, 2926, 2792, 1602, 1494, 1453, 1372, 1352, 1306, 1140, 1118, 1031, 790, 753, 733, 700 cm⁻¹; HRMS (MM:ESI-APCI+) *m/z* calc'd for C₁₆H₁₈N [M+H]⁺: 224.1434, found 224.1426; SFC Conditions: 20% IPA, 3.5 mL/min, Chiralpak AS-H column, λ = 210 nm, *t*_R (min): major = 2.16, minor = 2.62.

4.7.2.4 Product transformations



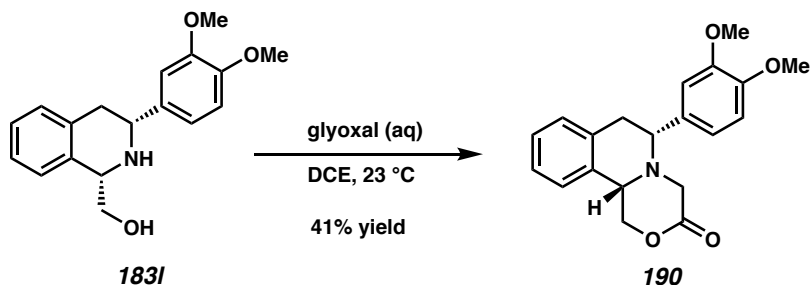
To a 1-dram vial equipped with a stir bar was added tetrahydroisoquinoline **183I** (20.0 mg, 0.067 mmol) in 1,2-dichloroethane (1.3 mL, 0.05 M). Formaldehyde solution (37 wt% in H₂O, 9.2 μ L, 0.124 mmol) was then added and the reaction was stirred for 15 minutes at room temperature. The reaction was then basified with K₂CO₃, and extracted with CH₂Cl₂. The collected organic layers were dried over Na₂SO₄, and concentrated under vacuum. The crude product was purified by column chromatography (50% EtOAc

in hexanes + 1% NEt₃) to afford **188** as a white solid (19.3 mg, 93% yield): $[\alpha]_D^{25} +134.8$ (*c* 1.03, CHCl₃); ¹H NMR (400 MHz, CDCl₃) δ 7.25 – 7.14 (m, 3H), 7.04 (d, *J* = 2.0 Hz, 1H), 7.02 – 6.90 (m, 2H), 6.83 (d, *J* = 8.2 Hz, 1H), 4.58 – 4.43 (m, 2H), 3.97 (t, *J* = 7.6 Hz, 1H), 3.94 – 3.87 (m, 2H), 3.89 (s, 6H), 3.83 (dd, *J* = 10.6, 4.8 Hz, 1H), 3.23 (dd, *J* = 16.8, 10.6 Hz, 1H), 3.11 (dd, *J* = 16.8, 4.8 Hz, 1H); ¹³C NMR (100 MHz, CDCl₃) δ 149.4, 148.7, 135.1, 134.7, 134.6, 128.6, 127.2, 126.3, 125.0, 119.6, 110.9, 110.2, 84.2, 71.5, 62.9, 61.3, 56.1, 56.0, 37.3; IR (Neat Film, NaCl) 2930, 1592, 1513, 1454, 1263, 1237, 1167, 1060, 1027, 918, 752, 680 cm⁻¹; HRMS (MM:ESI-APCI+) *m/z* calc'd for C₁₉H₂₂NO₃ [M+H]⁺: 312.1594, found 312.1594.



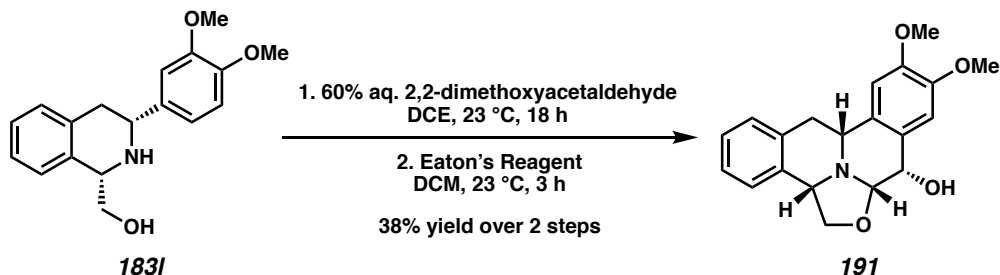
To a 1-dram vial equipped with a stir bar was added tetrahydroisoquinoline **183I** (10.0 mg, 0.033 mmol), THF (0.7 mL, 0.05 M), and CDI (21.7 mg, 0.134 mmol). The solution was stirred at 50 °C for 15 h. After complete conversion of the starting material monitored by TLC, the reaction concentrated and the crude product was purified by preparative-TLC (100% EtOAc) to afford **189** as a white solid (9.2 mg, 84% yield): $[\alpha]_D^{25} +71.4$ (*c* 0.76, CHCl₃); ¹H NMR (400 MHz, CDCl₃) δ 7.34 (dd, *J* = 8.3, 7.0 Hz, 1H), 7.30 – 7.23 (m, 1H), 7.08 (t, *J* = 6.6 Hz, 2H), 6.66 (d, *J* = 8.2 Hz, 1H), 6.52 (dd, *J* = 8.2, 2.1 Hz, 1H), 6.33 (d, *J* = 2.1 Hz, 1H), 5.14 – 5.02 (m, 2H), 4.92 (t, *J* = 7.9 Hz, 1H), 4.49 (dd, *J* = 10.1, 8.2 Hz, 1H), 3.78 (s, 3H), 3.60 (s, 3H), 3.36 (dd, *J* = 14.9, 6.4 Hz, 1H), 2.99 (dd, *J* = 14.9, 2.7 Hz, 1H); ¹³C NMR (100 MHz, CDCl₃) δ 156.1, 148.7, 148.3,

136.0, 134.2, 133.9, 129.4, 128.5, 127.5, 122.4, 118.5, 110.9, 109.3, 67.5, 55.9, 55.6, 54.6, 53.4, 36.8; IR (Neat Film, NaCl) 2933, 1756, 1515, 1464, 1396, 1260, 1234, 1139, 1025, 779, 762, 748 cm^{-1} ; HRMS (MM:ESI-APCI+) m/z calc'd for $\text{C}_{19}\text{H}_{20}\text{NO}_4$ $[\text{M}+\text{H}]^+$: 326.1387, found 326.1386.



To a 1-dram vial equipped with a stir bar was added tetrahydroisoquinoline **183I** (20.0 mg, 0.067 mmol) in 1,2-dichloroethane (1.3 mL, 0.05 M). Glyoxal solution (40 wt% in H_2O , 0.15 mL, 1.336 mmol) was then added, and the reaction was stirred at room temperature overnight. After complete conversion of the starting material monitored by TLC, the reaction was diluted with H_2O , and extracted with CH_2Cl_2 . The collected organic layers were dried over Na_2SO_4 , and concentrated under vacuum. The crude product was purified by preparative-TLC (50% EtOAc in hexanes) to afford **190** as a white solid (9.2 mg, 41% yield): $[\alpha]_{\text{D}}^{25} +187.8$ (c 0.61, CHCl_3); ^1H NMR (400 MHz, CDCl_3) δ 7.29 – 7.20 (m, 2H), 7.20 – 7.10 (m, 2H), 6.95 – 6.81 (m, 3H), 4.84 (dd, J = 10.5, 3.4 Hz, 1H), 4.33 (t, J = 10.7 Hz, 1H), 4.04 – 3.94 (m, 1H), 3.90 (s, 6H), 3.62 (d, J = 17.7 Hz, 1H), 3.43 (dd, J = 11.2, 3.2 Hz, 1H), 3.32 – 3.19 (m, 1H), 2.98 – 2.85 (m, 2H); ^{13}C NMR (100 MHz, CDCl_3) δ 167.7, 149.8, 149.1, 135.0, 132.8, 130.6, 129.1, 127.7, 126.7, 124.7, 120.5, 111.4, 110.2, 73.3, 63.8, 59.5, 56.1, 56.1, 54.9, 38.9; IR (Neat Film,

NaCl) 2932, 1745, 1511, 1463, 1421, 1263, 1242, 1137, 1028, 809, 746 cm^{-1} ; HRMS (MM:ESI-APCI+) m/z calc'd for $\text{C}_{20}\text{H}_{22}\text{NO}_4$ $[\text{M}+\text{H}]^+$: 340.1543, found 340.1545.

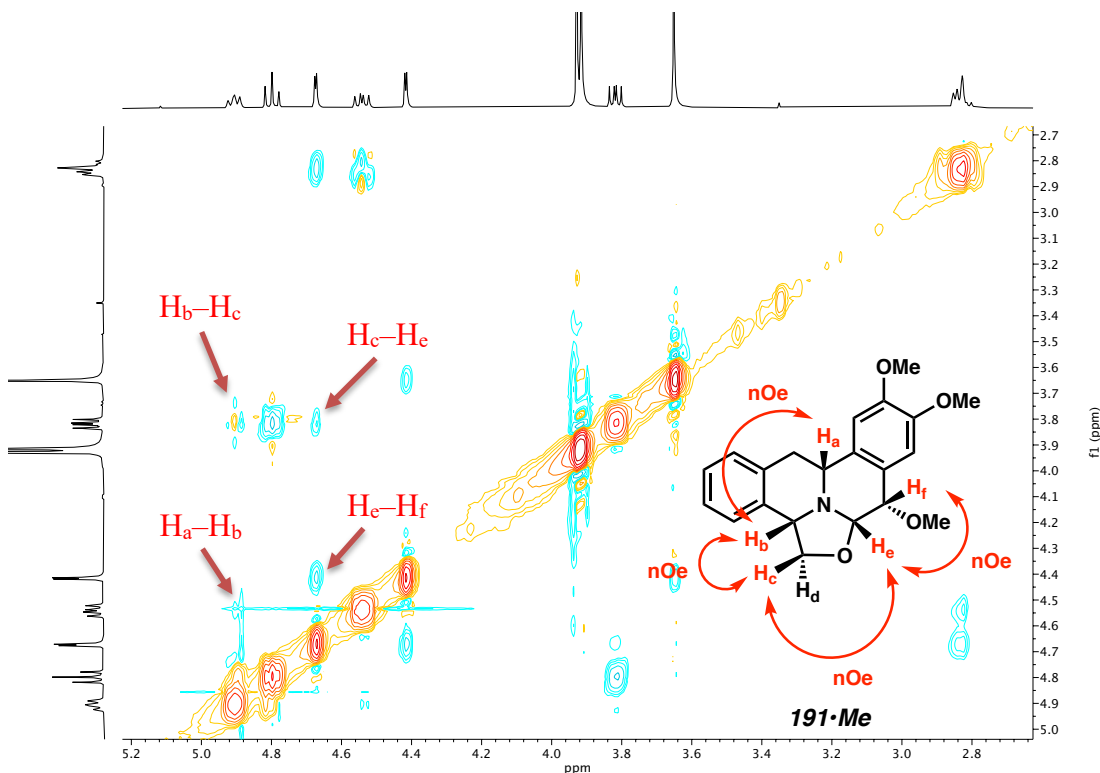


To a 1-dram vial equipped with a stir bar was added tetrahydroisoquinoline **183I** (10.0 mg, 0.033 mmol) in 1,2-dichloroethane (0.5 mL, 0.07 M). 2,2-Dimethoxyacetaldehyde solution (60 wt% in H_2O , 9.2 μL , 0.061 mmol) was then added and the reaction stirred at room temperature overnight. The reaction was then concentrated under vacuum to afford a yellow oil, which was then used in the next step without further purification.

To a 1-dram vial was added the crude product and CH_2Cl_2 (0.5 mL, 0.07 M). Eaton's reagent (0.28 mL, 0.134 mmol) was then added dropwise, and the reaction was stirred for 3 hours. The reaction was then quenched by slow addition of saturated aqueous NaHCO_3 , diluted with H_2O and extracted with CH_2Cl_2 . The collected organic phases were dried over Na_2SO_4 , and concentrated under vacuum. The crude product was purified by preparative-TLC (100% EtOAc) twice to afford **191** as a white solid as a single diastereomer (4.3 mg, 38% yield over 2 steps): $[\alpha]_{\text{D}}^{25} +32.0$ (c 0.29, CHCl_3); ^1H NMR (400 MHz, CDCl_3) δ 7.29 – 7.26 (m, 1H), 7.24 – 7.20 (m, 1H), 7.16 (d, J = 6.0 Hz, 1H), 7.08 (d, J = 6.8 Hz, 1H), 6.97 (s, 1H), 6.69 (s, 1H), 4.89 – 4.82 (m, 1H), 4.79 (t, J = 7.8 Hz, 1H), 4.71 (dd, J = 8.3, 2.1 Hz, 1H), 4.65 (d, J = 2.1 Hz, 1H), 4.47 (dd, J = 9.1, 7.0 Hz, 1H), 3.93 (s, 3H), 3.91 (s, 3H), 3.86 (dd, J = 7.9, 5.3 Hz, 1H), 2.89 – 2.87 (m, 2H),

2.79 (d, $J = 8.4$ Hz, 1H); ^{13}C NMR (100 MHz, CDCl_3) δ 149.4, 148.6, 136.5, 133.1, 130.9, 129.3, 127.3, 127.3, 126.8, 126.6, 113.6, 109.2, 86.7, 74.4, 67.9, 57.3, 56.2, 56.1, 54.2, 31.1; IR (Neat Film, NaCl) 3442, 2918, 1610, 1515, 1464, 1380, 1353, 1270, 1242, 1160, 1117, 1074, 1010, 868, 762, 732, 642 cm^{-1} ; HRMS (MM:ESI-APCI+) m/z calc'd for $\text{C}_{20}\text{H}_{22}\text{NO}_4$ $[\text{M}+\text{H}]^+$: 340.1543, found 340.1548.

The stereochemistry of **191** was assigned using diagnostic nOe correlations (highlighted arrows, *vide infra*). Due to the ambiguous nOe correlations observed in **191**, the stereochemistry was determined by derivatizing the hydroxyl group of **191** to the methoxy group.



2D NOESY NMR of compound **191•Me**.

4.7.3 Additional optimization results

Table 4.2 Additional Ligand Screen.

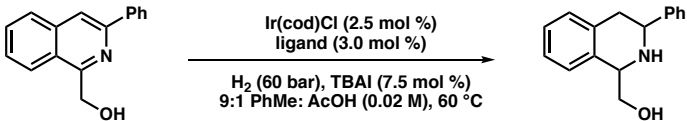
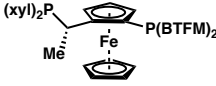
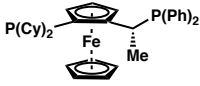
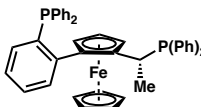
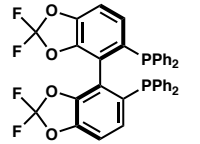
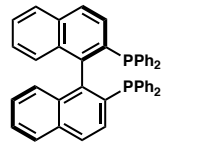
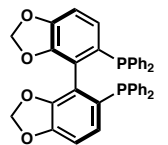
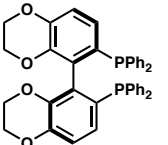
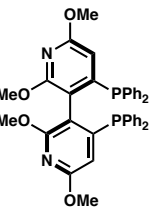
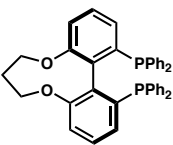
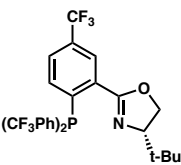
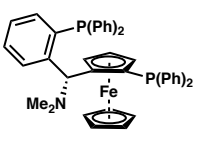
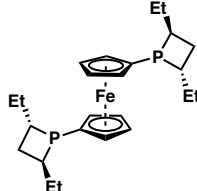
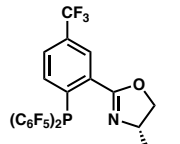
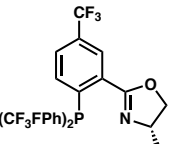
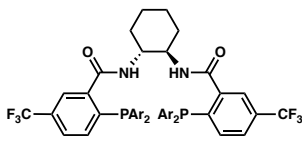
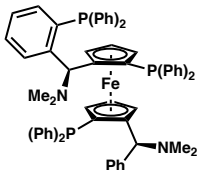
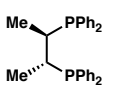
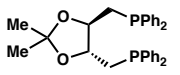
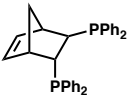
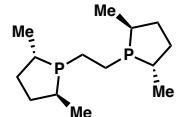
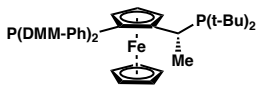
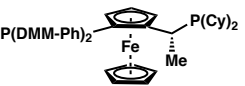
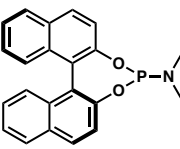
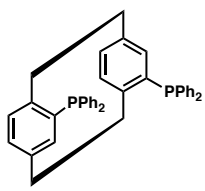
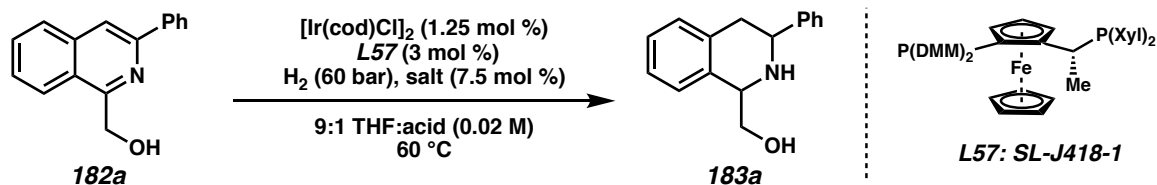
				
 SL-J008-2 > 95% conversion 86% yield, 49% ee	 SL-J004-1 56% conversion 37% yield, -61% ee	 Walphos (SL-002-1) 23% conversion 9% yield, ee ND	 59% conversion 59% yield, -61% ee	 36% conversion 23% yield, 19% ee
 50% conversion 20% yield, ee ND	 15% conversion 16% yield, ee ND	 59% conversion 46% yield, -41% ee	 50% conversion 20% yield, ee ND	 65% conversion 71% yield, 2% ee
 >95% conversion 80% yield, -40% ee	 >62% conversion 48% yield, -44% ee	 55% conversion 39% yield, -4% ee	 74% conversion 46% yield, 5% ee	 0% conversion 0% yield, ee ND
 SL-M001-2 > 61% conversion 51% yield, 49% ee	 (R, R)-chiralphos 78% conversion 57% yield, -37% ee	 (R, R)-DIOP 37% conversion 28% yield, 5% ee	 Norphos 31% conversion 20% yield, ee ND	 Me-BPE 22% conversion 10% yield, ee ND
 SL-J013-1 0% conversion 0% yield	 SL-J007-1 16% conversion 6% yield, ee ND	 Monophos 42% conversion 29% yield, 5% ee	 PhanePhos 67% conversion 74% yield, -19% ee	

Table 4.3 Additive Effects in Ir-Catalyzed Enantio- and Diastereoselective Hydrogenation.^a



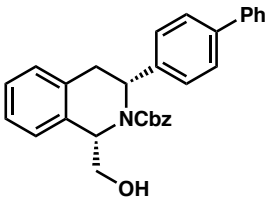
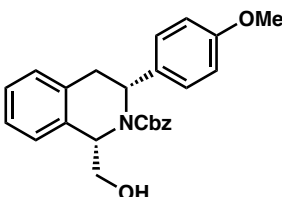
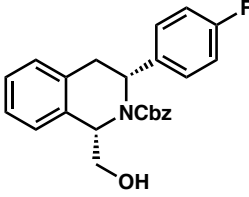
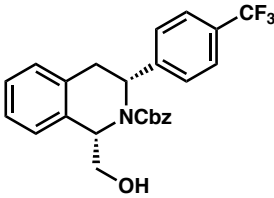
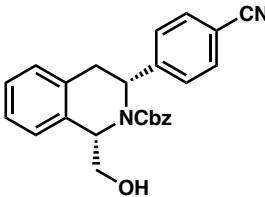
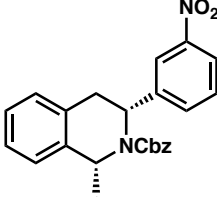
entry	salt additive	acid	% conversion ^b	cis:trans ^b	% ee of cis ^c
1	TBAI	AcOH	>95	10:1	89
2	Lil	AcOH	>95	10:1	89
3	NaI	AcOH	>95	10:1	90
4	KI	AcOH	92	10:1	87
5	TBACl	AcOH	>95	1:1.2	31
6	TBABr	AcOH	>95	1.2:1	63
7	none	AcOH	50	1:1	27
8	TBAI	none	31	ND	67
9	TBAI	TFA	>95	10:1	90
10	TBAI	(n-BuO) ₂ PO ₂ H	>95	7:1	84

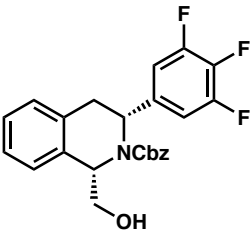
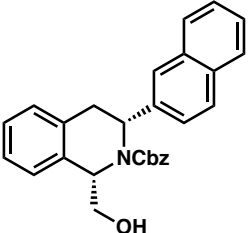
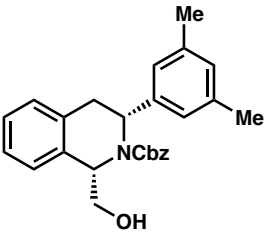
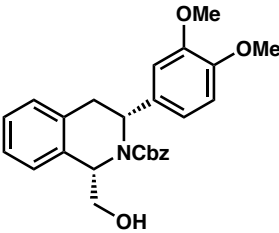
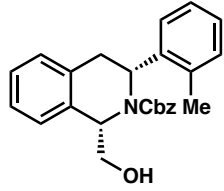
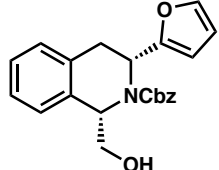
[a] Reactions conditions: 0.04 mmol of **182a**, 1.25 mol % [Ir(cod)Cl]₂, 3 mol % ligand, 7.5 mol % TBAI, 60 bar H₂ in 2.0 mL 9:1 solvent:AcOH. [b] Determined from crude ¹H NMR using 1,3,5-trimethoxybenzene as a standard. [c] Determined by chiral SFC analysis of Cbz-protected product.

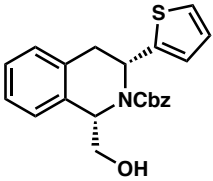
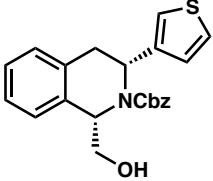
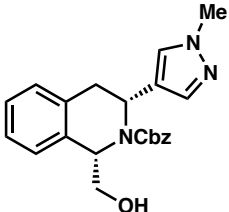
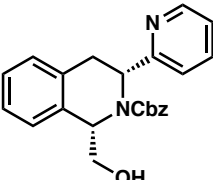
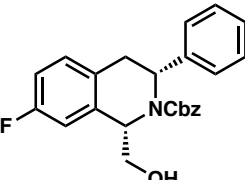
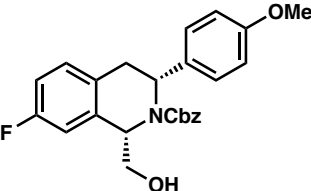
4.7.4 Determination of enantiomeric excess

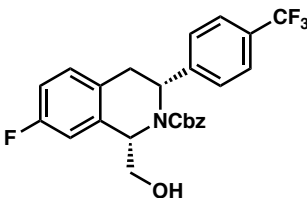
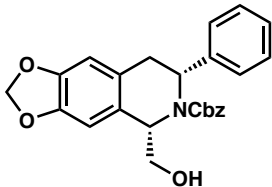
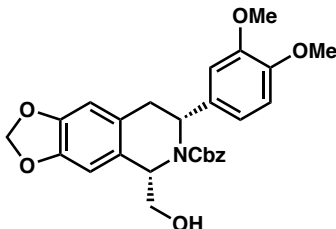
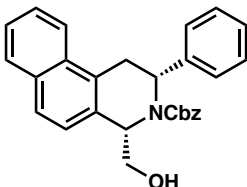
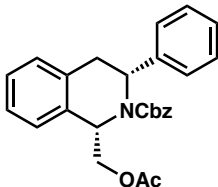
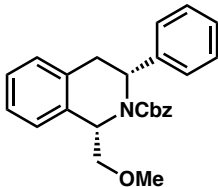
Table 4.4 Determination of Enantiomeric Excess.

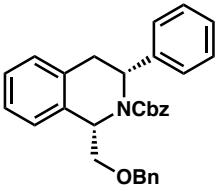
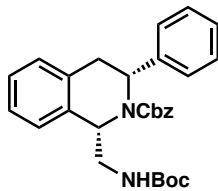
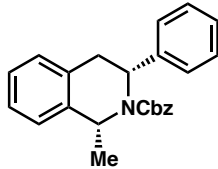
entry	compound	SFC analytic conditions	ee (%)
1	<p>183a-Cbz</p>	Chiralpak AD-H, λ = 210 nm 45% IPA/CO ₂ , 3.5 mL/min t _R (min) major 2.34, minor 4.02	92
2	<p>183b-Cbz</p>	Chiralpak AD-H, λ = 210 nm 45% IPA/CO ₂ , 3.5 mL/min t _R (min) major 1.81, minor 2.73	91

entry	compound	SFC analytic conditions	ee (%)
3	 <p>183c-Cbz</p>	Chiracel AD-H, $\lambda = 210$ nm 45% IPA/CO ₂ , 3.5 mL/min t _R (min) major 4.08, minor 5.18	92
4	 <p>183d-Cbz</p>	Chiralpak AD-H, $\lambda = 210$ nm 45% IPA/CO ₂ , 2.5 mL/min t _R (min) major 2.59, minor 3.61	92
5	 <p>183e-Cbz</p>	Chiralpak AD-H, $\lambda = 210$ nm 45% IPA/CO ₂ , 2.5 mL/min t _R (min) major 1.93, minor 2.87	93
6	 <p>183f-Cbz</p>	Chiralpak AD-H, $\lambda = 210$ nm 25% IPA/CO ₂ , 2.5 mL/min t _R (min) major 3.11, minor 5.54	92
7	 <p>183g-Cbz</p>	Chiralpak AD-H, $\lambda = 210$ nm 45% IPA/CO ₂ , 3.5 mL/min t _R (min) major 2.03, minor 3.33	82
8	 <p>183h-Cbz</p>	Chiralpak AD-H, $\lambda = 210$ nm 45% IPA/CO ₂ , 3.5 mL/min t _R (min) major 2.45, minor 3.23	86

entry	compound	SFC analytic conditions	ee (%)
9	 <p>183i-Cbz</p>	Chiralcel AD-H, $\lambda = 210$ nm 40% IPA/CO ₂ , 2.5 mL/min t_R (min) major 1.67, minor 2.20	89
10	 <p>183j-Cbz</p>	Chiralpak AD-H, $\lambda = 210$ nm 45% IPA/CO ₂ , 3.5 mL/min t_R (min) major 3.61, minor 5.81	95
11	 <p>183k-Cbz</p>	Chiralpak AD-H, $\lambda = 210$ nm 45% IPA/CO ₂ , 3.5 mL/min t_R (min) major 1.95, minor 3.02	92
12	 <p>183l-Cbz</p>	Chiralpak AD-H, $\lambda = 210$ nm 45% IPA/CO ₂ , 3.5 mL/min t_R (min) major 2.28, minor 2.93	88
13	 <p>183m-Cbz</p>	Chiralpak AD-H, $\lambda = 210$ nm 30% IPA/CO ₂ , 2.5 mL/min t_R (min) major 5.91, minor 6.39	49
14	 <p>183n-Cbz</p>	Chiralpak OJ-H, $\lambda = 210$ nm 35% IPA/CO ₂ , 2.5 mL/min t_R (min) major 1.52, minor 1.82	92

entry	compound	SFC analytic conditions	ee (%)
15	 <p>183o-Cbz</p>	Chiracel OJ-H, $\lambda = 210$ nm 35% IPA/CO ₂ , 2.5 mL/min t_R (min) major 2.86, minor 6.02	90
16	 <p>183p-Cbz</p>	Chiralpak AD-H, $\lambda = 210$ nm 45% IPA/CO ₂ , 3.5 mL/min t_R (min) major 3.19, minor 4.05	89
17	 <p>183q-Cbz</p>	Chiralpak OJ-H, $\lambda = 210$ nm 25% IPA/CO ₂ , 2.5 mL/min t_R (min) minor 1.84, major 2.60	87
18	 <p>183r-Cbz</p>	Chiralpak OD-H, $\lambda = 210$ nm 30% IPA/CO ₂ , 2.5 mL/min t_R (min) major 2.52, minor 2.79	85
19	 <p>185a-Cbz</p>	Chiralpak AD-H, $\lambda = 210$ nm 40% IPA/CO ₂ , 2.5 mL/min t_R (min) major 2.56, minor 3.04	93
20	 <p>185b-Cbz</p>	Chiralpak OJ-H, $\lambda = 210$ nm 30% IPA/CO ₂ , 2.5 mL/min t_R (min) major 1.93, minor 2.42	90

entry	compound	SFC analytic conditions	ee (%)
21	 <p>185c-Cbz</p>	Chiracel AD-H, $\lambda = 210$ nm 20% IPA/CO ₂ , 2.5 mL/min t _R (min) major 3.93, minor 4.46	94
22	 <p>185d-Cbz</p>	Chiralpak AD-H, $\lambda = 210$ nm 45% IPA/CO ₂ , 2.5 mL/min t _R (min) major 5.00, minor 7.22	58
23	 <p>185e-Cbz</p>	Chiralpak AD-H, $\lambda = 210$ nm 45% IPA/CO ₂ , 2.5 mL/min t _R (min) major 3.89, minor 5.16	54
24	 <p>185f-Cbz</p>	Chiralpak AD-H, $\lambda = 210$ nm 45% IPA/CO ₂ , 2.5 mL/min t _R (min) major 5.31, minor 10.01	82
25	 <p>187a-Cbz</p>	Chiralpak OJ-H, $\lambda = 210$ nm 20% IPA/CO ₂ , 2.5 mL/min t _R (min) major 3.32, minor 3.93	86
26	 <p>187b-Cbz</p>	Chiracel OD-H, $\lambda = 210$ nm 20% IPA/CO ₂ , 2.5 mL/min t _R (min) major 4.82, minor 5.25	89

entry	compound	SFC analytic conditions	ee (%)
27	 <p>187c-Cbz</p>	Chiralpak OD-H, $\lambda = 210$ nm 25% IPA/CO ₂ , 2.5 mL/min t_R (min) major 5.66, minor 6.38	88
28	 <p>187d-Cbz</p>	Chiralpak AD-H, $\lambda = 210$ nm 40% IPA/CO ₂ , 2.5 mL/min t_R (min) major 1.41, minor 1.76	90
29	 <p>187e-Cbz</p>	Chiralpak AS-H, $\lambda = 210$ nm 20% IPA/CO ₂ , 3.5 mL/min t_R (min) major 2.16, minor 2.62	90

4.7.5 Determination of relative and absolute configuration via VCD & OR

Method 1 – Vibrational Circular Dichroism (VCD)

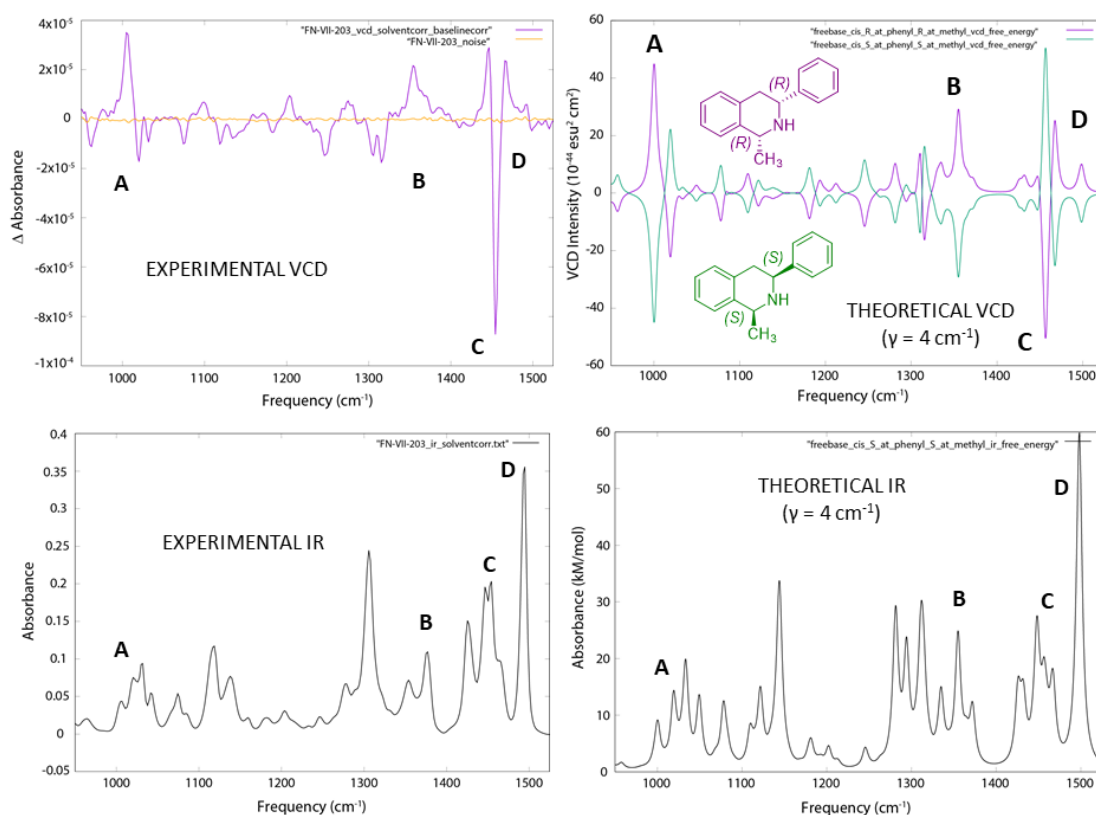
Experimental Protocol. A solution of **187e** (60 mg/mL) was prepared in CDCl₃ and loaded into a front-loading SL-4 cell (International Crystal Laboratories) possessing BaF₂ windows and 100 μ m path length. Infrared (IR) and VCD spectra were acquired on a BioTools ChiralIR-2X VCD spectrometer as a set of 27 one-hour blocks (27 blocks, 3120 scans per block) in dual PEM mode. A 15-minute acquisition of neat (-)- α -pinene control (separate 75 μ m BaF₂ cell) yielded a VCD spectrum in agreement with literature spectra. IR and VCD spectra were background-corrected using a 30-minute block IR acquisition of the empty instrument chamber under gentle N₂ purge, and were solvent corrected using an 8-hour (8 blocks, 3120 scans per block) IR/VCD acquisition of CDCl₃ in the same 100

$\mu\text{m BaF}_2$ cell as used for **187e**. The reported spectra represent the result of block averaging.

Computational Protocol. The arbitrarily chosen (*S,S*) stereoisomer of compound **187e** ((*S*) at methyl, (*S*) at phenyl; thus *cis*) was subjected to an exhaustive initial molecular mechanics-based conformational search (MMFF94 force field, 0.08 Å geometric RMSD cutoff, and 30 kcal/mol energy window) as implemented in MOE 2019.0102 (Chemical Computing Group, Montreal, CA). All conformers retained the (*S*) configuration at both centers. Separately, a study involving the *trans* stereoisomer possessing the (*R*) configuration at the methyl group and (*S*) configuration at phenyl was performed in identical fashion, with stereochemical integrity again retained throughout the stochastic conformational search. All MMFF94 conformers within a 10 kcal/mol energy window were then subjected to geometry optimization, harmonic frequency calculation, and VCD rotational strength evaluation using density functional theory. All quantum mechanical calculations first utilized the B3LYP functional, small 6-31G* basis, and IEFPCM model (chloroform solvent) as an initial filter, followed by subsequent optimization using B3PW91 functional, cc-pVTZ basis, and implicit IEFPCM chloroform solvation model on all IEFPCM-B3LYP/6-31G* conformers below 5 kcal/mol. All calculations were performed with the *Gaussian 16* program system (Rev. C.01; Frisch *et al.*, Gaussian, Inc., Wallingford, CT). Resultant IEFPCM-B3PW91/cc-pVTZ harmonic frequencies were scaled by 0.98. All structurally unique conformers possessing all positive Hessian eigenvalues were Boltzmann weighted by relative free energy at 298.15 K. The predicted IR and VCD frequencies and intensities of the retained conformers were convolved using Lorentzian line shapes ($\gamma = 4\text{ cm}^{-1}$) and summed using the respective Boltzmann weights

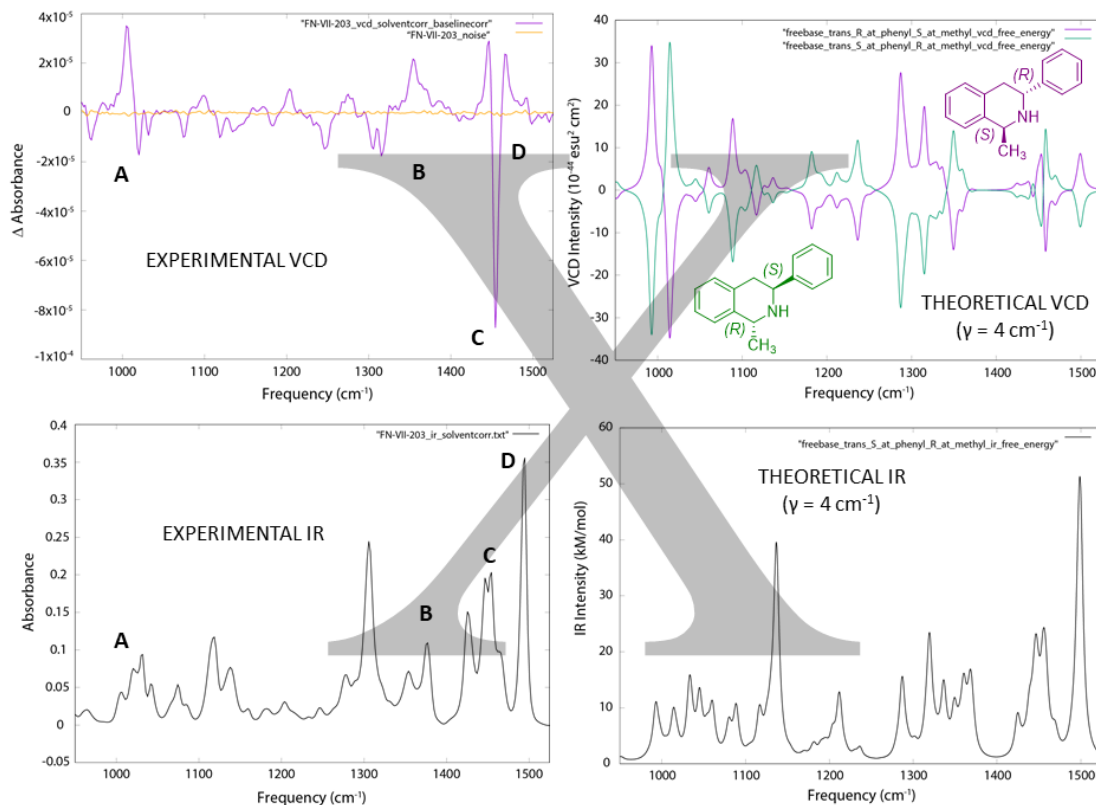
to yield the final predicted IR and VCD spectra of the species described above. The predicted VCD of the corresponding enantiomers were generated by inversion of sign. From a combination of (a) the best overall agreement of (*R,R*)-**187e** with experiment among all of the theoretical spectra in the useful range of the VCD (~ 1000 - 1450 cm^{-1} , regions **A-D**; see below) coupled with (b) support of this assignment by the agreement between predicted versus measured optical rotation (see Method 2) the absolute configuration of **6e** was established as *cis* and (*R,R*).

Figure 4.3 Experimental (left) and computed (right) IR and VCD spectra for the *cis* isomers of **187e**.



The better agreement with the (*R,R*) stereoisomer, upon alignment of the achiral IR spectra and correlation to VCD signals, is readily evident.

Figure 4.4 Experimental (left) and computed (right) IR and VCD spectra for the *trans* isomers of **187e**.

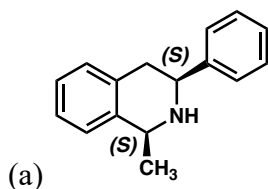


The worse agreement with experiment between either of the predicted *trans* stereoisomers, compared to the *cis*- and (*R,R*) stereoisomer above, can be seen. This assertion is further supported to an extent by the optical rotation data below.

Method 2 – Optical Rotation (OR)

Computational Protocol. The ensemble of unique IEFPCM-B3PW91/cc-pVTZ conformers of **187e** generated in Method 1 above were subjected to optical rotation calculation at 589.0 nm using the B3LYP hybrid density functional, the large and diffuse 6-311++G(2df,2pd) basis set, and the IEFPCM implicit chloroform solvent model. The computed IEFPCM-B3LYP/6-31++G(2df,2pd) optical rotations (weighted by IEFPCM-B3PW91/cc-pVTZ free energies at 298.15 K) along with those resulting from

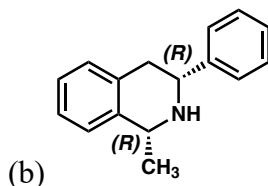
alternatively weighting by either the IEFPCM-B3PW91/cc-pVTZ total energies or IEFPCM-B3LYP/6-31++G(2df,2pd)/IEFPCM-B3PW91/cc-pVTZ total energies are reported in (a)-(d) below.



Predicted OR, weighted by IEFPCM-B3PW91/cc-pVTZ free energies: **-144.5°**

Predicted OR, weighted by IEFPCM-B3PW91/cc-pVTZ total energies: **-144.6°**

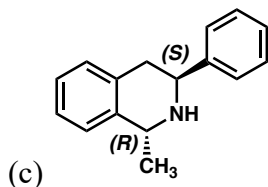
Predicted OR, weighted by IEFPCM-B3LYP/6-31++G(2df,2pd)/IEFPCM-B3PW91/cc-pVTZ total energies: **-147.0°**



Predicted OR, weighted by IEFPCM-B3PW91/cc-pVTZ free energies: **+144.5°**

Predicted OR, weighted by IEFPCM-B3PW91/cc-pVTZ total energies: **+144.6°**

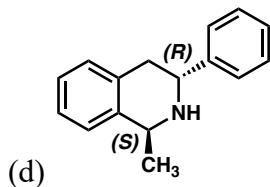
Predicted OR, weighted by IEFPCM-B3LYP/6-31++G(2df,2pd)/IEFPCM-B3PW91/cc-pVTZ total energies: **+147.0°**



Predicted OR, weighted by IEFPCM-B3PW91/cc-pVTZ free energies: **-94.5°**

Predicted OR, weighted by IEFPCM-B3PW91/cc-pVTZ total energies: **-101.0°**

Predicted OR, weighted by IEFPCM-B3LYP/6-31++G(2df,2pd)/IEFPCM-B3PW91/cc-pVTZ total energies: **-100.1°**



Predicted OR, weighted by IEFPCM-B3PW91/cc-pVTZ free energies: **+94.5°**

Predicted OR, weighted by IEFPCM-B3PW91/cc-pVTZ total energies: **+101.0°**

Predicted OR, weighted by IEFPCM-B3LYP/6-31++G(2df,2pd)/IEFPCM-B3PW91/cc-pVTZ total energies: **+100.1°**

Measured optical rotation: $[\alpha]_{\text{D}}^{25} +133.3$ (c 0.79, CHCl_3). Assuming only that the *sign* of the optical rotation is correctly predicted by theory, given the experimentally measured value of $+133.3^\circ$, the absolute configuration of **187e** must either be: (i) (*R*) at both chiral centers (and therefore *cis*); or (b) (*S*) at phenyl and (*R*) at methyl (*trans*). Scenario (b) is unlikely, given the wrong (opposite) directionality of the VCD signals in regions **C** and **D** of the experimental spectrum. Scenario (a) also gives rise to the best agreement between the predicted and measured VCD spectra.

4.8 REFERENCES AND NOTES

- (1) a) Taylor, R. D.; MacCoss, M.; Lawson, A. D. G. *J. Med. Chem.* **2014**, *57*, 5845.
b) Vitaku, E.; Smith, D. T.; Njardarson, J. T. *J. Med. Chem.* **2014**, *57*, 10257–10274. c) Lovering, F.; Bikker, J.; Humblet, C. *J. Med. Chem.* **2009**, *52*, 6752–

6756. d) Lovering, F. *Med. Chem. Commun.* **2013**, *4*, 515–519. e) Roughley, S. D.; Jordan, A. M. *J. Med. Chem.* **2011**, *54*, 3451–3479.
- (2) a) Zhou, Y.-G. *Acc. Chem. Res.* **2007**, *40*, 1357–1366. b) Wang, D.-S.; Chen, Q.-A.; Lu, S.-M.; Zhou, Y.-G. *Chem. Rev.* **2012**, *112*, 2557–2590.
- (3) a) Zhao, D.; Glorius, F. *Angew. Chem. Int. Ed.* **2013**, *52*, 9616–9618. b) Wiedner, E. S.; Chambers, M. B.; Pitman, C. L.; Bullock, R. M.; Miller, A. J. M.; Appel, A. M. *Chem. Rev.* **2016**, *116*, 8655–8692.
- (4) For Ir-catalyzed asymmetric hydrogenation of isoquinolines, see a) Lu, S. M.; Wang, Y. Q.; Han, X. W.; Zhou, Y.-G. *Angew. Chem. Int. Ed.* **2006**, *45*, 2260–2263. b) Shi, L. Ye, Z.-S.; Cao, L. L.; Guo, R. N.; Hu, Y.; Zhou, Y.-G. *Angew. Chem. Int. Ed.* **2012**, *51*, 8286–8289. c) Iimuro, A.; Yamaji, K.; Kandula, S.; Nagano, T.; Kita, Y.; Mashima, K. *Angew. Chem. Int. Ed.* **2013**, *52*, 2046–2050. d) Ye, Z.-S.; Guo, R.-N.; Cai, X.-F.; Chen, M.-W.; Shi, L.; Zhou, Y.-G. *Angew. Chem. Int. Ed.* **2013**, *52*, 3685–3689. e) Kita, Y.; Yamaji, K.; Higashida, K.; Sathaiah, K.; Iimuro, A.; Mashima, K. *Chem. Eur. J.* **2015**, *21*, 1915–1927. f) Guo, R.-N.; Cai, X.-F.; Shi, L.; Ye, Z.-S.; Chen, M.-W.; Zhou, Y.-G. *Chem. Commun.* **2013**, *49*, 8537–8539. g) Chen, M.-W.; Ji, Y.; Wang, J.; Chen, Q.-A.; Shi, L.; Zhou, Y.-G. *Org. Lett.* **2017**, *19*, 4988–4991. For Ru-Catalyzed Enantioselective Hydrogenation of Isoquinolines, see h) Wen, J.; Tan, R.; Liu, S.; Zhao, Q.; Zhang, X. *Chem. Sci.* **2016**, *7*, 3047–3051.
- (5) a) Scott, J. D.; Williams, R. M. *Chem. Rev.* **2002**, *102*, 1669–1730. b) Siengalewicz, P.; Rinner, U.; Mulzer, J. *Chem. Soc. Rev.* **2008**, *37*, 2676–2690.

- (6) Welin, E. R.; Ngamnthiporn, A.; Klatte, M.; Lapointe, G.; Pototschnig, G. M.; McDermott, M. S. J.; Conklin, D.; Gilmore, C. D.; Tadross, P. M.; Haley, C. K.; Negoro, K.; Glibstrup, E.; Grünanger, C. U.; Allan, K. M.; Virgil, S. C.; Slamon, D. J.; Stoltz, B. M. *Science*. **2019**, *363*, 270–275.
- (7) For C–H activation/annulation strategy, see a) Zhang, Z.-W.; Lin, A.; Yang, J. *J. Org. Chem.* **2014**, *79*, 7041–7050. For ketone enolate-arylation/annulation, see b) Donohoe, T. J.; Pilgrim, B. S.; Jones, G. R.; Bassuto, J. A. *Proc. Natl. Acad. Sci. U.S.A.* **2012**, *109*, 11605–11608. For benzannulation of isocoumarins, see c) Manivel, P. Probakaran, K.; Khan, F. N.; Jin, J. S. *Res. Chem. Intermed.* **2012**, *38*, 347–357.
- (8) Pilgrim, B. S.; Gatland, A. E.; Esteves, C. H. A.; McTernan, C. T.; Jones, G. R.; Tatton, M. R. Procopiou, P. A.; Donohoe, T. J. *Org. Biomol. Chem.* **2016**, *14*, 1065–1090.
- (9) Allan, K. M.; Hong, B. D.; Stoltz, B. M. *Org. Biomol. Chem.* **2009**, *7*, 4960–4964.
- (10) For example of transition-metal-catalyzed tandem C–H activation/annulation of arenes and alkynes, see a) Zhu, Z.; Tang, X.; Li, X.; Wu, W.; Deng, G.; Jiang, H. *J. Org. Chem.* **2016**, *81*, 1401–1409. b) Zhou, S.; Wang, M.; Wang, L.; Chen, K.; Wang, J.; Song, C.; Zhu, J. *Org. Lett.* **2016**, *18*, 5632–5635. c) Chinnagolla, R. K.; Pimparkar, S.; Jeganmohan, M. *Org. Lett.* **2012**, *14*, 3032–3035. d) Zhao, D.; Lied, F.; Glorius, F. *Chem. Sci.* **2014**, *5*, 2869–2873.
- (11) a) Chu, H.; Sun, S.; Yu, J.-T.; Cheng, J. *Chem. Commun.* **2015**, *51*, 13327. b) Arambasic, M.; Hooper, J. F.; Willis, M. C. *Org. Lett.* **2013**, *15*, 5162–5165.

- (12) See Table 4.3, Section 4.7.3 for additional results using other acids. Although further studies are required to fully understand the role of acid, we speculate that the acid helps promoting a) the tautomerization of enamine to imine prior to the second reduction and b) the dissociation of THIQ product from Ir-complex through protonation.
- (13) In a similar Ir-xylylphos system, it is reported that the alpha-alkoxy imine binds to the catalyst in a bidentate fashion, see a) Dorta, R.; Broggini, D.; Stoop, R.; R  gger, H. Spindler, F.; Togni, A. *Chem. Eur. J.* **2004**, *10*, 267–278. b) Dorta, R.; Broggini, D.; Kissner, R.; Togni, A. *Chem. Eur. J.* **2004**, *10*, 4546–4555.
- (14) Hopmann, K. H.; Bayer, A. *Organometallics*. **2011**, *30*, 2483–2497.
- (15) Increasing the catalyst loading to 2.5 mol % of [Ir(cod)Cl]₂ and 6 mol % of **L57** does not improve the conversion any further.
- (16) The absolute stereochemistry of product **187e** was determined via the combination of measured and computed vibrational circular dichroism (VCD) spectra and optical rotations. The configuration of **187e** (*R, R*) was found to be analogous to that determined for hydroxymethyl product **183a** and also observed crystallographically for **183p**.
- (17) a) Chrzanowska, M. Grajewska, A.; Rozwadowska, M. D. *Chem. Rev.* **2016**, *116*, 12369–12465. b) Carrillo, L.; Badia, D.; Dominguez, E.; Anakabe, E.; Osante, I.; Tellitu, I.; Vicario, J. L. *J. Org. Chem.* **1999**, *64*, 115–1120.
- (18) Haftchenary, S.; Nelson, S. D.; Furst, L.; Dandapani, S.; Ferrara, S. J.; Bo  kovi  , Z. V.; Laz  , S. F.; Guerrero, A. M.; Serrano, J. C.; Crews, D. K.; Brackeen, C.;

- Mowat, J.; Brumby, T.; Bauser, M.; Schreiber, S. L.; Phillips, A. J. *ACS. Comb. Sci.* **2016**, *18*, 569–574.
- (19) Alternatively, the oxazolidinone-fused product **189** could be synthesized utilizing a 2-step sequence. First is the Boc-protection of the amine. The Boc-protected product was subsequently cyclized to afford oxazolidinone-fused THIQ **189** under the Appel reaction conditions.
- (20) Zhang, G.-L.; Chen, C.; Xiong, Y.; Zhang, L.-H.; Ye, J.; Ye, X.-S. *Carbohydrate Research*. **2010**, *345*, 780–786.
- (21) Gadhiya, S. V.; Giri, R.; Cordone, P.; Karki, A.; Harding, W. W. *Curr. Org. Chem.* **2018**, *22*, 1893–1905.
- (22) Thimmaiah, S.; Ningegowda, M.; Shivananju, N. S.; Ningegowda, R.; Siddaraj, R.; Priya, B. S. *Eur. J. Chem.* **2016**, *7*, 391–396.
- (23) Guo, D.; Li, J.; Lin, H.; Zhou, Y.; Chen, Y.; Sun, H.; Zhang, D.; Li, H.; Shoichet, B. K.; Shan, L.; Xie, X.; Jiang, H.; Liu, H. *J. Med. Chem.* **2016**, *59*, 9489–9502.
- (24) Pangborn, A. M.; Giardello, M. A.; Grubbs, R. H.; Rosen, R. K.; Timmers, F. J. Safe and Convenient Procedure for Solvent Purification. *Organometallics*. **1996**, *15*, 1518–1520.
- (25) Bruno, N. C.; Tudge, M. T.; Buchwald, S. L. *Chem. Sci.* **2013**, *4*, 916–920.
- (26) Legault, C. Y.; Charette, A. B. *J. Am. Chem. Soc.* **2005**, *127*, 8966–8967.
- (27) Xu, Z.; Xu, X.; O’Laoi, R.; Ma, H.; Zheng, J.; Chen, S.; Luo, L.; Hu, Z.; He, S.; Li, J.; Zhang, H.; Zhang, X. *Bioorg. Med. Chem.* **2016**, *24*, 5861–5872.

APPENDIX 11

Spectra Relevant to Chapter 4:

Iridium-Catalyzed Enantioselective and Diastereoselective

Hydrogenation of 1,3-Disubstituted Isoquinolines

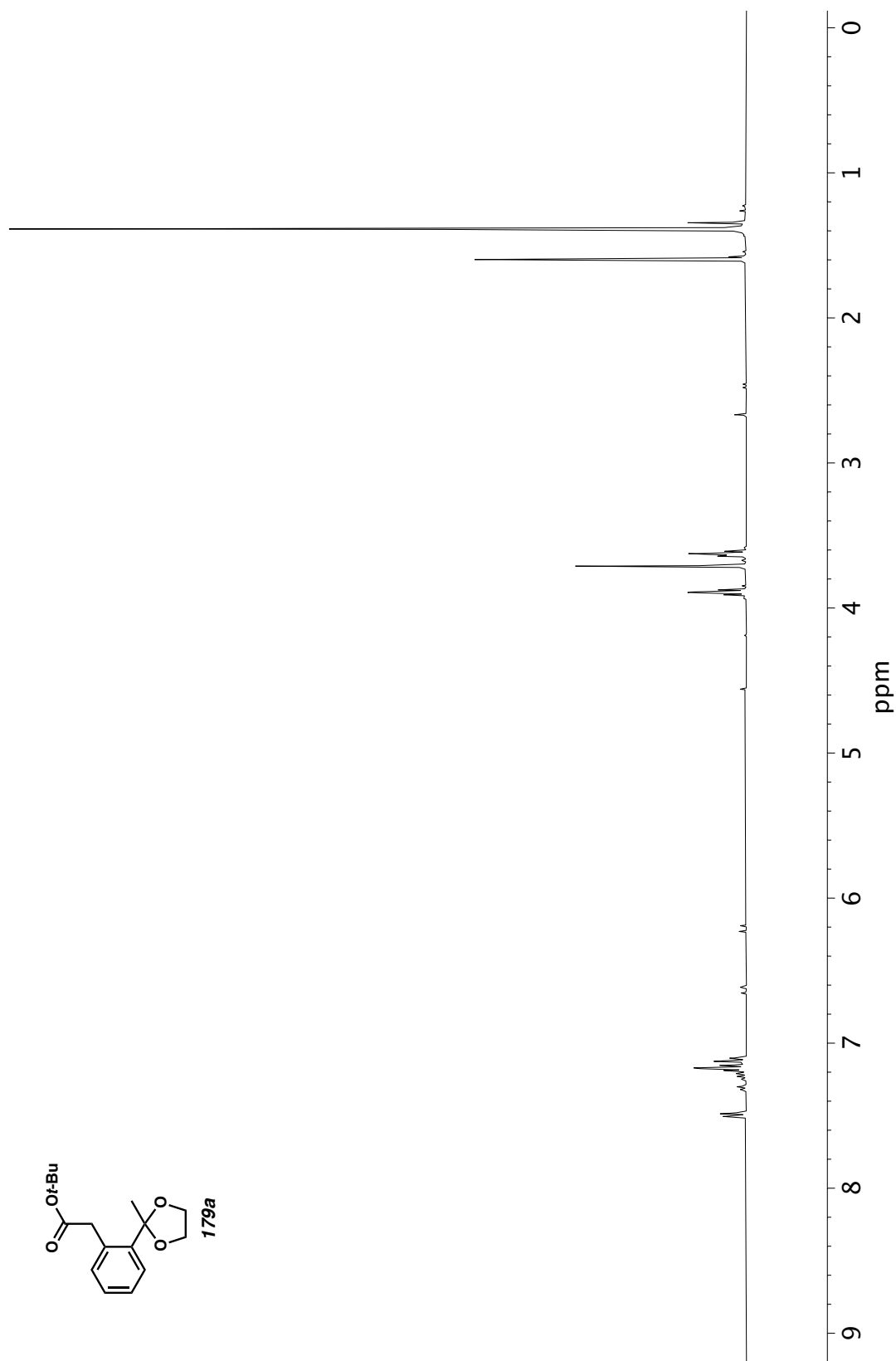


Figure A11.1 ¹H NMR (400 MHz, CDCl₃) of compound **179a**.

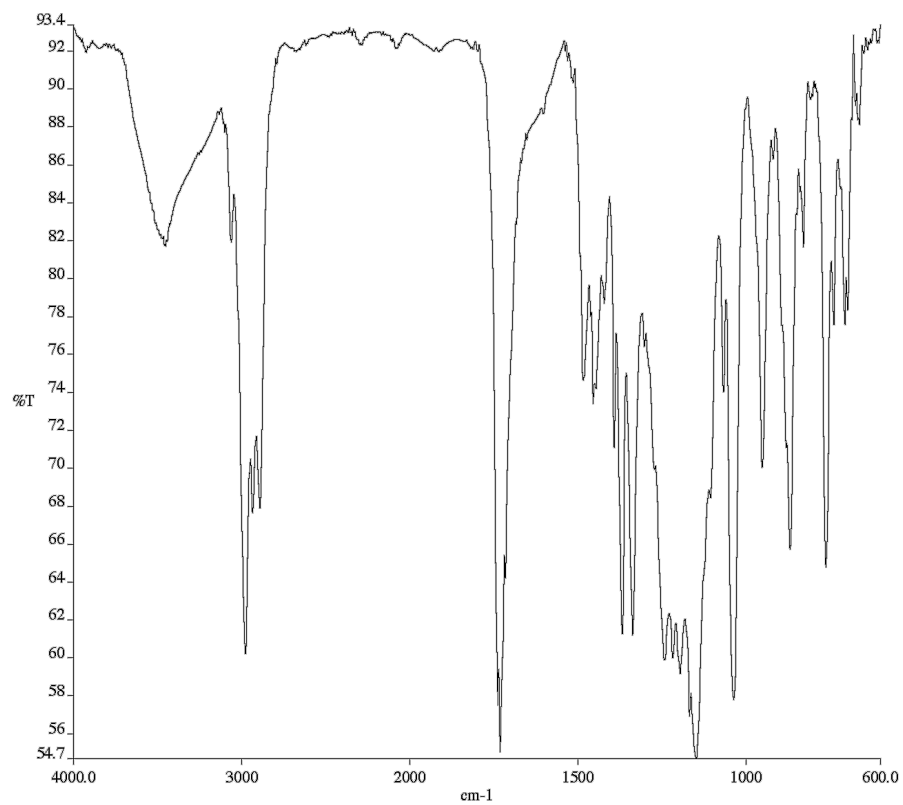


Figure A11.2 Infrared spectrum (Thin Film, NaCl) of compound **179a**.

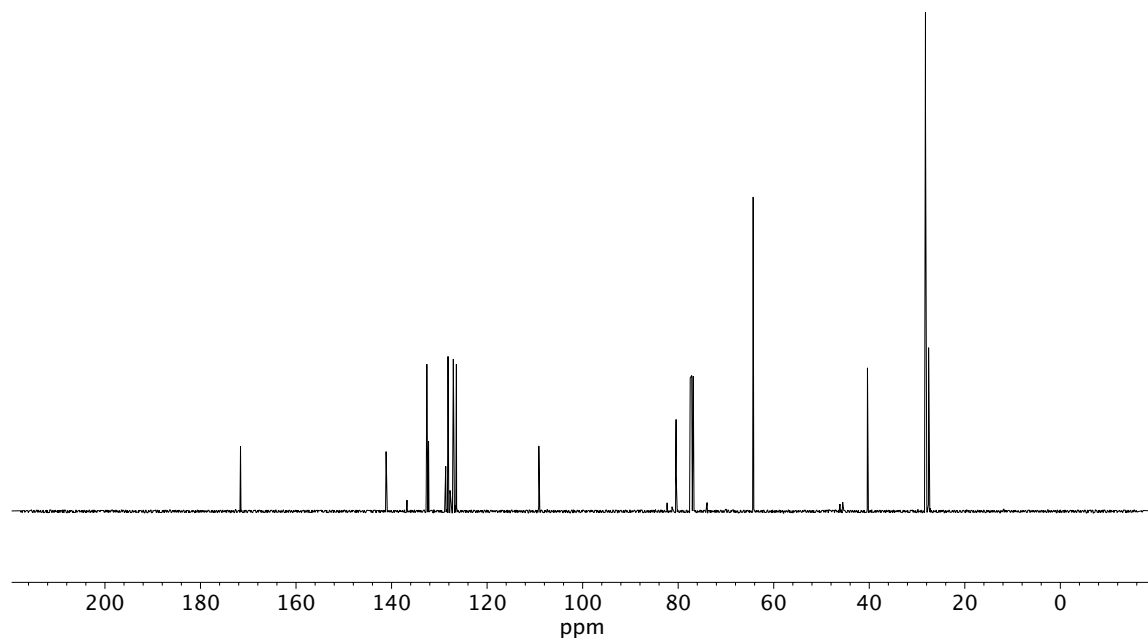


Figure A11.3 ¹³C NMR (100 MHz, CDCl₃) of compound **179a**.

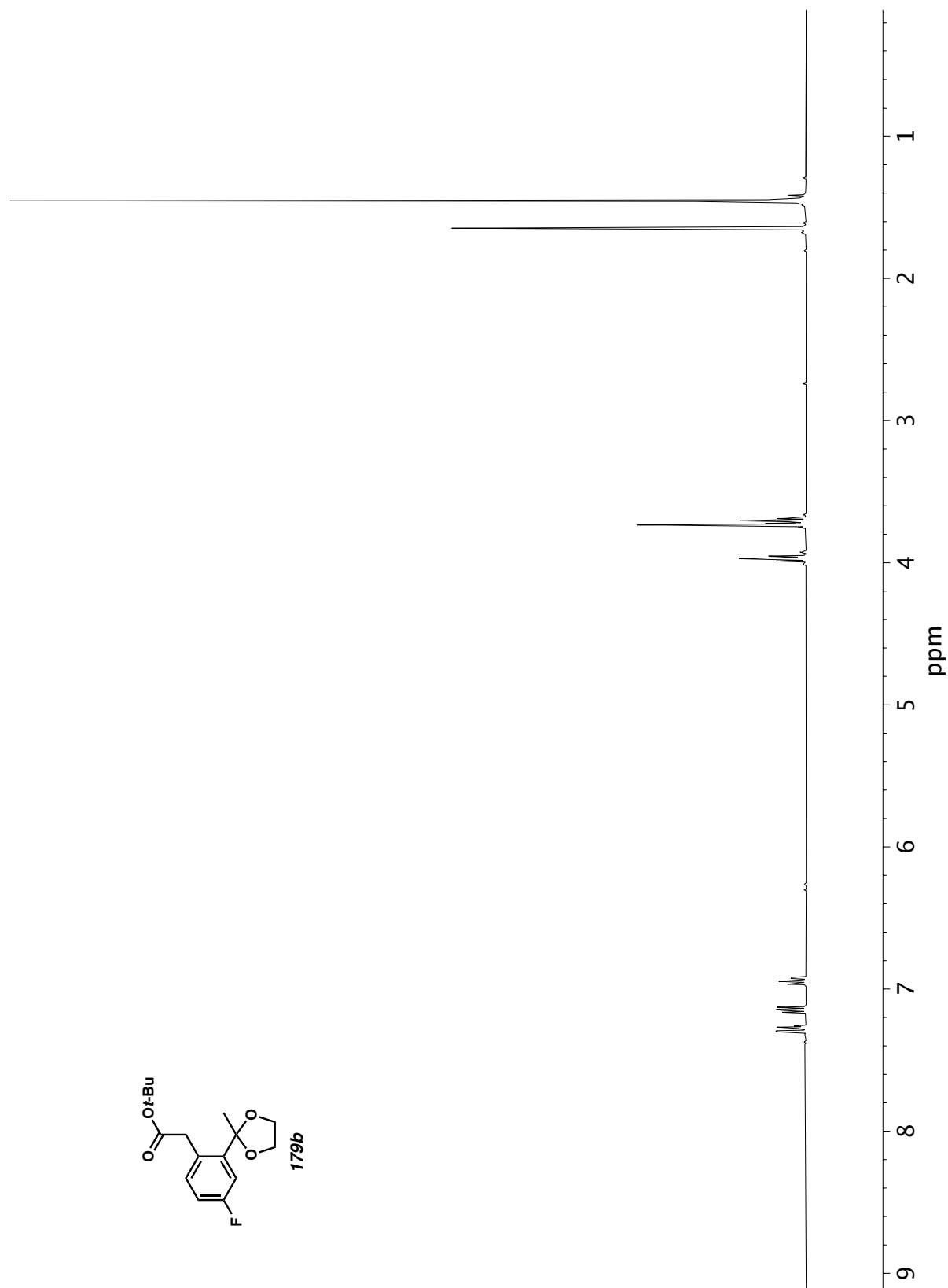


Figure A11.4 ¹H NMR (400 MHz, CDCl₃) of compound **179b**.

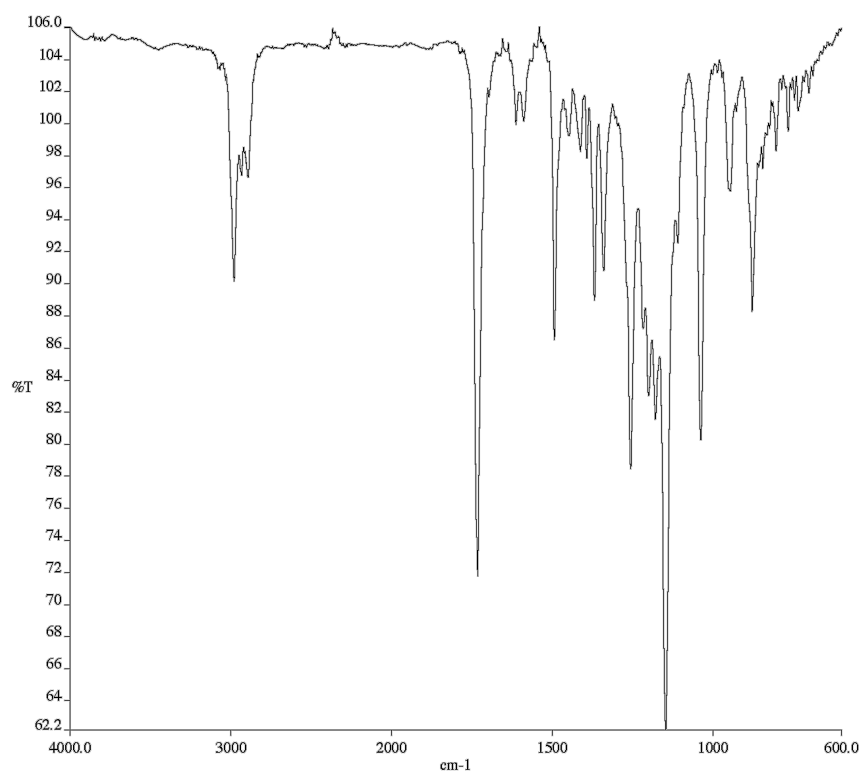


Figure A11.5 Infrared spectrum (Thin Film, NaCl) of compound **179b**.

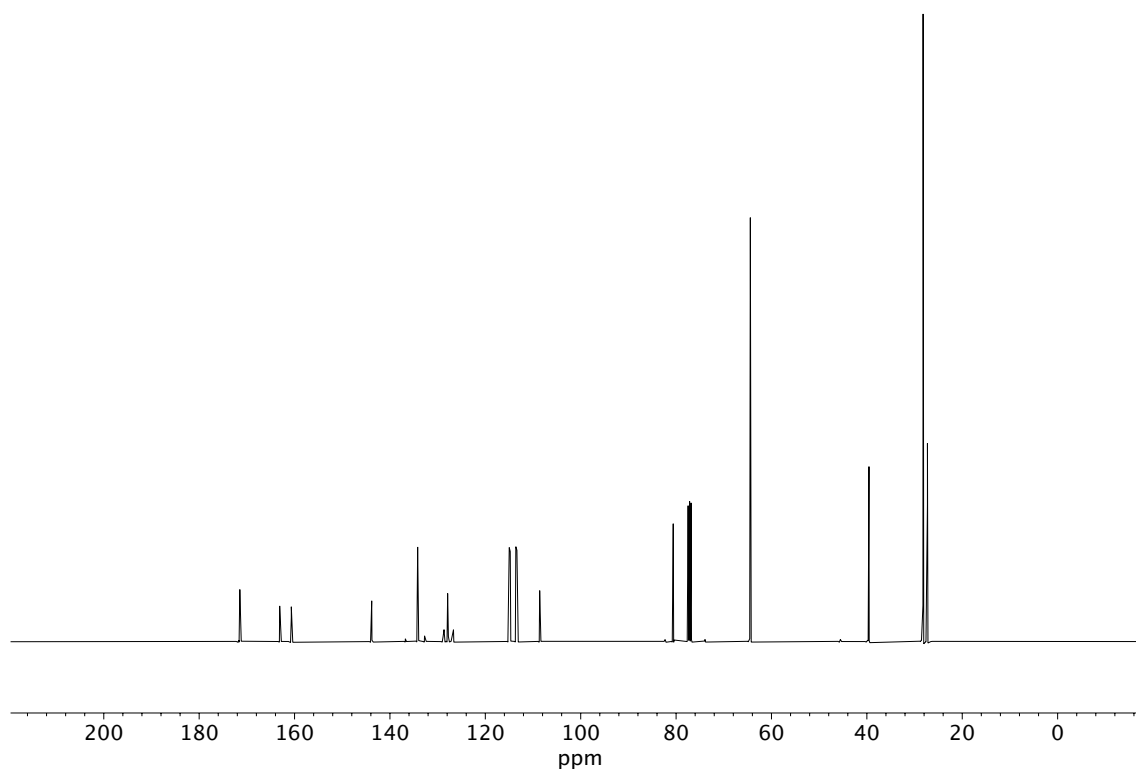


Figure A11.6 ¹³C NMR (100 MHz, CDCl₃) of compound **179b**.

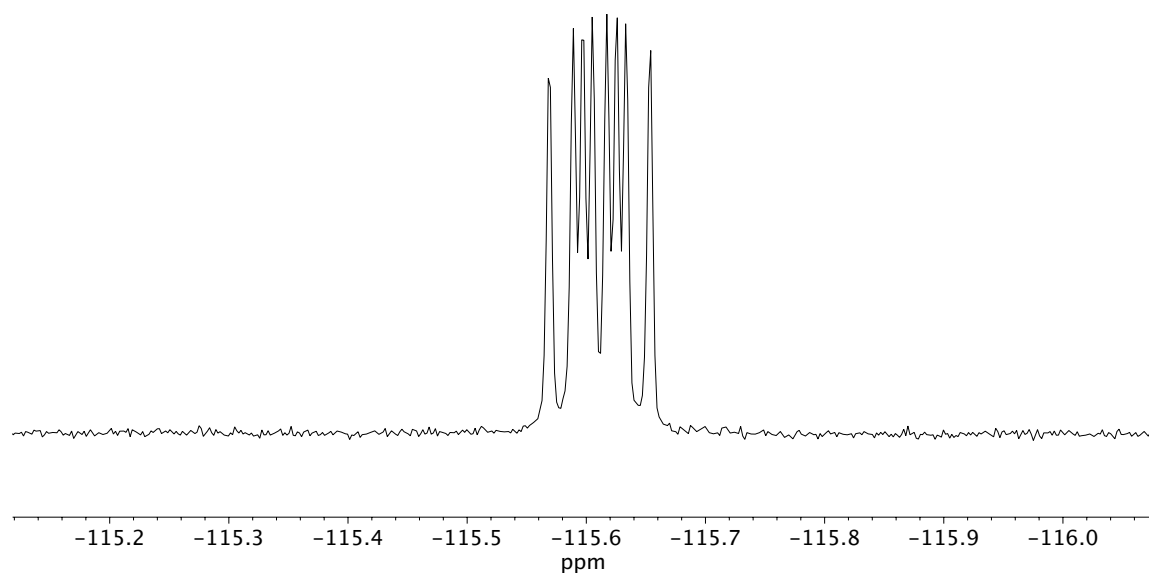


Figure A11.7 ^{19}F NMR (282 MHz, CDCl_3) of compound **179b**.

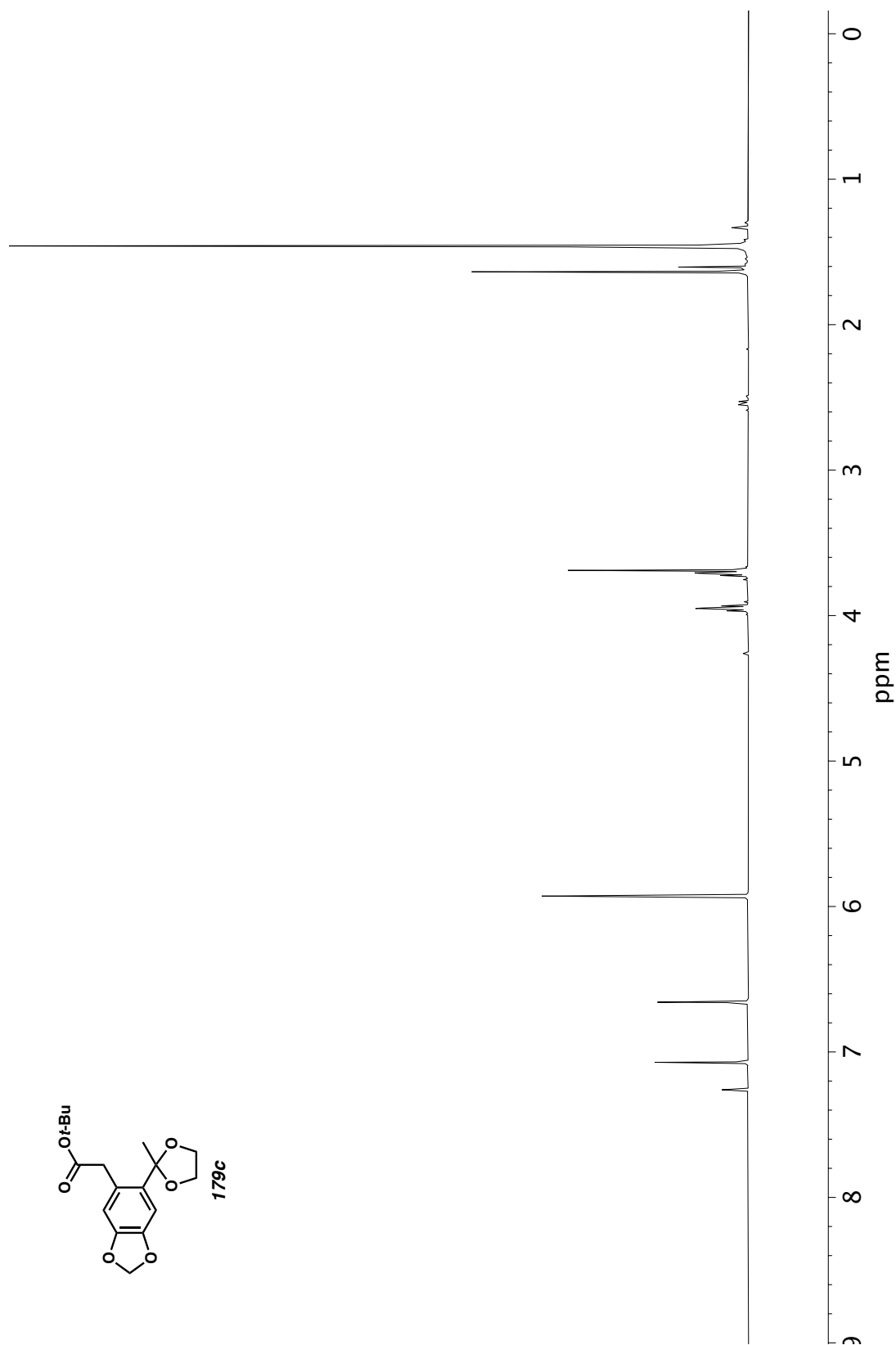


Figure A11.8 ^1H NMR (400 MHz, CDCl_3) of compound **179c**.

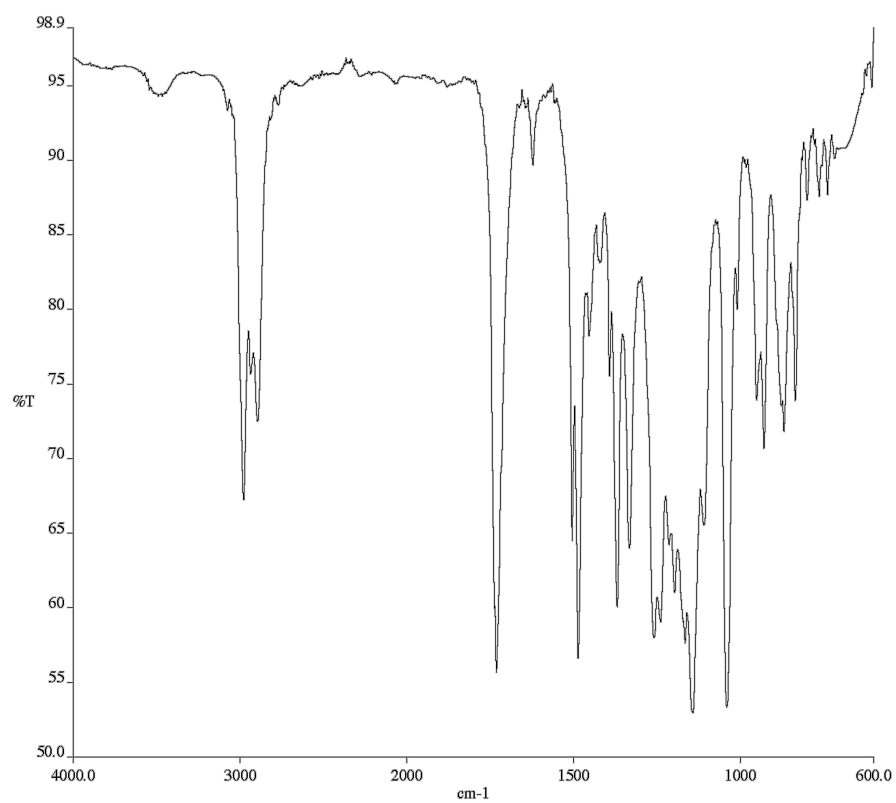


Figure A11.9 Infrared spectrum (Thin Film, NaCl) of compound **179c**.

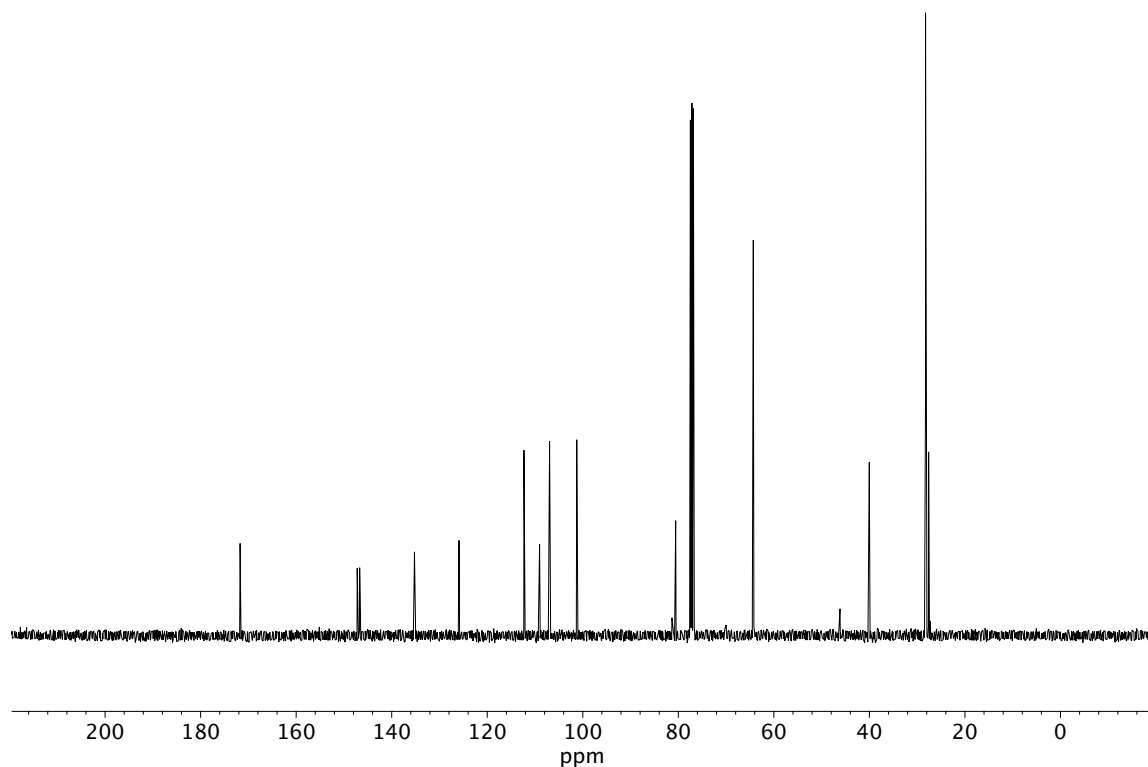


Figure A11.10 ¹³C NMR (100 MHz, CDCl₃) of compound **179c**.

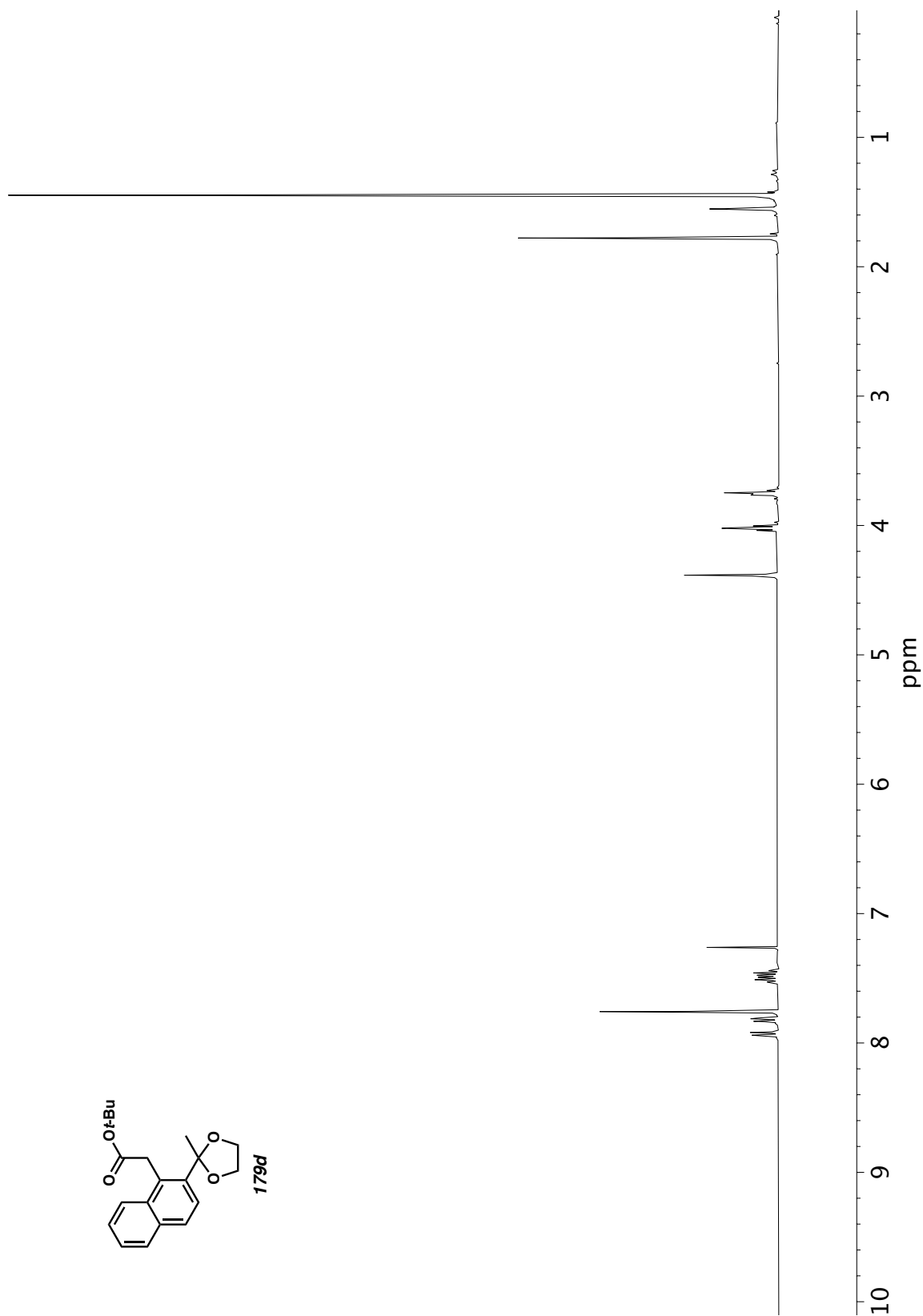


Figure A11.11 ^1H NMR (400 MHz, CDCl_3) of compound **179d**.

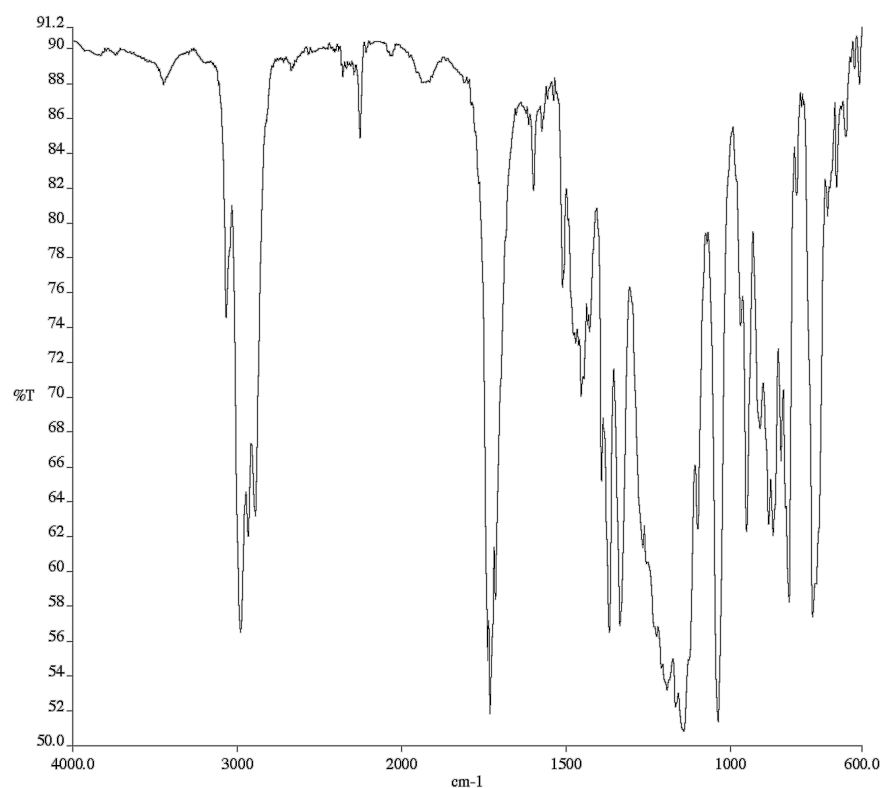


Figure A11.12 Infrared spectrum (Thin Film, NaCl) of compound **179d**.

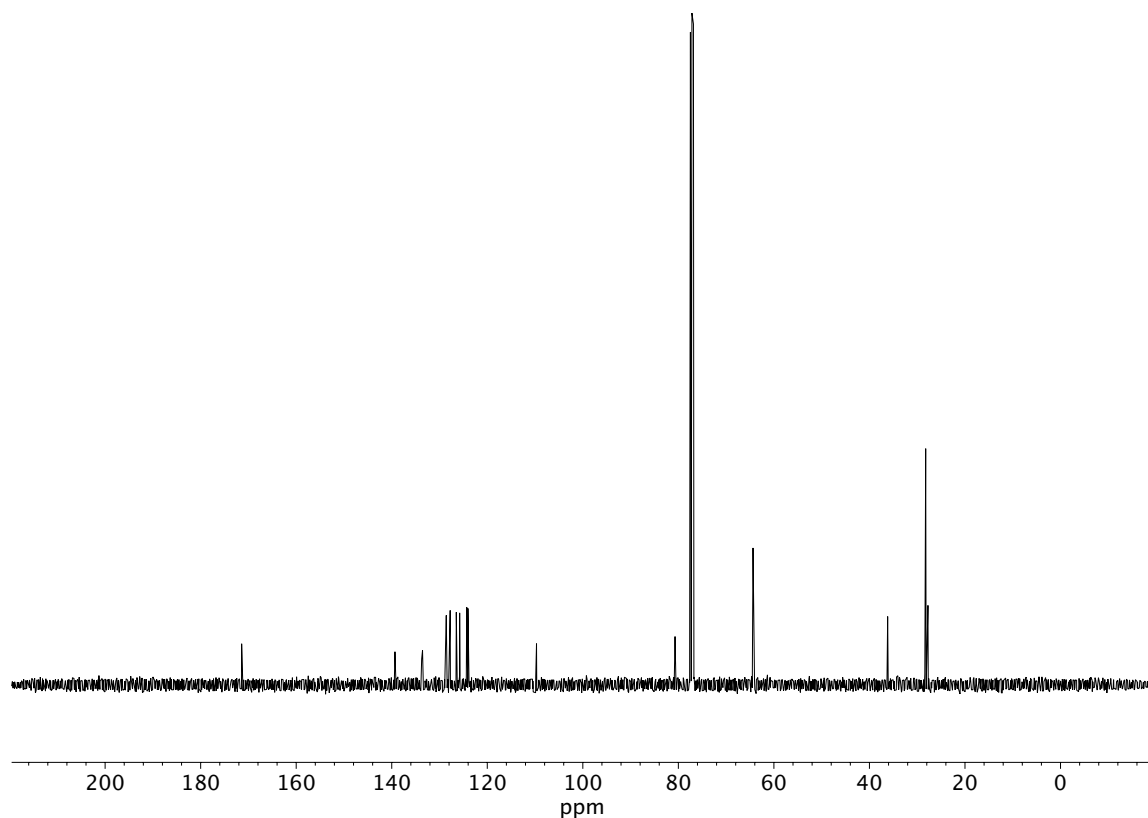


Figure A11.13 ¹³C NMR (100 MHz, CDCl₃) of compound **179d**.

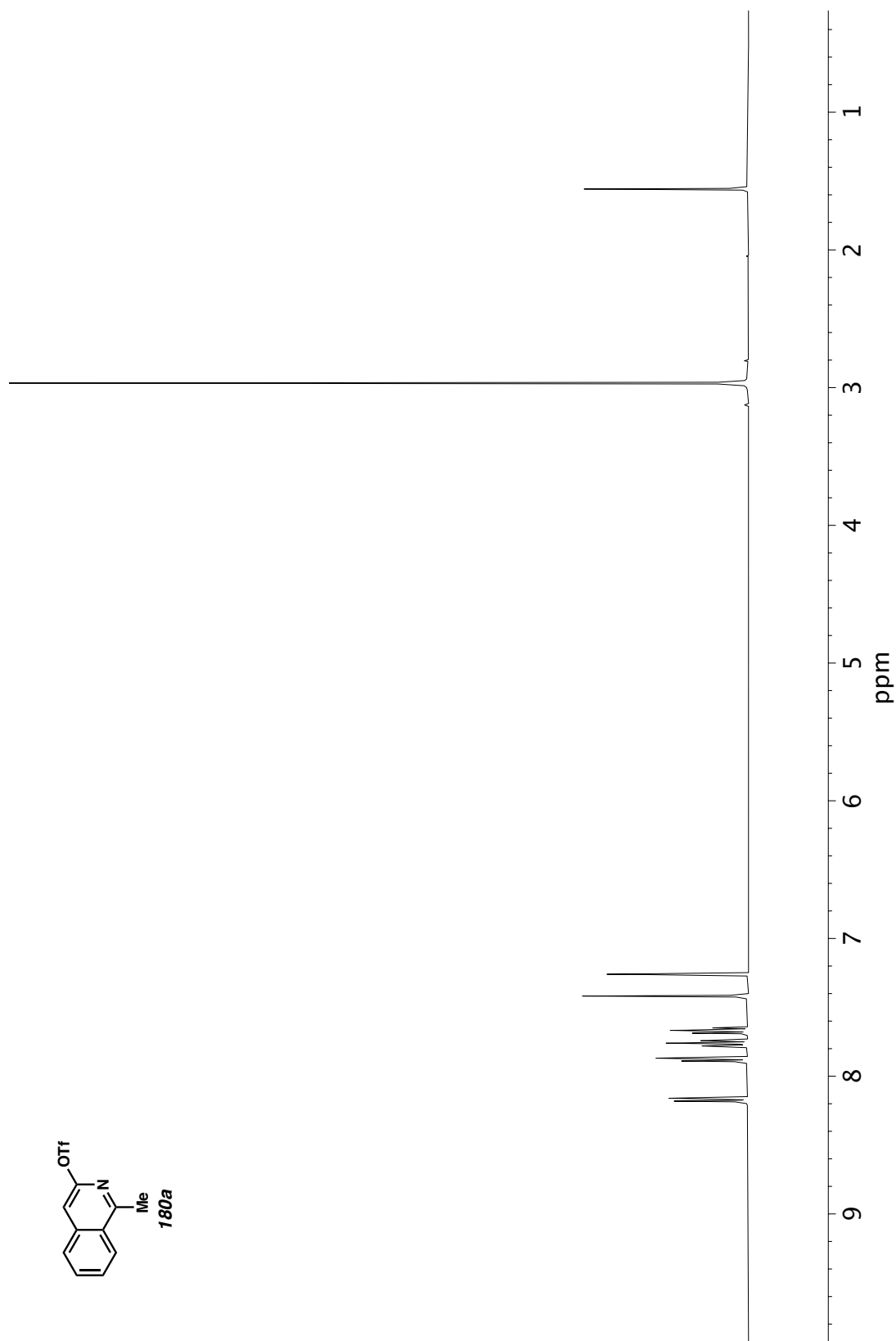


Figure A11.14 ^1H NMR (400 MHz, CDCl_3) of compound **180a**.

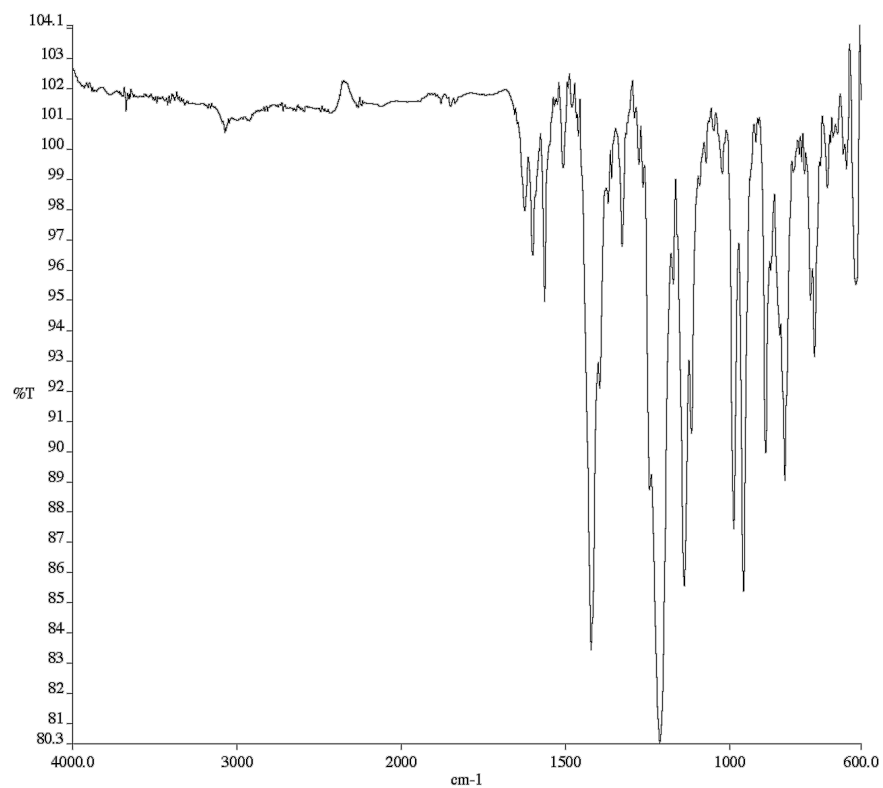


Figure A11.15 Infrared spectrum (Thin Film, NaCl) of compound **180a**.

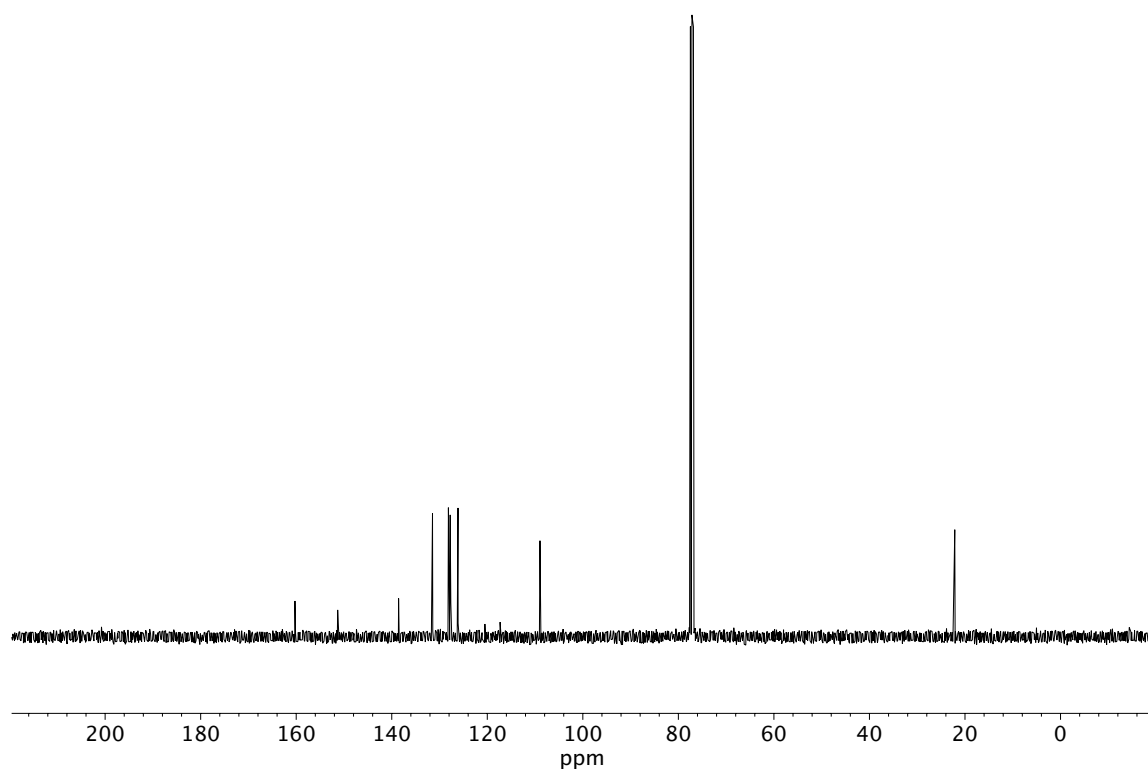


Figure A11.16 ¹³C NMR (100 MHz, CDCl₃) of compound **180a**.

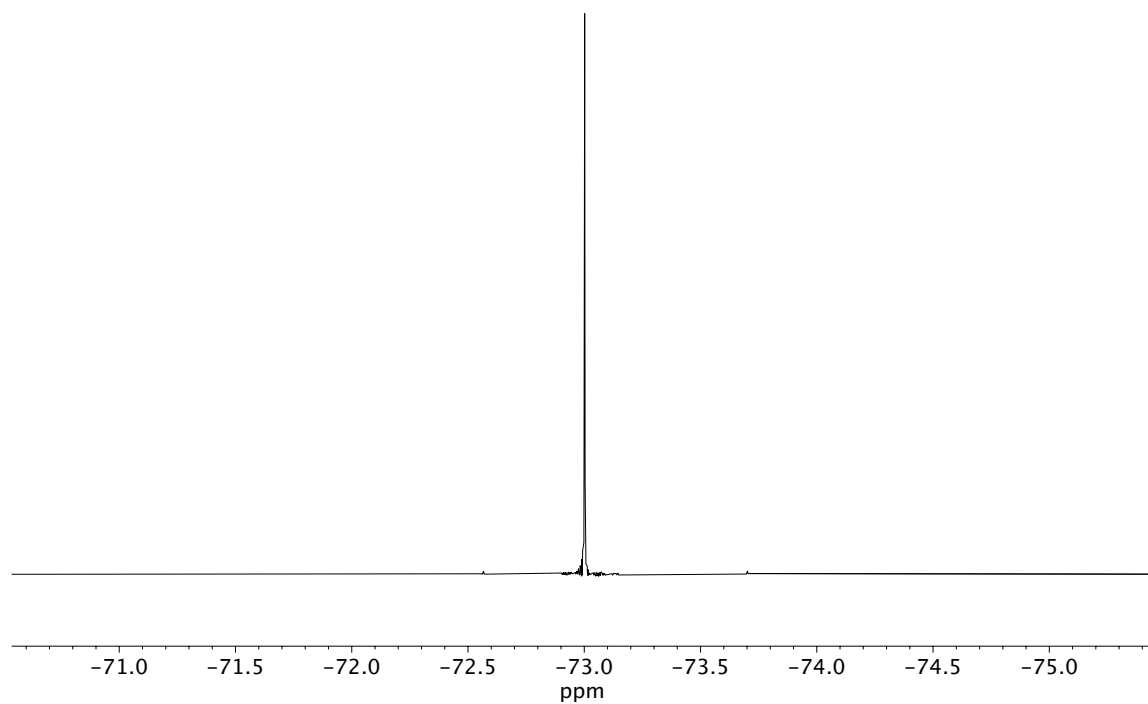


Figure A11.17 ^{19}F NMR (282 MHz, CDCl_3) of compound **180a**.

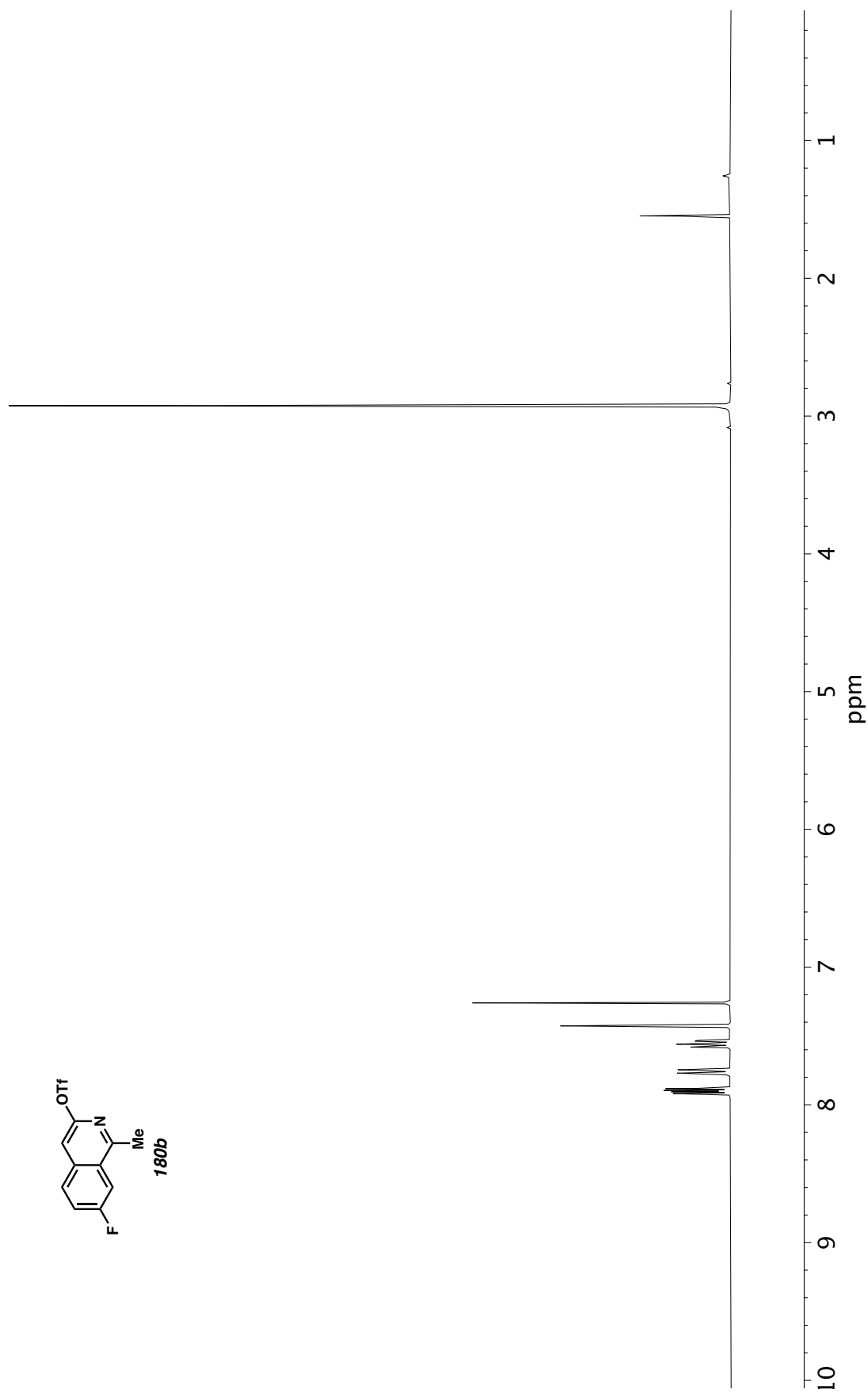


Figure A11.18 ¹H NMR (400 MHz, CDCl₃) of compound **180b**.

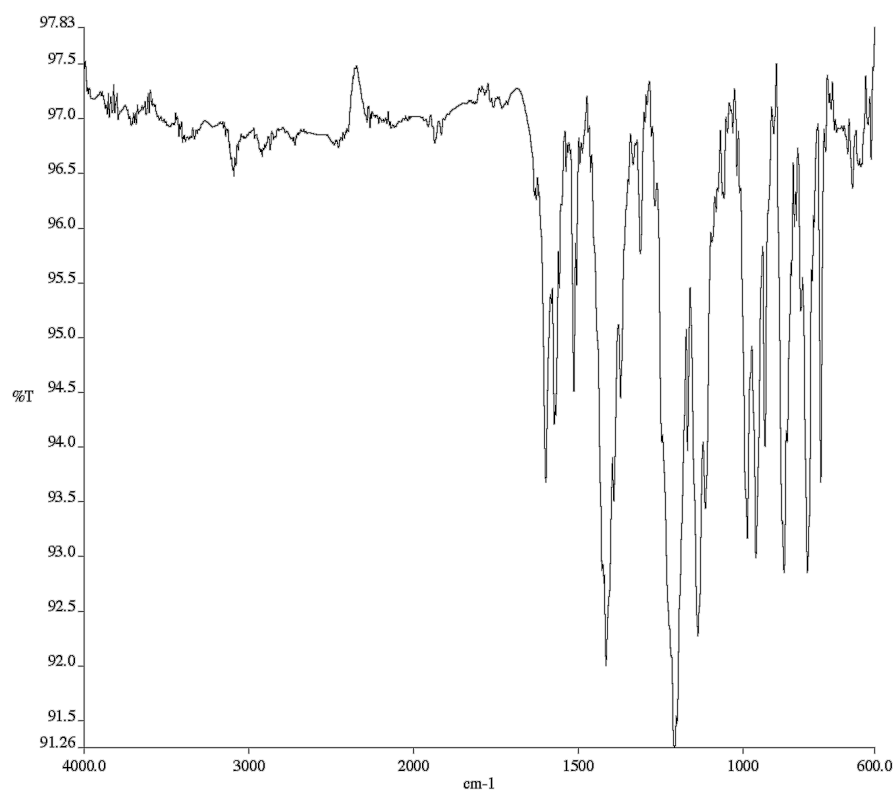


Figure A11.19 Infrared spectrum (Thin Film, NaCl) of compound **180b**.

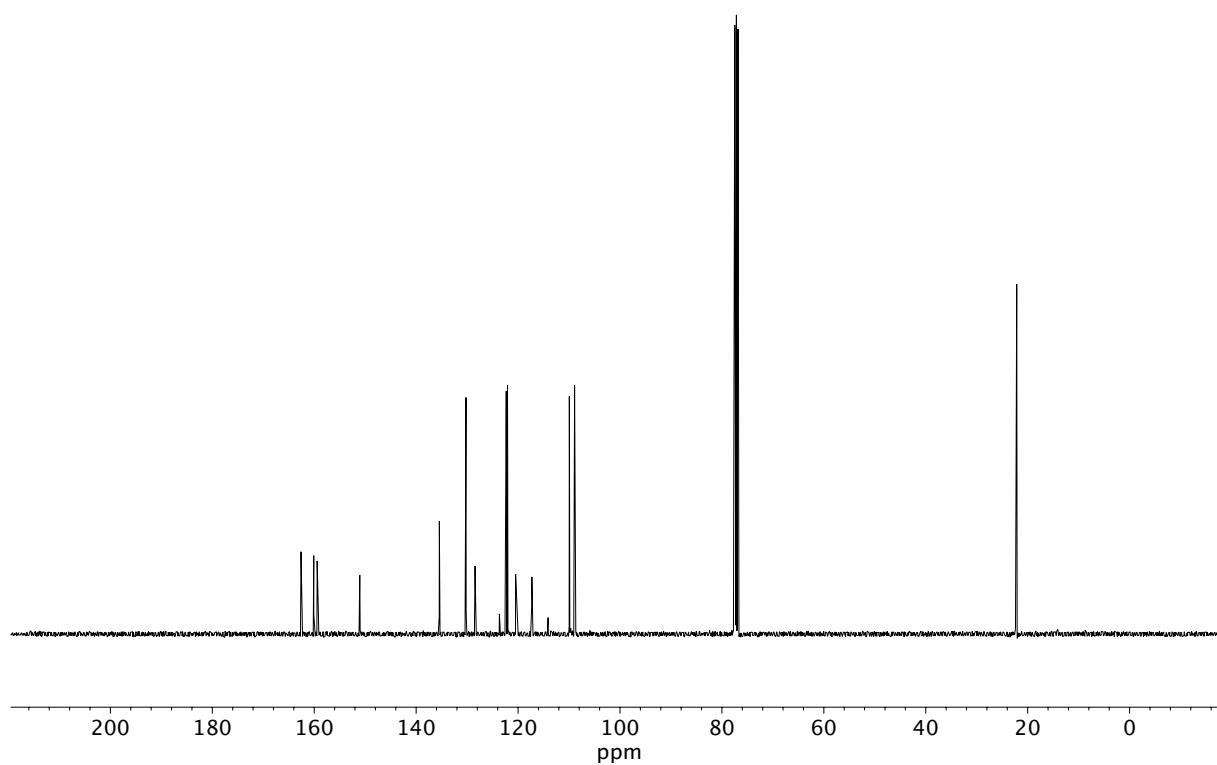


Figure A11.20 ¹³C NMR (100 MHz, CDCl₃) of compound **180b**.

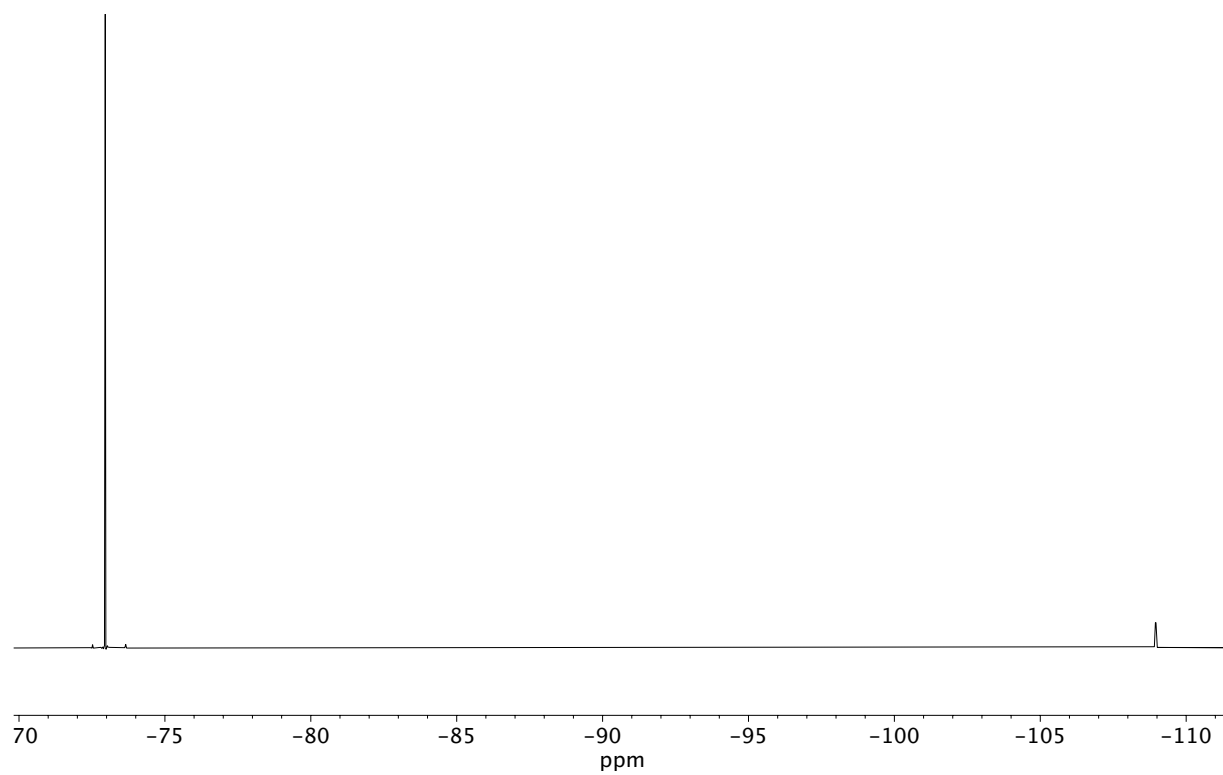


Figure A11.21 ^{19}F NMR (282 MHz, CDCl_3) of compound **180b**.

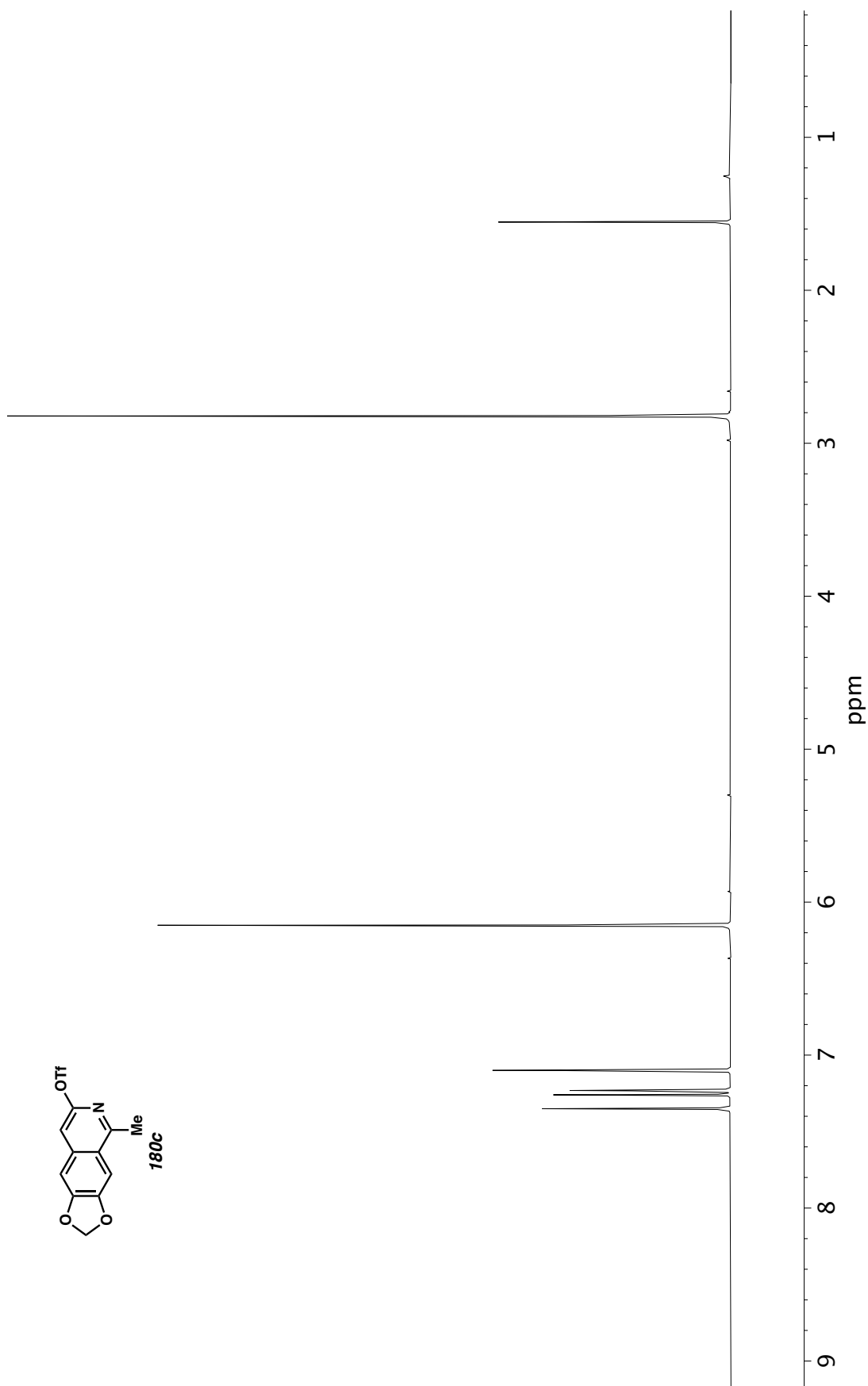


Figure A11.22 ^1H NMR (400 MHz, CDCl_3) of compound **180c**.

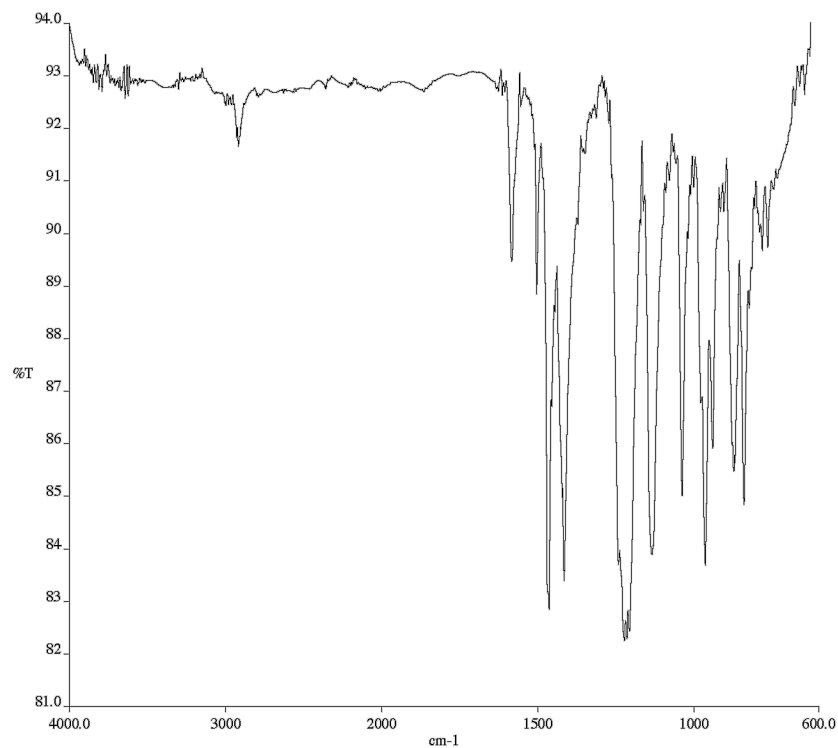


Figure A11.23 Infrared spectrum (Thin Film, NaCl) of compound **180c**.

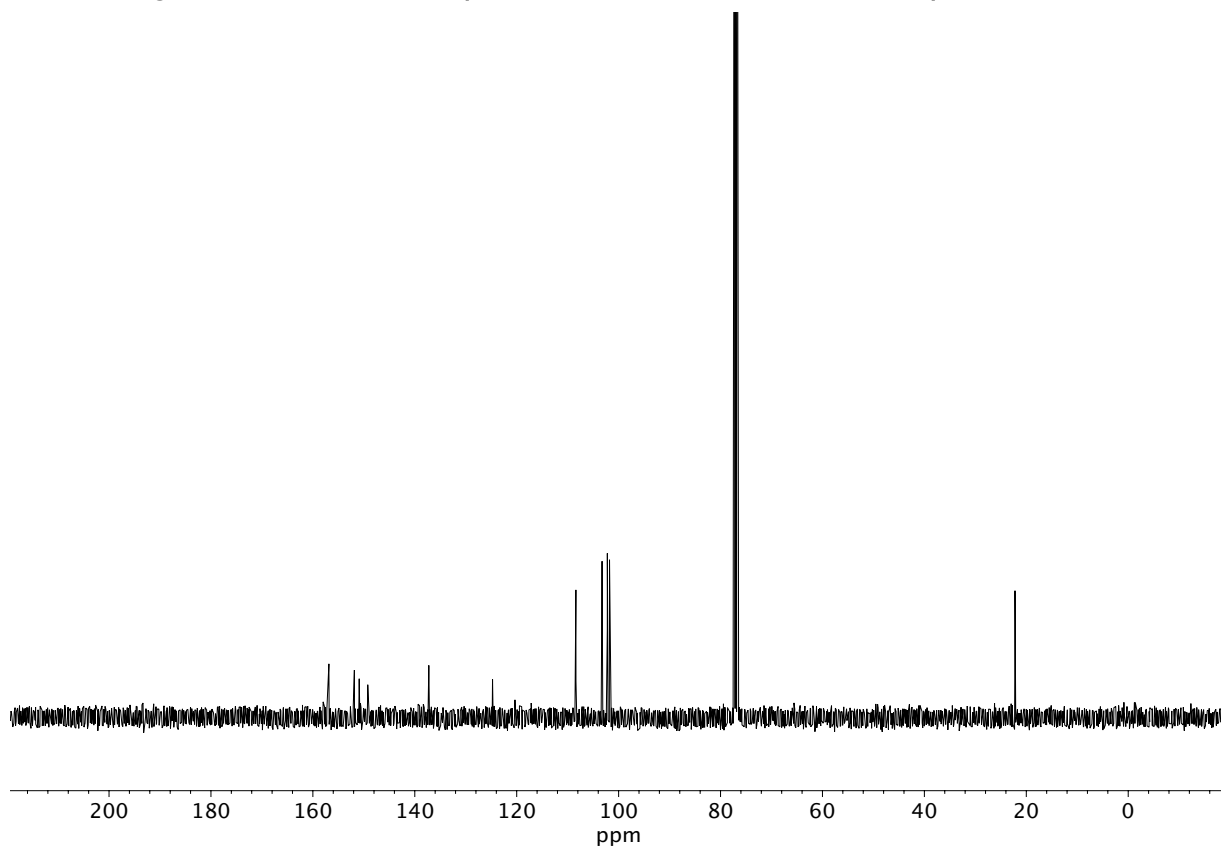


Figure A11.24 ¹³C NMR (100 MHz, CDCl₃) of compound **180c**.

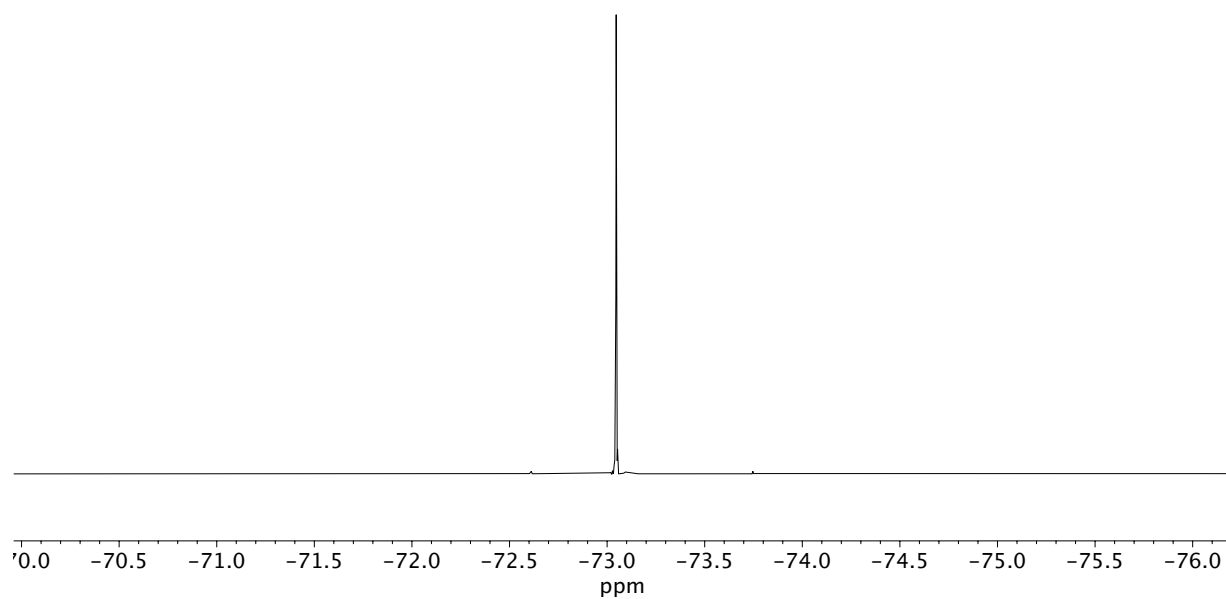


Figure A11.25 ^{19}F NMR (282 MHz, CDCl_3) of compound **180c**.

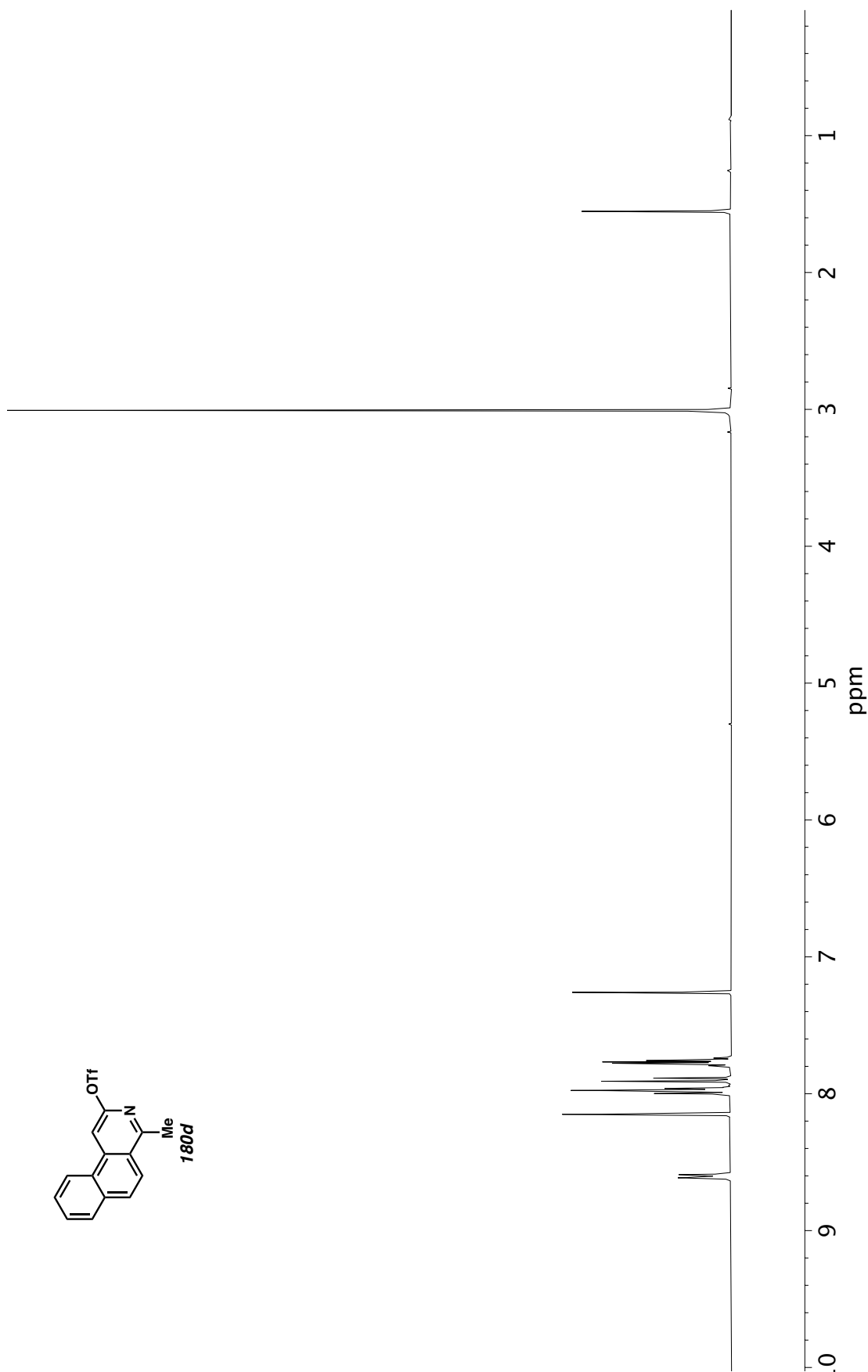


Figure A11.26 ^1H NMR (400 MHz, CDCl_3) of compound **180d**.

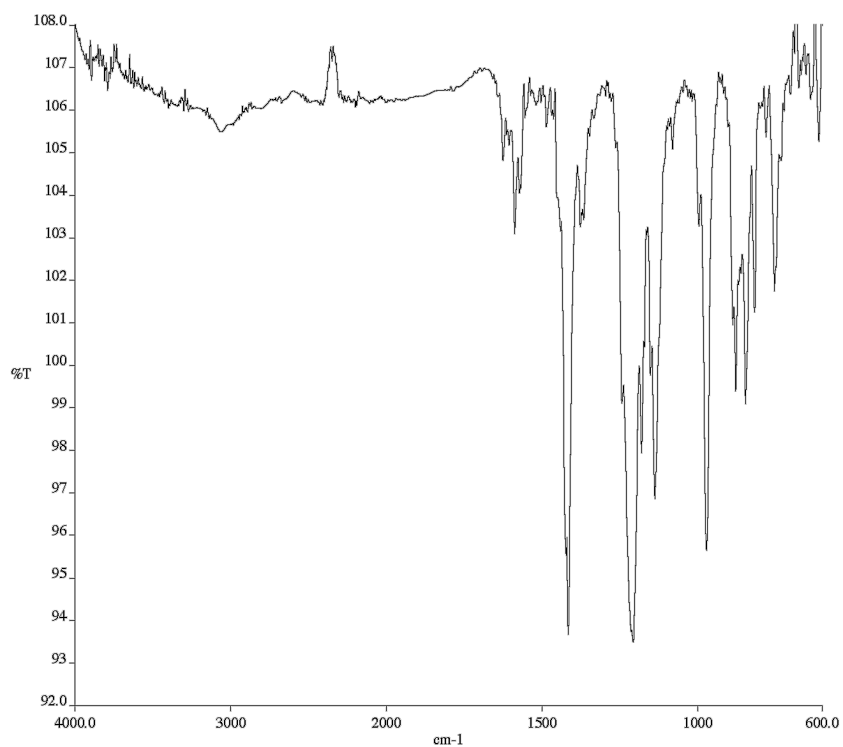


Figure A11.27 Infrared spectrum (Thin Film, NaCl) of compound **180d**.

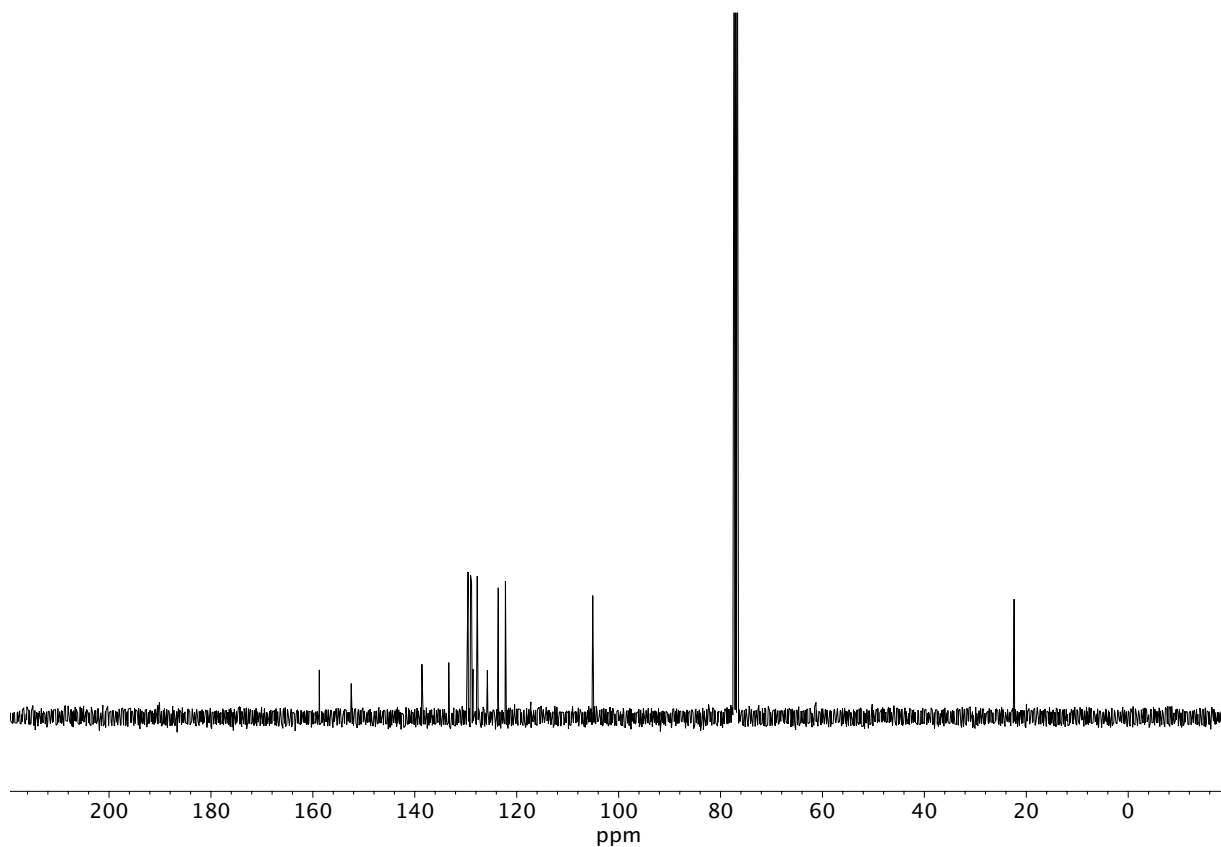


Figure A11.28 ¹³C NMR (100 MHz, CDCl₃) of compound **180d**.

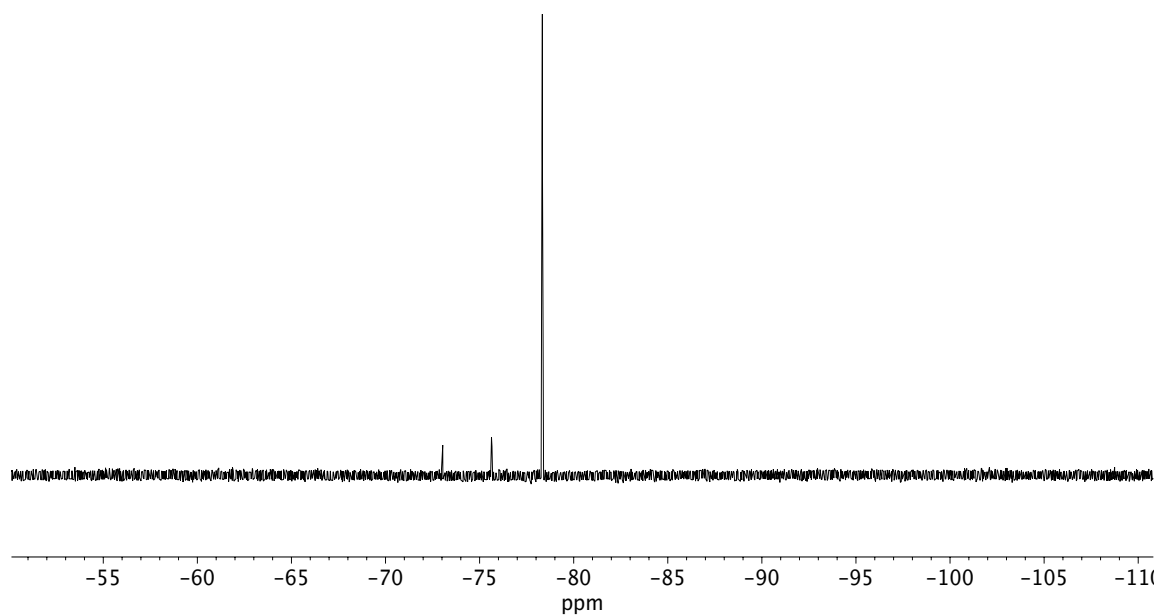


Figure A11.29 ^{19}F NMR (282 MHz, CDCl_3) of compound **180d**.

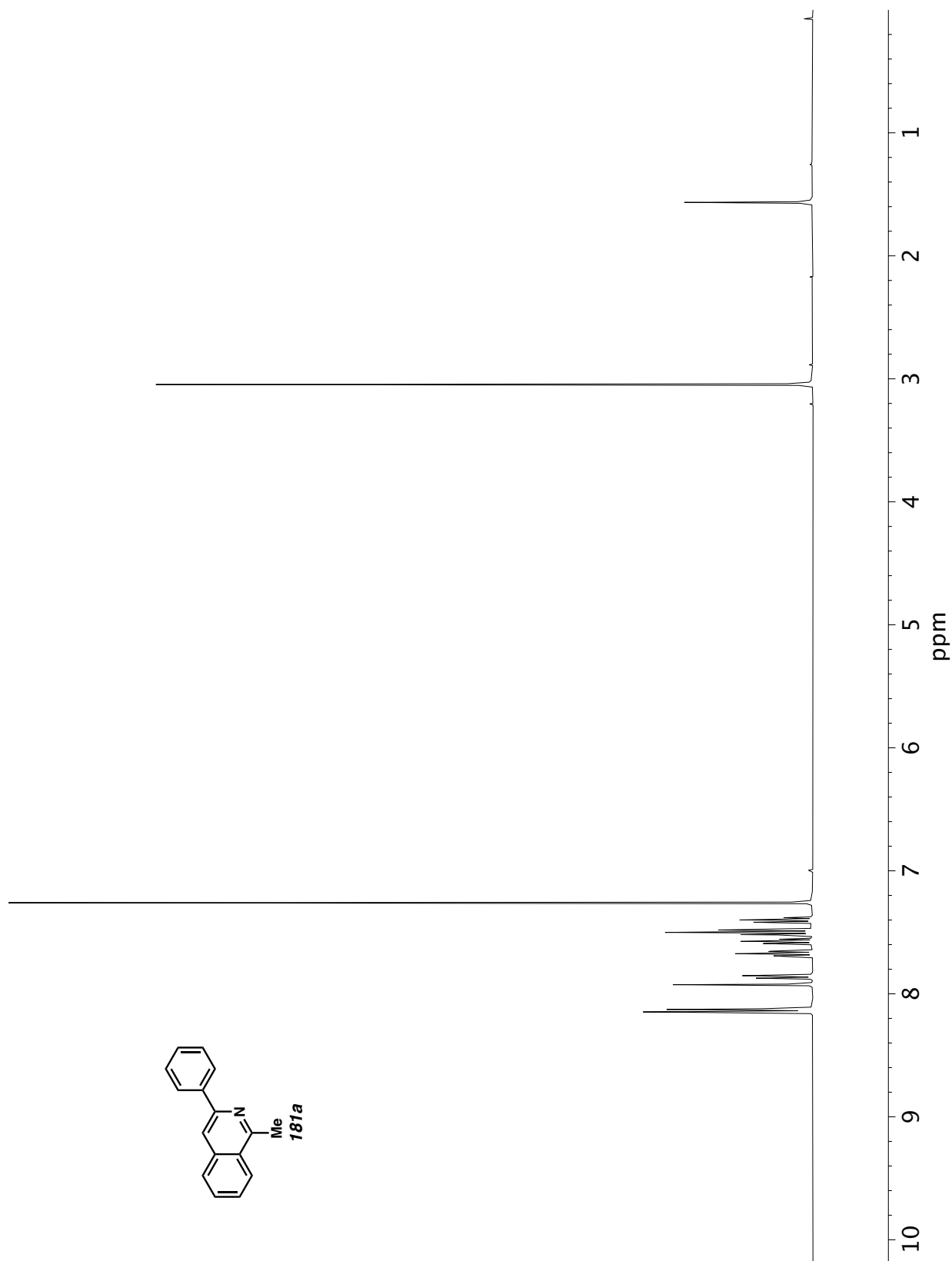


Figure A11.30 ^1H NMR (400 MHz, CDCl_3) of compound **181a**.

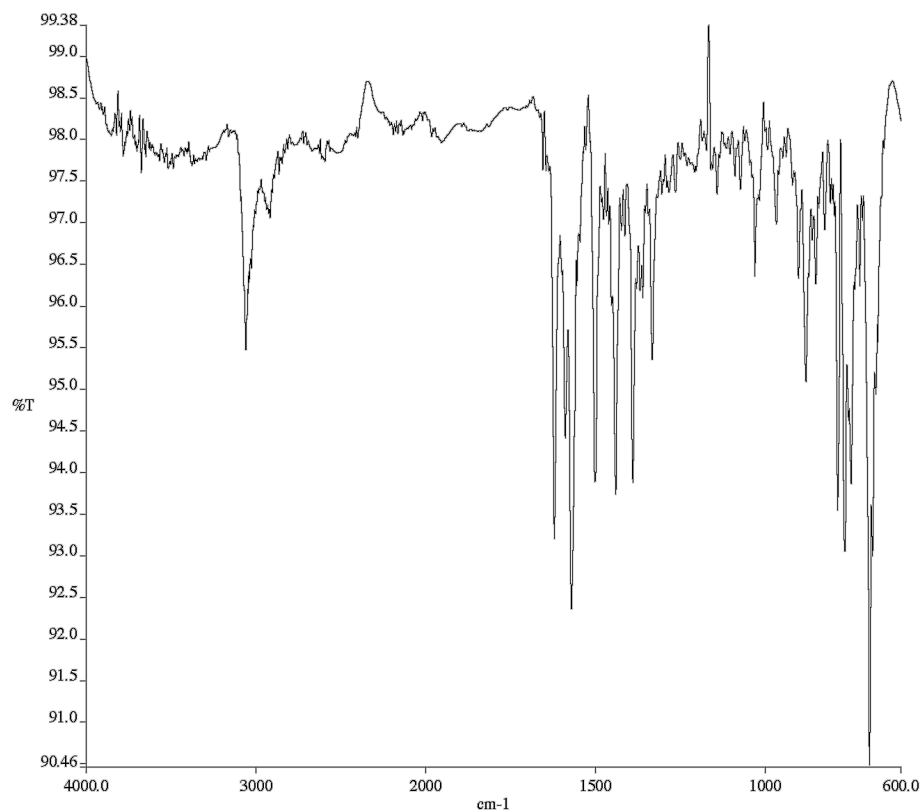


Figure A11.31 Infrared spectrum (Thin Film, NaCl) of compound **181a**.

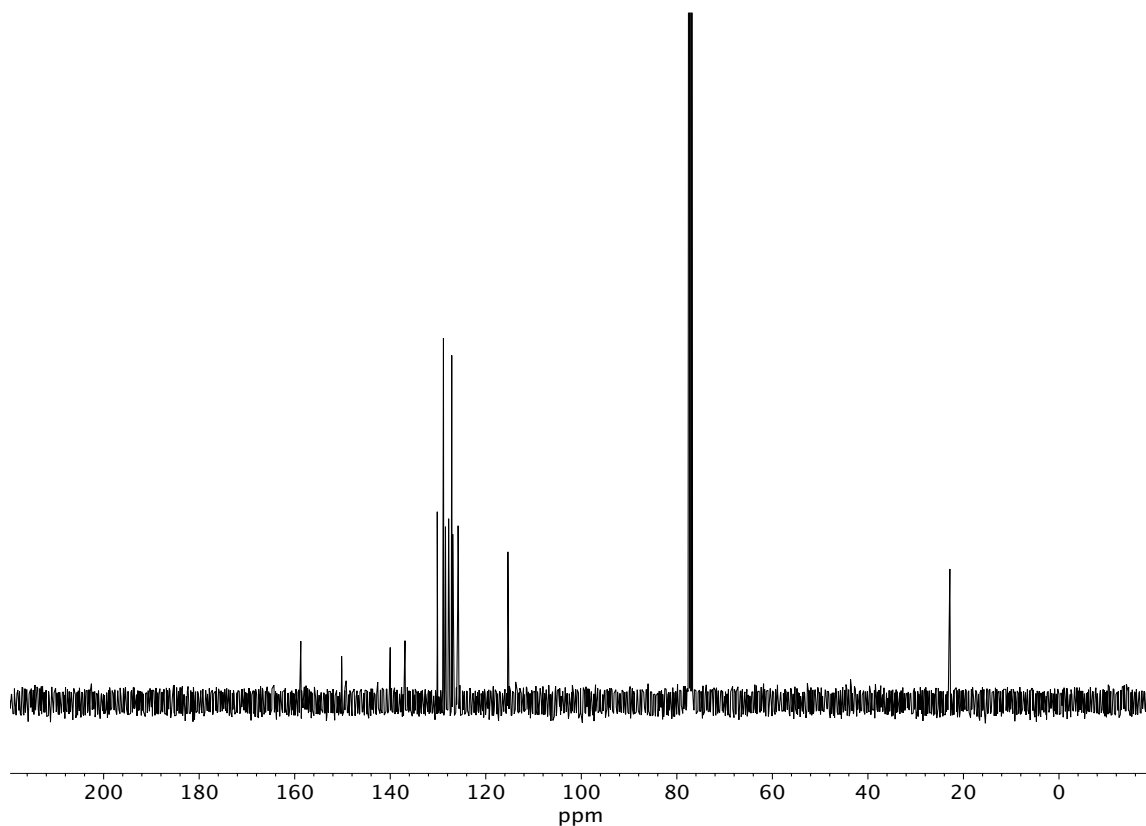


Figure A11.32 ¹³C NMR (100 MHz, CDCl₃) of compound **181a**.

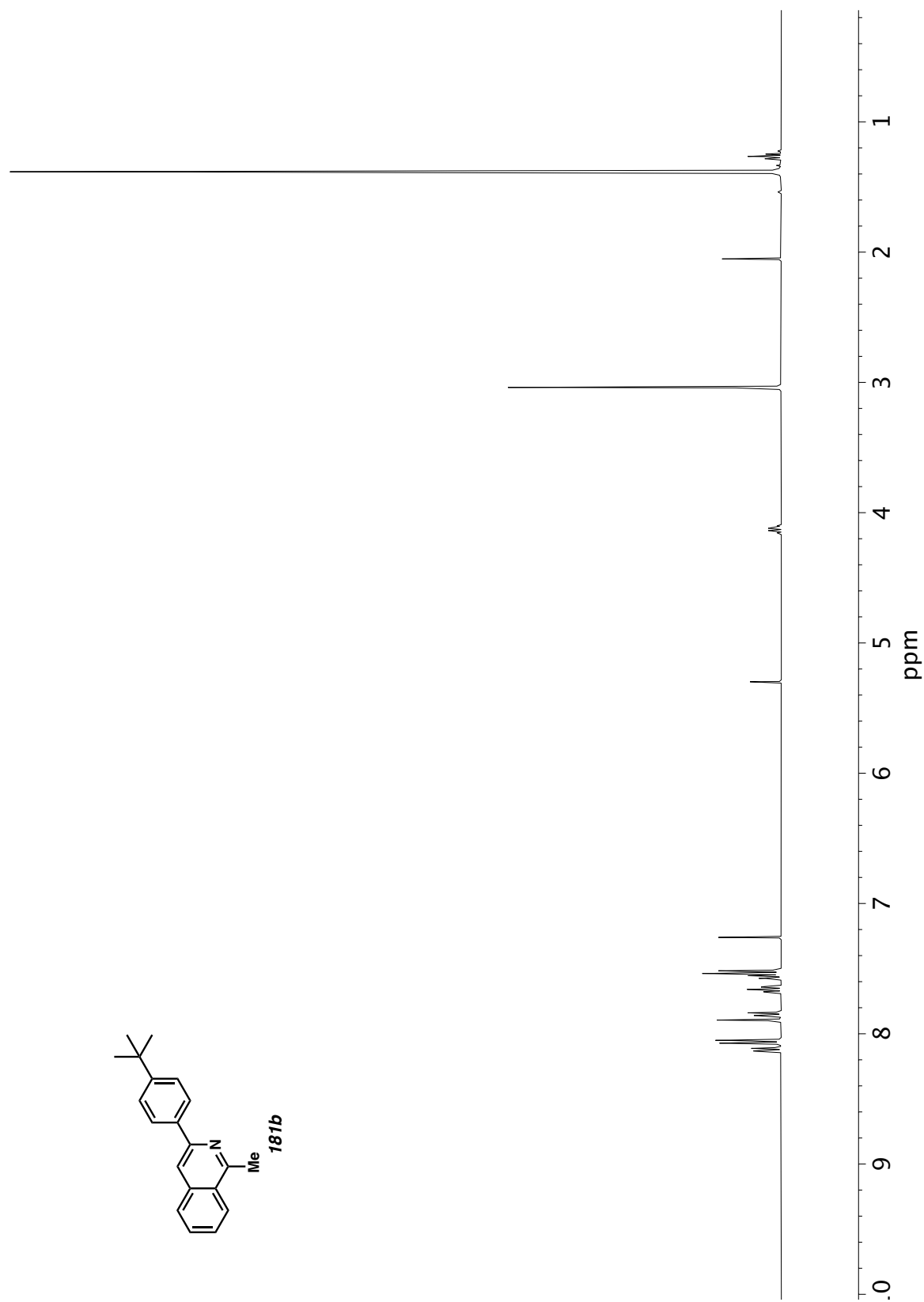


Figure A11.33 ^1H NMR (400 MHz, CDCl_3) of compound **181b**.

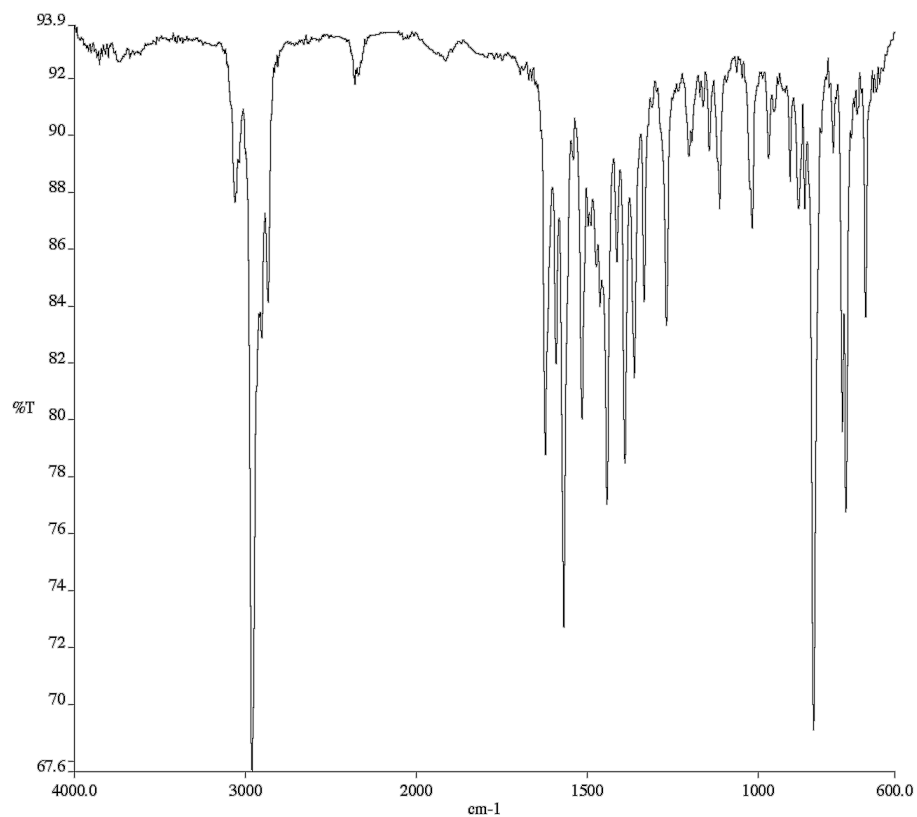


Figure A11.34 Infrared spectrum (Thin Film, NaCl) of compound **181b**.

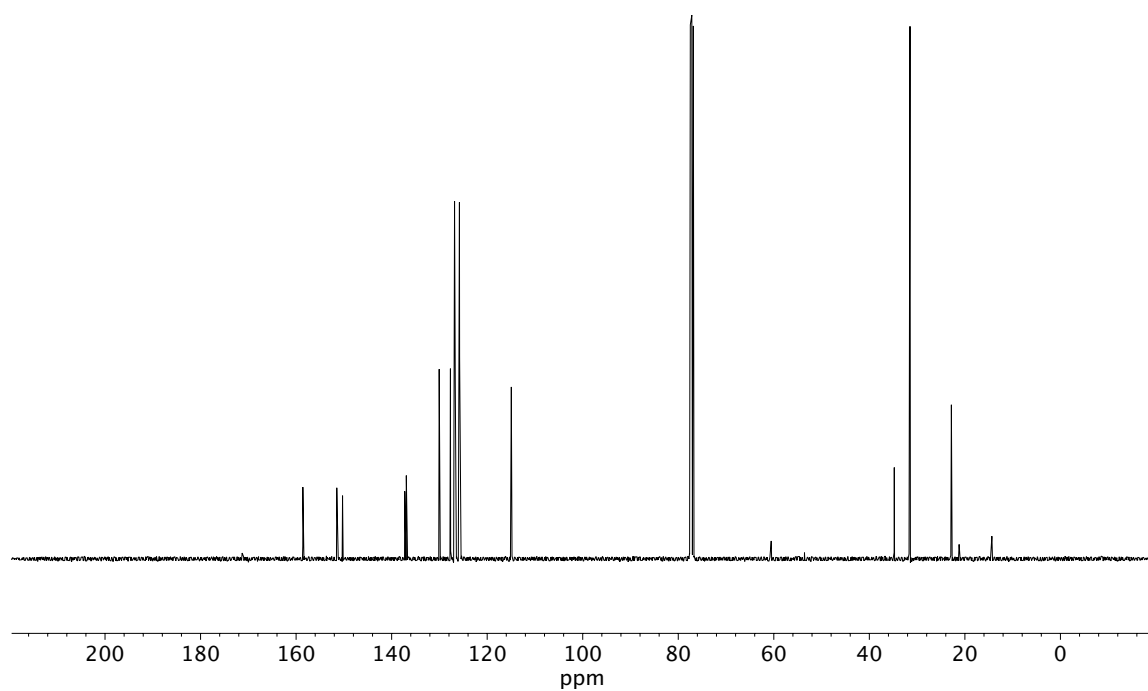


Figure A11.35 ¹³C NMR (100 MHz, CDCl₃) of compound **181b**.

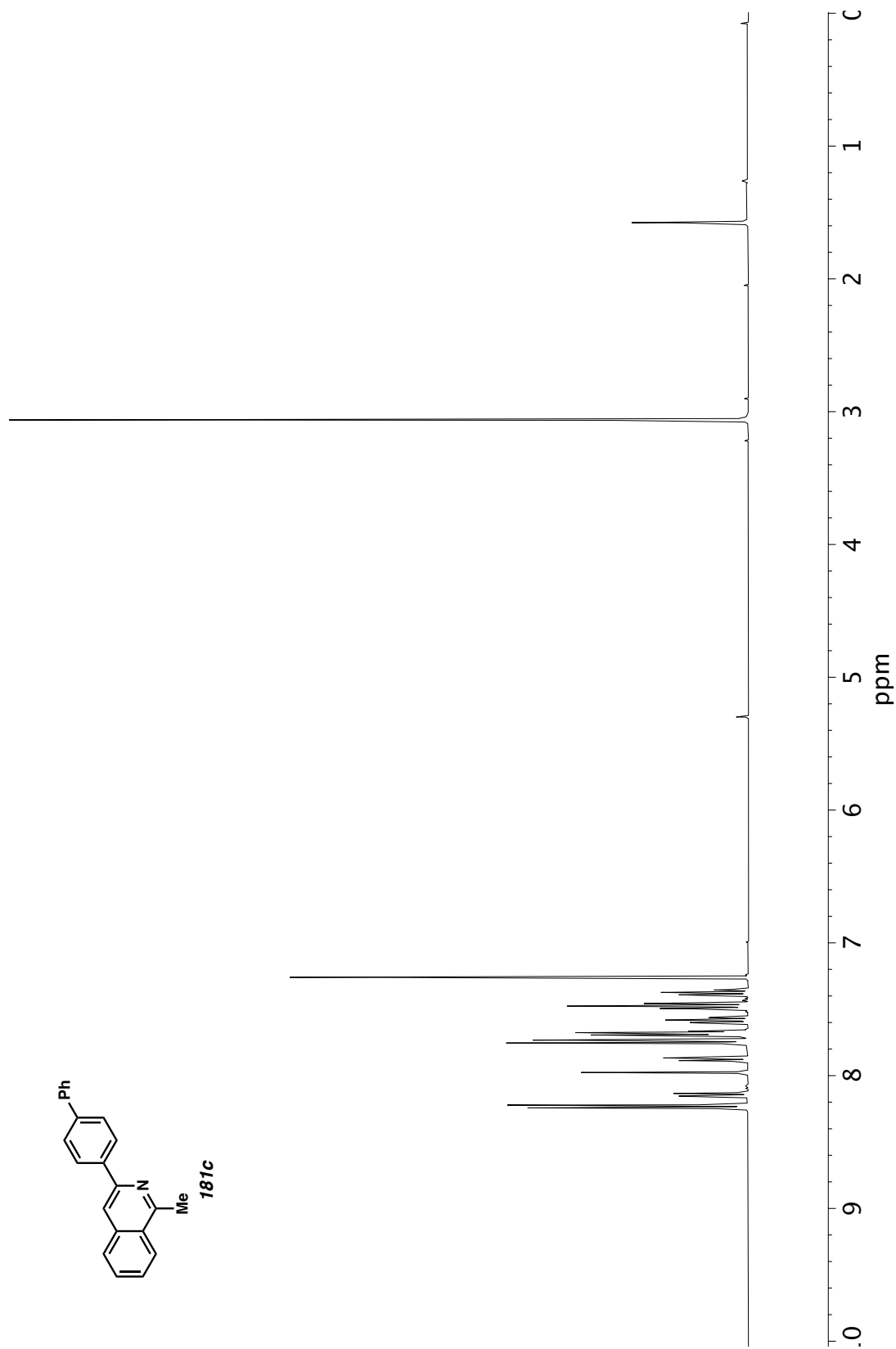


Figure A11.36 ^1H NMR (400 MHz, CDCl_3) of compound **181c**.

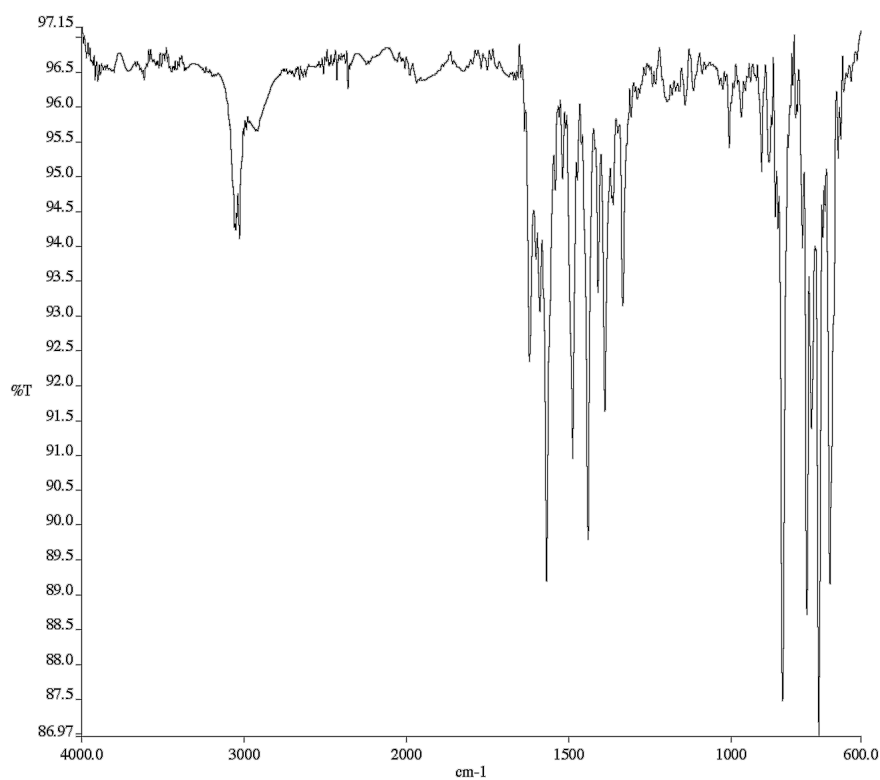


Figure A11.37 Infrared spectrum (Thin Film, NaCl) of compound **181c**.

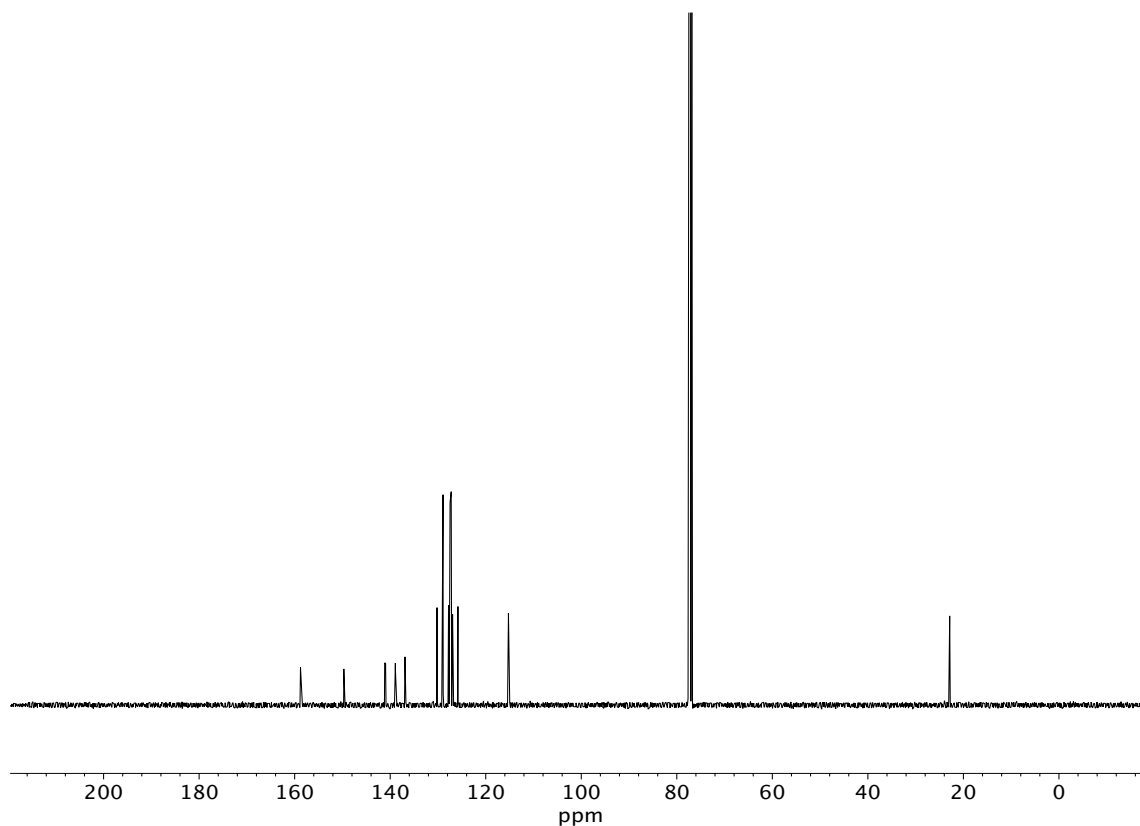


Figure A11.38 ¹³C NMR (100 MHz, CDCl₃) of compound **181c**.

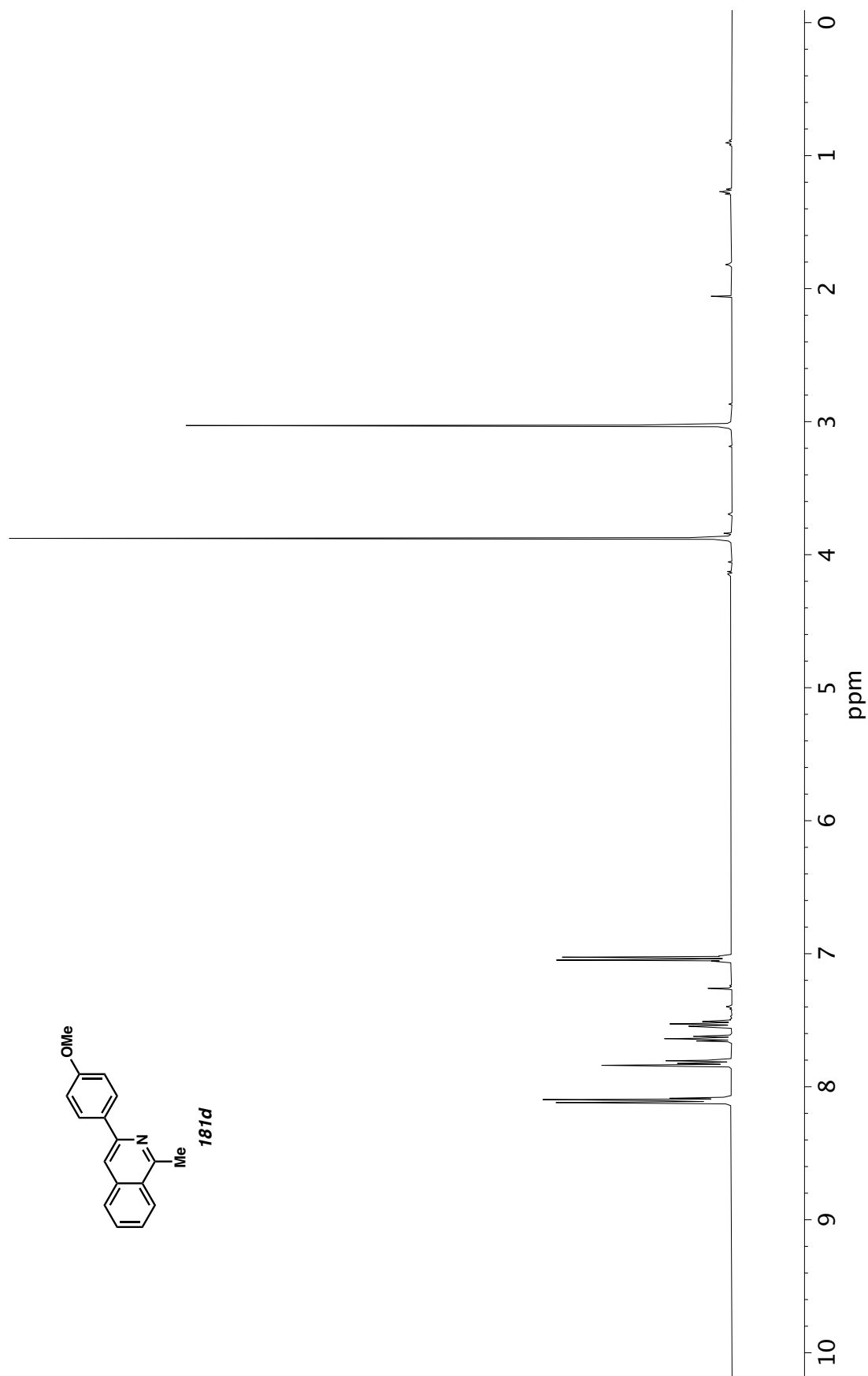


Figure A11.39 ^1H NMR (400 MHz, CDCl_3) of compound **181d**.

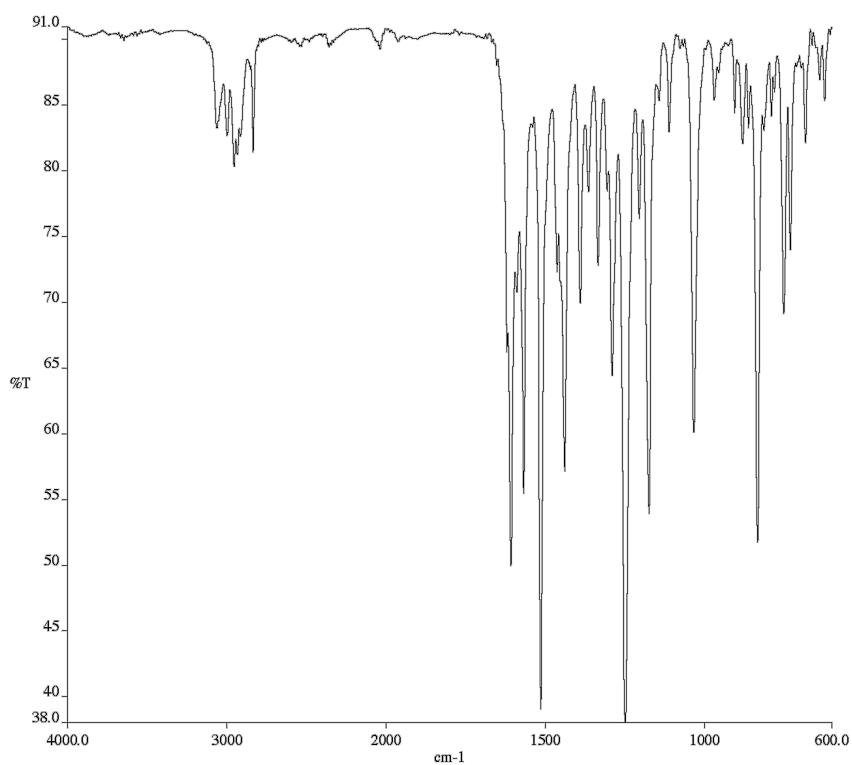


Figure A11.40 Infrared spectrum (Thin Film, NaCl) of compound **181d**.

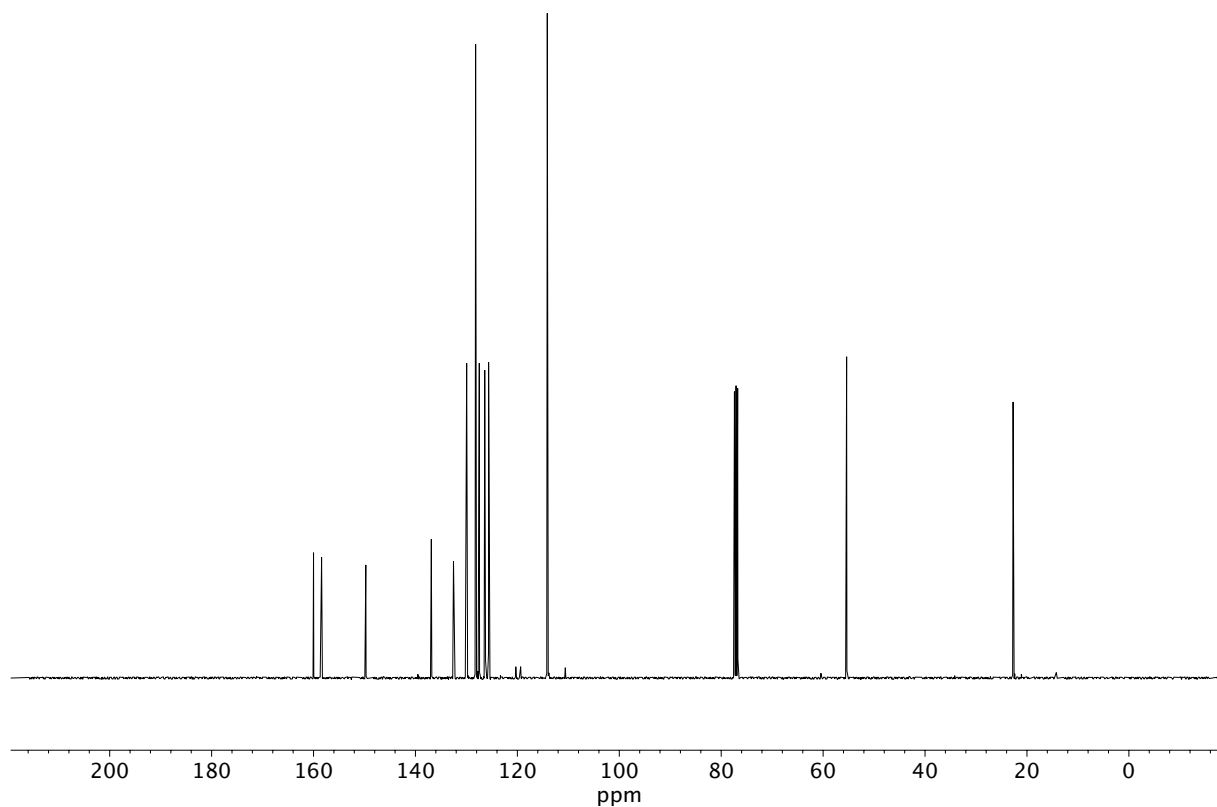


Figure A11.41 ¹³C NMR (100 MHz, CDCl₃) of compound **181d**.

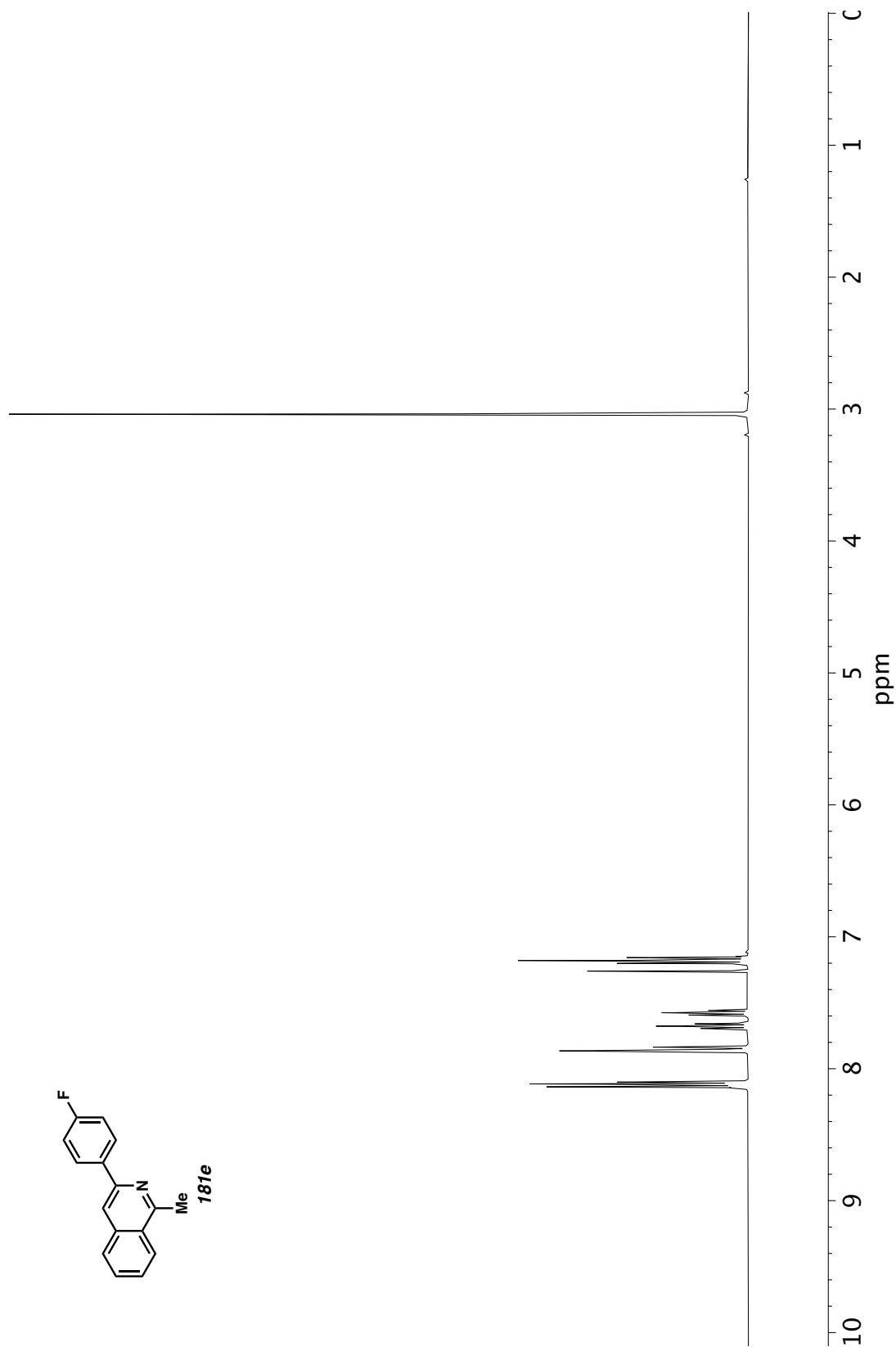


Figure A11.42 ¹H NMR (400 MHz, CDCl₃) of compound **181e**.

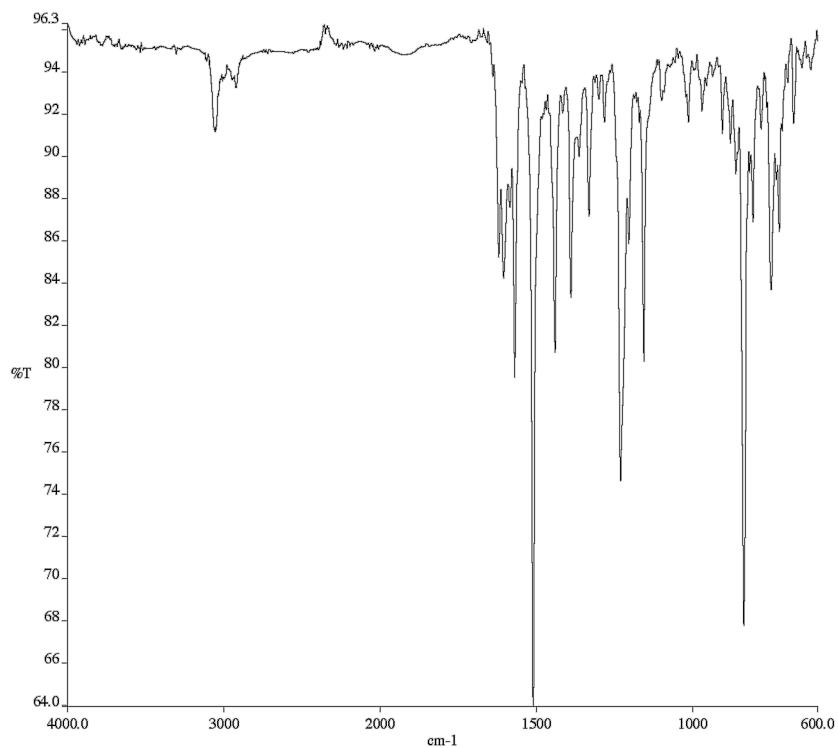


Figure A11.43 Infrared spectrum (Thin Film, NaCl) of compound **181e**.

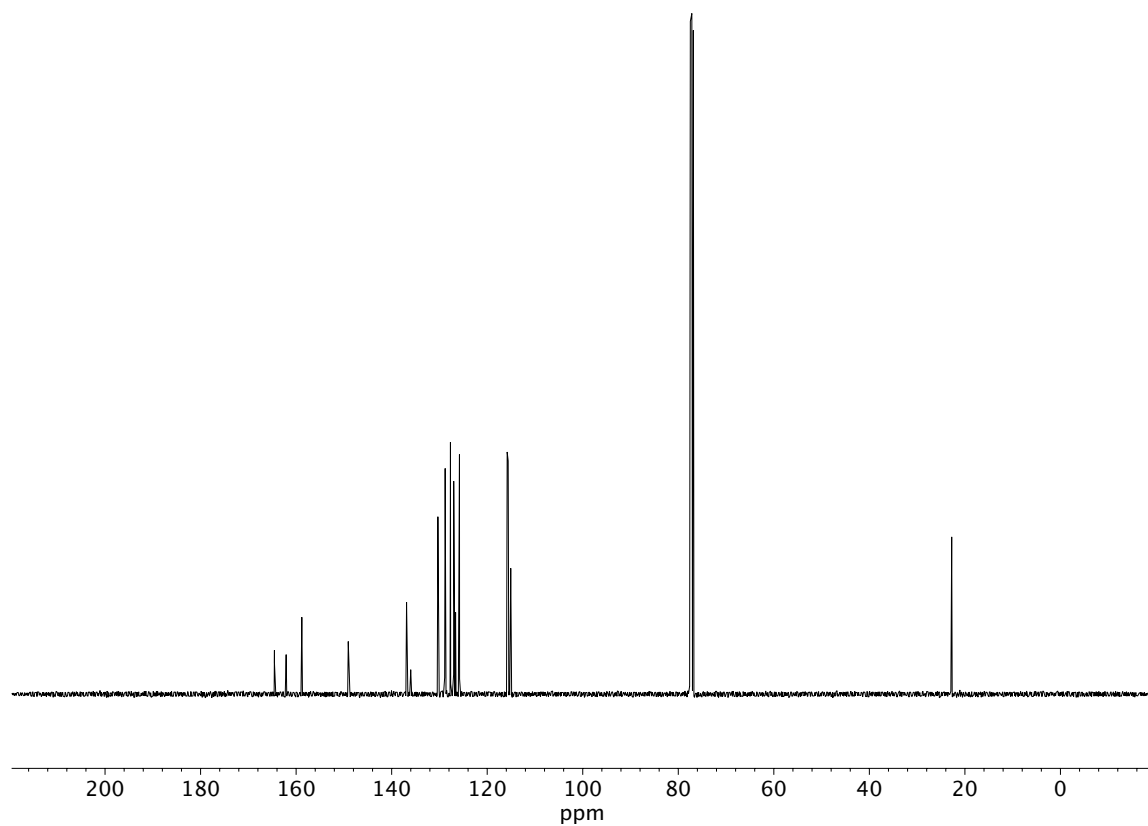


Figure A11.44 ¹³C NMR (100 MHz, CDCl₃) of compound **181e**.

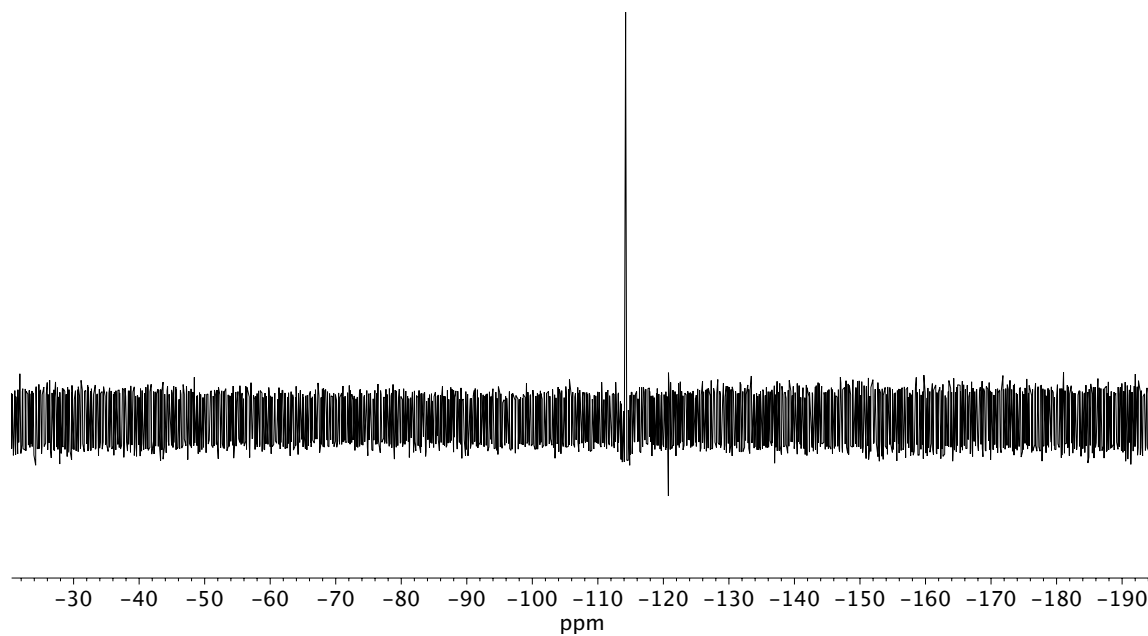


Figure A11.45 ^{19}F NMR (282 MHz, CDCl_3) of compound **181e**.

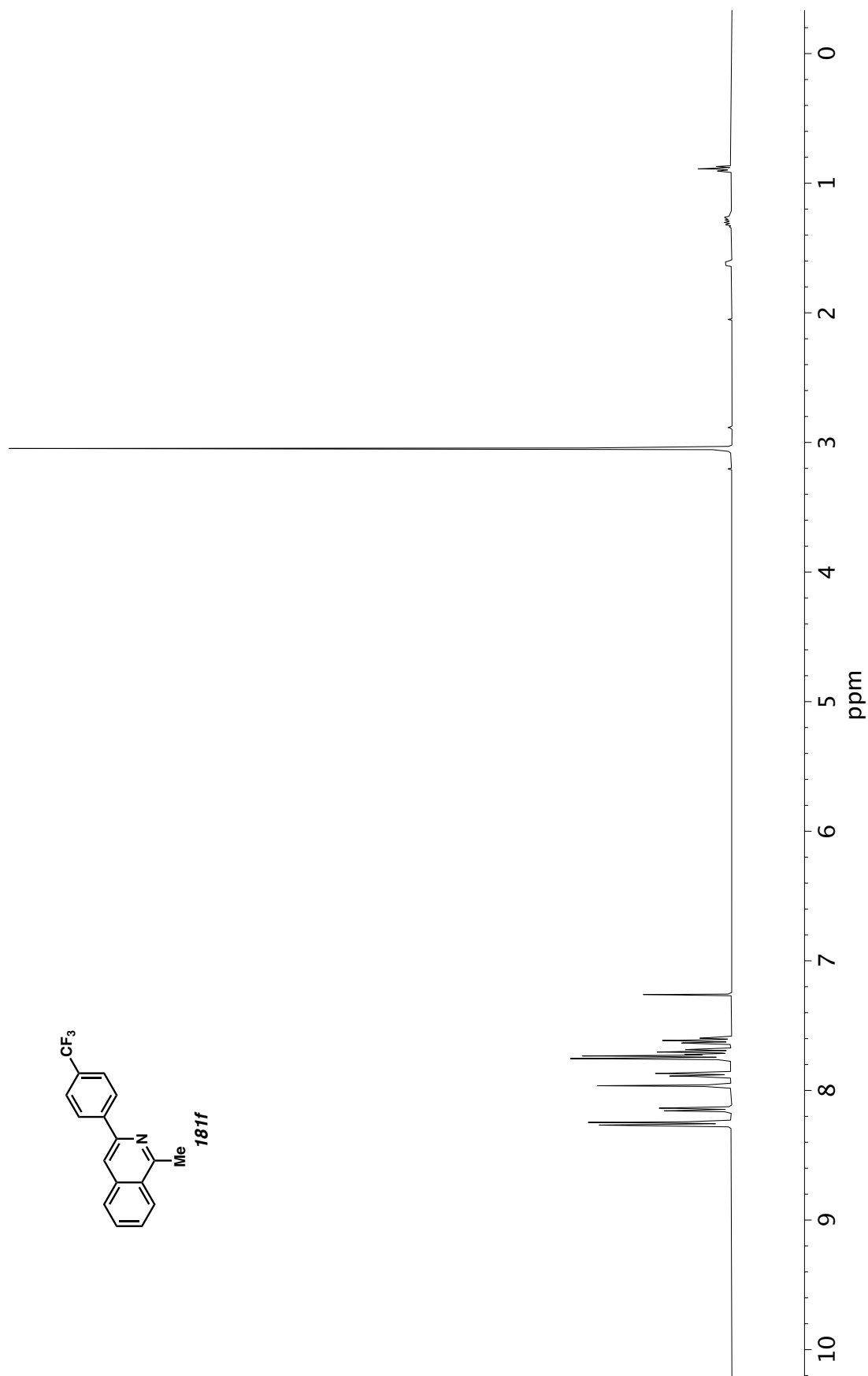


Figure A11.46 ¹H NMR (400 MHz, CDCl₃) of compound **181f**.

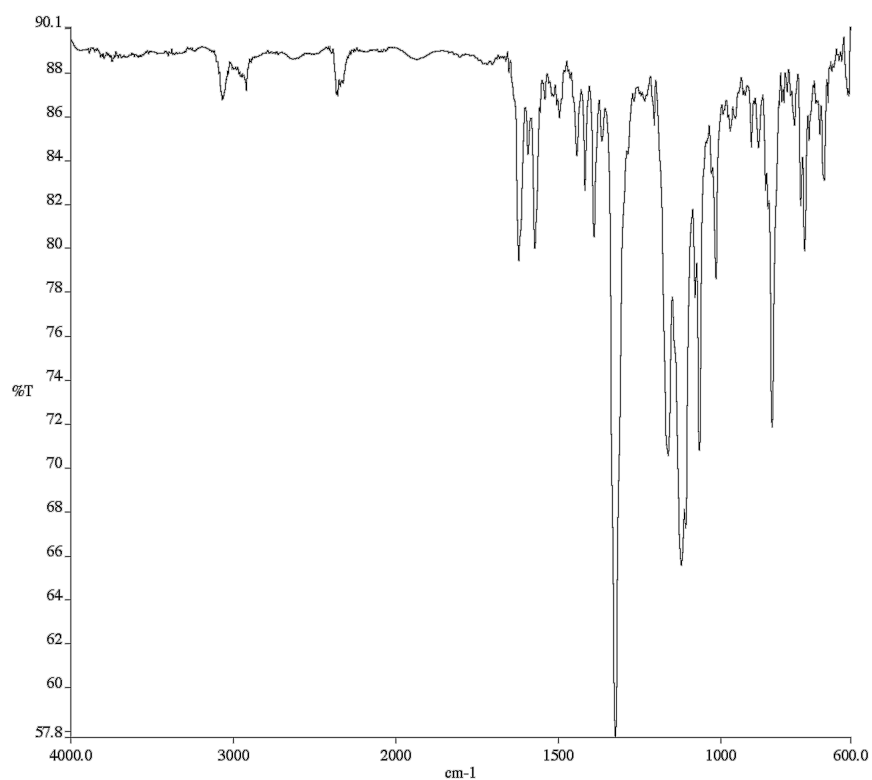


Figure A11.47 Infrared spectrum (Thin Film, NaCl) of compound **181f**.

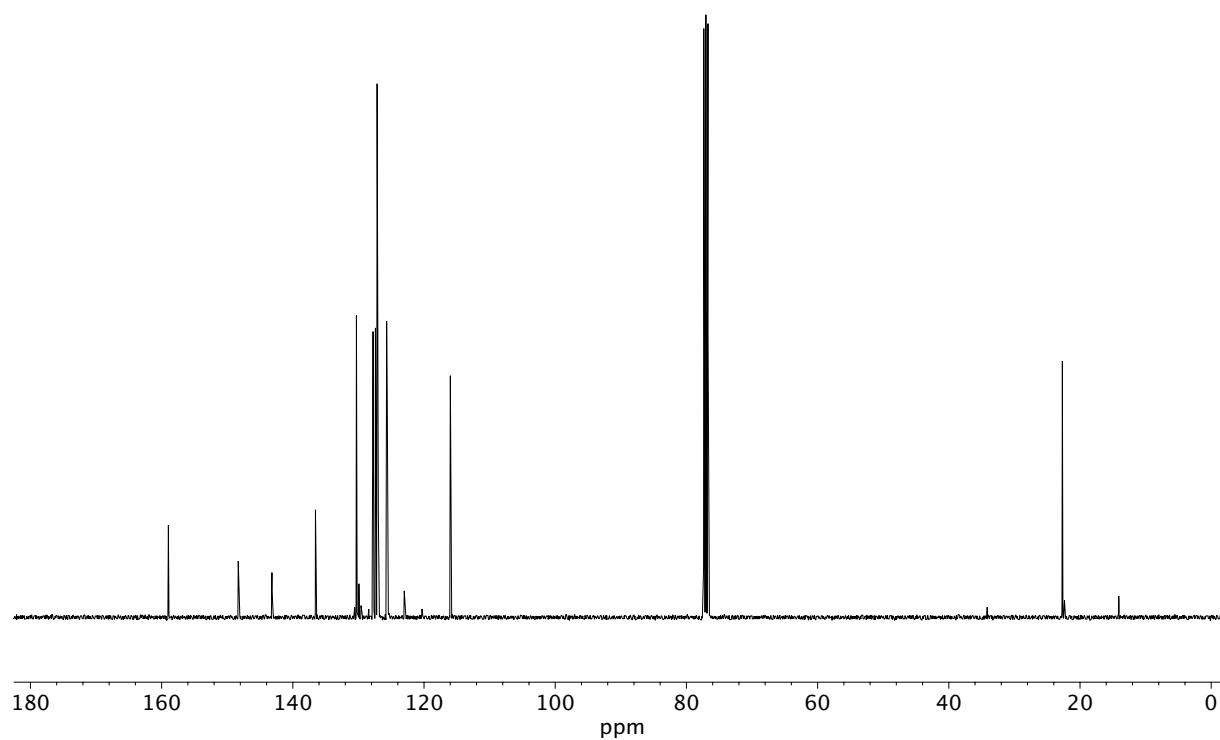


Figure A11.48 ¹³C NMR (100 MHz, CDCl₃) of compound **181f**.

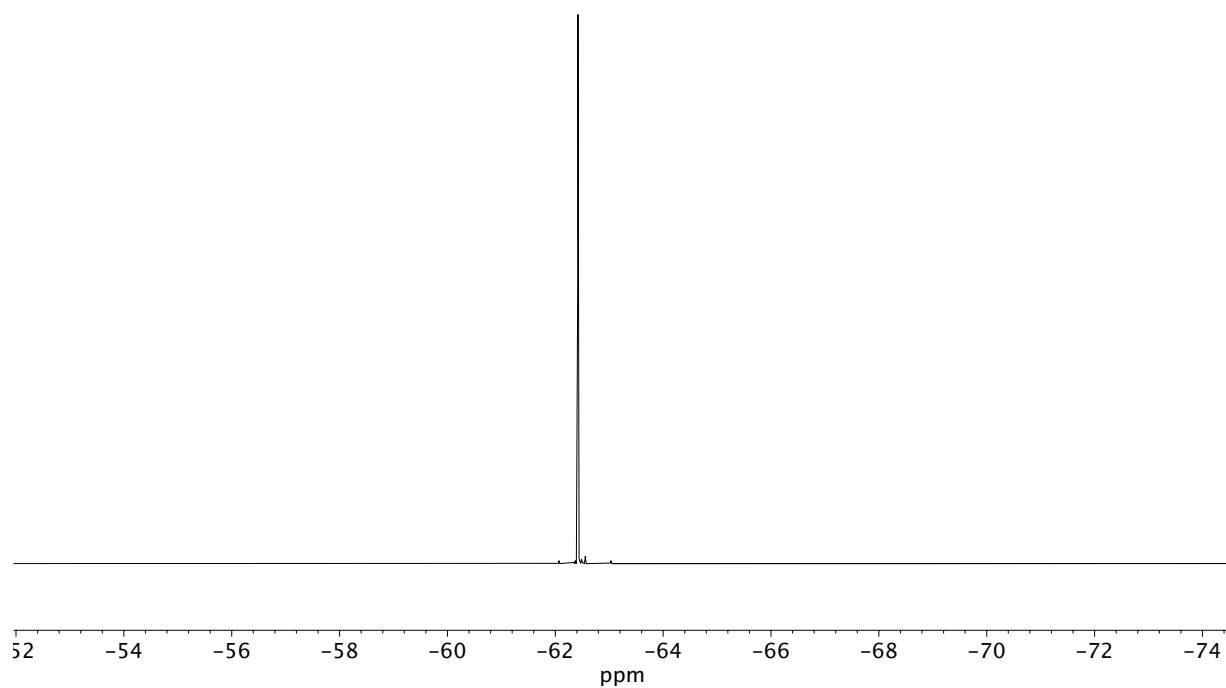


Figure A11.49 ^{19}F NMR (282 MHz, CDCl_3) of compound **181f**.

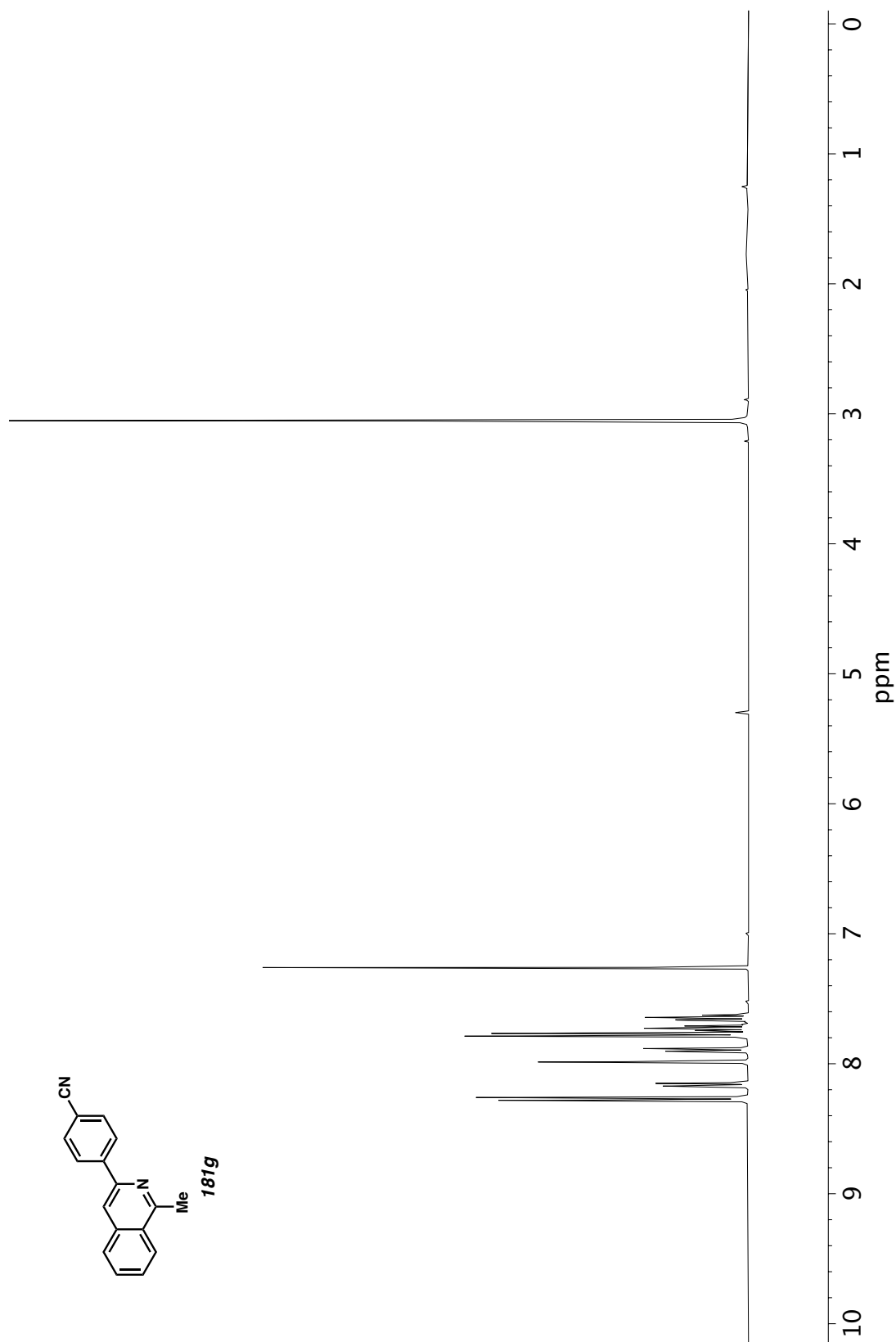


Figure A11.50 ^1H NMR (400 MHz, CDCl_3) of compound **181g**.

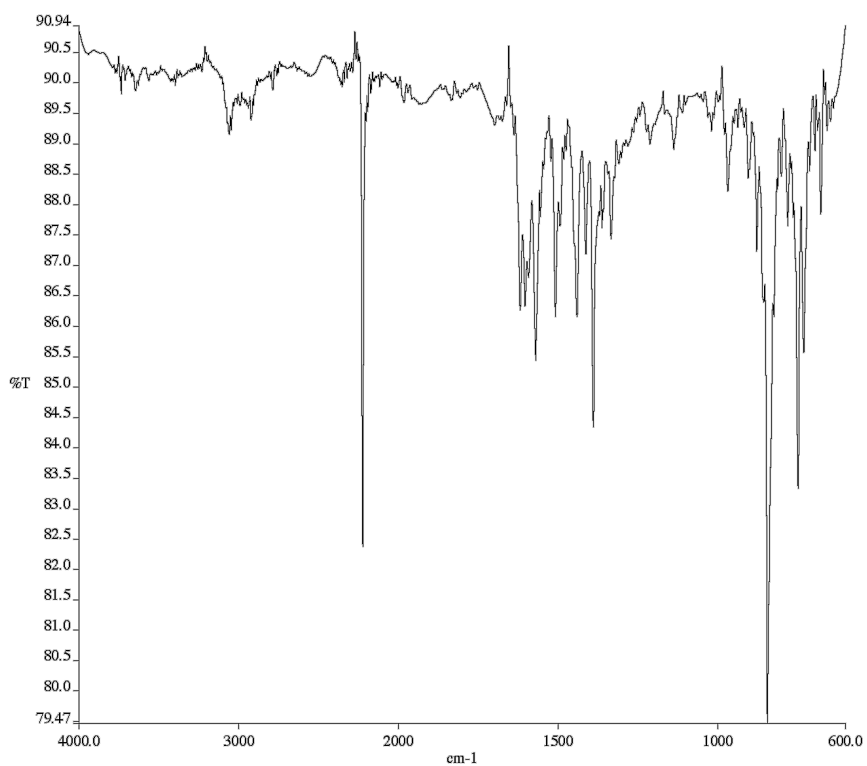


Figure A11.51 Infrared spectrum (Thin Film, NaCl) of compound **181g**.

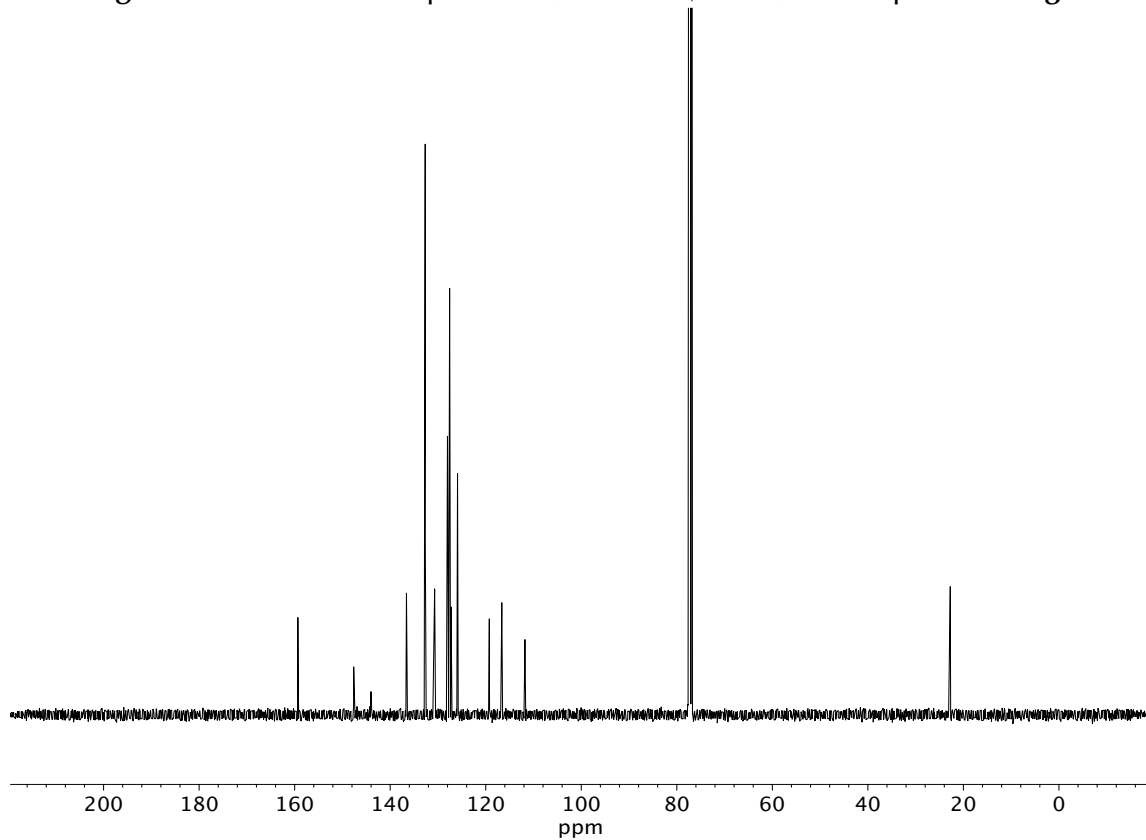


Figure A11.52 ^{13}C NMR (100 MHz, CDCl_3) of compound **181g**.

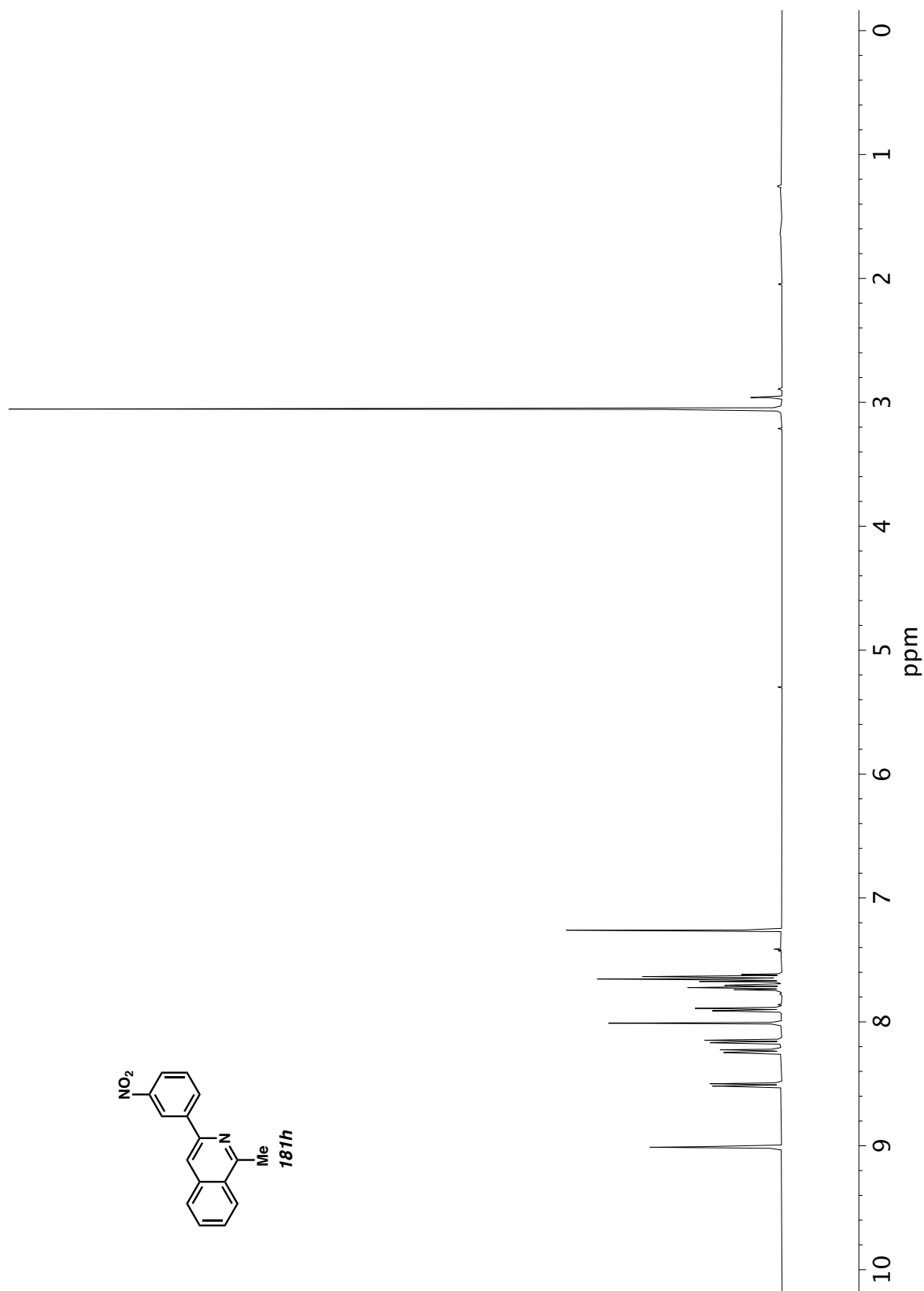


Figure A11.53 ^1H NMR (400 MHz, CDCl_3) of compound **181h**.

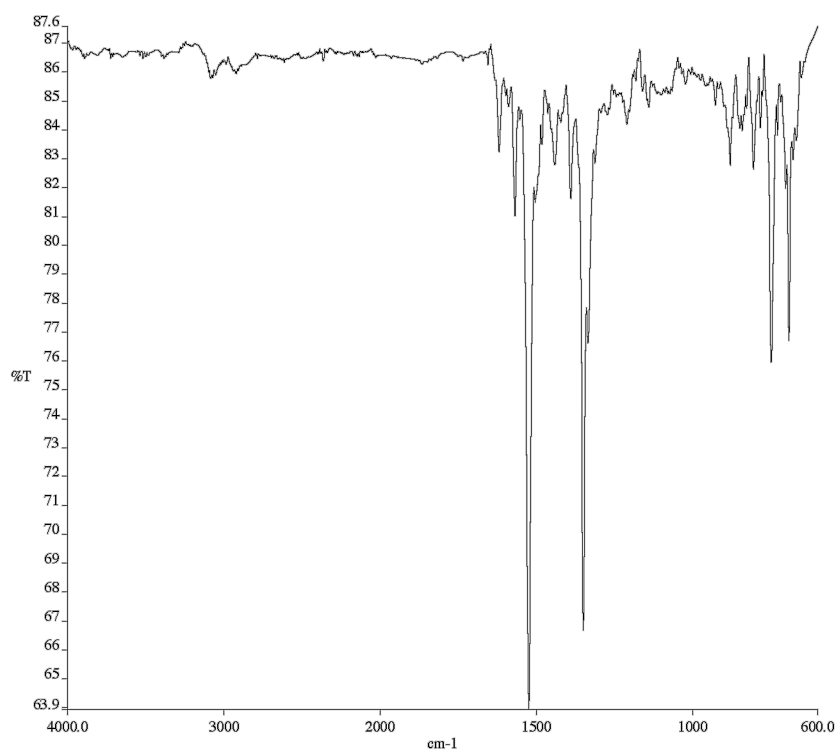


Figure A11.54 Infrared spectrum (Thin Film, NaCl) of compound **181h**.

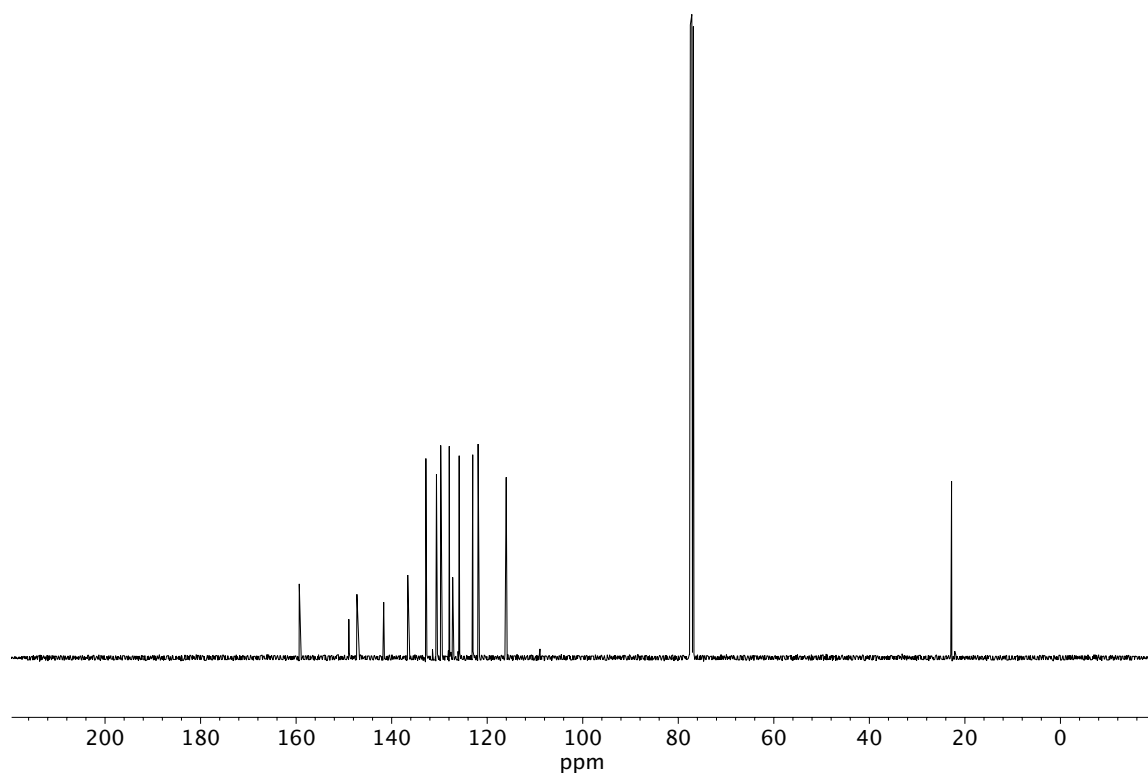


Figure A11.55 ¹³C NMR (100 MHz, CDCl₃) of compound **181h**.

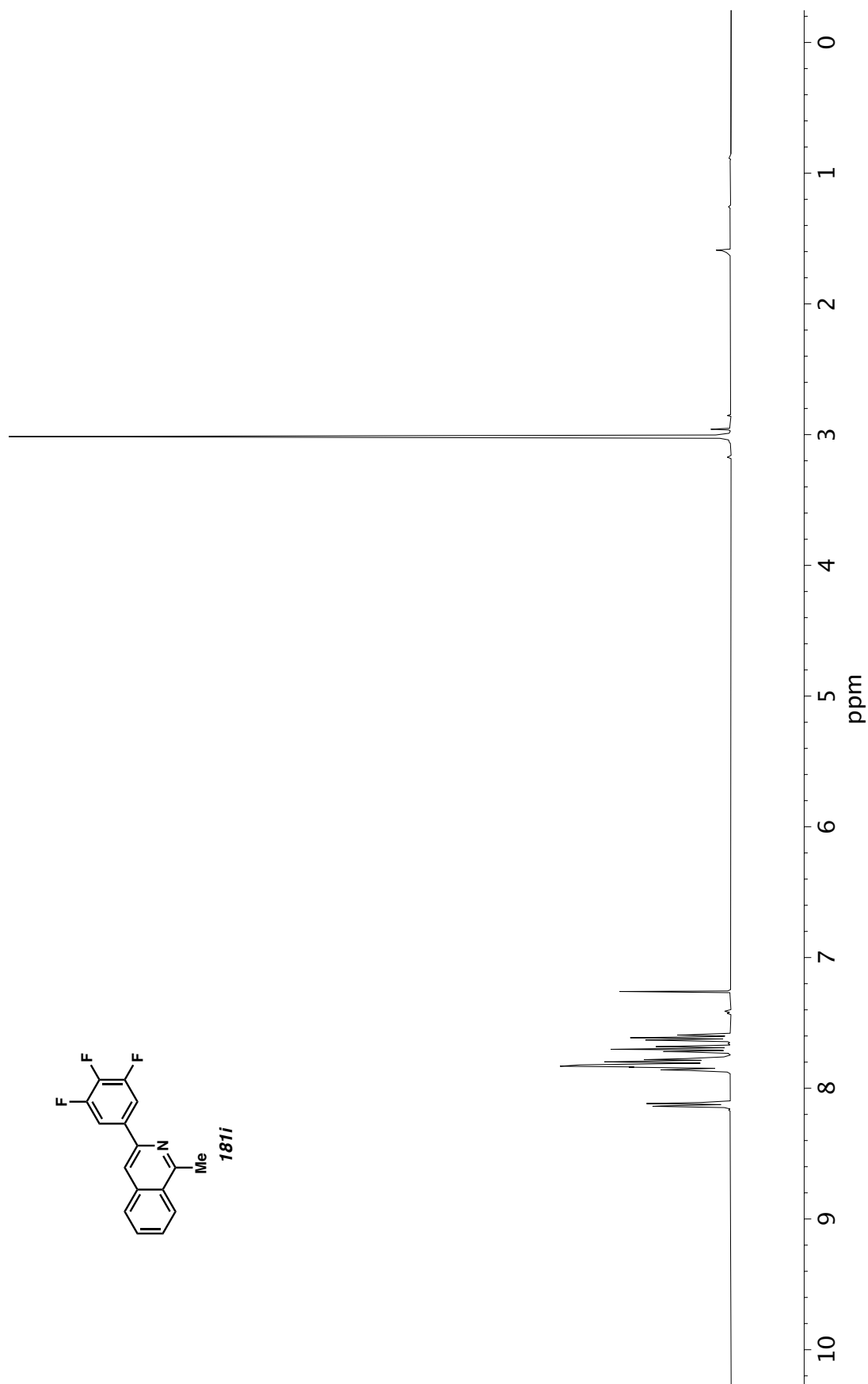


Figure A11.56 ^1H NMR (400 MHz, CDCl_3) of compound **181i**.

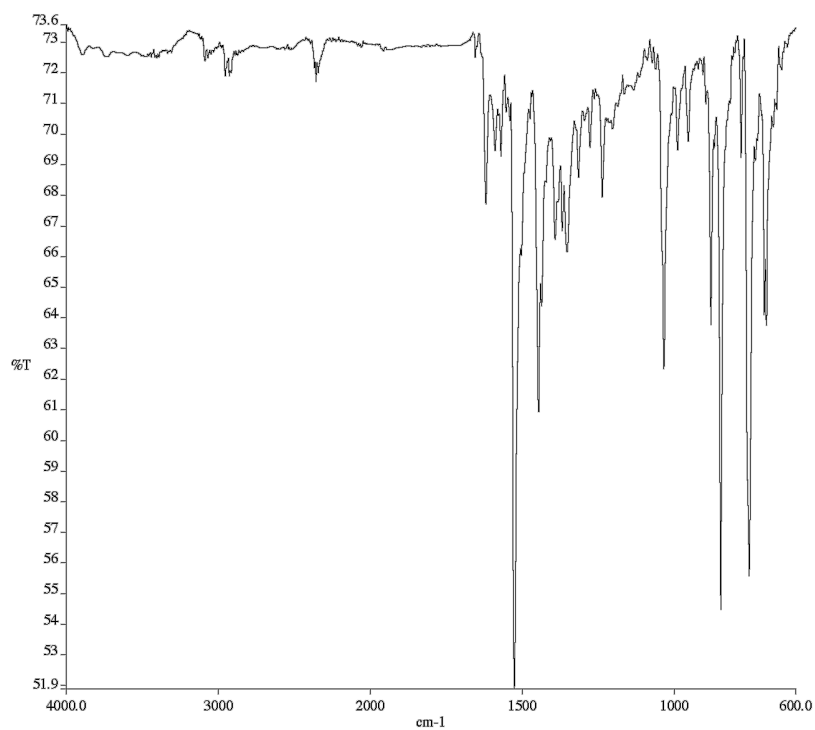


Figure A11.57 Infrared spectrum (Thin Film, NaCl) of compound **181i**.

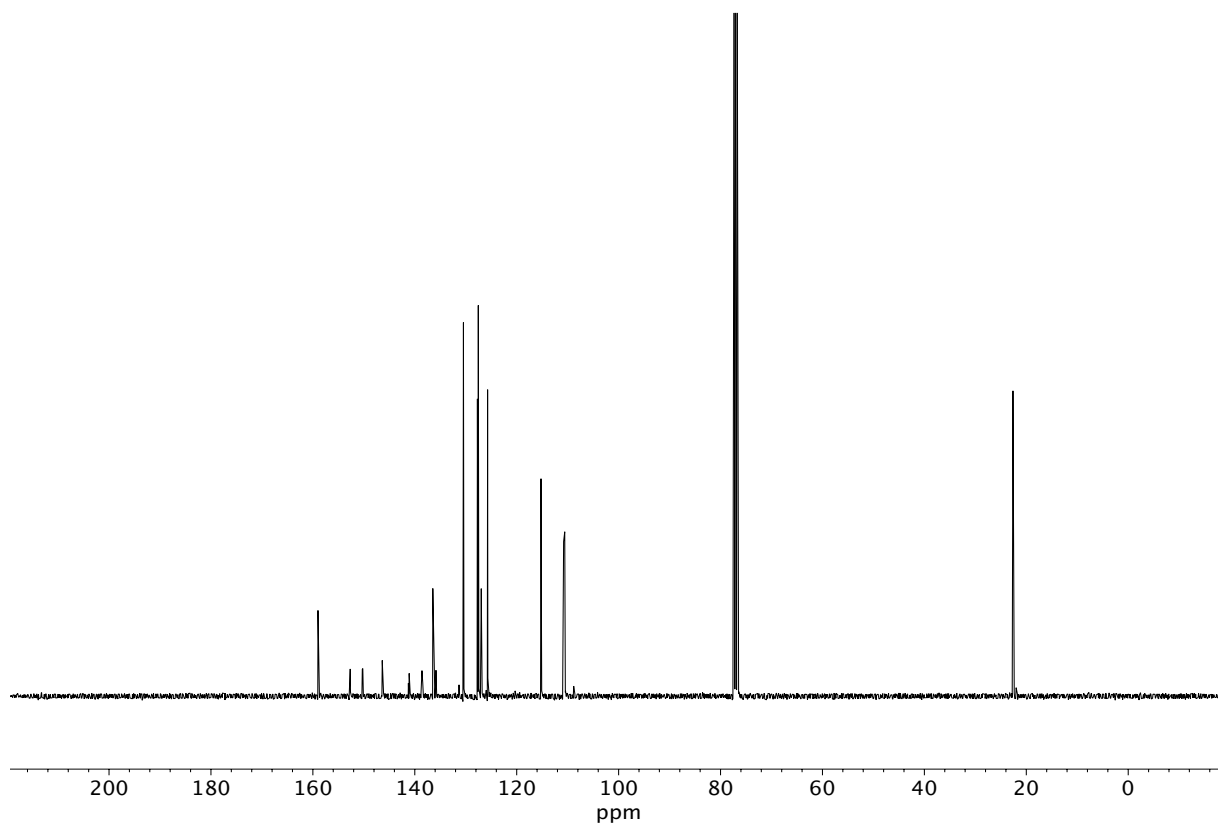


Figure A11.58 ¹³C NMR (100 MHz, CDCl₃) of compound **181i**.

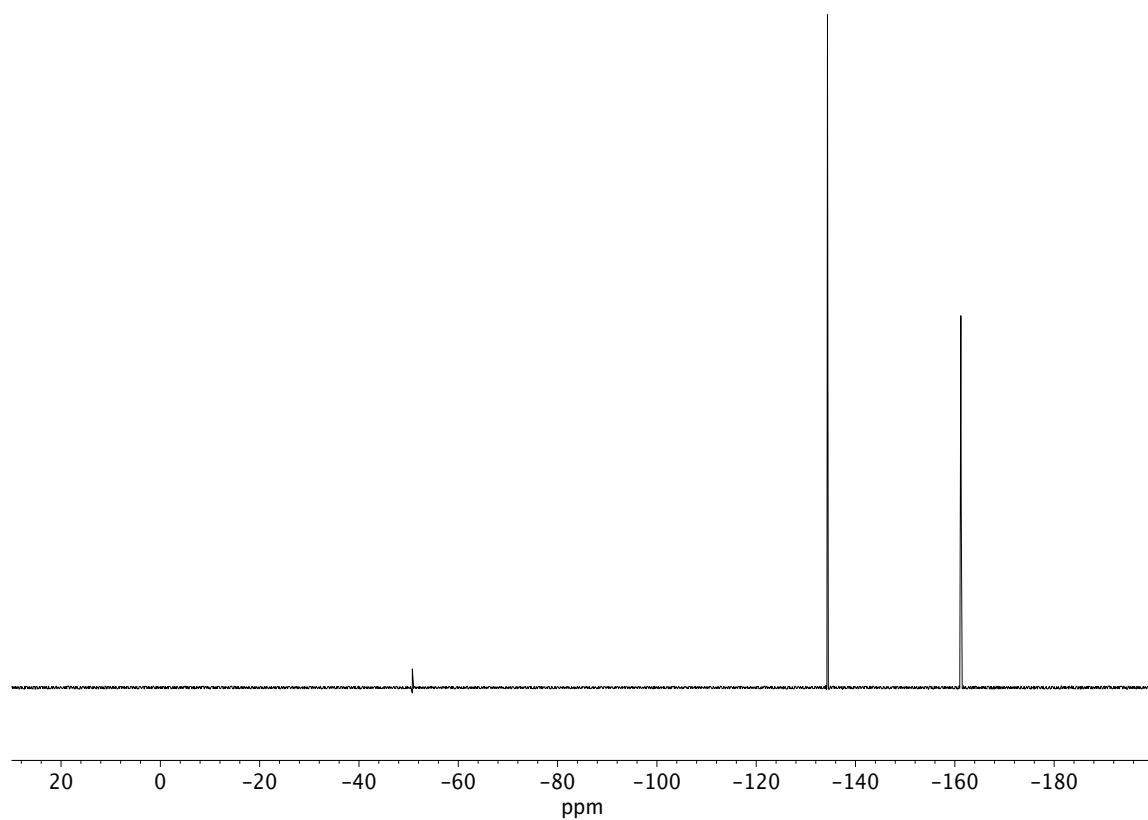


Figure A11.59 ^{19}F NMR (282 MHz, CDCl_3) of compound **181i**.

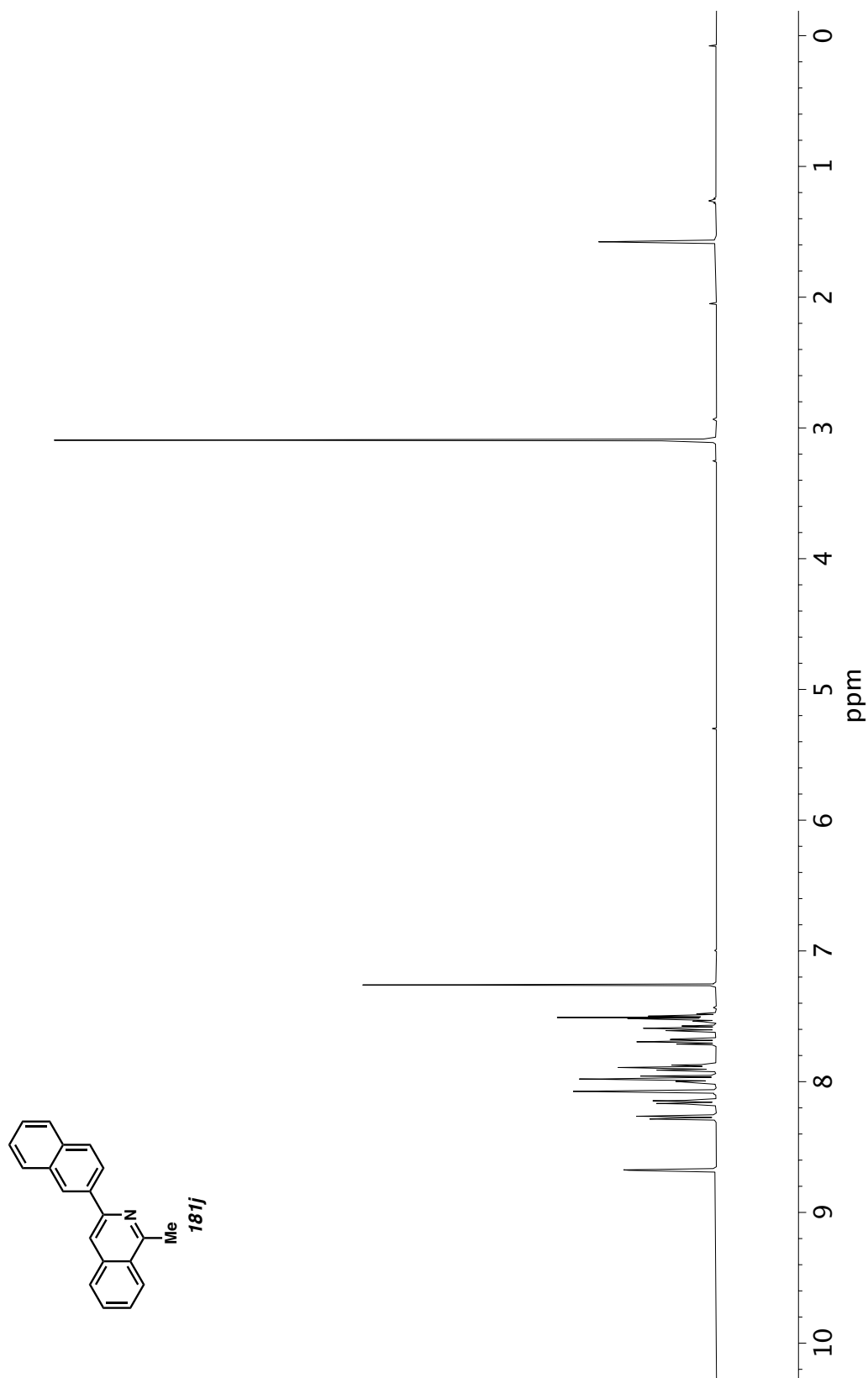


Figure A11.60 ^1H NMR (400 MHz, CDCl_3) of compound **181j**.

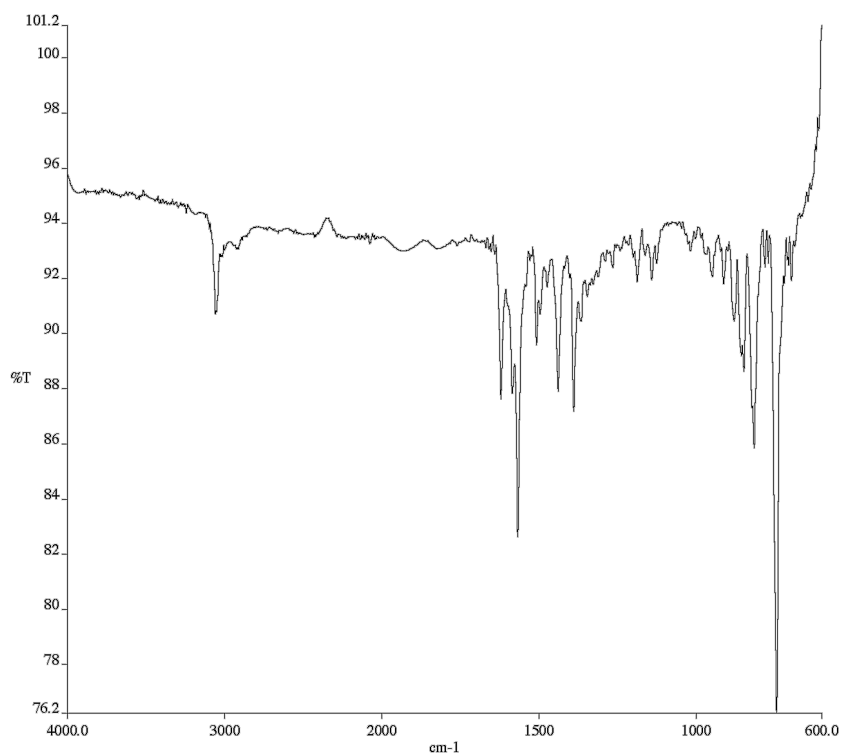


Figure A11.61 Infrared spectrum (Thin Film, NaCl) of compound **181j**.

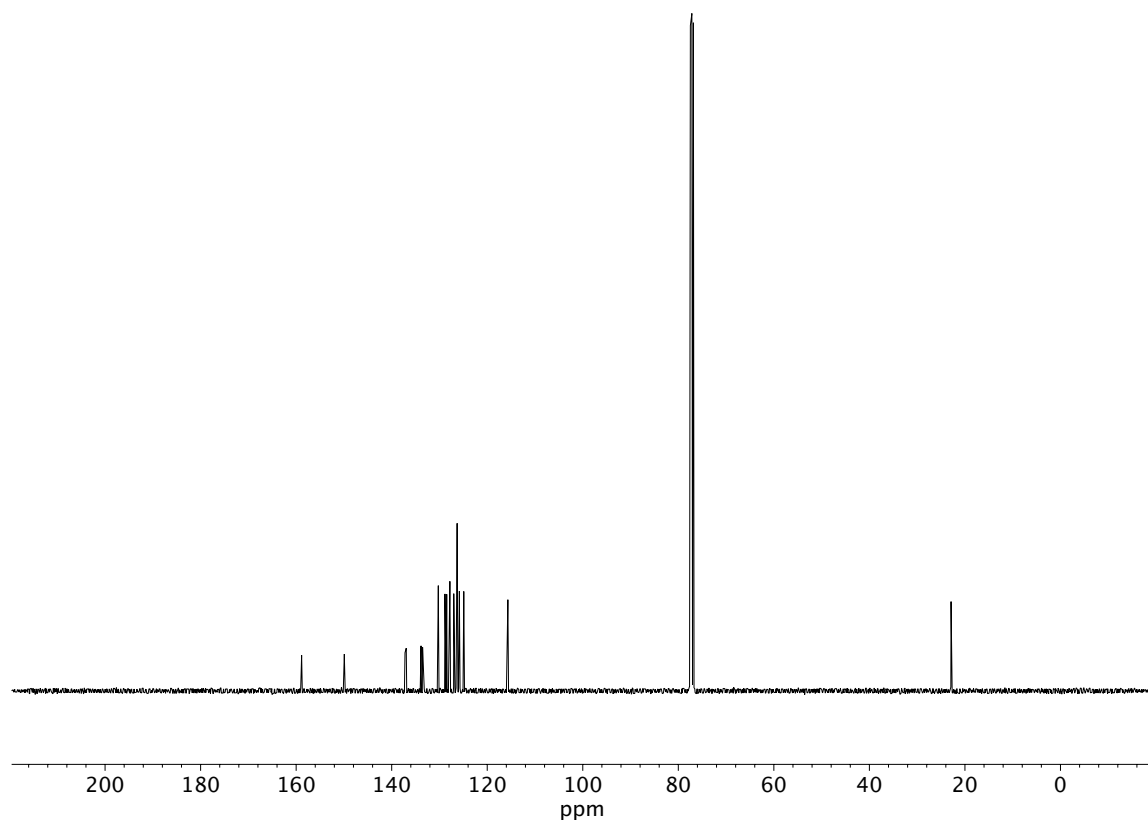


Figure A11.62 ¹³C NMR (100 MHz, CDCl₃) of compound **181j**.

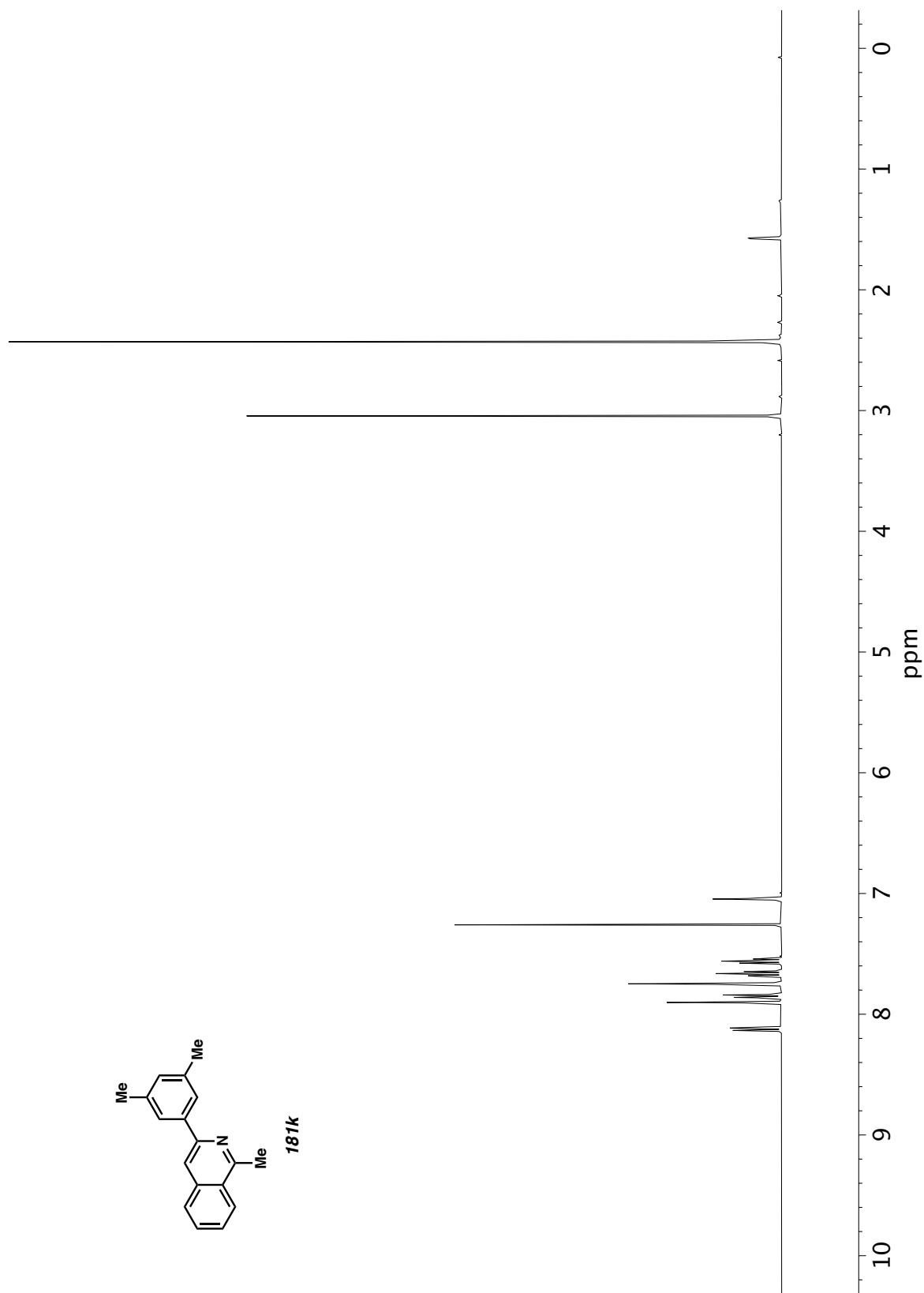


Figure A11.63 ^1H NMR (400 MHz, CDCl_3) of compound **181k**.

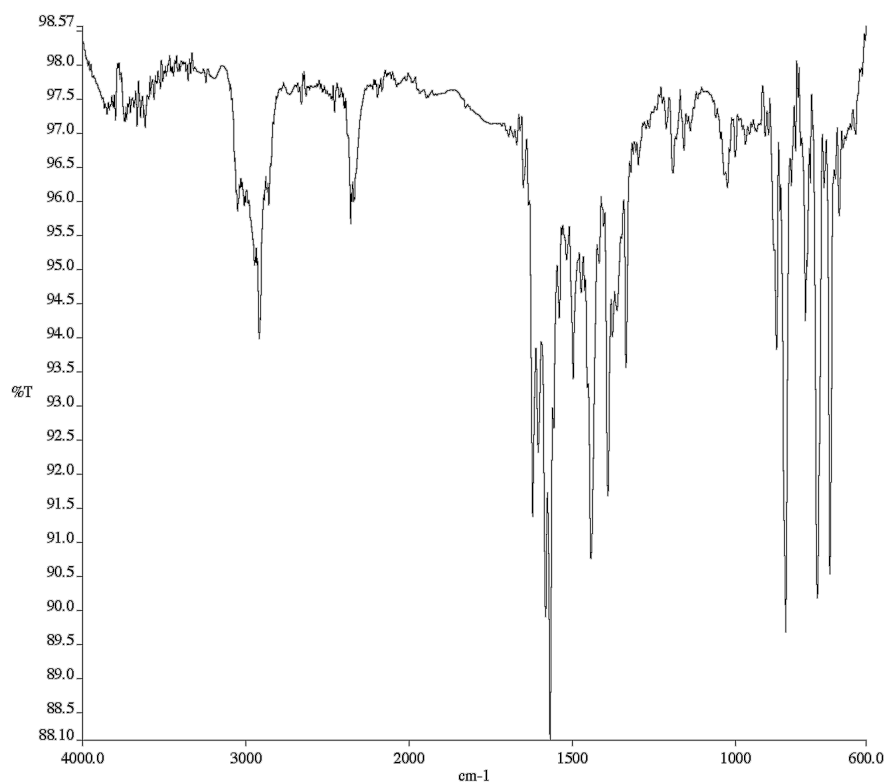


Figure A11.64 Infrared spectrum (Thin Film, NaCl) of compound **181k**.

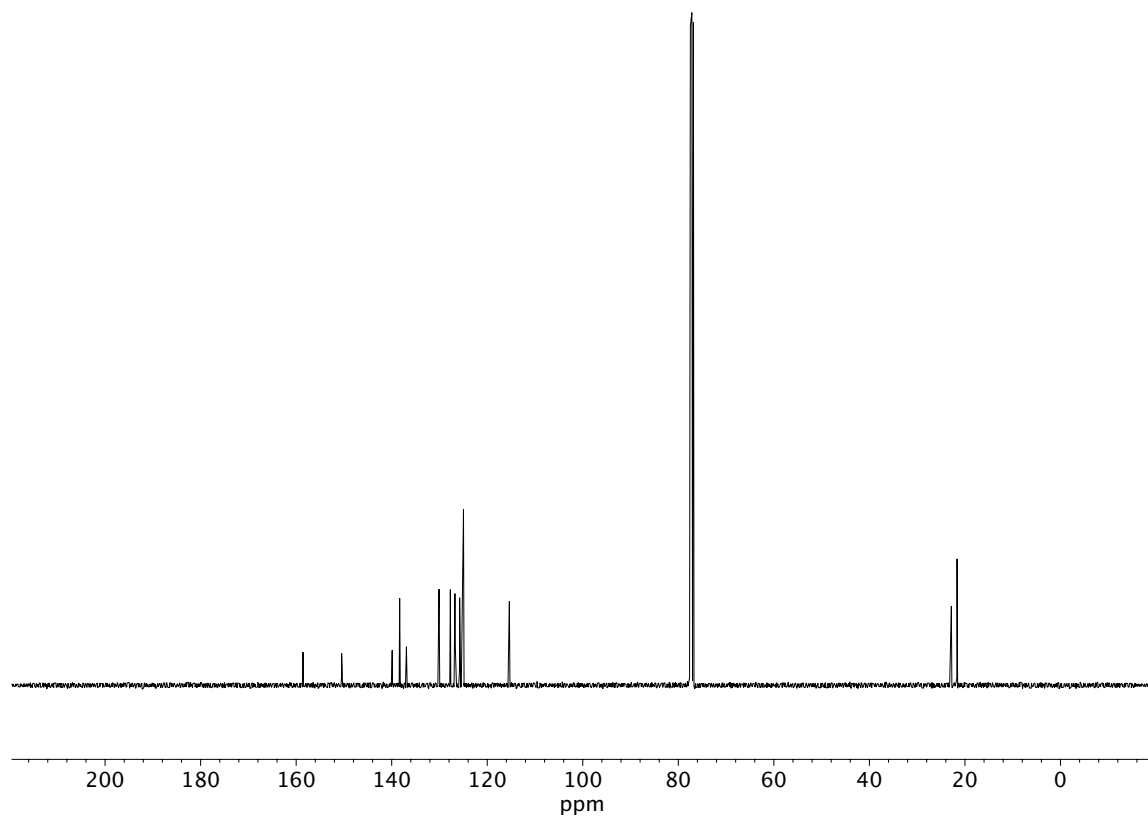


Figure A11.65 ¹³C NMR (100 MHz, CDCl₃) of compound **181k**.

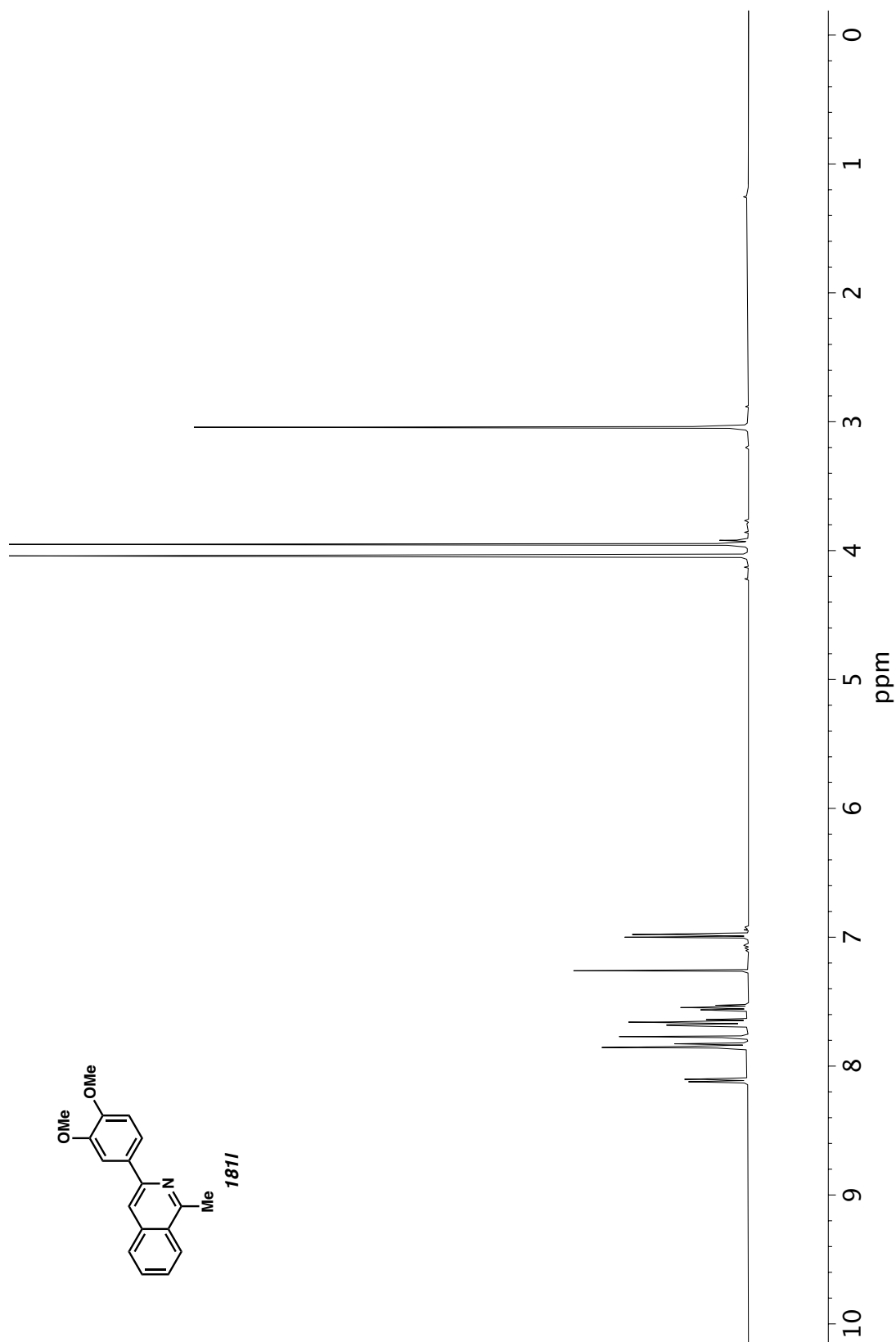


Figure A11.66 ^1H NMR (400 MHz, CDCl_3) of compound **181I**.

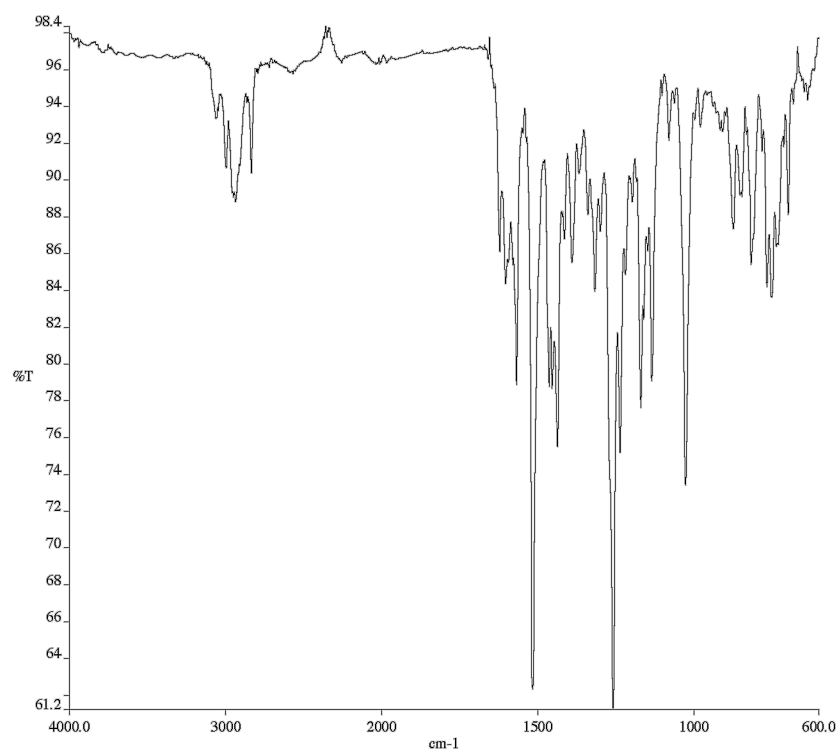


Figure A11.67 Infrared spectrum (Thin Film, NaCl) of compound **181I**.

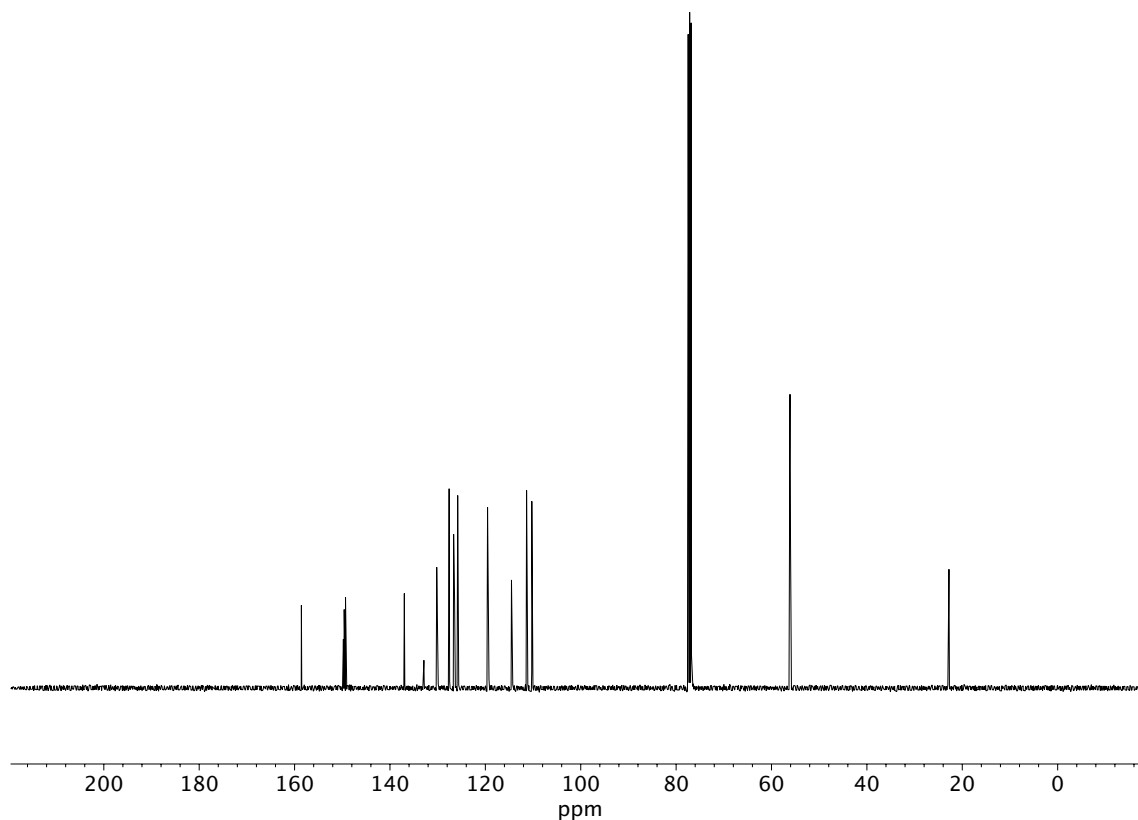


Figure A11.68 ¹³C NMR (100 MHz, CDCl₃) of compound **181I**.

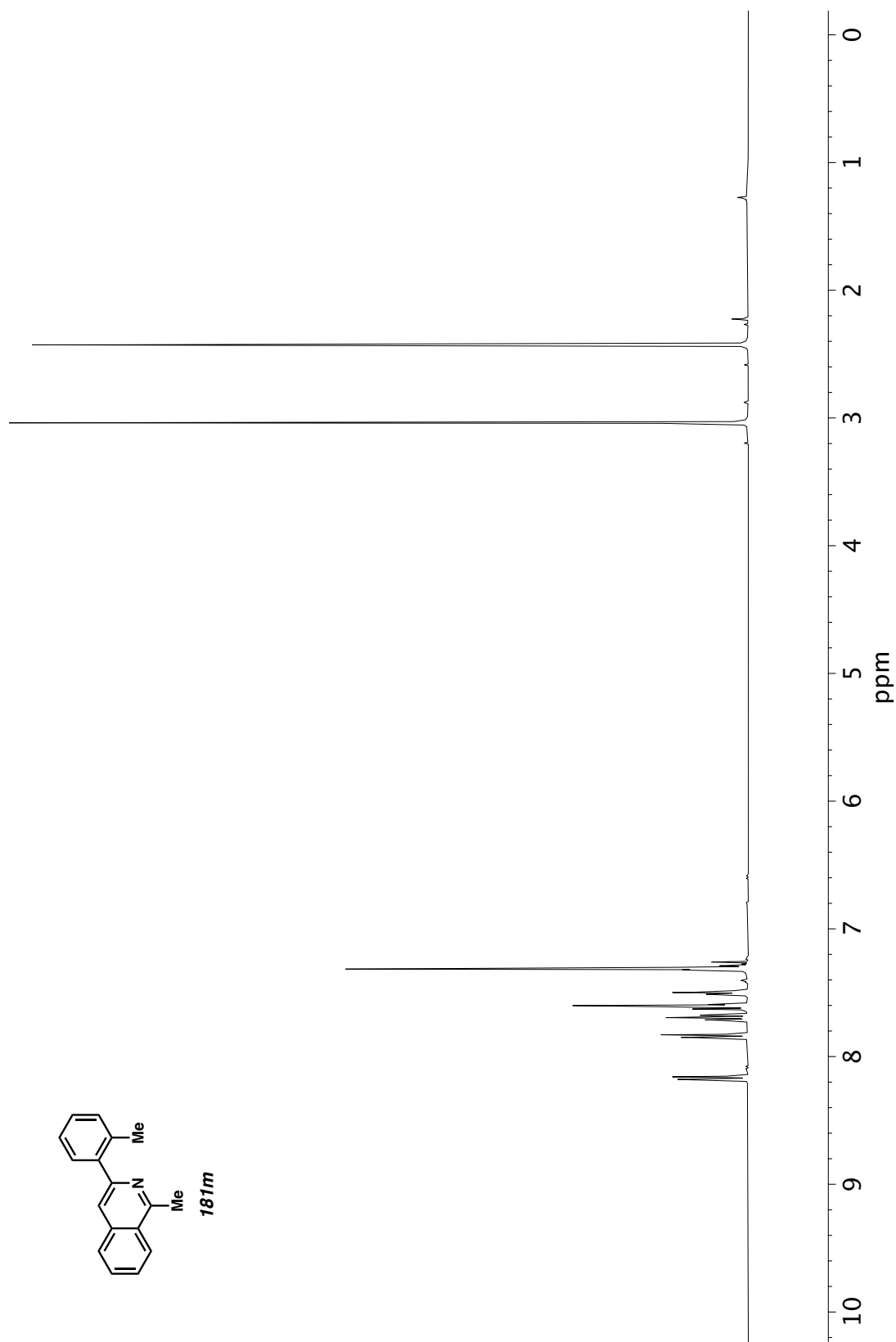


Figure A11.69 ^1H NMR (400 MHz, CDCl_3) of compound **181m**.

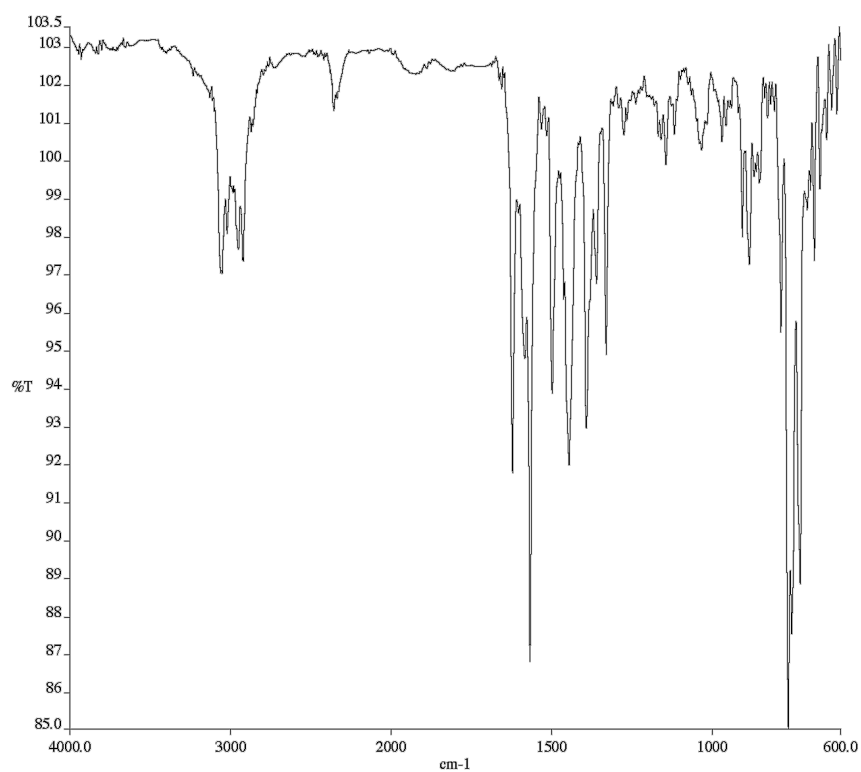


Figure A11.70 Infrared spectrum (Thin Film, NaCl) of compound

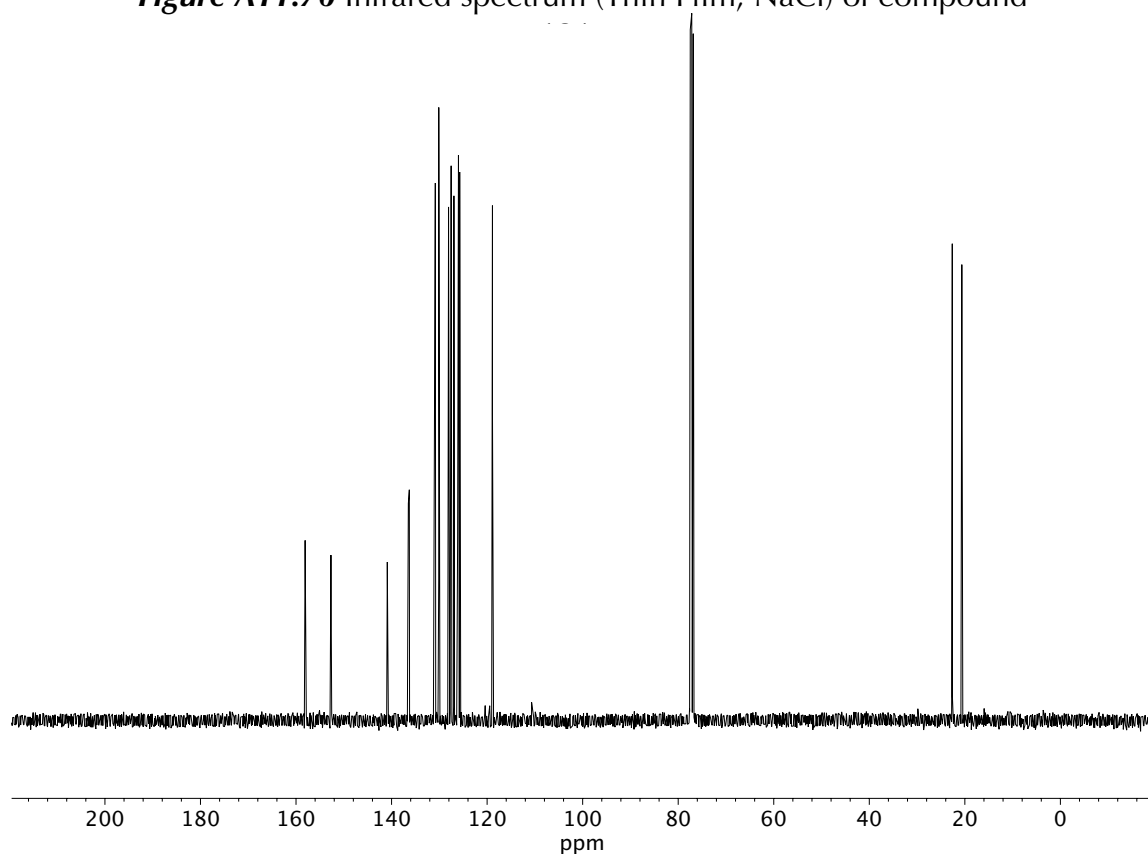


Figure A11.71 ¹³C NMR (100 MHz, CDCl₃) of compound **181m**.

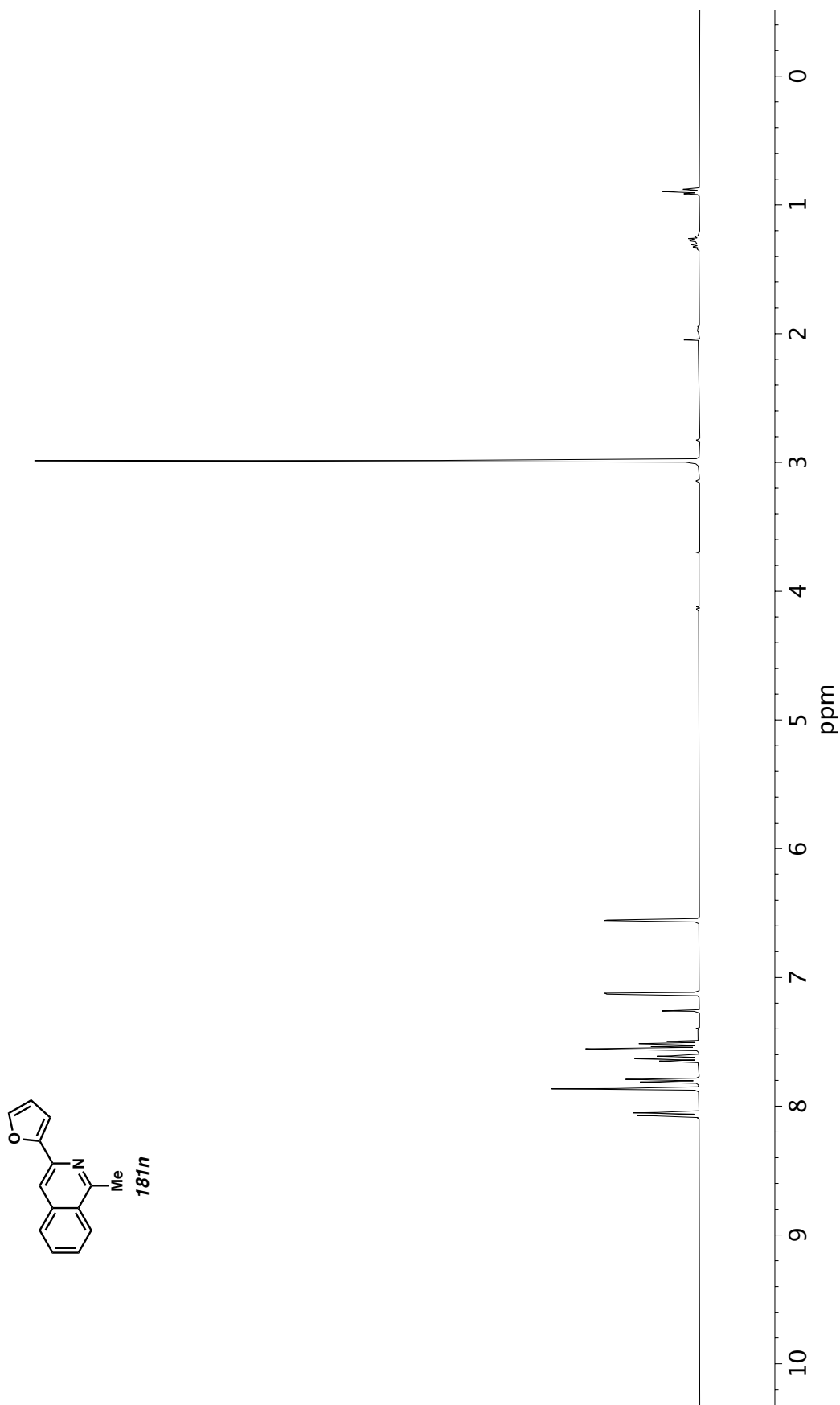


Figure A11.72 ^1H NMR (400 MHz, CDCl_3) of compound **181n**.

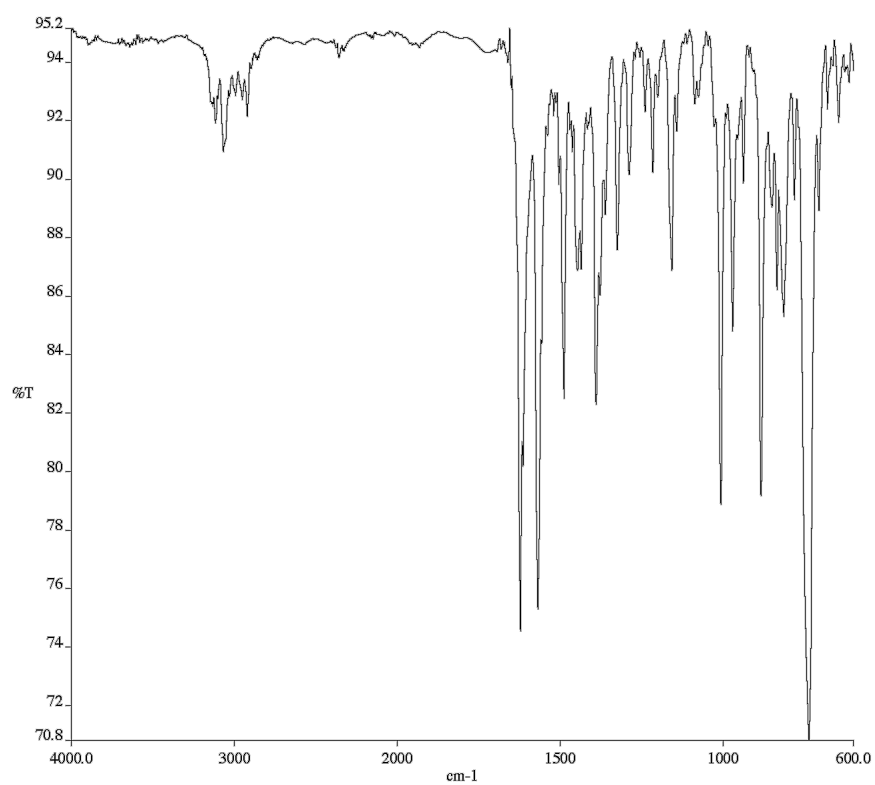


Figure A11.73 Infrared spectrum (Thin Film, NaCl) of compound **181n**.

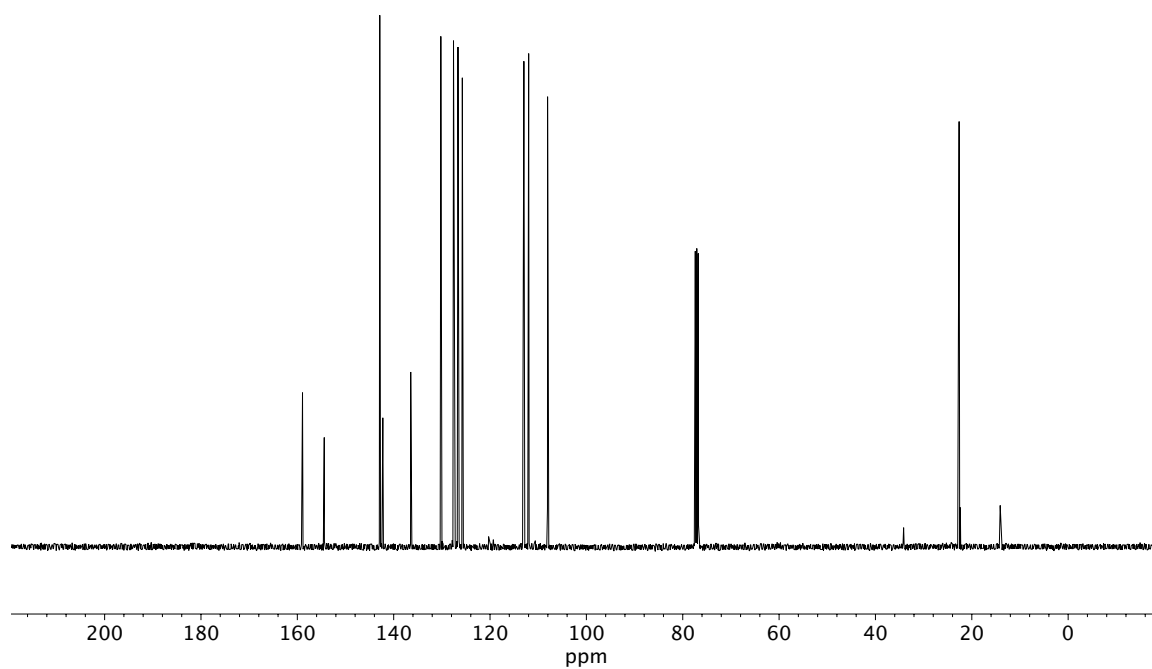


Figure A11.74 ¹³C NMR (100 MHz, CDCl₃) of compound **181n**.

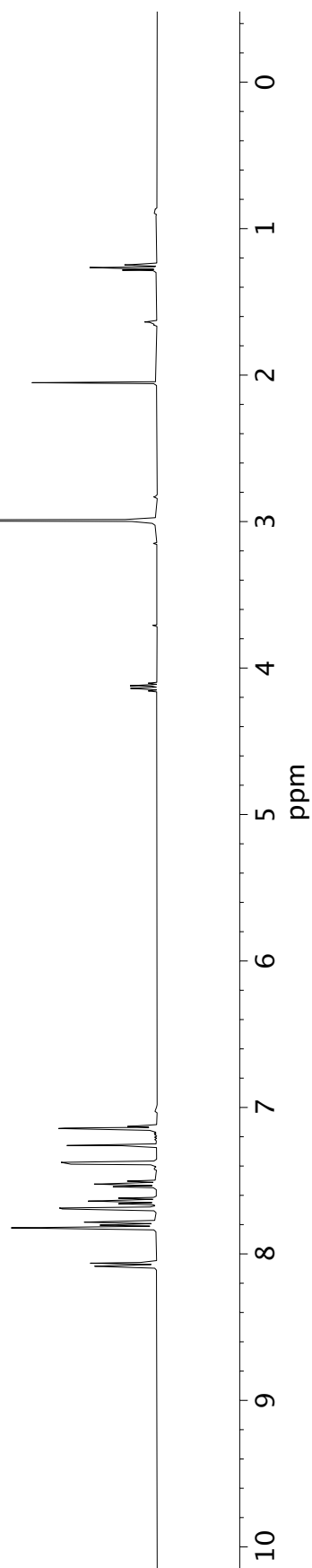
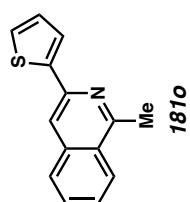


Figure A11.75 ^1H NMR (400 MHz, CDCl_3) of compound **181o**.

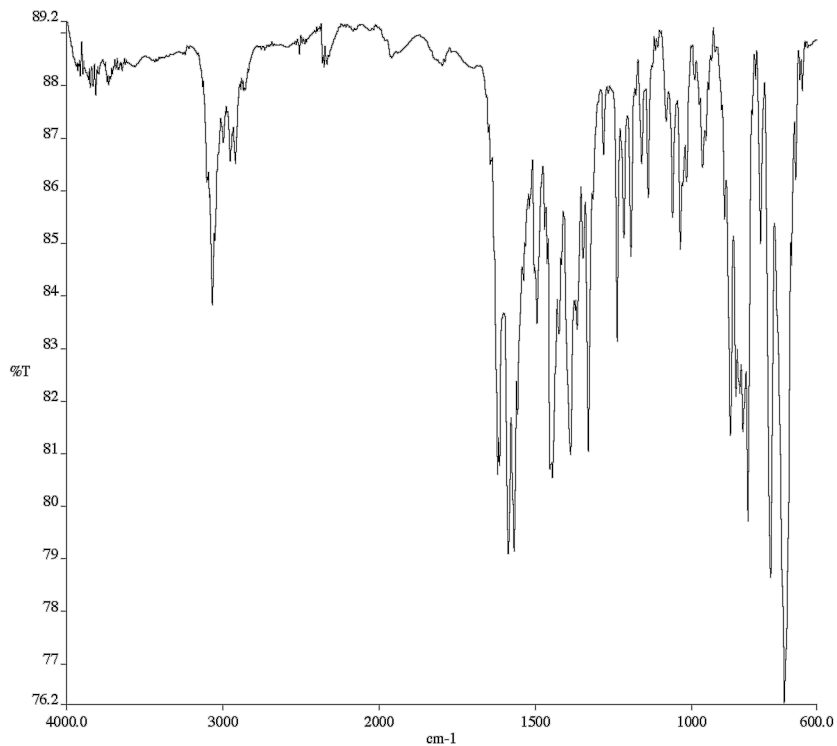


Figure A11.76 Infrared spectrum (Thin Film, NaCl) of compound **181o**.

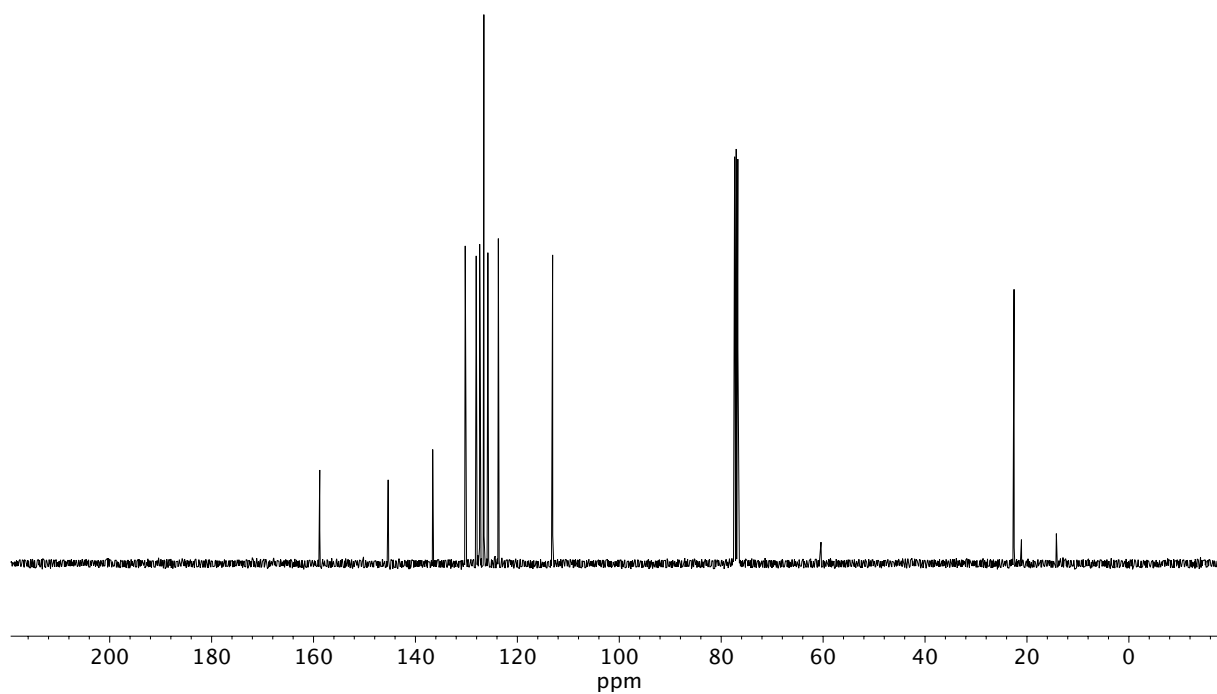


Figure A11.77 ¹³C NMR (100 MHz, CDCl₃) of compound **181o**.



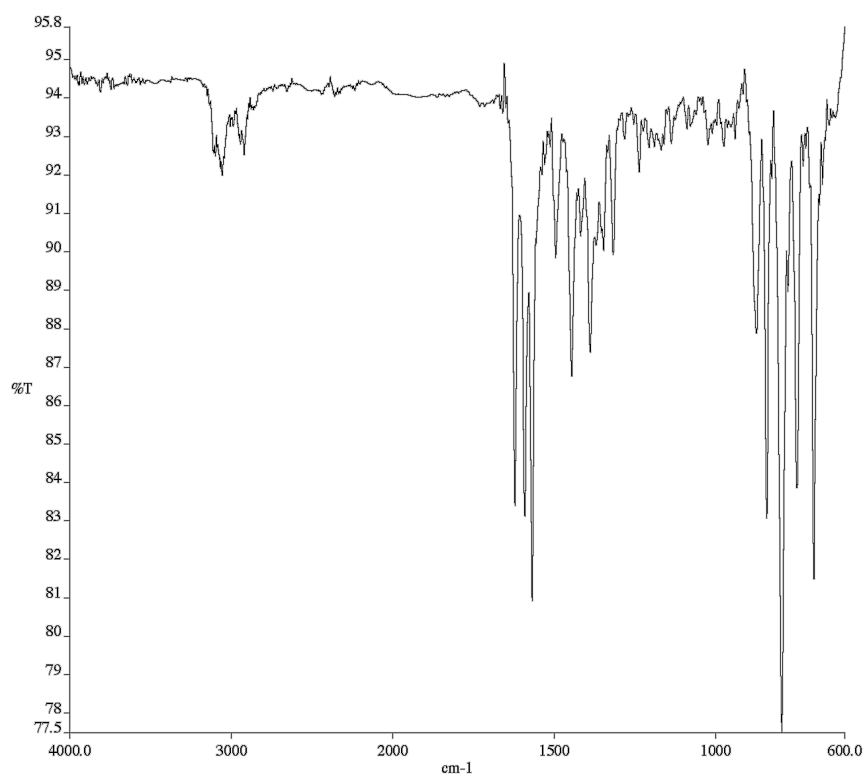


Figure A11.79 Infrared spectrum (Thin Film, NaCl) of compound **181p**.

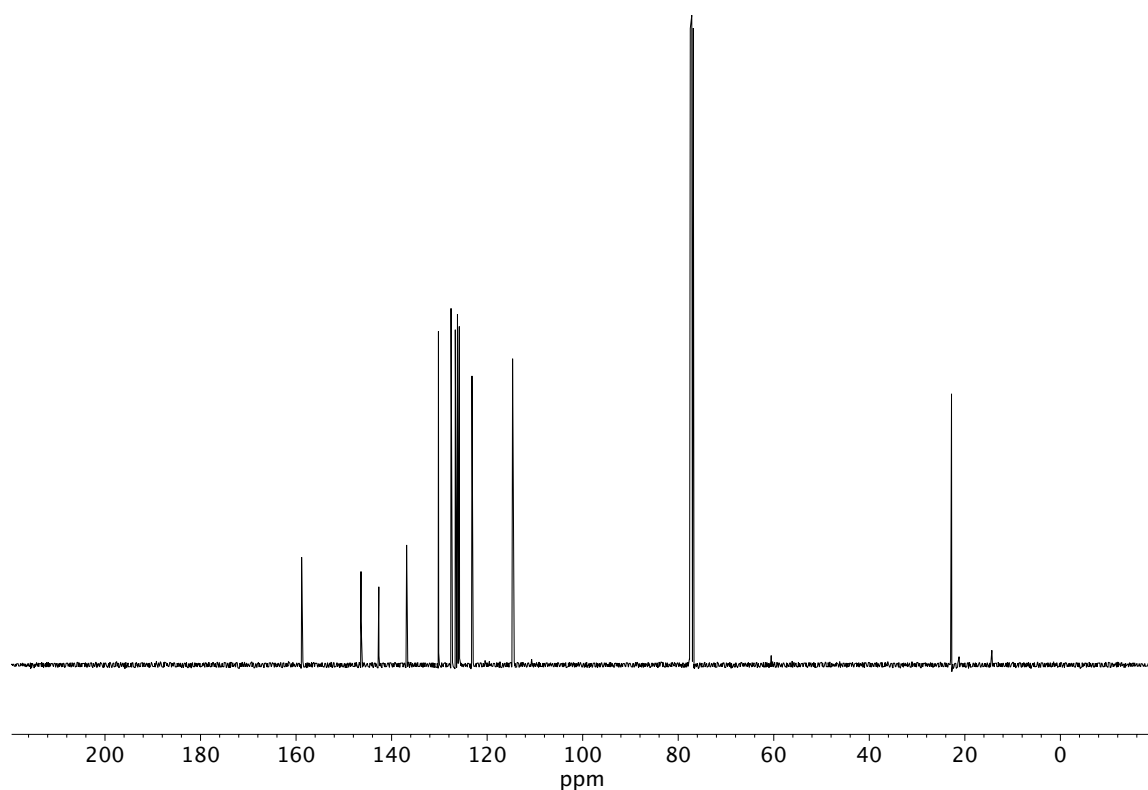


Figure A11.80 ¹³C NMR (100 MHz, CDCl₃) of compound **181p**.

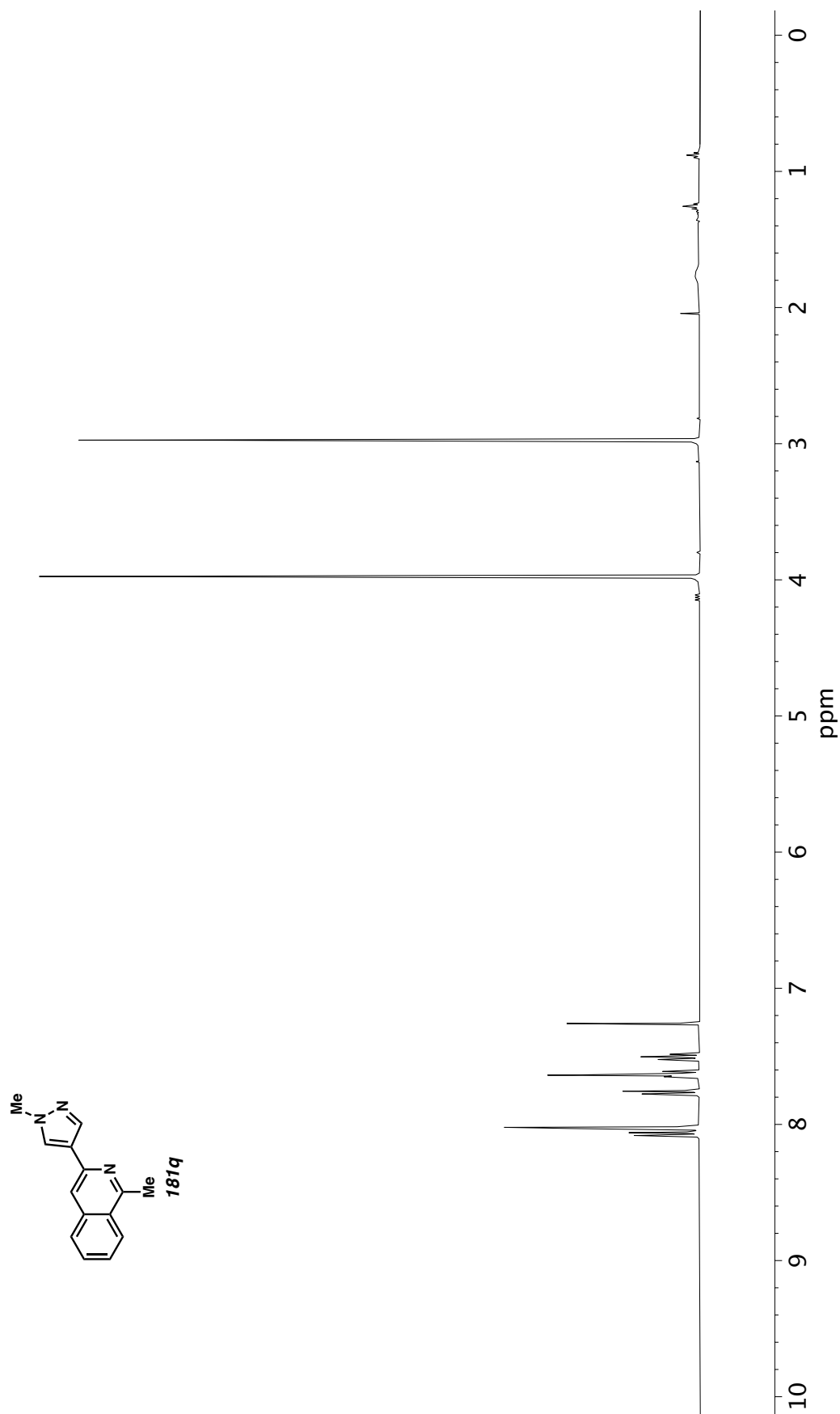


Figure A11.81 ^1H NMR (400 MHz, CDCl_3) of compound **181q**.

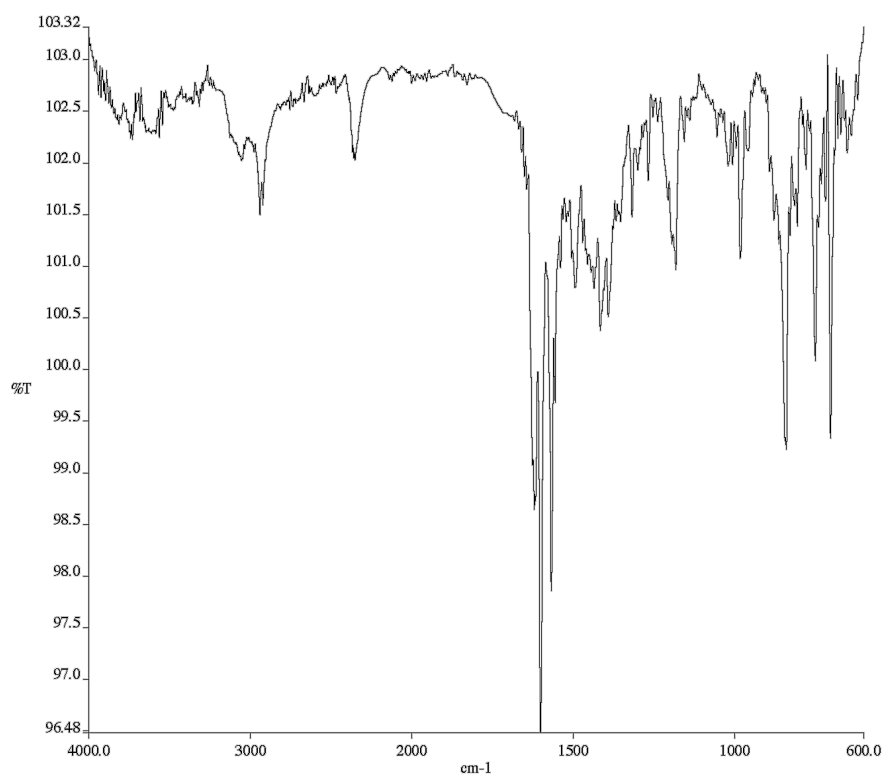


Figure A11.82 Infrared spectrum (Thin Film, NaCl) of compound **181q**.

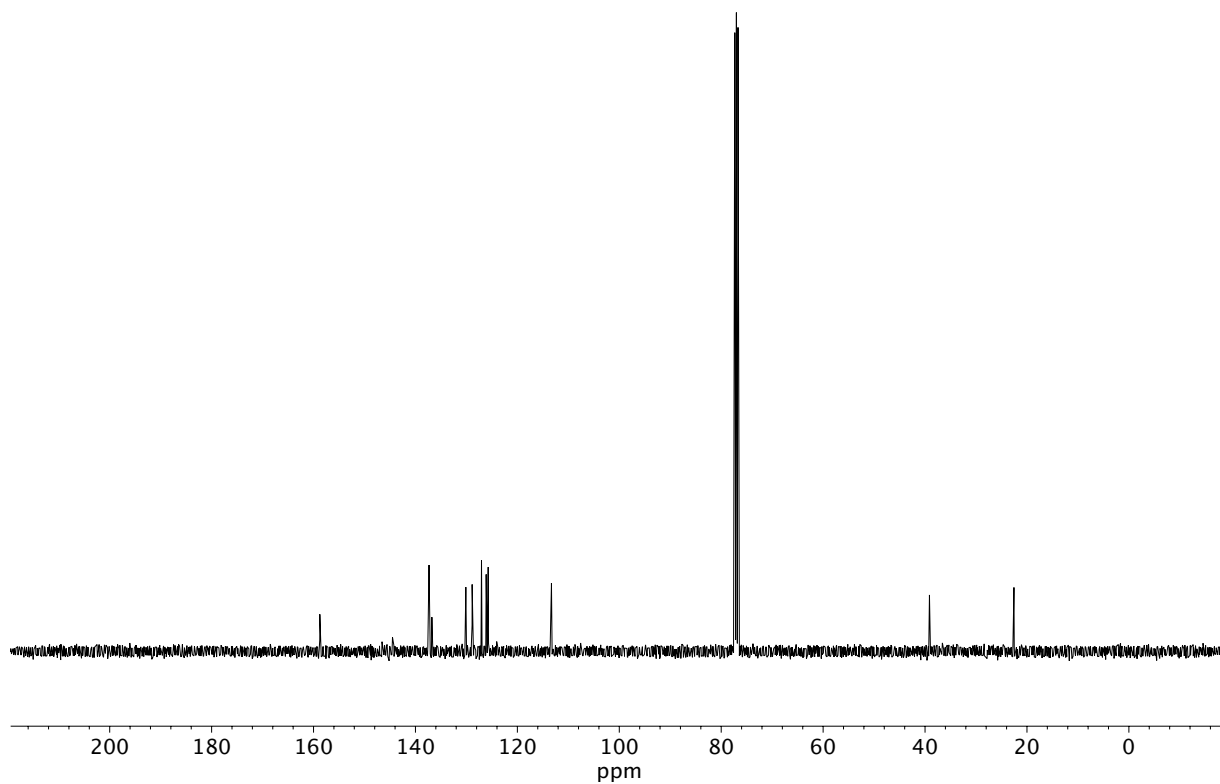


Figure A11.83 ¹³C NMR (100 MHz, CDCl₃) of compound **181q**.

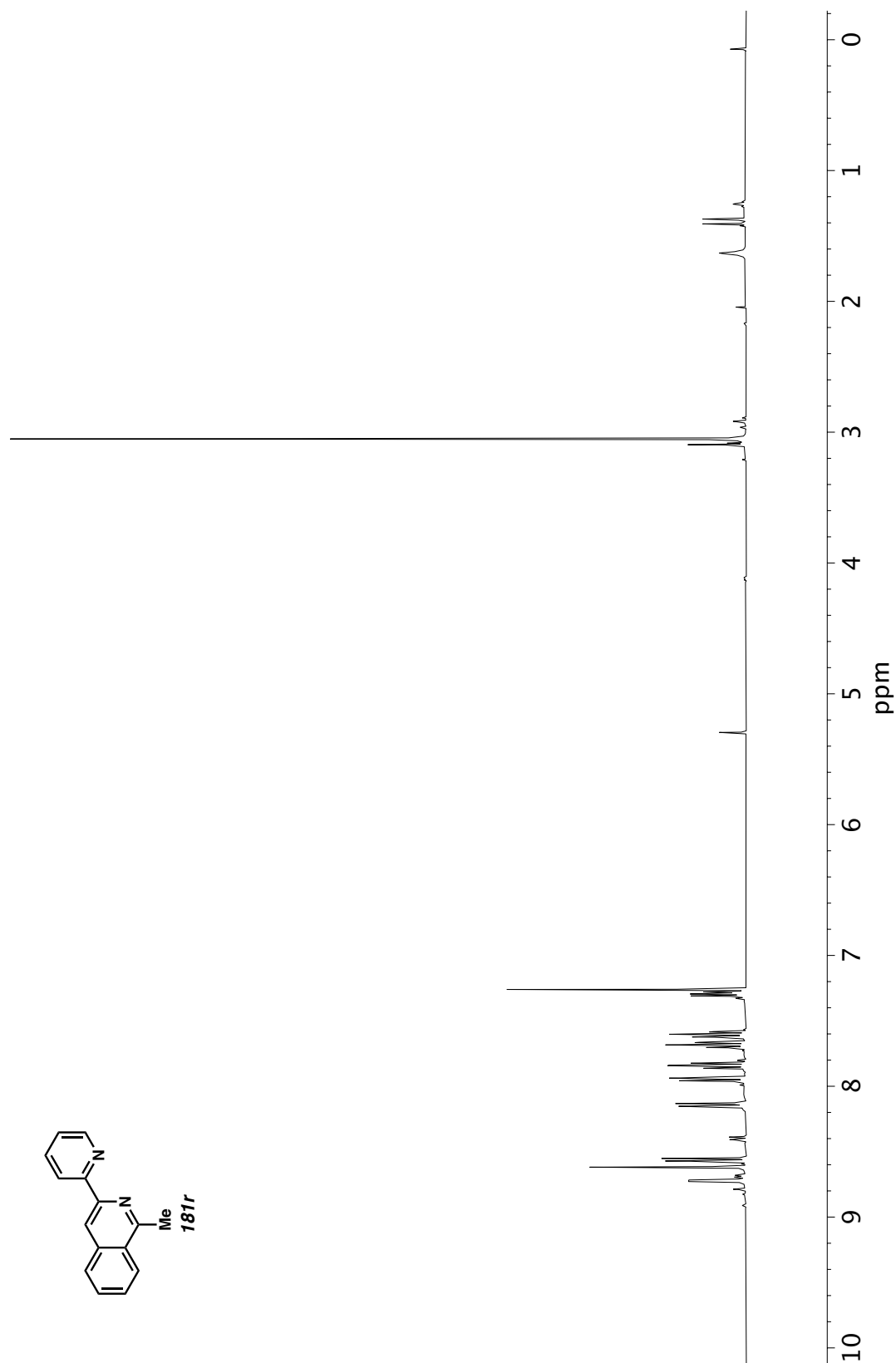


Figure A11.84 ¹H NMR (400 MHz, CDCl₃) of compound **181r**.

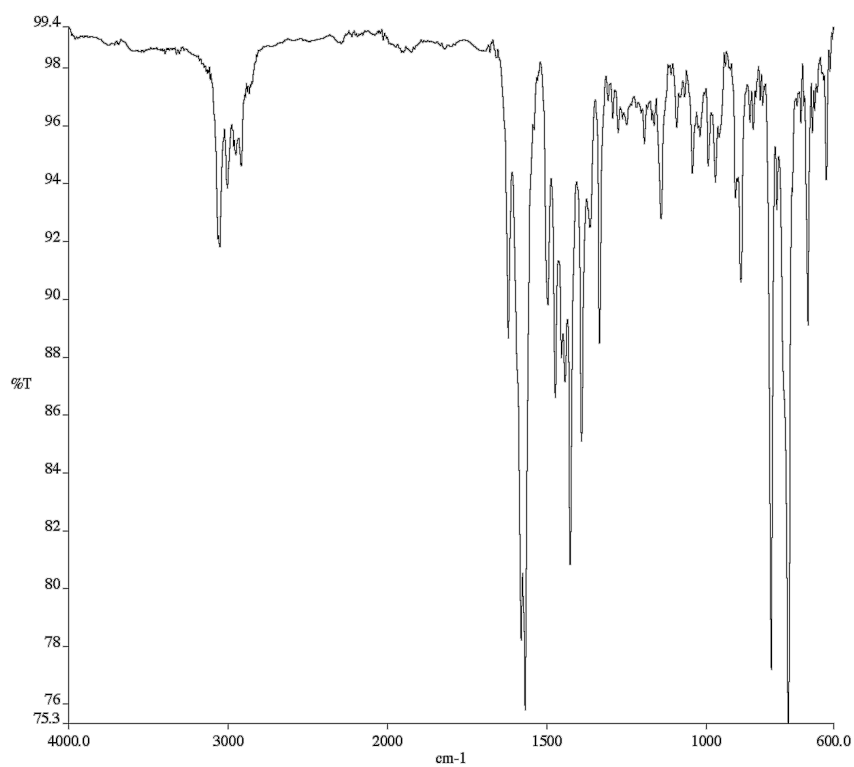


Figure A11.85 Infrared spectrum (Thin Film, NaCl) of compound **181r**.

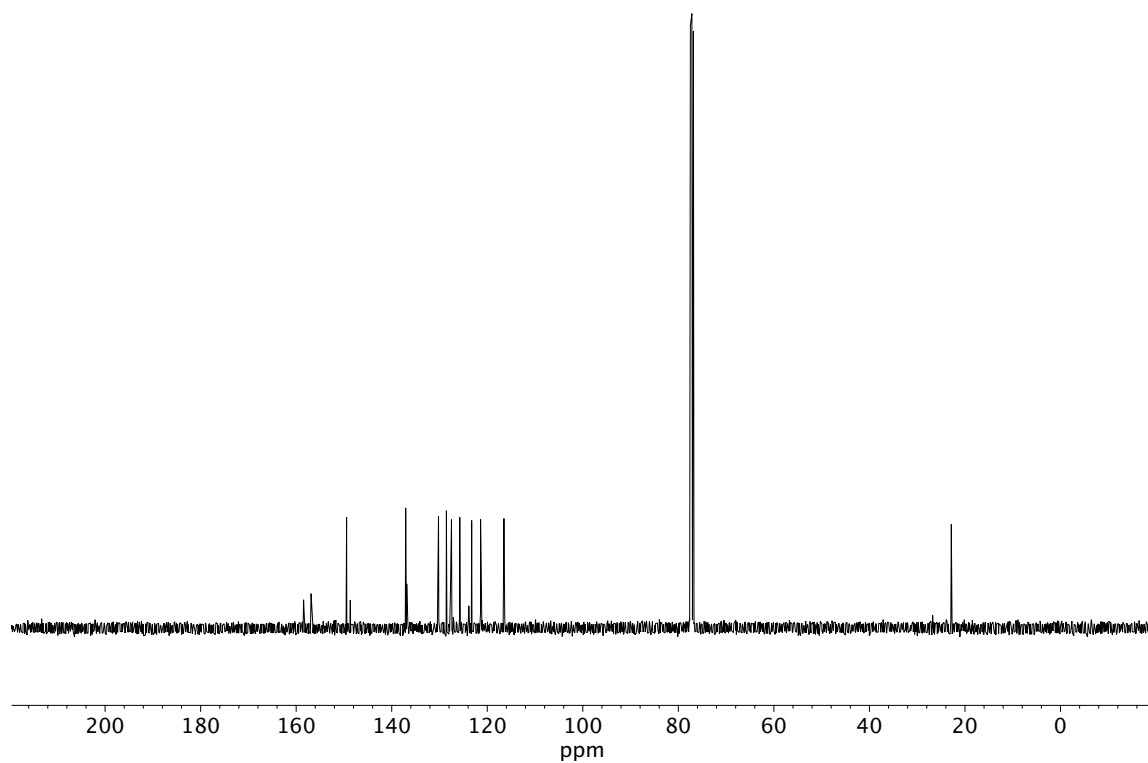


Figure A11.86 ¹³C NMR (100 MHz, CDCl₃) of compound **181r**.

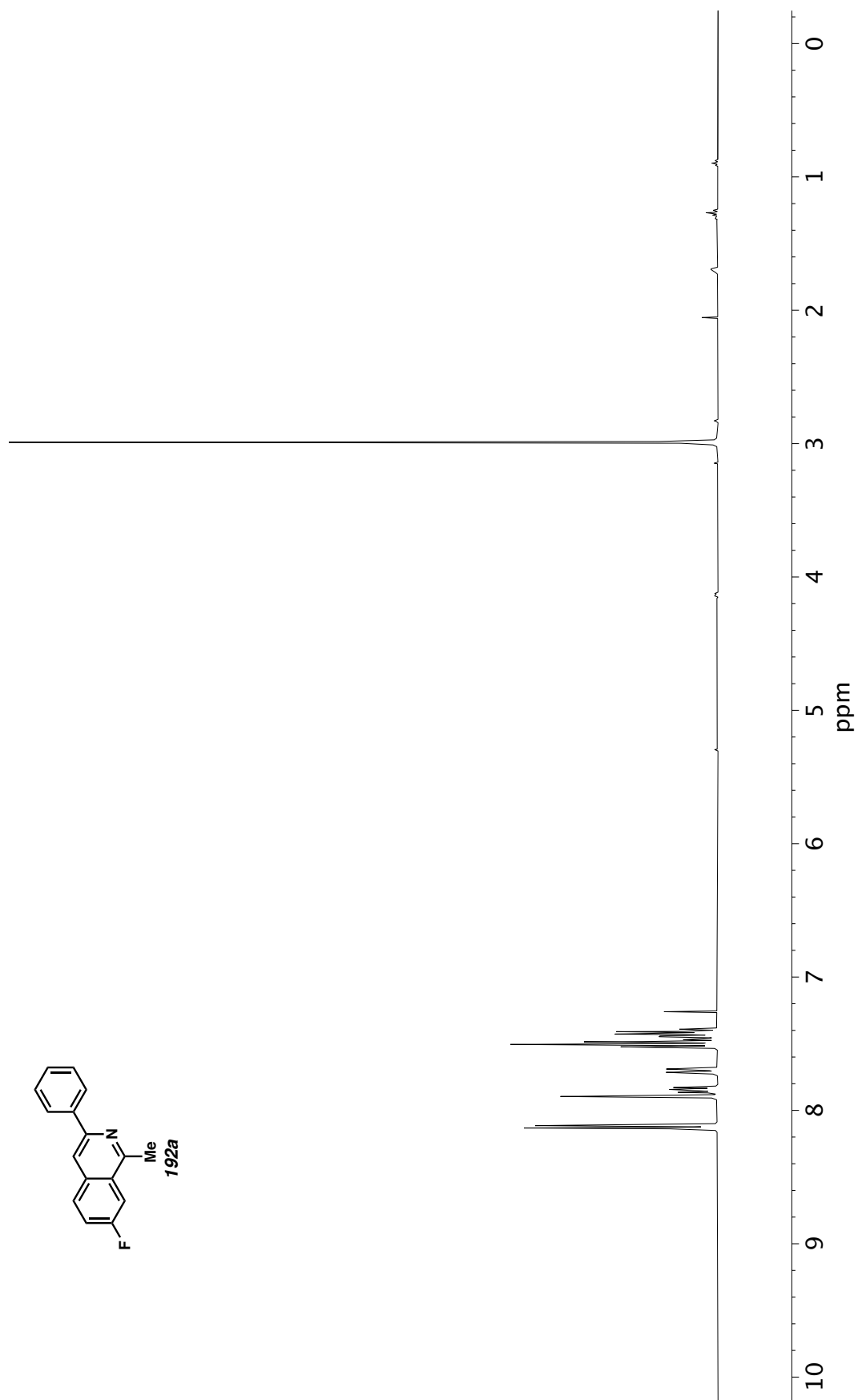


Figure A11.87 ^1H NMR (400 MHz, CDCl_3) of compound **192a**.

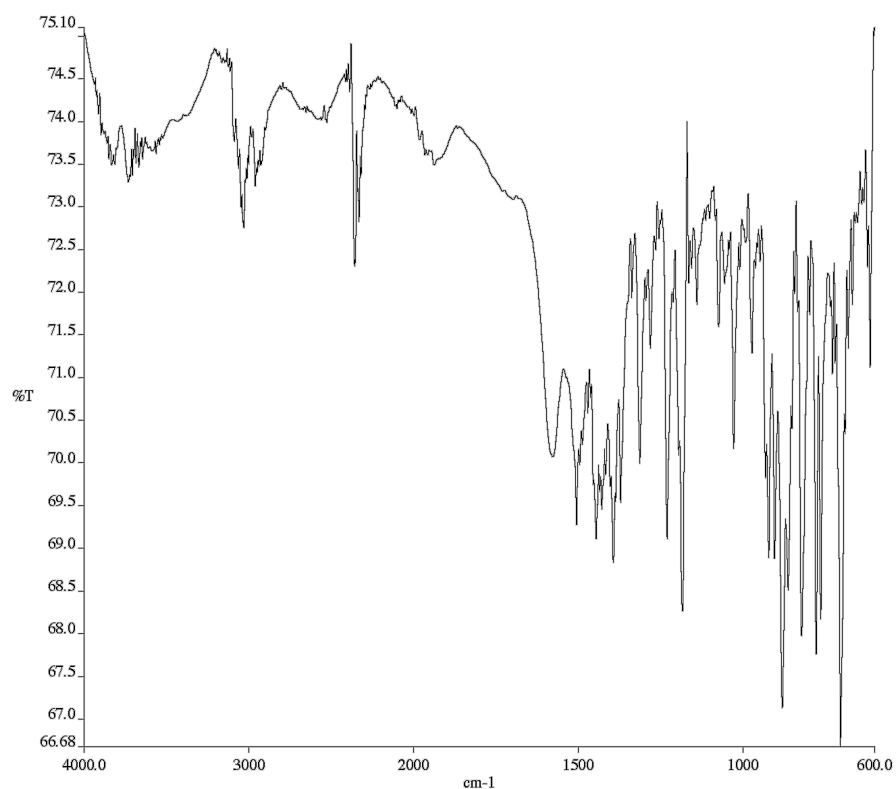


Figure A11.88 Infrared spectrum (Thin Film, NaCl) of compound **192a**.

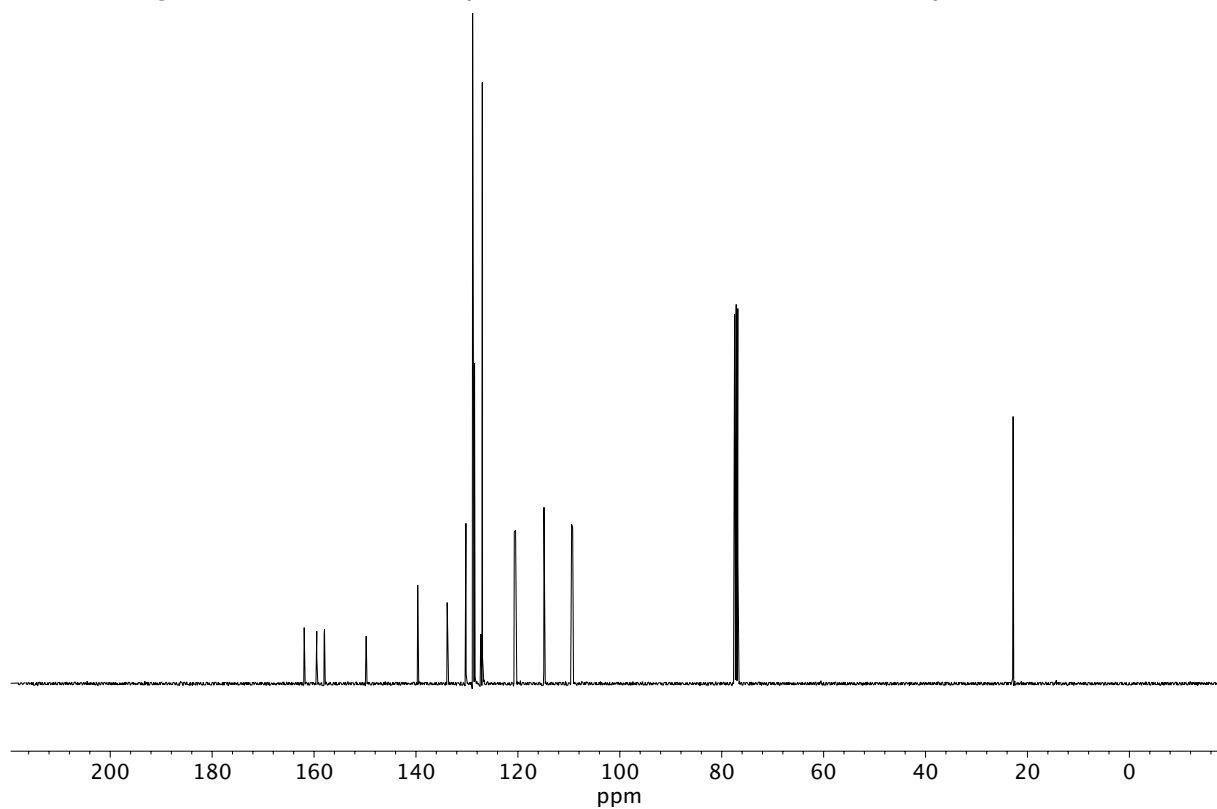


Figure A11.89 ¹³C NMR (100 MHz, CDCl₃) of compound **192a**.

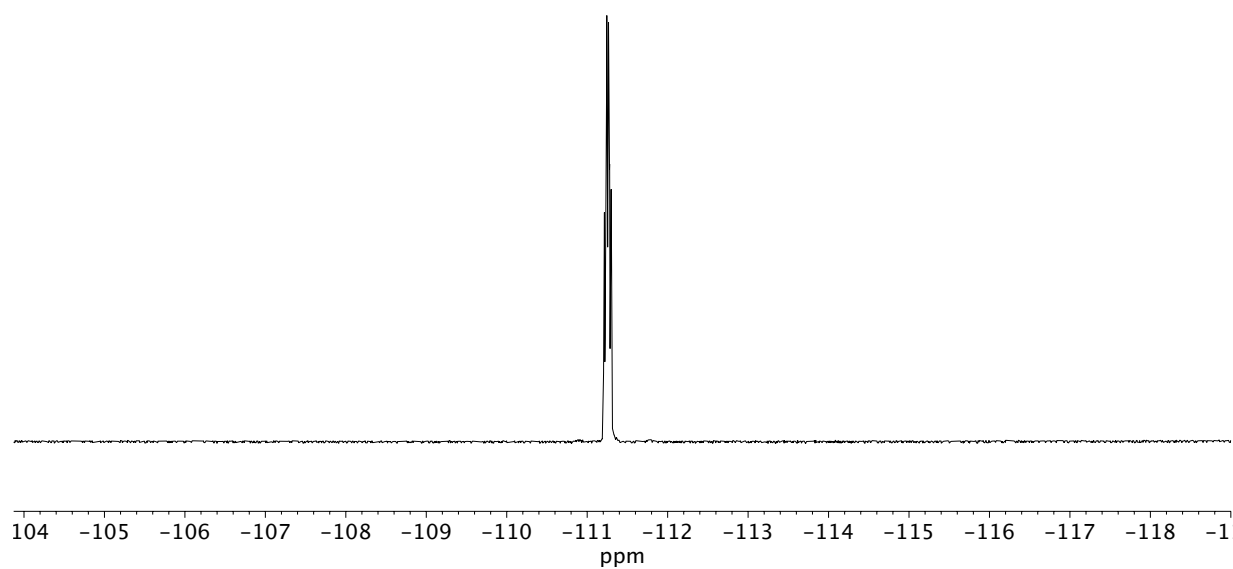


Figure A11.90 ^{19}F NMR (282 MHz, CDCl_3) of compound **192a**.

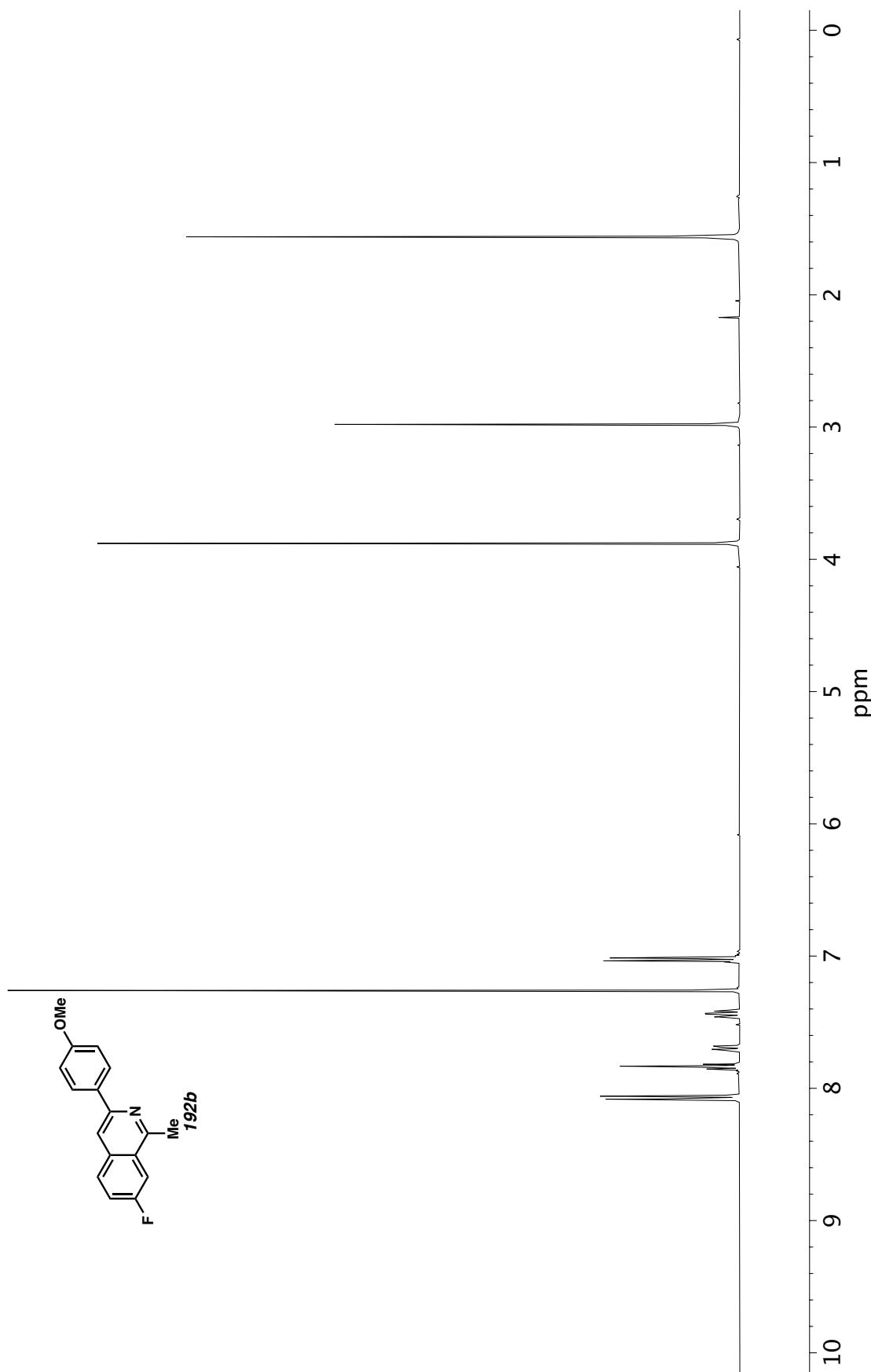


Figure A11.91 ¹H NMR (400 MHz, CDCl₃) of compound **192b**.

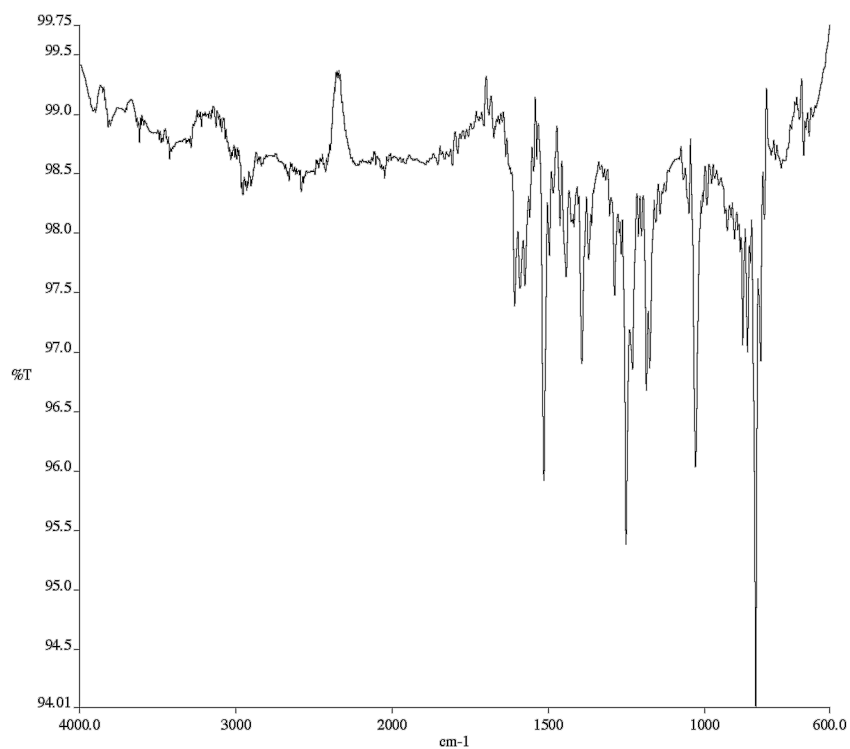


Figure A11.92 Infrared spectrum (Thin Film, NaCl) of compound **192b**.

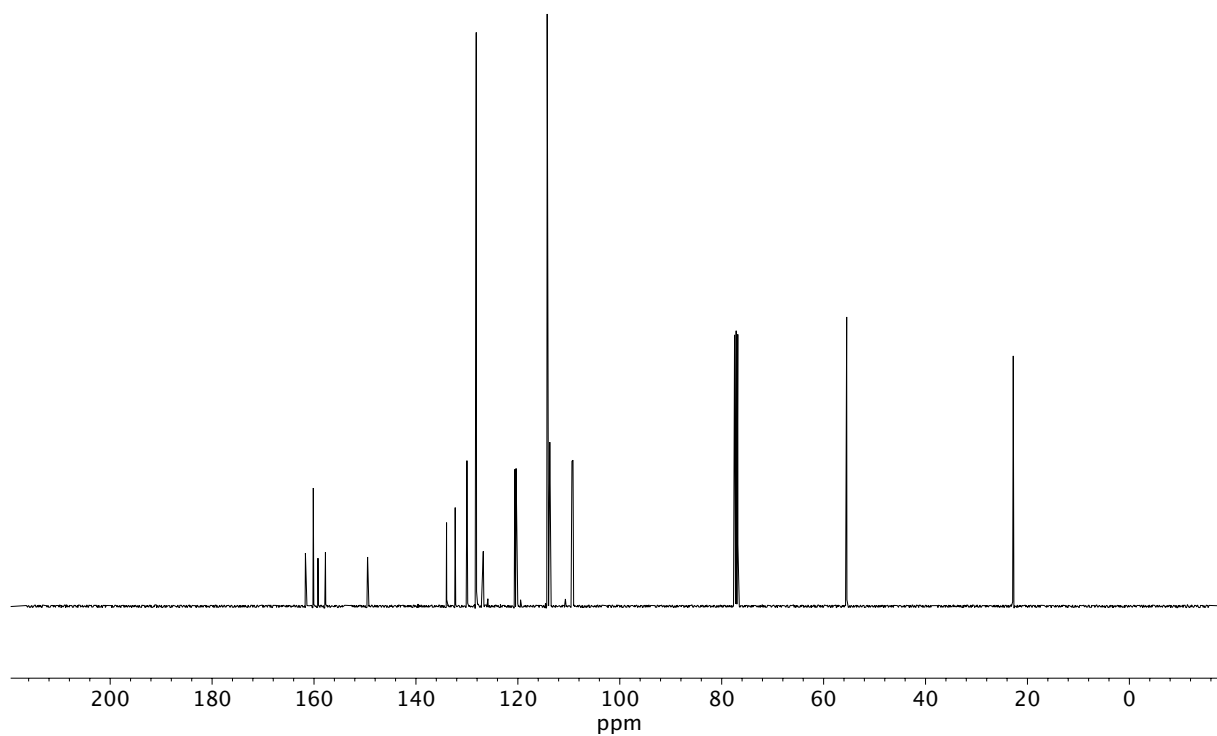


Figure A11.93 ¹³C NMR (100 MHz, CDCl₃) of compound **192b**.

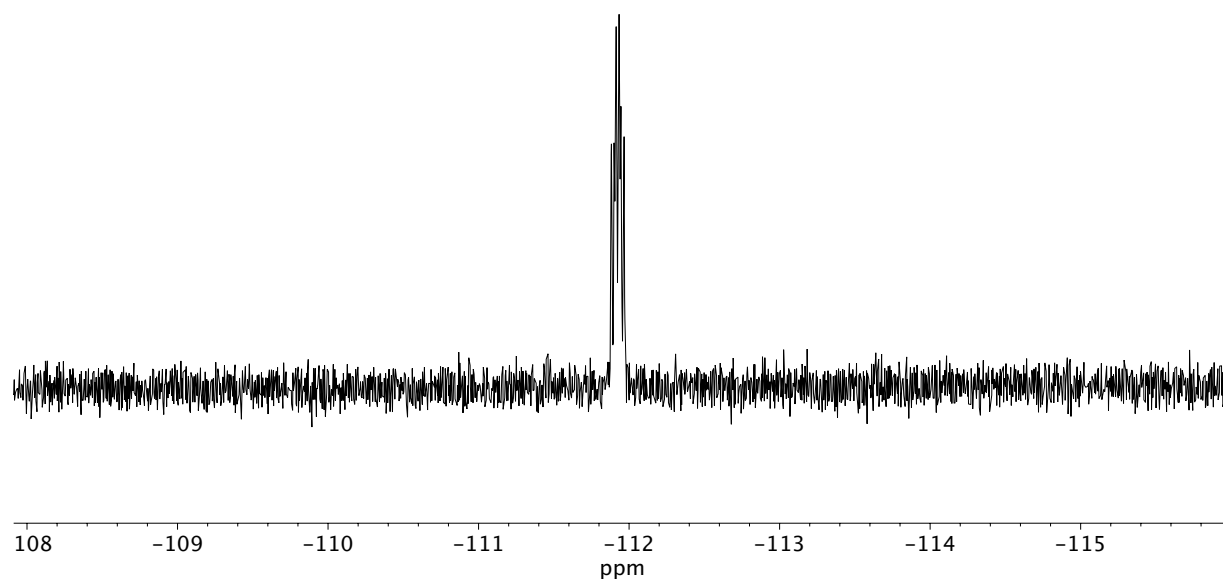


Figure A11.94 ^{19}F NMR (282 MHz, CDCl_3) of compound **192b**.

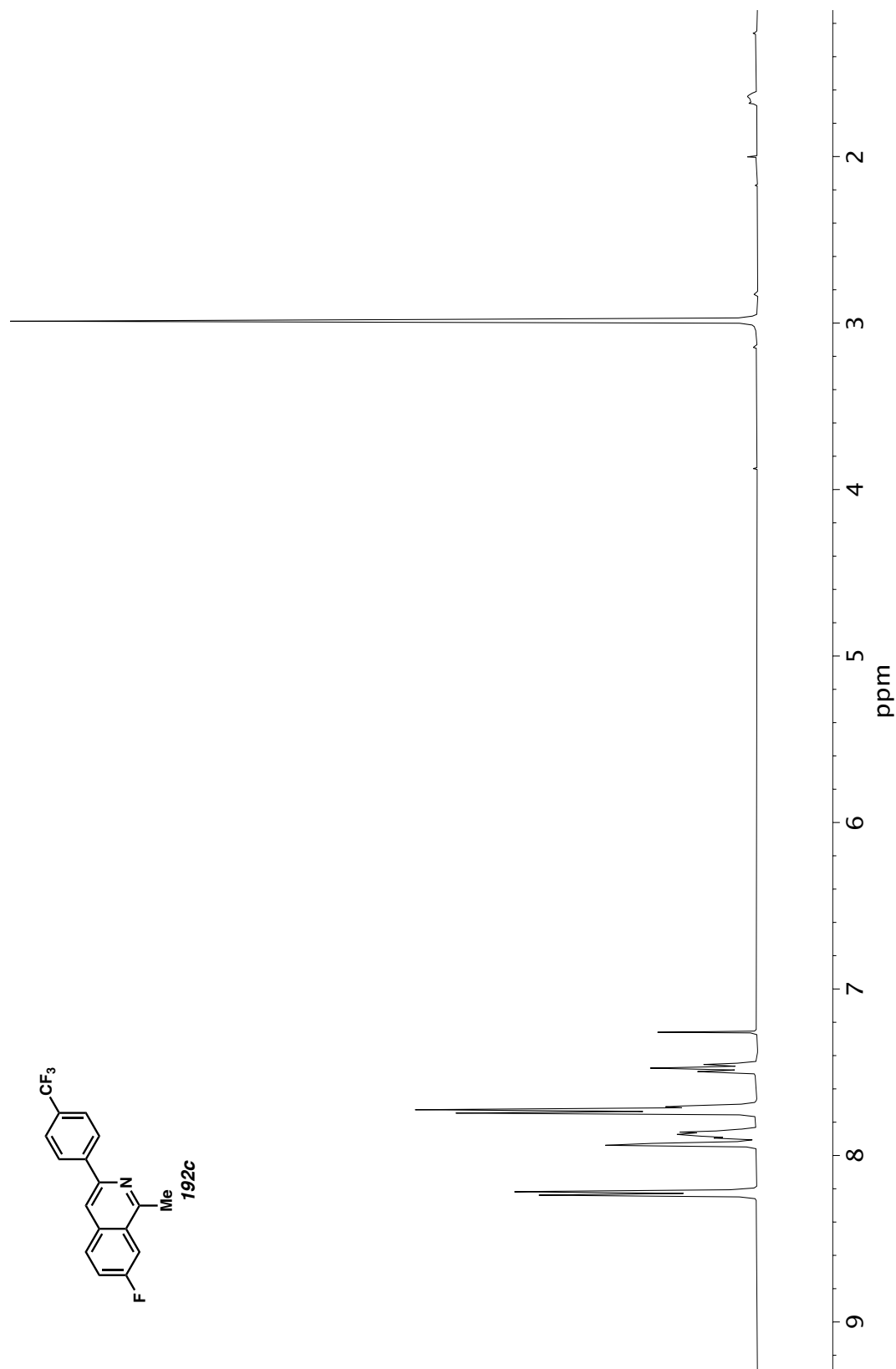


Figure A11.95 ^1H NMR (400 MHz, CDCl_3) of compound **192c**.

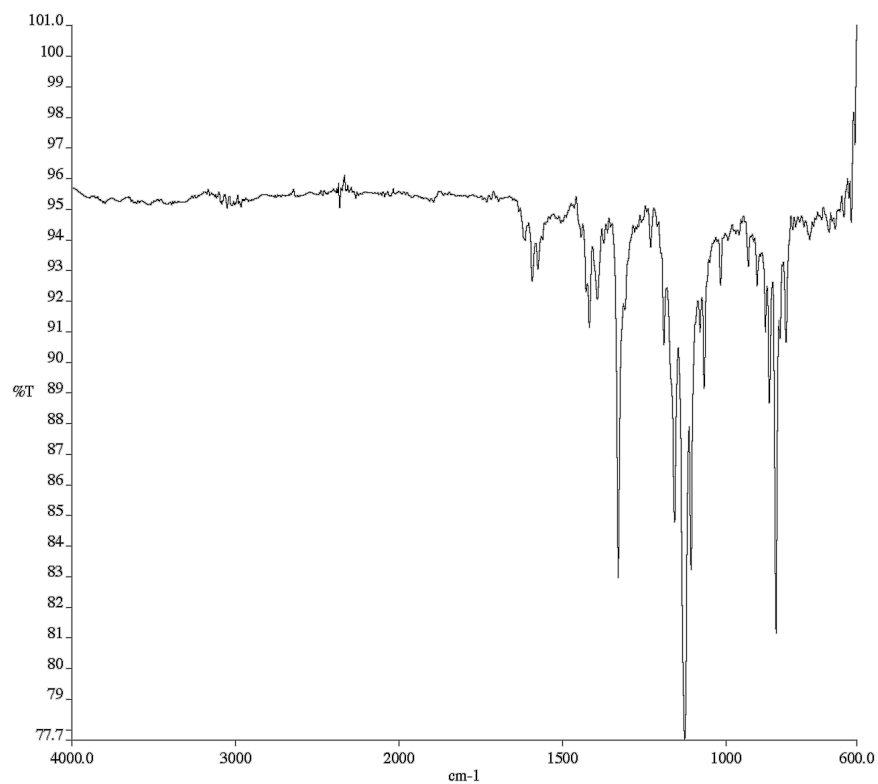


Figure A11.96 Infrared spectrum (Thin Film, NaCl) of compound **192c**.

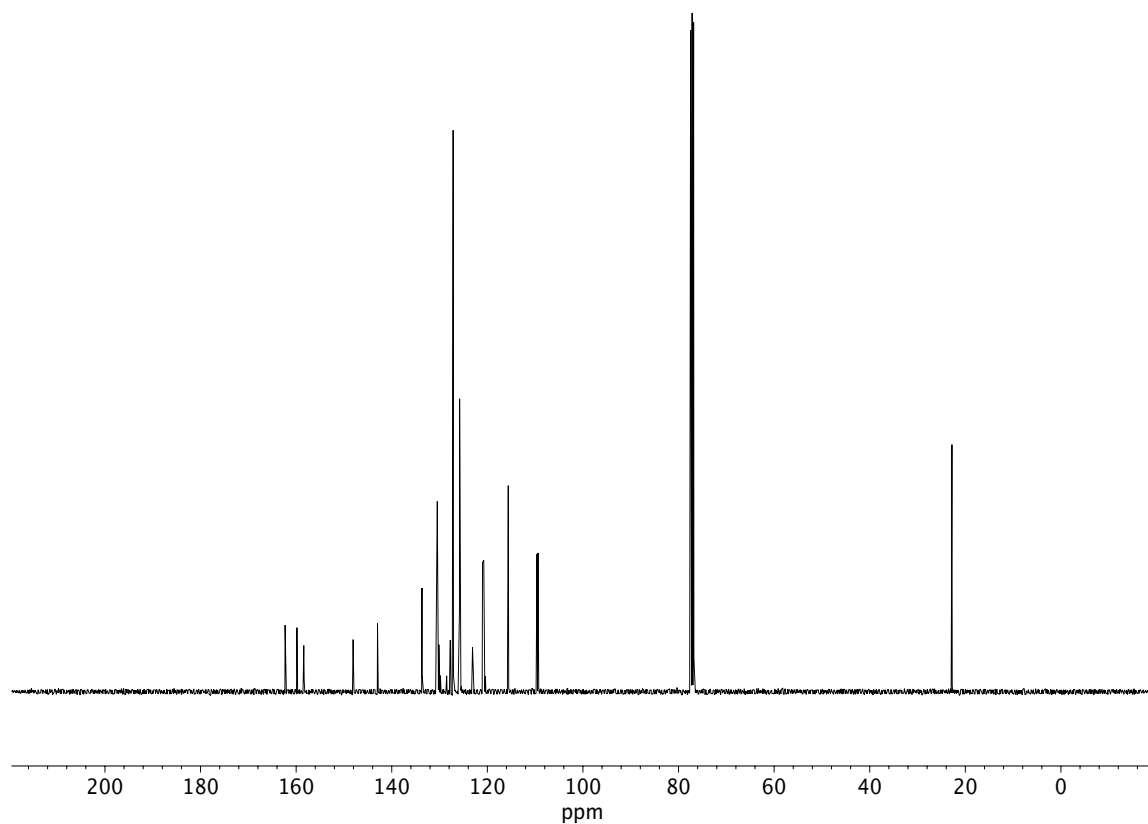


Figure A11.97 ¹³C NMR (100 MHz, CDCl₃) of compound **192c**.

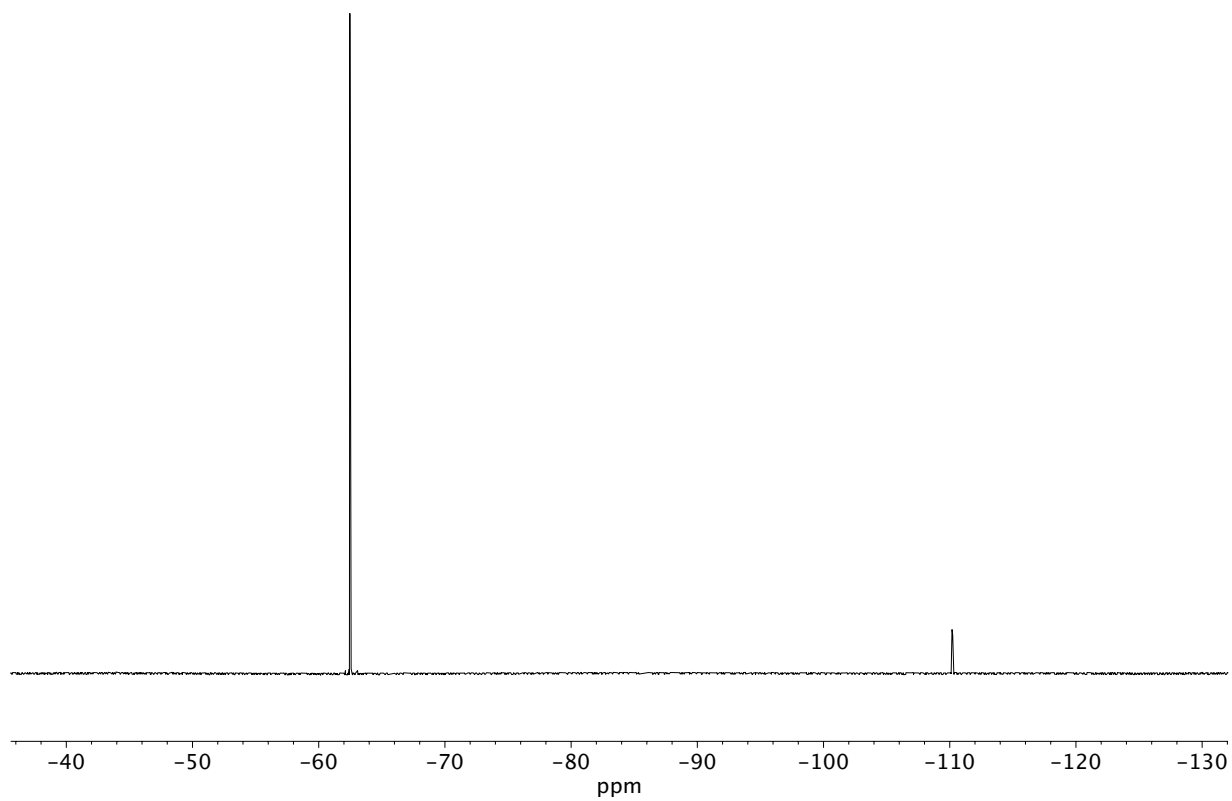


Figure A11.98 ^{19}F NMR (282 MHz, CDCl_3) of compound **192c**.

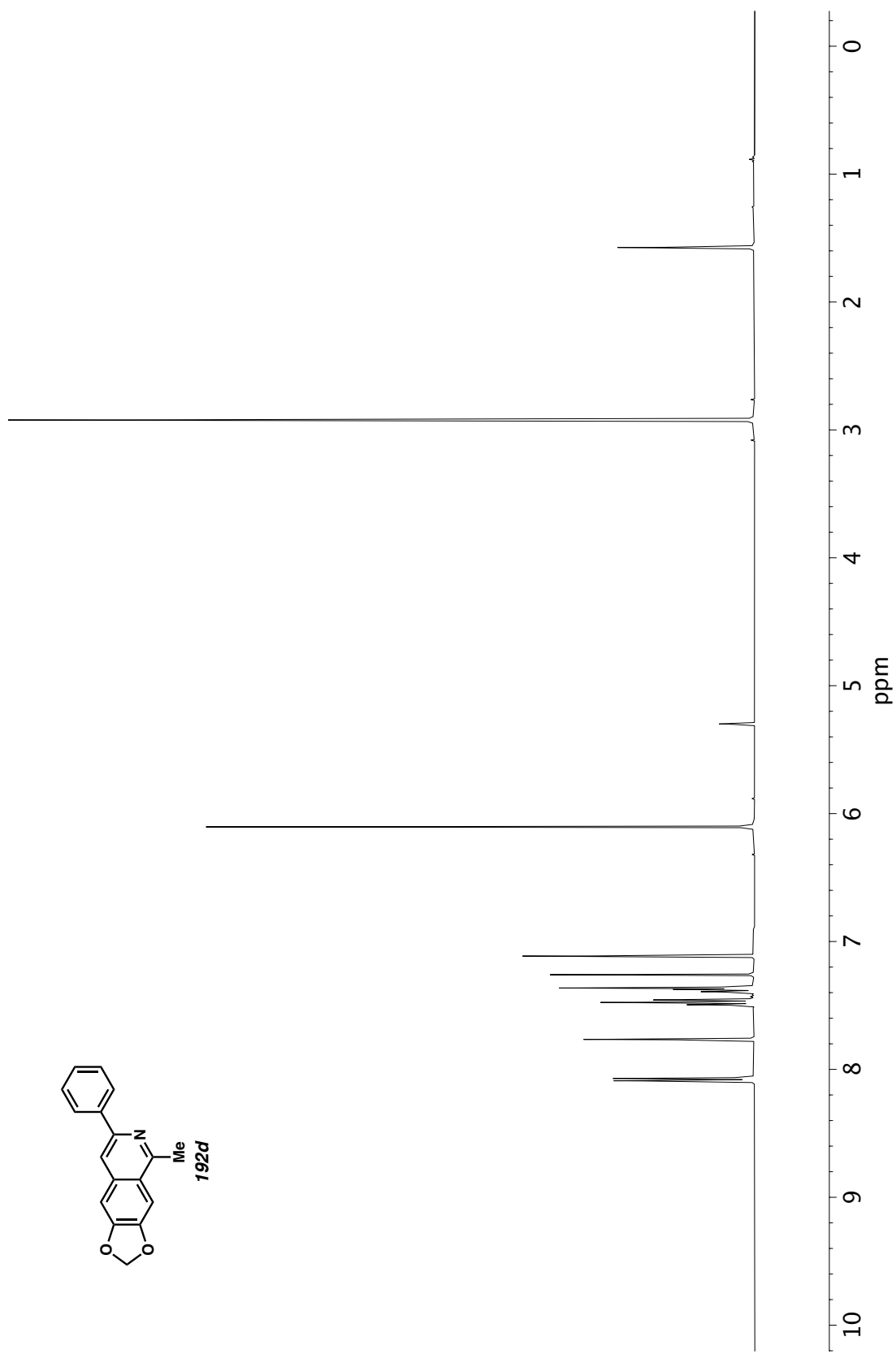


Figure A11.99 ^1H NMR (400 MHz, CDCl_3) of compound **192d**.

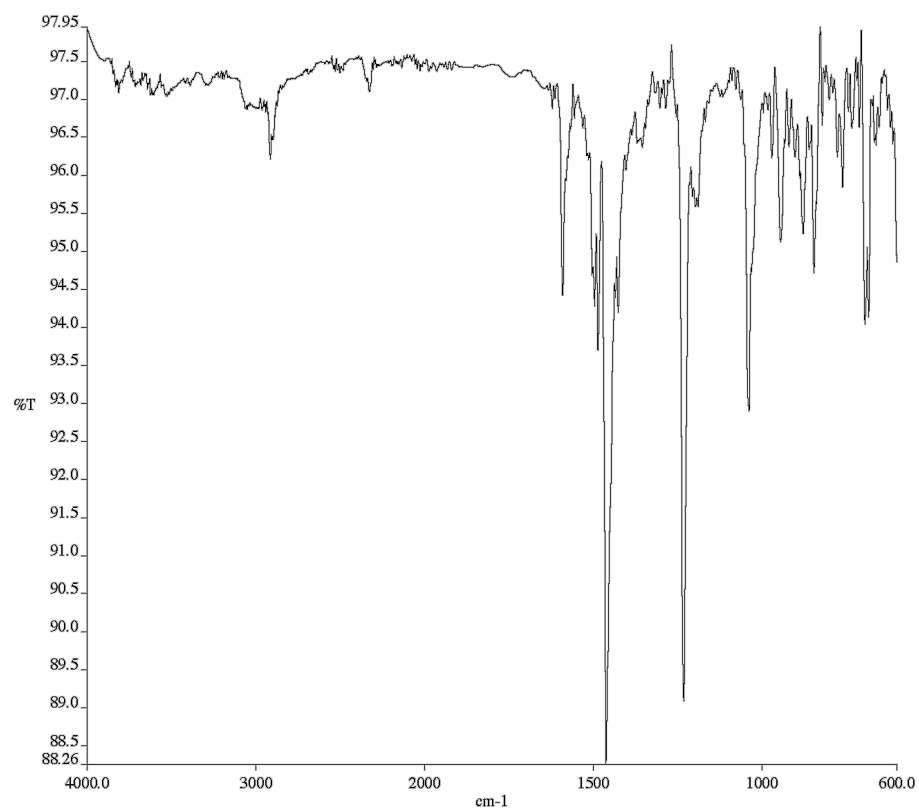


Figure A11.100 Infrared spectrum (Thin Film, NaCl) of compound

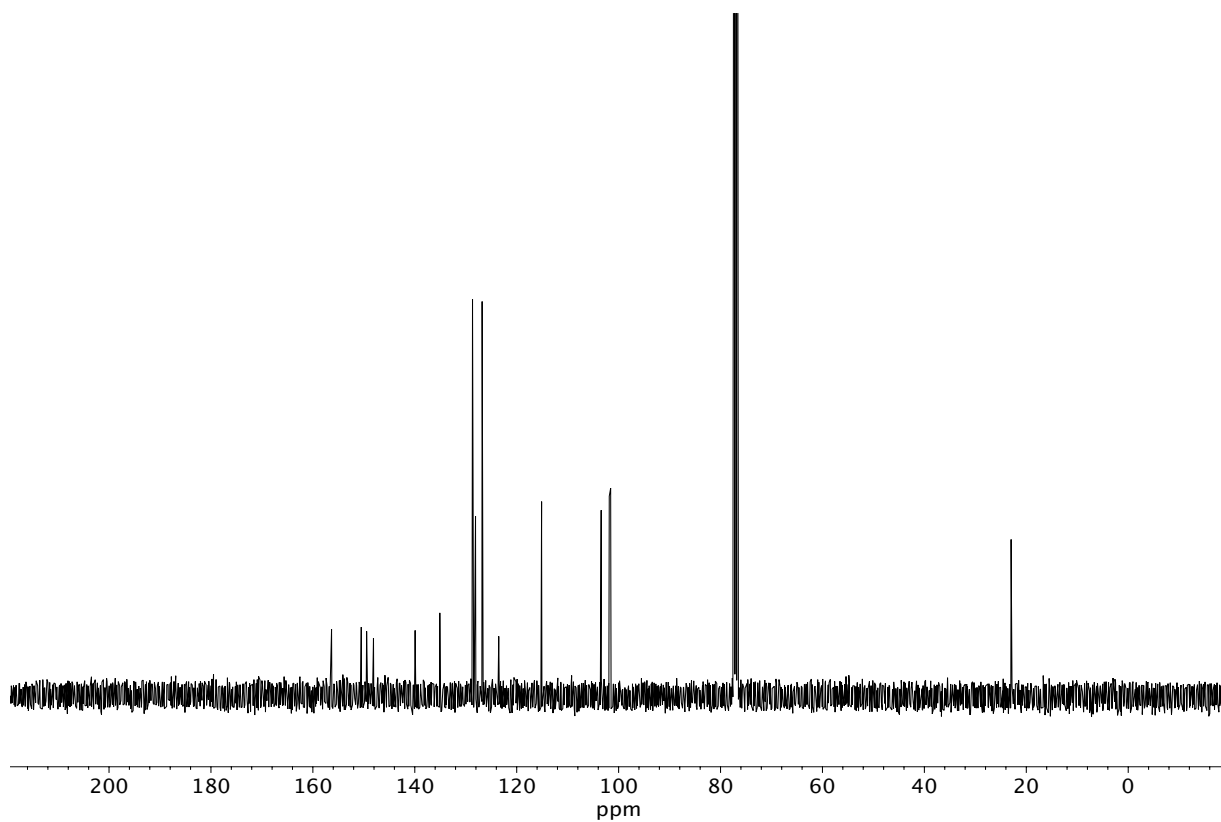


Figure A11.101 ¹³C NMR (100 MHz, CDCl₃) of compound **192d**.

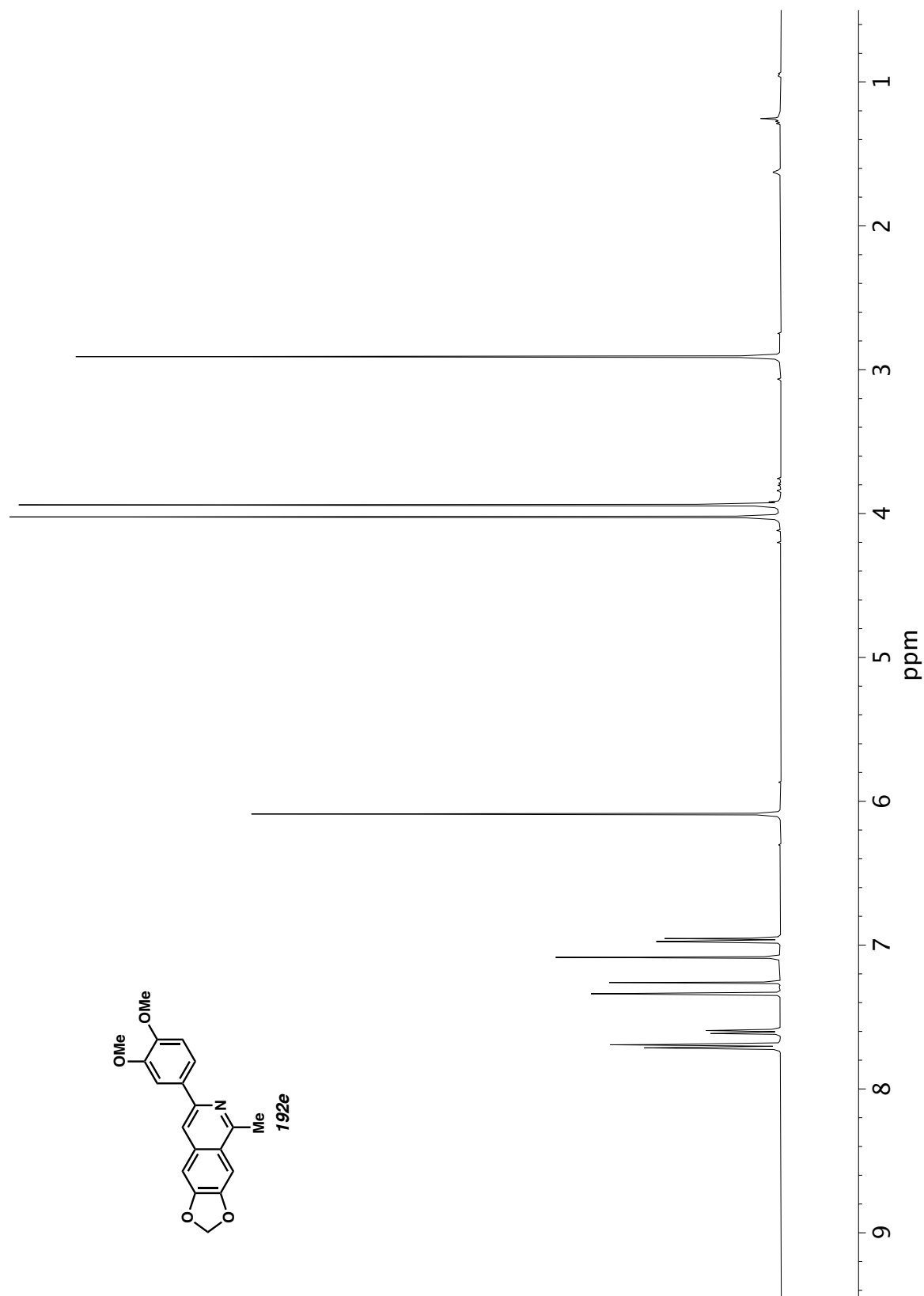


Figure A11.102 ^1H NMR (400 MHz, CDCl_3) of compound **192e**.

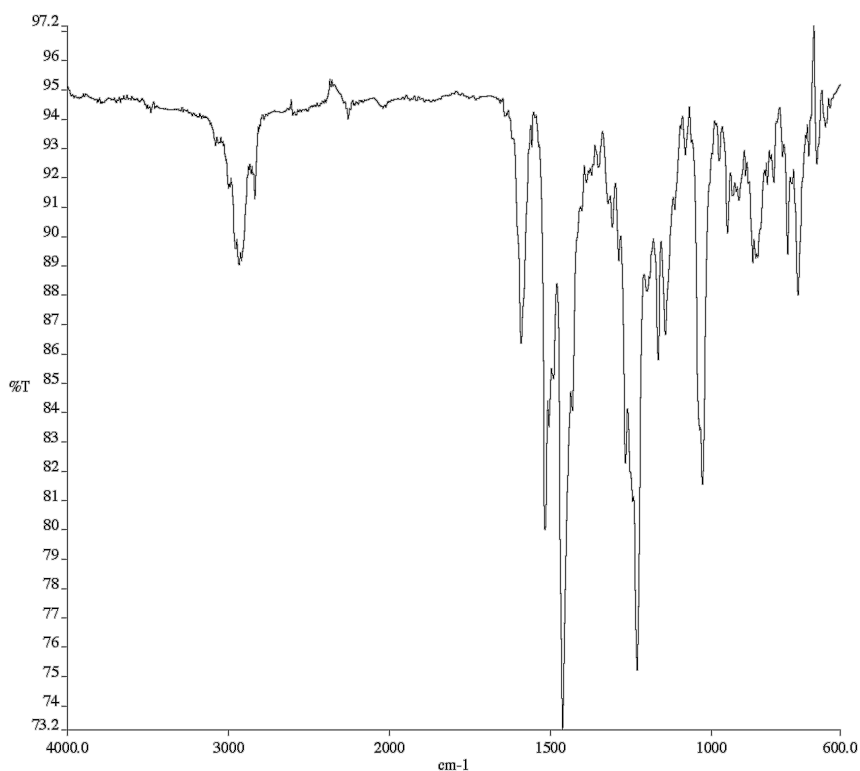


Figure A11.103 Infrared spectrum (Thin Film, NaCl) of compound

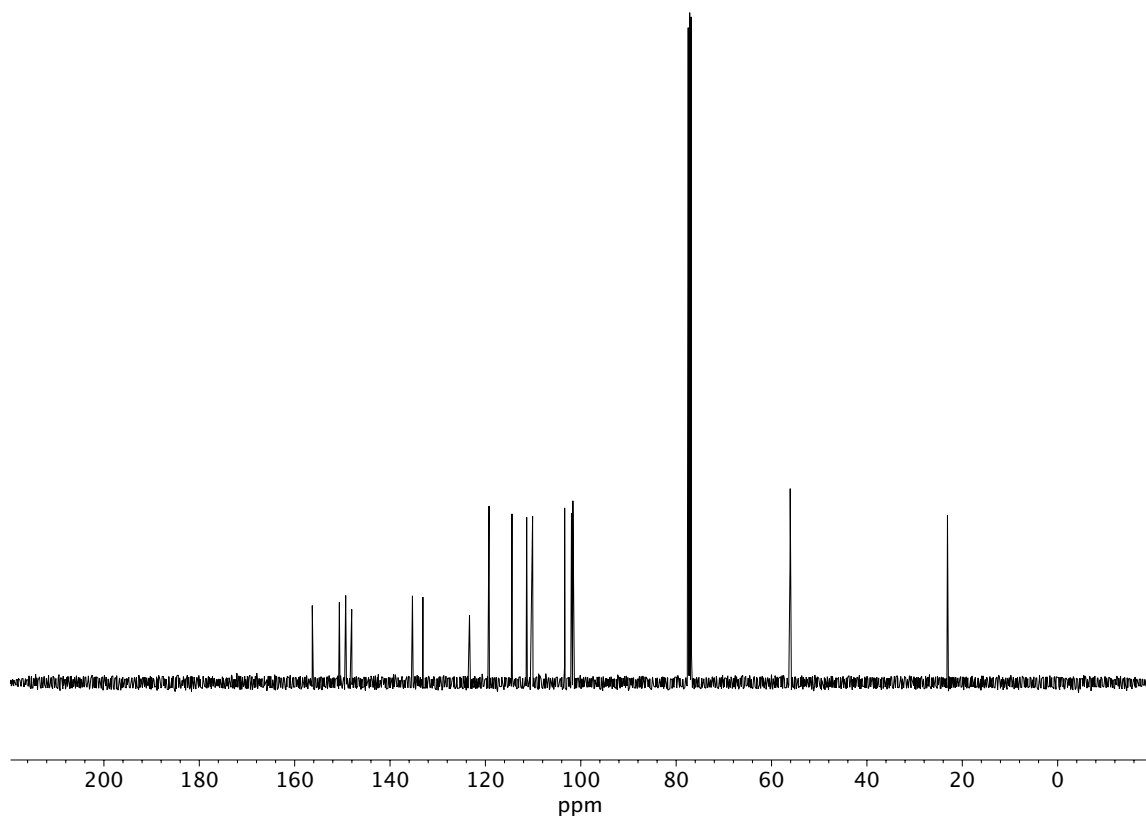


Figure A11.104 ¹³C NMR (100 MHz, CDCl₃) of compound **192e**.

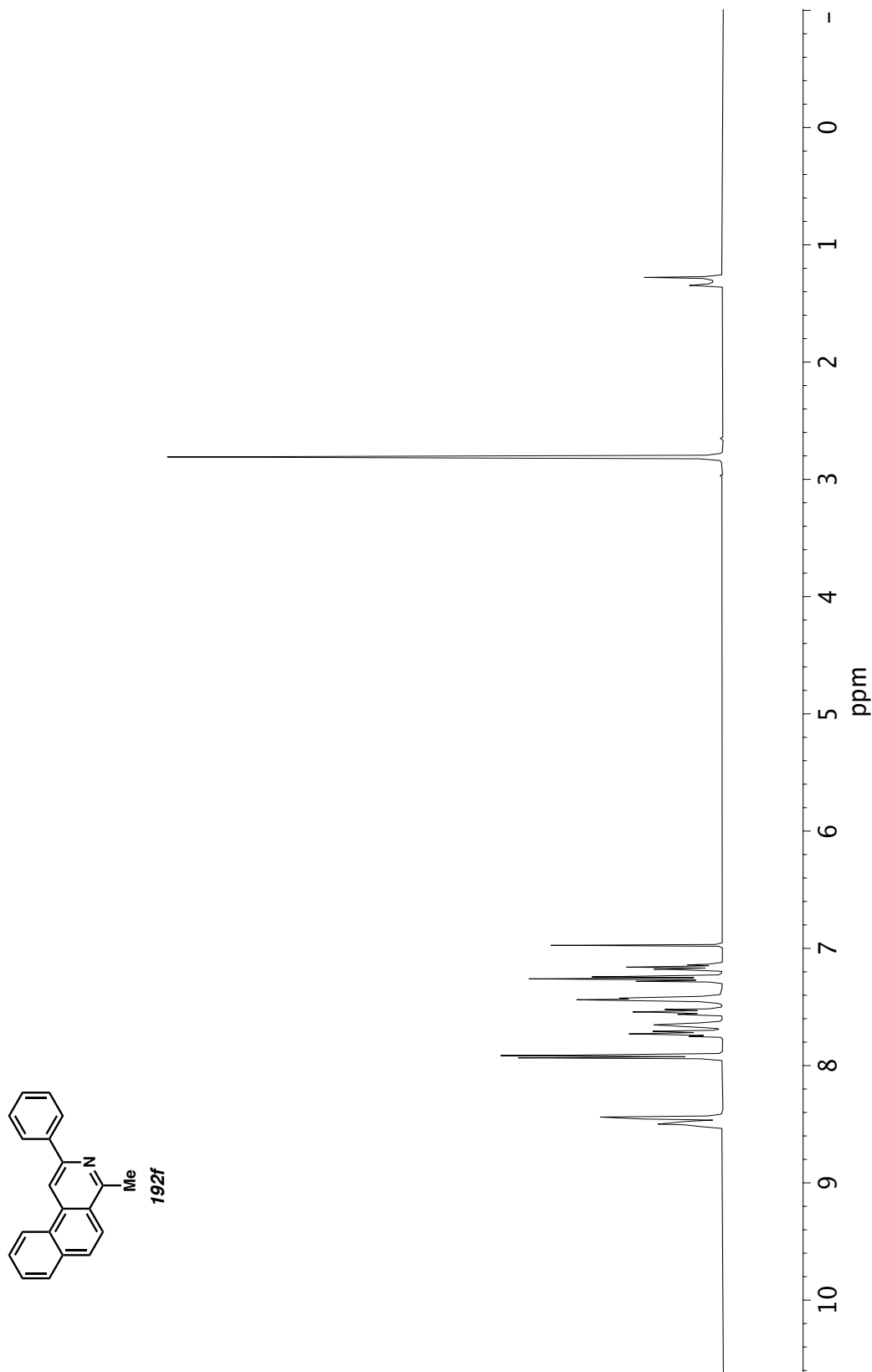


Figure A11.105 ^1H NMR (400 MHz, CDCl_3) of compound **192f**.

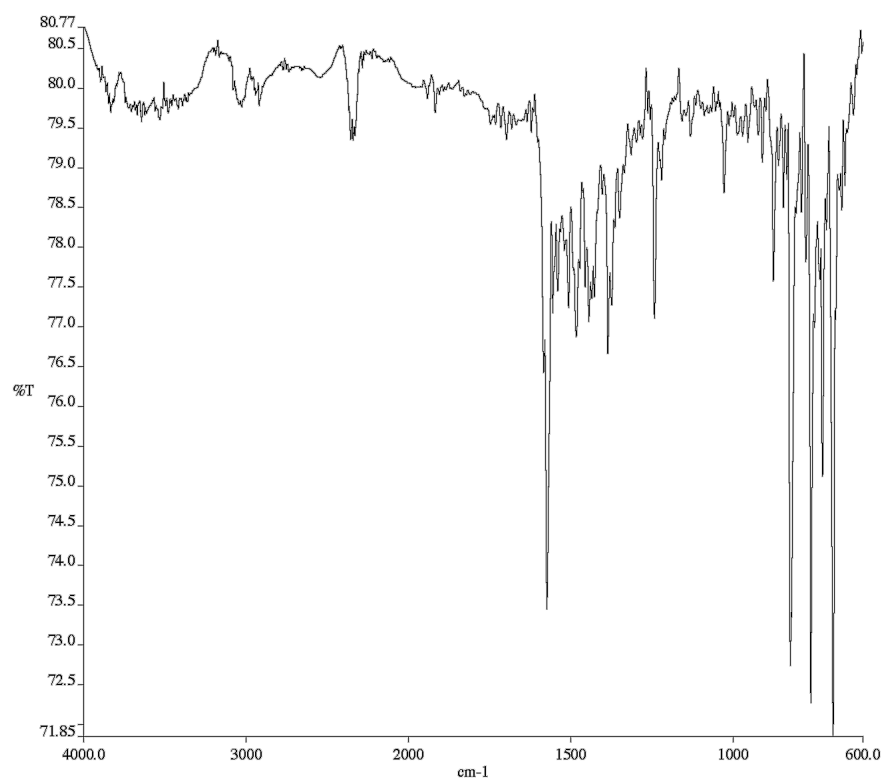


Figure A11.106 Infrared spectrum (Thin Film, NaCl) of compound

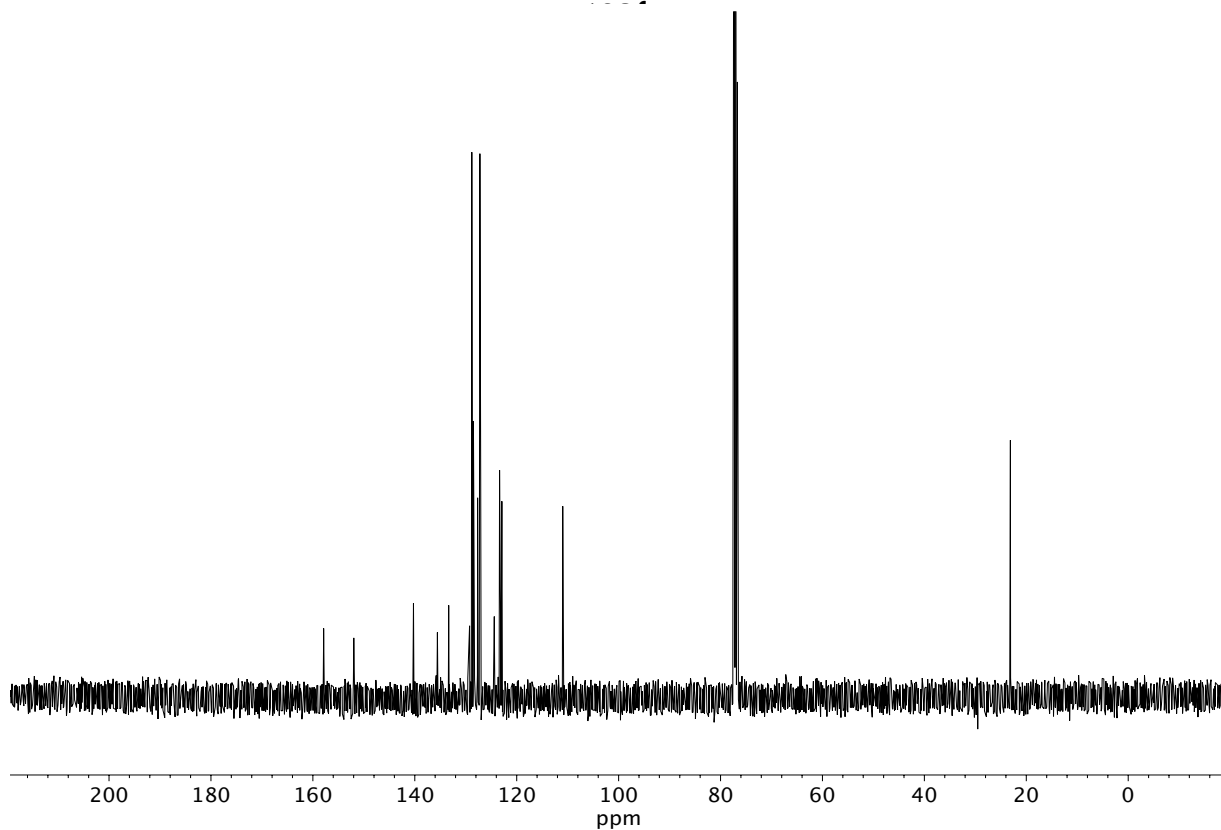


Figure A11.107 ¹³C NMR (100 MHz, CDCl₃) of compound **192f**.

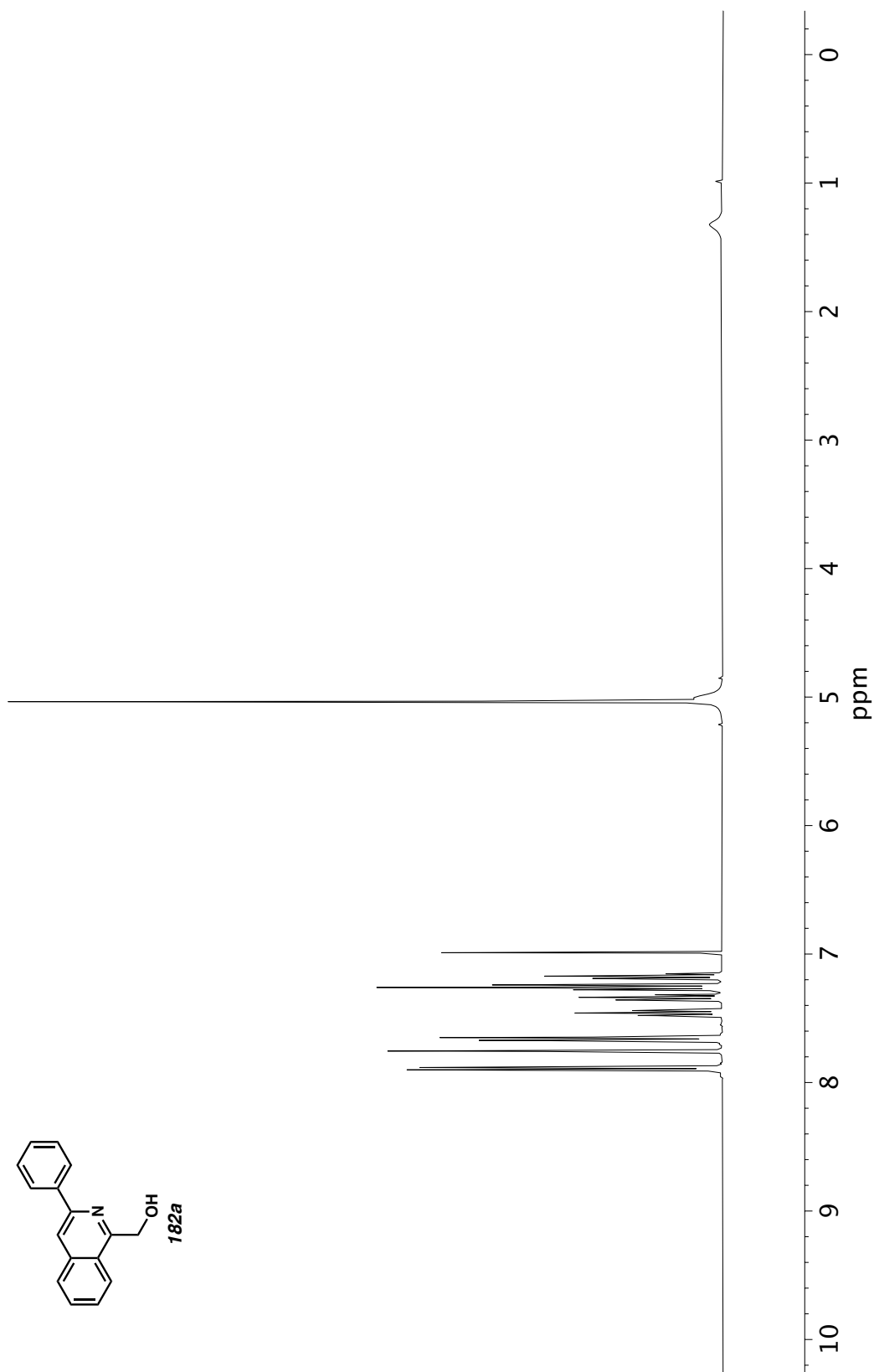


Figure A11.108 ¹H NMR (400 MHz, CDCl₃) of compound **182a**.

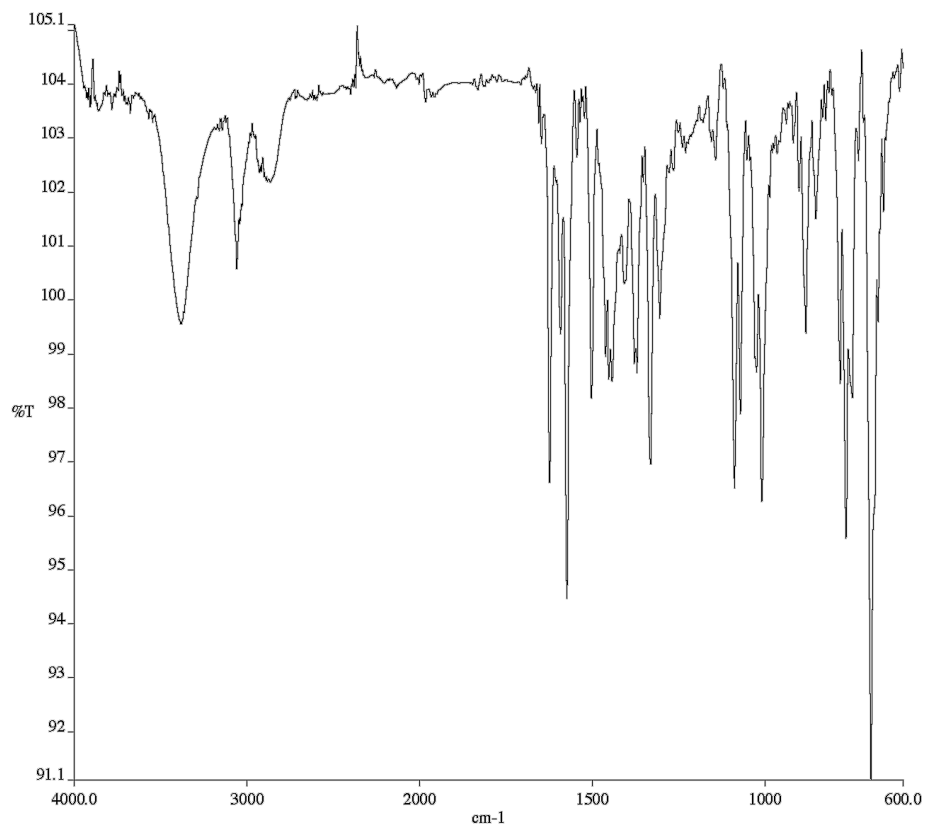


Figure A11.109 Infrared spectrum (Thin Film, NaCl) of compound

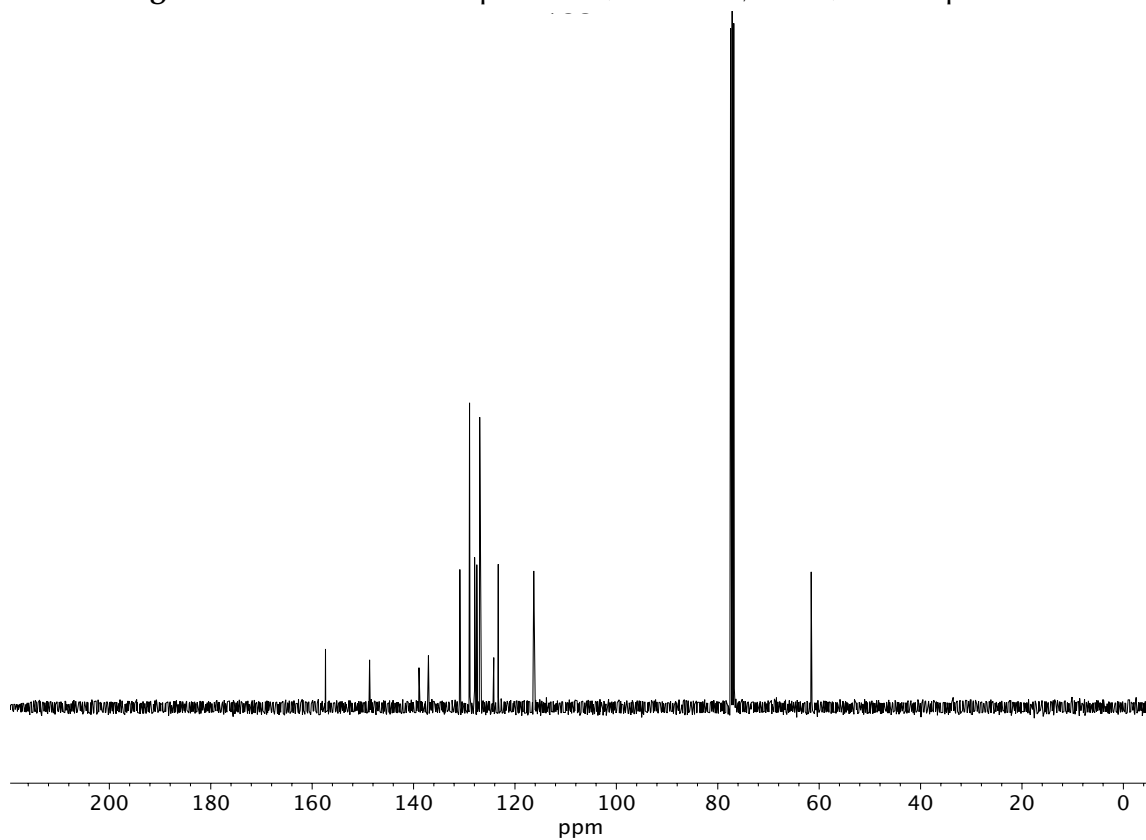


Figure A11.110 ¹³C NMR (100 MHz, CDCl₃) of compound **182a**.

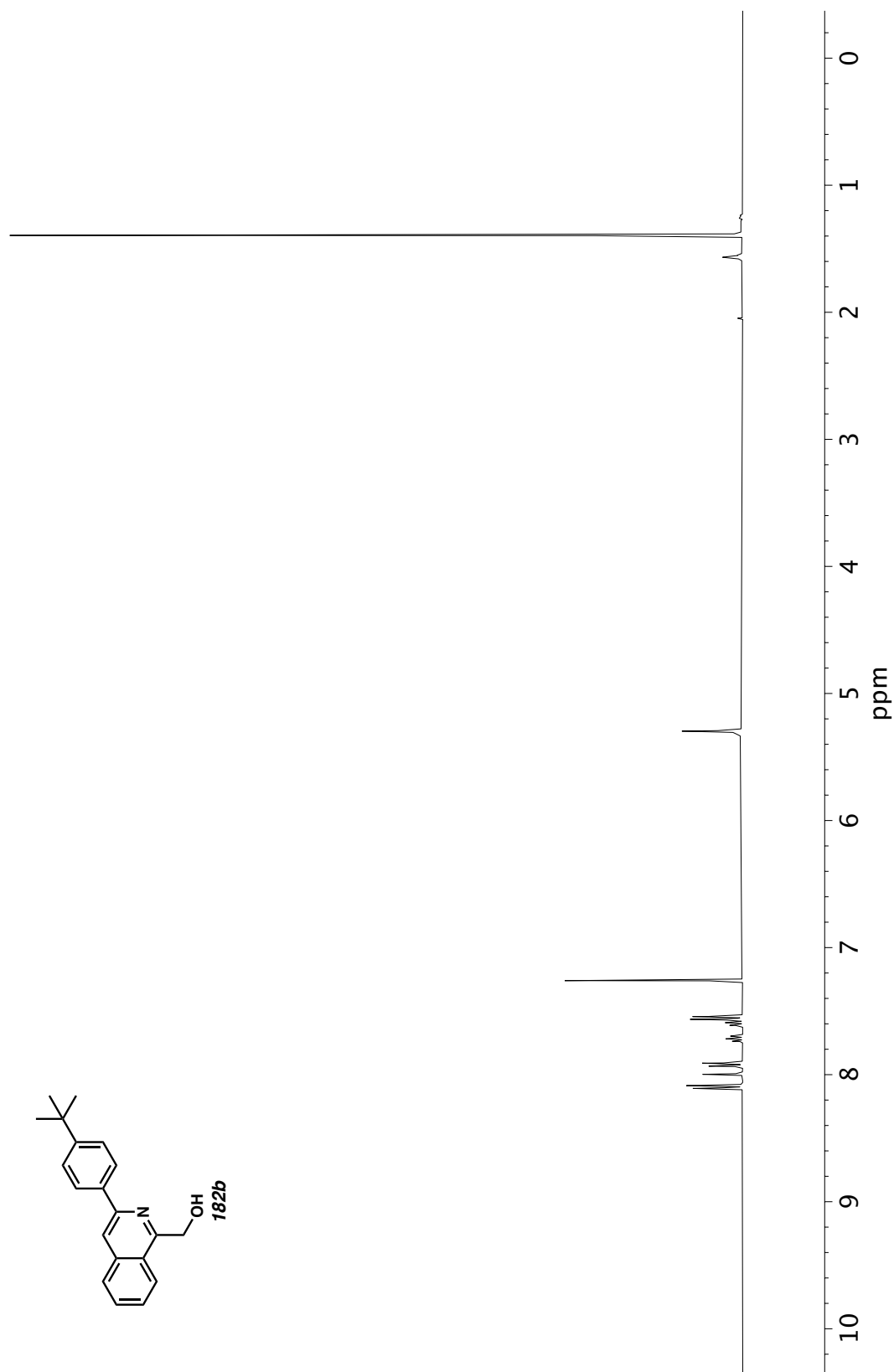


Figure A11.111 ¹H NMR (400 MHz, CDCl₃) of compound **182b**.

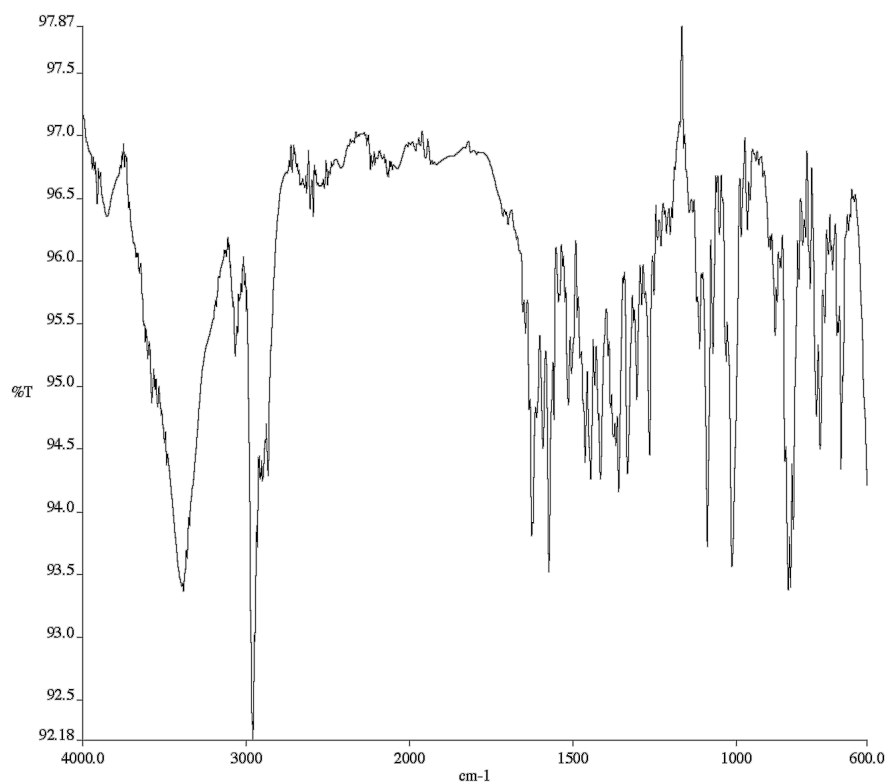


Figure A11.112 Infrared spectrum (Thin Film, NaCl) of compound

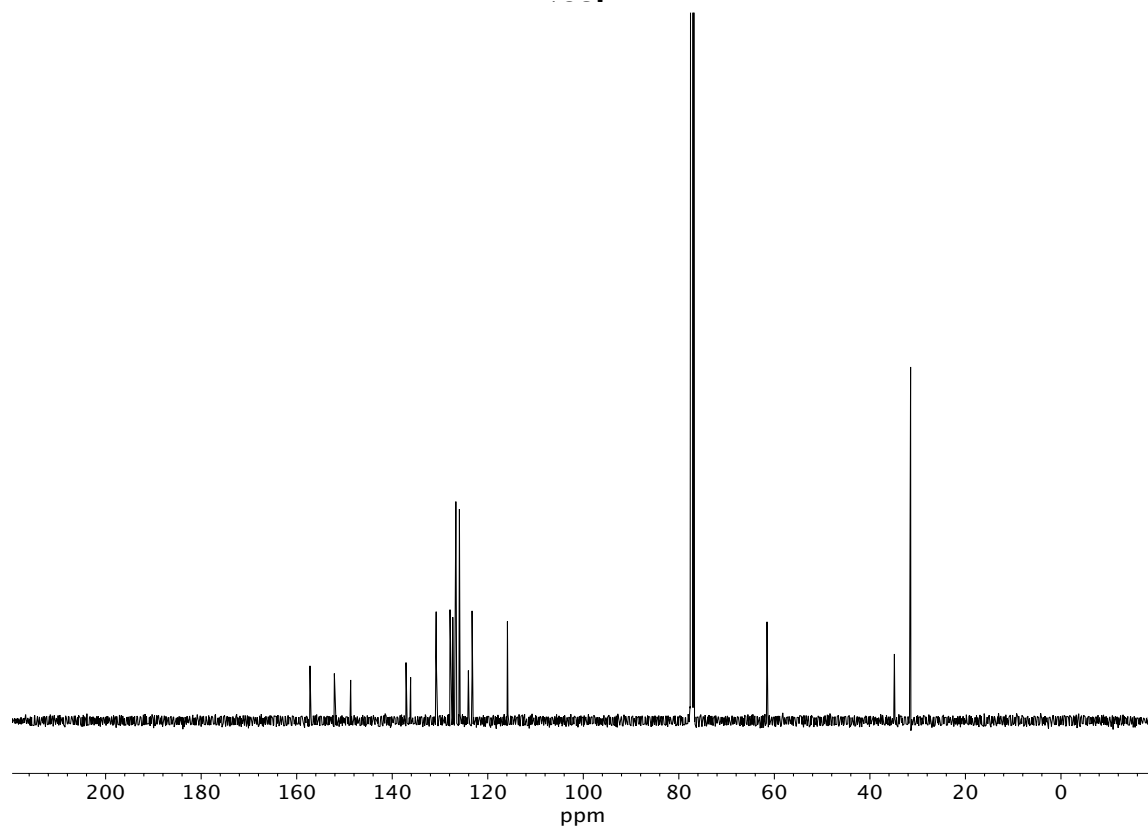


Figure A11.113 ¹³C NMR (100 MHz, CDCl₃) of compound **182b**.

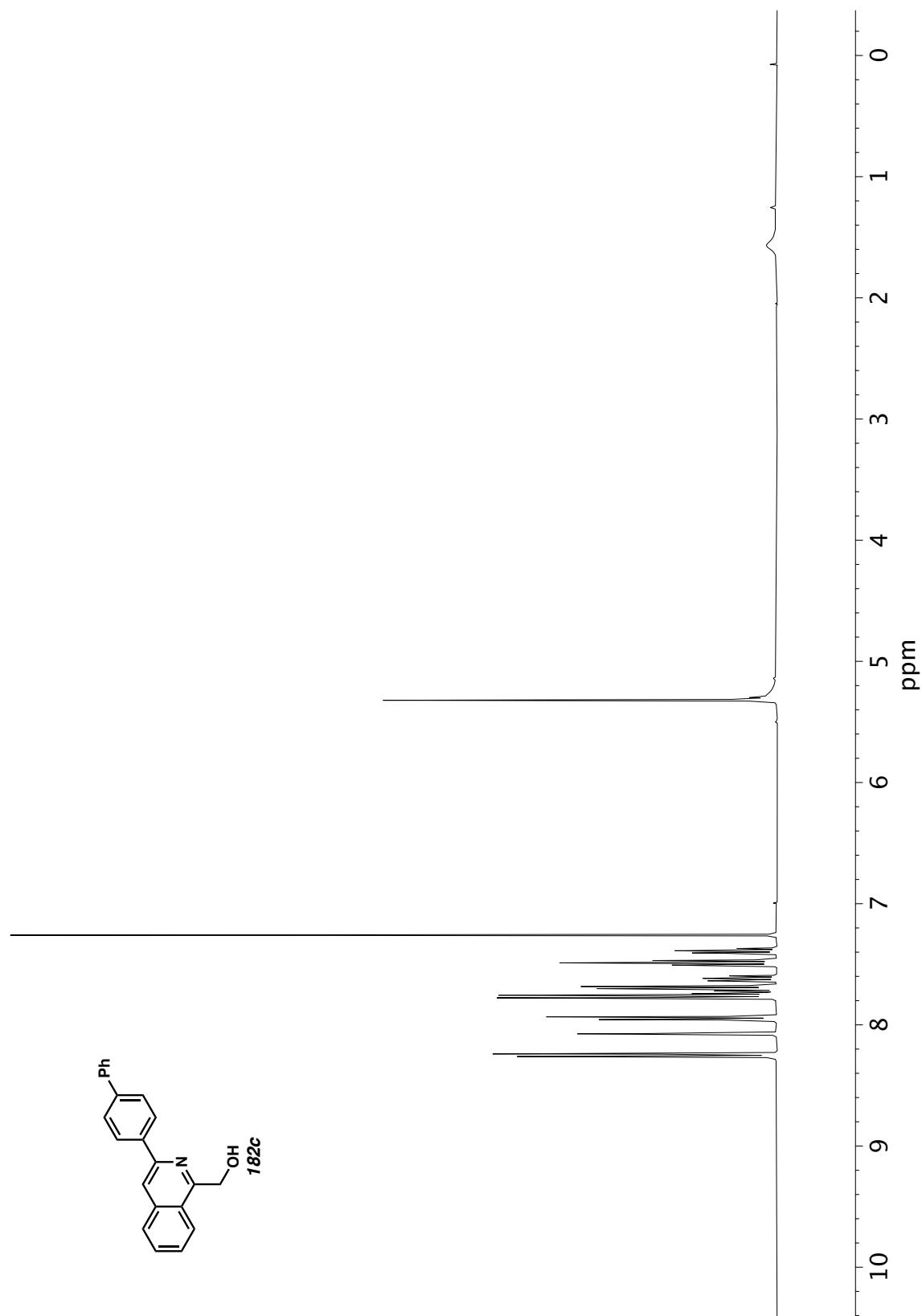


Figure A11.114 ^1H NMR (400 MHz, CDCl_3) of compound **182c**.

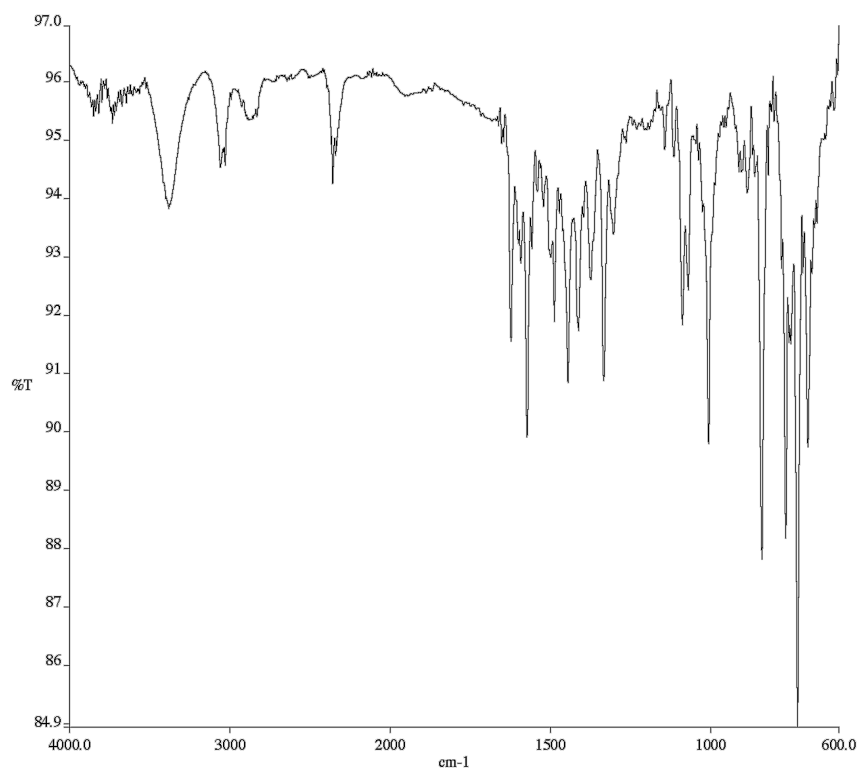


Figure A11.115 Infrared spectrum (Thin Film, NaCl) of compound

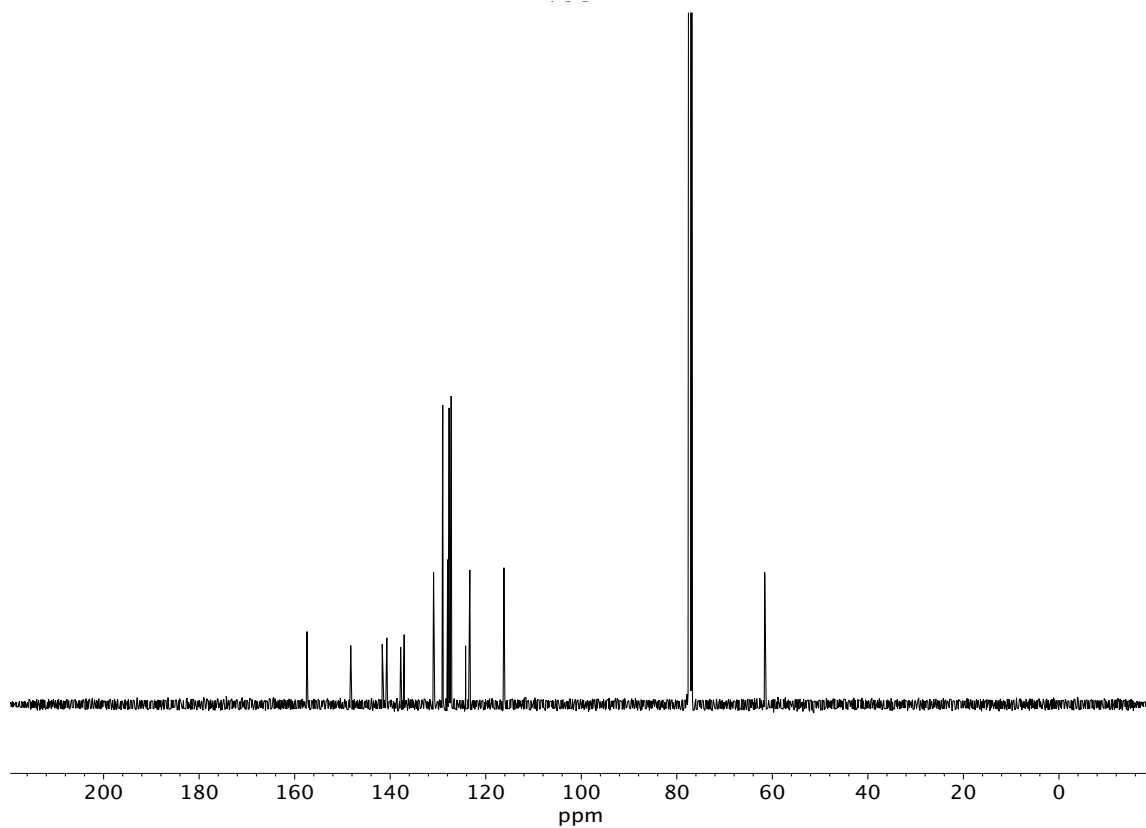


Figure A11.116 ¹³C NMR (100 MHz, CDCl₃) of compound **182c**.

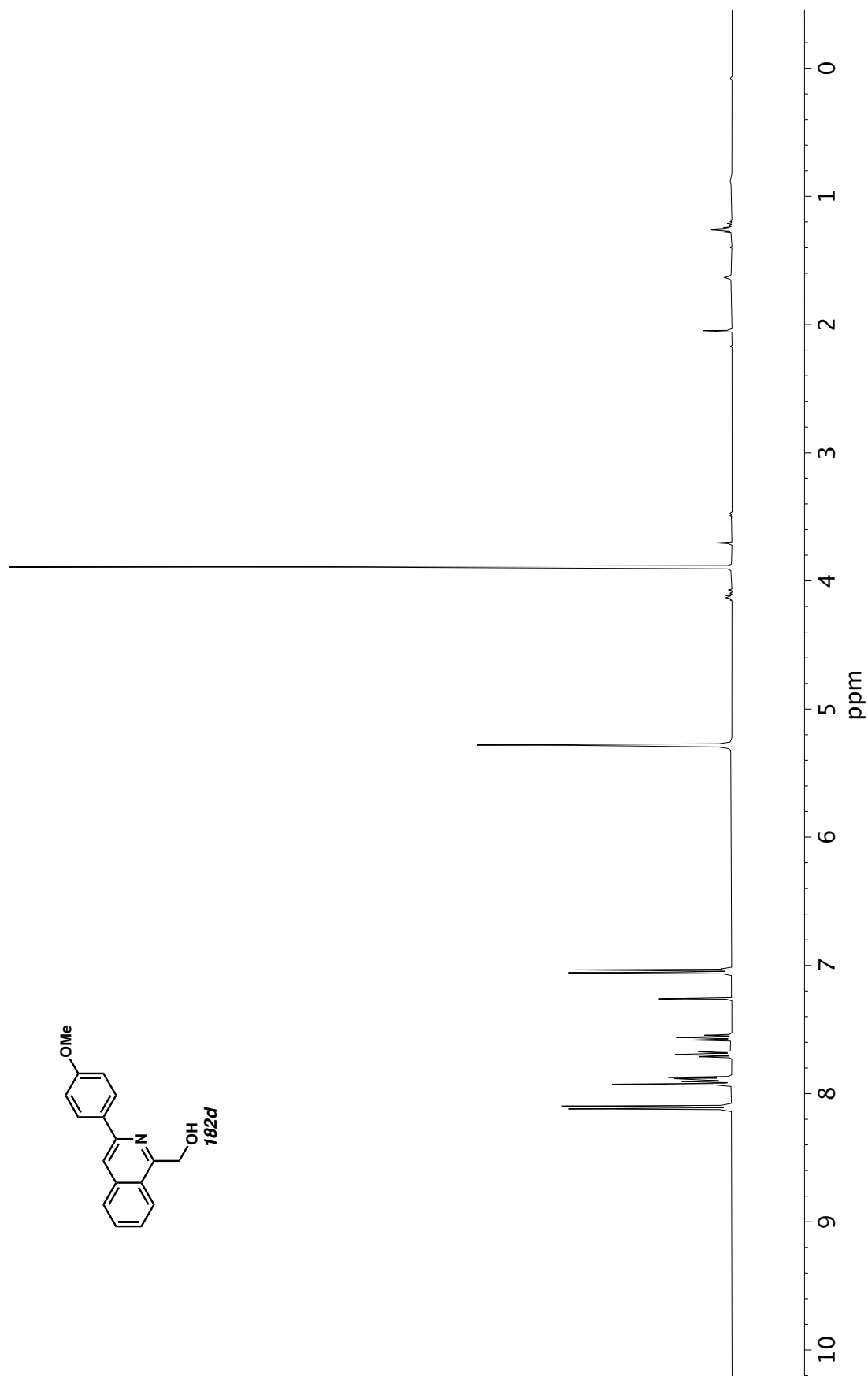


Figure A11.117 ¹H NMR (400 MHz, CDCl₃) of compound **182d**.

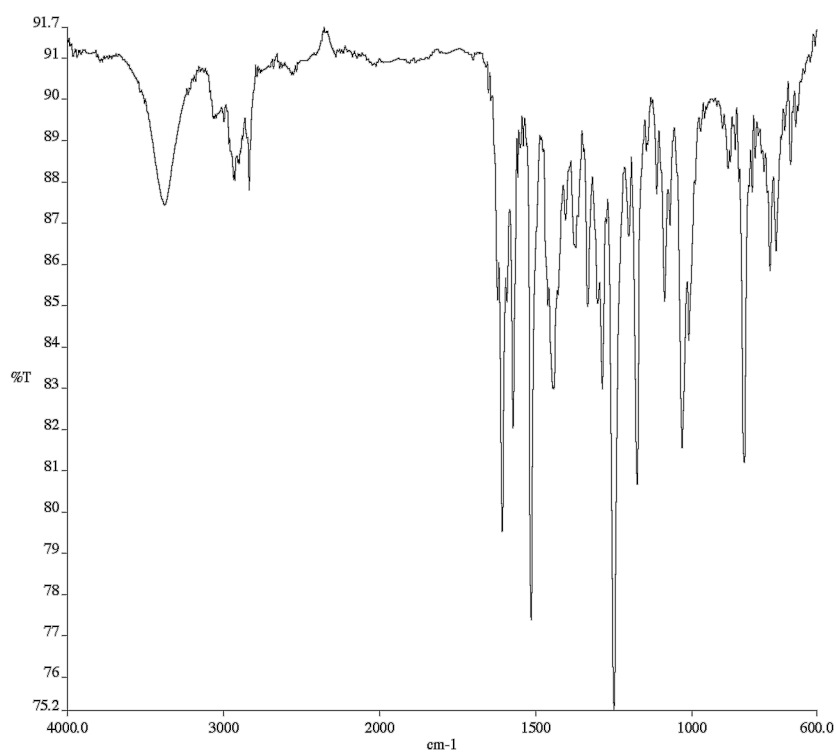


Figure A11.118 Infrared spectrum (Thin Film, NaCl) of compound

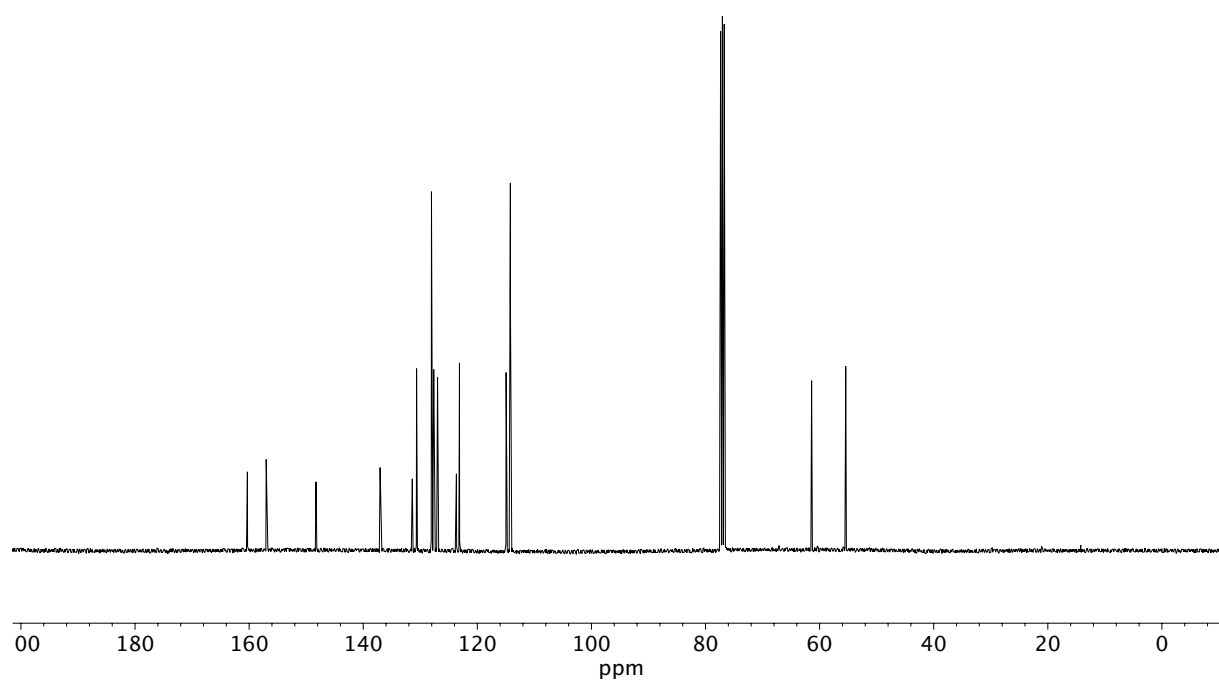


Figure A11.119 ¹³C NMR (100 MHz, CDCl₃) of compound **182d**.

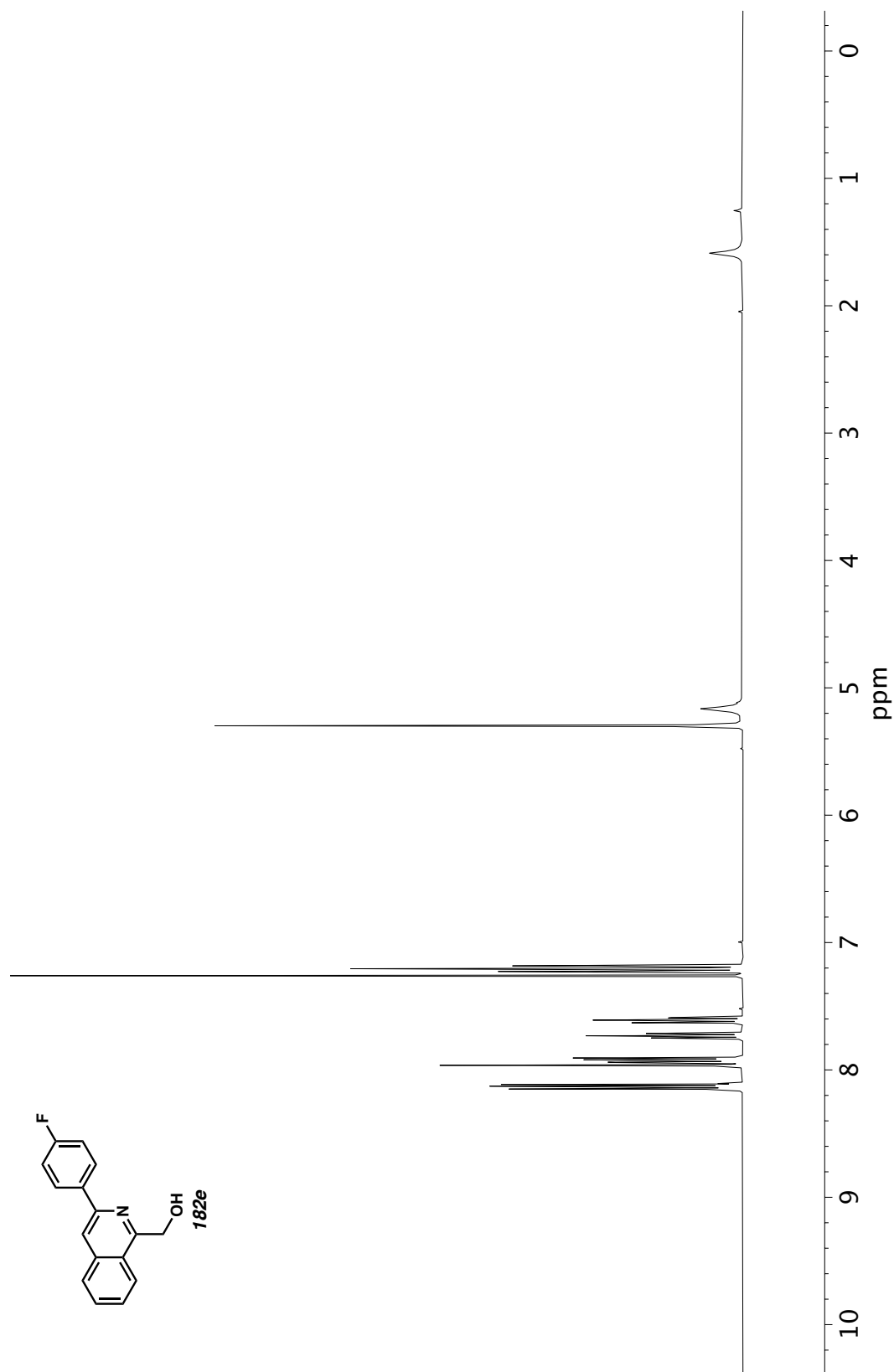


Figure A11.120 ¹H NMR (400 MHz, CDCl₃) of compound **182e**.

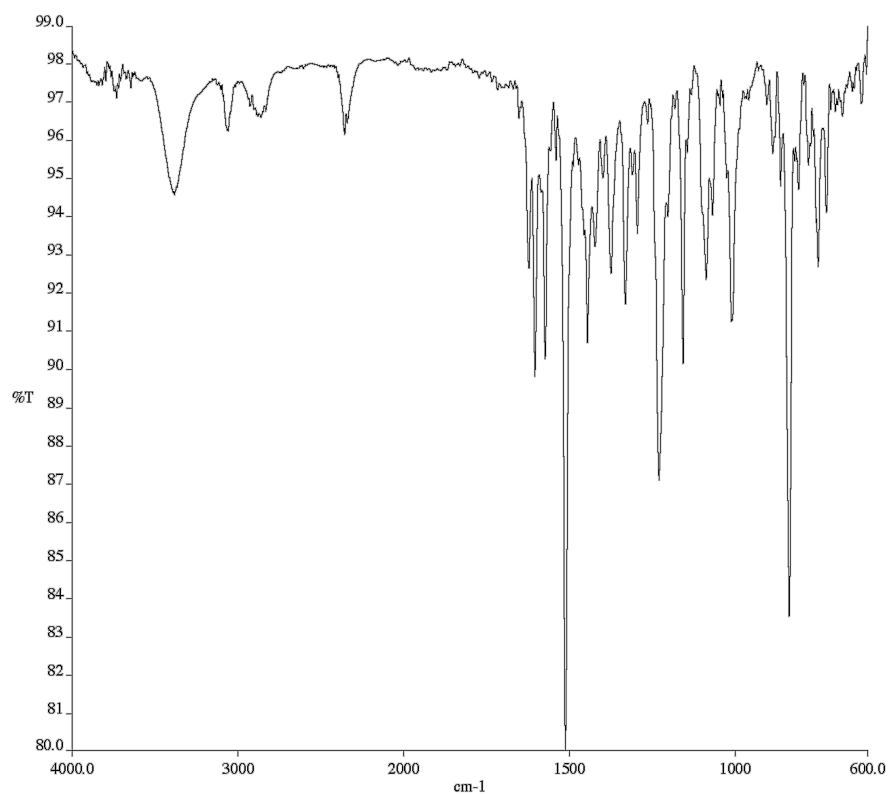


Figure A11.121 Infrared spectrum (Thin Film, NaCl) of compound

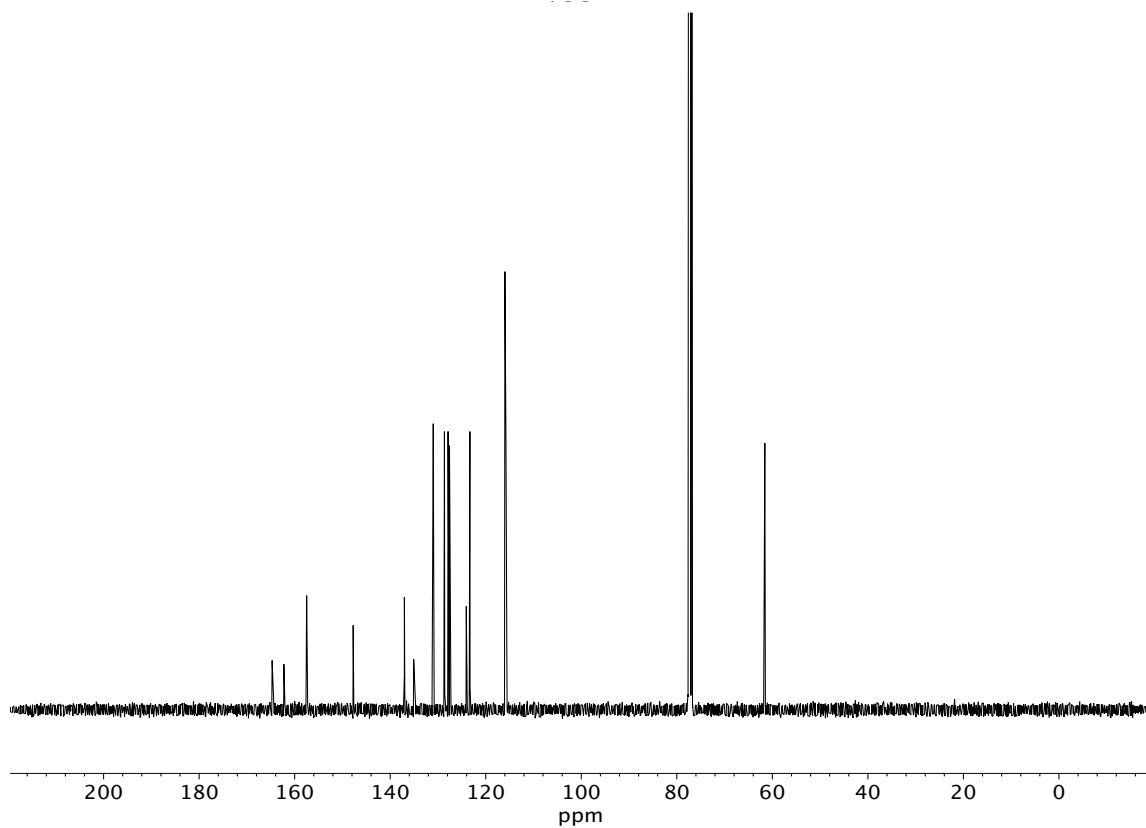


Figure A11.122 ¹³C NMR (100 MHz, CDCl₃) of compound **182e**.

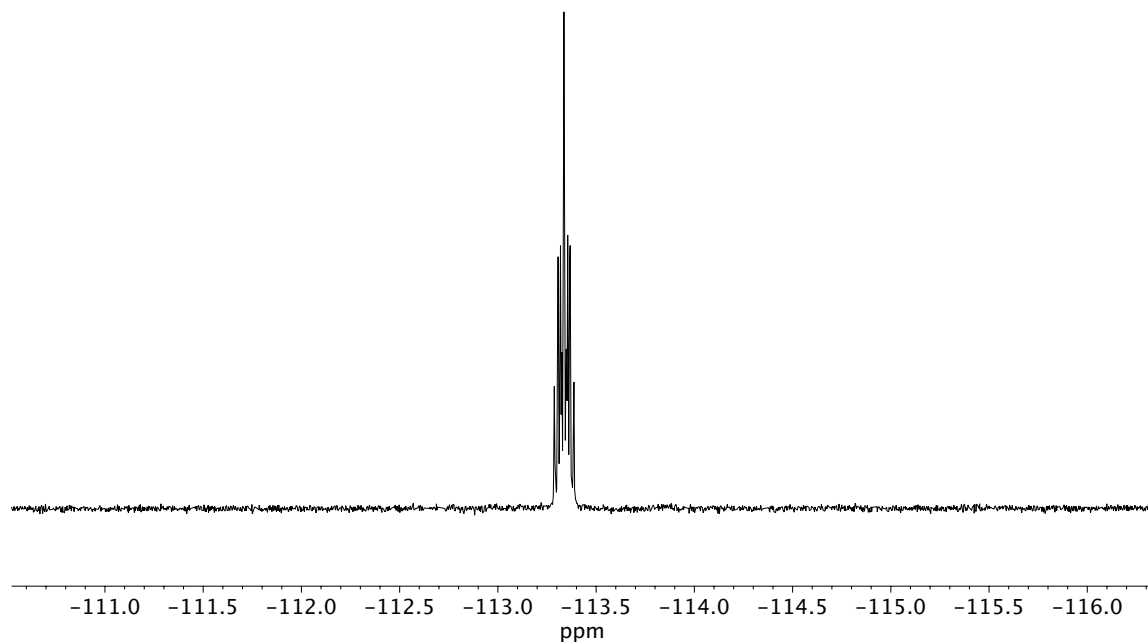


Figure A11.123 ^{19}F NMR (282 MHz, CDCl_3) of compound **182e**.

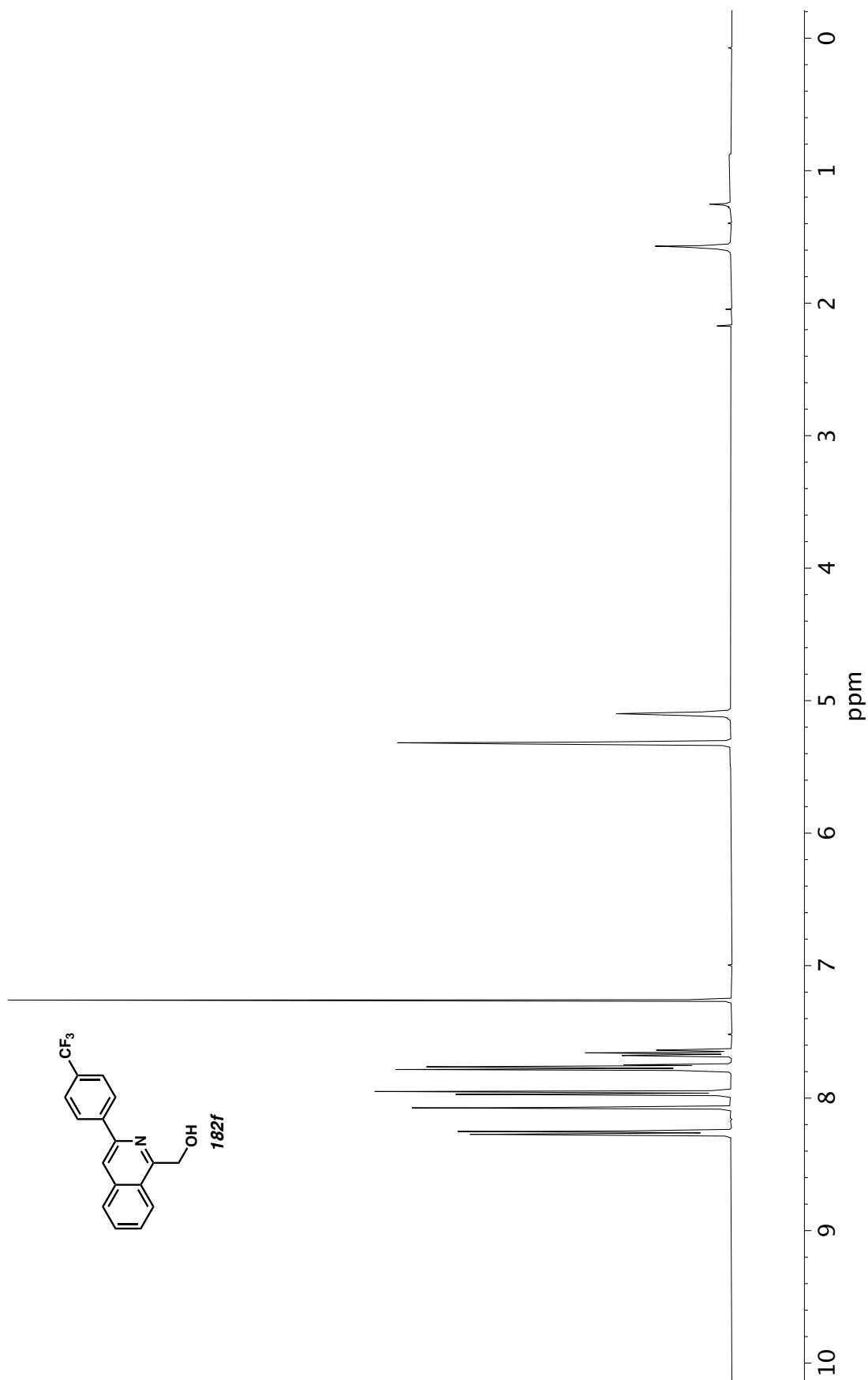


Figure A11.124 ^1H NMR (400 MHz, CDCl_3) of compound **182f**.

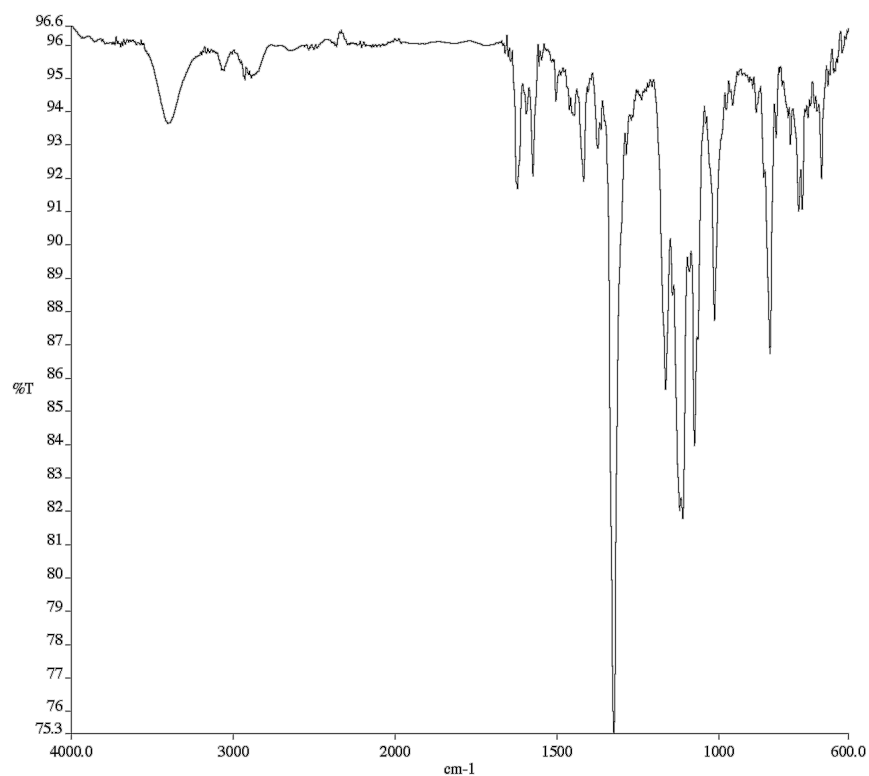


Figure A11.125 Infrared spectrum (Thin Film, NaCl) of compound

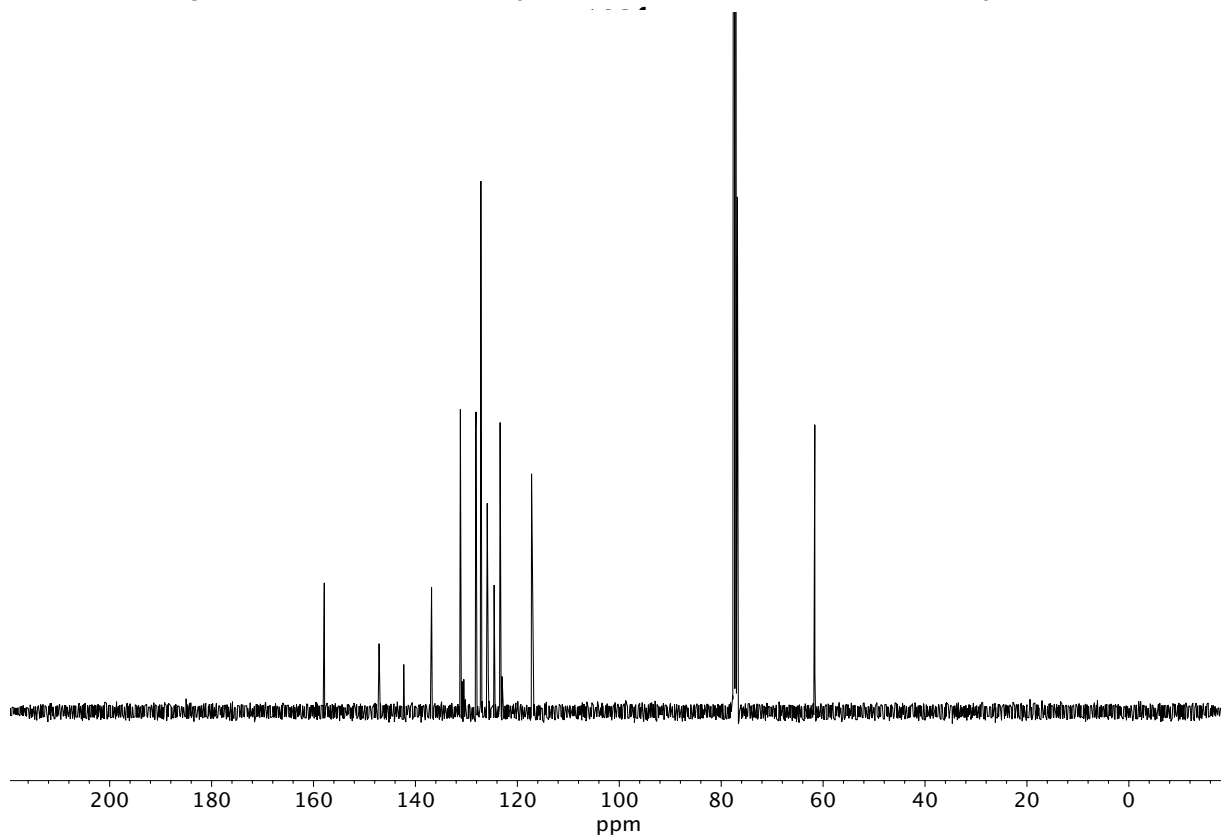


Figure A11.126 ¹³C NMR (100 MHz, CDCl₃) of compound **182f**.

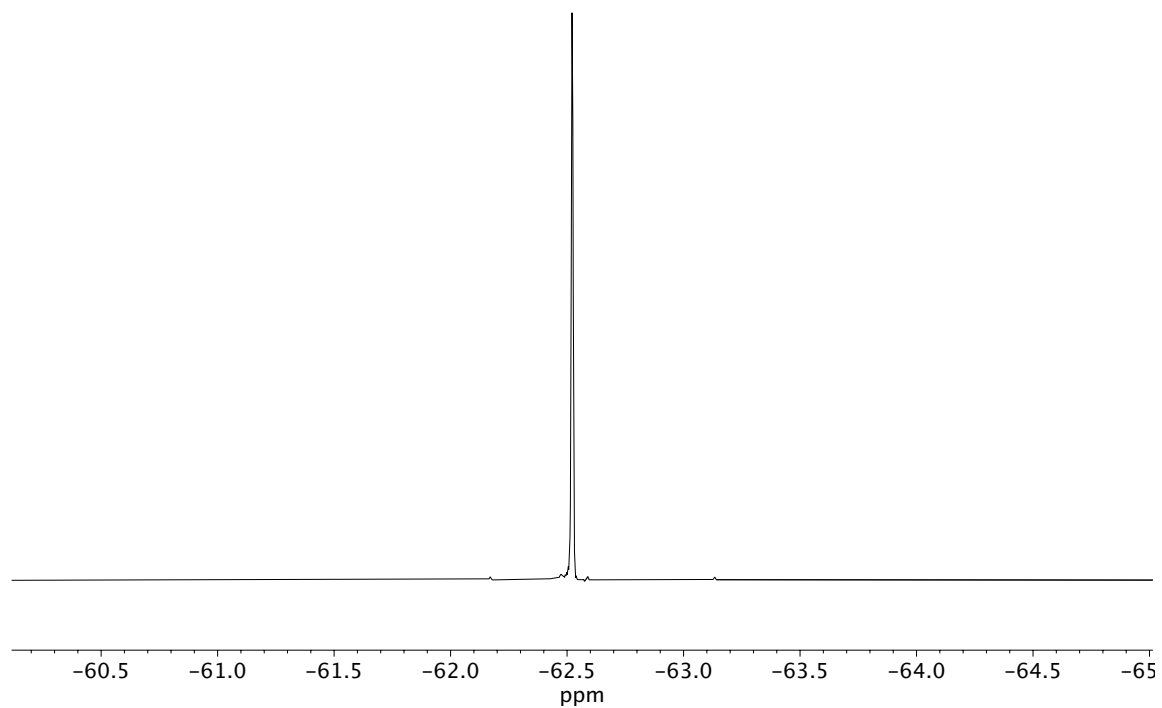


Figure A11.127 ^{19}F NMR (282 MHz, CDCl_3) of compound **182f**.

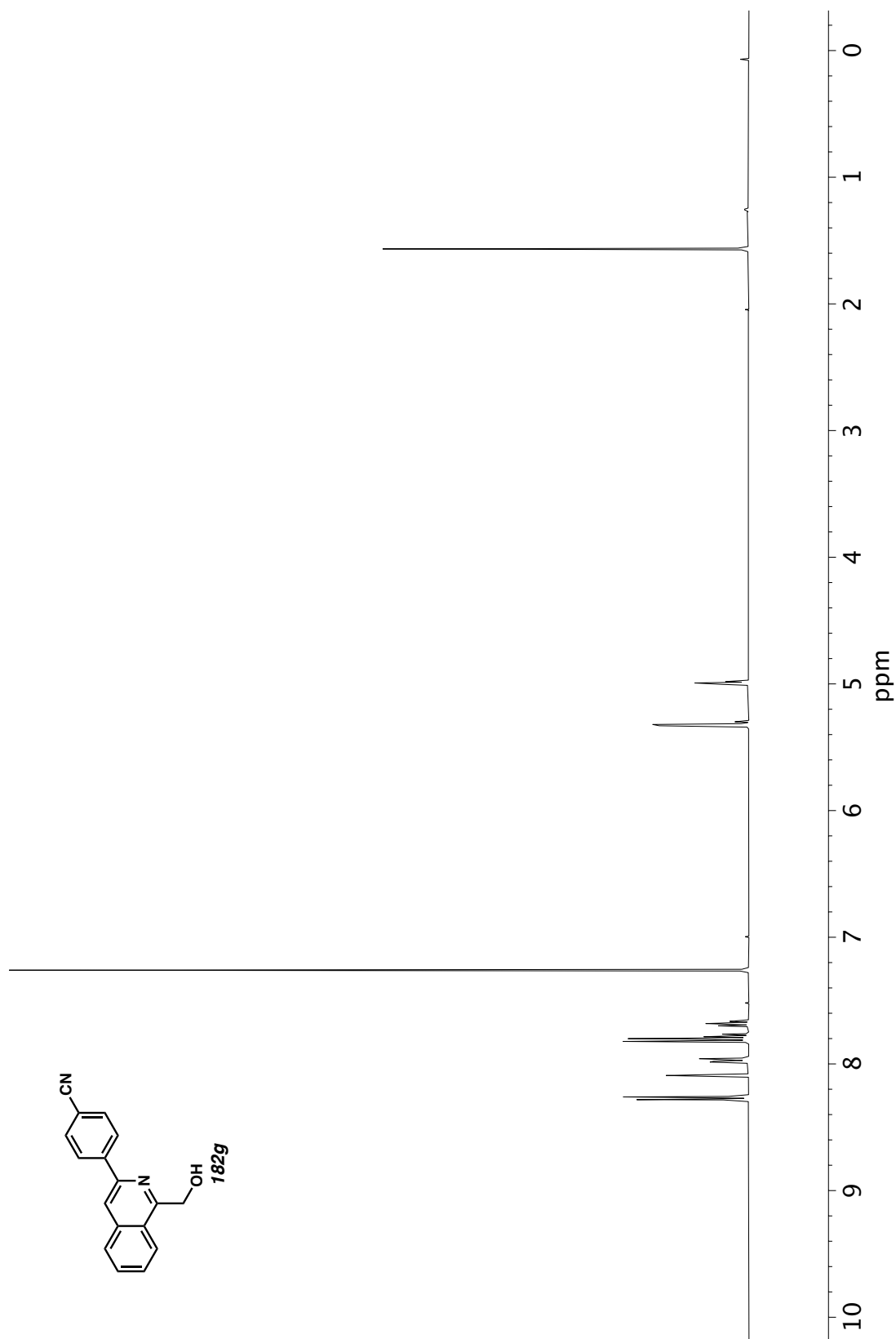


Figure A11.128 ^1H NMR (400 MHz, CDCl_3) of compound **182g**.

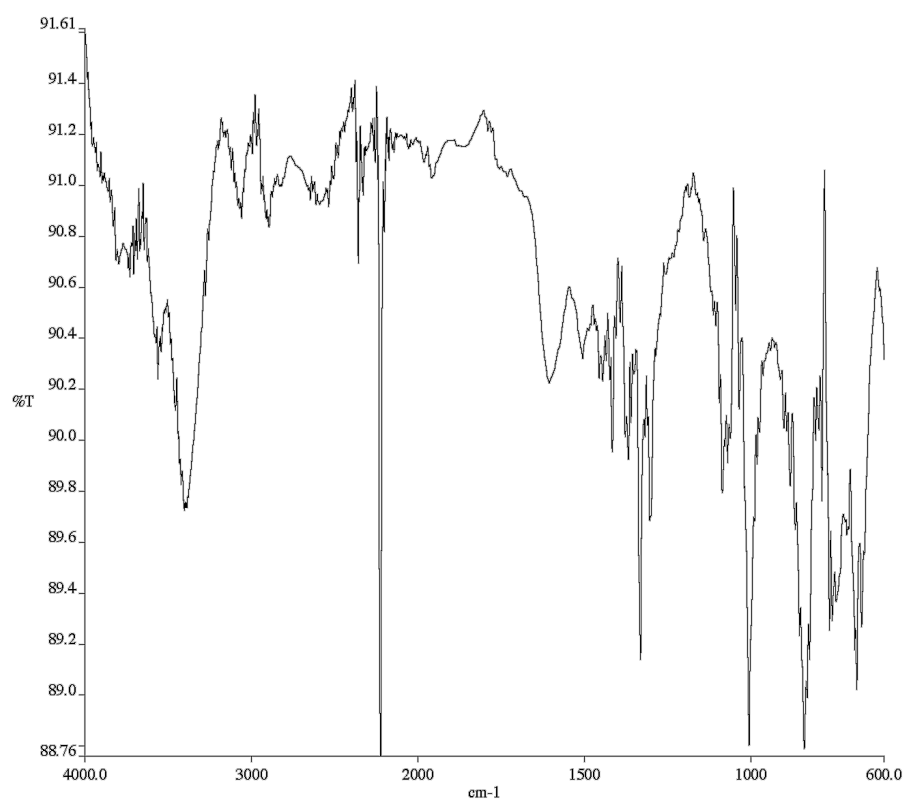


Figure A11.129 Infrared spectrum (Thin Film, NaCl) of compound

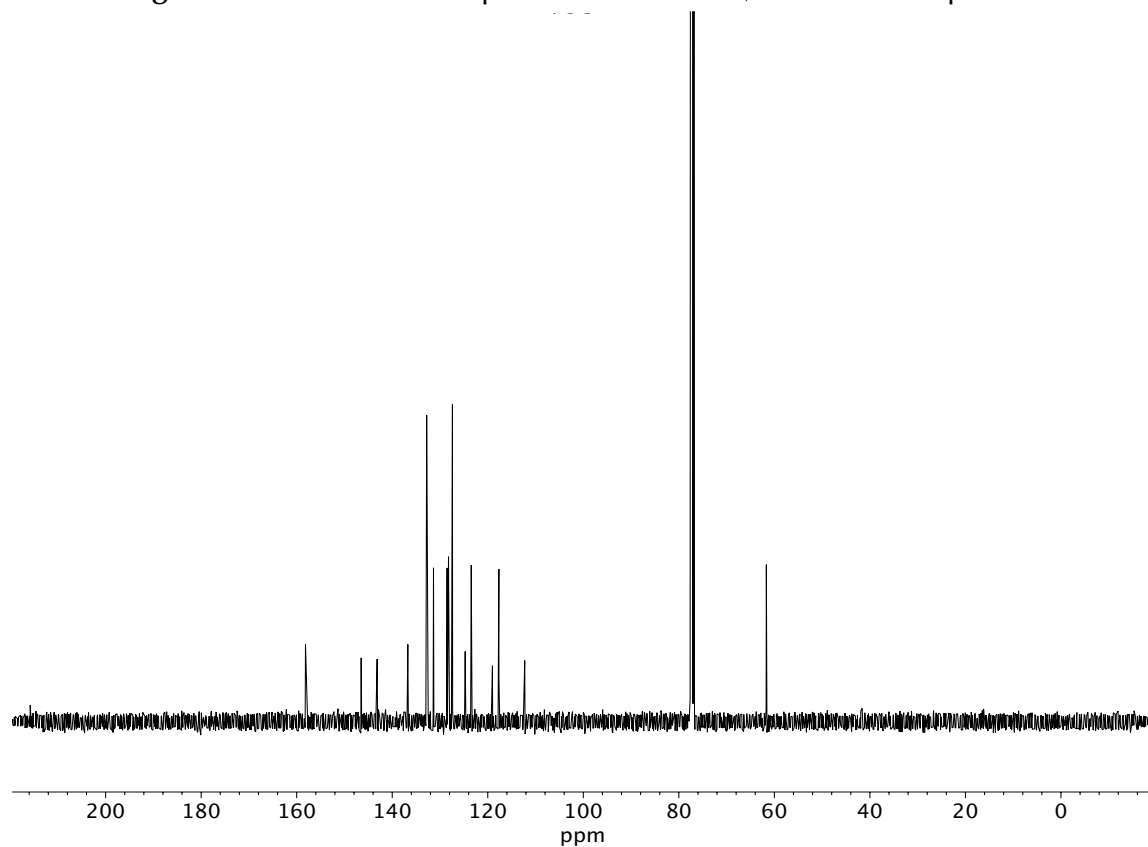


Figure A11.130 ¹³C NMR (100 MHz, CDCl₃) of compound **182g**.

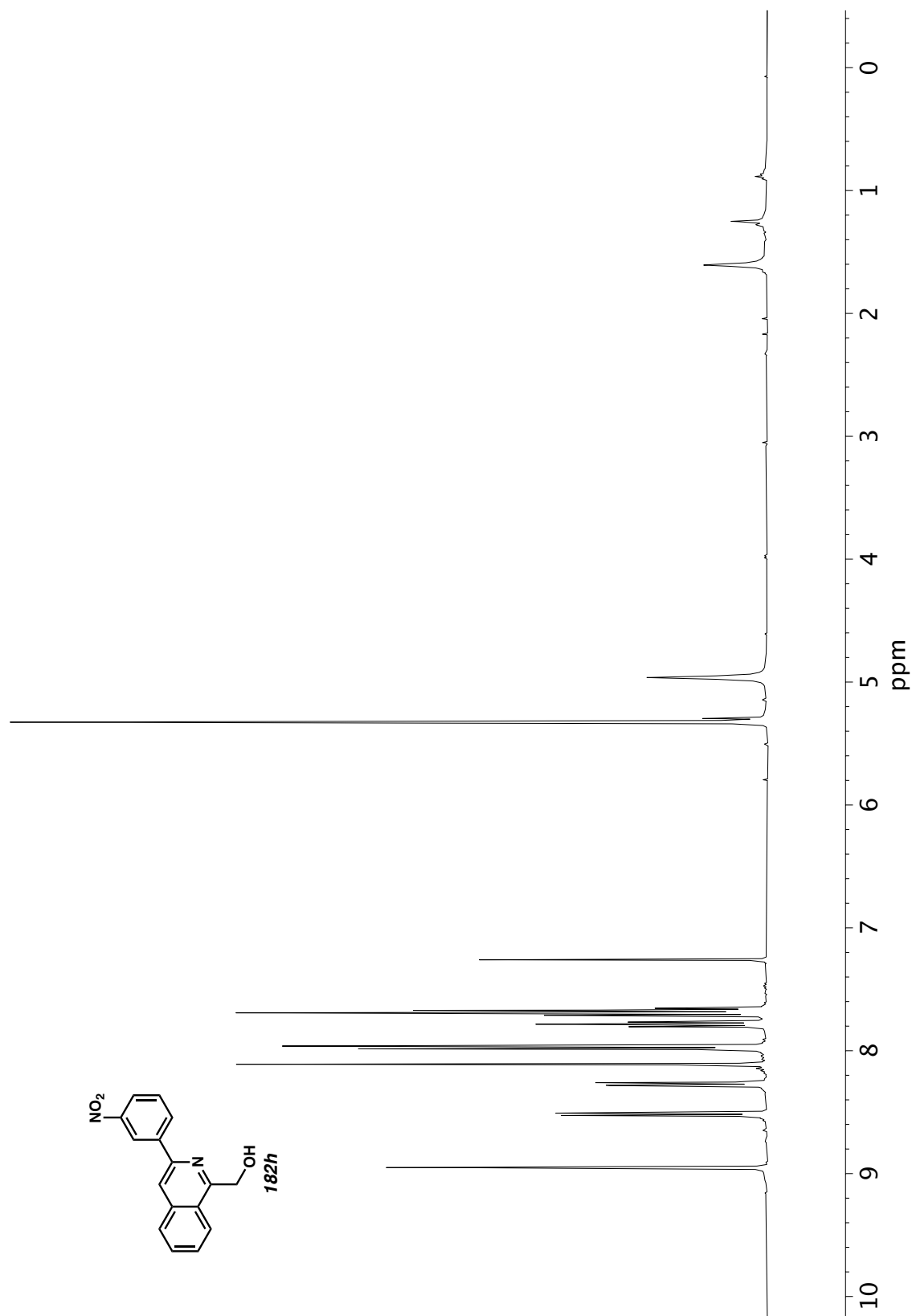


Figure A11.131 ^1H NMR (400 MHz, CDCl_3) of compound **182h**.

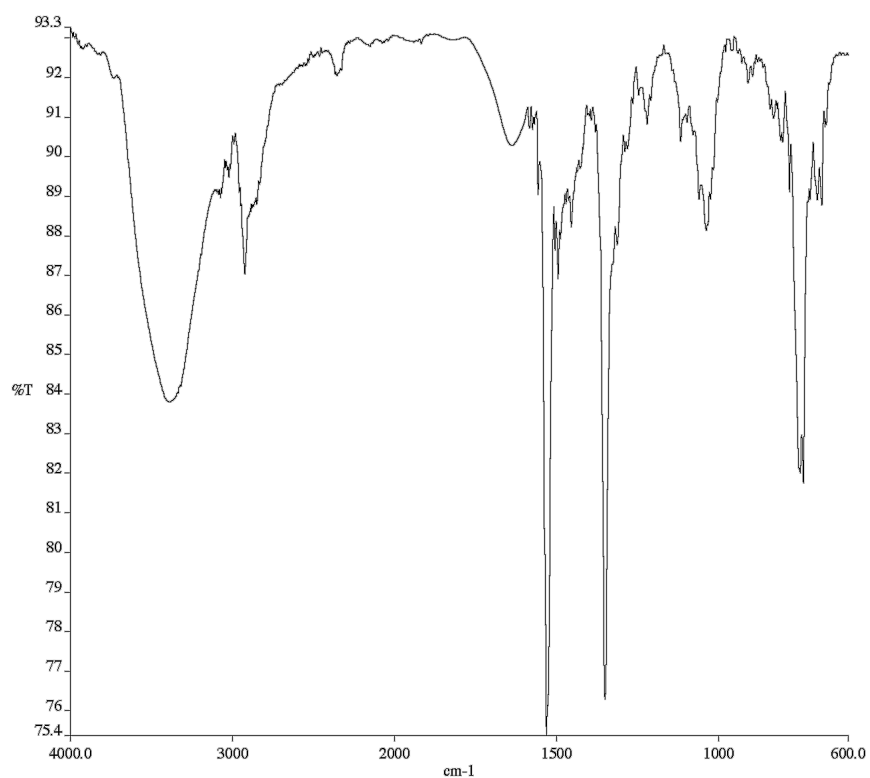


Figure A11.132 Infrared spectrum (Thin Film, NaCl) of compound

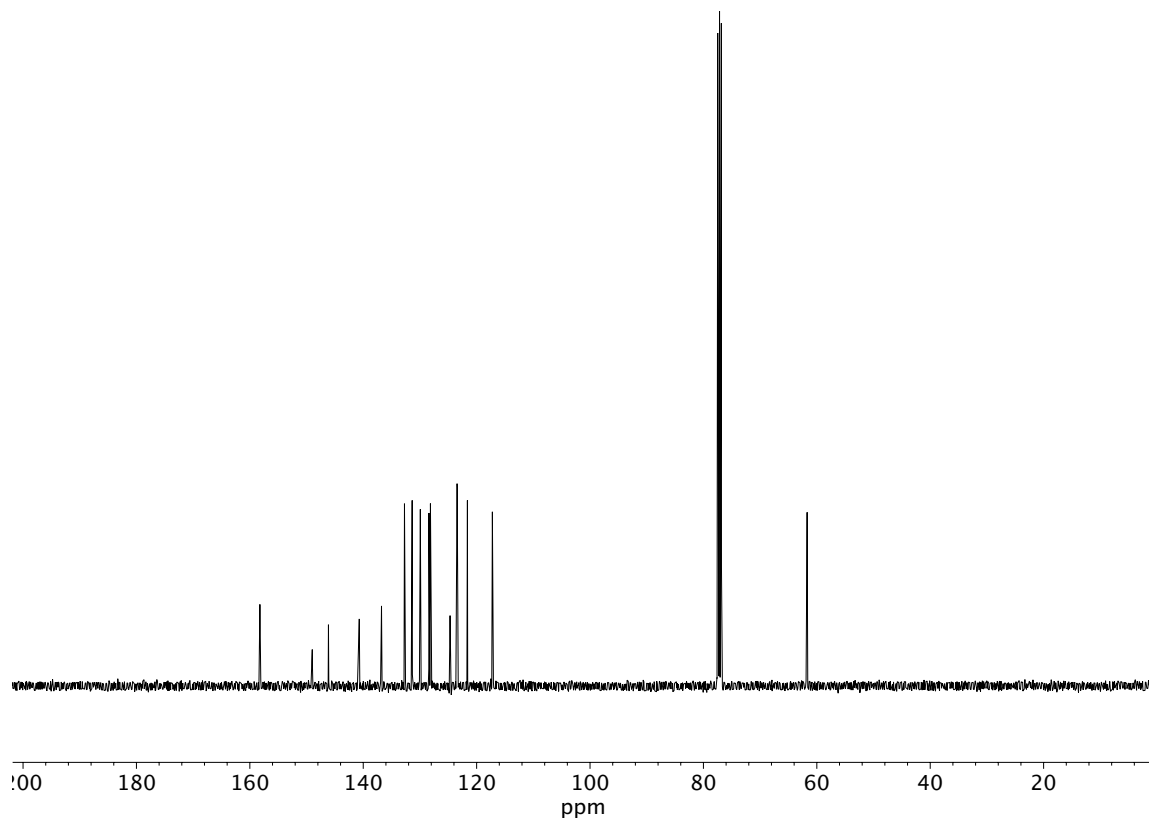


Figure A11.133 ¹³C NMR (100 MHz, CDCl₃) of compound **182h**.

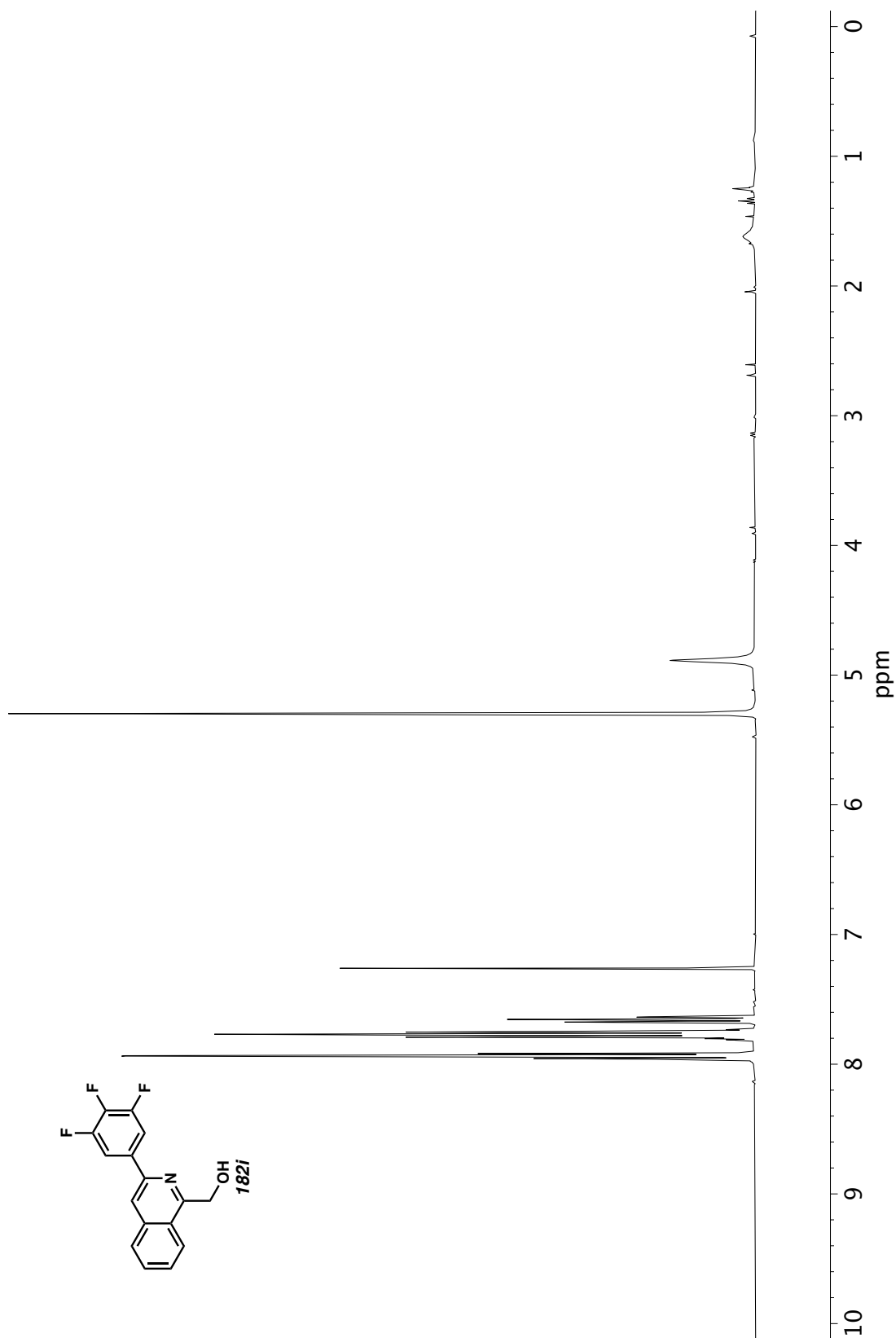


Figure A11.134 ¹H NMR (400 MHz, CDCl₃) of compound **182i**.

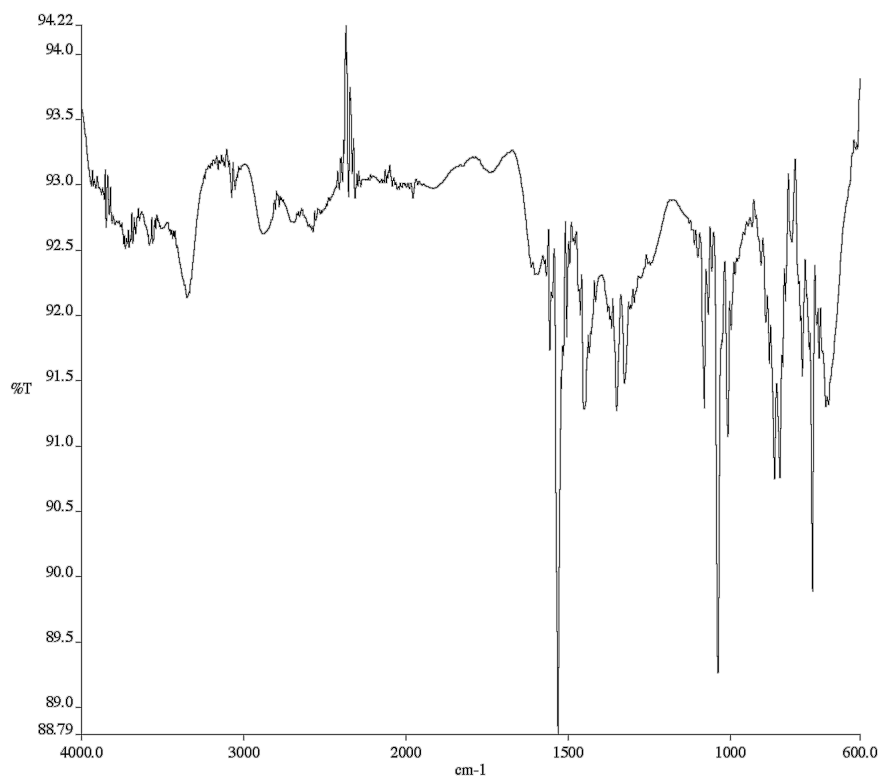


Figure A11.135 Infrared spectrum (Thin Film, NaCl) of compound

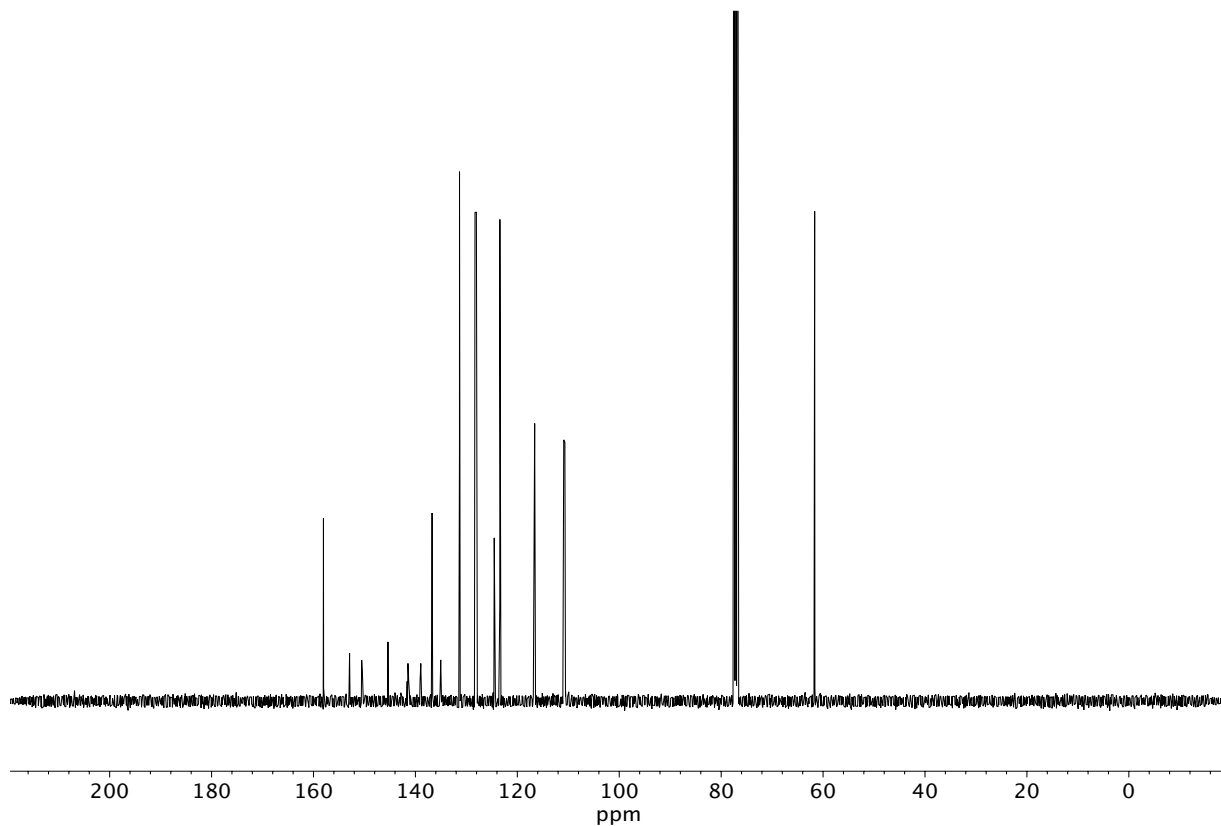


Figure A11.136 ¹³C NMR (100 MHz, CDCl₃) of compound **182i**.

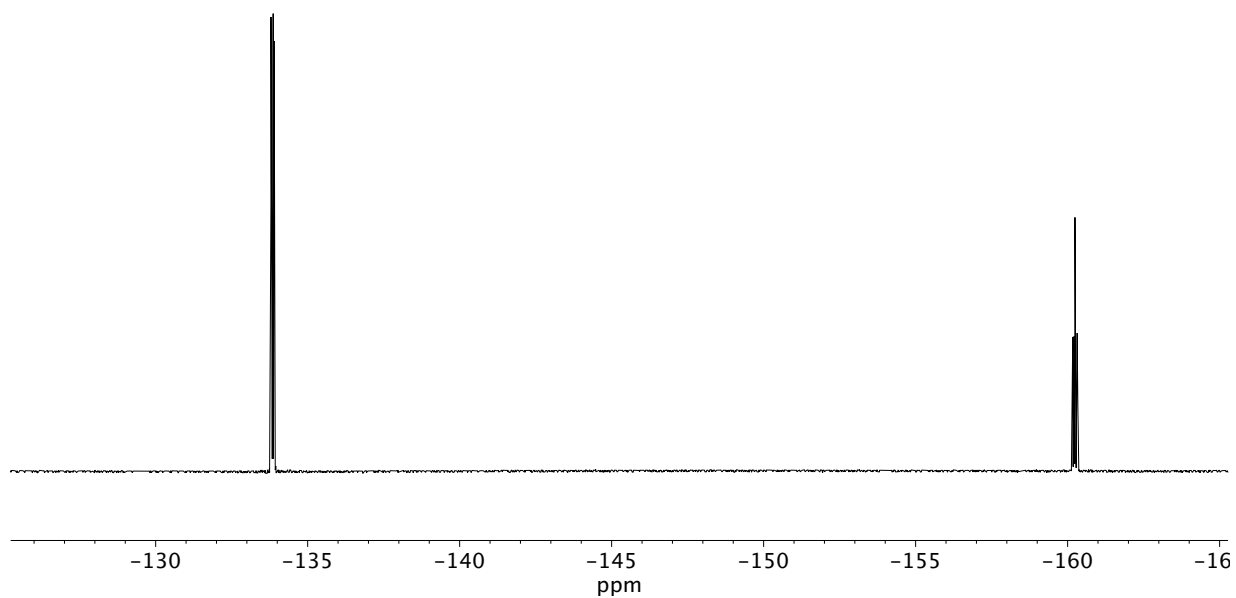


Figure A11.137 ^{19}F NMR (282 MHz, CDCl_3) of compound **182i**.

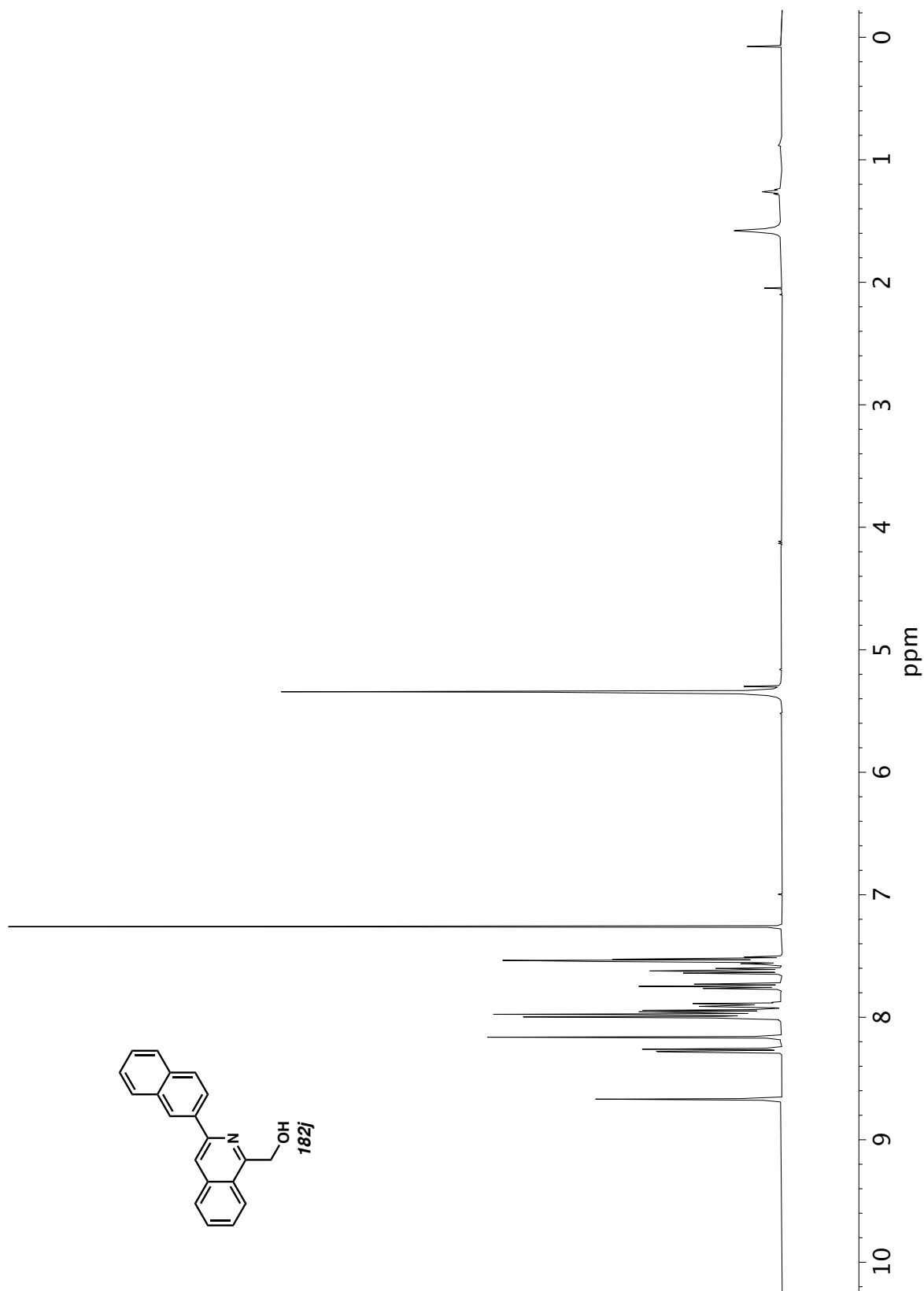


Figure A11.138 ^1H NMR (400 MHz, CDCl_3) of compound **182j**.

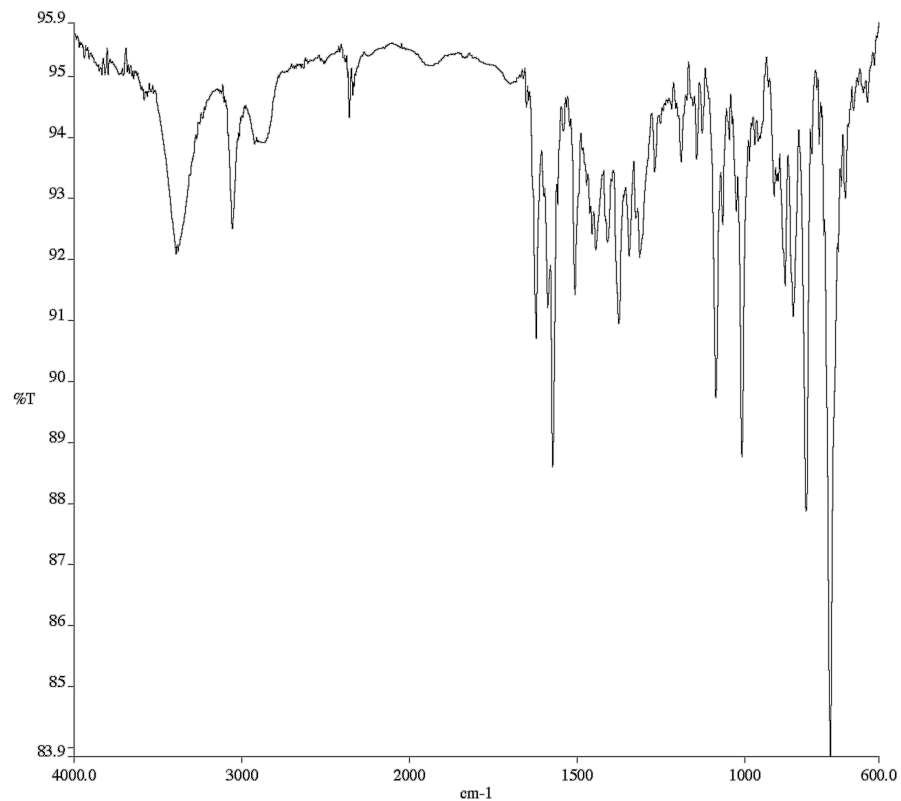


Figure A11.139 Infrared spectrum (Thin Film, NaCl) of compound

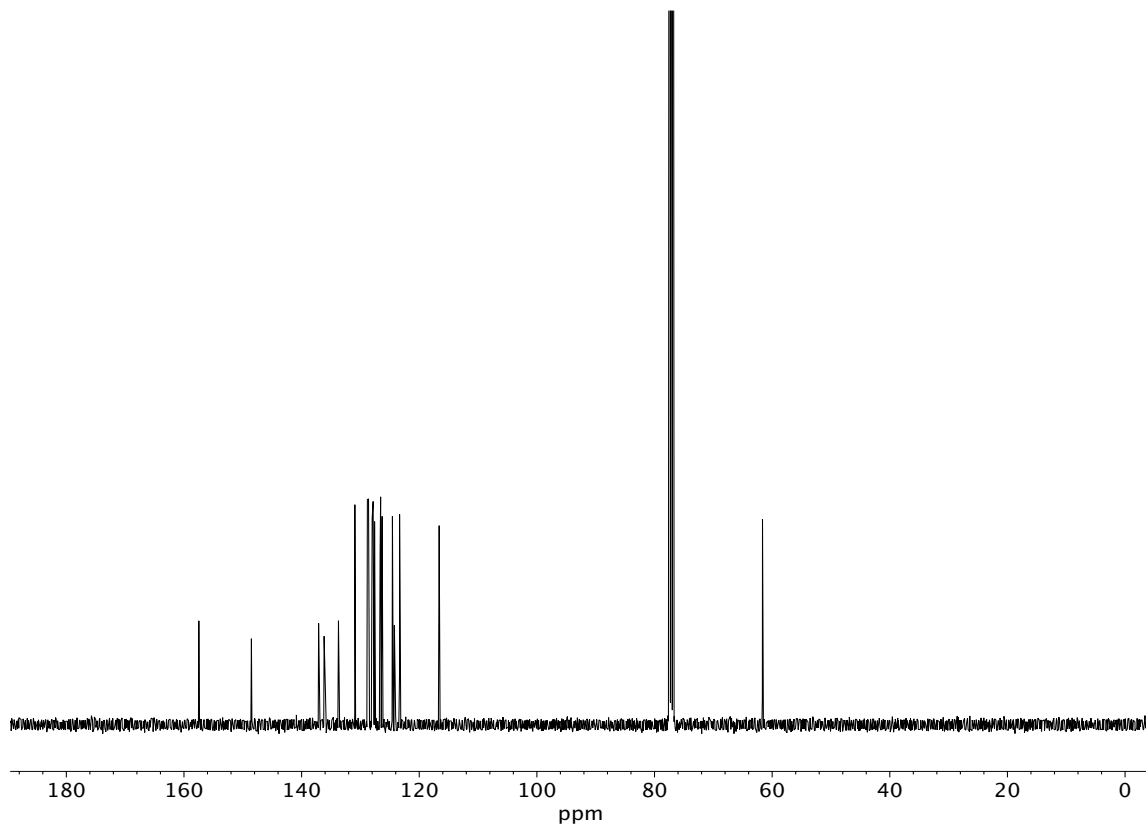


Figure A11.140 ¹³C NMR (100 MHz, CDCl₃) of compound **182j**.

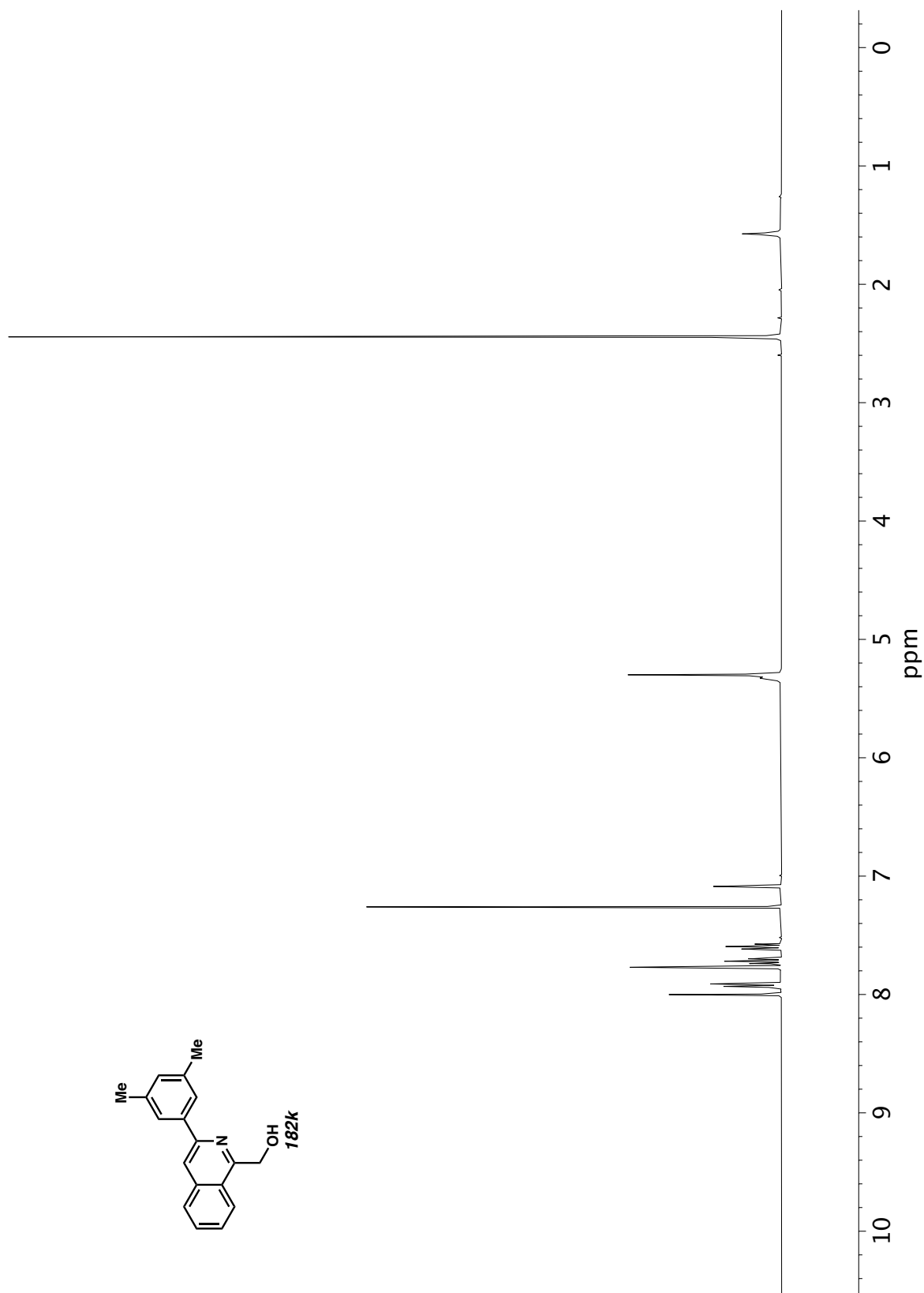


Figure A11.141 ^1H NMR (400 MHz, CDCl_3) of compound **182k**.

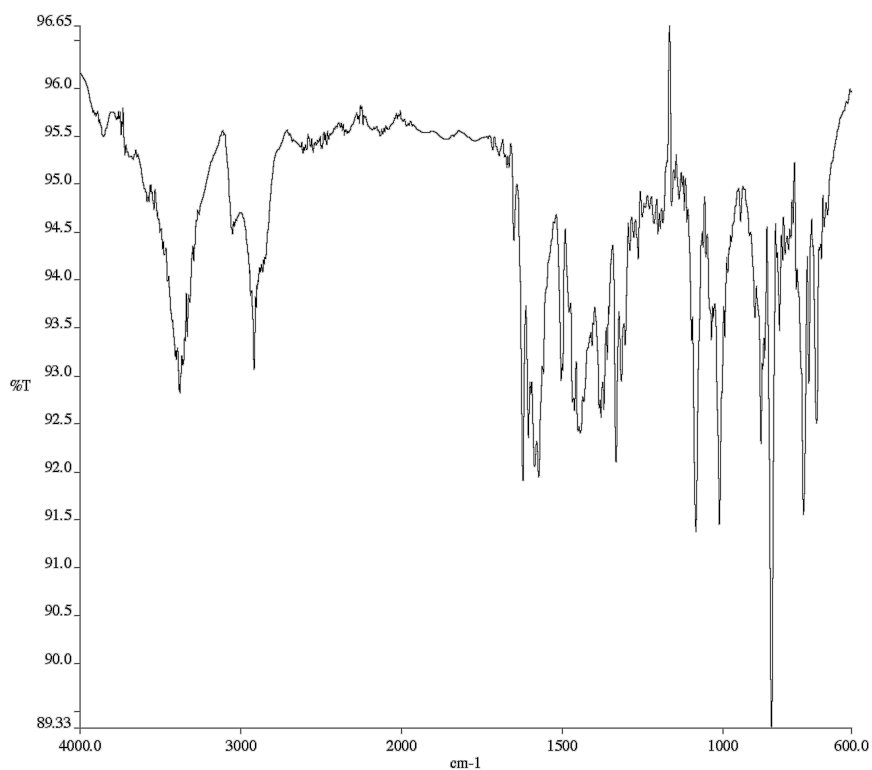


Figure A11.142 Infrared spectrum (Thin Film, NaCl) of compound

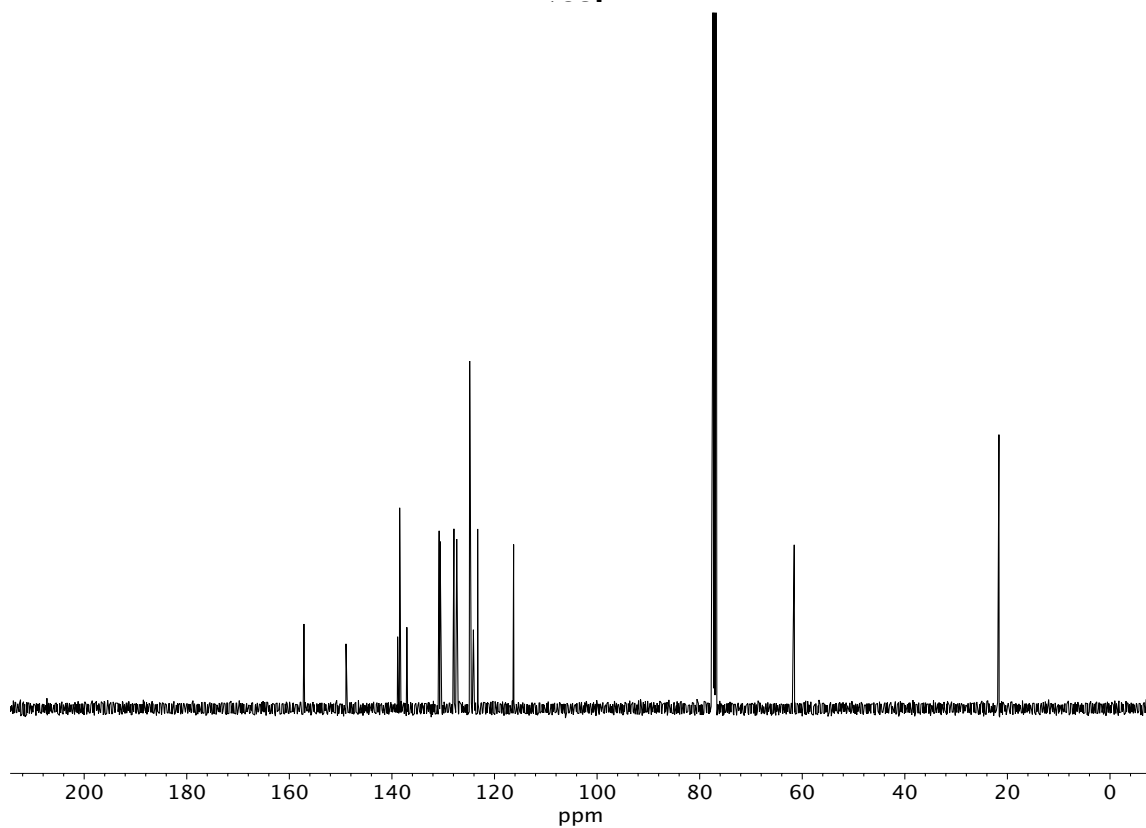


Figure A11.143 ¹³C NMR (100 MHz, CDCl₃) of compound **182k**.

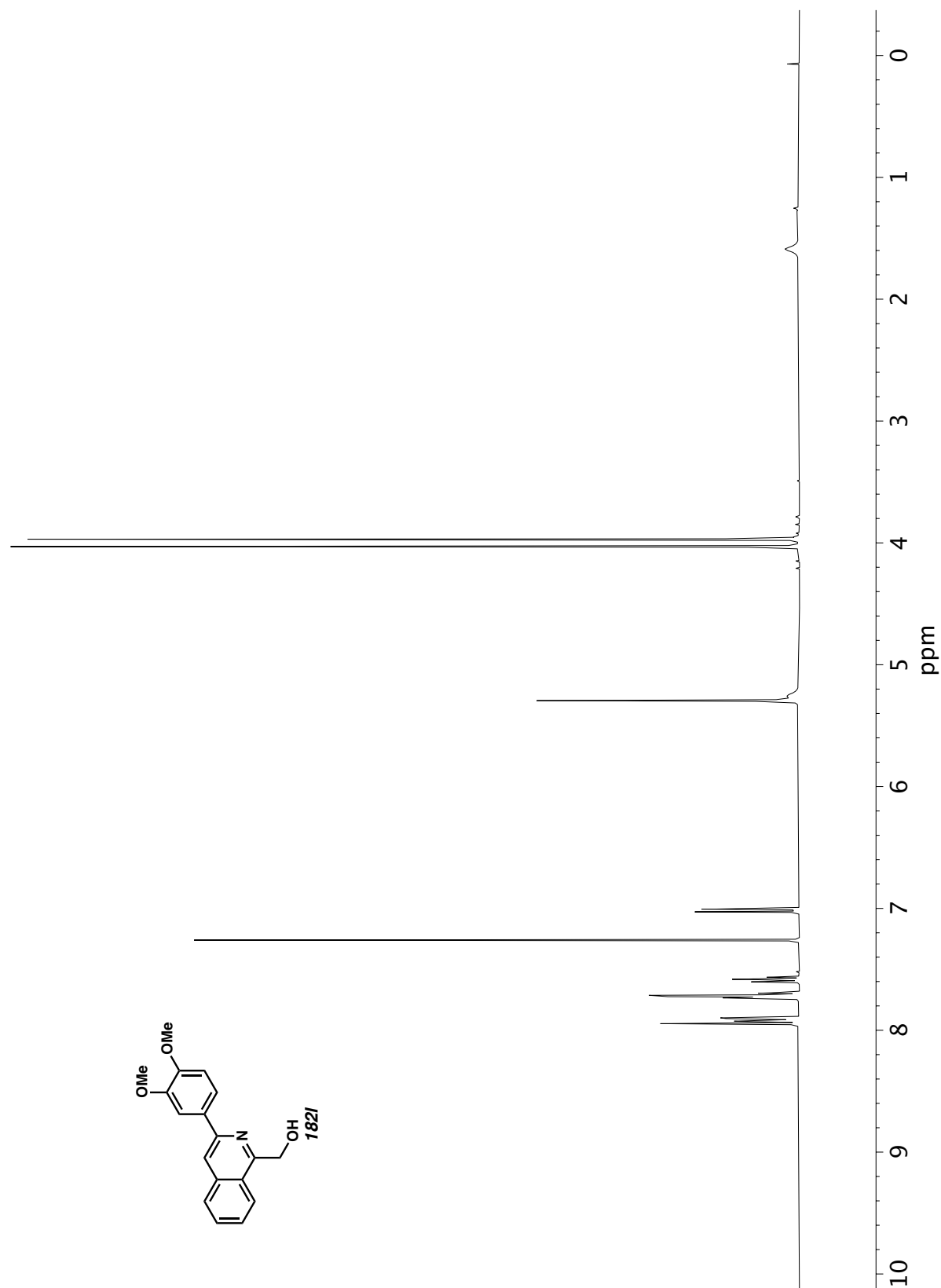


Figure A11.144 ¹H NMR (400 MHz, CDCl₃) of compound **182l**.

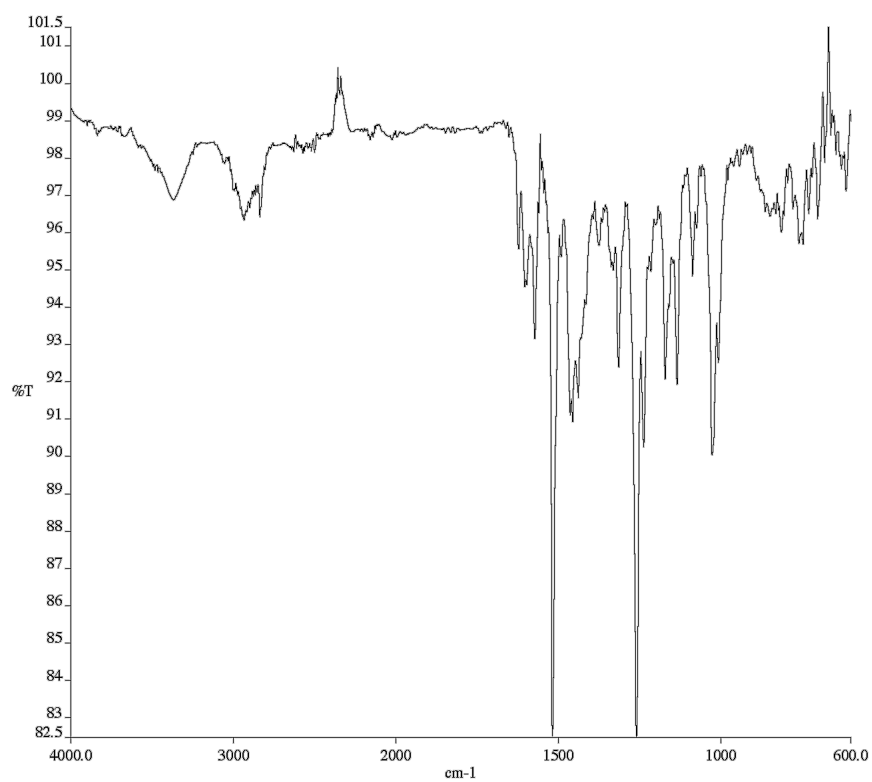


Figure A11.145 Infrared spectrum (Thin Film, NaCl) of compound

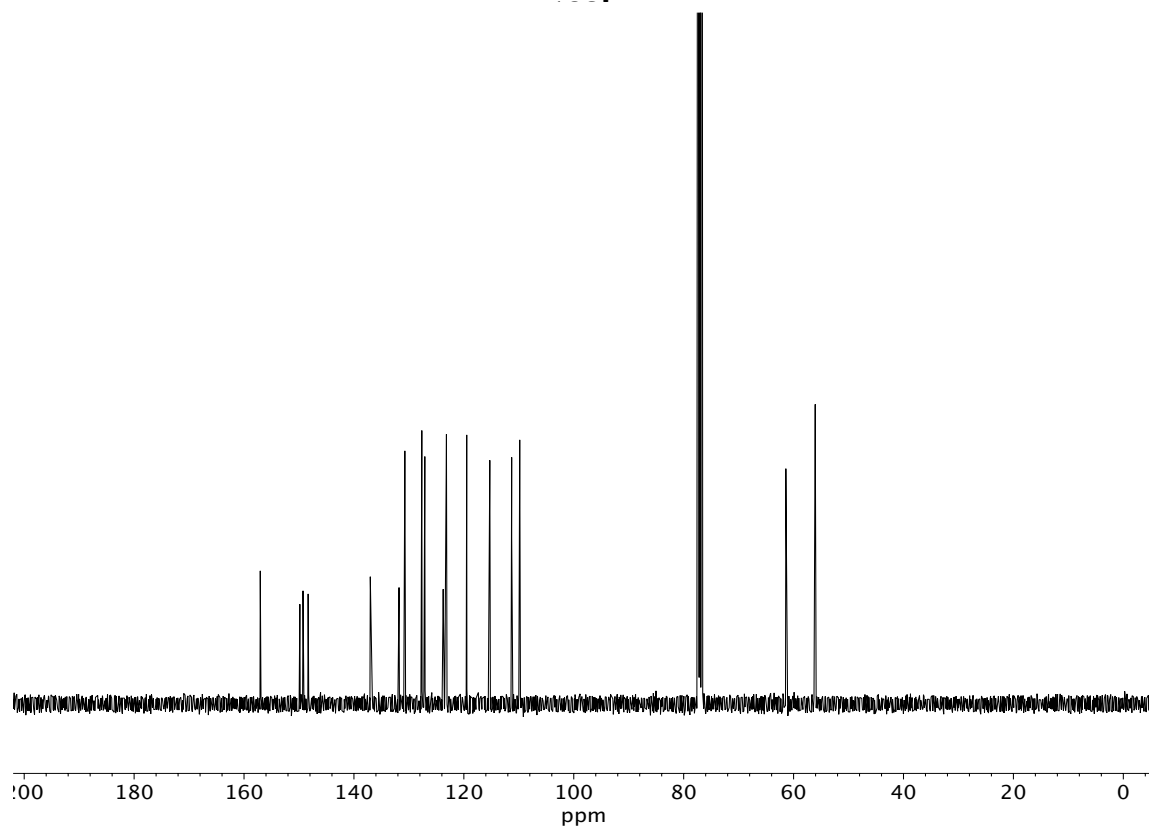
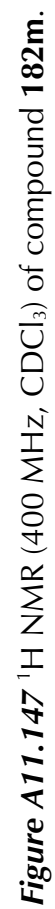


Figure A11.146 ¹³C NMR (100 MHz, CDCl₃) of compound **182l**.



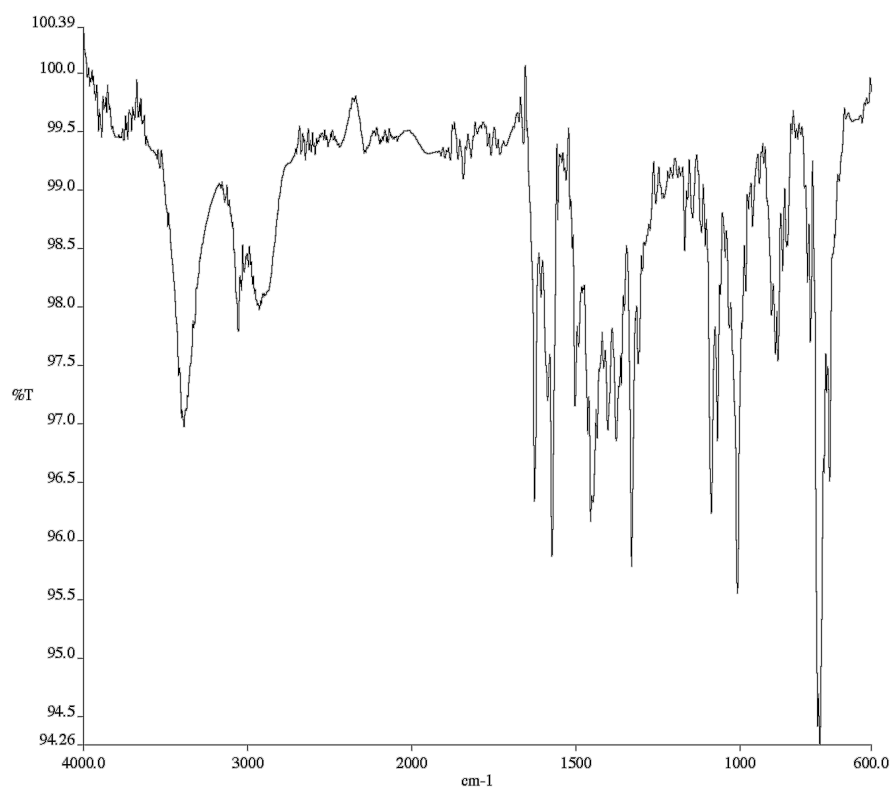


Figure A11.148 Infrared spectrum (Thin Film, NaCl) of compound **182m**.

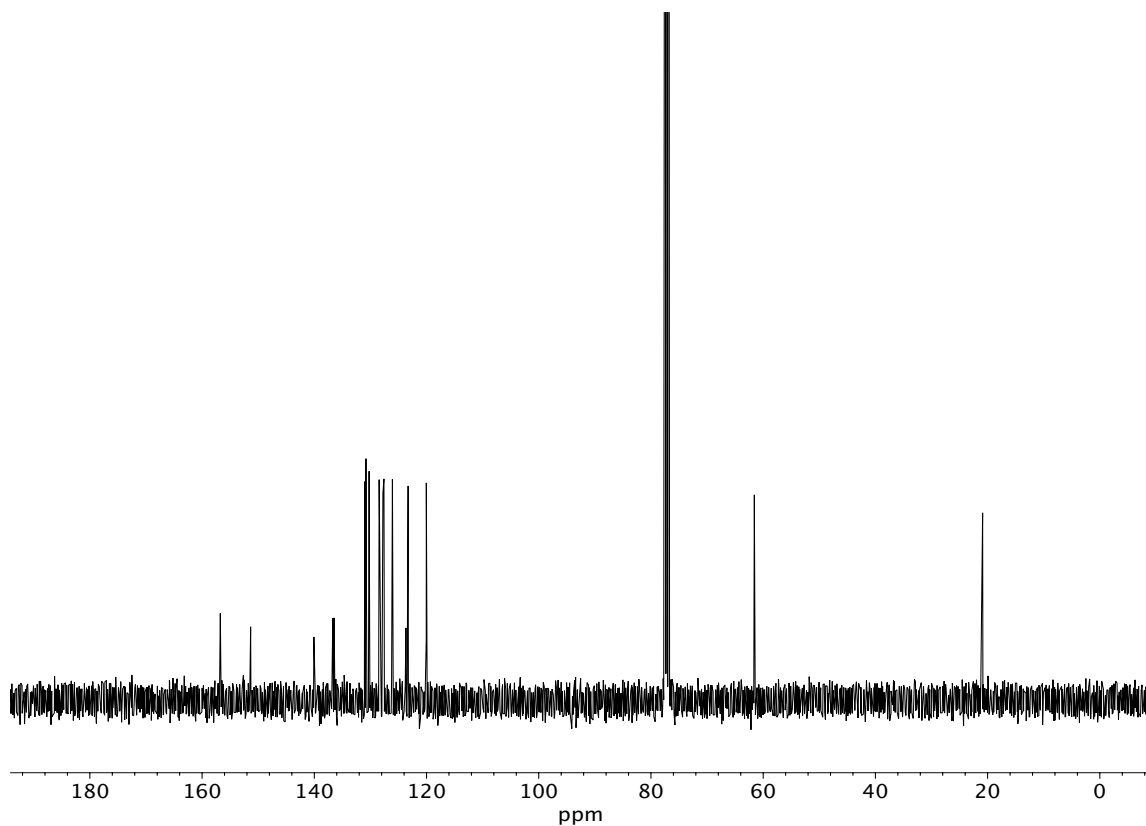


Figure A11.149 ¹³C NMR (100 MHz, CDCl₃) of compound **182m**.

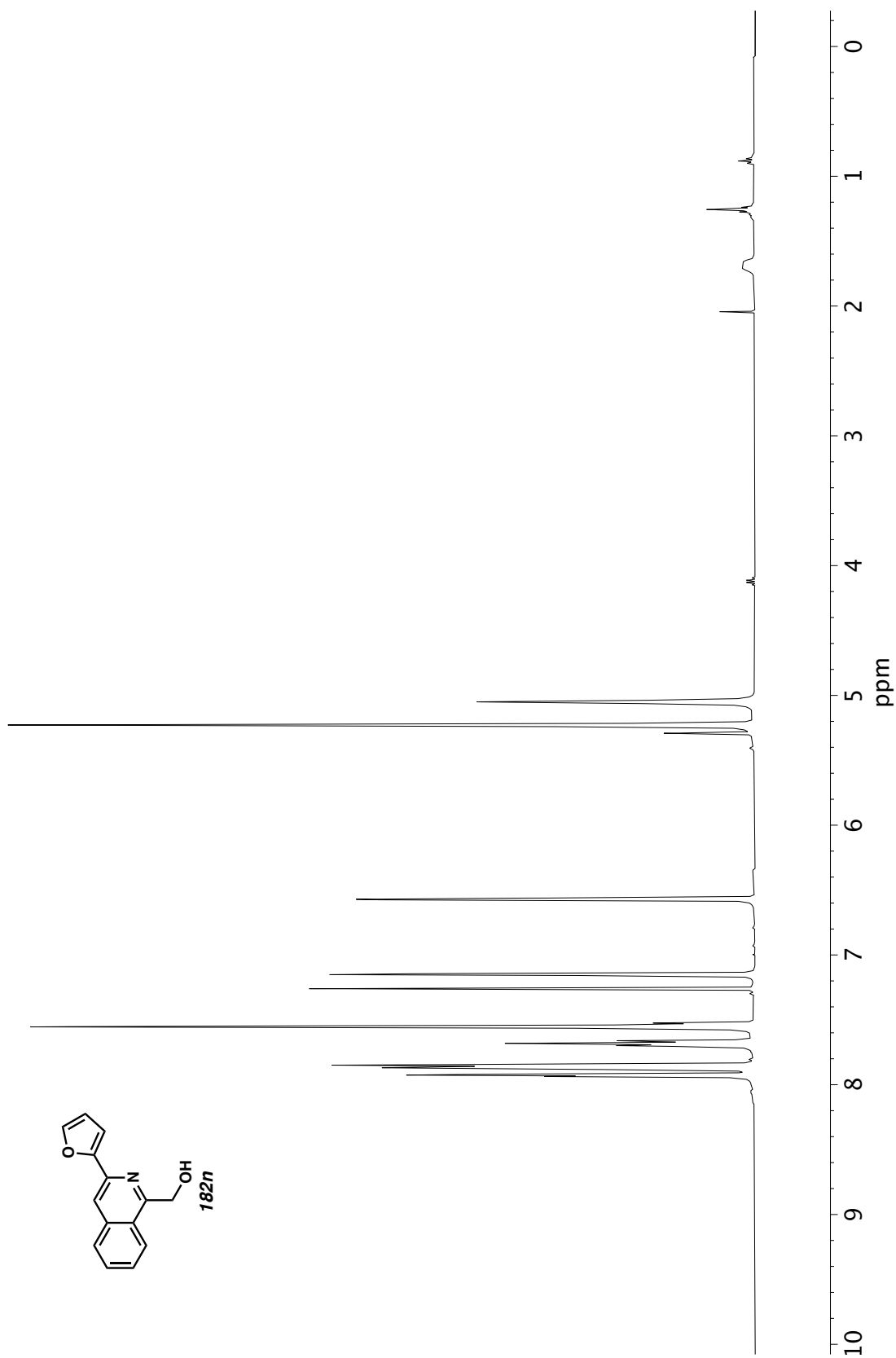


Figure A11.150 ^1H NMR (400 MHz, CDCl_3) of compound **182n**.

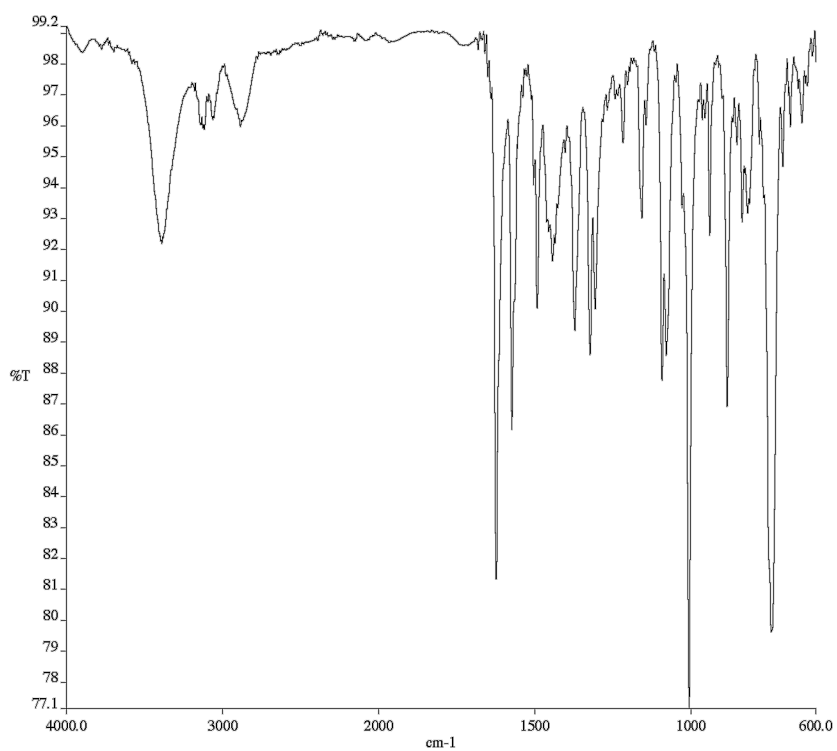


Figure A11.151 Infrared spectrum (Thin Film, NaCl) of compound

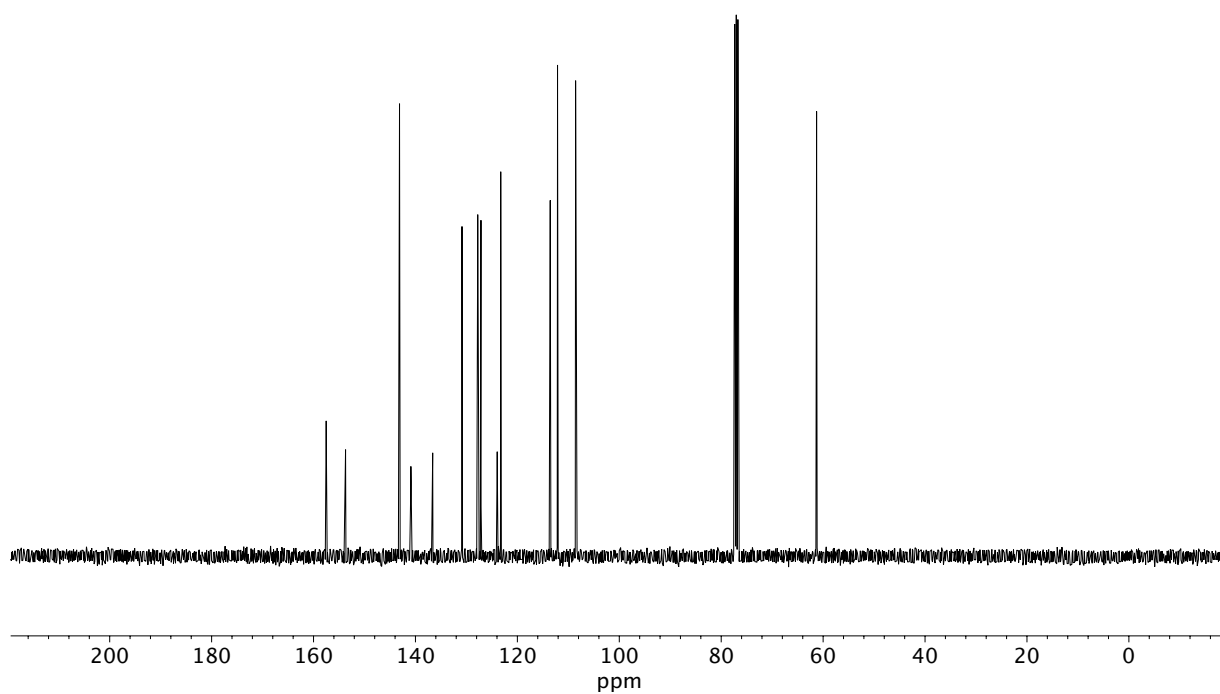


Figure A11.152 ¹³C NMR (100 MHz, CDCl₃) of compound **182n**.

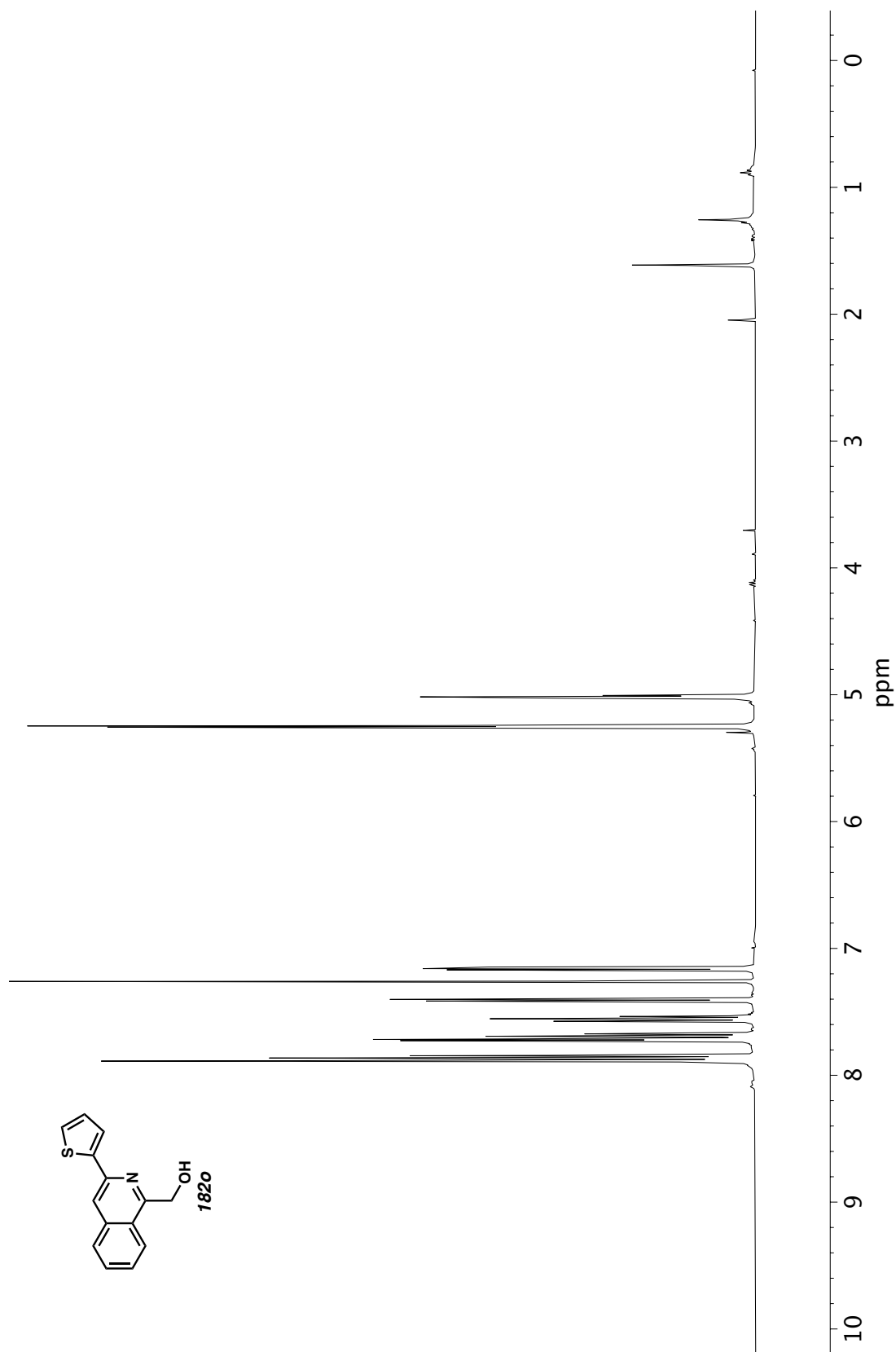


Figure A11.153 ¹H NMR (400 MHz, CDCl₃) of compound **182o**.

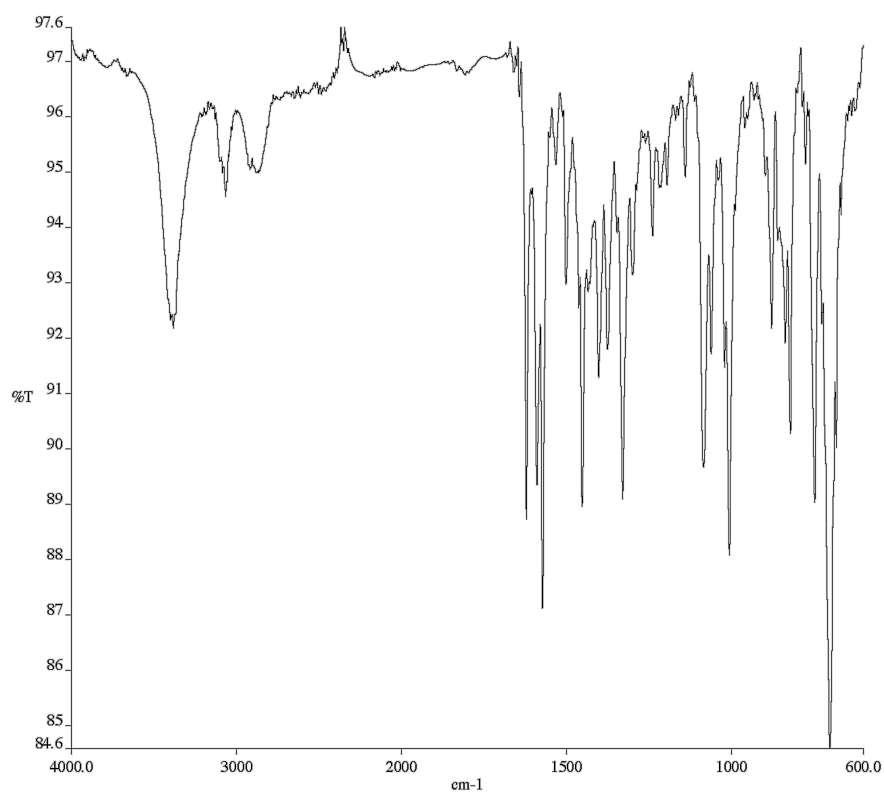


Figure A11.154 Infrared spectrum (Thin Film, NaCl) of compound

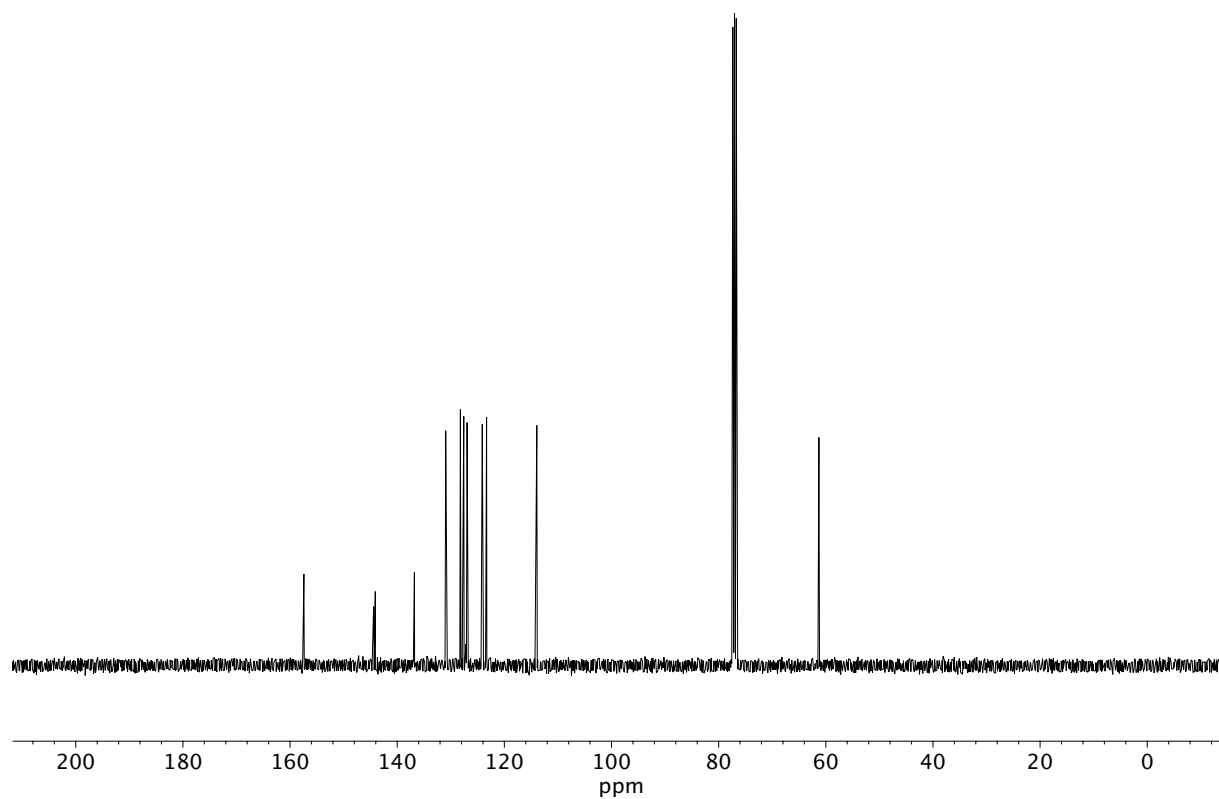


Figure A11.155 ¹³C NMR (100 MHz, CDCl₃) of compound **182o**.

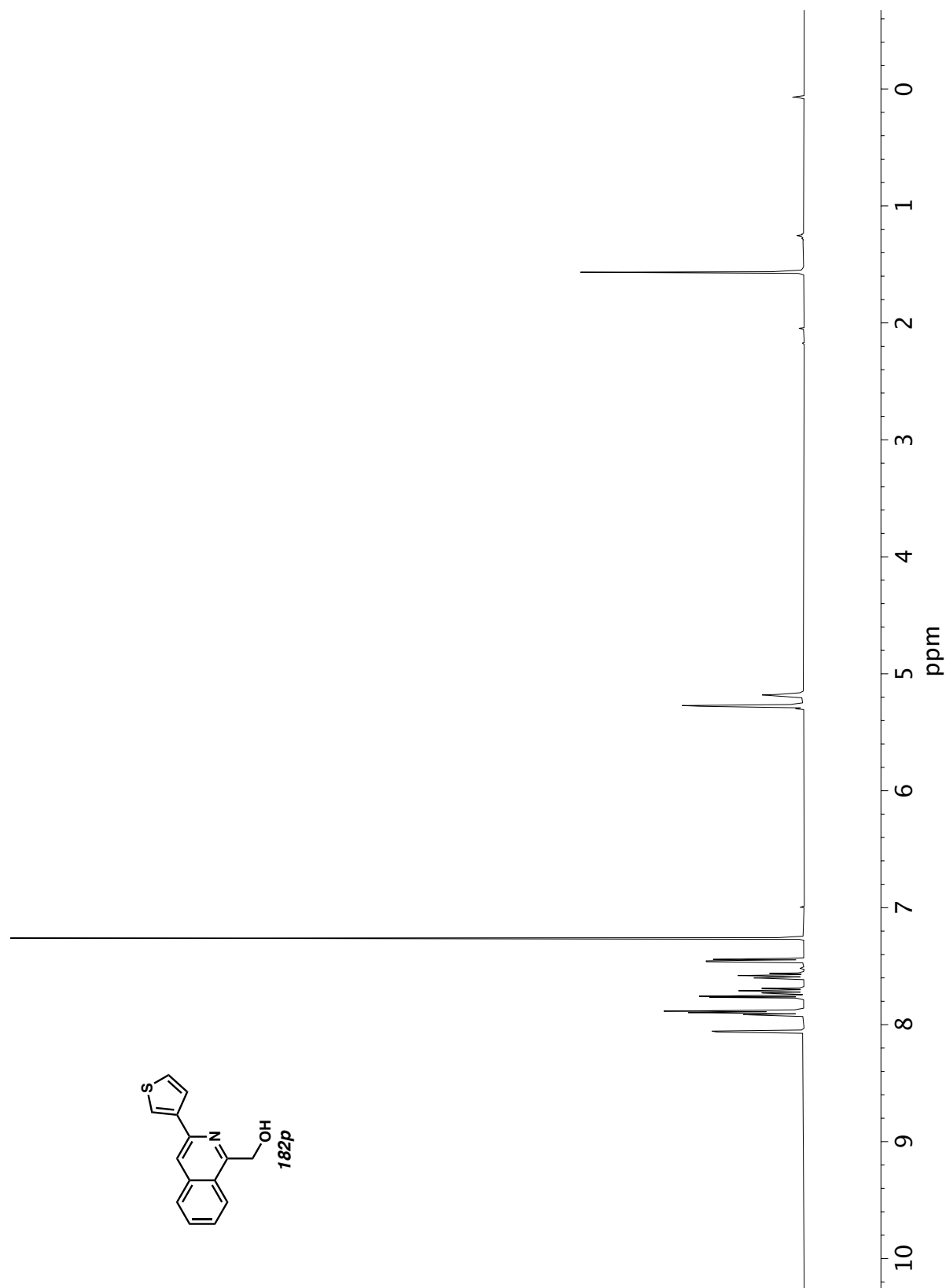


Figure A11.156 ¹H NMR (400 MHz, CDCl₃) of compound **182p**.

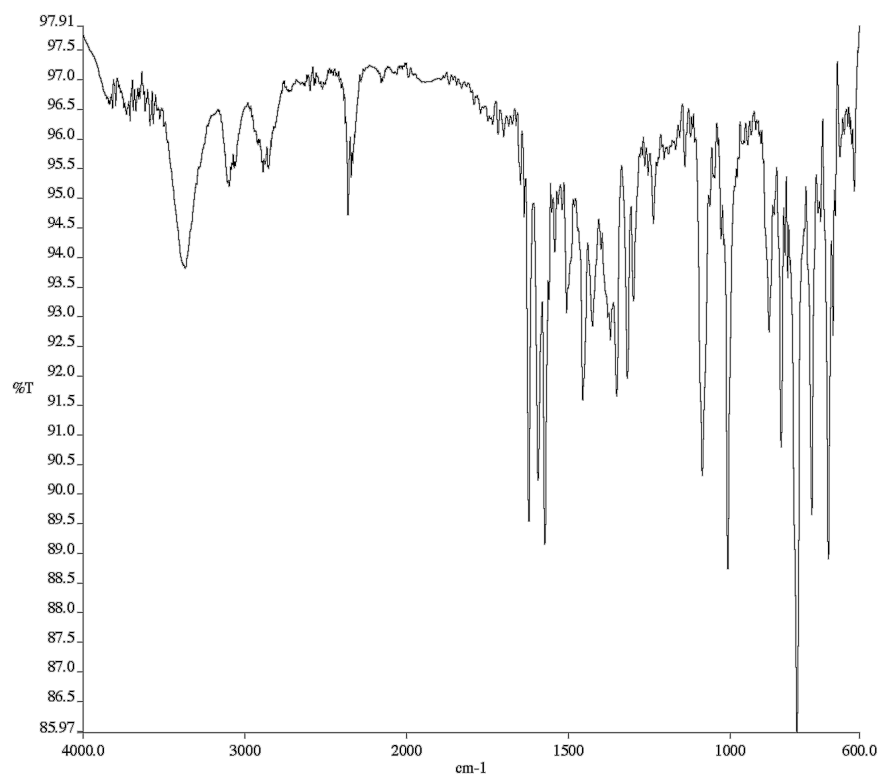


Figure A11.157 Infrared spectrum (Thin Film, NaCl) of compound

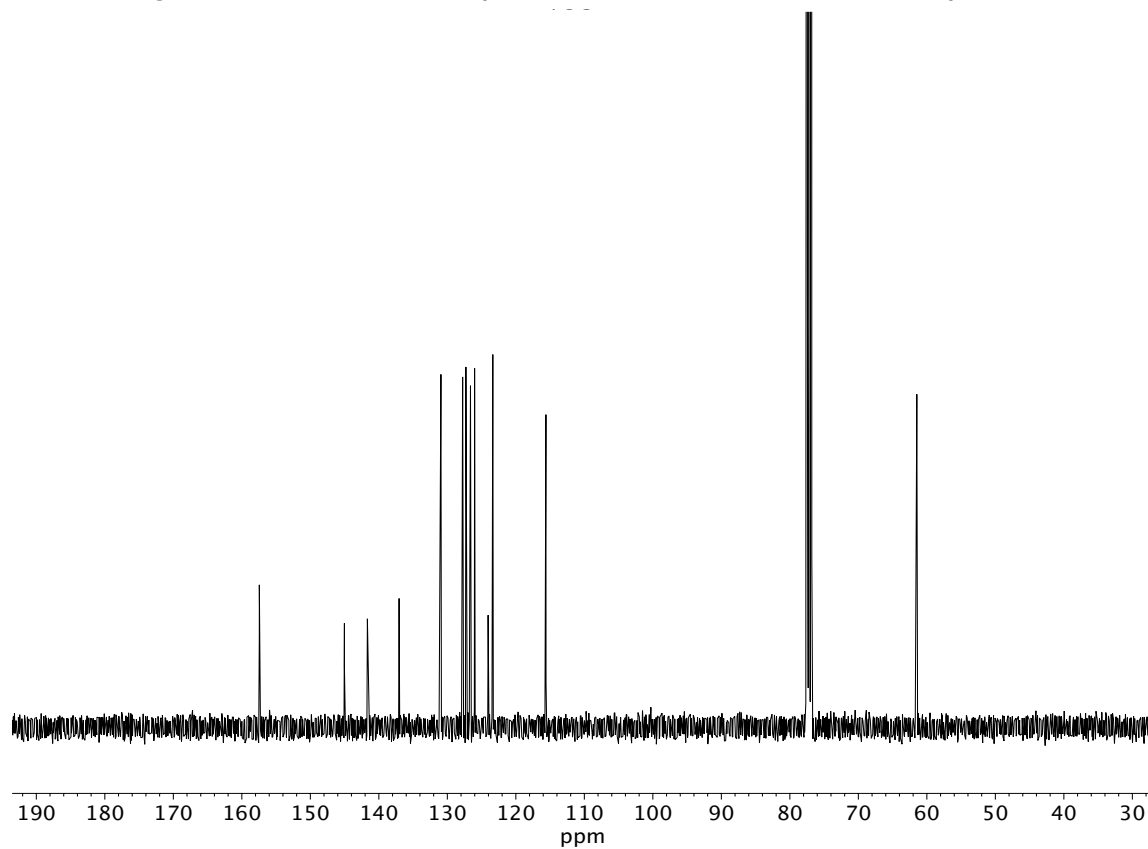


Figure A11.158 ^{13}C NMR (100 MHz, CDCl_3) of compound **182p**.

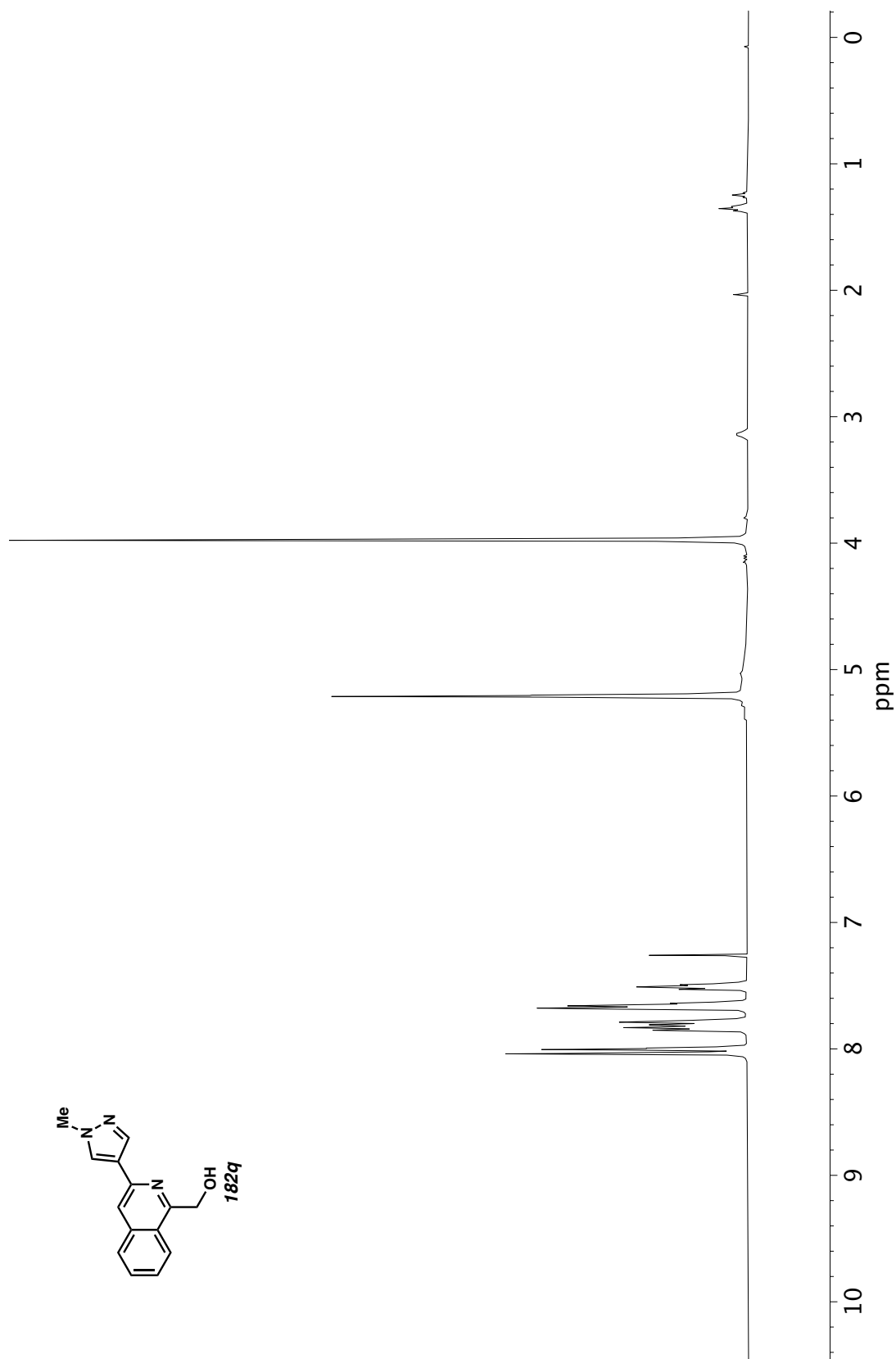


Figure A11.159 ¹H NMR (400 MHz, CDCl₃) of compound **182q**.

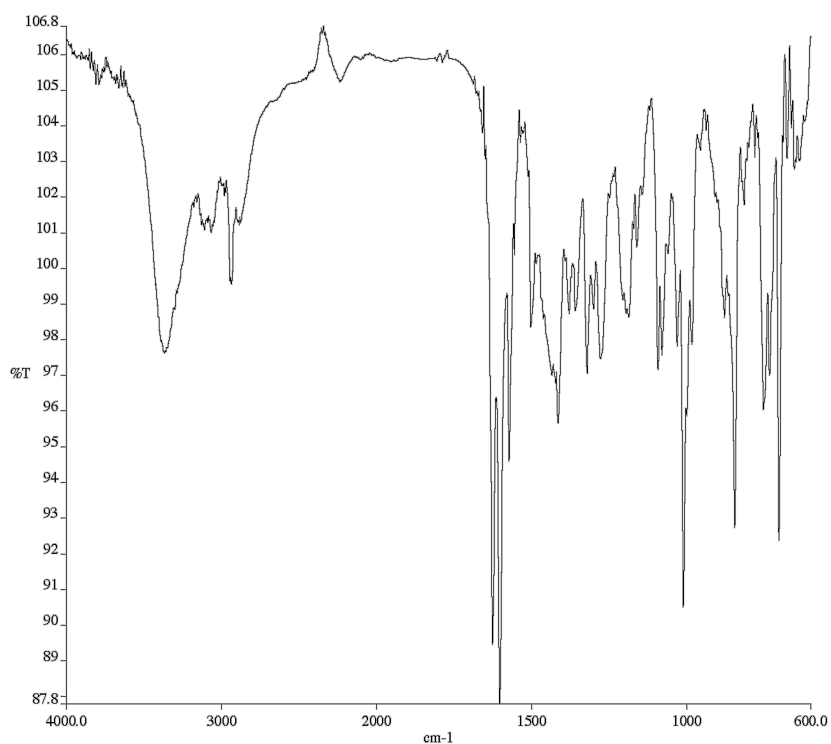


Figure A11.160 Infrared spectrum (Thin Film, NaCl) of compound

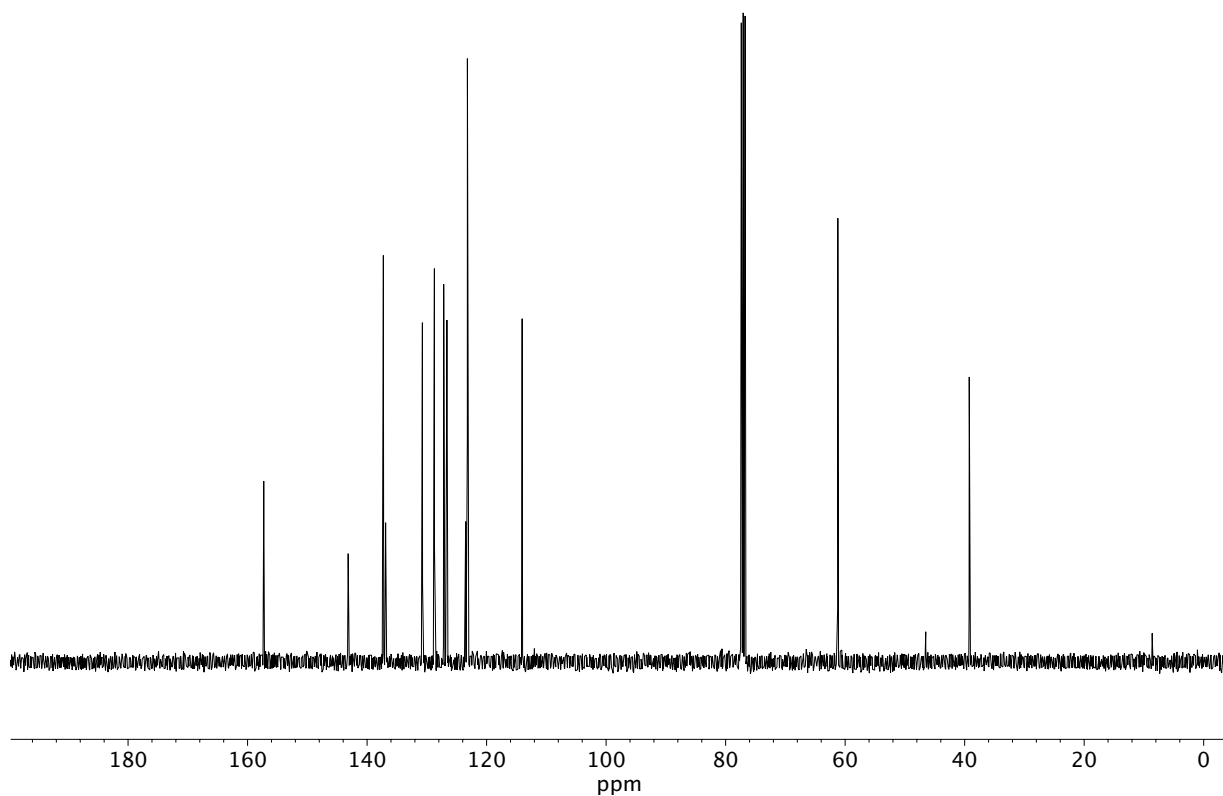


Figure A11.161 ¹³C NMR (100 MHz, CDCl₃) of compound **182q**.

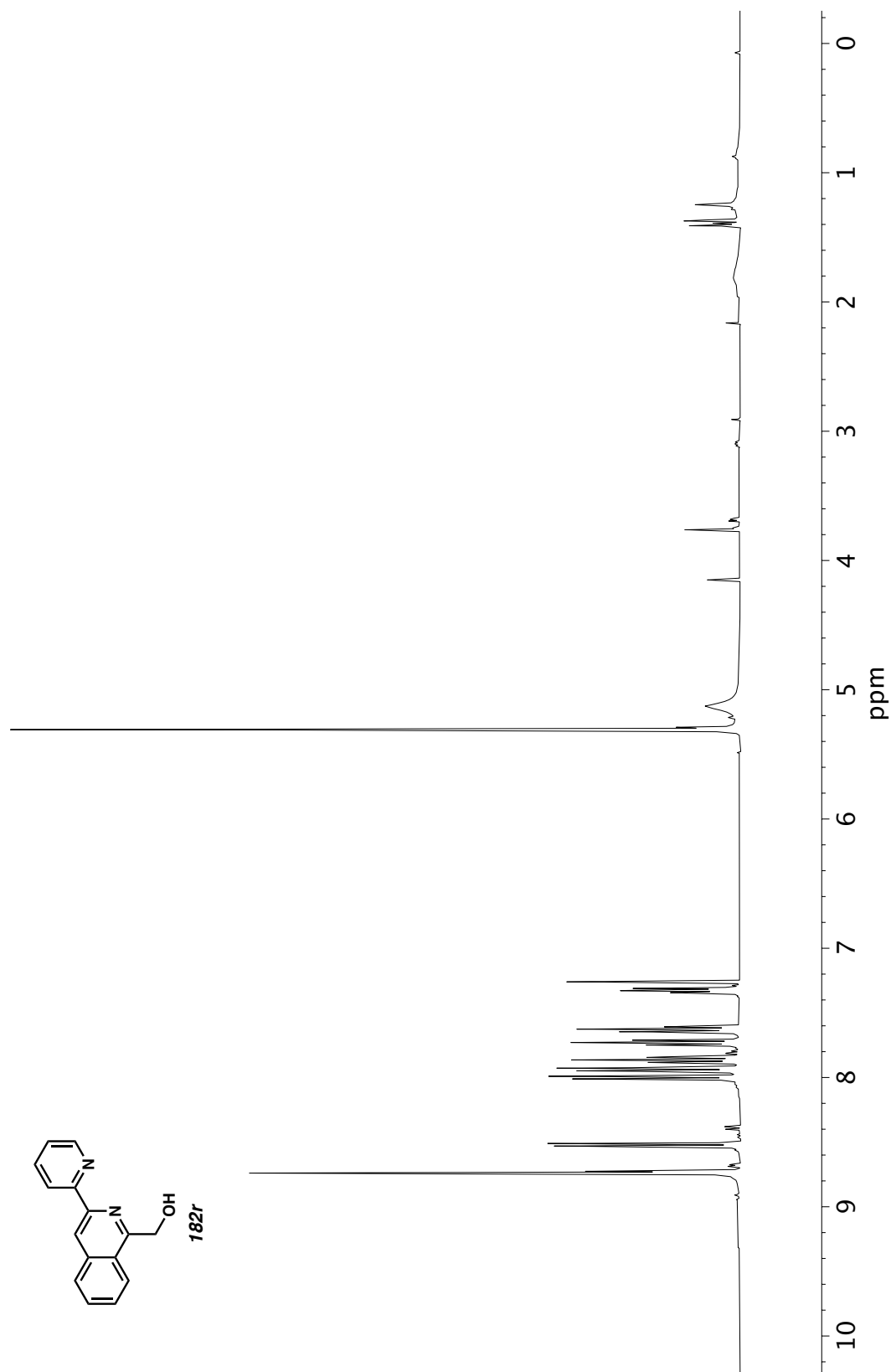


Figure A11.162 ¹H NMR (400 MHz, CDCl₃) of compound **182r**.

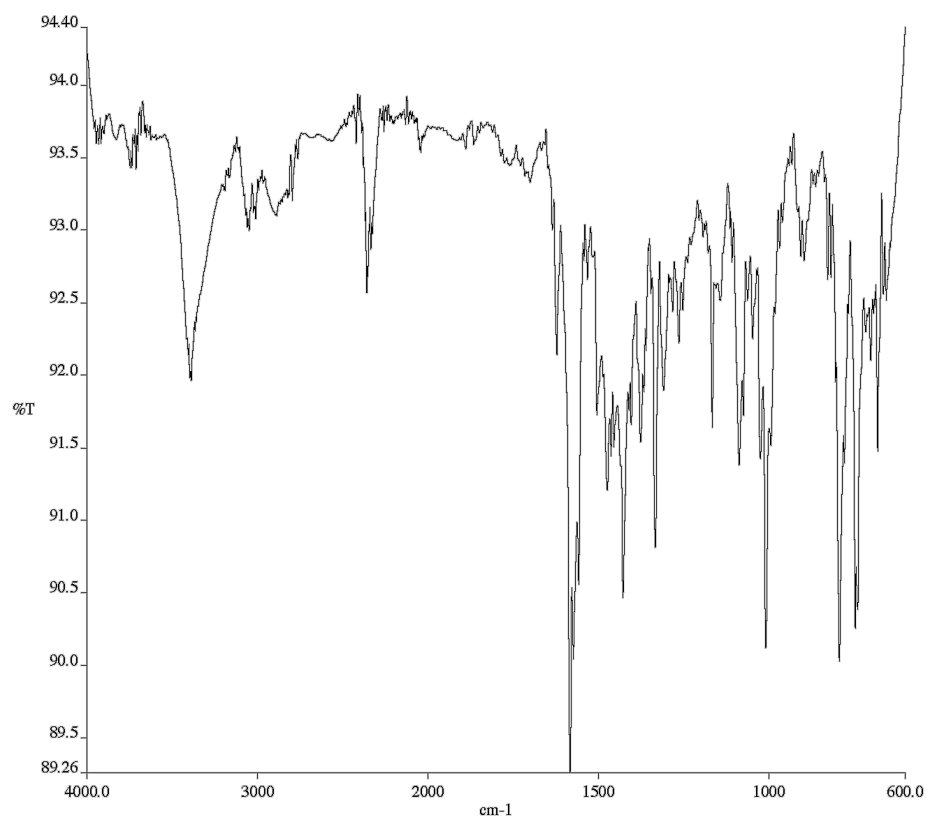


Figure A11.163 Infrared spectrum (Thin Film, NaCl) of compound

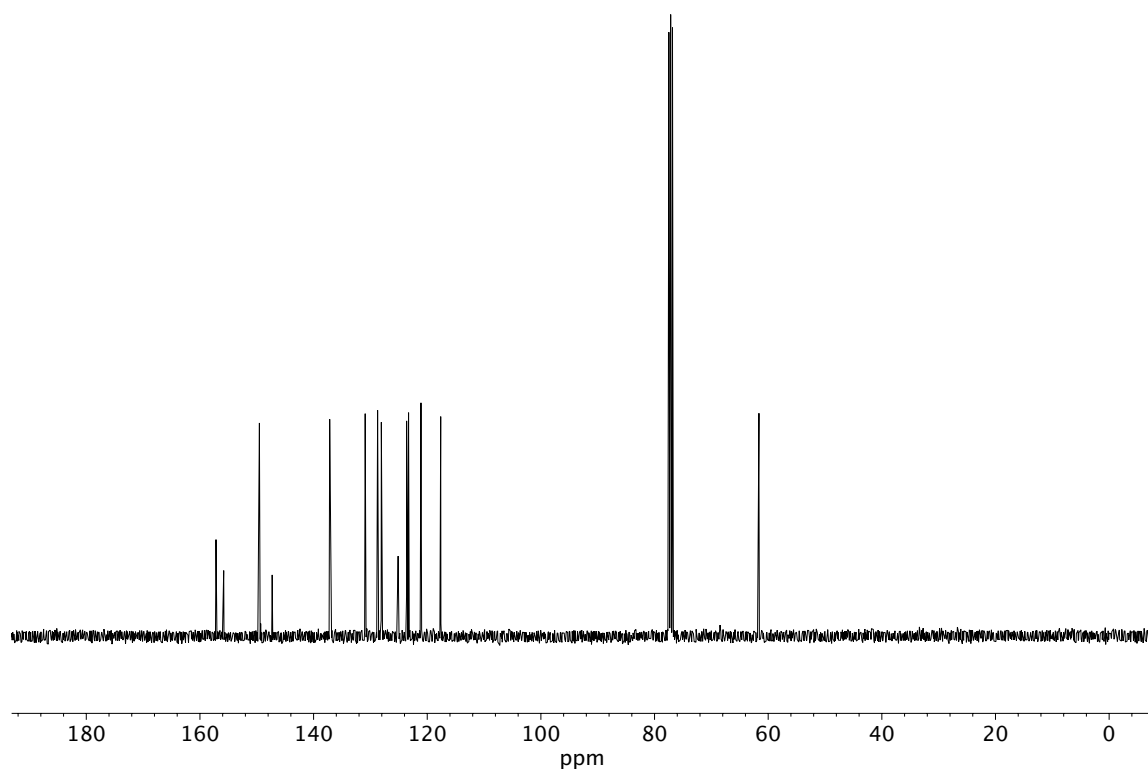


Figure A11.164 ¹³C NMR (100 MHz, CDCl₃) of compound **182r**.

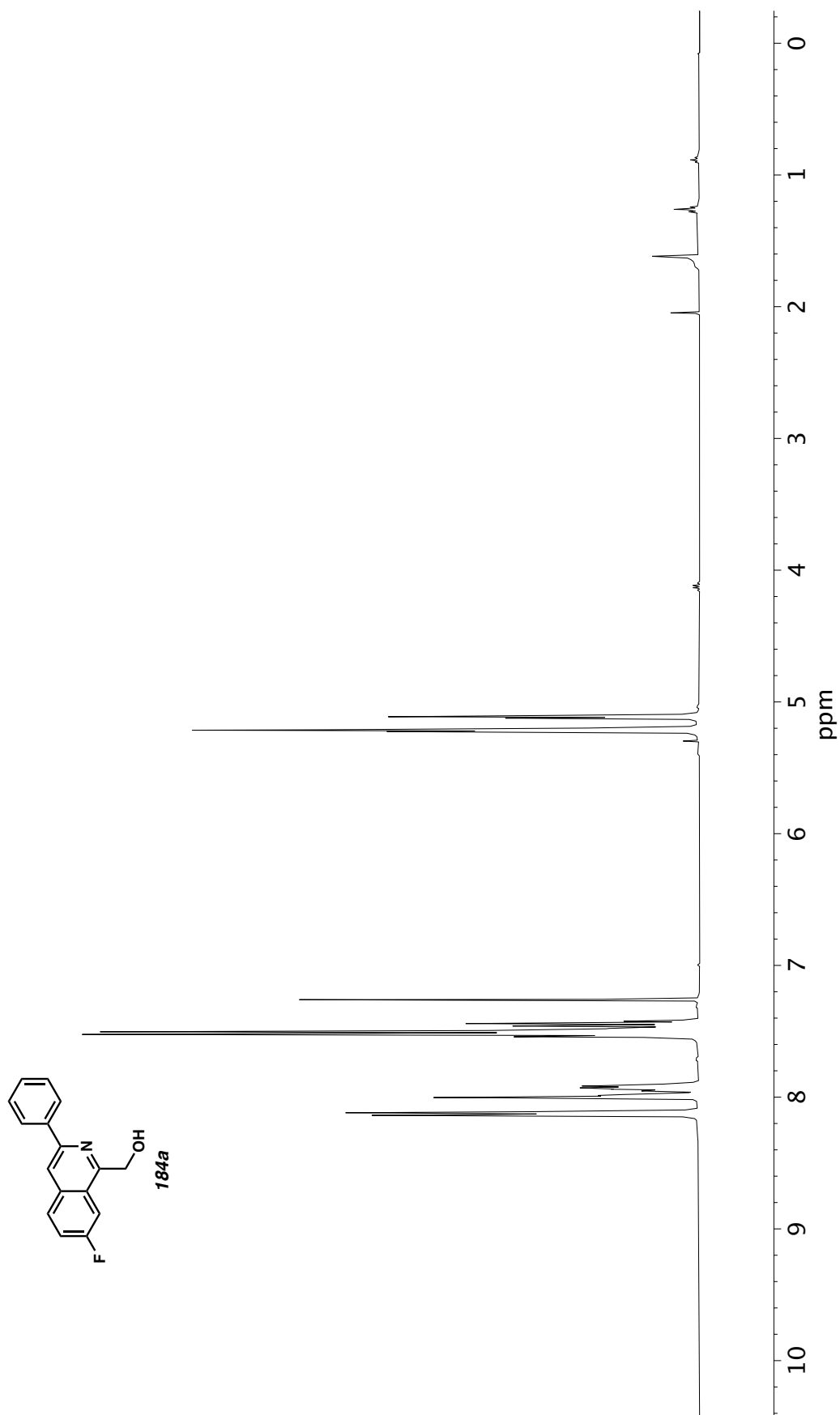


Figure A11.165 ¹H NMR (400 MHz, CDCl₃) of compound **184a**.

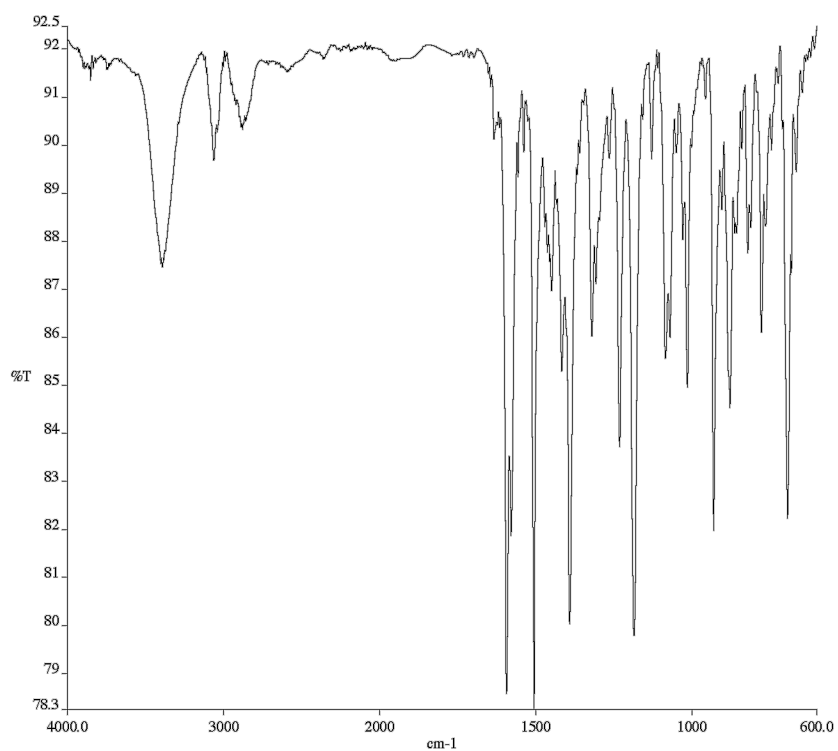


Figure A11.166 Infrared spectrum (Thin Film, NaCl) of compound

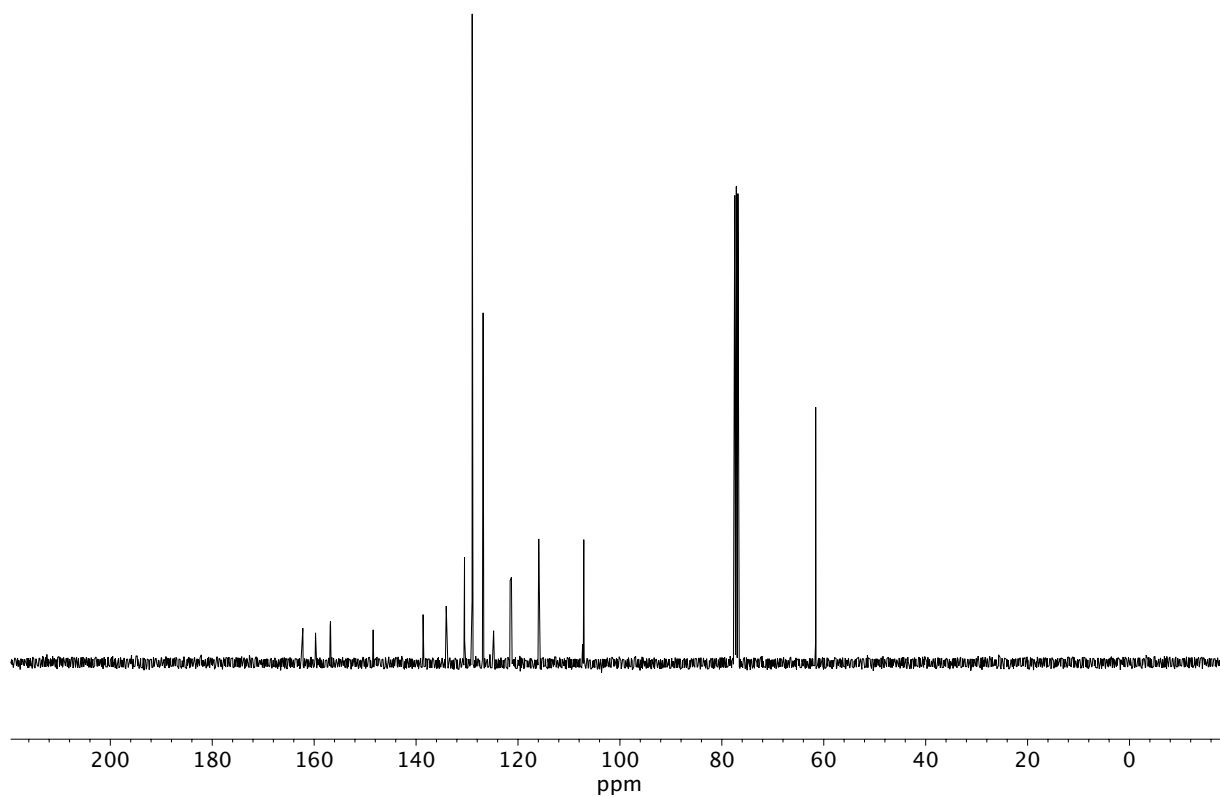


Figure A11.167 ¹³C NMR (100 MHz, CDCl₃) of compound **184a**.

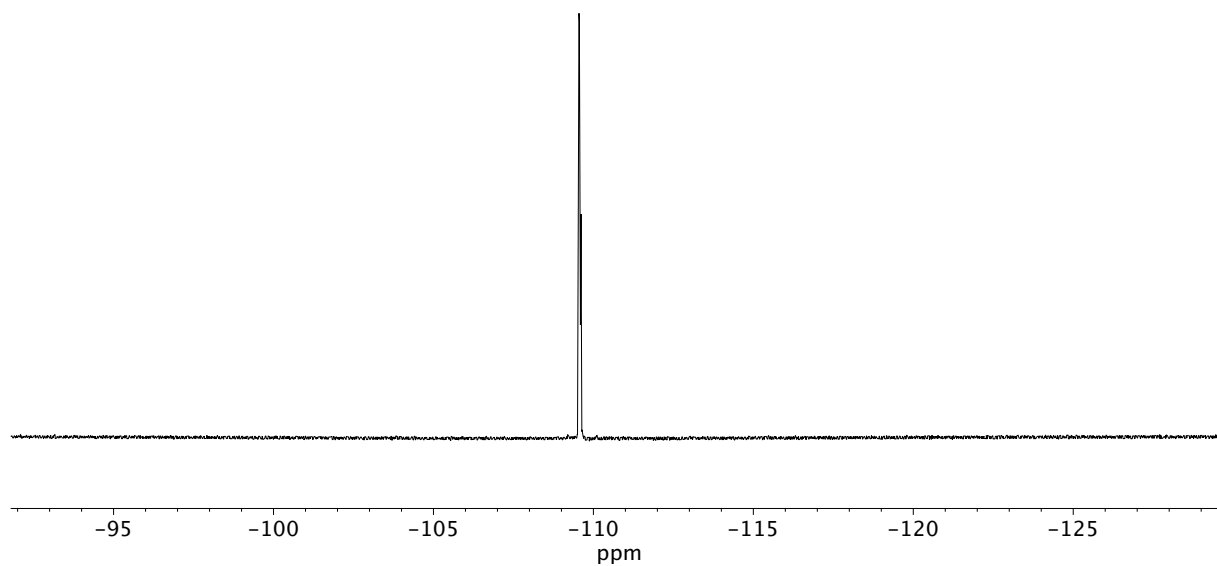


Figure A11.168 ^{19}F NMR (282 MHz, CDCl_3) of compound **184a**.

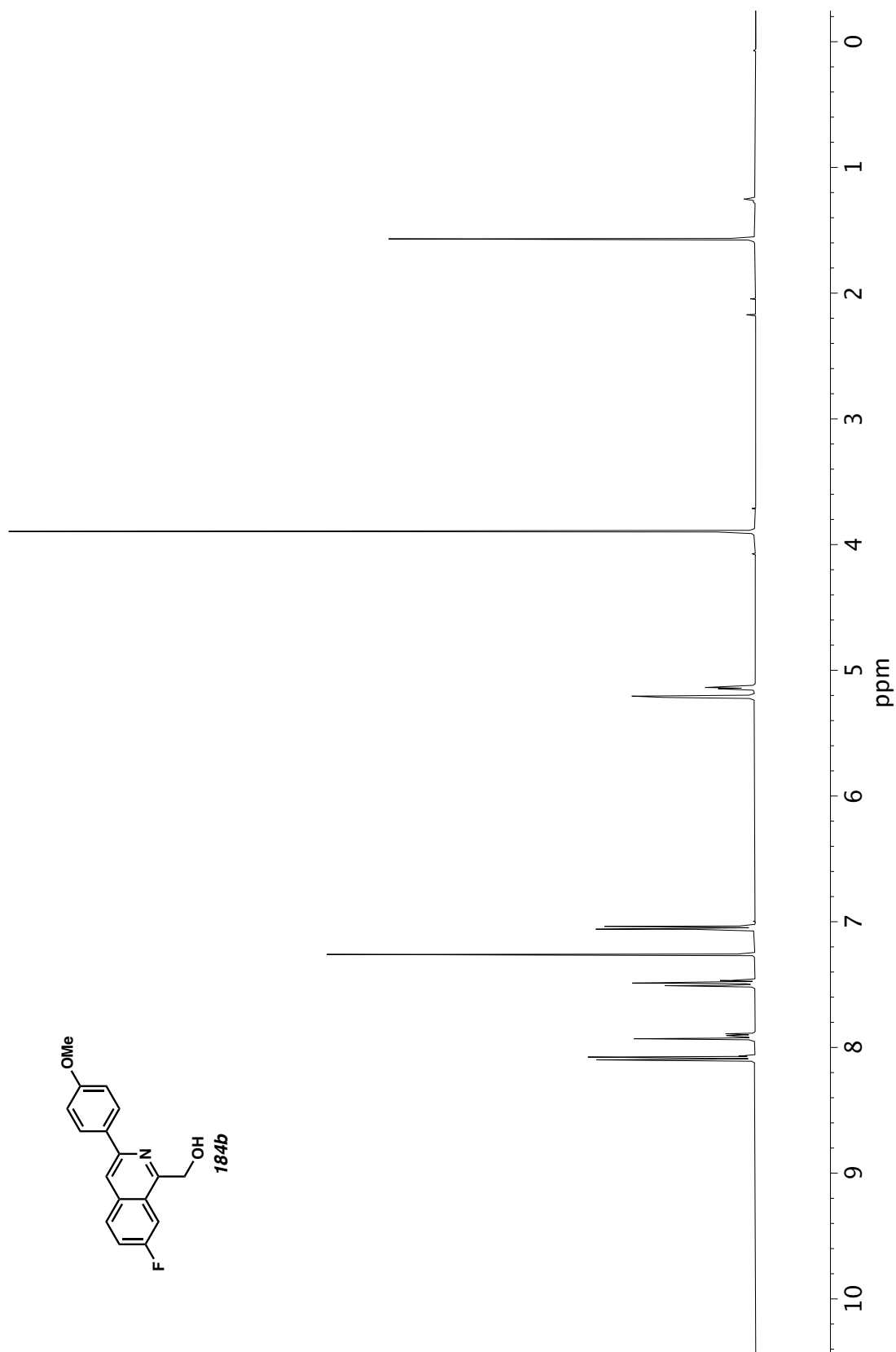


Figure A11.169 ^1H NMR (400 MHz, CDCl_3) of compound **184b**.

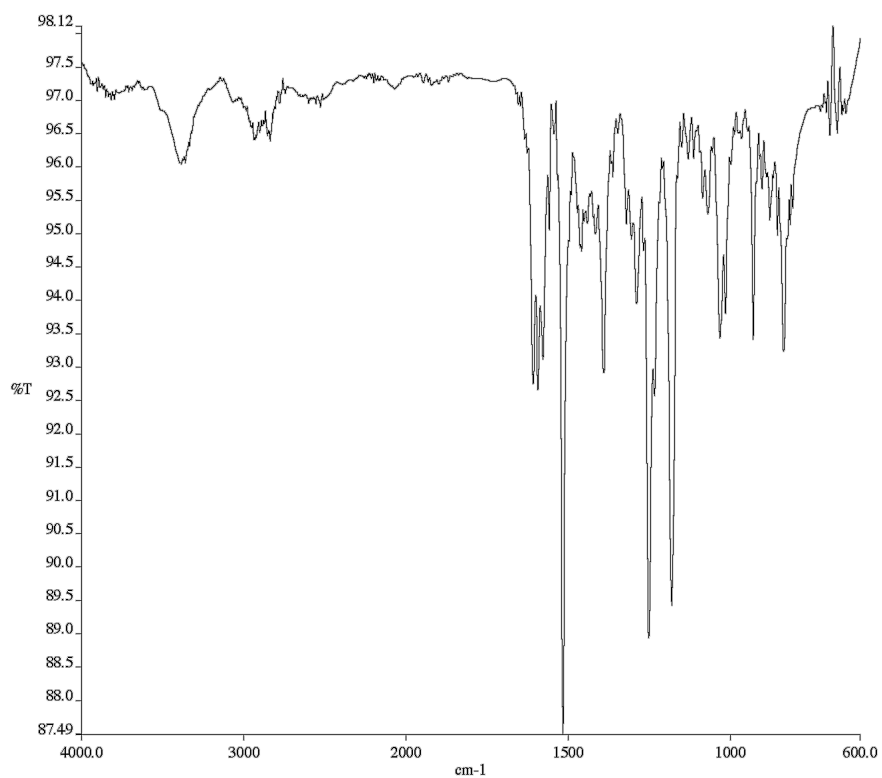


Figure A11.170 Infrared spectrum (Thin Film, NaCl) of compound

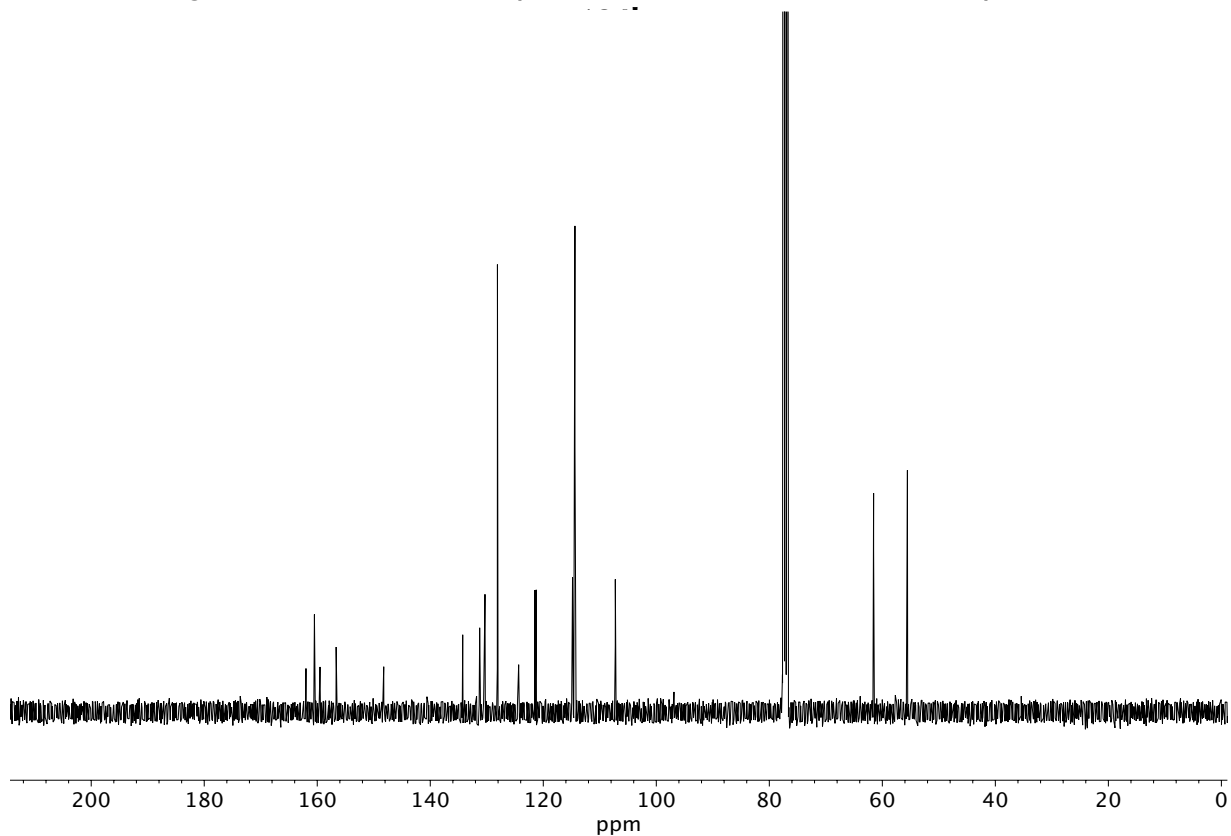


Figure A11.171 ¹³C NMR (100 MHz, CDCl₃) of compound **184b**.

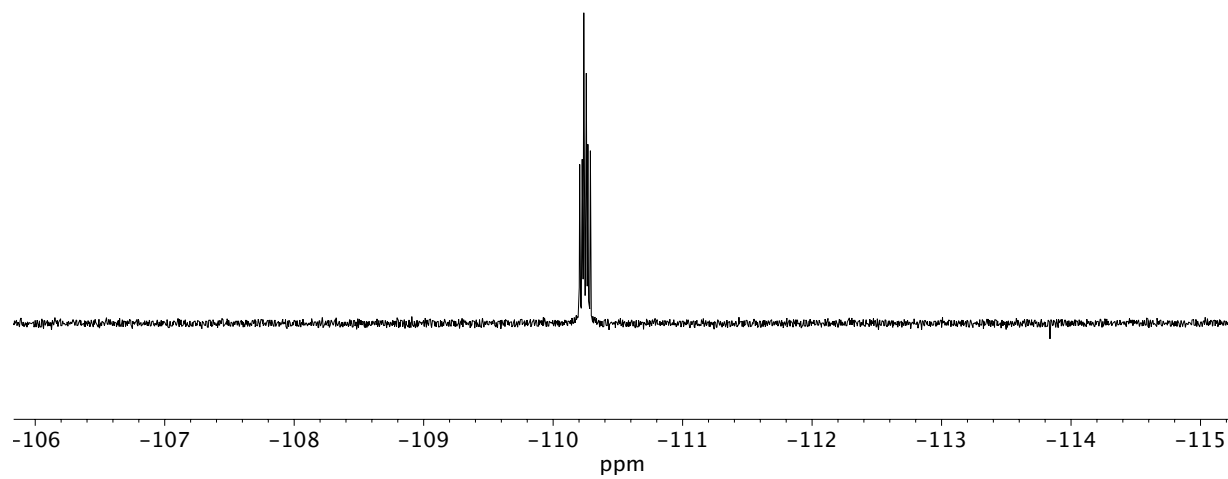


Figure A11.172 ^{19}F NMR (282 MHz, CDCl_3) of compound **184b**.

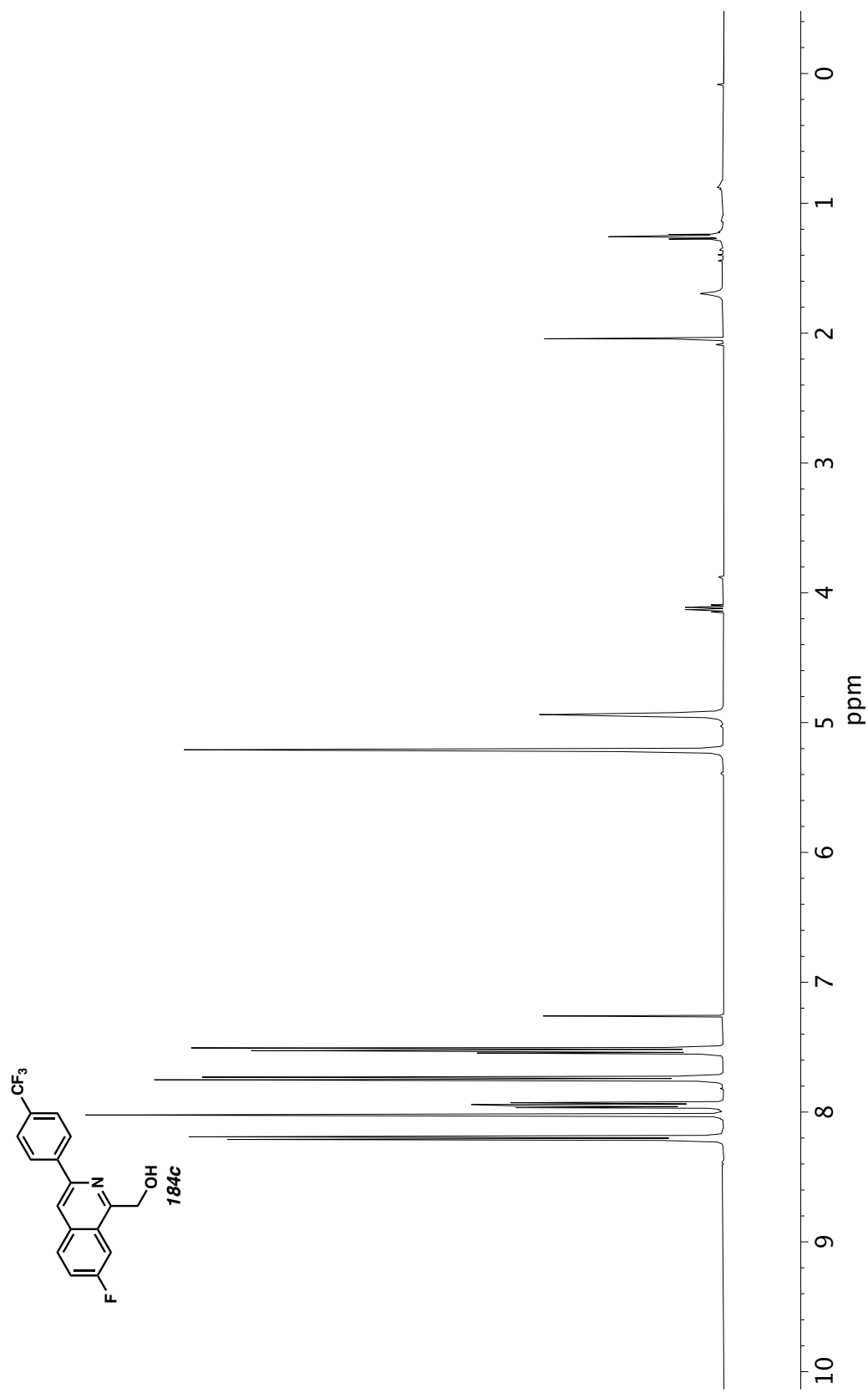


Figure A11.173 ¹H NMR (400 MHz, CDCl₃) of compound **184c**.

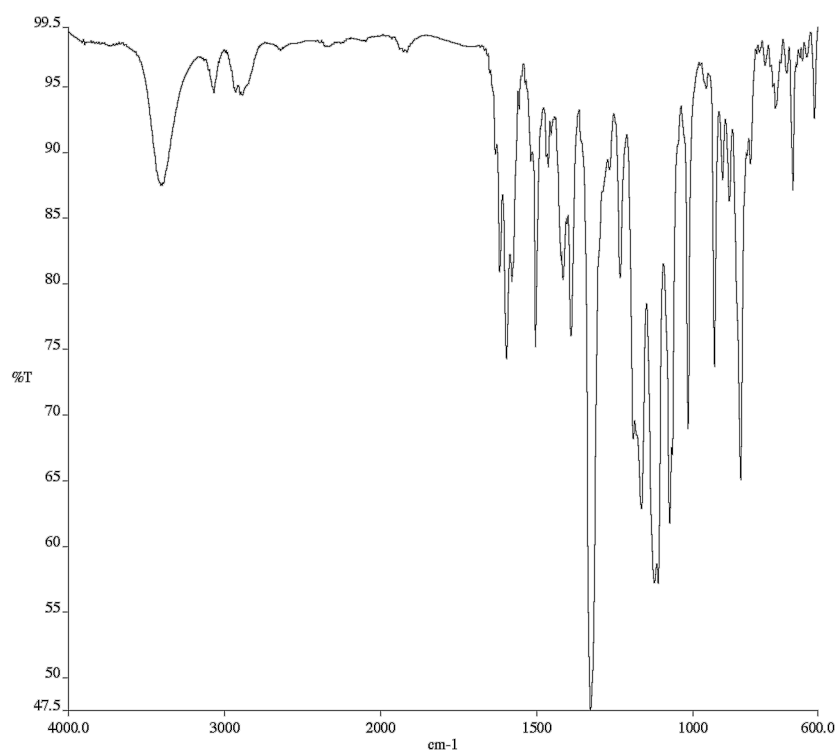


Figure A11.174 Infrared spectrum (Thin Film, NaCl) of compound

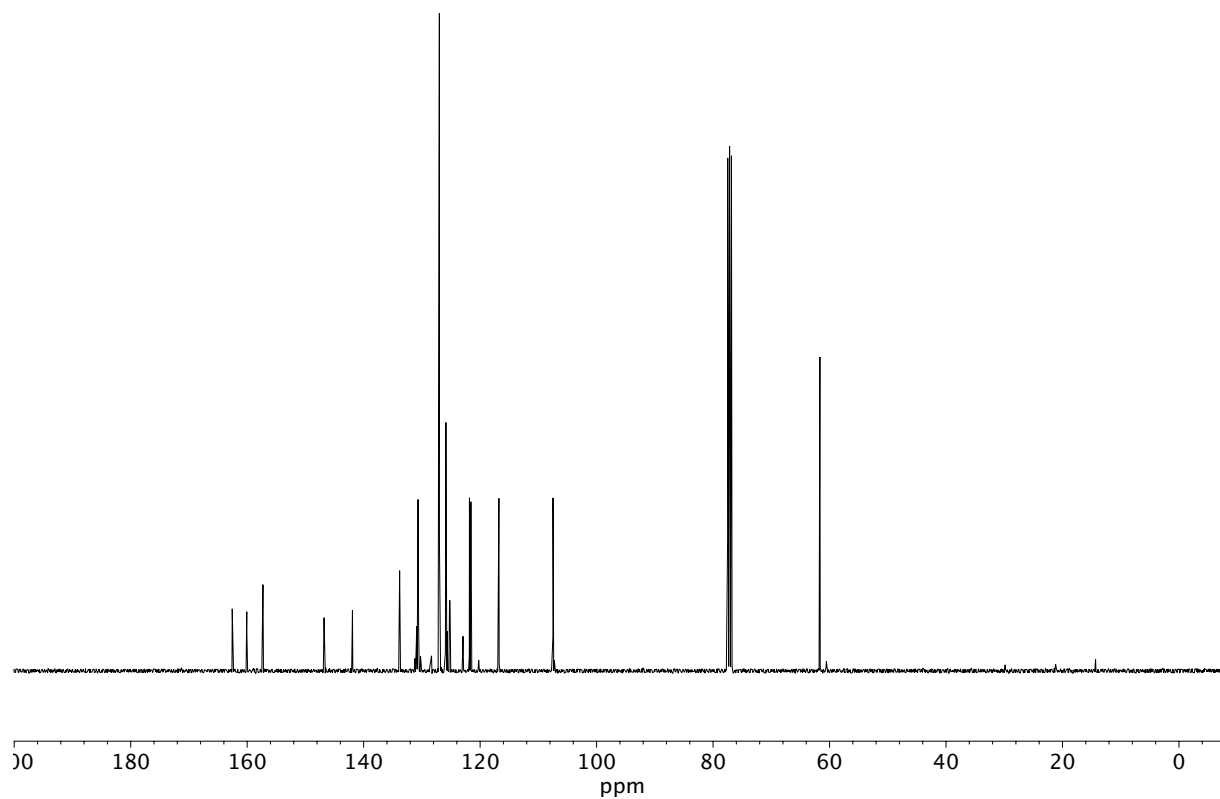


Figure A11.175 ¹³C NMR (100 MHz, CDCl₃) of compound **184c**.

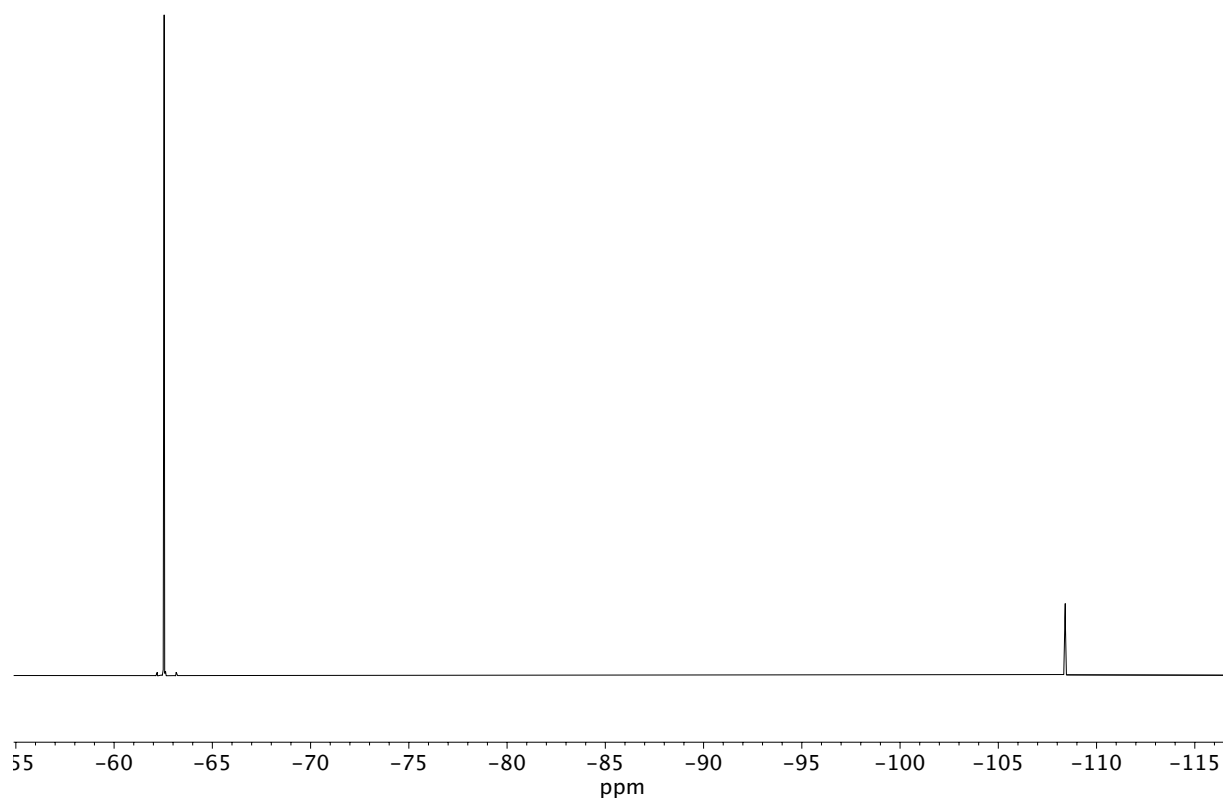


Figure A11.176 ^{19}F NMR (282 MHz, CDCl_3) of compound **184c**.

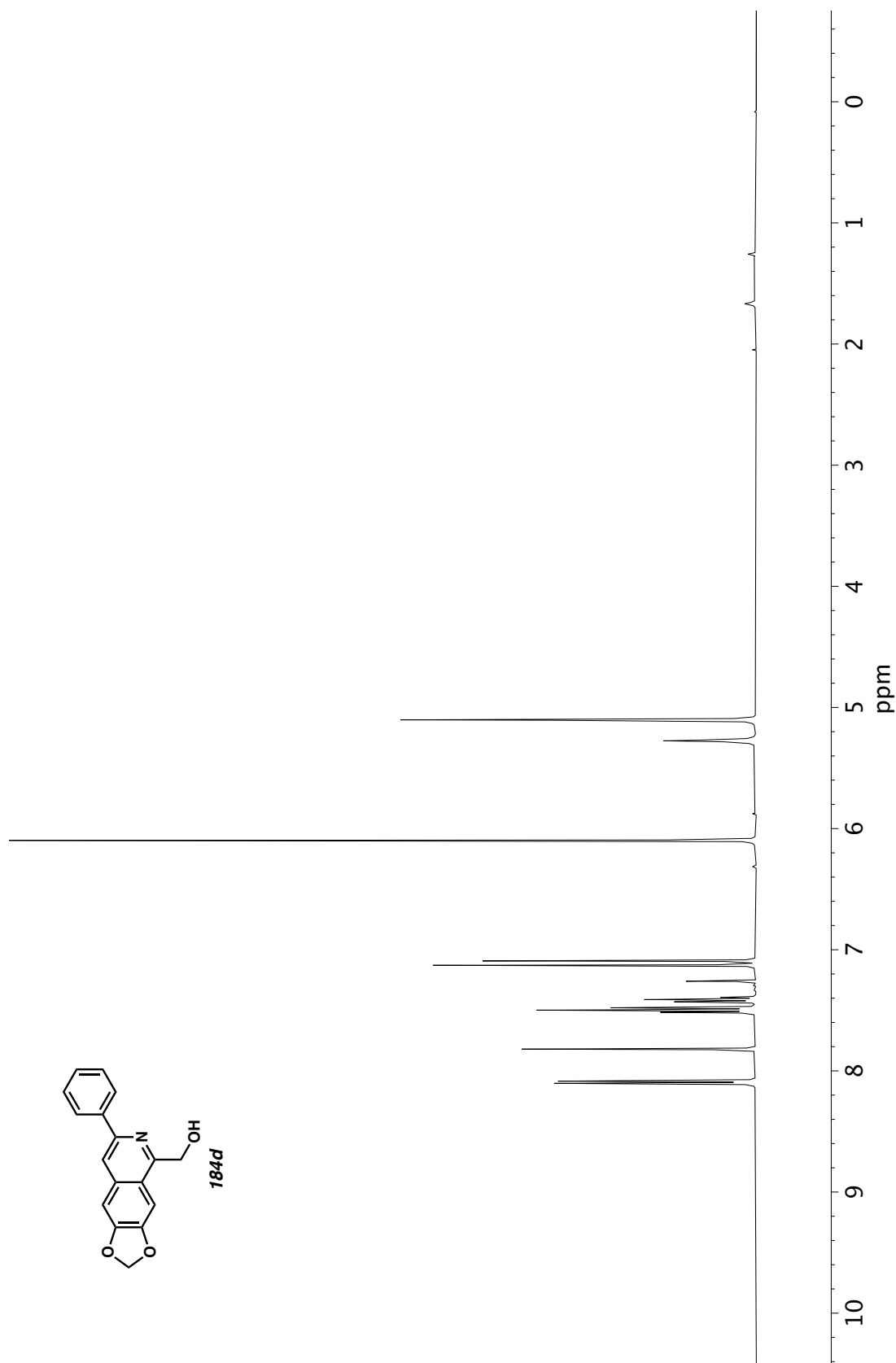


Figure A11.177 ^1H NMR (400 MHz, CDCl_3) of compound **184d**.

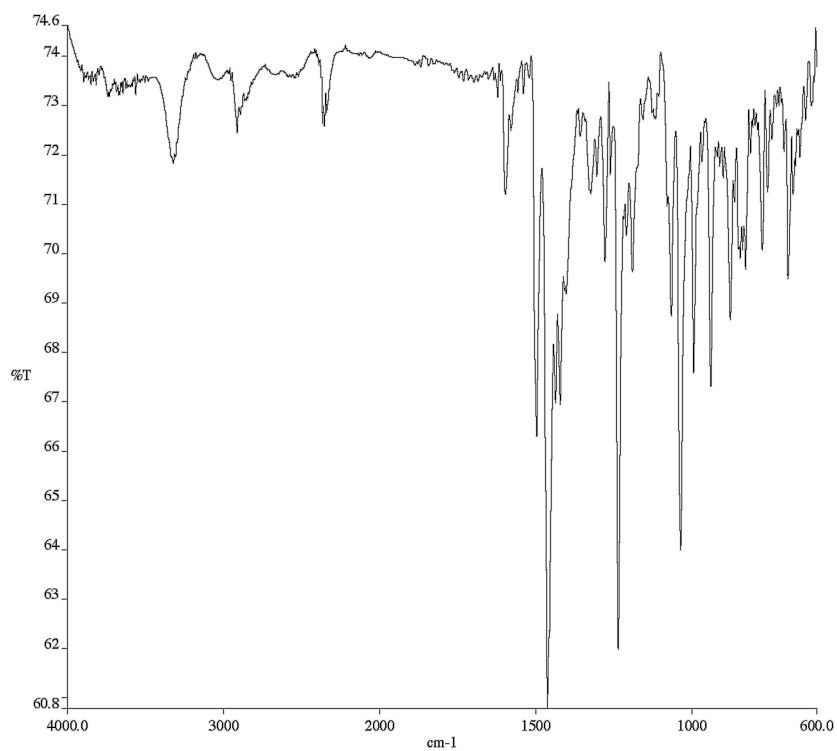


Figure A11.178 Infrared spectrum (Thin Film, NaCl) of compound

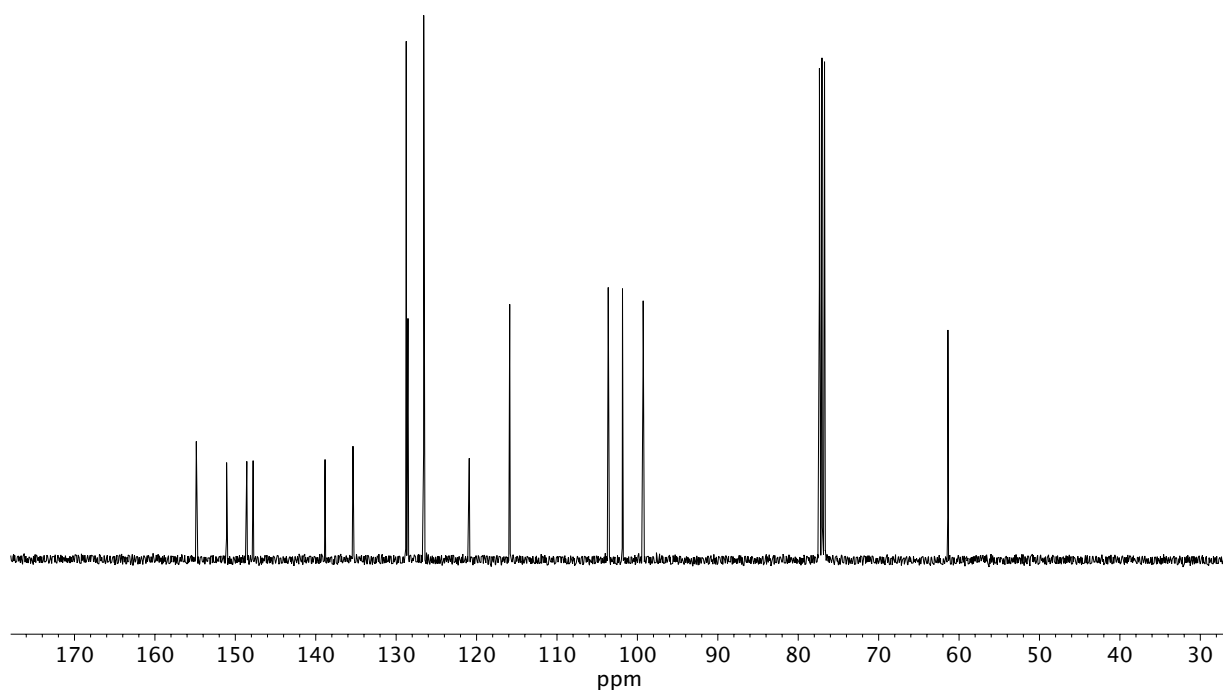


Figure A11.179 ¹³C NMR (100 MHz, CDCl₃) of compound **184d**.

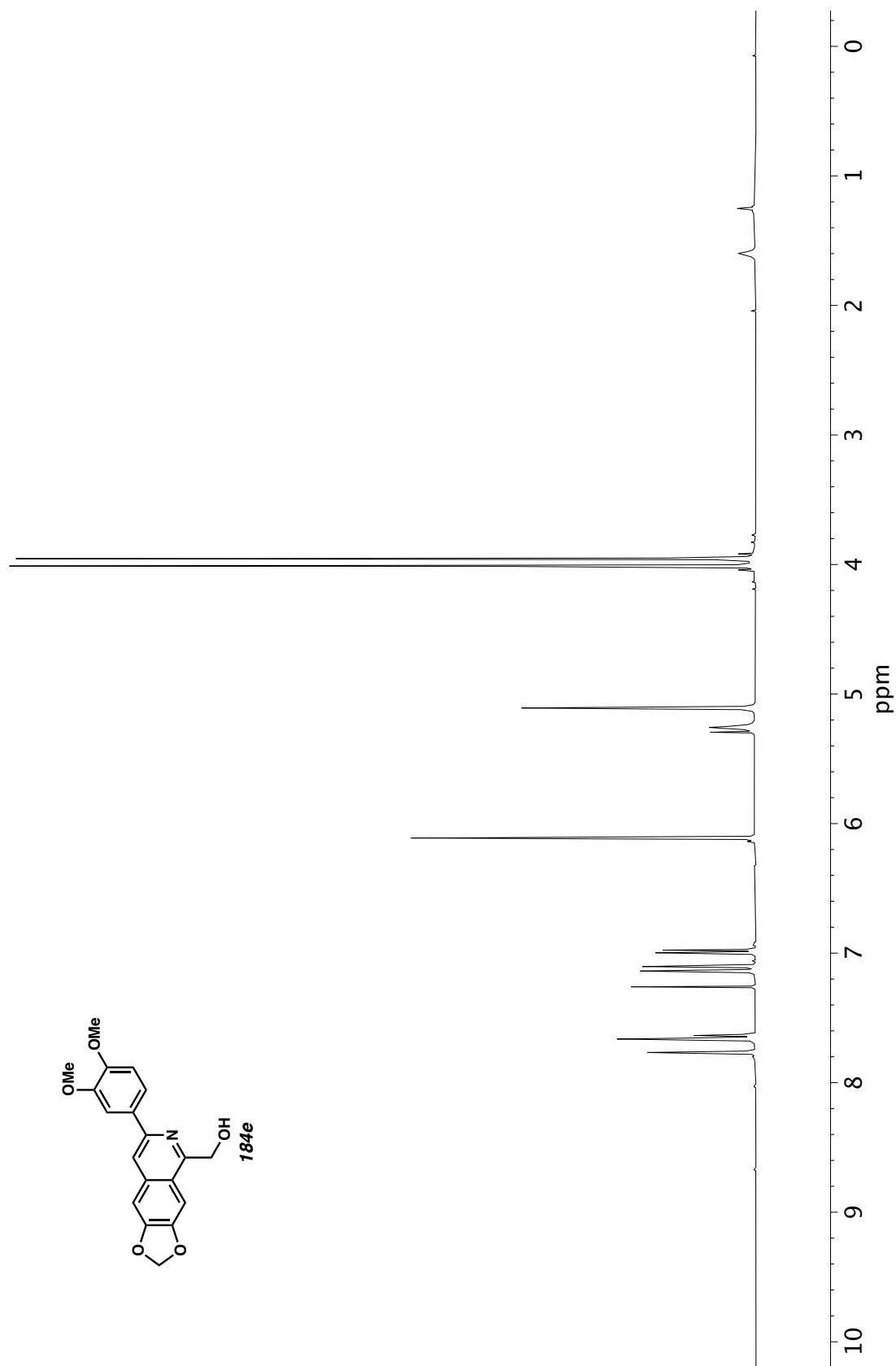


Figure A11.180 ^1H NMR (400 MHz, CDCl_3) of compound **184e**.

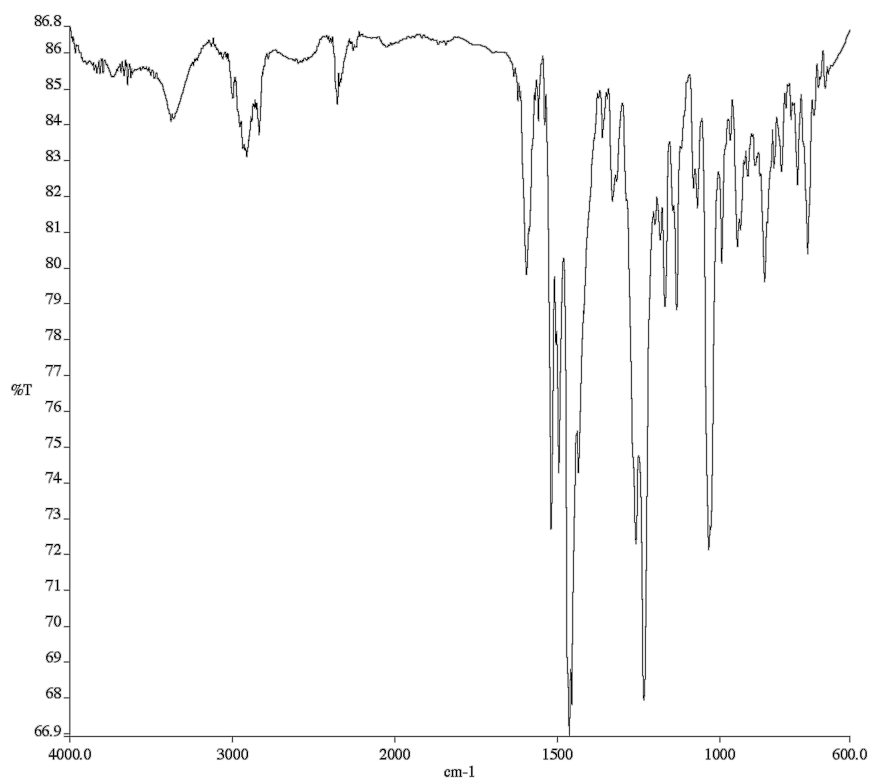


Figure A11.181 Infrared spectrum (Thin Film, NaCl) of compound

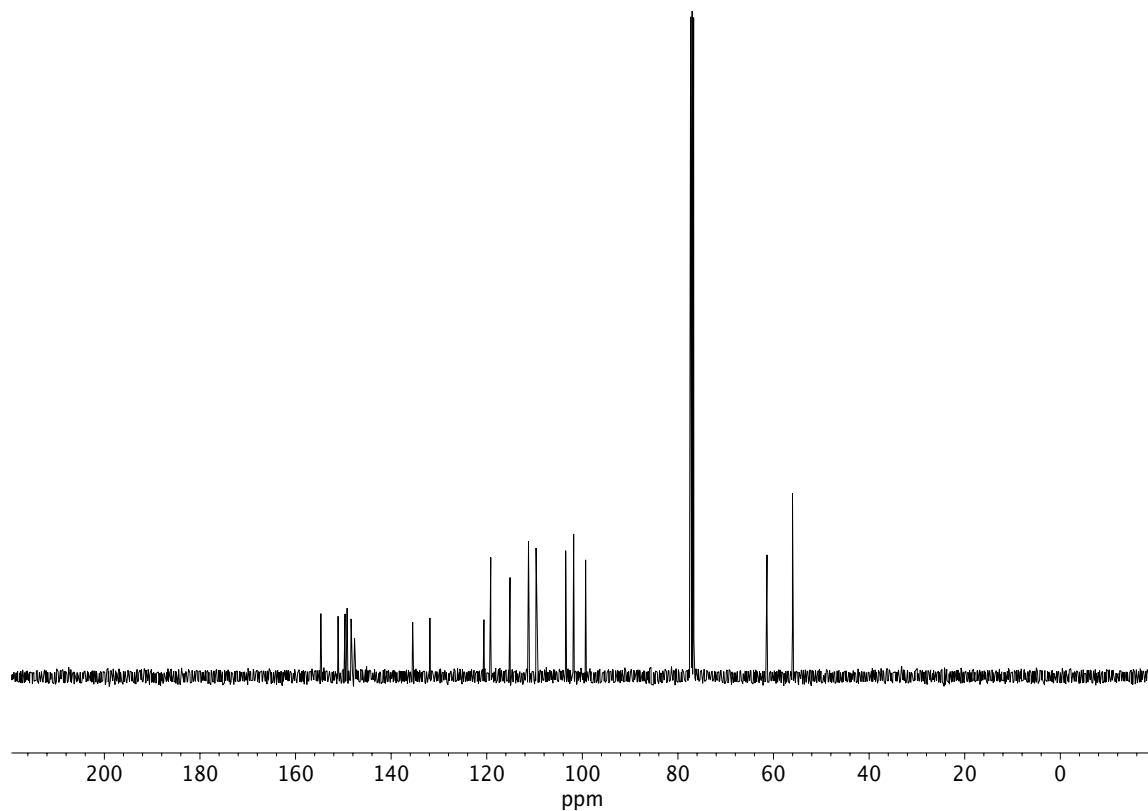


Figure A11.182 ¹³C NMR (100 MHz, CDCl₃) of compound **184e**.

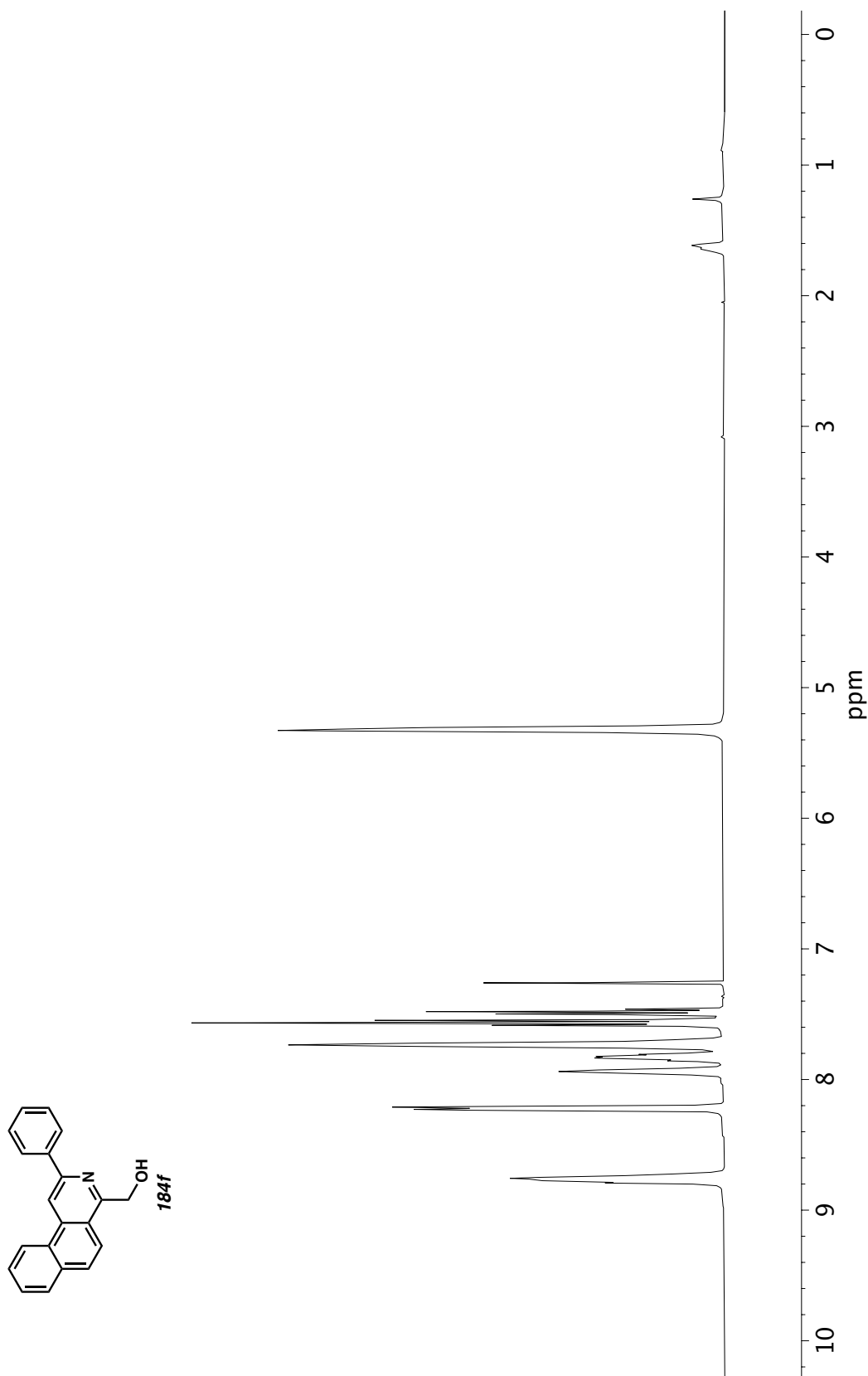


Figure A11.183 ¹H NMR (400 MHz, CDCl₃) of compound **184f**.

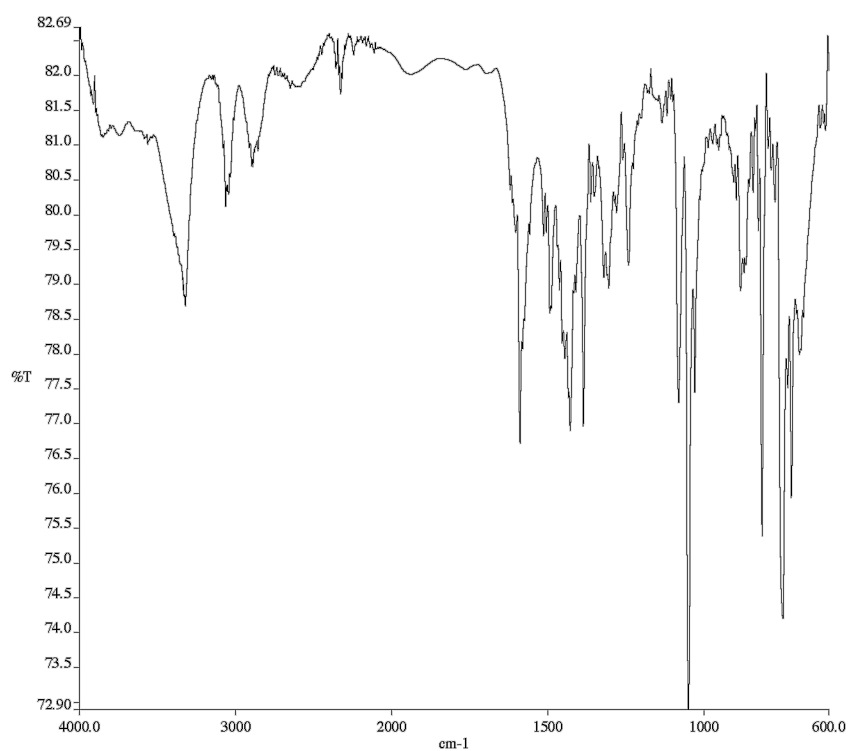


Figure A11.184 Infrared spectrum (Thin Film, NaCl) of compound

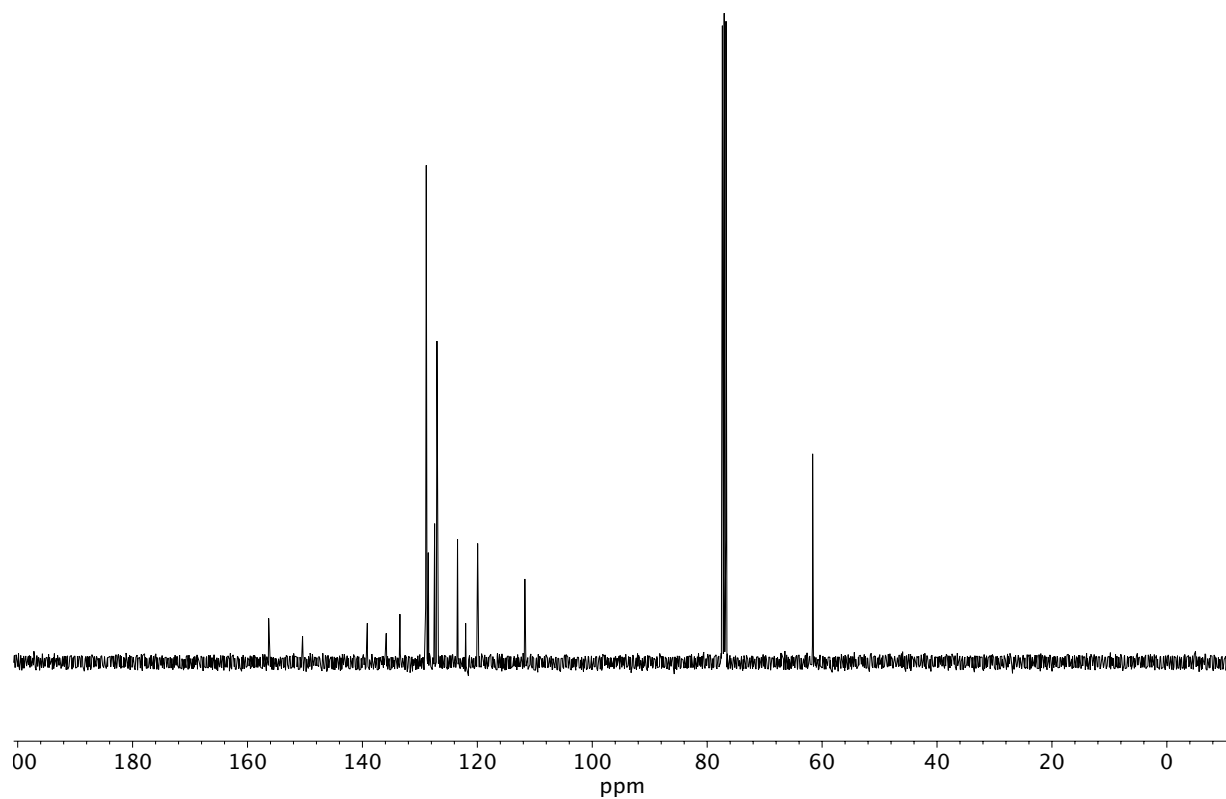


Figure A11.185 ¹³C NMR (100 MHz, CDCl₃) of compound **184f**.

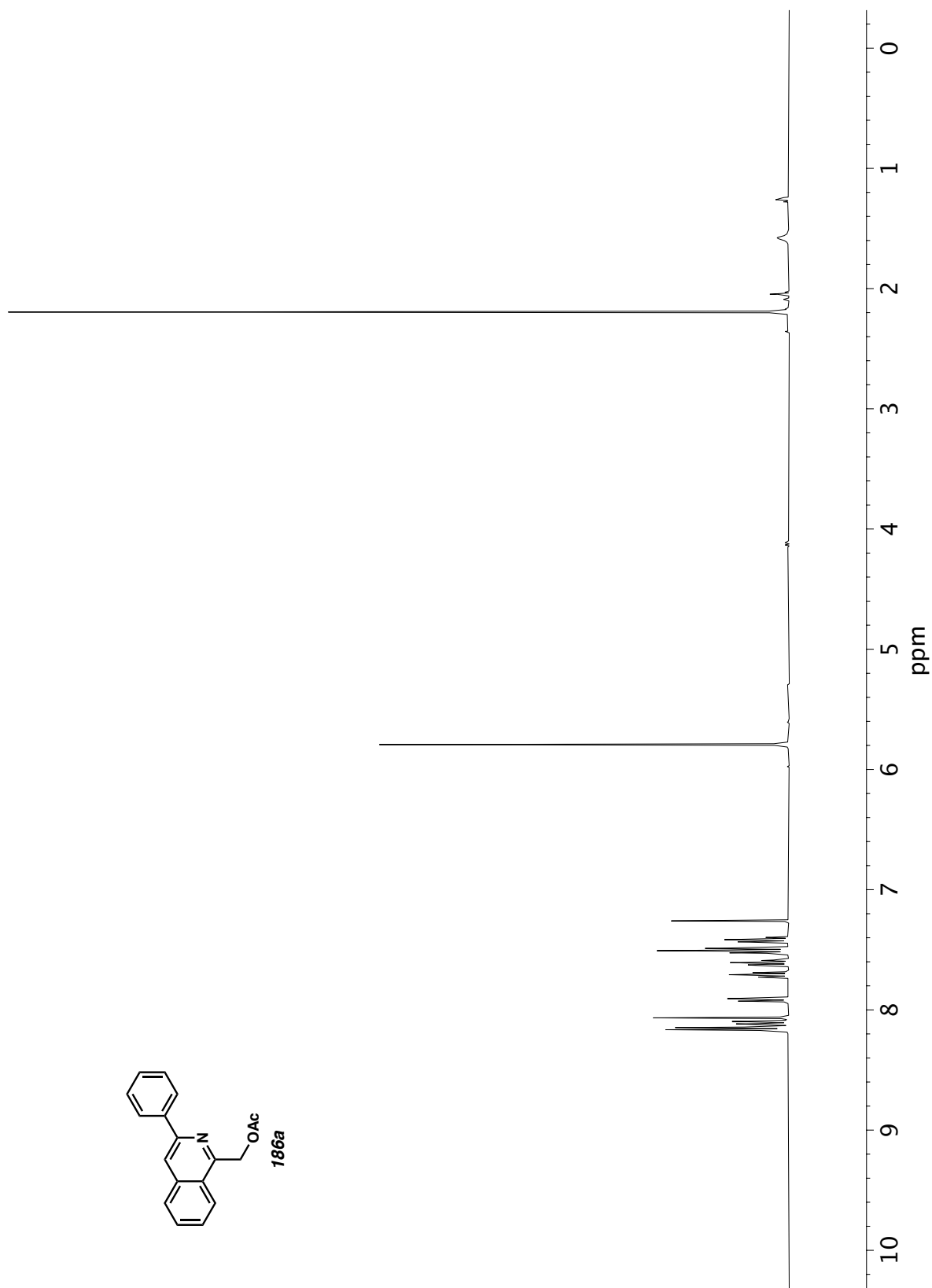


Figure A11.186 ^1H NMR (400 MHz, CDCl_3) of compound **186a**.

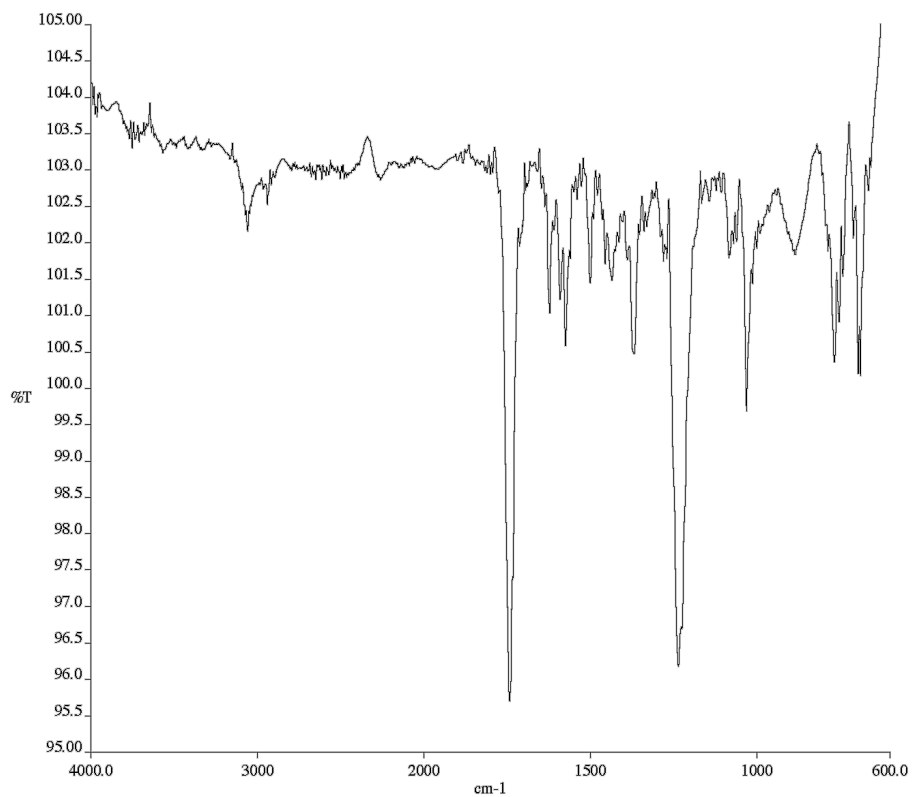


Figure A11.187 Infrared spectrum (Thin Film, NaCl) of compound

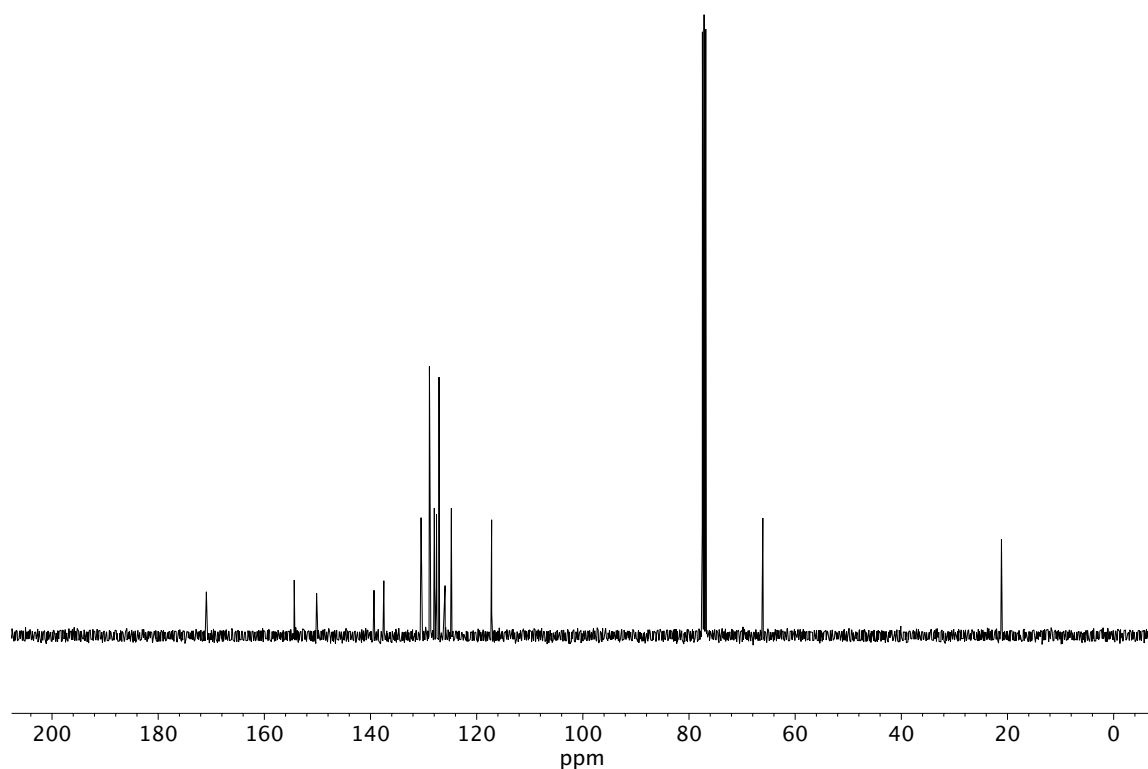


Figure A11.188 ¹³C NMR (100 MHz, CDCl₃) of compound **186a**.

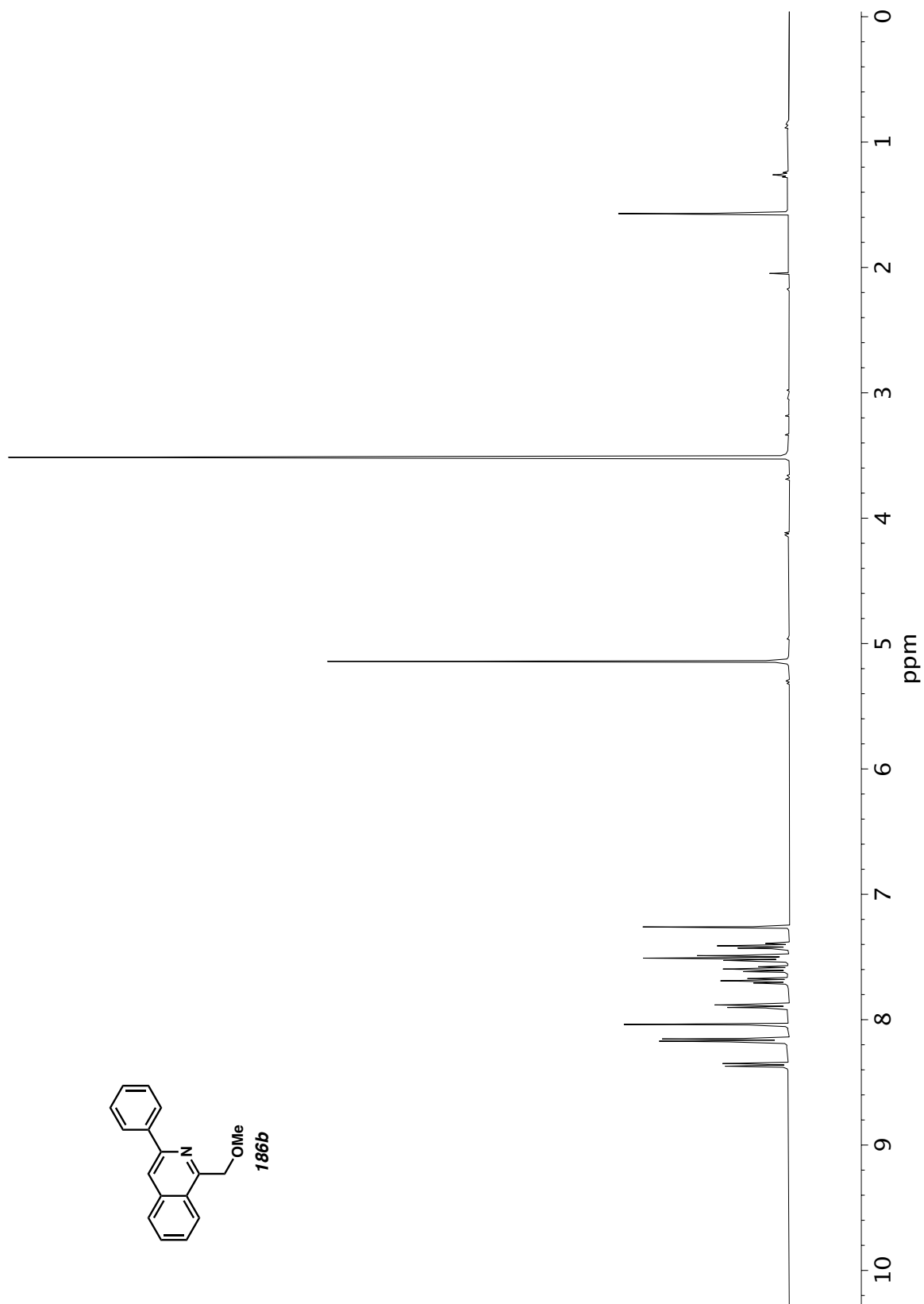


Figure A11.189 ^1H NMR (400 MHz, CDCl_3) of compound **186b**.

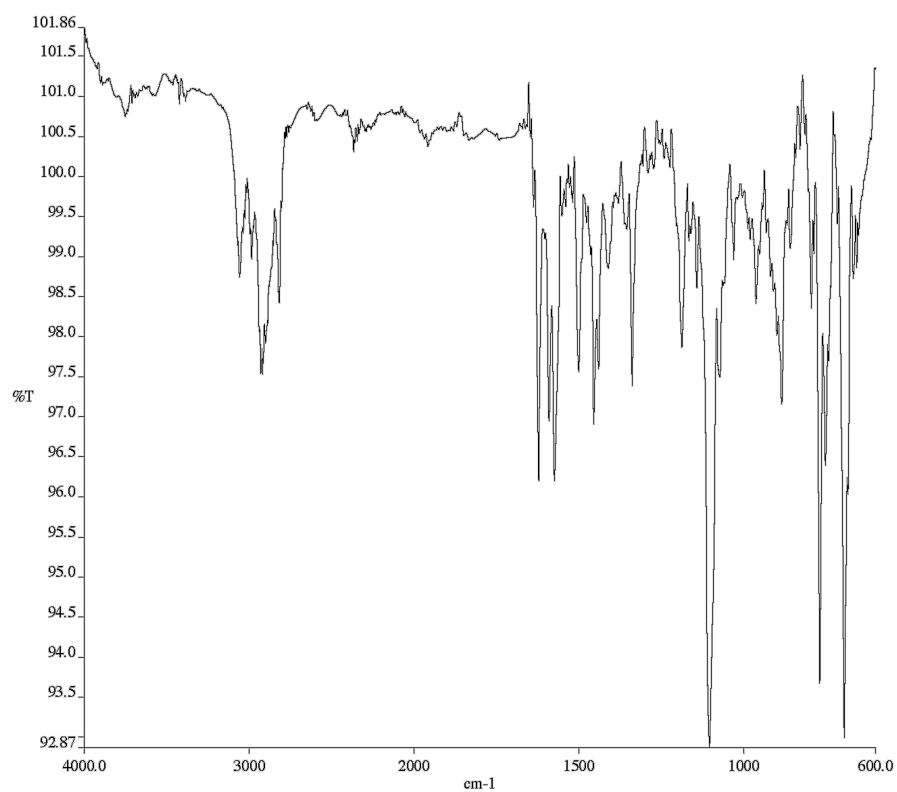


Figure A11.190 Infrared spectrum (Thin Film, NaCl) of compound

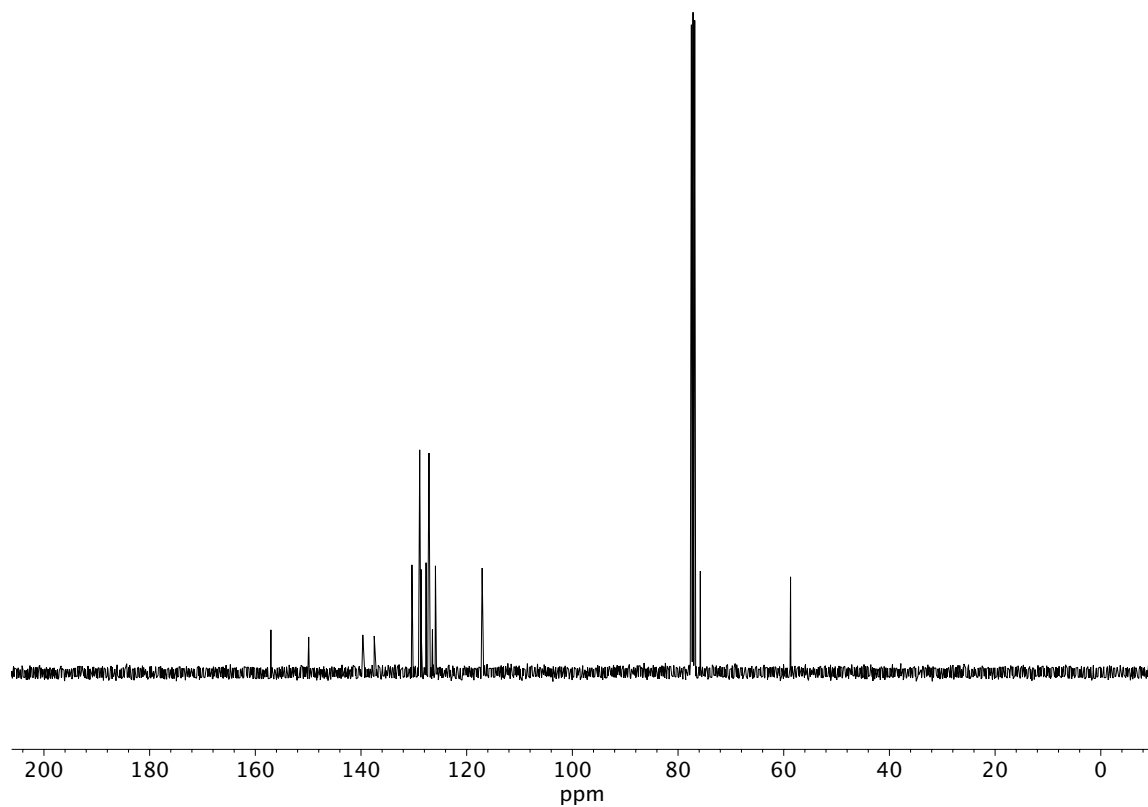


Figure A11.191 ¹³C NMR (100 MHz, CDCl₃) of compound **186b**.

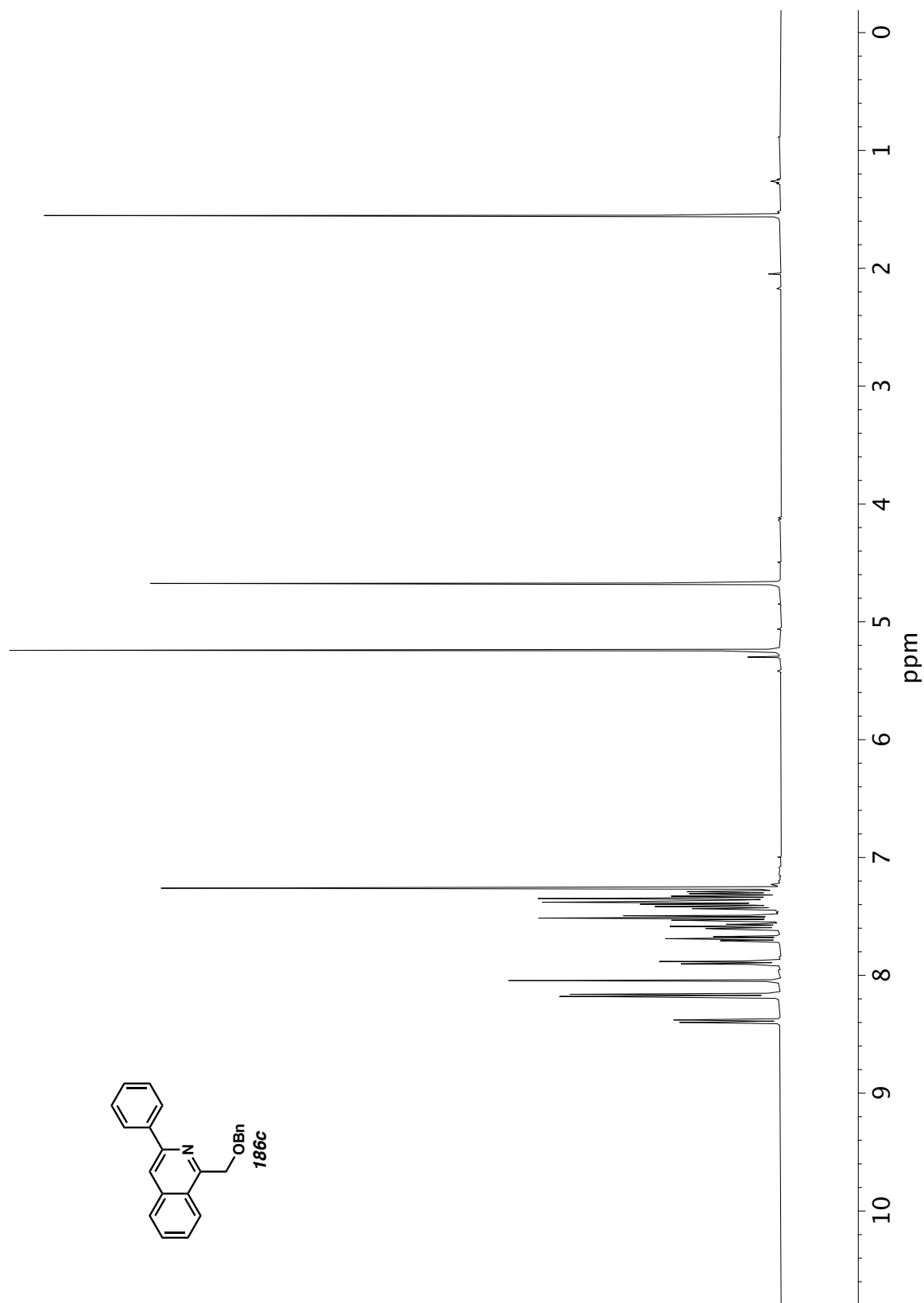


Figure A11.192 ¹H NMR (400 MHz, CDCl₃) of compound **186c**.

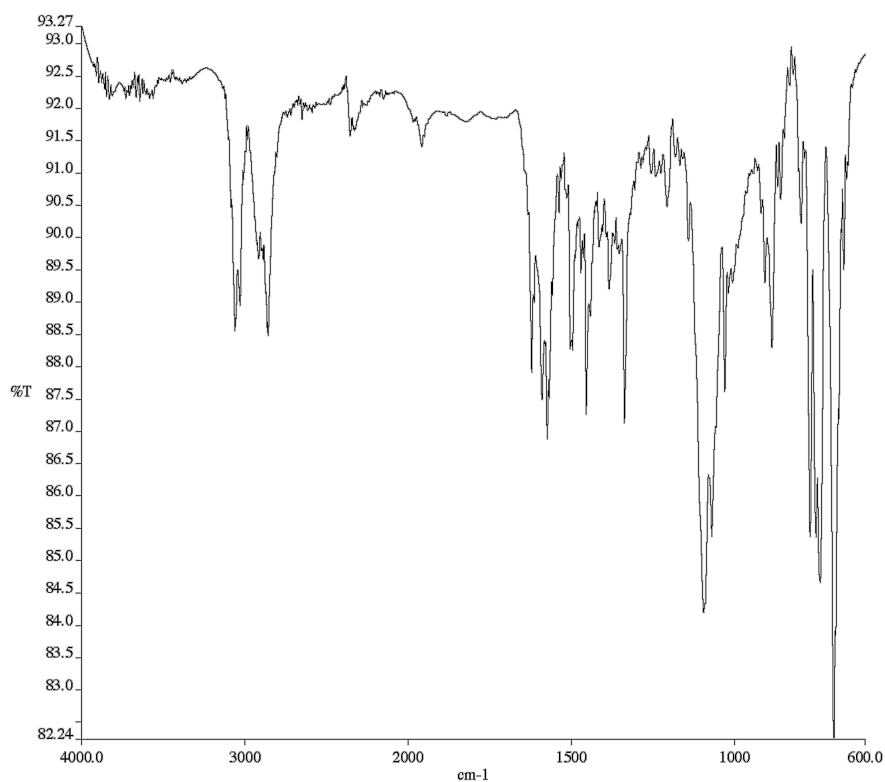


Figure A11.193 Infrared spectrum (Thin Film, NaCl) of compound

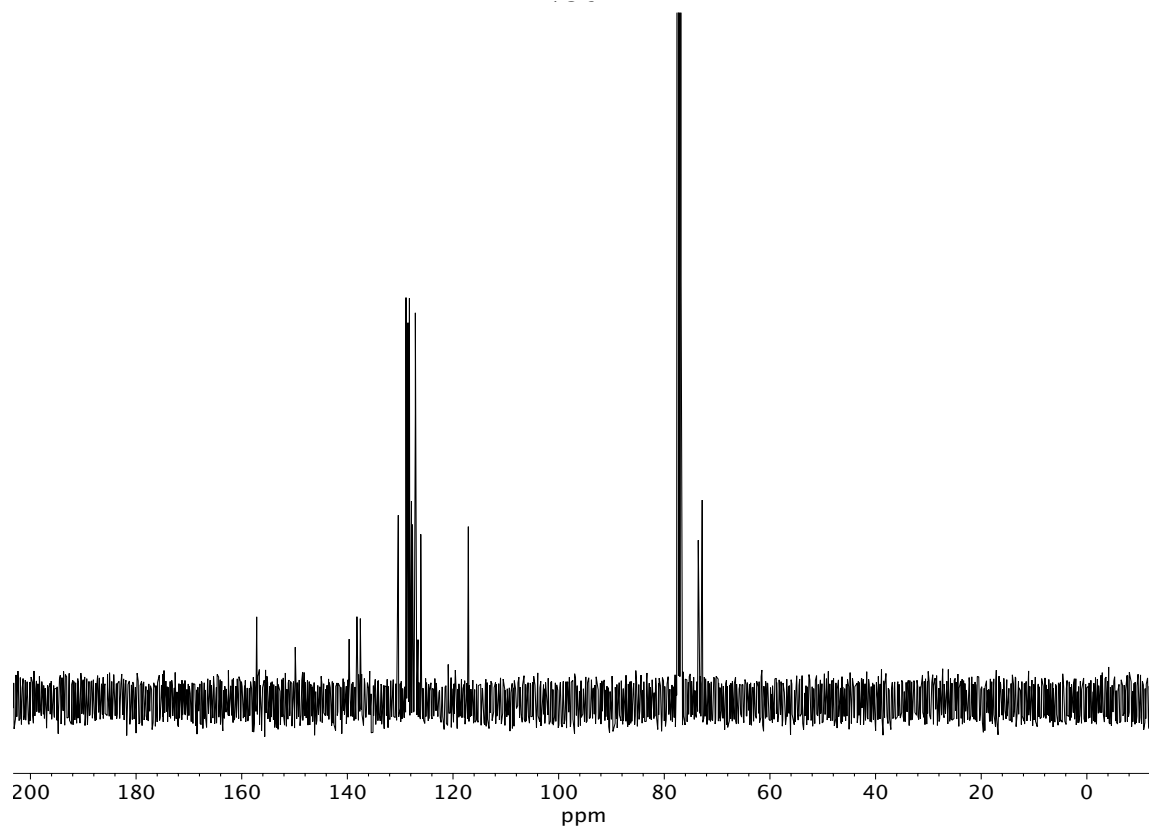


Figure A11.194 ¹³C NMR (100 MHz, CDCl₃) of compound **186c**.

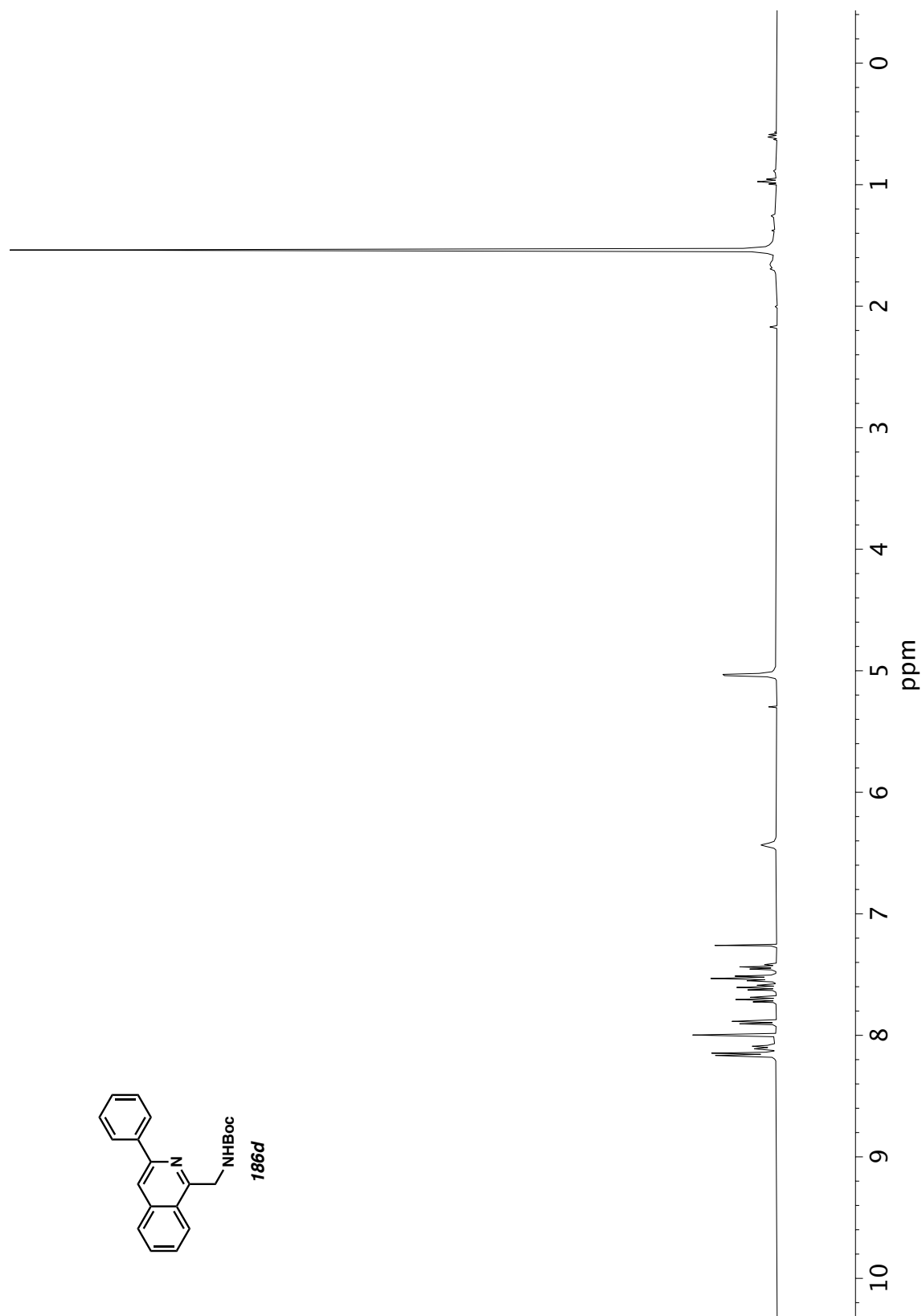


Figure A11.195 ^1H NMR (400 MHz, CDCl_3) of compound **186d**.

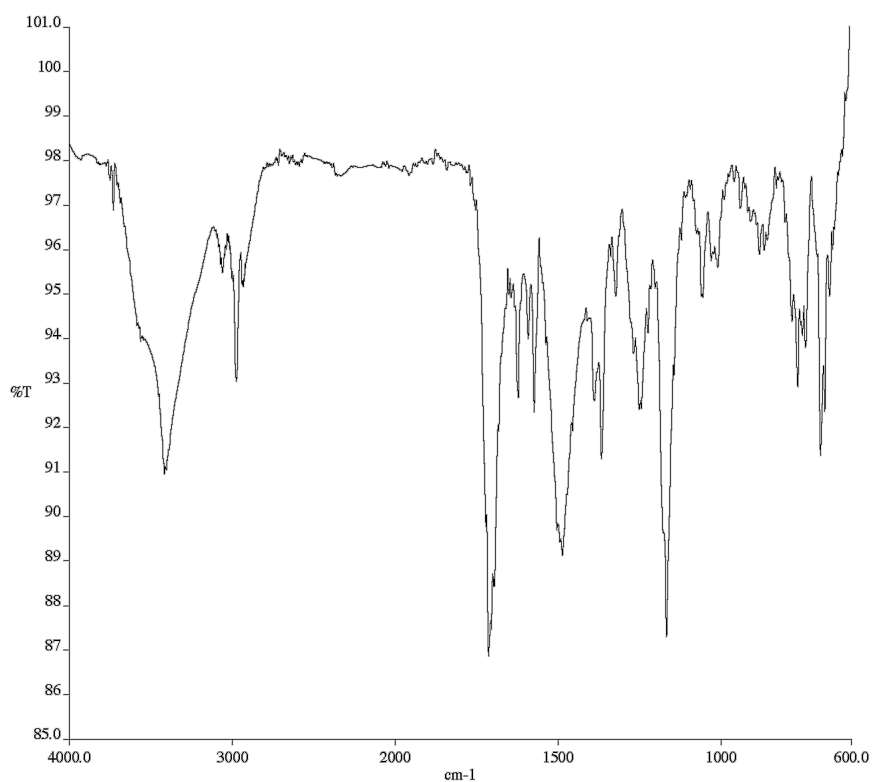


Figure A11.196 Infrared spectrum (Thin Film, NaCl) of compound

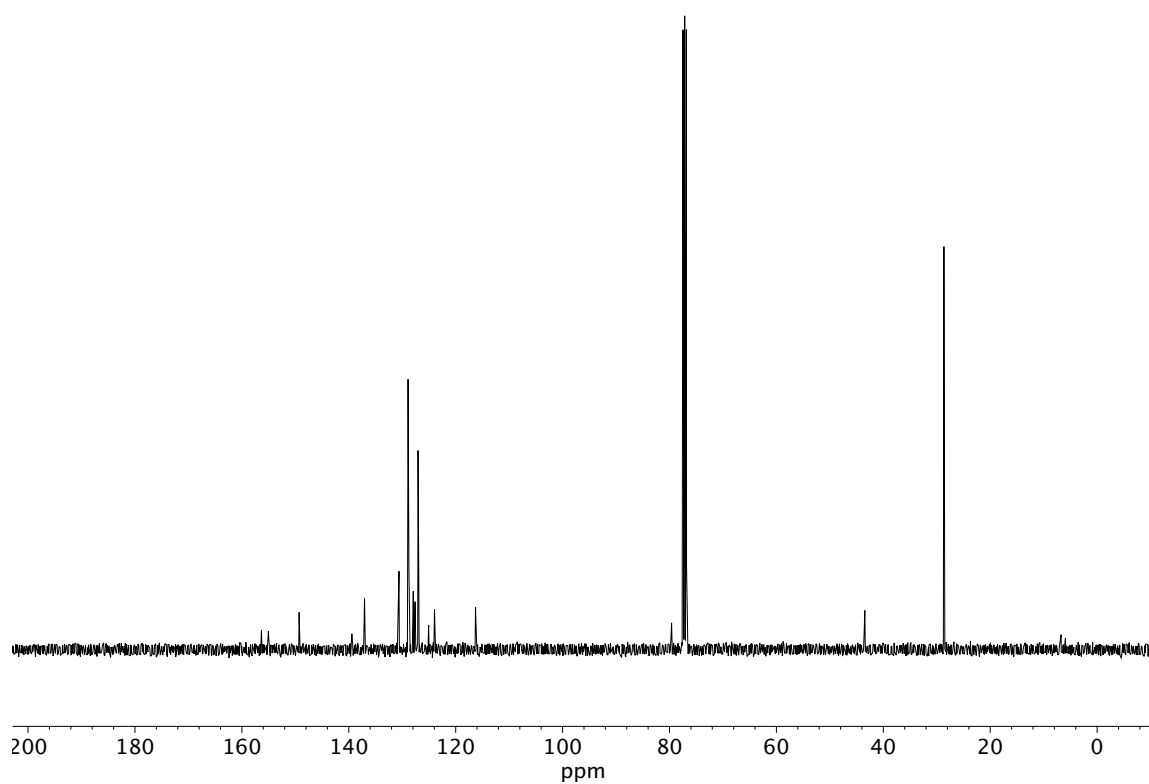


Figure A11.197 ¹³C NMR (100 MHz, CDCl₃) of compound **186d**.

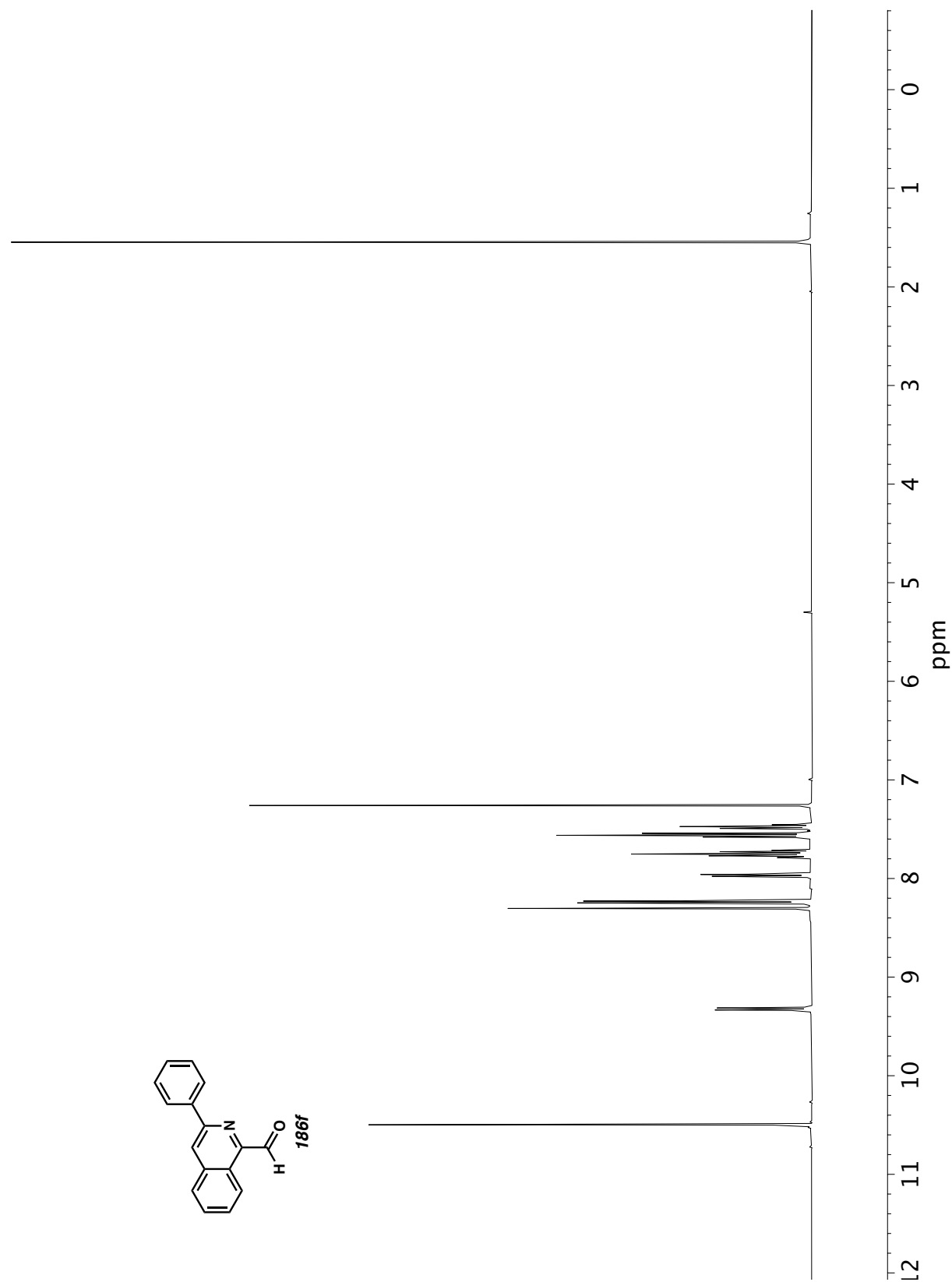


Figure A11.198 ^1H NMR (400 MHz, CDCl_3) of compound **186f**.

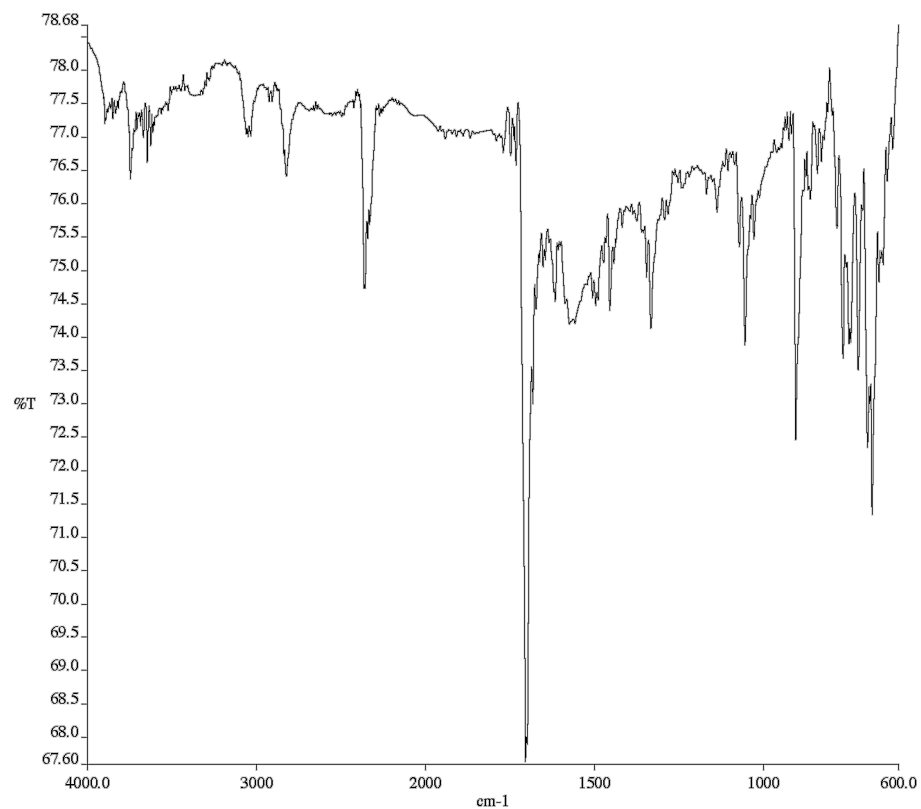


Figure A11.199 Infrared spectrum (Thin Film, NaCl) of compound

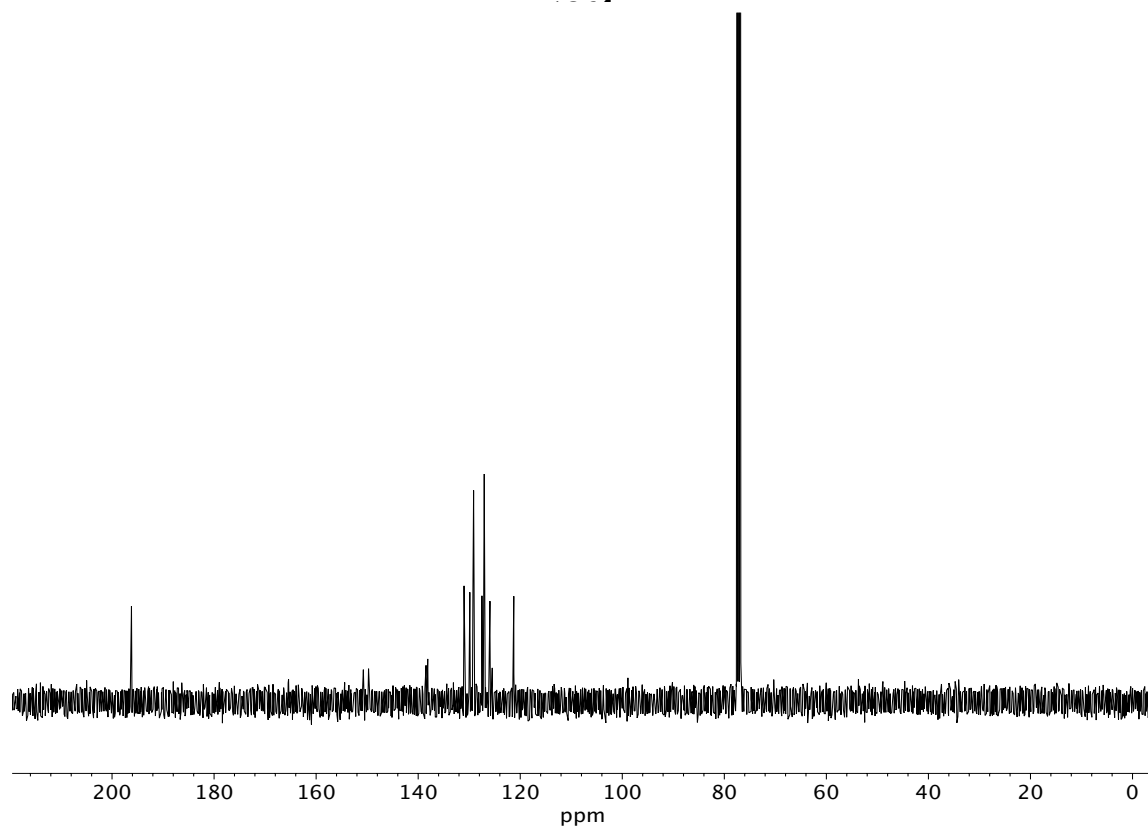


Figure A11.200 ^{13}C NMR (100 MHz, CDCl_3) of compound **186f**.

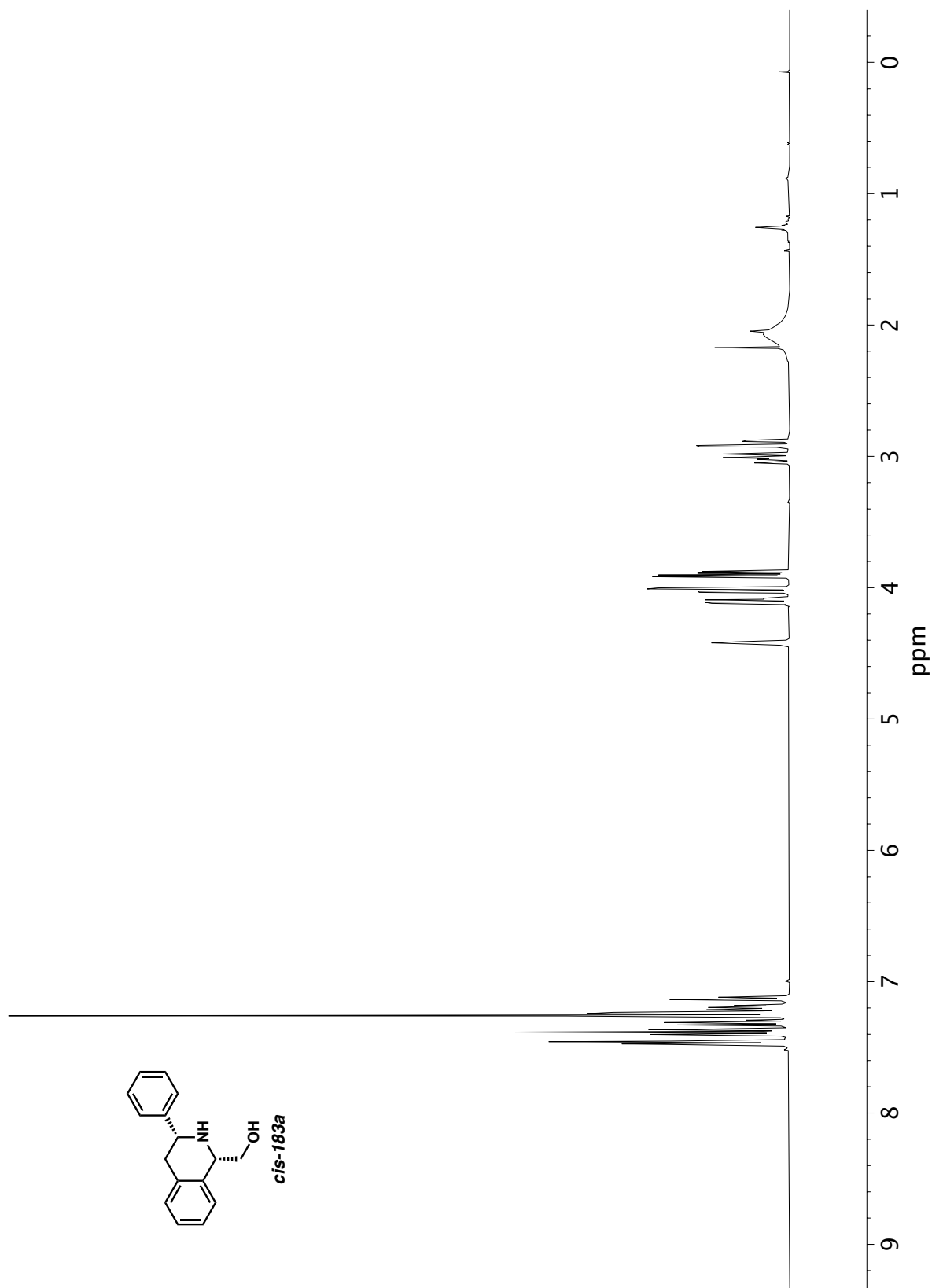


Figure A11.201 ¹H NMR (400 MHz, CDCl₃) of compound *Cis*-183a.

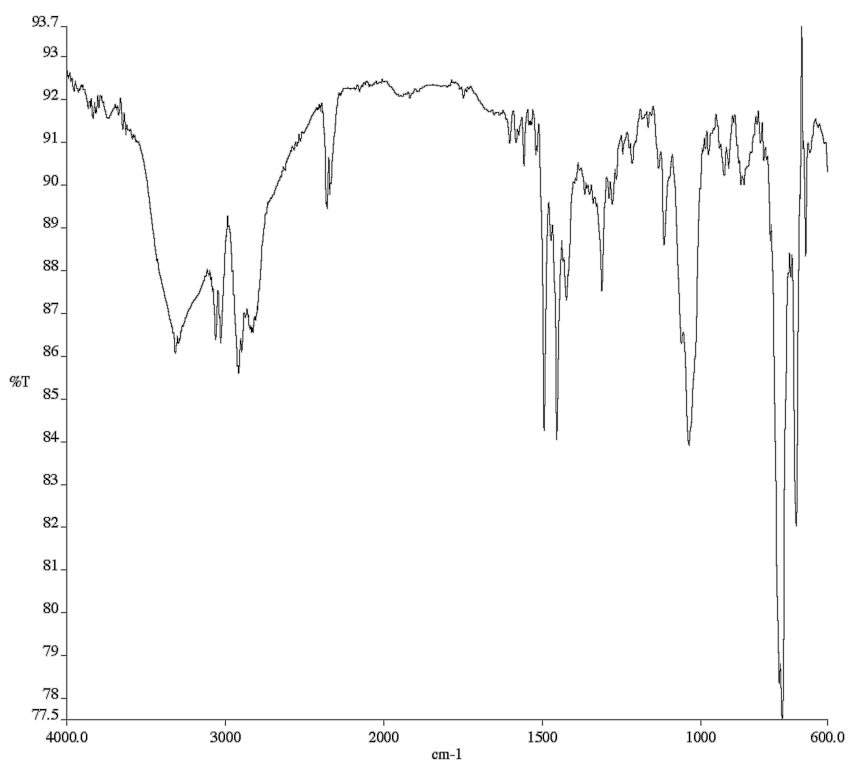


Figure A11.202 Infrared spectrum (Thin Film, NaCl) of compound

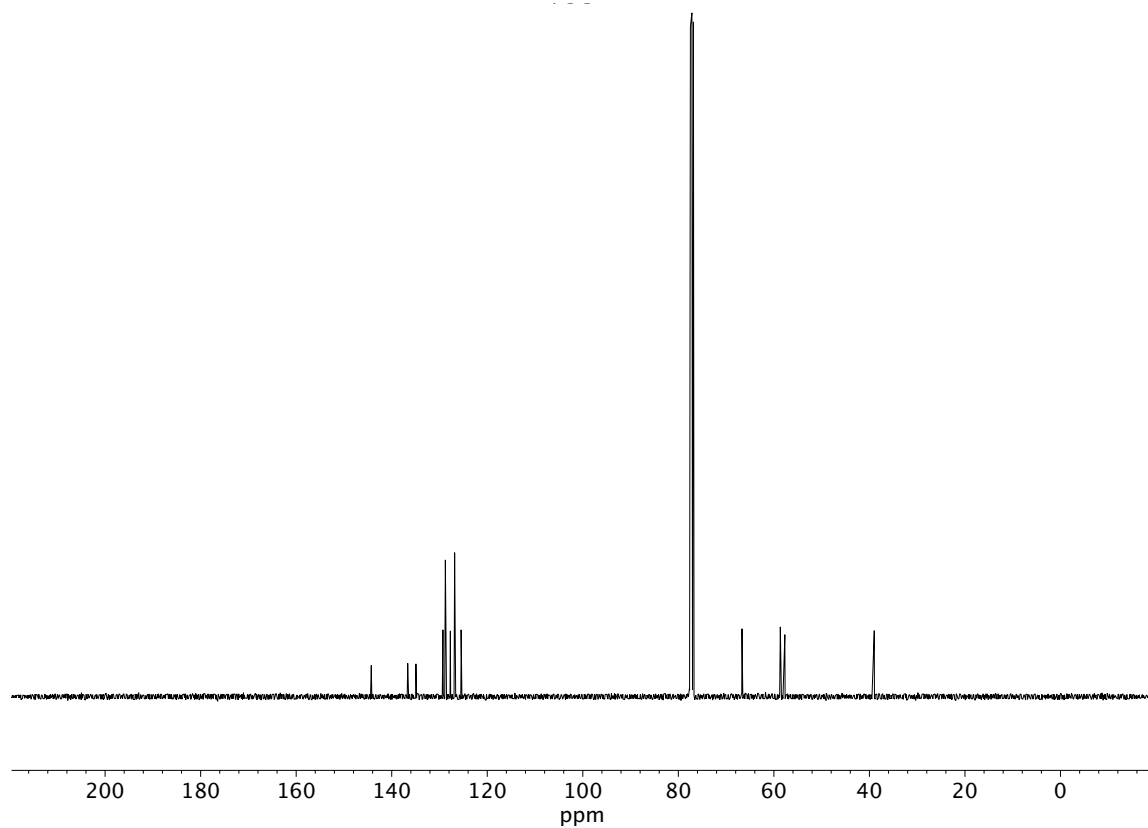


Figure A11.203 ^{13}C NMR (100 MHz, CDCl_3) of compound **183a**.

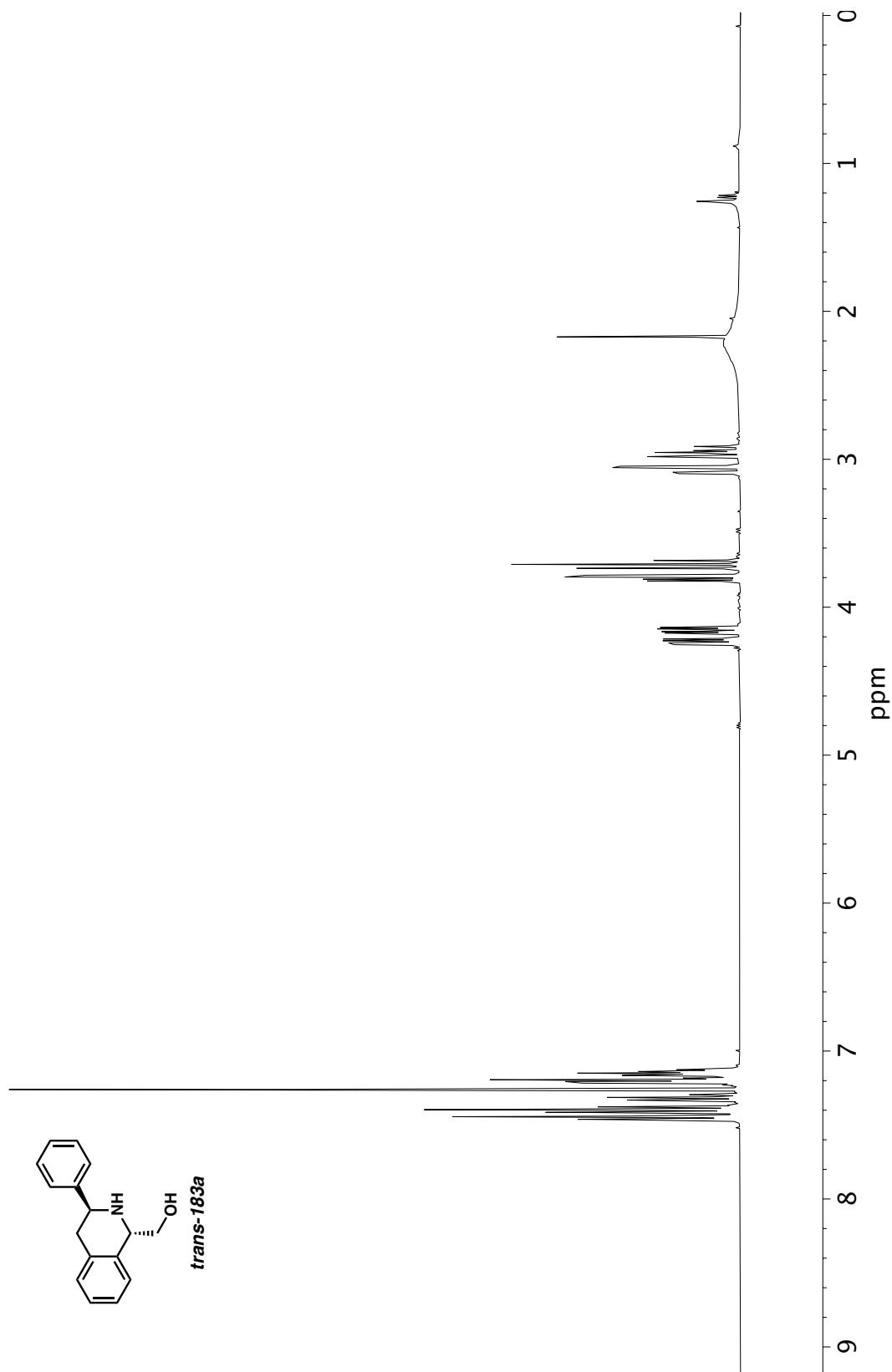


Figure A11.204 ^1H NMR (400 MHz, CDCl_3) of compound **Trans-183a**.

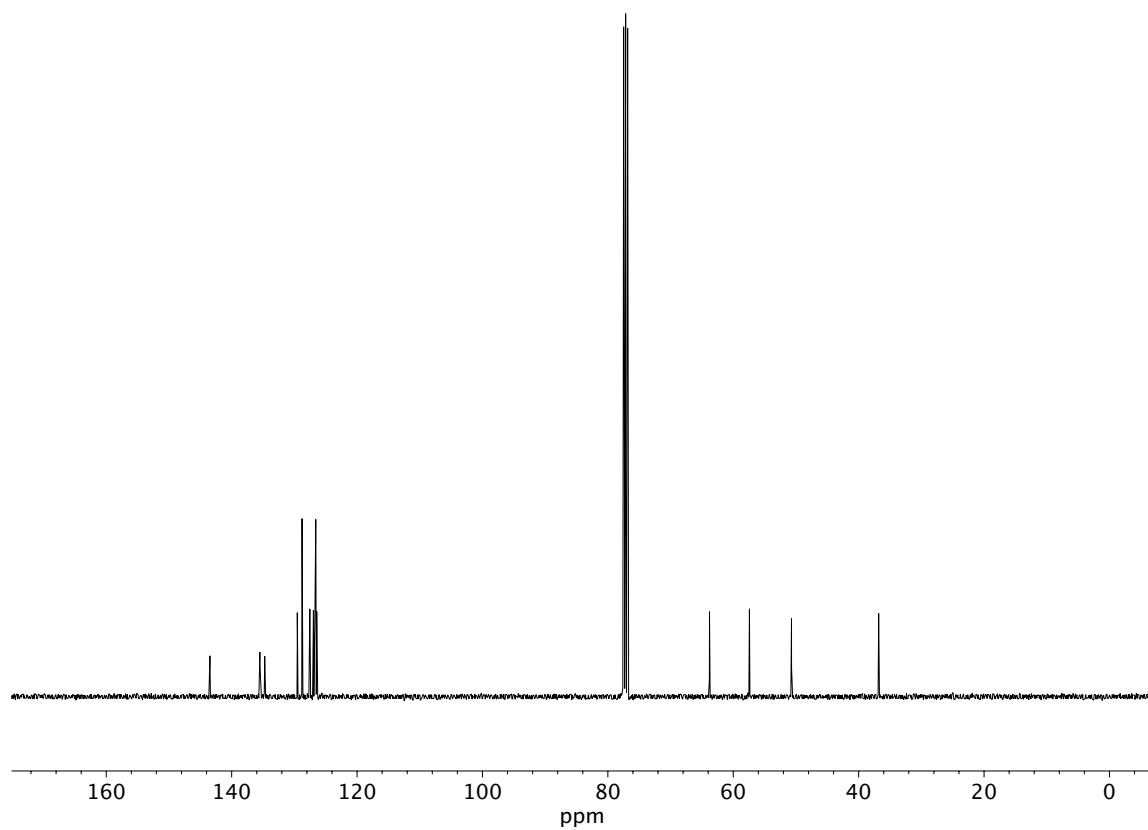


Figure A11.205 ^{13}C NMR (100 MHz, CDCl_3) of compound *Trans-*



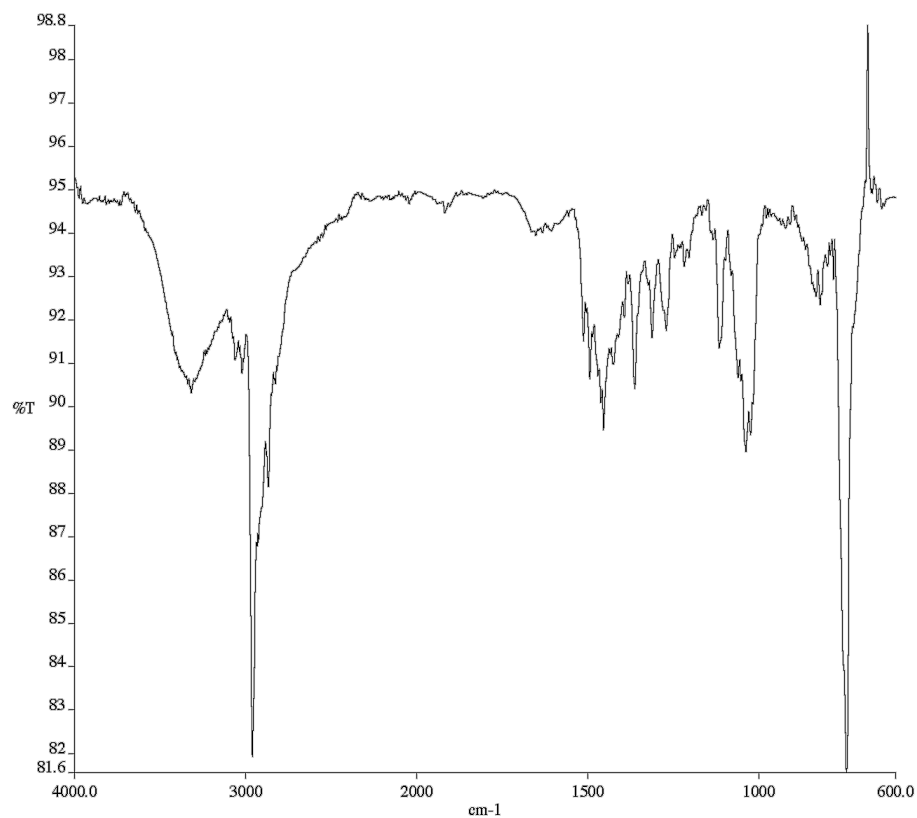


Figure A11.207 Infrared spectrum (Thin Film, NaCl) of compound

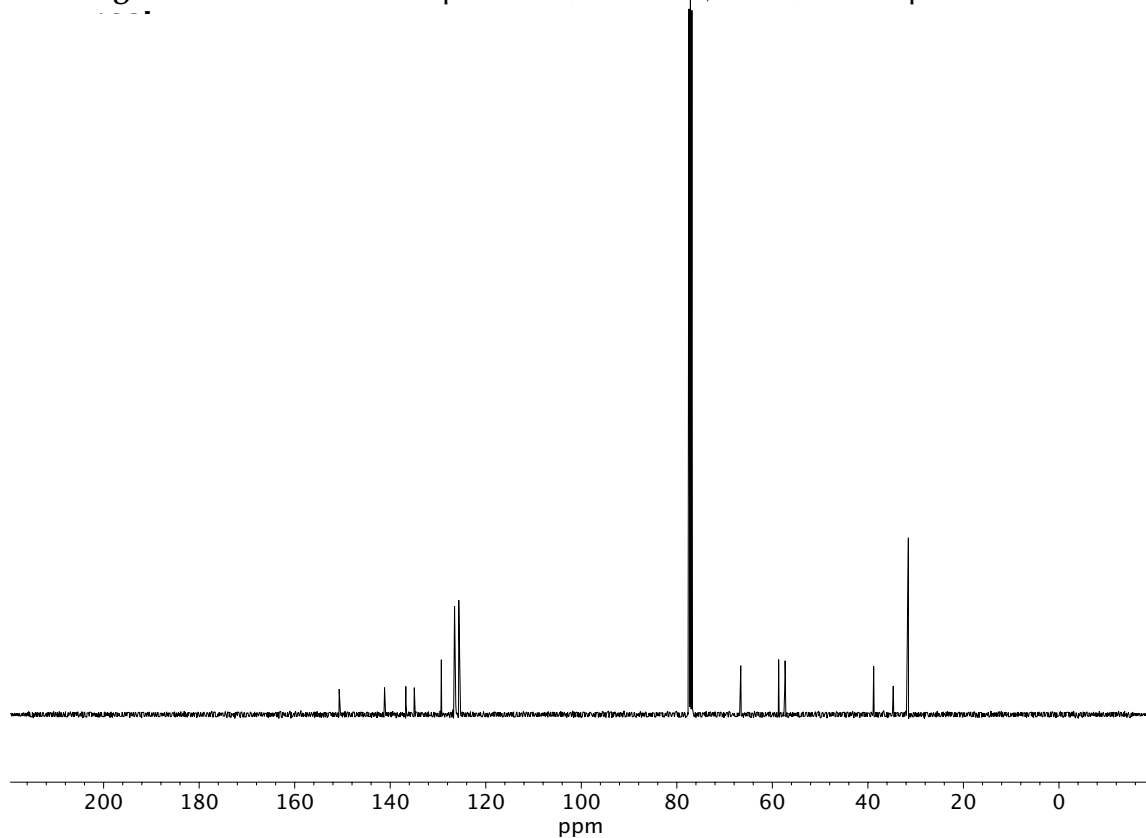


Figure A11.208 ¹³C NMR (100 MHz, CDCl₃) of compound **183b**.

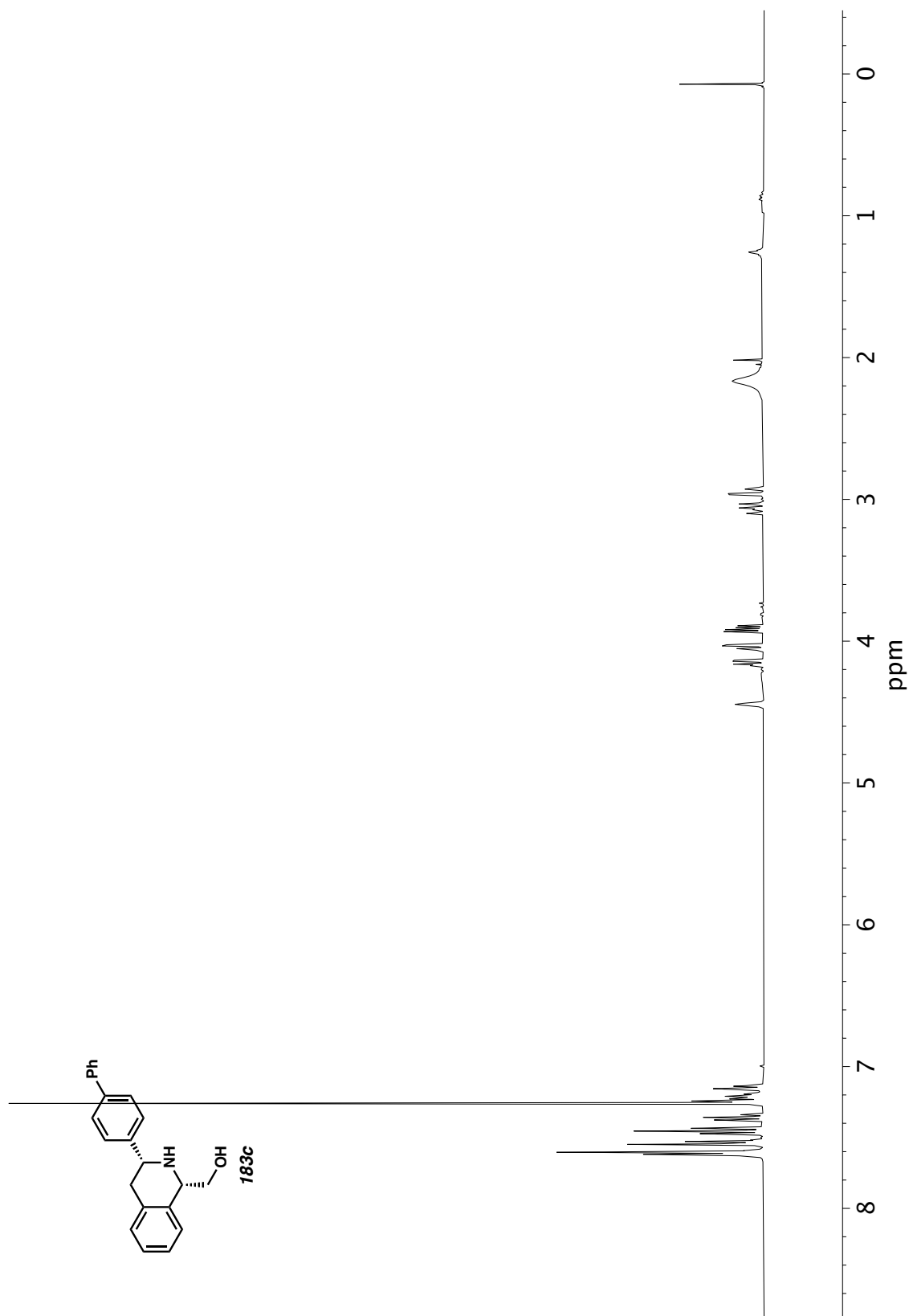


Figure A11.209 ^1H NMR (400 MHz, CDCl_3) of compound **183c**.

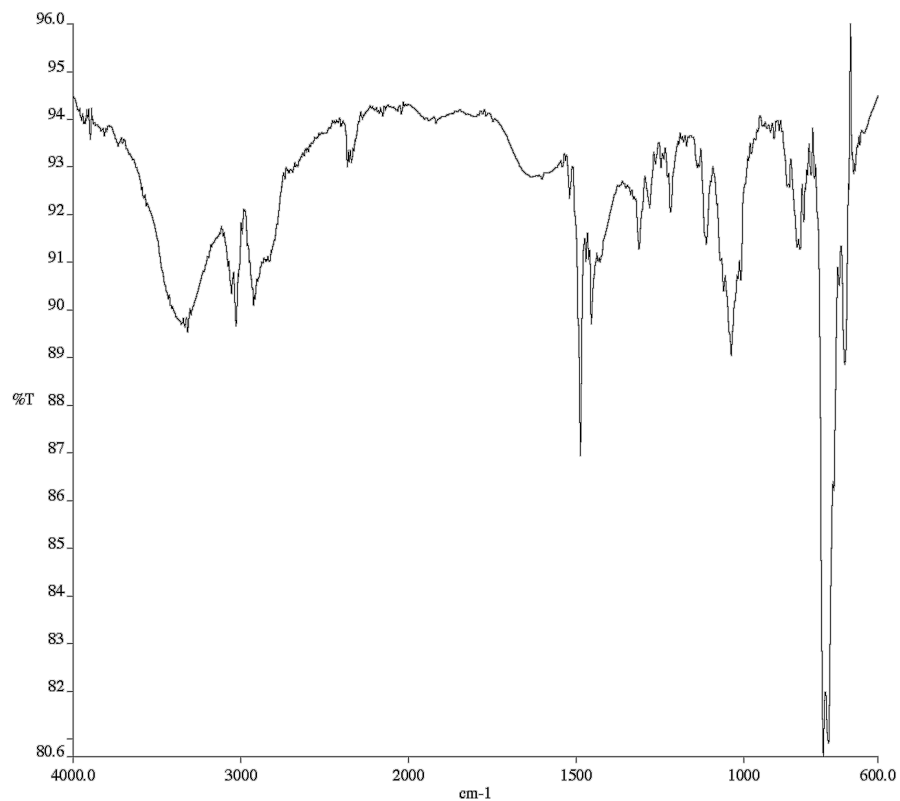


Figure A11.210 Infrared spectrum (Thin Film, NaCl) of compound

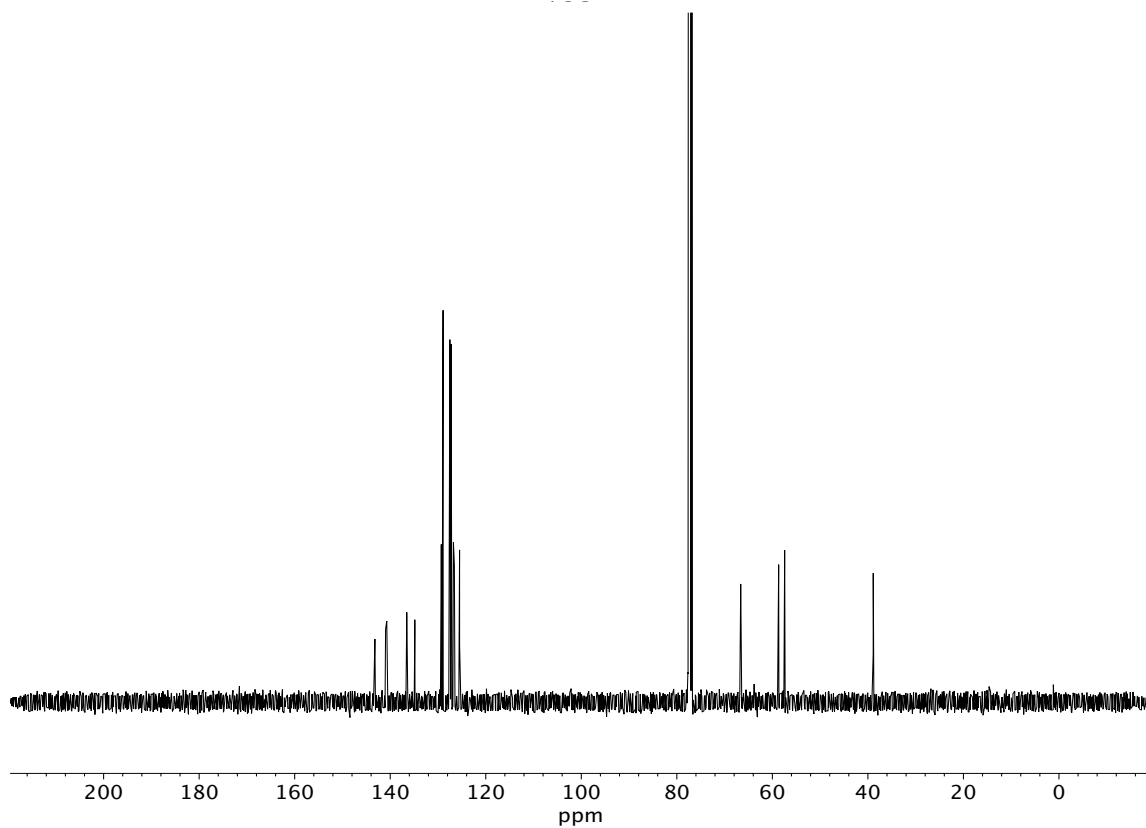


Figure A11.211 ^{13}C NMR (100 MHz, CDCl_3) of compound **183c**.

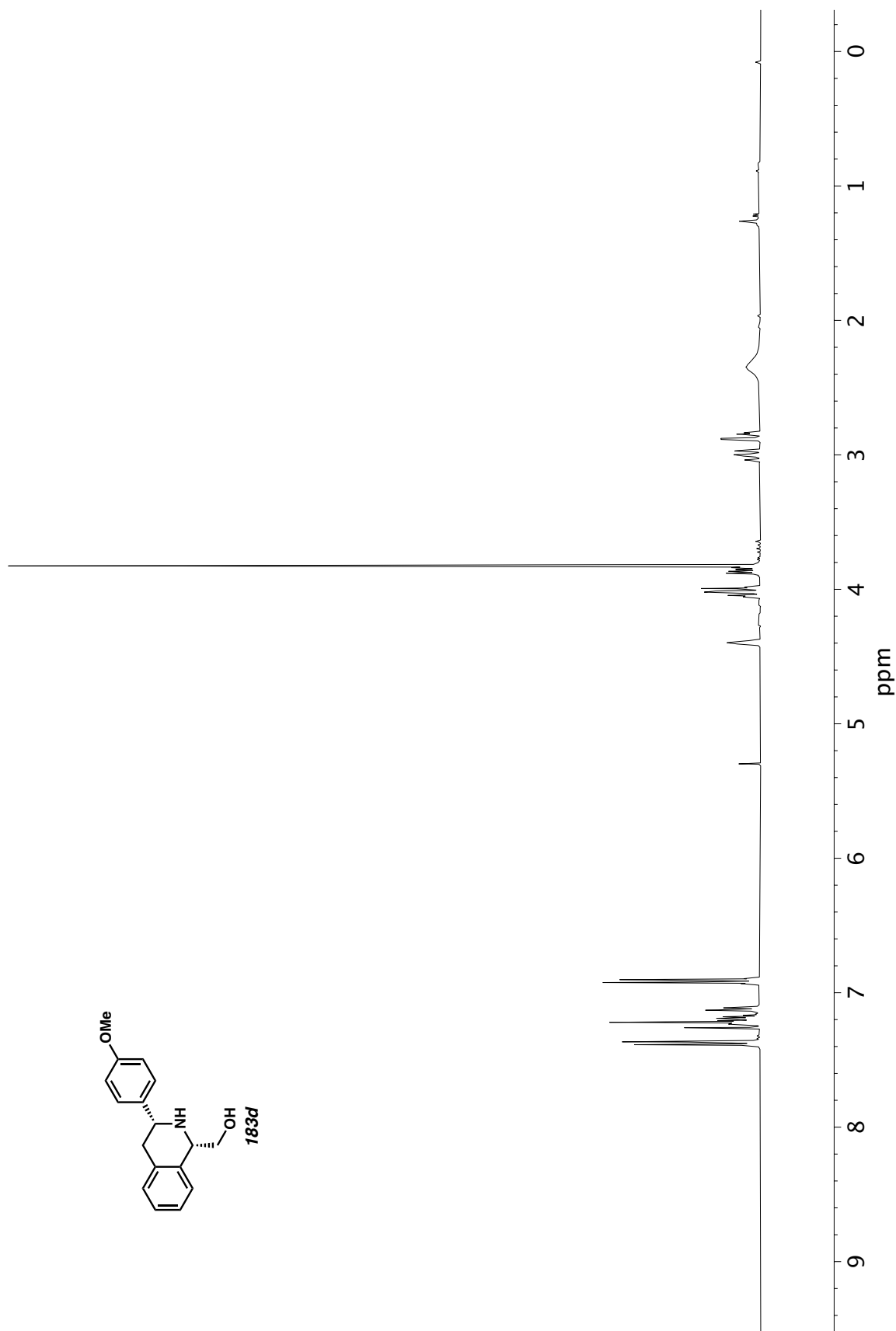


Figure A11.212 ^1H NMR (400 MHz, CDCl_3) of compound **183d**.

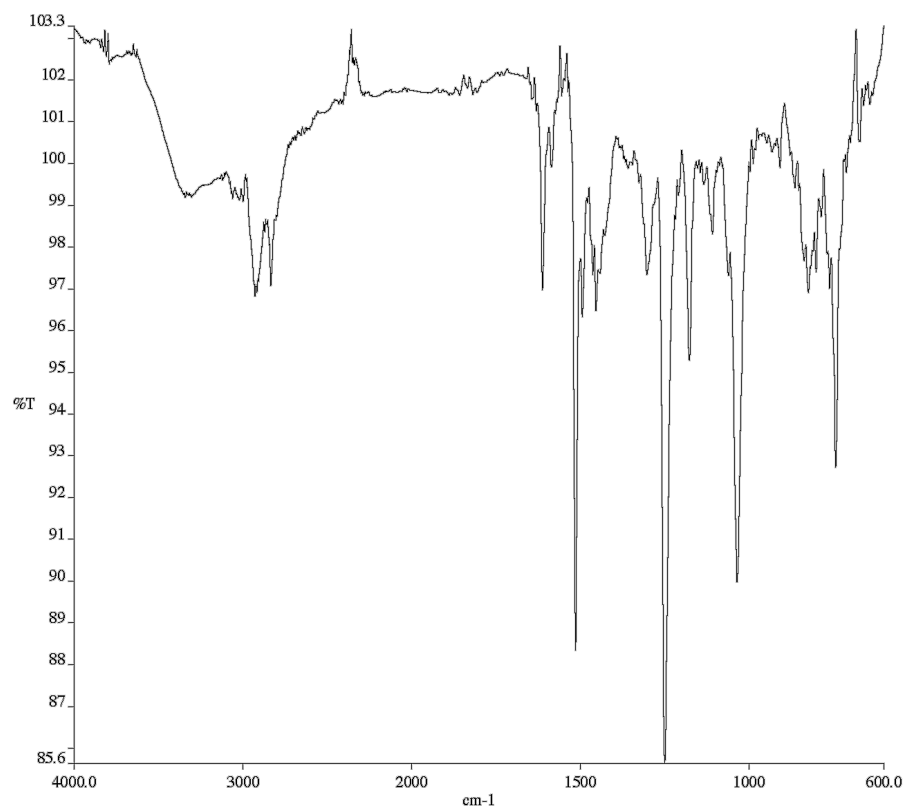


Figure A11.213 Infrared spectrum (Thin Film, NaCl) of compound

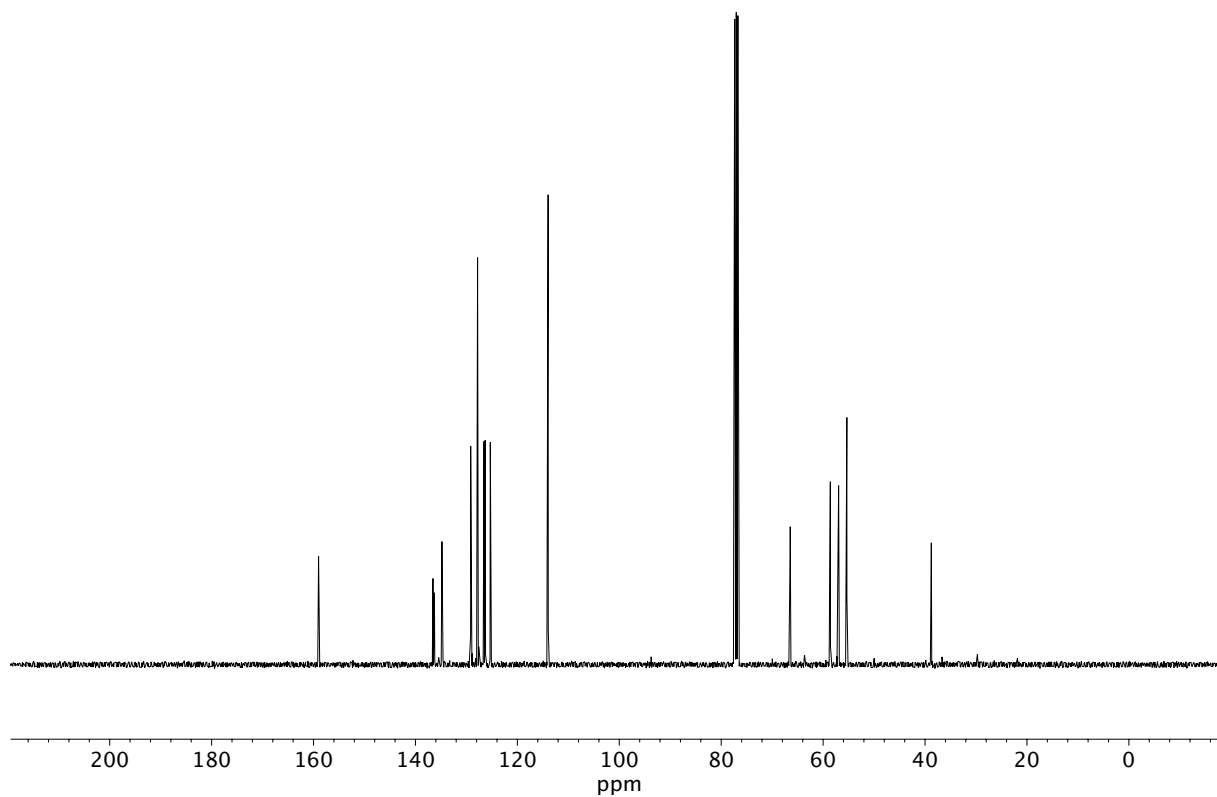


Figure A11.214 ¹³C NMR (100 MHz, CDCl₃) of compound **183d**.

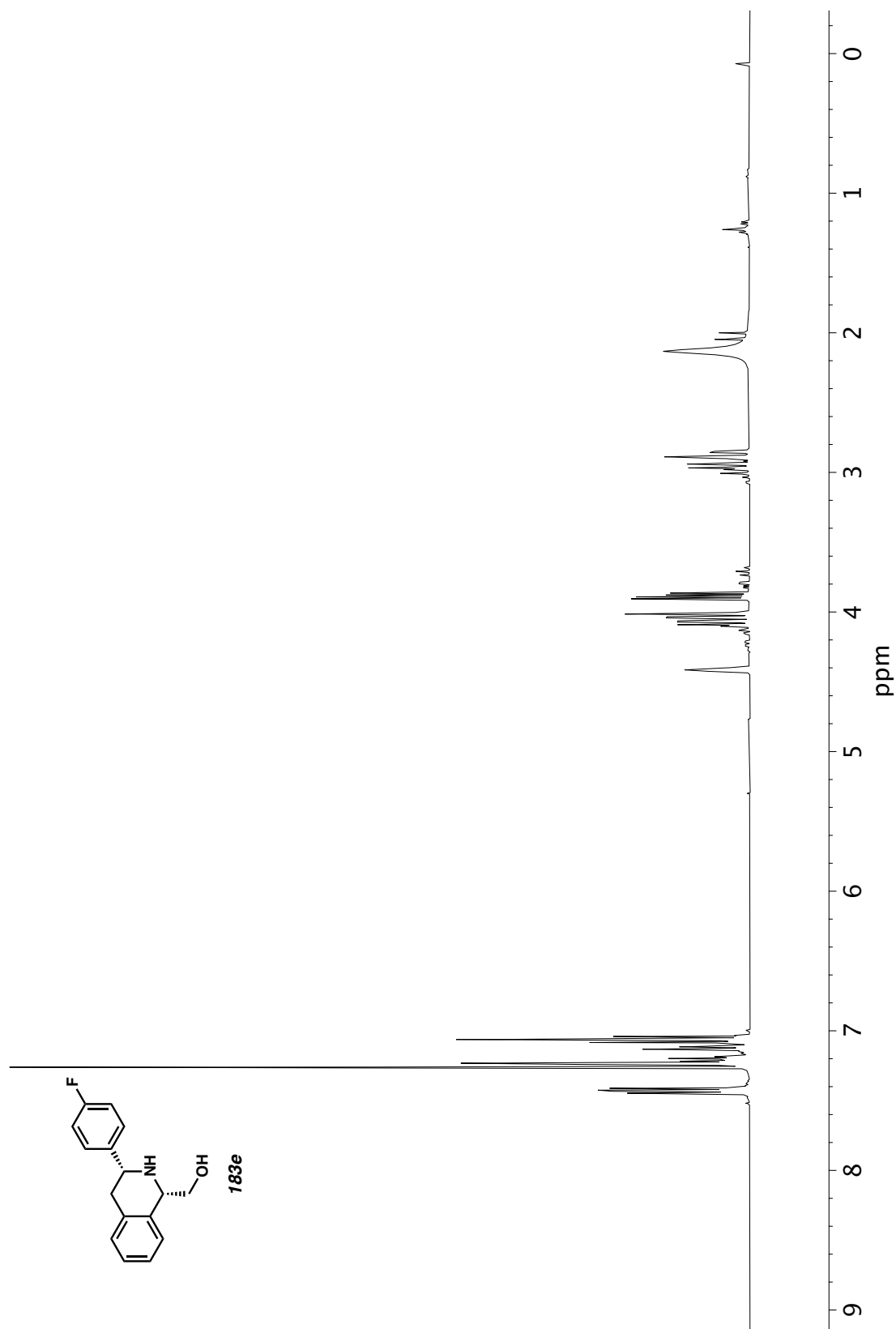


Figure A11.215 ¹H NMR (400 MHz, CDCl₃) of compound **183e**.

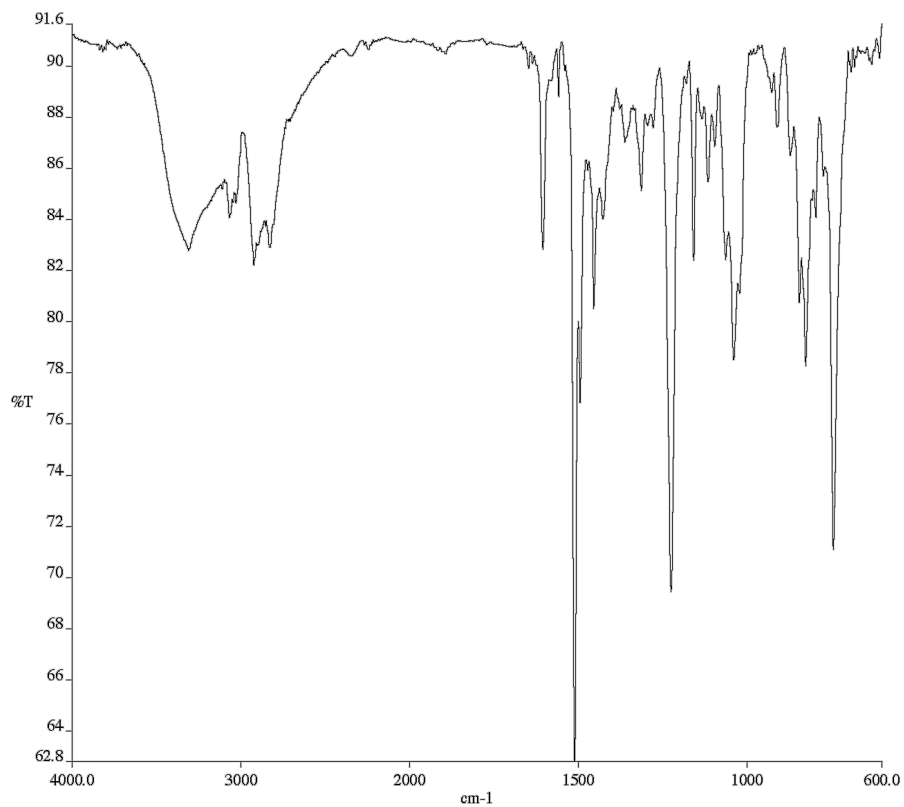


Figure A11.216 Infrared spectrum (Thin Film, NaCl) of compound

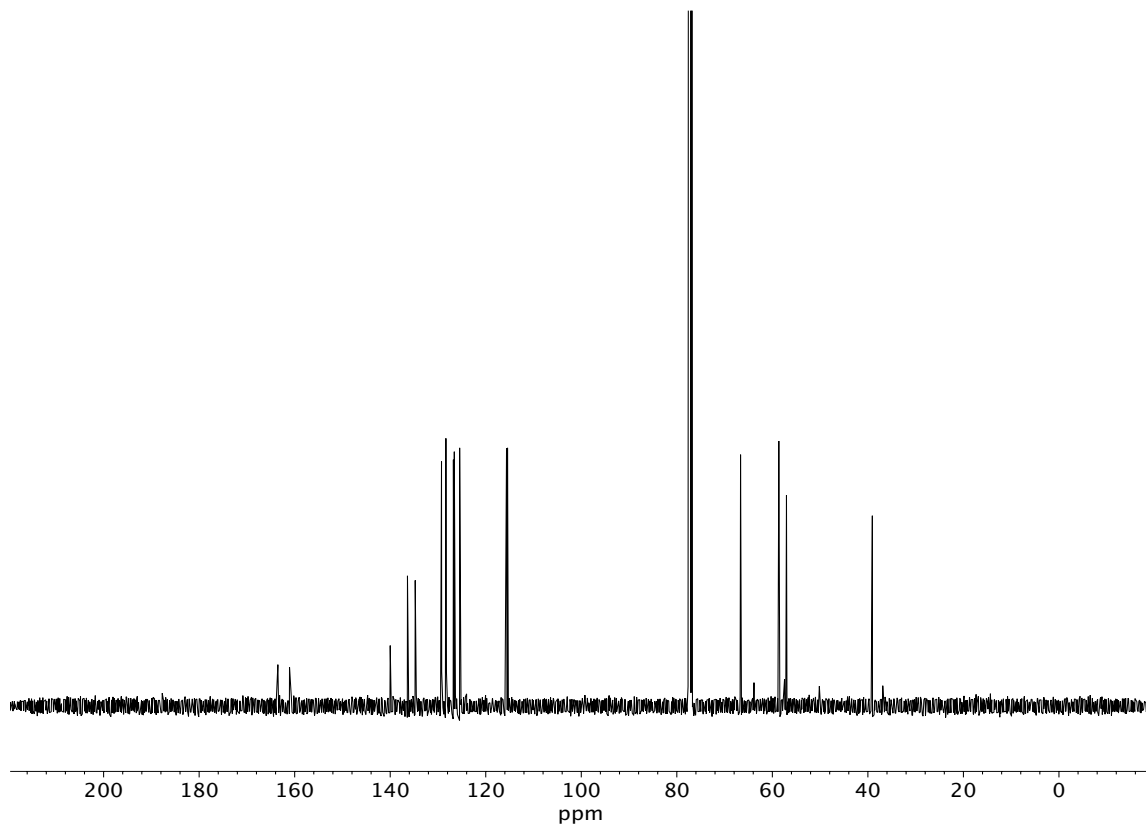


Figure A11.217 ¹³C NMR (100 MHz, CDCl₃) of compound **183e**.

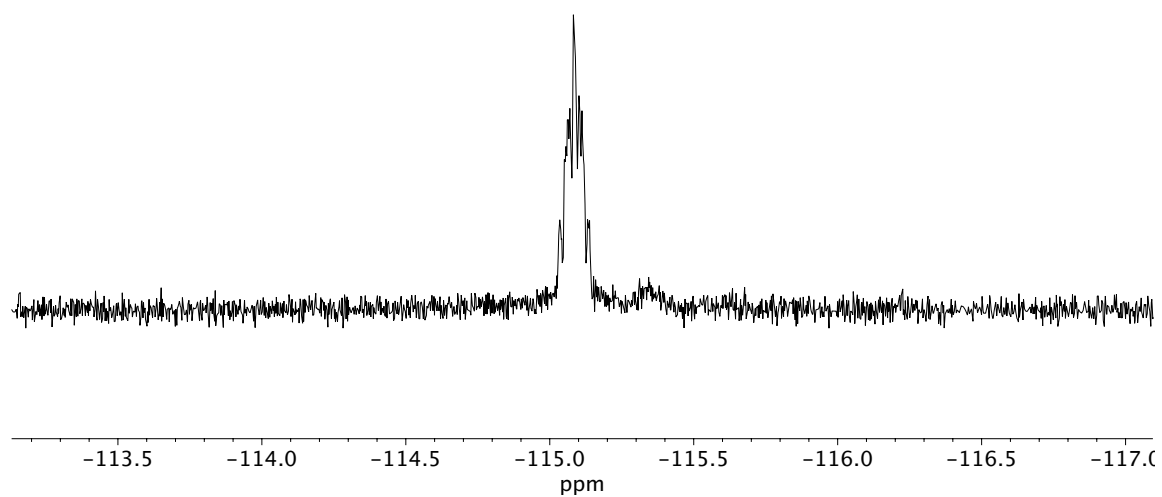


Figure A11.218 ^{19}F NMR (282 MHz, CDCl_3) of compound **183e**.

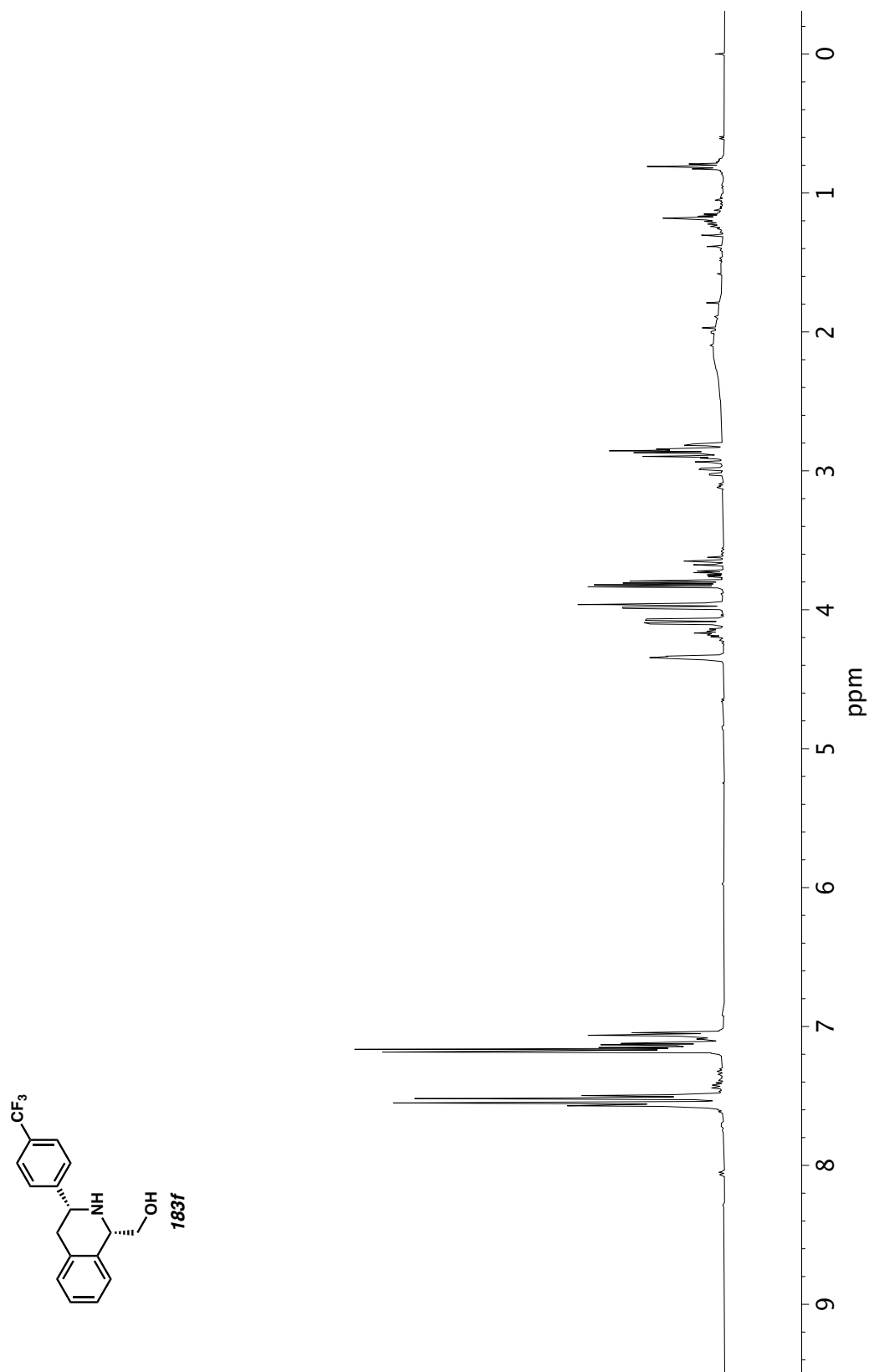


Figure A11.219 ¹H NMR (400 MHz, CDCl₃) of compound **183f**.

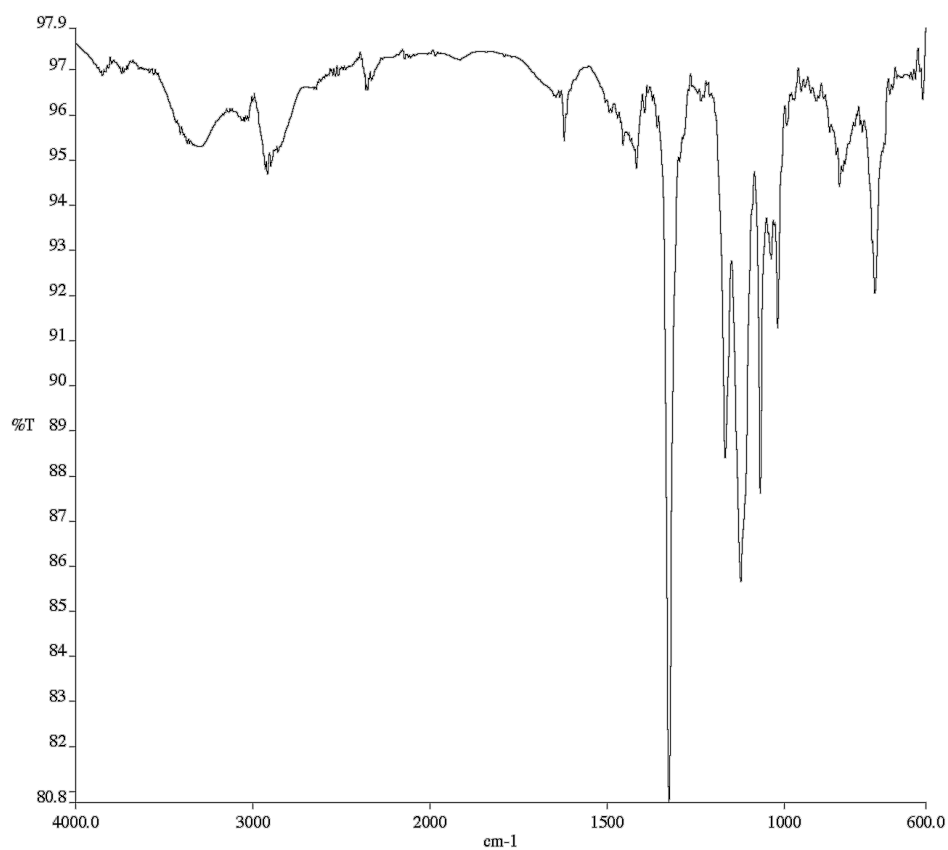


Figure A11.220 Infrared spectrum (Thin Film, NaCl) of compound

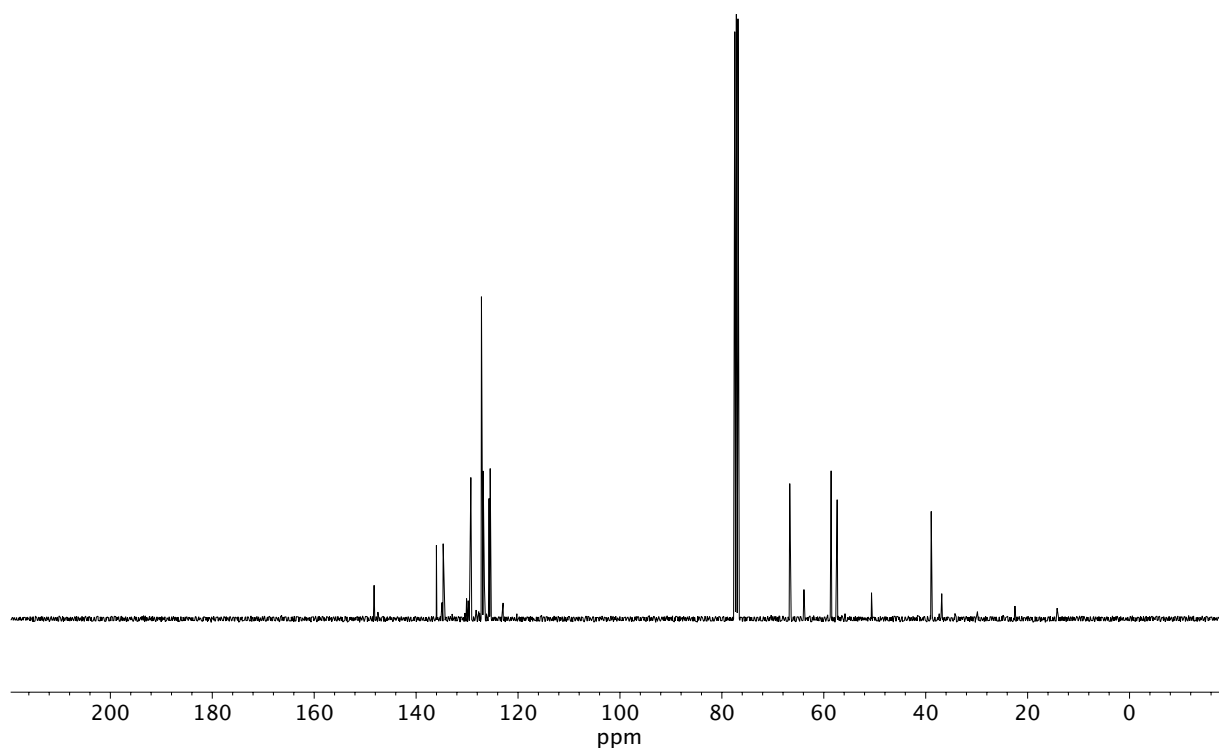


Figure A11.221 ¹³C NMR (100 MHz, CDCl₃) of compound **183f**.

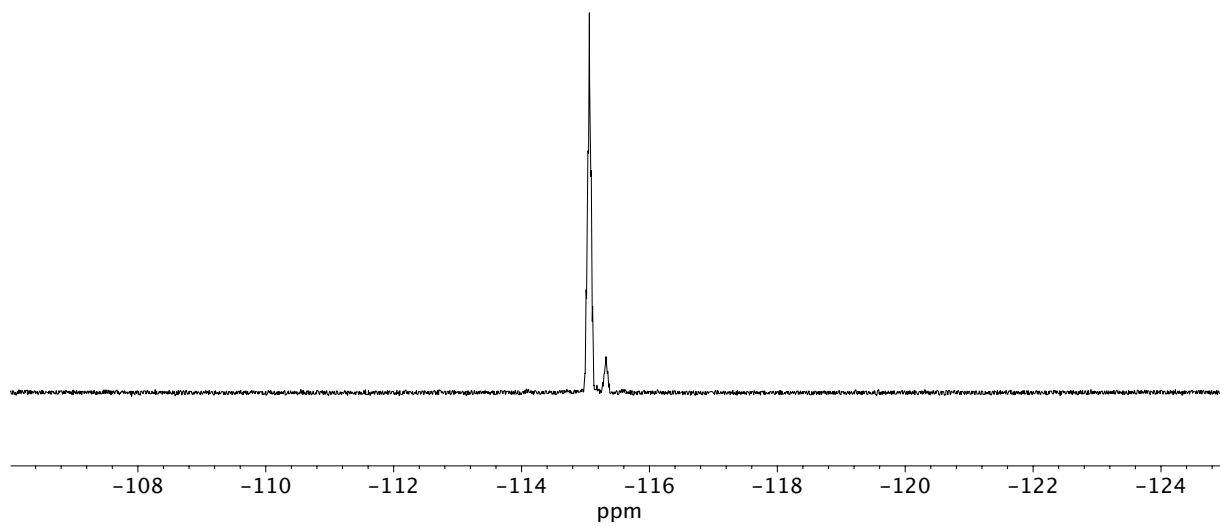


Figure A11.222 ^{19}F NMR (282 MHz, CDCl_3) of compound **183f**.

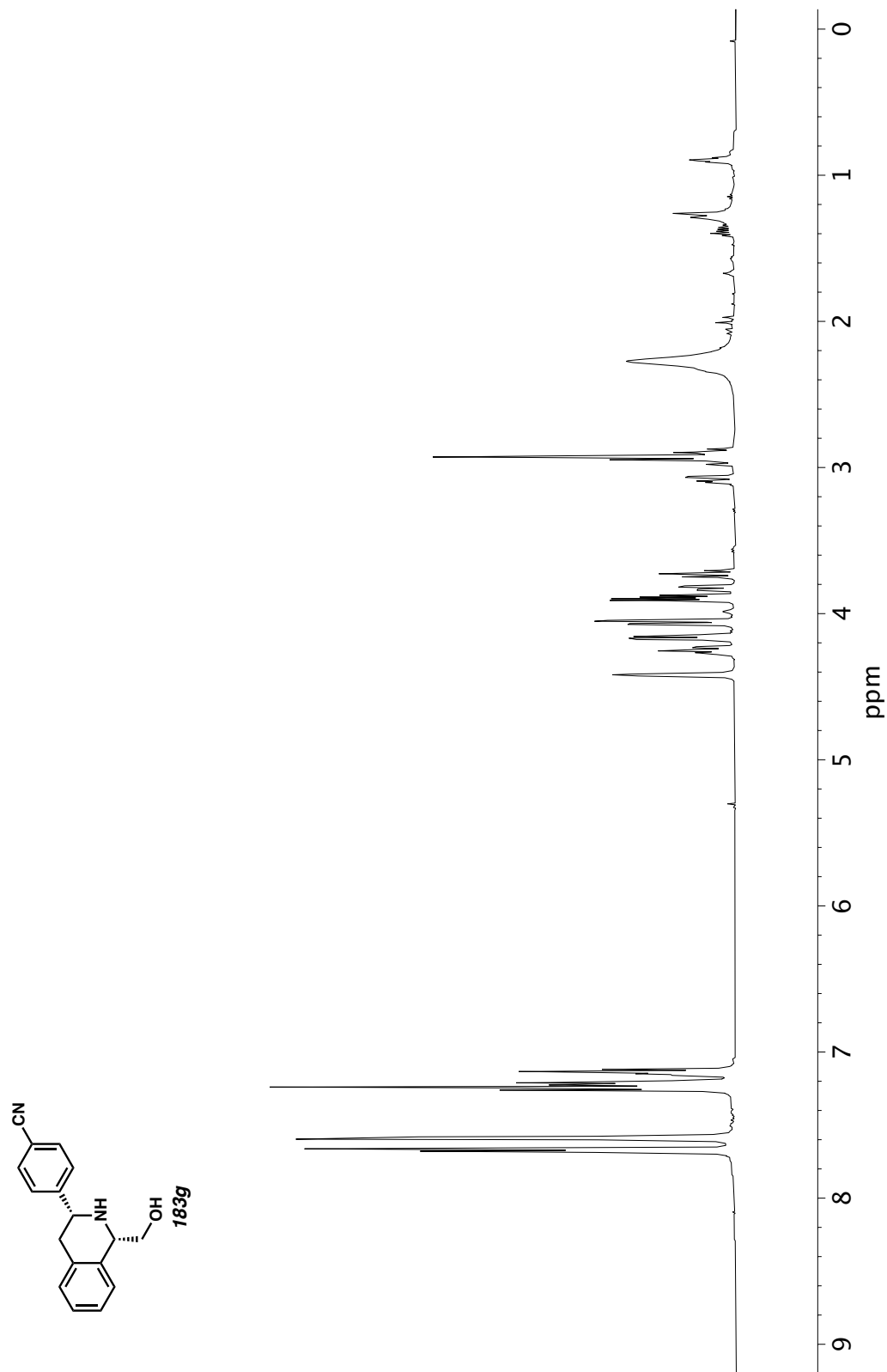


Figure A11.223 ^1H NMR (400 MHz, CDCl_3) of compound **183g**.

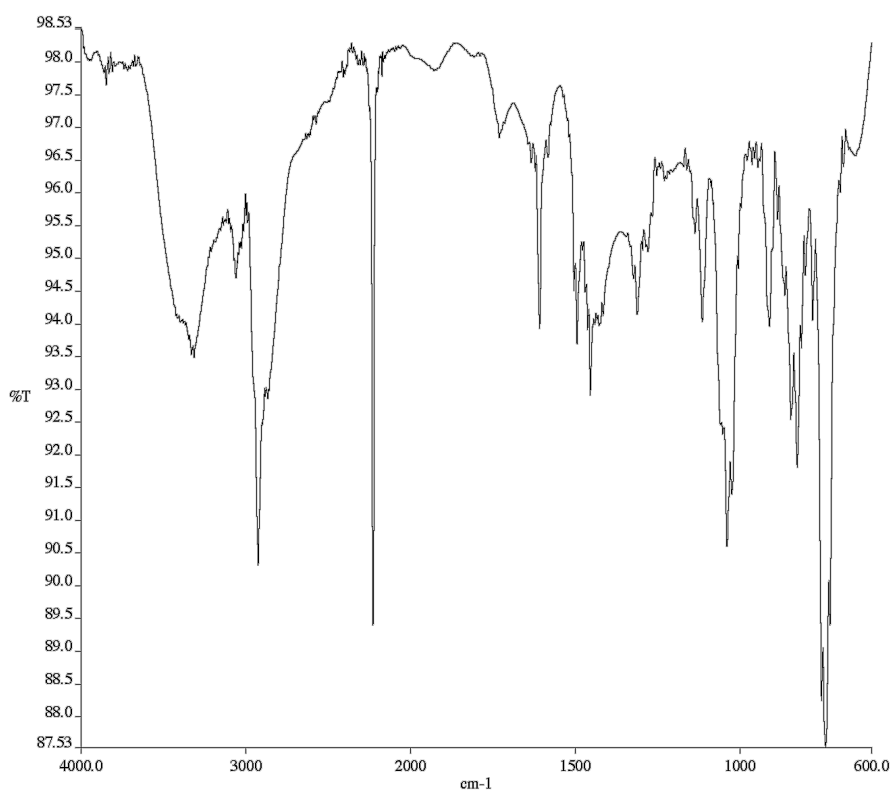


Figure A11.224 Infrared spectrum (Thin Film, NaCl) of compound

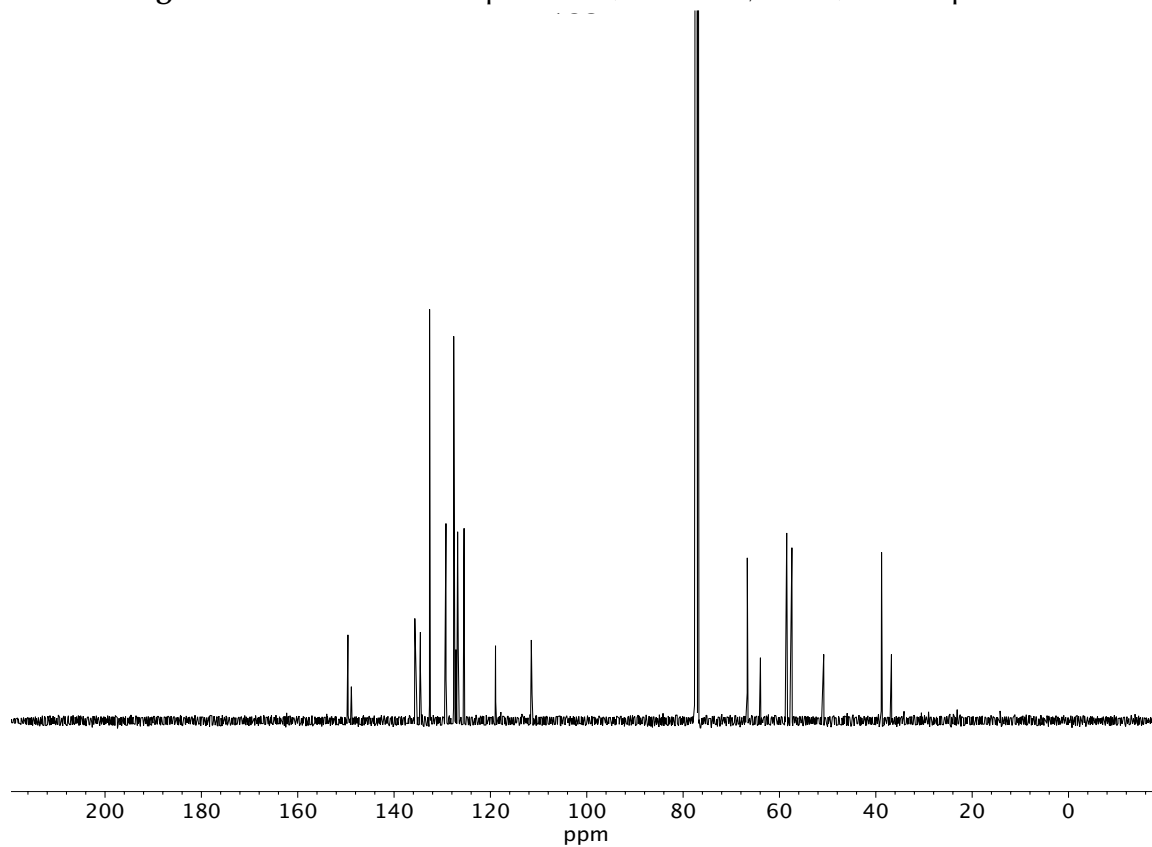


Figure A11.225 ¹³C NMR (100 MHz, CDCl₃) of compound **183g**.

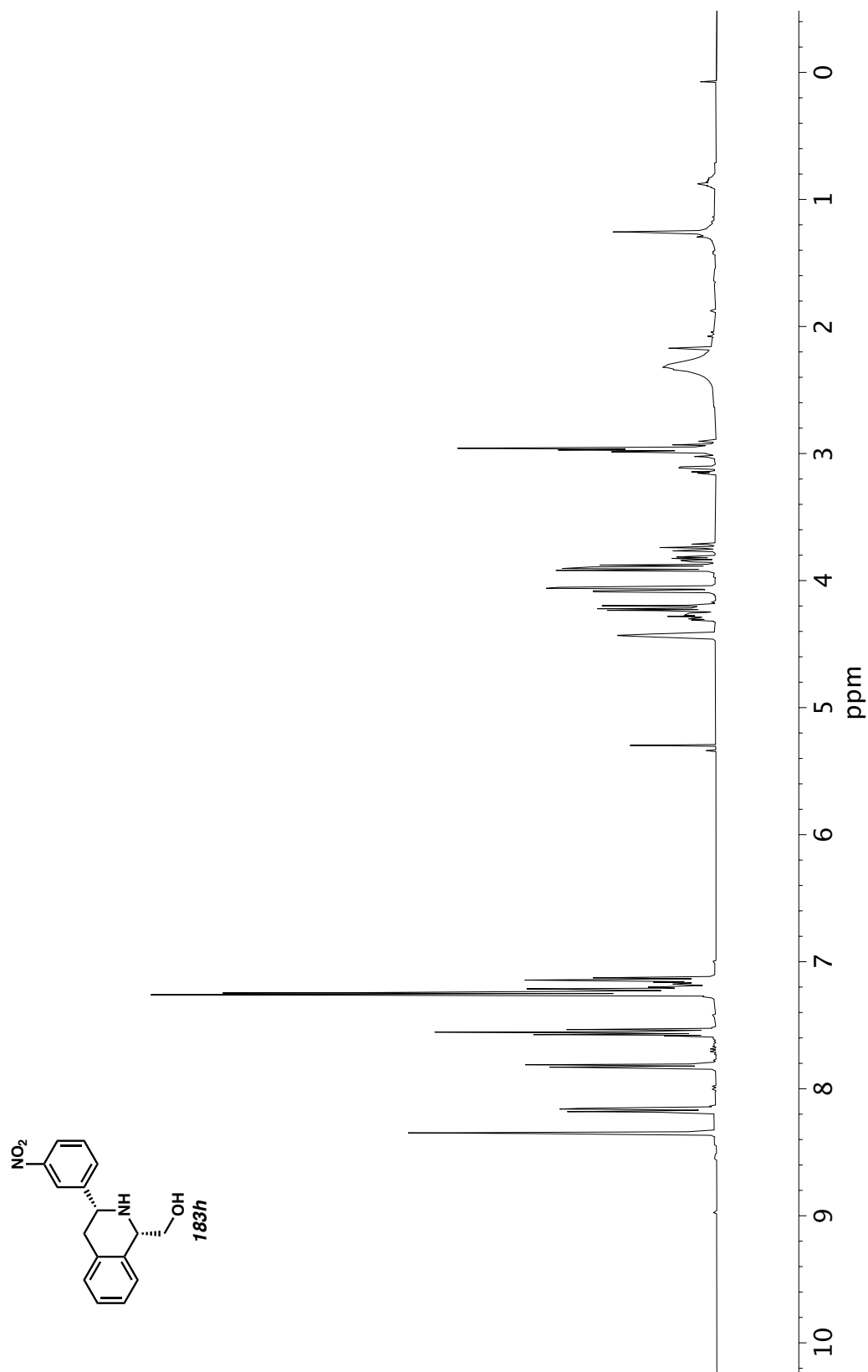


Figure A11.226 ¹H NMR (400 MHz, CDCl₃) of compound **183h**.

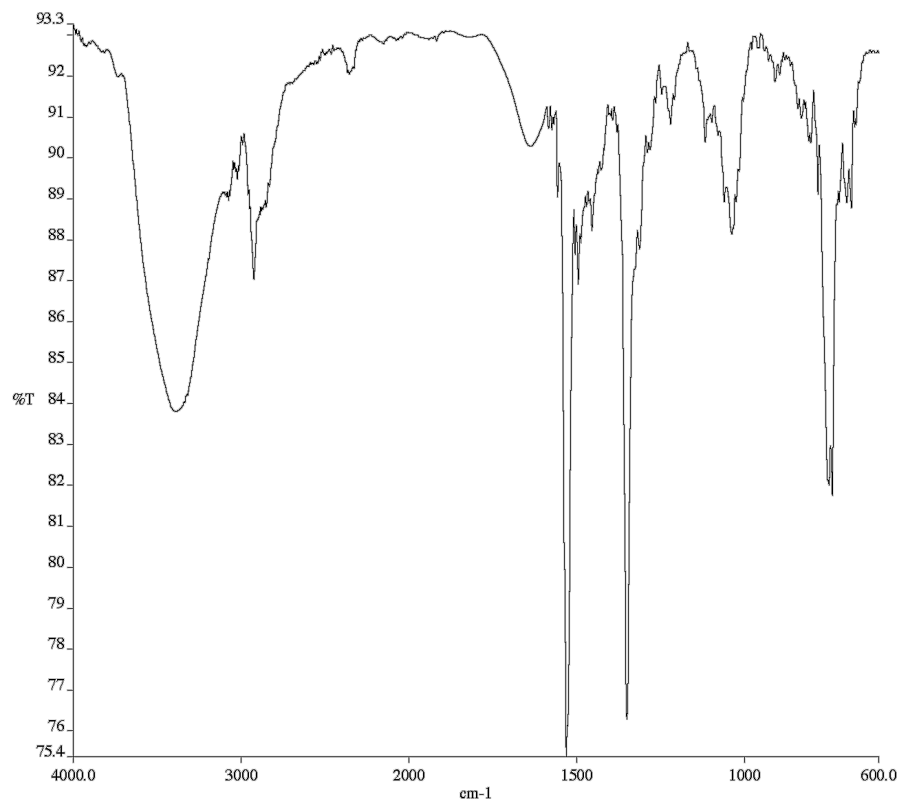


Figure A11.227 Infrared spectrum (Thin Film, NaCl) of compound

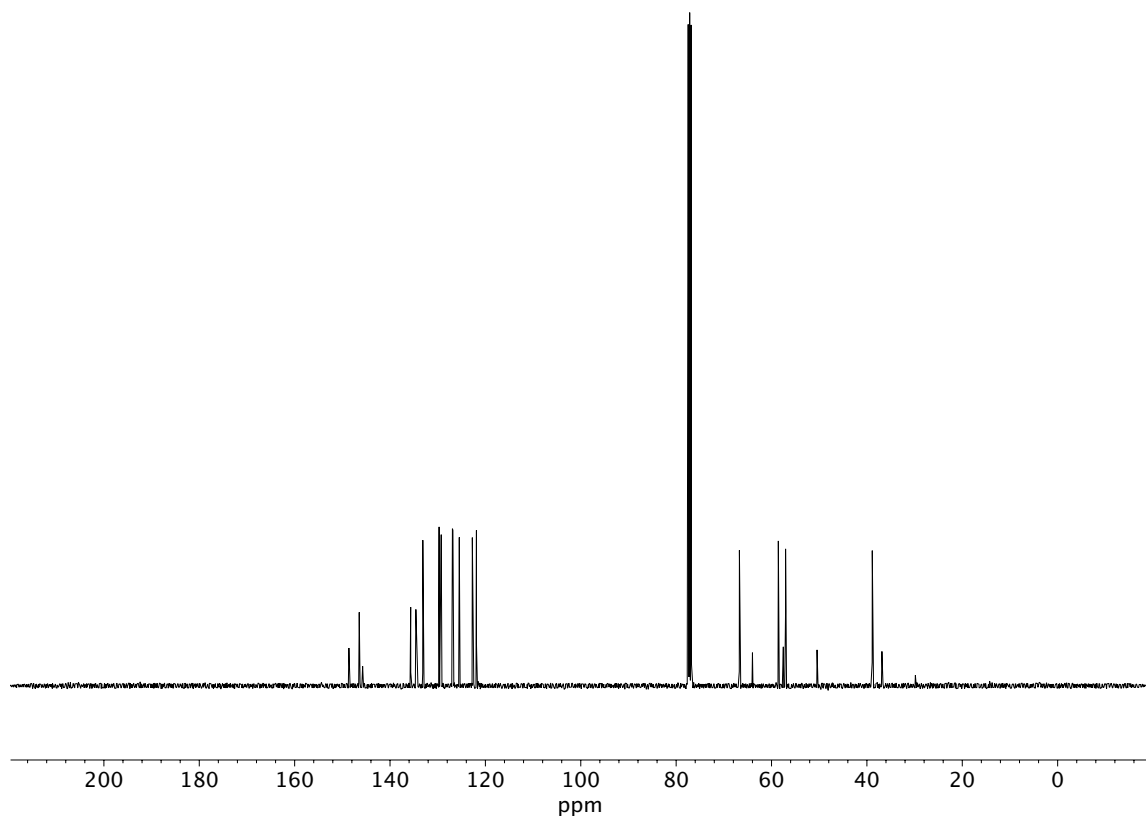


Figure A11.228 ¹³C NMR (100 MHz, CDCl₃) of compound **183h**.

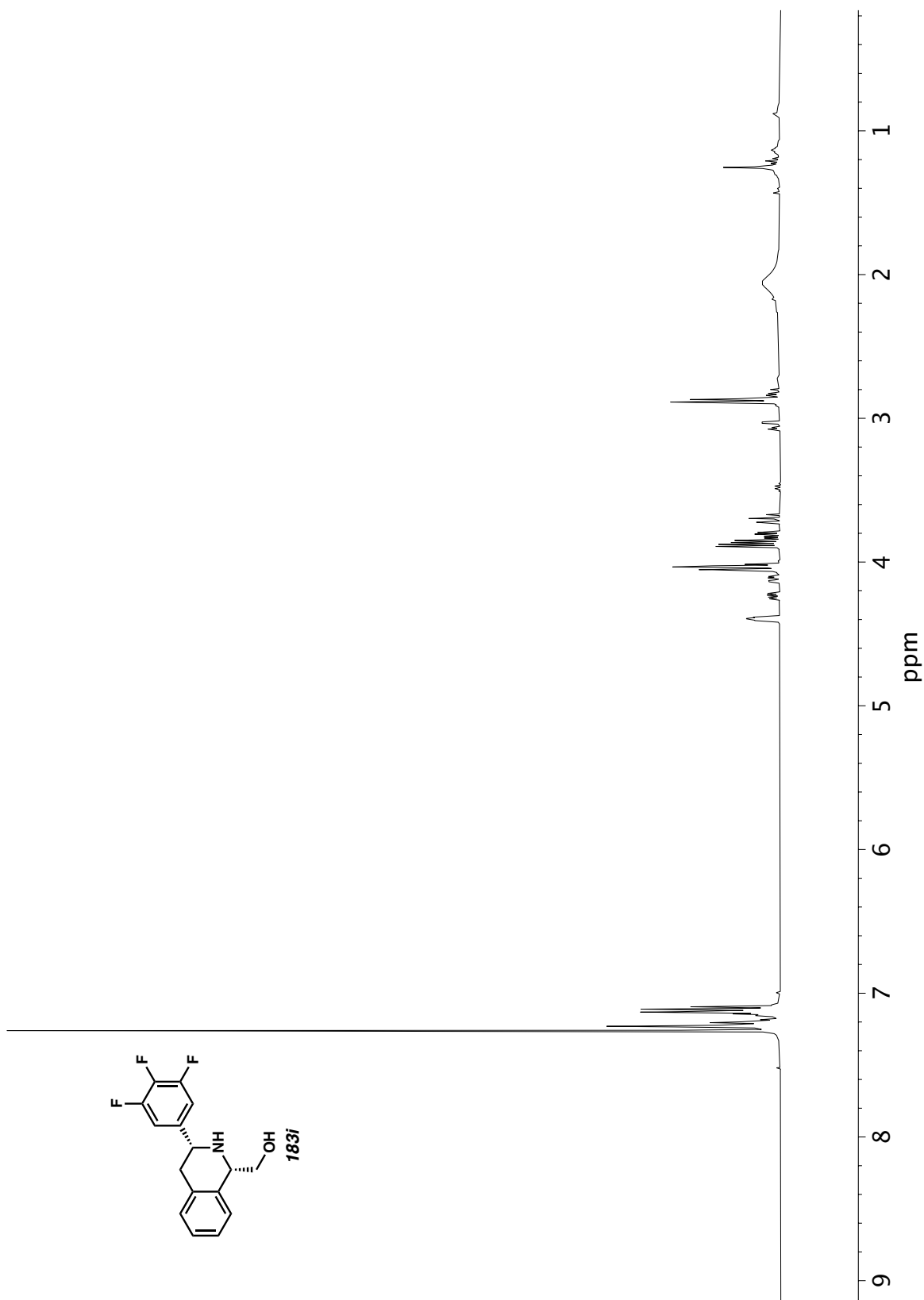


Figure A11.229 ¹H NMR (400 MHz, CDCl₃) of compound **183i**.

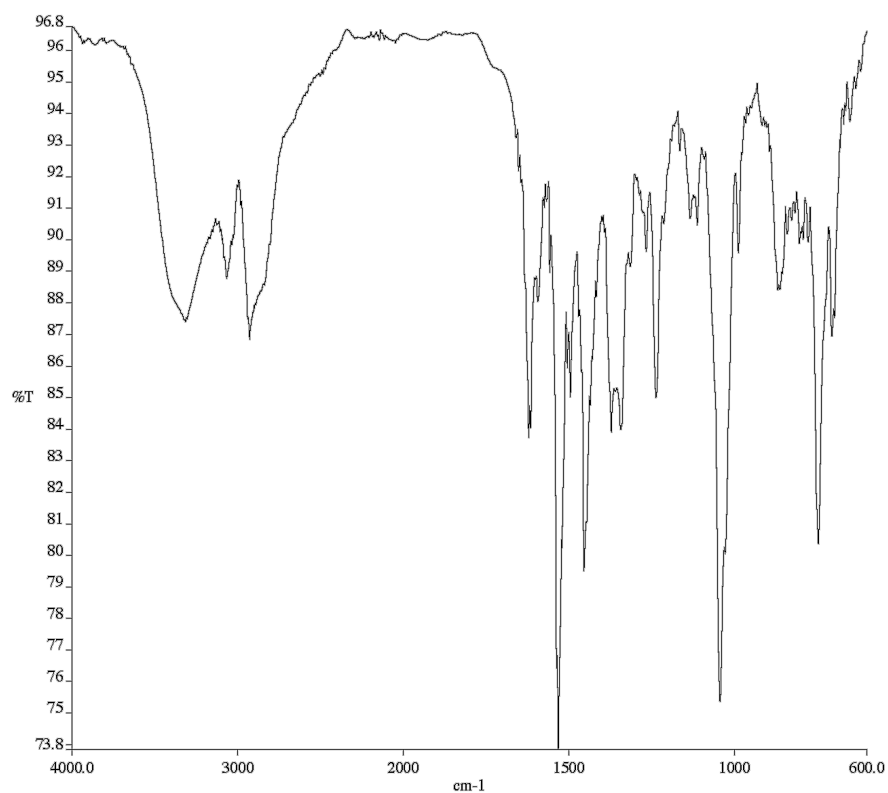


Figure A11.230 Infrared spectrum (Thin Film, NaCl) of compound

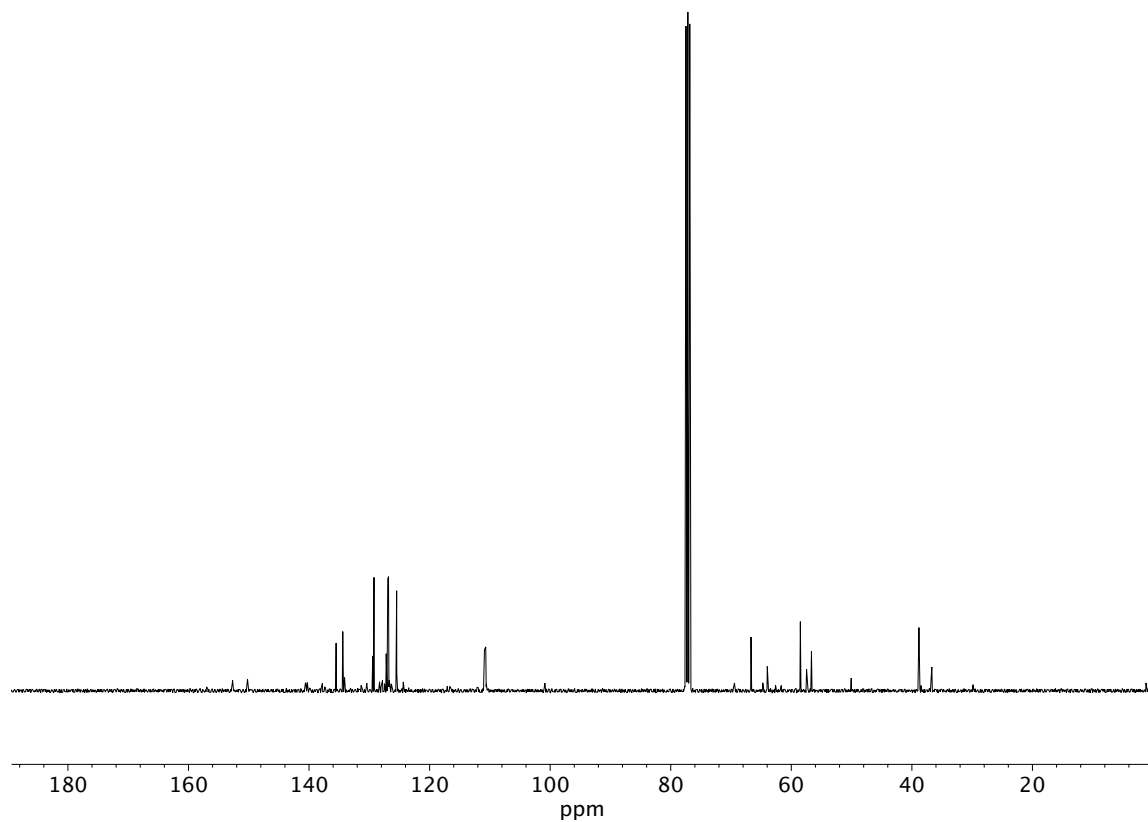


Figure A11.231 ¹³C NMR (100 MHz, CDCl₃) of compound **183i**.

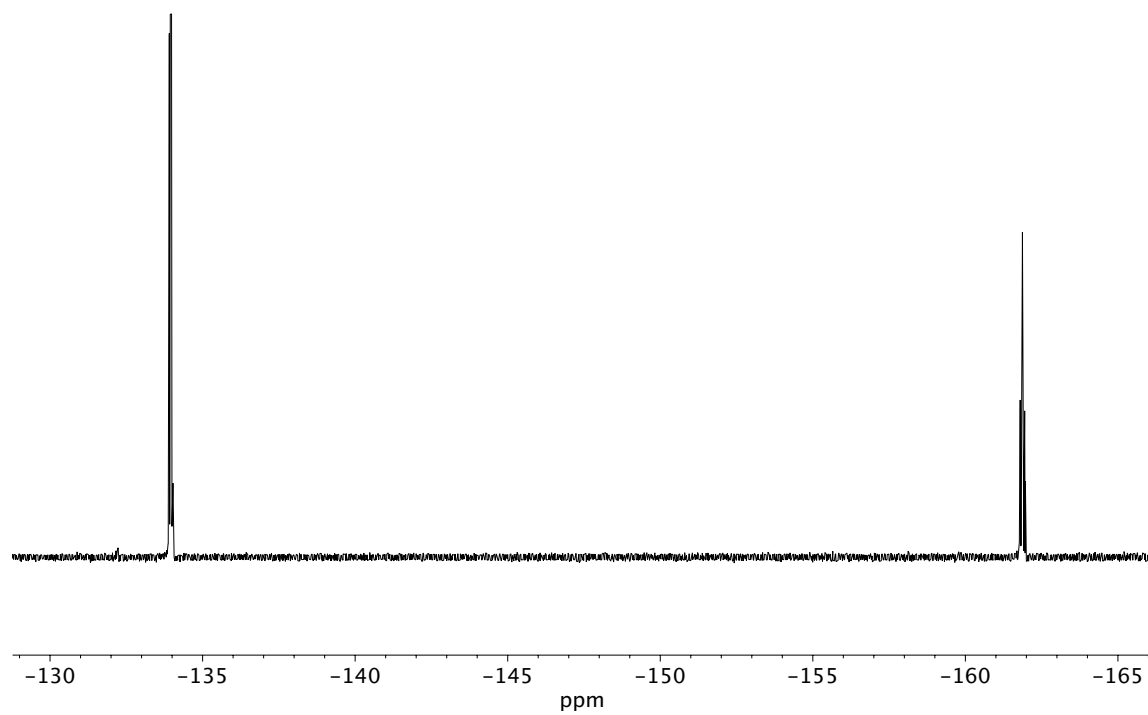


Figure A11.232 ^{19}F NMR (282 MHz, CDCl_3) of compound **183i**.

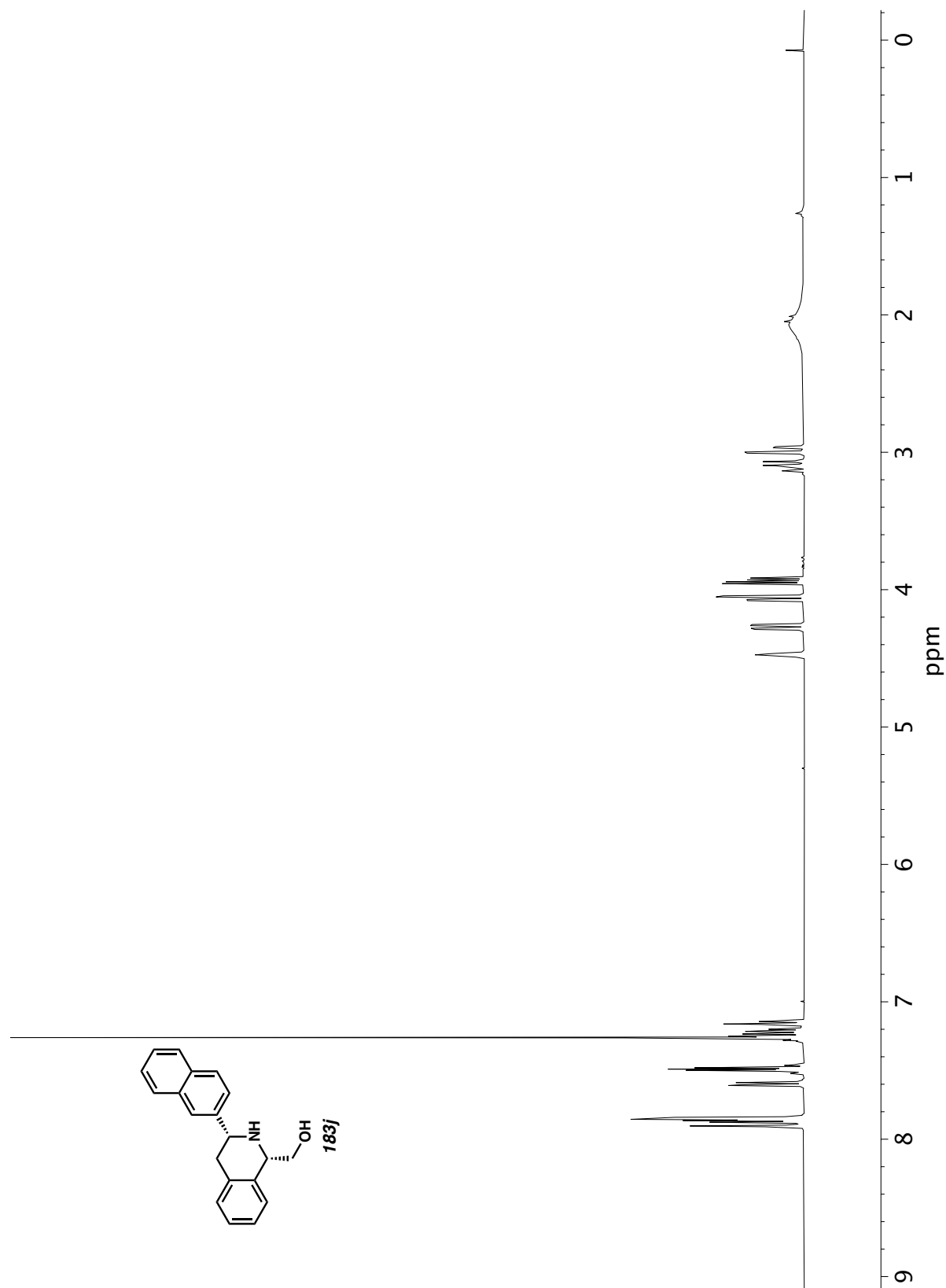


Figure A11.233 ^1H NMR (400 MHz, CDCl_3) of compound **183j**.

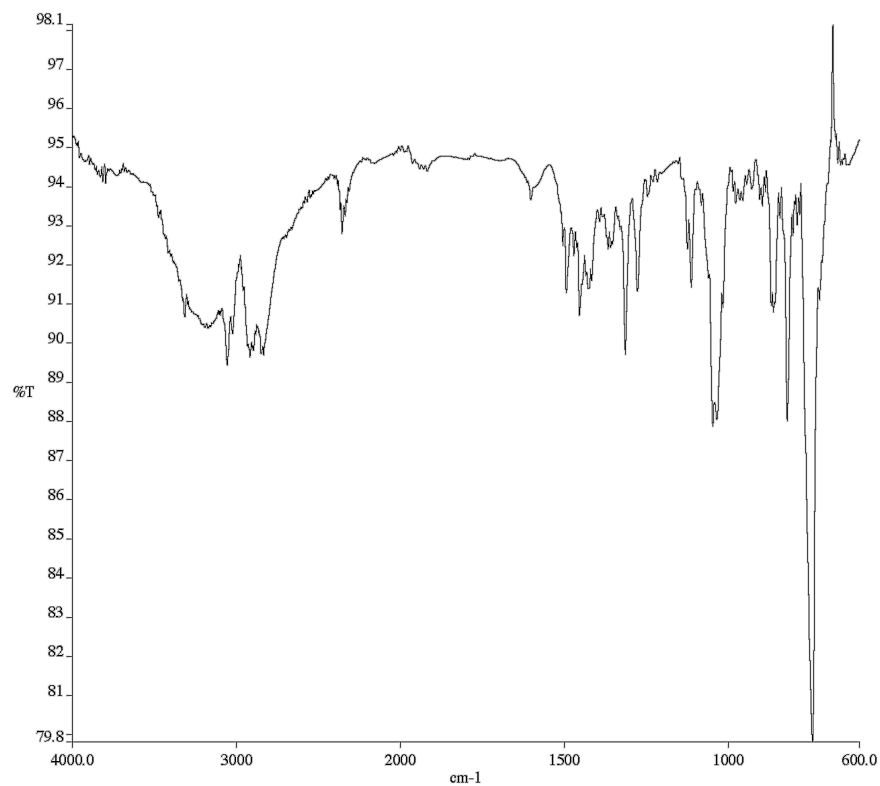


Figure A11.234 Infrared spectrum (Thin Film, NaCl) of compound

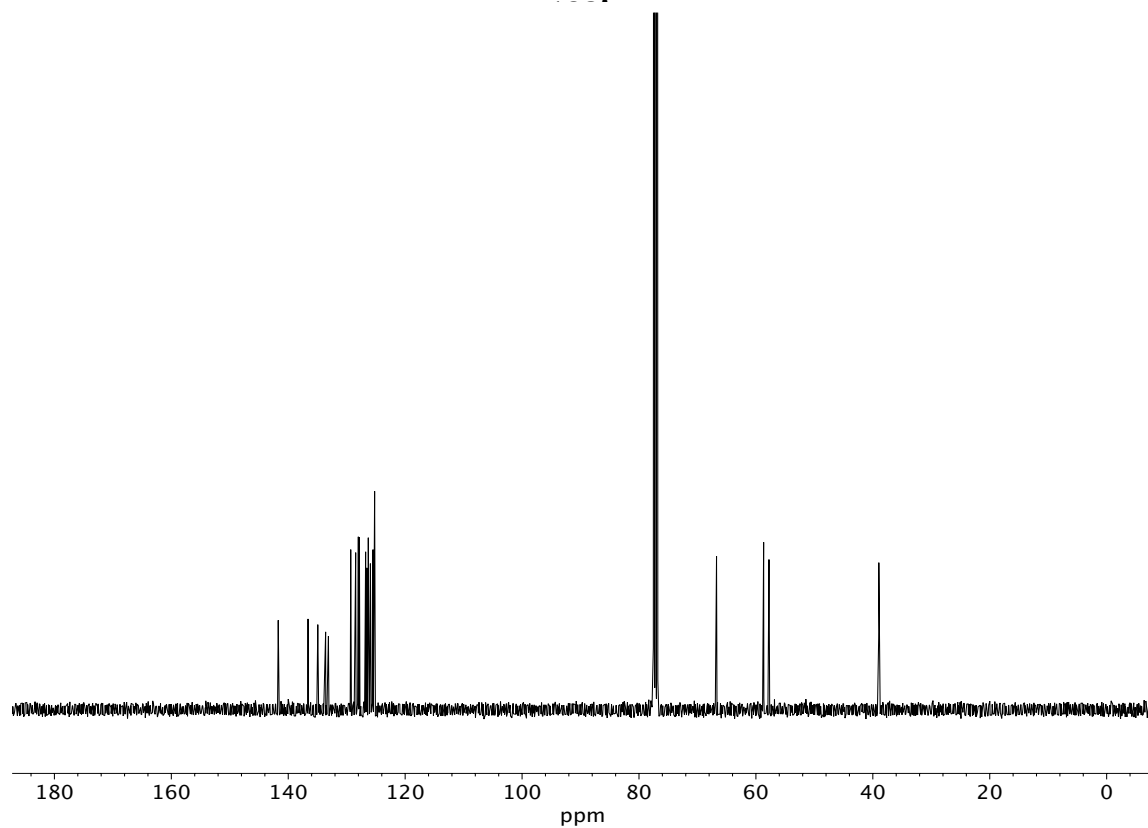


Figure A11.235 ¹³C NMR (100 MHz, CDCl₃) of compound **183j**.

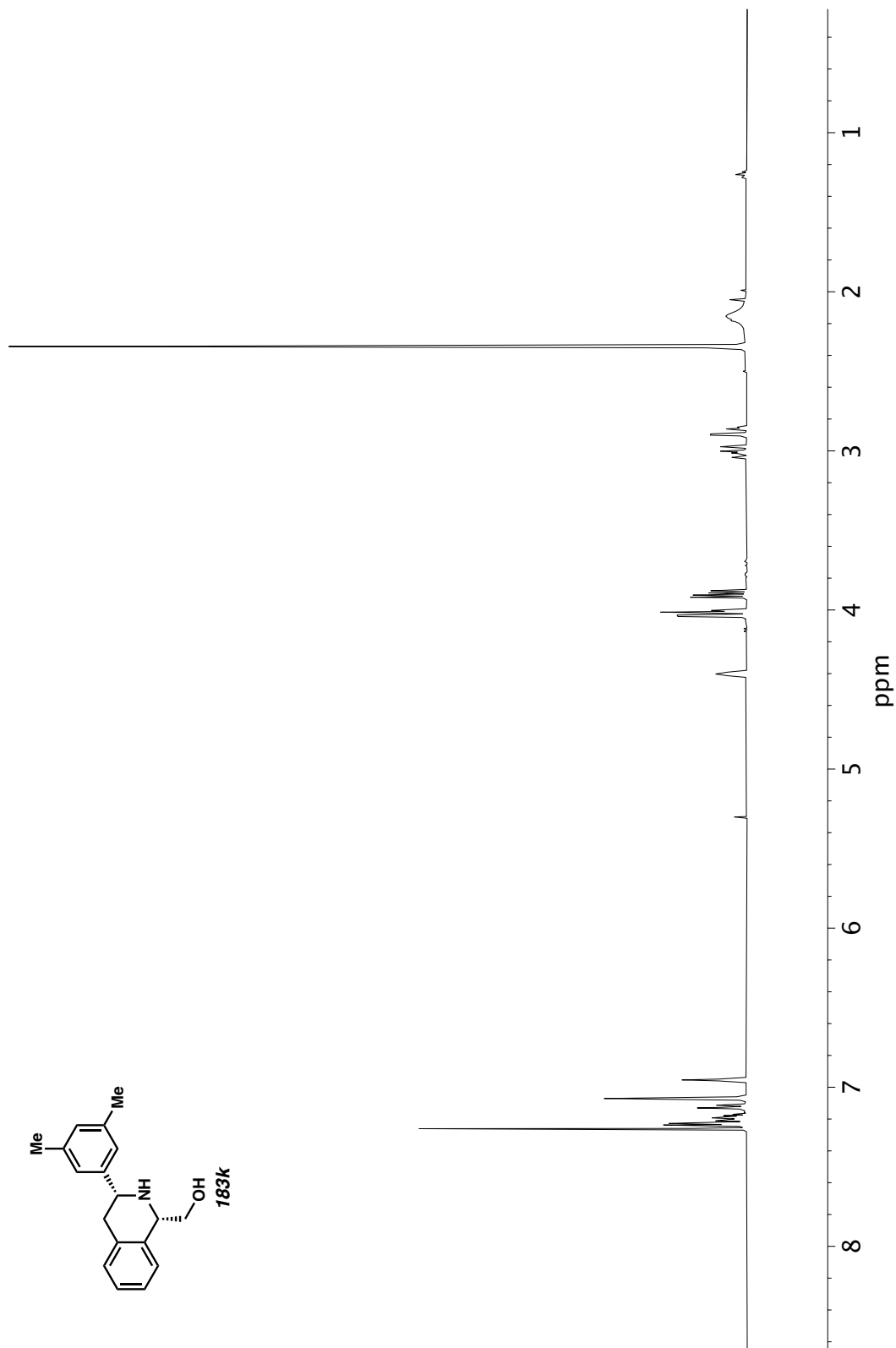


Figure A11.236 ^1H NMR (400 MHz, CDCl_3) of compound **183k**.

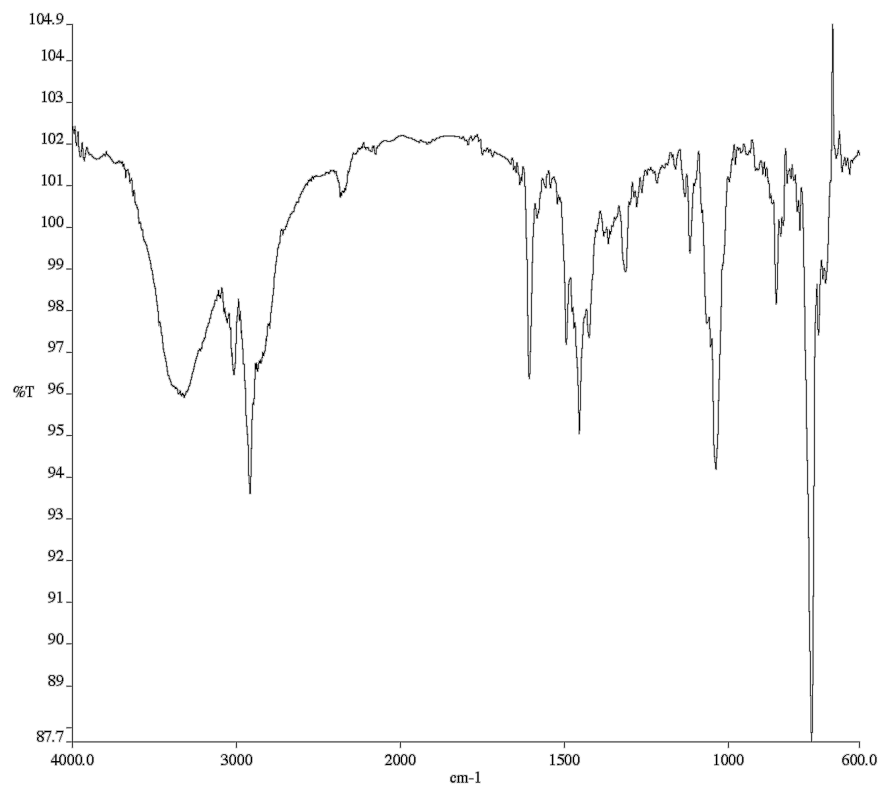


Figure A11.237 Infrared spectrum (Thin Film, NaCl) of compound

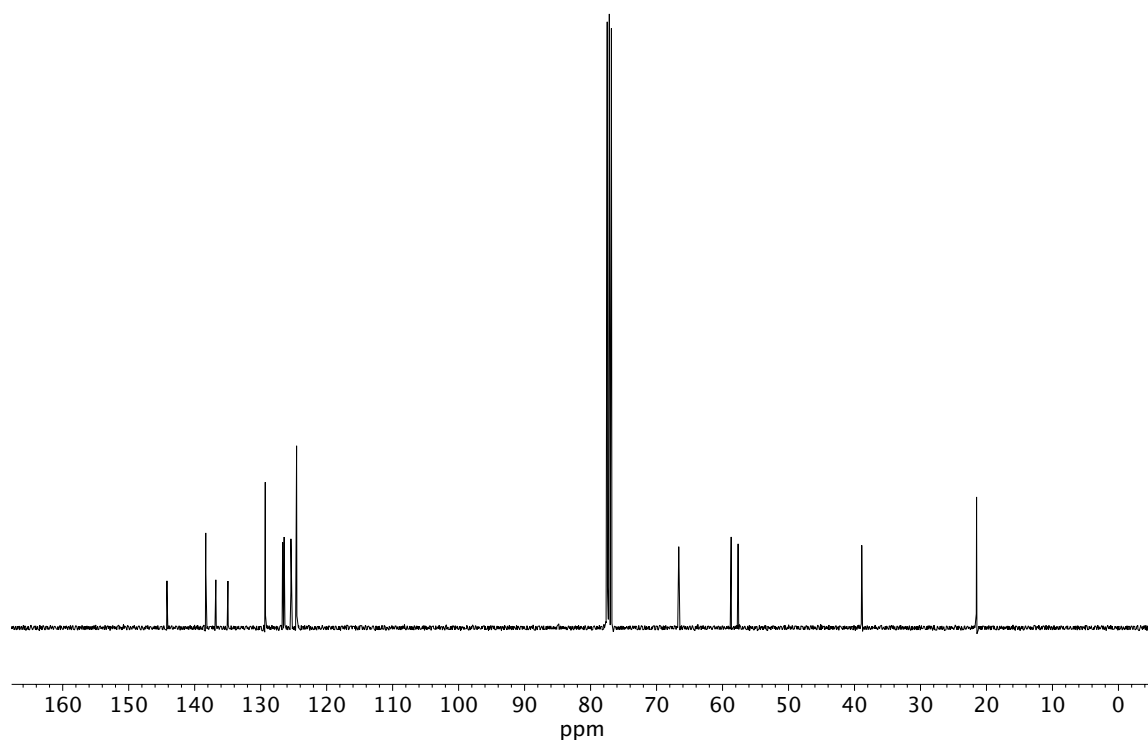


Figure A11.238 ¹³C NMR (100 MHz, CDCl₃) of compound **183k**.

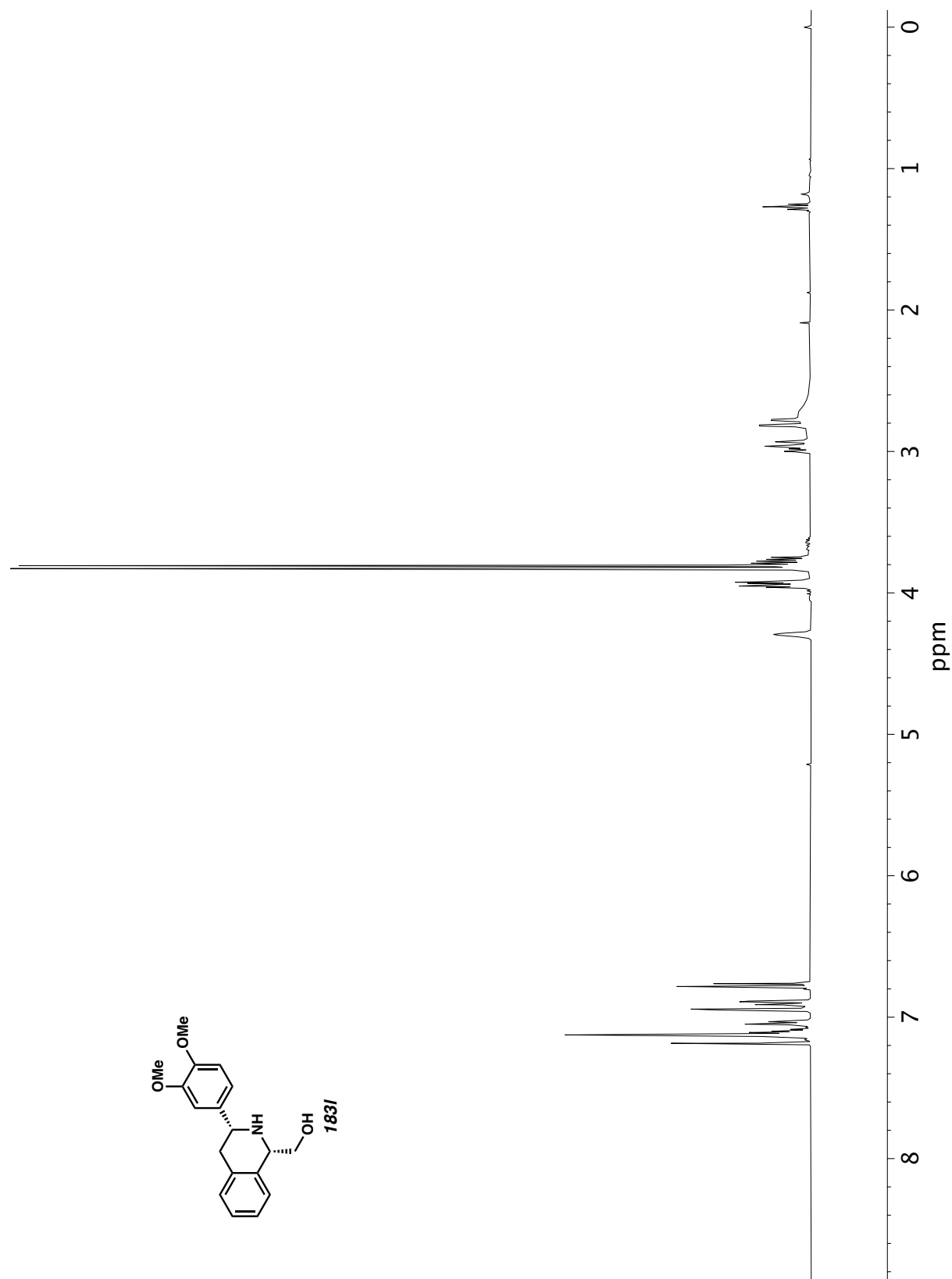


Figure A11.239 ¹H NMR (400 MHz, CDCl₃) of compound **183l**.

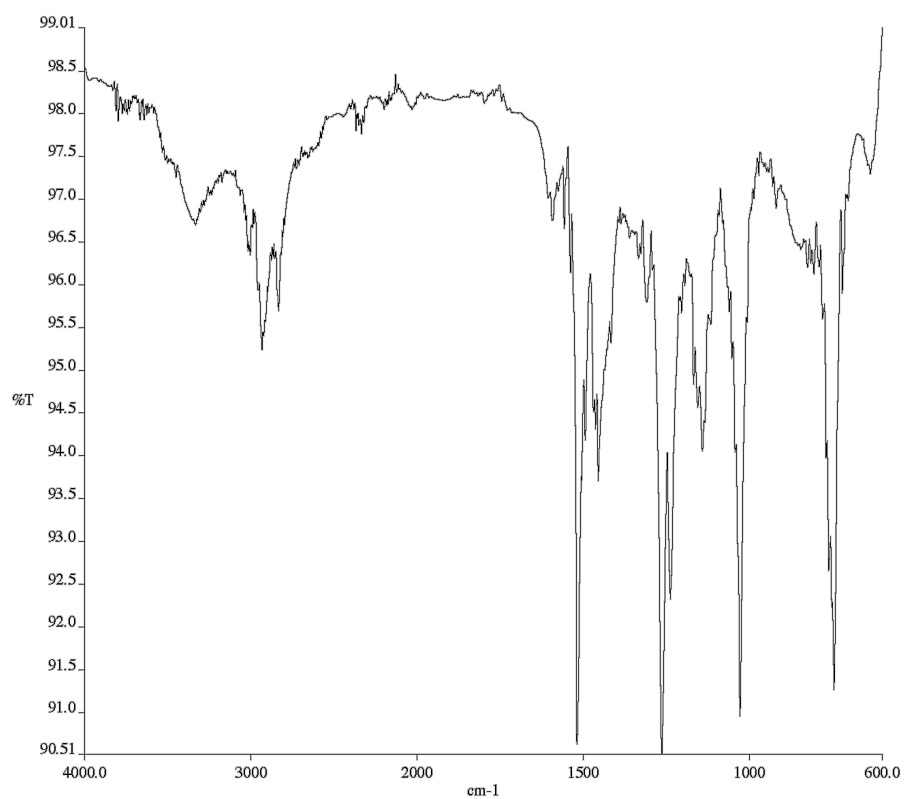


Figure A11.240 Infrared spectrum (Thin Film, NaCl) of compound

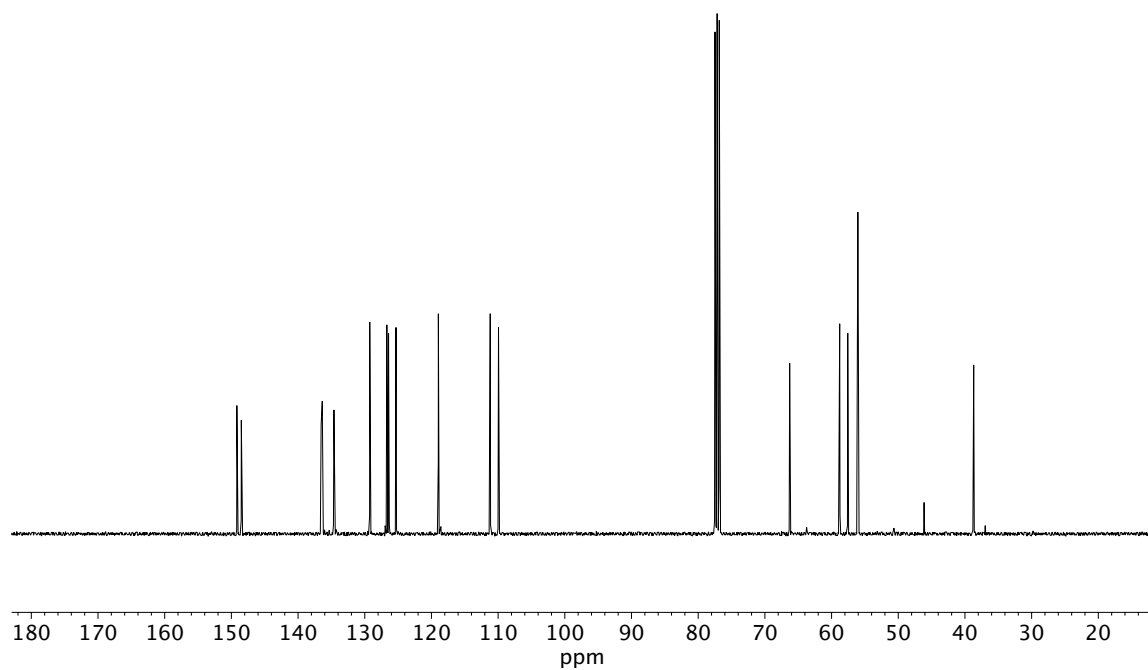


Figure A11.241 ¹³C NMR (100 MHz, CDCl₃) of compound **183l**.

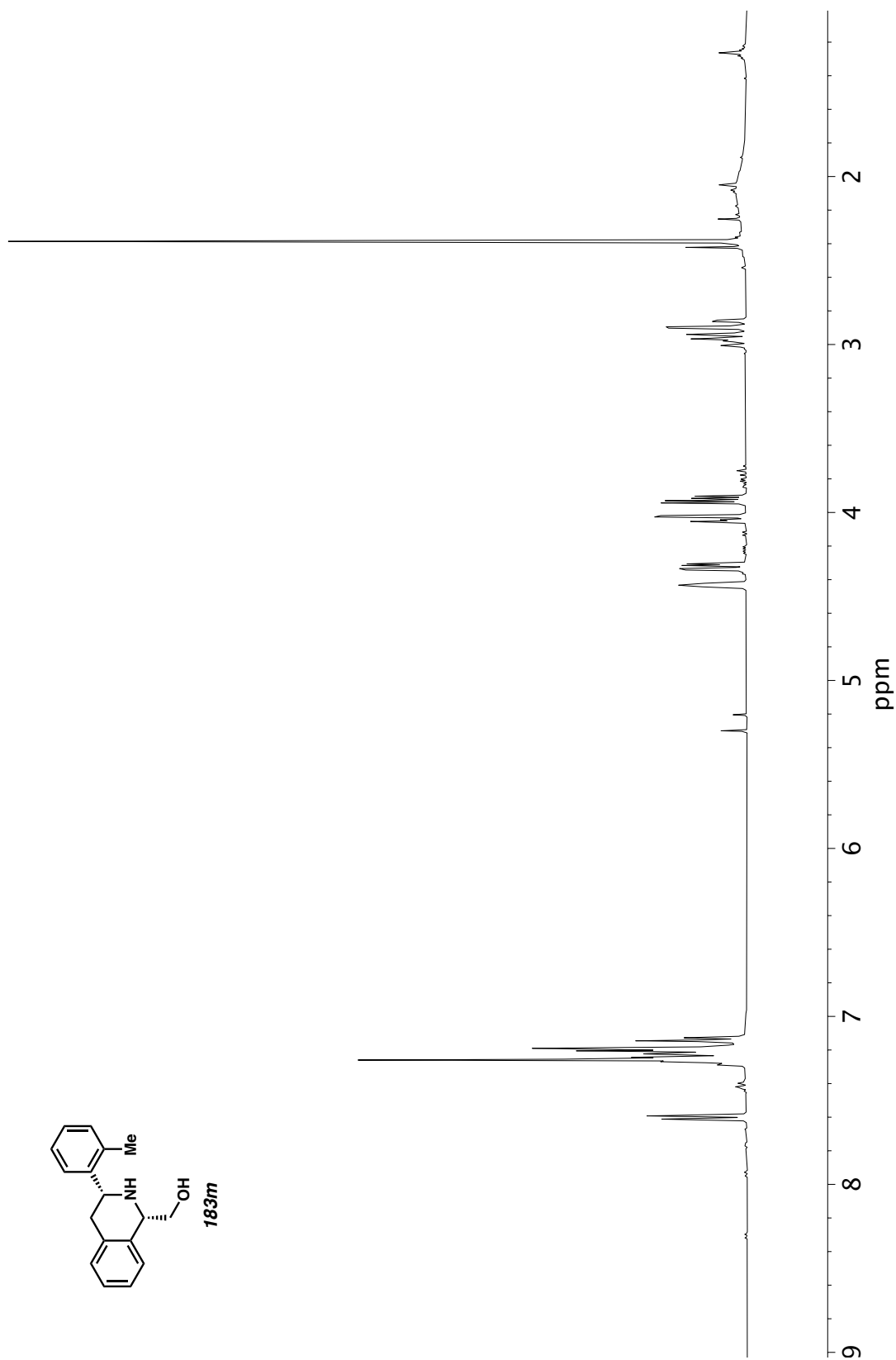


Figure A11.242 ^1H NMR (400 MHz, CDCl_3) of compound **183m**.

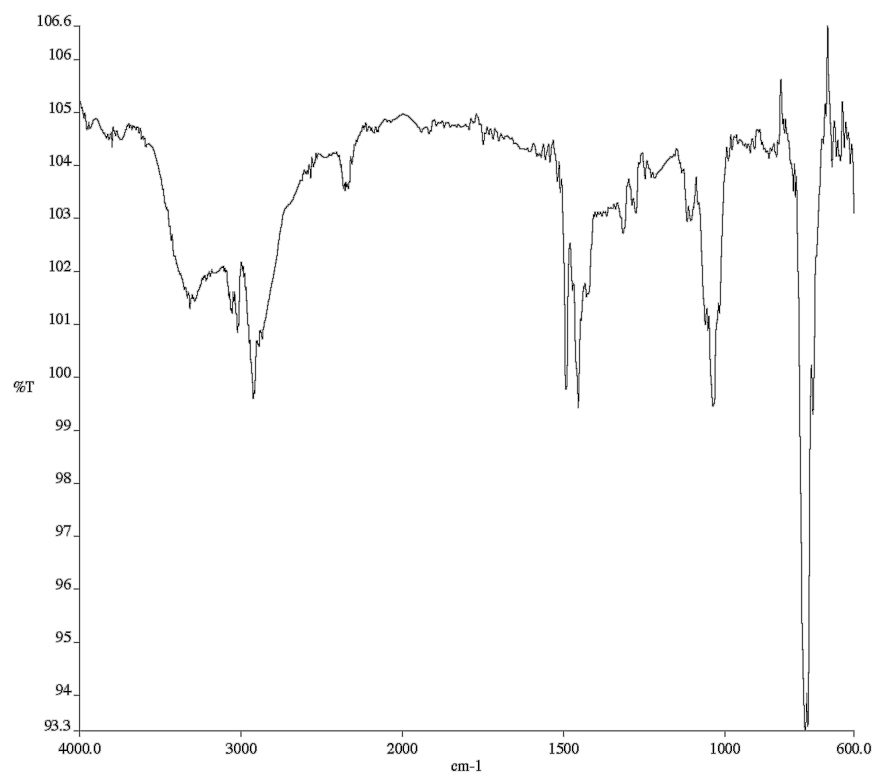


Figure A11.243 Infrared spectrum (Thin Film, NaCl) of compound

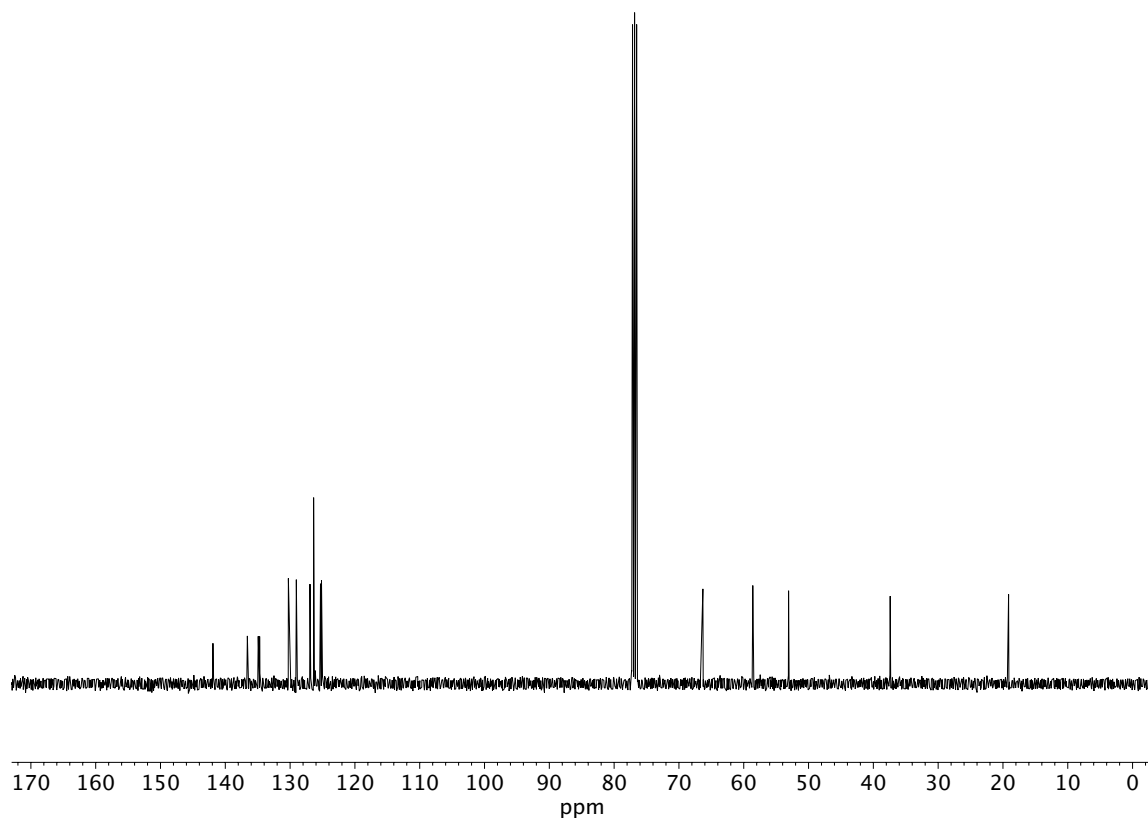


Figure A11.244 ¹³C NMR (100 MHz, CDCl₃) of compound **183m**.

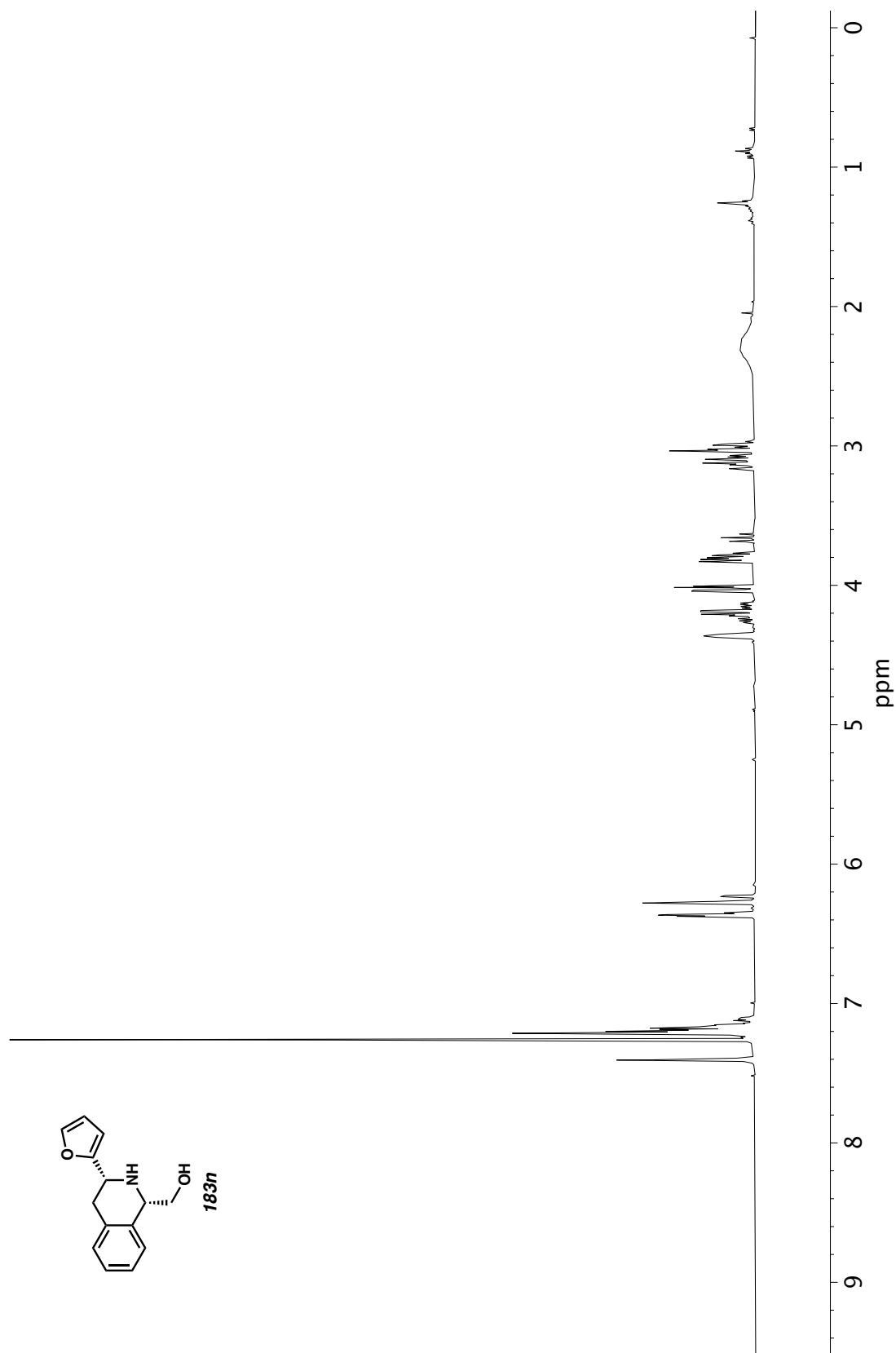


Figure A11.245 ¹H NMR (400 MHz, CDCl₃) of compound **183n**.

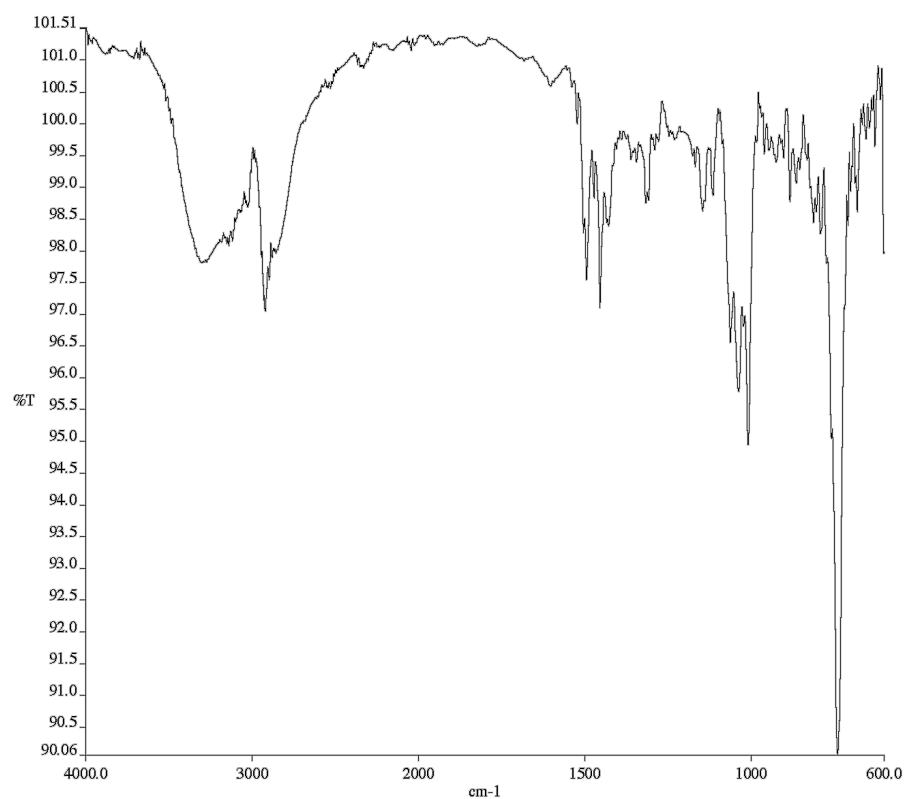


Figure A11.246 Infrared spectrum (Thin Film, NaCl) of compound

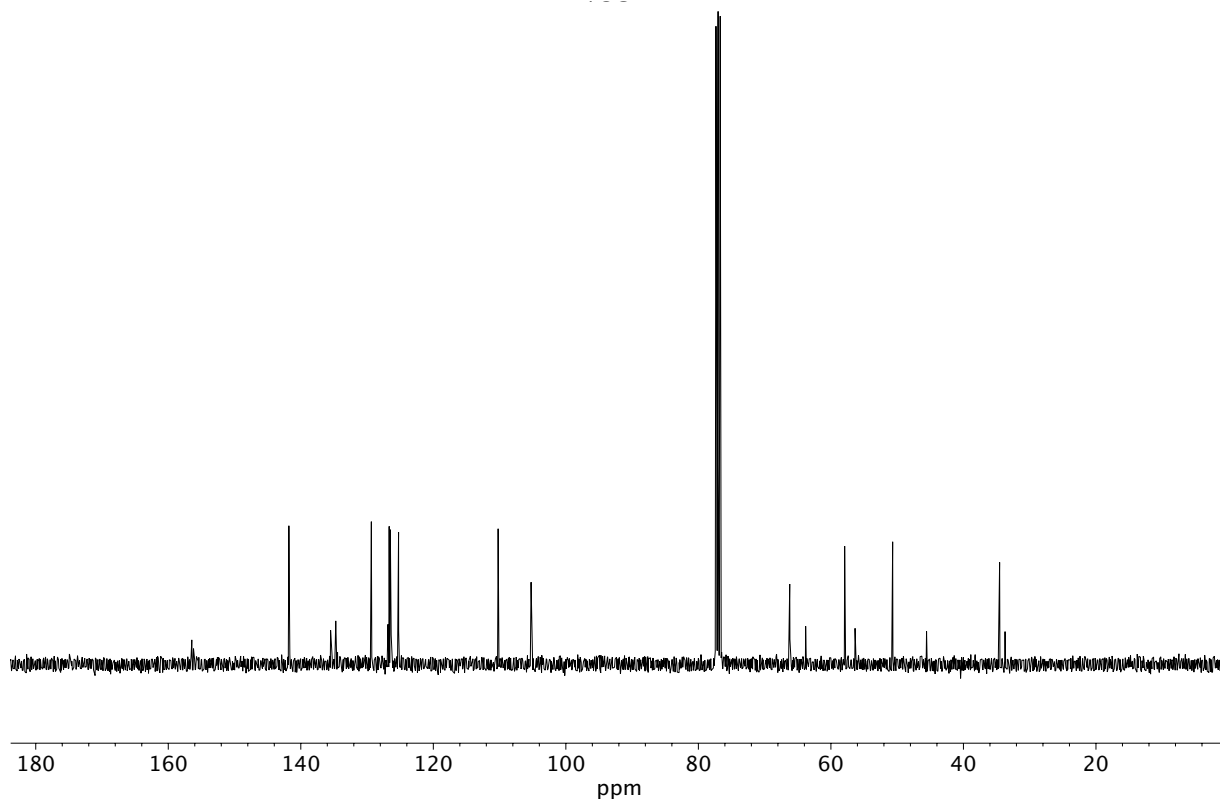


Figure A11.247 ¹³C NMR (100 MHz, CDCl₃) of compound **183n**.

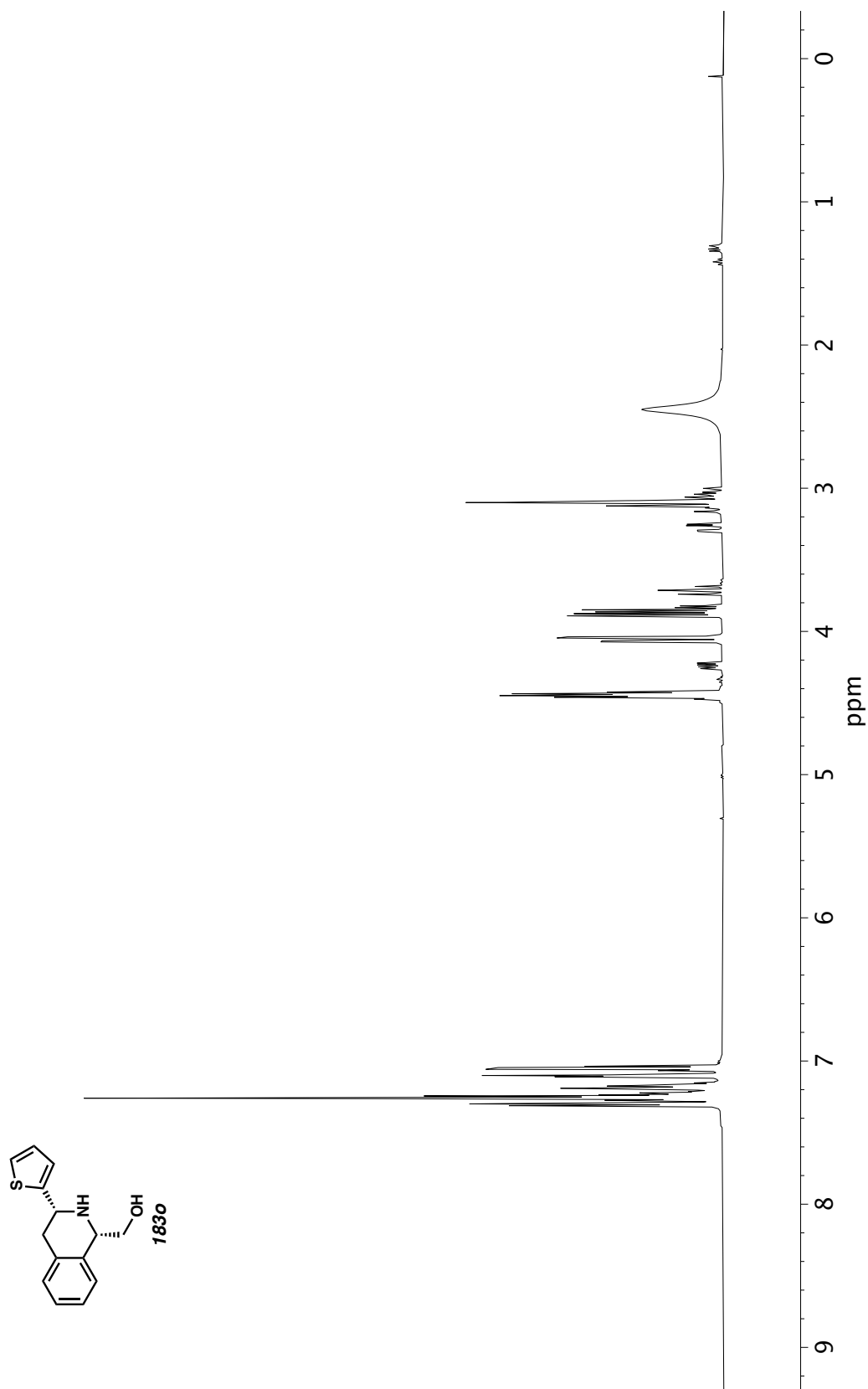


Figure A11.248 ¹H NMR (400 MHz, CDCl₃) of compound **183o**.

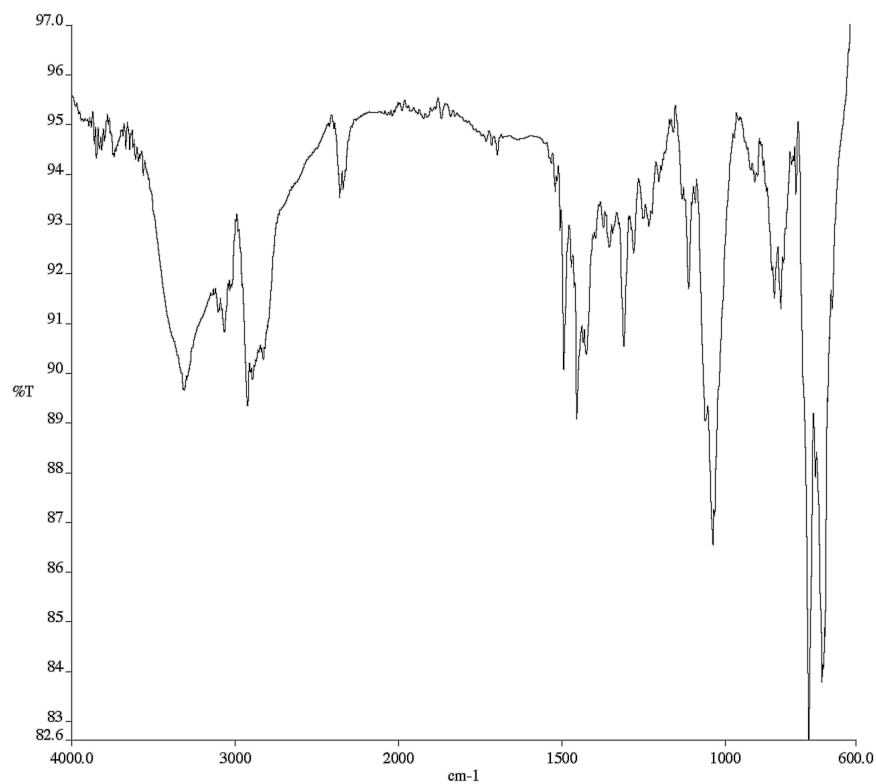


Figure A11.249 Infrared spectrum (Thin Film, NaCl) of compound

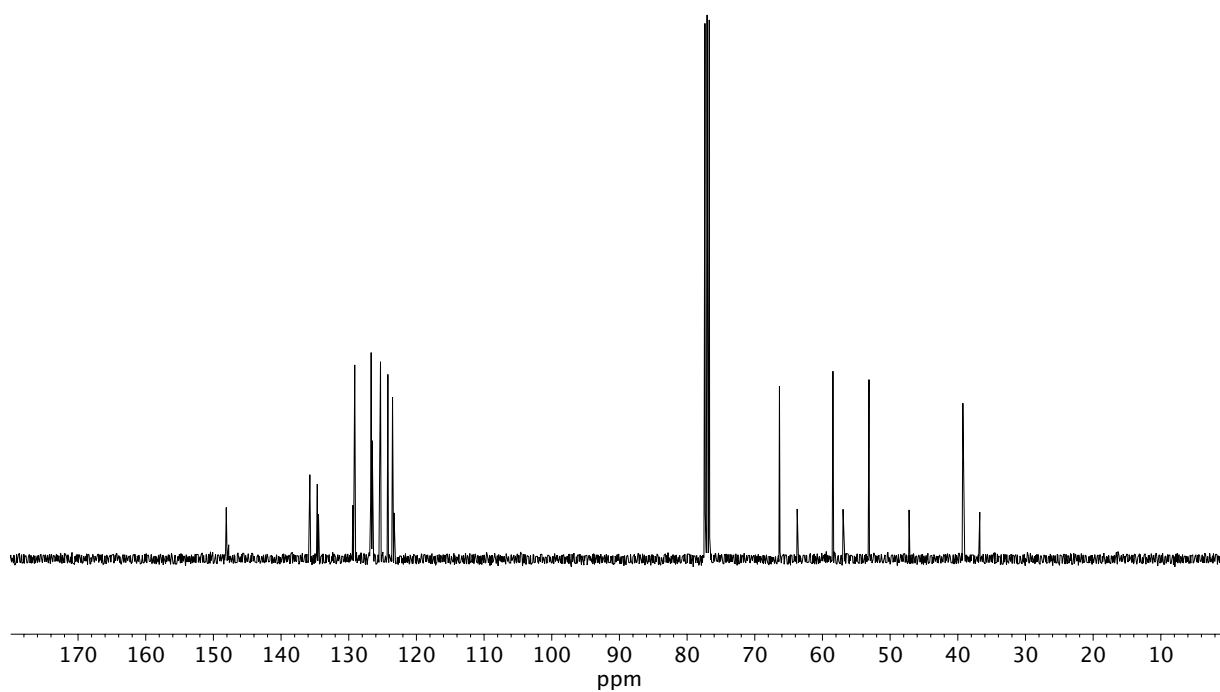


Figure A11.250 ¹³C NMR (100 MHz, CDCl₃) of compound **183o**.

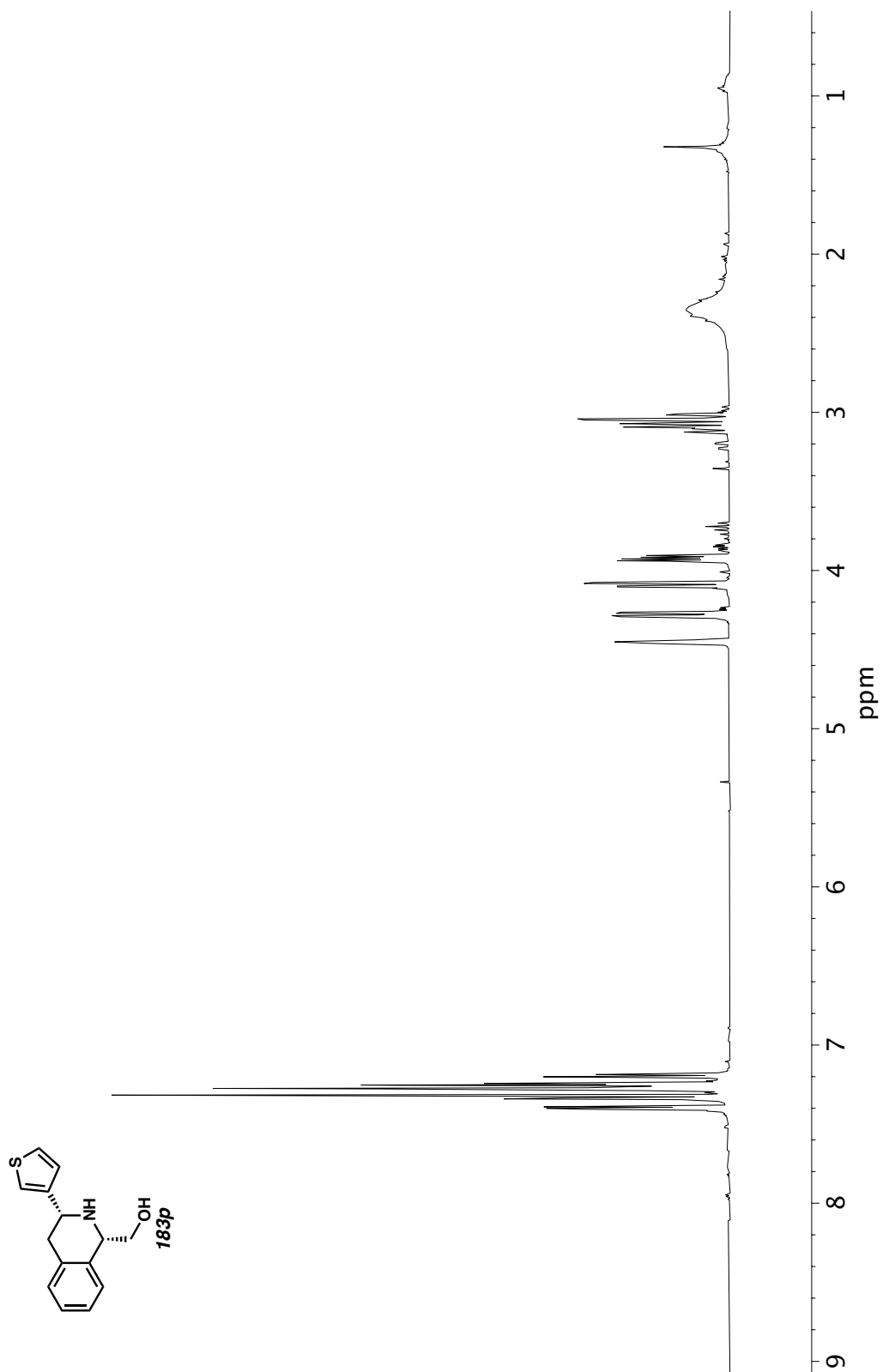


Figure A11.251 ^1H NMR (400 MHz, CDCl_3) of compound **183p**.

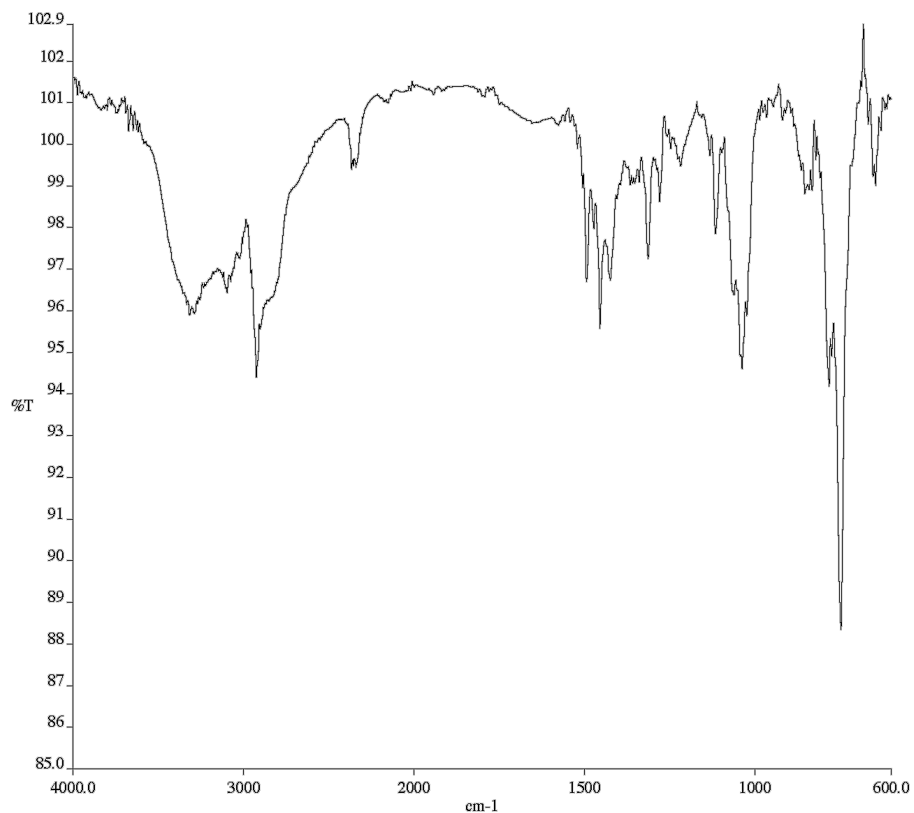


Figure A11.252 Infrared spectrum (Thin Film, NaCl) of compound

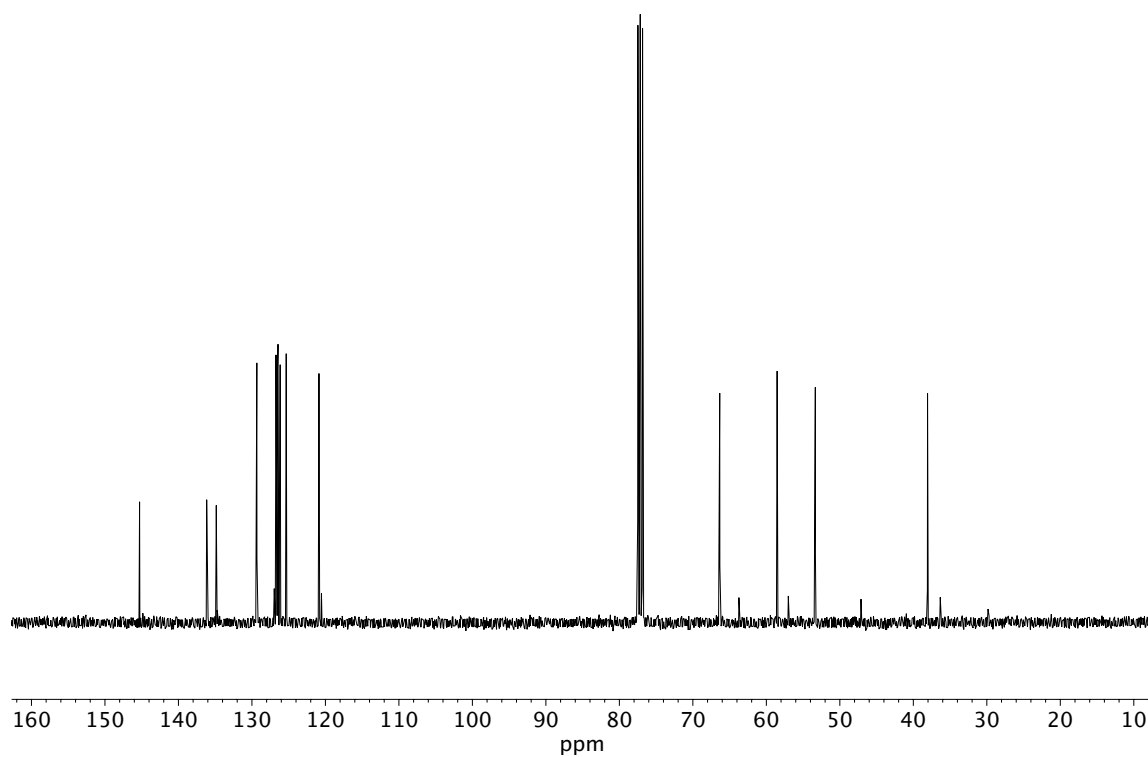


Figure A11.253 ¹³C NMR (100 MHz, CDCl₃) of compound **183p**.

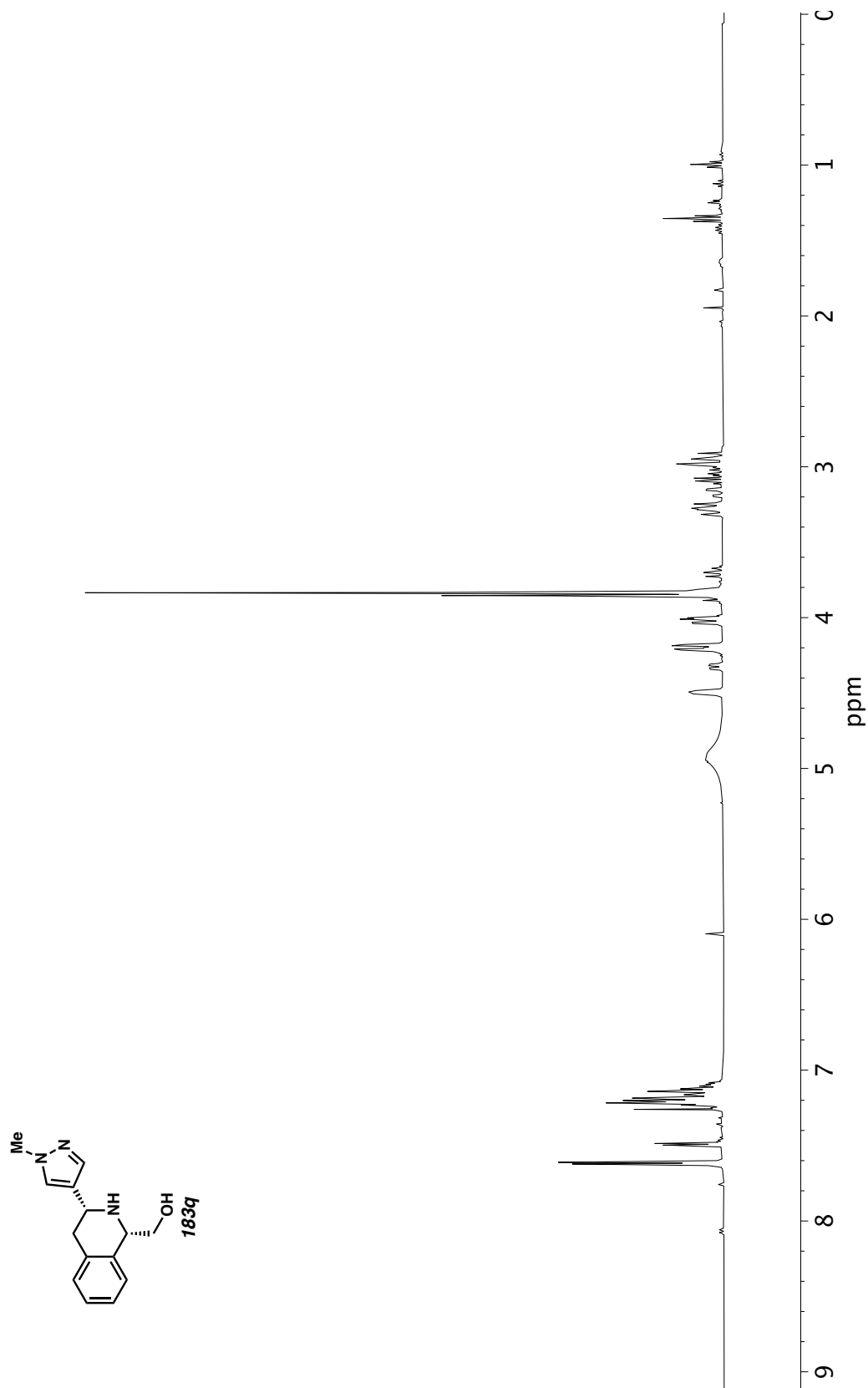


Figure A11.254 ^1H NMR (400 MHz, CDCl_3) of compound **183q**.

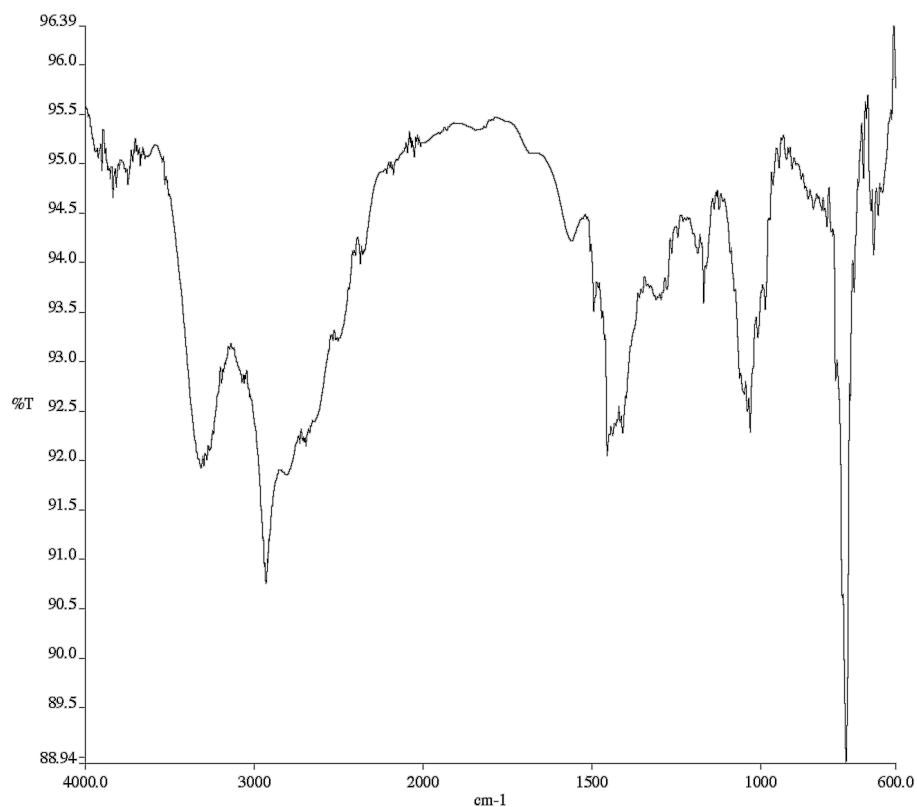


Figure A11.255 Infrared spectrum (Thin Film, NaCl) of compound

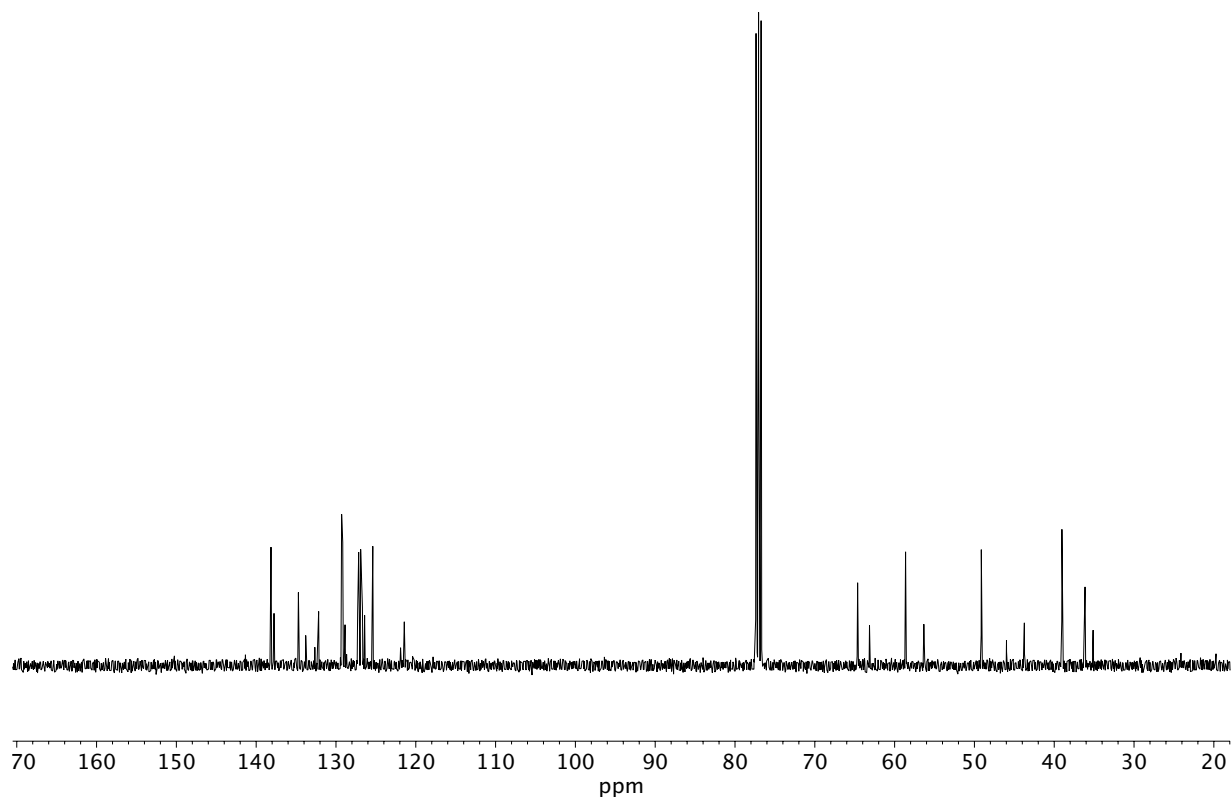


Figure A11.256 ¹³C NMR (100 MHz, CDCl₃) of compound **183q**.

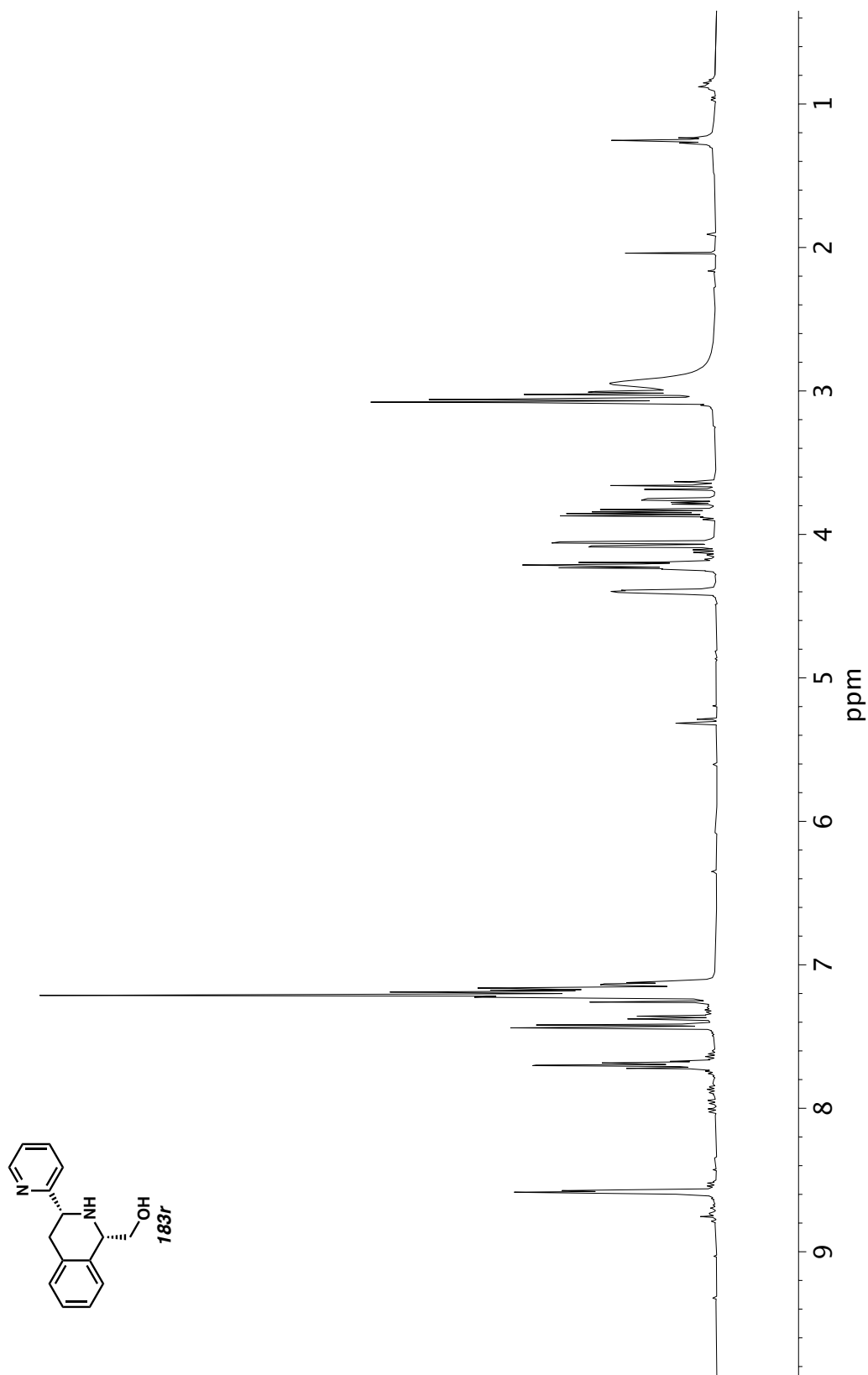


Figure A11.257 ^1H NMR (400 MHz, CDCl_3) of compound **183r**.

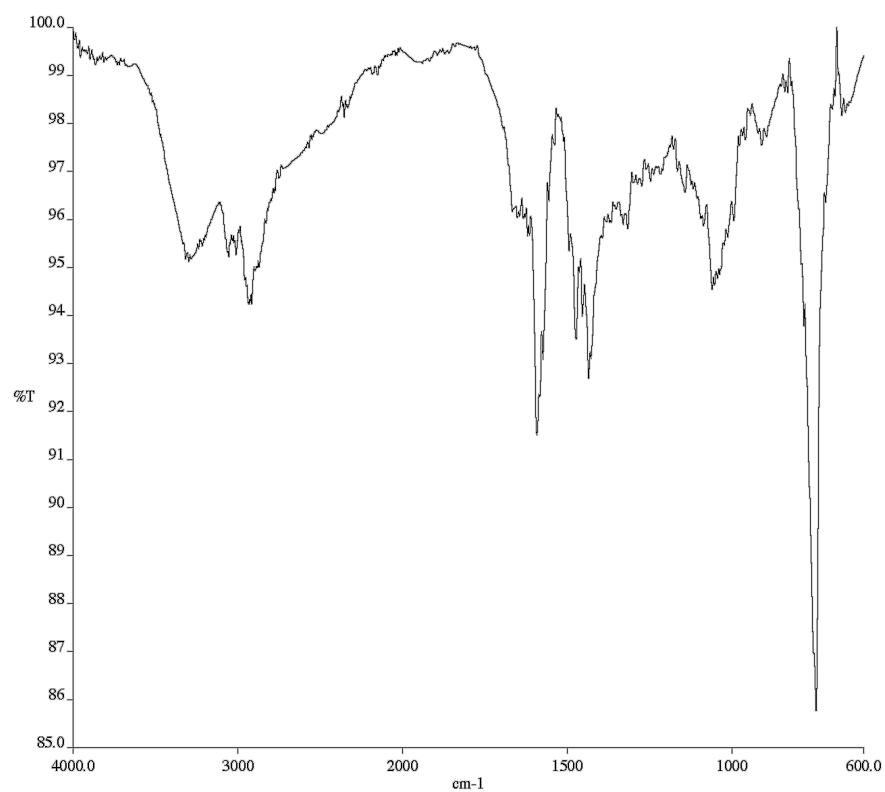


Figure A11.258 Infrared spectrum (Thin Film, NaCl) of compound

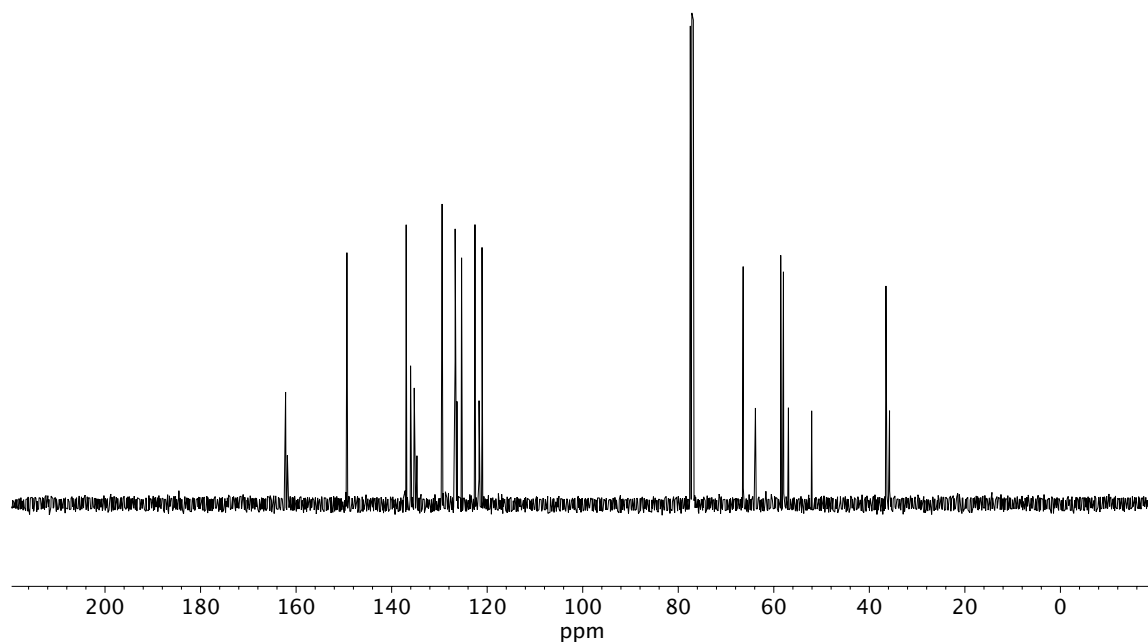


Figure A11.259 ¹³C NMR (100 MHz, CDCl₃) of compound **183r**.

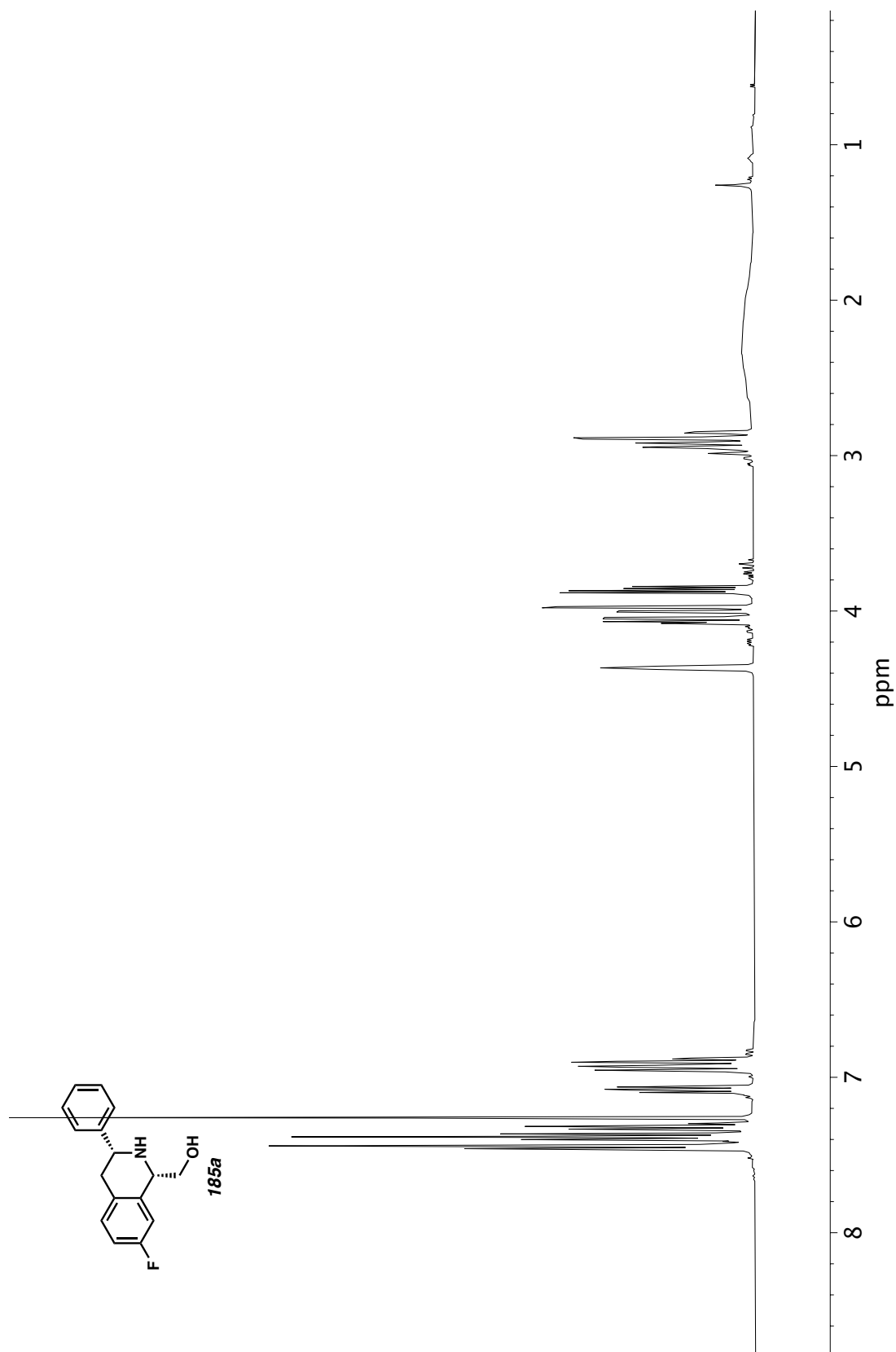


Figure A11.260 ^1H NMR (400 MHz, CDCl_3) of compound **185a**.

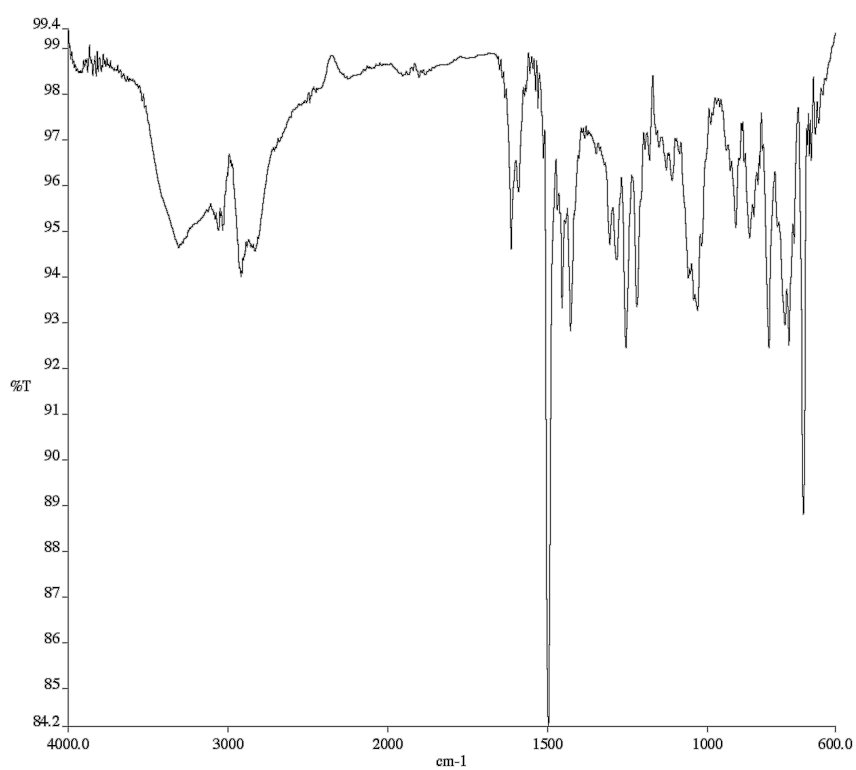


Figure A11.261 Infrared spectrum (Thin Film, NaCl) of compound

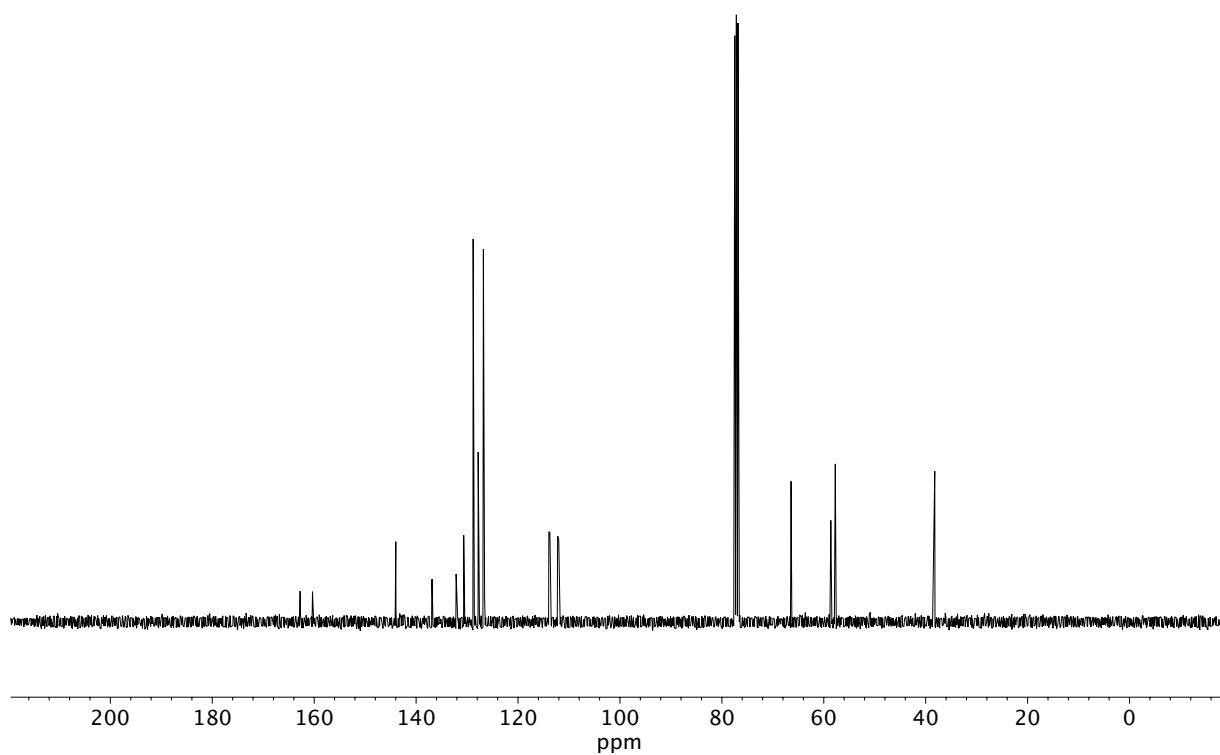


Figure A11.262 ¹³C NMR (100 MHz, CDCl₃) of compound **185a**.

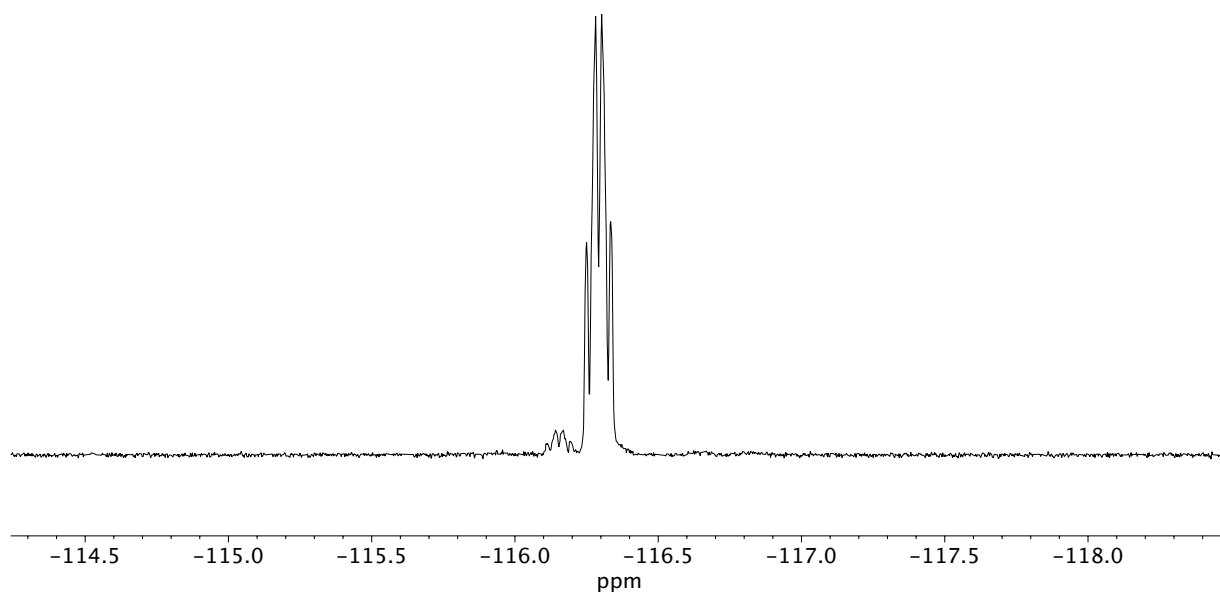


Figure A11.263 ^{19}F NMR (282 MHz, CDCl_3) of compound **185a**.

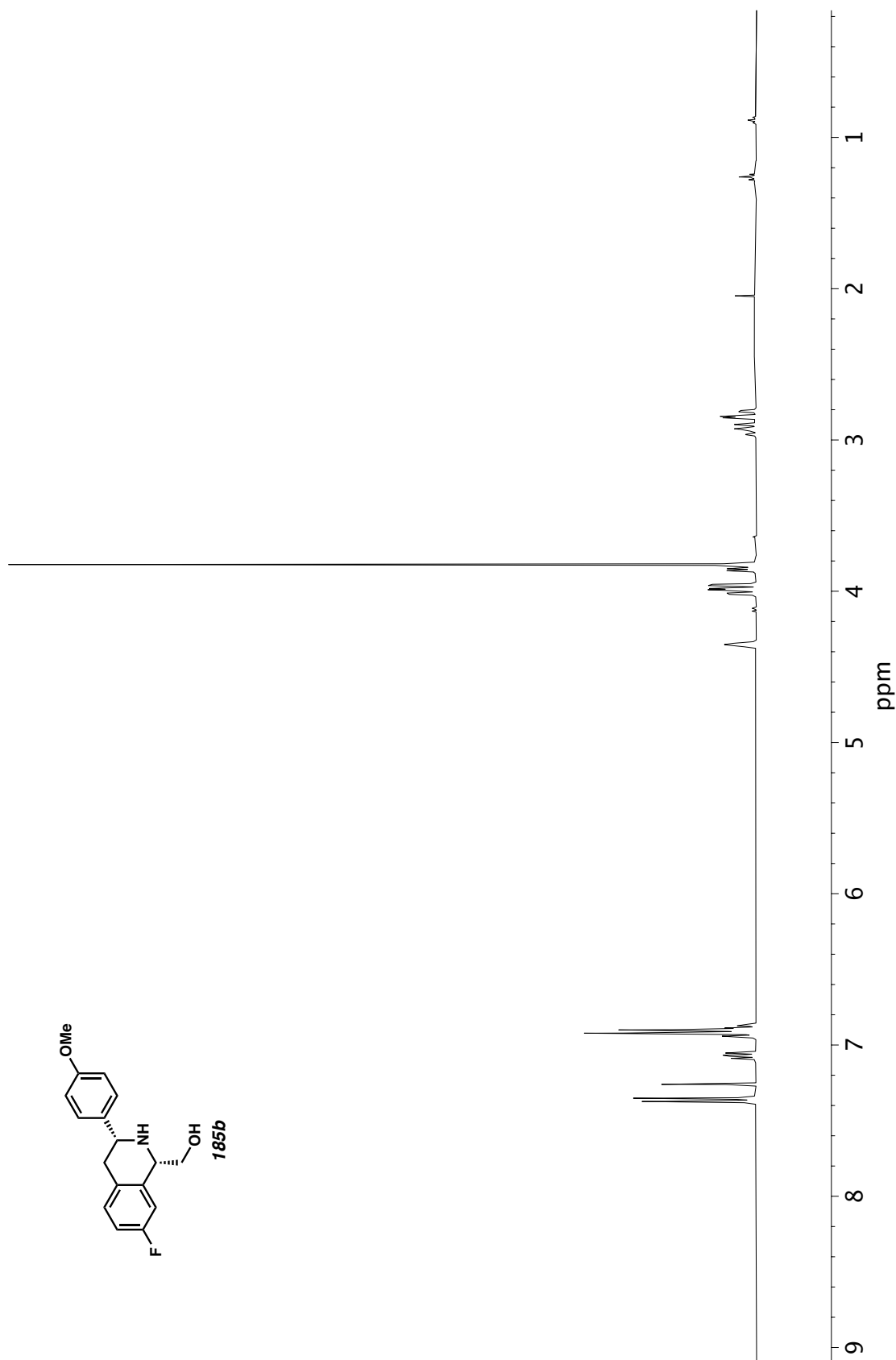


Figure A11.264 ¹H NMR (400 MHz, CDCl₃) of compound **185b**.

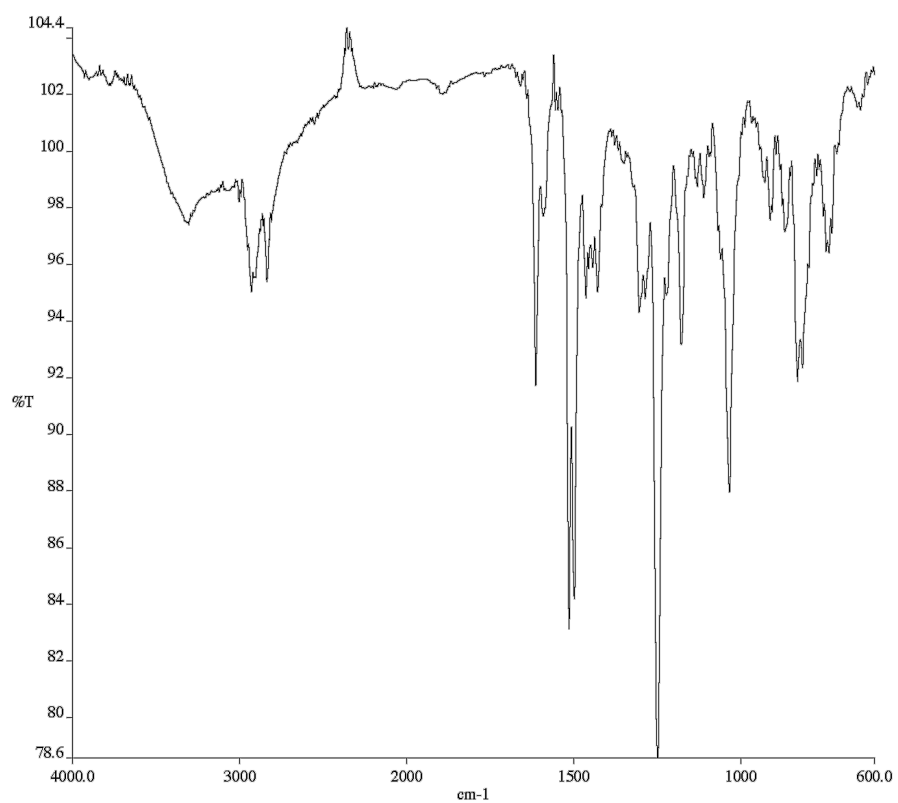


Figure A11.265 Infrared spectrum (Thin Film, NaCl) of compound

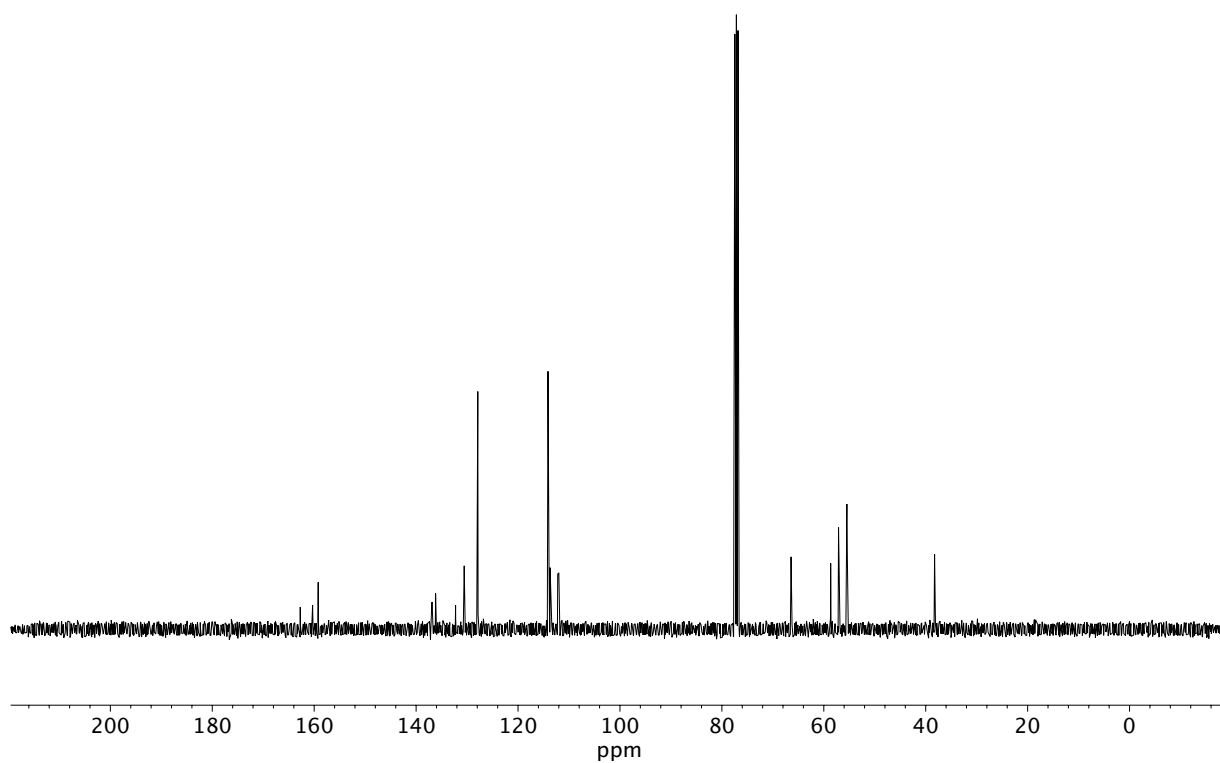


Figure A11.266 ¹³C NMR (100 MHz, CDCl₃) of compound **185b**.

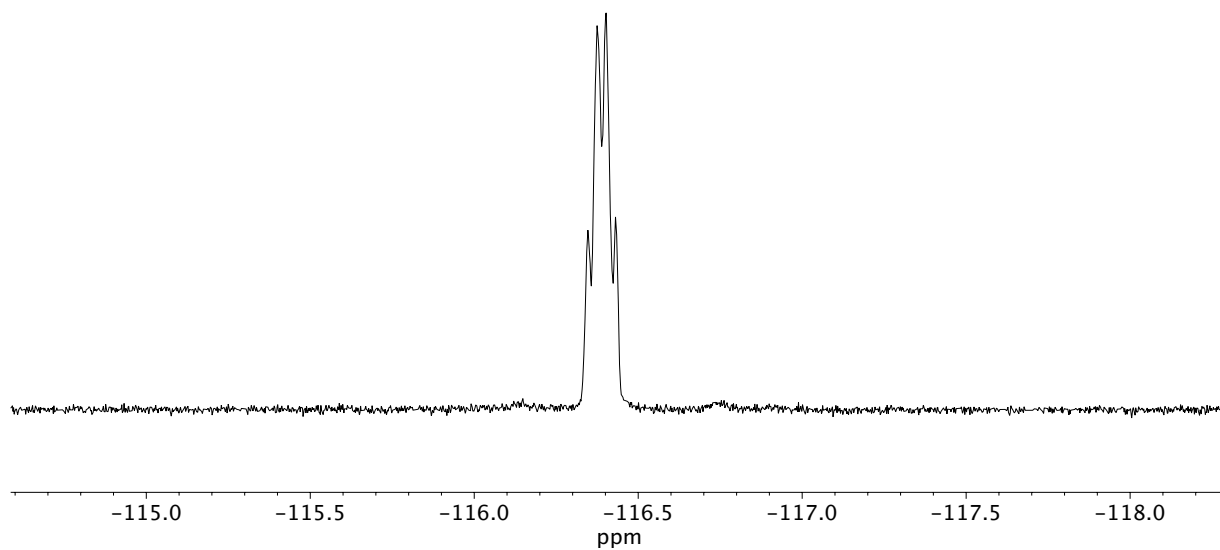


Figure A11.267 ^{19}F NMR (282 MHz, CDCl_3) of compound **185b**.

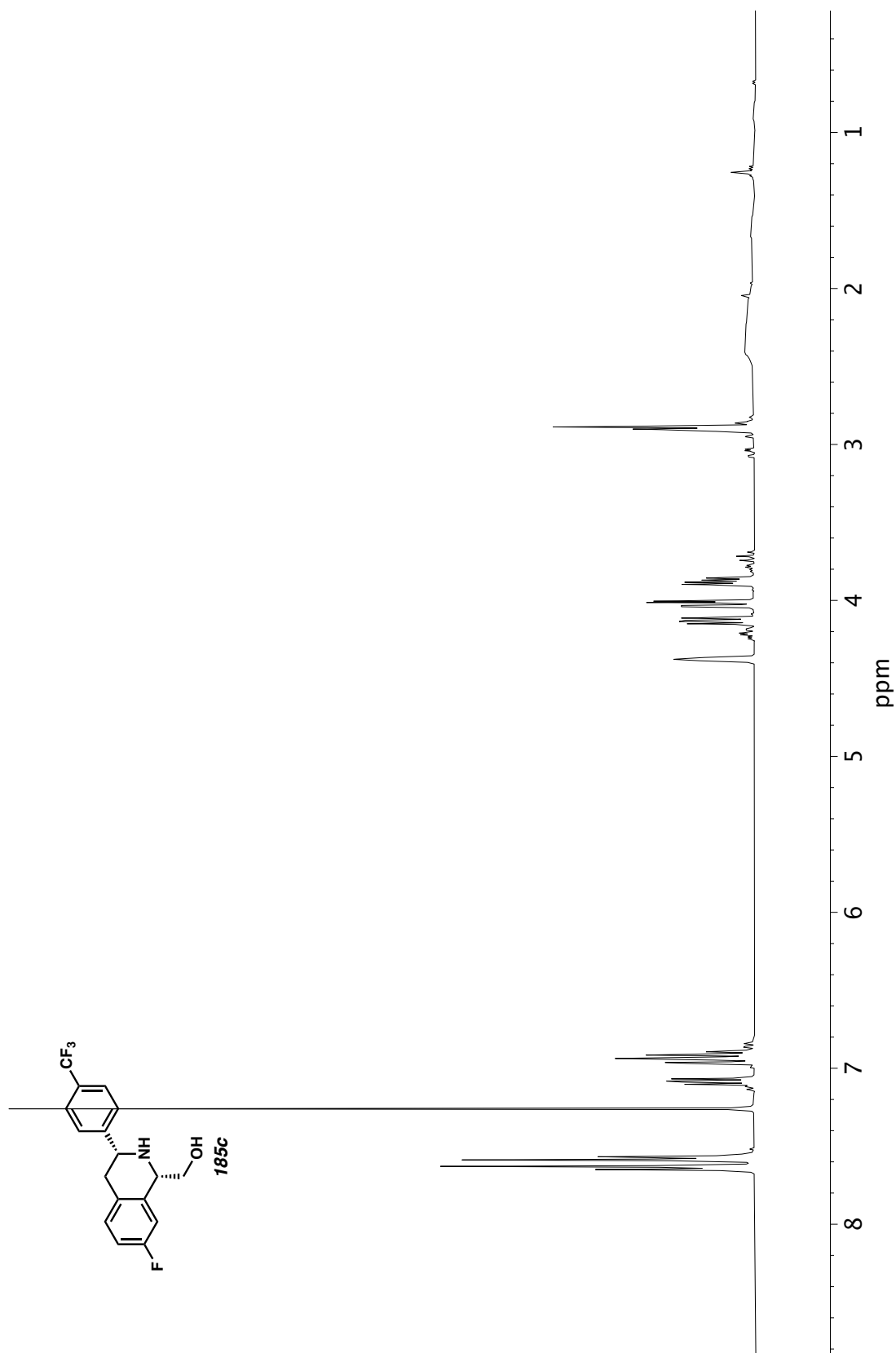


Figure A11.268 ¹H NMR (400 MHz, CDCl₃) of compound **185c**.

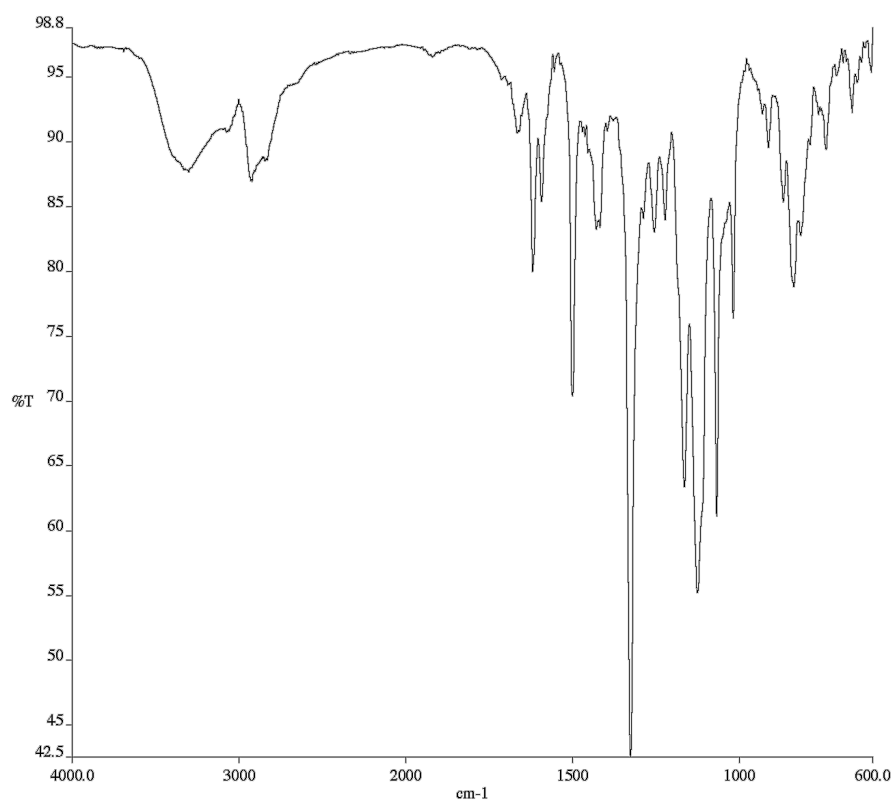


Figure A11.269 Infrared spectrum (Thin Film, NaCl) of compound

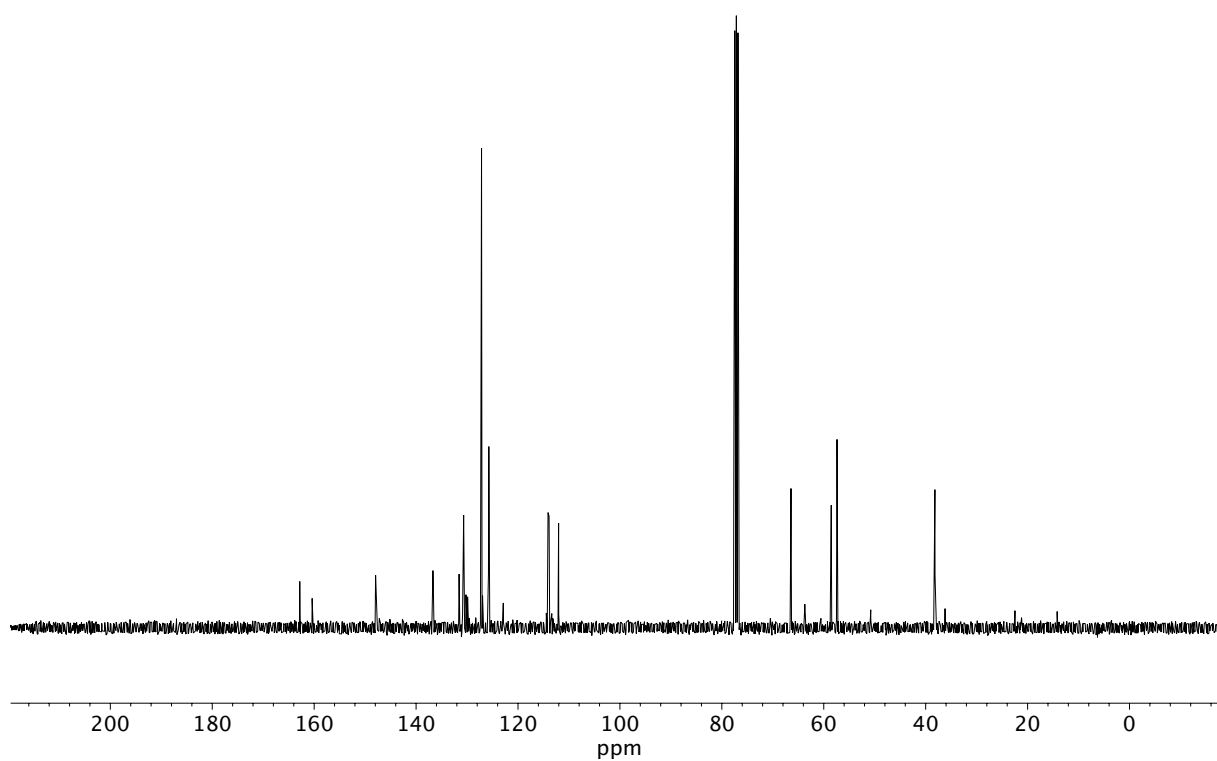


Figure A11.270 ¹³C NMR (100 MHz, CDCl₃) of compound **185c**.

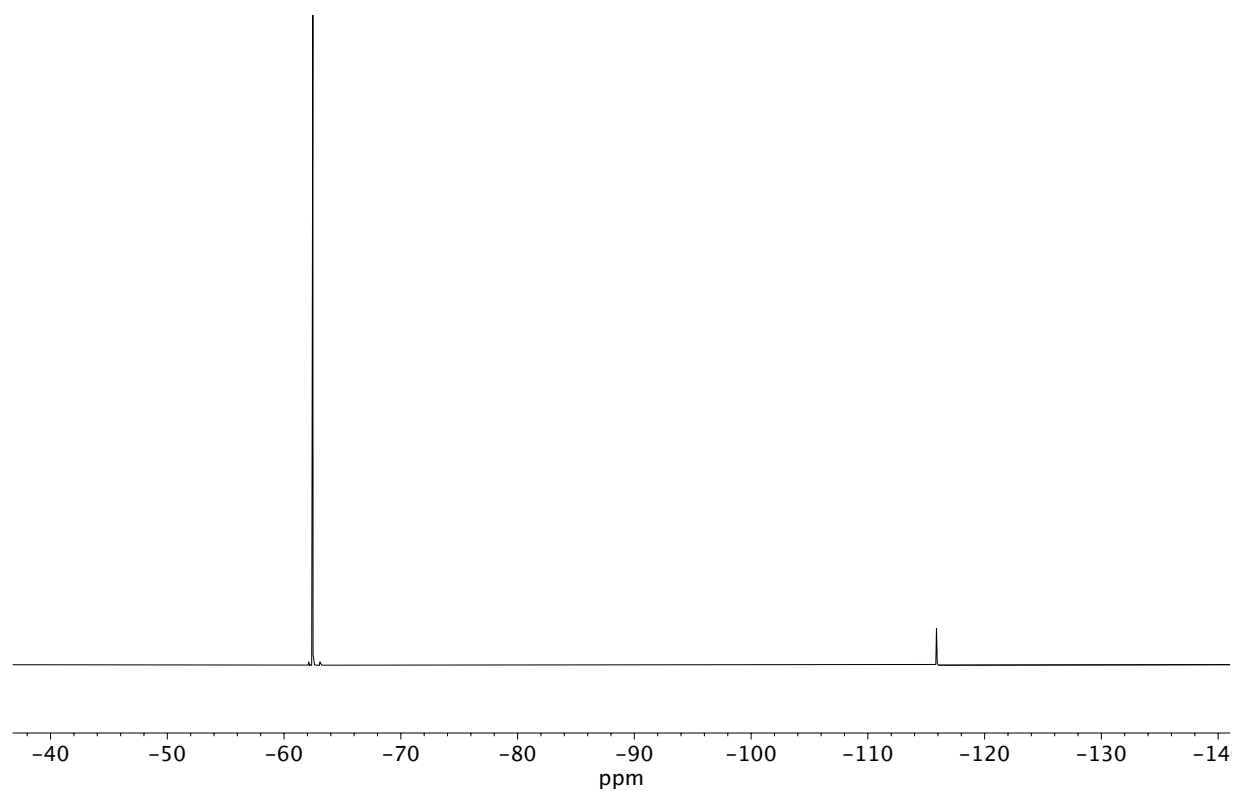


Figure A11.271 ^{19}F NMR (282 MHz, CDCl_3) of compound **185c**.

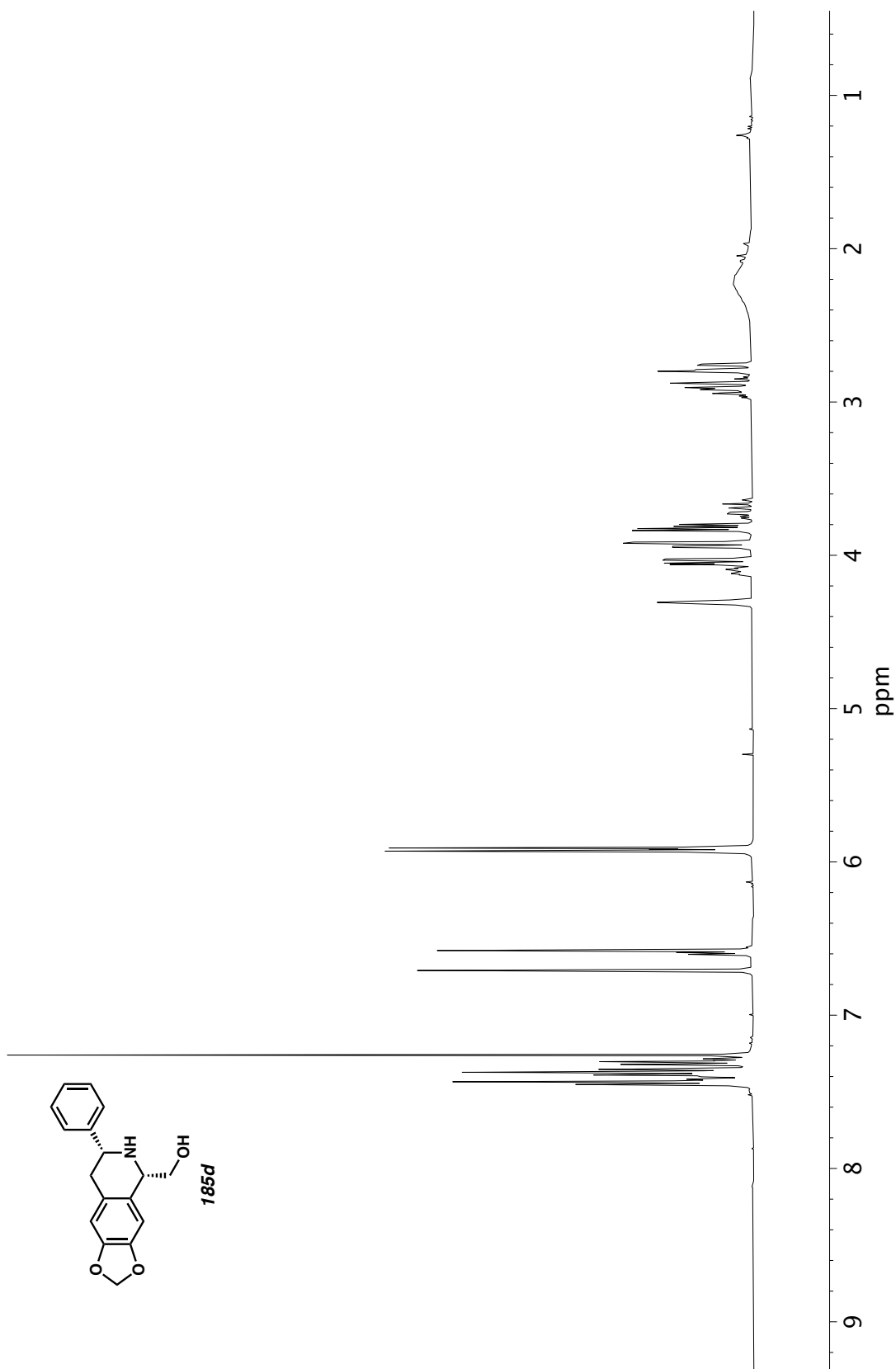


Figure A11.272 ^1H NMR (400 MHz, CDCl_3) of compound **185d**.

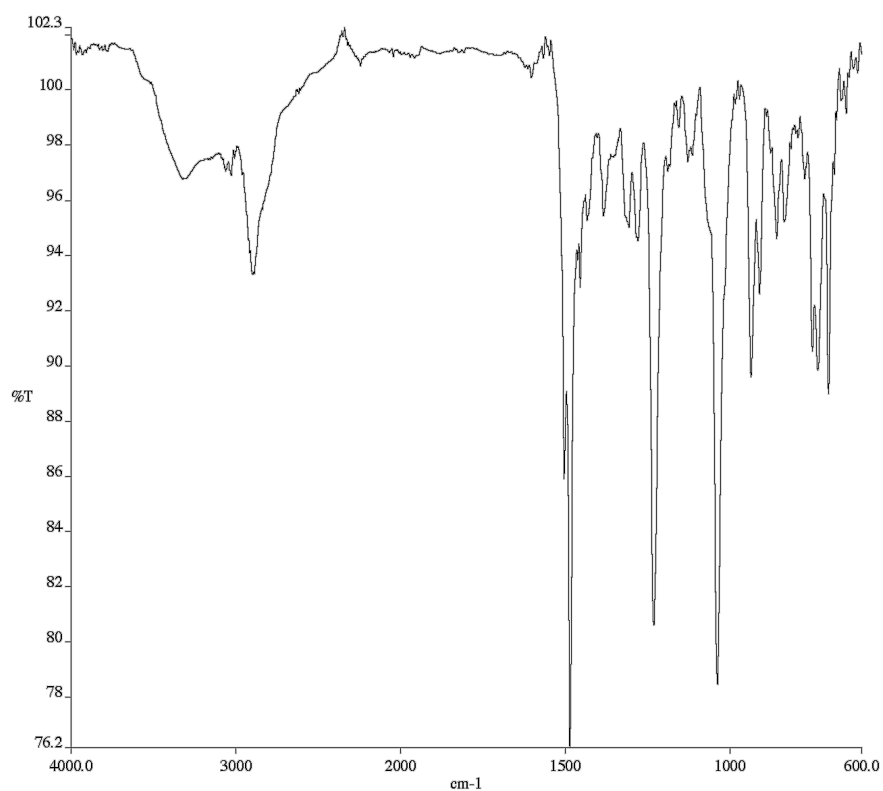


Figure A11.273 Infrared spectrum (Thin Film, NaCl) of compound

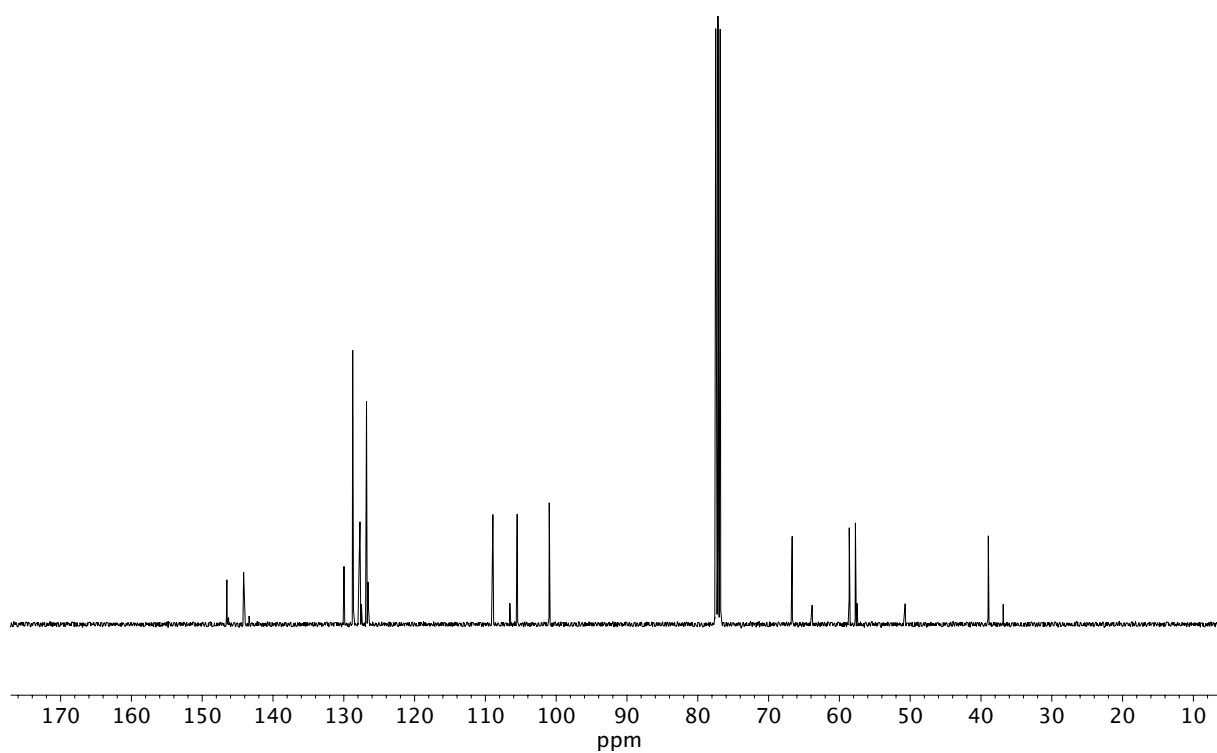


Figure A11.274 ¹³C NMR (100 MHz, CDCl₃) of compound **185d**.

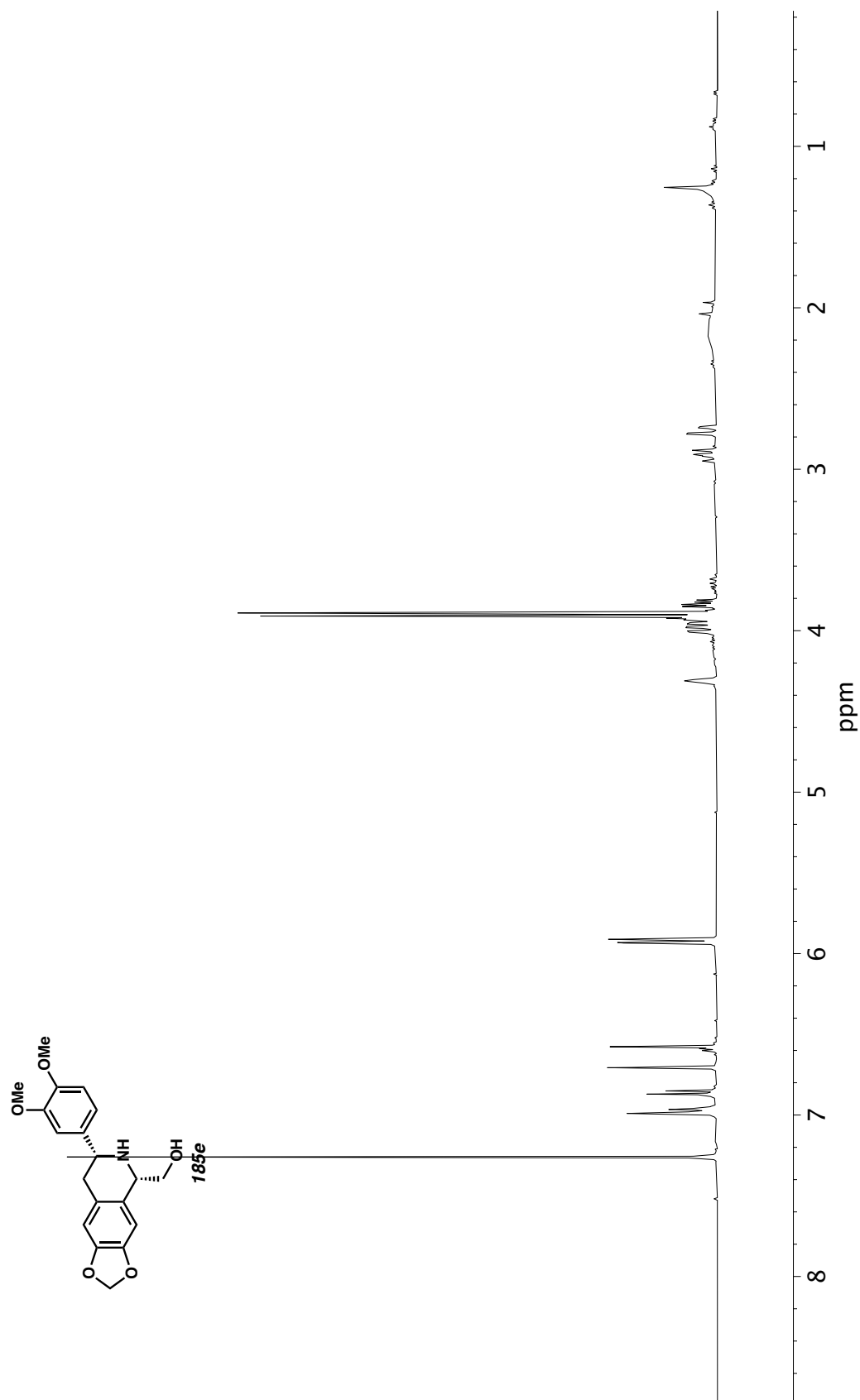


Figure A11.275 ^1H NMR (400 MHz, CDCl_3) of compound **185e**.

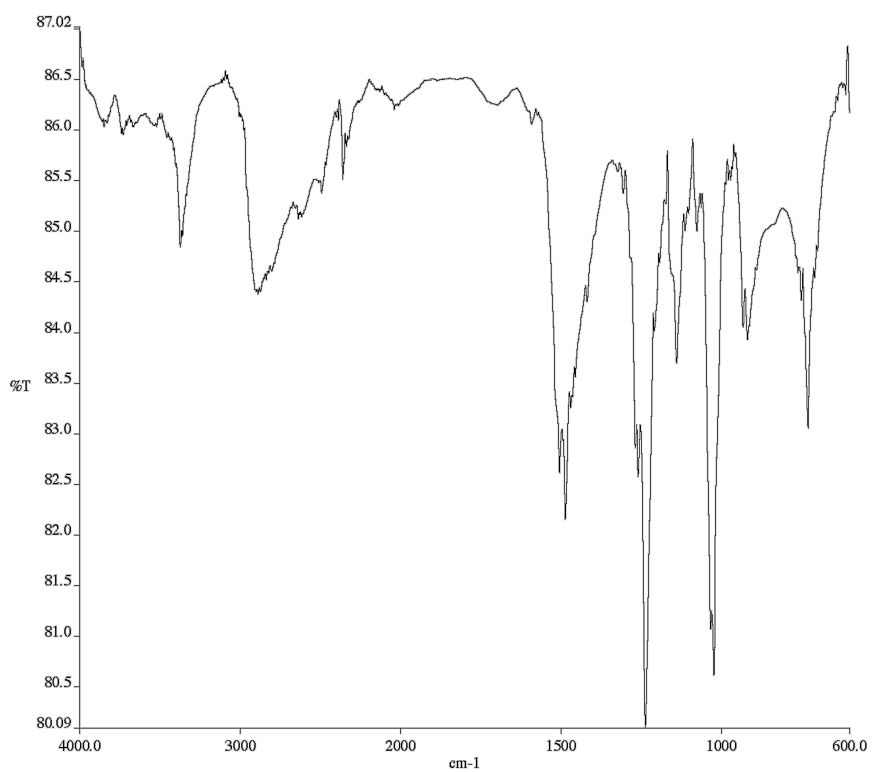


Figure A11.276 Infrared spectrum (Thin Film, NaCl) of compound

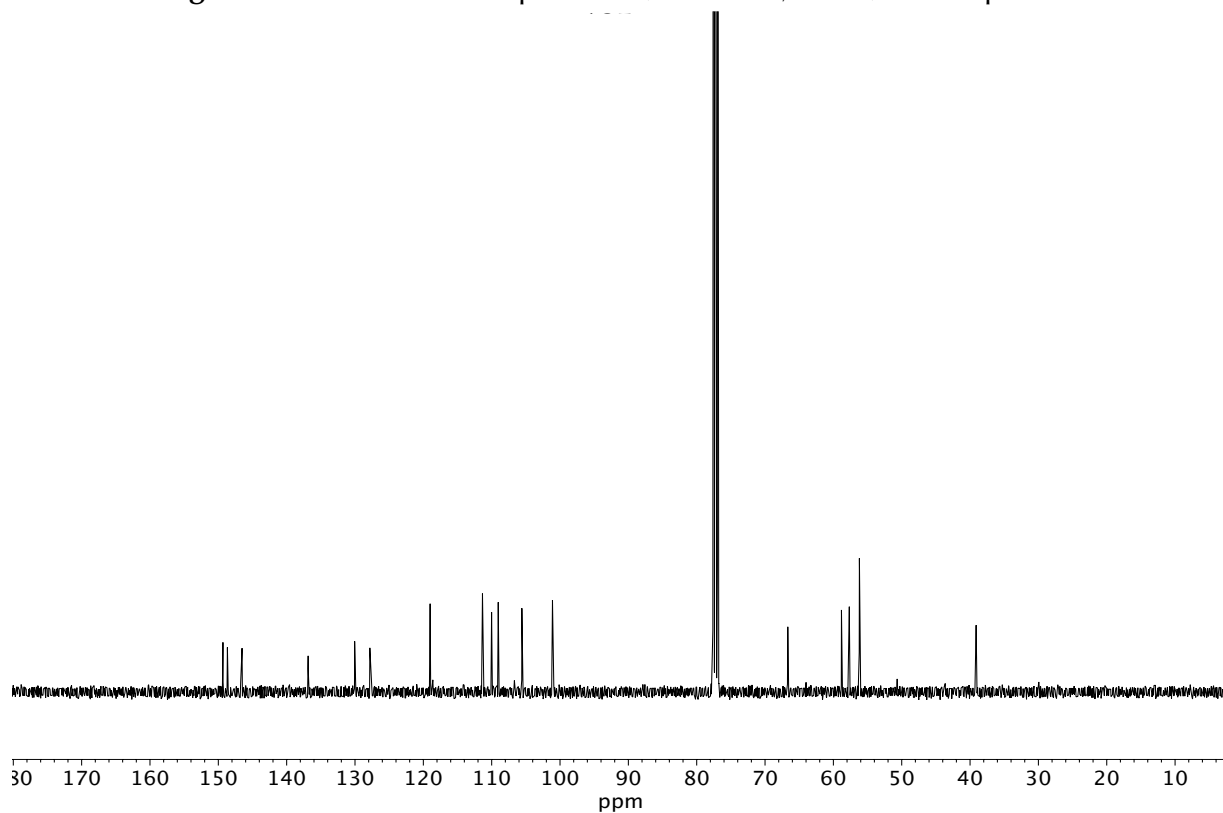


Figure A11.277 ¹³C NMR (100 MHz, CDCl₃) of compound **185e**.

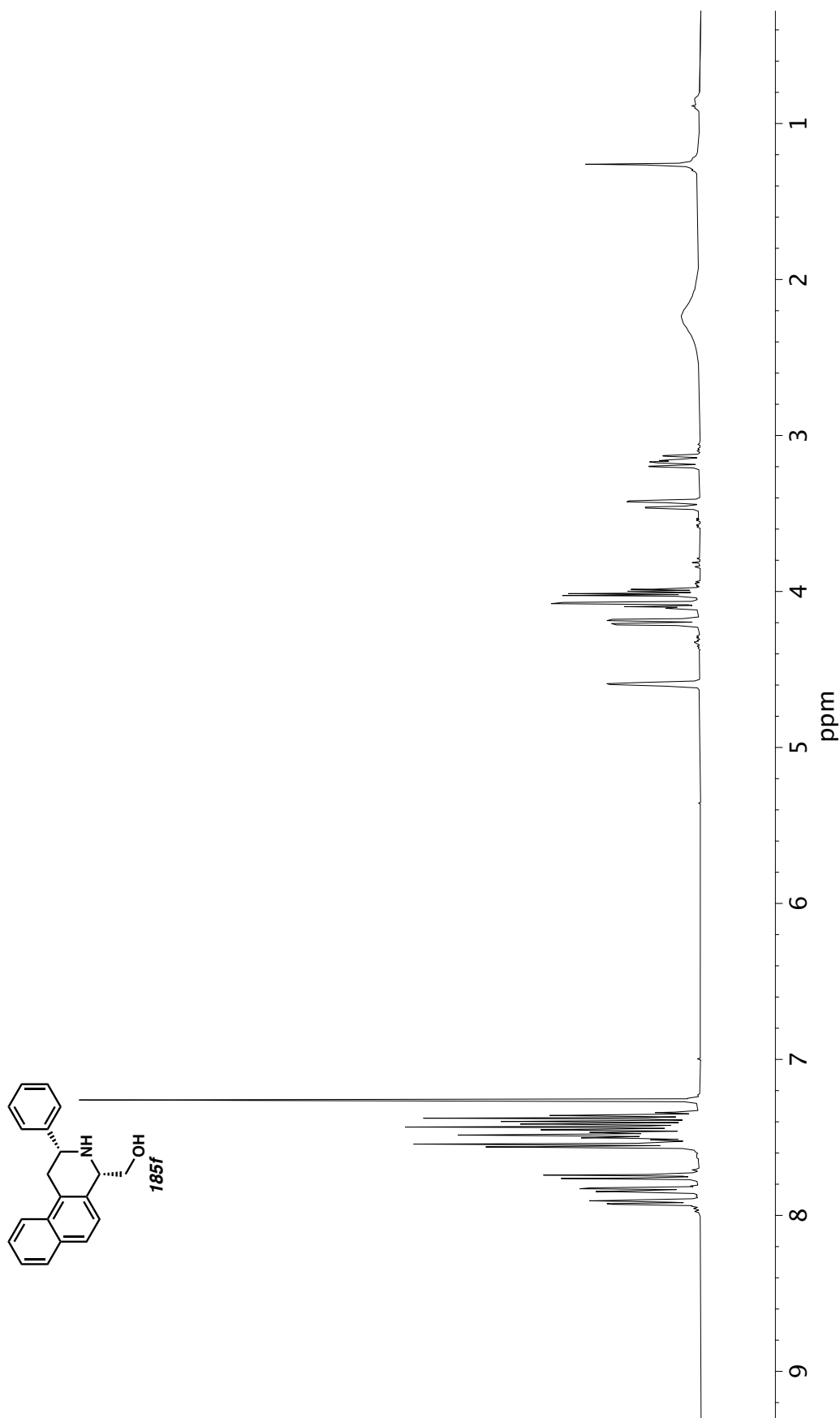


Figure A11.278 ^1H NMR (400 MHz, CDCl_3) of compound **185f**.

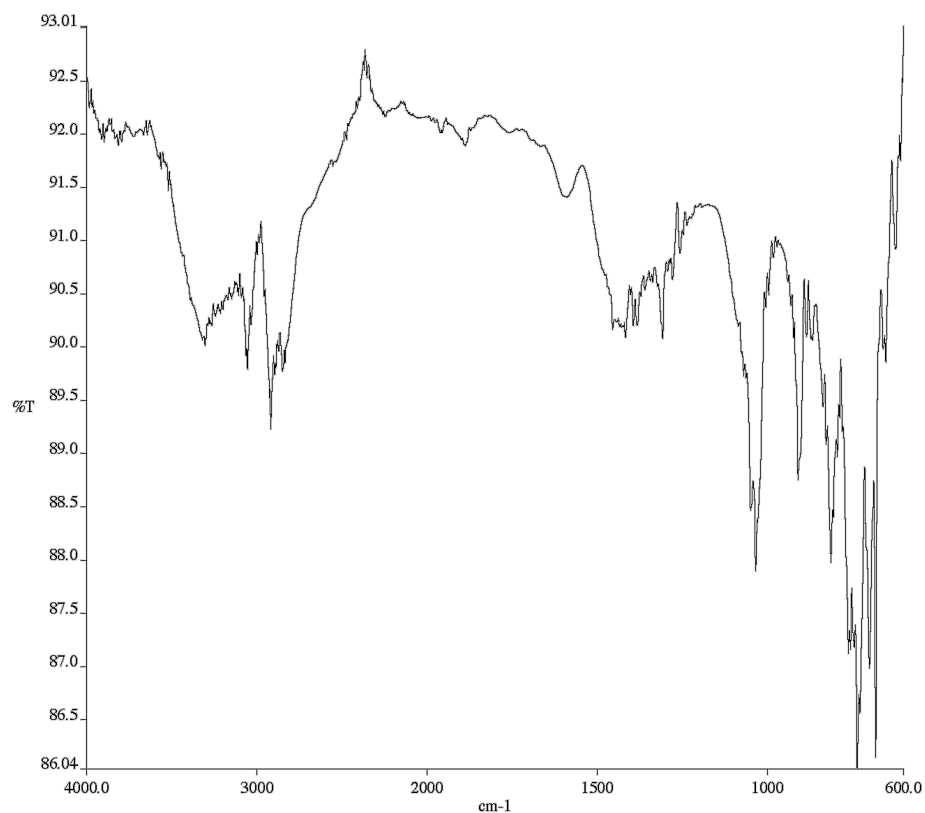


Figure A11.279 Infrared spectrum (Thin Film, NaCl) of compound

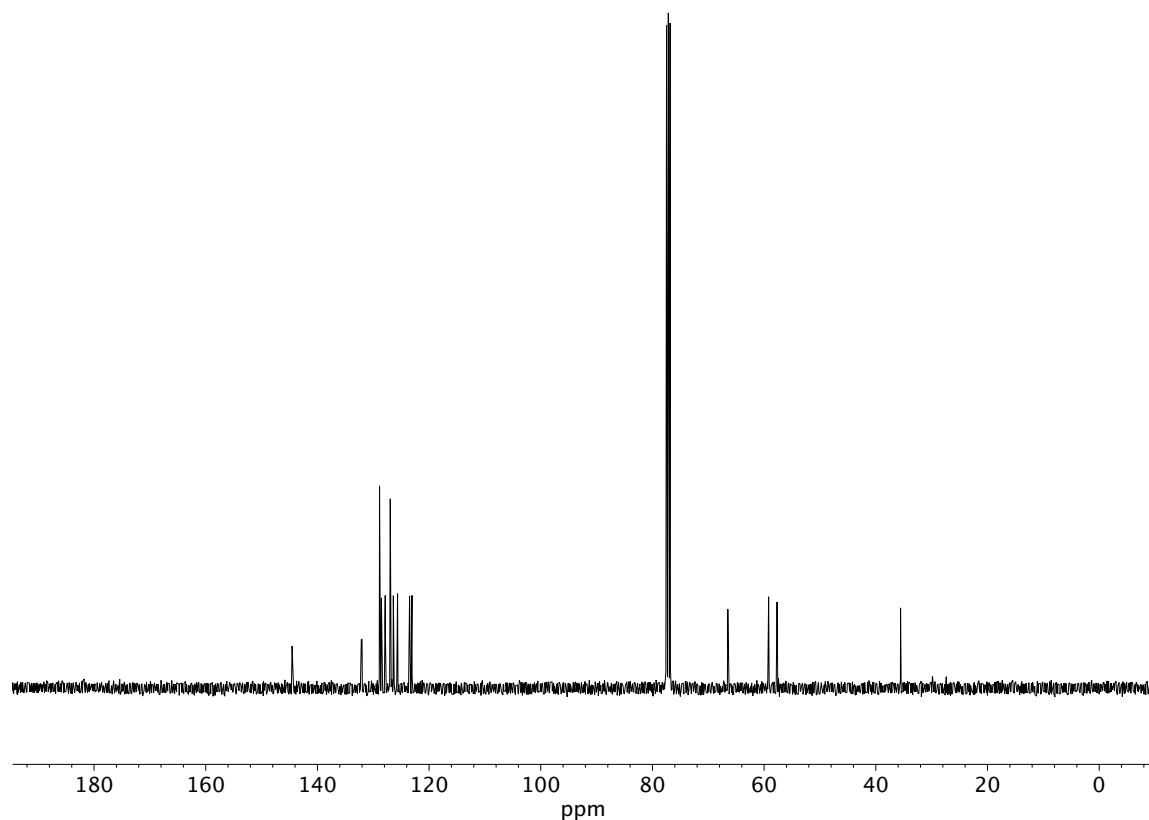


Figure A11.280 ¹³C NMR (100 MHz, CDCl₃) of compound **185f**.

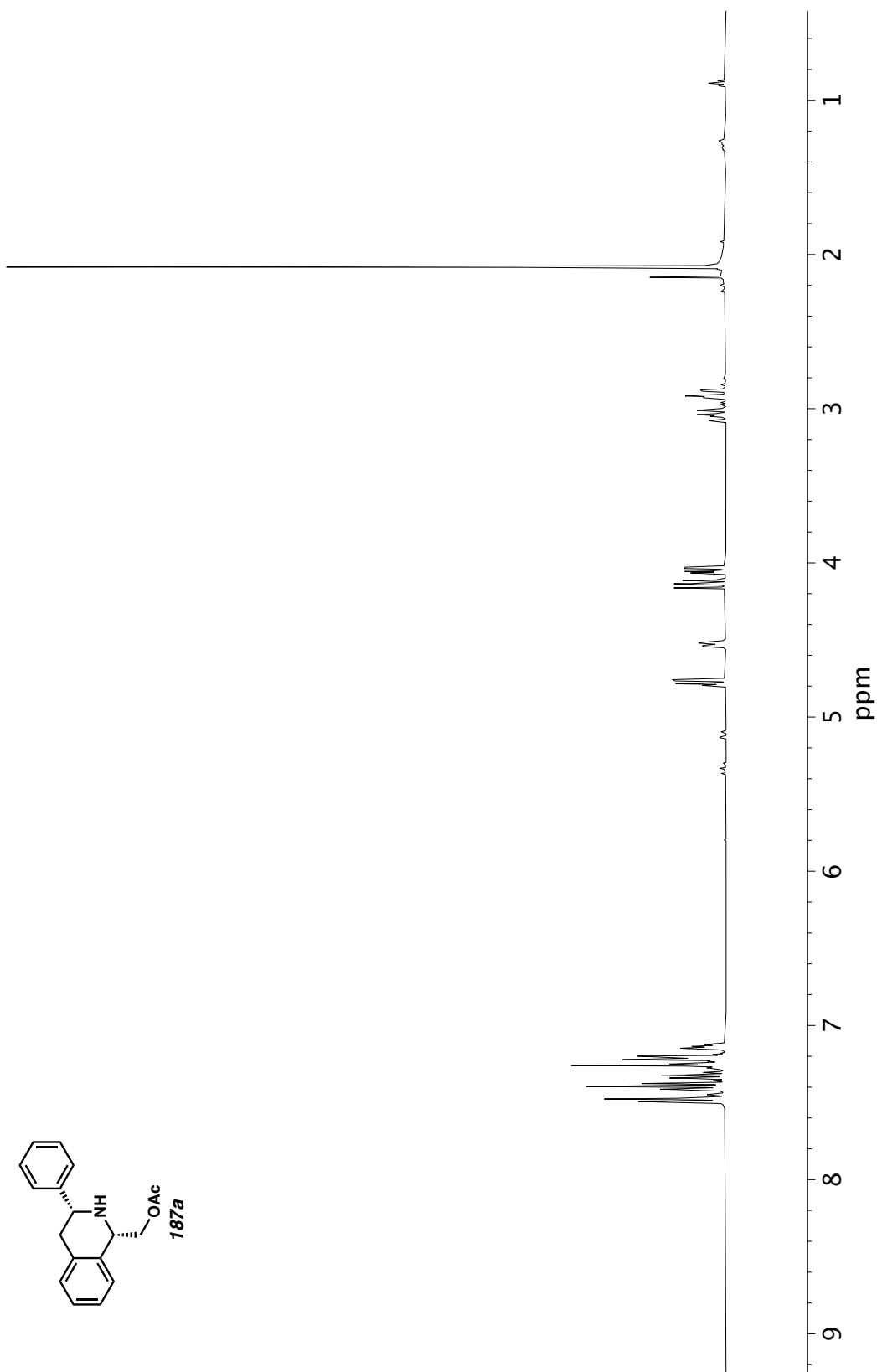


Figure A11.281 ^1H NMR (400 MHz, CDCl_3) of compound **187a**.

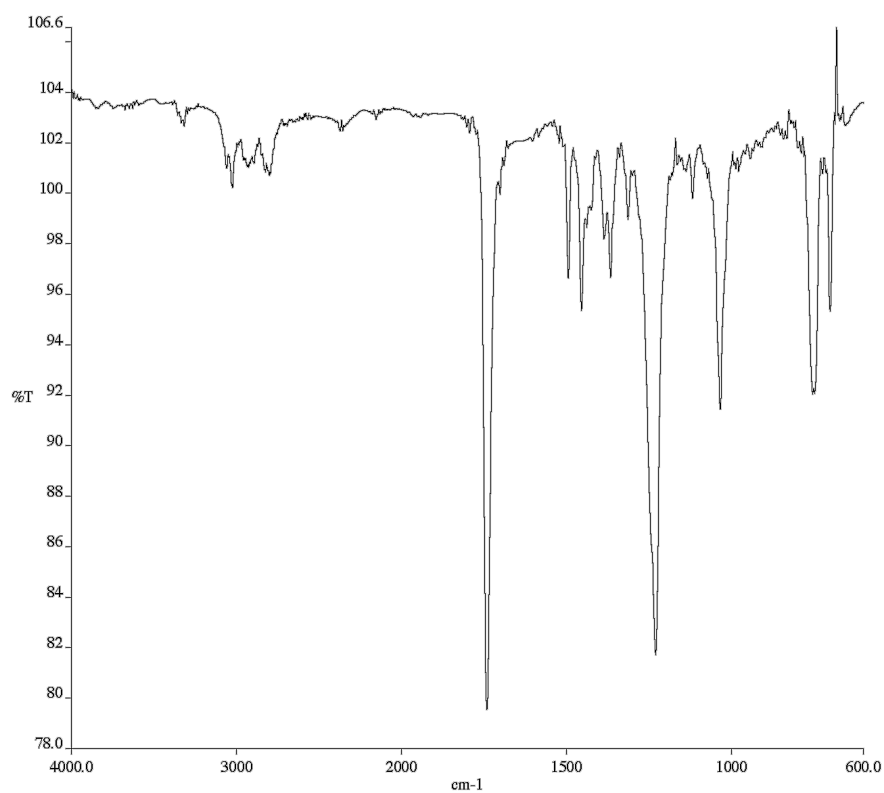


Figure A11.282 Infrared spectrum (Thin Film, NaCl) of compound

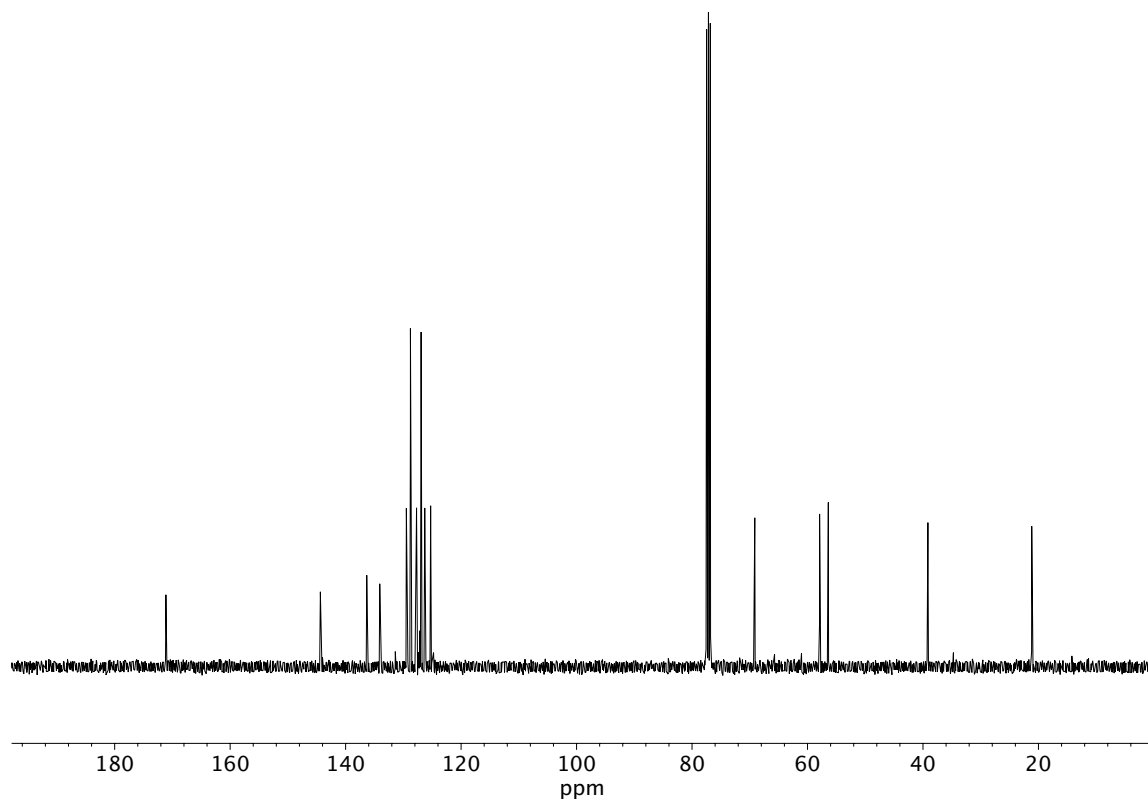


Figure A11.283 ¹³C NMR (100 MHz, CDCl₃) of compound **187a**.

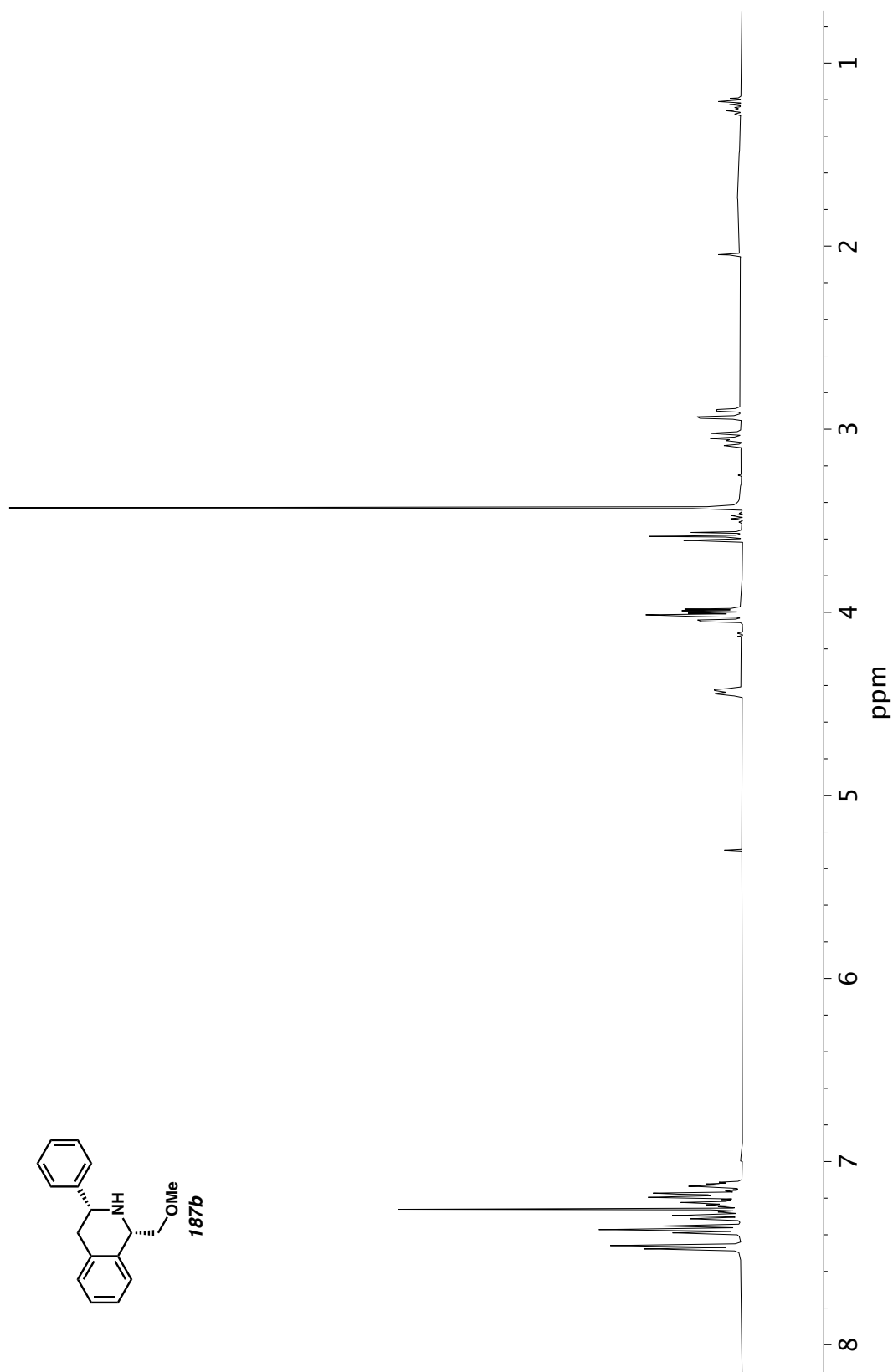


Figure A11.284 ^1H NMR (400 MHz, CDCl_3) of compound **187b**.

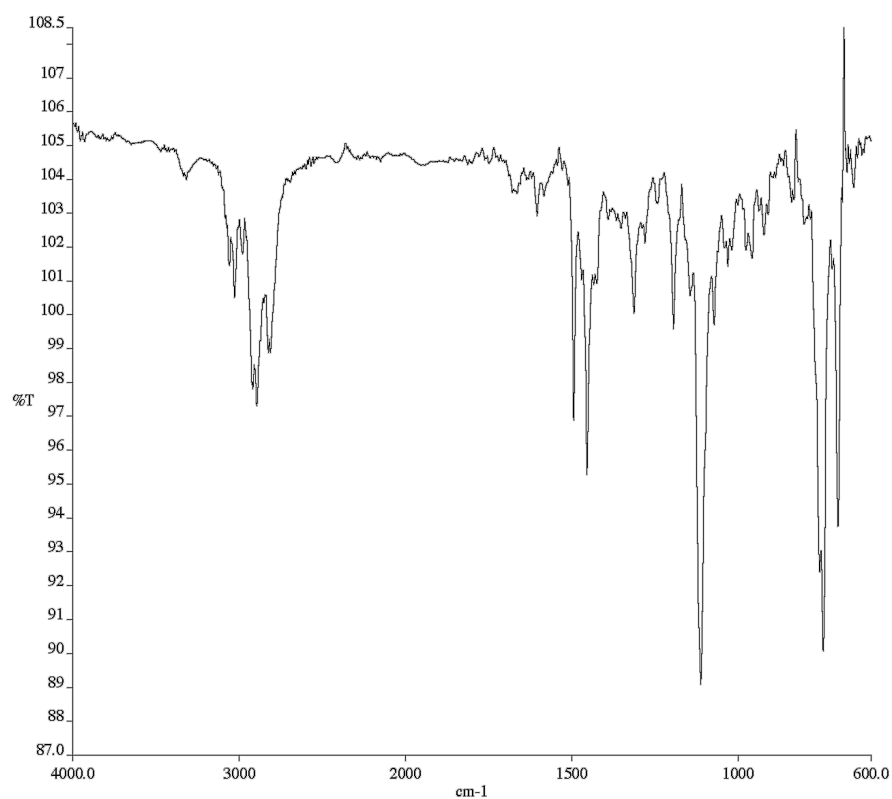


Figure A11.285 Infrared spectrum (Thin Film, NaCl) of compound

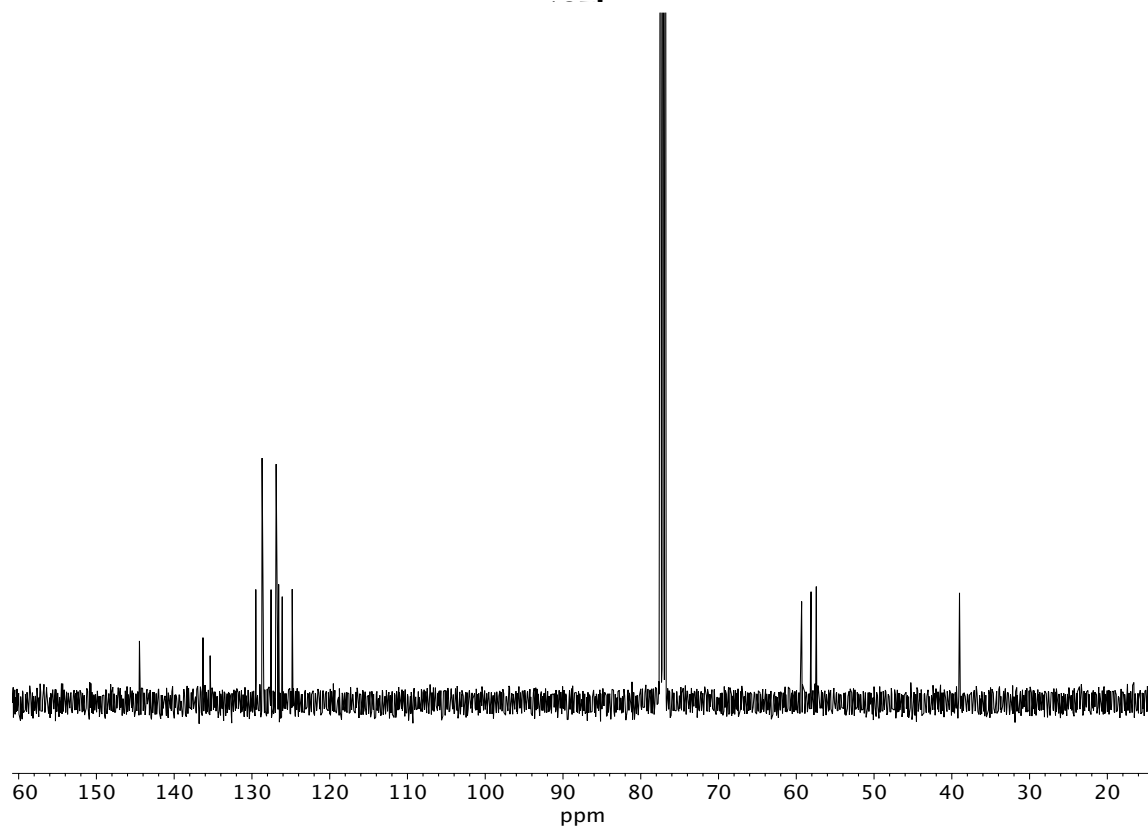


Figure A11.286 ¹³C NMR (100 MHz, CDCl₃) of compound **187b**.

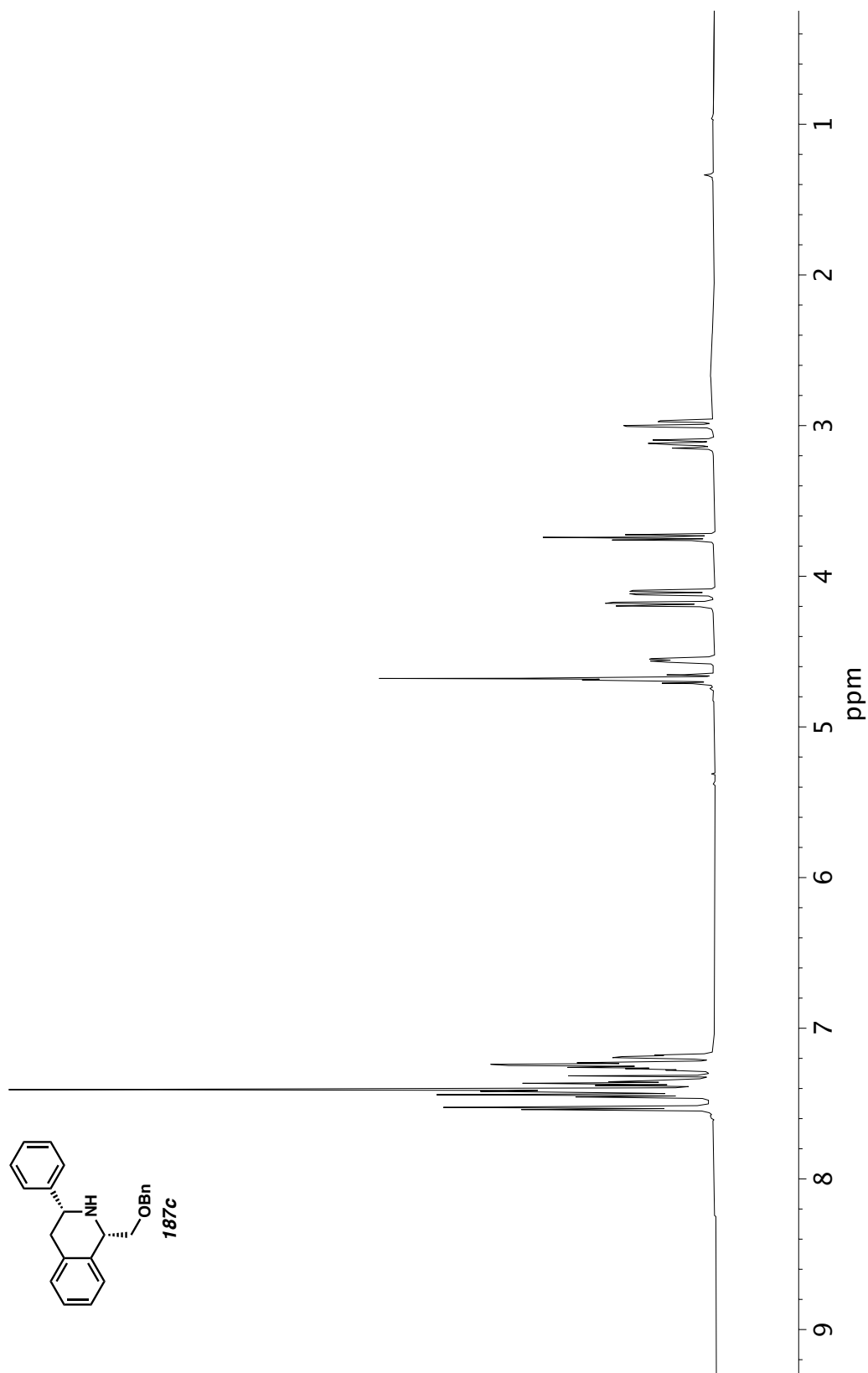


Figure A11.287 ^1H NMR (400 MHz, CDCl_3) of compound **187c**.

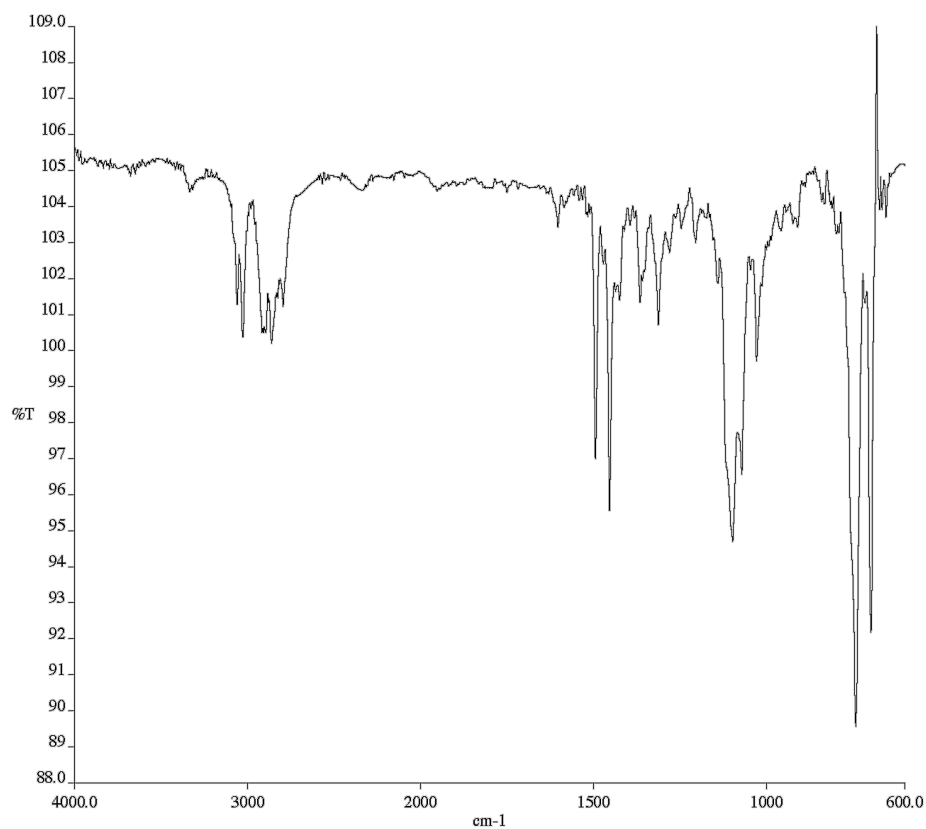


Figure A11.288 Infrared spectrum (Thin Film, NaCl) of compound

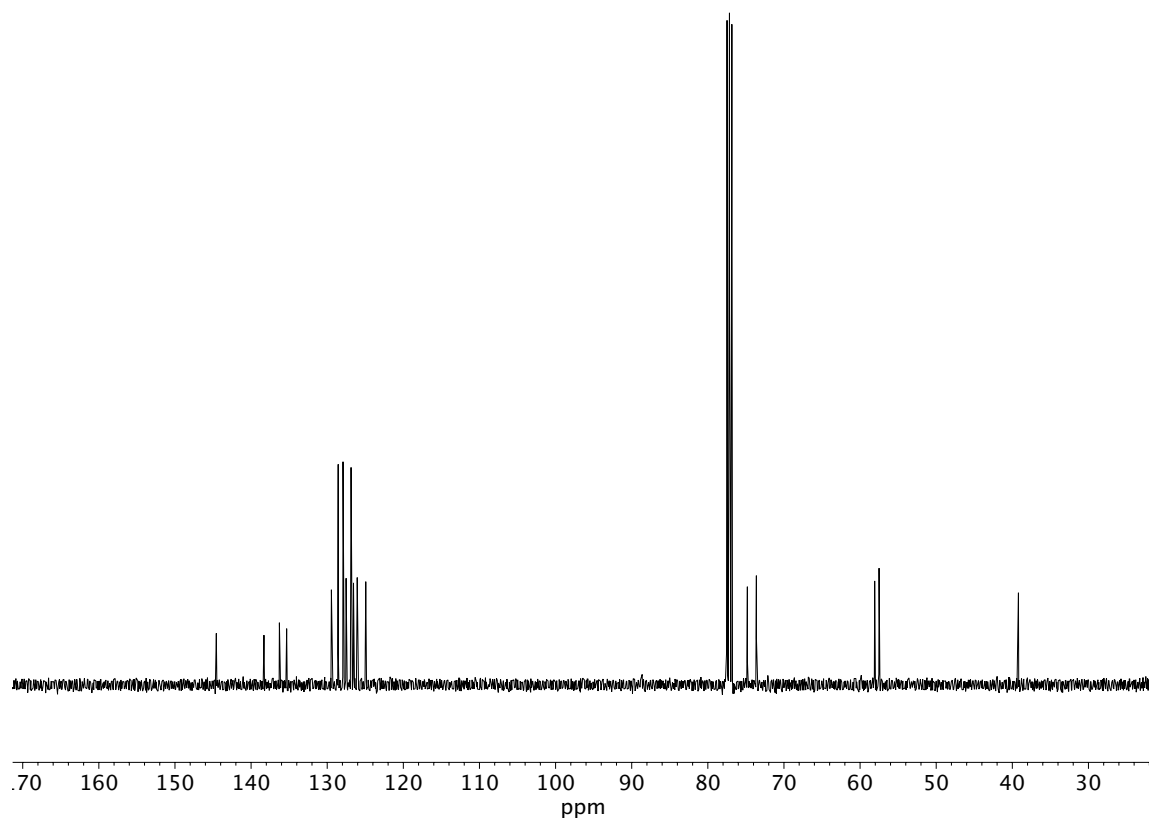


Figure A11.289 ¹³C NMR (100 MHz, CDCl₃) of compound **187c**.

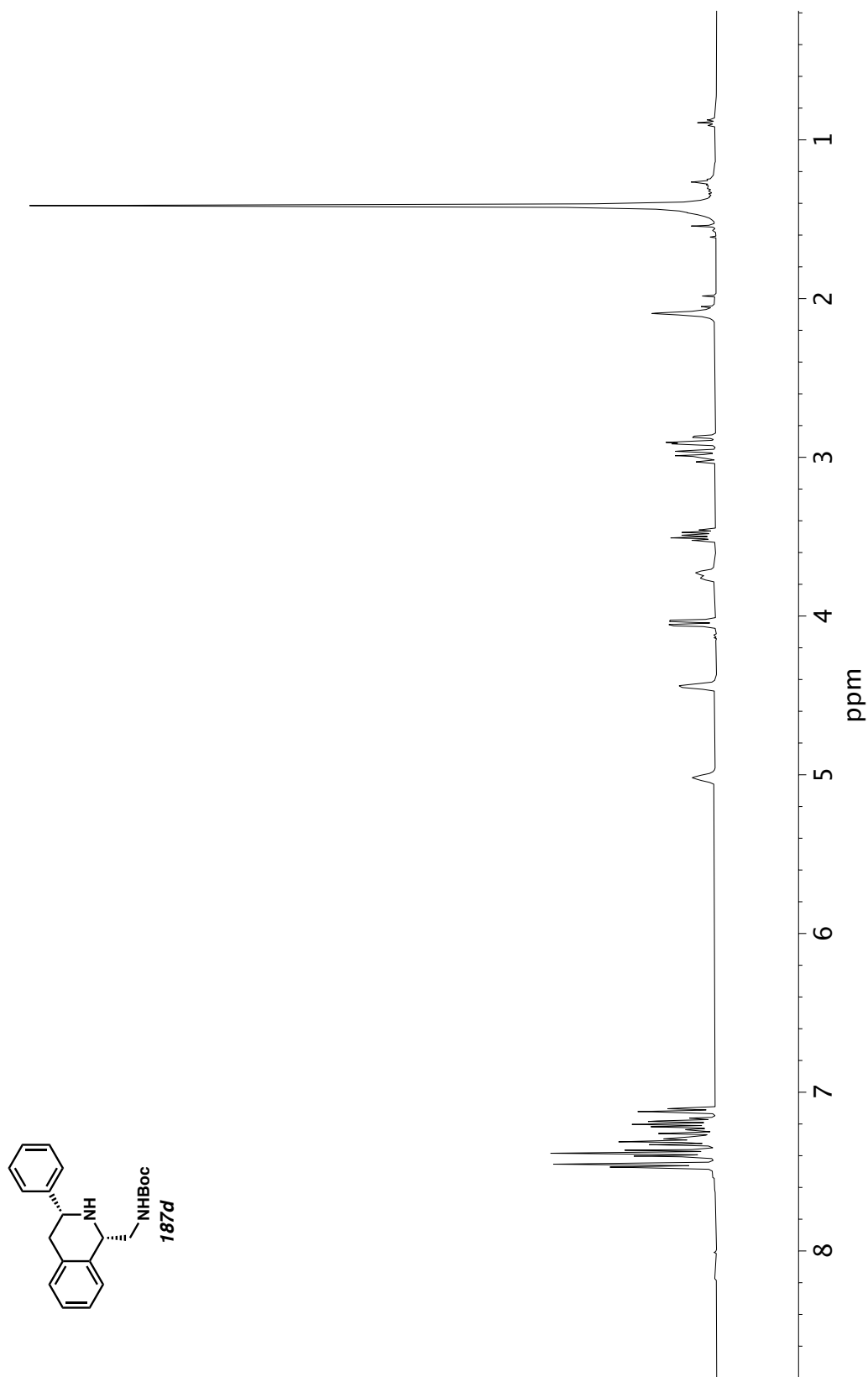


Figure A11.290 ^1H NMR (400 MHz, CDCl_3) of compound **187d**.

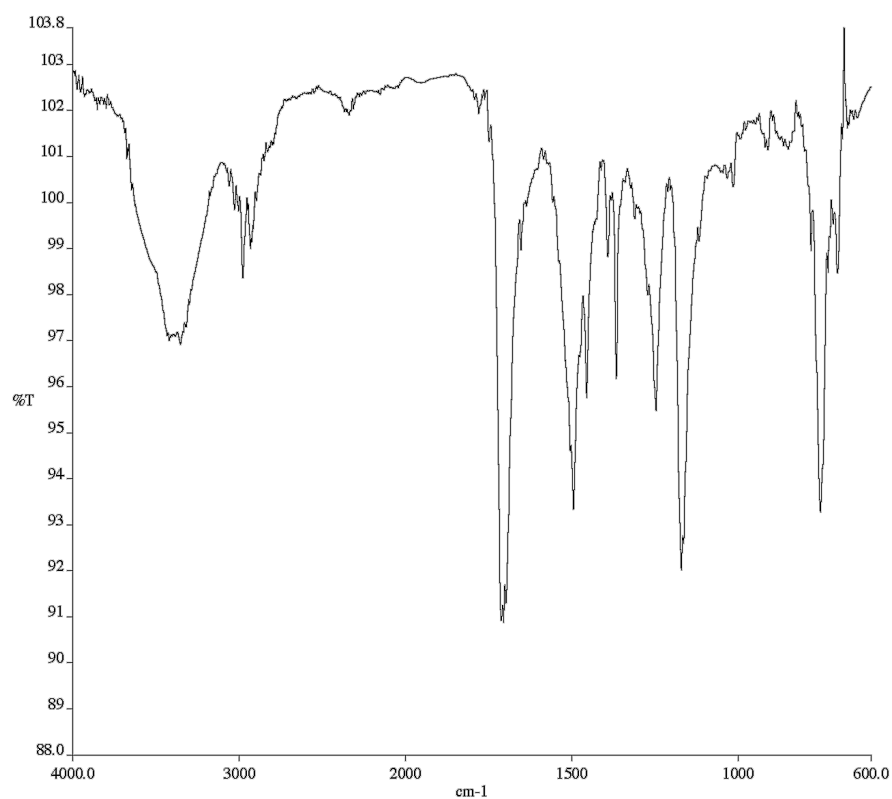


Figure A11.291 Infrared spectrum (Thin Film, NaCl) of compound

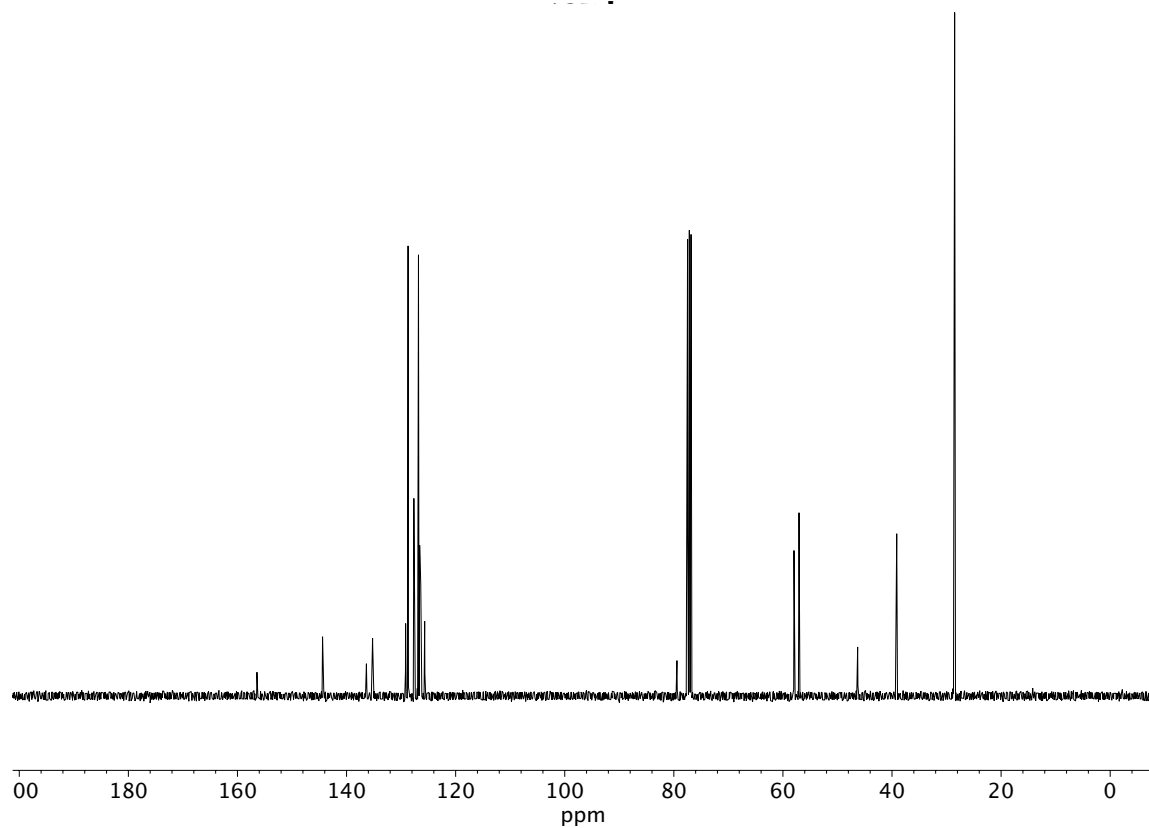


Figure A11.292 ¹³C NMR (100 MHz, CDCl₃) of compound **187d**.

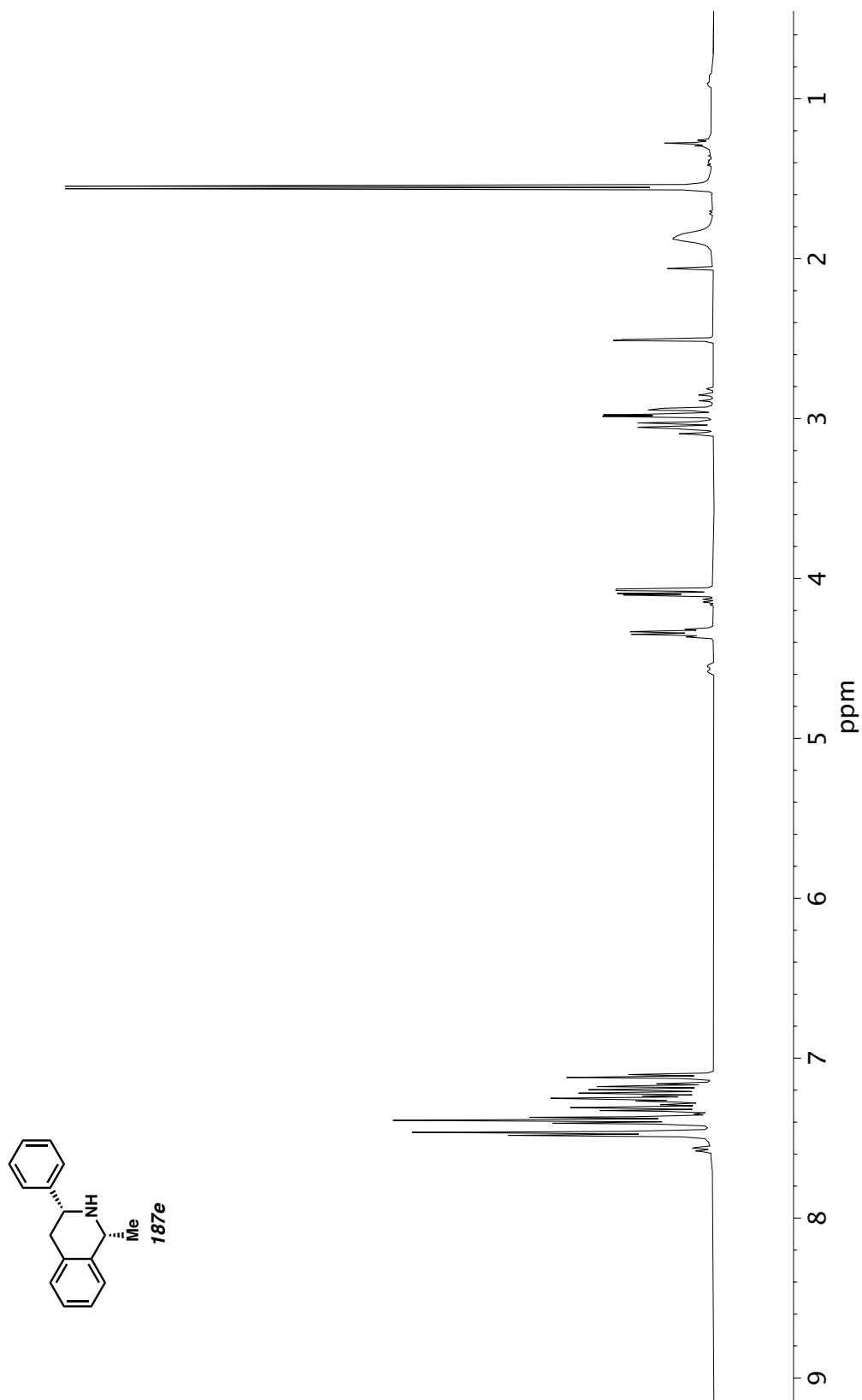


Figure A11.293 ^1H NMR (400 MHz, CDCl_3) of compound **187e**.

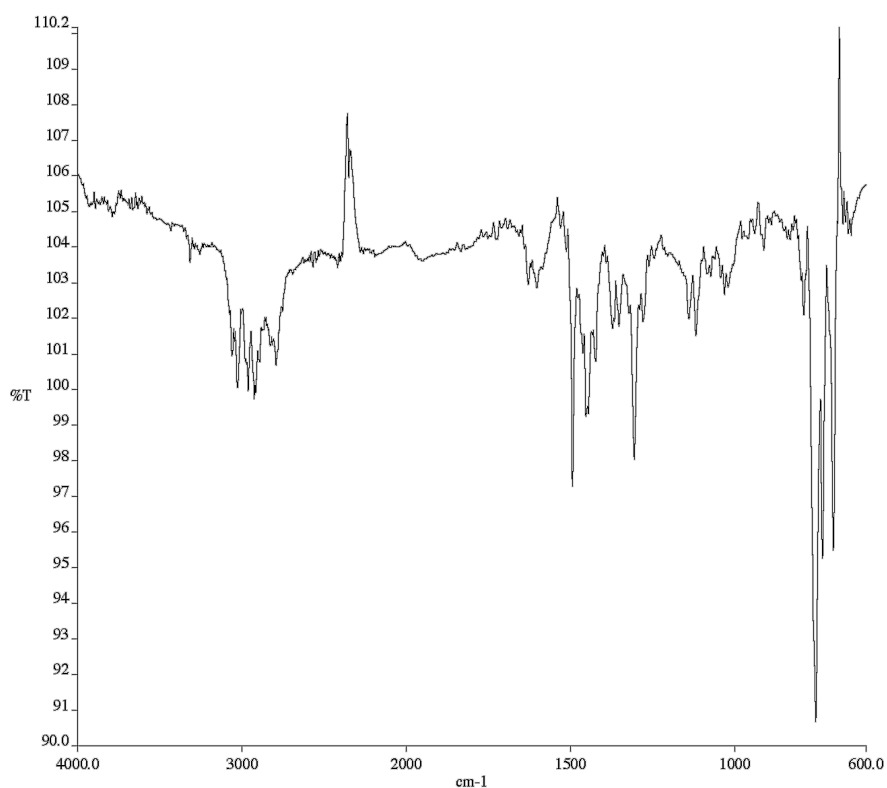


Figure A11.294 Infrared spectrum (Thin Film, NaCl) of compound

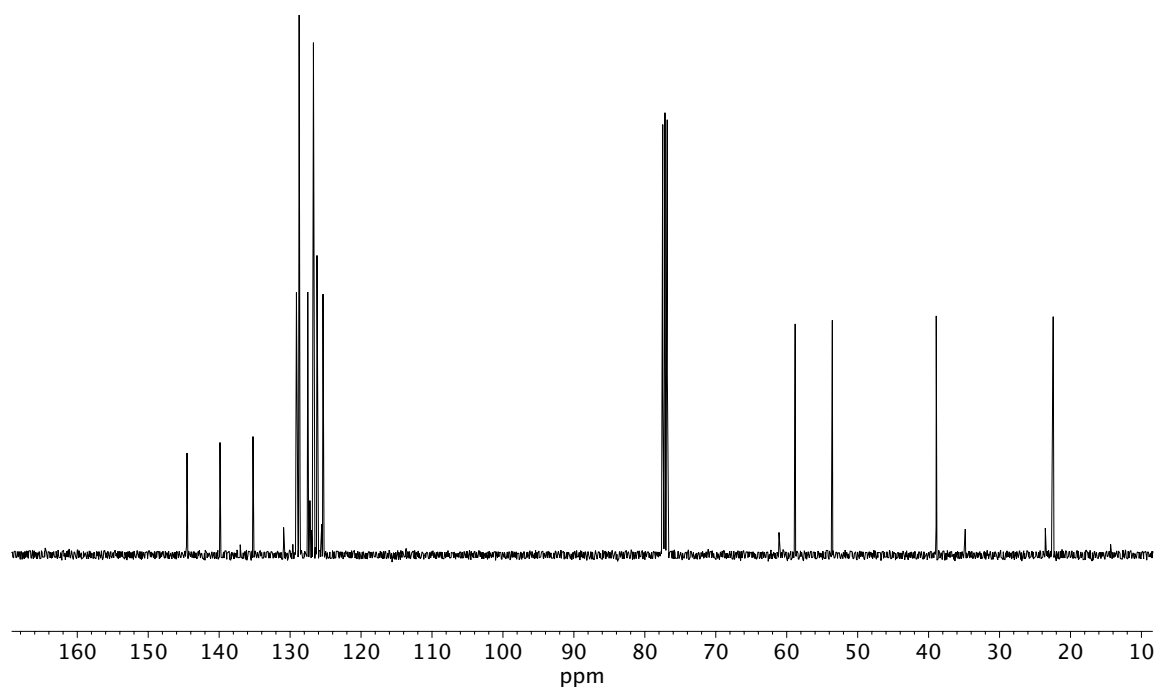


Figure A11.295 ¹³C NMR (100 MHz, CDCl₃) of compound **187e**.

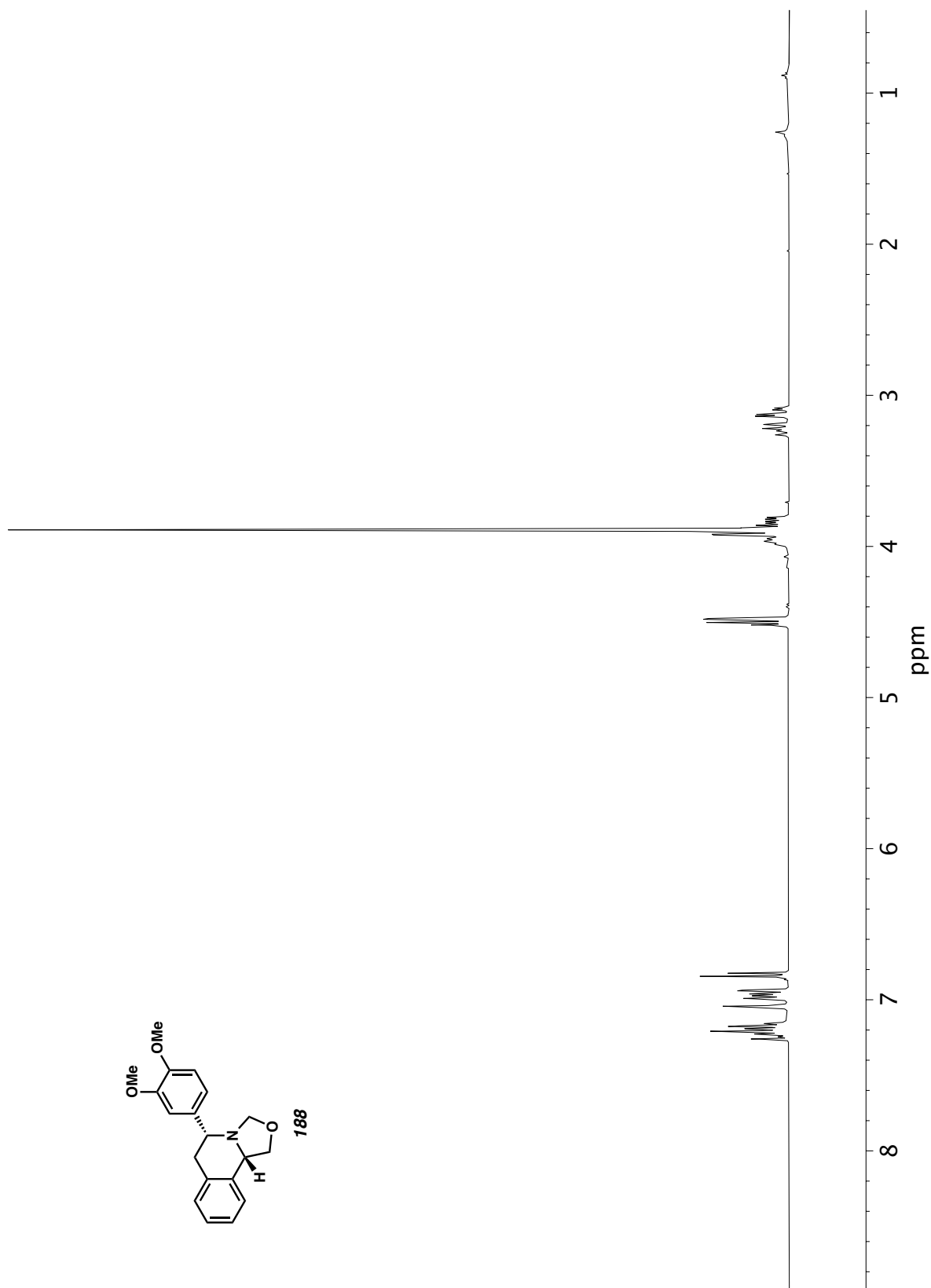


Figure A11.296 ^1H NMR (400 MHz, CDCl_3) of compound **188**.

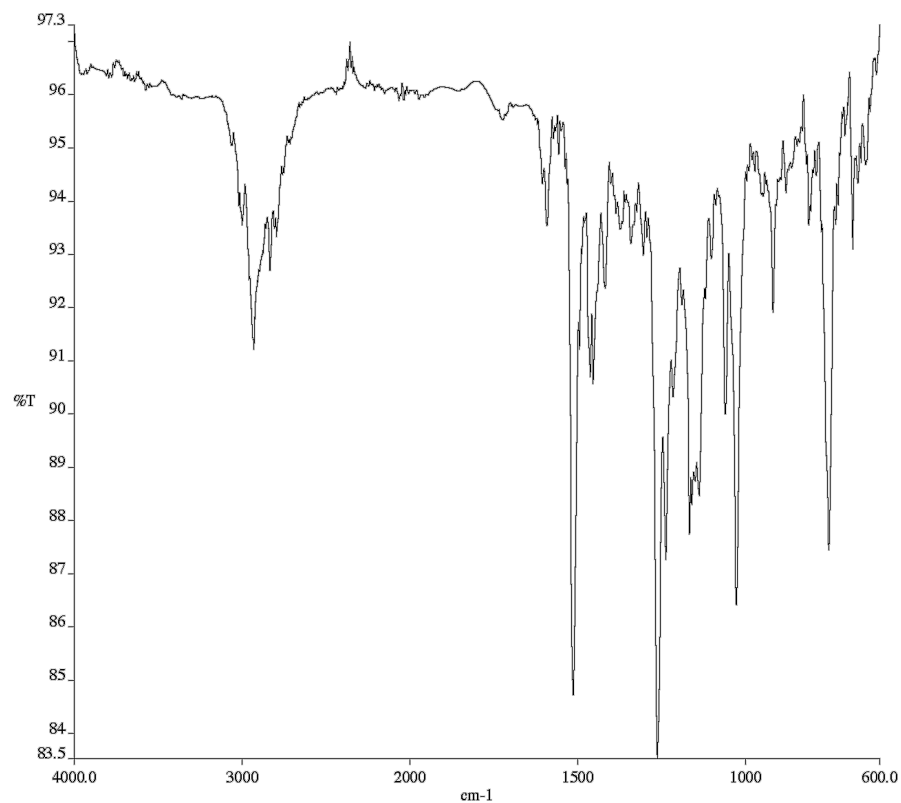


Figure A11.297 Infrared spectrum (Thin Film, NaCl) of compound **188**.

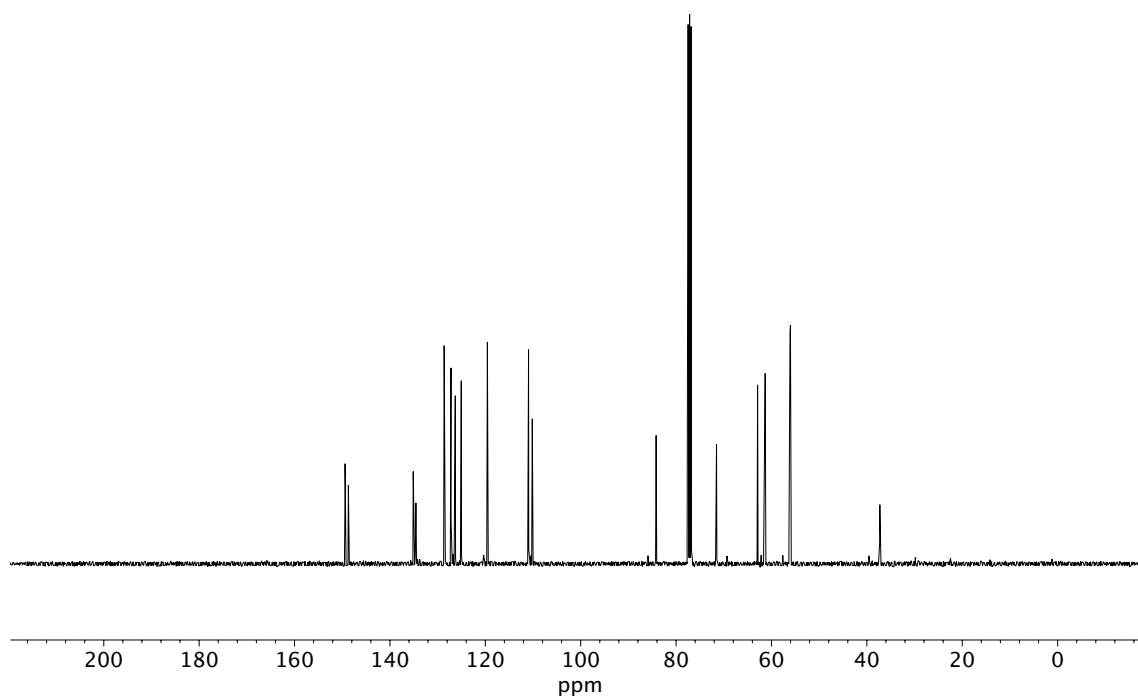


Figure A11.298 ¹³C NMR (100 MHz, CDCl₃) of compound **188**.

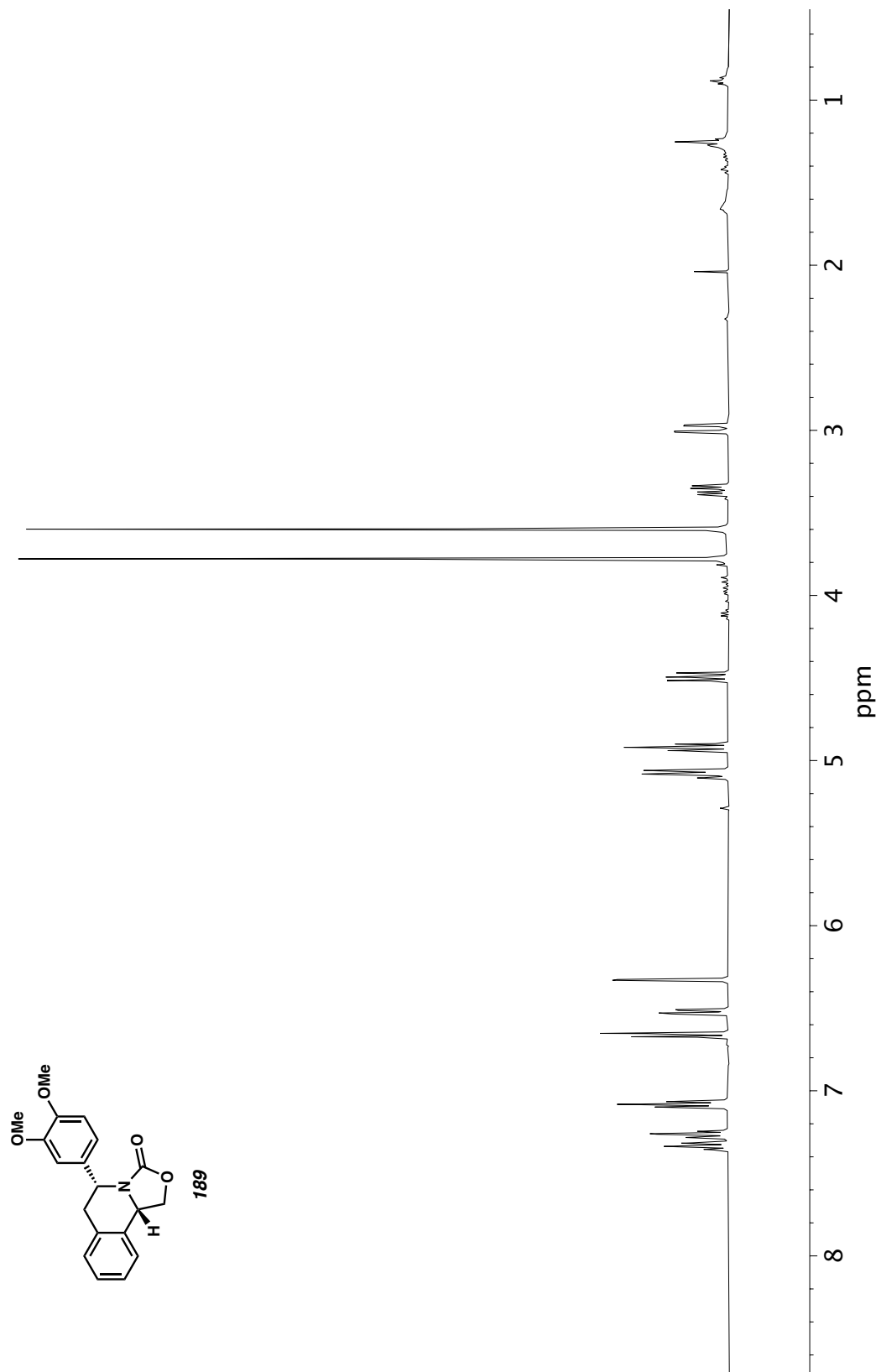


Figure A11.299 ^1H NMR (400 MHz, CDCl_3) of compound **189**.

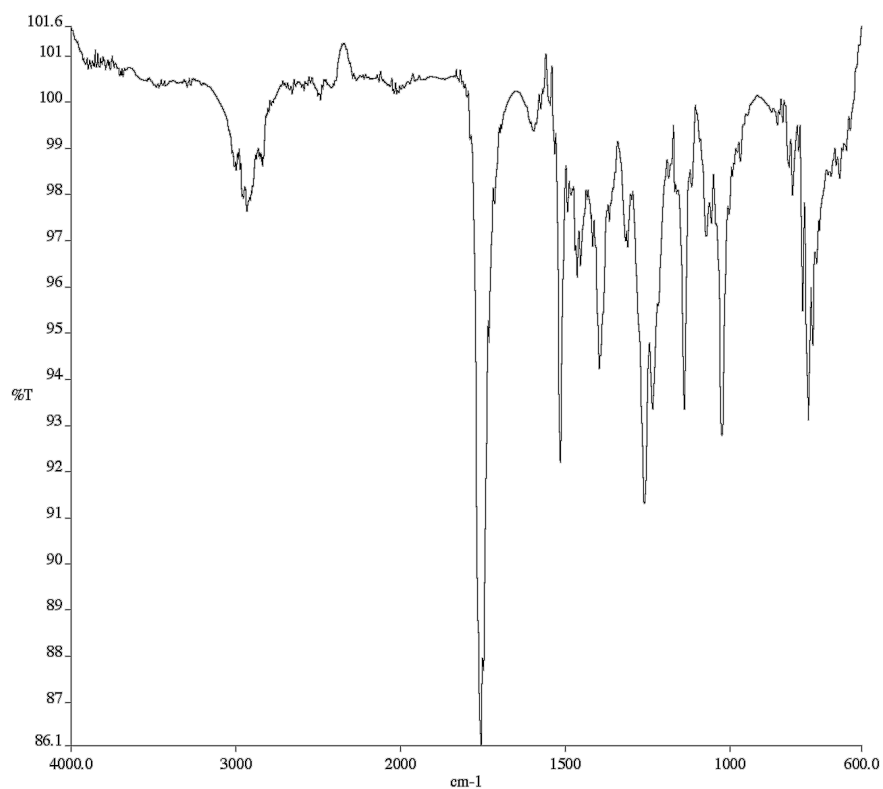


Figure A11.300 Infrared spectrum (Thin Film, NaCl) of compound **189**.

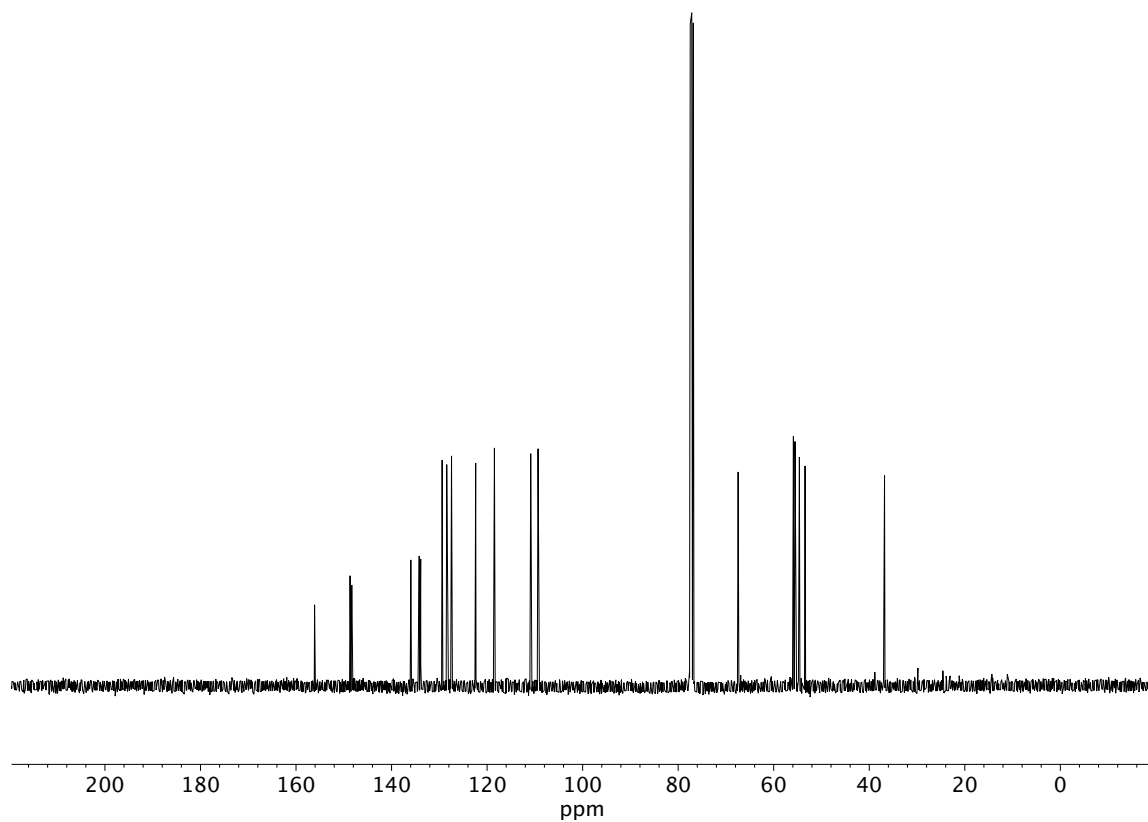


Figure A11.301 ¹³C NMR (100 MHz, CDCl₃) of compound **189**.

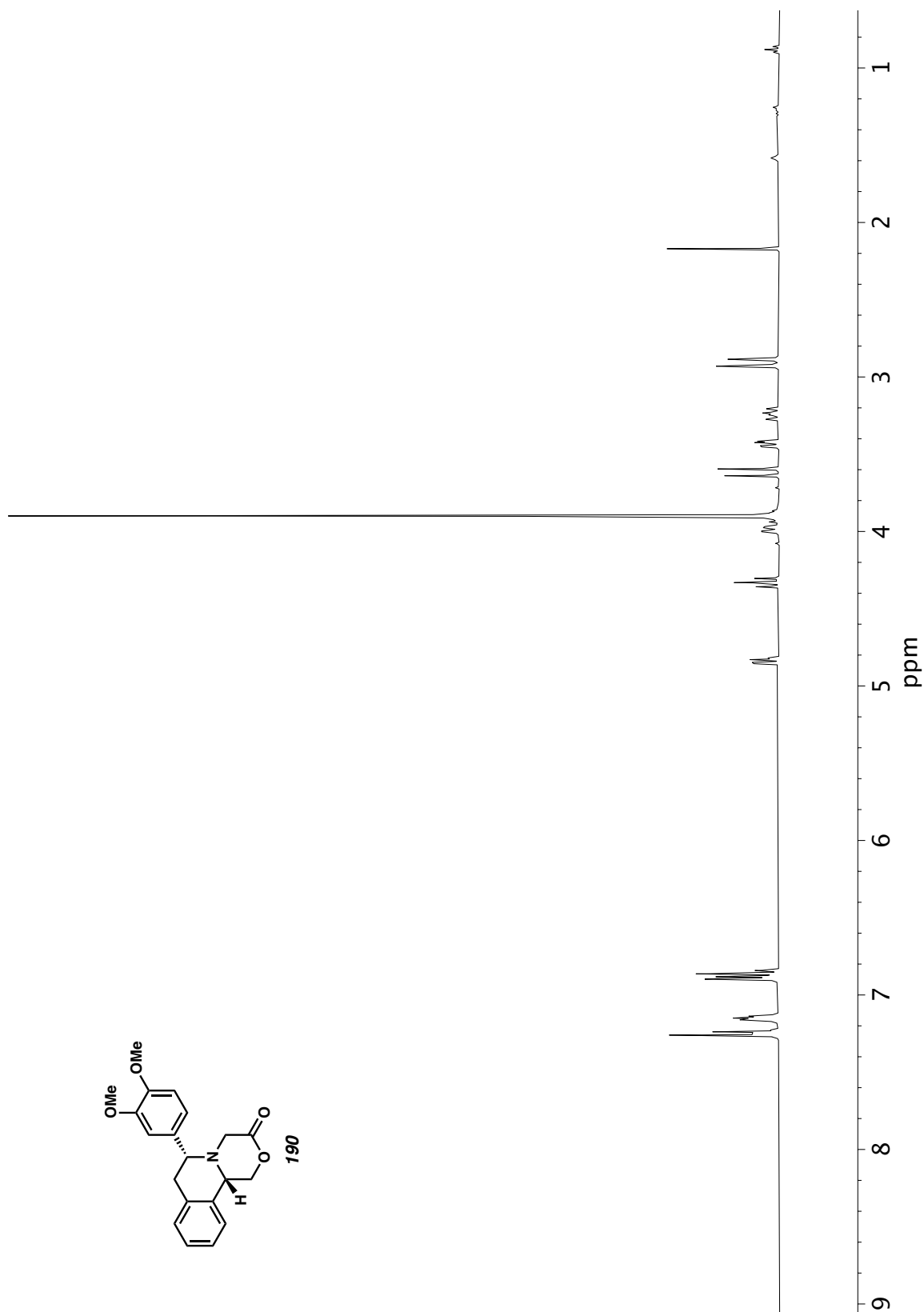


Figure A11.302 ¹H NMR (400 MHz, CDCl₃) of compound **190**.

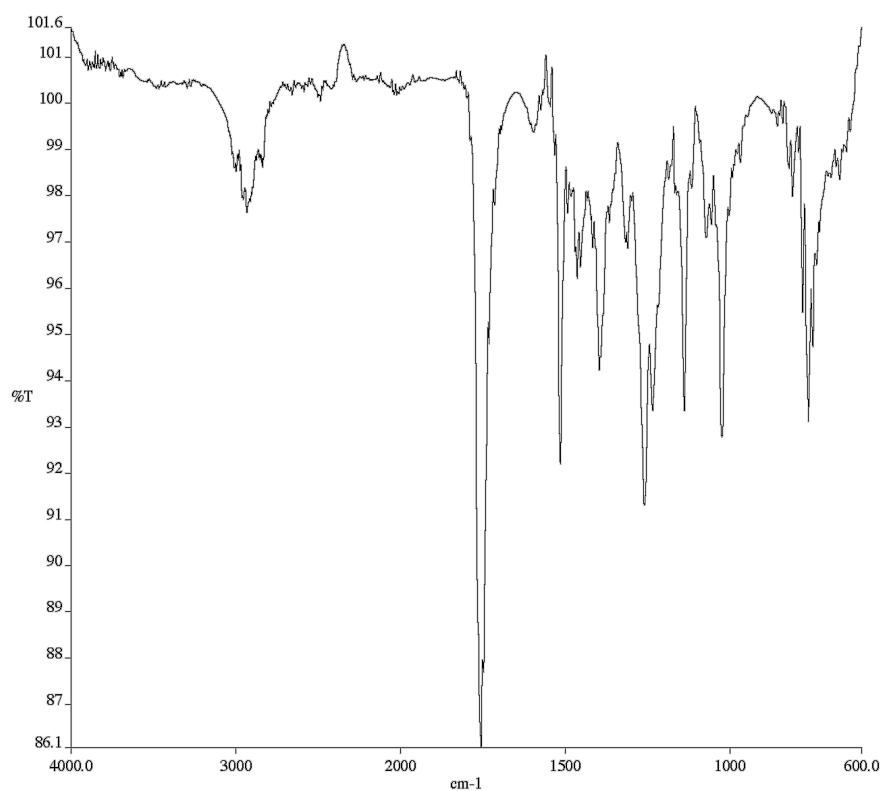


Figure A11.303 Infrared spectrum (Thin Film, NaCl) of compound **190**.

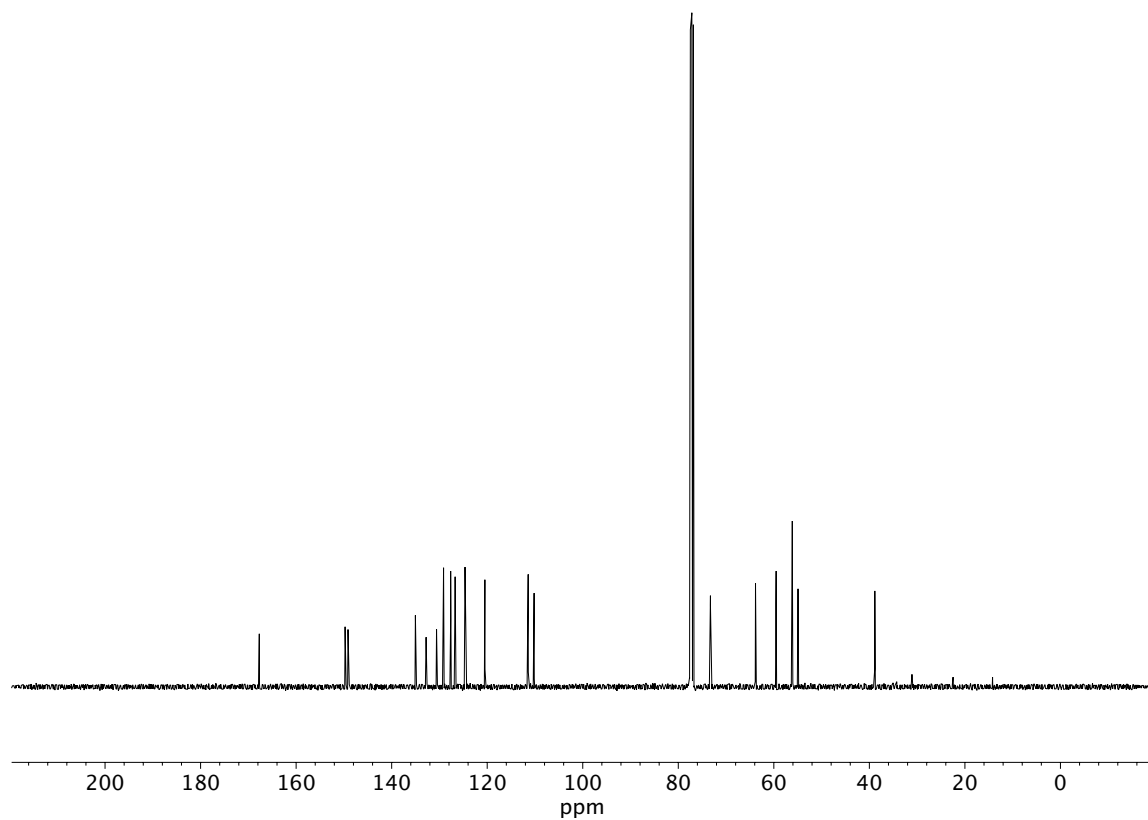


Figure A11.304 ¹³C NMR (100 MHz, CDCl₃) of compound **190**.

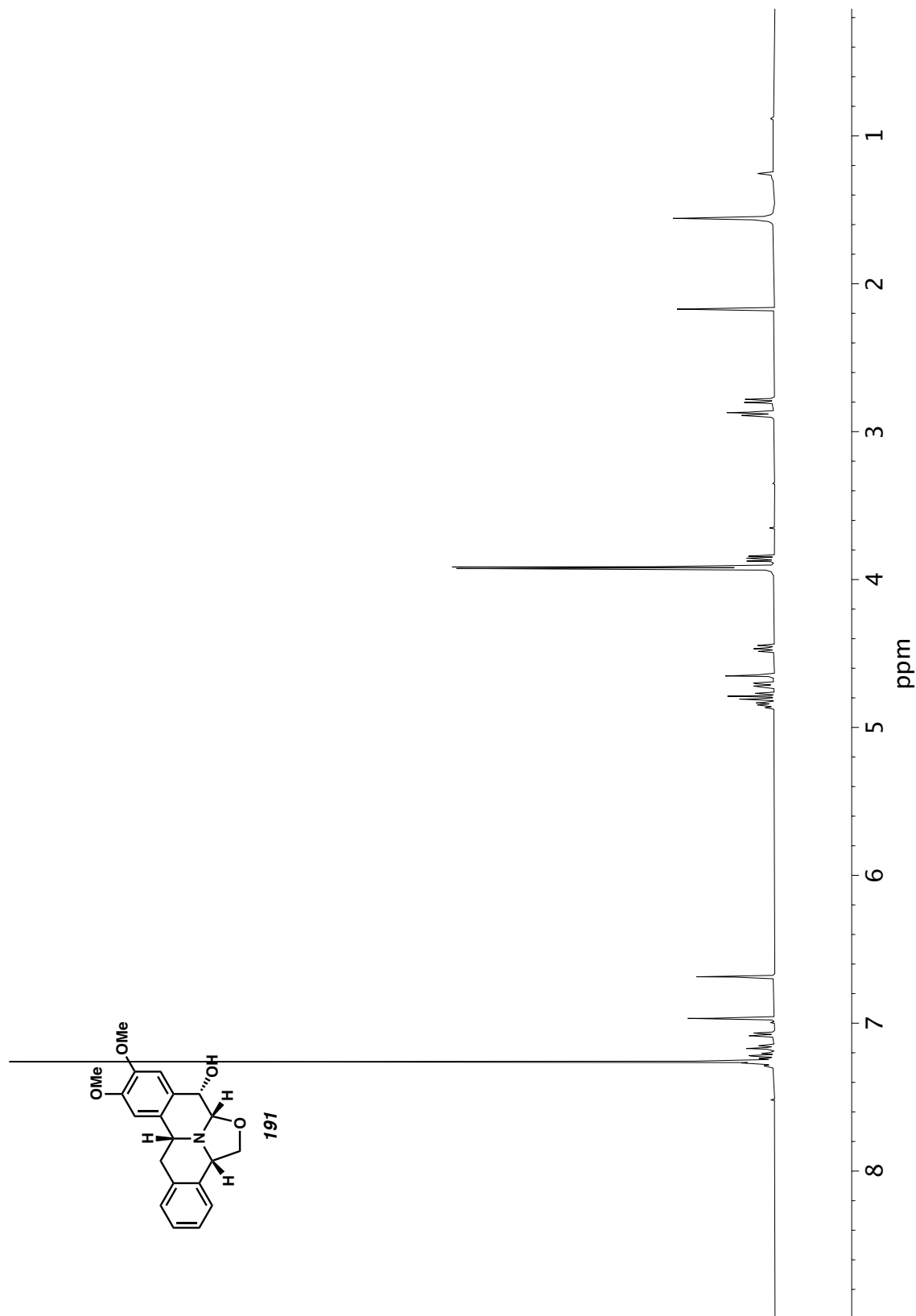


Figure A11.305 ^1H NMR (400 MHz, CDCl_3) of compound **191**.

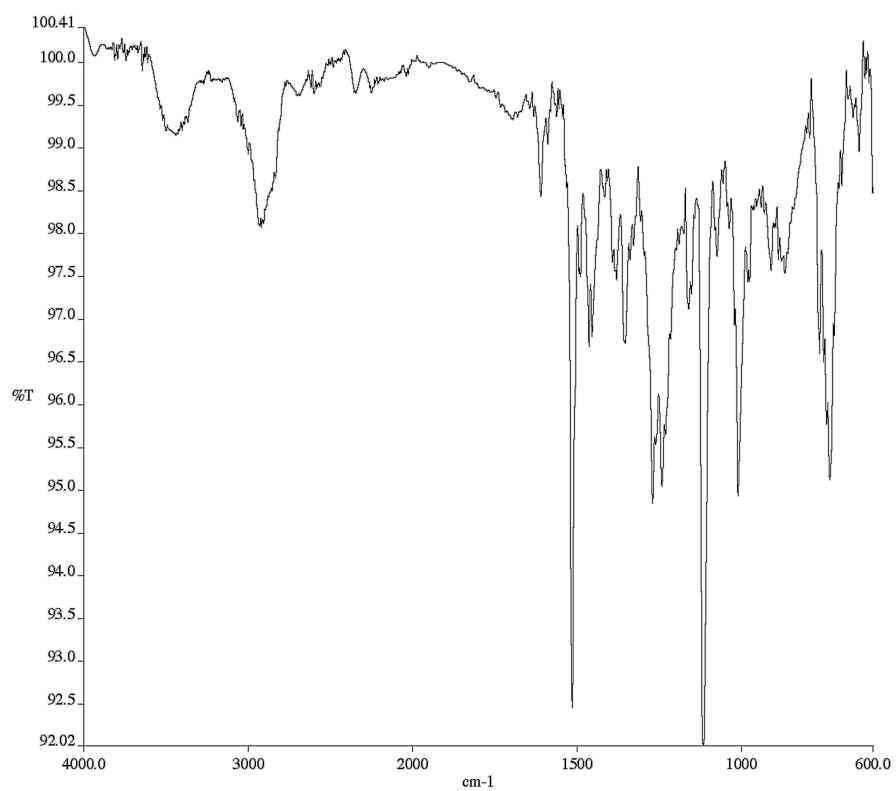


Figure A11.306 Infrared spectrum (Thin Film, NaCl) of compound **191**.

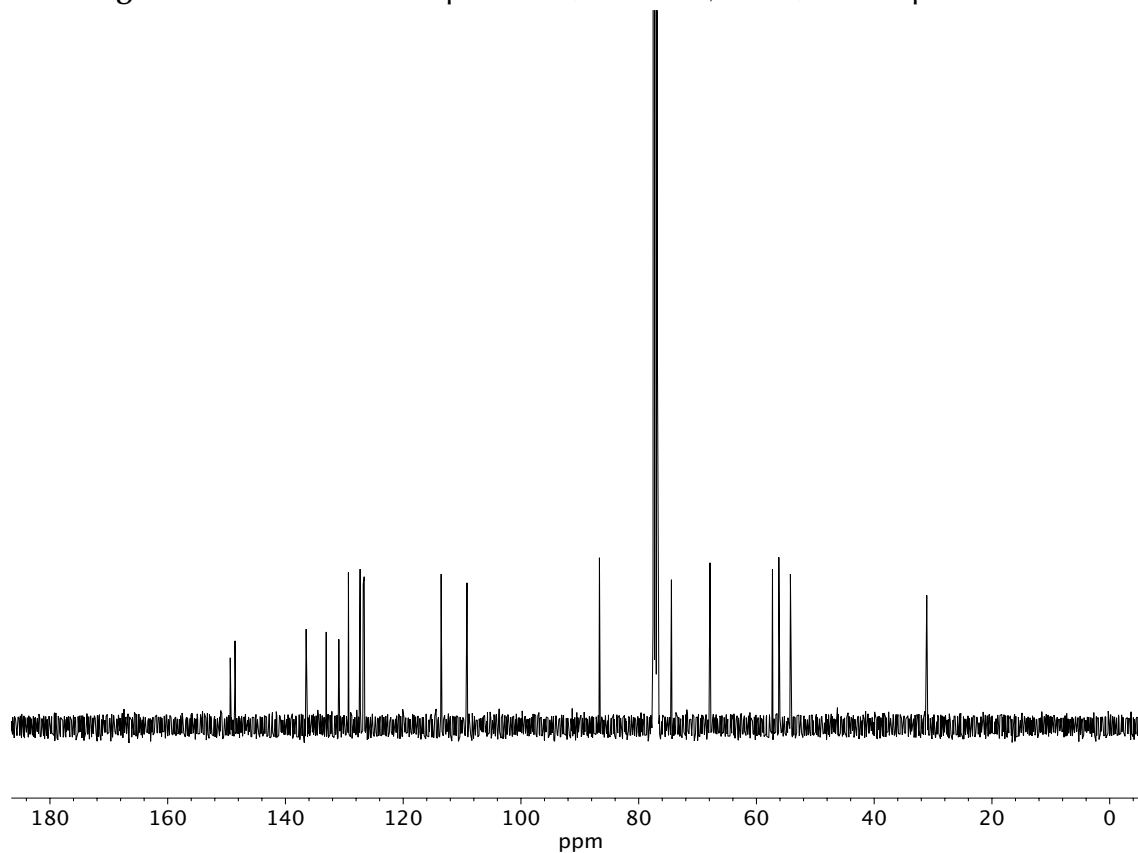


Figure A11.307 ¹³C NMR (100 MHz, CDCl₃) of compound **191**.

APPENDIX 12

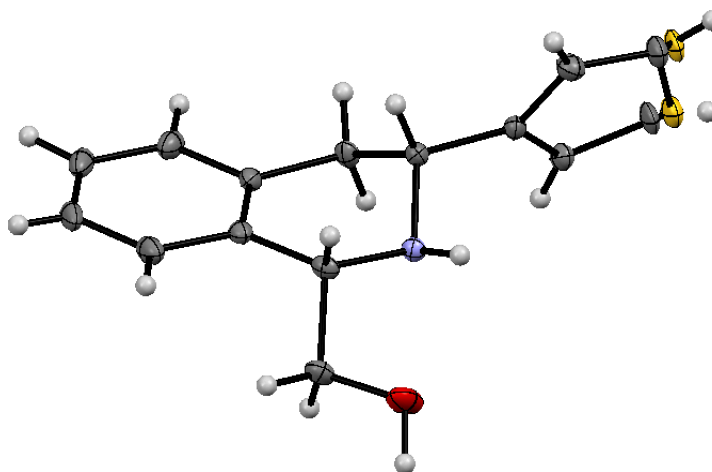
*X-Ray Crystallography Reports Relevant to Chapter 4:
Iridium-Catalyzed Enantioselective and Diastereoselective
Hydrogenation of 1,3-Disubstituted Isoquinolines*

A12.1 GENERAL EXPERIMENTAL

A crystal was mounted on a polyimide MiTeGen loop with STP Oil Treatment and placed under a nitrogen stream. Low temperature (100K) X-ray data were collected with a Bruker AXS KAPPA APEX II diffractometer running at 50 kV and 30 mA (Mo K_{α} = 0.71073 Å; PHOTON 100 CMOS detector with TRIUMPH graphite monochromator). All diffractometer manipulations, including data collection, integration, and scaling were carried out using the Bruker APEX3 software. An absorption correction was applied using SADABS in point group 2. The space group was determined and the structure solved by intrinsic phasing using XT. Refinement was full-matrix least squares on F^2 using XL. All non-hydrogen atoms were refined using anisotropic displacement parameters. Hydrogen atoms were placed in idealized positions and the coordinates refined (each of the two disordered pairs were constrained to the same position). The isotropic displacement parameters of all hydrogen atoms were fixed at 1.2 times (1.5 times for methyl groups and alcohol) the U_{eq} value of the bonded atom.

A12.2 X-RAY CRYSTAL STRUCTURE ANALYSIS OF THIQ 183P

The tetrahydroisoquinoline (THIQ) product **183p** (87% ee) was crystallized by slow evaporation from chloroform at 23 °C to provide crystals suitable for X-ray analysis. Compound d19110 (**183p**) crystallizes in the monoclinic space group $P2_1(\#4)$ with one molecule in the asymmetric unit. The S atom and one C atom were disordered 60:40; the anisotropic displacement parameters of each of the C–S bonded pairs were constrained to be the same.

Figure A12.1 X-ray crystal structure of THIQ **183p**.**Table A12.1** Crystal data and structure refinement for product **183p**.

Identification code	d19110	
Empirical formula	C ₁₄ H ₁₅ N O S	
Formula weight	245.33	
Temperature	100 K	
Wavelength	0.71073 Å	
Crystal system	Monoclinic	
Space group	P 1 2 ₁ 1	
Unit cell dimensions	a = 8.3309(19) Å	a = 90°
	b = 6.6556(18) Å	b = 96.337(8)°
	c = 10.916(3) Å	g = 90°
Volume	601.6(3) Å ³	
Z	2	
Density (calculated)	1.354 g/cm ³	
Absorption coefficient	0.251 mm ⁻¹	
F(000)	260	
Crystal size	0.38 x 0.17 x 0.08 mm ³	
Theta range for data collection	1.877 to 35.613°.	
Index ranges	-13 ≤ h ≤ 13, -10 ≤ k ≤ 10, -17 ≤ l ≤ 17	
Reflections collected	25734	

Independent reflections	5228 [R(int) = 0.0337]
Completeness to theta = 25.242°	99.5 %
Absorption correction	Semi-empirical from equivalents
Max. and min. transmission	1.0000 and 0.9299
Refinement method	Full-matrix least-squares on F ²
Data / restraints / parameters	5228 / 1 / 209
Goodness-of-fit on F ²	1.058
Final R indices [I>2sigma(I)]	R1 = 0.0383, wR2 = 0.0909
R indices (all data)	R1 = 0.0484, wR2 = 0.0960
Absolute structure parameter [Flack]	0.04(2)
Absolute structure parameter [Hooft]	0.03(2)
Extinction coefficient	n/a
Largest diff. peak and hole	0.457 and -0.227 e.Å ⁻³

Table A12.2 Atomic coordinates ($\times 10^5$) and equivalent isotropic displacement parameters ($\text{\AA}^2 \times 10^3$), and population for **183p**. $U(\text{eq})$ is defined as one third of the trace of the orthogonalized U^{ij} tensor.

	x	y	z	U(eq)	pop
S(1)	-1782(9)	10112(13)	8554(8)	192(2)	0.61(1)
S(1A)	-12835(17)	26880(20)	15351(16)	200(4)	0.40(1)
O(1)	46731(15)	90530(20)	2239(13)	250(3)	1
N(1)	38190(14)	60130(20)	16462(10)	126(2)	1
C(1)	31520(15)	47500(20)	25761(12)	119(2)	1
C(2)	45361(17)	34360(20)	31317(14)	146(2)	1
C(3)	59104(16)	47440(20)	36870(12)	135(2)	1
C(4)	69583(19)	40430(30)	46858(14)	193(3)	1
C(5)	81732(19)	52630(30)	52519(15)	236(3)	1
C(6)	83610(20)	71900(30)	48189(15)	243(4)	1
C(7)	73300(20)	79110(30)	38302(15)	210(3)	1
C(8)	60916(17)	66970(20)	32554(13)	140(2)	1

C(9)	49394(17)	75610(20)	22155(13)	133(2)	1
C(10)	58373(18)	84320(30)	11976(14)	174(3)	1
C(11)	16954(16)	36170(20)	20222(13)	127(2)	1
C(12)	17083(17)	18760(20)	13110(13)	147(2)	1
C(13)	-10370(60)	29940(90)	16190(50)	192(2)	0.61(1)
C(13A)	1840(80)	11730(130)	9760(70)	200(4)	0.40(1)
C(14)	1166(19)	42160(30)	21889(15)	177(3)	1

Table A12.3 Bond lengths [\AA] and angles [$^\circ$] for **183p**.

S(1)-C(12)	1.6959(16)
S(1)-C(13)	1.755(6)
S(1A)-C(13A)	1.746(9)
S(1A)-C(14)	1.6492(19)
O(1)-H(1)	0.93(3)
O(1)-C(10)	1.419(2)
N(1)-H(1A)	0.90(2)
N(1)-C(1)	1.4732(18)
N(1)-C(9)	1.4799(19)
C(1)-H(1B)	1.03(2)
C(1)-C(2)	1.5193(19)
C(1)-C(11)	1.4985(19)
C(2)-H(2A)	0.98(2)
C(2)-H(2B)	1.00(2)
C(2)-C(3)	1.511(2)
C(3)-C(4)	1.400(2)
C(3)-C(8)	1.396(2)
C(4)-H(4)	0.91(3)
C(4)-C(5)	1.389(2)
C(5)-H(5)	0.93(3)
C(5)-C(6)	1.382(3)

C(6)-H(6)	0.85(3)
C(6)-C(7)	1.388(3)
C(7)-H(7)	0.99(3)
C(7)-C(8)	1.403(2)
C(8)-C(9)	1.517(2)
C(9)-H(9)	0.99(2)
C(9)-C(10)	1.521(2)
C(10)-H(10A)	0.96(3)
C(10)-H(10B)	1.01(3)
C(11)-C(12)	1.395(2)
C(11)-C(14)	1.405(2)
C(12)-C(13A)	1.365(6)
C(12)-H(12)	0.94(2)
C(12)-H(12A)	0.94(2)
C(13)-H(13)	0.91(5)
C(13)-C(14)	1.357(5)
C(13A)-H(13A)	1.04(8)
C(14)-H(14A)	0.90(3)
C(14)-H(14)	0.90(3)

C(12)-S(1)-C(13)	91.08(18)
C(14)-S(1A)-C(13A)	91.0(2)
C(10)-O(1)-H(1)	112.9(17)
C(1)-N(1)-H(1A)	108.6(14)
C(1)-N(1)-C(9)	112.10(10)
C(9)-N(1)-H(1A)	106.4(15)
N(1)-C(1)-H(1B)	110.5(13)
N(1)-C(1)-C(2)	106.04(11)
N(1)-C(1)-C(11)	111.07(11)
C(2)-C(1)-H(1B)	108.3(12)
C(11)-C(1)-H(1B)	106.3(12)

C(11)-C(1)-C(2)	114.61(12)
C(1)-C(2)-H(2A)	112.8(13)
C(1)-C(2)-H(2B)	110.8(13)
H(2A)-C(2)-H(2B)	106(2)
C(3)-C(2)-C(1)	109.66(12)
C(3)-C(2)-H(2A)	108.2(13)
C(3)-C(2)-H(2B)	109.0(13)
C(4)-C(3)-C(2)	120.00(14)
C(8)-C(3)-C(2)	120.42(12)
C(8)-C(3)-C(4)	119.48(14)
C(3)-C(4)-H(4)	117.4(15)
C(5)-C(4)-C(3)	120.85(16)
C(5)-C(4)-H(4)	121.3(15)
C(4)-C(5)-H(5)	120.5(18)
C(6)-C(5)-C(4)	119.70(16)
C(6)-C(5)-H(5)	119.6(18)
C(5)-C(6)-H(6)	122.3(19)
C(5)-C(6)-C(7)	120.17(15)
C(7)-C(6)-H(6)	117.3(19)
C(6)-C(7)-H(7)	122.1(15)
C(6)-C(7)-C(8)	120.68(17)
C(8)-C(7)-H(7)	117.2(15)
C(3)-C(8)-C(7)	119.12(14)
C(3)-C(8)-C(9)	121.50(12)
C(7)-C(8)-C(9)	119.33(14)
N(1)-C(9)-C(8)	111.60(12)
N(1)-C(9)-H(9)	108.5(13)
N(1)-C(9)-C(10)	107.26(12)
C(8)-C(9)-H(9)	111.2(13)
C(8)-C(9)-C(10)	111.69(12)
C(10)-C(9)-H(9)	106.4(14)

O(1)-C(10)-C(9)	107.91(12)
O(1)-C(10)-H(10A)	111.9(15)
O(1)-C(10)-H(10B)	111.6(13)
C(9)-C(10)-H(10A)	109.0(14)
C(9)-C(10)-H(10B)	110.1(14)
H(10A)-C(10)-H(10B)	106(2)
C(12)-C(11)-C(1)	125.94(13)
C(12)-C(11)-C(14)	111.87(13)
C(14)-C(11)-C(1)	122.19(13)
S(1)-C(12)-H(12)	119.9(15)
C(11)-C(12)-S(1)	112.40(11)
C(11)-C(12)-H(12)	127.7(16)
C(11)-C(12)-H(12A)	127.7(16)
C(13A)-C(12)-C(11)	111.7(4)
C(13A)-C(12)-H(12A)	120.6(16)
S(1)-C(13)-H(13)	105(3)
C(14)-C(13)-S(1)	111.3(4)
C(14)-C(13)-H(13)	143(3)
S(1A)-C(13A)-H(13A)	105(3)
C(12)-C(13A)-S(1A)	112.0(5)
C(12)-C(13A)-H(13A)	143(4)
S(1A)-C(14)-H(14A)	120.7(15)
C(11)-C(14)-S(1A)	113.35(14)
C(11)-C(14)-H(14A)	125.9(15)
C(11)-C(14)-H(14)	125.9(15)
C(13)-C(14)-C(11)	113.4(3)
C(13)-C(14)-H(14)	120.7(15)

Table A12.4 Anisotropic displacement parameters ($\text{\AA}^2 \times 10^4$) for **183p**. The anisotropic displacement factor exponent takes the form: $-2\pi^2 [h^2 a^{*2} U^{11} + \dots + 2 h k a^* b^* U^{12}]$

	U ¹¹	U ²²	U ³³	U ²³	U ¹³	U ¹²
S(1)	146(4)	220(4)	204(4)	-44(3)	-7(3)	-76(3)
S(1A)	121(7)	246(7)	223(6)	-49(5)	-15(4)	-92(4)
O(1)	205(6)	302(7)	251(6)	151(5)	60(4)	14(5)
N(1)	133(5)	113(5)	131(5)	14(4)	8(4)	-15(4)
C(1)	109(5)	126(5)	121(5)	0(4)	13(4)	-11(4)
C(2)	129(6)	135(6)	168(6)	39(5)	-7(4)	-20(5)
C(3)	101(5)	182(6)	123(5)	1(5)	14(4)	5(5)
C(4)	157(6)	274(8)	144(6)	12(6)	2(5)	45(5)
C(5)	127(6)	437(10)	143(6)	-57(6)	2(5)	35(6)
C(6)	148(6)	416(11)	167(6)	-123(7)	23(5)	-95(6)
C(7)	191(7)	255(8)	193(6)	-75(6)	54(5)	-94(6)
C(8)	125(5)	173(6)	126(5)	-31(5)	35(4)	-21(5)
C(9)	150(6)	94(5)	161(6)	-5(5)	45(4)	-16(4)
C(10)	171(6)	166(6)	191(6)	30(5)	53(5)	-35(5)
C(11)	124(5)	138(6)	114(5)	5(4)	-2(4)	-20(4)
C(12)	150(6)	141(6)	147(6)	-16(5)	10(4)	-27(5)
C(13)	146(4)	220(4)	204(4)	-44(3)	-7(3)	-76(3)
C(13A)	121(7)	246(7)	223(6)	-49(5)	-15(4)	-92(4)
C(14)	153(6)	197(7)	186(6)	-13(5)	45(5)	-5(5)

Table A12.5 Hydrogen coordinates ($\times 10^4$) and isotropic displacement parameters ($\text{\AA}^2 \times 10^3$) for **183p**.

	x	y	z	U(eq)
H(1)	5130(30)	9700(50)	-410(30)	38
H(1A)	3010(30)	6680(40)	1220(20)	15
H(1B)	2770(20)	5620(40)	3270(20)	14

H(2A)	4220(30)	2540(40)	3780(20)	18
H(2B)	4930(30)	2550(40)	2490(20)	18
H(4)	6740(30)	2820(40)	5010(20)	23
H(5)	8820(30)	4820(50)	5950(20)	28
H(6)	9050(30)	8010(40)	5180(20)	29
H(7)	7390(30)	9310(40)	3530(20)	25
H(9)	4290(30)	8670(40)	2510(20)	16
H(10A)	6490(30)	9530(40)	1520(20)	21
H(10B)	6600(30)	7400(40)	910(20)	21
H(13)	-2130(60)	2800(70)	1480(40)	23
H(13A)	-450(70)	-40(120)	550(60)	24
H(12)	2610(30)	1210(40)	1060(20)	21
H(12A)	2610(30)	1210(40)	1060(20)	21
H(14A)	-150(30)	5310(40)	2600(20)	21
H(14)	-150(30)	5310(40)	2600(20)	21

Table A12.6 Torsion angles [°] for **183p**.

S(1)-C(13)-C(14)-C(11)	0.6(4)
N(1)-C(1)-C(2)-C(3)	58.56(14)
N(1)-C(1)-C(11)-C(12)	78.77(18)
N(1)-C(1)-C(11)-C(14)	-102.09(16)
N(1)-C(9)-C(10)-O(1)	52.73(16)
C(1)-N(1)-C(9)-C(8)	44.46(15)
C(1)-N(1)-C(9)-C(10)	167.09(12)
C(1)-C(2)-C(3)-C(4)	151.33(13)
C(1)-C(2)-C(3)-C(8)	-25.09(17)
C(1)-C(11)-C(12)-S(1)	179.50(12)
C(1)-C(11)-C(12)-C(13A)	178.1(4)
C(1)-C(11)-C(14)-S(1A)	-177.87(13)
C(1)-C(11)-C(14)-C(13)	-179.8(3)

C(2)-C(1)-C(11)-C(12)	-41.36(19)
C(2)-C(1)-C(11)-C(14)	137.77(14)
C(2)-C(3)-C(4)-C(5)	-176.42(14)
C(2)-C(3)-C(8)-C(7)	176.81(13)
C(2)-C(3)-C(8)-C(9)	-0.66(19)
C(3)-C(4)-C(5)-C(6)	-0.5(2)
C(3)-C(8)-C(9)-N(1)	-7.99(18)
C(3)-C(8)-C(9)-C(10)	-128.05(14)
C(4)-C(3)-C(8)-C(7)	0.4(2)
C(4)-C(3)-C(8)-C(9)	-177.09(13)
C(4)-C(5)-C(6)-C(7)	0.7(2)
C(5)-C(6)-C(7)-C(8)	-0.3(2)
C(6)-C(7)-C(8)-C(3)	-0.3(2)
C(6)-C(7)-C(8)-C(9)	177.26(14)
C(7)-C(8)-C(9)-N(1)	174.55(12)
C(7)-C(8)-C(9)-C(10)	54.49(17)
C(8)-C(3)-C(4)-C(5)	0.0(2)
C(8)-C(9)-C(10)-O(1)	175.30(13)
C(9)-N(1)-C(1)-C(2)	-71.23(14)
C(9)-N(1)-C(1)-C(11)	163.67(12)
C(11)-C(1)-C(2)-C(3)	-178.55(11)
C(11)-C(12)-C(13A)-S(1A)	0.4(6)
C(12)-S(1)-C(13)-C(14)	-0.3(4)
C(12)-C(11)-C(14)-S(1A)	1.37(18)
C(12)-C(11)-C(14)-C(13)	-0.6(3)
C(13)-S(1)-C(12)-C(11)	0.0(2)
C(13A)-S(1A)-C(14)-C(11)	-0.9(3)
C(14)-S(1A)-C(13A)-C(12)	0.3(5)
C(14)-C(11)-C(12)-S(1)	0.29(16)
C(14)-C(11)-C(12)-C(13A)	-1.1(4)

Table A12.7 Hydrogen bonds for **183p** [\AA and $^\circ$].

D-H...A	d(D-H)	d(H...A)	d(D...A)	<(DHA)
O(1)-H(1)...N(1)#1	0.93(3)	1.90(3)	2.8310(18)	177(2)

Symmetry transformations used to generate equivalent atoms: #1 -x+1,y+1/2,-z .

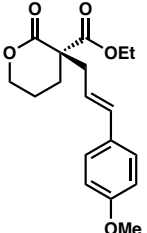
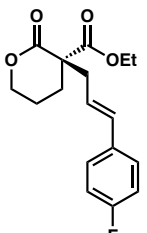
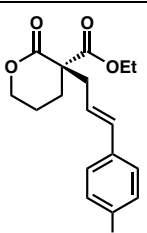
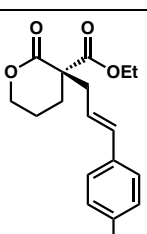
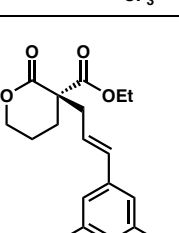
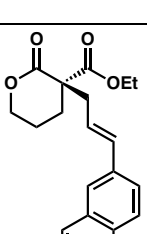
APPENDIX 13

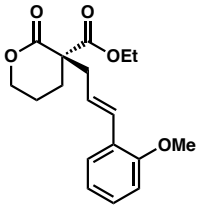
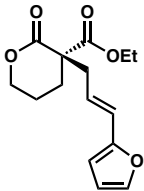
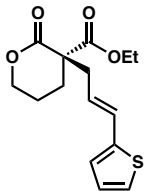
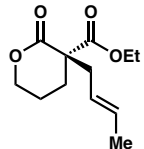
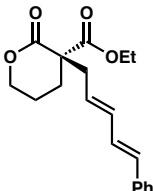
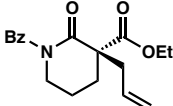
Notebook Cross-Reference for New Compounds

The following notebook cross-reference provides the file name for all original spectroscopic data obtained for new compounds presented within this thesis. The information is organized by chapter or appendix and sequentially by compound number. All ^1H NMR, ^{13}C NMR, as well as ^{19}F NMR and any two-dimensional NMR data, if applicable, are electronically stored on the Caltech NMR laboratory server (mangia.caltech.edu, most typically under the usernames ‘angamnit,’ ‘ewelin,’ ‘cjette,’ or ‘akim2’) and on the Stoltz group server. Electronic copies of all IR spectra can also be found on the Stoltz group server. All laboratory notebooks are stored in the Stoltz group archive.

Table A13.1 Notebook cross-reference for compounds in Chapter 1.

Compound	Chemical Structure	¹ H NMR	¹³ C NMR	IR
4a		FN-II-45 (florencia)	FN-II-45 (florencia)	FN-III-EthylLactam
4b		FN-III-187dry (florencia)	FN-III-187 (florencia)	FN-III-187
–		CIJ-III-291pc (florencia)	CIJ-III-291pc (florencia)	CIJ-III-291
–		CIJ-II-293-pc-phv- pro (florencia)	CIJ-II-293-pc-phv- carbon (florencia)	CIJ-II-293
–		FN-III-149 (florencia)	FN-III-149 (florencia)	FN-III-149
3aa		FN-III-53-1 (florencia)	FN-III-53-1 (florencia)	FN-III-53-1
3ba		FN-III-53-2 (florencia)	FN-III-53-2 (florencia)	FN-III-193
3ca		FN-III-53-4 (florencia)	FN-III-53-4 (florencia)	FN-III-53-4
3ab		FN-III-105-1 (florencia)	FN-III-105-1 (florencia)	FN-III-107-5
3ac		FN-III-107-2 (florencia)	FN-III-107-2 (florencia)	FN-III-107-2

Compound	Chemical Structure	¹ H NMR	¹³ C NMR	IR
3ad		FN-III-105-2 (Florence)	FN-III-105-2 (Florence)	FN-III-105-2
3ae		FN-III-113-1dry (florence) ¹⁹ F: FN-III-113-1-F (hg3)	FN-III-113-1dry (Florence)	FN-III-113-1
3af		FN-III-105-3 (Florence)	FN-III-105-3 (Florence)	FN-III-105-3
3ag		FN-III-107-4 (florence) ¹⁹ F: FN-III-107-4- CF3 (hg3)	FN-III-107-4 (Florence)	FN-III-107-4
3ah		FN-III-107-3 (florence)	FN-III-107-3 (florence)	FN-III-107-3
3ai		FN-III-113-2 (florence)	FN-III-113-2 (florence)	FN-III-113-2

Compound	Chemical Structure	¹ H NMR	¹³ C NMR	IR
3aj		FN-III-113-3 (florence)	FN-III-113-3 (florence)	FN-III-113-3
3ak		FN-III-105-4 (florence)	FN-III-105-4 (florence)	FN-III-105-4
3al		FN-III-107-1 (florence)	FN-III-107-1 (florence)	FN-III-107-1
3am		FN-III-275-3 (florence)	FN-III-275-3 (florence)	FN-III-275-3
3an		FN-III-113-4 (florence)	FN-III-113-4 (florence)	FN-III-113-4
5aa		FN-III-185-2 (florence)	FN-III-185-2 (florence)	FN-III-185-2

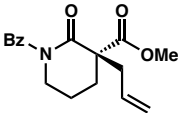
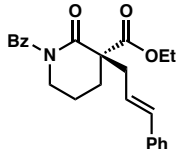
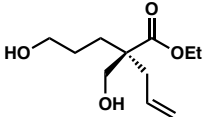
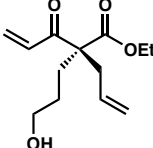
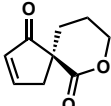
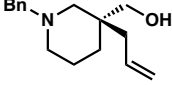
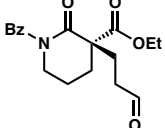
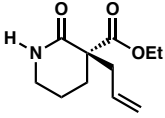
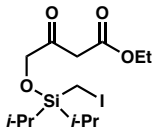
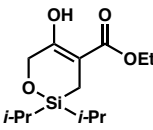
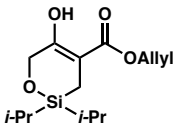
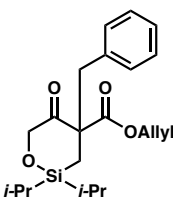
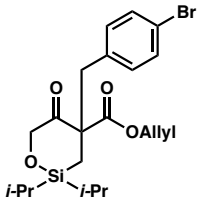
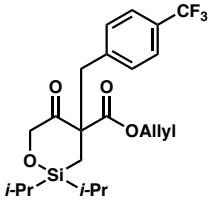
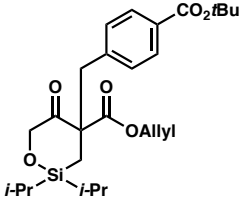
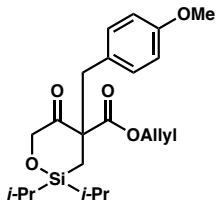
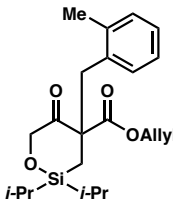
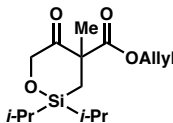
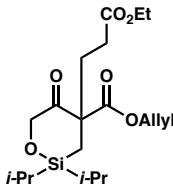
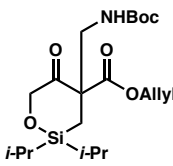
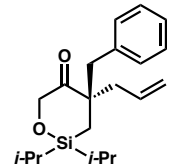
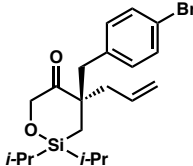
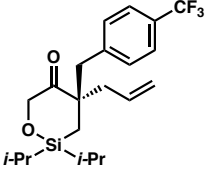
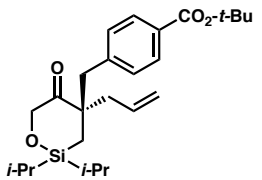
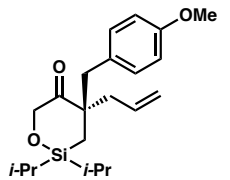
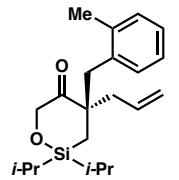
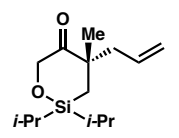
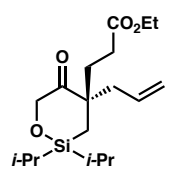
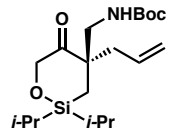
Compound	Chemical Structure	¹ H NMR	¹³ C NMR	IR
5ba		FN-III-211-1 (florencia)	FN-III-211-1 (florencia)	FN-III-211
5ab		FN-III-143-2 (florencia) *misabeled, actually from FN-III-173	FN-III-143-2 (florencia) *misabeled, actually from FN-III-173	FN-III-173-2
6		FN-III-221 (florencia)	FN-III-221 (florencia)	FN-III-243
7		CIJ-III-133pc (florencia)	CIJ-III-133pc (florencia)	CIJ_III_133
8		FN-III-261dry (florencia)	FN-III-261dry (florencia)	FN-III-261
9		CIJ-III-83-r2-pc (florencia)	CIJ-III-83-r2-pc (florencia)	CIJ_III_83
10		CIJ-III-137-r2-pc (florencia)	CIJ-III-137-r2-pc (florencia)	CIJ_III_137
11		CIJ-III-149-ptlc (florencia)	CIJ-III-149-ptlc (florencia)	CIJ_III_149

Table A13.2 Notebook cross-reference for compounds in Chapter 2.

Compound	Chemical Structure	¹ H NMR	¹³ C NMR	IR
14		FN-IV-197dry.1 (florencia)	FN-IV-197dry.2 (florencia)	FN-IV-197
23		FN-IV-205dry.1 (florencia)	FN-IV-205dry.2 (florencia)	FN-IV-205
15		FN-IV-253dry.1 (florencia)	FN-IV-253dry.2 (florencia)	FN-IV-253
16a		FN-IV-259.1 (florencia)	FN-IX-255-5a.2 (florencia)	FN-IV-259
16b		FN-III-289.3 (florencia)	FN-III-289.4 (florencia)	FN-III-289
16c		FN-III-291.1 (florencia) ¹⁹ F: FN-III-291 (hg3)	FN-III-291.2 (florencia)	FN-III-291
16d		FN-IV-47dry.1 (florencia) *mislabeled, actually from FN-IV-43	FN-IV-47dry.2 (florencia) *mislabeled, actually from FN-IV-43	FN-IV-47 *mislabeled, actually from FN-IV-43

Compound	Chemical Structure	¹ H NMR	¹³ C NMR	IR
16e		FN-III-281.1 (florencia)	FN-III-281.2 (florencia)	FN-III-281
16f		FN-IV-31.1 (florencia)	FN-IV-31.2 (florencia)	FN-IV-31
16g		FN-III-175.1 (florencia)	FN-III-175.2 (florencia)	FN-III-175
16h		FN-IV-29.1 (florencia)	FN-IV-29.2 (florencia)	FN-IV-29
16i		FN-IV-45.3 (florencia)	FN-IV-45.4 (florencia)	FN-IV-45
17a		FN-III-207.1 (florencia)	FN-III-207.2 (florencia)	FN-III-207
17b		FN-IV-53.1 (florencia)	FN-IV-53.2 (florencia)	FN-IV-53

Compound	Chemical Structure	¹ H NMR	¹³ C NMR	IR
17c		FN-IV-27col2.1 (florencia) ¹⁹ F: FN-IV-27col2 (hg3)	FN-IV-27col2.2 (florencia)	FN-IV-27
17d		FN-IV-57.1 (florencia)	FN-IV-57.2 (florencia)	FN-IV-57
17e		FN-IV-23col-OMe.1 (florencia)	FN-IV-23col-OMe.2 (florencia)	FN-IV-23
17f		FN-IV-37.1 (florencia) *mislabeled, actually from FN-IV-39	FN-IV-37.2 (florencia) *mislabeled, actually from FN-IV-39	FN-IV-39
17g		FN-III-223.1 (florencia)	FN-III-223.2 (florencia)	FN-III-223
17h		FN-IV-33.1 (florencia) *mislabeled, actually from FN-IV-35	FN-IV-33.2 (florencia) *mislabeled, actually from FN-IV-35	FN-IV-35
17i		FN-IV-61.1 (florencia)	FN-IV-61.2 (florencia)	FN-IV-61

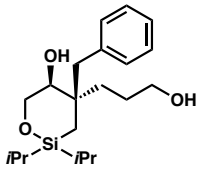
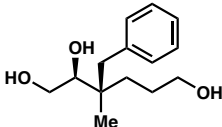
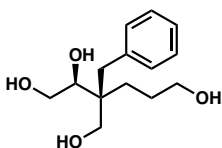
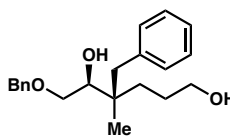
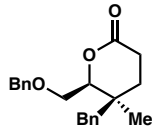
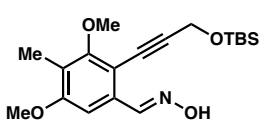
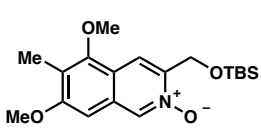
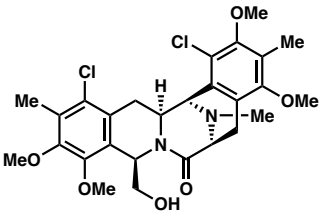
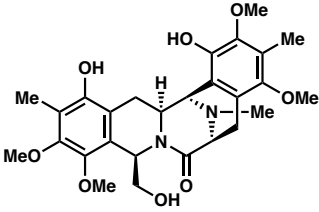
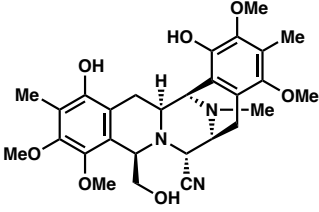
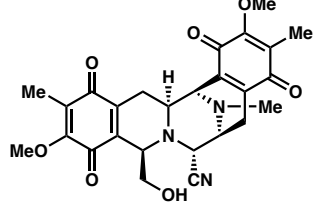
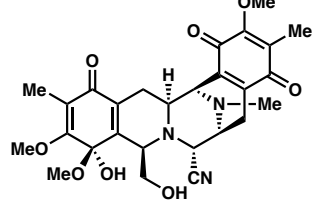
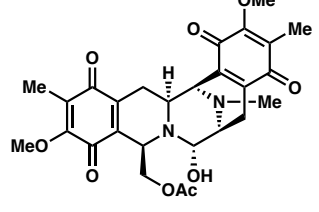
Compound	Chemical Structure	¹ H NMR	¹³ C NMR	IR
18		FN-IV-245dry.1 (florencia)	FN-IV-245dry.2 (florencia)	FN-IV-299
19		FN-IIX-259-MeOD (indy)	FN-IIX-259inMeOH.2 (florencia)	FN-IIX-259
20		FN-IIX-269prep.1 (florencia)	FN-IIX-269prep.2 (florencia)	FN-IIX-269
21		FN-IV-273.1 (florencia)	FN-IV-273.2 (florencia)	FN-IV-281
22		FN-IIX-267prep.1 (florencia)	FN-IIX-267prep.2 (florencia)	FN-IIX-267

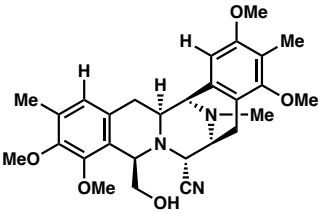
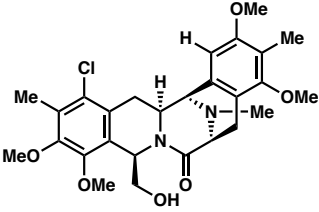
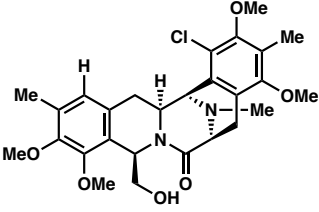
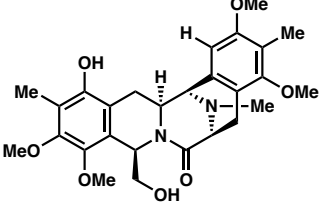
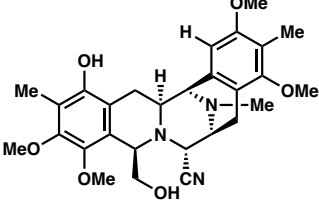
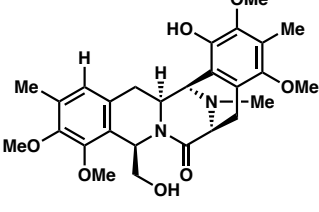
Table A13.3 Notebook cross-reference for compounds in Chapter 3.

Compound	Chemical Structure	¹ H NMR	¹³ C NMR	IR
88		ERW-3-289_col (indy)	ERW-3-289_col (florencia)	ERW-III-289
84		ERW-2-215 jan.1 (florencia)	ERW-2-215 jan.2 (florencia)	ERW-2-215

Compound	Chemical Structure	¹ H NMR	¹³ C NMR	IR
91		ERW-2-209 (hg3)	ERW-3-185 (indy)	ERW-3-185
85		ERW-3-189.1 (florencia) ¹⁹ F: ERW-1-97 (hg3)	ERW-3-189.2 (florencia)	ERW-3-189
93		ERW-3-191.1 (florencia)	ERW-3-191.2 (florencia)	ERW-3-191
114		ERW-4-33 (indy)	ERW-4-127 C.1 (florencia)	—
112		ERW-4-35.1 (florencia)	ERW-4-35.2 (florencia)	ERW-4-35
113		ERW-1-155.1 (florencia)	ERW-1-155.1 (florencia)	ERW-1-155

Compound	Chemical Structure	¹ H NMR	¹³ C NMR	IR
115 & 116 aldehyde+ hemiacetal		ERW-4-51.1 (florencia)	ERW-4-51.2 (florencia)	ERW-4-51
83 • DCM		ERW-4-53.1 (florencia)	ERW-4-53.2 (florencia)	ERW-4-53
95		FN-V-153.1 (florencia)	FN-V-153.2 (florencia)	FN-V-153
96		FN-V-193col- bottom.1 (florencia)	FN-V-193col- bottom.2 (florencia)	FN-V-193
81		ERW-3-221 (indy)	ERW-3-221 (indy)	ERW-3-221
117		ERW-3-259 (indy)	ERW-3-259 (indy)	ERW-3-239

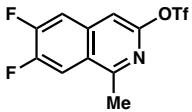
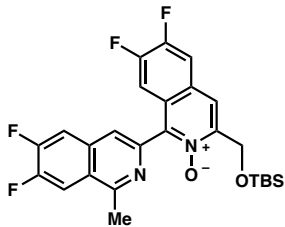
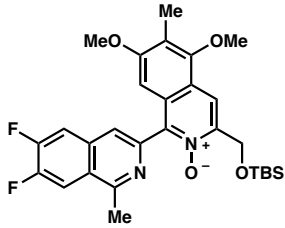
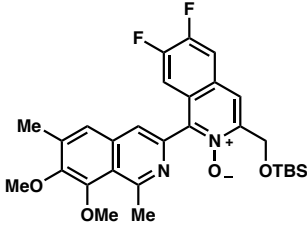
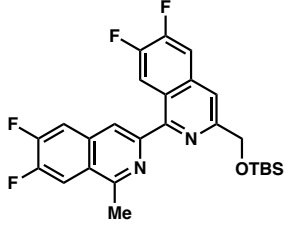
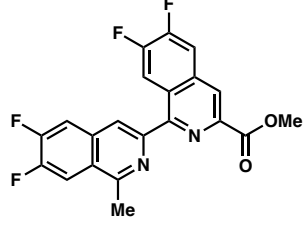
Compound	Chemical Structure	¹ H NMR	¹³ C NMR	IR
99		ERW-3-293_col (indy)	ERW-3-293_col (indy)	ERW-3-293
100		ERW-4-165 (indy)	ERW-4-165 (indy)	ERW-4-165
105		ERW-4-173.1 (florencia)	ERW-4-173.2 (florencia)	ERW-4-173
79		ERW-4-175 (indy)	ERW-4-175 (indy)	ERW-4-175
101		ERW-4-177 bypdt.1 (florencia)	ERW-4-177 bypdt.2 (florencia)	ERW-4-177- byproduct
77		ERW-4-179_pdt.1 (florencia)	ERW-4-179_pdt.2 (florencia)	ERW-4-179

Compound	Chemical Structure	¹ H NMR	¹³ C NMR	IR
102		ERW-3-261 (indy)	ERW-4-207.1 (florencia)	ERW-4-207
118		FN-V-163prep- mixed.3 (florencia)	FN-V-163prep- mixed.2 (florencia)	FN-V-163B
119		FN-V_163prep- C.2 (florencia)	FN-V_163prep- C.1 (florencia)	FN-V-163C
120		FN-V-171col.1 (florencia)	FN-V-171col.4 (florencia)	FN-V-171
103		FN-V-175 (fid)	FN-V-175.1 (florencia)	FN-V-175
121		FN-V-181prepA.1 (florencia)	FN-V-181prepA.1 (florencia)	FN-V-181prepA

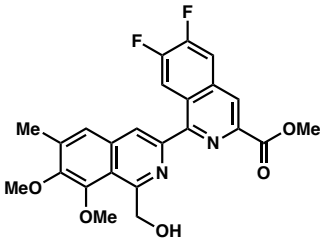
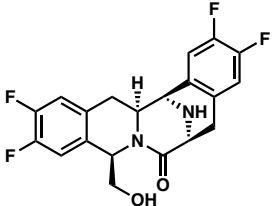
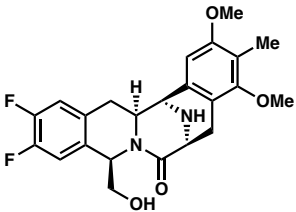
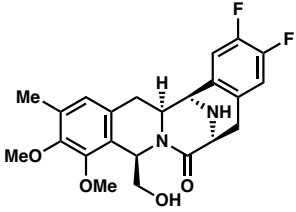
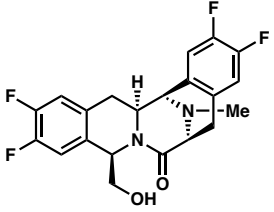
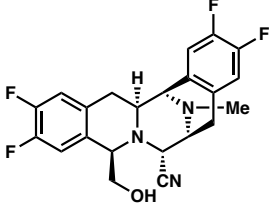
Compound	Chemical Structure	¹ H NMR	¹³ C NMR	IR
122		FN-V-181prepC.1 (florencia)	FN-V-181prepC.1 (florencia)	FN-V-181C
104		FN-V-197conc.1 (florencia)	FN-V-197conc.2 (florencia)	FN-V-197
98		ERW-3-45 (florencia)	—	—

Table A13.4 Notebook cross-reference for compounds in Appendix 7.

Compound	Chemical Structure	¹ H NMR	¹³ C NMR	IR
171		ERW-4-91 (indy)	gmp-iii-197-c.1 (florencia)	—
135		ERW-4-95 (hg3) *bad shimming	—	—
132		gmp-iii-259-2ndfraction (hg3) ¹⁹ F: GMP-iii-259 (hg3)	gmp-iii-259.1 (florencia) *bad S/N	—

Compound	Chemical Structure	¹ H NMR	¹³ C NMR	IR
133		FN-V-43col (indy)	—	—
138		gmp-iii-177c.1 (florencia)	gmp-iii-177c.3 (florencia)	—
139		FN-VI-37.1 (florencia) ¹⁹ F: FN-VI-37conc (hg3)	FN-VI-37.2 (indy)	FN-VI-37
140		ERW-4-239 (hg3) ¹⁹ F: ERW-4-239 (hg3)	—	—
141		FN-V-107.1 (florencia) ¹⁹ F: FN-V-107 (hg3)	FN-V-107.2 (florencia)	FN-V-107
142		FN-V-91 (hg3)	—	—

Compound	Chemical Structure	¹ H NMR	¹³ C NMR	IR
144		FN-V-115 (hg3)	—	—
146		FN-V-139crude (hg3) ¹⁹ F: FN-V-139crude (hg3)	—	FN-V-139
149		FN-VI-41col.1 (florencia) ¹⁹ F: FN-VI-41col (hg3)	FN-VI-41col.2 (florencia)	FN-VI-41
151		FN-VI-45.1 (florencia) ¹⁹ F: FN-VI-45col (hg3)	FN-VI-45.2 (florencia) *bad S/N	—
152		ERW-4-241 (indy)	ERW-4-241.2 (florencia)	—
153		ERW-4-247.1 (florencia) ¹⁹ F: ERW-4-247 (hg3)	ERW-4-247.2 (florencia)	—

Compound	Chemical Structure	¹ H NMR	¹³ C NMR	IR
155		ERW-4-251.1 (florencia) ¹⁹ F: ERW-4-251 (hg3)	ERW-4-251.2 (florencia)	—
129		FN-V-119dry.1 (florencia) ¹⁹ F: FN-V-119dry (hg3)	FN-V-119dry.2 (florencia)	FN-V-119
130		FN-VI-83.3 (florencia) ¹⁹ F: FN-VI-83 (hg3)	FN-VI-83.2 (florencia)	FN-VI-83
131		ERW-4-253A.1 (florencia)	ERW-4-253A.2 (florencia)	—
156		FN-V-229dry.1 (florencia) ¹⁹ F: FN-V-73crude (hg3)	FN-V-229dry.2 (florencia)	FN-V-229
126		FN-V-231.1 (florencia) ¹⁹ F: FN-V-231 (hg3)	FN-V-231.2 (florencia)	FN-V-231

Compound	Chemical Structure	¹ H NMR	¹³ C NMR	IR
157		ERW-4-215.1 (florencia) ¹⁹ F: ERW-4-215 (hg3) * ¹⁹ F in FN folder	ERW-4-215.2 (florencia)	—
158		ERW-4-221.1 (florencia) ¹⁹ F: ERW-4-221 (hg3) * ¹⁹ F in FN folder	ERW-4-221.2 (florencia)	—
159		FN-VI-87crude.1 (florencia) ¹⁹ F: FN-VI- 87crude (hg3)	FN-VI-87crude.2 (florencia) *bad S/N	—
160		FN-IX-159dry (indy)	FN-IX-159.2 (Florence) *bad S/N	—
173		FN-VI-107crude (indy)	—	—
174		FN-VI-113col.1 (Florence)	—	—
175		FN-VI-115col (hg3)	—	—

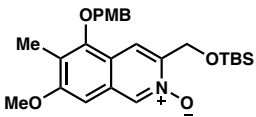
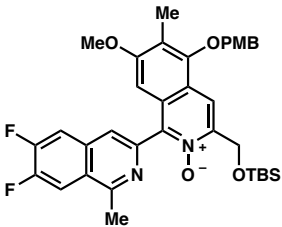
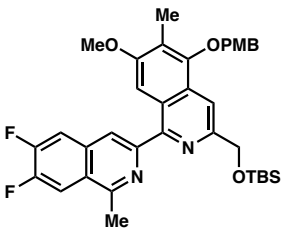
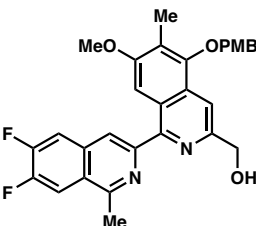
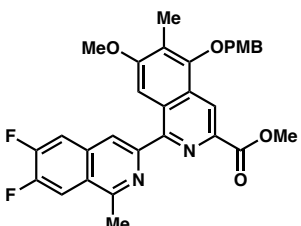
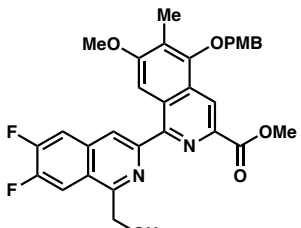
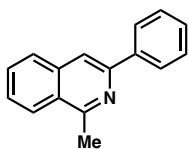
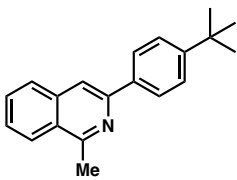
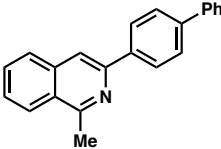
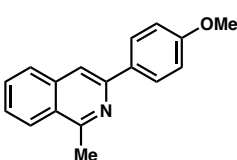
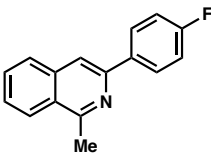
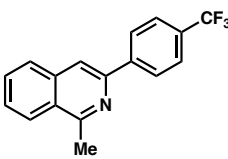
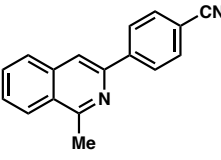
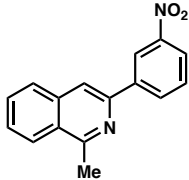
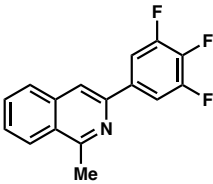
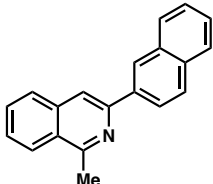
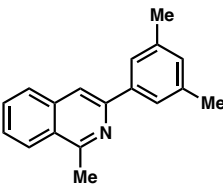
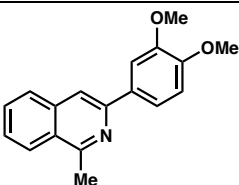
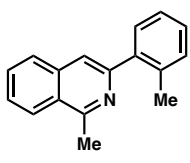
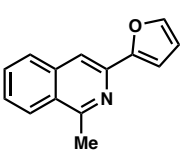
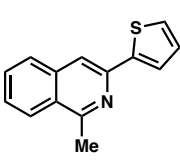
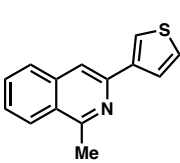
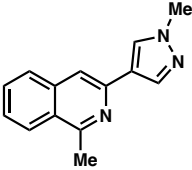
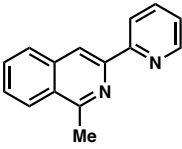
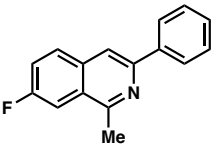
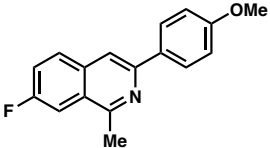
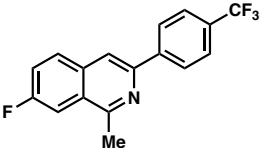
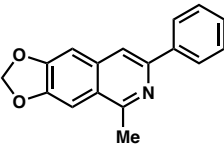
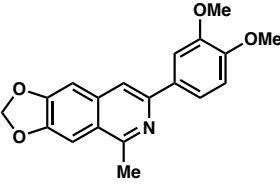
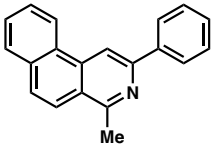
Compound	Chemical Structure	¹ H NMR	¹³ C NMR	IR
164		FN-VI-179col (hg3)	–	–
165		FN-IIX-283.1 (florencia)	–	–
176		FN-IIX-285 (indy)	–	–
177		FN-IIX-287crude- conc (indy)	–	–
166		FN-IIX-289major (indy)	–	–
167		FN-IIX-293flush (indy)	–	–

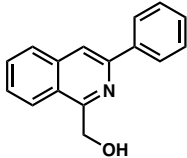
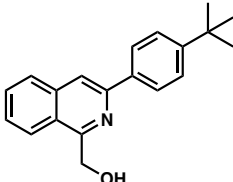
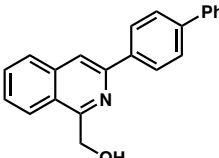
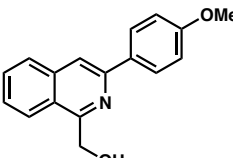
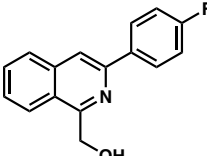
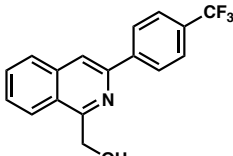
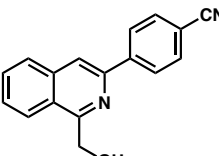
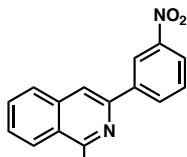
Table A13.5 Notebook cross-reference for compounds in Chapter 4.

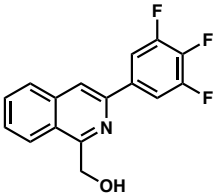
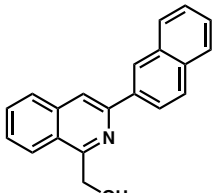
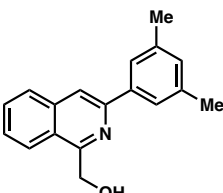
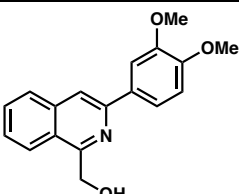
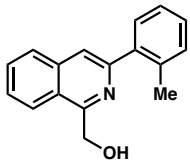
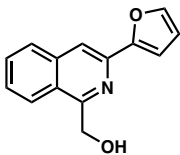
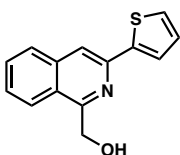
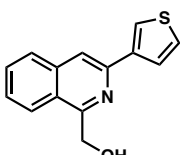
Compound	Chemical Structure	¹ H NMR	¹³ C NMR	IR
179a		FN-IIX-43.1 (florencia)	FN-IIX-43.2 (florencia)	FN-IIX-43
179b		FN-IIX-149col2.1 (florencia) ¹⁹ F: FN-IIX-149col (hg3)	FN-IIX-149col2.2 (florencia)	FN-IIX-149
179c		FN-IIX-45.1 (florencia)	FN-IIX-45.2 (florencia)	FN-IIX-45
179d		FN-IIX-47.1 (florencia)	FN-IIX-47.2 (florencia)	FN-IIX-47
180a		FN-hydrog-OTf.1 (florencia) ¹⁹ F: FN-hydrog- OTf (hg3)	FN-hydrog-OTf.2 (florencia)	FN-OTf
180b		AK-2-35- Fbackbone-OTf- 1H.3 (florencia) ¹⁹ F: AK-2-35- Fbackbone-OTf- 19F (hg3)	AK-F-OTf13C.1 (Florencia)	AK-2-35- Fbackbone-OTf
180c		AK-2-89- dioxolane-OTf- 1H.3 (florencia) ¹⁹ F: AK-2-89- dioxolane-19F (hg3)	AK-2-89- dioxolane-OTf- 1H.4 (florencia)	AK-2-89- dioxolane-OTf
180d		AK-2-93-naphthyl- OTf-1H.4 (florencia) ¹⁹ F: AK-2-93- naphthyl-OTf-19F (hg3)	AK-2-93-naphthyl- OTf-1H.5 (florencia)	AK-2-93-naphthyl- OTf

Compound	Chemical Structure	¹ H NMR	¹³ C NMR	IR
181a		FN-VII-199.1 (florencia)	FN-VII-199.2 (florencia)	FN-VI-211
181b		FN-VII-59.1 (florencia)	FN-VII-59.2 (florencia)	FN-VII-59
181c		FN-VII-55.1 (florencia)	FN-VII-55.1 (florencia)	FN-VII-55
181d		AK-1-279-pOMe- 1H.4 (florencia)	AK-1-279-pOMe- 13C.3 (florencia)	AK-1-279-pOMe
181e		FN-VII-73.3 (florencia) ¹⁹ F: FN-VII-73 (hg3)	FN-VII-73.4 (florencia)	FN-VII-73
181f		AK-1-281-pCF3- 1H.3 (florencia) ¹⁹ F: AK-1-281- pCF3 (hg3)	AK-1-281-pCF3- 13C.4 (florencia)	AK-pCF3-SM
181g		FN-VII-75.3 (florencia)	FN-VII-75.4 (florencia)	FN-VII-75
181h		FN-VII-81.1 (florencia)	FN-VII-81.2 (florencia)	FN-VII-81

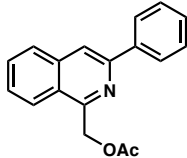
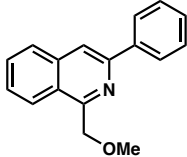
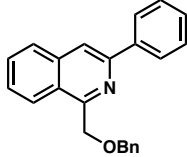
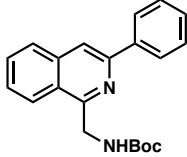
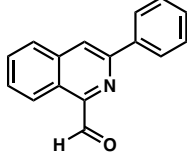
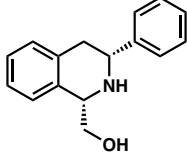
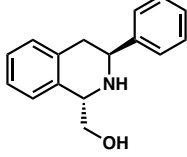
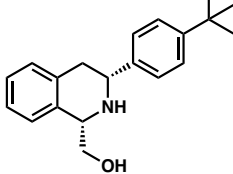
Compound	Chemical Structure	¹ H NMR	¹³ C NMR	IR
181i		AK-1-289-F3Ph-1H.4 (florencia) ¹⁹ F: AK-F3-suzuki (hg3)	AK-1-289-F3Ph-13C.5 (florencia)	AK-1-289-F3Ph
181j		FN-VII-53.1 (florencia)	FN-VII-53.2 (florencia)	FN-VII-53
181k		FN-VII-57.1 (florencia)	FN-VII-57.2 (florencia)	FN-VII-57
181l		FN-VII-71.3 (florencia)	FN-VII-71.4 (florencia)	FN-VII-71
181m		FN-VII-61.1 (florencia)	FN-VII-61.2 (florencia)	FN-IIX-61
181n		AK-2-51-furan-1H.3 (florencia)	AK-2-51-furan-13C.4 (florencia)	AK-2-51-furan
181o		AK-2-53-thiophene-1H.3 (florencia)	AK-2-53-thiophene-13C.4 (florencia)	AK-2-52-thiophene
181p		FN-VII-79.3 (florencia)	FN-VII-79.4 (florencia)	FN-VII-79

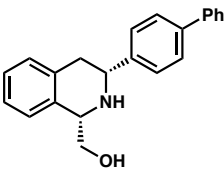
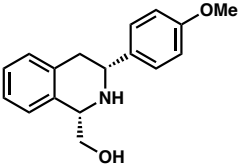
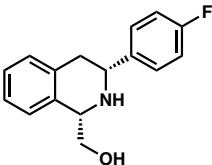
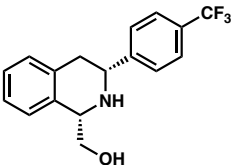
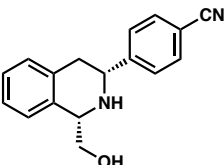
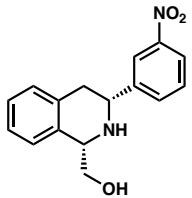
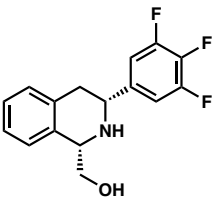
Compound	Chemical Structure	¹ H NMR	¹³ C NMR	IR
181q		AK-2-73-pyrazole-1H.3 (florencia)	AK-2-73-pyrazole-13C.4 (florencia)	AK-2-73-pyrazole
181r		FN-VII-295.1 (florencia)	FN-VII-295.2 (florencia)	FN-VII-295
192a		AK-2-41-Ph-F-1H.3 (florencia) ¹⁹ F: AK-2-41-Ph-F-19F (hg3)	AK-2-41-Ph-F-13C.4 (florencia)	AK-2-41-Ph-F
192b		AK-1-251-pOMe-F.1 (florencia) ¹⁹ F: AK-1-251-col (hg3)	AK-2-179-F-pOMe-13C.1 (florencia)	AK-1-251-pOMe-F
192c		AK-1-253-CF ₃ -F-2-1H.5 (florencia) ¹⁹ F: AK-1-253-col (hg3)	AK-1-253-CF ₃ -F-2-13C.6 (florencia)	AK-1-253-pCF ₃ -F
192d		AK-2-95-dioxolane-Ph-1H.3 (florencia)	AK-2-95-dioxolane-Ph-13C.4 (florencia)	AK-2-95-dioxolane-Ph
192e		AK-2-119-dioxolane-diOMe-1H.5 (florencia)	AK-2-119-dioxolane-diOMe-13C.6 (florencia)	AK-2-119-dioxolane-diOMe
192f		AK-2-99-naphthyl-1H.3 (florencia)	AK-2-99-naphthyl-13C.4 (florencia)	AK-2-99-naphthyl-Ph

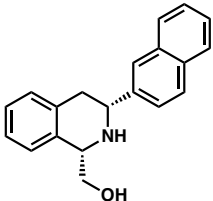
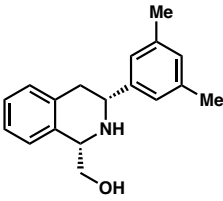
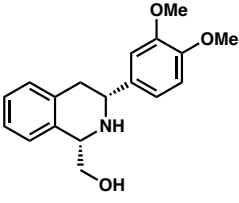
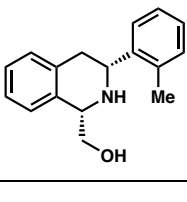
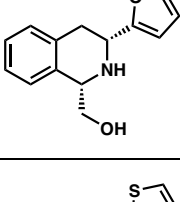
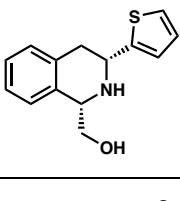
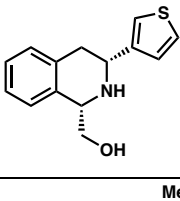
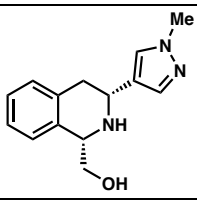
Compound	Chemical Structure	¹ H NMR	¹³ C NMR	IR
182a		FN-VI-243.1 (florencia)	FN-VI-243.2 (florencia)	FN-VI-243
182b		FN-VII-111.1 (florencia)	FN-VII-111.2 (florencia)	FN-VII-11 *misabeled, actually from FN- VII-111
182c		FN-VII-107.1 (florencia)	FN-VII-107.2 (florencia)	FN-VII-107
182d		AK-1-295-pOMe- 1H.5 (Florence)	AK-1-295-pOMe- 13C.6 (Florence)	AK-1-295-pOMe
182e		FN-VII-113.1 (florencia) ¹⁹ F: FN-VII-113 (hg3)	FN-VII-113.2 (florencia)	FN-VII-113
182f		AK-1-189-pCF3- 1H.3 (florencia) ¹⁹ F: AK-1-189-19F	AK-1-189-pCF3- 13C.4 (florencia)	AK-1-189-pCF3
182g		FN-VII-177.1 (florencia)	FN-VII-177.2 (florencia)	FN-VII-177
182h		FN-VII-277.3 (florencia)	FN-VII-277.4 (florencia)	FN-VII-277

Compound	Chemical Structure	¹ H NMR	¹³ C NMR	IR
182i		AK-2-27-F3-OH-1H.3 (Florence) ¹⁹ F: AK-2-27-F3	AK-2-27-F3-OH-13C.4 (Florence)	AK-2-27-F3-OH
182j		FN-VII-105.1 (florencia)	FN-VII-105.2 (florencia)	FN-VII-105
182k		FN-VII-109.1 (florencia)	FN-VII-109.2 (florencia)	FN-VII-109
182l		FN-VII-145.1 (florencia)	FN-VII-145.2 (florencia)	FN-VII-145
182m		FN-VII-279.1 (florencia)	FN-VII-279.2 (florencia)	FN-VII-279
182n		AK-2-61-furan-OH-1H.3 (florencia)	AK-2-61-furan-OH-13C.4 (florencia)	AK-2-61-furan-OH
182o		AK-2-65-thiophene-OH-1H.3 (florencia)	AK-2-65-thiophene-OH-13C.3 (florencia)	AK-2-65-thiophene-OH
182p		FN-VII-147.1 (florencia)	FN-VII-147.2 (florencia)	FN-VII-147

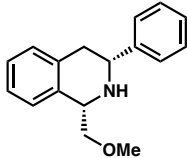
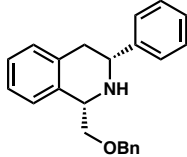
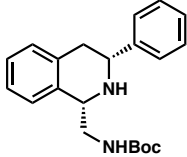
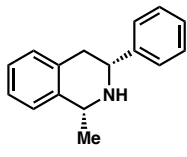
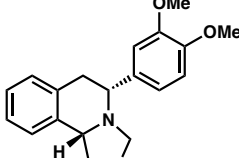
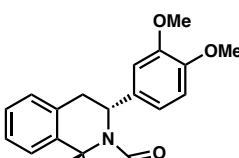
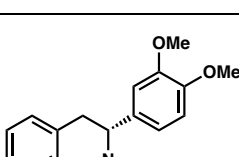
Compound	Chemical Structure	¹ H NMR	¹³ C NMR	IR
182q		AK-2-91-pyrazole-OH-1H.1 (florencia)	AK-2-91-pyrazole-OH-13C.4 (florencia)	AK-2-91-pyrazole-OH
182r		FN-11X-29.1 (florencia)	FN-11X-29.2 (florencia)	FN-2pyridine-hydrogSM
184a		AK-2-57-F-Ph-OH-1H.3 (florencia) ¹⁹ F: AK-2-57-F-Ph-OH (hg3)	AK-2-57-F-Ph-OH-13C.4 (florencia)	AK-2-57-F-Ph-OH
184b		AK-1-263-pOMe-F-OH-1H.1 (florencia) ¹⁹ F: AK-1-263-pOMe-F-OH-19F (hg3)	AK-1-263-pOMe-F-OH-13C.3 (Florencia)	AK-1-263-pOMe-F-OH
184c		AK-1-265-pCF3-F-OH-1H.3 (florencia) ¹⁹ F: AK-1-265-19F (hg3)	AK-1-265-pCF3-F-OH-13C.4 (florencia)	AK-1-265-pCF3-F-OH
184d		AK-2-105-dioxolane-Ph-OH-1H.3 (florencia)	AK-2-105-dioxolane-Ph-OH-13C.4 (florencia)	AK-2-105-dioxolane-Ph-OH
184e		AK-2-107-dioxolane-diOMe-OH-1H.3 (florencia)	AK-2-107-dioxolane-diOMe-OH-13C.4 (florencia)	AK-2-107-dioxolane-diOMe-OH
184f		AK-2-109-naphthylback-OH-1H.3 (florencia)	AK-2-109-naphthylback-OH-13C.4 (florencia)	AK-2-109-naphthylback-OH

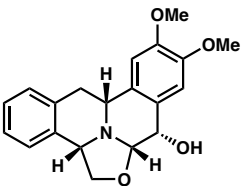
Compound	Chemical Structure	¹ H NMR	¹³ C NMR	IR
186a		FN-VII-231.1 (florence)	FN-VII-231.2 (florence)	FN-VII-231
186b		FN-VII-229.1 (florence)	FN-VII-229.2 (florence)	FN-VII-229
186c		FN-VII-243.1 (florence)	FN-VII-243.2 (florence)	FN-VII-243
186d		FN-VII-219.3 (florence)	FN-VII-219.4 (florence)	FN-VII-255
186f		FN-VII-211.1 (florence)	FN-VII-211.2 (florence)	FN-VII-211
183a		FN-VII-51.1 (florence)	FN-VII-51.2 (florence)	FN-VII-51
<i>trans</i> -183a		<i>trans</i> -FN-IIX-185prep.1 (florence)	<i>trans</i> -FN-IIX-185prep.2 (florence)	—
183b		FN-VII-129.1 (florence)	FN-VII-129.2 (florence)	FN-VII-129

Compound	Chemical Structure	¹ H NMR	¹³ C NMR	IR
183c		FN-VII-119.1 (florencia)	FN-VII-119.2 (florencia)	FN-VII-119
183d		AK-1-299A- pOMe-pdt-1H.3 (florencia)	AK-1-299A- pOMe-pdt-13C.4 (florencia)	AK-1-299A-pOMe- pdt
183e		FN-VII-131.1 (florencia) ¹⁹ F: FN-VII-131 (hg3)	FN-VII-131.2 (florencia)	AK-1-299c-pF-pdt
183f		AK-1-299B-pCF3- pdt-1H.3 (florencia) ¹⁹ F: AK-1-299B-2 (hg3)	AK-1-299B-pCF3- pdt-13C.4 (florencia)	AK-1-299B-pCF3- pdt
183g		FN-IX-77recol- dry (indy)	FN-IX-77recol.2 (florencia)	FN-IX-77
183h		FN-IX-205.1 (florencia)	FN-IX-205.2 (florencia)	FN-VII-183
183i		AK-2-47B-F3-pdt- final-1H.4 (florencia) ¹⁹ F: AK-2-47B- 19F (hg3)	AK-2-47B-triF- 13C.1 (florencia)	AK-2-47B-F3-pdt2

Compound	Chemical Structure	¹ H NMR	¹³ C NMR	IR
183j		FN-VII-121.1 (florencia)	FN-VII-121.2 (florencia)	FN-VII-121
183k		FN-VII-127.1 (florencia)	FN-VII-127.2 (florencia)	FN-VII-127
183l		FN-VII-159B.1 (florencia)	FN-VII-159B.2 (florencia)	FN-VII-159
183m		FN-VII-281.1 (florencia)	FN-VII-281.2 (florencia)	FN-VII-281
183n		AK-2-75B-furan- pdt-1H.3 (florencia)	AK-2-75B-furan- pdt-13C.4 (florencia)	AK-2-75B-furan- pdt
183o		AK-2-75D- thiophene-pdt- 1H.3 (florencia)	AK-2-75D- thiophene-pdt- 13C.4 (florencia)	AK-2-75D- thiophene-pdt
183p		FN-THIQ- 3thiophene (indy)	FN-VII-225.2 (florencia)	FN-VII-225
183q		AK-2-101B- pyrazole-pdt-1H.3 (florencia)	AK-2-101B- pyrazole-pdt- 13C.4 (florencia)	AK-2-101B- pyrazole-pdt

Compound	Chemical Structure	¹ H NMR	¹³ C NMR	IR
183r		FN-IIX-37washed.1 (florencia)	FN-IIX-37washed.2 (florencia)	FN-IIX-37
185a		AK-2-69B-F-Ph-pdt-1H.3 (florencia) ¹⁹ F: AK-2-69B-F-Ph (hg3)	AK-2-69B-F-Ph-pdt-13C.3 (florencia)	AK-2-69B-F-Ph-pdt
185b		AK-1-277B-pOMe-F-pdt-1H.3 (florencia) ¹⁹ F: AK-2-69C-F-pOMe-19F (hg3)	AK-2-69C-F-pOMe-pdt-13C.1 (florencia)	AK-1-277B-pOMe-F-pdt
185c		AK-2-69D-pCF3-F-pdt-1H.1 (florencia) ¹⁹ F: AK-1-277D (hg3)	AK-2-69D-pCF3-F-pdt-13C.1 (florencia)	AK-2-69D-pCF3-F-pdt
185d		AK-2-135-dioxolane-Ph-pdt-1H.3 (florencia)	AK-2-135-dioxolane-Ph-13C.4 (florencia)	AK-2-135-dioxolane-Ph-pdt
185e		AK-2-129B-dioxolane-diOMe-pdt-1H.3 (florencia)	AK-2-129B-dioxolane-diOMe-pdt-13C.4 (florencia)	AK-2-129B-dioxolane-diOMe-pdt
185f		AK-2-129D-naphthyl-OH-pdt-1H.3 (florencia)	AK-2-129D-naphthyl-OH-pdt-13C.4 (florencia)	AK-2-129D-naphthyl-pdt
187a		FN-VII-285.1 (florencia)	FN-VII-285.2 (florencia)	FN-VII-285

Compound	Chemical Structure	¹ H NMR	¹³ C NMR	IR
187b		FN-VII-261.1 (florence)	FN-VII-261.2 (florence)	FN-VII-261
187c		FN-THIQ-OBn (indy)	FN-VII-265.2 (florence)	FN-VII-265
187d		FN-IIX-39.1 (florence) *in AK folder	FN-IIX-39.2 (florence) *in AK folder	FN-IIX-39
187e		FN-VII-203.3 (florence)	FN-VII-203.2 (florence)	FN-VII-203
188		FN-IIX-107col.1 (florence)	FN-IIX-107col.2 (florence)	FN-IIX-107
189		FN-IIX-73col.1 (florence)	FN-IIX-73col.2 (florence)	FN-IIX-73
190		FN-IIX-127col.1 (florence)	FN-IIX-127col.2 (florence)	FN-IIX-127

Compound	Chemical Structure	¹ H NMR	¹³ C NMR	IR
191		AK-2-173B-prep2- 1H.3 (florencia)	AK-2-173B-prep2- 13C.4 (florencia)	AK-2-173B

COMPREHENSIVE BIBLIOGRAPHY

- Aeilts, S. L.; Cefalo, D. R.; Bonitatebus, P. J. Jr.; Houser, J. H.; Hoveyda, A. H.; Schrock, R. R. *Angew. Chem. Int. Ed.* **2001**, *40*, 1452–1456.
- Akula, R.; Guiry, P. J. *Org. Lett.* **2016**, *18*, 5472–5475.
- Alexy, E. J.; Fulton, T. J.; Zhang, H.; Stoltz, B. M. *Chem. Sci.* **2019**, *10*, 5996–6000.
- Alexy, E. J.; Virgil, S. C.; Bartberger, M. D.; Stoltz, B. M. *Org. Lett.* **2017**, *19*, 5007–5009.
- Alexy, E. J.; Zhang, H.; Stoltz, B. M. *J. Am. Chem. Soc.* **2018**, *140*, 10109–10112.
- Allan, K. M.; Hong, B. D.; Stoltz, B. M. *Org. Biomol. Chem.* **2009**, *7*, 4960–4964.
- Angus, R. O.; Schmidt, M. W.; Johnson, R. P.; *J. Am. Chem. Soc.* **1985**, *107*, 532–537.
- Arambasic, M.; Hooper, J. F.; Willis, M. C. *Org. Lett.* **2013**, *15*, 5162–5165.
- Asamdi, M.; Chikhalia, K. H. *Asian J. Org. Chem.* **2017**, *6*, 1331–1348.
- Atul, G.; Amit, K.; Ashutosh, R. *Chem. Rev.* **2013**, *113*, 1614–1640.
- Balskus, E. P.; Jacobsen, E. N. *Science* **2007**, *317*, 1736–1740.
- Barber, J. S.; Styduhar, E. D.; Pham, H. W.; McMahon, T. C.; Houk, K. N.; Garg, N. K. *J. Am. Chem. Soc.* **2016**, *138*, 2512–2515.
- Barber, J. S.; Yamano, M. M.; Ramirez, M.; Darzi, E. R.; Knapp, R. R.; Liu, F.; Houk, K. N.; Garg, N. K. *Nat. Chem.* **2018**, *10*, 953–960.
- Behenna, D. C.; Liu, Y.; Yurino, T.; Kim, J.; White, D. E.; Virgil, S. C.; Stoltz, B. M. *Nature Chem.* **2012**, *4*, 130–133.
- Behenna, D. C.; Mohr, J. T.; Sherden, N. H.; Marinescu, S. C.; Harned, A. M.; Tani, K.; Seto, M.; Ma, S.; Novák, Z.; Krout, M. R.; McFadden, R. M.; Roizen, J. L.; Enquist,

- J. A.; White, D. E.; Levine, S. R.; Petrova, K. V.; Iwashita, A.; Virgil, S. C.; Stoltz, B. M. *Chem. Eur. J.* **2011**, *17*, 14199–14223.
- Bernhard, Y.; Thomson, B.; Ferey, V.; Sauthier, M. *Angew. Chem. Int. Ed.* **2017**, *56*, 7460–7464; *Angew. Chem.* **2017**, *129*, 7568–7572.
- Beumer, J. H.; Rademaker-Lakhai, J. M.; Rosing, H.; Hillebrand, M. J. X.; Bosch, T. M.; Lopez-Lazaro, L.; Schellens, J. H. M.; Beijnen, J. H. *Cancer Chemother. Pharmacol.* **2007**, *59*, 825–837.
- Bhat, V.; Welin, E. R.; Guo, X.; Stoltz, B. M. *Chem. Rev.* **2017**, *117*, 4528–4561.
- Bhojgude, S. S.; Bhunia, A.; Biju, A. T. *Acc. Chem. Res.* **2016**, *49*, 1658–1670.
- Blakemore, D. C.; Castro, L.; Churcher, I.; Rees, D. C.; Thomas, A. W.; Wilson, D. M.; Wood, A. *Nat. Chem.* **2018**, *10*, 383–394.
- Boekelheide, V.; Linn, W. J.; *J. Am. Chem. Soc.* **1954**, *76*, 1286–1291.
- Bols, M.; Skrydstrup, T. *Chem. Rev.* **1995**, *95*, 1253–1277.
- Börgel, J.; Tanwar, L.; Berger, F.; Ritter, T. *J. Am. Chem. Soc.* **2018**, *140*, 16026–16031.
- Bracegirdle, S.; Anderson, E. A. *Chem. Soc. Rev.* **2010**, *39*, 4114–4129.
- Bruno, N. C.; Tudge, M. T.; Buchwald, S. L. *Chem. Sci.* **2013**, *4*, 916–920.
- Campeau, L.-C.; Schipper, D. J.; Fagnou, K. *J. Am. Chem. Soc.* **2008**, *130*, 3266–3267.
- Carrillo, L.; Badia, D.; Dominguez, E.; Anakabe, E.; Osante, I.; Tellitu, I.; Vicario, J. L. *J. Org. Chem.* **1999**, *64*, 115–1120.
- Carroll, F. I.; Robinson, T. P.; Brieady, L. E.; Atkinson, R. N.; Mascarella, S. W.; Damaj, M. I.; Martin, B. R.; Navarrio, H. A. *J. Med. Chem.* **2007**, *50*, 6383–6391.
- Carter, N. J.; Keam, S. J. *Drugs* **2010**, *70*, 355–376.

- Charupant, K.; Daikuhara, N.; Saito, E.; Amnuoypol, S.; Suwanborirux, K.; Owa, T.; Saito, N. *Bioorg. Med. Chem.* **2009**, *17*, 4548–4558.
- Charupant, K.; Suwanborirux, K.; Amnuaypol, S.; Saito, E.; Kubo, A.; Saito, N. *Chem. Pharm. Bull.* **2007**, *55*, 81–86.
- Chen, J.-P.; Ding, C.-H.; Liu, W.; Hou, X.-L.; Dai, L.-X. *J. Am. Chem. Soc.* **2010**, *132*, 15493–15495.
- Chen, M.-W.; Ji, Y.; Wang, J.; Chen, Q.-A.; Shi, L.; Zhou, Y.-G. *Org. Lett.* **2017**, *19*, 4988–4991.
- Chen, R.; Liu, H.; Chen, X. *J. Nat. Prod.* **2013**, *76*, 1789–1795.
- Chinnagolla, R. K.; Pimparkar, S.; Jeganmohan, M. *Org. Lett.* **2012**, *14*, 3032–3035.
- Christl, M.; Braun, M.; Wolz, E.; Wagner, W. *Chem. Ber.* **1994**, *127*, 1137–1142.
- Christl, M.; Fischer, H.; Arnone, M.; Engels, B. *Chem. Eur. J.* **2009**, *15*, 11266–11272.
- Chrzanowska, M.; Grajewska, A.; Rozwadowska, M. D. *Chem. Rev.* **2016**, *116*, 12369–12465.
- Chrzanowska, M.; Rozwadowska, M. D. *Chem. Rev.* **2004**, *104*, 3341–3370.
- Chu, H.; Sun, S.; Yu, J.-T.; Cheng, J. *Chem. Commun.* **2015**, *51*, 13327.
- Chupakhin, E. G.; Krasavin, M.Y. *Chem. Heterocycl. Compd.* **2018**, *54*, 483–501.
- Coe, J. W. et al., *Bioorg. Med. Chem. Lett.* **2005**, *15*, 4889–4897.
- Comins, D. L.; Brown, J. D.; *J. Org. Chem.* **1984**, *49*, 1078–1083.
- Corsello, M. A.; Kim, J.; Garg, N. K. *Nat. Chem.* **2017**, *9*, 944–949.
- Cossy, J.; de Filippis, A.; Pardo, D. G. *Org. Lett.* **2003**, *5*, 3037–3039.

- Crowley, B. M.; Mori, Y.; McComas, C. C.; Tang, D.; Boger, D. L. *J. Am. Chem. Soc.* **2004**, *126*, 4310–4317.
- Cuevas, C. *et al.*, *Org. Lett.* **2000**, *2*, 2545–2548.
- Cuevas, C.; Francesch, A. *Nat. Prod. Rep.* **2009**, *26*, 322–337.
- Daoust, K. J.; Hernandez, S. M.; Konrad, K. M.; Mackie, I.; Winstanley, J.; Johnson, R. P. *J. Org. Chem.* **2006**, *71*, 5708–5714.
- Davies, S. G.; Haggitt, J. R.; Ichihara, O.; Kelly, R. J.; Leech, M. A.; Mortimer, A. J. P.; Roberts, P. M.; Smith, A. D. *Org. Biomol. Chem.* **2004**, *2*, 2630–2649.
- Delhay, L.; Merschaert, A.; Diker, K.; Houppis, I. N. *Synthesis*, **2006**, *9*, 1437–1442.
- Deng, J. Z.; Paone, D. V.; Ginnetti, A. T.; Kurihara, H.; Dreher, S. D.; Weissman, S. A.; Stauffer, S. R. *Org. Lett.* **2009**, *11*, 345–347.
- Dhokale, R. A.; Mhaske, S. B. *Synthesis* **2018**, *50*, 1–16.
- Dillion, P. W.; Underwood, G. R.; *J. Am. Chem. Soc.* **1974**, *96*, 779–787.
- Dondorp, A. M. *et al.*, *N. Engl. J. Med.* **2009**, *361*, 455–467.
- Donohoe, T. J.; Pilgrim, B. S.; Jones, G. R.; Bassuto, J. A. *Proc. Natl. Acad. Sci. U.S.A.* **2012**, *109*, 11605–11608.
- Dorta, R.; Broggini, D.; Kissner, R.; Togni, A. *Chem. Eur. J.* **2004**, *10*, 4546–4555.
- Dorta, R.; Broggini, D.; Stoop, R.; Rüegger, H. Spindler, F.; Togni, A. *Chem. Eur. J.* **2004**, *10*, 267–278.
- Drinkuth, S.; Groetsch, S.; Peters, E.; Peters, K.; Christl, M. *Eur. J. Org. Chem.* **2001**, 2665–2670.
- Engels, B.; Schöneboom, J. C.; Münster, A. F.; Geoetsch, S.; Christl, M. *J. Am. Chem. Soc.* **2002**, *124*, 287–297.

- Feng, J.; Holmes, M.; Krische, M. J. *Chem. Rev.* **2017**, *117*, 12564–12580.
- Filippis, A.; Pardo, D. G.; Cossy, J. *Synthesis*. **2004**, *17*, 2930–2933.
- Finn, R. S.; Dering, J.; Conklin, D.; Kalous, O.; Cohen, D. J.; Desai, A. J.; Ginther, C.; Atefi, M.; Chen, I.; Fowst, C.; Los, G.; Slamon, D. J. *Breast Cancer Res.* **2009**, *11*, R77–R89.
- Fontana, A.; Cavaliere, P.; Wahidulla, S.; Naik, C. G.; Cimino, G. *Tetrahedron* **2000**, *56*, 7305–7308.
- Foot, J. S.; Kanno, H.; Giblin, G. M. P.; Taylor, R. J. K. *Synthesis* **2003**, *2003*, 1055–1064.
- Foti, C. J.; Comins, D. L., *J. Org. Chem.* **1995**, *60*, 2656–2657.
- Gadhiya, S. V.; Giri, R.; Cordone, P.; Karki, A.; Harding, W. W. *Curr. Org. Chem.* **2018**, *22*, 1893–1905.
- Gallagher, A. G.; Tian, H.; Torres-Herrera, O. A.; Yin, S.; Xie, A.; Lange, D. M.; Wilson, J. K.; Mueller, L. G.; Gau, M. R.; Carroll, P. J.; Martinez-Solorio, D. *Org. Lett.* **2019**, *21*, 8646–8651.
- Garnier, E. C.; Liebeskind, L.S. *J. Am. Chem. Soc.* **2008**, *130*, 7449–7458.
- Goetz, A. E.; Garg, N. K. *J. Org. Chem.* **2014**, *79*, 846–851.
- Goetz, A. E.; Silberstein, A. L.; Corsello, M. A.; Garg, N. K. *J. Am. Chem. Soc.* **2014**, *136*, 3036–3039.
- Gunaydin, H.; Altman, M. D.; Ellis, J. M.; Fuller, P.; Johnson, S. A.; Lahue, B.; Lapointe, B. *ACS Med. Chem. Lett.* **2018**, *9*, 528–533.
- Guo, D.; Li, J.; Lin, H.; Zhou, Y.; Chen, Y.; Sun, H.; Zhang, D.; Li, H.; Shoichet, B. K.; Shan, L.; Xie, X.; Jiang, H.; Liu, H. *J. Med. Chem.* **2016**, *59*, 9489–9502.
- Guo, R.-N.; Cai, X.-F.; Shi, L.; Ye, Z.-S.; Chen, M.-W.; Zhou, Y.-G. *Chem. Commun.* **2013**, *49*, 8537–8539.

- Ha, M. W.; Lee, H.; Yi, H. Y.; Park, Y.; Kim, S.; Hong, S.; Lee, M.; Kim, M.-h.; Kim, T.-s.; Park, H.-g. *Adv. Synth. Catal.* **2013**, *355*, 637–642.
- Haftchenary, S.; Nelson, S. D.; Furst, L.; Dandapani, S.; Ferrara, S. J.; Bošković, Z. V.; Lazú, S. F.; Guerrero, A. M.; Serrano, J. C.; Crews, D. K.; Brackeen, C.; Mowat, J.; Brumby, T.; Bauser, M.; Schreiber, S. L.; Phillips, A. J. *ACS. Comb. Sci.* **2016**, *18*, 569–574.
- Harmata, M.; Yang, W.; Barnes, C. L. *Tetrahedron Lett.* **2009**, *50*, 2326–2328.
- Hayashi, M.; Bachman, S.; Hashimoto, S.; Eichman, C. C.; Stoltz, B. M. *J. Am. Chem. Soc.* **2016**, *138*, 8997–9000.
- Hethcox, J. C.; Shockley, S. E.; Stoltz, B. M. *ACS Catal.* **2016**, *6*, 6207–6213.
- Hethcox, J. C.; Shockley, S. E.; Stoltz, B. M. *Angew. Chem. Int. Ed.* **2016**, *55*, 16092–16095.; *Angew. Chem.* **2016**, *128*, 16326–16329.
- Himeshima, Y.; Sonoda, T.; Kobayashi, H. *Chem. Lett.* **1983**, *12*, 1211–1214.
- Hong, A. Y.; Bennett, N. B.; Krout, M. R.; Jensen, T.; Harned, A. M.; Stoltz, B. M. *Tetrahedron* **2011**, *67*, 10234–10248.
- Hopmann, K. H.; Bayer, A. *Organometallics.* **2011**, *30*, 2483–2497.
- Hoshiya, N.; Takenaka, K.; Shuto, S.; Uenishi, J. *Org. Lett.* **2016**, *18*, 48–51.
- Hosseinzadeh, R.; Tajbakhsh, M.; Mohadjerani, M.; Mehdinejad, H. *Synlett.* **2004**, *9*, 1517–1520.
- Huang, C.; Ghavtadze, N.; Godoi, B.; Gevorgyan, V. *Chem. Eur. J.* **2012**, *18*, 9789–9792.
- Idiris, F. I. M.; Jones, C. R. *Org. Biomol. Chem.* **2017**, *15*, 9044–9056.
- Iimuro, A.; Yamaji, K.; Kandula, S.; Nagano, T.; Kita, Y.; Mashima, K. *Angew. Chem. Int. Ed.* **2013**, *52*, 2046–2050.

- Inoue, K.; Nakura, R.; Okano, K.; Mori, A. *Eur. J. Org. Chem.* **2018**, 3343–3347.
- Jacob, P. III. *J. Med. Chem.* **1981**, 24, 1348–1353.
- Jakubec, P.; Farley, A. J. M.; Dixon, D. J. *Beilstein J. Org. Chem.* **2016**, 12, 1096–1100.
- James, J.; Guiry, P. J. *ACS Catal.* **2017**, 1397–1402.
- James, J.; Jackson, M.; Guiry, P. J. *Adv. Synth. Catal.* **2019**, 361, 3016–3049.
- Jette, C. I.; Tong, Z. J.; Hadt, R. G.; Stoltz, B. M. *Angew. Chem. Int. Ed.* **2020**, 59, 2033–2038.
- Kim, K. E.; Li, J.; Grubbs, R. H.; Stoltz, B. M. *J. Am. Chem. Soc.* **2016**, 138, 13179–13182.
- Kita, Y.; Kavthe, R. D.; Oda, H.; Mashima, K. *Angew. Chem. Int. Ed.* **2016**, 55, 1098–1101; *Angew. Chem.* **2016**, 128, 1110–1113.
- Kita, Y.; Yamaji, K.; Higashida, K.; Sathaiah, K.; Iimuro, A.; Mashima, K. *Angew. Chem., Int. Ed.* **2013**, 52, 2046–2050.
- Kita, Y.; Yamaji, K.; Higashida, K.; Sathaiah, K.; Iimuro, A.; Mashima, K. *Chem. Eur. J.* **2015**, 21, 1915–1927.
- Klayman, D. L. *Science* **1985**, 228, 1049–1055.
- Klepacz, A.; Zwierzak, A. *Tetrahedron Lett.* **2002**, 43, 1079–1080.
- Kondo, H.; Maeno, M.; Hirano, K.; Shibata, N. *Chem. Commun.* **2018**, 54, 5522–5525.
- Kou, K. G. M.; Pflueger, J. J.; Kiho, T.; Morrill, L. C.; Fisher, E. L.; Clagg, K.; Lebold, T. P.; Kisunzu, J. K.; Sarpong, R. *J. Am. Chem. Soc.* **2018**, 140, 8105–8109.
- Lane, J. W.; Chen, Y.; Williams, R. M. *J. Am. Chem. Soc.* **2005**, 127, 12684–12690.
- Lavery, C. B.; Rotta-Loria, N. L.; McDonald, R.; Stradiotto, M. *Adv. Synth. Catal.* **2013**, 335, 981–987.

- Lee, E.; Song, H. Y.; Kang, J. W.; Kim, D.-S.; Jung, C.-K.; Joo, J. M. *J. Am. Chem. Soc.* **2002**, *124*, 384–385.
- Legault, C. Y.; Charette, A. B. *J. Am. Chem. Soc.* **2005**, *127*, 8966–8967.
- Li, X.-H.; Wan, S.-L.; Chen, D.; Liu, Q.; Ding, C.-H.; Fang, P.; Hou, X.-L. *Synthesis*, **2016**, *48*, 1568–1572.
- Li, X.; Sun, Y.; Huang, X.; Zhang, L.; Kong, L.; Peng, B. *Org. Lett.* **2017**, *19*, 838–841.
- Lian, W.-F.; Wang, C.-C.; Kang, H.-P.; Li, H.-L.; Feng, J.; Liu, S.; Zhang, Z.-W. *Tetrahedron Lett.* **2017**, *58*, 1399–1402.
- Lin, J. B.; Shah, T. J.; Goetz, A. E.; Garg, N. K.; Houk, K. N. *J. Am. Chem. Soc.* **2017**, *139*, 10447–10455.
- Liu, W.; Liao, X.; Dong, W.; Yan, Z.; Wang, N.; Liu, Z. *Tetrahedron* **2012**, *68*, 2759–2764.
- Liu, W.; Xu, D. D.; Repič, O.; Blacklock, T. J. *Tetrahedron Lett.* **2001**, 2439–2441.
- Liu, Y.; Han, S.-J.; Liu, W.-B.; Stoltz, B. M. *Acc. Chem. Res.* **2015**, *48*, 740–751.
- Lofstrand, V. A.; West, F. G. *Chem. Eur. J.* **2016**, *22*, 10763–10767.
- Loreto, A.; Migliorini, A.; Tardella, P. A.; Gambacorta, A. *Eur. J. Org. Chem.* **2007**, *14*, 2365–2371.
- Lovering, F. *Med. Chem. Commun.* **2013**, *4*, 515–519.
- Lovering, F.; Bikker, J.; Humblet, C. *J. Med. Chem.* **2009**, *52*, 6752–6756.
- Lown, J. W.; Joshua, A. V.; Lee, J. S. *Biochemistry* **1982**, *21*, 419–428.
- Lu, P.; Mailyan, A.; Gu, Z.; Guptill, D. M.; Wang, H.; Davies, H. M. L.; Zakarian, A. *J. Am. Chem. Soc.* **2014**, *136*, 17738–17749.

- Lu, S. M.; Wang, Y. Q.; Han, X. W.; Zhou, Y.-G. *Angew. Chem. Int. Ed.* **2006**, *45*, 2260–2263.
- Maki, B. E.; Chan, A.; Phillips, E. M.; Scheidt, K. A. *Org. Lett.* **2007**, *9*, 371–374.
- Manivel, P. Probakaran, K.; Khan, F. N.; Jin, J. S. *Res. Chem. Intermed.* **2012**, *38*, 347–357.
- Martinez, E. J.; Owa, T.; Schreiber, S. L.; Corey, E. J. *Proc. Natl. Acad. Sci. USA* **1999**, *96*, 3496–3501.
- Mauger, C. C.; Mignani, G. A. *Org. Proc. Res. Dev.* **2004**, *8*, 1065–1071.
- Miller, D. J.; Yu, F.; Knight, D. W.; Allemann, R. K. *Org. Biomol. Chem.* **2009**, *7*, 962–975.
- Mohr, J. T.; Stoltz, B. M. *Chem. Asian. J.* **2007**, *2*, 1476–1491.
- Montgomery, C. T.; Cassels, B. K.; Shamma, M. *J. Nat. Prod.* **1983**, *46*, 441–453.
- Müller, P. *Crystallography Reviews*, **2009**, *15*, 57–83.
- Myers, A. G.; Lanman, B. A. *J. Am. Chem. Soc.* **2002**, *124*, 12969–12971.
- Myers, A. G.; Plowright, A. T. *J. Am. Chem. Soc.* **2001**, *123*, 5114–5115.
- Neog, K.; Borah, A.; Gogoi, P. *J. Org. Chem.* **2016**, *81*, 11971–11977.
- Neumeyer, M.; Kopp, J.; Brückner, R. *Eur. J. Org. Chem.* **2017**, 2883–2915.
- Nevagi, R. J.; Dighe, S. N. *Eur. J. Med. Chem.* **2015**, *97*, 561–581.
- Newman, D. J.; Cragg, G. M. *J. Nat. Prod.* **2016**, *79*, 629–661.
- Ngamnithiporn, A.; Jette, C. I.; Bachman, S.; Virgil, S. C.; Stoltz, B. M. *Chem. Sci.* **2018**, *9*, 2547–2551.

- Nicolaou, K. C.; Rhoades, D.; Lamani, M.; Pattanayak, M. R.; Kumar, S. M. *J. Am. Chem. Soc.* **2016**, *138*, 7532–7535.
- Noyori, R.; Hashiguchi, S. *Acc. Chem. Res.* **1997**, *20*, 97–102.
- O'Brien, N. A.; McDonald, K.; Luo, T.; Euw, E.; Kalous, O.; Conklin, D.; Hurvitz, S. A.; Tomaso, E. D.; Schnell, C.; Linnartz, R.; Finn, R. S.; Hirawat, S.; Slamon, D. J. *Clin. Cancer Res.* **2014**, *20*, 3507–2510.
- Ocio, E. M. *et al.*, *Blood* **2009**, *113*, 3781–3791.
- Oliveira, M. N.; Fournier, J.; Arseniyadis, S.; Cossy, J. *Org. Lett.* **2017**, *19*, 14–17.
- Oliver, S.; Evans, P. A. *Synthesis*. **2013**, *45*, 3179–3198.
- Pangborn, A. B.; Giardello, M. A.; Grubbs, R. H.; Rosen, R. K.; Timmers, F. J. *Organometallics*, **1996**, *15*, 1518–1520.
- Parasram, M.; Iaroshenko, V. O.; Gevorgyan, V. *J. Am. Chem. Soc.* **2014**, *136*, 17926–17929.
- Park, Y.; Lee, Y. J.; Hong, S.; Kim, M.-h.; Lee, M.; Kim, T.-s.; Lee, J. K.; Jew, S.-s.; Park, H.-g. *Adv. Synth. Catal.* **2011**, *353*, 3313–3318.
- Parmar, D.; Duffy, L. A.; Sadasivam, D. V.; Matsubara, H.; Bradley, P. A.; Flowers II, R. A.; Procter, D. J. *J. Am. Chem. Soc.* **2009**, *131*, 15467–15473.
- Pérez-Ruixo, C.; Valenzuela, B.; Fernández Teruel, C.; González-Sales, M.; Miguel-Lillo, B.; Soto-Matos, A.; Pérez-Ruixo, J. J. *Cancer Chemother. Pharmacol.* **2012**, *69*, 15–24.
- Perez-Ruixo, J. J.; Zannikos, P.; Hirankam, S.; Stuyckens, K.; Ludwig, E. A.; Soto-Matos, A.; Lopez-Lazaro, L.; Owen, J. S. *Clin. Pharmacokinet.* **2007**, *46*, 867–884.
- Pilgrim, B. S.; Gatland, A. E.; Esteves, C. H. A.; McTernan, C. T.; Jones, G. R.; Tatton, M. R.; Procopiou, P. A.; Donohoe, T. J. *Org. Biomol. Chem.* **2016**, *14*, 1065–1090.

- Pommier, Y.; Kohlhagen, G.; Bailly, C.; Waring, M.; Mazumder, A.; Kohn, K. W. *Biochemistry* **1996**, *35*, 13303–13309.
- Quintana, I.; Peña, D.; Pérez, D.; Guitián, E. *Eur. J. Org. Chem.* **2009**, 5519–5524.
- Radadiya, A.; Shah, A. *Eur. J. Med. Chem.* **2015**, *97*, 356–376.
- Rath, C. M. *et al.*, *ACS Chem. Biol.* **2011**, *6*, 1244–1256.
- Reid, J. M.; Kuffel, M. J.; Ruben, S. L.; Morales, J. J.; Rinehart, K. L.; Squillace, D. P.; Ames, M. M. *Clin. Cancer Res.* **2002**, *8*, 2952–2962.
- Roberts, J. D.; Simmons, H. E.; Carlsmith, L. A.; Vaughn, C. W. *J. Am. Chem. Soc.* **1953**, *75*, 3290–3291.
- Roughley, S. D.; Jordan, A. M. *J. Med. Chem.* **2011**, *54*, 3451–3479.
- Ruzziconi, R.; Naruse, Y.; Schlosser, M. *Tetrahedron* **1991**, *47*, 4603–4610.
- Saito, N.; Tanaka, C.; Koizumi, Y.-i.; Suwanborirux, K.; Amnuoypol, S.; Pummangura, S.; Kubo, A. *Tetrahedron* **2004**, *60*, 3873–3881.
- Salaski, E. J. *et al.*, *J. Med. Chem.* **2009**, *52*, 2181–2184.
- Sauerberg, P.; Kindtler, J. W.; Nielsen, L.; Sheardown, M. J.; Honoré, T. *J. Med. Chem.* **1991**, *34*, 687–697.
- Schleth, F.; Vettiger, T.; Rommel, M.; Tobler, H. WO2011131544 A1, 2011.
- Schmidt, M. W.; Angus, R. O.; Johnson, R. P. *J. Am. Chem. Soc.* **1982**, *104*, 6838–6839.
- Schreck, M.; Christl, M. *Angew. Chem. Int. Ed.* **1987**, *26*, 690–692; *Angew. Chem.* **1987**, *99*, 720–721.
- Scott, J. D.; Williams, R. M. *Chem. Rev.* **2002**, *102*, 1669–1730.
- Sercel, Z. P.; Sun, A. W.; Stoltz, B. M. *Org. Lett.* **2019**, *21*, 9158–9161.

- Sha, C.-K.; Chiu, R.-T.; Yang, C.-F.; Yao, N.-T.; Tseng, W.-H.; Liao, F.-L.; Wang, S.-L. *J. Am. Chem. Soc.* **1997**, *119*, 4130–4135.
- Sha, S. C.; Mao, J.; Bellomo, A.; Jeong, S. A.; Walsh, P. J. *Angew. Chem. Int. Ed.* **2016**, *55*, 1070–1074; *Angew. Chem.* **2017**, *128*, 1082–1086.
- Shah, P.; Westwell, A. D. *Journal of Enzyme Inhibition and Medicinal Chemistry* **2007**, *22*, 527–540.
- Shah, T. K.; Medina, J. M.; Garg, N. K. *J. Am. Chem. Soc.* **2016**, *138*, 4948–4954.
- Shakespeare, W. C.; Johnson, R. P. *J. Am. Chem. Soc.* **1990**, *112*, 8578–8579.
- Sheldrick, G. M. *Acta Cryst.* **1990**, *A46*, 467–473.
- Sheldrick, G. M. *Acta Cryst.* **2008**, *A64*, 112–122.
- Sheldrick, G. M. *Acta Cryst.* **2015**, *C71*, 3–8.
- Shi, J.; Li, Y.; Li, Y. *Chem. Soc. Rev.* **2017**, *46*, 1707–1719.
- Shi, L.; Ye, Z.-S.; Cao, L.-L.; Guo, R.-N.; Hu, Y.; Zhou, Y.-G. *Angew. Chem., Int. Ed.* **2012**, *51*, 8286–8289.
- Shields, J. D.; Ahneman, D. T.; Graham, T. J. A.; Doyle, A. G. *Org. Lett.* **2014**, *16*, 142–145.
- Shockley, S. E.; Hethcox, J. C.; Stoltz, B. M. *Angew. Chem. Int. Ed.* **2017**, *56*, 11545–11548; *Angew. Chem.* **2017**, *129*, 11703–11706.
- Shvartsbart, A.; Smith, A. B., III. *J. Am. Chem. Soc.* **2015**, *137*, 3510–3519.
- Siengalewicz, P.; Rinner, U.; Mulzer, J. *Chem. Soc. Rev.* **2008**, *37*, 2676–2690.
- Sikriwal, D.; Kant, R.; Maulik, P. R.; Dikshit, D. K. *Tetrahedron* **2010**, *66*, 6167–6173.
- Simas, A. B. C.; Pais, K. C.; da Silva, A. A. T. *J. Org. Chem.* **2003**, *68*, 5426–5428.

Skardon-Duncan, J.; Sparenberg, M.; Bayle, A.; Alexander, S.; Stephen, C. J. *Org. Lett.* **2018**, *20*, 2782–2786.

Son, S.; Fu, G. C. *J. Am. Chem. Soc.* **2008**, *130*, 2756–2757.

Song, L.-Q.; Zhang, Y.-Y.; Pu, J.-Y.; Tang, M.-C.; Peng, C.; Tang, G.-L. *Angew. Chem., Int. Ed.* **2017**, *56*, 9116–9120.

Spencer, J. R.; Sendzik, M.; Oeh, J.; Sabbatini, P.; Dalrymple, S. A.; Magill, C.; Kim, H. M.; Zhang, P.; Squires, N.; Moss, K. G.; Sukbuntherng, J.; Graupe, D.; Eksterowicz, J.; Young, P. R.; Myers, A. G.; Green, M. J. *Bioorg. Med. Chem. Lett.* **2006**, *16*, 4884–4888.

Srinivas, H. D.; Zhou, Q.; Watson, M. P. *Org. Lett.* **2014**, *16*, 3596–3599.

Starkov, P.; Moore, J. T.; Duquette, D. C.; Stoltz, B. M.; Marek, I. *J. Am. Chem. Soc.* **2017**, *139*, 9615–9620.

Suljić, S.; Pietruszka, J. *Adv. Synth. Catal.* **2014**, *356*, 1007–1020.

Sun, A. W.; Hess, S. N.; Stoltz, B. M. *Chem. Sci.* **2019**, *10*, 788–792.

Surry, D. S.; Buchwald, S. L. *Angew. Chem. Int. Ed.* **2008**, *47*, 6338–6361; *Angew. Chem.* **2008**, *120*, 6438–6461.

Szosak, M.; Spain, M.; Choquette, K. A.; Flowers II, R. A.; Procter, D. J. *J. Am. Chem. Soc.* **2013**, *135*, 15702–15705.

Tadross, P. M.; Gilmore, C. D.; Bugga, P.; Virgil, S. C.; Stoltz, B. M. *Org. Lett.* **2010**, *12*, 1224–1227.

Takikawa, H.; Nishii, A.; Sakai, T.; Suzuki, K. *Chem. Soc. Rev.* **2018**, *47*, 8030–8056.

Tan, Y.; Barrios-Landeros, F.; Hartwig, J. F. *J. Am. Chem. Soc.* **2012**, *134*, 3683–3686.

Taylor, R. D.; MacCoss, M.; Lawson, A. D. G. *J. Med. Chem.* **2014**, *57*, 5845.

- Thimmaiah, S.; Ningegowda, M.; Shivananju, N. S.; Ningegowda, R.; Siddaraj, R.; Priya, B. S. *Eur. J. Chem.* **2016**, *7*, 391–396.
- Tomaszewski, Z. et al., *J. Med. Chem.* **2005**, *48*, 926–934.
- Trost, B. M. *J. Org. Chem.* **2004**, *69*, 5813–5837.
- Trost, B. M.; Ball, Z. T.; Laemmerhold, K. M. *J. Am. Chem. Soc.* **2005**, *127*, 10028–10038.
- Trost, B. M.; Crawley, M. L. *Chem Rev.* **2003**, *103*, 2921–2943.
- Trost, B. M.; Frederiksen, M. U. *Angew. Chem. Int. Ed.* **2005**, *44*, 308–310; *Angew. Chem.* **2005**, *117*, 312–314.
- Trost, B. M.; Radinov, R.; Grenzer, E. M. *J. Am. Chem. Soc.* **1997**, *119*, 7879–7880.
- Trost, B. M.; Van Vranken, D. L., *Chem Rev.* **1996**, *96*, 395–422.
- Trost, B. M.; Xu, J.; Schmidt, T. *J. Am. Chem. Soc.* **2009**, *131*, 18343–18357.
- Trost, B.; Schultz, J. E. *Synthesis* **2019**, *51*, 1–30.
- Tsuji, J.; Takahashi, H.; Morikawa, M. *Tetrahedron Lett.* **1965**, *6*, 4387–4388.
- Tunge, J. A. *Isr. J. Chem.* **2020**, *60*, 351–359.
- U.S. Food and Drug Administration, Center for Drug Evaluation and Research. ID No. 207953Orig1s000, Pharmacology Reviews.
- Vita, M. V.; Caramenti, P.; Waser, J. *Org. Lett.* **2015**, *17*, 5832–5835.
- Vitaku, E.; Smith, D. T.; Njardarson, J. T. *J. Med. Chem.* **2014**, *57*, 10257–10274.
- Wang, D.-S.; Chen, Q.-A.; Lu, S.-M.; Zhou, Y.-G. *Chem. Rev.* **2012**, *112*, 2557–2590.
- Wang, J.; Wang, P.; Wang, L.; Li, D.; Wang, K.; Wang, Y.; Zhu, H.; Yang, D.; Wang, R. *Org. Lett.* **2017**, *19*, 4826–4829.

- Weaver, J. D.; Recio, A.; Grenning, A. J.; Tunge, J. A. *Chem. Rev.* **2011**, *68*, 1846–1913.
- Welin, E. R.; Ngamnithiporn, A.; Klatte, M.; Lapointe, G.; Pototschnig, G. M.; McDermott, M. S. J.; Conklin, D.; Gilmore, C. D.; Tadross, P. M.; Haley, C. K.; Negoro, K.; Glibstrup, E.; Grünanger, C. U.; Allan, K. M.; Virgil, S. C.; Slamon, D. J.; Stoltz, B. M. *Science*. **2019**, *363*, 270–275.
- Wen, J.; Tan, R.; Liu, S.; Zhao, Q.; Zhang, X. *Chem. Sci.* **2016**, *7*, 3047–3051.
- Wiedner, E. S.; Chambers, M. B.; Pitman, C. L.; Bullock, R. M.; Miller, A. J. M.; Appel, A. M. *Chem. Rev.* **2016**, *116*, 8655–8692.
- Willis, P. G.; Pavlova, O. A.; Chefer, S. I.; Vaupel, D. B.; Mukhin, A. G.; Horti, A. G. *J. Med. Chem.* **2005**, *48*, 5813–5822.
- Wittig, G. *Naturwissenschaften* **1942**, *30*, 696–703.
- Wittig, G.; Fritze, P. *Angew. Chem. Int. Ed.* **1966**, *5*, 846; *Angew. Chem.* **1966**, *78*, 905.
- Wu, Y.-C.; Zhu, J. *Org. Lett.* **2009**, *11*, 5558–5561.
- Xie, J.-H.; Zhu, S.-F.; Zhou, Q.-L. *Chem. Rev.* **2011**, *111*, 1713–1760.
- Xing, C.; LaPorte, J. R.; Barbay, J. K.; Myers, A. G. *Proc. Natl. Acad. Sci. USA* **2004**, *101*, 5862–5866.
- Xu, S.; Wang, G.; Zhu, J.; Shen, C.; Yang, Z.; Yu, J.; Li, Z.; Lin, T.; Sun, X.; Zhang, F. A *Eur. J. Org. Chem.* **2017**, 2017, 975–983.
- Xu, Z.; Xu, X.; O’Laoi, R.; Ma, H.; Zheng, J.; Chen, S.; Luo, L.; Hu, Z.; He, S.; Li, J.; Zhang, H.; Zhang, X. *Bioorg. Med. Chem.* **2016**, *24*, 5861–5872.
- Yamano, M. M.; Knapp, R. R.; Ngamnithiporn, A.; Ramirez, M.; Houk, K. N.; Stoltz, B. M.; Garg, N. K. *Angew. Chem. Int. Ed.* **2019**, *58*, 5653–5657.
- Ye, Z.-S.; Guo, R.-N.; Cai, X.-F.; Chen, M.-W.; Shi, L.; Zhou, Y.-G. *Angew. Chem. Int. Ed.* **2013**, *52*, 3685–3689.

Yeom, H.-S.; Kim, S.; Shin, S. *Synlett* **2008**, 2008, 924–928.

Yoshida, S.; Hosoya, T. *Chem. Lett.* **2015**, 44, 1450–1460.

Zhang, G.-L.; Chen, C.; Xiong, Y.; Zhang, L.-H.; Ye, J.; Ye, X.-S. *Carbohydrate Research*. **2010**, 345, 780–786.

Zhang, S.; Reith, M. E. A.; Dutta, A. K. *Bioorg. Med. Chem. Lett.* **2003**, 13, 1591–1595.

Zhang, S.; Zhen, J.; Reith, M. E. A.; Dutta, A. K. *Bioorg. Med. Chem.* **2004**, 12, 6301–6315.

Zhang, Z.-W.; Lin, A.; Yang, J. *J. Org. Chem.* **2014**, 79, 7041–7050.

Zhang, Z.-W.; Wang, C.-C.; Xue, H.; Dong, Y.; Yang, J.-H.; Shouxin, L.; Wen-Qing, L.; Wei-Dong, Z. *Org. Lett.* **2018**, 20, 1050–1053.

Zhao, D.; Glorius, F. *Angew. Chem. Int. Ed.* **2013**, 52, 9616–9618.

Zhao, D.; Lied, F.; Glorius, F. *Chem. Sci.* **2014**, 5, 2869–2873.

Zhou, S.; Wang, M.; Wang, L.; Chen, K.; Wang, J.; Song, C.; Zhu, J. *Org. Lett.* **2016**, 18, 5632–5635.

Zhou, Y.-G. *Acc. Chem. Res.* **2007**, 40, 1357–1366.

Zhu, Z.; Tang, X.; Li, X.; Wu, W.; Deng, G.; Jiang, H. *J. Org. Chem.* **2016**, 81, 1401–1409.

INDEX

π

π -allyl 8

A

acyclic 2, 9, 130, 134–136

allene 229–241

alkyne 230, 233, 253, 428, 551

analog 251, 261, 263, 425–439

anticancer 250, 252, 261, 262

aryne 254, 274–275, 428, 443

B

bisphosphine 4, 7, 10, 131

Boekelheide 255

C

carboxylic acid 282, 430, 431, 451, 454

chirality transfer 232, 240, 241

computational/computations/computed 133, 165–169, 232–234, 644–646

cytotoxic 261–263, 425, 428

D

decarboxylative 2, 129, 131, 136, 171, 238–239

Diels–Alder 129, 234, 235, 239, 241, 248

dioxolane 558, 566, 568

E

enolate 1, 238, 551, 565, 650

F

Fagnou coupling..... 254, 427, 429, 437, 444

G

Grignard 9

H

hemiacetal260, 283–285

heteroaryl 7, 548, 551, 552, 565, 557

hydrogenation..... 252, 255–257, 259, 263, 317, 426, 427, 434, 437–438, 547–563

hydrolysis 296, 551

I

iridium..... 256, 549, 550, 555

isoquinoline.....249, 252–257, 428–430

L

lactam..... 1–3, 7–10, 14, 19, 23, 252, 253, 260, 435, 439

lactamization 257, 319, 434

lactone..... 1–10, 135–136

Lewis acid..... 562

Lewis basic260, 548–550, 560

M

metabolic stability..... 251, 426, 428, 439

metathesis..... 9, 129

N

N-oxide236, 253, 255, 428–430

O

oxime 253, 268, 269, 428, 441, 442, 471, 472

P

palladium 2, 128, 131, 149, 254, 260, 268, 278, 296, 311, 441, 445

Pictet-Spengler 250, 252, 561, 563

piperidine 2, 9

prochiral 1–3, 7

propargyl 428

S

siloxane 128–136

silver 253, 282, 301, 428, 430–431

Sonogashira 253, 428, 440

steric/sterically 133, 241, 260, 548, 555, 558

Suzuki 551, 565, 572

V

Vibrational Circular Dichroism (VCD) 133, 164–169, 608, 643–648

W

Wacker 10

ABOUT THE AUTHOR

Aurapat (Fa) Ngamnithiporn was born in Bangkok, Thailand on April 6th, 1992 to Somsak and Penchit Ngamnithiporn. She grew up with her twin sibling Auranan (Fern) in Thailand until she moved to study in the United States in 2010 at Shuttuck-St. Mary's School in Faribault, MN.

Fa decided to stay in Minnesota and attended Carleton College in the fall of 2011, where she developed her interest in organic chemistry. By taking inspiring organic chemistry classes and working in the laboratory of Professors David Alberg and Gretchen Hofmeister, she decided to pursue her studies in graduate school. She graduated with a B.A. degree in chemistry and her undergraduate research focused on the synthesis of transition state analogs that can be utilized as mechanistic probes to study organocatalytic desymmetrization reactions.

Upon completion of her undergraduate studies, Fa moved to Pasadena, CA to pursue her doctoral education at the California Institute of Technology in 2015. Under the guidance of Professor Brian Stoltz, her graduate work focused on the development of enantioselective transition-metal catalysis and the synthesis of bioactive natural products. Following completion of her doctoral research in March 2021, Fa will return to Thailand and begin her professional career as a research chemist at Chulabhorn Research Institute.